

# Liver Elastography

Clinical Use and Interpretation

Sebastian Mueller

*Editor*

# Liver Elastography

Sebastian Mueller  
Editor

# Liver Elastography

## Clinical Use and Interpretation

 Springer

*Editor*

Sebastian Mueller  
Department of Medicine and Center for Alcohol  
Research and Liver Diseases, Salem Medical Center  
University of Heidelberg  
Heidelberg  
Germany

ISBN 978-3-030-40541-0                      ISBN 978-3-030-40542-7 (eBook)  
<https://doi.org/10.1007/978-3-030-40542-7>

© Springer Nature Switzerland AG 2020

This work is subject to copyright. All rights are reserved by the Publisher, whether the whole or part of the material is concerned, specifically the rights of translation, reprinting, reuse of illustrations, recitation, broadcasting, reproduction on microfilms or in any other physical way, and transmission or information storage and retrieval, electronic adaptation, computer software, or by similar or dissimilar methodology now known or hereafter developed.

The use of general descriptive names, registered names, trademarks, service marks, etc. in this publication does not imply, even in the absence of a specific statement, that such names are exempt from the relevant protective laws and regulations and therefore free for general use.

The publisher, the authors and the editors are safe to assume that the advice and information in this book are believed to be true and accurate at the date of publication. Neither the publisher nor the authors or the editors give a warranty, express or implied, with respect to the material contained herein or for any errors or omissions that may have been made. The publisher remains neutral with regard to jurisdictional claims in published maps and institutional affiliations.

This Springer imprint is published by the registered company Springer Nature Switzerland AG  
The registered company address is: Gewerbestrasse 11, 6330 Cham, Switzerland



*To my wife Ana and my children Julian  
and Ainhoa*

*Discovery consists of seeing what everybody  
has seen, and thinking what nobody has  
thought.*

Albert Szent-Györgyi

# Preface to the First Edition

When asked by Springer Nature to publish a first-time book on liver stiffness and its clinical interpretation, I have been enthusiastic from the very beginning. Bedside measurement of liver stiffness by elastography, namely transient elastography, has been a breathless and inspiring journey since its first start in 2003. At this time, nobody could foresee that this rapid and noninvasive technique would not only drastically improve our abilities to screen patients for liver fibrosis, but also change and is still changing the daily management of patients with liver diseases. Without any exaggeration, it has become a silent but fascinating revolution in hepatology and can be considered essential for diagnosing and managing liver diseases today. Moreover, it has helped to rethink hitherto still poorly understood fundamentals of liver diseases, namely the pathology of cirrhosis and the role of pressure-related mechanisms.

In this first comprehensive book entitled *Liver Elastography: Its Clinical Use and Interpretation*, the major advances are presented by technical pioneers and clinical experts for a broad readership. The book is not only considered to be a first summary of our present knowledge, but also thought to identify unresolved problems and to provide future directions. Care has been taken to provide clinicians with practical algorithms and knowledge for daily usage and interpretation.

I owe gratitude not only to the many colleagues who have enthusiastically prepared the various chapters in time. This is also the moment to thank Laurent Sandrin, the inventor of transient elastography, for an intensive and inspiring journey over a decade between the edges of physics and medicine and a true franco-allemand friendship. I would also like to thank my Heidelberg team, especially Vanessa Rausch, Tessa Peccerella, Felix Piecha, Christian Dietrich, Gunda Millonig, and Johannes Mueller, for their support over many years. Special thanks go to Omar Elshaarawy who has supported me through many critical discussions, cross-reading, and suggestions. This is also the time to thank the Dietmar Hopp Foundation and the employees of Salem Medical Center for their long-standing support of my clinical studies and basic research projects that formed the basis of this book.

I would also like to thank Mrs. Evgenia Koutsouki and Mr. Anand Shanmugam from Springer Nature for their continued encouragement and the very pleasant and supportive interactions over the last 2 years.

Finally, I am deeply grateful to my wife Ana for her strong support, understanding, and tolerance for such a huge and long-term endeavor. The book is dedicated to her and my children Julian and Ainhoa.

Heidelberg, Germany  
November 13, 2019

Sebastian Mueller

# Contents

## Part I Introduction

<b>1</b>	<b>Introduction to Liver Stiffness: A Novel Parameter for the Diagnosis of Liver Disease</b> . . . . .	<b>3</b>
	Sebastian Mueller	

## Part II Techniques to Measure Liver Stiffness

<b>2</b>	<b>Liver Stiffness and Its Measurement</b> . . . . .	<b>13</b>
	Sebastian Mueller	
<b>3</b>	<b>Liver Stiffness Measurement Using Vibration-Controlled Transient Elastography</b> . . . . .	<b>29</b>
	Laurent Sandrin	
<b>4</b>	<b>Characterizing Liver Stiffness with Acoustic Radiation Force</b> . . . . .	<b>41</b>
	Mark L. Palmeri	
<b>5</b>	<b>Two Dimensional Shear Wave Elastography/Supersonic Shear Imaging</b> . . . . .	<b>51</b>
	Jeremy Bercoff	
<b>6</b>	<b>Liver Magnetic Resonance Elastography: Clinical Use and Interpretation</b> . . . . .	<b>69</b>
	Jing Guo, Ingolf Sack, and Stephan Rodrigo Marticorena Garcia	
<b>7</b>	<b>Liver Stiffness Measurements in Small Animals</b> . . . . .	<b>95</b>
	Omar Elshaarawy, Shami Alquzi, Felix Piecha, Laurent Sandrin, Cecil Bastard, and Sebastian Mueller	

## Part III Liver Stiffness and Various Etiologies of Liver Diseases

<b>8</b>	<b>Introduction to Fibrosis Assessment by Liver Stiffness in Different Etiologies</b> . . . . .	<b>105</b>
	Sebastian Mueller	

<b>9</b>	<b>Fibrosis Assessment in Patients with HCV or HBV Chronic Infection. . . . .</b>	<b>113</b>
	Cristina Stasi, Laura Gragnani, and Anna Linda Zignego	
<b>10</b>	<b>Fibrosis Assessment in Patients with NAFLD . . . . .</b>	<b>123</b>
	Victor de Ledinghen	
<b>11</b>	<b>Liver Stiffness in Alcoholic Liver Disease. . . . .</b>	<b>141</b>
	Sebastian Mueller	
<b>12</b>	<b>Liver and Spleen Stiffness in Schistosomiasis . . . . .</b>	<b>153</b>
	Zulane da Silva Tavares Veiga, Cristiane Alves Vilella Nogueira, and Flavia Ferreira Fernandes	
<b>13</b>	<b>Screening for Cystic Fibrosis Using Liver Stiffness Measurements . . . . .</b>	<b>161</b>
	Elke Roeb	
<b>14</b>	<b>Role of Liver Stiffness in Hematological Disorders: Assessment of Sinusoidal Obstruction Syndrome, Budd–Chiari Syndrome, and Treatment Complications. . . . .</b>	<b>169</b>
	Thomas Karlas	
<b>15</b>	<b>Liver and Spleen Stiffness in Patients with Portal Vein Thrombosis .</b>	<b>177</b>
	Praveen Sharma	
<b>16</b>	<b>Liver Stiffness in Autoimmune Hepatitis . . . . .</b>	<b>181</b>
	Johannes Hartl	
<b>17</b>	<b>Liver Fibrosis Assessment in Adults with Alpha1-Antitrypsin Deficiency . . . . .</b>	<b>187</b>
	Vitor Magno Pereira, Karim Hamesch, and Pavel Strnad	
<b>18</b>	<b>Fibrosis and Prognosis Assessment Using Liver Stiffness in Patients with PBC and PSC . . . . .</b>	<b>197</b>
	Christophe Corpechot	
<b>19</b>	<b>Liver Stiffness in Patients with Hereditary Hemochromatosis and Secondary Iron Overload. . . . .</b>	<b>209</b>
	Agustín Castiella and Eva Zapata	
<b>20</b>	<b>Liver Stiffness in Patients with Wilson’s Disease. . . . .</b>	<b>217</b>
	Thomas Karlas	
<b>Part IV Important (Patho)physiological Confounders of Liver Stiffness</b>		
<b>21</b>	<b>Introduction to Confounders of Elevated Liver Stiffness . . . . .</b>	<b>225</b>
	Sebastian Mueller	
<b>22</b>	<b>Histological Confounders of Liver Stiffness . . . . .</b>	<b>233</b>
	Sebastian Mueller and Carolin Lackner	

**23 Liver Stiffness Elevation in Patients with Heart Failure and Liver Congestion . . . . . 243**  
Gunda Millonig

**24 Modulation of Liver Stiffness by Arterial and Portal Pressure . . . . . 257**  
Felix Piecha and Sebastian Mueller

**25 Liver Stiffness and Cholestasis . . . . . 265**  
Sebastian Mueller

**26 Liver Stiffness and Nutrition . . . . . 271**  
Sebastian Mueller, Felix Piecha, and Omar Elshaarawy

**27 Genetic Confounders of Liver Stiffness and Controlled Attenuation Parameter . . . . . 277**  
Vanessa Rausch, Johannes Mueller, and Sebastian Mueller

**28 Liver Stiffness and Acute Liver Failure . . . . . 297**  
Aline Gottlieb and Ali Canbay

**29 Liver Stiffness and Pregnancy . . . . . 307**  
Omar Elshaarawy, Johannes Mueller, and Sebastian Mueller

**Part V Liver Stiffness and Important Clinical Endpoints**

**30 Liver Stiffness and Important Clinical Endpoints . . . . . 317**  
Sebastian Mueller

**31 Liver and Spleen Stiffness to Predict Portal Hypertension and Its Complications . . . . . 325**  
Yuly P. Mendoza, Giuseppe Murgia, Susana G. Rodrigues, Maria G. Delgado, and Annalisa Berzigotti

**32 Liver Stiffness and Hepatic Decompensation . . . . . 361**  
Omar Elshaarawy and Sebastian Mueller

**33 Spleen Stiffness to Liver Stiffness Ratio and Disease Etiology . . . . . 369**  
Omar Elshaarawy, Johannes Mueller, and Sebastian Mueller

**34 Prediction of HCC Using Liver Stiffness Measurements . . . . . 375**  
Grace Lai-Hung Wong

**35 Liver Stiffness as a Predictor for Survival . . . . . 383**  
Sebastian Mueller

**36 Role of Liver Stiffness in the Management of Liver Transplantation: First Experience and Clinical Practice . . . . . 393**  
Guido Piai, Giovanna Valente, and Luca Rinaldi

<b>Part VI Assessment of Hepatic Steatosis Using Controlled Attenuation Parameter (CAP)</b>	
<b>37 Steatosis Assessment by Controlled Attenuation Parameter (CAP™)</b> .....	413
Magali Sasso and Laurent Sandrin	
<b>38 Steatosis Assessment with Controlled Attenuation Parameter (CAP) in Various Diseases</b> .....	441
Charlotte Wernberg, Mie Balle Hugger, and Maja Thiele	
<b>39 Liver Steatosis (CAP) as Modifier of Liver Stiffness</b> .....	459
Thomas Karlas and Sebastian Mueller	
<b>Part VII How to Use Liver Stiffness in Clinical Practice</b>	
<b>40 Introducing to Liver Stiffness Measurement in Clinical Practice</b> ...	471
Sebastian Mueller	
<b>41 Quality Criteria for Liver Stiffness Measurement by Transient Elastography</b> .....	479
Jérôme Boursier	
<b>42 Interpretation of Shear Wave Propagation Maps (Elastogram) Using Transient Elastography</b> .....	495
Sebastian Mueller, Johannes Mueller, and Omar Elshaarawy	
<b>43 Liver Stiffness Measurement in Patients with Hepatic Versus Non-hepatic Ascites</b> .....	509
Sebastian Mueller	
<b>44 Use of XL Probe in Obese and Non-obese Patients</b> .....	517
Omar Elshaarawy and Sebastian Mueller	
<b>45 Comparison of Various Elastographic Techniques for Liver Fibrosis Assessment</b> .....	523
Ioan Sporea	
<b>46 Adaptation of Liver Stiffness Cutoff Values to Inflammation, Cholestasis, and Congestion</b> .....	537
Sebastian Mueller	
<b>47 Screening for Liver Fibrosis in General or At-Risk Populations Using Transient Elastography</b> .....	545
Dominique Roulot	
<b>48 Elastography in Combination with Other Biomarkers: Role of Algorithms</b> .....	551
Maja Thiele and Katrine Prier Lindvig	

**49 Fibrosis Assessment via Liver Stiffness Measurements: How Many Patients Are Spared from a Liver Biopsy? . . . . .** 563  
 Amine Benmassaoud and Giada Sebastiani

**50 Performance of Liver and Spleen Stiffness Measurements in Predicting Postoperative Hepatic Decompensation After HCC Resection . . . . .** 589  
 Horia Stefanescu, Oana Nicoara-Farcau, Andreea Ardelean, and Bogdan Procopet

**51 Liver Stiffness Changes in Patients with Established Liver Cirrhosis . . . . .** 599  
 Felix Piecha and Sebastian Mueller

**52 Therapeutic Monitoring of Portal Pressure Lowering Drugs Using Liver Stiffness . . . . .** 605  
 Omar Elshaarawy, Felix Piecha, and Sebastian Mueller

**53 Clinical Cases: Application and Interpretation of Liver Stiffness . . .** 615  
 Sebastian Mueller

**Part VIII Molecular Basis of Liver Stiffness and Cell Biology**

**54 Introduction to the Molecular Basis of Liver Stiffness and Its Relation to Mechano-signaling . . . . .** 631  
 Sebastian Mueller

**55 Stiffness and Hepatocytes Function In Vitro . . . . .** 645  
 Srivatsan Kidambi

**56 Liver Mechanics and the Profibrotic Response at the Cellular Level . . . . .** 661  
 Rebecca G. Wells

**57 Role of Sinusoidal Pressure and Arterialization in Driving Fibrosis Progression . . . . .** 671  
 Sebastian Mueller

**Part IX Future Directions and Open Questions**

**58 Future Applications and Directions of Liver Stiffness Studies . . . . .** 687  
 Sebastian Mueller, Omar Elshaarawy, and Felix Piecha

**Appendix . . . . .** 695

**Index . . . . .** 727



# Abbreviations

A2M	alpha-2-Macroglobulin
AAT	Alpha-1 antitrypsin
AATD	Alpha-1 antitrypsin deficiency
ACLD	Advanced chronic liver disease
AFLP	Acute fatty liver of pregnancy
AH	Alcoholic hepatitis
AIH	Autoimmune hepatitis
AJ	Adherence junctions
ALD	Alcoholic liver disease
ALF	Acute liver failure
ALT	Alanine aminotransferase or Alanine transaminase
AML	Angiomyolipomas
AMUSE	Attenuation measuring ultrasound shearwave elastography
AOCLF	Acute-on-chronic liver
ApoA1	Apolipoprotein A-1
APRI	AST to Platelet Ratio Index
ARFI	Acoustic radiation force impulse
ASH	Alcoholic steatohepatitis
ASQ	Acoustic Structure Quantification™
AST	Aspartate aminotransferase or Aspartate transaminase
AUROC	Area under the receiver operating characteristic curve
BCLC	Barcelona Clinic Liver Cancer staging system
BI-RADS	Breast Imaging Reporting and Data System
BIVAD	Biventricular assist device
BLEP	Bright liver echo pattern
BMI	Body mass index
cACLD	Compensated advanced chronic liver disease
CAP	Controlled attenuation parameter
ChREBP	Carbohydrate responsive element-binding protein
CKD	Chronic kidney disease
CLD	Chronic liver disease

CSPH	Clinically significant portal hypertension
CT	Computed tomography
CVP	Central vein pressure or Central vein pressure
CYP	Cytochrome P450
DAA	Direct-acting antiviral
DM	Diabetes mellitus
DNA	Deoxyribonucleic acid
DRE	Digital rectal examination
E	Young's modulus
EASL	European Association for the Study of the Liver
EBV	Epstein–Barr virus
ECM	Extracellular matrix
EFSUMB	European Federation of Societies for Ultrasound in Medicine and Biology
EHPVO	Extrahepatic portal vein obstruction
EHS	Engelbreth–Holm–Swarm gel
ELF	Enhanced Liver Fibrosis score
Elpho	Serum electrophoresis
ERCP	Endoscopic retrograde cholangiopancreatography
ES	Elasticity score
ESBRA	European Society for Biomedical Studies on Alcoholism
EUS	Endoscopic ultrasound
EV	Esophageal varices
FLD	Fatty liver disease
FLL	Focal liver lesion
FNA	Fine needle aspiration
FOV	Field of view
G	Shear force
GGT	Gamma-glutamyl transferase
GPT	Glutamate pyruvate transaminase
GOT	Glutamate oxaloacetate transaminase
GSH	Reduced glutathione
GSSG	Oxidized glutathione
GWAS	Genome-wide association studies
HA	Hyaluronic acid
HABR	Hepatic arterial buffer response
HBV	Hepatitis B virus
HCC	Hepatocellular carcinoma
HCV	Hepatitis C virus
HD	Hepatic decompensation
HE	Hepatic encephalopathy
HELLP syndrome	Hemolysis, elevated liver enzymes, and low platelets syndrome
HES	Hepatosplenic schistosomiasis
HFE	Hereditary hemochromatosis protein, HFE=High Ferritin

HG	Hyperemesis gravidarum
HH	Hereditary hemochromatosis
HIF-1 alpha	Hypoxia-inducible factor 1-alpha
HIV	Human immuno deficiency virus
HNF4a	Hepatocyte nuclear factor 4-alpha
HR	Heart rate or hazard ratio
HRS	Hepatorenal syndrome
HSC	Hepatic stellate cell
HSD17B13	Hydroxysteroid 17-beta dehydrogenase 13
HVPG	Hepatic venous pressure gradient
IAP	Intra-abdominal pressure
ICC	Intraclass correlation coefficient
ICP	Intrahepatic cholestasis of pregnancy
ICU	Intensive care unit
INR	International normalized ratio
IQR	Interquartile range
IQR/M	Interquartile range/median
IRI	Ischemia/reperfusion injury
KCC	King's College Criteria
LDLT	Living donor liver transplantation
LEV	Large esophageal varices
LME	Liver microenvironment
LR	Likelihood ratio
LS	Liver stiffness
LSEC	Liver sinus endothelial cells
LSM	Liver stiffness measurements
LTX	Liver transplantation
LVAD	Left ventricular assist device
LXR	Liver X receptor
MAP	Mean arterial pressure
MBOAT7	Membrane bound O-acyltransferase domain containing protein 7
MCV	Mean corpuscular volume
MELD	Model for end-stage liver disease
MetS	Metabolic syndrome
MMPs	Matrix metalloproteinases
MR	Magnetic resonance
MRE	Magnetic resonance elastography
MRI	Magnetic resonance imaging
MRI-PDFF	Magnetic resonance imaging proton density fat fraction
MRS	Magnetic resonance spectroscopy or MR spectroscopy
NAFLD	Non-alcoholic fatty liver disease
NFS	NAFLD fibrosis score
NP	Not provided
NPV	Negative predictive value

NSBB	Non-selective beta-blockers
NT-proBNP	N-terminal fragment in the prohormone brain natriuretic peptide
PBC	Primary biliary cirrhosis
PCD	Probe-to-capsula distance
PCF	Pericellular fibrosis
PDEI-5	Phosphodiesterase type 5 inhibitors
PDFF	Proton density fat fraction
PDMS	Polydimethylsiloxane
PH	Portal hypertension
PHLF	Post-hepatectomy liver failure
PNPLA3	Patatin-like phospholipase domain-containing 3 or adiponutrin
PPV	Positive predictive value
PSA	Prostate-specific antigen
PSC	Primary sclerosing cholangitis
pSWE	Point shear wave elastography
PVA	Polyvinyl alcohol hydrogels
PVP	Portal vein pressure
QIBA	Quantitative Imaging Biomarkers Alliance
RCC	Renal cell carcinoma
RF	Radio frequency
RIMP	Right ventricular index of myocardial performance
ROI	Region of interest (used in MRE or 2D-SWE)
RR	Relative risk
RTS	Room-temperature susceptometry or Room-temperature susceptometer
RV	Right ventricle
RVEF	Right ventricular ejection fraction
2D-SWE	Two-dimensional shear wave elastography
SBP	Spontaneous bacterial peritonitis
SD/M	Standard deviation/mean ratio
SE	Strain elastography
SI	Strain index
SL	Spleen length
SNPs	Small nucleotide polymorphisms
SP	Sinusoidal pressure
SPH	Sinusoidal pressure hypothesis
SPSS	Spontaneous porto-systemic shunts
SQUID	Superconducting quantum interference device
SR	Strain ratio
SREBP-1c	Sterol regulatory element-binding protein 1c
SS	Spleen stiffness
SSM	Spleen stiffness measurement
SVR	Sustained virologic response

SWI	Shear wave imaging
SWS	Shear wave speed
SWV	Shear wave velocity
1D-TE	One-dimensional transient elastography
TACE	Transarterial chemoembolization
TAPSE	Tricuspid annular plane systolic excursion
TE	Transient elastography
TG	Triglycerides
TGF- $\beta$	Transforming growth factor- $\beta$
THE	Time-harmonic elastography
TIMP	Tissue inhibitor of metalloproteinases
TIMPs	Tissue inhibitors of MMPs
TIPS	Transjugular intrahepatic portosystemic shunt
TJ	Tight junctions
TM6SF2	Transmembrane 6 Superfamily 2
TME	Transient micro-elastography
TOF	Time of flight
TRUS	Transrectal ultrasonography
US	Ultrasound
USE	Ultrasound-based elastography
VCTE	Vibration-controlled transient elastography
VTI	Virtual Touch™ Imaging
VTQ	Virtual Touch™ Quantification
WFUMB	World Federation for Ultrasound in Medicine and Biology
WHO	World Health Organization

**Part I**  
**Introduction**

# Chapter 1

## Introduction to Liver Stiffness: A Novel Parameter for the Diagnosis of Liver Disease



Sebastian Mueller

### Introduction

This is the first comprehensive book on liver stiffness, its usage, and clinical interpretation after a 15-year-long worldwide inspiring and intensive experience. It has been written for both newcomers and experienced users. Likewise, it should be educative for experts in various technical, biological, medical, and clinical areas. It is supposed to provide an overview demonstrating established findings but also to highlight points of controversies while I have taken the freedom to draw potential solutions to my best knowledge. It should also provide great support in daily clinical practice, and, pave the way for future directions.

Although liver cirrhosis is a major health care problem worldwide, the diagnosis of this deadly disease has been a challenge and it still is in many parts of the developed world. One problem is the fact that chronic liver diseases are typically asymptomatic, present with almost normal laboratory tests and ultrasound imaging to general practitioners and normally slowly progress to cirrhosis over many years. Cirrhosis is then typically unmasked after decompensation (ascites, encephalopathy, bleeding, jaundice) or occasionally in routine lab test or by ultrasound. The diagnosis is further complicated by the fact that so-called typical or sure signs of cirrhosis are often normal in imaging analysis. For these reasons, cirrhosis remains highly underestimated by health care statistics and clinicians.

In this context, the introduction of ultrasound-based transient elastography (TE) using Fibroscan<sup>®</sup> in 2003 has revolutionized the diagnosis of liver diseases, namely liver cirrhosis [1]. Meanwhile, many alternative techniques such as acoustic radiation force imaging (ARFI), two-dimensional shear wave elastography (2D-SWE), or magnetic resonance elastography (MRE) have been pushed forward.

---

S. Mueller (✉)

Department of Medicine and Center for Alcohol Research and Liver Diseases,  
Salem Medical Center, University of Heidelberg, Heidelberg, Germany  
e-mail: [sebastian.mueller@urz.uni-heidelberg.de](mailto:sebastian.mueller@urz.uni-heidelberg.de)

**Fig. 1.1** Annual rate of published articles (PUBMED) on liver stiffness (LS) and controlled attenuation parameter (CAP) by February 2020 since their first publications (arrows)

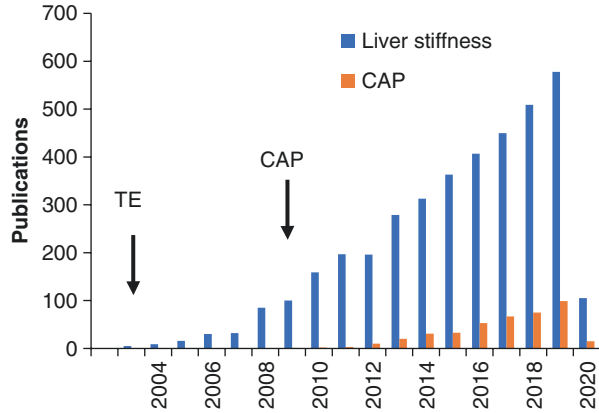


**Table 1.1** History of elastography

Year	What	Reference
1500 BC	Manual palpation	Egyptian Ebers and Edwin Smith Papyrus
Ancient Greece	Palpation of breast, wounds, bowels, ulcers, uterus, skin, and tumors	Hippocrates
1970s	Strain imaging named elastography	[2]
1970s	Ultrasonic assessment of tissue elasticity	[3]
1987	Ultrasound propagation in anisotropic soft tissues	[4]
2000	MRE	[5]
2003	TE	[1]
2004	SWE	[6]
2008	ARFI	[7]

Figure 1.1 demonstrates the still increasing publication rate on liver stiffness in scientific databases, now reaching more than 1500 articles. While there has been a lot of excitement about the evolution of liver stiffness measurements, it remains paradox while it has taken so long to technically assess the stiffness of the liver. A closer look, however, reveals that manual palpation of the liver dates back at least to 1500 BC, with the Egyptian Ebers Papyrus and Edwin Smith Papyrus both giving instructions on diagnosis with palpation (see Table 1.1). In ancient Greece, Hippocrates gave instructions on many forms of diagnosis using palpation, including palpation of the wounds, bowels, ulcers, uterus, skin, and tumors. In the modern Western world, palpation became considered a respectable method of diagnosis in the 1930s. Many basic physiologically parameters have been initially addressed in the nineteenth century during evolution of experimental modern physiology with first continuous blood pressure recording by Carl Ludwig [8] or the noninvasive assessment of arterial blood pressure by Riva-Rocci [9]. Other prominent examples of tissue stiffness are the arterial wall stiffness during progression of atherosclerosis, its association with pulse wave speed [10], the compliance and function of lungs [11] and, of course, the palpation of the liver during a medical examination since



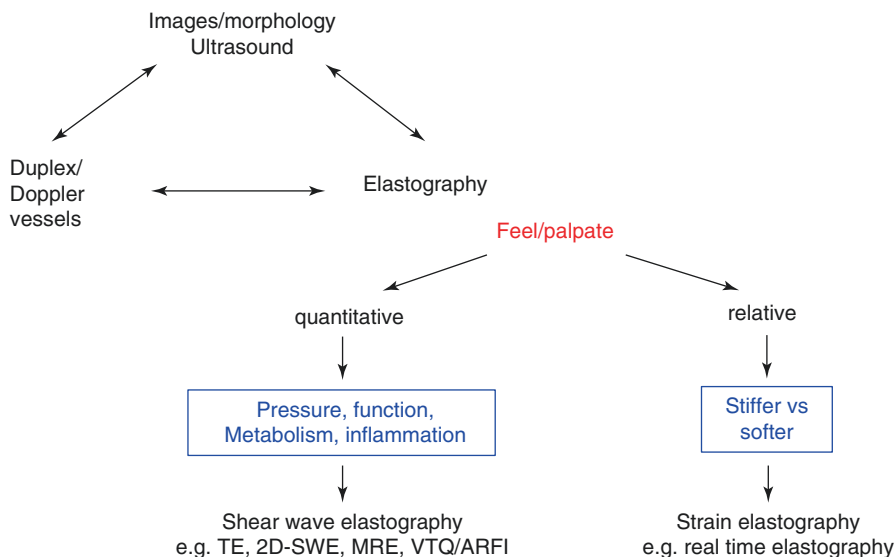


**Fig. 1.2** Ultrasound-based elastography provides novel bedside information on function and pressure next to other ultrasound-based information such as imaging and duplex. The measured stiffness not only detects fibrosis stage many years before manifestation of cirrhosis but is a highly sensitive surrogate marker of (patho)physiological activities of liver tissue including function, pressure, metabolism, and inflammation. For more details on elastographic techniques see also Appendix Table A.2

ancient times. First electric methods to assess tissue stiffness have been reported ca. 100 years ago while measuring skin stiffness [12]. The sophisticated ultrasound techniques and on-time shear wave speed measurements have required an evolution of electronics that have prevented the earlier introduction of liver stiffness measurements. Although MRE has been already introduced in the early 2000s, its high costs, complex technique, and interpretation did not allow a more widespread use [13].

In 2003, Sandrin introduced TE [1] which rapidly became the first true non-invasive bedside procedure to measure LS and screen for fibrosis. It is now clear that elastographic techniques add a new dimension to ultrasound which has been a highly important technology in improving diagnosis and point of care in medicine starting from monitoring of pregnancy complications, diseases in internal medicine, and many others. As shown in Fig. 1.2, with elastography, ultrasound not only provides images of anatomical structures, blood flow (Duplex) but pathophysiological activities such as pressures, inflammation, and even metabolism. This new dimension of elastography and stiffness should be readily conceived and its association with perfusion, tissue structure, and pressure is further highlighted in Fig. 1.3. The liver, probably due to its easy accessibility, has now evolved as the first role model organ for stiffness measurements and it is quite clear that important findings can be also transferred to other organs. Although the term organ stiffness may sound quite straight forward and simple,

**Fig. 1.3** Fundamental dependence of liver stiffness on perfusion, tissue structure, and pressure

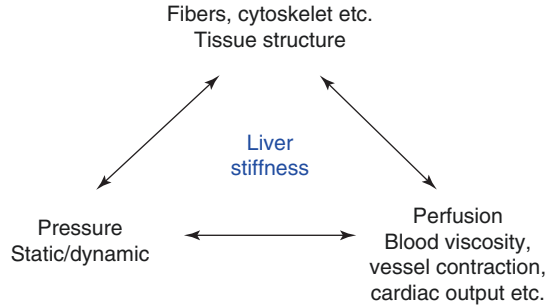


**Table 1.2** Stiffness of various materials and living tissues

Tissue/material	Stiffness
Fat tissue	0.7 kPa
Brain, gray matter	1.4 kPa
Brain, white matter	1.9 kPa
Liver	4 kPa
0.3% Gelatin hydrogel	6 kPa
Kidney	6–20 kPa
Spleen	13–20 kPa
Elastin	500–600 kPa
Skin	600 kPa
Rubber	1000–1400 kPa
Collagen	1 GPa
Wood	10 GPa
Bone	18 GPa
Concrete	47 GPa
Aluminum	70 GPa
Carbonated apatite	70 GPa
Steel	210 GPa
Diamond	1200 GPa

a rather complex area of physics is entered that requires cross-disciplinary thinking. As a result of last 15 years of liver stiffness measurements, a more sophisticated interpretation of LS requires some basic knowledge about the physics behind LS and its measurement through shear wave assessment. Material stiffness, however, has a long and important foundation not only in material physics but also engineering. Table 1.2 shows a list of various stiffness values from the living and nonliving world and spanning an incredible huge range. Accordingly, liver can be considered a rather soft tissue.

This book is not limited to TE but will focus on it for one simple reason: TE has been the first true bedside technique to reproducibly screen for liver fibrosis. It has an excellent interobserver variability, small sampling error, and good reproducibility. Moreover, these properties have allowed to easily validate findings between different centers and countries, and it has been the major technique to collect first time

experience in the confounders of stiffness elevation. In fact, it is no exaggeration to state that TE meanwhile serves as hidden novel gold standard when validating novel alternatives. We should also not forget that in many healthcare structures worldwide, gastroenterologists are not performing abdominal ultrasound by themselves but refer patients to e.g., radiologists. The technique of TE, however, has enabled liver stiffness measurements even for non-sonographers, which is an important step forward in terms of integrated patient care. With regard to worldwide screening strategies for liver fibrosis, it still remains open where technically developments will lead us and at which cost. Here, Appendix Table A.1 provides a rough and not complete overview about factors to be considered for using different methods as screening tools.

LS has been proven as an excellent surrogate marker of advanced fibrosis (F3) and cirrhosis (F4) outscoring all previous noninvasive approaches to detect cirrhosis. LS values below 6 kPa are considered as normal and exclude ongoing liver disease. LS of 8 and 12.5 kPa represent generally accepted cut-off values for F3 and F4 fibrosis. Moreover, LS highly correlates with portal pressure and predicts complications such as esophageal varices, HCC, or survival. These settled cut-off values have proven highly valuable and effective for screening strategies, follow-up strategies after therapy, etc. Importantly, based on LS, effective decisions and recommendations can be made to patients and important information for the management of health care systems are expected:

1. Thus, at a very early asymptomatic state, patients can be screened for esophageal varices or HCC which is now the most common and severe complication in central Europe.
2. There are indications that LS measurements can have a direct impact on the patient's compliance e.g., for controlling alcohol consumption, losing weight, and following other treatment recommendations.
3. It is expected that true prevalence data of cirrhosis will be obtained for general populations for the first time.
4. There are clear indications that LS per se can become an important parameter that does not necessarily need to be translated e.g., into histology scores. First survival data seem to confirm this.
5. It is also expected that LS measurements will optimize the management of liver involvement in other areas such as cardiology (right heart failure), intensive care medicine, gynecology (preeclampsia), hematology (hepatic manifestations), and surgery (preoperative assessment).

One of the major four reasons of the success of TE is:

1. It is rapidly measured within less than 5 min.
2. It is noninvasive.
3. It has a low sample error allowing for follow-up measurements.
4. Both technical artifacts or clinical confounders other than fibrosis will always cause LS elevation but never LS decrease. Consequently, a normal LS excludes ongoing liver manifestations and has an excellent negative predictive value.

On the other side, it has been rapidly learnt in the last decade that an elevated LS should not be taken as manifest liver cirrhosis [14]. Rather and irrespective of cirrhosis, it can be due to many other confounding factors such as inflammation or pressure changes. While these confounders have caused quite some confusion even among experts, it now seems clear that an elevated LS is “in any way an unfavorable prognostic sign.” This is a clear indication that LS measurements will play an increasing role in the future even in the GP or nurse care setting or potentially even in self-diagnosis settings for screening purposes. At the moment, this is limited by the costs, but will quickly become more affordable with the more widespread use and commercial competition.

This book tries to cover all aspects in the most comprehensive way. It is divided into major book sections I-X (techniques, etiologies, confounders, algorithms, future directions, etc.). Some redundancies between chapters have been intentionally left to underline the different perspectives. Book section VII is specifically written for the usage of LSM in daily clinical practice including a chapter of patient cases that demonstrate the usefulness of LSM even in previously unforeseen clinical situations.

On a personal note, I have been especially happy being able to include section VIII on the “Molecular basis of liver stiffness and cell biology.” These chapters look far into the future and summarize the present knowledge of molecular mechanisms behind the “clinical parameter” liver stiffness. In addition, there are exciting and first indications that liver stiffness and its physiological correlate “*sinusoidal pressure*” seem to be one of the major driving forces of fibrosis progression [15].

## References

1. Sandrin L, Fourquet B, Hasquenoph J-M, Yon S, Fournier C, Mal F, et al. Transient elastography: a new non-invasive method for assessment of hepatic fibrosis. *Ultrasound Med Biol.* 2003;29(12):1705–13.
2. Ophir J, Alam SK, Garra B, Kallel F, Konofagou E, Krouskop T, et al. Elastography: ultrasonic estimation and imaging of the elastic properties of tissues. *Proc Inst Mech Eng.* 1999;213(3):203–33.
3. Bamber JC. Ultrasound elasticity imaging: definition and technology. *Eur Radiol.* 1999;9(Suppl 3):S327–30.
4. Levinson SF. Ultrasound propagation in anisotropic soft tissues: the application of linear elastic theory. *J Biomech.* 1987;20(3):251–60.
5. Kruse SA, Smith JA, Lawrence AJ, Dresner MA, Manduca A, Greenleaf JF, et al. Tissue characterization using magnetic resonance elastography: preliminary results. *Phys Med Biol.* 2000;45(6):1579–90.
6. Bercoff J, Tanter M, Fink M. Supersonic shear imaging: a new technique for soft tissue elasticity mapping. *IEEE Trans Ultrason Ferroelectr Freq Control.* 2004;51(4):396–409.
7. Palmeri ML, Wang MH, Dahl JJ, Frinkley KD, Nightingale KR, Zhai L. Quantifying hepatic shear modulus in vivo using acoustic radiation force. *Ultrasound Med Biol.* 2008;34(4):546–58.
8. Ding XR, Zhao N, Yang GZ, Pettigrew RI, Lo B, Miao F, et al. Continuous blood pressure measurement from invasive to nonobtrusive: celebration of 200th birth anniversary of Carl Ludwig. *IEEE J Biomed Health Inform.* 2016;20(6):1455–65.

9. Riva-Rocci S. Un nuovo sfigmomanometro. *Gazz Med Torino*. 1896;47:1001–17.
10. Fung YC. *Biomechanics: mechanical properties of living tissues*. 2nd ed. New York: Springer; 2019.
11. Schmidt RF, Thews G. *Physiologie des menschen*. 23rd ed. Heidelberg: Springer; 1987.
12. Gildemeister M, Hoffmann L. Über elastizität und innendruck der gewebe. *Pflüger Arch*. 1922;195:153–66.
13. Manduca A, Oliphant TE, Dresner MA, Mahowald JL, Kruse SA, Amromin E, et al. Magnetic resonance elastography: non-invasive mapping of tissue elasticity. *Med Image Anal*. 2001;5(4):237–54.
14. Mueller S, Sandrin L. Liver stiffness: a novel parameter for the diagnosis of liver disease. *Hepatic Med Evid Res*. 2010;2:49–67.
15. Mueller S. Does pressure cause liver cirrhosis? The sinusoidal pressure hypothesis. *World J Gastroenterol*. 2016;22(48):10482.

**Part II**  
**Techniques to Measure Liver Stiffness**

# Chapter 2

## Liver Stiffness and Its Measurement



Sebastian Mueller

### What Is Stiffness?

*Stiffness* is the extent to which an object resists deformation in response to an applied force and it is given in Pascal (Pa). The complementary concept is flexibility or *compliance* e.g., lung compliance which is given in 1/Pa. Stiffness and compliance are connected by the following simple equation: Stiffness = 1/compliance. Table 2.1 provides the definitions of some important biomechanical parameters. The stiffer a tissue is the less compliant it is. For an elastic body with a single degree of freedom (for example, a metal spring, see Fig. 2.1) stretching of this spring, the force expressed in Newton is defined as: Force = stiffness  $\times$  displacement ( $F = k \times x$ ) where displacement  $x$  is the displacement (in meter) produced by the force along the same degree of freedom (for instance, the change in length of the depicted stretched spring) and the stiffness is the spring stiffness usually expressed in Newton per meter. In Appendix Fig. A.1 more common equations and symbols are discussed. It should be noted that a displacement can occur along multiple degrees of freedom e.g., the  $x$ ,  $y$ , and  $z$  coordinates. Figure 2.2 shows the resulting moduli whether it is resulting from extension (Young's modulus  $E$ ), shear stress (shear modulus  $G$  or  $\mu$ ), or compression (bulk modulus  $K$  or  $\lambda$ ). Different symbols are sometimes used throughout the literature. The term modulus is derived from the Latin word "modus" which means measure. The two most important elastic moduli are the Young's and the shear modulus, which can be only obtained for solids. In contrast, the bulk modulus can be given for all matter states: solids, liquids, and gases. The shear modulus is also called rigidity. With the assumption of a homogenous, isotropic,

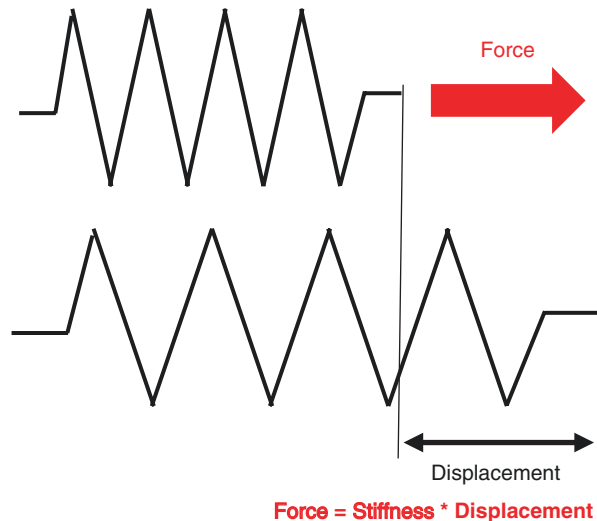
---

S. Mueller (✉)

Department of Medicine and Center for Alcohol Research and Liver Diseases, Salem Medical Center, University of Heidelberg, Heidelberg, Germany  
e-mail: [sebastian.mueller@urz.uni-heidelberg.de](mailto:sebastian.mueller@urz.uni-heidelberg.de)

**Table 2.1** Important biomechanical parameters

Parameter	Description
Elasticity	The ability of a body to resist a distorting influence and to return to its original size and shape when that influence or force is removed. Units are Pascals = Pa
Stiffness	Stiffness is the extent to which an object resists deformation in response to an applied force. Units are Pa
Compliance	Compliance is the opposite of stiffness. Units are 1/Pa
Strain	Strain is a description of deformation in terms of relative displacement of particles in the body that excludes rigid-body motions
Elastic deformations	Deformations which are recovered after the stress field has been removed
Plastic deformation	remain even after stresses have been removed. Occurs in material bodies after stresses have attained a certain threshold value known as the elastic limit or yield stress, and are the result of slip, or dislocation mechanisms at the atomic level.
Viscous deformation	Another type of irreversible deformation, which is the irreversible part of viscoelastic deformation
Viscosity	Viscosity of a fluid is a measure of its resistance to deformation at a given rate; SI unit of dynamic viscosity is the pascal-second (Pa s) and the opposite is fluidity. Irreversible energy loss

**Fig. 2.1** Stiffness of a metal spring

and purely elastic tissue, soft tissue like liver tissue shows a simple relation between Young's modulus and shear modulus which is  $E = 3G$ . More details are provided in the appendix but are not needed for understanding basic principles of LS measurement.



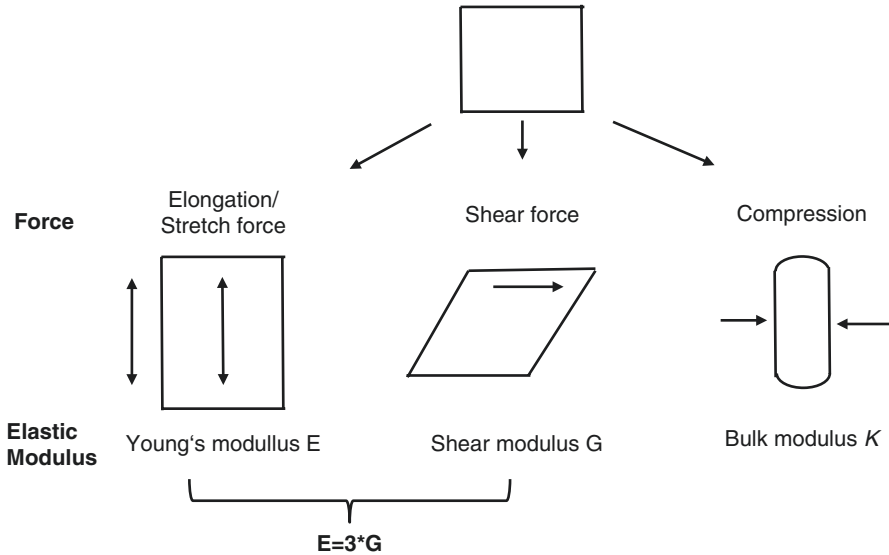


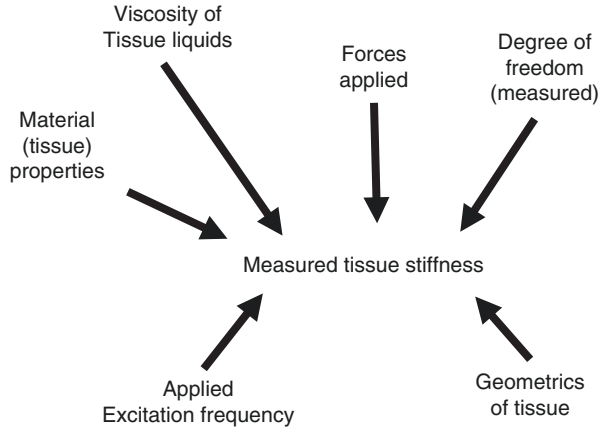
Fig. 2.2 Comparison of different forces, resulting moduli used for stiffness measurements

## General Considerations About Stiffness and Other Biomechanical Terms

The stiffness of a structure is of principal importance in many engineering applications and often a primary property for material selection. In biology, the stiffness of the extracellular matrix is important for resisting forces such as pressure or for guiding the migration of cells in a phenomenon called durotaxis. Another application of stiffness finds itself in skin biology. The skin maintains its structure due to its intrinsic tension, contributed to by collagen, an extracellular protein which accounts for approximately 75% of its dry weight [1]. The *pliability* or simplified softness of skin is a parameter that represents its firmness and extensibility, encompassing characteristics such as elasticity, stiffness, and adherence. In traumatic injuries to the skin, the pliability can be reduced due to the formation and replacement of healthy skin tissue by a pathological scar which can be assessed e.g., by using a cutometer. This device assesses stiffness by applying a vacuum to the skin to measure the extent to which it can be vertically distended [2].

While *elasticity* describes just the ability of a body to return to its original size and shape after removal of the force, stiffness includes the information about the necessary force to achieve a certain displacement. In contrast, *viscosity* of a fluid is a measure of its resistance to deformation at a given rate. For liquids, it corresponds to the informal concept of “thickness”: for example, syrup has a higher viscosity than water. Viscosity can be seen as quantifying the frictional force that arises between adjacent layers of fluid that are in relative motion. A fluid that has no resistance to shear stress is known as an ideal or inviscid fluid. Zero viscosity is observed

**Fig. 2.3** Factors affecting stiffness



only at very low temperatures in superfluids. Superfluidity is the characteristic property of a fluid with zero viscosity which therefore flows without loss of kinetic energy.

Since tissues like liver tissue is composed in a complex manner including fluids, their viscosity adds to the biomechanical properties as will be briefly discussed in Part VIII “Molecular basis of liver stiffness and cell biology.” In addition, stiffness is affected by many other factors. For instance, the stiffness of a spring, as shown in Fig. 2.1, is affected by five major factors: material, length and thickness of spring, diameter of coils, and arrangement of springs. In contrast tissue stiffness is more complex in biological organs as multiple structures, filaments, membrane boundaries, and other structures such as water phase and fat have an effect on it. Moreover, the stiffness properties are modulated at the cellular, intracellular, and super cellular level by viscous and other elastic aspects that are still largely unexplored (see Part VIII). Viscosity and other tissue properties will also affect the ultimately measured stiffness (see Fig. 2.3).

## General Strategies to Measure Tissue Stiffness

To measure or image the tissue stiffness, its behavior needs to be analyzed when deformed in response to a *distortion/mechanic stress* such as we do it by palpating an unknown body with our fingers. There are several ways to induce mechanical stress (Fig. 2.4) and, principally, two mechanical solicitations are possible which is either static or dynamic. Static approaches pushing/deform while dynamic solicitations apply, e.g., a *vibration of the surface* of the liver with a probe. These distortions can also be created by normal physiological processes, e.g., pulse, breathing movements, or heartbeat. The dynamic excitation can be over a short time period, which is then called transient, or it can be a continuous vibration which is often called harmonic excitation. Second, *radiation force* of focused ultrasound can be used to remotely create a mechanical solicitation inside the tissue. This can be done in normal direction and with a single or multiple focal zones (pSWE vs 2D-SWE).

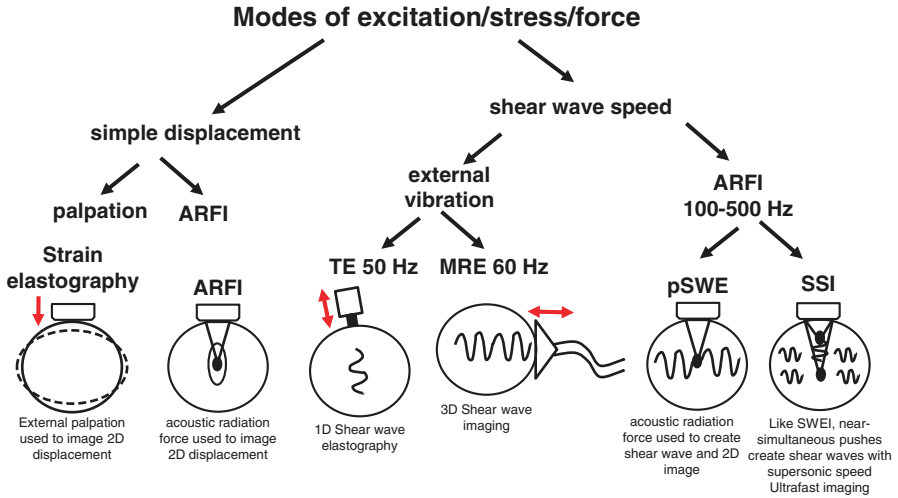


Fig. 2.4 Elastographic techniques classified by modes of excitation

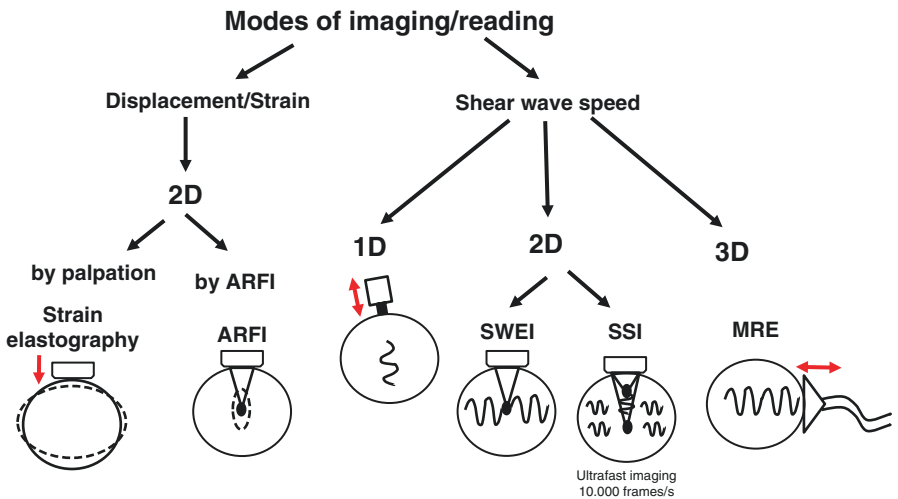


Fig. 2.5 Elastographic techniques classified by modes of reading/imaging

The response of the tissue, the strain, or displacement, needs then to be observed (Fig. 2.5). The primary way through which elastographic techniques are categorized is by the type of imaging used to record the response whether it is ultrasound, magnetic resonance imaging (MRI), or pressure/stress sensors in tactile imaging using tactile sensors. In addition, the tissue response can be observed at various dimensions e.g., simply a value (0D), a line (1D), a plane (2D), or the whole volume (3D). The result can be conveniently displayed to the operator along with a conventional image of the tissue, which overlays the anatomical image with the stiffness map.

Most elastography techniques find the stiffness of tissue based on one of two main principles: For a given applied force (stress), stiffer tissue deforms (strains) less than do softer tissues. Some techniques are able to quantitate the modulus, while others can only provide qualitative or relative results. Various techniques have been introduced to induce a mechanic shear wave and to determine its velocity. Figure 2.4 shows the principle of commonly used ultrasound techniques to measure stiffness using strain imaging by manual compression, longitudinal wave in the B-Mode, or shear wave speed. In addition, tactile imaging involves translating the results of a digital “touch” into an image. Many other physical principles have been explored for the realization of tactile sensors: resistive, inductive, capacitive, optoelectric, magnetic, piezoelectric, and electroacoustic principles, in a variety of configurations [3]. Atomic force microscopy is the today's standard to analyze stiffness in a microscopic microenvironment [4]. Table 2.2 provides an overview of types of elastography, the used excitation mode, dimensions, and producers.

## LS Measurement by Strain Elastography

Strain elastography or quasistatic elastography, sometimes also called simply “elastography” for historical reasons is one of the earliest elastography techniques [5]. In this technique, an external compression is applied to the tissue, and the ultrasound images before and after the compression are compared (Table 2.2, Figs. 2.4, 2.5, and 2.6). The areas of the image that are least deformed are the ones that are the stiffest, while the most deformed areas are the least stiff. Generally, what is displayed to the operator is an image of the relative distortions (strains), which is often of clinical utility. From the relative distortion image, however, making a quantitative stiffness map is often desired. To do this requires that assumptions be made about the nature of the soft tissue being imaged and about tissue outside of the image. Additionally, under compression, objects can move into or out of the image or around in the image, causing problems with interpretation. Another limit of this technique is that like manual palpation, it has difficulty with organs or tissues that are not close to the surface or easily compressed.

Moreover, the manually or physiologically applied stress is not quantifiable, but by assuming uniform normal stress, the measured normal strain provides a qualitative measure of Young's modulus  $E$  and thus tissue elasticity (Fig. 2.2). The strain measurements can be displayed as a semitransparent color map called an elastograph, which is overlaid on the B-mode image. Typically, low strain (stiff tissue) is displayed in blue, and high strain (soft tissue) is displayed in red. A pseudo-quantitative measurement called the strain ratio can be used, which is the ratio of strain measured in adjacent (usually normal) reference tissue region of interest

**Table 2.2** Types of elastography: excitation mode, dimensions. and producers

Type of elastography	Excitation	Elastography type	Dimension	Company/brand
Strain imaging/ elastography	Manual compression	Strain elastography	2D	
		ElaXto	2D	Esaote
		Real-time elastography	2D	Hitachi Aloka
		Elastography	2D	GE, Philips, Mindray Toshiba, Ultrasonix
		ElastoScan	2D	Samsung
		eSieTouch elasticity imaging	2D	Siemens
	Controlled compression	Atomic force microscopy	2D	Bruker, Hitachi, etc.
	Acoustic radiation force (single focus)	Acoustic radiation force impulse (ARFI) strain imaging	2D	
		VirtualTouch imaging (VTI/ARFI)	2D	Siemens
Shear wave imaging/ elastography	Acoustic radiation force (single focus)	Point shear wave measurements (pSWE/ ARFI quantification)	2D	
		VirtualTouch quantification (VTQ/ ARFI)	2D	Siemens
		ElastPQ	2D	Philips
	Acoustic radiation force (single focus)	Virtual touch image quantification (VTIQ/ ARFI)	2D	Siemens 2008, Philips, Toshiba 2013, GE
	Acoustic radiation force (multiple- zonated focus)	2D-shear wave elastography (2D-SWE) or supersonic shear imaging (SSI)	2D	SuperSonic Imagine
	Controlled external vibration	Transient elastography (TE)	1D	
		Fibroscan®	1D	Echosens 2003
		Magnetic resonance elastography (MRE)	3D	Hitachi, Siemens etc.

(ROI) to strain measured in a target lesion ROI. Today, qualitative strain elastography which was first introduced by Hitachi is mostly used to detect e.g., stiff nodules in large tissues e.g., the liver, thyroid, prostate, or breasts but it performs less well when trying to quantitate stiffness.

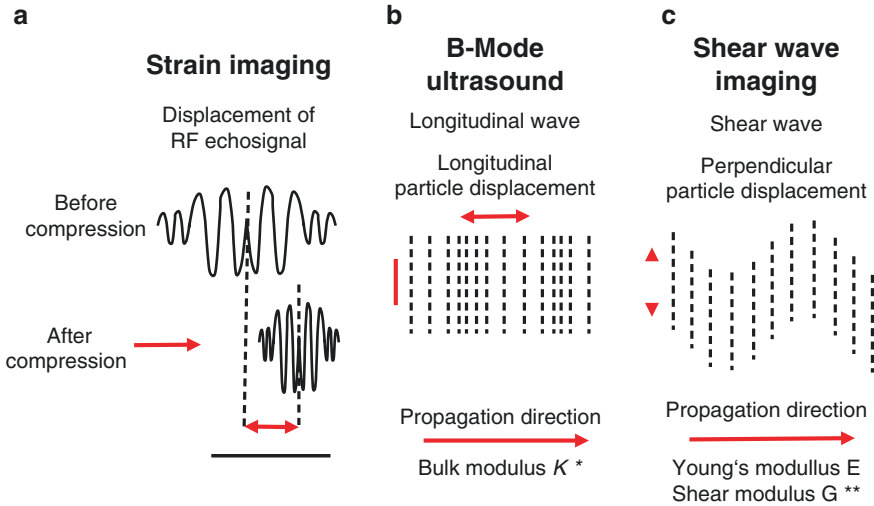


**Fig. 2.6** Ultrasound measurement methods for stiffness. In strain imaging (a), tissue displacement is measured by correlation of radiofrequency (RF) echo signals before and after compression. In B-mode ultrasound (b), particle motion is parallel to the direction of wave propagation, with longitudinal wave speed related to bulk modulus  $K$  (\* sometimes also  $\lambda$ ). In shear wave imaging (c), particle motion is perpendicular to the direction of wave propagation in the far field, with shear wave speed related to shear modulus  $G$  (\*\* sometimes also  $\mu$ )

## Measurement of Liver Stiffness Using Shear Waves

Today, most techniques (ultrasound and MRI) induce shear waves in the liver and measure their speed. Shear waves are mechanic waves (see Table 2.3 and Figs. 2.7 and 2.8) with perpendicular displacement with regard to the direction of wave propagation. In compression waves (also called pressure, compression or density waves) like sound waves, the medium displacement occurs along the direction of propagation (Fig. 2.8). It has to be mentioned that these statements are only true for the so-called far field. In the near field, coupling between compression and shear waves can occur [6]. Unlike compression waves, the slower shear wave only propagates through solid media and in the case of a soft tissue, its speed depends on the elastic properties of the tissue, i.e., the tissue stiffness. The shear modulus depends on the shear wave speed by  $G = \text{density} \times (\text{shear velocity})^2$ . Since the density of liver tissue can be assumed with close to 1 it follows for the liver stiffness (Young's modulus) under the assumption of a purely elastic, homogeneous, and isotropic soft tissue:  $E = 3G = 3(\text{shear wave velocity})^2$ . An overview of the ultrasound techniques that use shear waves are given in Tables 2.2 and 2.4. As shown in Fig. 2.9, the shear wave can be induced by external vibration with a controlled frequency of usually 50 Hz as is the case of liver transient elastography or 100 Hz for spleen stiffness measurements. In this special case, shear waves are followed along the same propagation

**Table 2.3** Classification of waves

Wave/synonym	Definition	Example
Mechanical wave	Oscillation of matter. Mechanical waves transport energy. Can be produced only in media (in contrast to electromagnetic waves) which possess elasticity and inertia	Water waves, sound waves, seismic waves
Electromagnetic waves	Electromagnetic waves require no medium, but can still travel through one	Radio waves, microwaves, infrared, (visible) light, ultraviolet, X-rays, and gamma rays
Body waves	Travel through the interior of a body along paths controlled by the material properties in terms of density and modulus (stiffness). The density and modulus according to temperature, composition, and material phase. Two types of particle motion result in two types of body waves: primary and secondary waves	
P-wave Primary waves Compressional waves Pressure waves	P-wave longitudinally ca. 1.7 times faster than other waves hence the name "Primary." In air, they travel at the speed of sound. Typical speeds are 330 m/s in air, 1450 m/s in water, and about 5000 m/s in granite	Sound waves
S-wave Secondary waves Transverse waves	S-waves are shear waves displace the ground perpendicular to the direction of propagation. S-waves can travel only through solids, as fluids (liquids and gases) do not support shear stresses. S-waves are typically around 60% of that of P-waves in any given material	
Surface waves	Surface waves travel along a surface e.g., earth or water. They are a form of mechanical surface waves and diminish as they get further from the surface. They travel more slowly than P and S-waves	

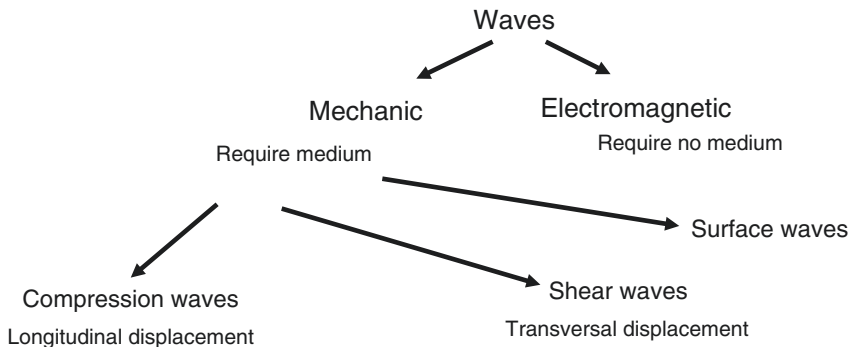


**Fig. 2.7** Classification of waves. Note that in reality waves can be of mixed type (e.g., compression and shear waves) and this depends on the distance from the excitation/solicitation (near field versus far field)

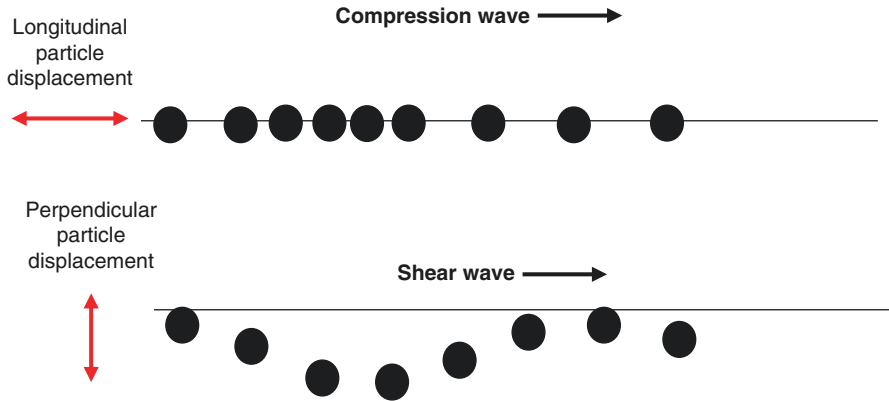


**Fig. 2.8** Compression versus shear wave (in the far field)

**Table 2.4** Comparison of the different ultrasound-based shear wave elastographic techniques

	1D-TE	pSWE	2D-SWE
Excitation	Dynamic stress by a mechanical vibrating device	Dynamic stress by ARFI in normal direction and single focal location	Dynamic stress by ARFI in normal direction and with multiple focal zones
Shear wave measurement	Shear waves measured parallel to excitation	Shear waves measured perpendicular to plane of excitation	Shear waves measured perpendicular to plane of excitation
Modulus	Shear wave speed converted to E	Shear wave speed converted to E, but often the shear wave speed is given	Multiple focal zones are interrogated in rapid succession faster than shear wave speed allowing real-time monitoring of shear waves in 2D, shear wave speed converted to E
Positioning	Operator selects area using time motion ultrasound	Operator can use B-mode to visualize ROI	Operator can use B-mode to visualize ROI
Image?	No image	No image	Quantitative shear wave images
Guidance	Stiffness estimated along ultrasonic A line in a fixed region, no image guidance, but 1D B-mode guidance	Performed on conventional ultrasound machine with standard probes	Operator has both anatomical and tissue stiffness information
History	First system commercially available in 2005, most widely used and validated for liver fibrosis	Available since 2008, multiple organs	Newest SWE methods, multiple organs



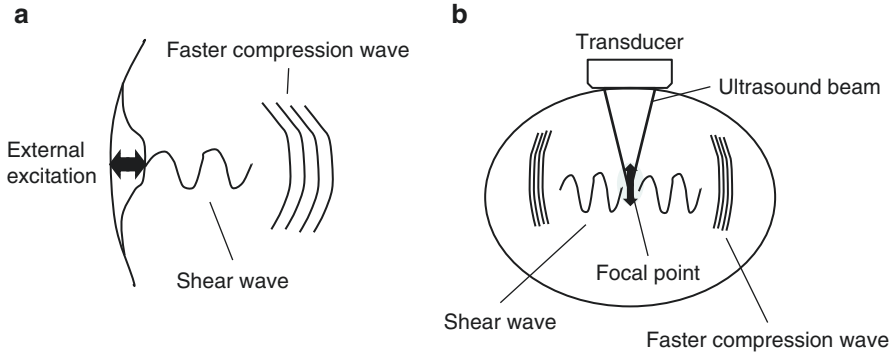


**Fig. 2.9** Shear wave excitation by (a) external excitation or (b) acoustic radiation force excitation

direction as the compression waves. The shear wave speed is then tracked by linear monochromatic ultrasound imaging.

## Transient Elastography (TE)

TE was initially called time-resolved pulse elastography [7], when it was introduced in the late 1990s. TE was the first commercially available method to measure LS and is to date the most widely used and validated technique to assess liver fibrosis. TE was introduced by Echosens/Paris under the brand Fibroscan<sup>®</sup>, and many clinicians simply refer to transient elastography as “Fibroscan<sup>®</sup>.” The technique relies on a transient mechanical vibration which is used to induce a shear wave into the tissue. The propagation of the shear wave is tracked using ultrasound in order to assess the shear wave speed from which the Young’s modulus is deduced under the assumption of homogeneity, isotropy, and pure elasticity. Transient elastography gives a quantitative one-dimensional (i.e., a line) image of tissue stiffness. The progression of the shear wave is imaged as it passes deeper into the body using a 1D ultrasound beam. The ultrasound images per time are then displayed in a two-dimensional diagram which is called shear wave propagation map or elastogram. From the elastogram, the shear wave speed is automatically derived with software-based algorithms and converted into the Young’s modulus. An important advantage of TE compared to harmonic elastography techniques is the separation of shear waves and compression waves. A specific implementation of 1D-TE called VCTE has been developed to assess the average liver stiffness which correlates to liver fibrosis assessed by liver biopsy [8]. This technique is implemented in the Fibroscan<sup>®</sup> which can also assess the *controlled attenuation parameter (CAP)* parameter which is good surrogate marker of liver steatosis (see Part VI).

## **Acoustic Radiation Force Impulse Imaging (ARFI)**

ARFI [9] uses ultrasound to create a qualitative two-dimensional map of tissue stiffness. It does so by creating a “push” inside the tissue using the acoustic radiation force from a focused ultrasound beam. The amount the tissue along the axis of the beam is pushed down is reflective of tissue stiffness; softer tissue is more easily pushed than stiffer tissue. ARFI shows a qualitative stiffness value along the axis of the pushing beam. By pushing in many different places, a map of the tissue stiffness is built up. ARFI can be used both in a strain elastography setting or to generate shear waves (see Table 2.2).

## ***Shear Wave Elasticity Imaging (SWEI)***

In SWEI, similar to ARFI, a “push” is induced deep in the tissue by acoustic radiation force. The disturbance created by this push travels sideways through the tissue as a shear wave. By using an image modality like ultrasound or MRI to see how fast the wave gets to different lateral positions, the stiffness of the intervening tissue is inferred. Since the terms “elasticity imaging” and “elastography” are synonyms, the original term SWEI denoting the technology for elasticity mapping using shear waves is often replaced by SWE. The principal difference between SWEI and ARFI is that SWEI is based on the use of shear waves propagating laterally from the beam axis and creating elasticity map by measuring shear wave propagation parameters whereas ARFI gets elasticity information from the axis of the pushing beam and uses multiple pushes to create a 2D stiffness map. No shear waves are involved in ARFI and no axial elasticity assessment is involved in SWEI. Producers such as Siemens (VTQ), Philips (ElastPQ) or GE (2D SWI GE) use a SWEI technique that is also called *point shear wave elastography (pSWE)* by inducing dynamic stress by ARFI in normal direction and a single focal location. Lateral shear waves are then mapped in a quantitative manner.

## ***Supersonic Shear Imaging (SSI or 2D-SWE)***

In contrast, in SSI or 2D-SWE [10], the most recent development, stress is induced by ARFI using multiple focal zones that are interrogated in rapid succession faster than shear wave speed. This allows real-time monitoring of shear waves in two dimensions. 2D-SWE gives a quantitative, real-time two-dimensional map of tissue stiffness. Local tissue velocity maps are obtained with a conventional speckle tracking technique and provide a full movie of the shear wave propagation through the tissue. By using many near-simultaneous pushes, SSI creates a source of shear waves which is moved through the medium at a supersonic speed. The generated shear wave is visualized by using ultrafast imaging technique. Using inversion algorithms, the shear elasticity of medium is mapped quantitatively from the wave propagation movie. SSI reaches more than 10,000 frames per second of deep-seated

organs. SSI provides a set of quantitative and in vivo parameters describing the tissue mechanical properties such as Young's modulus, viscosity, anisotropy although comparative studies have just started.

## **Magnetic Resonance Elastography (MRE)**

Magnetic resonance elastography (MRE) was introduced in the mid-1990s, and multiple clinical applications have been investigated [11]. In MRE, a mechanical vibrator is used on the surface of the patient's body; this creates shear waves that travel into the patient's deeper tissues. An imaging acquisition sequence that measures the velocity of the waves is used, and this is used to infer the tissue's stiffness often and historically given as shear modulus. The result of an MRE scan is a quantitative three-dimensional map of the tissue stiffness, as well as a conventional 3D MRI image. One strength of MRE is the resulting 3D elasticity map, which can cover an entire organ. Because MRI is not limited by air or bone, it can access some tissues ultrasound cannot, notably the brain. It also has the advantage of being more uniform across operators and less dependent on operator's skill than most methods of ultrasound elastography. MRE has made significant advances over the past few years with acquisition times down to a minute or less and has been used in a variety of medical applications including cardiology research on living human hearts. MREs short acquisition time also make it competitive with other elastography techniques.

## **Need for Standardization**

So far, with very few exceptions, the various producers of elastographic devices have done little to strictly specify the conditions to measure LS. Moreover, different moduli or different units are provided. This has caused enormous confusion among users including clinicians and even expert review articles. For example, widely used TE reports the stiffness by calculating the Young's modulus and results are reported in kPa. MRE also provides stiffness in kPa, however, usually the shear modulus  $G$  is given. Consequently, MRE data are about three times lower than for TE. Shear wave elasticity imaging reports values usually as shear wave speed in meters per second. ARFI and strain imaging is qualitative and displays different relative stiffnesses as different contrasts. Some authors advocate reporting results as shear wave speed in m/s as part of a standardized approach [12]. From clinical praxis point, however, it is less important whether shear wave speed or modulus is provided but rather the actual conditions of measurement and the device/technique used. An initiative by the Quantitative Imaging Biomarkers Alliance (QIBA) is attempting to use phantoms to standardize quantitative measurements from different elastographic techniques. An overview of the different methods and their reported units is given in Appendix Table A.3. In addition, Appendix Table A.4 provides comparable cut-off values and estimated formulas obtained from face-to-face comparative studies.

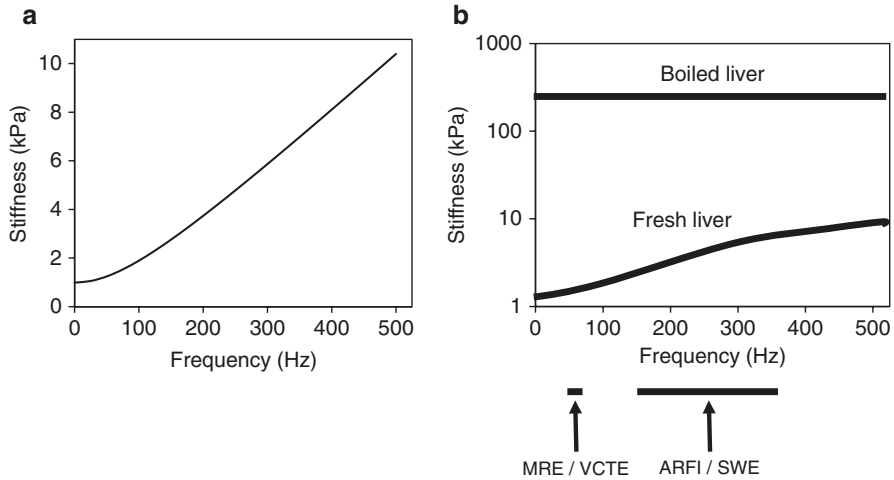


**Fig. 2.10** Dependence of stiffness on the excitation frequency in (a) a viscoelastic experimental model (Voigt's body) and (b) liver. (a) Simulated stiffness depends on the frequency for a so-called Voigt's tissue with a shear modulus of 3 kPa. (b) In living biological tissues such as fresh liver, stiffness varies as a function of frequency of the applied excitation probe. This frequency is tightly controlled in MRE/TE while a frequency spectrum is applied by ARFI/SWE. The frequency spectrum is filtered by the biological tissue in an uncontrolled manner

While it is technically easy to convert between  $E$  and  $G$  via equation  $E = 3G$  (under some assumptions), estimations of these values depend on the used frequency of excitation. Figure 2.10a further demonstrates that shear modulus and Young's modulus also depend on the (center-) frequency of the shear wave. In this example, so-called viscoelastic Voigt's tissue is used which is typically explored when simulating tissue in ultrasound experiments [13]. In Fig. 2.10b, the dependence of obtained LS on the excitation frequency is shown. These findings are important since techniques such as ARFI are applying a frequency spectrum which can also be filtered through the tissue in an uncontrolled manner. In contrast, external mechanical generation of shear waves (MRE, VCTE) allows for shear wave frequency control (50–60 Hz). This could also explain why conversion equations from TE to SWE differ between pSWE and 2D-SWE.

Liver stiffness like any other soft tissue stiffness depends on many factors. First and main factor is the extracellular matrix of the organ. The extracellular matrix is a deformable structure that transfers the external forces through the liver. It can be compared to the foundation of a building. A second factor is the constraints that are applied on the organ. The more pressure is applied to the liver at its boundaries, the stiffer it gets. A third factor is the internal pressure inside the organ, if blood or another liquid is coming in and out then stiffness will depend on the resistance that the organ applies to the flow. A fourth and important factor is the viscous effects which influence the time constant over which stiffness is tested. This effect is linked to above mentioned frequency, i.e., stiffness depends on frequency. While liver is soft at very low frequency (on the order of several hertz) which corresponds to

manual palpation time constant, it tends to be much harder at high frequencies (over several tens of kilohertz) (see also Fig. 2.10).

Finally, for most elastographic techniques, core assumptions are not always fulfilled. Thus, it is assumed that tissue is:

1. linear; resulting strain linearly increases as a function of incremental stress.
2. elastic; tissue deformation is not dependent on stress rate, and tissue returns to original non-deformed equilibrium state.
3. isotropic; the tissue is symmetrical/homogeneous and responds to stress the same from all directions.
4. incompressible; the overall volume of tissue remains the same under stress applied.

These assumptions have worked quite well for the diagnosis of liver fibrosis. However, fat content either within the tissue or its surrounding could strongly interfere with it. Moreover, mechanical properties of the liver are complex, the structure is heterogeneous with both a viscous and an elastic mechanical response.

Table 2.5 provides an overview of the still challenging issues that need to be addressed for a better standardization and comparability in the future. For now, measurements should be performed under standardized examination conditions (see section VII) and LS should be given together with the device brand and actual version.

**Table 2.5** Points to be addressed for further standardization of elastography

Problem	Explanation/potential interference
Platforms provide different units and moduli	MRE provides shear modulus while TE, 2D/pSWE provide Young's modulus. How does the actual methods of shear wave orientation and generation influence the resulting stiffness?
Control of external and internal excitation such as frequency and energy	Tissues can filter frequencies and thus cause uncontrolled excitation. How is this frequency filter affecting measurement outcomes?
Role of probe pressure (e.g., ARFI) or heat in pSWE for shear wave speed	It is not yet clear, how tissue compression or heat changes by ARFI affect shear wave propagation.
Viscoelastic properties	Liver tissue is not solely elastic but viscoelastic. It is not clear how filament stabilization of cellular structures, lipid droplets and their size, interstitial fluid are affecting LS.
Role of anatomical structures such as capsule or vessels	The liver capsule may compress surface-near tissue and change shear wave behavior. Vessel structures may be stiffer (artery) and "contaminate" the surrounding. This applies also to the question which distance from the surface is optimal to measure LS [14].
Role of fat	Fat has important specific properties that cause mechanic wave attenuation but also fluidity.
Spatial stiffness distribution in the liver	There are still major controversies about spatial stiffness distributions, since objective validation of each method is challenging. This applies to whether the right/left lobe should be measured or which depth should be used.

## References

1. Chattopadhyay S, Raines RT. Review collagen-based biomaterials for wound healing. *Biopolymers*. 2014;101(8):821–33.
2. Nedelec B, Correa JA, de Oliveira A, LaSalle L, Perrault I. Longitudinal burn scar quantification. *Burns*. 2014;40(8):1504–12.
3. Tegin J, Wikander J. Tactile sensing in intelligent robotic manipulation—a review. *Ind Robot*. 2005;32(1):64–70.
4. Ebert A, Tittmann BR, Du J, Scheuchenzuber W. Technique for rapid in vitro single-cell elastography. *Ultrasound Med Biol*. 2006;32(11):1687–702.
5. Ophir J, Cespedes I, Ponnekanti H, Yazdi Y, Li X. Elastography: a quantitative method for imaging the elasticity of biological tissues. *Ultrason Imaging*. 1991;13(2):111–34.
6. Sandrin L, Cassereau D, Fink M. The role of the coupling term in transient elastography. *J Acoust Soc Am*. 2004;115(1):73–83.
7. Sandrin L, Catheline S, Tanter M, Hennequin X, Fink M. Time-resolved pulsed elastography with ultrafast ultrasonic imaging. *Ultrason Imaging*. 1999;21(4):259–72.
8. Sandrin L, Fourquet B, Hasquenoph J-M, Yon S, Fournier C, Mal F, et al. Transient elastography: a new non-invasive method for assessment of hepatic fibrosis. *Ultrasound Med Biol*. 2003;29(12):1705–13.
9. Nightingale K, Palmeri N, Nightingale R, Trahey G. On the feasibility of remote palpation using acoustic radiation force. *J Acoust Soc Am*. 2001;110:625–34.
10. Bercoff J, Tanter M, Fink M. Supersonic shear imaging: a new technique for soft tissue elasticity mapping. *IEEE Trans Ultrason Ferroelectr Freq Control*. 2004;51(4):396–409.
11. Fowlkes JB, Emelianov SY, Pipe JG, Skovoroda AR, Carson PL, Adler RS, et al. Magnetic-resonance imaging techniques for detection of elasticity variation. *Med Phys*. 1995;22(11 Pt 1):1771–8.
12. Barr RG, Ferraioli G, Palmeri ML, Goodman ZD, Garcia-Tsao G, Rubin J, et al. Elastography assessment of liver fibrosis: society of radiologists in ultrasound consensus conference statement. *Ultrasound Q*. 2016;32(2):94–107.
13. Ahuja AS. Tissue as a Voigt body for propagation of ultrasound. *Ultrason Imaging*. 1979;1(2):136–43.
14. Sporea I, Sirlu RL, Deleanu A, Popescu A, Focsa M, Danila M, et al. Acoustic radiation force impulse elastography as compared to transient elastography and liver biopsy in patients with chronic hepatopathies. *Ultraschall Med*. 2011;32(Suppl 1):S46–52.

# Chapter 3

## Liver Stiffness Measurement Using Vibration-Controlled Transient Elastography



Laurent Sandrin

### Introduction

Initial developments on transient elastography (TE) started in the late 1990s [1–3]. At that time the elastography research field was dominated by sonoelastography [2] using ultrasound and magnetic resonance elastography (MRE) [4]. Both sonoelastography and MRE were using harmonic excitations to induce elastic waves into the tissues which results in the superimposition of shear and compression waves. The main limitation of harmonic techniques is the superimposition of both compression and shear waves which makes a straightforward computation of shear wave speed difficult. TE was introduced to overcome the limitations of harmonic elastography techniques [5–7]. TE allows the separation in time of shear and compression components of the elastic waves by inducing a transient mechanical solicitation. As a matter of fact, in soft tissues, the shear wave speed is much lower than the compression speed which allows the temporal separation as far as the mechanical solicitation is transient and the ultrasound modality operates at a very high frame rate. The development of a high frame rate ultrasound modality was achieved in parallel of the development of TE [8–10].

### A Bit of History

Far from mainstream applications of elastography, TE was initially tested on yogurt in 1998 and 1999 within the context of a research contract between the Laboratoire Onde et Acoustique and a major player of the milk industry. The purpose was to

---

L. Sandrin (✉)  
Echosens, Paris, France  
e-mail: [laurent.sandrin@echosens.com](mailto:laurent.sandrin@echosens.com)

develop a device that would assess yogurt's viscoelastic properties in real time at the manufacturing site. Although the experiments were quite successful in the laboratory on the yogurts that were purchased in grocery stores, the project did not succeed for a very simple reason: the absence of ultrasound backscattered signal in fresh to-be-measured yogurt. Another possible application that remained at the stage of idea was the assessment of the stiffness of "Camembert" cheese directly at the grocery store as a quantitative alternative to the well-known French way of testing Camembert by pressing on the cheese surface with the thumb. This led to the so-called "cheese story" of FibroScan development.

Echosens was founded in Paris in 2001 with the first objective to still find potential applications for the technology that was still at a very early stage. At that time, the majority of research projects in elastography would focus on breast and prostate cancers, the most deadly cancers in women and men, respectively. A meeting took place in June 2001 at the Institut Mutualiste Montsouris (IMM, Paris, France) in the context of a market survey. The few physicians who were attending the meeting suggested a possible application to liver chronic diseases. The pilot study started just a few months later at the IMM Institute. In parallel, the electronic platform and the core algorithms were being developed. This was the real beginning of the development of the technology behind FibroScan, the first commercially available elastography device. The pilot study consisted in a comparison between histological findings and liver stiffness [10]. The area under the ROC (AUROC) curves was 0.88 and 0.99 for significant fibrosis ( $F \geq 2$ ) and cirrhosis ( $F = 4$ ), respectively. These initial results paved the way for a larger multicenter study, which started in 2002 in several hospitals in France (Hospital Jean Verdier, Bondy, Hospital Beaujon, Clichy, Hospital Henri Mondor, Créteil, Hospital Haut Lévêque, Pessac). The first clinical paper on chronic hepatitis C was published in 2005 [11]. Finally, a review in 2010 could identify important clinical confounders of LS irrespective of fibrosis stage and introduce a potential association between intrahepatic pressure (or sinusoidal pressure) and fibrosis itself [12].

## A Shear Wave Story

Whatever the imaging modality (ultrasound, optics, and magnetic resonance), quantitative elastography techniques rely on shear waves. Actually, in soft tissues, shear wave speed has a very interesting property: it can be expressed as a function of only two independent parameters. One may decide to use the Lamé's coefficients ( $\lambda$  and  $\mu$ ) or the Young's modulus and the Poisson ratio ( $E$  and  $\nu$ ). Given that soft tissues are nearly incompressible, the Poisson ratio is very close to 1/2. In such conditions, the relationship between the shear wave speed, the Young's modulus,  $E$  expressed in kPa, and the tissue density,  $\rho$  which is roughly constant in soft tissues ( $\rho = 1000 \text{ kg/m}^3$ ) is:

$$E = 3\rho V_s^2 \quad (3.1)$$



In theory, this equation is only true under the assumptions that the tissue is homogeneous, linear, and purely elastic which is very unlikely for a biological complex medium such as liver tissue. However, the application of TE to liver stiffness measurement is indeed very useful. This may be due to the relatively favorable condition of chronic liver diseases, which are diffuse diseases that affect the organ globally. This is obviously a very good condition for an average liver stiffness measurement device like FibroScan.

FibroScan uses ultrasound as an imaging modality to track the shear waves. A single-element disk shape ultrasound transducer is mounted on the axis of an electrodynamic actuator (vibrator). The shear wave is induced mechanically when the actuator triggers a transient motion of mild amplitude. In other words, not only the ultrasound transducer emits and receives ultrasound, it also vibrates at low frequency to induce the shear wave propagation. In FibroScan, both ultrasound and shear wave propagations are fully axisymmetric. All displacements on the symmetry axis are therefore longitudinal (parallel to the direction of propagation). For many physicists, the physics behind FibroScan may appear weird or even wrong as the device tracks the longitudinal component of a shear wave. *How can one measure the longitudinal component of a shear wave?* This frequent question is due to the fact that shear waves are often named transverse waves. But shear waves are only purely transverse in the far field. Since the answer to this question goes far beyond the scope of this paper, curious readers may be referred to the existing literature [13].

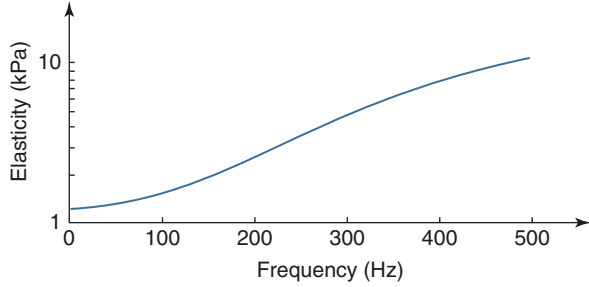
## **VCTE Technology**

The technology behind FibroScan is called VCTE which stands for vibration-controlled transient elastography. VCTE is an improved implementation of TE in which special controls were implemented in order to ensure that the measurements are reproducible. VCTE controls include the control of the force applied by the operator at the surface of the skin, the control of the shape of the transient excitation as a function of time on the full range of applied force, the control of the acoustic output power, and the control of the validity of the measurements.

### ***Force Applied by the Operator***

The force applied by the operator at the surface of the skin must remain in a given range to trigger a stiffness measurement. Indeed, an excessive force may result in a distortion of the vibration and an insufficient force would impair the mechanical coupling between the probe tip and the tissue preventing the vibration to be properly transmitted. The acceptable applied force range varies depending on the probe used.

**Fig. 3.1** Normal liver stiffness frequency dependence. (Courtesy of Rheolution Inc., Canada)



Obviously the deeper the liver, the more difficult the mechanical coupling is. Therefore, the minimum applied force is higher with the probe for adults than with the probe for pediatric applications (see also Appendix Table A.13).

### *Shape and Frequency of the Transient Excitation*

The control of the center frequency of the shear wave excitation is crucial since biological tissue properties are frequency dependent. In the case of the liver, as shown in Fig. 3.1, stiffness increases with shear wave frequency. In VCTE, the shape of the transient excitation is controlled in order to ensure that the center frequency of the excitation be constant whatever the applied force and probe-to-skin contact characteristics. This is a prerequisite to be able to define quantitative liver stiffness thresholds that can be used in clinical practice to differentiate patients. In FibroScan, this control is obtained by using a position sensor which tracks the position of the tip in real time. This position is fed into a servo-controller which is used to adapt the command of the actuator located inside the probe in order to precisely reproduce the expected excitation. Actually, with a device that would not precisely control the excitation, an increased applied force would likely induce a distorted excitation along with a decrease of the center frequency. As liver stiffness increases with frequency, a shift toward the lower frequency would result in a decrease of liver stiffness measurement.

### *Acoustic Output Power*

Contrary to ultrasound scanners which are using a high acoustic output power to induce shear waves by radiation force mechanism [14], VCTE based FibroScan requires very low acoustic output power. The acoustic output exposure levels of FibroScan device are below the limits set by the FDA amendment:  $I_{\text{SPTA},3} < 720 \text{ mW/cm}^2$  and  $I_{\text{SPPA},3} < 190 \text{ W/cm}^2$ . It means that there are absolutely no contraindications on using FibroScan device even for long period of examinations allowing its application in sensitive medical situations such as pregnancy [15].

## ***Measurements Validity***

In VCTE, each shear wave propagation map is associated with a quality factor which is used to automatically reject measurements when the quality of the shear wave propagation is not sufficient. In such a case, the measurement is identified as invalid and the counter of invalid measurements is increased by one.

## **CAP Technology**

In 2011, Echosens introduced an important new feature on FibroScan: the assessment of liver steatosis through a new technology called CAP (see also book Part VI). CAP stands for Controlled Attenuation Parameter assessing ultrasound attenuation at 3.5 MHz. The development of CAP was initiated in order to propose a surrogate marker of liver steatosis. As a matter of fact it is well known that ultrasound attenuation correlates with fat content [16]. However, at that time there was no ultrasound attenuation measurement device commercially available. CAP measurement is performed during the stiffness examination with FibroScan device. At the end of the examination, two numerical values are available: liver stiffness measurement (in kPa) and liver attenuation measurement called CAP (in dB/m). CAP measurement is processed from the same ultrasound data than the one used to track the shear waves. Therefore, the assessments of fibrosis and steatosis are made at the same location in the liver. The first study on CAP [17] reported good to excellent performances for the assessment of liver steatosis using liver biopsy as a gold standard. Meanwhile, CAP technology has been made compatible with obese patients [18]. There is now a wide body of evidence showing that CAP is a good surrogate marker of steatosis [19] that is superior in comparison to conventional ultrasound [20].

## **Operation**

The FibroScan device (Fig. 3.2) consists of a main unit connected to up to three probes (M-probe for adults, S-probe for children, and XL-probe for obese patients) which are designed to fit different patient morphology. Each probe corresponds to different settings in term of ultrasound center frequency and measurement depth. The characteristics of the probes are detailed in Appendix Table A.13. As shown in this table, the tip diameter is 7, 9, and 13 mm for the children, adults, and obese patients' probes respectively. These changes in tip diameter values are important for the ultrasound focus characteristics. They are also important to cope with the intercostal space, which is obviously smaller in children than in adult obese patients. Appendix Table A.13 provides more details about the different FibroScan probes.



**Fig. 3.2** Left: FibroScan 630 Expert device. Right: XL-probe, M-probe, and S-probe

### ***Liver Localization and Probe Selection***

During a VCTE examination, the patient is lying in a dorsal decubitus position with the right arm in maximal abduction in order to enlarge the intercostal space (Fig. 3.3). Before starting to trigger stiffness measurements, the operator needs to locate the liver which is performed with the ultrasound imaging mode of the device. Two graphs are displayed on the FibroScan: an A-mode (A = amplitude mode) and a TM-mode (TM = time motion) (Fig. 3.4). These two graphs are refreshed every 50 ms. They are used by the operator to find a measurement spot which must be homogeneous, exempt from vessel interfaces, exhibiting a linear decrease of the ultrasound signal versus depth. Using these graphs, the operator can observe the movement of the liver due to the respiratory motion which is depicted on the TM-mode graph. A probe selection tool (Fig. 3.4) recommends the to-be-used probe to the operator based on the measurement of the probe-to-capsula distance (PCD). The operator monitors the force applied at the tip of the probe (see Fig. 3.4).



**Fig. 3.3** VCTE examination setting with a FibroScan device. (Courtesy of Echosens, Paris, France)

### *Measurement Sequence of Stiffness and CAP*

When the operator presses the probe button and the applied force is within the approved range, a measurement is triggered. As shown in Fig. 3.5, the measurement sequence consists in applying a transient vibration at the tip of the probe (Fig. 3.5a). The shape of the displacement of the tip is a period of sinusoid at 50 Hz. The peak-to-peak amplitude of the transient vibration is 1 mm, 2 mm, and 3 mm, with the S,

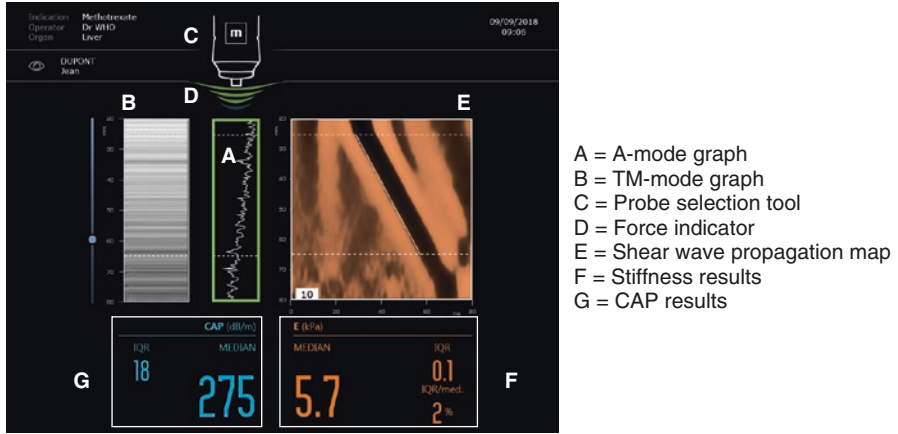
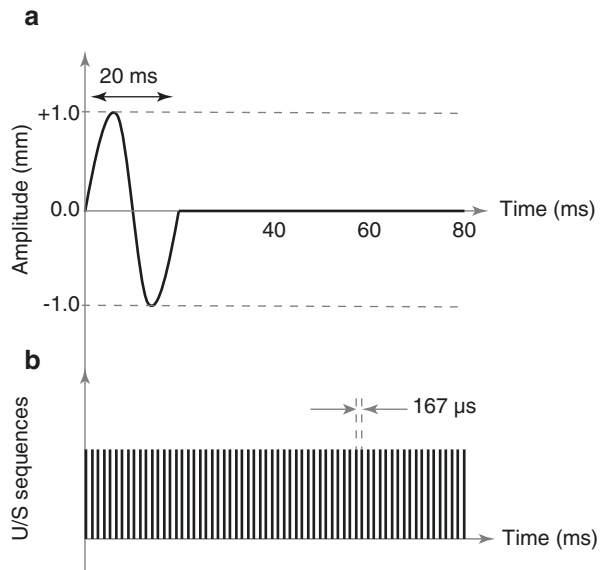


Fig. 3.4 FibroScan device examination screen

Fig. 3.5 Measurement sequence: vibration (a) and ultrasound (b)



M, and XL-probe, respectively. Starting with the vibration and lasting 80 ms, ultrasound lines are acquired at a rate of 6000 Hz (Fig. 3.4B), which corresponds to a periodicity of 167 μs. In total, 480 ultrasound lines are thereafter processed in order to compute the stiffness and CAP parameters. The displacements induced in the liver by the shear wave propagation as a function of depth and time are obtained using correlation techniques applied to the ultrasound lines. The *shear wave propagation map* (Fig. 3.4) is processed using a time-of-flight algorithm to estimate the shear wave speed,  $V_s$ , from which the stiffness or Young’s modulus,  $E$  expressed in kPa, is deduced using Eq. (3.1). The shear wave

propagation map will be also termed elastograph in this book. As already mentioned, invalid measurements are automatically rejected using an algorithm that checks that a proper shear wave propagation is detected. The CAP parameter is derived from the same ultrasound data as stiffness. CAP is an estimate of the total ultrasonic attenuation (go-and-return path) at 3.5 MHz and is expressed in dB/m. The CAP measurement is guided by the stiffness measurement since the CAP value extracted from the set of ultrasound data of a stiffness measurement is rejected if the associated stiffness measurement is identified as invalid. The results are the median of valid stiffness and CAP measurements (see Fig. 3.4).

### ***Final Results***

Echosens recommends that the operator performs 10 valid stiffness measurements before ending the exam. As the liver moves in front of the probe tip during respiration, the 10 measurements will be representative of a large portion of the liver. The median of the 10 valid stiffness measurements is the final stiffness result. The stiffness value is an estimate of the average stiffness. With the latest FibroScan devices, a complete exam typically lasts about 1 min.

### **Spleen Stiffness Measurement with VCTE @ 100 Hz**

Several clinical studies refer to the use of FibroScan devices to assess spleen stiffness [21–23]. However, these studies showed some limitations of VCTE settings tailored for liver stiffness assessment. Actually, the liver stiffness measurement range (1.5–75.0 kPa) is not adapted since the spleen is generally stiffer than the liver. A dedicated exam type was developed to perform spleen stiffness measurements (SSM) [24]. The spleen exam is performed with an M-probe. A higher shear wave frequency of 100 Hz is used to improve the accuracy of the stiffness measurement. The maximum stiffness value is increased to 100.0 kPa and the depths of measurement set to 25–55 mm. With the spleen dedicated settings, the overall performance of VCTE is significantly improved and supports the role of SSM as a surrogate marker of portal hypertension that could be used for the management of patients at risk of developing esophageal varices.

### **Fibroscan-Based Scores**

Another noninvasive alternative to liver biopsy is the blood tests which consist in scores computed from several, usually circulating, biomarkers to assess fibrosis. An important difference with LSM is that blood tests are designed to reflect liver fibrosis as they are trained for that purpose. However, LSM generally outperforms

blood tests which are more influenced by extrahepatic conditions given they are using circulating biomarkers. In 2014, a combination of circulating biomarkers with LSM [25] was introduced under the name FibroMeter VCTE to further increase accuracy (see also book Part IV “confounders of liver stiffness”).

More recently, a NASH score was developed under the name FAST<sup>TM</sup>. The FAST<sup>TM</sup> score aims at identifying at-risk NASH patients with a fibrosis stage of  $F \geq 2$  and  $NAS \geq 4$ . FAST<sup>TM</sup> combines LSM by VCTE, CAP, and AST which reflect fibrosis, steatosis, and inflammation, respectively. This combination of two very specific physical biomarkers directly measured in the liver (E and CAP) together with a sensitive circulating biomarker (AST) shows an excellent performance with AUROC ranging from 83% in the training cohort to 92% in the validation cohorts (to be published). For further reading on the role of AST levels and overestimation of fibrosis stage see also book Part IV “confounders of liver stiffness.”

## Conclusion

Initially introduced on the market in 2003, VCTE<sup>TM</sup> is by far the most clinically validated technology in the field of liver elastography. Due to easy bedside handling, short training period, and high reproducibility, FibroScan device has become a standard in the field of liver diseases. Considered as a good surrogate marker of liver fibrosis at first, LSM by VCTE<sup>TM</sup> at 50 Hz plays more and more a role on its own as a more general liver health status biomarker. As the technology improved, FibroScan<sup>®</sup> devices now embed the measurement of new surrogate markers: liver steatosis and portal hypertension, to improve the management of patients with chronic liver diseases. The combination of FibroScan-based biomarkers with simple blood biomarkers is proposed as a means to develop high performances, easy-to-use and widely available tests.

## References

1. Krouskop T. A pulsed doppler ultrasonic system for making noninvasive measurements of the mechanical properties of soft tissues. *J Rehabil Res Dev*. 1987;24:1–8.
2. Yamakoshi Y, Suzuki M, Sato T. Imaging the elastic properties using low frequency vibration and probing ultrasonic wave. *Japanese Meetings of Applied Physics*, Tokyo. 1987.
3. Parker KJ, Huang S, Musulin R, Lerner R. Tissue response to mechanical vibrations for “sono-elasticity imaging”. *Ultrasound Med Biol*. 1990;16(3):241–6.
4. Muthupillai R, Lomas D, Rossman P, Greenleaf J, Manduca A, Ehman R. Magnetic resonance elastography by direct visualization of propagating acoustic strain waves. *Science*. 1995;269:1854–7.
5. Catheline S, Thomas JL, Wu F, Fink MA. Diffraction field of a low frequency vibrator in soft tissues using transient elastography. *IEEE Trans Ultrason Ferroelectr Freq Control*. 1999;46(4):1013–9.



6. Catheline S, Wu F, Fink M. A solution to diffraction biases in sonoelasticity: the acoustic impulse technique. *J Acoust Soc Am*. 1999;105(5):2941–50.
7. Sandrin L, Catheline S, Tanter M, Hennequin X, Fink M. Time-resolved pulsed elastography with ultraFAST™ ultrasonic imaging. *Ultrason Imaging*. 1999;21(4):259–72.
8. Sandrin L, Tanter M, Catheline S, Fink M. Shear modulus imaging with 2-D transient elastography. *IEEE Trans Ultrason Ferroelectr Freq Control*. 2002;49(4):426–35.
9. Sandrin L, Tanter M, Gennisson JL, Catheline S, Fink M. Shear elasticity probe for soft tissues with 1-D transient elastography. *IEEE Trans Ultrason Ferroelectr Freq Control*. 2002;49(4):436–46.
10. Sandrin L, Fourquet B, Hasquenoph J-M, Yon S, Fournier C, Mal F, et al. Transient elastography: a new non-invasive method for assessment of hepatic fibrosis. *Ultrasound Med Biol*. 2003;29(12):1705–13.
11. Ziol M, Handra-Luca A, Kettaneh A, Christidis C, Mal F, Kazemi F, et al. Noninvasive assessment of liver fibrosis by measurement of stiffness in patients with chronic hepatitis C. *Hepatology*. 2005;41(1):48–54.
12. Mueller S, Sandrin L. Liver stiffness: a novel parameter for the diagnosis of liver disease. *Hepatic Med Evid Res*. 2010;2:49–67.
13. Sandrin L, Cassereau D, Fink M. The role of the coupling term in transient elastography. *J Acoust Soc Am*. 2004;115(1):73–83.
14. Nightingale K, Palmeri N, Nightingale R, Trahey G. On the feasibility of remote palpation using acoustic radiation force. *J Acoust Soc Am*. 2001;110:625–34.
15. Ammon FJ, Kohlhaas A, Elshaarawy O, Mueller J, Bruckner T, Sohn C, et al. Liver stiffness reversibly increases during pregnancy and independently predicts preeclampsia. *World J Gastroenterol*. 2018;24(38):4393–402.
16. Kuc R. Clinical application of an ultrasound attenuation coefficient estimation technique for liver pathology characterization. *IEEE Trans Biomed Eng*. 1980;27(6):312–9.
17. Sasso M, Beaugrand M, de Ledinghen V, Douvin C, Marcellin P, Poupon R, et al. Controlled attenuation parameter (CAP): a novel VCTE guided ultrasonic attenuation measurement for the evaluation of hepatic steatosis: preliminary study and validation in a cohort of patients with chronic liver disease from various causes. *Ultrasound Med Biol*. 2010;36(11):1825–35.
18. Sasso M, Audiere S, Kengang A, Gaouar F, Corpechot C, Chazouilleres O, et al. Liver steatosis assessed by controlled attenuation parameter (CAP) measured with the XL probe of the fibroscan: a pilot study assessing diagnostic accuracy. *Ultrasound Med Biol*. 2016;42(1):92–103.
19. Karlas T, Petroff D, Sasso M, Fan JG, Mi YQ, de Ledinghen V, et al. Individual patient data meta-analysis of controlled attenuation parameter (CAP) technology for assessing steatosis. *J Hepatol*. 2017;66(5):1022–30.
20. Thiele M, Rausch V, Fluhr G, Kjærgaard M, Piecha F, Mueller J, et al. Controlled attenuation parameter and alcoholic hepatic steatosis: diagnostic accuracy and role of alcohol detoxification. *J Hepatol*. 2018;68(5):1025–32.
21. Stefanescu H, Grigorescu M, Lupsor M, Procopet B, Maniu A, Badea R. Spleen stiffness measurement using Fibroscan for the noninvasive assessment of esophageal varices in liver cirrhosis patients. *J Gastroenterol Hepatol*. 2011;26(1):164–70.
22. Fraquelli M, Rigamonti C, Colombo M. Spleen stiffness measured by transient elastography accurately predicts esophageal varices in liver cirrhosis. *Gastroenterology*. 2012;143(4):e23; author reply e-4.
23. Calvaruso V, Bronte F, Conte E, Simone F, Craxi A, Di Marco V. Modified spleen stiffness measurement by transient elastography is associated with presence of large oesophageal varices in patients with compensated hepatitis C virus cirrhosis. *J Viral Hepat*. 2013;20(12):867–74.
24. Bastard C, Miette V, Cales P, Stefanescu H, Festi D, Sandrin L. A novel FibroScan examination dedicated to spleen stiffness measurement. *Ultrasound Med Biol*. 2018;44(8):1616–26.
25. Cales P, Boursier J, Ducancelle A, Oberti F, Hubert I, Hunault G, et al. Improved fibrosis staging by elastometry and blood test in chronic hepatitis C. *Liver Int*. 2014;34(6):907–17.

# Chapter 4

## Characterizing Liver Stiffness with Acoustic Radiation Force



Mark L. Palmeri

### Introduction

Methods to characterize the elastic properties of the liver typically have two means of introducing mechanical perturbations into liver to then monitor the liver's response and estimate its stiffness: (1) external vibration—such as transient elastography and MR elastography—and (2) an internally applied acoustic radiation force. For more details see also other chapters of the book section II “Techniques to measure liver stiffness.” While external sources of vibration can be well-controlled at fixed frequencies with external vibrators and couple relatively strong waves into the body, these waves must couple from the skin surface, through superficial tissues (i.e., skin, subcutaneous fat, muscle), into the liver. These propagating external waves can be distorted through interactions with these tissues surrounding the liver, and in some circumstances, such as abdominal ascites, cannot couple through fluids into the liver. Given some of the challenges that external vibration sources can face when characterizing the liver, there was parallel development in the 1990s and early 2000s to develop acoustic radiation force methods that would generate sources of mechanical perturbation in the focal zone of an ultrasonic excitation inside the target tissue of interest and not relying on coupling external mechanical energy into the patient. These acoustic radiation force methods have been developed and deployed on standard diagnostic ultrasound scanners as software features, allowing clinicians to evaluate the liver without any additional hardware.

---

M. L. Palmeri (✉)

Department of Biomedical Engineering, Duke University, Durham, NC, USA

Department of Anesthesiology, Duke University, Durham, NC, USA

e-mail: [mark.palmeri@duke.edu](mailto:mark.palmeri@duke.edu)

## What Is Acoustic Radiation Force?

Acoustic radiation force is a phenomenon that was first described in the acoustics literature by Nyborg in 1965 in the context of acoustic streaming [1] and further by Apfel and Chu in 1985 [2]. Acoustic radiation force is generated in the direction of propagation of an acoustic wave in a lossy (attenuating) medium, where the loss of momentum of the propagating wave results in an impulse transfer to the tissue. The direction and magnitude of acoustic radiation force ( $\vec{F}$ ) can be represented as:

$$\vec{F} = \frac{2a\vec{I}}{c},$$

where  $a$  is the acoustic attenuation of the tissue,  $\vec{I}$  is the acoustic intensity vector, and  $c$  is the sound speed of the tissue [1, 3, 4].

The application of acoustic radiation force to tissue results in a transient displacement of the tissue, where the magnitude of that displacement is related to the magnitude of the acoustic radiation force applied to the tissue, and the stiffness of the tissue. Stiffer tissues resist deformation than more compliant tissues and, therefore, experience less induced displacement. The transient, impulsive application of acoustic radiation force also leads to the generation of shear waves that emanate out from the region of acoustic radiation force application, and the speed of these shear waves can also be related to the stiffness of the tissue they are propagating in [5–7]. While acoustic radiation force is associated with all ultrasonic insonification of tissue (e.g., B-mode and Doppler imaging), the ultrasonic pulses for acoustic radiation force-based elasticity imaging must be intense and/or long enough to generate tissue displacements that can be estimated ultrasonically (on the order of microns) [8]. Commercial implementations of acoustic radiation force imaging methods that are described in this chapter have traditionally adhered to U.S. Food and Drug Administration diagnostic ultrasound output limits [9, 10], but new research efforts are exploring the benefits of using elevated acoustic output for more robust imaging performance, especially in the difficult to image demographic, such as those with high Body Mass Indices [11].

## Acoustic Radiation Force Impulse (ARFI) Imaging

ARFI imaging refers to images of tissue displacement (or metrics related to tissue displacement, such a time-to-peak displacement or maximum displacement) that result from the application of impulsive acoustic radiation force excitations [3, 12]. The “impulsive” nature of the excitation refers to an insonification time that is less than the mechanical response time of tissue, which is related to the tissue’s stiffness, with stiffer tissues reacting faster [12]. For liver tissue, this typical impulsive excitation lasts for less than 1 ms [12].

A single A-line of an ARFI image typically involves the following sequence:

1. A single, B-mode-like tracking pulse to determine the RF data associated with the tissue pre-ARFI-induced deformation;
2. A impulsive ARFI excitation either at a single focal depth, or over a range of focal depths to extend the effective depth-of-field of the excitation energy [13];
3. A series of B-mode-like tracking pulses at a relatively high pulse repetition frequency (typically 5–10 kHz) to track the tissue displacement and recovery from the ARFI excitation using correlation, phase-shift, or more complex displacement estimation methods [8, 14–19].

To form a 2D ARFI image, the A-line sequence is repeated at laterally offset positions from one another to form an image. Displacement estimation can be affected by motion (and other) artifacts, include those related to respiratory and cardiac motion. While clinical imaging protocols may recommend techniques like suspended breathing to minimize these effects [20, 21], most scanner post-processing includes motion filtering, through means of temporal profile shape-fitting [22], or frequency-domain filtering. While ARFI images can utilize elasticity as a mechanism of contrast not present in B-mode images, ARFI images are not typically used to estimate absolute stiffness of tissues (i.e., relating displacement amplitude to elastic modulus) since the magnitude of the acoustic radiation force is a function of acoustic attenuation [23], which is not easily estimated for different imaging targets/tissues. Additionally, the acoustic radiation force magnitude is not constant as a function of depth, and instead varies as a function of focal depth, requiring some depth-dependent normalization scheme to be applied to compensate for these force gradients [3].

## Shear Wave Elasticity Imaging (SWEI)

SWEI was first described in the literature by Saravazyan et al. [24] as novel approach to generating shear wave with acoustic radiation force and measuring the resultant shear wave propagation and shear wave speed to ultimately reconstruct an elastic modulus. Unlike ARFI images that can generate images of relative tissue stiffness differences, SWEI allows for absolute metrics of stiffness to be estimated in tissue. The typical assumptions surrounding the reconstruction of an elastic modulus ( $E$ , Young's modulus, or  $\mu$ , shear modulus) from shear wave speed ( $c_T$ ) include the tissue being linear, isotropic, incompressible, and having a density of water ( $\rho = 1.0 \text{ g/cm}^3$ ), such that the following relationships can hold [25]:

$$E = 3\mu = 3\rho c_T^2.$$

The incompressibility assumption allows the Young's modulus to be simply related to the shear modulus by a factor of 3. For more details see also book Part II "Techniques to measure liver stiffness." It should be noted that the relationship

between elastic moduli and shear wave speed is quadratic, and therefore, when statistical analyses are performed on data acquired on systems that report different metrics, retrospective conversion of reported thresholds for diagnostic purposes should not be attempted with simple linear scaling. Instead, thresholds for significance and confidence intervals should be recalculated as they may change with this nonlinear relationship. Like ARFI imaging, the acoustic radiation force excitations used for SWEI can involve single or multiple focal zones, depending the depth-of-field being characterized by the shear wave propagation. Rapid firing of multiple focal zone excitations such that a virtual extended shear wave front is launched is referred to as a “supersonic” shear excitation, which was popularized by SuperSonic Shear Wave™ Elastography [26].

One challenge with SWEI can be the distance over which shear wave propagate with displacements that can be reliably tracked. Greater distances can be achieved with stronger radiation force excitations [27, 28], more advanced displacement estimation approaches [29, 30], or creative implementations of interspersed acoustic radiation force excitation, tracking, and directional filtering to tease apart the complexities of intersecting propagating wave fields [31, 32].

Unlike MR elastography, which can measure displacement components in three dimensions and reconstruct a resultant (complex) shear modulus from these data using the Helmholtz equation [33], ultrasonic shear wave methods have a much higher resolution for displacement estimation in the single direction orthogonal to the transducer face, and have instead utilized time-of-flight methods to estimate shear wave speed [26, 34–39]. These shear wave speed estimation methods applied over 2D regions of interest (ROI) can be used to generate two types of quantitative images:

1. *Point Shear Wave Elastography (pSWE)* utilizes all the propagation data in the 2D ROI to estimate a consensus shear wave speed in that region [3, 21]. Typically, a singleton shear wave speed metric is reported per measurement, and clinical studies have supported using a median value across 12 repeated measurements to report as a representative measurement for diagnostic purposes [20, 21]. Quality metrics can be reported along with the shear wave speed to increase diagnostic confidence.
2. *2D-shear wave Elastography (2D-SWE)* breaks the ROI into smaller shear wave reconstruction kernels to generate 2D images of shear wave speed to characterize local variabilities in elasticity [21, 40].

As the confounding factors—viscosity, nonlinearity, anisotropy, structural boundaries—surrounding accurate reconstruction of an elastic modulus from shear wave speed became more well understood, many derivatives of SWEI have settled on directly reporting shear wave speed instead of making additional assumptions to report an elastic modulus. Thus, additional details about the conditions under which an elastic modulus has been estimated must be provided (e.g., the frequency of excitation used in transient elastography or MR elastography) [41, 42]. Given the complexities and nuances surrounding the different commercial implementations of

**Table 4.1** Frequency content of different shear wave elastography methods

Method	Frequency content of shear wave
Transient elastography (TE)	50–60 Hz
Point shear wave elastography (pSWE)	100–500 Hz
2D shear wave elastography (2D-SWE)	100–500 Hz
MR elastography (MRE)	60 Hz

SWEI for liver characterization, guidelines have been established for its recommended clinical usage by the World Federation of Ultrasound in Medicine and Biology [20] and the Society of Radiologists in Ultrasound [21].

**Viscosity** Tissue viscosity is a material property that makes the shear wave speed dependent on the frequency content of the shear wave, and is a confounding factor when assuming that liver tissue is purely elastic (shear wave speed is independent of the shear wave frequency content) [43]. It is known that different elasticity imaging methods can generate shear waves of differing frequency content [21] (see also Table 4.1). The frequency differences can lead to different reconstructed group shear wave speeds in viscoelastic media [44], which can be a source of discrepancy when comparing measurements with different elasticity imaging modalities [41]. Additionally, the processing methods used by each manufacturer—specifically the use of displacement versus velocity data—can also influence the estimated speeds in the presence of viscosity. Velocity data are effectively high pass filtered displacement profiles, and this higher frequency bias can lead to an increase in the estimated shear wave speed.

Some investigators have sought to characterize the viscosity of liver tissue as a measurement of hepatic steatosis or inflammation [45–47], but no conclusive conclusions have been drawn to date.

In addition to the elastography guidelines and consensus documents that have been published, the Radiological Society of North America (RSNA) Quantitative Imaging Biomarker Alliance (QIBA) establishes an Ultrasonic Shear Wave Speed (US SWS) working group in 2012 to study the factors that influence the consistent reconstruction of the shear wave speed metric across different manufacturer systems [41, 48, 49]. This working group is composed of international researchers, manufacturers, and regulatory members, and a profile guiding best practices for manufacturers to achieve consistent measurements across different systems is available for consultation.

Another resource generated through the RSNA QIBA US SWS effort has been the generation and public release of digital phantom data generated through finite element method models of shear wave propagation in elastic and viscoelastic materials for shear wave reconstruction development validation [50]. Additionally, standardized sequences for generating and processing shear waves using the Verasonics ultrasound research platform have also been released for public use [51].

**Table 4.2** Publicly released digital phantom data and standardized sequences for generating and processing shear waves

Webpage
<a href="https://github.com/RSNA-QIBA-US-SWS/QIBA-DigitalPhantoms">https://github.com/RSNA-QIBA-US-SWS/QIBA-DigitalPhantoms</a>
<a href="https://doi.org/10.7924/r4sj1f98c">https://doi.org/10.7924/r4sj1f98c</a>
<a href="https://github.com/RSNA-QIBA-US-SWS/VerasonicsPhantomSequences">https://github.com/RSNA-QIBA-US-SWS/VerasonicsPhantomSequences</a>

Another resource generated through the RSNA QIBA US SWS effort has been the generation and public release of digital phantom data generated through finite element method models of shear wave propagation in elastic and viscoelastic materials for shear wave reconstruction. Additionally, standardized sequences for generating and processing shear waves using the Verasonics ultrasound research platform have also been released for public use

One confounding factor discovered by the QIBA group in calibrated elastic and viscoelastic phantom studies has been the presence of a negative bias in shear wave speed as a function of increasing focal depth when using curvilinear arrays. The relative magnitude of these biases has been  $<4\%$  for focal depths ranging from 3 to 7 cm (<https://github.com/RSNA-QIBA-US-SWS/>).

Another resource generated through the RSNA QIBA US SWS effort has been the generation and public release of digital phantom data generated through finite element method models of shear wave propagation in elastic and viscoelastic materials for shear wave reconstruction development validation [50]. Additionally, standardized sequences for generating and processing shear waves using the Verasonics ultrasound research platform have also been released for public use [51]. The web-links to this information is provided in Table 4.2.

## Conclusions

Acoustic radiation force elasticity imaging methods have become a viable clinical option to noninvasively evaluate liver stiffness. Unlike external vibration-base methods, acoustic radiation force excitations can be focused directly in the tissue of interest, while also providing real-time, ultrasonic B-mode imaging guidance and clinical evaluation. Acoustic radiation force methods are also available to screen for and characterize liver masses. Efforts to standardize and provide more consistent measurements between different manufacturer systems is being addressed by consensus documents and guideline documents, and the RSNA QIBA Ultrasonic Shear Wave Speed group is taking important steps toward characterizing the performance of these systems in calibrated elastic and viscoelastic media.



## References

1. Nyborg WLM, Litovitz T, Davis C. Acoustic streaming, vol. IIA. New York: Academic Press; 1965. p. 265–331.
2. Apfel RE, Chu BT. Acoustic radiation pressure produced by a beam of sound. *J Acoust Soc Am.* 1982;72(6):1673–87.
3. Doherty JR, Trahey GE, Nightingale KR, Palmeri ML. Acoustic radiation force elasticity imaging in diagnostic ultrasound. *IEEE Trans Ultrason Ferroelectr Freq Control.* 2013;60(4):685–701.
4. Shiina T, Nightingale KR, Palmeri ML, Hall TJ, Bamber JC, Barr RG, et al. WFUMB guidelines and recommendations for clinical use of ultrasound elastography: part 1: basic principles and terminology. *Ultrasound Med Biol.* 2015;41(5):1126–47.
5. Sandrin L, Tanter M, Gennisson JL, Catheline S, Fink M. Shear elasticity probe for soft tissues with 1-D transient elastography. *IEEE Trans Ultrason Ferroelectr Freq Control.* 2002;49(4):436–46.
6. Sandrin L, Tanter M, Catheline S, Fink M. Shear modulus imaging with 2-D transient elastography. *IEEE Trans Ultrason Ferroelectr Freq Control.* 2002;49(4):426–35.
7. Sandrin L, Fourquet B, Hasquenoph J-M, Yon S, Fournier C, Mal F, et al. Transient elastography: a new non-invasive method for assessment of hepatic fibrosis. *Ultrasound Med Biol.* 2003;29(12):1705–13.
8. Pinton GF, Dahl JJ, Trahey GE. Rapid tracking of small displacements with ultrasound. *IEEE Trans Ultrason Ferroelectr Freq Control.* 2006;53(6):1103–17.
9. Nightingale KR, Church CC, Harris G, Wear KA, Bailey MR, Carson PL, et al. Conditionally increased acoustic pressures in nonfetal diagnostic ultrasound examinations without contrast agents: a preliminary assessment. *J Ultrasound Med.* 2015;34(7):1–41.
10. Ncrp. report No. 113: exposure criteria for medical diagnostic ultrasound: I. Criteria based on thermal mechanisms: National Council on Radiation Protection and Measurements; 2002.
11. Deng Y, Palmeri ML, Rouze NC, Rosenzweig SJ, Abdelmalek MF, Nightingale KR. Analyzing the impact of increasing mechanical index and energy deposition on shear wave speed reconstruction in human liver. *Ultrasound Med Biol.* 2015;41(7):1948–57.
12. Palmeri ML, McAleavey SA, Fong KL, Trahey GE, Nightingale KR. Dynamic mechanical response of elastic spherical inclusions to impulsive acoustic radiation force excitation. *IEEE Trans Ultrason Ferroelectr Freq Control.* 2006;53(11):2065–79.
13. Rosenzweig SJ, Palmeri ML, Nightingale KR. Analysis of rapid multi-focal zone ARFI imaging. *IEEE Trans Ultrason Ferroelectr Freq Control.* 2015;62(2):280–9.
14. Kasai C, Koroku N, Koyano A, Omoto R. Real-time two-dimensional blood flow imaging using an autocorrelation technique. *IEEE Trans Ultrason Control.* 1985;32(3):458–63.
15. Loupas T, Powers JT, Gill RW. An axial velocity estimator for ultrasound blood flow imaging, based on a full evaluation of the Doppler equation by means of a two-dimensional autocorrelation approach. *IEEE Trans Ultrason Ferroelectr Freq Control.* 1995;42(4):672–88.
16. Pesavento A, Perrey C, Krueger M, Ermert H. A time-efficient and accurate strain estimation concept for ultrasonic elastography using iterative phase zero estimation. *IEEE Trans Ultrason Ferroelectr Freq Control.* 1999;46(5):1057–67.
17. Byram B, Trahey G, Palmeri M. Bayesian speckle tracking. Part I: an implementable perturbation to the likelihood function for ultrasound displacement estimation. *IEEE Trans Ultrason Ferroelectr Freq Control.* 2013;60(1):132–43.
18. Byram B, Trahey G, Palmeri M. Bayesian speckle tracking. Part II: biased ultrasound displacement estimation. *IEEE Trans Ultrason Ferroelectr Freq Control.* 2013;60(1):144–57.
19. Palmeri M, McAleavey S, Trahey G, Nightingale K. Ultrasonic tracking of acoustic radiation force-induced displacements in homogeneous media. *IEEE Trans Ultrason Ferroelectr Freq Control.* 2006;53(7):1300–13.



20. Ferraioli G, Filice C, Castera L, Choi BI, Sporea I, Wilson SR, et al. WFUMB guidelines and recommendations for clinical use of ultrasound elastography: part 3: liver. *Ultrasound Med Biol.* 2015;41(5):1161–79.
21. Barr RG, Ferraioli G, Palmeri ML, Goodman ZD, Garcia-Tsao G, Rubin J, et al. Elastography assessment of liver fibrosis: society of radiologists in ultrasound consensus conference statement. *Ultrasound Q.* 2016;32(2):94–107.
22. Giannantonio DM, Dumont DM, Trahey GE, Byram BC. Comparison of physiological motion filters for in vivo cardiac ARFI. *Ultrason Imaging.* 2011;33(2):89–108.
23. Palmeri ML, Frinkley KD, Oldenburg KG, Nightingale KR. Characterizing acoustic attenuation of homogeneous media using focused impulsive acoustic radiation force. *Ultrason Imaging.* 2006;28(2):114–28.
24. Sarvazyan AP, Rudenko OV, Swanson SD, Fowlkes JB, Emelianov SY. Shear wave elasticity imaging: a new ultrasonic technology of medical diagnostics. *Ultrasound Med Biol.* 1998;24(9):1419–35.
25. Lai WM, Rubin DEK. Introduction to continuum mechanics. Woburn: Butterworth-Heinemann; 1999.
26. Bercoff J, Tanter M, Fink M. Supersonic shear imaging: a new technique for soft tissue elasticity mapping. *IEEE Trans Ultrason Ferroelectr Freq Control.* 2004;51(4):396–409.
27. Deng Y, Palmeri ML, Rouze NC, Trahey GE, Haystead CM, Nightingale KR. Quantifying image quality improvement using elevated acoustic output in B-mode harmonic imaging. *Ultrasound Med Biol.* 2017;43(10):2416–25.
28. Deng Y, Palmeri ML, Rouze NC, Haystead CM, Nightingale KR. Evaluating the benefit of elevated acoustic output in harmonic motion estimation in ultrasonic shear wave elasticity imaging. *Ultrasound Med Biol.* 2018;44(2):303–10.
29. Dumont DM, Byram BC. Robust tracking of small displacements with a Bayesian estimator. *IEEE Trans Ultrason Ferroelectr Freq Control.* 2016;63(1):20–34.
30. Dumont DM, Walsh KM, Byram BC. Improving displacement signal-to-noise ratio for low-signal radiation force elasticity imaging using Bayesian techniques. *Ultrasound Med Biol.* 2016;42(8):1986–97.
31. Song P, Zhao H, Manduca A, Urban M, Greenleaf J, Chen S. Comb-push ultrasound shear elastography (CUSE): a novel method for two-dimensional shear elasticity imaging of soft tissues. *IEEE Trans Med Imaging.* 2012;31:1821–32.
32. Lipman SL, Rouze NC, Palmeri ML, Nightingale KR. Evaluating the improvement in shear wave speed image quality using multidimensional directional filters in the presence of reflection artifacts. *IEEE Trans Ultrason Ferroelectr Freq Control.* 2016;63(8):1049–63.
33. Huwart L, Sempoux C, Vicaut E, Salameh N, Annet L, Danse E, et al. Magnetic resonance elastography for the noninvasive staging of liver fibrosis. *Gastroenterology.* 2008;135(1):32–40.
34. Palmeri ML, Wang MH, Dahl JJ, Frinkley KD, Nightingale KR, Zhai L. Quantifying hepatic shear modulus in vivo using acoustic radiation force. *Ultrasound Med Biol.* 2008;34(4):546–58.
35. Wang MH, Palmeri ML, Rotemberg VM, Rouze NC, Nightingale KR. Improving the robustness of time-of-flight based shear wave speed reconstruction methods using RANSAC in human liver in vivo. *Ultrasound Med Biol.* 2010;36(5):802–13.
36. Rouze NC, Wang MH, Palmeri ML, Nightingale KR. Robust estimation of time-of-flight shear wave speed using a Radon sum transformation. *IEEE Trans Ultrason Ferroelectr Freq Control.* 2010;57(12):2662–70.
37. Song P, Manduca A, Zhao H, Urban MW, Greenleaf JF, Chen S. Fast shear compounding using robust 2-d shear wave speed calculation and multi-directional filtering. *Ultrasound Med Biol.* 2014;40(6):1343–55.
38. Song P, Urban MW, Manduca A, Greenleaf JF, Chen S. Coded excitation plane wave imaging for shear wave motion detection. *IEEE Trans Ultrason Ferroelectr Freq Control.* 2015;62(7):1356–72.
39. Song P, Macdonald M, Behler R, Lanning J, Wang M, Urban M, et al. Two-dimensional shear-wave elastography on conventional ultrasound scanners with time-aligned sequential tracking (TAST) and comb-push ultrasound shear elastography (CUSE). *IEEE Trans Ultrason Ferroelectr Freq Control.* 2015;62(2):290–302.

40. Rouze NC, Wang MH, Palmeri ML, Nightingale KR. Parameters affecting the resolution and accuracy of 2-D quantitative shear wave images. *IEEE Trans Ultrason Ferroelectr Freq Control*. 2012;59(8):1729–40.
41. Palmeri M, Nightingale K, Fielding S, Rouze N, Deng YF, Lynch T, et al. RSNA QIBA ultrasound shear wave speed phase II phantom study in viscoelastic media. *IEEE Int Ultra Sym*. 2015.
42. Rouze NC, Palmeri ML, Nightingale KR, editors. Estimation of model parameters characterizing dispersion in ARFI induced shear waves in in vivo human liver. In: 2014 IEEE International Ultrasonics Symposium; 2014.
43. Nightingale K, Rouze N, Rosenzweig S, Wang M, Abdelmalek M, Guy C, et al. Derivation and analysis of viscoelastic properties in human liver: impact of frequency on fibrosis and steatosis staging. *IEEE Trans Ultrason Ferroelectr Freq Control*. 2015;62(1):165–75.
44. Rouze NC, Deng Y, Trutna CA, Palmeri ML, Nightingale KR. Characterization of viscoelastic materials using group shear wave speeds. *IEEE Trans Ultrason Ferroelectr Freq Control*. 2018;65(5):780–94.
45. Asbach P, Klatt D, Hamhaber U, Braun J, Somasundaram R, Hamm B, et al. Assessment of liver viscoelasticity using multifrequency MR elastography. *Magn Reson Med*. 2008;60:373–9.
46. Chen S, Sanchez W, Callstrom MR, Gorman B, Lewis JT, Sanderson SO, et al. Assessment of liver viscoelasticity by using shear waves induced by ultrasound radiation force. *Radiology*. 2012;266(3):964–70.
47. Chen X, Shen Y, Zheng Y, Lin H, Guo Y, Zhu Y, et al. Quantification of liver viscoelasticity with acoustic radiation force: a study of hepatic fibrosis in a rat model. *Ultrasound Med Biol*. 2013;39(11):2091–102.
48. Hall TJ, Milkowski A, Garra B, Carson P, Palmeri M, Nightingale K, et al. RSNA/QIBA: Shear wave speed as a biomarker for liver fibrosis staging. In: 2013 IEEE International Ultrasonics Symposium (IUS); 2013, pp. 397–400.
49. Deng Y, Rouze NC, Palmeri ML, Nightingale KR. On system-dependent sources of uncertainty and bias in ultrasonic quantitative shear-wave imaging. *IEEE Trans Ultrason Ferroelectr Freq Control*. 2016;63(3):381–93.
50. Palmeri ML, Qiang B, Chen S, Urban MW. Guidelines for finite-element modeling of acoustic radiation force-induced shear wave propagation in tissue-mimicking media. *IEEE Trans Ultrason Ferroelectr Freq Control*. 2017;64(1):78–92.
51. Deng Y, Rouze NC, Palmeri ML, Nightingale KR. Ultrasonic shear wave elasticity imaging sequencing and data processing using a verasonics research scanner. *IEEE Trans Ultrason Ferroelectr Freq Control*. 2017;64(1):164–76.

# Chapter 5

## Two Dimensional Shear Wave Elastography/Supersonic Shear Imaging



Jeremy Bercoff

### Introduction

Elastography has been one of the most fruitful fields in the ultrasound community in the past two decades. Its aim is to digitize and standardize one of the most ancient medical acts, the manual palpation, in order to detect pathologies inducing stiffness abnormalities. If multiple elastography techniques have been invented by researchers around the world, only a few had made their journeys up to the medical device industry and the routine clinical use. The first one was strain elastography in the early 2000s (2003), almost 20 years after its academic proof of principle [1]. Strain elastography relies on a manual stress applied by the user on the organ and calculates and then displays the induced strain within the image area. The strain map is indirectly related to tissue stiffness with the assumption that the induced stress is spatially homogeneous and that tissue stiffness heterogeneity is fairly simple (a harder nodule for example). With interesting results for breast cancer diagnostic [2], strain elastography is barely usable in the liver as the induction of a controlled stress by the user on an internal organ remains a key challenge. In 2004, the company Echosens introduced the FibroScan, a dedicated tool for quantitative liver stiffness assessment. The FibroScan relies on transient elastography, a technique developed in the mid-1990s by Institut Langevin in Paris [3]. The technique differs substantially from strain imaging, as the vibration is now automatically generated by an external vibrator. The vibrator applies at the body surface a transient pulse that induces mechanical waves propagating in the liver. The mechanical waves are tracked using a single circular ultrasound transducer, and their speeds are measured over a cylindrical region of interest, providing a global assessment of liver stiffness in kPa. FibroScan has been widely adopted by hepatologists to assess liver stiffness and has contributed in dramatically reducing the need for liver biopsies to perform

---

J. Bercoff (✉)  
SUPERSONIC IMAGINE, S.A., Aix-en-Provence, France  
e-mail: [jeremy.bercoff@supersonicimagine.com](mailto:jeremy.bercoff@supersonicimagine.com)

fibrosis staging. A few years later (2008), two dimensional shear wave elastography (2D-SWE) has been introduced by SuperSonic Imagine (SSI) on the Aixplorer ultrasound system. Relying on the combination of radiation force-induced shear waves and ultrafast ultrasound imaging to track their propagation, 2D-SWE was the first ultrasound technique capable of providing real-time imaging of tissue stiffness for a wide range of organs: breast, liver, prostate, thyroid, scrotum, muscles, and tendon.

## Shear Wave Elastography Basics

Prior to the introduction of shear wave elastography, two clinical solutions were available for the clinician or the radiologist to assess liver stiffness:

- Strain elastography, as a complementary imaging mode of traditional ultrasound systems.
- Transient elastography, through the Fibroscan, as a dedicated tool for global liver stiffness assessment.

Strain elastography has the advantage to provide an image, despite not quantitative, of tissue stiffness distribution. It is however extremely difficult to use in the liver as sufficient and homogeneous stress needs to be induced in the liver from the external ultrasound probe.

Transient elastography (TE) provides a quantitative value of the global liver stiffness but cannot deal with liver stiffness variability and potential artefacts (pulsating vessels, reverberation, motion). The aim of shear wave elastography is to overcome the limitations of these approaches by providing both a high-resolution image and quantitative measurements of liver stiffness.

2D-SWE is based on the supersonic shear imaging technique [4] from Institute Langevin and combines two innovative concepts to induce and image shear waves with the goal to provide the user with maximal ease of use and reliability:

- Automatic and supersonic shear wave generation
- Ultrafast ultrasound imaging.

## Automatic and Supersonic Shear Wave Generation

The generation of shear waves in the body is not performed using an external solicitation like in strain or transient elastography techniques. It leverages the physical properties of ultrasound wave propagation in human tissue to induce them. Ultrasound waves act like a wind inside the body, pushing tissue in their propagation direction. The wind force is linked to medium ultrasound attenuation and ultrasound beam intensity ( $F = 2\alpha I/c$ , where  $I$  is the ultrasound beam intensity,  $\alpha$  the

ultrasound attenuation, and  $c$  the ultrasound speed of sound). This phenomenon called radiation force is very well known in wave physics but has never been used so far in medical ultrasound. In order to obtain a noticeable effect (typically a few micron displacement), the ultrasound beam must be spatially focused at a given location, and its intensity must be increased compared to traditional ultrasound imaging beam. Typically, the ultrasound “push” pulse has the same amplitude but is 100 times longer than the imaging pulse.

Using such beams, ultrasound waves act, at the focus point, as virtual fingers pushing the tissue in the direction of their propagation and generating shear waves as illustrated in Fig. 5.1a. Thanks to this technology, shear waves can be automatically generated in tissue anywhere without any actions from the user and without any changes in its workflow (the user uses the probe as in all other ultrasound imaging modes). The system automatically generates the shear waves by programming and sending appropriate focused pushing beams in the liver.

A big drawback of the method is the small amplitude of the induced shear waves and their resulting fast attenuation, making the detection of the displacements only possible at focus (such as in ARFI based methods [5]) or in the few millimeters near the focus. To compensate for the shear wave weakness, a solution could be to increase the ultrasound beam intensity, but the relevance of this strategy is reduced by the medical acoustic power and intensity limitations that are imposed to any

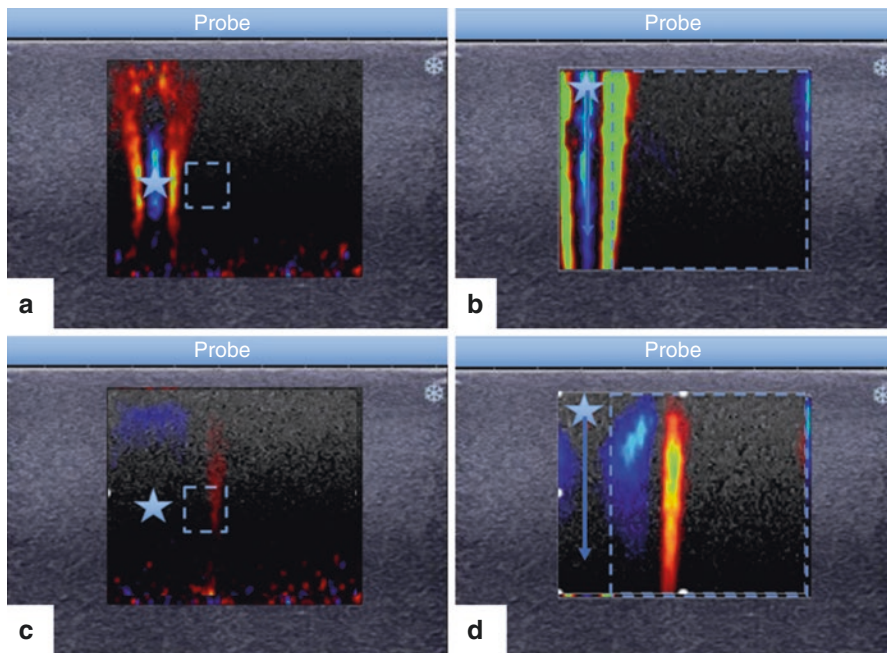


**Fig. 5.1** (a) Single push-induced shear wave at 2 ms. (b) Supersonic push-induced shear wave at 2 ms. (c) Single push-induced shear wave at 6 ms. (d) Supersonic push-induced shear wave at 6 ms

commercially available medical devices. 2D-SWE uses properties of wave propagation. The focused beam (or virtual palpating finger) is moved in the medium at a supersonic speed (i.e., faster than the induced shear waves) and creates a shear wave bang (like the sonic bang of supersonic airplanes). The shear waves are then confined along a Mach cone and their amplitude summed up in a coherent manner to generate higher amplitude shear waves without increasing the beam intensity itself. Figure 5.1a, c illustrate a shear wave induced by a typical single focused “pushing” beam. The induced shear wave displacements are of a few microns amplitude in the vicinity of the beam. Figure 5.1b, d show the same movie using a supersonic source. The amplitude of the induced shear wave is clearly higher and the propagation area much larger (blue square dots). Supersonic-induced waves are of enough amplitudes to propagate in soft tissue through several centimeters. The region of interest area is multiplied by 12–16. The supersonic generation of shear waves is a key contributor of the robustness and reliability of 2D-SWE.

## Ultrafast Ultrasound Imaging of Shear Waves

Shear wave frequencies vary between 20 and 2000 Hz in the body. To correctly analyze shear wave propagation and calculate their speeds (without bias or artefacts), they should be imaged at frame rates at least twice higher than their maximum frequency (Nyquist sampling rule), typically 4000–5000 images/s. This is way faster than the current capabilities of ultrasound systems (capable of reaching 50–100 images/s). In order to reach such frame rates, the way an ultrasound image is built needs to be rethought. Instead of firing focused beams and successively reconstructing ultrasound lines, the body is insonified with tilted plane waves and a specific algorithm is used to reconstruct the ultrasound images from the multiple plane wave insonification scheme (illustrated in Fig. 5.2e).

A good quality image can be built with 1–5 tilted insonifications instead of 200 for the focused approach increasing potentially the maximum frame rate achievable by typically a factor of 50 [6]. Ultrafast imaging capabilities are used to capture shear waves and measure their propagation speed. Depending on the application and depth of interest, ultrafast achievable frame rates can vary from 5000 images/s in the liver to 20,000 images/s in the breast or 40,000 images/s in MSK. From the propagation movie, the system calculates the shear wave speed at each pixel and displays an elasticity map as illustrated in the Fig. 5.2d. The elasticity map is calculated assuming a purely elastic medium where stiffness and shear wave speed are directly linked with the formula:

$$E = 3G = \rho V^2 \quad (5.1)$$

$E$  is the Young’s modulus, traditionally used to measure tissue stiffness.  $G$  is the shear modulus,  $V$  is the shear wave group velocity, and  $\rho$  is the tissue density assumed constant. For more details, see also other chapters in the book Part II



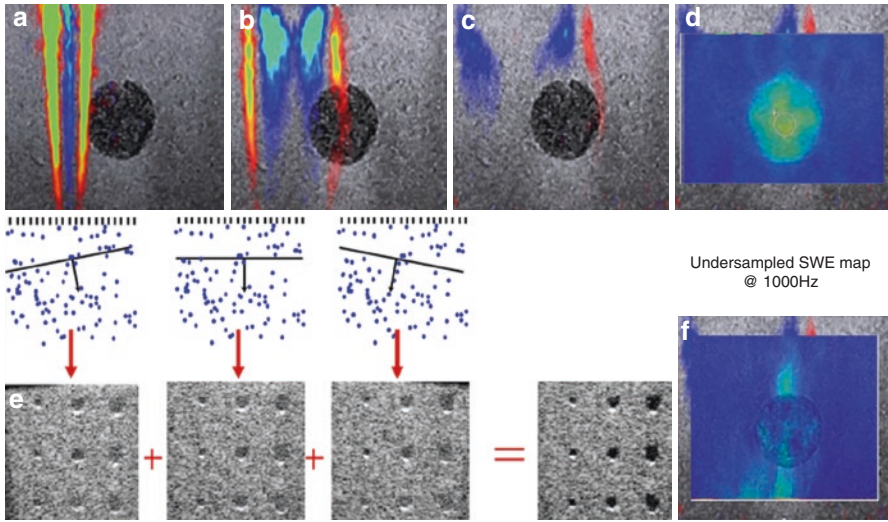


**Fig. 5.2** (a) Supersonic push-induced shear wave at 2 ms induced in a medium containing a harder inclusion. Ultrafast imaging to track shear wave is performed at 6000 Hz. (b) Supersonic push-induced shear wave at 6 ms. The shear wave accelerates in the harder inclusion. (c) Supersonic push-induced shear wave at 10 ms. (d) 2D-SWE map deduced from the propagation movie. The harder inclusion clearly appears in green. (e) Ultrafast acquisition sequence. (f) 2D-SWE map obtained if the imaging frame rate is reduced to 1000 Hz. The stiffer inclusion cannot be visualized

“Techniques to Measure Liver Stiffness”. Figure 5.2a–c show a shear wave propagation captured by Aixplorer® ultrafast camera in medium containing a harder inclusion. A Mach cone of plane shear waves propagates laterally. The 2D-SWE map clearly displays the harder inclusion in Fig. 5.2d. The combination of supersonic shear wave generation and ultrafast imaging is the most efficient and robust way to perform reliable and real-time imaging of tissue stiffness. Single-push strategies are barely usable in vivo given the weakness of the shear wave induced and traditional frame rates are insufficient to track the shear wave propagation. Figure 5.2f illustrates the bias introduced on the stiffness mapping when the frame rate is lowered to 1000 Hz inducing non-trustable results and bad clinical outcomes.

## Reinventing Ultrasound Technology

For its effective implementation on commercial products, the 2D-SWE mode requires to rethink the architecture and design of an ultrasound system. A traditional ultrasound system is not able to generate supersonic pushing sequences nor capable of reaching ultrafast frame rates. Two key components must be rethought: the power supply to be able to deliver higher intensity supersonic pushing beams and the beamforming (or image formation) architecture that requires fully parallelized

processing capabilities. The Aixplorer family (Aixplorer, Aixplorer Ultimate) and its new generation (Aixplorer Mach 30 and 20) are the only commercially available systems that have been designed with the goal to perform ultrafast imaging and 2D-SWE. They leverage the extremely high processing capabilities of modern CPUs and GPU to perform image beamforming in software instead of relying on single-line processing through electronic board. The switch from a hardware design to a fully software-based ultrasound system is a major technology shift that allows clinical availability and performance of 2D-SWE but also opens many perspectives to major clinical evolutions of ultrasound.

## 2D-SWE for Liver Stiffness Assessment

Shear wave elastography is proposed to the clinician as a real-time ultrasound imaging mode on Aixplorer family systems. The image is displayed in a wide box using a quantitative color-coded scale, overlaid on the B mode image. The real-time B mode is also shown in a duplex view as displayed in Figs. 5.3a and 5.4a. On Aixplorer Mach 30, typical 2D-SWE imaging frame rates vary from 1 to 3 Hz depending on the scanning conditions. B mode frame rates are the same as in stand-alone B mode (around 20–30 Hz). To specifically address the liver application, three curved array transducers are available in order to fit all morphologies specificities. The C6-1X probe (3 MHz central frequency) is designed for normal to high BMI patients, the C9-2X probe is specified for thin patients with low intercostal space, the micro convex MC12-3 probe is available for pediatric applications. Liver

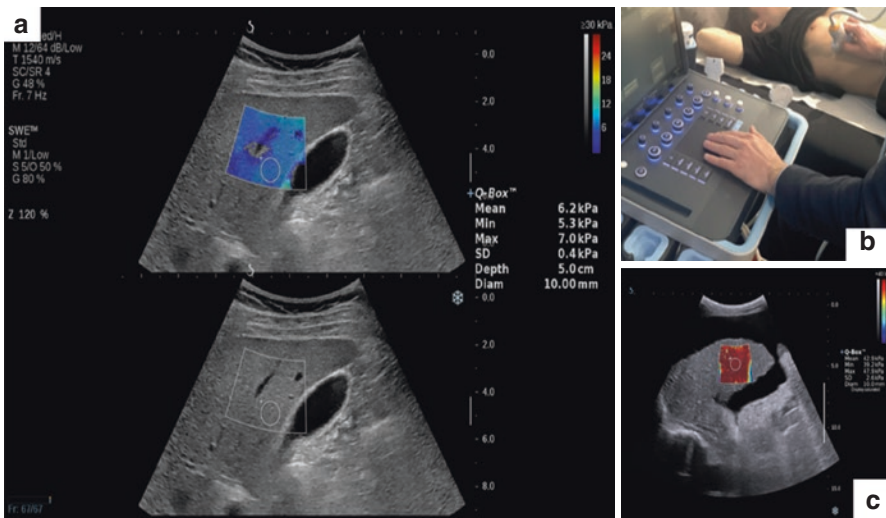


**Fig. 5.3** (a) 2D-SWE mode on Aixplorer Mach 30, (b) acquisition protocol using Aixplorer Mach 30, (c) 2D-SWE example on cirrhosis with ascites



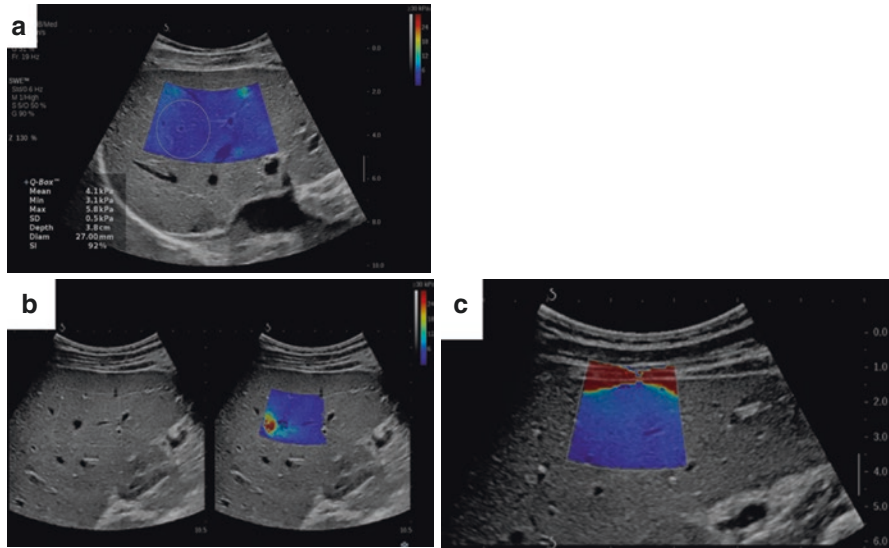


**Fig. 5.4** (a) 2D-SWE on liver. Real-time, quantitative on a large ROI. (b) Pulsating vessel artefact: a red area just near the vessel. (c) Capsule red artefact. For avoidance, guidelines recommend to place the box a few millimeters below it

stiffness can be assessed in a wide region of interest with a high resolution (1–3 mm resolution depending on the probe) as illustrated on Fig. 5.3a. Liver stiffness measurements are performed using the Q-Box tool: a circular ROI can be positioned anywhere in the 2D-SWE box, and its size can be set by the user. Stiffness measurements made in the Q-box area are provided: mean, max, min stiffness (kPa), and standard deviation over all the pixels of the Q-box area. In each Q-box, a stability index (SI) is also provided in percentage, indicating the quality of the 2D-SWE measurement. Measurements should be discarded if the SI is lower than 90%. Average stiffness and ratios over multiple Q-boxes are also available for the user.

### *Typical Guidelines for 2D-SWE in the Liver*

To perform proper stiffness measurement using 2D-SWE in the liver, a few scanning guidelines need to be followed.

- The patient should fast for a minimum of 2 h and rest for a minimum of 10 min before undergoing liver stiffness measurement.
- The patient needs to lie supine with the right arm in maximal abduction.
- The probe needs to be placed between the ribs (seventh to ninth right intercostal space), parallel to the intercostal space.
- The optimal window should be found using real-time B mode. The image quality should be high, the probe surface should be parallel to the ribs and the image should not contain major liver vessels.

- Sufficient pressure on the probe needs to be applied to avoid acoustic shadowing.
- Just before launching the 2D-SWE mode, the patient must stop breathing.
- The 2D-SWE box must be positioned in order to contain an area of uniform parenchyma. Measurements should target segment 6 and 8 of the right lobe.
- Stabilize the real 2D-SWE image over 3 s and then freeze the image.

The measurements can then be performed using the Q-Box tool. A dedicated reporting solution for liver is available for the user including dedicated labelled measurements, automatic calculation of statistical data from several measurements, selection of dedicated fibrosis publications by etiology with cut-offs for diagnosis.

### *Artefacts and Ways to Overcome Them*

Liver stiffness measurement can be affected by multiple artefacts [7]. Among them, the most important ones are:

- (a) A bad scanning window reducing the capacity to induce efficient vibrations inducing instabilities in the 2D-SWE real time image.
- (b) High heart beating rate that will create natural shear waves and interfere with the 2D-SWE-induced shear wave. This will also result in instabilities.
- (c) Patient motion (movement, breathing) that could induce instability in stiffness measurements.
- (d) Glisson capsule artefacts when the SWE box is positioned too close to it.
- (e) The presence of pulsating vessels that will interfere with the elastography technique.

An illustration of the two last artefacts is shown in Fig. 5.4b, c. The above guidelines allow significant reduction of instability-related artefacts (Fig. 5.4a–c). Furthermore, 2D-SWE provides a full set of tools and guidelines to make sure stiffness measurements are free of artefacts and are accurate and trustable. First the B mode allows precise monitoring of the scanning area in order to optimize the scanning window and eliminate the presence of pulsating vessels or lesions at the center of the image. Second, the 2D-SWE real-time capabilities help the user ensure that the stiffness measurement is accurate (stable image over time) and free of artefacts (artefacts linked to vessels or liver capsule can be easily avoided looking at the image). The stability index is provided for each measurement to help eliminate the acquisitions of insufficient quality (below 90%). Third, stiffness measurement can be performed using the Q-Box tool at any location within the 2D-SWE box with an adjustable measurement area. Typical Q-Box measurement area is 2 cm<sup>2</sup> wide and relies on the average value of more than 500-pixel values from the 2D-SWE image (compared to one measurement per acquisition with FibroScan). To be fully efficient, they must be inserted in specific scanning guidelines that have been overseen above (see Fig. 5.3).

## Clinical Impact of 2D-SWE in the Liver

Since its introduction and commercialization in 2008, 2D-SWE has been extensively used for liver disease assessment, leading to more than 160 peer-reviewed clinical publications and several thousands of cases reported. The clinical performances and the clinical value of 2D-SWE have been documented, and a review of main published results is done below.

### *2D-SWE Provides Reliable and Reproducible Measurements*

2D-SWE provides a high technical success rate (TSR) in various liver pathologies. Hudson et al. found a 98% TSR in healthy patients [8]. TSR above 97.5 was demonstrated in studies involving hepatitis B or C recruitment [9–12]. Even in cirrhotic patients, Cassinotto found a 93.8 TSR over 401 patients [13]. In patients with various chronic liver diseases, TSR has been kept in the 90–100% range depending on the studies and recruitment [14]. **Intra-operator reproducibility** has also been demonstrated as excellent with intraclass correlation coefficients (ICC) ranging from 0.93 to 0.96 depending on the qualification of the operator and the type of disease [9, 13, 15]. Ferraioli [10] demonstrated that the mean difference between measurements during a given scanning session was 0.01 kPa, significantly below the precision required to stage fibrosis. **Inter-operator reproducibility** was reported with ICC above 0.83 [8] up to 0.94 [13]. Cassinotto also demonstrated higher ICC for liver (0.94) than for spleen (0.87) [13].

With higher TSR and reproducibility than FibroScan, 2D-SWE interestingly shows similar threshold values for hepatitis C virus-related patients. This was demonstrated in 2017 by Piscaglia et al. [16]. The study reported a good concordance in terms of precision and accuracy between 2D-SWE and FibroScan (0.90 precision coefficient and 0.99 accuracy coefficient) for measurements taken into two intercostal spaces. The concordance was significantly lower for shear wave-based ultrasound elastography techniques provided by other manufacturers (typically 0.7 and 0.5 precision and accuracy coefficient).

### *A Fast Acquisition Protocol*

In all techniques other than 2D-SWE, ten consecutive measurements are recommended by the manufacturer to perform a liver stiffness measurement. This constrain slows down and significantly complicates the scanning workflow. Huang et al. demonstrated that 2D-SWE has the same diagnostic performances [17] with 1 or 10 measurements. For BMI > 27 kg/m<sup>2</sup>, three measurements are recommended.

The typical full 2D-SWE liver protocol (scan, perform 2D-SWE, quantify, report) can be performed in less than 60 s.

Publication results show that the technological superiority of 2D-SWE (supersonic shear wave generation and ultrafast imaging) brings significant value to the clinician by reducing the examination time and increasing the accuracy and robustness of the measurements.

As we will show below, it also translates into high value clinical results.

### ***Liver Stiffness Assessment with 2D-SWE Is Correlated with Fibrosis Stage***

The correlation of stiffness assessment with 2D-SWE with fibrosis severity has been established in multiple studies [14, 18–20]. An overview of diagnostic performance of 2D-SWE among different comparative studies with mixed etiologies is shown on Fig. 5.4a. AUROCs above 0.86 have been systematically demonstrated to assess significant fibrosis ( $F \geq 2$ ). AUROCs are above 0.91 for severe fibrosis ( $F \geq 3$ ) and above 0.92 for cirrhosis. Performance is very similar (a bit higher) if the focus is on a specific pathology such as HCV, HBV, or NASH/ASH. Those studies have been confirmed by several meta-analysis published in 2016 [21–23]. For example, Jiang et al. found AUROCs of 0.87 for significant fibrosis detection and of 0.94 on cirrhosis over 2303 patients. Figure 5.5b shows the range of diagnostic cut-off values from the literature to evaluate liver fibrosis severity using 2D-SWE. The ranges per fibrosis stage are clearly not overlapping for Hep B and C diseases-based recruitments. Figure 5.5c shows the cut-off values in terms of sensitivity and specificity.

More recently, Wang et al. [24] demonstrated on 398 patients that the use of deep learning radiomics on 2D-SWE images could increase diagnostic performance of 2D-SWE for fibrosis assessment. AUROCs were found up to be 0.98 for severe fibrosis and 0.97 for cirrhosis. This preliminary paper shows the great potential of combining high-quality 2D-SWE images with artificial intelligence but requires further confirmation. Similar results have been found for the pediatric population. Franchi et al. [25] found that 2D-SWE correlated better than FibroScan for fibrosis assessment (AUROCs of 0.8 vs. 0.75).

### ***Beyond Liver Fibrosis Assessment***

2D-SWE can also be considered as an efficient clinical tool for other indications than fibrosis assessment, particularly in cirrhotic patients. Publications have demonstrated that the combination of liver and spleen stiffness using 2D-SWE could indicate prognosis. Jansen et al. [26] showed that liver and spleen stiffness above certain

thresholds predict clinically significant portal hypertension (CSPH). Kim et al. [27] showed that 2D-SWE can non-invasively predict the presence of esophageal varices, more accurately than platelet count versus spleen diameter ratio. 2D-SWE can also be used for liver treatment monitoring, such as anti-portal hypertension therapy [28] or for transplantation planning and monitoring [29]. No data are yet available on spleen stiffness (or spleen size) to liver stiffness ratio which could help to localize the histological side of inflammation and predict disease-specific complications as shown recently in a FibroScan based study [30].

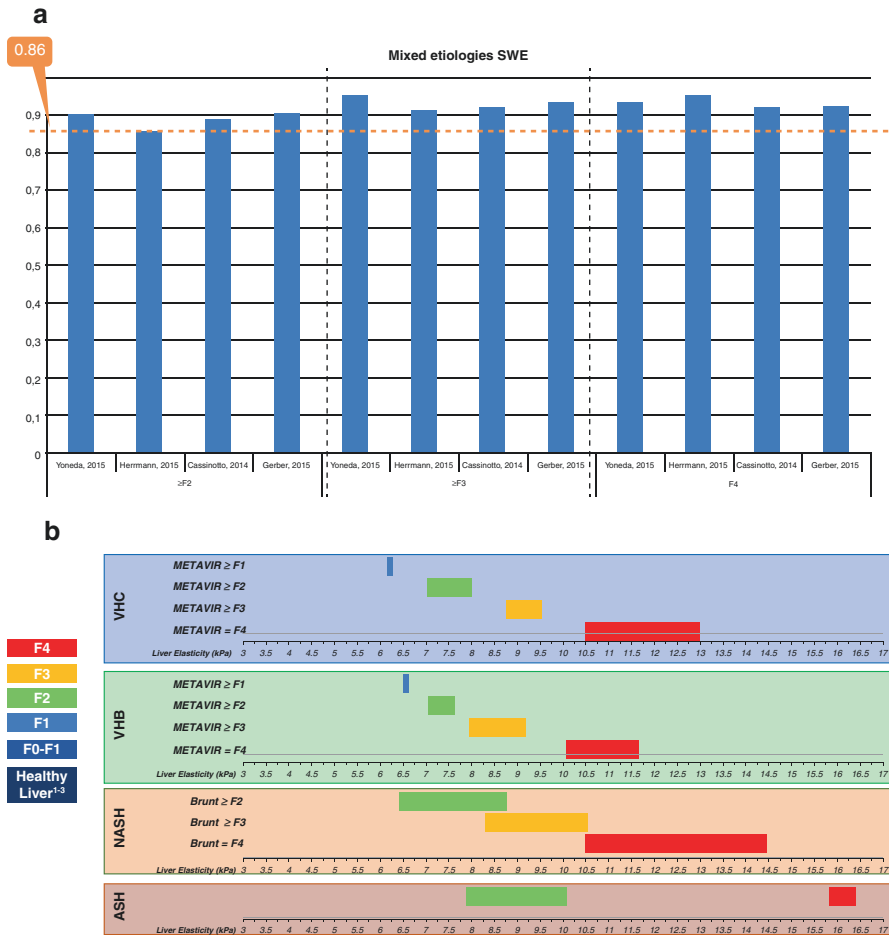


**Fig. 5.5** (a) Diagnostic performance of 2D-SWE among different comparative studies with mixed etiologies in different studies. (b) Range of diagnostic cut-off values from the literature to evaluate liver fibrosis severity using 2D-SWE. (c) Cut-off performances in terms of sensitivity and specificity from different studies. For sake of clarity, references are directly inserted in the figures

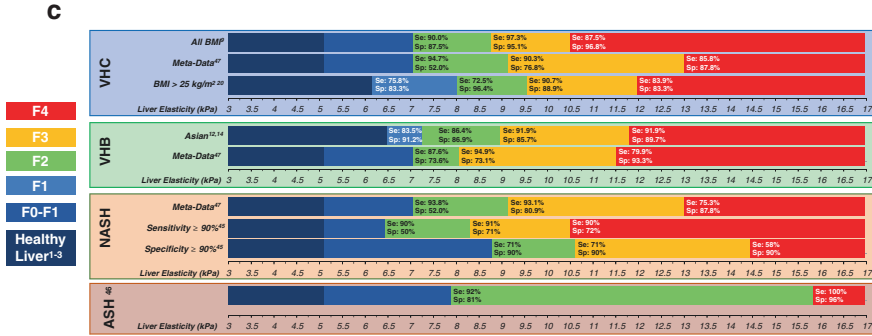


Fig. 5.5 (continued)

## Beyond 2D-SWE

Many confounding factors should be taken into account such as liver pathological evolution before fibrosis, blood pressure, congestion, BMI, and cardiac insufficiency [31–37]. For more details, see also the book Part IV “Important (Patho) physiological Confounders of LS.” Thus, it would be highly desirable, if steatosis and necro-inflammatory activity could be also assessed in addition to fibrosis. Complementary quantitative tools for better noninvasive assessment of liver diseases are therefore needed comparable to the controlled attenuation parameter (CAP) run on the FibroScan platform. For more details, see also the book Part VI “Assessment of Hepatic Steatosis Using CAP.” On Aixplorer Mach 30, 2D-SWE is complemented with many other ultrasound markers with the goal to assess liver disease in its globality.

## Viscosity

Human tissue can be considered as viscoelastic materials. Viscosity refers to the tissue capacity to attenuate or absorb vibrations. If 2D-SWE measures the elastic properties of tissues (elasticity or stiffness can be considered as the same information), viscosity remains an unknown. When tissues have viscous properties, shear waves of different frequencies propagate at different speeds (the so-called dispersion effect). This is illustrated in equations below.

$$v_{\phi}(\omega) = \sqrt{\frac{\mu}{\rho}} \quad v_{\phi}(\omega) = \sqrt{\frac{2(\mu^2 + \eta^2 \omega^2)}{\rho(\mu + \sqrt{\mu^2 + \eta^2 \omega^2})}} \quad (5.2)$$

Equation 5.1 is for purely elastic medium and Eq. 5.2 for viscoelastic medium, where  $\mu$  is the shear modulus,  $\eta$  is the viscosity, and  $\rho$  is the medium density. When the medium is purely elastic, the wave speed is directly linked to tissue elasticity. When the medium is viscoelastic (Voigt model), the wave speed depends on medium elasticity, viscosity, and the frequency of the wave

Shear waves induced by the 2D-SWE contain multiple frequencies (typically from 20 to 400 Hz in the liver). This is not the case for strain elastography (a static compression corresponds to a zero-frequency wave) or FibroScan (the vibration is generated at 50 Hz). By adding a new processing algorithm to 2D-SWE data, shear wave speed can be estimated at multiple frequencies, and a quantitative viscosity image can be provided to the user without changing anything to its protocol. Figure 5.6a shows the new 2D-SWE mode on Aixplorer Mach 30 with viscosity imaging provided as a complementary information to elasticity.

### *Ultrasound Attenuation and Ultrasound Speed of Sound*

Despite being an active field in the research arena for many decades, ultrasound image quantification has never really been adopted by the medical industry. One reason seems to be the technical challenge to provide accurate and unbiased estimation of ultrasound body properties. Recently, a re-interest has been observed for breast and liver imaging. In the liver, CAP (controlled attenuation parameter), proposed on the Fibroscan [38], is one of the first tools to assess a global liver ultrasound attenuation. Aixplorer Mach 30 leverage its ultrafast architecture to propose in addition to its 2D-SWE mode (including elasticity and viscosity quantification), a tool able to accurately quantify ultrasound attenuation and ultrasound speed of sound within the liver. Both parameters have been shown to be correlated to liver steatosis according to preliminary studies [39, 40]. Figure 5.6b shows the new ultrasound quantification mode.

### *Vascularization*

As part of a complete ultrasound solution, real-time Doppler imaging and Angio PL.U.S. (ultrasensitive Doppler imaging) are available on Aixplorer Mach 30. Angio PL.U.S. is a new Doppler imaging mode based on ultrafast technology [41] and allows small vessel detection and mapping in the liver. Figure 5.5c shows the comparison between traditional Doppler and Angio PL.U.S. on a focal nodular hyperplasia (FNH). The bike wheel pattern is clearly identified on the Angio PL.U.S. image, making the mode a very neat help to detect and characterize such liver lesions. Vascular analysis with contrast agent imaging (CEUS) is also available



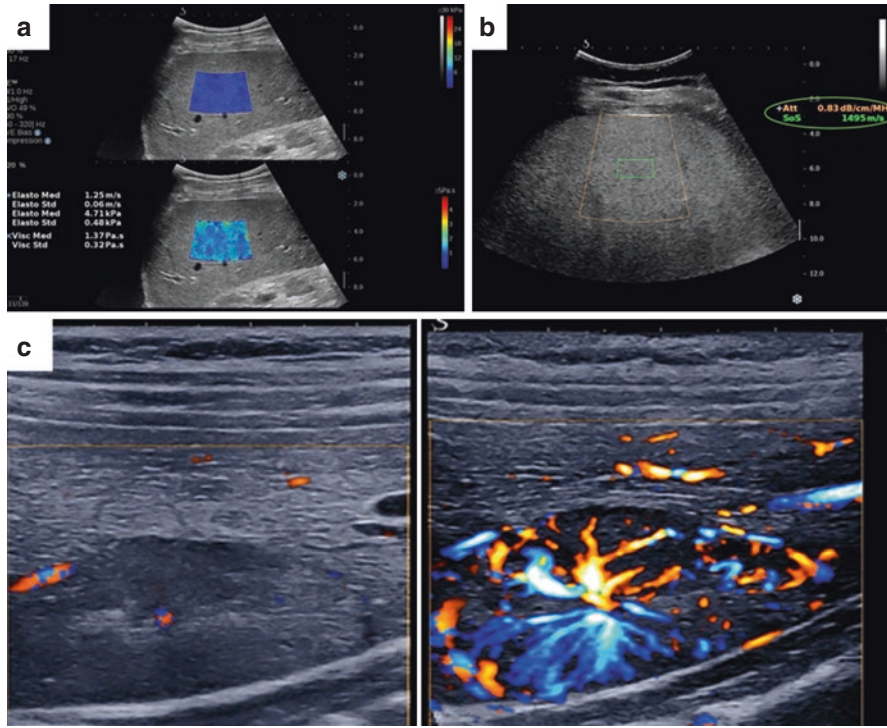


**Fig. 5.6** (a) 2D-SWE mode with quantitative stiffness (top) and viscosity imaging (bottom). (b) Liver ultrasound quantification (attenuation and speed of sound). All features from Aixplorer Mach 30. (c) Classical Doppler vs. Angio PL.U.S on a FNH

and is particularly relevant for liver nodule characterization indication. The complement of 2D-SWE stiffness assessment with vascularization imaging and three new ultrasound quantitative markers open the possibility to improve non-invasive diffuse liver management. The combination of such imaging modes and markers with machine learning or deep learning techniques could hopefully lead to accurate assessment of steatosis and necro-inflammatory activity. Clinical studies are ongoing to assess the relevance of these new parameters for liver disease management.

## Conclusion

2D-SWE is an accurate, easy to use, and reliable tool to assess liver fibrosis, and it has better or equivalent performances as compared to other methods. It is recognized by FDA as a clinical tool in the management of patients with liver diseases. 2D-SWE could be regarded as a first step of quantitative ultrasound imaging where ultrasound imaging is switching from a purely morphological imaging system to a fully quantitative imaging device of several tissue and flow markers.



## References

1. Krouskop T, Dougherty D, Vinson F. A pulsed Doppler ultrasonic system for making non-invasive measurements of the mechanical properties of soft tissue. *J Rehabil Res Dev*. 1987;24(2):1–8.
2. Itoh A, Ueno E, Tohno E, Kamma H, Takahashi H, Shiina T, et al. Breast disease: clinical application of US elastography for diagnosis. *Radiology*. 2006;239(2):341–50.
3. Sandrin L, Fourquet B, Hasquenoph J-M, Yon S, Fournier C, Mal F, et al. Transient elastography: a new non-invasive method for assessment of hepatic fibrosis. *Ultrasound Med Biol*. 2003;29(12):1705–13.
4. Bercoff J, Tanter M, Fink M. Supersonic shear imaging: a new technique for soft tissue elasticity mapping. *IEEE Trans Ultrason Ferroelectr Freq Control*. 2004;51(4):396–409.
5. Fahey BJ, Nightingale KR, Nelson RC, Palmeri ML, Trahey GE. Acoustic radiation force impulse imaging of the abdomen: demonstration of feasibility and utility. *Ultrasound Med Biol*. 2005;31(9):1185–98.
6. Montaldo G, Tanter M, Bercoff J, Benech N, Fink M. Coherent plane-wave compounding for very high frame rate ultrasonography and transient elastography. *IEEE Trans Ultrason Ferroelectr Freq Control*. 2009;56(3):489–506.
7. Bruce M, Kolokythas O, Ferraioli G, Filice C, O'Donnell M. Limitations and artifacts in shear-wave elastography of the liver. *Biomed Eng Lett*. 2017;7(2):81–9.
8. Hudson JM, Milot L, Parry C, Williams R, Burns PN. Inter- and intra-operator reliability and repeatability of shear wave elastography in the liver: a study in healthy volunteers. *Ultrasound Med Biol*. 2013;39(6):950–5.
9. Ferraioli G, Tinelli C, Dal Bello B, Zicchetti M, Filice G, Filice C. Accuracy of real-time shear wave elastography for assessing liver fibrosis in chronic hepatitis C: a pilot study. *Hepatology*. 2012;56(6):2125–33.
10. Ferraioli G, Tinelli C, Zicchetti M, Above E, Poma G, Di Gregorio M, et al. Reproducibility of real-time shear wave elastography in the evaluation of liver elasticity. *Eur J Radiol*. 2012;81(11):3102–6.
11. Gao Y, Zheng J, Liang P, Tong M, Wang J, Wu C, et al. Liver fibrosis with two-dimensional US shear-wave elastography in participants with chronic hepatitis b: a prospective multicenter study. *Radiology*. 2018;289(2):407–15.
12. Leung VY, Shen J, Wong VW, Abrigo J, Wong GL, Chim AM, et al. Quantitative elastography of liver fibrosis and spleen stiffness in chronic hepatitis B carriers: comparison of shear-wave elastography and transient elastography with liver biopsy correlation. *Radiology*. 2013;269(3):910–8.
13. Cassinotto C, Charrie A, Mouries A, Lapuyade B, Hiriart J-B, Vergniol J, et al. Liver and spleen elastography using supersonic shear imaging for the non-invasive diagnosis of cirrhosis severity and oesophageal varices. *Dig Liver Dis*. 2015;47(8):695–701.
14. Gerber L, Kasper D, Fitting D, Knop V, Vermehren A, Sprinzl K, et al. Assessment of liver fibrosis with 2-D shear wave elastography in comparison to transient elastography and acoustic radiation force impulse imaging in patients with chronic liver disease. *Ultrasound Med Biol*. 2015;41(9):2350–9.
15. Yoon JH, Lee JM, Han JK, Choi BI. Shear wave elastography for liver stiffness measurement in clinical sonographic examinations: evaluation of intraobserver reproducibility, technical failure, and unreliable stiffness measurements. *J Ultrasound Med*. 2014;33(3):437–47.
16. Piscaglia F, Salvatore V, Mulazzani L, Cantisani V, Colecchia A, Di Donato R, et al. Differences in liver stiffness values obtained with new ultrasound elastography machines and fibroscan: a comparative study. *Dig Liver Dis*. 2017;49(7):802–8.
17. Huang Z-P, Zhang X-L, Zeng J, Zheng J, Wang P, Zheng R-Q. Study of detection times for liver stiffness evaluation by shear wave elastography. *World J Gastroenterol*. 2014;20(28):9578.

18. Cassinotto C, Lapuyade B, Mouries A, Hiriart J-B, Vergniol J, Gaye D, et al. Non-invasive assessment of liver fibrosis with impulse elastography: comparison of Supersonic Shear Imaging with ARFI and FibroScan®. *J Hepatol.* 2014;61(3):550–7.
19. Yoneda M, Thomas E, Sclair SN, Grant TT, Schiff ER. Supersonic shear imaging and transient elastography with the XL probe accurately detect fibrosis in overweight or obese patients with chronic liver disease. *Clin Gastroenterol Hepatol.* 2015;13(8):1502–9. e5.
20. Herrmann E, De Ledinghen V, Cassinotto C, Chu W-W, Leung V-F, Ferraioli G, et al. 2D-shear wave elastography is equivalent or superior to transient elastography for liver fibrosis assessment: results from an individual patient databased meta-analysis. *J Hepatol.* 2015;62(Suppl):S199–200.
21. Feng J-C, Li J, Wu X-W, Peng X-Y. Diagnostic accuracy of SuperSonic shear imaging for staging of liver fibrosis: a meta-analysis. *J Ultrasound Med.* 2016;35(2):329–39.
22. Jiang T, Tian G, Zhao Q, Kong D, Cheng C, Zhong L, et al. Diagnostic accuracy of 2D-shear wave elastography for liver fibrosis severity: a meta-analysis. *PLoS One.* 2016;11(6):e0157219.
23. Li Y, Huang YS, Wang ZZ, Yang ZR, Sun F, Zhan SY, et al. Systematic review with meta-analysis: the diagnostic accuracy of transient elastography for the staging of liver fibrosis in patients with chronic hepatitis B. *Aliment Pharmacol Ther.* 2016;43(4):458–69.
24. Wang K, Lu X, Zhou H, Gao Y, Zheng J, Tong M, et al. Deep learning radiomics of shear wave elastography significantly improved diagnostic performance for assessing liver fibrosis in chronic hepatitis B: a prospective multicentre study. *Gut.* 2019;68(4):729–41.
25. Franchi-Abella S, Corno L, Gonzales E, Antoni G, Fabre M, Ducot B, et al. Feasibility and diagnostic accuracy of supersonic shear-wave elastography for the assessment of liver stiffness and liver fibrosis in children: a pilot study of 96 patients. *Radiology.* 2015;278(2):554–62.
26. Jansen C, Bogs C, Verlinden W, Thiele M, Möller P, Görtzen J, et al. Shear-wave elastography of the liver and spleen identifies clinically significant portal hypertension: a prospective multicentre study. *Liver Int.* 2017;37(3):396–405.
27. Kim TY, Kim TY, Kim Y, Lim S, Jeong WK, Sohn JH. Diagnostic performance of shear wave elastography for predicting esophageal varices in patients with compensated liver cirrhosis. *J Ultrasound Med.* 2016;35(7):1373–81.
28. Choi SY, Jeong WK, Kim Y, Kim J, Kim TY, Sohn JH. Shear-wave elastography: a noninvasive tool for monitoring changing hepatic venous pressure gradients in patients with cirrhosis. *Radiology.* 2014;273(3):917–26.
29. Yoon JH, Lee JY, Woo HS, Yu MH, Lee ES, Joo I, et al. Shear wave elastography in the evaluation of rejection or recurrent hepatitis after liver transplantation. *Eur Radiol.* 2013;23(6):1729–37.
30. Elshaarawy O, Mueller J, Guha IN, Chalmers J, Harris R, Krag A, et al. Spleen stiffness to liver stiffness ratio significantly differs between ALD and HCV and predicts disease-specific complications. *JHEP Reports.* 2019;1(2):99–106.
31. Millonig G, Friedrich S, Adolf S, Fonouni H, Golriz M, Mehrabi A, et al. Liver stiffness is directly influenced by central venous pressure. *J Hepatol.* 2010;52(2):206–10.
32. Millonig G, Reimann FM, Friedrich S, Fonouni H, Mehrabi A, Büchler MW, et al. Extrahepatic cholestasis increases liver stiffness (FibroScan) irrespective of fibrosis. *Hepatology.* 2008;48(5):1718–23.
33. Piecha F, Mandorfer M, Peccerella T, Ozga AK, Poth T, Vonbank A, et al. Pharmacological decrease of liver stiffness is pressure-related and predicts long-term clinical outcome. *Am J Physiol Gastrointest Liver Physiol.* 2018;315(4):G484–G94.
34. Piecha F, Peccerella T, Bruckner T, Seitz HK, Rausch V, Mueller S. Arterial pressure suffices to increase liver stiffness. *Am J Physiol Gastrointest Liver Physiol.* 2016;311(5):G945–G53.
35. Elshaarawy O, Alquzi S, Mueller J, Rausch V, Silva I, Peccerella T, et al. Response of liver and spleen stiffness to portal pressure lowering drugs in a rat model of cirrhosis. *J Hepatol.* 2019;70:E14–E5.
36. Mueller S, Englert S, Seitz HK, Badea RI, Erhardt A, Bozaari B, et al. Inflammation-adapted liver stiffness values for improved fibrosis staging in patients with hepatitis C virus and alcoholic liver disease. *Liver Int.* 2015;35(12):2514–21.

37. Mueller S, Sandrin L. Liver stiffness: a novel parameter for the diagnosis of liver disease. *Hepatic Med Evid Res.* 2010;2:49–67.
38. Sasso M, Miette V, Sandrin L, Beaugrand M. The controlled attenuation parameter (CAP): a novel tool for the non-invasive evaluation of steatosis using Fibroscan®. *Clin Res Hepatol Gastroenterol.* 2012;36(1):13–20.
39. Imbault M, Faccinetto A, Osmanski B-F, Tissier A, Deffieux T, Gennisson J-L, et al. Robust sound speed estimation for ultrasound-based hepatic steatosis assessment. *Phys Med Biol.* 2017;62(9):3582.
40. de Ledinghen V, Vergniol J, Capdepon M, Chermak F, Hiriart JB, Cassinotto C, et al. Controlled attenuation parameter (CAP) for the diagnosis of steatosis: a prospective study of 5323 examinations. *J Hepatol.* 2014;60(5):1026–31.
41. Bercoff J, Montaldo G, Loupas T, Savery D, Mézière F, Fink M, et al. Ultrafast compound Doppler imaging: providing full blood flow characterization. *IEEE Trans Ultrason Ferroelectr Freq Control.* 2011;58(1):134–47.

# Chapter 6

## Liver Magnetic Resonance Elastography: Clinical Use and Interpretation



Jing Guo, Ingolf Sack, and Stephan Rodrigo Marticorena Garcia

### Technical Introduction

Magnetic resonance elastography (MRE) is a phase-contrast-based MRI technique that can measure displacement due to propagating mechanical waves, from which material properties such as shear modulus can be calculated [1]. It is motivated by the clinical importance of palpation, which has been used for centuries to detect diseased tissue. MRE gains increasingly clinical importance, in particular for the diagnosis and staging of liver fibrosis [2–4]. However, many groups are reporting MRE results in terms of different parameters, and numerous types of acquisitions and processing techniques are currently in use [1]. The diversity of techniques and terminology can lead to confusion as to the meaning of certain terms or how to interpret or compare MRE results. Therefore, standardization and guidelines in MRE including recent technological advancements such as multifrequency MRE, tomoelastography, and stable actuation methods are necessary to further improve the applicability and consistency of MRE in clinical examinations, in particular for the liver [5]. Since the number of publications in MRE of the liver expands far beyond a compact overview within this textbook, we recommend further reading of the following review articles and meta-analyses [3, 4, 6–20].

---

J. Guo (✉) · I. Sack · S. R. Marticorena Garcia  
Department of Radiology, Charité—Universitätsmedizin Berlin, Berlin, Germany  
e-mail: [jing.guo@charite.de](mailto:jing.guo@charite.de); [ingolf.sack@charite.de](mailto:ingolf.sack@charite.de); [stephan.marticorena-garcia@charite.de](mailto:stephan.marticorena-garcia@charite.de)

## *Driver, Sequences, and Post-processing*

There are three main technical components to MRE: (a) the generation of the mechanical waves and their delivery to the relevant part of the body, (b) the MR pulse sequence used to acquire data, and (c) the inversion algorithm to recover one or more mechanical parameters from the displacement data [1].

Several approaches have been used to generate mechanical waves for MRE. MRE of the liver typically uses pneumatic drivers either coupled with commercially available loudspeaker systems (Resoundant Inc., Rochester, MN) [4] or operated by compressed air drivers [1, 21]. Other studies used piezoelectrical actuators [22], rigid piston drivers [23] or electromagnetic induction coils [24] to generate motion in the liver. Irrespective of the way of introducing shear waves into the liver, MRE relies on the full penetration of the liver and abdominal cavity with time-harmonic vibrations [1]. Care has to be taken to avoid insufficient wave penetration of the liver leading to artifacts and noise in parameter maps (elastograms) [25]. Therefore, multiple drivers placed around the abdomen have been proposed to further improve the reproducibility of MRE in clinical examinations [26]. The frequencies of the vibrations are typically in the range between 30 and 60 Hz [1]. The commercial Resoundant system uses 60 Hz [3] while several studies have demonstrated the benefit of using multifrequency MRE protocols by introducing several frequencies for analyzing viscoelastic dispersion of liver tissue [23, 27] or for high-resolution parameter mapping [15, 22].

MRE pulse sequences are typically based on gradient-echo (GRE-MRE) or spin-echo sequences (SE-MRE) with Cartesian readout which is favored by the rectangular field-of-view given in transversal slices through the abdomen [1]. Motion is encoded by oscillating gradients (MEG) either in synchrony to the induced mechanical vibration or having a shorter period time than the stimulated harmonic vibration [28]. Encoding by short MEG is often required in order to keep echo times short and to minimize T2-signal relaxation. Motion encoding gradients which are shorter than a vibration period are referred to as fractional encoding schemes which are increasingly applied in MRE of the liver [29]. Currently, spin-echo echo-planar imaging (SE-EPI) MRE is becoming a routine clinical protocol for imaging the liver at 1.5 and 3 T [30]. MRE captures shear wave images within several seconds in two dimensions or within minutes in three dimensions including full-field acquisition. Scan times exceeding 20 s are often segmented to fit into breath hold windows, which significantly prolongs measure time. Therefore, free breathing protocols have been established in larger cohorts demonstrating good stability of values across all patients and diseases [31]. Reasons for the relative insensitivity of MRE to breathing artifacts might relate to typical post-processing strategies in MRE in which only harmonic motions are selected and unwanted stochastic motions are suppressed. Here, automated motion correction routines based on image registration prior to the specific MRE post-processing might help to further improve the consistency of MRE in the liver at shorter scan times similar to motion correction applied to the brain [32].

A central part of post-processing in MRE is the solution of the inverse problem of time-harmonics waves [33]. The wave equation governs the propagation of wave

fields in which shear and compression components overlap. Usually, Helmholtz decomposition is applied to separate shear from compression components followed by solving the scalar shear wave equation for the complex shear modulus [34]. This procedure is named direct inversion (DI) and is used in many MRE examinations of the liver [1]. However, Helmholtz decomposition combined with DI is known to be very sensitive to noise due to finite difference operators in second or third orders [34]. Therefore, DI-inherent difference operators are often replaced by bandpass-filters. Local frequency estimation (LFE) relies on filter banks yielding stable results with, however, limited spatial resolution of anatomical details [34]. A better approach has been introduced recently, named tomoelastography, which uses spatiotemporal filtering combined with single-order derivative operators to solve the equation of plane waves for wave numbers [15]. As a result, tomoelastography delivers maps of inverse wave numbers times actuation frequency (shear wave speed,  $c$  in m/s) as a surrogate of stiffness [21]. Both DI and tomoelastography can be extended to multifrequency reconstruction methods [21, 22]. It has been shown that combining multifrequency wave fields prior to inversion permits alleviation of wave voids and amplitude nulls at single frequency yielding an overall improved quality of parameter maps [35].

### *Elasticity and Viscosity*

The complex shear modulus  $G^*$  as measured by MRE provides a basic description of mechanical tissue properties. Stiffness is often referred to the magnitude modulus ( $|G^*|$ ), while elasticity and viscosity are quantified by storage (real part of  $G^*$ ) and loss modulus (imaginary part of  $G^*$ ). Viscosity is a material's ability to convert mechanical energy into heat. An alternative description of viscosity is based on the phase angle  $\varphi$  of the complex modulus (also known as loss angle) which indicates fluidity. Conceptually, fluidity signifies the conversion of a solid into a fluid within a continuous range of values from 0 to  $\pi/2$ . Materials of  $\varphi < \pi/4$  behave predominantly solid while materials of  $\varphi > \pi/4$  are thought to be dominated by fluid properties. Some studies of MRE of the liver also reported volumetric strain. Unlike shear strain, which is commonly evaluated in MRE, volumetric strain relates to compression. As will be shown later, compression of liver tissue can change with portal hypertension and increased intrahepatic pressure gradient. Beyond shear modulus, MRE holds great promise for future applications aiming at physiologically and pathologically altered pressure. More reading on MRE parameters can be found in [1].

In summary, current MRE technology for the liver is well established in clinical routine providing mechanical parameters such as shear modulus for the detection of abnormal hepatic stiffness due to fibrosis. Technical improvements addressed deep penetration of abdominal tissues by shear waves, fast imaging sequences to avoid motion artifacts and noise-robust inversion routines to better depict anatomical details. Multifrequency-based tomoelastography of abdominal organs including the liver based on compressed air drivers has recently been demonstrated as viable approach to address those challenges [15, 21, 31, 36].

## MRE in Liver Fibrosis

Liver fibrosis is a dynamic process characterized by the accumulation of extracellular matrix (ECM) elements such as collagen, fibronectin, proteoglycans, and glycosaminoglycans in response to chronic inflammation. Major reasons for liver fibrosis comprise alcohol abuse, metabolic disorders, and viral infections. The volume fraction of liver-ECM is in the order of 3% in healthy livers but can increase up to a factor of ten due to advanced fibrosis [37]. Fibrosis progresses very slowly, typically within 5–50 years, in an asymptomatic course [38]. However, significant liver reorganization can occur already at early stages of fibrosis [39]. Advanced fibrosis is characterized by end-stage fibrous scar tissue with hepatocellular dysfunction, known as cirrhosis. Cirrhosis is typically associated with elevated intrahepatic resistance to blood flow, varicose veins, portal hypertension, and hepatic insufficiency. There are two general categories of cirrhosis: compensated and decompensated cirrhosis. In compensated cirrhosis, the liver is still able to perform vital functions without major complications and clinical symptoms. Progression from compensated to decompensated cirrhosis is marked by symptoms such as ascites, variceal bleeding, hepatic encephalopathy, and hepatic failure. Furthermore, liver fibrosis is associated with increased risk of the development of hepatocellular carcinoma (HCC) [40, 41].

Staging of liver fibrosis is essential for the prognosis and treatment planning of chronic liver diseases. Liver biopsy is considered the reference standard for staging fibrosis despite its invasiveness and associated risks. Different histopathological staging scores are used in clinical routine. The most commonly used scores are Meta-analysis of Histological Data in Viral Hepatitis (METAVIR) [42], Classification of the International Association for the Study of the Liver (IASL) [43], and the Ishak score [44], which combine a representation of the extent of fibrosis and inflammation. However, the diagnostic accuracy of liver biopsy is still under debate since biopsy covers only a fraction of 1/150,000 of the entire liver parenchyma and thus is susceptible for sampling errors [45, 46]. Furthermore, histopathological analysis is often subjective and therefore limited by inter- and intraobserver variability [47]. Finally, the application of biopsy in follow-up examinations suffers from low patient acceptance [46].

Advanced imaging modalities are used in the clinical routine for diagnosing fibrosis, such as sonography, MRI with dynamic extracellular, or hepatobiliary contrast medium-enhancement, MRI-based perfusion and diffusion quantification, as well as T1- and T2-Mapping [48, 49].

In this context, MRE is unique as it provides quantitative, biophysical, and system-independent parameters of structure and composition of soft tissues. MRE in the liver is particularly successful as reflected by the high number of publications. Clinical MRE studies in patients with liver fibrosis have been validated by tissue studies of bovine liver [50], human tissue [51], and animal models [52–54] showing the high sensitivity of MRE to structural changes in the course of liver disease.



Several studies demonstrated the value of MRE for a noninvasive detection of liver fibrosis and the potential of MRE for distinguishing different fibrosis stages [16–19]. For simplicity, we will present fibrosis stages according to the METAVIR-score [42]: stage 1 = any fibrosis; stage 2 = significant fibrosis; stage 3 = advanced fibrosis; stage 4 = cirrhosis. An example of using multifrequency MRE with tomoelastography post-processing [15] is provided in Fig. 6.1. A recent meta-analysis, which included 26 studies with a total of 3200 patients, reported a very

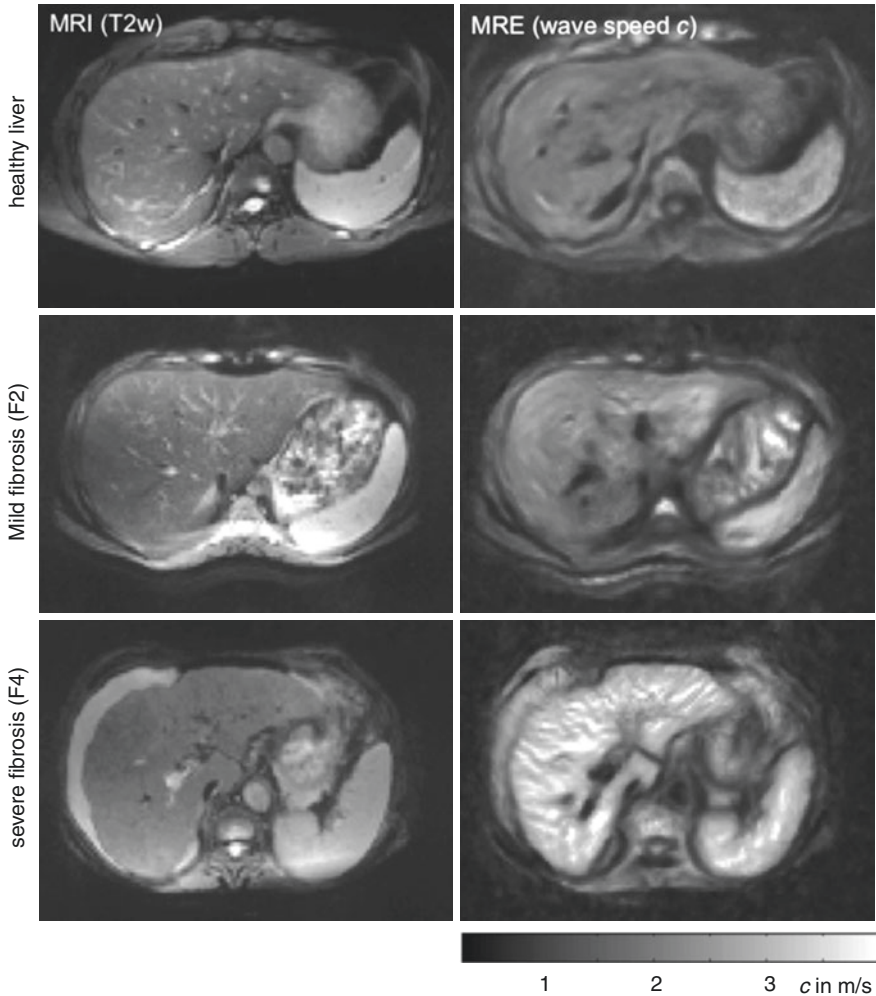


**Fig. 6.1** T2w images (left) and shear wave speed maps (elastograms, right) of a healthy liver, and patients with stage 2 and 4 fibrosis. Increased shear wave speed values with higher fibrosis stage are clearly visible. (Reproduced from H. Tzschätzsch et al. [15] with permission)

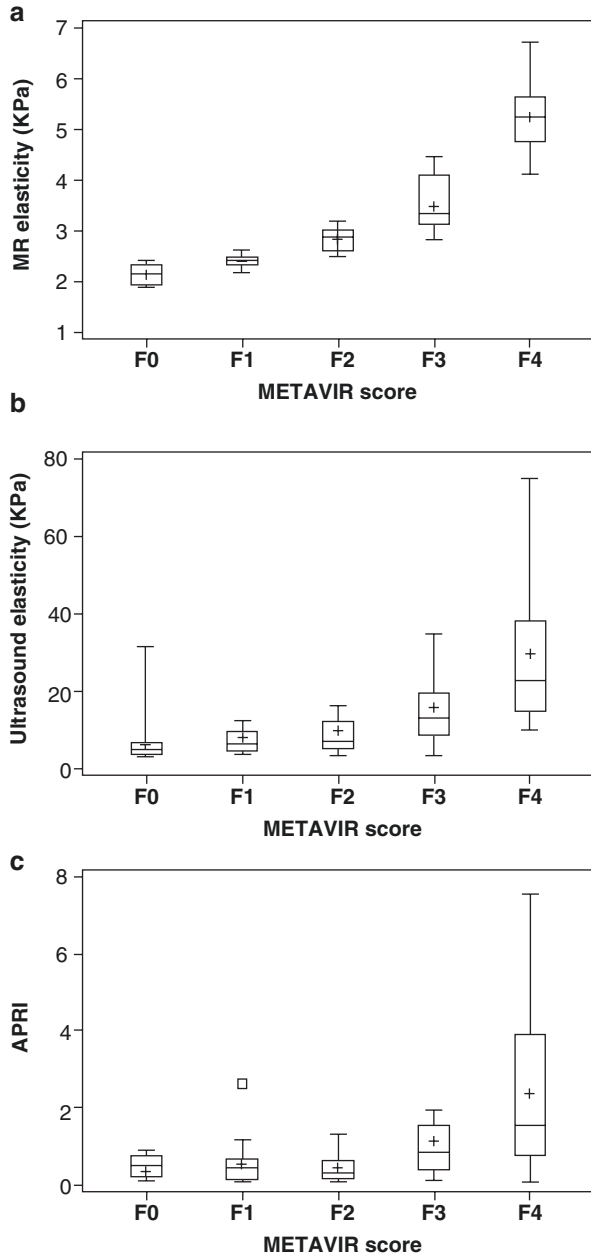


good diagnostic performance of MRE with area under the receiver operating curve (AUC) values of 0.93, 0.95, 0.94, and 0.92 for GRE-MRE, and 0.94, 0.94, 0.95, and 0.93 for SE-EPI MRE in detecting fibrosis  $\geq F1$ ,  $\geq F2$ ,  $\geq F3$ , and  $\geq F4$  [17]. Similarly, L.N. Su et al. reported AUC-values of 0.95, 0.97, 0.96, and 0.99 (including 13 studies comprising a total of 989 patients) [19] while Y. Guo et al. reported 0.94, 0.97, 0.96, and 0.97 (including 11 studies comprising a total of 982 patients) [16] for detection of fibrosis stages  $\geq F1$ ,  $\geq F2$ ,  $\geq F3$ , and  $\geq F4$ , respectively. Another meta-analysis reported lower AUC-values of 0.84, 0.88, 0.93, and 0.92 for the detection of fibrosis  $\geq F1$ ,  $\geq F2$ ,  $\geq F3$ , and  $\geq F4$  [18]. However, liver stiffness can be influenced by several physiological effects such as water intake [21] and liver fat deposition [21, 31]. Different MRE methods and study protocols prevent the calculation of general cutoff values yielding to recommendation of systems-specific thresholds [16–19].

As compared to MRE, ultrasound-based elastography (USE) is more widely used and recommended by guidelines [7]. Liver stiffness obtained by USE provides reliable fibrosis assessment in chronic liver disease [55, 56]. The major advantages of USE are wide availability, low cost, and real-time performance. However, a better diagnostic performance in detection of hepatic fibrosis  $\geq F1$ ,  $\geq F2$ ,  $\geq F3$ , and  $\geq F4$  was found for MRE (AUC = 0.96, 0.99, 0.99, and 1.00) compared to ultrasound-based transient elastography (TE, Fibroscan) (0.80, 0.84, 0.91, and 0.93) and laboratory parameter-based scores including aspartate aminotransferase (AST) and aspartate aminotransferase-to-platelet ratio Index (APRI) (0.68, 0.71, 0.82, and 0.82) [57], as shown in Fig. 6.2. G. Xiao et al. performed a meta-analysis for detection of advanced fibrosis in NAFLD including 64 studies with overall 15,515 patients reporting excellent AUC-values for MRE (0.96) and ultrasound-based shear wave elastography (SWE) (0.95) followed by TE (0.85 and 0.88, depending on M or XL probe), laboratory parameter based fibrosis-4 index (FIB-4) [58] (0.84), APRI (0.77), NAFLD score (NFS) [59] (0.84), and BARD-score [60] (0.76) [20] (see Fig. 6.3). A meta-analysis demonstrated a better diagnostic performance of MRE in staging F0–F1 vs F2–F4 and F0–F2 vs F3–F4 (AUC = 0.98 and 0.98) than diffusion weighted imaging (DWI, AUC, 0.83 and 0.86) [61]. These findings agree with a recent article in which the diagnostic performance of MRE and DWI in detecting hepatic fibrosis was analyzed finding AUC-values of 0.99, 0.99, and 0.98 and 0.72, 0.83, and 0.79 for fibrosis stages  $\geq F2$ ,  $\geq F3$  and F4, respectively [62]. MRE was highly reproducible as demonstrated by intraclass correlation coefficients (ICC) of 0.84 [63] and 0.85 [64]. MRE is currently considered the most accurate method for diagnosing liver fibrosis noninvasively [8].

In summary, MRE is a promising noninvasive biomarker for assessing fibrosis of different etiologies allowing a precise prediction of different fibrosis stages. However, further development is needed to allow for a better comparability of different MRE-systems and to gain deeper knowledge of the micro-architectural contributions to macroscopic stiffness changes in the liver [65].

**Fig. 6.2** Staging liver fibrosis with (a) MRE, (b) TE (ultrasound), and (c) APRI (laboratory tests). Best differentiation between fibrosis stages was performed by MRE. (Reproduced from L. Huwart et al. [57] with permission)



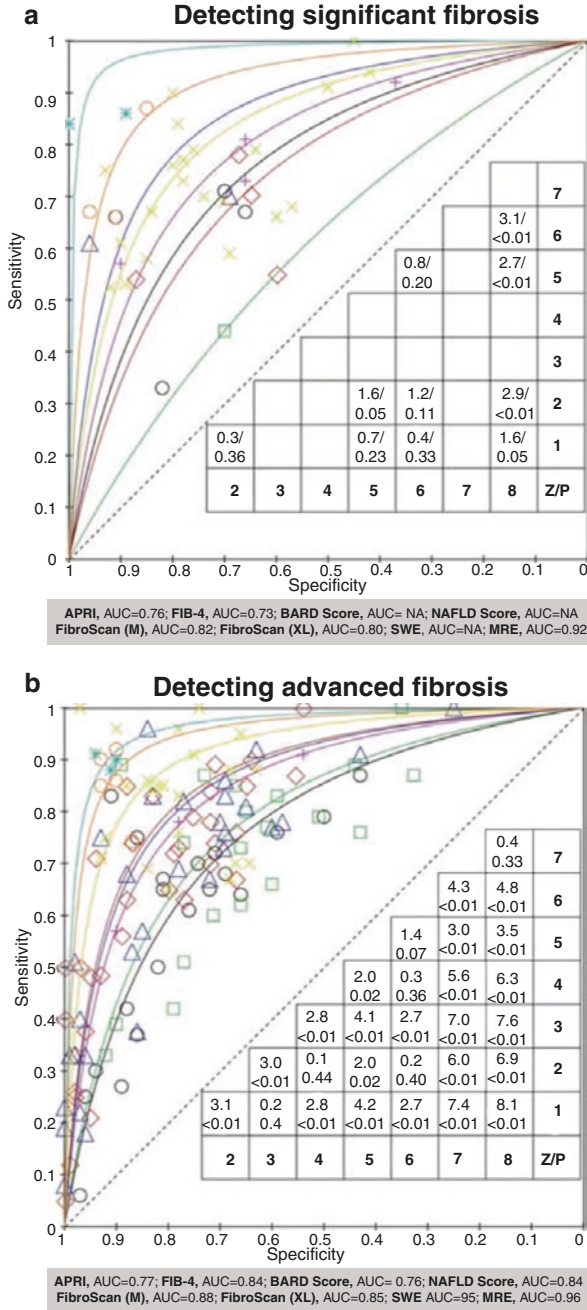


**Fig. 6.3** Summary ROC plots of detecting (a) significant fibrosis, (b) advanced fibrosis, and (c) cirrhosis. SWE and MRE demonstrated the highest summary AUC. (Reproduced from G. Xiao et al. [20] with permission)

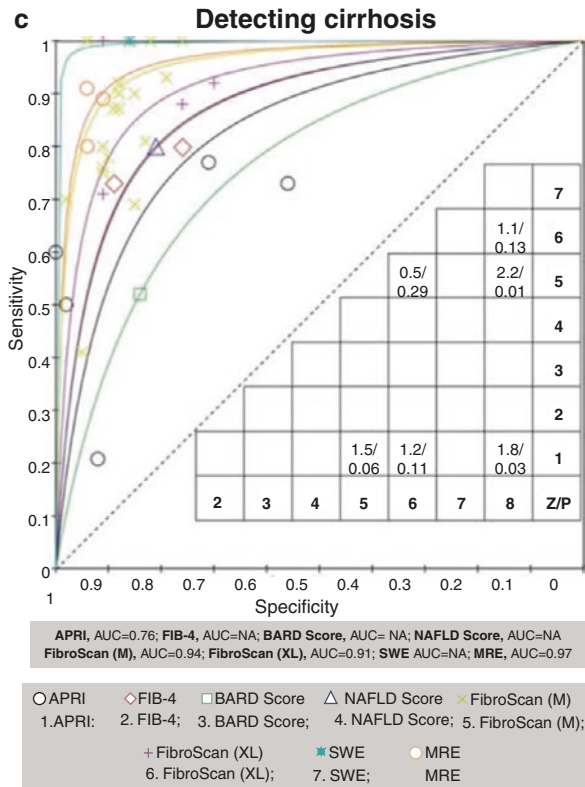


Fig. 6.3 (continued)

### MRE in NAFLD/NASH

Nonalcoholic fatty liver disease [66] is associated with obesity, insulin resistance, and metabolic syndrome [67]. During NAFLD development, the liver accumulates fat (mainly triglycerides) in the hepatocytes by an increased load of fatty acids, increased hepatic triglyceride synthesis, and a decreased degradation and export of fats [68]. NAFLD is the most prevalent chronic hepatic disease. The incidence of NAFLD is estimated to be 20–30% in Western countries and 5–18% in Asia [69]. Although the progression of NAFLD is itself benign and reversible, in 20% of patients with NAFLD, a more server condition involving hepatocyte necrosis and inflammation called nonalcoholic steatohepatitis (NASH) develops [70]. The rapid progression of NASH is a major risk factor for liver failure, cirrhosis, and hepatocellular carcinoma (HCC) as well as for hepatic decompensation [71, 72].

Liver biopsy and histological analysis are considered the reference standard for the diagnosis of NAFLD [73]. However, due to its invasive nature, liver biopsy should be limited to patients who are more likely to progress to NASH [74]. There are some noninvasive imaging modalities available for initial screening, detecting, or even quantifying the fat content of the liver, such as sonography, CT, and MRI. MRE has been extensively used for noninvasive quantification of liver fibrosis, which is strongly associated to the progression of NAFLD [75]. In [76], 117 patients with biopsy-proven NAFLD were prospectively enrolled for testing the diagnostic performance of MRE. The authors revealed that MRE has a very good diagnostic performance for separating advanced and severe fibrosis (F3–4) from insignificant or early stages (F0–2) (AUC = 0.0924). A recent review article that evaluates nine individual MRE studies with a total of 232 patients with NAFLD reports AUC-values of 0.86, 0.87, 0.90, and 0.91 for the diagnosis of any, significant or advanced fibrosis and cirrhosis, respectively [18].

Steatosis and inflammation, two other main pathological components of NAFLD, have also been investigated by MRE. An early study suggested, based on data from 58 NAFLD patients, that hepatic stiffness measured by MRE is higher in patients with inflammation than those with simple steatosis leading to good diagnostic accuracy (AUC = 0.93) in discriminating patients with NASH from those with simple steatosis [77].

More attention has recently been paid to the diagnosis of pediatric NAFLD due to the increased obesity and high prevalence of fatty liver in children and adolescents [78]. Considering that the histopathologic patterns in pediatric NAFLD patient differ from the adult cohort [79], a few MRE studies were conducted in order to evaluate the diagnostic performance of MRE for the detection of fibrosis and steatosis in children with NAFLD. A good correlation was found between MRE and liver fibrosis based on a dual-center study including 99 pediatric NAFLD patients [80]. However, this study also showed that MRE is limited in children compared to adults, probably due to lacking cooperation, motion artefacts and inconsistent breathing encountered in children. A recent study used tomoelastography to study both fibrosis and steatosis in pediatric NAFLD [31]. The authors derived shear wave speed  $c$  and penetration rate  $a$ , as surrogate markers of liver stiffness and viscosity, respectively [31]. Two maps of  $c$  and  $a$  are shown in Fig. 6.4a, b for two patients with various degrees of fibrosis and steatosis. Hudert et al. [31] reported that  $c$  and  $a$  are independently responsive to fibrosis and steatosis allowing to distinguish different stages of these disease components (Fig. 6.4c, d). Furthermore, the authors reported a very good diagnostic accuracy of these two parameters in detecting moderate ( $\geq F2$ , AUC = 0.91) and advanced fibrosis ( $\geq F3$ , AUC = 0.90) as well as moderate ( $\geq S2$ , AUC = 0.87) and severe steatosis (S3, AUC = 0.87) [31]. The combination of MRE-measured  $a$  with other MRI imaging markers such as hepatic fat fraction (HFF) improved the diagnostic accuracy for severe steatosis [31]. Notably in the same study, 48 patients were also examined by ultrasound time-harmonic elastography (THE) [81] showing a slightly lower diagnostic power of MRE than THE. Again, this difference is probably attributable to limitations with respect to motion and breathing artifacts encountered of children during longer MRE scans as compared to ultrashort THE examination times (in seconds).

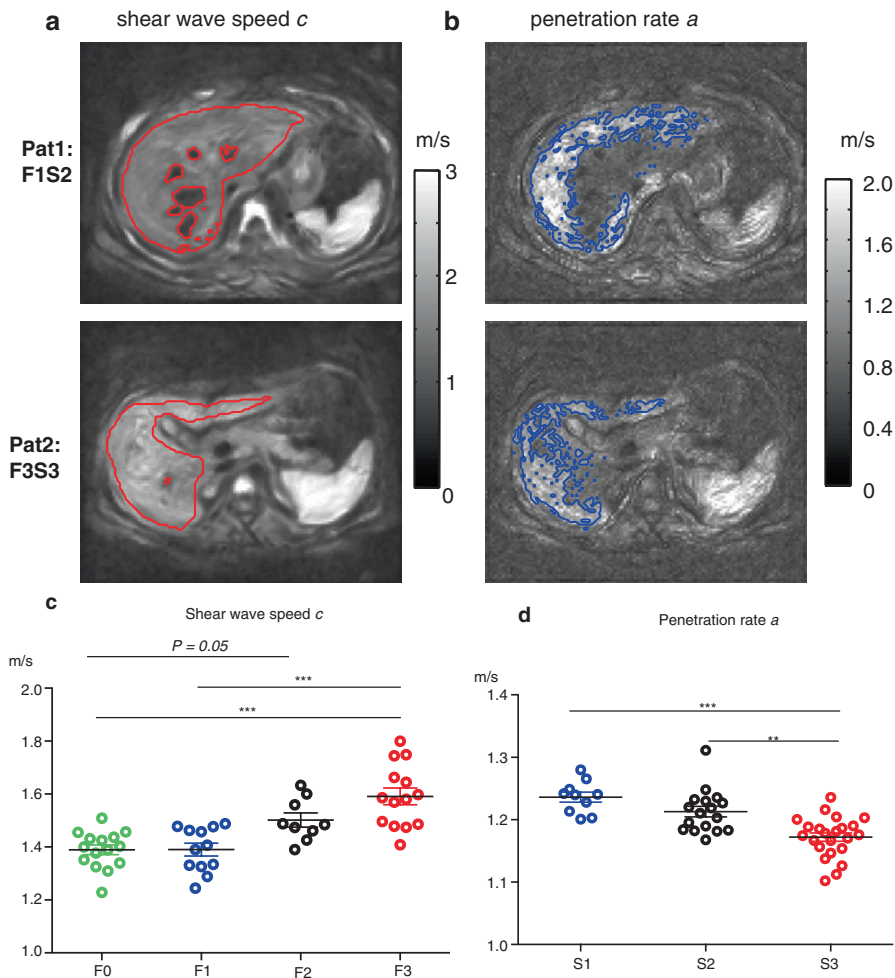


**Fig. 6.4** Maps of shear wave speed  $c$  (a) and penetration rate  $a$  (b) of two patients with different degree of fibrosis and steatosis: patient #1 has stage 1 fibrosis and grade 2 steatosis (Pat1: F1S2) and patient #2 has stage 3 fibrosis and grade 3 steatosis (Pat2: F3S3). Scatter plots of shear wave speed  $c$  (c) and penetration rate  $a$  (d) grouped by fibrosis stage and steatosis grade, respectively. \*\* $P < 0.01$ . \*\*\* $P < 0.001$ . (Figures are adapted from [31] and rearranged with permission)

As has been demonstrated, the diagnostic power of MRE in adults with chronic liver disease is excellent while MRE in pediatric NAFLD is limited and data are sparse for younger cohorts. Therefore, the two pediatric NAFLD studies are yet to be followed by larger studies to validate the outcomes and establish pediatric-based cutoffs. In addition, the MRE technique and protocols need to be optimized, e.g., by implementing navigators for motion correction, reducing measurement time as proposed in [82] or using image registration for motion correction within the post-processing. These strategies might further improve the diagnostic accuracy of MRE in the liver in pediatric patients in the future.

To summarize, MRE is a promising imaging marker for assessing fibrosis in patients with NAFLD and can provide valuable information on inflammation and steatosis. MRE has been demonstrated to be accurate in discriminating NASH from NAFLD. However, MRE needs further development, validation, and prospective evaluation in pediatric patients with NAFLD.

## MRE in Viral Hepatitis

Chronic liver hepatitis is associated with an increased risk of liver fibrosis [83], which in turn increases the prevalence of HCC [84, 85]. Specifically, chronic hepatitis B (HBV) and C virus [86] infections are considered the primary risk factors for HCC [87].

Knowledge about the stage of liver fibrosis is important for the prognosis of viral hepatitis [10]. Particularly, detection of significant fibrosis (METAVIR, F2) is important for antiviral treatment planning [88]. Therefore, most MRE studies in patients with HBV and HCV infection focused on the staging of liver fibrosis. In 63 patients with HBV, MRE could discriminate fibrosis stages  $\geq F1$ ,  $\geq F2$ ,  $\geq F3$ , and F4 with excellent accuracy (AUC: 0.99, 0.99, 0.99, and 0.98, respectively) [89] which outperformed serum fibrosis markers [89]. In 85 patients with hepatitis (65 HBV, 19 HCV) MRE had a similar accuracy as ultrasound-based transient elastography [90] with AUC-values of 0.909 and 0.914 for separating F0–F1 from F2–F4 [90].

The development of direct-acting antiviral drugs in chronically HCV-infected patients revolutionized the treatment options in HCV [91, 92]. Various studies based on ultrasound elastography showed softening of the liver after the application of direct-acting antivirals [93–97]. These results suggest that inflammation contributes to the stiffening of liver tissue, which was confirmed by MRE in a longitudinal study design [26]. Figure 6.5 presents an example of liver softening due to antiviral therapy in patients with HCV.

In summary, MRE is effective for noninvasive detection and staging of liver fibrosis associated with viral hepatitis. MRE can also be applied for monitoring the response of antiviral treatment to liver stiffness, in order to detect and quantify a possible regression of fibrosis and inflammatory activity.

## MRE in Liver Tumors

Liver cancer is the sixth most common cancer worldwide [98] among which HCC is most prevalent [84]. Major risk factors for HCC are alcohol abuse, chronic infections with hepatitis B or C, nonalcoholic fatty liver disease and aflatoxin consumption [84, 98]. Chronic liver diseases promote tissue scarring and cirrhosis, which in turn foster hepatocarcinogenesis [84, 85].



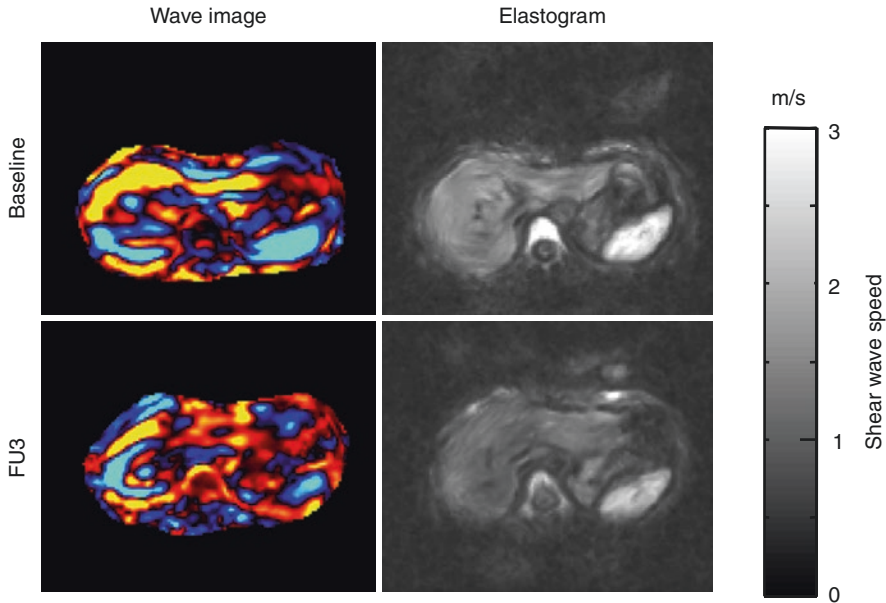


**Fig. 6.5** Wave images at 50 Hz and elastograms of one patient with hepatitis C virus infection at baseline (before treatment) and at 3 months after end of treatment (FU3) with direct-acting antiviral medication. Decrease in overall liver stiffness is visible after direct-acting antiviral medication as a surrogate of anti-inflammatory response. (Figures are adapted from [26] and rearranged with permission)

Noninvasive imaging techniques for liver cancer comprise sonography with and without contrast medium, dynamic contrast medium-enhanced computed tomography (CT), dynamic gadolinium-enhanced MRI, and positron emission (PET) CT/MRI with fluorodeoxyglucose (FDG) [49, 99–101]. However, in clinical routine, liver metastases are still diagnosed by biopsy and pathohistological analysis. A recent meta-analysis showed that gadolinium-enhanced MRI has the highest sensitivity for the detection of colorectal liver metastasis (93.1% vs. CT, 82.1%, and PET/CT, 74.1%) with similar specificity as PET-CT (87.3% vs. 93.9%) but higher specificity than CT (73.5%) [102]. For detection of HCC, gadolinium-enhanced MRI is the reference standard, without need of biopsy. Preferably hepatobiliary contrast media are used for the MRI-based detection of HCC at early stages providing a sensitivity of 91–93% [49, 103]. The American College of Radiology developed a standardized reporting and data collection system, Liver Reporting & Data System (Li-RADS) [104].

Among quantitative MRI techniques, MRE is of particular interest for the characterization of liver tumors. In general, tumor growth is associated with extensive alterations of tissue structures resulting from a number of processes such as neo-vascularization, accumulation of cells, and remodeling of the extracellular matrix [105, 106]. Furthermore, leaky tumor blood vessels and impaired lymphatic drain-



age lead to interstitial fluid accumulation and elevated hydrostatic pressure. The altered structure and fluid turnover is mirrored by significant changes in the effective shear modulus as measured by MRE [1]. The incidence of HCC increases with progression of liver fibrosis indicating the relevance of biophysical tissue properties for tumor development. A one-kilopascal increase of liver stiffness is associated with 4% higher incidence of HCC [107] and increases the risk for tumor recurrence by 16.3% [108]. Notwithstanding these impressive numbers, MRE-data on liver malignancies are sparse. So far, elastography in liver tumors has predominantly been demonstrated by ultrasound techniques providing sensitivity and specificity for the differentiation of malignant from benign tumors of 82% and 80% [109]. Surgeons normally feel liver tumors by palpation as stiff masses: This is mirrored by MRE which also detects malignant lesions as being stiffer than surrounding liver tissue (see Table 6.1) [36, 110–112]. Compared to benign lesions, malignant tumors in the liver are stiffer [110–112]. Examples of stiff cholangiocarcinoma and soft benign hepatic adenoma are shown in Fig. 6.6. Further details of MRE-measured stiffness in liver lesions, diagnostic performance and cutoffs are summarized in Tables 6.1 and 6.2. In a recent study also vascular invasion and absent tumor capsule were identified as independent factors for increased stiffness [108]. A trend toward increased HCC stiffness with the tumor grade (HCC, well/moderately vs poorly differentiated) was reported by Thompson et al. ( $6.5 \pm 1.2$  kPa vs  $4.9 \pm 1.2$  kPa;  $P = 0.01$ ) [113] and Wang et al. ( $4.91$  [4.01–6.48] kPa vs.  $7.28$  [5.68–9.80] kPa) [108].

Detection of liver lesions by MRE is considered to be limited at lesion diameters smaller than 10 mm [108, 110, 111] while higher resolution and improved MRE-based detection of smaller lesions (<10 mm) has been recently demonstrated by tomoelastography [36]. MRE is potentially relevant for an objectified characterization of liver tumors. The excellent interobserver agreement of MRE in liver tumors was shown by [112] and [110] with ICC's between 0.93 and 0.99 raising the prospect of therapy monitoring of liver tumors by MRE. A preliminary study demonstrated that HCC-therapy can be monitored by MRE showing softening of HCC after locoregional therapy from  $6.9 \pm 3.4$  kPa in an untreated state toward  $3.9 \pm 1.8$  kPa after treatment ( $P = 0.006$ ) [114].

Beside stiffness, MRE can measure viscosity, which is of great interest in tumors since tumors often accumulate extracellular fluid and build up their own vascular system leading to abnormal viscous properties. In fact, HCC have a larger loss modulus than surrounding tissue or benign entities as reported in [110] ( $2.25 \pm 0.26$  vs  $1.05 \pm 0.13$  kPa,  $P < 0.001$ ). The same study could not reveal a significant difference HCC and benign tumors based on storage modulus ( $2.37 \pm 0.15$  vs  $2.11 \pm 0.11$  kPa,  $P = 0.16$ ). This observation is in agreement with preliminary reports by [36] on abnormal loss angle of complex shear modulus in malignant liver tumors while stiffness appeared to be less significantly changed in the process of tumorigenesis. As mentioned above, the loss angle is a measure of fluidity of the tissue with being zero in pure solids and  $\pi/2$  in pure fluids. MRE might be useful for detecting the shift of tissue properties from a more solid state to a more fluid state during the development of malignancies [36].

**Table 6.1** Comparison of malignant liver lesions to benign lesions and liver

Parameter	Benign lesion	Malignant lesion	Normal liver	Fibrotic liver	P value			References
					Malignant vs benign	Malignant vs normal liver	Malignant vs fibrotic liver	
G' (kPa)	2.41 ± 0.15	3.38 ± 0.26	–	–	<0.01	–	–	[110]
IG*1 (kPa)	2.7 ± 0.4	10.1 ± 3.6	2.3 ± 0.3	5.9 ± 2.5	<0.001	<0.001	<0.001	[111]
IG*1 (kPa) <sup>a</sup>	3.1 kPa <sup>a</sup>	7.9 kPa <sup>a</sup>	–	–	<0.001	–	–	[112]
c (m/s)	1.41–2.08	2.34 ± 0.48 to 2.57 ± 0.90	1.37 ± 0.13 to 1.72 ± 0.29	1.97 ± 0.49	<0.001	<0.001	–	[36]

<sup>a</sup>No standard deviation was reported

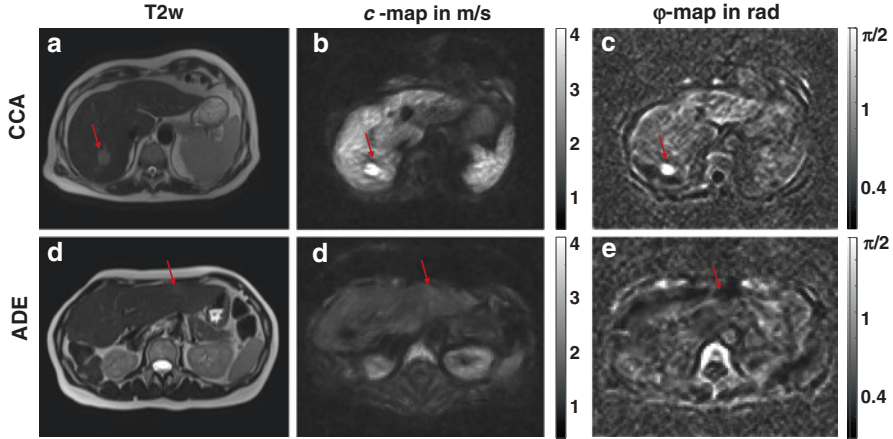


**Fig. 6.6** T2w images and reconstructed  $c$ -map (shear wave speed) of a malignant cholangiocarcinoma (CCA) and a benign hepatic adenoma (ADE). Malignancy is clearly visible as stiff lesion, even the surrounding liver tissue is fibrotic with high stiffness. In contrast, a benign lesion appears soft, not distinguishable from surrounding liver tissue. Lesions are indicated by red arrows. (Figures are adapted from [36] and rearranged with permission)

**Table 6.2** Diagnostic performance in distinguishing malignant from benign liver lesions

AUC	Cutoff	Sensitivity/specificity	Reference
0.72	–	–	[110]
–	5.0 kPa	100% accuracy <sup>a</sup>	[111]
0.98	4.54 kPa	96%/96%	[112]
0.85	1.75 m/s	94%/78%	[36]

AUC area under the receiver operating characteristic curve

<sup>a</sup>No sensitivity and specificity were reported

To summarize, MRE holds promise as a quantitative, biophysical imaging marker for noninvasive characterization of liver tumors. Combined with stiffness, MRE-measured viscosity and fluidity can provide valuable information about the mechanical consistency of the tissue and abnormal variations during tumor progression. Within multiparametric imaging protocols, MRE can contribute to improved diagnostic decisions and therapy monitoring.

## MRE in Portal Hypertension

In patients with liver cirrhosis, the hepatic vasculature is known to become irregular and tortuous [115]. The distorted vascular structure increases resistance to blood flow, which leads to elevated pressure in the portal venous system, defined as portal hypertension [116]. Hepatic venous pressure gradient (HVPG) is a gold standard for

portal hypertension quantification and has an important prognostic relevance since it can be associated with severe complications such as variceal bleeding, ascites or hepatic encephalopathy [117]. In clinical practice, HVPG is normally measured with catheters through the internal jugular vein, femoral vein, or cubital vein access under local anesthesia [118]. Due to the invasiveness and potential risk of the HVPG measurement, there is a clinical need for developing noninvasive imaging markers to substitute or reduce the need for HVPG measurements.

In the past, MRE parameters such as shear modulus, shear wave speed, and volumetric strain were used to noninvasively assess portal hypertension [119–122]. All these mechanical parameters have been found to correlate to hepatic fibrosis and HVPG in patients with portal hypertension. In a recent study, 33 patients with chronic liver disease were prospectively investigated with MRE [122]. In these patients of various stages of fibrosis and HVPG, a positive correlation between liver stiffness and HVPG was reported. The authors also proposed a new parameter ratio of liver stiffness and liver upslope (LSLU), which is associated with liver perfusion and acquired by dynamic contrast-enhanced (DCE)-MRI. This new parameter improved the diagnosis of portal hypertension (with sensitivity of 78% and specificity of 100%) [122]. Another MRE study in 36 patients with liver cirrhosis reported the loss modulus of the liver to be correlated with HVPG [121].

Blood flow in portal hypertension is significantly affected by an altered vasculature. The altered blood flow may lead to the hyperdynamic circulatory syndrome [123] which also affects mechanical parameters measured by MRE. The mechanical coupling between fluid and solid phases in the liver tissue results in a sensitivity of MRE to tissue pressure. This was demonstrated in an MRE study in patients with portal hypertension before and after transjugular intrahepatic portosystemic shunt (TIPS) treatment indicating the influence of blood flow-related parameters on MRE-measured liver stiffness [119]. During TIPS implantation, the liver experienced instantaneous portal decompression, resulting in a reduction in HVPG with a concomitant increase in both arterial and total liver perfusion [124]. The authors observed a significant reduction in liver stiffness after TIPS treatment [119] similar to studies using transient elastography [125, 126]. The marked changes of hepatic stiffness due to TIPS placement are clearly visible in the MRE elastograms of Fig. 6.7a. The softening of liver tissue 48–72 h after TIPS implantation points toward the relationship between hepatic stiffness and portal pressure due to biphasic solid–fluid interactions. In this context, the shear modulus of the liver should be understood as an effective mechanical property that integrates solid mechanical matrix properties, fluid mechanical properties of the blood pool and vessel–matrix interactions [127]. Volumetric strain, a compression-related parameter that can be measured by MRE, offers a direct link to fluid pressure. A pilot study investigated the sensitivity of volumetric strain in a group of 13 patients with portal hypertension before and after TIPS implantation [120]. The authors observed that volumetric strain increased after TIPS placement indicating tissue decompression ( $P < 0.001$ , Fig. 6.7b). Furthermore, relative changes of volumetric strain after TIPS were significantly correlated with both pre-TIPS HVPG ( $R^2 = 0.726$ ,  $P < 0.001$ ) and portal venous pressure ( $R^2=0.503$ ,  $P < 0.01$ ) [120].

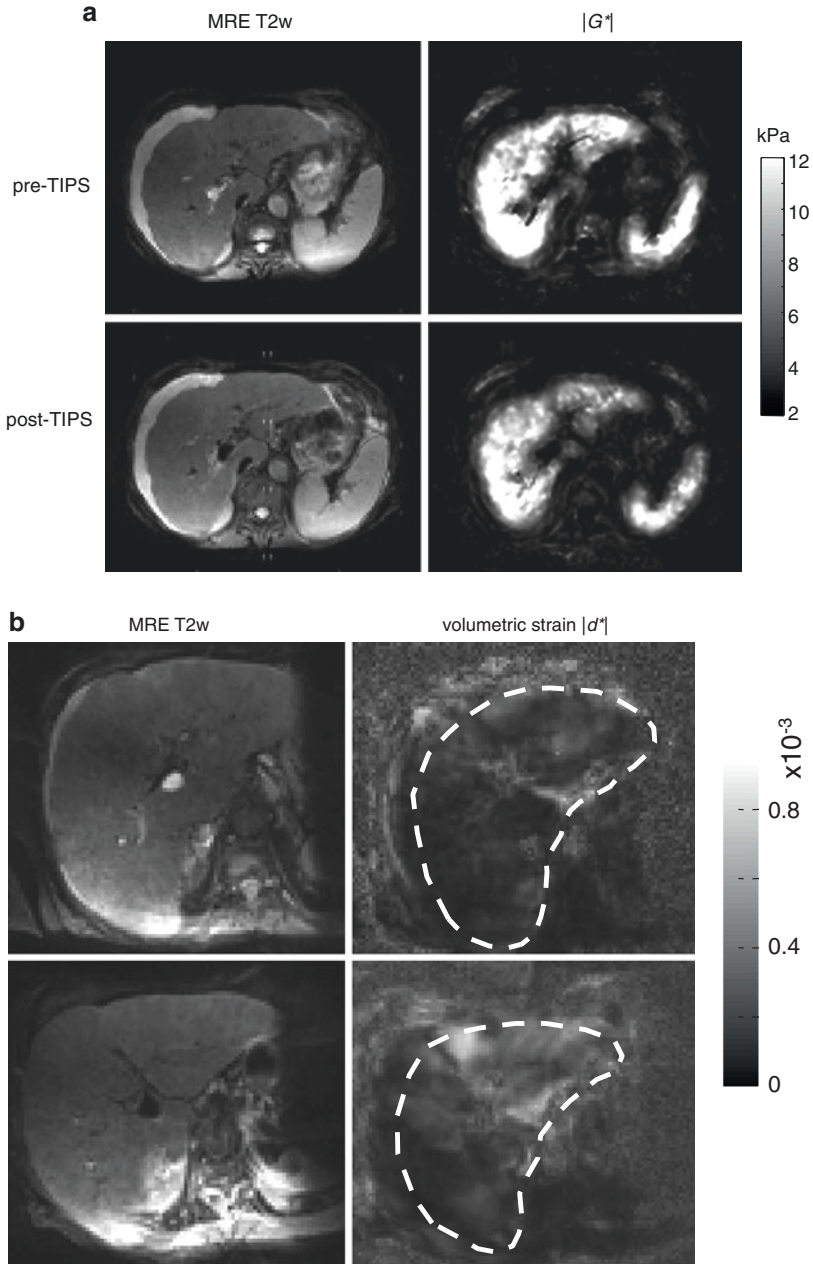


**Fig. 6.7** (a) MRE T2w image and reconstructed  $|G^*|$  map reflecting the liver stiffness of a patient with portal hypertension before and after TIPS treatment. Softening of liver is clearly visible from the  $|G^*|$  map. The images are adapted from [119] and replotted in gray scale for consistency. (b) MRE T2w image and maps of the volumetric strain in one patient with portal hypertension before and after TIPS placement. Increased volumetric strain is apparent after TIPS treatment. (Figures adapted from [120] and rearranged with permission)

It should be noted that hepatic and splenic circulations belong to the splanchnic circulation causing a pathologically altered hepatic blood flow to influence also the flow through the splenic veins [128]. The spleen is often later involved in chronic disease and has less advanced fibrosis than the liver. Therefore, splenic stiffness is more sensitive to portal decompression and disease progression than hepatic stiffness in cirrhotic liver [119, 121].

To summarize, MRE-measured mechanical parameters of the liver such as shear stiffness and volumetric strain are sensitive to changes in HVPG due to disease progression and therapy. MRE could serve as a useful noninvasive imaging marker for the assessment of portal hypertension.

## References

1. Hirsch S, Braun J, Sack I. Magnetic resonance elastography: physical background and medical applications. Weinheim: Wiley-VCH; 2017.
2. Venkatesh SK. Magnetic resonance elastography: an update. *Top Magn Reson Imaging*. 2018;27(5):303.
3. Venkatesh SK, Ehman RL. Magnetic resonance elastography of liver. *Magn Reson Imaging Clin N Am*. 2014;22(3):433–46.
4. Venkatesh SK, Ehman RL. Magnetic resonance elastography of abdomen. *Abdom Imaging*. 2015;40(4):745–59.
5. Manduca A. MR elastography: standardizing terminology and setting guidelines. In: *Proceedings of the 1st International MRE Workshop, Berlin, Germany; 2017*. p. 12.
6. Barr RG, Ferraioli G, Palmeri ML, Goodman ZD, Garcia-Tsao G, Rubin J, et al. Elastography assessment of liver fibrosis: Society of Radiologists in ultrasound consensus conference statement. *Ultrasound Q*. 2016;32(2):94–107.
7. Dietrich CF, Bamber J, Berzigotti A, Bota S, Cantisani V, Castera L, et al. EFSUMB guidelines and recommendations on the clinical use of liver ultrasound elastography, update 2017 (long version). *Ultraschall Med*. 2017;38(4):e16–47.
8. Horowitz JM, Kamel IR, Arif-Tiwari H, Asrani SK, Hindman NM, Expert Panel on Gastrointestinal I, et al. ACR appropriateness criteria((R)) chronic liver disease. *J Am Coll Radiol*. 2017;14(5S):S103–S17.
9. Hoodeshenas S, Yin M, Venkatesh SK. Magnetic resonance elastography of liver: current update. *Top Magn Reson Imaging*. 2018;27(5):319–33.
10. Kennedy P, Wagner M, Castera L, Hong CW, Johnson CL, Sirlin CB, et al. Quantitative elastography methods in liver disease: current evidence and future directions. *Radiology*. 2018;286(3):738–63.
11. Manka P, Zeller A, Syn WK. Fibrosis in chronic liver disease: an update on diagnostic and treatment modalities. *Drugs*. 2019;79(9):903–27.
12. Sack I. Magnetic resonance elastography 2.0: high resolution imaging of soft tissue elasticity, viscosity and pressure. *Dtsch Med Wochenschr*. 2013;138(47):2426–30.
13. Terrault NA, Lok ASF, McMahon BJ, Chang KM, Hwang JP, Jonas MM, et al. Update on prevention, diagnosis, and treatment of chronic hepatitis B: AASLD 2018 hepatitis B guidance. *Hepatology*. 2018;67(4):1560–99.
14. Venkatesh SK, Talwalkar JA. When and how to use magnetic resonance elastography for patients with liver disease in clinical practice. *Am J Gastroenterol*. 2018;113(7):923–6.
15. Tzschatzsch H, Guo J, Dittmann F, Hirsch S, Barnhill E, Johrens K, et al. Tomoelastography by multifrequency wave number recovery from time-harmonic propagating shear waves. *Med Image Anal*. 2016;30:1–10.

16. Guo Y, Parthasarathy S, Goyal P, McCarthy RJ, Larson AC, Miller FH. Magnetic resonance elastography and acoustic radiation force impulse for staging hepatic fibrosis: a meta-analysis. *Abdom Imaging*. 2015;40(4):818–34.
17. Kim YS, Jang YN, Song JS. Comparison of gradient-recalled echo and spin-echo echo-planar imaging MR elastography in staging liver fibrosis: a meta-analysis. *Eur Radiol*. 2018;28(4):1709–18.
18. Singh S, Venkatesh SK, Loomba R, Wang Z, Sirlin C, Chen J, et al. Magnetic resonance elastography for staging liver fibrosis in non-alcoholic fatty liver disease: a diagnostic accuracy systematic review and individual participant data pooled analysis. *Eur Radiol*. 2016;26(5):1431–40.
19. Su LN, Guo SL, Li BX, Yang P. Diagnostic value of magnetic resonance elastography for detecting and staging of hepatic fibrosis: a meta-analysis. *Clin Radiol*. 2014;69(12):e545–52.
20. Xiao G, Zhu S, Xiao X, Yan L, Yang J, Wu G. Comparison of laboratory tests, ultrasound, or magnetic resonance elastography to detect fibrosis in patients with nonalcoholic fatty liver disease: a meta-analysis. *Hepatology*. 2017;66(5):1486–501.
21. Dittmann F, Tzschätzsch H, Hirsch S, Barnhill E, Braun J, Sack I, et al. Tomoelastography of the abdomen: tissue mechanical properties of the liver, spleen, kidney, and pancreas from single MR elastography scans at different hydration states. *Magn Reson Med*. 2017;78(3):976–83.
22. Hirsch S, Guo J, Reiter R, Papazoglou S, Kroencke T, Braun J, et al. MR elastography of the liver and the spleen using a piezoelectric driver, single-shot wave-field acquisition, and multifrequency dual parameter reconstruction. *Magn Reson Med*. 2014;71(1):267–77.
23. Asbach P, Klatt D, Schlosser B, Biermer M, Muehe M, Rieger A, et al. Viscoelasticity-based staging of hepatic fibrosis with multifrequency MR elastography. *Radiology*. 2010;257(1):80–6.
24. Huwart L, Sempoux C, Salameh N, Jamart J, Annet L, Sinkus R, et al. Liver fibrosis: non-invasive assessment with MR elastography versus aspartate aminotransferase-to-platelet ratio index. *Radiology*. 2007;245(2):458–66.
25. Wagner M, Corcuera-Solano I, Lo G, Esses S, Liao J, Besa C, et al. Technical failure of MR elastography examinations of the liver: experience from a large single-center study. *Radiology*. 2017;284(2):401–12.
26. Garcia SM, Tzschätzsch H, Althoff C, Burkhardt C, Dürr M, Halleck F, et al. Assessment of treatment outcome in chronic hepatitis C virus infected patients with liver stiffness measured by magnetic resonance elastography. In: Joint annual meeting ISMRM-ESMRMB. Paris: ISMRM; 2018.
27. Asbach P, Klatt D, Hamhaber U, Braun J, Somasundaram R, Hamm B, et al. Assessment of liver viscoelasticity using multifrequency MR elastography. *Magn Reson Med*. 2008;60:373–9.
28. Dittmann F, Hirsch S, Tzschätzsch H, Guo J, Braun J, Sack I. In vivo wideband multifrequency MR elastography of the human brain and liver. *Magn Reson Med*. 2016;76(4):1116–26.
29. Rump J, Klatt D, Braun J, Warmuth C, Sack I. Fractional encoding of harmonic motions in MR elastography. *Magn Reson Med*. 2007;57(2):388–95.
30. Serai SD, Dillman JR, Trout AT. Spin-echo echo-planar imaging MR elastography versus gradient-echo mr elastography for assessment of liver stiffness in children and young adults suspected of having liver disease. *Radiology*. 2017;282(3):761–70.
31. Hudert CA, Tzschätzsch H, Rudolph B, Blaker H, Loddenkemper C, Muller HP, et al. Tomoelastography for the evaluation of pediatric nonalcoholic fatty liver disease. *Investig Radiol*. 2018;54(4):198–203.
32. Fehlnner A, Hirsch S, Weygandt M, Christophel T, Barnhill E, Kadobianskyi M, et al. Increasing the spatial resolution and sensitivity of magnetic resonance elastography by correcting for subject motion and susceptibility-induced image distortions. *J Magn Reson Imaging*. 2017;46(1):134–41.



33. Doyley MM. Model-based elastography: a survey of approaches to the inverse elasticity problem. *Phys Med Biol.* 2012;57(3):R35–73.
34. Manduca A, Oliphant TE, Dresner MA, Mahowald JL, Kruse SA, Amromin E, et al. Magnetic resonance elastography: non-invasive mapping of tissue elasticity. *Med Image Anal.* 2001;5(4):237–54.
35. Papazoglou S, Hirsch S, Braun J, Sack I. Multifrequency inversion in magnetic resonance elastography. *Phys Med Biol.* 2012;57(8):2329–46.
36. Shahryari M, Tzschätzsch H, Guo J, Garcia SRM, Böning G, Fehrenbach U, et al. Tomoelastography distinguishes non-invasively between benign and malignant liver lesions. *Cancer Res.* 2019;79(22):5704–10.
37. Schiff ER, Maddrey WC, Reddy KR. Schiff's diseases of the liver. Oxford: Wiley; 2018.
38. Pinzani M, Romanelli RG, Magli S. Progression of fibrosis in chronic liver diseases: time to tally the score. *J Hepatol.* 2001;34(5):764–7.
39. Shiratori Y, Imazeki F, Moriyama M, Yano M, Arakawa Y, Yokosuka O, et al. Histologic improvement of fibrosis in patients with hepatitis C who have sustained response to interferon therapy. *Ann Intern Med.* 2000;132(7):517–24.
40. Bataller R, Brenner DA. Liver fibrosis. *J Clin Invest.* 2005;115(2):209–18.
41. Tsukada S, Parsons CJ, Rippe RA. Mechanisms of liver fibrosis. *Clin Chim Acta.* 2006;364(1-2):33–60.
42. Bedossa P, Poynard T. An algorithm for the grading of activity in chronic hepatitis C. The METAVIR Cooperative Study Group. *Hepatology.* 1996;24(2):289–93.
43. Desmet VJ, Gerber M, Hoofnagle JH, Manns M, Scheuer PJ. Classification of chronic hepatitis: diagnosis, grading and staging. *Hepatology.* 1994;19(6):1513–20.
44. Ishak K, Baptista A, Bianchi L, Callea F, De Groote J, Gudat F, et al. Histological grading and staging of chronic hepatitis. *J Hepatol.* 1995;22(6):696–9.
45. Bedossa P, Dargere D, Paradis V. Sampling variability of liver fibrosis in chronic hepatitis C. *Hepatology.* 2003;38(6):1449–57.
46. Regev A, Berho M, Jeffers LJ, Milikowski C, Molina EG, Pyrsopoulos NT, et al. Sampling error and intraobserver variation in liver biopsy in patients with chronic HCV infection. *Am J Gastroenterol.* 2002;97(10):2614–8.
47. The French METAVIR Cooperative Study Group. Intraobserver and interobserver variations in liver biopsy interpretation in patients with chronic hepatitis C. *Hepatology.* 1994;20(1 Pt 1):15–20.
48. Ippolito D, Inchingolo R, Grazioli L, Drago SG, Nardella M, Gatti M, et al. Recent advances in non-invasive magnetic resonance imaging assessment of hepatocellular carcinoma. *World J Gastroenterol.* 2018;24(23):2413–26.
49. Navin PJ, Venkatesh SK. Hepatocellular carcinoma: state of the art imaging and recent advances. *J Clin Transl Hepatol.* 2019;7(1):72–85.
50. Klatt D, Friedrich C, Korth Y, Vogt R, Braun J, Sack I. Viscoelastic properties of liver measured by oscillatory rheometry and multifrequency magnetic resonance elastography. *Biorheology.* 2010;47(2):133–41.
51. Reiter R, Freise C, Jöhrens K, Kamphues C, Seehofer D, Stockmann M, et al. Wideband MRE and static mechanical indentation of human liver specimen: sensitivity of viscoelastic constants to the alteration of tissue structure in hepatic fibrosis. *J Biomech.* 2014;47(7):1665–74.
52. Salameh N, Peeters F, Sinkus R, Abarca-Quinones J, Annet L, Ter Beek LC, et al. Hepatic viscoelastic parameters measured with MR elastography: correlations with quantitative analysis of liver fibrosis in the rat. *J Magn Reson Imaging.* 2007;26(4):956–62.
53. Yin M, Glaser KJ, Manduca A, Mounajjed T, Malhi H, Simonetto DA, et al. Distinguishing between hepatic inflammation and fibrosis with MR elastography. *Radiology.* 2017;284(3):694–705.
54. Yin M, Woollard J, Wang X, Torres VE, Harris PC, Ward CJ, et al. Quantitative assessment of hepatic fibrosis in an animal model with magnetic resonance elastography. *Magn Reson Med.* 2007;58(2):346–53.



55. Mueller S, Millonig G, Sarovska L, Friedrich S, Reimann FM, Pritsch M, et al. Increased liver stiffness in alcoholic liver disease: differentiating fibrosis from steatohepatitis. *World J Gastroenterol.* 2010;16(8):966–72.
56. Mueller S, Sandrin L. Liver stiffness: a novel parameter for the diagnosis of liver disease. *Hepatic Med Evid Res.* 2010;2:49–67.
57. Huwart L, Sempoux C, Vicaud E, Salameh N, Annet L, Danse E, et al. Magnetic resonance elastography for the noninvasive staging of liver fibrosis. *Gastroenterology.* 2008;135(1):32–40.
58. Sterling RK, Lissen E, Clumeck N, Sola R, Correa MC, Montaner J, et al. Development of a simple noninvasive index to predict significant fibrosis in patients with HIV/HCV coinfection. *Hepatology.* 2006;43(6):1317–25.
59. Angulo P, Hui JM, Marchesini G, Bugianesi E, George J, Farrell GC, et al. The NAFLD fibrosis score: a noninvasive system that identifies liver fibrosis in patients with NAFLD. *Hepatology.* 2007;45(4):846–54.
60. Harrison SA, Oliver D, Arnold HL, Gogia S, Neuschwander-Tetri BA. Development and validation of a simple NAFLD clinical scoring system for identifying patients without advanced disease. *Gut.* 2008;57(10):1441–7.
61. Wang QB, Zhu H, Liu HL, Zhang B. Performance of magnetic resonance elastography and diffusion-weighted imaging for the staging of hepatic fibrosis: a meta-analysis. *Hepatology.* 2012;56(1):239–47.
62. Hennedige TP, Wang G, Leung FP, Alsaif HS, Teo LL, Lim SG, et al. Magnetic resonance elastography and diffusion weighted imaging in the evaluation of hepatic fibrosis in chronic hepatitis B. *Gut Liver.* 2017;11(3):401–8.
63. Rusak G, Zawada E, Lemanowicz A, Serafin Z. Whole-organ and segmental stiffness measured with liver magnetic resonance elastography in healthy adults: significance of the region of interest. *Abdom Imaging.* 2015;40(4):776–82.
64. Lee DH, Lee JM, Han JK, Choi BI. MR elastography of healthy liver parenchyma: normal value and reliability of the liver stiffness value measurement. *J Magn Reson Imaging.* 2013;38(5):1215–23.
65. de Schellenberger AA, Tzschatsch H, Polchlopek B, Bertalan G, Schrank F, Garczynska K, et al. Sensitivity of multifrequency magnetic resonance elastography and diffusion-weighted imaging to cellular and stromal integrity of liver tissue. *J Biomech.* 2019;88:201–8.
66. Krawczyk M, Rau M, Schattenberg JM, Bantel H, Pathil A, Demir M, et al. Combined effects of the PNPLA3 rs738409, TM6SF2 rs58542926, and MBOAT7 rs641738 variants on NAFLD severity: a multicenter biopsy-based study. *J Lipid Res.* 2017;58(1):247–55.
67. Kim D, Touro A, Kim WR. Nonalcoholic fatty liver disease and metabolic syndrome. *Clin Liver Dis.* 2018;22(1):133–40.
68. Kawano Y, Cohen DE. Mechanisms of hepatic triglyceride accumulation in non-alcoholic fatty liver disease. *J Gastroenterol.* 2013;48(4):434–41.
69. Sayiner M, Koenig A, Henry L, Younossi ZM. Epidemiology of nonalcoholic fatty liver disease and nonalcoholic steatohepatitis in the United States and the rest of the world. *Clin Liver Dis.* 2016;20(2):205–14.
70. Hughes AN, Oxford JT. A lipid-rich gestational diet predisposes offspring to nonalcoholic fatty liver disease: a potential sequence of events. *Hepatic Med Evid Res.* 2014;6:15–23.
71. Caldwell SH, Oelsner DH, Iezzoni JC, Hespenheide EE, Battle EH, Driscoll CJ. Cryptogenic cirrhosis: clinical characterization and risk factors for underlying disease. *Hepatology.* 1999;29(3):664–9.
72. Angulo P. Obesity and nonalcoholic fatty liver disease. *Nutr Rev.* 2007;65(6 Pt 2):S57–63.
73. Nalbantoglu IL, Brunt EM. Role of liver biopsy in nonalcoholic fatty liver disease. *World J Gastroenterol.* 2014;20(27):9026–37.
74. Perumpail BJ, Khan MA, Yoo ER, Cholankeril G, Kim D, Ahmed A. Clinical epidemiology and disease burden of nonalcoholic fatty liver disease. *World J Gastroenterol.* 2017;23(47):8263–76.

75. Ekstedt M, Nasr P, Kechagias S. Natural history of NAFLD/NASH. *Curr Hepatol Rep.* 2017;16(4):391–7.
76. Loomba R, Wolfson T, Ang B, Hooker J, Behling C, Peterson M, et al. Magnetic resonance elastography predicts advanced fibrosis in patients with nonalcoholic fatty liver disease: a prospective study. *Hepatology.* 2014;60(6):1920–8.
77. Chen J, Talwalkar JA, Yin M, Glaser KJ, Sanderson SO, Ehman RL. Early detection of non-alcoholic steatohepatitis in patients with nonalcoholic fatty liver disease by using MR elastography. *Radiology.* 2011;259(3):749–56.
78. Anderson EL, Howe LD, Jones HE, Higgins JP, Lawlor DA, Fraser A. The prevalence of non-alcoholic fatty liver disease in children and adolescents: a systematic review and meta-analysis. *PLoS One.* 2015;10(10):e0140908.
79. Schwimmer JB, Behling C, Newbury R, Deutsch R, Nievergelt C, Schork NJ, et al. Histopathology of pediatric nonalcoholic fatty liver disease. *Hepatology.* 2005;42(3):641–9.
80. Schwimmer JB, Behling C, Angeles JE, Paiz M, Durelle J, Africa J, et al. Magnetic resonance elastography measured shear stiffness as a biomarker of fibrosis in pediatric nonalcoholic fatty liver disease. *Hepatology.* 2017;66(5):1474–85.
81. Hudert CA, Tzschatzsch H, Guo J, Rudolph B, Blaker H, Loddenkemper C, et al. US time-harmonic elastography: detection of liver fibrosis in adolescents with extreme obesity with nonalcoholic fatty liver disease. *Radiology.* 2018;288(1):99–106.
82. Ebersole C, Ahmad R, Rich AV, Potter LC, Dong H, Kolipaka A. A bayesian method for accelerated magnetic resonance elastography of the liver. *Magn Reson Med.* 2018;80(3):1178–88.
83. Sebastiani G, Gkouvatsos K, Pantopoulos K. Chronic hepatitis C and liver fibrosis. *World J Gastroenterol.* 2014;20(32):11033–53.
84. El-Serag HB, Rudolph KL. Hepatocellular carcinoma: epidemiology and molecular carcinogenesis. *Gastroenterology.* 2007;132(7):2557–76.
85. Nishida N, Goel A. Genetic and epigenetic signatures in human hepatocellular carcinoma: a systematic review. *Curr Genomics.* 2011;12(2):130–7.
86. Panel A-IHG. Hepatitis C guidance 2018 update: AASLD-IDSAs recommendations for testing, managing, and treating hepatitis C virus infection. *Clin Infect Dis.* 2018;67(10):1477–92.
87. Bosch FX, Ribes J, Cleries R, Diaz M. Epidemiology of hepatocellular carcinoma. *Clin Liver Dis.* 2005;9(2):191–211, v.
88. Mendes LC, Stucchi RS, Vigani AG. Diagnosis and staging of fibrosis in patients with chronic hepatitis C: comparison and critical overview of current strategies. *Hepatic Med Evid Res.* 2018;10:13–22.
89. Venkatesh SK, Wang G, Lim SG, Wee A. Magnetic resonance elastography for the detection and staging of liver fibrosis in chronic hepatitis B. *Eur Radiol.* 2014;24(1):70–8.
90. Bohte AE, de Niet A, Jansen L, Bipat S, Nederveen AJ, Verheij J, et al. Non-invasive evaluation of liver fibrosis: a comparison of ultrasound-based transient elastography and MR elastography in patients with viral hepatitis B and C. *Eur Radiol.* 2014;24(3):638–48.
91. Nelson DR, Cooper JN, Lalezari JP, Lawitz E, Pockros PJ, Gitlin N, et al. All-oral 12-week treatment with daclatasvir plus sofosbuvir in patients with hepatitis C virus genotype 3 infection: ALLY-3 phase III study. *Hepatology.* 2015;61(4):1127–35.
92. Sulkowski MS, Gardiner DF, Rodriguez-Torres M, Reddy KR, Hassanein T, Jacobson I, et al. Daclatasvir plus sofosbuvir for previously treated or untreated chronic HCV infection. *N Engl J Med.* 2014;370(3):211–21.
93. Bachofner JA, Valli PV, Kroger A, Bergamin I, Kunzler P, Baserga A, et al. Direct antiviral agent treatment of chronic hepatitis C results in rapid regression of transient elastography and fibrosis markers fibrosis-4 score and aspartate aminotransferase-platelet ratio index. *Liver Int.* 2017;37(3):369–76.
94. Chan J, Gogela N, Zheng H, Lammert S, Ajayi T, Fricker Z, et al. Direct-acting antiviral therapy for chronic HCV infection results in liver stiffness regression over 12 months post-treatment. *Dig Dis Sci.* 2018;63(2):486–92.

95. Fernandes FF, Piedade J, Guimaraes L, Nunes EP, Chaves U, Goldenzon RV, et al. Effectiveness of direct-acting agents for hepatitis C and liver stiffness changing after sustained virological response. *J Gastroenterol Hepatol.* 2019;34(12):2187–95.
96. Ogasawara N, Kobayashi M, Akuta N, Kominami Y, Fujiyama S, Kawamura Y, et al. Serial changes in liver stiffness and controlled attenuation parameter following direct-acting antiviral therapy against hepatitis C virus genotype 1b. *J Med Virol.* 2018;90(2):313–9.
97. Tada T, Kumada T, Toyoda H, Mizuno K, Sone Y, Kataoka S, et al. Improvement of liver stiffness in patients with hepatitis C virus infection who received direct-acting antiviral therapy and achieved sustained virological response. *J Gastroenterol Hepatol.* 2017;32(12):1982–8.
98. Bray F, Ferlay J, Soerjomataram I, Siegel RL, Torre LA, Jemal A. Global cancer statistics 2018: GLOBOCAN estimates of incidence and mortality worldwide for 36 cancers in 185 countries. *CA Cancer J Clin.* 2018;68(6):394–424.
99. Guang Y, Xie L, Ding H, Cai A, Huang Y. Diagnosis value of focal liver lesions with SonoVue(R)-enhanced ultrasound compared with contrast-enhanced computed tomography and contrast-enhanced MRI: a meta-analysis. *J Cancer Res Clin Oncol.* 2011;137(11):1595–605.
100. Heiken JP. Distinguishing benign from malignant liver tumours. *Cancer Imaging.* 2007;7:S1–S14.
101. Kartalis N, Brehmer K, Loizou L. Multi-detector CT: liver protocol and recent developments. *Eur J Radiol.* 2017;97:101–9.
102. Choi SH, Kim SY, Park SH, Kim KW, Lee JY, Lee SS, et al. Diagnostic performance of CT, gadoxetate disodium-enhanced MRI, and PET/CT for the diagnosis of colorectal liver metastasis: systematic review and meta-analysis. *J Magn Reson Imaging.* 2018;47(5):1237–50.
103. Park MJ, Kim YK, Lee MW, Lee WJ, Kim YS, Kim SH, et al. Small hepatocellular carcinomas: improved sensitivity by combining gadoxetic acid-enhanced and diffusion-weighted MR imaging patterns. *Radiology.* 2012;264(3):761–70.
104. Radiology ACo. Liver Reporting & Data System. <https://www.acr.org/Clinical-Resources/Reporting-and-Data-Systems/LI-RADS2019>.
105. Butcher DT, Alliston T, Weaver VM. A tense situation: forcing tumour progression. *Nat Rev Cancer.* 2009;9(2):108–22.
106. Levental KR, Yu H, Kass L, Lakins JN, Egeblad M, Erler JT, et al. Matrix crosslinking forces tumor progression by enhancing integrin signaling. *Cell.* 2009;139(5):891–906.
107. Singh S, Fujii LL, Murad MH, Wang Z, Asrani SK, Ehman RL, et al. Liver stiffness is associated with risk of decompensation, liver cancer, and death in patients with chronic liver diseases: a systematic review and meta-analysis. *Clin Gastroenterol Hepatol.* 2013;11(12):1573–84.e2.
108. Wang J, Shan Q, Liu Y, Yang H, Kuang S, He B, et al. 3D MR elastography of hepatocellular carcinomas as a potential biomarker for predicting tumor recurrence. *J Magn Reson Imaging.* 2019;49(3):719–30.
109. Jiao Y, Dong F, Wang H, Zhang L, Xu J, Zheng J, et al. Shear wave elastography imaging for detecting malignant lesions of the liver: a systematic review and pooled meta-analysis. *Med Ultrason.* 2017;19(1):16–22.
110. Garteiser P, Doblaz S, Daire JL, Wagner M, Leitao H, Vilgrain V, et al. MR elastography of liver tumours: value of viscoelastic properties for tumour characterisation. *Eur Radiol.* 2012;22(10):2169–77.
111. Venkatesh SK, Yin M, Glockner JF, Takahashi N, Araoz PA, Talwalkar JA, et al. MR elastography of liver tumors: preliminary results. *AJR Am J Roentgenol.* 2008;190(6):1534–40.
112. Hennemige TP, Hallinan JT, Leung FP, Teo LL, Iyer S, Wang G, et al. Comparison of magnetic resonance elastography and diffusion-weighted imaging for differentiating benign and malignant liver lesions. *Eur Radiol.* 2016;26(2):398–406.
113. Thompson SM, Wang J, Chandan VS, Glaser KJ, Roberts LR, Ehman RL, et al. MR elastography of hepatocellular carcinoma: correlation of tumor stiffness with histopathology features—preliminary findings. *Magn Reson Imaging.* 2017;37:41–5.
114. Gordic S, Ayache JB, Kennedy P, Besa C, Wagner M, Bane O, et al. Value of tumor stiffness measured with MR elastography for assessment of response of hepatocellular carcinoma to locoregional therapy. *Abdom Radiol (NY).* 2017;42(6):1685–94.

115. Iwakiri Y, Shah V, Rockey DC. Vascular pathobiology in chronic liver disease and cirrhosis - current status and future directions. *J Hepatol.* 2014;61(4):912–24.
116. Banerjee JK. Portal hypertension. *Med J Armed Forces India.* 2012;68(3):276–9.
117. Sanyal AJ, Bosch J, Blei A, Arroyo V. Portal hypertension and its complications. *Gastroenterology.* 2008;134(6):1715–28.
118. Bosch J, Abraldes JG, Berzigotti A, García-Pagan JC. The clinical use of HVPG measurements in chronic liver disease. *Nat Rev Gastroenterol Hepatol.* 2009;6(10):573–82.
119. Guo J, Buning C, Schott E, Kroncke T, Braun J, Sack I, et al. In vivo abdominal magnetic resonance elastography for the assessment of portal hypertension before and after transjugular intrahepatic portosystemic shunt implantation. *Investig Radiol.* 2015;50(5):347–51.
120. Hirsch S, Guo J, Reiter R, Schott E, Buning C, Somasundaram R, et al. Towards compression-sensitive magnetic resonance elastography of the liver: sensitivity of harmonic volumetric strain to portal hypertension. *J Magn Reson Imaging.* 2014;39(2):298–306.
121. Ronot M, Lambert S, Elkrief L, Doblas S, Rautou PE, Castera L, et al. Assessment of portal hypertension and high-risk oesophageal varices with liver and spleen three-dimensional multifrequency MR elastography in liver cirrhosis. *Eur Radiol.* 2014;24(6):1394–402.
122. Wagner M, Hectors S, Bane O, Gordic S, Kennedy P, Besa C, et al. Noninvasive prediction of portal pressure with MR elastography and DCE-MRI of the liver and spleen: preliminary results. *J Magn Reson Imaging.* 2018;48(4):1091–103.
123. Blendis L, Wong F. The hyperdynamic circulation in cirrhosis: an overview. *Pharmacol Ther.* 2001;89(3):221–31.
124. Weidekamm C, Cejna M, Kramer L, Peck-Radosavljevic M, Bader TR. Effects of TIPS on liver perfusion measured by dynamic CT. *AJR Am J Roentgenol.* 2005;184(2):505–10.
125. Jansen C, Moller P, Meyer C, Kolbe CC, Bogs C, Pohlmann A, et al. Increase in liver stiffness after transjugular intrahepatic portosystemic shunt is associated with inflammation and predicts mortality. *Hepatology.* 2018;67(4):1472–84.
126. Piecha F, Paech D, Sollors J, Seitz HK, Rossle M, Rausch V, et al. Rapid change of liver stiffness after variceal ligation and TIPS implantation. *Am J Physiol Gastrointest Liver Physiol.* 2018;314(2):G179–G87.
127. Leiderman R, Barbone PE, Oberai AA, Bamber JC. Coupling between elastic strain and interstitial fluid flow: ramifications for poroelastic imaging. *Phys Med Biol.* 2006;51(24):6291–313.
128. Bolognesi M, Merkel C, Sacerdoti D, Nava V, Gatta A. Role of spleen enlargement in cirrhosis with portal hypertension. *Dig Liver Dis.* 2002;34(2):144–50.

# Chapter 7

## Liver Stiffness Measurements in Small Animals



Omar Elshaarawy, Shami Alquzi, Felix Piecha, Laurent Sandrin, Cecil Bastard, and Sebastian Mueller

### Introduction to Transient Micro-Elastography

Transient elastography (TE) determines LS by measuring shear wave velocity generated by a transducer [1, 2]. A low frequency vibration of 50 Hz is generated by an ultrasonic transducer 9 mm in diameter which is used as a piston. However, in the near field zone and due to diffraction effects, the LS is overestimated (i.e., under 25 mm for a 50 Hz excitation) [3]. Because of the morphology of small animal models, measurements have to be performed very close to the vibration source, where diffraction effects are likely to occur. Echosens developed a transient micro-elastography (TME) device to allow LSM within millimeters of the probe [4]. In addition, in the non-commercial prototype, the probe can directly touch the liver surface without any positive pressure. TME includes a microprobe as seen in Fig. 7.1 and a control unit for data analysis (Fig. 7.2). The microprobe has an ultrasonic transducer (Imasonic, Besançon, France), used as both the receiver and the

---

O. Elshaarawy · S. Alquzi · S. Mueller (✉)

Department of Medicine and Center for Alcohol Research and Liver Diseases, Salem Medical Center, University of Heidelberg, Heidelberg, Germany

e-mail: [oelshaarawy@liver.menofia.edu.eg](mailto:oelshaarawy@liver.menofia.edu.eg); [sebastian.mueller@urz.uni-heidelberg.de](mailto:sebastian.mueller@urz.uni-heidelberg.de)

F. Piecha

I. Department of Medicine, University Medical Center Hamburg-Eppendorf, Hamburg, Germany

e-mail: [f.piecha@uke.de](mailto:f.piecha@uke.de)

L. Sandrin · C. Bastard

Echosens, Paris, France

e-mail: [laurent.sandrin@echosens.com](mailto:laurent.sandrin@echosens.com)



**Fig. 7.1**  $\mu$ FibroScan probe

emitter, which is mounted on a mechanical vibrator to produce a low frequency shear wave. The electronic system is fully programmable and allows sampling of the radiofrequency data at a frequency up to 200 MHz with a 12-bit precision. Diffraction effects were reduced by increasing the frequency of vibration to 300 Hz and reducing the diameter of the piston (2 mm) [4].

TME uses an increased ultrasound frequency of 12 MHz to improve the resolution for the calculation of displacements [4]. During the propagation of the low



Fig. 7.2  $\mu$ FibroScan lab processing unit

frequency shear wave, the radiofrequency (RF) data were acquired at a repetition frequency of 15,000 Hz. An autocorrelation method and a time-of-flight algorithm are used similar in TE to calculate the LS from the shear wave velocity [5]. The LS or Young's modulus  $E$  is calculated from  $E = 3\rho V_s^2$  where  $E$ ,  $\rho$  ( $1 \text{ kg/dm}^3$ ), and  $V_s$  are the Young's modulus, the mass density, and the shear wave velocity, respectively [4]. Figure 7.3 shows a typical elastogram obtained with TME. TME allows LSM between 0.5 and 170 kPa. However, for high stiffness values ( $>100 \text{ kPa}$ ), the computational step is larger and the measurement is less accurate [4].

## Liver and Spleen Stiffness Measurements in Small Animal Models

TME has been used in mice and rats [4, 6–8], and recently also for SS in rats [9]. It has confirmed that LS of small animals is comparable to those of humans and pigs (see also Appendix Table A.12). The basic settings of TME are specified by the manufacturer and cannot be changed. Only the depth at which the liver stiffness should be measured by the user can be adjusted. In a preliminary experiment, it was determined that a measuring depth of 2–4 mm provides the smallest IQR on the rat liver and spleen. Analogous to the criteria of the LS in humans, ten consecutive successful measurements with IQR  $<30\%$  of the median range were regarded as a valid measurement [10]. TME can also be used in the so-called continuous mode allowing for continuous LSM every 3 s. The TME probe was also attached to a tripod, to ensure a uniform contact pressure of the ultrasonic head in the liver and spleen and at the same time to minimize possible disturbances such as motion, which would inevitably occur during measurements by hand. The tip of the probe should be placed in contact with the tissue without applying any pressure as it is very sensitive to pressure.



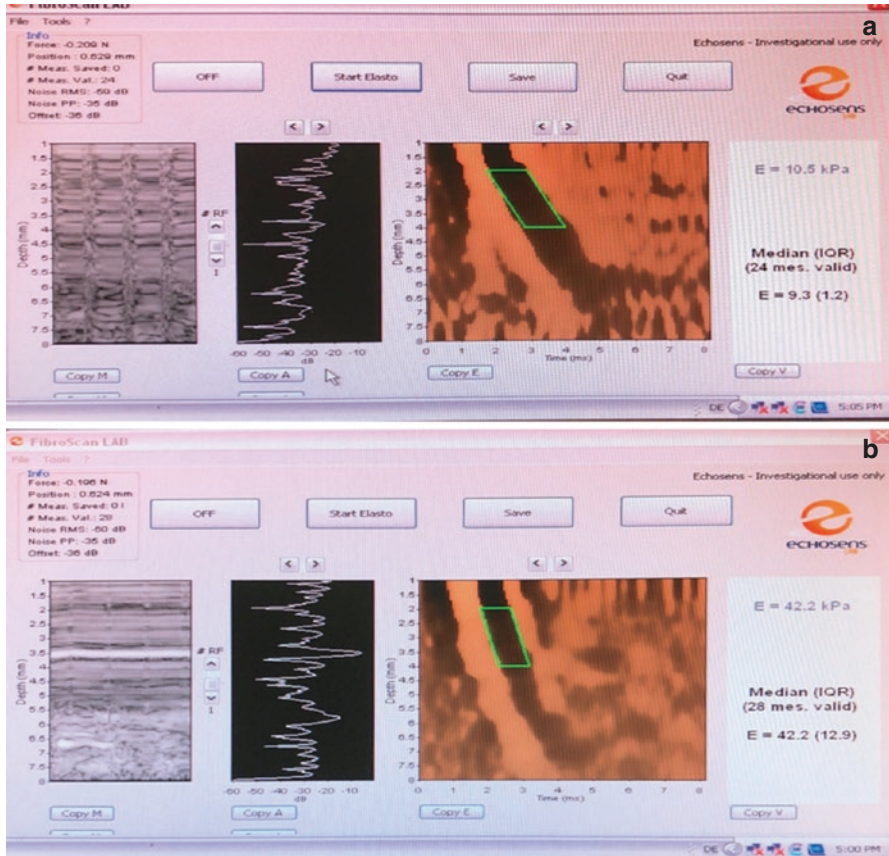


Fig. 7.3 Screenshot of valid LS (a) and SS (b) measurements in a cirrhotic rat

### TME Measurements in Rats

The probe is placed perpendicular to the liver surface at the center of the left lateral lobe which constitute the largest lobe of the four lobes of the rat liver. Sometimes, after induction of cirrhosis using TAA, some livers show nodules which would cover the surface of the liver. During LSM, you should avoid placing the probe on such nodules as it gives higher LSM which are not representative to the actual fibrosis stage of the liver.

### Spleen Stiffness Measurements in Rats

The spleen is slightly placed in the epigastric area after displacing the stomach and the intestine. Then, the probe is placed perpendicular to the spleen surface at a point which is midway between the upper and lower borders and midway between the



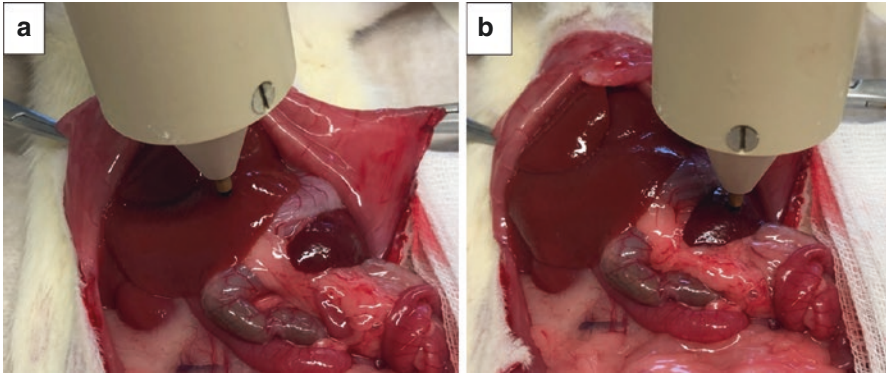


**Fig. 7.4** Site of measurements for LS (a) and SS (b) using  $\mu$ FibroScan

spleen hilum and the anterior pole. This site was selected precisely after several experiments and was found the most representative of the whole spleen tissue, as the measurements could be extreme at the borders and the hilum. Also, measurements at this selected site were reproducible and showed no interobserver discrepancies. This was found to be due to the decreasing spleen thickness at the borders and the impact of high blood flow at the hilum. Surface of the spleen should be kept wet with saline solution to prevent drying out of the spleen which will lead to inaccurate SSM. The positions for LS and SS measurements are illustrated in Fig. 7.4.

## Pharmacological Modulation Experiments

TME has been successfully used to study LS and SS in response to pressure-modulating drugs and to compare it with invasively assessed portal, central venous, and arterial pressure [6, 7, 9]. Before the start of the experiment, the rat is taken out of the cage and weighed. Thereafter, it is placed in an anesthesia box connected to isoflurane inhalation device (Dräger, Germany). Anesthesia dose is adjusted to 2.5% isoflurane and 1% O<sub>2</sub> is used, for anesthesia maintenance dose to 1.7% isoflurane and 0.5% O<sub>2</sub> were adjusted. Then, the animal is placed supine on a heating pad, and the abdomen is shaved. Before the first incision, you should again check whether the deep reflexes as flexion reflex is lost. The abdomen is opened with an extended median laparotomy incision. Immediately after opening the abdomen, the liver and spleen stiffness is detected at least at two different points, to obtain base value before further manipulation and detect a possible change due to the operation. The operation field is further increased by two lateral dissections in the lower third of the abdomen. Thereafter, the stomach and the intestines were wrapped in a piece of gauze soaked in warm saline and kept laterally to access the retroperitoneal abdominal aorta and vena cava. The retroperitoneum was opened by blunt dissection using two cotton swabs. With the aid of a surgical microscope, the vena cava and the abdominal aorta were having a micro-scissors completely exposed. For invasive blood pressure

measurement, 24-gauge indwelling catheters of the company BD (Becton, Dickinson and Company, USA) were inserted into the vessels and connected to the blood pressure sensors. In order to prevent thrombus formation within the catheter, they were wetted with heparin prior to puncture from the inside. After successful catheterization, the system was additionally washed with saline to remove any air bubbles. Catheters were then left without further fixation such as ligatures in the vessels, to avoid possible artifacts. Five minutes were waited before beginning the actual measurements and to ensure stabilization of the cardiovascular system. Thereafter, the TME was then switched on and at least 10 valid successive measurements were achieved for both LS and SS. Then, the medication was injected intravenously directly into the vena cava. After 15 min of drug injection, the probe was repositioned to perform both LSM and SSM, and the same step was repeated again at 30 min.

## Cirrhosis and Portal Hypertension Assessment by TME

In a TAA-induced cirrhosis model, the cirrhotic rats showed significantly higher liver and spleen stiffness than controls (18.6 vs. 4 kPa, 50.5 vs. 23.5 kPa, respectively,  $P < 0.001$ , see also Fig. 7.5). Likewise, the cirrhotic rats had heavier and bigger spleens than the controls (5.9 vs. 4 cm, 2.2 vs. 1.1 g,  $P < 0.001$ , see Fig. 7.5). Besides, the portal vein pressure (PVP) was significantly higher in cirrhotic rats in comparison to controls (15.5 vs. 10.1 mmHg,  $P < 0.001$ ). In general, the change of LS and SS followed strictly the change in PVP ( $r = 0.642$  and  $0.859$ ,  $P < 0.01$ , respectively).

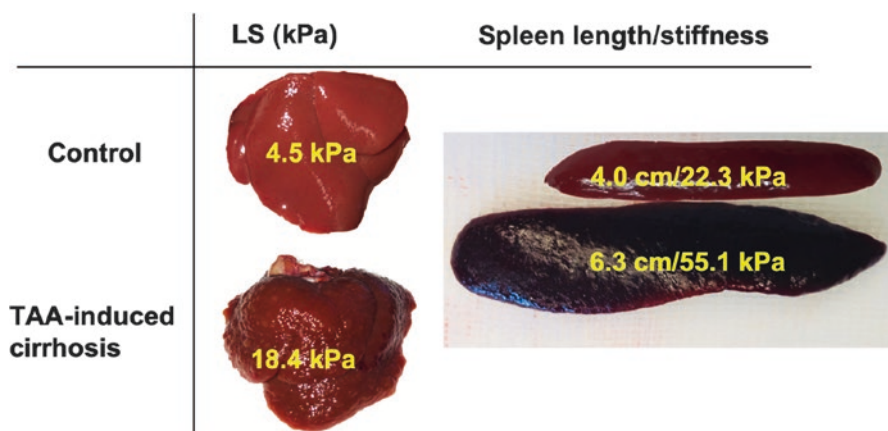


**Fig. 7.5** TAA-induced cirrhosis rats have higher LS and SS and bigger spleen lengths in comparison to control rats

## Experimental Applications of TME

The novel probe was validated in a classical fibrosis model (CCl<sub>4</sub>) and in a transgenic murine model of systemic amyloidosis by Bastard et al. in 2011 [4]. Interestingly, LS values of control mice ( $4.4 \pm 1.3$  kPa) were comparable to those of healthy humans, which should be below 6 kPa. These LS values are also consistent with those found in rodents using other techniques such as MRE or ARFI [11–13]. These findings emphasize that normal LS seems to be below 6 kPa, which is independent of liver size. It has been recently demonstrated in humans that hepatic amyloidosis can drastically increase LS up to the detection limit of TE [14, 15]. Here, Bastard et al. reproduced these data in a transgenic murine model of amyloidosis using TME and showed significant correlation between histological and serum markers of amyloidosis. Thus, in contrast to visual assessment and manual palpation, TME allowed the detection of the early stage 1 of the disease. Piecha et al. studied the effect of acute hemodynamic changes on LS (measured by  $\mu$ FibroScan) in a rodent model of cirrhosis in response to pharmacological modulation of portal pressure (PP) by losartan, nitric oxide (NO) donors, and propranolol [6]. In the animal model, cirrhosis induction resulted in a significant increase of LS and PP. After losartan or NO application, an LS decrease of 25% was strongly correlated with a concomitant decrease of mean arterial pressure and PP. They concluded that LS is efficiently modulated by changes in portal venous and systemic pressures in an animal model of liver cirrhosis irrespective of baseline LS and portal pressure values [6]. Recently, Elshaarawy et al. studied for the first time SS in addition to LS in TAA-induced cirrhosis rat models after exposure to portal hypertension-lowering drugs using the same platform ( $\mu$ FibroScan) [9]. They investigated the following drug groups: metoprolol, udenafil, enalapril, carvedilol, and terlipressin. All drugs showed significant decrease of the portal pressure. Surprisingly, LS and SS significantly decreased in all drug groups except terlipressin. Of note, SS is correlated to portal and arterial pressures better than LS and allows better monitoring of portal pressure than LS. These experiments concluded that the optimal non-invasive monitoring of portal-pressure lowering drugs should require pulse, arterial pressure and combined LS/SS measurements [9].

In conclusion, TME allows the measurement of LS and SS in small animal models in a fast and reproducible manner. TME could be a powerful tool for studying fibrosis in murine models, and in transgenic and knockout mice in longitudinal studies. It will help to better understand determinants of LS as well as SS. Noteworthy, TME could be a useful tool that opens new horizons toward the development of new anti-fibrotic strategies.

## References

1. Ziolkowski M, Handra-Luca A, Kettaneh A, Christidis C, Mal F, Kazemi F, et al. Noninvasive assessment of liver fibrosis by measurement of stiffness in patients with chronic hepatitis C. *Hepatology*. 2005;41(1):48–54.

2. Sandrin L, Tanter M, Gennisson JL, Catheline S, Fink M. Shear elasticity probe for soft tissues with 1-D transient elastography. *IEEE Trans Ultrason Ferroelectr Freq Control*. 2002;49(4):436–46.
3. Sandrin L, Cassereau D, Fink M. The role of the coupling term in transient elastography. *J Acoust Soc Am*. 2004;115(1):73–83.
4. Bastard C, Bosisio MR, Chabert M, Kalopissis AD, Mahrouf-Yorgov M, Gilgenkrantz H, et al. Transient micro-elastography: a novel non-invasive approach to measure liver stiffness in mice. *World J Gastroenterol*. 2011;17(8):968–75.
5. Sandrin L, Fourquet B, Hasquenoph J-M, Yon S, Fournier C, Mal F, et al. Transient elastography: a new non-invasive method for assessment of hepatic fibrosis. *Ultrasound Med Biol*. 2003;29(12):1705–13.
6. Piecha F, Mandorfer M, Peccerella T, Ozga AK, Poth T, Vonbank A, et al. Pharmacological decrease of liver stiffness is pressure-related and predicts long-term clinical outcome. *Am J Physiol Gastrointest Liver Physiol*. 2018;315(4):G484–G494.
7. Piecha F, Peccerella T, Bruckner T, Seitz HK, Rausch V, Mueller S. Arterial pressure suffices to increase liver stiffness. *Am J Physiol Gastrointest Liver Physiol*. 2016;311(5):G945–G953.
8. Piecha F, Peccerella T, Seitz HK, Rausch V, Mueller S. Pharmacological vasodilatation efficiently decreases LS in rats with TAA-induced liver cirrhosis. In: *EASL Abstract SAT443*; 2016.
9. Elshaarawy O, Alquzi S, Mueller J, Rausch V, Silva I, Peccerella T, et al. Response of liver and spleen stiffness to portal pressure lowering drugs in a rat model of cirrhosis. *J Hepatol*. 2019;70:E14–E5.
10. Boursier J, Zarski JP, de Ledinghen V, Rousselet MC, Sturm N, Lebaill B, et al. Determination of reliability criteria for liver stiffness evaluation by transient elastography. *Hepatology*. 2013;57(3):1182–91.
11. Yin M, Talwalkar JA, Glaser KJ, Manduca A, Grimm RC, Rossman PJ, et al. Assessment of hepatic fibrosis with magnetic resonance elastography. *Clin Gastroenterol Hepatol*. 2007;5(10):1207–13.e2.
12. Salameh N, Peeters F, Sinkus R, Abarca-Quinones J, Annet L, Ter Beek LC, et al. Hepatic viscoelastic parameters measured with MR elastography: correlations with quantitative analysis of liver fibrosis in the rat. *J Magn Reson Imaging*. 2007;26(4):956–62.
13. Nightingale K, Soo MS, Nightingale R, Trahey G. Acoustic radiation force impulse imaging: in vivo demonstration of clinical feasibility. *Ultrasound Med Biol*. 2002;28(2):227–35.
14. Janssens F, de Suray N, Piessevaux H, Horsmans Y, de Timary P, Starkel P. Can transient elastography replace liver histology for determination of advanced fibrosis in alcoholic patients: a real-life study. *J Clin Gastroenterol*. 2010;44(8):575–82.
15. Lanzi A, Gianstefani A, Mirarchi MG, Pini P, Conti F, Bolondi L. Liver AL amyloidosis as a possible cause of high liver stiffness values. *Eur J Gastroenterol Hepatol*. 2010;22(7):895–7.

**Part III**  
**Liver Stiffness and Various Etiologies**  
**of Liver Diseases**

# Chapter 8

## Introduction to Fibrosis Assessment by Liver Stiffness in Different Etiologies



Sebastian Mueller

### General Cutoff Values Versus Disease-Specific Cutoff Values?

This book section provides an overview of the many histology-proven studies on liver stiffness (LS) in different liver diseases. In addition, it tries to provide a rational how to interpret LS in daily clinical practice. LS measurements succeeded early on since it performed better than other e.g., serum biomarkers or imaging tools in face to face comparisons (see Appendix Fig. A.2). Correlation coefficients for LS with histological fibrosis stage F0-F4 are typical  $>0.7$  and AUROCs for F4 cirrhosis  $>0.9$ . On the other side, the report of so many different cutoff values either in patients with the same liver disease or between different etiologies has caused some confusion and it certainly has prevented an easier access to the concept of liver stiffness. Table 8.1 provides a representative but not complete list of mean cutoff values for F3 and F4 fibrosis which are 9.6 and 14.0 kPa, respectively (Fig. 8.1). These values are clearly higher as reported in earlier meta-analysis [1] which were 8 and 12.5 kPa. Especially data on ALD has underlined the role of inflammation. In contrast to viral hepatitis or NAFLD, inflammation is even more volatile in drinkers due to noncontinuous drinking (see also the chapter 11 on ALD). Consequently, the F4 cutoff values range from 11.5 to 22.6 kPa. To provide a better standardization of inflammation, cutoff values have been calculated both for HCV and ALD as a function of AST levels that correlated best with LS in both diseases [2]. Figure 8.2 shows these cutoff values for fibrosis stages F0-F4 in patients with chronic HCV. It is striking to see how these cutoff values increase with increasing AST levels. Most interestingly, at no inflammation/no AST elevation, cutoff values were almost identical between HCV and ALD (see Appendix Fig. A.3) [2]. Consequently, studies should take into consideration the degree and distribution of inflammation.

---

S. Mueller (✉)

Department of Medicine and Center for Alcohol Research and Liver Diseases, Salem Medical Center, University of Heidelberg, Heidelberg, Germany  
e-mail: [sebastian.mueller@urz.uni-heidelberg.de](mailto:sebastian.mueller@urz.uni-heidelberg.de)

**Table 8.1** Estimated cutoff values for F3 fibrosis and F4 cirrhosis for different etiologies

Etiology	F3 LS cutoff value (kPa)	F4 LS cutoff value (kPa)	References
NASH	9.6 (8–11.4)	13.7 (10.2–14)	[8–11]
ALD	10.5 (8–12.9)	17.6 (11.5–22.6)	[3, 12–14]
HCV	10.8	14.8	[15–17]
HBV	8.1	10.9	[18–21]
AIH	10.4	16	[22, 23]
PSC	9.6	14.4	[24]
PBC	10.7	16.3	[25, 26]
HFE	13.9	17.9	[27]
Wilson’s disease	8.25	13	[28]
Cardiac hepatopathy	7.6	13.0	[29]
AATD	7.8 (7.2–8.4)	14	[30, 31]
Cystic fibrosis		7.95	[32]
ALL <sup>a</sup>	<b>9.6 kPa</b>	<b>14.0 kPa</b>	
ALL <sup>b</sup>	<b>8 kPa</b>	<b>12.5 kPa</b>	

Note that mean values are shown from selected, representative studies without being complete. For some etiologies such as NAFLD or HCV a range is provided. This range gives an impression of the variability between studies most likely due to confounders such as inflammation (e.g. ALD) and/or cholestasis (e.g. PBC)

<sup>a</sup>Mean values of this table

<sup>b</sup>Mean values in the absence of inflammation

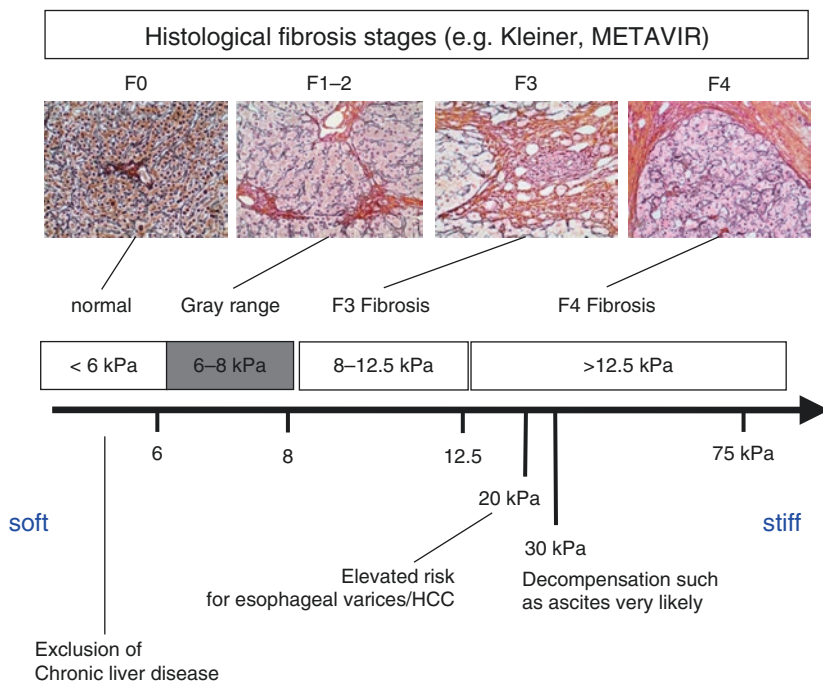
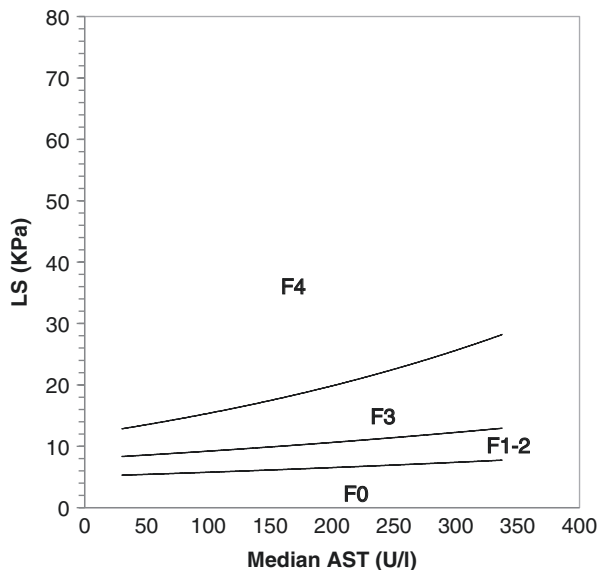


**Fig. 8.1** Liver stiffness range for transient elastography and important cutoff values for liver fibrosis and complications. More information about histological fibrosis scores is shown in Appendix Tables A.21, A.22, A.23, and A.24

**Fig. 8.2** Inflammation-adapted cutoff values for chronic HCV (modified from [2]). See also Appendix Fig. A.3. Actual AST levels cause exponential increase of LS cutoff values for fibrosis stages. Usage of these charts will avoid overestimation of fibrosis stage due to inflammation



Even more convincing are the data on the response of LS toward resolution of inflammation with targeted therapies. A selected list is shown in Table 8.2 for various liver diseases. For instance, in heavy drinkers, LS decreased from 20.1 to 16.5 kPa within 1 week of detoxification [3]. The mean decrease of LS was 17% in this study and rather short time interval. However, extreme responses have been observed and the largest absolute drop was 26 kPa (from 72 to 45 kPa). The largest relative decrease was 65% (from 12.2 to 4.3 kPa). In viral hepatitis with long-term follow-up, LS decreases of 40% have been observed after successful virus elimination by DAAs. Significant reduction of LS was generally associated with milder fibrosis stage, longer treatment duration, sustained virological response, and higher alanine aminotransferase levels [4]. In patients with chronic HBV infection, comparable to ALD, large LS decreases from 28.8 to 8.8 have been described within 9 months of treatment (nucleoside analogues) corresponding to an absolute change of 20 kPa and percentage change of almost 70% [5]. In NAFLD patients, weight loss is the key strategy for therapy and bariatric surgery can be regarded as the most efficient intervention to achieve weight loss. In a recent study of patients undergoing bariatric surgery, BMI decreased from 48.6 to 34.1 kg/m<sup>2</sup> within 12 months. In the same time interval, LS fell from 12.9 to 7.1 kPa [6]. This LS decrease of 41% is comparable to those with ALD. Finally, personal observations include the complete normalization of LS in acute viral hepatitis including the more frequent acute hepatitis A [7]. These typical spontaneous remissions can reach up to 30 kPa when presented to hospitals in case of jaundice. In addition, acute hepatitis A infection never becomes chronic and typically normalizes within 4–6 weeks which underlines the role of elevated perfusion pressure for fibrosis progression (see section book Part VIII, “Molecular basis of LS”).

Based on these arguments, general cutoff values should be used as a first line of elastographic interpretation and rough orientation. However, and this is discussed in



**Table 8.2** Changes of liver stiffness in response to various treatments. In addition, typical time intervals are provided for the LS changes observed

Etiology	Intervention	LS decrease before and after treatment	LS decrease (%)	Time	Ref.
HCV	HCV therapy	10.6–8.8 kPa	17%	2 years	[4, 33–36]
		15.4–10.4 kPa	32%	4 weeks	
HBV	HBV therapy	12.6–7.3 kPa	42%	1–4 years	[5, 38]
AIH	Immunosuppressive therapy	Decrease	6.2–11.7%	12 months	[39]
Heart failure	Diuretics	22.0–14.8 kPa	32%	6.4 days	[7] <i>n</i> = 25
Congestion		30.9–18.6 kPa	40%	7 days	[40] <i>n</i> = 10
ALD	Alcohol detoxification	20.1–16.5 kPa	17%	5.3 days	[41]
		20.5–10.5	48%	5.5 years	[7] <i>n</i> = 23
NAFLD	Bariatric	12.9–7.1 kPa	41%	12 months	[6]
	Weight loss 5% weight reduction	2.8–2.3 kPa (MRE)	15–19%	26 months	[42]
Acute hepatitis A	Spontaneous remission	25.0–5.1 kPa	79%	6 weeks	[7]

The table shows the decrease of LS in response to treatment for various liver diseases. Note that absolute and relative LS decreases of 20 kPa or 80% can be observed including complete normalization. LS decrease depend on initial LS, disease etiology, treatment duration and observation interval. It has been even observed that heavy drinkers with long-term abstaining from alcohol show LS improvement even after 2–5 years of abstinence

the various sections of the book (namely IV, V and VII), interpretation should be done with caution within the clinical context. Under perfect conditions, an on-time laboratory (transaminase levels) and ultrasound imaging should be available for a more sophisticated interpretation. Finally, it should be noted that ratio of spleen stiffness (SS) to LS and its relation to portal hypertension or disease-specific complications [37] will be discussed in parts VI and V.

## References

1. Friedrich-Rust M, Ong MF, Martens S, Sarrazin C, Bojunga J, Zeuzem S, et al. Performance of transient elastography for the staging of liver fibrosis: a meta-analysis. *Gastroenterology*. 2008;134(4):960–74.e8.
2. Mueller S, Englert S, Seitz HK, Badea RI, Erhardt A, Bozaari B, et al. Inflammation-adapted liver stiffness values for improved fibrosis staging in patients with hepatitis C virus and alcoholic liver disease. *Liver Int*. 2015;35(12):2514–21.
3. Mueller S, Millonig G, Sarovska L, Friedrich S, Reimann FM, Pritsch M, et al. Increased liver stiffness in alcoholic liver disease: differentiating fibrosis from steatohepatitis. *World J Gastroenterol*. 2010;16(8):966–72.

4. Arima Y, Kawabe N, Hashimoto S, Harata M, Nitta Y, Murao M, et al. Reduction of liver stiffness by interferon treatment in the patients with chronic hepatitis C. *Hepatol Res.* 2010;40(4):383–92.
5. Stasi C, Salomoni E, Arena U, Corti G, Montalto P, Bartalesi F, et al. Non-invasive assessment of liver fibrosis in patients with HBV-related chronic liver disease undergoing antiviral treatment: a preliminary study. *Eur J Pharmacol.* 2017;806:105–9.
6. Nickel F, Tapking C, Benner L, Sollors J, Billeter AT, Kenngott HG, et al. Bariatric surgery as an efficient treatment for non-alcoholic fatty liver disease in a prospective study with 1-year follow-up: BariScan study. *Obes Surg.* 2018;28(5):1342–50.
7. Mueller S. personal observation; 2019.
8. Eddowes PJ, Sasso M, Allison M, Tsochatzis E, Anstee QM, Sheridan D, et al. Accuracy of FibroScan controlled attenuation parameter and liver stiffness measurement in assessing steatosis and fibrosis in patients with nonalcoholic fatty liver disease. *Gastroenterology.* 2019;156(6):1717–30.
9. Yoneda M, Mawatari H, Fujita K, Endo H, Iida H, Nozaki Y, et al. Noninvasive assessment of liver fibrosis by measurement of stiffness in patients with nonalcoholic fatty liver disease (NAFLD). *Dig Liver Dis.* 2008;40(5):371–8.
10. Cassinotto C, Boursier J, de Ledinghen V, Lebigot J, Lapuyade B, Cales P, et al. Liver stiffness in nonalcoholic fatty liver disease: a comparison of supersonic shear imaging, FibroScan, and ARFI with liver biopsy. *Hepatology.* 2016;63(6):1817–27.
11. Imajo K, Kessoku T, Honda Y, Tomeno W, Ogawa Y, Mawatari H, et al. Magnetic resonance imaging more accurately classifies steatosis and fibrosis in patients with nonalcoholic fatty liver disease than transient elastography. *Gastroenterology.* 2016;150(3):626–37.e7.
12. Nahon P, Kettaneh A, Tengher-Barna I, Zioli M, de Ledinghen V, Douvin C, et al. Assessment of liver fibrosis using transient elastography in patients with alcoholic liver disease. *J Hepatol.* 2008;49(6):1062–8.
13. Nguyen-Khac E, Chatelain D, Tramier B, Decrombecque C, Robert B, Joly JP, et al. Assessment of asymptomatic liver fibrosis in alcoholic patients using fibroscan: prospective comparison with seven non-invasive laboratory tests. *Aliment Pharmacol Ther.* 2008;28(10):1188–98.
14. Thiele M, Detlefsen S, Sevelsted Møller L, Madsen BS, Fuglsang Hansen J, Fiolla AD, et al. Transient and 2-dimensional shear-wave elastography provide comparable assessment of alcoholic liver fibrosis and cirrhosis. *Gastroenterology.* 2016;150(1):123–33.
15. Arena U, Vizzutti F, Abralde JG, Corti G, Stasi C, Moscarella S, et al. Reliability of transient elastography for the diagnosis of advanced fibrosis in chronic hepatitis C. *Gut.* 2008;57(9):1288–93.
16. Castera L, Vergniol J, Foucher J, Le Bail B, Chanteloup E, Haaser M, et al. Prospective comparison of transient elastography, Fibrotest, APRI, and liver biopsy for the assessment of fibrosis in chronic hepatitis C. *Gastroenterology.* 2005;128(2):343–50.
17. Ferraioli G, Tinelli C, Dal Bello B, Zicchetti M, Lissandrini R, Filice G, et al. Performance of liver stiffness measurements by transient elastography in chronic hepatitis. *World J Gastroenterol.* 2013;19(1):49–56.
18. Cai YJ, Dong JJ, Wang XD, Huang SS, Chen RC, Chen Y, et al. A diagnostic algorithm for assessment of liver fibrosis by liver stiffness measurement in patients with chronic hepatitis B. *J Viral Hepat.* 2017;24(11):1005–15.
19. Marcellin P, Zioli M, Bedossa P, Douvin C, Poupon R, de Ledinghen V, et al. Non-invasive assessment of liver fibrosis by stiffness measurement in patients with chronic hepatitis B. *Liver Int.* 2009;29(2):242–7.
20. Sporea I, Sirlin R, Deleanu A, Tudora A, Popescu A, Curescu M, et al. Liver stiffness measurements in patients with HBV vs HCV chronic hepatitis: a comparative study. *World J Gastroenterol.* 2010;16(38):4832–7.
21. Zhang D, Zhang S, Wan M, Wang S. A fast tissue stiffness-dependent elastography for HIFU-induced lesions inspection. *Ultrasonics.* 2011;51(8):857–69.
22. Sun LL, Dong G, Wang B, Zheng Q, Wang S, Zhang RF. Real-time shear wave elastography and APRI index for evaluating autoimmune hepatitis fibrosis. *J Biol Regul Homeost Agents.* 2016;30(4):1019–21.

23. Hartl J, Denzer U, Ehlken H, Zenouzi R, Peiseler M, Sebode M, et al. Transient elastography in autoimmune hepatitis: timing determines the impact of inflammation and fibrosis. *J Hepatol.* 2016;65(4):769–75.
24. Corpechot C, Gaouar F, El Naggar A, Kemgang A, Wendum D, Poupon R, et al. Baseline values and changes in liver stiffness measured by transient elastography are associated with severity of fibrosis and outcomes of patients with primary sclerosing cholangitis. *Gastroenterology.* 2014;146(4):970–9; quiz e15-6.
25. Corpechot C, Carrat F, Poujol-Robert A, Gaouar F, Wendum D, Chazouilleres O, et al. Noninvasive elastography-based assessment of liver fibrosis progression and prognosis in primary biliary cirrhosis. *Hepatology.* 2012;56(1):198–208.
26. Gomez-Dominguez E, Mendoza J, Garcia-Buey L, Trapero M, Gisbert JP, Jones EA, et al. Transient elastography to assess hepatic fibrosis in primary biliary cirrhosis. *Aliment Pharmacol Ther.* 2008;27(5):441–7.
27. Legros L, Bardou-Jacquet E, Latournerie M, Guillygomarc'h A, Turlin B, Le Lan C, et al. Non-invasive assessment of liver fibrosis in C282Y homozygous HFE hemochromatosis. *Liver Int.* 2015;35(6):1731–8.
28. Behairy BE-S, Sira MM, Zalata KR, Salama E-SE, Abd-Allah MA. Transient elastography compared to liver biopsy and morphometry for predicting fibrosis in pediatric chronic liver disease: does etiology matter? *World J Gastroenterol.* 2016;22(16):4238–49.
29. Colli A, Pozzoni P, Berzuini A, Gerosa A, Canovi C, Molteni EE, et al. Decompensated chronic heart failure: increased liver stiffness measured by means of transient elastography. *Radiology.* 2010;257(3):872–8.
30. Guillaud O, Dumortier J, Traclet J, Restier L, Joly P, Chapuis-Cellier C, et al. Assessment of liver fibrosis by transient elastography (Fibroscan((R))) in patients with A1AT deficiency. *Clin Res Hepatol Gastroenterol.* 2019;43(1):77–81.
31. Clark VC, Marek G, Liu C, Collinsworth A, Shuster J, Kurtz T, et al. Clinical and histologic features of adults with alpha-1 antitrypsin deficiency in a non-cirrhotic cohort. *J Hepatol.* 2018;69(6):1357–64.
32. Karlas T, Neuschulz M, Oltmanns A, Guttler A, Petroff D, Wirtz H, et al. Non-invasive evaluation of cystic fibrosis related liver disease in adults with ARFI, transient elastography and different fibrosis scores. *PLoS One.* 2012;7(7):e42139.
33. Macias J, del Valle J, Rivero A, Mira JA, Camacho A, Merchante N, et al. Changes in liver stiffness in patients with chronic hepatitis C with and without HIV co-infection treated with pegylated interferon plus ribavirin. *J Antimicrob Chemother.* 2010;65(10):2204–11.
34. Wang J-H, Changchien C-S, Hung C-H, Tung W-C, Kee K-M, Chen C-H, et al. Liver stiffness decrease after effective antiviral therapy in patients with chronic hepatitis C: longitudinal study using FibroScan. *J Gastroenterol Hepatol.* 2010;25(5):964–9.
35. Martinez SM, Foucher J, Combis J-M, Métivier S, Brunetto M, Capron D, et al. Longitudinal liver stiffness assessment in patients with chronic hepatitis c undergoing antiviral therapy. *PLoS One.* 2012;7(10):e47715.
36. Stasi C, Arena U, Zignego AL, Corti G, Monti M, Triboli E, et al. Longitudinal assessment of liver stiffness in patients undergoing antiviral treatment for hepatitis C. *Dig Liver Dis.* 2013;45(10):840–3.
37. Elshaarawy O, Mueller J, Guha IN, Chalmers J, Harris R, Krag A, et al. Spleen stiffness to liver stiffness ratio significantly differs between ALD and HCV and predicts disease-specific complications. *JHEP Reports.* 2019;1(2):99–106.
38. Ogawa E, Furusyo N, Murata M, Ohnishi H, Toyoda K, Taniai H, et al. Longitudinal assessment of liver stiffness by transient elastography for chronic hepatitis B patients treated with nucleoside analog. *Hepatol Res.* 2011;41(12):1178–88.
39. Hartl J, Ehlken H, Sebode M, Peiseler M, Krech T, Zenouzi R, et al. Usefulness of biochemical remission and transient elastography in monitoring disease course in autoimmune hepatitis. *J Hepatol.* 2018;68(4):754–63.

40. Millonig G, Friedrich S, Adolf S, Fonouni H, Golriz M, Mehrabi A, et al. Liver stiffness is directly influenced by central venous pressure. *J Hepatol.* 2010;52(2):206–10.
41. Mueller S, Sandrin L. Liver stiffness: a novel parameter for the diagnosis of liver disease. *Hepat Med Evid Resarch.* 2010;2:49–67.
42. Patel NS, Hooker J, Gonzalez M, Bhatt A, Nguyen P, Ramirez K, et al. Weight loss decreases magnetic resonance elastography estimated liver stiffness in nonalcoholic fatty liver disease. *Clin Gastroenterol Hepatol.* 2017;15(3):463–4.

# Chapter 9

## Fibrosis Assessment in Patients with HCV or HBV Chronic Infection



Cristina Stasi, Laura Gragnani, and Anna Linda Zignego

### Introduction

Chronic hepatitis C Virus (HCV) or hepatitis B Virus (HBV) – related hepatitis are still widespread in the world with very high morbidity and mortality rates. The severity of the liver disease is represented by its capacity for fibrotic evolution.

Currently, several drugs are available to treat HCV-infected patients, and the cure rates are continuously improving. These new molecules are able to treat more than 90% of HCV-infected patients and positive results in terms of fibrosis regression have been described for patients achieved sustained virological response [1, 2]. However, the fibrosis regression is still a matter of discussion as regards the natural history of cirrhosis [3].

Several evidences suggest that in HBV patients the long-term complete suppression of HBV replication by nucleosides/nucleotides results in an improved survival and quality of life by preventing disease progression, and consequently hepatocellular carcinoma (HCC) development [4]. Moreover, a longitudinal assessment of liver fibrosis showed a histologically proven regression of liver fibrosis during entecavir or tenofovir therapy [5].

Transient elastography (TE) is considered a reliable method for the diagnosis of cirrhosis in patients with chronic liver diseases that performs better at ruling out than ruling in cirrhosis (with negative predictive value higher than 90%). The detection of cirrhosis represents the most relevant clinical endpoint, because affected patients should be monitored for complications related to portal hypertension and regularly screened for HCC [6].

---

C. Stasi · L. Gragnani · A. L. Zignego (✉)  
Interdepartmental Hepatology Center MASVE, Department of Clinical and Experimental  
Medicine, University of Florence, Florence, Italy  
e-mail: [a.zignego@dmf.unifi.it](mailto:a.zignego@dmf.unifi.it)

## The Baseline Assessment of Liver Fibrosis in Chronic HBV Infection

Clinical practice guidelines for chronic hepatitis therapy recommend evaluating liver fibrosis to aid in treatment decision-making and proper treatment timing EASL [7]. Meanwhile, elastographic techniques [1, 7–11] (Tables 9.1, 9.2, and 9.3) are the novel standard for the diagnosis of severe fibrosis and cirrhosis (F3 or F4 according to METAVIR scoring system, respectively) and for the exclusion of significant fibrosis, with transient elastography (TE) being the most common elastographic technique explored so far. In fact, LS was used as a “diagnostic discriminator” to establish clinical priorities and reduce the number of liver biopsies. In a meta-analysis by Tsochatzis et al. [11], the cut-off values were 7.6 (range

**Table 9.1** LS cut-off values for F2 fibrosis mainly in chronic HCV infected patients

Cut-off stiffness values						
Authors	Etiology	$\geq$ F2	Sensitivity [%]	Specificity [%]	PPV [%]	NPV [%]
Castera et al. 2005 [38]	HCV	7.1	67	89	95	48
Ziol et al. 2005 [39]	HCV	8.8	56	91	88	56
Carrion et al. 2006 [40]	HCV post-LT	8.5 <sup>a</sup>	90	81	79	92
Foucher et al. 2006 [8]	CLD	7.2	64	85	90	52
Gomez-Dominguez et al. 2006 [41]	CLD	4	94	33	88	50
Kim et al. 2007 [42]	CLD	7.3	79	88	96	50
Arena et al. 2007 [12]	HCV	7.8	83	82	83	79

For details of histological fibrosis scores, see also Tables A.19–A.24

Cut-off stiffness values in relation to  $\geq$ F2 METAVIR score

<sup>a</sup>Optimal liver stiffness cut-off values used for the diagnosis of significant fibrosis (F2–F4)

**Table 9.2** LS cut-off values for F3 fibrosis mainly in chronic HCV infected patients

Cut-off stiffness values						
Authors	Etiology	$\geq$ F3	Sensitivity [%]	Specificity [%]	PPV [%]	NPV [%]
Castera et al. 2005 [38]	HCV	9.5	73	91	87	81
Ziol et al. 2005 [39]	HCV	9.6	86	85	71	93
Foucher et al. 2006 [8]	CLD	12.5	65	95	90	80
Gomez-Dominguez et al. 2006 [41]	CLD	11	58	89	78	76
Kim et al. 2007 [42]	CLD	8.8	95	78	78	95
Arena et al. 2007 [12]	HCV	10.8	91	94	89	95

For details of histological fibrosis scores, see also Tables A.19–A.24

Cut-off stiffness values in relation to  $\geq$ F3 METAVIR score

**Table 9.3** LS cut-off values for F4 cirrhosis mainly in chronic HCV infected patients

Cut-off stiffness values						
Authors	Etiology	≥F4	Sensitivity [%]	Specificity [%]	PPV [%]	NPV [%]
Castera et al. 2005 [38]	HCV	12.5	87	91	77	95
Ziol et al. 2005 [39]	HCV	14.6	86	96	78	97
Carrion et al. 2006 [40]	HCV post-LT	12.5	100	87	50	100
Foucher et al. 2006 [8]	CLD	17.6	77	97	91	92
Gomez-Dominguez et al. 2006 [41]	CLD	16	89	96	80	98
Kim et al. 2007 [42]	CLD	15	80	78	33	97
Arena et al. 2007 [12]	HCV	14.8	94	92	73	98

For details of histological fibrosis scores, see also Tables A.19–A.24

Cut-off stiffness values in relation to ≥F4 METAVIR score

5.1–10.1), 10.9 (range 8.0–15.4), and 15.3 (range 11.9–26.5) kPa for  $F = 2, 3,$  and 4, respectively, in chronic HCV infection. Our previous studies [1, 10] demonstrated that LS was a strong pre-treatment predictor of response to both dual (peginterferon plus ribavirin) and triple therapy (peginterferon plus ribavirin plus boceprevir) and was an extremely useful tool for the accurate selection of patients for treatment before the era of new direct-acting antiviral drugs (DAAs). Although TE is characterized by low intra- and interobserver variability [9], LS values can be significantly influenced by the degree of necroinflammation, in particular in the absence of extensive fibrosis [8, 9, 12–14]. A higher accuracy for fibrosis assessment can be reached by using so-called AST-adapted cut-off values [15]. The role of food intake and other important clinical confounders will be discussed in detail in the book Part IV “Important (Patho)physiological Confounders of LS.”

## Longitudinal Evaluation of Chronic HCV Infection

The reversibility of liver fibrosis is possible after the removal of the causal agent. In fact, the regression of fibrosis has been demonstrated in patients with chronic HCV infection, after viral eradication [2, 10]. Several drugs (DAA) are currently available to treat HCV-infected patients, and a sustained virological response is continually improving with >90% at the moment. However, fibrosis regression is still a matter of discussion [16]. Therefore, the precise distinction between advanced fibrosis and cirrhosis is of fundamental importance in terms of both diagnostic and therapeutic approaches [3]. The impact of fibrosis stage on a patient’s response to HCV treatment has been explored in several studies [10, 17–21]. An international multicenter study by Sporea et al. compared the reliability of ARFI with liver biopsy and TE [22]. Here, TE performed better at predicting all stages of fibrosis ≥F1 and cirrhosis F4, while a similar performance was seen for significant (≥F2) and severe fibrosis (≥F3). Poynard

et al. [23] assessed the performance of a new test Elasto-FibroTest® (EFT) that combines FibroTest® and LS measurement. The performance of the EFT for the diagnosis of cirrhosis was higher than the FibroTest or FibroScan® alone, but no improvement in performance has been observed for the diagnosis of advanced fibrosis. Recently, Giannini et al. demonstrated that in patients with advanced, compensated chronic liver disease, LS significantly improved in the long term after an SVR. The LS improvement was accompanied by an amelioration of indirect indices of liver fibrosis function but also parameters of portal hypertension [24]. Ravioli et al. showed that spleen stiffness measurements closely reflect changes in portal hypertension and could represent a useful non-invasive test in the follow-up of these patients [25]. A recent 2-year follow-up study Flisiak et al. confirmed the durability of virologic response after HCV infection treatment with DAAs [26]. It was accompanied by a significant improvement in hepatic function and the reduction of LS. However, successful therapy did not prevent hepatic decompensation, HCC, or death in cirrhotic patients who needed to be monitored for possible disease progression for longer than 2 years.

## The Baseline Assessment of Liver Fibrosis in HBV

The proposed algorithm for the use of transient elastography in treatment-naive patients with chronic HBV infection by the EASL and ALEH guidelines in the measurement of liver stiffness considered normal ALT versus elevated ALT ( $5 \times \text{ULN}$ ) [6]. In the case of normal ALT the cut-off values of  $<6$  kPa, 6–9 kPa, and  $>9$  kPa corresponded to non-significant fibrosis, gray area, and severe fibrosis/cirrhosis, respectively. In the case of elevated ALT, the cut-off values of  $<6$  kPa, 6–12 kPa, and  $>12$  kPa corresponded to non-significant fibrosis, gray area, and severe fibrosis/cirrhosis, respectively.

The meta-analysis including 26 studies by Li et al. showed that the cut-off values for detecting liver fibrosis in hepatitis B virus (HBV)-infected patients ranged from 5.85 to 8.8, 7.0 to 13.5, and 9.0 to 16.9 kPa for  $F \geq 2$ ,  $F \geq 3$ , and  $F = 4$  respectively [27].

Cai et al. investigated the impact of steatosis on liver stiffness in HBV-infected patients and developed a diagnostic algorithm for the prediction of liver fibrosis from liver stiffness based on a controlled attenuation parameter [28]. A total of 488 HBV-infected patients who underwent clinical examination, FibroScan, and liver biopsy were prospectively enrolled. The best liver stiffness (kPa) cut-off value for significant fibrosis (Ishak score  $F \geq 3$ ) and advanced fibrosis ( $F \geq 4$ ) were 8.1 and 10.9, respectively. The presence of steatosis may lead to an overestimation of fibrosis assessed by liver stiffness measurement. For Ishak score, see also Fig. A.19.

In a total of 466 patients including 31 patients with acute-on-chronic liver failure (ACLF), and 435 patients with chronic hepatitis B among whom 82 patients were diagnosed with liver cirrhosis from clinical manifestations and liver B-type ultrasonic inspection were enrolled at Tongji Hospital from April to December 2009 [29]. All of these patients underwent transient elastography. In this study the authors



evaluated the possible influencing factors concerning the patients' clinical data including age, gender, and liver inflammation represented by alanine transaminase total bilirubin levels, HBV replication (HBV DNA loads), portal vein pressure, splenic thickness, and body mass index (BMI) [5]. The authors concluded that patients' gender should be taken into consideration during liver stiffness assessment and the avoidance of possible influencing factors including liver inflammation (high levels of ALT and total bilirubin), and obesity (high BMI) is advised.

Xie et al. determined the collagen proportionate area (CPA) of resected liver tissue samples from patients with HBV-related decompensated cirrhosis using digital image analysis and analyzed the relationship between the CPA and liver functional reserve in 53 resected liver tissue samples from liver transplant patients with chronic hepatitis B-induced decompensated cirrhosis [30]. Lower CPA values were found in patients who had mainly macronodular cirrhosis. In these patients, liver transplants were performed mainly due to severe portal hypertension (gastrointestinal bleeding) even though their liver functional reserve was still at the compensated stage. Given that the number of hepatocytes decreases with an increasing number of fibers and CPA value, this study demonstrated a strong correlation between MELD score, serum total bilirubin level, INR, and CPA and showed significant differences among three CPA groups ( $<0.22$ ,  $0.22-0.48$ , and  $>0.48$ ).

Liang et al. retrospectively evaluated patients with HBV, and they demonstrated that combining routine markers improves the accuracy of transient elastography for cirrhosis detection in these patients [31].

## Longitudinal Evaluation of Chronic HBV Infection

Ogawa et al. [32] in chronic HBV infected patients showed that liver stiffness significantly decreased at 1, 2, and 3 years after treatment compared to pre-treatment stiffness values, and they provided information on the impact of successful antiviral treatment 3–5 years after the start of treatment.

The results of the study by Stasi et al. in chronic HBV infected patients are in a substantial agreement with those for HCV patients undergoing treatment and provide valuable information regarding successful antiviral treatment over a period of 2 years [5]. However, in HBV patients undergoing therapy, a significant decrease in liver stiffness was only observed at 18 and 24 months, probably due to fibrosis regression. The greatest degree of stiffness reduction, which Stasi et al. [5] found 2 years after therapy compared to that found by Ogawa et al., was due to potent analogues with a high genetic barrier [32]. In fact, in our study the patients received entecavir/tenofovir in 100% of cases, whereas in the study by Ogawa et al. the patients received lamivudine in 84.4% and entecavir in only 15.6% [32].

In the study by Wu et al. were enrolled 438 patients, all of whom underwent entecavir-based antiviral therapy. The aforementioned patients were followed up every 26 weeks for 2 years [33]. This study demonstrated that pre-treatment liver stiffness measurement can predict risks concerning liver-related events. In fact, liver

stiffness measurement significantly decreased after entecavir treatment. The authors suggested that changes in liver stiffness values in the first 26 weeks could be an important predictor of liver-related events such as HCC development, which may help to identify high-risk patients requiring further optimal surveillance and intervention strategies.

Kim et al. demonstrated that dynamic changes in liver stiffness values in follow-ups may aid in assessing the risk of liver-related events in subjects with HBV-related advanced liver fibrosis receiving antiviral therapy [34]. In a longitudinal study, Wang et al. evaluated the predictors of advanced liver fibrosis in patients with chronic HBV infection with persistently normal alanine aminotransferase, or persistently or intermittently mild elevated ALT [35]. In this study, the proportion of patients with liver fibrosis in the persistently normal alanine aminotransferase group was significantly higher compared to the persistently or intermittently mild elevated group. The authors suggest that normal ALT levels do not always indicate the absence of hepatic fibrosis, but a combination of ALT levels, sex and serum HBV DNA viral load may identify patients with chronic HBV infection at a high risk of developing fibrosis more effectively. Qi et al. analyzed the correlation between pre-operative liver stiffness values and survival, and they found that liver stiffness values can be considered as an independent prognostic factor for HBV-positive HCC after curative resection [36]. Jeon et al. identified a significant association between the sub-cirrhotic range of liver stiffness value (<13 kPa) and a lower risk of HCC development in patients with clinically evident chronic HBV-related cirrhosis [37].

## Conclusions

In patients with viral hepatitis, measurement of LS is now considered essential for the correct management of patients with long life expectancies after anti-HCV eradicating therapy or during anti-HBV treatment, especially by allowing non invasive evaluation of liver fibrosis regression and the risk of severe complications of liver cirrhosis.

## References

1. Stasi C, Piluso A, Arena U, Salomoni E, Montalto P, et al. Evaluation of the prognostic value of liver stiffness in patients with hepatitis C virus treated with triple or dual antiviral therapy: A prospective pilot study. *World J Gastroenterol.* 2015;21:3013–9.
2. Stasi C, Sadalla S, Carradori E, Monti M, Petracchia L, Madia F, Gragnani L, Zignego AL. Longitudinal evaluation of liver stiffness and outcomes in patients with chronic hepatitis C before and after short- and long-term IFN-free antiviral treatment. *Curr Med Res Opin.* 2020;36:245–9.
3. Stasi C, Milani S. Evolving strategies for liver fibrosis staging: the non-invasive assessment. *World J Gastroenterol.* 2017;23(2):191–6.

4. Lampertico P, Agarwal K, Berg T, Buti M, Janssen HLA, Papatheodoridis G, et al. EASL 2017 Clinical Practice Guidelines on the management of hepatitis B virus infection. *J Hepatol.* 2017;67(2):370–98.
5. Stasi C, Salomoni E, Arena U, Corti G, Montalto P, Bartalesi F, et al. Non-invasive assessment of liver fibrosis in patients with HBV-related chronic liver disease undergoing antiviral treatment: a preliminary study. *Eur J Pharmacol.* 2017;806:105–9.
6. European Association for Study of Liver, Asociacion Latinoamericana para el Estudio del Hígado. EASL-ALEH clinical practice guidelines: non-invasive tests for evaluation of liver disease severity and prognosis. *J Hepatol.* 2015;63:237–64.
7. Pawlotsky J-M, Negro F, Aghemo A, Berenguer M, Dalgard O, Dusheiko G, et al. EASL recommendations on treatment of hepatitis C 2018. *J Hepatol.* 2018;69(2):461–511.
8. Foucher J, Chanteloup E, Vergniol J, Castera L, Le Bail B, Adhoute X, et al. Diagnosis of cirrhosis by transient elastography (FibroScan): a prospective study. *Gut.* 2006;55(3):403–8.
9. Fraquelli M, Rigamonti C, Casazza G, Conte D, Donato MF, Ronchi G, et al. Reproducibility of transient elastography in the evaluation of liver fibrosis in patients with chronic liver disease. *Gut.* 2007;56(7):968–73.
10. Stasi C, Arena U, Zignego AL, Corti G, Monti M, Triboli E, et al. Longitudinal assessment of liver stiffness in patients undergoing antiviral treatment for hepatitis C. *Dig Liver Dis.* 2013;45(10):840–3.
11. Tsochatzis EA, Gurusamy KS, Ntaoula S, Cholongitas E, Davidson BR, Burroughs AK. Elastography for the diagnosis of severity of fibrosis in chronic liver disease: a meta-analysis of diagnostic accuracy. *J Hepatol.* 2011;54(4):650–9.
12. Arena U, Vizzutti F, Abraldes JG, Corti G, Stasi C, Moscarella S, et al. Reliability of transient elastography for the diagnosis of advanced fibrosis in chronic hepatitis C. *Gut.* 2008;57(9):1288–93.
13. Coco B, Oliveri F, Maina AM, Ciccorossi P, Sacco R, Colombatto P, et al. Transient elastography: a new surrogate marker of liver fibrosis influenced by major changes of transaminases. *J Viral Hepat.* 2007;14(5):360–9.
14. Sagir A, Heintges T, Akyazi Z, Oette M, Erhardt A, Haussinger D. Therapy outcome in patients with chronic hepatitis C: role of therapy supervision by expert hepatologists. *J Viral Hepat.* 2007;14(9):633–8.
15. Mueller S, Englert S, Seitz HK, Badea RI, Erhardt A, Bozaari B, et al. Inflammation-adapted liver stiffness values for improved fibrosis staging in patients with hepatitis C virus and alcoholic liver disease. *Liver Int.* 2015;35(12):2514–21.
16. Desmet VJ, Roskams T. Cirrhosis reversal: a duel between dogma and myth. *J Hepatol.* 2004;40(5):860–7.
17. Ogawa E, Furusyo N, Toyoda K, Takeoka H, Maeda S, Hayashi J. The longitudinal quantitative assessment by transient elastography of chronic hepatitis C patients treated with pegylated interferon alpha-2b and ribavirin. *Antivir Res.* 2009;83(2):127–34.
18. Arima Y, Kawabe N, Hashimoto S, Harata M, Nitta Y, Murao M, et al. Reduction of liver stiffness by interferon treatment in the patients with chronic hepatitis C. *Hepatol Res.* 2010;40(4):383–92.
19. Macias J, del Valle J, Rivero A, Mira JA, Camacho A, Merchante N, et al. Changes in liver stiffness in patients with chronic hepatitis C with and without HIV co-infection treated with pegylated interferon plus ribavirin. *J Antimicrob Chemother.* 2010;65(10):2204–11.
20. Wang J-H, Changchien C-S, Hung C-H, Tung W-C, Kee K-M, Chen C-H, et al. Liver stiffness decrease after effective antiviral therapy in patients with chronic hepatitis C: longitudinal study using FibroScan. *J Gastroenterol Hepatol.* 2010;25(5):964–9.
21. Martinez SM, Foucher J, Combis J-M, Métivier S, Brunetto M, Capron D, et al. Longitudinal liver stiffness assessment in patients with chronic hepatitis C undergoing antiviral therapy. *PLoS One.* 2012;7(10):e47715.
22. Sporea I, Bota S, Peck-Radosavljevic M, Sirlin R, Tanaka H, Iijima H, et al. Acoustic Radiation Force Impulse Elastography for fibrosis evaluation in patients with chronic hepatitis C: an international multicenter study. *Eur J Radiol.* 2012;81(12):4112–8.

23. Poynard T, de Ledinghen V, Zarski JP, Stanciu C, Munteanu M, Vergniol J, et al. Performances of Elasto-FibroTest(®), a combination between FibroTest(®) and liver stiffness measurements for assessing the stage of liver fibrosis in patients with chronic hepatitis C. *Clin Res Hepatol Gastroenterol*. 2012;36(5):455–63.
24. Giannini EG, Crespi M, Demarzo M, Bodini G, Furnari M, Marabotto E, et al. Improvement in hepatitis C virus patients with advanced, compensated liver disease after sustained virological response to direct acting antivirals. *Eur J Clin Invest*. 2018;49(3):e13056.
25. Ravaioli F, Colecchia A, Dajti E, Marasco G, Alemanni LV, Tamè M, et al. Spleen stiffness mirrors changes in portal hypertension after successful interferon-free therapy in chronic-hepatitis C virus patients. *World J Hepatol*. 2018;10(10):731–42.
26. Flisiak R, Janczewska E, Łucejko M, Karpińska E, Zarebska-Michaluk D, Nazzal K, et al. Durability of virologic response, risk of de novo hepatocellular carcinoma, liver function and stiffness 2 years after treatment with ombitasvir/paritaprevir/ritonavir±dasabuvir±ribavirin in the AMBER, real-world experience study. *J Viral Hepatitis*. 2018;25(11):1298–305.
27. Li Y, Huang YS, Wang ZZ, Yang ZR, Sun F, Zhan SY, et al. Systematic review with meta-analysis: the diagnostic accuracy of transient elastography for the staging of liver fibrosis in patients with chronic hepatitis B. *Aliment Pharmacol Ther*. 2015;43(4):458–69.
28. Cai YJ, Dong JJ, Wang XD, Huang SS, Chen RC, Chen Y, et al. A diagnostic algorithm for assessment of liver fibrosis by liver stiffness measurement in patients with chronic hepatitis B. *J Viral Hepat*. 2017;24(11):1005–15.
29. Ding H, Wu T, Ma K, Wang X, Wu Z, Guo W, et al. Noninvasive measurement of liver fibrosis by transient elastography and influencing factors in patients with chronic hepatitis B—a single center retrospective study of 466 patients. *J Huazhong Univ Sci Technolog Med Sci*. 2012;32(1):69–74.
30. Xie S-B, Ma C, Lin C-S, Zhang Y, Zhu J-Y, Ke W-M. Collagen proportionate area of liver tissue determined by digital image analysis in patients with HBV-related decompensated cirrhosis. *Hepatobiliary Pancreat Dis Int*. 2011;10(5):497–501.
31. Liang XE, Dai L, Yang SL, Zhong CX, Peng J, Zhu YF, et al. Combining routine markers improves the accuracy of transient elastography for hepatitis B cirrhosis detection. *Dig Liver Dis*. 2016;48(5):512–8.
32. Ogawa E, Furusyo N, Murata M, Ohnishi H, Toyoda K, Taniiai H, et al. Longitudinal assessment of liver stiffness by transient elastography for chronic hepatitis B patients treated with nucleoside analog. *Hepatol Res*. 2011;41(12):1178–88.
33. Wu S, Kong Y, Piao H, Jiang W, Xie W, Chen Y, et al. On-treatment changes of liver stiffness at week 26 could predict 2-year clinical outcomes in HBV-related compensated cirrhosis. *Liver Int*. 2017;38(6):1045–54.
34. Kim BK, Oh HJ, Park JY, Kim DY, Ahn SH, Han KH, et al. Early on-treatment change in liver stiffness predicts development of liver-related events in chronic hepatitis B patients receiving antiviral therapy. *Liver Int*. 2013;33(2):180–9.
35. Wang D, Zhang P, Zhang M. Predictors for advanced liver fibrosis in chronic hepatitis B virus infection with persistently normal or mildly elevated alanine aminotransferase. *Exp Ther Med*. 2017;14(6):5363–70.
36. Qi M, Chen Y, Zhang GQ, Meng YJ, Zhao FL, Wang J, et al. Clinical significance of preoperative liver stiffness measurements in primary HBV-positive hepatocellular carcinoma. *Future Oncol*. 2017;13(30):2799–810.
37. Jeon MY, Lee HW, Kim SU, Heo JY, Han S, Kim BK, et al. Subcirrhotic liver stiffness by FibroScan correlates with lower risk of hepatocellular carcinoma in patients with HBV-related cirrhosis. *Hepatol Int*. 2017;11(3):268–76.
38. Castera L, Vergniol J, Foucher J, Le Bail B, Chanteloup E, Haaser M, et al. Prospective comparison of transient elastography, Fibrotest, APRI, and liver biopsy for the assessment of fibrosis in chronic hepatitis C. *Gastroenterology*. 2005;128(2):343–50.
39. Ziolk M, Handra-Luca A, Kettaneh A, Christidis C, Mal F, Kazemi F, et al. Noninvasive assessment of liver fibrosis by measurement of stiffness in patients with chronic hepatitis C. *Hepatology*. 2005;41(1):48–54.

40. Carrión JA, Navasa M, Bosch J, Bruguera M, Gilibert R, Forns X. Transient elastography for diagnosis of advanced fibrosis and portal hypertension in patients with hepatitis C recurrence after liver transplantation. *Liver Transpl.* 2006;12(12):1791–8.
41. Gomez-Dominguez E, Mendoza J, Rubio S, Moreno-Monteaquedo JA, Garcia-Buey L, Moreno-Otero R. Transient elastography: a valid alternative to biopsy in patients with chronic liver disease. *Aliment Pharmacol Ther.* 2006;24(3):513–8.
42. Kim KM, Choi W-B, Park SH, Yu E, Lee SG, Lim Y-S, et al. Diagnosis of hepatic steatosis and fibrosis by transient elastography in asymptomatic healthy individuals: a prospective study of living related potential liver donors. *J Gastroenterol.* 2007;42(5):382–8.

# Chapter 10

## Fibrosis Assessment in Patients with NAFLD



Victor de Ledinghen

### Introduction

The unrelenting challenge of obesity has resulted in nonalcoholic fatty liver disease (NAFLD) becoming the most common cause of chronic liver disease in the industrialized countries. Based on extensive previous data [1], the estimated prevalence of NAFLD in the United States is approximately 24%. The vast majority of large, population-based studies assessing the burden of NAFLD are derived from the National Health and Nutrition Examination Survey (NHANES) III between 1988 and 1994, when obesity rates were estimated at 22.9% of the population [2]. However, the prevalence of obesity has continued to increase steeply beyond this time frame in all representative age and sex groups. Based on the most recent NHANES estimates from 2013 to 2014, 35% of men, 40% of women, and 17% of children and adolescents are obese [3].

In this context, NAFLD is a major public health problem afflicting approximately one billion individuals worldwide. In the USA, NASH has already become the second or third leading cause of end-stage liver disease and hepatocellular carcinoma (HCC) [4]. Liver biopsy is heavily relied upon to assess the severity of NAFLD, select patients for pharmacological treatment, monitor disease progression or treatment response, and develop new drugs. However, it is invasive, has high interobserver variability, and is associated with adverse effects, including pain, infection and, albeit rarely, death. It is also impractical because of the large number of individuals who have NAFLD. Over the last two decades, tremendous advances have been made in the assessment of NAFLD by noninvasive imaging. In this review, we will discuss the different noninvasive imaging modalities available to assess liver fibrosis.

---

V. de Ledinghen (✉)

Centre d'Investigation de la Fibrose hépatique, Hôpital Haut-Lévêque, Pessac, France  
e-mail: [victor.deledinghen@chu-bordeaux.fr](mailto:victor.deledinghen@chu-bordeaux.fr)

## Diagnosis of Liver Fibrosis

Based on disease severity, NAFLD is divided into nonalcoholic fatty liver (NAFL) and nonalcoholic steatohepatitis (NASH). The latter is characterized by histological lobular inflammation and hepatocyte ballooning, and is associated with faster fibrosis progression than NAFL [5]. With ongoing liver injury, some patients will progress to cirrhosis and develop various liver-related complications. The presence of advanced fibrosis identifies patients in need of in-depth hepatological investigation, including, on a case-by-case basis, confirmatory biopsy and intensive therapies. Monitoring of fibrosis progression is also necessary at variable time intervals. One other possible solution is to compare the correlations of noninvasive methods with clinical outcomes such as hepatocellular carcinoma, cirrhotic complications, and liver-related death.

## Liver Stiffness Measurement Using TE/FibroScan

FibroScan (TE, transient elastography) measures the velocity of an elastic shear wave propagating through the liver [6]. This velocity is directly related to tissue stiffness, which in turn is related to the degree of fibrosis; the stiffer the tissue, the faster the shear wave propagates. The measurement procedure is considered to have failed when no value is obtained after ten attempts. The results are expressed in kilopascals (kPa) and range from 1.5 to 75 kPa, with normal values around 5 kPa. More details are provided in book Part II “Techniques to measure Liver stiffness.” The summary AUROC values using FibroScan M and XL probes for diagnosing advanced fibrosis in NAFLD are 0.88 and 0.85, respectively [7]. The XL probe was designed to cater for patients who are obese, and produces similar diagnostic accuracy as the M probe in nonobese patients [8, 9]. Performances of liver stiffness measurement with FibroScan are indicated in Table 10.1.

Although FibroScan has excellent negative predictive value to exclude advanced fibrosis, its positive predictive value to rule in advanced fibrosis or cirrhosis is modest. At a fixed sensitivity, a cutoff of 6.5 kPa can exclude advanced fibrosis with a negative predictive value of 0.91, and a cutoff LSM of 12.1 kPa can exclude cirrhosis with a negative predictive value of 0.99. At a fixed specificity, liver stiffness can identify patients with advanced fibrosis with a positive predictive value of 0.71 and patients with cirrhosis with a positive predictive value of 0.41 [10].

Albeit transient elastography is a highly sensitive screening test to exclude F3-4 fibrosis in nonalcoholic fatty liver disease patients, one-third of patients with high liver stiffness may have normal results on repeated examination [11]. Therefore, in case of suspected abnormal high liver stiffness value, a new measurement, a few weeks later, can help to avoid liver biopsy. This elevated LS can be due to clinical confounders such as inflammation. For more details see also book Part IV “Important (patho)physiological confounders of LS.” At last, liver stiffness is not affected by hepatic steatosis or necroinflammation but could be affected by high ALT level [9, 12].

**Table 10.1** Performance of transient elastography (FibroScan) for the diagnosis of liver fibrosis in NAFLD

Study	Year	N	AUROC F2F3F4 (95% CI)	AUROC F3F4 (95% CI)	AUROC F4 (95% CI)
Eddowes PJ [12]	2019	373	0.77 (0.72–0.82)	0.80 (0.75–0.84)	0.89 (0.84–0.93)
Siddiqui MS [10]	2019	393		0.83 (0.79–0.87)	0.93 (0.90–0.97)
Jiang W [54]	2018	Meta-analysis 1753	0.85 (0.82–0.88)	0.92 (0.89–0.94)	0.94 (0.93–0.97)
Chen J [20]	2017	111	0.81 (0.69–0.89)	0.87 (0.76–0.94)	0.92 (0.73–0.98)
Lee MS [55]	2017	94	0.757 (0.645–0.867)	0.870 (0.774–0.965)	0.882 (0.737–0.931)
Petta S [25]	2017	761		0.863 (0.837–0.889)	
Petta S [56]	2017	324	0.808	0.861	
Park CC [19]	2017	94	0.86 (0.77–0.95)	0.80 (0.67–0.93)	0.69 (0.45–0.94)
Loong TCW [57]	2017	215	0.851 ± 0.029	0.940 ± 0.016	0.916 ± 0.027
Boursier J [29]	2016	452	0.842 ± 0.019	0.831 ± 0.019	0.864 ± 0.024
Tapper EB [58]	2016	164		0.93 (0.86–0.96)	
Imajo K [18]	2016	127	0.82 (0.74–0.89)	0.88 (0.79–0.97)	0.92 (0.86–0.98)
Petta S [24]	2015	321		0.857 (0.790–0.924)	
Wong V [8]	2012	193 M probe	0.83 (0.76–0.89)	0.87 (0.82–0.93)	0.89 (0.82–0.97)
Wong V [8]	2012	193 XL probe	0.80 (0.74–0.87)	0.85 (0.79–0.91)	0.91 (0.85–0.96)
Petta S [59]	2011	146	0.79	0.87	
Wong V [9]	2010	246	0.84 (0.79–0.90)	0.93 (0.89–0.96)	0.95 (0.91–0.99)

AUROC area under the ROC curve, CI confidence interval

## Liver Stiffness Measurement Using Acoustic Radiation Force Impulse (ARFI)

Point shear wave elastography (pSWE), also known as acoustic radiation force impulse (ARFI) involves mechanical excitation of tissue using short-duration acoustic pulses that propagate shear waves and generate localized, micron-scale displacements in tissue. For more details see also book Part II “Techniques to measure Liver stiffness.” ARFI (Antares or Acuson S2000, Siemens Medical Solutions, Mountain view, CA) elastography is integrated into a conventional ultrasound device and provides an estimate of liver stiffness in shear wave speed (m/s). The exact location where measurements are obtained can be selected by the operator. A



**Table 10.2** Performance of ARFI for the diagnosis of liver fibrosis in NAFLD

Study	Year	<i>N</i>	AUROC F2F3F4 (95% CI)	AUROC F3F4 (95% CI)	AUROC F4 (95% CI)
Lee MS [55]	2017	94	0.657 (0.545–0.758)	0.873 (0.777–0.968)	0.920 (0.849–0.990)
Cassinotto C [14]	2016	291	0.77	0.84	0.84
Cui J [21]	2016	125	0.848 (0.776–0.921)	0.896 (0.824–0.968)	0.862 (0.721–1.000)
Palmeri ML [60]	2011	172		0.90	

*AUROC* area under the ROC curve, *CI* confidence interval

major advantage of pSWE/ARFI is that it can be easily implemented on modified commercial ultrasound machines. One may therefore assess liver fibrosis and examine the liver parenchyma during the same examination. Values obtained with pSWE/ARFI are expressed in m/s and have a narrow range (0.5–4.4 m/s), which limits the definitions of cutoff values for discriminating certain fibrosis stages and thus for making management decisions. Only few studies have evaluated pSWE using ARFI in patients with NAFLD with diagnostic accuracies of 84–98% for advanced fibrosis. A systematic review of 7 studies having included 723 NAFLD patients, reported a summary diagnostic accuracy, sensitivity, and specificity of 90%, 80%, and 85%, respectively for the detection of significant fibrosis. No data were available for advanced fibrosis and cirrhosis [13]. However, Cassinotto et al showed that pSWE/ARFI performance is better for severe fibrosis and cirrhosis than for less severe fibrosis [14]. Performances of ARFI for the diagnosis of liver fibrosis in NAFLD patients are indicated in Table 10.2.

## 2D-Shear Wave Elastography

2D-Shear wave elastography (2D-SWE) (ElastQ; Philips, Andover, MA. Logiq E9; GE Healthcare, Wauwatosa, WI. Aixplorer; Supersonic Imagine, Aix-en-Provence, France) is an FDA approved technique that adapts ultrasound imaging to produce liver stiffness measurement. For more details see also book Part II “Techniques to measure Liver stiffness.” Similar to ARFI, the 2D-SWE operator must define a large, vessel-free region of interest in ultrasonic B-mode imaging using curved abdominal probe during breath hold, and take a series of measurements (typically seven to eleven), then a median of those values is obtained. 2D-SWE is based on the combination of a radiation force induced in tissues by focused ultrasonic beams and a very high frame rate ultrasound imaging sequence capable of catching in real time the transient propagation of resulting shear waves. The size of the region of interest can be chosen by the operator. 2D-SWE also has the advantage of being implemented on a commercially available ultrasound machine with results expressed either in m/s or in kPa across a wide range of values (2–150 kPa). As other methods,

**Table 10.3** Performance of shear wave elastography for the diagnosis of liver fibrosis in NAFLD

Study	Year	<i>N</i>	AUROC F2F3F4 (95% CI)	AUROC F3F4 (95% CI)	AUROC F4 (95% CI)
Takeuchi H [61]	2018	71	0.75 0.62–0.85	0.82 0.70–0.90	0.90 0.78–0.96
Hermann E [62]	2018	156	0.855	0.928	0.917
Lee MS [55]	2017	94	0.759 (0.641, 0.854)	0.809 (0.697, 0.894)	0.906 (0.811, 0.963)
Xiao G [7]	2017	Meta-analysis 429		0.95	
Cassinotto C [14]	2016	291	0.86	0.89	0.88

AUROC area under the ROC curve, CI confidence interval

2D-SWE performance is better for severe fibrosis and cirrhosis than for less severe fibrosis [14]. Performances of 2D-SWE for the diagnosis of liver fibrosis in NAFLD patients are indicated in Table 10.3.

## Magnetic Resonance Elastography

Magnetic resonance elastography (MRE) is expected to become one of the most promising methods of hepatology in the future. The principle of MRE was reported by the Mayo Clinic in 1995, and MRE was first approved by the FDA in 2009; it is now available as a commercial upgrade for standard magnetic resonance imaging (MRI) systems. For more details see also book Part II “Techniques to measure Liver stiffness.” MRE uses a modified phase-contrast method to image the propagation of the shear wave in the liver parenchyma. It can assess the entire liver, irrespective of body habitus, and mechanical parameters for shear stiffness have been standardized. Performances of MRE for the diagnosis of liver fibrosis in NAFLD patients are indicated in Table 10.4. A meta-analysis of nine studies comprising 232 patients with NAFLD found that MRE detected fibrosis with a high level of accuracy, independent of liver inflammation and BMI with AUROC values of 0.86–0.91 for all stages of fibrosis [15].

In a head to head comparison between 3D MRE versus 2D MRE, 3D MRE at 40 Hz was superior to 2D MRE at 60 Hz with an AUROC for the detection for advanced fibrosis of 0.97 [16]. However, even though 2D and 3D MRE are able to overcome all these issues except for iron overload or acute inflammation, MRE is limited by restricted accessibility at many centers, especially worldwide, and the required expertise needed to obtain adequate results in the setting of 3D MRE. Currently, accurate imaging is a trade-off between specificity, accessibility, and ease of use such that as specificity goes up, accessibility and ease of use go down.

**Table 10.4** Performance of magnetic resonance elastography for the diagnosis of liver fibrosis in NAFLD

Study	Year	N	AUROC F2F3F4 (95% CI)	AUROC F3F4 (95% CI)	AUROC F4 (95% CI)
Costa Silva L [48]	2018	49	0.932 (0.823–0.984)	0.928 (0.817–0.982)	0.964 (0.867–0.996)
Chen J [20]	2017	111	0.93 (0.85, 0.97)	0.92 (0.82, 0.97)	0.95 (0.85, 0.99)
Xiao G [7]	2017	Meta-analysis 384	0.92	0.96	0.97
Park CC [19]	2017	94	0.89 (0.83–0.96)	0.87 (0.78–0.96)	0.87 (0.71–1.00)
Imajo K [18]	2016	142	0.89 (0.85–0.94)	0.89 (0.83–0.95)	0.97 (0.94–1.00)
Cui J [21]	2016	125	0.885 (0.816–0.953)	0.934 (0.863–1.000)	0.882 (0.729–1.000)
Loomba R [49]	2014	117	0.856	0.924	0.894

AUROC area under the ROC curve, CI confidence interval

## Multiparametric MRI

In the past few years, a multiparametric magnetic resonance technique (LiverMultiScan, Oxford, UK) has been established that includes T1 mapping for fibrosis and inflammation imaging, T2\* mapping for liver iron quantification and <sup>1</sup>H-MRS for liver fat quantification. The T1 measurements are adjusted for the iron level, as high iron levels in the presence of fibrosis can lead to “pseudo-normal” T1 values. LiverMultiScan is a quick and noninvasive test that does not require injection of any intravenous contrast agent. In a study published in 2017, the AUROC using liver inflammation and fibrosis for the diagnosis of NAFLD-related cirrhosis was 0.85 [17]. However, at this time, further validation studies are needed.

## Comparison of Different Methods

MRE and transient elastography have been compared head to head in patients with biopsy-proven NAFLD in a small number of studies. MRE is more accurate than FibroScan in detecting F2 fibrosis (AUROC 0.86–0.89 versus AUROC 0.84, respectively) and F4 fibrosis (AUROC 0.88–0.97 versus AUROC 0.95) [18]. In a prospective, cross-sectional study of more than 100 patients, C.C. Park et al. found that MRE is more accurate than FibroScan in identification of liver fibrosis (stage 1 or more), using biopsy analysis as the standard [19]. However, in this study, only a few patients had advanced fibrosis. In obese patient population, both MRE and FibroScan have an excellent diagnostic performance in the assessment of liver fibrosis [20].

Another study evaluated the performances of MRE versus ARFI for diagnosing fibrosis in NAFLD patients [21]. For diagnosing any fibrosis ( $\geq$ stage 1), the MRE AUROC was 0.799 (95% confidence interval [CI] 0.723–0.875), significantly higher than the ARFI AUROC of 0.664 (95% CI 0.568–0.760). In stratified analysis by presence or absence of obesity, MRE was superior to ARFI for diagnosing any fibrosis in obese patients but not in nonobese patients. Unfortunately, the comparison of MRE and ARFI for the diagnosis of advanced fibrosis was not evaluated. In a recent meta-analysis, it was shown that MRE and SWE have the highest diagnostic accuracy for staging fibrosis in NAFLD patients [7].

In conclusion, all of these methods have a good performance to exclude advanced liver fibrosis in NAFLD patients. They can be used in clinical practice according to their availability in each area or center. For the diagnosis of liver fibrosis in NAFLD patients, AASLD Guidelines are as follows: FibroScan or MRE, used for liver stiffness measurement, are clinically useful tools for identifying advanced fibrosis in patients with NAFLD [22]. AGA Guidelines are as follow: In adults with NAFLD and a lower risk of cirrhosis, the AGA makes no recommendation regarding the role of MRE or VCTE for detection of cirrhosis. However, in adults with NAFLD and a higher risk of cirrhosis (advanced age, obesity, particularly central adiposity, diabetes, alanine elevated  $>23$  upper limit of normal), the AGA suggest using MRE, rather than VCTE, for detection of cirrhosis [23].

## Combination of Liver Stiffness Measurement and Blood Marker

A lot of serum markers (AST to Platelet Ratio Index (APRI), BARD, FIB-4, and NAFLD fibrosis score (NFS)) are easy and reliable scores proposed to be used in clinical practice. There is no consensus on thresholds or strategies for their use in clinical practice when trying to avoid liver biopsy [6]. Some data suggest that the combination of elastography and serum markers performs better than either method alone.

In 2015, Petta et al. evaluated combinations using liver stiffness measurement with FibroScan and FIB-4 or NFS (two complementary, easy-to-perform, and widely available tools) in 179 Sicilian patients [24]. They showed that the combination of liver stiffness measurement with NFS was able to accurately diagnose or exclude the presence of severe liver fibrosis, also reducing of about 50–60% the number of needed diagnostic liver biopsies.

Two years later, in a multicenter study, Petta et al. evaluated these combinations, liver stiffness measurement with FIB-4 or NFS [25]. Again, the paired combination of liver stiffness measurement with NFS or FIB-4 strongly reduced the likelihood of wrongly classified patients (ranging from 2.7% to 2.6%), at the price of a high uncertainty area (ranging from 54.1% to 58.2%), and of a low overall accuracy (ranging from 43% to 39.1%). The serial combination with the second test used in patients in the grey area of the first test and in those with high liver stiffness measurement values

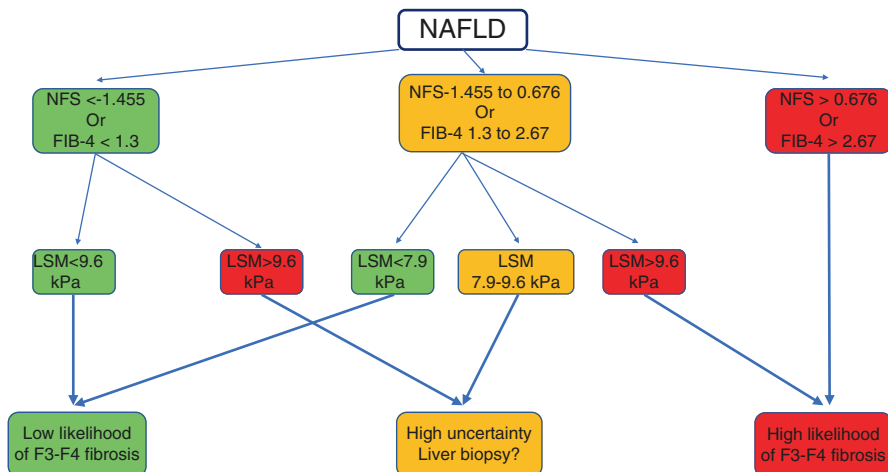


**Fig. 10.1** Suggested algorithm for the noninvasive assessment of F3-F4 fibrosis in patients with NAFLD [25]. *LSM* liver stiffness measurement. *NFS* NAFLD fibrosis score

(>9.6 kPa) or low NFS or FIB-4 values (<1.455 and <1.30, respectively) overall increased the diagnostic performance generating an accuracy ranging from 69.8% to 70.1%, an uncertainty area ranging from 18.9% to 20.4% and a rate of wrong classification ranging from 9.2% to 11.3%. They proposed an algorithm for the diagnosis of advanced fibrosis in NAFLD patients (Fig. 10.1).

At this time, there are no guidelines that recommend the combination of liver stiffness measurement with any biomarker.

## Prognosis of NAFLD Patients

The risk of death from liver disease increases by a factor of 50–80 for patients with NAFLD who have F3 or F4 fibrosis, as compared with those who have NAFLD with little or no fibrosis [26]. In 2015, experts at the Baveno VI Consensus Workshop recommended LSM cutoffs of 10 and 15 kPa to rule out and rule in compensated advanced chronic liver disease (cACLD), respectively [27]. Only a few studies evaluated the role of liver stiffness as prognostic factor in NAFLD patients.

A recent study validated Baveno VI criteria in 790 patients with NAFLD-related compensated cirrhosis. The best thresholds to rule out varices needing treatment were identified as platelet count >110,000/mm<sup>3</sup> and liver stiffness <30 kPa for M probe, and platelet count >110,000/mm<sup>3</sup> and liver stiffness <25 kPa for XL probe [28]. Further studies are needed to evaluate the role of spleen stiffness measurement for the diagnosis and follow-up of portal hypertension.

Another study showed the prognosis accuracy of liver stiffness measurement with FibroScan for the prediction of mortality from liver-related complication in

360 NAFLD patients [29]. In this study, the prognostic accuracy of liver stiffness was 0.725 (0.659–0.782) for all-cause mortality, 0.885 (0.818–0.947) for mortality from liver-related complication, and 0.704 (0.630–0.776) for mortality from extra-hepatic cause.

However, prospective cohort studies are needed to examine the longitudinal association between baseline imaging-based modalities and their longitudinal change over time and incident development of cirrhosis, risk of hepatic decompensation, need for liver transplant, and liver-related mortality.

## Fibrosis Assessment in Children with NAFLD

Only a few studies are available for the evaluation of liver fibrosis in NAFLD children. In a prospective study of 67 adolescents (age range, 10–17 years; mean body mass index, 34.7 kg/m<sup>2</sup>) with biopsy-proven NAFLD, liver stiffness was measured by using time-harmonic elastography. This method uses a bed-type actuator device for stimulation and real-time analysis of continuous multifrequency vibrations, allowing liver stiffness measurement of the entire liver for depths of up to 14 cm. Unlike classic US-based elastography methods, which use transient stimulations, time-harmonic elastography exploits a continuous flux of shear wave energy generated by a vibration bed. The continuous influx of wave energy ensures the entire liver is illuminated by shear waves. The displayed quantity is shear wave speed similar to acoustic radiation force impulse-based methods; however, it is distinct from transient elastography (which measures Young moduli) and MR elastography (which classically displays shear modulus maps) [30]. Time-harmonic elastography was feasible in all patients (0% failure rate), including 70% ( $n = 47$ ) of individuals with extreme obesity (body mass index above the 99.5th percentile). AUC analysis for the detection of any fibrosis ( $\geq$ stage F1), moderate fibrosis ( $\geq$ stage F2), and advanced fibrosis ( $\geq$ stage F3) was 0.88 (95% confidence interval [CI]: 0.80, 0.96), 0.99 (95% CI: 0.98, 1.00), and 0.88 (95% CI: 0.80, 0.96), respectively.

A retrospective study included 86 patients younger than 21 years of age who underwent MRE and liver biopsy within 3 months [31]. Fifty-one patients (59.3%) had Ludwig stage 2 or higher fibrosis (only 2 children with cirrhosis). The area under the ROC curve for Ludwig stage 0–1 versus stage 2 or higher fibrosis was 0.70 (95% confidence interval 0.59–0.81). Optimal stiffness cutoff was 2.27 kPa with 68.6% sensitivity (95% CI: 57.2%, 80.1%) and 74.3% specificity (95% CI: 63.5%, 85.1%). In this study, steatosis or inflammation were confounding factors for the diagnosis of liver fibrosis.

At last, a retrospective cohort study including 65 children evaluated the progression of liver fibrosis using MRE [32]. Time from first to last MRE was  $27 \pm 14$  months. Liver stiffness decreased in 20% of patients, and increased in 22% of patients. There was no correlation between change in liver stiffness and change in ALT.

In 2019, liver stiffness measurement is not recommended in clinical practice for the diagnosis of liver fibrosis in NAFLD children.

## Liver Stiffness as Screening Tool

There is mounting evidence that besides increasing the risk of cirrhosis, end-stage liver disease, and hepatocellular carcinoma, nonalcoholic fatty liver disease (NAFLD) also affects risk of disease in organs beyond the liver [33]. For example, NAFLD is an independent risk factor for cardiovascular disease (CVD) [34], type 2 diabetes [35], and chronic kidney disease [36]. Moreover, the prevalence of NAFLD could be around 25% in general population. Therefore, screening of liver fibrosis or cirrhosis in all these populations should be evaluated.

A population-based, cross-sectional study was performed in the Barcelona metropolitan area [37]. Subjects aged 18–75 years old were identified randomly from citizens included in the primary health care registry. Liver fibrosis was estimated by measuring liver stiffness with transient elastography in 3076 subjects. Prevalence estimate of increased liver stiffness  $>9.0$  kPa was 3.6%. Factors independently associated with increased liver stiffness were male sex, abdominal obesity, type 2 diabetes, serum glucose, high-density lipoprotein, and triglyceride levels. They propose a value less than 9.2 kPa to be used for screening purposes.

In a community-based diabetic population, liver stiffness was measured in 705 patients [38]. Overall, 7.3% exhibited advanced fibrosis (liver stiffness  $\geq 9.6$  kPa). By multivariate analysis, factors associated with severe fibrosis were age, overweight, and high GGT.

In another study, screening diabetic patients for nonalcoholic fatty liver disease with liver stiffness measurement was performed in a prospective cohort study of 1884 patients [39]. The proportion of patients with increased liver stiffness measurement was 17.7% (95% CI 16.0% to 19.5%). By multivariable analysis, longer duration of diabetes, higher body mass index, increased ALT, and spot urine albumin: creatinine ratio and lower high-density lipoprotein-cholesterol were associated with increased LSM. They concluded that diabetic patients with high BMI and dyslipidemia are at particularly high risk and may be the target for liver assessment.

Another prospective study evaluated 277 patients hospitalized for their diabetes [40]. Severe fibrosis was predicted when FibroTest (blood marker) was  $>0.59$  or liver stiffness  $>8.7$  kPa. The prevalence of severe fibrosis was 15.5%. By multivariate analysis, factors associated with severe fibrosis were age  $>50$  years, type 2 diabetes, no retinopathy, and past history of foot ulcer.

A cross-sectional analysis of a prospective study that included 100 consecutively enrolled diabetics was performed using MRE [41]. The prevalence of advanced fibrosis (defined as MRE  $\geq 3.6$  kPa) was 7.1%. Patients with NAFLD were younger and had higher mean BMI, waist circumference, and prevalence of metabolic syndrome. Only 26% of those with NAFLD had elevated alanine aminotransferase. However, its wider application is limited by cost and availability. In particular, these drawbacks make it unlikely that MRE can be applied as a screening test.

A study evaluated the utility of liver stiffness measurement (FibroScan, XL probe) for assessment of liver fibrosis in 76 morbidly obese individuals (mean body mass index  $45.2 \pm 7.1$  kg/m<sup>2</sup>). FibroScan success rate was 87.9%. Area under



receiver operator characteristic curve of liver stiffness measurement for prediction of significant fibrosis and advanced fibrosis was 0.65 (95% confidence interval [CI]: 0.52–0.77) and 0.83 (95% CI: 0.72–0.94), respectively [42].

According to these studies, EASL-EASD-EASO guidelines are as follow: in patients with type 2 diabetes, the presence of NAFLD should be looked for irrespective of liver enzyme levels, since type 2 diabetes patients are at high risk of disease progression (A2) [43].

However, AASLD Guidance Statements are quite different [22]. Routine screening for NAFLD in high-risk groups attending primary care, diabetes, or obesity clinics is not advised at this time because of uncertainties surrounding diagnostic tests and treatment options, along with lack of knowledge related to long-term benefits and cost-effectiveness of screening. There should be a high index of suspicion for NAFLD and NASH in patients with type 2 diabetes. Clinical decision aids such as NFS or fibrosis-4 index (FIB-4) or vibration controlled transient elastography (FibroScan) can be used to identify those at low or high risk for advanced fibrosis (bridging fibrosis or cirrhosis).

At this time, there are no specific guidelines for the screening of patients with a past history of cardiovascular event.

## How to Use Liver Stiffness in Clinical Practice?

In clinical practice, at bedside, a recurrent question is “which cutoff should we use?” The choice of a cutoff depends on disease and objective. Indeed, cutoffs are often different according to the disease for each stage of liver fibrosis. For example, cutoffs in HBV patients should consider ALT level. Moreover, in some cases, the objective is to have a more sensitive cutoff and, in some cases, the objective is to have a more specific cutoff.

With FibroScan, the cutoff of 8.7 kPa for the diagnosis of advanced fibrosis has a sensitivity of 88.4%, a specificity of 62.9%, a negative predictive value of 89.8% and a positive predictive value of 59.4% [29]. At a cutoff <8 kPa, FibroScan has a 94% to 100% negative predictive value. At a cutoff value of 7.9 kPa, the sensitivity, specificity, and positive and negative predictive values for advanced fibrosis or greater disease are 91%, 75%, 52%, and 97%, respectively [9]. At last, a meta-analysis proposed a cutoff of 7.2 kPa with a negative predictive value to exclude advanced fibrosis or cirrhosis of 89% (95% CI 84–95%) [44]. To rule in advanced fibrosis or cirrhosis, a cutoff of 9.3 kPa was proposed with the XL probe [8]. Using the latest model of FibroScan, probe selection can be done automatically. A recent study performed in US, Youden cutoff proposed values for  $F \geq F2$ ,  $F \geq F3$  and  $F = F4$  were 8.2 kPa, 9.7 kPa, and 13.6 kPa, respectively [12]. Recently, Wong et al. proposed simple liver stiffness measurement cutoffs of <10 kPa and  $\geq 15$  kPa to exclude and diagnose compensated advanced chronic liver disease, respectively [45].

With ARFI, the proposed cutoffs are 1.55–1.61 m/s for advanced fibrosis and 1.80–1.87 m/s for cirrhosis [46, 47]. With Aixplorer, the cutoff values with sensitivity



above 90% are 8.3 kPa, and 10.5 kPa for advanced fibrosis and cirrhosis, respectively [14].

With MRE, a threshold  $>4.39$  kPa results in a sensitivity of 90.9% and a specificity of 97.3% for diagnosing advanced fibrosis [48]. Using a stiffness cutoff of 3.63 kPa, MRE has a sensitivity of 0.86 (95% confidence interval [CI], 0.65–0.97), a specificity of 0.91 (95% CI, 0.83–0.96), a PPV of 0.68 (95% CI, 0.48–0.84), and a NPV of 0.97 (95% CI, 0.91–0.99) with an AUROC of 0.924 for diagnosing advanced fibrosis [20, 49].

## Follow-Up With or Without Treatment

One of the important surrogates for advanced liver disease, especially in NAFLD, is documentation of progressive liver fibrosis. In a recent meta-analysis, fibrosis progression in patients with histological NASH at baseline showed a mean annual fibrosis progression rate of 0.09 (95% CI, 0.06–0.12) [1]. Importantly, longitudinal data correlating changes in histological severity and in noninvasive measurements are urgently needed.

A recent study shown that approximately 15–19% relative reduction in MRE-derived liver stiffness corresponds to a 5% reduction in body weight (usually the lower threshold associated with improvement in liver histology in NASH) [50]. However, the exact clinical significance of a change in liver stiffness measurement still remains to be defined.

Recently, data from patients with NASH and stage 2 or 3 fibrosis enrolled in a phase II study of selonsertib were evaluated. Pre- and posttreatment assessments included centrally read MRE, and liver biopsies evaluated according to the NASH Clinical Research Network classification and the nonalcoholic fatty liver disease activity score (NAS). Among 54 patients with MRE and biopsies at baseline and week 24, 18 (33%) had fibrosis improvement ( $\geq 1$ -stage reduction) after undergoing 24 weeks of treatment with the study drug. The area under the receiver operating characteristic curve (AUROC) of MRE to predict fibrosis improvement was 0.62 (95% CI 0.46–0.78) and the optimal threshold was a  $\geq 0\%$  relative reduction. At this threshold, MRE had 67% sensitivity, 64% specificity, 48% positive predictive value, 79% negative predictive value. These preliminary data support the further evaluation of MRE for the longitudinal assessment of histologic response in patients with NASH [51].

In another study from Japan, LSM by TE was carried out for 97 biopsy-proven NAFLD patients and 34 patients underwent 10-year LSM reassessments, 14 of them with paired biopsies [52]. Over a 10-year period, 32.4% had LS progression, 50% had static disease, and 17.6% had LS improvement. From among the initially diagnosed nonalcoholic steatohepatitis patients, 18% had progressed to F4 (cirrhosis) 10 years later. In this cohort, none of the patients who had been initially diagnosed as F0 by TE had progressed to cirrhosis 10 years later. The changes in LS were correlated with the change in the histological fibrosis stage, the NAFLD

activity score, and the change in the sum of the steatosis, activity, and fibrosis score. Improving more than 1 BMI (body mass index in  $\text{kg}/\text{m}^2$ ) and having a higher initial aspartate aminotransferase, alanine aminotransferase (ALT), or ALT responder ( $>30\%$  improvement or reduction to less than 40 IU/L) were factors contributing to LS improvements ( $\geq 2$  kPa) [52].

In a recent study [53] on 2251 prospectively recruited NAFLD patients, the median follow-up time was 27 months. During the study period, 55 patients died, and three patients had liver transplantation. Only 0.9% of patients ( $n = 21$ ) had liver-related event (either decompensation or HCC) while 142 (6.3%) developed cancer (excluding HCC). 151 (6.7%) had a cardiovascular event during follow-up. Overall survival significantly decreased with increasing baseline LS. On multivariate analysis, independent predictors (adjusted HR = aHR) for overall survival were: baseline LSM with aHR = 2.85, age with aHR = 1.11 and male sex with aHR = 2.05. Patients with elevated LS showed more significant cardiovascular and liver events but no other cancers. Interestingly, there was no cutoff for no risk of HCC. Thus, the incidence of HCC increased with baseline LS ( $<12$  kPa: 0.32%; 12–18 kPa: 0.58%; 18–38 kPa 9.26% and  $>38$  kPa: 13.3%). Taken together, this study concludes to use initial LS values to predict survival, cardiovascular, and liver complications [53].

## Unresolved Issues to Be Addressed in the Future

Further advances are needed to identify patients at risk of fibrosis progression and at risk of complications. The evolution of liver stiffness (increase/decrease) over time needs to be described and understood. The diagnosis of NASH is a keypoint in the management of patients with NAFLD. The usefulness of liver stiffness for the diagnosis of NASH is a challenge for the next years. The cost-effectiveness of utilizing MRE vs FibroScan vs other methods and/or biopsy must also be evaluated to develop optimal diagnostic strategies for diagnosing NAFLD-associated fibrosis. At last, cost-effectiveness studies are needed to evaluate different strategies, for example the sequential use of biomarker (e.g. FIB-4) followed by liver stiffness measurement.

## Conclusion

For equipped centers, ultrasound-based elastography such as FibroScan and shear wave elastography has moderate to high accuracy in diagnosing advanced fibrosis or cirrhosis and can be used in routine clinical practice. MRE has a higher success rate and accuracy than ultrasound-based technologies, but is limited by cost and availability. Moreover, it is not practical to be used in routine clinical care across the millions of individuals who are at risk of advanced fibrosis. However, it can be used in clinical trials to identify drugs with potential antifibrotic effects. FibroScan offers

real-time results and is performed as a point-of-care test. It can be used as a practical tool for identifying patients with NAFLD at high as well as minimal risk for advanced fibrosis. This approach adds value to the clinic visit as it allows for in-clinic counseling and a decision to pursue a liver biopsy can be made expeditiously. This information can help clinicians better manage their patients with NAFLD. Similar to FibroScan, SWE or ARFI may also be utilized for risk stratification of patients with NAFLD, based upon their availability and local expertise and familiarity with their cutoff points for the presence of advanced fibrosis, shear wave speed or stiffness, respectively. Furthermore, a discussion with the local hepatologist and/or radiologist should be performed to decide on the preferred techniques, requirements for operator experience, and pre-specified criteria for reporting to ensure correct interpretation of results.

## References

1. Younossi ZM, Koenig AB, Abdelatif D, Fazel Y, Henry L, Wymer M. Global epidemiology of nonalcoholic fatty liver disease-meta-analytic assessment of prevalence, incidence, and outcomes. *Hepatology*. 2016;64(1):73–84.
2. Flegal KM, Carroll MD, Ogden CL, Johnson CL. Prevalence and trends in obesity among US adults, 1999-2000. *JAMA*. 2002;288(14):1723–7.
3. Ogden CL, Carroll MD, Lawman HG, Fryar CD, Kruszon-Moran D, Kit BK, et al. Trends in obesity prevalence among children and adolescents in the United States, 1988–1994 through 2013–2014. *JAMA*. 2016;315(21):2292–9.
4. Goldberg D, Ditah IC, Saeian K, Lalehzari M, Aronsohn A, Gorospe EC, et al. Changes in the prevalence of hepatitis C virus infection, nonalcoholic steatohepatitis, and alcoholic liver disease among patients with cirrhosis or liver failure on the waitlist for liver transplantation. *Gastroenterology*. 2017;152(5):1090–9.e1.
5. Singh S, Allen AM, Wang Z, Prokop LJ, Murad MH, Loomba R. Fibrosis progression in nonalcoholic fatty liver vs nonalcoholic steatohepatitis: a systematic review and meta-analysis of paired-biopsy studies. *Clin Gastroenterol Hepatol*. 2015;13(4):643–54.e1-9; quiz e39-40.
6. European Association for Study of Liver; Asociacion Latinoamericana para el Estudio del Hígado. EASL-ALEH clinical practice guidelines: non-invasive tests for evaluation of liver disease severity and prognosis. *J Hepatol*. 2015;63(1):237–64.
7. Xiao G, Zhu S, Xiao X, Yan L, Yang J, Wu G. Comparison of laboratory tests, ultrasound, or magnetic resonance elastography to detect fibrosis in patients with nonalcoholic fatty liver disease: a meta-analysis. *Hepatology*. 2017;66(5):1486–501.
8. Wong VW, Vergniol J, Wong GL, Foucher J, Chan AW, Chermak F, et al. Liver stiffness measurement using XL probe in patients with nonalcoholic fatty liver disease. *Am J Gastroenterol*. 2012;107(12):1862–71.
9. Wong VW, Vergniol J, Wong GL, Foucher J, Chan HL, Le Bail B, et al. Diagnosis of fibrosis and cirrhosis using liver stiffness measurement in nonalcoholic fatty liver disease. *Hepatology*. 2010;51(2):454–62.
10. Siddiqui MS, Yamada G, Vuppalanchi R, Van Natta M, Loomba R, Guy C, et al. Diagnostic accuracy of noninvasive fibrosis models to detect change in fibrosis stage. *Clin Gastroenterol Hepatol*. 2019;17(9):1877–85.e5.
11. Chow JC, Wong GL, Chan AW, Shu SS, Chan CK, Leung JK, et al. Repeating measurements by transient elastography in non-alcoholic fatty liver disease patients with high liver stiffness. *J Gastroenterol Hepatol*. 2019;34(1):241–8.

12. Eddowes PJ, Sasso M, Allison M, Tsochatzis E, Anstee QM, Sheridan D, et al. Accuracy of FibroScan controlled attenuation parameter and liver stiffness measurement in assessing steatosis and fibrosis in patients with nonalcoholic fatty liver disease. *Gastroenterology*. 2019;156(6):1717–30.
13. Liu H, Fu J, Hong R, Liu L, Li F. Acoustic radiation force impulse elastography for the non-invasive evaluation of hepatic fibrosis in non-alcoholic fatty liver disease patients: a systematic review & meta-analysis. *PLoS One*. 2015;10(7):e0127782.
14. Cassinotto C, Boursier J, de Ledinghen V, Lebigot J, Lapyuyade B, Cales P, et al. Liver stiffness in nonalcoholic fatty liver disease: a comparison of supersonic shear imaging, FibroScan, and ARFI with liver biopsy. *Hepatology*. 2016;63(6):1817–27.
15. Singh S, Venkatesh SK, Wang Z, Miller FH, Motosugi U, Low RN, et al. Diagnostic performance of magnetic resonance elastography in staging liver fibrosis: a systematic review and meta-analysis of individual participant data. *Clin Gastroenterol Hepatol*. 2015;13(3):440–51.e6.
16. Loomba R, Cui J, Wolfson T, Haufe W, Hooker J, Szeverenyi N, et al. Novel 3D magnetic resonance elastography for the noninvasive diagnosis of advanced fibrosis in NAFLD: a prospective study. *Am J Gastroenterol*. 2016;111(7):986–94.
17. Pavlides M, Banerjee R, Tunnicliffe EM, Kelly C, Collier J, Wang LM, et al. Multiparametric magnetic resonance imaging for the assessment of non-alcoholic fatty liver disease severity. *Liver Int*. 2017;37(7):1065–73.
18. Imajo K, Kessoku T, Honda Y, Tomeno W, Ogawa Y, Mawatari H, et al. Magnetic resonance imaging more accurately classifies steatosis and fibrosis in patients with nonalcoholic fatty liver disease than transient elastography. *Gastroenterology*. 2016;150(3):626–37.e7.
19. Park CC, Nguyen P, Hernandez C, Bettencourt R, Ramirez K, Fortney L, et al. Magnetic resonance elastography vs transient elastography in detection of fibrosis and noninvasive measurement of steatosis in patients with biopsy-proven nonalcoholic fatty liver disease. *Gastroenterology*. 2017;152(3):598–607.e2.
20. Chen J, Yin M, Talwalkar JA, Oudry J, Glaser KJ, Smyrk TC, et al. Diagnostic performance of MR elastography and vibration-controlled transient elastography in the detection of hepatic fibrosis in patients with severe to morbid obesity. *Radiology*. 2017;283(2):418–28.
21. Cui J, Heba E, Hernandez C, Haufe W, Hooker J, Andre MP, et al. Magnetic resonance elastography is superior to acoustic radiation force impulse for the Diagnosis of fibrosis in patients with biopsy-proven nonalcoholic fatty liver disease: a prospective study. *Hepatology*. 2016;63(2):453–61.
22. Chalasani N, Younossi Z, Lavine JE, Charlton M, Cusi K, Rinella M, et al. The diagnosis and management of nonalcoholic fatty liver disease: Practice guidance from the American Association for the Study of Liver Diseases. *Hepatology*. 2018;67(1):328–57.
23. Lim JK, Flamm SL, Singh S, Falck-Ytter YT, Clinical Guidelines Committee of the American Gastroenterological A. American Gastroenterological Association Institute Guideline on the role of elastography in the evaluation of liver fibrosis. *Gastroenterology*. 2017;152(6):1536–43.
24. Petta S, Vanni E, Bugianesi E, Di Marco V, Camma C, Cabibi D, et al. The combination of liver stiffness measurement and NAFLD fibrosis score improves the noninvasive diagnostic accuracy for severe liver fibrosis in patients with nonalcoholic fatty liver disease. *Liver Int*. 2015;35(5):1566–73.
25. Petta S, Wong VW, Camma C, Hiriart JB, Wong GL, Vergniol J, et al. Serial combination of non-invasive tools improves the diagnostic accuracy of severe liver fibrosis in patients with NAFLD. *Aliment Pharmacol Ther*. 2017;46(6):617–27.
26. Diehl AM, Day C. Cause, pathogenesis, and treatment of nonalcoholic steatohepatitis. *N Engl J Med*. 2017;377(21):2063–72.
27. de Franchis R. Expanding consensus in portal hypertension - report of the Baveno VI Consensus Workshop: stratifying risk and individualizing care for portal hypertension. *J Hepatol*. 2015;63(3):743–52.
28. Petta S, Sebastiani G, Bugianesi E, Vigano M, Wong VW, Berzigotti A, et al. Non-invasive prediction of esophageal varices by stiffness and platelet in non-alcoholic fatty liver disease cirrhosis. *J Hepatol*. 2018;69(4):878–85.

29. Boursier J, Vergniol J, Guillet A, Hiriart JB, Lannes A, Le Bail B, et al. Diagnostic accuracy and prognostic significance of blood fibrosis tests and liver stiffness measurement by FibroScan in non-alcoholic fatty liver disease. *J Hepatol.* 2016;65(3):570–8.
30. Hudert CA, Tzschatzsch H, Guo J, Rudolph B, Blaker H, Loddenkemper C, et al. US time-harmonic elastography: detection of liver fibrosis in adolescents with extreme obesity with nonalcoholic fatty liver disease. *Radiology.* 2018;288(1):99–106.
31. Trout AT, Sheridan RM, Serai SD, Xanthakos SA, Su W, Zhang B, et al. Diagnostic performance of MR elastography for liver fibrosis in children and young adults with a spectrum of liver diseases. *Radiology.* 2018;287(3):824–32.
32. Mouzaki M, Trout AT, Arce-Clachar AC, Bramlage K, Kuhnell P, Dillman JR, et al. Assessment of nonalcoholic fatty liver disease progression in children using magnetic resonance imaging. *J Pediatr.* 2018;201:86–92.
33. Byrne CD, Targher G. NAFLD: a multisystem disease. *J Hepatol.* 2015;62(1 Suppl):S47–64.
34. Targher G, Byrne CD, Lonardo A, Zoppini G, Barbui C. Non-alcoholic fatty liver disease and risk of incident cardiovascular disease: a meta-analysis. *J Hepatol.* 2016;65(3):589–600.
35. Mantovani A, Byrne CD, Bonora E, Targher G. Nonalcoholic fatty liver disease and risk of incident Type 2 diabetes: a meta-analysis. *Diabetes Care.* 2018;41(2):372–82.
36. Mantovani A, Zaza G, Byrne CD, Lonardo A, Zoppini G, Bonora E, et al. Nonalcoholic fatty liver disease increases risk of incident chronic kidney disease: a systematic review and meta-analysis. *Metabolism.* 2018;79:64–76.
37. Caballeria L, Pera G, Arteaga I, Rodríguez L, Aluma A, Morillas RM, et al. High prevalence of liver fibrosis among european adults with unknown liver disease: a population-based study. *Clin Gastroenterol Hepatol.* 2018;16(7):1138–45.e5.
38. Roulot D, Roudot-Thoraval F, Kouacou N, Costes JL, Elourimi G, et al. Concomitant screening for liver fibrosis and steatosis in French type 2 diabetic patients using Fibroscan. *Liver Int.* 2017;37(12):1897–906.
39. Kwok R, Choi KC, Wong GL, Zhang Y, Chan HL, Luk AO, et al. Screening diabetic patients for non-alcoholic fatty liver disease with controlled attenuation parameter and liver stiffness measurements: a prospective cohort study. *Gut.* 2016;65(8):1359–68.
40. de Ledinghen V, Vergniol J, Gonzalez C, Foucher J, Maury E, Chemineau L, et al. Screening for liver fibrosis by using FibroScan((R)) and FibroTest in patients with diabetes. *Dig Liver Dis.* 2012;44(5):413–8.
41. Doycheva I, Cui J, Nguyen P, Costa EA, Hooker J, Hofflich H, et al. Non-invasive screening of diabetics in primary care for NAFLD and advanced fibrosis by MRI and MRE. *Aliment Pharmacol Ther.* 2016;43(1):83–95.
42. Garg H, Aggarwal S, Shalimar, Yadav R, Datta Gupta S, Agarwal L, et al. Utility of transient elastography (fibroscan) and impact of bariatric surgery on nonalcoholic fatty liver disease (NAFLD) in morbidly obese patients. *Surg Obes Relat Dis.* 2018;14(1):81–91.
43. EASL. EASL-EASD-EASO clinical practice guidelines for the management of non-alcoholic fatty liver disease. *J Hepatol.* 2016;64(6):1388–402.
44. Kwok R, Tse YK, Wong GL, Ha Y, Lee AU, Ngu MC, et al. Systematic review with meta-analysis: non-invasive assessment of non-alcoholic fatty liver disease--the role of transient elastography and plasma cytokeratin-18 fragments. *Aliment Pharmacol Ther.* 2014;39(3):254–69.
45. Wong VW, Irls M, Wong GL, Shili S, Chan AW, Merrouche W, et al. Unified interpretation of liver stiffness measurement by M and XL probes in non-alcoholic fatty liver disease. *Gut.* 2019;68(11):2057–64.
46. Friedrich-Rust M, Nierhoff J, Lupsor M, Sporea I, Fierbinteanu-Braticcivici C, Strobel D, et al. Performance of acoustic radiation force impulse imaging for the staging of liver fibrosis: a pooled meta-analysis. *J Virul Hepat.* 2012;19(2):e212–9.
47. Nierhoff J, Chavez Ortiz AA, Herrmann E, Zeuzem S, Friedrich-Rust M. The efficiency of acoustic radiation force impulse imaging for the staging of liver fibrosis: a meta-analysis. *Eur Radiol.* 2013;23(11):3040–53.
48. Costa-Silva L, Ferolla SM, Lima AS, Vidigal PVT, Ferrari TCA. MR elastography is effective for the non-invasive evaluation of fibrosis and necroinflammatory activity in patients with nonalcoholic fatty liver disease. *Eur J Radiol.* 2018;98:82–9.

49. Loomba R, Wolfson T, Ang B, Hooker J, Behling C, Peterson M, et al. Magnetic resonance elastography predicts advanced fibrosis in patients with nonalcoholic fatty liver disease: a prospective study. *Hepatology*. 2014;60(6):1920–8.
50. Patel NS, Hooker J, Gonzalez M, Bhatt A, Nguyen P, Ramirez K, et al. Weight loss decreases magnetic resonance elastography estimated liver stiffness in nonalcoholic fatty liver disease. *Clin Gastroenterol Hepatol*. 2017;15(3):463–4.
51. Jayakumar S, Middleton MS, Lawitz EJ, Mantry PS, Caldwell SH, Arnold H, et al. Longitudinal correlations between MRE, MRI-PDFF, and liver histology in patients with non-alcoholic steatohepatitis: Analysis of data from a phase II trial of selonsertib. *J Hepatol*. 2019;70(1):133–41.
52. Nogami A, Yoneda M, Kobayashi T, Kessoku T, Honda Y, Ogawa Y, et al. Assessment of 10-year changes in liver stiffness using vibration-controlled transient elastography in non-alcoholic fatty liver disease. *Hepatol Res*. 2019;49(8):872–80.
53. Shili S, Wong GL-H, Jean-Baptiste H, Liu L, Chermak F, Shu S, et al. SAT-288-Liver stiffness measurement predicts long-term survival and complications in non-alcoholic fatty liver disease. *J Hepatol*. 2019;70(1):e763.e4.
54. Jiang W, Huang S, Teng H, Wang P, Wu M, Zhou X, et al. Diagnostic accuracy of point shear wave elastography and transient elastography for staging hepatic fibrosis in patients with non-alcoholic fatty liver disease: a meta-analysis. *BMJ Open*. 2018;8(8):e021787.
55. Lee MS, Bae JM, Joo SK, Woo H, Lee DH, Jung YJ, et al. Prospective comparison among transient elastography, supersonic shear imaging, and ARFI imaging for predicting fibrosis in nonalcoholic fatty liver disease. *PLoS One*. 2017;12(11):e0188321.
56. Petta S, Wong VW, Camma C, Hiriart JB, Wong GL, Marra F, et al. Improved noninvasive prediction of liver fibrosis by liver stiffness measurement in patients with nonalcoholic fatty liver disease accounting for controlled attenuation parameter values. *Hepatology*. 2017;65(4):1145–55.
57. Loong TC, Wei JL, Leung JC, Wong GL, Shu SS, Chim AM, et al. Application of the combined FibroMeter vibration-controlled transient elastography algorithm in Chinese patients with non-alcoholic fatty liver disease. *J Gastroenterol Hepatol*. 2017;32(7):1363–9.
58. Tapper EB, Challies T, Nasser I, Afdhal NH, Lai M. The performance of vibration controlled transient elastography in a US cohort of patients with nonalcoholic fatty liver disease. *Am J Gastroenterol*. 2016;111(5):677–84.
59. Petta S, Di Marco V, Camma C, Butera G, Cabibi D, Craxi A. Reliability of liver stiffness measurement in non-alcoholic fatty liver disease: the effects of body mass index. *Aliment Pharmacol Ther*. 2011;33(12):1350–60.
60. Palmeri ML, Wang MH, Rouze NC, Abdelmalek MF, Guy CD, Moser B, et al. Noninvasive evaluation of hepatic fibrosis using acoustic radiation force-based shear stiffness in patients with nonalcoholic fatty liver disease. *J Hepatol*. 2011;55(3):666–72.
61. Takeuchi H, Sugimoto K, Oshiro H, Iwatsuka K, Kono S, Yoshimasu Y, et al. Liver fibrosis: noninvasive assessment using supersonic shear imaging and FIB4 index in patients with non-alcoholic fatty liver disease. *J Med Ultrason*. 2018;45(2):243–9.
62. Herrmann E, de Ledinghen V, Cassinotto C, Chu WC, Leung VY, Ferraioli G, et al. Assessment of biopsy-proven liver fibrosis by two-dimensional shear wave elastography: an individual patient data-based meta-analysis. *Hepatology*. 2018;67(1):260–72.

# Chapter 11

## Liver Stiffness in Alcoholic Liver Disease



Sebastian Mueller

### Specific Diagnostic Challenges in Patients with ALD

Alcohol-related liver disease (ALD) is the most frequent cause of severe liver diseases in Europe and according to WHO, more than 40% of the liver deaths are attributed to alcohol [1]. In addition, the number of liver transplantation for patients with ALD-related cirrhosis has increased over the past two decades, both in Europe and in the USA [2, 3]. Despite this high burden of ALD, it is unfortunate that most patients are diagnosed at the decompensation stage normally presenting with ascites or jaundice. Moreover, a large proportion of newly diagnosed patients with cirrhosis had recent consultations in primary care or emergency units [4], without any intervention. ALD includes a wide spectrum of lesions ranging from steatosis to steatohepatitis, progressive liver fibrosis, cirrhosis and its complications [1]. Although steatosis is almost constant in heavy drinkers, it is estimated that only 10–20% will eventually develop cirrhosis [5]. Since the presence of advanced fibrosis or cirrhosis in compensated patients is the main predictor of long-term survival, it is of clinical importance to diagnose those patients with advanced fibrosis before decompensated stage, in order to promote abstinence and improve survival [6]. Liver diseases are in general hard to detect and commonly show no or only mild symptoms. Even end-stage liver cirrhosis remains undetected in routine laboratory testing or ultrasound screening in ca. 40% [7]. The diagnosis of ALD is further complicated by three major challenges: (1) underreporting by patients, (2) lack of good biomarkers for alcohol consumption, and (3) a rather diverse clinical presentation. These are the reasons why ALD is routinely underestimated both by physicians and health statistics [8, 9]. Therefore, the diagnosis of ALD normally must rely on a combination of clinical, laboratory,

---

S. Mueller (✉)

Department of Medicine and Center for Alcohol Research and Liver Diseases, Salem Medical Center, University of Heidelberg, Heidelberg, Germany  
e-mail: [sebastian.mueller@urz.uni-heidelberg.de](mailto:sebastian.mueller@urz.uni-heidelberg.de)



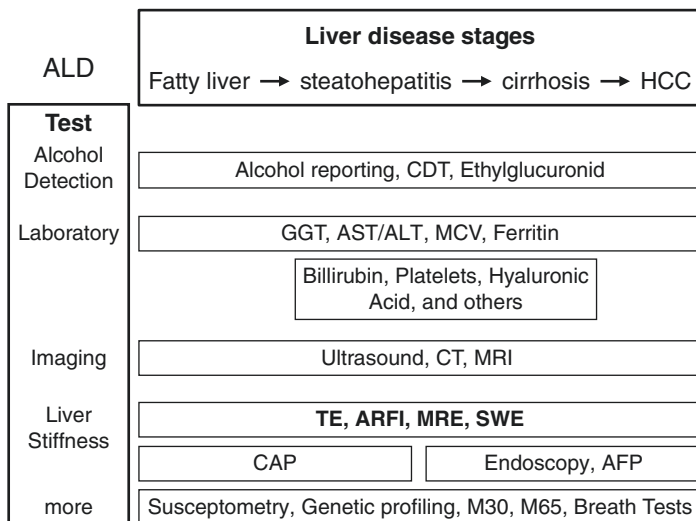


**Fig. 11.1** Role of various diagnostic measures for the assessment of ALD in different disease stages

elastographic, and imaging findings (Fig. 11.1) where elastography has gained an important novel role for early screening and follow-up.

### Elastography in Comparison to Other Alternative Methods to Assess Fibrosis

Although ALD follows the typical sequence of chronic liver diseases including alcoholic fatty liver, steatohepatitis, fibrosis, and eventually cirrhosis (Fig. 11.2), the early recognition of severe steatohepatitis and alcoholic cirrhosis is most important since it will save lives, prevent complications, and initiate follow-up programs [7]. Most important clinical end points are alcoholic liver cirrhosis and the rare and clinically defined alcoholic hepatitis (AH, ASH1). ASH1 should not be mismatched with the commonly and histologically detectable steatohepatitis (ASH, ASH2) (Fig. 11.2).

Since AH/ASH1 is very rare and there are still no early predictors, screening for liver problems in heavy drinkers should primarily focus on the screening for fibrosis [7].

In hepatology, liver biopsy is still essential in establishing the definite diagnosis or in ruling out additional or other causes of the disease. However, liver biopsy is an invasive procedure, with significant complications in up to 7% [10] and, with regard to fibrosis assessment, a sampling error of up to 30% [11–15]. Complications can encompass mild (pain and small bleedings in 6%) or severe (0.1%) complications and rarely fatal perforations and bleedings [16, 17]. In addition, and the context of



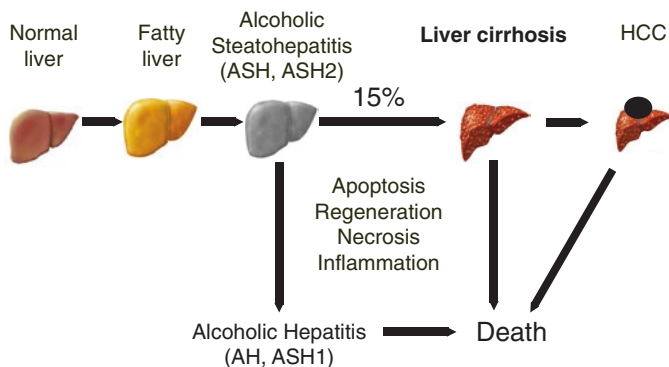


**Fig. 11.2** Natural course of ALD and importance to early detect liver fibrosis

ALD, heavy drinkers are typically less likely to see doctors and to undergo invasive diagnostic procedures. For instance, it has been estimated that less than 1% of patients with suspected ASH1/AH are biopsied although required according to international guidelines [18].

With respect to fibrosis assessment, all imaging techniques must rely on so-called “sure morphological signs of cirrhosis” such as nodular aspect of the liver or recanalization of the umbilical vein while splenomegaly or ascites are not specific. These imaging signs are only available in about half of ALD patients with manifest cirrhosis [7]. Serum markers have been long thought to allow for easy fibrosis screening [7, 19]. In ALD, however, a previous study clearly showed superiority of TE with regard to various serum markers [20]. Moreover, this was achieved without sophisticated algorithms. Although this will not be discussed in detail here, serum markers have important advantages (see Appendix Table A.1) when e.g., looking for affordable screening tools to be applied worldwide, especially in third world countries.

## Elastographic Assessment of Fibrosis in ALD

Several studies have been performed to directly compare the performance of TE with ARFI or 2D-SWE, however, no robust data are available on ALD. Therefore, this chapter focuses on TE. In contrast to popular liver diseases such as viral hepatitis, the performance of LS in ALD was assessed rather late. The major biopsy-proven studies on LS in patients with ALD are listed in Table 11.1. Early direct comparison with serum fibrosis markers showed a better performance of TE in patients with ALD [20] and AUROCs are typically  $>0.9$  to detect F4 cirrhosis. Although an excellent performance could be shown in all studies, they differ quite drastically regarding the cutoff values ranging from 11.5 to 25.8 kPa. This is primarily related to the presence of inflammation as assessed by transaminase levels [21]. In this study, it was shown that LS decreases in patients with ALD during alcohol

**Table 11.1** Liver stiffness and fibrosis stages in ALD (biopsy-proven studies)

Reference	Number of patients ( <i>n</i> )	Correlation	AUROC F4	Cutoff F4
Nahon et al. [39]	174	0.70, <i>P</i> < 0.0001	0.87	22.6
Nguyen-Khac et al. [20]	103	0.72, <i>P</i> < 0.014	0.92	19.5
Kim et al. [40]	45		0.97	25.8
Boursier et al. [41]	217	0.87, <i>P</i> < 0.02	0.91	17.3
Mueller et al. [21]	101	0.72, <i>P</i> < 0.001	0.92	11.5
Janssens et al. [42]	49		0.86	21.1
Fernandez et al. [43]	15		0.93	18.0
Thiele et al. [44]	199		0.94	16.9
Voican et al. [45]	217		0.73, <i>P</i> < 0.0001	0.93

**Table 11.2** Liver stiffness in response to alcohol detoxification and in relapsers

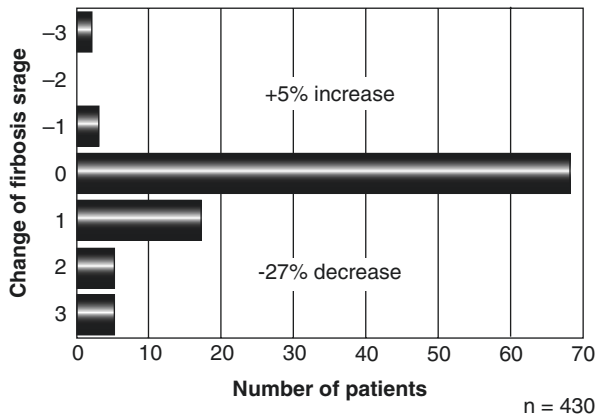
Ref.	Year/mean alcohol consumed/day	Patient number/ intervention	LS decrease before and after abstinence	Mean LS decrease (%)	Time of abstinence/ relapse
Mueller [33]	2010	50/detoxification	Mean LS 20.1–16.5 kPa	–17%	5.3 days
Gelsi et al. [24]	2011	23/abstinence relapse		–27%/D7 –20% D8–D60 abst. + 32% D8–D60 relapsers	7 days 9 weeks 9 weeks
	2012/150 g/day	137/abstinence	Median LS 7.2–6.1 kPa		7 days
Mueller et al. [22]	2019/98 g/day	Reduction of 45 g/day total alcohol consumption during 12 weeks treatment with Selincro (Nalmefene)	Mean LS 10.5–8.7 kPa Median LS 6.0–5.4 kPa	–13%	12 weeks
Mueller [34]	2019/181 g/day	23/complete abstinence	Mean LS 20.5–10.5 kPa	–48%	5.7 years
Mueller [34]	2019/194 g/day	23/continued drinking	Mean LS 14.8–18.1 kPa	+22% increase	5.3 years

D7 = day 7 of alcohol detoxification

withdrawal [21]. For more details see also the Chap. “Clinical Cases: Application and Interpretation of Liver Stiffness” in book part VII “How to Use LS in Clinical Practice.”

Table 11.2 summarizes the data on alcohol withdrawal/relapse and LS. Absolute alcohol withdrawal leads to ca. 20% decrease of LS within 1 week of alcohol detoxification which improves fibrosis stages in 27% (see Fig. 11.3).

**Fig. 11.3** Changes of fibrosis stage as assessed by liver stiffness after 1 week of alcohol detoxification. In 27%, a lower fibrosis stage is diagnosed due to resolution of inflammation. Unpublished data are from the Heidelberg cohort (n=430)



Even a 2 months reduction of alcohol consumption by 40% significantly reduced LS by 17% as shown recently using Selincro (Nalmefene) [22]. In another study, LS decreased significantly in 62 patients (45.3%) after complete alcohol detoxification, and there was a reduction in the estimated stage of fibrosis in 32 (23.3%). In contrast, an increase of LS was observed in 11.7% [23]. The proportion of patients with a significant decrease of LS after alcohol withdrawal increased from 41.7% to 66.7% with the duration of abstinence from 1 week to 9 weeks [24]. There are preliminary observations that long-term abstinence is even more beneficial as LS decreased by 50% if abstained from alcohol for 5 years [25].

As shown in Appendix Fig. A.7, AST levels show the best correlation with LS among other hepatitis markers both in patients with HCV and ALD for different fibrosis stages [26]. Why AST has this special impact on LS, is still not completely clear and may also be related to extrahepatic conditions as AST also occurs in muscle cells and erythrocytes. In the absence of elevated transaminases, cutoff values were almost identical between HCV and ALD for F1-2, F3 and F4 (HCV: 5.1, 9.0 and 11.9 kPa vs ALD: 4.9, 8.1 and 10.5 kPa). These cutoff values increase exponentially as a function of median AST level. The impact of AST on LS is higher in lobular-pronounced ALD as compared to portal tract-localized HCV (see Table 11.3, Fig. 11.5a and Appendix Fig. A.3).

In ALD, AST levels are typically higher as compared to ALT and in ca. 70% of patients the AST/ALT ratio is higher than two [27]. However, AST levels higher than 300 IU/L are rarely detected. In cirrhotic stages, transaminases may normalize while AST levels may be continuously increased despite the absence of alcohol consumption [26]. Appendix Fig. A.7 shows three-dimensionally the dependence of LS upon AST levels and fibrosis stage.

Other important confounders of elevated LS in heavy drinkers are signs of ballooning as assessed by caspase 3-cleaved cytokeratin 18 fragments (M30) levels and bilirubin levels at more advanced stages [28, 29]. Notably, M30/65 levels are

**Table 11.3** Exponential equations to define AST-adapted cutoff values for various fibrosis stages in patients with ALD or HCV. Note that equations correspond to Fig. 11.5a and also allow automated fibrosis scoring e.g. in Excel sheets or through web pages

Fibrosis stage	ALD	HCV
	AST-adapted LS cutoff value (kPa)	AST-adapted LS cutoff value (kPa)
F0 vs F1-2	$4.9 \times \exp(0.0022 \times \text{AST})$	$5.1 \times \exp(0.0018 \times \text{AST})$
F1-2 vs F3	$8.1 \times \exp(0.0046 \times \text{AST})$	$9.0 \times \exp(0.0023 \times \text{AST})$
F3 vs F4	$0.5 \times \exp(0.0069 \times \text{AST})$	$11.9 \times \exp(0.0035 \times \text{AST})$

Example of how to use equations e.g., for individual calculations or in databases with multiple patients: (a) determine AST-adapted cutoff values (F0 vs F1-2, F1-2 vs F3, F3 vs F4) using all three formulas. (b) Score fibrosis stage by comparing the original LS with the GOT-adapted cut of values

**Table 11.4** AUROCs and cutoff values of M30 and M65 for various important histological parameters

Histological parameter	M30		M65	
	Cutoff (U/L)	AUROC	Cutoff (U/L)	AUROC
Ballooning 1	334	0.787	926	0.789
Ballooning 2	426	0.795	972	0.786
Steatohepatitis 1	291	0.850	720	0.828
Steatohepatitis 2	334	0.776	926	0.784

All  $P < 0.05$

more sensitive as compared to transaminases and more specifically detect apoptotic cell death [28]. In contrast to M65 and AST levels, M30 levels significantly increase during alcohol withdrawal which highlights the specific role of apoptosis in ALD [28]. Table 11.4 provides cutoff values and AUROCS to detect important histological activity markers such as ballooning or steatohepatitis for M30 and M65.

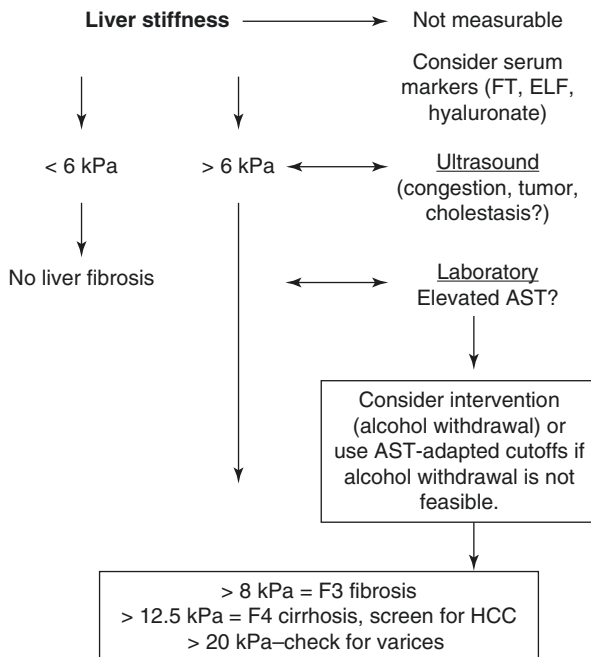
Finally, in the above mentioned actual meta-analysis [29] using more than 1000 patients, AST but also bilirubin concentrations had a significant effect on LS. The presence of histological features of asymptomatic and non-severe alcoholic hepatitis was associated with increased LS ( $P < 0.0001$ ). In a multivariate analysis, AST ( $P < 0.0001$ ) and bilirubin ( $P = 0.0002$ ) concentrations, and prothrombin activity ( $P = 0.01$ ), were independently associated with the presence of histological features of asymptomatic and non-severe alcoholic hepatitis. It remains to be confirmed whether bilirubin levels really improve the overall performance of LS-based fibrosis scoring, since ALD patients develop jaundice in end-stage cirrhosis where LS normally is higher than 30 kPa and the status of cirrhosis remains undoubted. In contrast, the so-called clinical alcoholic hepatitis (AH, ASH1) may develop high levels of bilirubin in the absence of drastic LS elevation.

## Clinical Practice with Available Ultrasound: Fibrosis Assessment in ALD Using LS

The findings above have been implemented in clinical algorithms to easily and accurately screen for fibrosis/cirrhosis in drinkers. Figure 11.4 shows a typical interpretation of LS if ultrasound and laboratory testing is available. After suspicion of ALD either by patients reporting, clinical, or laboratory signs, TE is performed directly after the abdominal ultrasound and routine blood tests. A minimum time of 5 min in horizontal position should be allowed for stable hemodynamics. During the ultrasound, liver size, spleen size, morphology, abnormalities such as congestion, cholestasis, morphological signs of cirrhosis, the presence of ascites, and the diameter of the inferior vena cava are assessed. TE is then performed either with the M probe or in cases of M probe failure, obvious obesity or ascites with the XL probe [30, 31]. Ascites is no contraindication for the XL probe and performs well [30]. If LS is elevated and patients have AST >100 U/ml, alcohol withdrawal for at least 2 weeks (optimal 4 weeks) is recommended followed by a second LS measurement. In patients with LS >30 kPa, the diagnosis of cirrhosis is settled despite steatohepatitis as measured by elevated transaminase levels. At these levels, the development of ascites is very likely.

This approach allows definitive noninvasive assessment of fibrosis stage in ca. 95%. Compared to conventional routine ultrasound, TE identifies twice as many patients with advanced fibrosis/cirrhosis (S. Mueller, unpublished) and has a smaller

**Fig. 11.4** Practical algorithm to assess fibrosis stage in patient with excessive alcohol consumption. AST-adapted cutoff values can be obtained from Fig. 11.5b or using the equations given in Table 11.3



sample error as compared to histology (3–5% versus 20–50%). In a recent French elastography screening study on more than 1000 apparently healthy people older than 45 years, 7.5% had a pathologically increased liver stiffness >8 kPa with 36% of them eventually being due to ALD [32]. Therefore, it is anticipated that these novel noninvasive screening tools will improve the early recognition and follow-up of patients with ALD, the most common and unfortunately too often underestimated liver disease.

## Fibrosis Assessment with TE Using Inflammation Adapted Cutoff Values

We have recently developed an algorithm to avoid repetitive reassessment of LS in ALD patients with elevated AST levels (Fig. 11.5). In this multicenter study with more than 2000 biopsy-proven patients with ALD and HCV, cutoff values for fibrosis increased exponentially as a function of median AST level. The impact of AST on LS was higher in lobular-pronounced ALD as compared to portal tract-localized HCV. Most notably, Cohen's weighted Kappa displayed an improved agreement of the novel AST-dependent cutoff values with histological fibrosis stage both for HCV (0.68 vs 0.65) and ALD (0.80 vs 0.76) [26]. While AST-adapted cutoff values allow an immediate assessment of fibrosis stage even in patients with pronounced steatohepatitis and avoid overestimation of fibrosis stages, it remains unclear why AST is

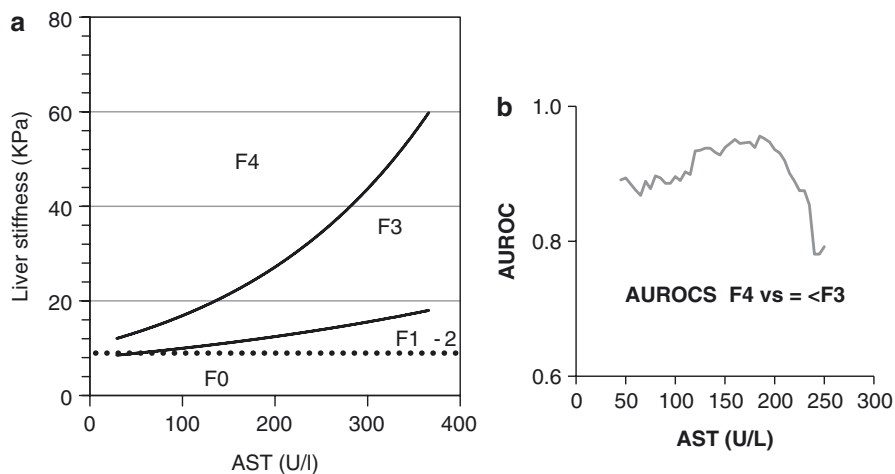


**Fig. 11.5** (a) AST-adapted cutoff values for LS in patients with ALD and (b) corresponding AUROC's to discriminate between F3 and F4 fibrosis. Note that cutoff values increase with AST elevation. Up to AST = 150–200, AST-adaptation shows improved diagnostic accuracy. Note that AST-adapted cutoff values can be also calculated using equations from Table 11.3

intensively correlated with LS since AST may not only be derived from hepatocytes but also myocytes and erythrocytes. It also remains to be studied whether indeed all patients with elevated AST levels will necessarily develop LS elevation.

## LS Follow-Up in Patients with ALD

LS measurement allows to monitor drinking activity and ALD progression since LS encompasses the sum of all pathological features from inflammation, ballooning to fibrosis. LS improved shortly after alcohol withdrawal in more than 80% [33]. As shown in Table 11.2, first unpublished preliminary data indicate that LS continues to decrease after further abstaining from alcohol up to 5 years. Thus, in 23 heavy drinkers who were followed-up for 5.5 years, LS decreased by almost 50%. Preliminary unpublished mortality data from a 10-year survey shows that LS seems to be the best univariate predictor of death in heavy drinkers [34]. A preliminary Kaplan Meier curve is shown in Appendix Fig. A.7. Accordingly, LS predict mortality independently from bilirubin and INR. A LS >12.5 is associated with 64% survival after 5 years.

## CAP and Steatosis in ALD

Controlled attenuation parameter (CAP) is a novel tool to noninvasively assess liver steatosis, which measures ultrasound attenuation when travelling through fatty liver tissue, compared to normal liver [35]. More details are provided in part VI of this book. In an individual data meta-analysis, CAP technology was shown to diagnose moderate and severe steatosis with diagnostic accuracies between 0.85 and 0.90 in 2735 patients with mixed liver disease etiologies (mainly viral hepatitis and NAFLD) [36]. In a recent European multicenter prospective study including 562 ALD patients who underwent CAP, regular US and liver biopsy [37], CAP diagnosed mild, moderate, and severe steatosis with AUC of 0.77, 0.78, and 0.82, respectively. A CAP value above 290 dB/m ruled in any steatosis with 88% specificity. Moreover, CAP was shown to be superior to regular US to diagnose steatosis in ALD patients. CAP technology appears therefore as an interesting tool to diagnose steatosis: the procedure is noninvasive, non-ionizing, easy to perform, and provides immediate results. In addition, CAP can be performed simultaneously to liver stiffness measurement, allowing for simultaneous evaluation of both fibrosis and steatosis [38]. However, diagnostic accuracy appears to be poorer at low steatosis stages and seems lower in ALD compared to other liver disease etiologies. Moreover, optimal cutoffs to rule in, rule out and stage steatosis are varying in the different studies performed.

One reason of this variation of CAP within multicenter studies seems to be the rapid response of CAP to drinking dynamics [37]. In case of sequential measurements of CAP in the same cohort, much better accuracy has been observed. It is therefore assumed that the specific challenges inherent of ALD studies have also contributed to the rather poor performance of CAP in ALD as compared to NAFLD.

## References

1. World Transplant Registry reports. La Moncloa; 2018. <https://www.lamoncloa.gob.es/lang/en/gobierno/news/Paginas/2018/20180829transplants.aspx>.
2. Wong RJ, Aguilar M, Cheung R, Perumpail RB, Harrison SA, Younossi ZM, et al. Nonalcoholic steatohepatitis is the second leading etiology of liver disease among adults awaiting liver transplantation in the United States. *Gastroenterology*. 2015;148(3):547–55.
3. Burra P, Senzolo M, Adam R, Delvart V, Karam V, Germani G, et al. Liver transplantation for alcoholic liver disease in Europe: a study from the ELTR (European Liver Transplant Registry). *Am J Transplant*. 2010;10(1):138–48.
4. Hazeldine S, Hynes T, Sheron N. Alcoholic liver disease - the extent of the problem and what you can do about it. *Clin Med*. 2015;15(2):179–85.
5. Teli MR, Day CP, Burt AD, Bennett MK, James OF. Determinants of progression to cirrhosis or fibrosis in pure alcoholic fatty liver. *Lancet*. 1995;346(8981):987–90.
6. Lackner C, Spindelboeck W, Haybaeck J, Douschan P, Rainer F, Terracciano L, et al. Histological parameters and alcohol abstinence determine long-term prognosis in patients with alcoholic liver disease. *J Hepatol*. 2017;66(3):610–8.
7. Mueller S, Seitz HK, Rausch V. Non-invasive diagnosis of alcoholic liver disease. *World J Gastroenterol*. 2014;20(40):14626–41.
8. Seitz HK, Mueller S. Alcoholic liver disease. In: Dancygier H, editor. *Clinical hepatology: principles and practice of hepatobiliary diseases*. Heidelberg: Springer; 2009. p. 1111–52.
9. European Association for the Study of Liver. EASL clinical practical guidelines: management of alcoholic liver disease. *J Hepatol*. 2012;57(2):399–420.
10. Filingeri V, Francioso S, Sforza D, Santopaolo F, Oddi FM, Tisone G. A retrospective analysis of 1.011 percutaneous liver biopsies performed in patients with liver transplantation or liver disease: ultrasonography can reduce complications? *Eur Rev Med Pharmacol Sci*. 2016;20(17):3609–17.
11. Abdi W, Millan JC, Mezey E. Sampling variability on percutaneous liver biopsy. *Arch Intern Med*. 1979;139(6):667–9.
12. Bedossa P, Dargere D, Paradis V. Sampling variability of liver fibrosis in chronic hepatitis C. *Hepatology*. 2003;38(6):1449–57.
13. Cadranel JF, Rufat P, Degos F. Practices of liver biopsy in France: results of a prospective nationwide survey. For the Group of Epidemiology of the French Association for the Study of the Liver (AFEF). *Hepatology*. 2000;32(3):477–81.
14. Maharaj B, Maharaj RJ, Leary WP, Cooppan RM, Naran AD, Pirie D, et al. Sampling variability and its influence on the diagnostic yield of percutaneous needle biopsy of the liver. *Lancet*. 1986;1(8480):523–5.
15. Regev A, Berho M, Jeffers LJ, Milikowski C, Molina EG, Pyrsopoulos NT, et al. Sampling error and intraobserver variation in liver biopsy in patients with chronic HCV infection. *Am J Gastroenterol*. 2002;97(10):2614–8.
16. Gilmore IT, Burroughs A, Murray-Lyon IM, Williams R, Jenkins D, Hopkins A. Indications, methods, and outcomes of percutaneous liver biopsy in England and Wales: an audit by the British Society of Gastroenterology and the Royal College of Physicians of London. *Gut*. 1995;36(3):437–41.



17. McGill DB, Rakela J, Zinsmeister AR, Ott BJ. A 21-year experience with major hemorrhage after percutaneous liver biopsy. *Gastroenterology*. 1990;99(5):1396–400.
18. Mathurin P, Hadengue A, Bataller R, Addolorato G, Burra P, Burt A, et al. EASL clinical practice guidelines: management of alcoholic liver disease. *J Hepatol*. 2012;57:399–420.
19. Moreno C, Mueller S, Szabo G. Non-invasive diagnosis and biomarkers in alcohol-related liver disease. *J Hepatol*. 2019;70(2):273–83.
20. Nguyen-Khac E, Chatelain D, Tramier B, Decrombecque C, Robert B, Joly JP, et al. Assessment of asymptomatic liver fibrosis in alcoholic patients using fibroscan: prospective comparison with seven non-invasive laboratory tests. *Aliment Pharmacol Ther*. 2008;28(10):1188–98.
21. Mueller S, Sandrin L. Liver stiffness: a novel parameter for the diagnosis of liver disease. *Hepatic Med Evid Res*. 2010;2:49–67.
22. Mueller S, Luderer M, Zhang D, Meulien D, Steiniger Brach B, Brix Schou M. Open-label study with nalmefene as needed use in alcohol dependent patients with evidence of elevated liver stiffness and/or hepatic steatosis. *Alcohol Alcohol*. 2019. <https://doi.org/10.1093/alcalc/agz078>.
23. Trabut JB, Thepot V, Nalpas B, Lavielle B, Cosconea S, Corouge M, et al. Rapid decline of liver stiffness following alcohol withdrawal in heavy drinkers. *Alcohol Clin Exp Res*. 2012;36(8):1407–11.
24. Gelsi E, Dainese R, Truchi R, Marine-Barjoan E, Anty R, Autuori M, et al. Effect of detoxification on liver stiffness assessed by fibroscan® in alcoholic patients. *Alcohol Clin Exp Res*. 2011;35(3):566–70.
25. Mueller J, Rausch V, Silva I, Peccerella T, Piecha F, Dietrich C, et al. PS-171-survival in a 10 year prospective cohort of heavy drinkers: liver stiffness is the best long-term prognostic parameter. *J Hepatol*. 2019;70(1):E107.
26. Mueller S, Englert S, Seitz HK, Badea RI, Erhardt A, Bozaari B, et al. Inflammation-adapted liver stiffness values for improved fibrosis staging in patients with hepatitis C virus and alcoholic liver disease. *Liver Int*. 2015;35(12):2514–21.
27. Mukai M, Ozasa K, Hayashi K, Kawai K. Various S-GOT/S-GPT ratios in nonviral liver disorders and related physical conditions and life-style. *Dig Dis Sci*. 2002;47(3):549–55.
28. Mueller S, Nahon P, Rausch V, Peccerella T, Silva I, Yagmur E, et al. Caspase-cleaved keratin-18 fragments increase during alcohol withdrawal and predict liver-related death in patients with alcoholic liver disease. *Hepatology*. 2017;66(1):96–107.
29. Nguyen-Khac E, Thiele M, Voican C, Nahon P, Moreno C, Boursier J, et al. Non-invasive diagnosis of liver fibrosis in patients with alcohol-related liver disease by transient elastography: an individual patient data meta-analysis. *Lancet Gastroenterol Hepatol*. 2018;3(9):614–25.
30. Kohlhaas A, Durango E, Millionig G, Bastard C, Sandrin L, Golriz M, et al. Transient elastography with the XL probe rapidly identifies patients with non-hepatic ascites. *Hepatic Med Evid Res*. 2012;4:11–8.
31. Durango E, Dietrich C, Seitz HK, Kunz CU, Pomier-Layrargues GT, Duarte-Rojo A, et al. Direct comparison of the FibroScan XL and M probes for assessment of liver fibrosis in obese and nonobese patients. *Hepatic Med Evid Res*. 2013;5:43–52.
32. Roulot D, Costes JL, Buyck JF, Warzocha U, Gambier N, Czernichow S, et al. Transient elastography as a screening tool for liver fibrosis and cirrhosis in a community-based population aged over 45 years. *Gut*. 2011;60(7):977–84.
33. Mueller S, Millionig G, Sarovska L, Friedrich S, Reimann FM, Pritsch M, et al. Increased liver stiffness in alcoholic liver disease: differentiating fibrosis from steatohepatitis. *World J Gastroenterol*. 2010;16(8):966–72.
34. Mueller S. personal observation. 2019.
35. Sasso M, Beaugrand M, de Ledinghen V, Douvin C, Marcellin P, Poupon R, et al. Controlled attenuation parameter (CAP): a novel VCTE guided ultrasonic attenuation measurement for the evaluation of hepatic steatosis: preliminary study and validation in a cohort of patients with chronic liver disease from various causes. *Ultrasound Med Biol*. 2010;36(11):1825–35.

36. Karlas T, Petroff D, Sasso M, Fan JG, Mi YQ, de Ledinghen V, et al. Individual patient data meta-analysis of controlled attenuation parameter (CAP) technology for assessing steatosis. *J Hepatol.* 2017;66(5):1022–30.
37. Thiele M, Rausch V, Fluhr G, Kjærgaard M, Piecha F, Mueller J, et al. Controlled attenuation parameter and alcoholic hepatic steatosis: diagnostic accuracy and role of alcohol detoxification. *J Hepatol.* 2018;68(5):1025–32.
38. de Ledinghen V, Vergniol J, Capdepon M, Chermak F, Hiriart JB, Cassinotto C, et al. Controlled attenuation parameter (CAP) for the diagnosis of steatosis: a prospective study of 5323 examinations. *J Hepatol.* 2014;60(5):1026–31.
39. Nahon P, Kettaneh A, Tenger-Barna I, Ziol M, de Ledinghen V, Douvin C, et al. Assessment of liver fibrosis using transient elastography in patients with alcoholic liver disease. *J Hepatol.* 2008;49(6):1062–8.
40. Kim SG, Kim YS, Jung SW, Kim HK, Jang JY, Moon JH, et al. The usefulness of transient elastography to diagnose cirrhosis in patients with alcoholic liver disease. *Korean J Hepatol.* 2009;15(1):42–51.
41. Boursier J, Vergniol J, Sawadogo A, Dakka T, Michalak S, Gallois Y, et al. The combination of a blood test and Fibroscan improves the non-invasive diagnosis of liver fibrosis. *Liver Int.* 2009;29(10):1507–15.
42. Janssens F, Piessevaux H, Horsmans Y, de Timary P, Starkel P. Can transient elastography replace liver histology for determination of advanced fibrosis in alcoholic patients: a real-life study. *J Clin Gastroenterol.* 2010;44(8):575–82.
43. Fernandez M, Trepo E, Degre D, Gustot T, Verset L, Demetter P, et al. Transient elastography using Fibroscan is the most reliable noninvasive method for the diagnosis of advanced fibrosis and cirrhosis in alcoholic liver disease. *Eur J Gastroenterol Hepatol.* 2015;27(9):1074–9.
44. Thiele M, Detlefsen S, Sevelsted Møller L, Madsen BS, Fuglsang Hansen J, Fiolla AD, et al. Transient and 2-dimensional shear-wave elastography provide comparable assessment of alcoholic liver fibrosis and cirrhosis. *Gastroenterology.* 2016;150(1):123–33.
45. Voican CS, Louvet A, Trabut JB, Njike-Nakseu M, Dharancy S, Sanchez A, et al. Transient elastography alone and in combination with FibroTest® for the diagnosis of hepatic fibrosis in alcoholic liver disease. *Liver Int.* 2017;37(11):1697–705.

# Chapter 12

## Liver and Spleen Stiffness in Schistosomiasis



Zulane da Silva Tavares Veiga, Cristiane Alves Vilella Nogueira,  
and Flavia Ferreira Fernandes

### Introduction

Schistosomiasis is a neglected tropical disease prevalent in low-to-middle income countries. Its transmission has been reported from 78 countries and the World Health Organization (WHO) estimates that more than 206 million individuals required preventive treatment worldwide in 2016 [1]. There are six species of *Schistosoma* in the world—*Schistosoma mansoni*, *Shistosoma haematobium*, *Schistosoma japonicum*, *Schistosoma intercalatum*, *Shistosoma mekongi*, and *Schistosoma malayensis*. *Schistosoma mansoni* is the most widespread and prevalent species. It is endemic in 52 countries and territories of South America, Africa, Caribbean, and Eastern Mediterranean [2]. Schistosomiasis is a disease typically associated with poverty and lack of adequate sanitation which forces people to contact unprotected natural freshwater sources where transmission occurs [1]. The socioeconomic impact generated by this disease should not be underestimated since it affects productive young adults and school-age children, which may hamper growth and development [1, 2]. Despite advances in control and substantial decreases in morbidity and mortality, schistosomiasis continues to be an important public health issue in endemic countries.

The transmission occurs when schistosome cercariae—released into water by intermediate host snails—penetrates human skin during contact with contaminated water [1]. In the body, cercariae develop into adult schistosomes, which mate, migrate to the mesenteric veins, and release eggs. These eggs, which are trapped in the tissues, deflagrate immunogenic inflammatory, granulomatous and fibrotic reac-

---

Z. da Silva Tavares Veiga (✉) · F. F. Fernandes  
Gastroenterology and Hepatology Unit, Bonsucesso Federal Hospital (Ministry of Health),  
Rio de Janeiro, Brazil

C. A. V. Nogueira  
Department of Internal Medicine, Clementino Fraga Filho University Hospital, Federal  
University of Rio de Janeiro, Rio de Janeiro, Brazil

tions that cause intestinal, hepatosplenic, or urinary disease which may evolve over many years [3].

Schistosomiasis presents as a large spectrum of manifestations since asymptomatic to acute and chronic disease. Up to 10% of infected individuals develop the severe form of the disease known as hepatosplenic schistosomiasis (HES) which is characterized by portal hypertension and hepatic periportal fibrosis [2]. The most serious complication is bleeding from esophageal varices, a condition that may be life-threatening.

## Diagnosis

Diagnosis can be made by direct methods (parasitological examination of feces, rectal biopsy, hepatic or other sites, fecal PCR) or indirect methods (serological tests, screening of circulating antigens). The diagnosis of active *Schistosoma* infection is based on the demonstration of egg excretion by parasitological methods such as Kato-Katz [4]. This technique is low-cost, easy to perform and allows visualization and counting of eggs per gram of feces, providing a reliable indicator of parasite load, infection intensity, and treatment efficacy [4]. However, in low endemicity areas or in patients with low parasite load, sometimes it is not possible to detect eggs by this technique. New diagnostic methods such as DNA detection assays and serological tests have been developed and proposed as complementary or in substitution to K-K in these scenarios [5].

## Hepatosplenic Schistosomiasis

Schistosomal hepatopathy is a peculiar form of chronic liver disease where the main feature is periportal fibrosis in the absence of significant hepatocellular injury [4]. In contrast to cirrhotic portal hypertension, the liver parenchyma usually preserves its normal architecture [3, 4]. In clinical practice, it is sometimes difficult to distinguish portal hypertension due to cirrhosis from that related to hepatosplenic schistosomiasis.

Historically, liver biopsy has been considered the reference for staging hepatic fibrosis. However, this invasive method has been challenged by poor acceptance by patients, potential complications, and low quality of specimen [6, 7]. In HES, the gold standard method to evaluate schistosomal hepatic fibrosis is wedge liver biopsy, taken during abdominal surgery for portal hypertension, but not justified in nonsurgical patients. Percutaneous liver biopsy has low sensitivity because it retrieves insufficient and fragmented tissue samples with few portal tracts [6]. Besides, most patients with HES are thrombocytopenic which implies an additional risk of bleeding. Considering these limitations, most attention has been focused on whether noninvasive methods can detect clinically significant fibrosis or cirrhosis.

Abdominal ultrasound (US) has become the most consolidated tool for the evaluation of liver fibrosis in HES because of its availability and sensitivity [8, 9]. US has been widely used in population studies and in the evaluation of patients with the disease since the 80s [9]. Studies have demonstrated that the sensitivity and specificity of ultrasonography in the recognition of schistosomiasis-related liver fibrosis—also known as Symmers fibrosis—is closely related to histological examination [10]. Among the ultrasound findings, periportal fibrous thickening is the most frequent and characteristic alteration of the disease, being evidenced as an area of periportal hyperechogenicity [11]. In order to standardize and quantify periportal fibrosis in schistosomiasis patients, ultrasound criteria were developed for the evaluation of periportal fibrosis by the World Health Organization (WHO) at Cairo in 1990, revised at Niamey in 1996 [12]. The criteria used are both of qualitative and quantitative nature. Qualitative criteria take into account the hepatic texture while quantitative measures include the wall thickness of branches of the portal vein. According to this protocol, periportal fibrosis can be classified as absent (pattern A), mild (B, C, D and Dc), moderate (E and Ec), or intense (F). Despite being a noninvasive, safe, and low-cost diagnostic method, US presents some limitations such as interobserver variation and operator's expertise to apply the WHO protocol for US assessment [13].

## Liver Elastography in Schistosomiasis

In HES, the applicability of liver elastography is still not well established. Periportal fibrosis induced by schistosomiasis has been evaluated by a few studies so far [14–20]. Recently our group compared liver and spleen stiffness among HES and HCV-cirrhotic patients with control patients using TE [14]. Our data showed lower LS values in HES patients when compared with HCV-cirrhotics (9.7 vs 27.0 kPa) as shown in Fig. 12.1. In the HES group, only 30% of individuals presented high values above 12.5 kPa on TE. The low LS values observed in most of the patients in the HES group are of high relevance in clinical practice as patients with portal hypertension and low values of LS may be distinguished from cirrhotic patients through a noninvasive, easy-to-perform, and reproducible tool. Thus, in the scenario of portal hypertension (PH) our results are very valuable in distinguishing between sinusoidal and presinusoidal etiologies of portal hypertension. We concluded that TE may be a useful tool to differentiate cirrhosis from HES. In this study, we found no association between liver stiffness and dopplerfluxometric parameters of portal hypertension. Similarly, no association was identified with grading of periportal fibrosis by US (Niamey), possibly because dopplerfluxometric parameters are related to portal hypertension and not liver fibrosis.

In a study on 30 HES patients, Shiha et al. [15] also found most LS values below of cirrhotic threshold in the majority of patients with a mean value of 9.4 kPa. In this study the main aim was to compare TE results in patients with and without esophageal varices and splenomegaly. They concluded that TE would not be useful to diagnose liver

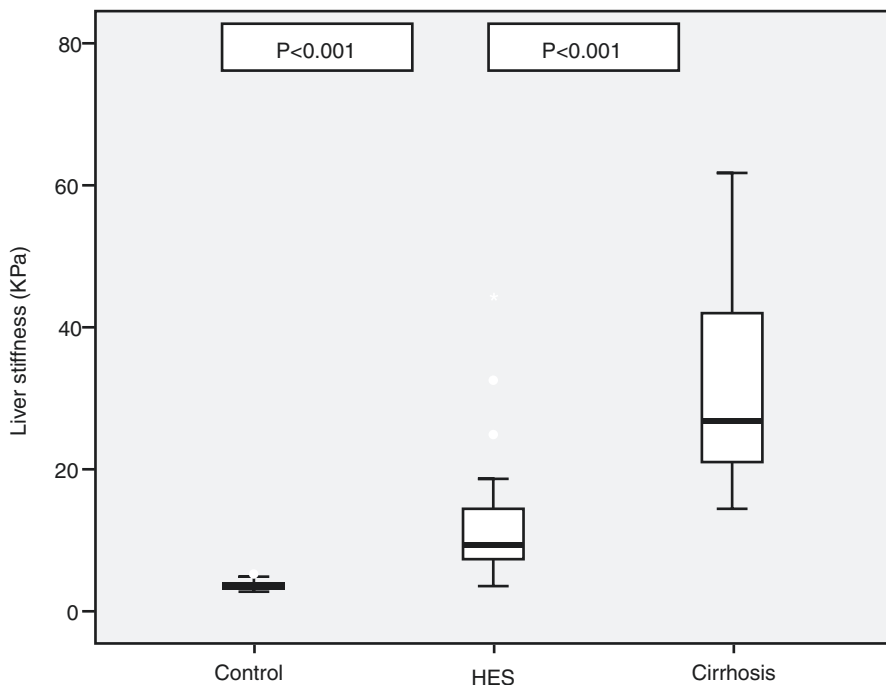


**Fig. 12.1** Boxplot shows liver stiffness values for controls, HES patients, and HCV patients with cirrhosis. The length of the boxes represents the interquartile range where 50% of values occur. Bars show the minimum and maximum values, median, and quartiles. The line through the middle of each box represents the median. HES, Hepatosplenic schistosomiasis

fibrosis and esophageal varices in patients with pure schistosomiasis. Recently, Shengd Wu [16] et al. assessed diagnostic performance of TE for evaluating fibrosis stages in 73 patients with biopsy-confirmed advanced schistosomiasis japonica. Significant differences were found for LS for the different stages of fibrosis. The optimal cutoff LS values were 8.0 kPa, 9.5 kPa, and 18.0 kPa for significant fibrosis, advanced fibrosis, and cirrhosis, respectively. They concluded that LS is a reliable parameter for assessing the risk of liver fibrosis in patients with advanced schistosomiasis japonica.

Ramzy et al. [17] aimed to evaluate effectiveness of TE for staging hepatic fibrosis in 358 chronic HCV—schistosomiasis co-infected patients enrolled in three groups: Group 1: chronic HCV without antischistosomal antibody (122 patients), Group 2: chronic HCV with positive antischistosomal antibodies and without periportal tract thickening (122 patients), Group 3: chronic HCV with positive antischistosomal antibodies and ultrasonographic picture of periportal tract thickening (108 patients). They found that schistosomal antigen, antischistosomal antibody, and periportal tract thickening did not have significant impact on the agreement between biopsy and FibroScan and that only higher antischistosomal antibody titers may impair this agreement. They concluded that TE is a reliable and noninvasive tool for staging hepatic fibrosis in HES regardless of periportal tract thickening.

Similarly, Esmat et al. [18] assessed liver elastography by TE in 231 patients HCV patients out of which 29% with positive schistosomal serology. Positive schistosomal serology status was significantly associated with the disagreement between the results of liver biopsy (Metavir) and the LS results. They concluded that although the sensitivity for the detection of intermediate fibrosis stages (F2 and F3) was impaired in patients with positive schistosomal serology, fibrosis stages (F0-F1 and F4) were the most independent factors associated with the agreement between FibroScan and liver biopsy.

Point shear wave (pSWE) using acoustic radiation force imaging, also has been applied to assess liver fibrosis in schistosomiasis [19]. Santos et al. [20] evaluated the performance of pSWE for predicting significant periportal fibrosis (PPF) in 358 patients with schistosomiasis. The pSWE measurements were compared to the US patterns of periportal fibrosis, as gold standard, according to the Niamey classification. Eighty-six patients were classified as having mild PPF and 272 patients as having significant PPF. The median pSWE of the significant fibrosis group was higher (1.40 m/s) than that of mild fibrosis group (1.14 m/s,  $P < 0.001$ ). They found 1.11 m/s as the best cutoff value for excluding significant PPF and 1.39 m/s as the best cutoff value for confirming significant PPF. They concluded that pSWE was able to differentiate significant from mild PPF and therefore, was a potential tool for noninvasive assessment of disease severity in patients with schistosomiasis mansoni.

## Spleen Elastography in Schistosomiasis

Noninvasive assessment of portal hypertension has become an issue of interest over the past few years. Recently, spleen stiffness was identified as a potential surrogate marker of portal hypertension in cirrhotic patients. Some studies have shown that spleen stiffness measurement by transient elastography can predict the presence and size of esophageal varices as well as clinical complications in compensated cirrhosis [21–24].

Our study [14] compared spleen stiffness measurement (SSM) among HES, HCV-cirrhotic patients, and controls. We found similar median values of SSM in both HES and cirrhotic patients (Fig. 12.2), suggesting that this parameter is not useful to differentiate cirrhotic from non-cirrhotic portal hypertension. When compared to several US dopplerfluxometric variables, high SSM was associated with right liver lobe diameter, higher values of the splenic artery resistance index, portal vein diameter, portal vein area, portal vein congestion index, splenic vein diameter, and spleen longitudinal diameter.

We concluded that, differently from LSM, the association of high SSM with several US Doppler parameters suggests that SSM may be considered a potential surrogate marker of portal hypertension in this population.

In conclusion, LSM may be a reliable parameter for assessing liver fibrosis in HES patients. The low values of LSM observed in most of studies indicate that it

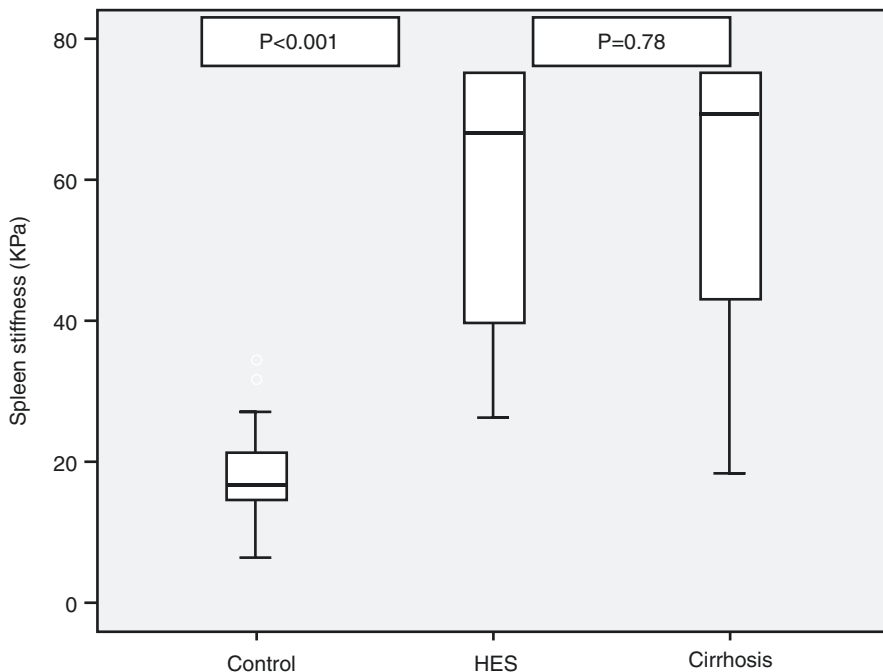


**Fig. 12.2** Boxplot shows spleen stiffness values for controls, HES patients, and HCV patients with cirrhosis. The length of the boxes represents the interquartile range where 50% of values occur. Bar shows the minimum and maximum values, median, and quartiles. The line through the middle of each box represents the median. *HES* Hepatosplenic schistosomiasis

may help to differentiate cirrhosis from HES. The association of high SS with several US Doppler parameters suggests that SS may be a potential surrogate marker of portal hypertension in patients with HES.

## References

1. Organization WH. WHO. Schistosomiasis: fact sheet no 115. Geneva. 2017.
2. Organization WH. WHO technical report series 830 - The control of schistosomiasis- second report of WHO Experts Committee. 1993.
3. Gryseels B. Schistosomiasis. *Infect Dis Clin N Am*. 2012;26(2):383–97.
4. Saúde MD. Vigilância da esquistossomose mansoni - Diretrizes técnicas. quarta edição. 2014.
5. Cavalcanti MG, Silva LF, Peralta RHS, Barreto MGM, Peralta JM. Schistosomiasis in areas of low endemicity: a new era in diagnosis. *Trends Parasitol*. 2013;29(2):75–82.
6. Lambertucci JR. Revisiting the concept of hepatosplenic schistosomiasis and its challenges using traditional and new tools. *Rev Soc Bras Med Trop*. 2014;47(2):130–6.
7. Bedossa P, Dargere D, Paradis V. Sampling variability of liver fibrosis in chronic hepatitis C. *Hepatology*. 2003;38(6):1449–57.
8. Cerri GG, Alves VA, Magalhães A. Hepatosplenic schistosomiasis mansoni: ultrasound manifestations. *Radiology*. 1984;153(3):777–80.



9. Lambertucci JR, Silva LCS, Andrade LM, de Queiroz LC, Carvalho VT, Voietta I, et al. Imaging techniques in the evaluation of morbidity in schistosomiasis mansoni. *Acta Trop.* 2008;108(2-3):209–17.
10. Homeida M, Bennett JL, Ibrahim SZ, Dafalla AA, Arbab BMO, Abdel-Salam IM, et al. Diagnosis of pathologically confirmed symmers' periportal fibrosis by ultrasonography: a prospective blinded study. *Am J Trop Med Hyg.* 1988;38(1):86–91.
11. Machado MM, Rosa ACF, Oliveira IRS, Cerri GG. Ultrasound findings in hepatosplenic schistosomiasis. *Radiol Bras.* 2002;35(1):41–5.
12. Richter J, Hatz C, Campagne G, Bergquist NR, Jenkins JM, et al. Ultrasound in schistosomiasis: a practical guide to the standard use of ultrasonography for assessment of schistosomiasis-related morbidity. 2000.
13. Silva LCS, Andrade LM, LCd Q, Voietta I, Azeredo LM, Antunes CMF, et al. Schistosoma mansoni: magnetic resonance analysis of liver fibrosis according to WHO patterns for ultrasound assessment of schistosomiasis-related morbidity. *Mem Inst Oswaldo Cruz.* 2010;105(4):467–70.
14. Veiga ZST, Villela-Nogueira CA, Fernandes FF, Cavalcanti MG, Figueiredo FA, Pereira JL, et al. Transient elastography evaluation of hepatic and spleen stiffness in patients with hepatosplenic schistosomiasis. *Eur J Gastroenterol Hepatol.* 2017;29(6):730–5.
15. Gamal S, Samir W, Soliman R, Elbasiony M, Ahmed N, Helmy A. Transient elastography (FibroScan) is not useful in the diagnosis of schistosomal hepatic fibrosis. *Med J Viral Hepatitis.* 2016;1(2):1–10.
16. Wu S, Tseng Y, Xu N, Yin X, Xie X, Zhang L, et al. Evaluation of transient elastography in assessing liver fibrosis in patients with advanced schistosomiasis japonica. *Parasitol Int.* 2018;67(3):302–8.
17. Ramzy I, Elsharkawy A, Fouad R, Hafez HA, El Raziky M, El Akel W, et al. Impact of old Schistosomiasis infection on the use of transient elastography (Fibroscan) for staging of fibrosis in chronic HCV patients. *Acta Trop.* 2017;176:283–7.
18. Esmat G, Elsharkawy A, El Akel W, Fouad A, Helal K, Mohamed MK, et al. Fibroscan of chronic HCV patients coinfecting with schistosomiasis. *Arab J Gastroenterol.* 2013;14(3):109–12.
19. Parfieniuk-Kowerda A, Lapinski TW, Rogalska-Plonska M, Swiderska M, Panasiuk A, Jaroszewicz J, et al. Serum cytochrome c and m30-neoepitope of cytokeratin-18 in chronic hepatitis C. *Liver Int.* 2014;34(4):544–50.
20. Carvalho Santos J, Dória Batista A, Maria Mola Vasconcelos C, Souza Lemos R, Romão de Souza Junior V, Dessein A, et al. Liver ultrasound elastography for the evaluation of periportal fibrosis in schistosomiasis mansoni: a cross-sectional study. *PLoS Negl Trop Dis.* 2018;12(11):e0006868.
21. Stefanescu H, Grigorescu M, Lupsor M, Procopet B, Maniu A, Badea R. Spleen stiffness measurement using Fibroscan for the noninvasive assessment of esophageal varices in liver cirrhosis patients. *J Gastroenterol Hepatol.* 2011;26(1):164–70.
22. Sharma P, Kirnake V, Tyagi P, Bansal N, Singla V, Kumar A, et al. Spleen stiffness in patients with cirrhosis in predicting esophageal varices. *Am J Gastroenterol.* 2013;108(7):1101–7.
23. Colecchia A, Montrone L, Scaiola E, Bacchi-Reggiani ML, Colli A, Casazza G, et al. Measurement of spleen stiffness to evaluate portal hypertension and the presence of esophageal varices in patients with hcv-related cirrhosis. *Gastroenterology.* 2012;143(3):646–54.
24. Colecchia A, Colli A, Casazza G, Mandolesi D, Schiumerini R, Reggiani LB, et al. Spleen stiffness measurement can predict clinical complications in compensated HCV-related cirrhosis: a prospective study. *J Hepatol.* 2014;60(6):1158–64.

# Chapter 13

## Screening for Cystic Fibrosis Using Liver Stiffness Measurements



Elke Roeb

### Introduction to Hepatic Involvement in Cystic Fibrosis

CFLD is a manifestation of cystic fibrosis with increasing frequency [1]. Patients also increasingly suffer from the complications of cystic fibrosis-associated hepatopathy. Transient elastography (TE) has been tested in some studies, however, is not yet the subject of a current guideline for the diagnosis of CFLD. Up to now (May 2019) 36 papers were published in PubMed when searching for “Cystic Fibrosis AND elastography.” Eight of them are dealing with the method ARFI and 21 papers with CFLD, the cystic fibrosis liver disease. Since 2009 when the first reports were published, various longitudinal studies were conducted and TE has been combined with several methods to enhance its diagnostic value and relevance.

In addition, there is still no ubiquitous cutoff value, that could be used to diagnose CFLD or to rule it out. So far there is no serum marker, which is determined by default on suspicion of CFLD. Especially in children, it must be considered whether any ursodesoxycholic acid (UDCA) therapy including all complications and risks offers more advantages than disadvantages. Children are generally burdened with the chronic disease and must take numerous medications. It is desirable to find the optimal time to start therapy with UDCA to avoid premature drug administration. The therapy should begin at an early stage to prevent the progression to manifest fibrosis. This point emphasizes once again the urgency of having a regular, and in the best case noninvasive, diagnostic approach to monitor patients, as there are no established therapies for advanced hepatopathy yet.

---

E. Roeb (✉)

Gastroenterology, Justus Liebig University Giessen, University Hospital UKGM,  
Giessen, Germany

e-mail: [Elke.Roeb@innere.med.uni-giessen.de](mailto:Elke.Roeb@innere.med.uni-giessen.de)

## Transient Elastography in Cystic Fibrosis/CFLD

Our group prospectively studied 145 CF patients (75 children, 70 adults) of our CF unit by TE and several biomarkers [2]. CFLD was diagnosed according to the guidelines from 2012. In addition, serum concentrations of YKL-40, HA, PIIIP, MMP-9, TIMP-1, and TIMP-2 were determined by ELISA. In this study, TE was increased in adults and children with CFLD compared to those without and exhibited a high diagnostic accuracy [2] (see Fig. 13.1). In adults with portal hypertension, LS was further elevated. Diagnostic sensitivities were increased when elastography and respective biomarkers were combined for the detection of CF hepatopathy and portal hypertension. In another study, TE was performed in 66 CF patients. Age-specific cutoff values were determined in a control population ( $n = 59$ ). The measurements were correlated with clinical data, biyearly biochemistry and ultrasound. Here, Fibroscan was easy to perform in this patient population. There were 14 patients (21%) with abnormal LSM. LS was significantly increased in patients with clinical CFLD (11.2 vs. 5.1 kPa), biochemical CFLD (7.4 vs. 5.4 kPa), or ultrasonographical CFLD (8.2 vs. 4.3 kPa) ( $P < 0.02$  for all). The authors concluded that TE is an objective measure and is easy to perform in CF patients, even in children, and could provide a valuable tool to detect and quantify CFLD.

A total of 134 consecutive patients with documented CF were prospectively studied by Menten et al. in order to compare TE and transabdominal US scanning in

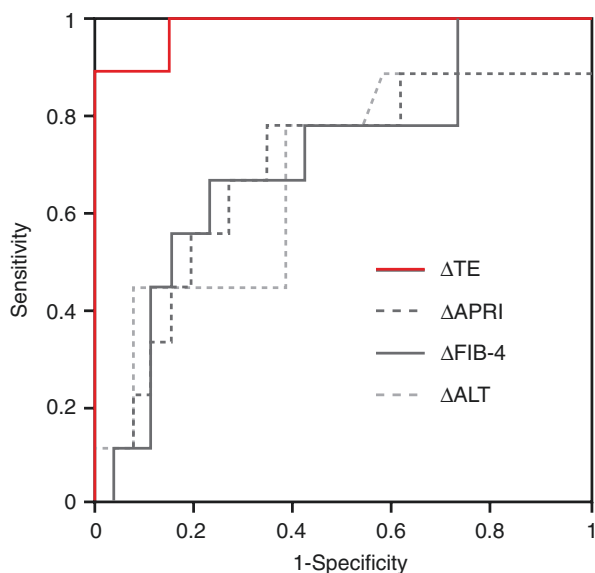


**Fig. 13.1** AUROCs for different diagnostic methods in 36 pediatric patients followed up over 5 years. *TE* transient elastography, *APRI* aspartate aminotransferase to platelet ratio index, *FIB-4* simple noninvasive index to predict significant fibrosis including age, AST, ALT, platelet count, *ALT* alanin-aminotransferase

children and adults attending a CF clinic. In that study median elasticity in CF patients was significantly higher in males (4.7 kPa) than in females (3.9 kPa) ( $P = 0.0013$ ) [3]. Both values however were rather low and within normal ranges.

Karlas et al. examined ARFI, TE, and laboratory-based fibrosis indices in 55 adult CF patients of whom 15 met CFLD criteria. ARFI, TE, and serum markers correlated with each other and detected CFLD related liver cirrhosis in these adult CF patients. CF specific cutoff TE values for cirrhosis in adults were lower than in non-cirrhotic patients (TE: 7.9 vs. 4.2 kPa;  $P = 0.02$ ) [4].

An Australian study measured LS using TE in 50 adult patients with and without CFLD. Median LS values were higher in those with CFLD (8.1 vs. 5.0 kPa  $P < 0.001$ ). In addition, LS was the only variable associated with CFLD (OR 2.74, 95% CI 1.53–4.89;  $P = 0.001$ ). AUROC for LS predicting CFLD was 0.87 (95% CI 0.77–0.98) and a LS  $\geq 6.8$  kPa predicted CFLD with 76.0% sensitivity and 92.0% specificity. Median LS was higher in case of portal hypertension (15.7 kPa (IQR 9.2–17.2) vs. 5.4 kPa (IQR 4.3–6.8);  $P < 0.001$ ) [5]. In a similar Canadian study at a threshold of  $>5.2$  kPa, the sensitivity, specificity, positive, and negative predictive values of LSM for detecting CFLD were 67%, 83%, 40%, and 94%, respectively [6]. In this study, the definition of CFLD relied on noninvasive criteria (i.e., abnormal liver biochemistry and ultrasonography), rather than on liver biopsy. However, there was no universally accepted definition of what constitutes CFLD.

A retrospective study from Belgium (2007–2013) aimed to detect CFLD using consecutive LSM by TE. The median LS value in CFLD was 14 kPa (8.7–32.2) compared with 5.3 (4.9–5.7) in cystic fibrosis patients without liver disease (CFnoLD;  $P = 0.0001$ ). In CFnoLD, LS was correlated with age ( $P = 0.031$ ) [7]. In their retrospective study, patients with developing CFLD had progressively increasing consecutive LSM [7]. A LS  $>6.8$  kPa had a sensitivity of 91.5% and a specificity of 91.7% in predicting CFLD. Again, this study confirmed rather low values for CFLD. LS values in patients with CFLD were significantly higher than in those without CFLD despite both groups having relatively low median LS values as already mentioned before by Sadler (6.4 vs. 3.9 kPa) [6].

We recently aimed to identify new experimental biomarkers for the detection of CFLD [8]. Forty-five CF patients were included in the study and received TE. Differential regulation of 220 different serum proteins was assessed in a subgroup of patients with and without CFLD. Most interesting candidate proteins were further quantified and validated by ELISA in the whole patient cohort.

Forty-three serum proteins differed at least twofold in patients with CFLD compared to those without liver disease as identified in proteome profiling. In ELISA quantifications, TIMP-4 and Endoglin were significantly upregulated in patients with CFLD as diagnosed by clinical guidelines or increased liver stiffness. Serum TIMP-4 and Endoglin showed highest values in HCV patients with liver cirrhosis compared to those with fibrosis but without cirrhosis. At a cutoff value of 6.3 kPa, TE compassed a very high diagnostic accuracy and specificity for the detection of CFLD. Among the biomarkers, TIMP-4 and Endoglin exhibited a high diagnostic accuracy for CFLD. Diagnostic sensitivities and negative predictive values were increased when TE and TIMP-4 and Endoglin were combined for the detection of CFLD. As shown

**Table 13.1** Diagnostic performance of TE and serum fibrosis markers for detection of cystic fibrosis liver disease

Elastography	Cutoff	Sensitivity	Specificity	PPW	NPW
TE	5.5 kPa	53.3 (34.6–71.2)	77.8 (62.5–88.3)	61.5 (40.7–79.1)	71.4 (56.5–83)
TIMP-4	139 pg/mL	72.7 (39.3–92.7)	72.2 (46.4–89.3)	61.5 (32.3–84.9)	81.3 (53.7–95)
TE + TIMP-4	5.5 kPa/139 pg/mL	95.2 (74.1–99.8)	47.8 (27.4–68.9)	62.5 (43.7–78.3)	91.7 (59.8–96)

in Table 13.1, we concluded that determination of TIMP-4 and Endoglin together with TE can increase the sensitivity for the noninvasive diagnosis of CFLD [8].

## Long-Term Follow-Up of CF Patients by TE

Cystic fibrosis associated liver disease (CFLD) is a relatively frequent and early complication of CF developing in 5–10% of children within the first life decade and with a high incidence of cirrhosis. The early diagnosis of CFLD is urgently needed since patients suffering from early stage liver disease are more likely to benefit from therapy. Our recent study from 2017 presented prospective data showing that transient elastography (TE) is a sensitive diagnostic tool for the identification of patients at risk for progressing CFLD [9]. Within this study we aimed to prospectively identify patients at risk for development of CFLD by longitudinal analysis of liver stiffness and fibrosis scores in a 5-year follow-up. Thirty-six pediatric and 16 adult patients with initial liver stiffness below the cutoff value indicative of CFLD (6.3 kPa) were examined by transient elastography for 4–5 years. TE, APRI-, and FIB-4-scores were assessed and compared by Kruskal–Wallis test and receiver operating characteristic (ROC)-analysis. Among the 36 patients participating in this study, a subgroup of 9 patients developed liver stiffness >6.3 kPa after 4–5 years with an annual LS increase of >0.38 kPa. For the first time it was shown that the noninvasive longitudinal assessment of TE allows identification of patients with progression of CFLD in a subgroup of juvenile but not in adult CF patients. Comparing TE to conventional fibrosis-scores underlined the strength of the continuous assessment of liver stiffness for the exact diagnosis of progressive CFLD (see Fig. 13.1). One year later our data were confirmed by Gomion et al. The aim of her retrospective study was to assess the progression of liver stiffness measurement (LSM) in pediatric patients with CF expressed as kPa/year and %/year, measured by (Fibroscan®) in 82 children with CF (median age:  $6.8 \pm 5.8$  years), the mean time interval between the two LSM was 3.5 years. Median initial liver stiffness was  $3.7 \pm 1.3$  kPa, and then progressed by 0.23 kPa/year, that is, 6%/year. The study demonstrated that the slope of worsening of liver stiffness was greater in patients who will develop CFLD [10]. These authors also, suggest that annual transient elastography may be useful to detect risk of severe liver disease, that is CFLD, at an earlier stage (Table 13.2).

**Table 13.2** LS cutoff values in different studies for diagnosis of cystic fibrosis liver disease and its performance in addition to patients' characteristics

Study	Number of patients	Number of CFLD	LS cutoff value for diagnosis of CFLD ( $\geq$ kPa)	Sensitivity % (95% CI)	Specificity % (95% CI)	LS cutoff AUROC	Mean ALT (IU/L)	AST(IU/L)	Mean GGT (IU/L)	Mean Platelet count ( $\times 10^9/L$ )	Mean APRI score
Friedrich-Rust et al. 2013 [11]	106	24	7.1	46 (82–96)	91 (82–96)	–	48	46.4	73	242	0.479
Karlas et al. 2012 [4]	55	14	5.9	43 (18–71)	97 (85–100)	0.68	36	36	67	211	0.426
Kitson et al. 2013 [5]	50	25	5.5	76 (55–91)	92 (74–99)	0.87	31.9	31.1	108.7	212	0.366
Rath et al. 2012 [2]	145	68	5.5	52 (40–65)	81 (71–89)	0.68	34.35	–	43.4	311	–
Sadler et al. 2015 [6]	127	18	5.3	67 (41–87)	83 (74–89)	0.78	31	28	41	218	0.50
Van Biervliet et al. 2016 [7]	150	20	6.8	90 (85–96)	92 (85–96)	0.97	28	–	55	–	–

## Transient Elastography in Other Organs

For patients with cystic fibrosis, the imaging of the pancreas is crucial for the early detection of replacement by fibrofatty tissue and lipomatous hypertrophy up to different forms of cystic transformation. A comparative study between magnetic resonance imaging (MRI) and sonographic pancreas sonography was presented recently [12]. They showed that ultrasound was superior to MRI in case of complete fibrofatty transformation of the parenchyma and for evaluation of the pancreatic duct. Point shear wave elastography, however, did not correlate directly with measured intensities of pancreatic parenchyma in MRI, neither in the whole CF collective nor in subgroups of fatty transformation of the parenchyma. The study was planned as a single center study and a total of 19 patients were only included [12].

## CAP and CF

Controlled attenuation parameter (CAP) measurement during transient elastography (TE) semi-quantifies liver steatosis. The relationship between CAP and CFLD severity, clinical factors and liver stiffness measurements was evaluated in 129 CF patients [13]. In conclusion there was no CAP difference between subjects with no CFLD and those with CFLD and portal hypertension. Thus, the semi-quantification of liver steatosis does not improve the diagnosis of CFLD [13].

## References

1. Sakiani S, Kleiner DE, Heller T, Koh C. Hepatic manifestations of cystic fibrosis. *Clin Liver Dis.* 2019;23(2):263–77.
2. Rath T, Menendez KM, Kügler M, Hage L, Wenzel C, Schulz R, et al. TIMP-1/-2 and transient elastography allow non invasive diagnosis of cystic fibrosis associated liver disease. *Dig Liver Dis.* 2012;44(9):780–7.
3. Menten R, Leonard A, Clapuyt P, Vincke P, Nicolae A-C, Lebecque P. Transient elastography in patients with cystic fibrosis. *Pediatr Radiol.* 2010;40(7):1231–5.
4. Karlas T, Neuschulz M, Oltmanns A, Guttler A, Petroff D, Wirtz H, et al. Non-invasive evaluation of cystic fibrosis related liver disease in adults with ARFI, transient elastography and different fibrosis scores. *PLoS One.* 2012;7(7):e42139.
5. Kitson MT, Kemp WW, Iser DM, Paul E, Wilson JW, Roberts SK. Utility of transient elastography in the non-invasive evaluation of cystic fibrosis liver disease. *Liver Int.* 2013;33(5):698–705.
6. Sadler MD, Crotty P, Fatovich L, Wilson S, Rabin HR, Myers RP. Noninvasive methods, including transient elastography, for the detection of liver disease in adults with cystic fibrosis. *Can J Gastroenterol Hepatol.* 2015;29(3):139–44.
7. Van Biervliet S, Verdievel H, Vande Velde S, De Bruyne R, De Looze D, Verhelst X, et al. Longitudinal transient elastography measurements used in follow-up for patients with cystic fibrosis. *Ultrasound Med Biol.* 2016;42(4):848–54.

8. Rath T, Hage L, Kügler M, Menendez Menendez K, Zachoval R, Naehrlich L, et al. Serum proteome profiling identifies novel and powerful markers of cystic fibrosis liver disease. *PLoS One*. 2013;8(3):e58955.
9. Klotter V, Gunchick C, Siemers E, Rath T, Hudel H, Naehrlich L, et al. Assessment of pathologic increase in liver stiffness enables earlier diagnosis of CFLD: results from a prospective longitudinal cohort study. *PLoS One*. 2017;12(6):e0178784-e.
10. Gominon A-L, Frison E, Hiriart J-B, Vergniol J, Clouzeau H, Enaud R, et al. Assessment of liver disease progression in cystic fibrosis using transient elastography. *J Pediatr Gastroenterol Nutr*. 2018;66(3):455–60.
11. Friedrich-Rust M, Schlueter N, Smaczny C, Eickmeier O, Rosewich M, Feifel K, et al. Non-invasive measurement of liver and pancreas fibrosis in patients with cystic fibrosis. *J Cyst Fibros*. 2013;12(5):431–9.
12. Kloth C, Fabricius D, Wendlik I, Schmidt SA, Pfahler M, Lormes E, et al. Diagnostic accuracy of MRI with MRCP and B-Mode-sonography with elastography of the pancreas in patients with cystic fibrosis: a point-to-point comparison. *BMC Res Notes*. 2019;12(1):150.
13. Bader RM, Jonas MM, Mitchell PD, Wiggins S, Lee CK. Controlled attenuation parameter: a measure of hepatic steatosis in patients with cystic fibrosis. *J Cyst Fibros*. 2019;18(2):280–5.



# Chapter 14

## Role of Liver Stiffness in Hematological Disorders: Assessment of Sinusoidal Obstruction Syndrome, Budd–Chiari Syndrome, and Treatment Complications



Thomas Karlas

### Considerations on Liver Stiffness in Hematology

Liver stiffness measurement (LSM) is often solely regarded as a noninvasive fibrosis surrogate marker while the role of other clinical confounders such as liver perfusion and inflammation are underestimated [1]. For more details see also book Part IV “Important (Patho)physiological Confounders of LS.” Moreover, diffuse malignant infiltration and deposition of proteins such as amyloid in the hepatic tissue can significantly modulate LS [2, 3].

Hematological malignancies and proliferative disorders are systemic diseases that frequently affect liver function. In addition, several of these etiologies are associated with liver complications such as liver vein outflow obstruction and portosinusoidal disease. These liver disorders potentially represent major targets for a LSM-based diagnostic workup [4], which shall not only focus on the initial diagnosis but may also play an important role in monitoring and guiding therapeutic decisions (Fig. 14.1). The scientific evidence on LSM applications in hematology is still limited, but recent publications support the further evaluation of elastography techniques in this field. This chapter gives an overview on current developments and future trends.

---

T. Karlas (✉)

Division of Gastroenterology, Medical Department II, University of Leipzig Medical Center, Leipzig, Germany

e-mail: [thomas.karlas@medizin.uni-leipzig.de](mailto:thomas.karlas@medizin.uni-leipzig.de)

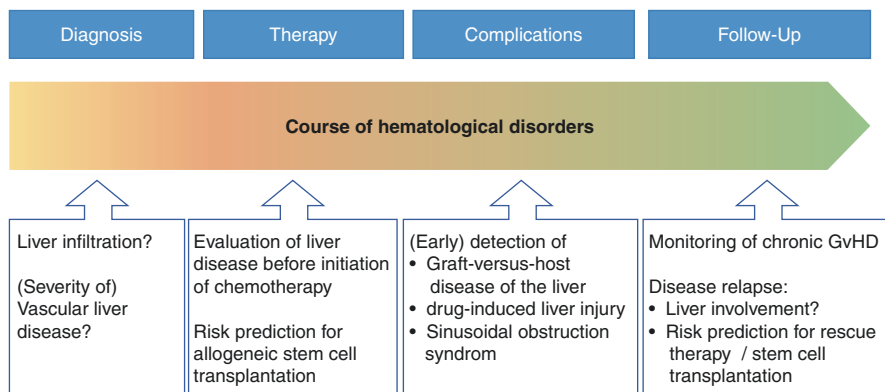


**Fig. 14.1** Current and potential future diagnostic utility of liver stiffness measurement in hematology

## Liver Stiffness Measurement in Budd–Chiari Syndrome

Budd–Chiari syndrome (BCS) is a rare disorder caused by obstruction of hepatic venous outflow. It is often associated with myeloproliferative neoplasms but may also occur in patients with congenital venous malformation or even without further predisposing risk factors. Clinical symptoms are dominated by portal hypertension and cirrhosis including increased risk of hepatocellular carcinoma [5]. Diagnosis of BCS can be challenging, especially in cases with incomplete venous obstruction where advanced imaging modalities are required. Early diagnosis is crucial for optimal treatment which usually comprises of anticoagulation and recanalization including placement of a transjugular portosystemic stent shunt (TIPS) [5].

Recent case series and monocentric studies provide first evidence of liver stiffness modulation in BCS: Manifestation of hepatic venous outflow obstruction is regularly accompanied by a strong increase of LS values [6] that decrease rapidly after successful recanalization [7, 8]. Both transient elastography and shear-wave-based methods seem appropriate for assessment of BCS [7, 8] and can already be used to complement the diagnostic assessment and monitoring of affected patients. However, considering the low incidence and the individual characteristics of BCS, it is unlikely that dedicated LS cutoff values for diagnosis will be established in the near future. Moreover, and in line with right heart failure patients [9], venous outflow obstruction can easily reach LS higher than 50 kPa. In a recent study using 2D-SWE, LS was measured in patients with BCS 2 days before angioplasty and 2 days, 3, and 6 months after angioplasty. Mean LS values for these time points were  $35.1 \pm 10.6$ ,  $20.1 \pm 5.5$ ,  $15.4 \pm 4.3$ , and  $15.7 \pm 5.6$  kPa. While LS decreased significantly in the first 3 months after angioplasty, there was no further change between month 3 and 6. Unfortunately, these stable LS values were in the cirrhotic range [8]. For another case (case no. 20), see also the Chap. 53 on clinical cases in this book.

Taken together, LS elevation in patients with BCS is an important and early sign. It also responds rapidly to recanalization and, therefore, is a promising noninvasive follow-up parameter in these patients. Since LS correlates highly with the venous pressure in BCS patients, the sustained LS elevation after 3 months of angioplasty indicates that this time period is critical. Longer pressure elevation seems to cause permanent collagen deposition in line with the sinusoidal pressure hypothesis [1]. For more details see also book Part VIII “Molecular Basis of Liver Stiffness and Cell Biology.”

## **Liver Stiffness as a Diagnostic Parameter in the Stem Cell Transplantation Setting**

Allogeneic stem cell transplantation (alloSCT) is the treatment of choice for a variety of hematological etiologies including rescue-approaches after failure of previous treatment strategies [10]. Due to the high risk of severe and potentially life-threatening side effects, indications for alloSCT are usually restricted to younger patients with poor prognosis at conventional therapy [10–12]. However, modified alloSCT regimens also provide new opportunities as first line approach and to elderly patients [11, 12].

Complications of alloSCT comprise of infections, toxic side effects of the conditioning chemotherapy and various manifestation of graft-versus-host reactions. Liver-related complications contribute significantly to morbidity and mortality, especially in the early course after alloSCT [13]. Notably, drug-induced liver injury (DILI), acute graft-versus-host disease (GvHD) of the liver, and sinusoidal obstruction syndrome (SOS, also veno-occlusive disease/VOD) are frequently observed during the first 3 months after alloSCT. Although these etiologies show distinct histological patterns, diagnosis is usually established by clinical symptoms and liver function tests. Therefore, differential diagnosis can be challenging due to overlapping clinical definitions of DILI, liver GvHD, and SOS [11, 13–15]. Because these liver complications can alter liver stiffness by inflammatory processes and modulation of liver perfusion, LSM is potentially helpful for diagnosis and monitoring. However, due to the restricted number of patients undergoing alloSCT, current knowledge is still limited to single center experiences, and derives from data of different elastography methods with restricted comparability [16].

## **Diagnosis of Sinusoidal Obstruction Syndrome in the Transplant Setting**

So far, only few studies have analyzed the diagnostic potential of LSM for detection of various liver-related complications e.g. [3, 17], whereas the majority of published data specifically focus on sinusoidal obstruction syndrome (SOS), which is commonly caused by condition therapy-related damage of the sinusoids in central areas

[18]. Given its potentially fatal course and the possibility of a specific pharmacological intervention, this disorder is of special interest in the care of transplanted patients [11].

Data from animal models have been able to recapitulate LS elevation in animal models of SOS [19, 20]. It is usually accompanied by a rapid and intense increase of previously normal liver stiffness, which can precede clinical symptoms by several days. When treatment is successfully performed, liver stiffness declines quite fast and may normalize within 2–3 weeks. Table 14.1 gives an overview of the current stand on LSM for SOS characterization.

**Table 14.1** Overview of studies evaluating liver stiffness measurement (LSM) for the diagnosis and management of sinusoidal obstruction syndrome (SOS)

Author/year	Study type	Method(s)	Cohort size	Main finding(s)	Further commentary
Fontanilla et al. (2011) [25]	Case series	Point-shear wave elastography (pSWE), serial measurements	Two adult patients with SOS	Increased shear wave velocities at diagnosis normalized after successful treatment	Comprehensive diagnostic workup including contrast enhanced and Doppler ultrasound
Colecchia et al. 2016 [26]	Interim analysis of a monocentric prospective study with systematic follow-up for 30 days after allogeneic (SCT)	LSM assessed with transient elastography (TE) prior HCT and on days +7–10, +17–20 and +27–30	22 pediatric patients; four patients developed SOS	A sudden increase of LSM was noted in SOS patients before the appearance of SOS	
Reddivalla et al. 2018 [27]	Monocentric prospective study with systematic follow-up for 24 days after allogeneic SCT	2D-Shearwave elastography (SWE) was performed at three predefined time points	25 pediatric patients; five patients developed SOS	SOS patients had a marked increase of LSM between day 10 and 20 after SCT	LSM changes occurred prior to further observations in imaging and laboratory tests
Colecchia et al. 2019 [28]	Monocentric prospective study with systematic follow-up for 24 days after allogeneic SCT	LSM assessed with transient elastography (TE) prior HCT and on days +9/10, +15/17 and +23/24	Total cohort = 78 patient; four developed SOS	A sudden increase of LSM was observed in all SOS patients 2–12 days prior to the onset of clinical symptoms	LSM increase was only observed in SOS cases, but not in other types of hepatobiliary complications

**Table 14.1** (continued)

Author/ year	Study type	Method(s)	Cohort size	Main finding(s)	Further commentary
Karlas et al. 2019 [3]	Monocentric prospective study with systematic follow-up for 3 months	LSM assessed with TE and pSWE including spleen- pSWE. Evaluation before allogeneic SCT and at the onset of hepatic symptoms	Total cohort = 106; nine developed SOS	Patients with confirmed SOS and/or severe other hepatic complications had elevated LSM compared to those without confirmed liver event	No specific stratification between liver GvHD, drug-induced liver injury, and SOS
Lazzari et al. 2019 [29]	Case report	TE and 2D-SWE at SOS diagnosis, serial LSM during treatment	Adult patient	Maximum LSM values were measured at SOS diagnosis	Normalized LSM values within 100 days after SCT
Zama et al. 2019 [30]	Case series	Serial measurements with TE and 2D-SWE	Three pediatric patients	SOS was associated with a major increase of LSM.	LSM normalized within 2 weeks after successful treatment

## Predictive Value of Liver Stiffness

The risk of liver-related complications of alloSCT is difficult to predict in individual patients, but is usually enhanced in cases with preexisting chronic liver disease [18, 21]. LSM reliably identifies patients with advanced chronic liver disease, but can also indicate overall prognosis in critically ill patients at intensive care units [22]. Auberger et al. described in an early pilot study the potential of LSM to predict the occurrence of liver morbidity in patients undergoing alloSCT [23]. This idea has been followed by Karlas et al. who assessed the predictive value of LSM in a large monocentric cohort [3]. The data show that LSM assessed with either pSWE or transient elastography predicts short-term liver-related and overall morbidity and mortality. Notably, increased baseline LSM was predictive of 1-year survival, especially when combined with liver function tests.

## Future Perspectives and Open Questions

The above-mentioned data identify two major fields where LSM can guide therapeutic decisions in alloSCT: First, LSM can be included in the diagnostic workup for preparation of patients undergoing alloSCT and may complement the risk strat-

ification [15]. Today, the decision to perform alloSCT in a patient with highly elevated LSM should be carefully taken. Further studies have to verify the results from monocentric cohorts [3] and need to provide reasonable, specific cutoff values. Second, the observations of very early LSM dynamics in the onset of SOS indicate that LSM-guided treatment with defibrotide may be beneficial for affected patients (Table 14.1). However, the low incidence of SOS poses considerable challenges for the design of interventional trials of such kind. Moreover, SOS patients frequently need reverse isolation and intensive care treatment, which impair the access to conventional ultrasound units. In the future, portable elastography device may help to overcome such limitations.

In addition to these important questions, diagnosis and monitoring of liver GvHD may be complemented by LSM in the early phase [3, 17] and the long-term course after alloSCT [24], but further data is needed before any recommendation can be given. Considering the complexity of alloSCT treatment [10, 12] and the technical background of LSM as a new diagnostic modality, the further development of LSM application in hematology will require a close collaboration of experts in hematology, hepatology, and ultrasound.

## References

1. Mueller S. Does pressure cause liver cirrhosis? The sinusoidal pressure hypothesis. *World J Gastroenterol.* 2016;22(48):10482.
2. Adolf S, Millonig G, Seitz HK, Reiter A, Schirmacher P, Longerich T, et al. Systemic mastocytosis: a rare case of increased liver stiffness. *Case Rep Hepatol.* 2012;2012:1–6.
3. Karlas T, Weisse T, Petroff D, Beer S, Dohring C, Gnatzy F, et al. Predicting hepatic complications of allogeneic hematopoietic stem cell transplantation using liver stiffness measurement. *Bone Marrow Transplant.* 2019;54(11):1738–46.
4. De Gottardi A, Rautou PE, Schouten J, Rubbia-Brandt L, Leebeek F, Trebicka J, et al. Porto-sinusoidal vascular disease: proposal and description of a novel entity. *Lancet Gastroenterol Hepatol.* 2019;4(5):399–411.
5. Hernández-Gea V, De Gottardi A, Leebeek FWG, Rautou P-E, Salem R, Garcia-Pagan JC. Current knowledge in pathophysiology and management of Budd-Chiari syndrome and non-cirrhotic non-tumoral splanchnic vein thrombosis. *J Hepatol.* 2019;71(1):175–99.
6. Dajti E, Ravaioli F, Colecchia A, Marasco G, Vestito A, Festi D. Liver and spleen stiffness measurements for assessment of portal hypertension severity in patients with Budd Chiari syndrome. *Can J Gastroenterol Hepatol.* 2019;2019:1673197.
7. Mukund A, Pargewar SS, Desai SN, Rajesh S, Sarin SK. Changes in liver congestion in patients with Budd–Chiari syndrome following endovascular interventions: assessment with transient elastography. *J Vasc Interv Radiol.* 2017;28(5):683–7.
8. Wang HW, Shi HN, Cheng J, Xie F, Luo YK, Tang J. Real-time shear wave elastography (SWE) assessment of short- and long-term treatment outcome in Budd-Chiari syndrome: a pilot study. *PLoS One.* 2018;13(5):e0197550.
9. Millonig G, Friedrich S, Adolf S, Fonouni H, Golriz M, Mehrabi A, et al. Liver stiffness is directly influenced by central venous pressure. *J Hepatol.* 2010;52(2):206–10.
10. Copelan EA. Hematopoietic stem-cell transplantation. *N Engl J Med.* 2006;354(17):1813–26.
11. Mohty M, Malard F, Abecassis M, Aerts E, Alaskar AS, Aljurf M, et al. Sinusoidal obstruction syndrome/veno-occlusive disease: current situation and perspectives—a position statement

- from the European Society for Blood and Marrow Transplantation (EBMT). *Bone Marrow Transplant.* 2015;50(6):781–9.
12. Sureda A, Bader P, Cesaro S, Dreger P, Duarte RF, Dufour C, et al. Indications for allo- and auto-SCT for haematological diseases, solid tumours and immune disorders: current practice in Europe, 2015. *Bone Marrow Transplant.* 2015;50(8):1037–56.
  13. McDonald GB. Hepatobiliary complications of hematopoietic cell transplantation, 40 years on. *Hepatology.* 2010;51(4):1450–60.
  14. Chalasani NP, Hayashi PH, Bonkovsky HL, Navarro VJ, Lee WM, Fontana RJ. ACG clinical guideline: the diagnosis and management of idiosyncratic drug-induced liver injury. *Am J Gastroenterol.* 2014;109(7):950–66.
  15. Dietrich CF, Trenker C, Fontanilla T, Görg C, Hausmann A, Klein S, et al. New ultrasound techniques challenge the diagnosis of sinusoidal obstruction syndrome. *Ultrasound Med Biol.* 2018;44(11):2171–82.
  16. Piscaglia F, Salvatore V, Mulazzani L, Cantisani V, Schiavone C. Ultrasound shear wave elastography for liver disease. A critical appraisal of the many actors on the stage. *Ultraschall Med.* 2016;37(1):1–5.
  17. Karlas T, Weber J, Nehring C, Kronenberger R, Tenckhoff H, Mössner J, et al. Value of liver elastography and abdominal ultrasound for detection of complications of allogeneic hemopoietic SCT. *Bone Marrow Transplant.* 2014;49(6):806–11.
  18. Strouse C, Zhang Y, Zhang M-J, DiGilio A, Pasquini M, Horowitz MM, et al. Risk score for the development of veno-occlusive disease after allogeneic hematopoietic cell transplant. *Biol Blood Marrow Transplant.* 2018;24(10):2072–80.
  19. Han H, Yang J, Li X, Zhuge YZ, Zhu CK, Chen J, et al. Role of virtual touch tissue imaging quantification in the assessment of hepatic sinusoidal obstruction syndrome in a rat model. *J Ultrasound Med.* 2018;38(8):2039–46.
  20. Park SH, Lee SS, Sung J-Y, Na K, Kim HJ, Kim SY, et al. Noninvasive assessment of hepatic sinusoidal obstructive syndrome using acoustic radiation force impulse elastography imaging: a proof-of-concept study in rat models. *Eur Radiol.* 2017;28(5):2096–106.
  21. Corbacioglu S, Jabbour EJ, Mohty M. Risk factors for development of and progression of hepatic veno-occlusive disease/sinusoidal obstruction syndrome. *Biol Blood Marrow Transplant.* 2019;25(7):1271–80.
  22. Koch A, Horn A, Dückers H, Yagmur E, Sanson E, Bruensing J, et al. Increased liver stiffness denotes hepatic dysfunction and mortality risk in critically ill non-cirrhotic patients at a medical ICU. *Crit Care.* 2011;15(6):R266.
  23. Auberger J, Graziadei I, Clausen J, Vogel W, Nachbaur D. Non-invasive transient elastography for the prediction of liver toxicity following hematopoietic SCT. *Bone Marrow Transplant.* 2012;48(1):159–60.
  24. Zhang M, Mendiratta-Lala M, Maturen KE, Wasnik AP, Wang SS, Assad H, et al. Quantitative assessment of liver stiffness using ultrasound shear wave elastography in patients with chronic graft-versus-host disease after allogeneic hematopoietic stem cell transplantation: a pilot study. *J Ultrasound Med.* 2018;38(2):455–61.
  25. Fontanilla T, Hernando CG, Claros JCV, Bautista G, Minaya J, del Carmen Vega M, et al. Acoustic radiation force impulse elastography and contrast-enhanced sonography of sinusoidal obstructive syndrome (veno-occlusive disease). *J Ultrasound Med.* 2011;30(11):1593–8.
  26. Colecchia A, Marasco G, Ravaioli F, Kleinschmidt K, Masetti R, Prete A, et al. Usefulness of liver stiffness measurement in predicting hepatic veno-occlusive disease development in patients who undergo HSCT. *Bone Marrow Transplant.* 2016;52(3):494–7.
  27. Reddivalla N, Robinson AL, Reid KJ, Radhi MA, Dalal J, Opfer EK, et al. Using liver elastography to diagnose sinusoidal obstruction syndrome in pediatric patients undergoing hematopoietic stem cell transplant. *Bone Marrow Transplant* 2018. <https://doi.org/10.1038/s41409-017-0064-6>.
  28. Colecchia A, Ravaioli F, Sessa M, Alemanni VL, Dajti E, Marasco G, et al. Liver stiffness measurement allows early diagnosis of veno-occlusive disease/sinusoidal obstruction syndrome in

- adult patients who undergo hematopoietic stem cell transplantation: results from a monocentric prospective study. *Biol Blood Marrow Transplant.* 2019;25(5):995–1003.
29. Lazzari L, Marra P, Greco R, Giglio F, Clerici D, Venturini E, et al. Ultrasound elastography techniques for diagnosis and follow-up of hepatic veno-occlusive disease. *Bone Marrow Transplant.* 2019;54(7):1145–7.
  30. Zama D, Bossu G, Ravaioli F, Masetti R, Prete A, Festi D, et al. Longitudinal evaluation of liver stiffness in three pediatric patients with veno-occlusive disease. *Pediatr Transplant.* 2019;23(5):e13456.



# Chapter 15

## Liver and Spleen Stiffness in Patients with Portal Vein Thrombosis



Praveen Sharma

### Introduction

Besides cirrhosis, portal vein thrombosis (PVT) is the second most common cause of portal hypertension (PH) both in developing and developed countries [1, 2]. Non-tumoral thrombosis of the portal vein (PV) and associated splanchnic vein can occur from a variety of reasons which includes portal hypertension due to cirrhosis, hypercoagulable state, and vascular endothelial injury. Anatomically, PVT can occur in the intra- or extrahepatic tract and/or involve the superior mesenteric vein and/or the spleen vein [3]. It is important in clinical practice to distinguish between the common cirrhosis-related PVT and the uncommon non-cirrhotic-related PVT. This distinction is critical, as the evaluation, prognosis, and treatment are different. Extrahepatic portal vein obstruction (EHPVO) is a vascular disorder of the liver defined by obstruction of the extrahepatic portal vein with or without involvement of the intrahepatic portal veins or spleen or superior mesenteric vein [3]. Patients with PVT can present in variable forms and range from asymptomatic incidental findings of splenomegaly to severe complications of portal hypertension like variceal bleeding. Normally, imaging like abdominal ultrasound with Doppler study of splenoportal axis clinches the diagnosis of EHPVO and is considered as modality of choice for diagnosis [3–5]. However, in the long-term, the liver contours change in patients with PVT and most radiologists often cannot differentiate between portal vein thrombosis due to cirrhosis or EHPVO.

---

P. Sharma (✉)  
Sir Ganga Ram Hospital, New Delhi, India

## Liver and Spleen Stiffness in Patients with Portal Vein Thrombosis

There are limited studies evaluating LS and SS in patients with PVT. Moreover, it is not known how PVT will affect LS and SS in patients with cirrhosis. Sharma et al. [5] evaluated 65 patients with EHPVO (with bleeding,  $n = 45$ ; without bleeding,  $n = 20$ ; mean age,  $25.4 \pm 10.7$  years; 29 men, 36 women) were enrolled. Twenty-two (34%) had splenomegaly. LS and SS were significantly higher in patients with EHPVO ( $6.7 \pm 2.3$  and  $51.7 \pm 21.5$  kPa, respectively) than in control subjects ( $4.6 \pm 0.7$  and  $16.0 \pm 3.0$  kPa, respectively). Patients with events of bleeding had higher SS than those without bleeding ( $60.4 \pm 5.4$  vs.  $30.3 \pm 14.2$  kPa,  $P = 0.01$ ). There was no significant difference in age and median duration of disease in patients with bleeding versus those without. With a cutoff value of 5.9 kPa for LS, sensitivity and specificity for detection of a variceal bleeding were 67% and 75%, respectively. A SS cutoff of 42.8 kPa yielded a sensitivity and specificity of 88% and 94%, respectively. It was concluded that SSM measurement is a useful tool for predicting esophageal varices.

Another study by Madhusudhan KS [6] evaluated SS using 2D-SWE in 52 patients with EHPVO with a mean age of 22.3 years. Here, the mean SS was  $44.9 \pm 12.3$  kPa. There was no significant difference between the mean SS of patients with high-grade varices (44.3 kPa;  $n = 25$ ) and those with low-grade varices (46.9 kPa;  $n = 20$ ). The analysis showed a poor area under the curve (AUROC) of 0.477 for the prediction of high-grade varices by SS. In addition, SS did not show any significant correlation with other ultrasonography parameters except spleen size. They concluded that the SS measured by 2D-SWE is not an accurate predictor of variceal grade and bleeding in patients of EHPVO. Same author also studied LS in 50 patients of EHPVO and 25 healthy volunteers by 2D-SWE. LS did not differ significantly between patients with EHPVO and healthy volunteers (5.9 vs. 5.5 kPa,  $P = 0.093$ ). There was no significant correlation between LS with duration of symptoms, hematemesis, esophageal varices, total bilirubin, serum alkaline phosphatase, and AST levels in the EHPVO group [7]. Hence, it seems that LS remains normal or near normal in patients with portal hypertension and extrahepatic portal vein obstruction [7, 8].

## Elevated Liver Stiffness in Patients with PVT

However, a case report of a patient with PVT found high LS by TE in the presence of normal or near normal liver biopsy. It was hypothesized that the hepatic arterial buffer response (HABR) accounted for LS elevation by a compensatory increase of arterial perfusion [9].

In a study by Sutton et al. [10] 15 children with a median age of 10 years underwent TE measurements. Median SS and LS in PVT were 4.7 (2–65.2) kPa and 57.5

(11–75) kPa. SS was significantly different between patients with clinical significant varices versus those with no clinical significant varices (62.8 vs. 13.2 kPa). No difference was found in LSM (19.4 vs. 8.7 kPa). In this study, children with PVT had LS values which ranged from 2 to 65.2 kPa. However, no details about histology were provided. In another study in patients with non-cirrhotic portal hypertension by Vuppalanchi et al. [11], 13 cases had portal hypertension secondary to PVT. Here, mean LS was  $8.4 \pm 5.4$  kPa with a range from 3.6 to 18.8 kPa.  $LS > 6.5$  kPa was seen in 31%. Eleven patients underwent portal pressure measurements and 45% had elevated LS. In those with abnormal LS, the free hepatic vein pressure was significantly higher with  $11 \pm 3$  vs.  $6 \pm 4$  mmHg ( $P = 0.033$ ). No differences were found with regard to right atrial pressure, wedge hepatic vein pressure, and hepatic vein pressure gradient between PVT patients with normal and abnormal LS. They assumed that the elevated LS is likely due to an elevated free hepatic vein pressure (FHVP). Increased FHVP may be possibly related to hyperdynamic circulation due to development of collateral vessels and altered hepatic artery blood flow as it is inversely related to portal vein flow. Moreover, compression by choledochal or periportal varices of the extrahepatic biliary tree from chronic PVT may be associated with increased biliary pressure.

Seijo et al. [12] retrospectively studied 39 cases of idiopathic portal hypertension patients. For other chapters on portal hypertension, see also book Part V “LS and Important Clinical Endpoints.” Hepatic vein catheterization and LSM were compared to matched patients with either cirrhosis-related portal hypertension or non-cirrhotic portal vein thrombosis. Mean LS in idiopathic portal hypertension was with  $8.4 \pm 3.3$  kPa significantly higher than in non-cirrhotic portal vein thrombosis ( $6.4 \pm 2.2$  kPa,  $P = 0.009$ ), but lower than in cirrhosis ( $40.9 \pm 20.5$  kPa,  $P = 0.005$ ). FHVP was  $7.5 \pm 3.0$  mmHg which was not significantly different between patients with cirrhosis and idiopathic portal hypertension. In conclusion, it still remains poorly understood why LS increases in patients with PVT but normal biopsy. One explanation could be learnt from animal models [13]. In this study, portal vein ligation resulted in liver fibrosis. According to the sinusoidal pressure hypothesis [14], portal vein ligation causes a compensatory elevated arterial flow via the hepatic arterial buffer response that exposes the sinusoidal bed permanently to high pressure. It is evident that LS may not be able to discriminate between PVT and onset cirrhosis by other etiologies. For more details see also book Part VIII “Molecular Basis of Liver Stiffness and Cell Biology.”

## References

1. Khanna R, Sarin SK. Idiopathic portal hypertension and extrahepatic portal venous obstruction. *Hepatol Int.* 2018;12(S1):148–67.
2. Sarin SK, Agarwal SR. Extrahepatic portal vein obstruction. *Semin Liver Dis.* 2002;22(1):043–58.
3. Sarin SK, Sollano JD, Chawla YK, Amarapurkar D, Hamid S, Hashizume M, et al. Consensus on extra-hepatic portal vein obstruction. *Liver Int.* 2006;26(5):512–9.

4. Baba M, Furuya K, Bandou H, Kasai K, Sadaoka K. Discrimination of individuals in a general population at high-risk for alcoholic and non-alcoholic fatty liver disease based on liver stiffness. *BMC Gastroenterol.* 2011;11(1):70.
5. Sharma P, Mishra SR, Kumar M, Sharma BC, Sarin SK. Liver and spleen stiffness in patients with extrahepatic portal vein obstruction. *Radiology.* 2012;263(3):893–9.
6. Madhusudhan KS, Kilambi R, Shalimar SP, Sharma R, Srivastava DN, et al. Measurement of spleen stiffness by 2D-shear wave elastography in patients with extrahepatic portal vein obstruction. *Br J Radiol.* 2018;91(1092):20180401.
7. Madhusudhan KS, Sharma R, Kilambi R, Shylendran S, Shalimar SP, et al. 2D Shear wave elastography of liver in patients with primary extrahepatic portal vein obstruction. *J Clin Exp Hepatol.* 2017;7(1):23–7.
8. Sharma P, Kirnake V, Tyagi P, Bansal N, Singla V, Kumar A, et al. Spleen stiffness in patients with cirrhosis in predicting esophageal varices. *Am J Gastroenterol.* 2013;108(7):1101–7.
9. Huang R, Gao Z-H, Tang A, Sebastiani G, Deschenes M. Transient elastography is an unreliable marker of liver fibrosis in patients with portal vein thrombosis. *Hepatology.* 2018;68(2):783–5.
10. Sutton H, Fitzpatrick E, Davenport M, Burford C, Alexander E, Dhawan A, et al. Transient elastography measurements of spleen stiffness as a predictor of clinically significant varices in children. *J Pediatr Gastroenterol Nutr.* 2018;67(4):446–51.
11. Vuppalanchi R, Mathur K, Pyko M, Samala N, Chalasani N. Liver stiffness measurements in patients with noncirrhotic portal hypertension—the devil is in the details. *Hepatology.* 2018;68(6):2438–40.
12. Seijo S, Reverter E, Miquel R, Berzigotti A, Abraldes JG, Bosch J, et al. Role of hepatic vein catheterisation and transient elastography in the diagnosis of idiopathic portal hypertension. *Dig Liver Dis.* 2012;44(10):855–60.
13. Yamasaki M, Ikeda K, Nakatani K, Yamamoto T, Kawai Y, Hirohashi K, et al. Phenotypical and morphological alterations to rat sinusoidal endothelial cells in arterialized livers after portal branch ligation. *Arch Histol Cytol.* 1999;62(5):401–11.
14. Mueller S. Does pressure cause liver cirrhosis? The sinusoidal pressure hypothesis. *World J Gastroenterol.* 2016;22(48):10482.

# Chapter 16

## Liver Stiffness in Autoimmune Hepatitis



Johannes Hartl

### Introduction

Autoimmune hepatitis (AIH) is a chronic non-resolving disorder of the immune system characterized by loss of immunological tolerance against hepatocytes which induces chronic inflammation [1]. Today, immunosuppression is the cornerstone for disease control or cure. The prognosis of treated AIH is generally good; however, insufficient treatment or too late diagnosis harbors a significant risk of fibrosis progression and adverse outcome [2–4]. Therefore, patients with AIH require close, life-long monitoring. Hence, there is a need for noninvasive surrogate markers for disease progression in AIH, and monitoring liver stiffness (LS) seems to be a promising tool for early screening and follow-up.

### Liver Stiffness Is a Reliable Surrogate Marker for Fibrosis Staging in AIH Patients Under Immunosuppression

Since autoimmune hepatitis is a relatively rare disease, the diagnostic accuracy of LSM as a surrogate for liver fibrosis has been assessed in a limited number of studies [5–11]. In a first study with 45 included patients with AIH we have observed an excellent accuracy for the detection of significant ( $F > 1$  according to Desmet and Scheuer, see Appendix) and severe liver fibrosis ( $F > 2$ ) by transient elastography (TE) with an AUROC of 0.89 and 0.93, respectively [7]. Subsequent studies have consistently confirmed these results [6, 8–10].

---

J. Hartl (✉)  
Medizinische Klinik und Poliklinik, Universitätsklinikum Hamburg-Eppendorf,  
Hamburg, Germany

**Table 16.1** Cutoff values for TE and SWE for fibrosis staging in AIH from [7]

Histological staging	Liver stiffness by TE [ $n = 94$ ]*		
	$F > 1$	$F > 2$	$F = 4$
Optimal cutoff	5.80	10.40	16.00
AUROC	0.87	0.93	0.96
Sensitivity	0.90	0.83	0.88
Specificity	0.72	0.98	1.00

A subsequent study found a comparable diagnostic performance of TE, but slightly lower cutoff values for the detection of liver cirrhosis [1]

\* Correlation between histological staging and liver stiffness:  $\rho = 0.777$ ,  $P < 0.0001$

Hence, the diagnostic accuracy of fibrosis staging by TE seems to be comparable to other more extensively studied liver diseases, such as viral hepatitis C [5]. Besides the more established TE, new ultrasound-based techniques such as 2D-SWE and pSWE are emerging as novel methods to noninvasively assess liver fibrosis. Unlike TE, 2D-SWE and pSWE provide a conventional B-mode image without any extra equipment. Therefore, hepatic parenchyma and hepatic fibrosis can be assessed simultaneously. Both, 2D-SWE and pSWE, have been relatively well studied in other chronic liver diseases, in which a comparable diagnostic performance to TE was found [12, 13]. In AIH, limited but promising data on these novel ultrasound-based methods are available: A study by Sun et al. comprising 112 AIH patients reported an AUROC of 0.91 for the detection of significant fibrosis [ $F > 1$ ] by 2D-SWE [10], and LS assessed by pSWE (ARFI) strongly correlated with the histological fibrosis stage in a small cohort of 31 AIH patients [9]. Unfortunately, neither techniques have been directly compared with TE or with each other in AIH. Cutoff values for TE are given in Table 16.1.

## Impact of Hepatic Inflammation on Liver Stiffness in AIH

It is well-known that hepatic inflammation can increase liver stiffness independent of fibrosis stage [5, 14–17] and that LS decreases after resolution of inflammation [17]. AIH was also suggested to be particularly prone to potential bias introduced by hepatic inflammation. Some patients with AIH show considerable inflammatory disease activity on histological assessment, even without markedly elevated liver enzymes [3]. Moreover, it has been demonstrated that histological resolution of disease activity may lack behind by several months after normalization of serum aminotransferases [18].

Accordingly, we found that LS assessed by TE correlated better with histological grading than with staging within the first weeks after initiation of immunosuppression [7]. Along the same line, a sharp decrease of LS is paralleled by a decrease of serum aminotransferases within the first weeks under immunosuppression [7]. However, after a time interval of 6 months under immunosuppression, LS correlated most reliably with histological fibrosis stage but not with grading. Most importantly,

**Table 16.2** Correlation of liver stiffness assessed by TE with histological grading and staging depending on the time interval between initiation of immunosuppression and liver stiffness measurement [7]

Parameters	Time interval between TE and initiation of immunosuppression		
	<3 months [n = 34] Group 1	6–18 months [n = 25] Group 2	>4 years [n = 27] Group 3
ALT, U/L*	70 ± 51 [8–191]	37 ± 43 [15–108]	38 ± 47 [15–94]
IgG, g/L	15.7 ± 2.9 [10–21]	13.4 ± 4.7 [9–27]	13.0 ± 5.3 [9.6–23]
Grading, according to Desmet and Scheuer**	2.8 [3]	1.8 [2]	1.7 [2]
Correlation TE and grading, Spearman coefficient	$\rho = 0.558$ , $P = 0.001$	$\rho = 0.404$ , $P = 0.062$	$\rho = 0.422$ , $P = 0.045$
Correlation TE and staging, Spearman coefficient	$\rho = 0.399$ , $P = 0.19$	$\rho = 0.809$ , $P < 0.0001$	$\rho = 0.850$ , $P < 0.0001$

\* The difference between group 1 vs. group 2 and group 1 vs. group 3 was significant ( $P = 0.016$  and  $P = 0.014$ , respectively)

\*\* The difference between group 1 vs. group 2 and group 1 vs. group 3 was significant ( $P = 0.024$  and  $P < 0.0001$ , respectively)

there was no difference in the diagnostic performance of TE between patients in complete biochemical remission and those with moderately elevated liver enzymes (serum transaminases <4× upper limit of normal). Hepatic inflammation usually resolves in patients under immunosuppression for at least 6 months and without a severe disease flare. Similar findings have been reported by Xu et al. in patients with AIH [11]. For other liver diseases such as alcoholic hepatitis and viral hepatitis, it has been reported that hepatic inflammation has little impact on liver stiffness in patients with ALT < 100 U/L [17]. Table 16.2 displays the association between LS and histological grading and staging depending on the duration of immunosuppressive treatment [7]. For other inflammatory liver diseases, such as viral hepatitis C and alcoholic hepatitis, it has been shown that inflammation-adapted liver stiffness cutoffs based on serum transaminases can correct for a bias introduced by hepatic inflammation [19]. Similar data are so far missing for AIH. However, the vast majority of treated AIH patients have normal or only moderately elevated serum transaminases, and the diagnostic performance of fibrosis staging by LS is excellent in these patients.

## LS an Excellent Parameter to Predict Disease Progression in AIH

In the view of the reliable diagnostic performance of LSM, we consider yearly follow-up measurements as sufficient for disease monitoring in most patients, especially to assure a lack of disease progression.

In clinical practice, treatment monitoring in AIH is principally guided by biochemical markers for hepatic inflammation. Besides serum aminotransferases, it has been shown that elevated immunoglobulin G (IgG) levels and gamma-globulins are also associated with ongoing inflammatory disease activity [3, 11, 20]. Therefore, most current treatment guidelines define complete biochemical remission as repeatedly normal serum aminotransferases and IgG levels as a main treatment goal in AIH [21]. In our experience, this definition of complete biochemical remission is a reliable surrogate of low histological disease activity [8].

Nevertheless, AIH is characterized by a fluctuating disease course and disease progression might be missed if biochemical parameters are assessed infrequently [21]. We therefore believe that yearly liver stiffness measurements in addition to biochemical remission help to exclude disease progression, thereby reducing the need of follow-up liver biopsies. In addition, we have reported that AIH patients in complete biochemical remission have a high chance of fibrosis regression, which can be documented by a decrease of LS [8]. This can be a very motivating finding for patients, especially when the initial diagnosis of AIH had been established at an advanced fibrosis stage. First data on the long-term prognosis of LS in other liver diseases are promising and suggest a similar performance for AIH [22].

In other patients, complete biochemical remission is difficult to achieve, and the risk of disease progression needs to be weighed against potential side effects of intensified immunosuppressed treatment. Moreover, some treatment regimens may cause drug-induced liver injury (DILI). In these patients, follow-up liver biopsies are usually required at some point to guide the intensity of immunosuppressive treatment. Follow-up liver stiffness measurement might be helpful in order to find the right timing for follow-up liver biopsies. Figure 16.1 depicts the change of LS over time in AIH depending on the fibrosis stage at baseline and whether patients are in stable biochemical remission [8].

In summary, LS can reliably detect fibrosis in AIH and annual follow-up LSM provides helpful information in order to exclude disease progression, thereby minimizing the need of follow-up liver biopsies. During the first weeks after initiation of immunosuppression, liver stiffness should be interpreted with caution in terms of fibrosis stage, since hepatic inflammation can lead to an increase of LS. Besides TE, novel ultrasound-based techniques such as 2D-SWE and pSWE seem to have a reliable diagnostic accuracy, albeit limited data is available in AIH.



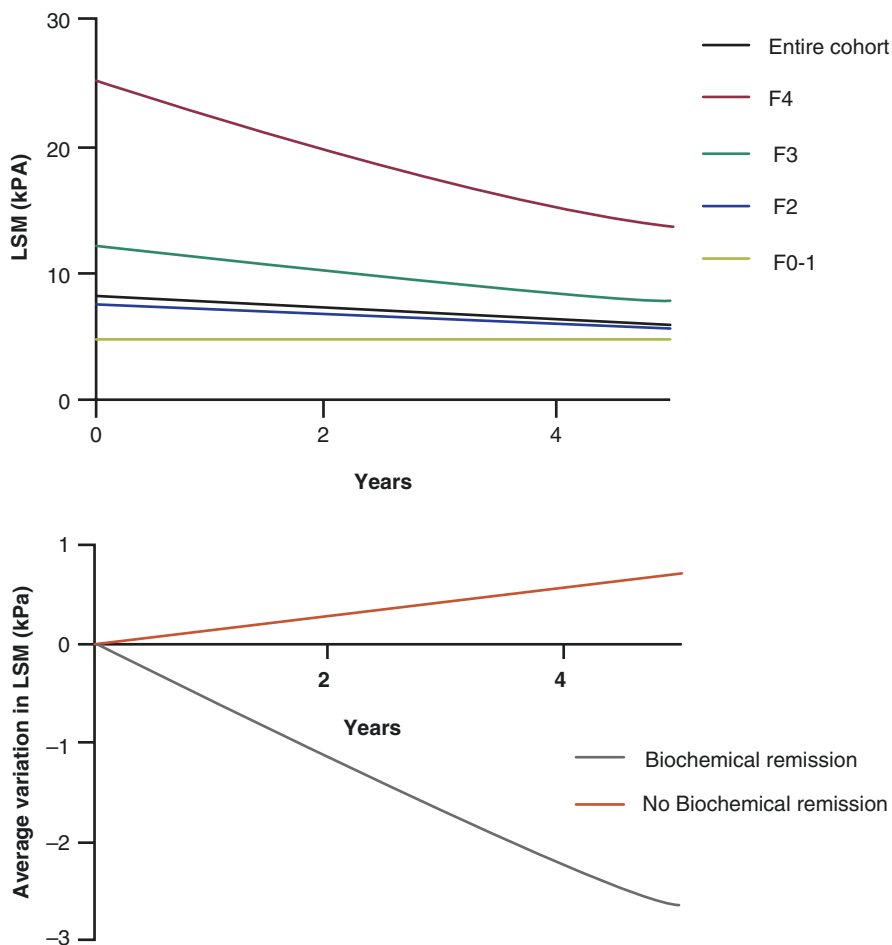


**Fig. 16.1** Changes of liver stiffness in treated AIH as assessed by TE. **(a)** Change of liver stiffness depending on the fibrosis stage at baseline according to Desmet and Scheuer classification; **(b)** Changes of liver stiffness in dependence whether patients achieved complete biochemical remission [8]

## References

1. Krawitt EL. Autoimmune hepatitis. *N Engl J Med.* 2006;354(1):54–66.
2. Czaja AJ, Carpenter HA. Progressive fibrosis during corticosteroid therapy of autoimmune hepatitis. *Hepatology.* 2004;39(6):1631–8.
3. Dhaliwal HK, Hoeroldt BS, Dube AK, McFarlane E, Underwood JCE, Karajeh MA, et al. Long-term prognostic significance of persisting histological activity despite biochemical remission in autoimmune hepatitis. *Am J Gastroenterol.* 2015;110(7):993–9.
4. Grønbaek L, Vilstrup H, Jepsen P. Autoimmune hepatitis in Denmark: incidence, prevalence, prognosis, and causes of death. A nationwide registry-based cohort study. *J Hepatol.* 2014;60(3):612–7.

5. Goertz RS, GaBmann L, Strobel D, Wildner D, Schellhaas B, Neurath MF, et al. Acoustic Radiation Force Impulse (ARFI) elastography in autoimmune and cholestatic liver diseases. *Ann Hepatol.* 2019;18(1):23–9.
6. Guo L, Zheng L, Hu L, Zhou H, Yu L, Liang W. Transient elastography (FibroScan) performs better than non-invasive markers in assessing liver fibrosis and cirrhosis in autoimmune hepatitis patients. *Med Sci Monit.* 2017;23:5106–12.
7. Hartl J, Denzer U, Ehlken H, Zenouzi R, Peiseler M, Sebode M, et al. Transient elastography in autoimmune hepatitis: timing determines the impact of inflammation and fibrosis. *J Hepatol.* 2016;65(4):769–75.
8. Hartl J, Ehlken H, Sebode M, Peiseler M, Krech T, Zenouzi R, et al. Usefulness of biochemical remission and transient elastography in monitoring disease course in autoimmune hepatitis. *J Hepatol.* 2018;68(4):754–63.
9. Park DW, Lee YJ, Chang W, Park JH, Lee KH, Kim YH, et al. Diagnostic performance of a point shear wave elastography (pSWE) for hepatic fibrosis in patients with autoimmune liver disease. *PLoS One.* 2019;14(3):e0212771.
10. Sun LL, Dong G, Wang B, Zheng Q, Wang S, Zhang RF. Real-time shear wave elastography and APRI index for evaluating autoimmune hepatitis fibrosis. *J Biol Regul Homeost Agents.* 2016;30(4):1019–21.
11. Xu Q, Sheng L, Bao H, Chen X, Guo C, Li H, et al. Evaluation of transient elastography in assessing liver fibrosis in patients with autoimmune hepatitis. *J Gastroenterol Hepatol.* 2017;32(3):639–44.
12. Bota S, Herkner H, Sporea I, Salzl P, Sirlu R, Neghina AM, et al. Meta-analysis: ARFI elastography versus transient elastography for the evaluation of liver fibrosis. *Liver Int.* 2013;33(8):1138–47.
13. Poynard T, Pham T, Perazzo H, Munteanu M, Luckina E, Elaribi D, et al. Real-time shear wave versus transient elastography for predicting fibrosis: applicability, and impact of inflammation and steatosis. A non-invasive comparison. *PLoS One.* 2016;11(10):e0163276.
14. EASL-ALEH clinical practice guidelines: non-invasive tests for evaluation of liver disease severity and prognosis. *J Hepatol.* 2015;63(1):237–64.
15. Coco B, Oliveri F, Maina AM, Ciccorossi P, Sacco R, Colombatto P, et al. Transient elastography: a new surrogate marker of liver fibrosis influenced by major changes of transaminases. *J Viral Hepat.* 2007;14(5):360–9.
16. Tapper EB, Cohen EB, Patel K, Bacon B, Gordon S, Lawitz E, et al. Levels of alanine aminotransferase confound use of transient elastography to diagnose fibrosis in patients with chronic hepatitis C virus infection. *Clin Gastroenterol Hepatol.* 2012;10(8):932–7.e1.
17. Mueller S, Millonig G, Sarovska L, Friedrich S, Reimann FM, Pritsch M, et al. Increased liver stiffness in alcoholic liver disease: differentiating fibrosis from steatohepatitis. *World J Gastroenterol.* 2010;16(8):966–72.
18. Soloway RD, Summerskill WHJ, Baggenstoss AH, Geall MG, Gitnick GL, Elveback LR, et al. Clinical, biochemical, and histological remission of severe chronic active liver disease: a controlled study of treatments and early prognosis. *Gastroenterology.* 1972;63(5):820–33.
19. Mueller S, Englert S, Seitz HK, Badea RI, Erhardt A, Bozaari B, et al. Inflammation-adapted liver stiffness values for improved fibrosis staging in patients with hepatitis C virus and alcoholic liver disease. *Liver Int.* 2015;35(12):2514–21.
20. Lüth S, Herkel J, Kanzler S, Frenzel C, Galle PR, Dienes HP, et al. Serologic markers compared with liver biopsy for monitoring disease activity in autoimmune hepatitis. *J Clin Gastroenterol.* 2008;42(8):926–30.
21. Corrigendum to “EASL Clinical Practice Guidelines: Autoimmune hepatitis” [*J Hepatol* 2015;63:971–1004]. *J Hepatol.* 2015;63(6):1543–4.
22. Mueller J, Rausch V, Silva I, Peccerella T, Piecha F, Dietrich C, et al. PS-171-Survival in a 10 year prospective cohort of heavy drinkers: liver stiffness is the best long-term prognostic parameter. *J Hepatol.* 2019;70(1):E107-E.

# Chapter 17

## Liver Fibrosis Assessment in Adults with Alpha1-Antitrypsin Deficiency



Vítor Magno Pereira, Karim Hamesch, and Pavel Strnad

### Abbreviations

AAT	Alpha1-antitrypsin
AATD	Alpha1-antitrypsin deficiency
CAP	Controlled attenuation parameter
LSM	Liver stiffness measurements
Pi*M	Normal AAT allele
Pi*MM	Normal AAT genotype
Pi*MZ	AAT genotype with heterozygosity for the Pi*Z variant
Pi*S/Pi*Z	Mutant AAT allele variants
TE	Transient elastography (FibroScan(R))

### Introduction

Alpha1-antitrypsin (AAT) is an important inhibitor of multiple serine proteases including neutrophil elastase and proteinase 3 and protects the tissues from proteolytic damage [1]. Genetic variants in AAT often lead to its retention in the endoplasmic reticulum of hepatocytes, thereby causing decreased levels in the systemic circulation [1, 2]. Because of the latter, the resulting disorder was termed AAT

---

V. Magno Pereira  
Department of Gastroenterology, Centro Hospitalar do Funchal, Madeira, Portugal

K. Hamesch · P. Strnad (✉)  
Coordinating Center for Alpha1-Antitrypsin Deficiency-Related Liver Disease of the European Reference Network on Hepatological Diseases (ERN-RARE-LIVER) and the European Association for the Study of the Liver Registry Group “Alpha1-Liver”, Aachen, Germany

Medical Clinic III, Gastroenterology, Metabolic Diseases and Intensive Care, University Hospital RWTH Aachen, Aachen, Germany  
e-mail: [khamesch@ukaachen.de](mailto:khamesch@ukaachen.de); [pstrnad@ukaachen.de](mailto:pstrnad@ukaachen.de)

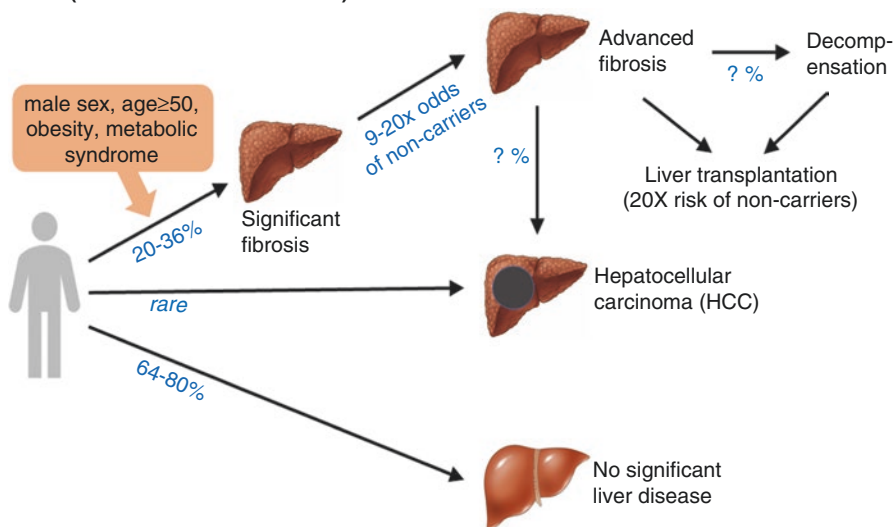
deficiency (AATD) and constitutes one of the most common, potentially fatal genetic diseases [1, 2].

Every tenth Caucasian carries an AAT mutation and, up to date, more than 100 variants in the AAT gene have been described [3]. Among them, Pi\*Z (a substitution of lysine for glutamic acid at codon 342; rs28929474) and Pi\*S (a substitution of valine for glutamic acid at codon 264; rs17580) variants are the most clinically relevant ones, while the wild-type allele is termed Pi\*M. Pi\*S and Pi\*Z display a differing geographic distribution. Pi\*Z is more common in Northern (prevalence up to 8%) and Pi\*S in the Southern Europe (prevalence up to 20%; [4]). Pi\*Z is the more deleterious variant and accordingly, Pi\*ZZ (i.e. the homozygous presence of Pi\*Z allele) is the classic cause of severe AATD and has a prevalence of 1:2000 to 1:4000 in Caucasians [2, 3]. Pi\*ZZ carriers regularly display the histological hallmark of the disease—the presence of accumulated AAT that can be recognized as roundish, intracellular aggregates in periodic-acid-Schiff-diastase staining [5]. On the other hand, Pi\*SZ (compound heterozygosity; i.e. a simultaneous presence of both variants) is even more common but, at least with regard to the lung phenotype, seems to be less damaging [6]. In line with that, Pi\*SS (i.e. the homozygous presence of Pi\*S allele) is considered to result in only a mild lung phenotype [7].

Loss of AAT is particularly apparent in the lungs, where it predisposes to the development of lung emphysema and chronic obstructive pulmonary disease (COPD). Notably, the lung involvement represents the major cause of death in AATD [1, 3]. In contrast, the accumulation of misfolded protein in the liver leads to a “gain-of-function” toxicity and promotes the development of liver cirrhosis as well as hepatocellular carcinoma [8, 9]. Additionally, AAT constitutes an important immunomodulatory protein and individuals carrying AAT variants are at higher risk to develop immune-related disorders such as ANCA-positive vasculitis or panniculitis [3].

## Liver Disease in AATD

Liver involvement constitutes the second most common cause of death in AATD and has been particularly well studied in Pi\*ZZ carriers [8]. It may become apparent already in neonates, in that some Pi\*ZZ babies suffer a prolonged neonatal cholestasis. While it typically resolves within months, up to 5% of children may progress to end-stage liver disease and require a liver transplantation during a preschool or early school age [8, 10]. Accordingly, severe AATD accounts for 3.5% of paediatric liver transplantations [11]. Children who survive this critical period typically improve and during adolescence, most Pi\*ZZ individuals display normal liver function [12]. However, some Pi\*ZZ individuals develop liver disease during adulthood, often after 50 years of age. To that end, two large cross-sectional studies demonstrated the presence of significant liver fibrosis in 20–36% of Pi\*ZZ carriers [5, 13] and advanced liver fibrosis was 9–20 times more frequent in Pi\*ZZ individuals compared to subjects not carrying any AAT mutation (termed Pi\*MM) (Fig. 17.1; [13]).

**Pi\*ZZ (1:2000-1:4000 Caucasians)**

**Fig. 17.1** Liver phenotype in individuals with a severe, homozygous alpha1-antitrypsin mutation (Pi\*ZZ genotype). “?” indicates that the exact rate of the development of the described event is not known

In line with that, Pi\*ZZ individuals are 20 times more likely to require liver transplantation than noncarriers [14]. Notably, Pi\*ZZ-related liver disease is highly heterogeneous and the majority of Pi\*ZZ carriers never develop a clinically relevant liver disease (Fig. 17.1). While the exact factors contributing to disease progression remain unknown, male sex, age  $\geq 50$  years, obesity, and presence of diabetes/metabolic syndrome seem to play an important role [5, 13, 15] (Fig. 17.1). Despite the recent efforts and the above described studies, AATD-associated liver disease remains greatly understudied, which is particularly striking given that it is more prevalent than several more established liver disorders such as autoimmune hepatitis or primary sclerosing cholangitis [13]. In that respect, individuals with a heterozygous Pi\*MZ mutation (genotype Pi\*MZ) need to be also taken into the account, since they constitute 2–4% of Caucasian population and are susceptible to development of advanced liver fibrosis/liver cirrhosis after a second hit (Fig. 17.2).

## Noninvasive Methods to Assess Liver Fibrosis in Patients with Alpha1-Antitrypsin Deficiency

Blood tests and various elastography methods have been developed to noninvasively estimate the amount of liver fibrosis. As shown in Table 17.1, Clark et al. systematically evaluated 94 non-cirrhotic Pi\*ZZ adults from North America and demonstrated clinically significant liver fibrosis (i.e. fibrosis stage of at least 2 on a 0–4 METAVIR

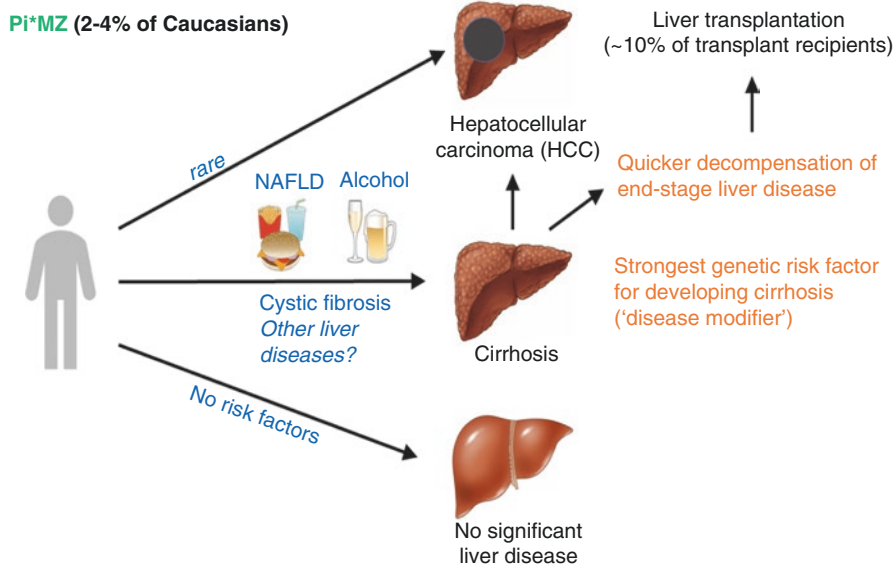


**Fig. 17.2** Heterozygous carriage of the Pi\*Z variant in alpha1-antitrypsin (Pi\*MZ genotype) as a risk factor for liver disease development

**Table 17.1** Overview of published studies using noninvasive methods to evaluate liver fibrosis in alpha1-antitrypsin-related liver disease

Reference	Number of patients	Main findings	Limitations
Kim et al. 2016 [17]	11 Pi*ZZ adults	MRE $\geq 3.0$ kPa is useful to predict existence of histologically proven liver fibrosis ( $F \geq 1$ ): 89% accuracy, 80% sensitivity and 100% specificity, AUROC 0.9	Small sample size
Clark et al. 2018 [5]	94 Pi*ZZ adults	Comparison of noninvasive liver fibrosis assessment methods with liver histology. TE > 5.45 kPa AUROC for $F \geq 2$ : 0.70; TE > 8.45 kPa AUROC for $F \geq 3$ : 0.92. $F \geq 2$ associates with metabolic syndrome	Only 6 patients with F3 fibrosis, no cirrhotic patients
Janciauskiene et al. 2011 [28]	52 Pi*ZZ adults with 34 years of age, 81 Pi*MM	Analysis of serum fibrosis test [29] and hepatocellular injury markers (M30 and M65) 81% correct classification of Pi*ZZ and Pi*MM cases (73% of sensitivity and 86% specificity)	No histology, small sample size, restricted age

**Table 17.1** (continued)

Reference	Number of patients	Main findings	Limitations
Mostafavi et al. 2017 [19]	32 Pi*ZZ, 15 Pi*SZ adults	Noninvasive liver fibrosis assessment via ARFI elastography in a population-based cohort; liver stiffness significantly higher in Pi*ZZ men and Pi*SZ men compared with Pi*MM men.	Small sample size, patient age 37–40 years, no liver histology
Mandorfer et al. 2018 [20]	31 Pi*ZZ/SZ, 11 Pi*MZ/MS adults	Analysis of liver fibrosis/steatosis via TE/CAP, measurement of HVPG. Liver stiffness was higher in Pi*ZZ men and Pi*SZ men compared with Pi*MM men.	Small sample size, no histology.
Reiter et al. 2018 [26]	11 Pi*ZZ, 4 Pi*MZ, 16 Pi*MM adults	Parallel evaluation of MRE, ARFI and 2D-SWE, strong correlation between the methods.	No histology, small sample size.
Diaz et al. 2018 [25]	29 Pi*ZZ 12 Pi*SZ 42 Pi*MM adults, 37–40 years old	Noninvasive liver fibrosis assessment via ARFI elastography. No significant difference in ARFI values between the Pi*ZZ carriers and noncarriers.	No histology, small sample size and restricted age
Guillaud et al. 2019 [21]	29 Pi*ZZ adults	Noninvasive liver fibrosis assessment via TE, 18% with TE > 7.2 kPa (suggesting significant fibrosis) 7% with TE > 14 kPa (suggesting advanced fibrosis)	No histology, small sample size
Karim Hamesch et al. 2019 [13]	554 Pi*ZZ, 234 Pi*MM adults	Noninvasive liver fibrosis assessment via TE, APRI and HepaScore. Significant fibrosis 20–36% of Pi*ZZ, advanced fibrosis: 9–20× more common in Pi*ZZ vs. Pi*MM. Severe steatosis (CAP-based) 39% of Pi*ZZ	No histology (but extensive cross-validation between different noninvasive methods)

Abbreviations: *2D-SWE* two-dimensional shear wave elastography, *APRI* AST-to-platelet ratio index, *CAP* controlled attenuation parameter (Fibroscan-based), *ELF* Enhanced Liver Fibrosis Test (serum-based noninvasive assessment of liver fibrosis), *HVPG* hepatic venous pressure gradient, *MRE* magnetic resonance elastography, *Pi\*MM* non-mutated alpha1-antitrypsin genotype, *Pi\*SZ* compound heterozygous alpha1-antitrypsin deficiency genotype, *Pi\*ZZ* classic severe alpha1-antitrypsin deficiency genotype, *TE* transient elastography (Fibroscan-based)

scale) in 35% of them [5]. This cross-sectional study also tested several noninvasive parameters. Here, gamma-glutamyl transferase (GGT) was the best one to detect significant fibrosis (i.e.  $F \geq 2$ ) with an AUROC of 0.77, while liver stiffness by TE and AST-to-platelet ratio indices (APRI) were less well suited (AUROC 0.69–0.7). On the other hand, LS constituted the best parameter to distinguish advanced liver fibrosis i.e.  $F \geq 3$  versus  $F \leq 2$  with an AUROC of 0.92. This is not surprising since LSM is known to be useful to detect advanced liver fibrosis but is less well able to demarcate mild or significant liver fibrosis stages (i.e.  $F \leq 2$ ) [16].

Kim et al. assessed the usefulness of magnetic resonance elastography (MRE) in 11 Pi\*ZZ adults and demonstrated that MRE might be suitable to exclude the presence of liver fibrosis [17]. Unfortunately, the described studies are the only ones that directly compared noninvasive methods with liver biopsies. Notably, the cutoffs used for detection of the corresponding fibrosis stages were rather low compared to other etiologies [5, 16]; thereby suggesting that use of LSM with commonly recommended etiology-unspecific cutoffs may under- rather than over-estimate the amount of liver fibrosis in Pi\*ZZ individuals. In fact, Clark et al. suggested the cutoff of 5.45 kPa for discriminating significant liver fibrosis (i.e.  $F \geq 2$  compared to  $F < 2$ ; AUROC 0.69), however, this cutoff does not seem to be useful for clinical routine as values  $>5.45$  kPa are seen in  $>50\%$  of Pi\*ZZ individuals [13].

Two large studies [18, 19] demonstrated, that normal serum liver enzyme activities are not sufficient to exclude advanced liver fibrosis and should be combined with other, ideally noninvasive methods. The largest body of evidence is available for LSM, that was assessed in three studies totalling  $>670$  Pi\*ZZ individuals [5, 13, 20]. The largest of them included 554 Pi\*ZZ adults without known liver disease from 9 European countries, that were compared against 234 adults not carrying any AAT mutation. Significant fibrosis was defined as  $LSM \geq 7.1$  kPa and was present in 24% of Pi\*ZZ carriers. Advanced liver fibrosis, defined as  $LSM \geq 10.0$  kPa, was seen in 14% of Pi\*ZZ individuals and was 9–20 times more common in Pi\*ZZ subjects compared to noncarriers [13]. Two other smaller studies revealed similar amount of Pi\*ZZ carriers (i.e. 15–25%) with LSM suggestive of significant liver fibrosis, but only  $<10\%$  of individuals were estimated to have advanced fibrosis [20, 21]. While these data are not sufficient to clearly determine the amount of liver fibrosis in individual subjects, it allows to stratify patients into low-, intermediate-, and high-risk groups. This stratification should be then put into a clinical context including age, sex, presence of comorbidities, etc. to decide, what patients would benefit from a histological evaluation and what individuals will be further monitored noninvasively.

The above described, large international study also evaluated APRI and revealed that it displays a moderate correlation with LSM [13]. However, since Clark et al. demonstrated that APRI displays an inferior correlation with histological fibrosis scores compared to LS, we suggest using it only as a supplemental evaluation method. For example, it might be a useful adjunct criterium for patients with intermediate LSM values (i.e. 5–7 kPa). A similar conclusion can be drawn for HepaScore, that consists of age, sex, alpha2-macroglobulin, hyaluronic acid, bilirubin, and gamma-glutamyl transferase [22]. While HepaScore has also been systematically assessed in the hitherto largest study [13], it displayed only a moderate correlation with LSM and was never directly compared with liver biopsies in AATD patients [13]. Therefore, further studies are needed to determine its usefulness in Pi\*ZZ individuals. In contrast, FIB-4 (i.e. score consisting of AST, ALT, age, and platelet count) was assessed in a biopsy-controlled study but was equal to or inferior to all other analyzed markers [5].

A small study used pSWE [23] to estimate liver fibrosis in 37 individuals from the Swedish national neonatal A1AT screening program. While this analysis took



advantage of the only population-based cohort of AATD individuals, it included only 47 subjects (32 Pi\*ZZ and 15 Pi\*SZ). The authors found an increased liver stiffness among Pi\*ZZ men in comparison with Pi\*MM men, but no significant differences were found in females [19]. Moreover, two important limitations need to be stressed out: (1) pSWE [23] is less widely available than TE [24] and was never directly compared to liver biopsies in AATD; (2) the analysed patients were relatively young since significant liver fibrosis often develops in adults >50 years old [13]. Another small report from a similar cohort of young adults did not detect a difference in pSWE [23] values between Pi\*ZZ carriers and noncarriers [25]. Notably, a small study found a strong correlation between different elastography methods including MRE, pSWE and 2D-SWE [26].

## Noninvasive Screening for Steatosis in Patients with Alpha1-Antitrypsin Deficiency

Ca. 44% Pi\*ZZ carriers display histological liver steatosis [5]. Similar data were found using transient elastography-based controlled attenuation parameter (CAP) as a surrogate of liver steatosis [27]. In particular, CAP  $\geq 280$  dB/m, suggesting severe steatosis, were detected in 39% of Pi\*ZZ carriers vs. 31% of noncarriers while CAP  $\geq 248$  dB/m suggesting the presence of steatosis grade  $\geq 1$  were present in 61% of Pi\*ZZ subjects [13]. Another small study using CAP detected steatosis grade  $\geq 1$  in 65% of Pi\*ZZ/Pi\*SZ patients and grade  $\geq 2$  in 52% of individuals [20]. However, it needs to be pointed out, that the accuracy of CAP for predicting histological steatosis has not been validated in AATD. As a potential underlying mechanism, Pi\*ZZ individuals displayed lower serum triglyceride, VLDL, and LDL cholesterol concentrations than noncarriers which raised the suspicion that they may experience impaired hepatic lipid secretion. These findings were strengthened by the observations in transgenic mice overexpressing the Pi\*Z mutation, that also harboured mild liver steatosis [13].

**Acknowledgements** P.S. is supported by the Deutsche Forschungsgemeinschaft (DFG) consortium SFB/TRR57 “Liver fibrosis” and unrestricted research grants from Grifols and CSL Behring.

## References

1. Silverman EK, Sandhaus RA. Clinical practice. Alpha1-antitrypsin deficiency. *N Engl J Med*. 2009;360(26):2749–57.
2. Greene CM, Marciniak SJ, Teckman J, Ferrarotti I, Brantly ML, Lomas DA, et al. Alpha1-antitrypsin deficiency. *Nat Rev Dis Primers*. 2016;2:16051.
3. Miravittles M, Dirksen A, Ferrarotti I, Koblizek V, Lange P, Mahadeva R, et al. European Respiratory Society statement: diagnosis and treatment of pulmonary disease in alpha1-antitrypsin deficiency. *Eur Respir J* 2017;50(5).

4. de Serres FJ, Blanco I. Prevalence of alpha1-antitrypsin deficiency alleles PI\*S and PI\*Z worldwide and effective screening for each of the five phenotypic classes PI\*MS, PI\*MZ, PI\*SS, PI\*SZ, and PI\*ZZ: a comprehensive review. *Ther Adv Respir Dis*. 2012;6(5):277–95.
5. Clark VC, Marek G, Liu C, Collinsworth A, Shuster J, Kurtz T, et al. Clinical and histologic features of adults with alpha-1 antitrypsin deficiency in a non-cirrhotic cohort. *J Hepatol*. 2018;69(6):1357–64.
6. Blanco I, Bueno P, Diego I, Perez-Holanda S, Casas-Maldonado F, Esquinas C, et al. Alpha-1 antitrypsin Pi\*Z gene frequency and Pi\*ZZ genotype numbers worldwide: an update. *Int J Chron Obstruct Pulmon Dis*. 2017;12:561–9.
7. Strnad P, Nuraldeen R, Guldiken N, Hartmann D, Mahajan V, Denk H, et al. Broad spectrum of hepatocyte inclusions in humans, animals, and experimental models. *Compr Physiol*. 2013;3(4):1393–436.
8. Townsend SA, Edgar RG, Ellis PR, Kantas D, Newsome PN, Turner AM. Systematic review: the natural history of alpha-1 antitrypsin deficiency, and associated liver disease. *Aliment Pharmacol Ther*. 2018;47(7):877–85.
9. Kuscuoğlu D, Janciauskiene S, Hamesch K, Haybaeck J, Trautwein C, Strnad P. Liver—master and servant of serum proteome. *J Hepatol*. 2018;69(2):512–24.
10. Teckman JH, Qu D, Perlmutter DH. Molecular pathogenesis of liver disease in alpha1-antitrypsin deficiency. *Hepatology*. 1996;24(6):1504–16.
11. Fromme M, Oliverius M, Strnad P. DEFI-ALFA: the French key to the alpha1 mystery? *Liver Int*. 2019;39(6):1019–21.
12. Sveger T, Eriksson S. The liver in adolescents with  $\alpha$ -antitrypsin deficiency. *Hepatology*. 1995;22(2):514–7.
13. Hamesch K, Mandorfer M, Vítor M, Pereira, Moeller LS, Pons M, et al. Liver fibrosis and metabolic alterations in adults with homozygous alpha1-antitrypsin deficiency (Pi\*ZZ genotype)—a multi-national study. *Gastroenterology*. 2019;157:705–19 e18.
14. Adam R, Karam V, Delvar V, O’Grady J, Mirza D, Klempnauer J, et al. Evolution of indications and results of liver transplantation in Europe. A report from the European Liver Transplant Registry (ELTR). *J Hepatol*. 2012;57(3):675–88.
15. Tanash HA, Piitulainen E. Liver disease in adults with severe alpha-1-antitrypsin deficiency. *J Gastroenterol*. 2019;54(6):541–8.
16. Friedrich-Rust M, Poynard T, Castera L. Critical comparison of elastography methods to assess chronic liver disease. *Nat Rev Gastroenterol Hepatol*. 2016;13(7):402–11.
17. Kim RG, Nguyen P, Bettencourt R, Dulai PS, Haufe W, Hooker J, et al. Magnetic resonance elastography identifies fibrosis in adults with alpha-1 antitrypsin deficiency liver disease: a prospective study. *Aliment Pharmacol Ther*. 2016;44(3):287–99.
18. Clark VC, Dhanasekaran R, Brantly M, Rouhani F, Schreck P, Nelson DR. Liver test results do not identify liver disease in adults with alpha(1)-antitrypsin deficiency. *Clin Gastroenterol Hepatol*. 2012;10(11):1278–83.
19. Mostafavi B, Diaz S, Tanash HA, Piitulainen E. Liver function in alpha-1-antitrypsin deficient individuals at 37 to 40 years of age. *Medicine (Baltimore)*. 2017;96(12):e6180.
20. Mandorfer M, Bucsecs T, Hutyá V, Schmid-Scherzer K, Schaefer B, Zoller H, et al. Liver disease in adults with  $\alpha$ 1-antitrypsin deficiency. *United Eur Gastroenterol J*. 2018;6(5):710–8.
21. Guillaud O, Dumortier J, Traclét J, Restier L, Joly P, Chapuis-Cellier C, et al. Assessment of liver fibrosis by transient elastography (Fibroscan(R)) in patients with A1AT deficiency. *Clin Res Hepatol Gastroenterol*. 2019;43(1):77–81.
22. Adams LA, Bulsara M, Rossi E, DeBoer B, Speers D, George J, et al. Hepascore: an accurate validated predictor of liver fibrosis in chronic hepatitis C infection. *Clin Chem*. 2005;51(10):1867–73.
23. Parfieniuk-Kowierda A, Lapinski TW, Rogalska-Plonska M, Swiderska M, Panasiuk A, Jaroszewicz J, et al. Serum cytochrome c and m30-neoepitope of cytokeratin-18 in chronic hepatitis C. *Liver Int*. 2014;34(4):544–50.

24. Castera L, Friedrich-Rust M, Loomba R. Noninvasive assessment of liver disease in patients with nonalcoholic fatty liver disease. *Gastroenterology*. 2019;156(5):1264–81 e4.
25. Diaz S, Mostafavi B, Tanash HA, Piitulainen E. Acoustic radiation force impulse (ARFI) elastography in a cohort of alpha-1 antitrypsin-deficient individuals and healthy volunteers. *Acta Radiol Open*. 2018;7(4):2058460118768363.
26. Reiter R, Wetzel M, Hamesch K, Strnad P, Asbach P, Haas M, et al. Comparison of non-invasive assessment of liver fibrosis in patients with alpha1-antitrypsin deficiency using magnetic resonance elastography (MRE), acoustic radiation force impulse (ARFI) Quantification, and 2D-shear wave elastography (2D-SWE). *PLoS One*. 2018;13(4):e0196486.
27. Karlas T, Petroff D, Sasso M, Fan JG, Mi YQ, de Ledinghen V, et al. Individual patient data meta-analysis of controlled attenuation parameter (CAP) technology for assessing steatosis. *J Hepatol*. 2017;66(5):1022–30.
28. Janciauskiene S, Wallmark A, Piitulainen E, Kohnlein T, Welte T, Sveger T. Performance of enhanced liver fibrosis plasma markers in asymptomatic individuals with ZZ alpha1-antitrypsin deficiency. *Eur J Gastroenterol Hepatol*. 2011;23(8):716–20.
29. Mazza A, Fruci B, Garinis GA, Giuliano S, Malaguarnera R, Belfiore A. The role of metformin in the management of NAFLD. *Exp Diabetes Res*. 2012;2012:716404.

# Chapter 18

## Fibrosis and Prognosis Assessment Using Liver Stiffness in Patients with PBC and PSC



Christophe Corpechot

### Introduction

Primary biliary cholangitis and primary sclerosing cholangitis (PSC) are the two most prevalent cholestatic liver diseases in adults. Both are chronic cholangiopathies that naturally progress toward liver fibrosis and cirrhosis as a main result of defective bile secretion (cholestasis). In both diseases, severe fibrosis and cholestasis are predictive of poor prognosis. Histological evaluation of liver biopsy remains the gold standard procedure of fibrosis assessment in PBC/PSC. Besides the poor acceptability of this invasive and potentially risky method, the heterogeneous distribution of fibrotic scars within the liver, a typical histopathological feature of cholangiopathies, is a significant source of sampling errors and of low reproducibility of fibrosis measurements. In the last 20 years, several non-invasive methods of fibrosis assessment have been developed, among which elastography-based methods, using liver stiffness measurement (LSM) as a surrogate marker of fibrosis, have shown acceptable to high performance in determining fibrosis stage in a broader range of chronic liver diseases. In this chapter, we will address specifically the utility and limitations of these methods in PBC/PSC and will describe how cholestasis, a characteristic feature of these diseases, can alter liver stiffness irrespective of fibrosis extent.

---

C. Corpechot (✉)

Reference Center for Inflammatory Biliary Diseases and Autoimmune Hepatitis,  
Saint-Antoine Hospital, Assistance Publique—Hôpitaux de Paris, Paris, France

Inserm UMR\_S938, Saint-Antoine Research Center (CRSA), Sorbonne University,  
Paris, France

e-mail: [christophe.corpechot@aphp.fr](mailto:christophe.corpechot@aphp.fr)

## Influence of Cholestasis on Liver Stiffness

Cholestasis, defined as a defect in bile secretion, can result from different mechanisms, including the obstruction of the common bile duct by gallstones, tumors, or strictures (extrahepatic cholestasis) and broader hepatocellular and/or small bile duct injuries within the liver (intrahepatic cholestasis). Both mechanisms lead to the accumulation of toxic bile acids in the liver that generates cell apoptosis, necro-inflammatory reaction, and ductular proliferation that eventually promote fibrosis development if cholestasis is not cured. PBC is typically associated with intrahepatic cholestasis while PSC can be associated with intra- or extrahepatic cholestasis.

There is now clear evidence that extrahepatic cholestasis increases liver stiffness (LS) per se, regardless of the assessment method used [1–5]. This effect, which is strongly correlated with serum levels of total bilirubin, most likely results from the increased hydrostatic pressure into the liver since the increase in LSM is quickly and fully reversible after biliary drainage [1]. These findings have important implications for the interpretation of elevated LSM, particularly in patients with PSC and elevated total bilirubin level in whom liver imaging must absolutely be performed prior to assessing LSM to exclude a dominant stricture of the common bile duct [6].

Intrahepatic cholestasis may also contribute to increased liver stiffness irrespective of any other hepatic conditions like fibrosis or inflammation, explaining the especially high cut-off values of 17.3 kPa for cirrhosis observed in patients with PBC or PSC [7]. Interestingly, liver stiffness has recently been shown to be increased in pregnant women with intrahepatic cholestasis of pregnancy, a transient condition characterized by pure, estrogen-induced, and reversible hepatocellular cholestasis, as compared to healthy pregnancies with similar gestation time [8]. This observation strongly supports that bile acid overload in hepatocytes and related hepatocellular changes (cell ballooning and clarification, Mallory bodies, etc.) may be sufficient to increase LS without requiring other superimposed factors. On the other side, pregnancy itself is able to increase LS which is highly associated with intrahepatic cholestasis of pregnancy (ICP), preeclampsia, and most likely related to pressure/perfusion changes than inflammation [9]. However, in patients with non-elevated serum bilirubin level, the effect of cholestasis on LS does not seem to compete significantly with fibrosis extent [7].

## Liver Stiffness Measurement in PBC: Evaluation of Fibrosis

Since 2006, a dozen of studies including 564 patients with histologically assessed fibrosis stage, have been conducted to assess the performance of elastography-based techniques in assessing liver fibrosis in PBC (Table 18.1). Most of these studies used vibration-controlled transient elastography (VCTE) as the main method, including two cohorts of >100 patients each [10–15]. Alternative methods, including acoustic radiation force impulse elastography, real-time tissue elastography (RTE), and point shear wave elastography (pSWE), involved less than 170 patients [14, 16–18]. In all

**Table 18.1** Performance of elastography-based techniques for the diagnosis of histologically proven severe fibrosis and cirrhosis in PBC

Reference	Technique	Patients	Severe fibrosis AUROC (cut-off)	Cirrhosis AUROC (cut-off)
Gomez, 2008 [10]	VCTE	55	0.86 (14.7 kPa)	0.96 (15.6 kPa)
Friedrich, 2010 [11]	VCTE	45	N/A (N/A)	0.95 (N/A)
Floreani, 2011 [12]	VCTE	120	0.88 (7.6 kPa)	0.99 (11.4 kPa)
Corpechot, 2012 [13]	VCTE	103	0.95 (10.7 kPa)	0.99 (16.9 kPa)
Zhang, 2014 [16]	ARFI	61	0.93 (1.79 m/s)	0.91 (2.01 m/s)
Koizumi, 2017 [14]	VCTE	44	0.91 (N/A)	0.91 (N/A)
Koizumi, 2017 [14]	RTE	44	0.95 (N/A)	0.97 (N/A)
Wu, 2018 [15]	VCTE	70	0.91 (10.5 kPa)	0.97 (14.5 kPa)
Goertz, 2019 [17]	ARFI	26	N/A (N/A)	N/A (N/A)
Park, 2019 [18]	pSWE	41	0.91 (6.04 kPa)	N/A (N/A)

VCTE vibration-controlled transient elastography, ARFI acoustic radiation force impulse elastography, RTE real-time tissue elastography, pSWE point shear wave elastography, AUROC area under the ROC curve

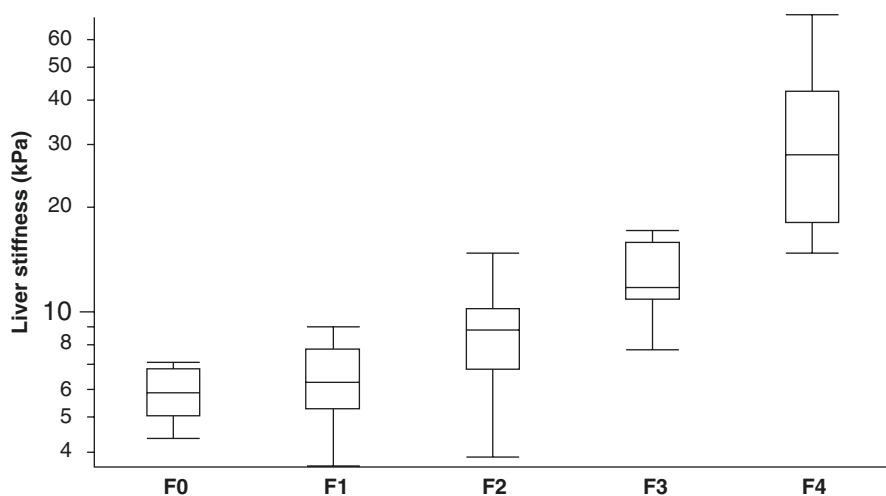


**Fig. 18.1** Distribution of liver stiffness measurement across METAVIR fibrosis stages in PBC. Box plot of liver stiffness measured by VCTE (logarithm scale) depending on biopsy fibrosis stage. The bottom and top of the boxes are the first and third quartiles, and the band inside the boxes is the median. The ends of the whiskers are the minimum and maximum of the data. (Adapted from Corpechot C et al. [13]; with permission)

studies but one [17], LSM strongly correlated with histological fibrosis stage (Fig. 18.1) and showed high performance (AUROC > 0.95) for the diagnosis of cirrhosis, and very good performance (AUROC > 0.85) for the diagnosis of severe fibrosis (i.e., septal fibrosis, Ludwig's stage 3, or METAVIR fibrosis stage F3). However, the rates of failure or of unreliable results vary across studies from 5 to 22% [12, 13]. In addition, inconsistent results regarding diagnostic VCTE thresholds

may reflect discrepancies in populations studied and histological scoring systems. However,  $>15$  and  $>10$  kPa are reasonable thresholds for the diagnosis of cirrhosis and of severe fibrosis, respectively, in keeping with VCTE thresholds reported in other chronic liver diseases. Finally, intra- and interobserver reproducibility of LSM in patients with PBC remains unestablished. Since the use of liver biopsy for PBC diagnosis is no longer mandatory, large series of biopsy-elastography couples are very unlikely to be conducted in the future. A meta-analysis based on individual data from previously published studies may help in better assessing VCTE thresholds in PBC. Alternative methods like ARFI elastography seem to have similar diagnostic performance for assessing fibrosis in PBC but data currently available are too limited to draw any recommendations regarding these techniques.

Elastography (mainly VCTE) was compared to a number of serum fibrosis markers, including AST-to-platelet ratio index (APRI), FIB-4, FibroTest, Forns score, hyaluronic acid, AST/ALT ratio, and GGT-to-platelet ratio, for the non-invasive assessment of fibrosis in PBC [11–15, 18]. In all studies, AUROCs of liver stiffness for the diagnosis of severe fibrosis and cirrhosis were higher than those of serum markers, showing that elastography-based techniques have higher performance in detecting advanced-stage PBC than serum fibrosis markers alone. LSM and enhanced liver fibrosis (ELF) score, the only serum fibrosis marker so far validated in PBC, have never been compared.

Measures of splenic stiffness (SS) in patients with PBC have been reported in only one small-sized study using both VCTE and RTE [14]. SS seems to associate with clinically significant fibrosis stages, but these data need to be confirmed in larger studies.

## Liver Stiffness and Prognosis in Patients with PBC

Until now, the prognostic value of LSM has been assessed in only two retrospective studies [13, 14]. In the former one, 150 patients, all treated with ursodeoxycholic acid (UDCA), had been followed-up for up to 5 years after last LSM [13]. Baseline LS was significantly associated with an increased risk of liver-related complications or death with an optimal predictive threshold of  $>9.6$  kPa (hazard ratio 5.1, 95% CI: 1.5–15.9), thus identifying patients with severe fibrosis as at high risk of poor outcomes (Fig. 18.2). All disease stages and adequate-vs.-inadequate response to UDCA taken together, LS was increasing over time ( $0.48 \pm 0.21$  kPa/year,  $P = 0.02$ ), this increase being related to a high progression rate ( $4.06 \pm 0.73$  kPa/year,  $P < 0.001$ ) of LS in cirrhotic patients while, in contrast, LSM remained stable in non-cirrhotic patients. The progression rate of LSM was a major independent predictive factor of adverse clinical outcomes, suggesting that LSM could be used as a clinically relevant surrogate marker of PBC progression. These findings, however, deserve validation in prospective studies. In the second study, 36 asymptomatic PBC patients were followed-up for an average of 16 months (up to 32 months) and the incident rate of liver-related symptoms was studied in connection with liver and splenic stiffness assessed by VCTE and RTE [14]. Spleen stiffness as assessed by

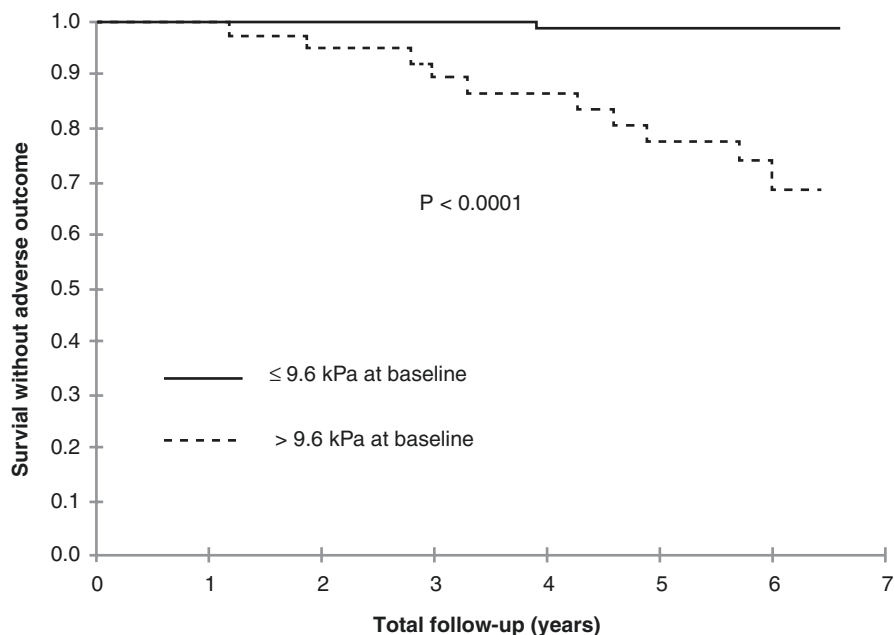


**Fig. 18.2** Survival rates without adverse outcome in patients with PBC depending on baseline liver stiffness measurement. Kaplan–Meier estimated survival by LSM as assessed with VCTE in 150 patients with PBC treated with UDCA. (Adapted from Corpechot C et al. [13]; with permission)

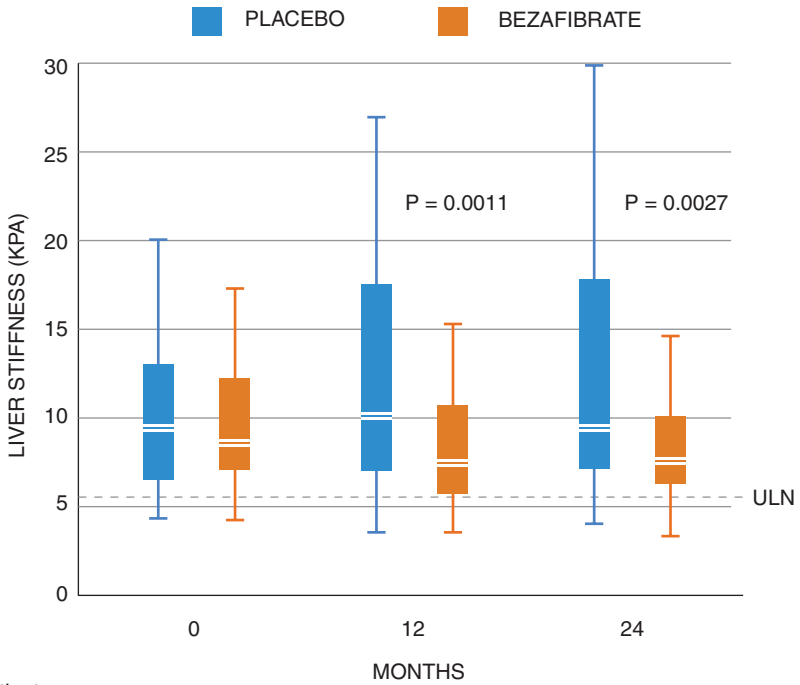
RTE was the only independent predictive factor of symptom development in this small-sized study.

Recently, the measure of liver stiffness was used as a secondary endpoint in the BEZURSO trial, a placebo-controlled, phase-3 study of bezafibrate therapy (lipid-lowering agent) in combination with UDCA in PBC patients who had an inadequate biochemical response to UDCA alone [19]. At the end of study, there was a significant difference in the progression rate of LS (assessed with VCTE) between the two groups, with a 15% reduction from baseline in the bezafibrate group and a 22% increase in the placebo group (difference,  $-36\%$ ; 95% CI,  $-64$  to  $-8\%$ ) (Fig. 18.3). This observation was consistent with the result of the primary outcome (increased rate of complete biochemical response in the bezafibrate group as compared to the placebo group) and confirmed that LS can be used as a surrogate endpoint in clinical trials with adequately selected PBC patients.

## Liver Stiffness Measurement in PSC: Evaluation of Fibrosis

Studies that aimed to assess the performance of elastography-based techniques for the diagnosis of histological fibrosis stage in patients with PSC are still scarce and of limited size (Table 18.2). A positive correlation between histological fibrosis stage





No. of Patients

Placebo	45	34	41
Bezafibrate	44	39	41

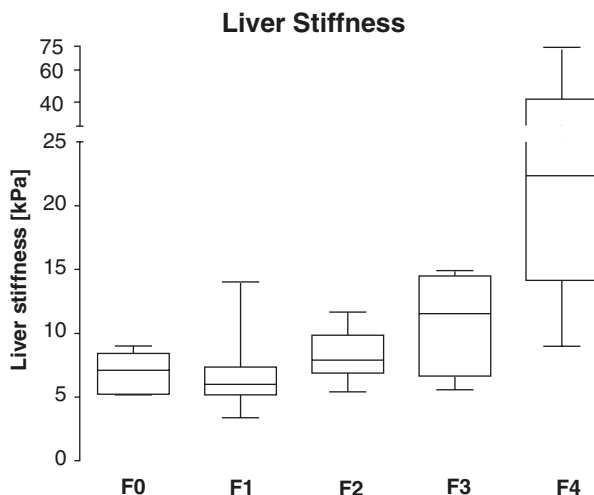
**Fig. 18.3** Liver stiffness measurement according to time and treatment group in patients who participated in the BEZURSO trial. Box plot of liver stiffness measured by VCTE depending on time and treatment group. The bottom and top of the boxes are the first and third quartiles, and the band inside the boxes is the median. The bars are 1.5 times the interquartile range. Bezafibrate and placebo were administered with standard-of-care ursodeoxycholic acid. ULN denotes upper limit of the normal range. (Adapted from Corpechot C et al. [19]; with permission)

**Table 18.2** Performance of elastography-based techniques for the diagnosis of histologically proven severe fibrosis and cirrhosis in PSC

Reference	Technique	Patients	Severe fibrosis AUROC (cut-off)	Cirrhosis AUROC (cut-off)
Corpechot, 2014 [20]	VCTE	73	0.93 (9.6 kPa)	0.95 (14.4 kPa)
Ehlken, 2016 [21]	VCTE	62	0.95 (9.6 kPa)	0.98 (14.1 kPa)
Eaton, 2016 [22]	MRE	20	0.97 (3.26 kPa)	0.99 (4.93 kPa)
Krawczyk, 2017 [23]	VCTE	30	N/A (N/A)	0.90 (13.7 kPa)
Goertz, 2019 [17]	ARFI	19	N/A (N/A)	N/A (N/A)

VCTE vibration-controlled transient elastography, MRE magnetic resonance elastography, ARFI acoustic radiation force impulse elastography, AUROC area under the ROC curve

**Fig. 18.4** Distribution of liver stiffness measurement across histological fibrosis stages in PSC. Box plot of liver stiffness measured by VCTE depending on Desmet and Scheuer fibrosis stage. The bottom and top of the boxes are the first and third quartiles, and the band inside the boxes is the median. The ends of the whiskers are the minimum and maximum of the data. (Adapted from Ehlken H et al. [21]; with permission)



and LSM was shown in all of them (Fig. 18.4). VCTE is the main method used in these studies, followed by ARFI elastography and magnetic resonance elastography (MRE) [17, 20–23]. Two studies were of acceptable size ( $n > 50$ ) to assess the ability of LSM in distinguishing between histological fibrosis stages [20, 21]. In both studies, LS assessed by VCTE has shown high performance (AUROC  $> 0.90$ ) for the diagnosis of severe fibrosis and cirrhosis, with optimal cut-offs close to 10 kPa and 14 kPa, respectively, in accordance with thresholds found in other chronic liver diseases. Failure or unreliable results of VCTE have been reported in 8% of patients [20]. Interobserver reproducibility and concordance of VCTE results between adjacent measurement sites have been reported to be excellent (intra-class correlation  $\geq 0.90$ ). In one study, the performance of LS, as assessed by VCTE, was superior to APRI and FIB-4 score in differentiating patients with significant or severe fibrosis from those without [20]. Since fibrosis is patchily distributed in the liver of PSC patients, MRE may appear as a more adequate method than VCTE to assess the severity of fibrosis on the whole liver (Fig. 18.5) [22, 24–26]. So far, however, there is no face-to-face comparison in PSC although superiority of MRE in assessing liver fibrosis has been shown from a variety of other etiologies [27, 28]. The comparison of VCTE and MRE performance with non-elastography-based techniques like diffusion-weighted MR imaging, MR spectroscopy, or validated serum markers (ELF score) deserves consideration. Finally, there are very few data on SS in patients with PSC [29]. These limited data did not show statistical differences between patients and healthy controls.

## Liver Stiffness and Prognosis in Patients with PSC

The prognostic value of LSM in PSC has been evaluated in three retrospective studies, two based on VCTE as a reference technique and one on MRE [20–22]. In 168 patients followed-up for a mean period of 4 years (range, 1–7 years), baseline LS

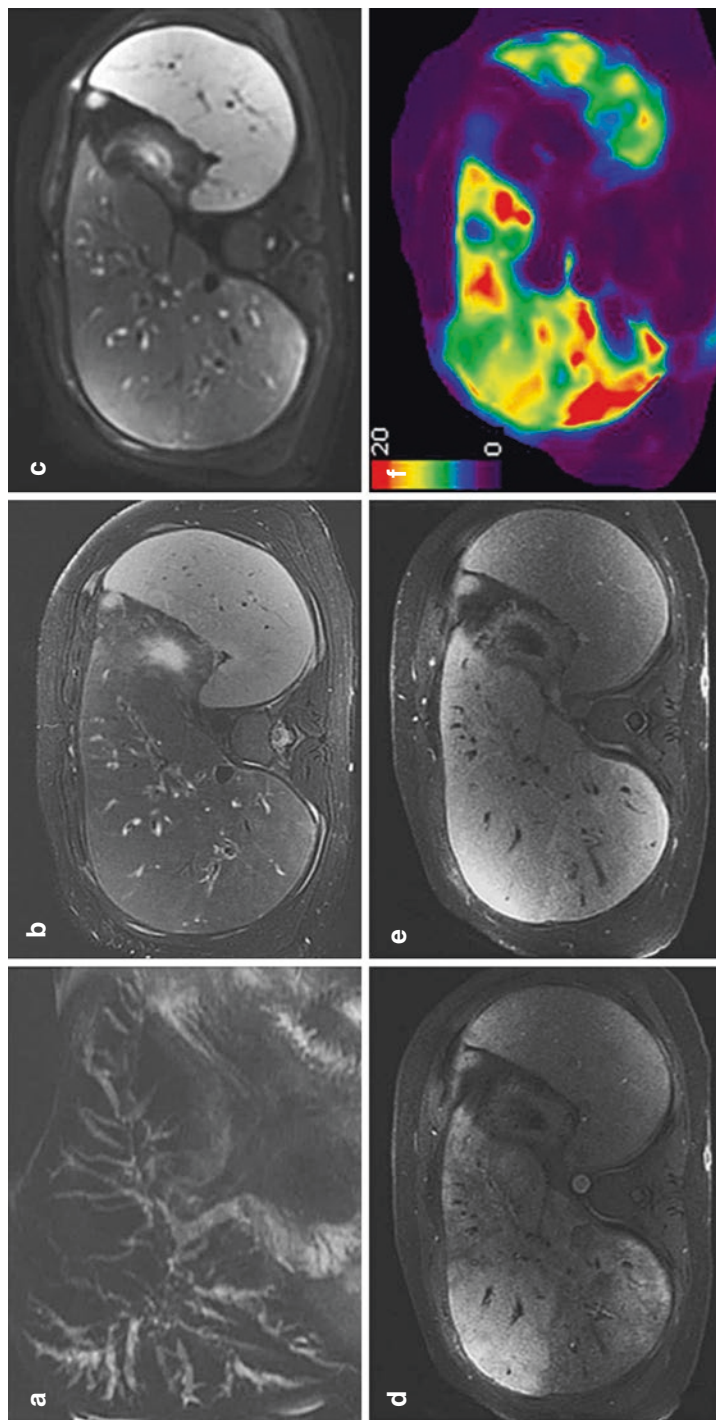
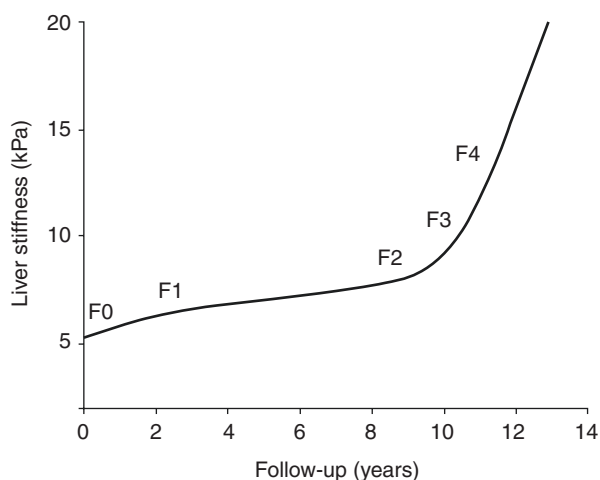


**Fig. 18.5** Example of global liver stiffness measurement using MR elastography in PSC. **(a)** Radial single-shot spin echo sequence image shows multiple strictures of intrahepatic ducts, right and left main ducts, and intrahepatic ducts in both lobes. **(b–e)** Corresponding axial sections on T2W, DWI, arterial phase, and delayed phase images, respectively. T2W and DWI images do not show any significant parenchymal signal abnormalities except a subtle patchy hyperintensity on T2W images. Heterogeneous hyperenhancement of the parenchyma in the arterial and delayed phases. Note dilated ducts in both lobes. **(f)** MRE stiffness map (0–20 kPa scale) shows diffusely stiff liver with heterogeneous distribution of stiffness in both right and left lobes and a mean stiffness of 12.8 kPa consistent with cirrhosis. (Adapted from Bookwalter C et al. [24]; with permission)

assessed by VCTE strongly associated with the risk of developing adverse outcomes, including death, liver transplantation, cirrhotic decompensation, or primary liver cancer [20]. In this study, LS and total bilirubin were the only two independent prognostic factors at baseline. The optimal LS threshold for predicting poor outcomes was  $>18.5$  kPa (HR, 11.9; 95% CI, 5.2–27.4). Thresholds as low as  $>6.5$  kPa continued to split the patients into distinct prognostic groups despite lower predictive performance. This strong association between baseline LS and long-term prognosis in PSC has been confirmed in an independent cohort of 130 PSC patients followed-up for an average of 3.6 years [21]. In this cohort, the optimal predictive threshold of baseline LS for the risk of adverse outcomes was  $>12.4$  kPa. In parallel, LS assessed by MRE was shown to associate with the development of decompensated liver disease in 266 patients with PSC followed-up for a median of 2 years (HR, 1.55; 95% CI, 1.41–1.70) [22]. In this study, both MRE-LSM and Mayo risk score had independent prognostic values at baseline. The optimal LS thresholds that stratified patients at a low, medium, and high risk for hepatic decompensation were  $<4.5$  kPa, 4.5–6.0 kPa, and  $>6.0$  kPa, respectively. Taken together, these three studies provide consistent data supporting the prognostic value of LSM in PSC. The results of the ongoing international prospective FICUS study, specifically designed to assess the prognostic value of LS in PSC, are still awaited.

Changes in LSM have been assessed in PSC in a longitudinal retrospective study of 142 patients monitored with VCTE for a mean period of 4 years [20]. These changes varied as a function of initial LS values and corresponding fibrosis stage. The progression rates of LS estimated from F0, F1, F2, F3, and F4 stages (as diagnosed by VCTE) were  $0.47 \pm 0.45$  kPa/year ( $P = \text{NS}$ ),  $0.25 \pm 0.67$  kPa/year ( $P = \text{NS}$ ),  $1.64 \pm 0.78$  kPa/year ( $P = 0.0368$ ),  $3.40 \pm 0.89$  kPa/year ( $P = 0.0002$ ), and  $4.37 \pm 0.76$  kPa/year ( $P = 0.0001$ ), respectively, thus indicating an exponential increase (acceleration) in LSM over time from F2 to F4 and beyond (Fig. 18.6). The progression rate of LS was an independent predictive

**Fig. 18.6** Natural course of liver stiffness measurement in PSC as assessed by VCTE. Modeling of liver stiffness progression in PSC as a continuous-time function derived from data of 142 patients repeatedly assessed with VCTE. (Adapted from Corpechot C et al. [20]; with permission)



factor of adverse outcomes with an optimal predictive threshold at 1.3 kPa/year (HR, 10.4; 95% CI, 3.0–36.5). These data suggest that in PSC repeated measures of LS can be used as a surrogate marker of disease progression and a predictor of long-term outcomes.

## Conclusion

Irrespective of used technique, elastography-based assessment of LS has high performance in both diagnosing severe fibrosis or cirrhosis and predicting long-term outcomes in PBC and PSC. These techniques should therefore be considered in clinical practice to assess the severity of the disease and its progression [30]. They may be considered as well for risk stratification and definition of surrogate endpoints in clinical trials.

**Acknowledgment** *Conflict of Interest:* None.

## References

1. Millonig G, Reimann FM, Friedrich S, Fonouni H, Mehrabi A, Büchler MW, et al. Extrahepatic cholestasis increases liver stiffness (FibroScan) irrespective of fibrosis. *Hepatology*. 2008;48(5):1718–23.
2. Harata M, Hashimoto S, Kawabe N, Nitta Y, Murao M, Nakano T, et al. Liver stiffness in extrahepatic cholestasis correlates positively with bilirubin and negatively with alanine aminotransferase. *Hepatol Res*. 2011;41(5):423–9.
3. Trifan A, Sfarti C, Cojocariu C, Dimache M, Cretu M, Hutanasu C, et al. Increased liver stiffness in extrahepatic cholestasis caused by choledocholithiasis. *Hepat Mon*. 2011;11(5):372–5.
4. Attia D, Pischke S, Negm AA, Rifai K, Manns MP, Gebel MJ, et al. Changes in liver stiffness using acoustic radiation force impulse imaging in patients with obstructive cholestasis and cholangitis. *Dig Liver Dis*. 2014;46:625.
5. Pfeifer L, Strobel D, Neurath MF, Wildner D. Liver stiffness assessed by acoustic radiation force impulse (ARFI) technology is considerably increased in patients with cholestasis. *Ultraschall Med*. 2014;35(4):364–7.
6. Ehlken H, Lohse AW, Schramm C. Transient elastography in primary sclerosing cholangitis—the value as a prognostic factor and limitations. *Gastroenterology*. 2014;147(2):542–3.
7. Corpechot C, El Naggar A, Poujol-Robert A, Ziol M, Wendum D, Chazouilleres O, et al. Assessment of biliary fibrosis by transient elastography in patients with PBC and PSC. *Hepatology*. 2006;43(5):1118–24.
8. Cetin O, Karaman E, Arslan H, Akbudak I, Yildizhan R, Kulusari A. Maternal liver elasticity determined by acoustic radiation force impulse elastosonography in intrahepatic cholestasis of pregnancy. *J Med Ultrason* (2001). 2017;44(3):255–61.
9. Ammon FJ, Kohlhaas A, Elshaarawy O, Mueller J, Bruckner T, Sohn C, et al. Liver stiffness reversibly increases during pregnancy and independently predicts preeclampsia. *World J Gastroenterol*. 2018;24(38):4393–402.
10. Gomez-Dominguez E, Mendoza J, Garcia-Buey L, Trapero M, Gisbert JP, Jones EA, et al. Transient elastography to assess hepatic fibrosis in primary biliary cirrhosis. *Aliment Pharmacol Ther*. 2008;27(5):441–7.

11. Friedrich-Rust M, Muller C, Winckler A, Kriener S, Herrmann E, Holtmeier J, et al. Assessment of liver fibrosis and steatosis in PBC with FibroScan, MRI, MR-spectroscopy, and serum markers. *J Clin Gastroenterol.* 2010;44(1):58–65.
12. Floreani A, Cazzagon N, Martines D, Cavalletto L, Baldo V, Chemello L. Performance and utility of transient elastography and noninvasive markers of liver fibrosis in primary biliary cirrhosis. *Dig Liver Dis.* 2011;43(11):887–92.
13. Corpechot C, Carrat F, Poujol-Robert A, Gaouar F, Wendum D, Chazouilleres O, et al. Noninvasive elastography-based assessment of liver fibrosis progression and prognosis in primary biliary cirrhosis. *Hepatology.* 2012;56(1):198–208.
14. Koizumi Y, Hirooka M, Abe M, Tokumoto Y, Yoshida O, Watanabe T, et al. Comparison between real-time tissue elastography and vibration-controlled transient elastography for the assessment of liver fibrosis and disease progression in patients with primary biliary cholangitis. *Hepato Res.* 2017;47(12):1252–9.
15. Wu HM, Sheng L, Wang Q, Bao H, Miao Q, Xiao X, et al. Performance of transient elastography in assessing liver fibrosis in patients with autoimmune hepatitis-primary biliary cholangitis overlap syndrome. *World J Gastroenterol.* 2018;24(6):737–43.
16. Zhang DK, Chen M, Liu Y, Wang RF, Liu LP, Li M. Acoustic radiation force impulse elastography for non-invasive assessment of disease stage in patients with primary biliary cirrhosis: a preliminary study. *Clin Radiol.* 2014;69(8):836–40.
17. Goertz RS, GaBmann L, Strobel D, Wildner D, Schellhaas B, Neurath MF, et al. Acoustic radiation force impulse (ARFI) elastography in autoimmune and cholestatic liver diseases. *Ann Hepatol.* 2019;18(1):23–9.
18. Park DW, Lee YJ, Chang W, Park JH, Lee KH, Kim YH, et al. Diagnostic performance of a point shear wave elastography (pSWE) for hepatic fibrosis in patients with autoimmune liver disease. *PLoS One.* 2019;14(3):e0212771.
19. Corpechot C, Chazouilleres O, Rousseau A, Le Gruyer A, Habersetzer F, Mathurin P, et al. A placebo-controlled trial of bezafibrate in primary biliary cholangitis. *N Engl J Med.* 2018;378(23):2171–81.
20. Corpechot C, Gaouar F, El Naggar A, Kemgang A, Wendum D, Poupon R, et al. Baseline values and changes in liver stiffness measured by transient elastography are associated with severity of fibrosis and outcomes of patients with primary sclerosing cholangitis. *Gastroenterology.* 2014;146(4):970–9. quiz e15–6.
21. Ehliken H, Wroblewski R, Corpechot C, Arrive L, Rieger T, Hartl J, et al. Validation of transient elastography and comparison with spleen length measurement for staging of fibrosis and clinical prognosis in primary sclerosing cholangitis. *PLoS One.* 2016;11(10):e0164224.
22. Eaton JE, Dzyubak B, Venkatesh SK, Smyrk TC, Gores GJ, Ehman RL, et al. Performance of magnetic resonance elastography in primary sclerosing cholangitis. *J Gastroenterol Hepatol.* 2016;31(6):1184–90.
23. Krawczyk M, Ligocka J, Ligocki M, Raszeja-Wyszomirska J, Milkiewicz M, Szparecki G, et al. Does transient elastography correlate with liver fibrosis in patients with PSC? Laennec score-based analysis of explanted livers. *Scand J Gastroenterol.* 2017;52(12):1407–12.
24. Bookwalter CA, Venkatesh SK, Eaton JE, Smyrk TD, Ehman RL. MR elastography in primary sclerosing cholangitis: correlating liver stiffness with bile duct strictures and parenchymal changes. *Abdom Radiol (NY).* 2018;43:3260.
25. Jhaveri KS, Hosseini-Nik H, Sadoughi N, Janssen H, Feld JJ, Fischer S, et al. The development and validation of magnetic resonance elastography for fibrosis staging in primary sclerosing cholangitis. *Eur Radiol.* 2019;29(2):1039–47.
26. Hoodeshenas S, Welle CL, Navin PJ, Dzyubak B, Eaton JE, Ehman RL, et al. Magnetic resonance elastography in primary sclerosing cholangitis: interobserver agreement for liver stiffness measurement with manual and automated methods. *Acad Radiol.* 2019;26:1625.
27. Ichikawa S, Motosugi U, Morisaka H, Sano K, Ichikawa T, Tatsumi A, et al. Comparison of the diagnostic accuracies of magnetic resonance elastography and transient elastography for hepatic fibrosis. *Magn Reson Imaging.* 2015;33(1):26–30.

28. Park CC, Nguyen P, Hernandez C, Bettencourt R, Ramirez K, Fortney L, et al. Magnetic resonance elastography vs transient elastography in detection of fibrosis and noninvasive measurement of steatosis in patients with biopsy-proven nonalcoholic fatty liver disease. *Gastroenterology*. 2017;152(3):598–607 e2.
29. Mjelle AB, Mulabecirovic A, Hausken T, Havre RF, Gilja OH, Vesterhus M. Ultrasound and point shear wave elastography in livers of patients with primary sclerosing cholangitis. *Ultrasound Med Biol*. 2016;42(9):2146–55.
30. European Association for Study of Liver; Asociacion Latinoamericana para el Estudio del Hígado. EASL-ALEH Clinical Practice Guidelines: Non-invasive tests for evaluation of liver disease severity and prognosis. *J Hepatol*. 2015;63(1):237–64. <https://doi.org/10.1016/j.jhep.2015.04.006>.



# Chapter 19

## Liver Stiffness in Patients with Hereditary Hemochromatosis and Secondary Iron Overload



Agustín Castiella and Eva Zapata

### Introduction

Hereditary hemochromatosis (HH) is an autosomal recessive genetic disease mostly due to mutations in the HFE gene with (C282Y) being the most frequent [1, 2]. Clinical penetration of the mutation can be as low as 10% and strongly depends on innate factors (sex and other mutations involved in iron metabolism) and acquired factors (alcohol, metabolic syndrome, and viruses) [1, 3]. Major target organ for iron accumulation is the liver, with the development of chronic liver disease and cirrhosis if treatment is delayed, and with an increased risk of hepatocellular carcinoma [1]. Liver biopsy with histopathological assessment and liver iron concentration quantification by spectrophotometry have long been the gold standard for the diagnosis and prognosis of hemochromatosis [4, 5]. Other techniques such as superconducting quantum interference device (SQUID) or room temperature susceptometry (RTS) have also been successfully explored for non-invasive detection of hepatic iron [6, 7]. Our understanding of the molecular basis in iron overload diseases has drastically improved in the last 20 years, especially with the discovery of the *HFE* gene and the mutation (C282Y/C282Y) responsible for hereditary hemochromatosis. Magnetic resonance imaging (MRI) for the study of liver iron concentration and non-invasive liver fibrosis prediction with laboratory tests [2, 8, 9] have considerably diminished the role of hepatic biopsies for the diagnosis of hemochromatosis, and it is more commonly used for prognosis purposes only [10]. However, quantitative MRI platforms are still not readily available in many countries, and the technique is still too expensive for population screening. The development of liver cirrhosis is a key factor for hemochromatosis patients, since it significantly deterio-

---

A. Castiella (✉) · E. Zapata  
Gastroenterology Service, Donostia University Hospital, Donostia, Spain  
e-mail: [evamaria.zapatamorcillo@osakidetza.eus](mailto:evamaria.zapatamorcillo@osakidetza.eus)



rates prognosis, the management of the disease and constitutes an additional risk for cancer [11]. However, liver biopsy is invasive and harbours a relative mortality of around 1/1000 to 1/10,000 [12, 13]. Moreover, biopsies show a rather high sampling error. About 10–30% of patients will be incorrectly classified for fibrosis by at least one stage in 20–30% [11–14]. Concerns about complications and sampling errors have resulted in the research for non-invasive tests for cirrhosis [8].

Today, most hemochromatosis cases are identified through laboratory screening, normally by an elevated serum ferritin level or transferrin saturation. Figure 19.1 gives an overview about all diagnostic aspects of the so-called hyperferritinaemia. It underlines the many diverse aetiologies that can account for elevated ferritin levels ranging from the rare hereditary hyperferritinaemia cataract syndrome [15] to the most common liver diseases such as alcoholic and non-alcoholic fatty liver disease [16]. For these and many other reasons, the introduction of elastography has drastically improved fibrosis screening in hepatology including patients with iron overload (Table 19.1). At present, transient elastography (TE) is available in many hospitals and worldwide the most commonly used technique. We here review the elastography data for fibrosis screening in the context of iron overload and hereditary hemochromatosis.

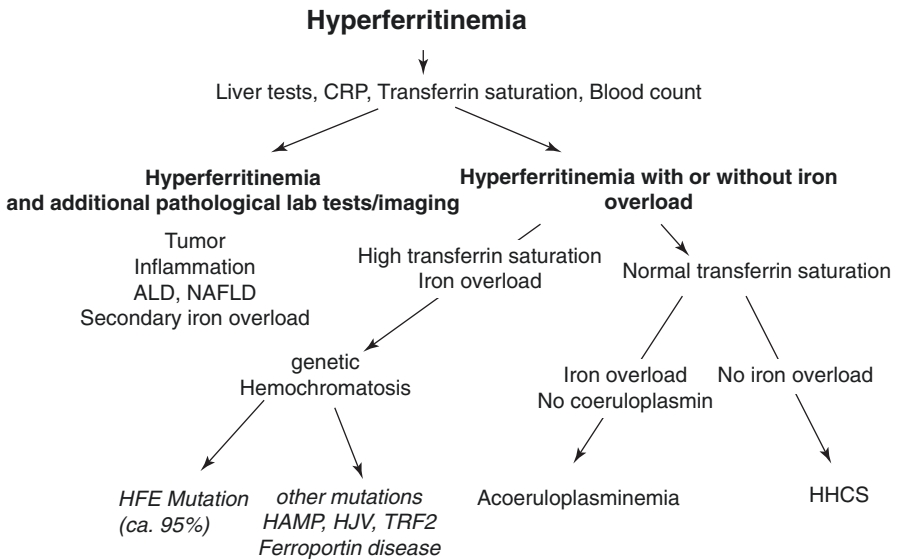


**Fig. 19.1** Differential diagnosis of elevated serum ferritin levels (hyperferritinaemia). Today, most hemochromatosis cases are identified through laboratory screening, normally by an elevated serum ferritin level or transferrin saturation. Many diverse aetiologies can account for elevated ferritin levels ranging from the rare hereditary hyperferritinaemia cataract syndrome (HHCS) to the most common liver diseases such as alcoholic and non-alcoholic fatty liver disease (ALD and NAFLD)

**Table 19.1** Liver stiffness in patients with hereditary hemochromatosis (HH)

Parameters	Adhoue [17]	Legros [18]
No. of patients with HH	57	61
Controls	46	No
Biopsy	No	Yes
Median LS value (kPa)	5.20	
LS cut-off value (kPa) for significant fibrosis	>7.1	>13.9
Sex (men)	58%	71.4%
Age (mean)	54.3 ± 13.7	50
BMI	25.0 ± 3.5	26
Recent diagnosis HH	17.5%	100%
Iron-depleted HH	82.5%	0%

## Transient Elastography (FibroScan) in Hereditary Hemochromatosis

So far, no LS cut-off values in biopsy-proven studies have been published due to the limited number of patients, and LSM is still not taken up by guidelines [1]. However, there is clear evidence that LS is elevated in patients with HH and that it decreases in response to phlebotomy.

In 2008 Adhoue et al. [17] published the first prospective study on FibroScan (EchoSens, Paris, France) in patients with hereditary hemochromatosis. During the study period from 2004 to 2006, 57 patients with hereditary hemochromatosis were included, all with the homozygous C282Y mutation. In addition, 46 controls were used. The study included ten recently diagnosed patients before initiating phlebotomy treatment and a group of iron-depleted patients that had been treated with phlebotomies for months or years. LS could be determined during follow-up of their disease. The control group consisted of patients with elevated transaminase levels (ALT) that had no fibrosis on liver biopsy. In addition, they were all negative for HIV, HCV, and HBV, alcohol abuse, and other causes of chronic liver disease. In this study, an LS >7.1 kPa was considered as the cut-off for significant fibrosis. Median LS was similar in both hemochromatosis and controls with 5.2 kPa (range 2.3–7.5) vs. 4.9 kPa (range 2.6–7.0), respectively. No differences with respect to biochemical markers were observed between hemochromatosis patients and controls.

Four patients in the hemochromatosis group (7%) and none in the control group were excluded because of LSM failure. A strong correlation was found between LS and biomarkers such as Fibrotest, GUCI, Hepascore, and Forns score, but not with APRI, FIB-4, or Lok score. Serum ferritin levels did not correlate with LS values. In 22.8% ( $n = 13$ ) of the hemochromatosis patients, LS values were higher than 7.1 kPa while none of the controls showed elevated LS ( $P < 0.0001$ ). Presence of diabetes and a serum ferritin value greater than 150 ng/mL were the two factors

associated with LS elevation in the hemochromatosis group. Notably, 44 hemochromatosis patients were annually followed-up for up to 2 years (7 recent diagnoses and 37 iron-depleted). In the group of patients with a recent diagnosis, five had initial values of less than 6 kPa without changes after 1–2 years. LS decreased from 8.8 to 4.9 kPa in one patient after 1 year. The only patient with an initially very high LS of 21.1 kPa, had 21.3 kPa after 1 year and 8.8 kPa after 2 years. In the iron-depleted group, LS values did not differ significantly in the follow-up period.

In 2015 Legros et al. [18] studied prospectively LS by TE between 2005 and 2013 in 77 C282Y homozygous patients that underwent a liver biopsy based on elevated serum ferritin levels >1000 ng/mL and raised transaminases (according to the guidelines). Patients previously treated with phlebotomies or with chronic hepatitis B or C were excluded. All of them had clinical and biological evaluation, including hyaluronic acid measurement in 52 cases. From the 77 patients with liver biopsy and LSM, 49 (63.6%) were overweight (BMI  $\geq$  25 kg/m<sup>2</sup>) and 11 (14.3%) were obese (BMI  $\geq$  30 kg/m<sup>2</sup>). Eight patients had excessive alcohol consumption. Fibrosis stage of hemochromatosis patients was F0 in 11 (14.3%), F1 in 33 (42.9%), F2 in 18 (23.4%), F3 in 2 (2.5%), and F4 in 13 (16.9%). A total of 19.5% of the patients had F3–F4 severe fibrosis. Hyaluronic acid was higher in patients with severe fibrosis but did not accurately predict severe fibrosis. Transient elastography was successful in 90.9% of the patients (70/77) due to obesity. Nine patients had no valid LSM with an IQR >30%. Therefore, valid LS values were available from 61 patients (79.2%).

Transient elastography was significantly higher in patients with severe fibrosis (17.2 vs. 4.9 kPa;  $P < 0.05$ ). In 38 patients (62.3%), LS was <6.4 kPa. None of them had severe liver fibrosis. Nine patients (14.8%) had a LS  $\geq$  13.9 kPa. All of them had severe liver fibrosis on histology. Fourteen patients (22.9%) had an LS between 6.4 and 13.9 kPa, and the prevalence of histological severe fibrosis was 5/14 (35.7%). Thus, using these two cut-off values, TE was able to accurately predict fibrosis stage in 77%. Efficient assessment of severe fibrosis was not possible in patients with intermediate values.

Consequently, this algorithm, based on the use of serum ferritin >1000 ng/mL and LS > 13.9 kPa, accurately classifies severe fibrosis in 61% of patients.

## Transient Elastography in Secondary Hemochromatosis

Transient elastography has also been explored in patients with secondary iron overload due to blood transfusions [19–21]. In addition, two publications have reported in histological fibrosis determination in patients with liver iron overload of secondary origin [20, 21].

Mirault et al. [20] studied 15 chronically transfused patients (13 beta-thalassemia major; 1 sickle cell disease, 1 myelodysplastic syndrome) and compared the results obtained by transient elastography with those of liver biopsy (METAVIR). Mean LS

values significantly differed in patients with severe fibrosis (F3/F4) from those with mild or no fibrosis (F0–F2) ( $9.4 \pm 3.7$  kPa vs.  $5.9 \pm 1.8$  kPa).  $LS > 6.25$  kPa identified patients at risk for severe fibrosis (NPP 88%; PPV 57%). They concluded that TE is a reliable tool for liver fibrosis evaluation in post-transfusion iron overload. Fraquelli et al. [21] studied 115 patients with beta-thalassemia major or intermedia. Histological data were available in only 14 cases. In these patients, a significant correlation was observed between LS and histological fibrosis stage. Severe fibrosis was diagnosed with a sensitivity of 60% and a specificity of 89%. Cirrhosis was detected with 100% sensitivity and 92% specificity.

## Real-Time Elastography

In 2013, Paparo et al. [19] published a prospective monocentric study to determine the value of real-time elastography (RTE) for the assessment of liver fibrosis in patients with iron overload, using transient elastography as a reference standard. The study included 67 patients with iron overload determined by MRI. Transient elastography and RTE were performed on the same day. Seven patients were excluded because of invalid transient elastography or RTE. The remaining 60 patients encompassed 37 homozygous beta-thalassaemic patients, 13 with beta-thalassemia intermedia, six with hereditary hemochromatosis, and four with myelodysplastic syndromes. They concluded that RTE allows the discrimination between F0/F1 and F3–F4 with reasonable diagnostic accuracy in patients with iron overload determined by MRI.

## ARFI Elastography

In 2013, Muniz et al. [22] studied two cases of patients with hemochromatosis with ultrasound, Doppler and liver elastography virtual touch (ARFI), and they commented that ARFI could collaborate in monitoring patients with hemochromatosis.

## MR Elastography (MRE)

MRE is a promising technique, but with limitations due to costs and availability [23]. It requires patient collaboration because MRE is a breath-hold procedure, similar to other MRI-related liver sequences [24]. In patients that suffer from moderate or high liver iron overload (hemosiderosis-hemochromatosis), the MRI liver signal may be very low, and waves cannot be visualised with a gradient-echo-based MRE sequence. This is an important clinical problem because iron deposition is a coexis-

tent condition in different diseases, such as hemochromatosis, thalassemia but also metabolic liver diseases [25]. Moreover, low MRI signal intensity in the liver is the major reason for measurement failures (approximately 70%). Advanced MRE in patients with mild or moderate liver iron overload [26], implementing alternative pulse sequences with shorter echo times such as spin-echo (SE), echo-planar imaging (EPI)-based MRE. However, no studies in HH patients have been published so far.

## Conclusion

LSM in combination with serum ferritin levels provide a highly accurate diagnosis of fibrosis in an important number of hereditary hemochromatosis patients, reducing the need of liver biopsy for prognosis evaluation. Figure 19.2 provides an actual working scheme and algorithm for the diagnosis of iron overload disease with liver stiffness being a central parameter for therapeutic guidance. More prospective studies are needed, but elastography should become an essential part of next guideline recommendations [1]. Other techniques, such as MR elastography, will provide unique opportunities in the future, namely in combination with iron detection by MRI. The first single patient observations demonstrate LS resolution after consequent initiation of phlebotomy.

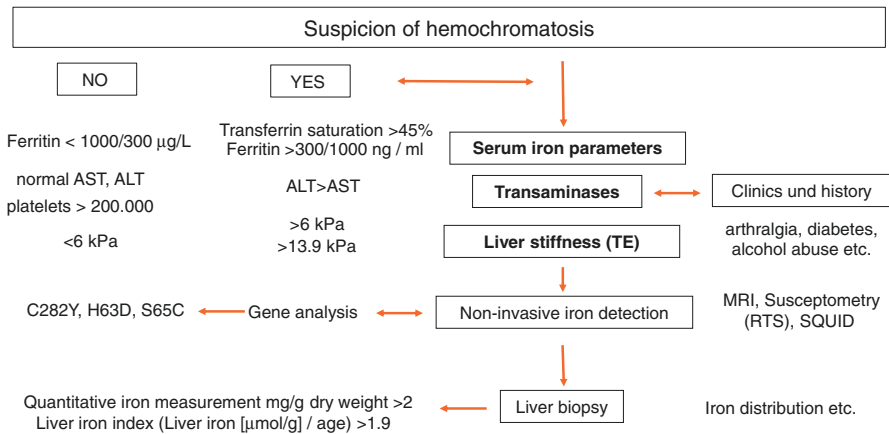


**Fig. 19.2** Actual proposed diagnostic algorithm and central role of liver stiffness for the diagnosis of iron overload disease. Hemochromatosis should be suspected in the presence of high ferritin levels in combination with signs of liver injury (elevated transaminase levels) and within the clinical context. LS values >6 kPa are a clear indication for a more intense search for iron overload. This can include non-invasive techniques such as MRI or RTS, if available, or genetic screening for common mutations. Today, liver biopsy is only performed in cases of doubt or to exclude the co-existence of other pathologies

## References

1. European Association For The Study Of The L. EASL clinical practice guidelines for HFE hemochromatosis. *J Hepatol.* 2010;53(1):3–22.
2. Feder JN, Gnirke A, Thomas W, Tsuchihashi Z, Ruddy DA, Basava A, et al. A novel MHC class I-like gene is mutated in patients with hereditary haemochromatosis. *Nat Genet.* 1996;13(4):399–408.
3. Mueller S, Mueller J, Raisi H, Sollors J, Rausch V. Hämochromatose. *Falk Gastrokolleg. Leber und Gallenwege;* 2015:1–15.
4. Castiella A, Zapata E, Alustiza JM. Non-invasive methods for liver fibrosis prediction in hemochromatosis: one step beyond. *World J Hepatol.* 2010;2(7):251–5.
5. Pietrangelo A. Hereditary Hemochromatosis—a new look at an old disease. *N Engl J Med.* 2004;350(23):2383–97.
6. Mueller J, Raisi H, Rausch V, Peccerella T, Simons D, Ziener CH, et al. Sensitive and non-invasive assessment of hepatocellular iron using a novel room-temperature susceptometer. *J Hepatol.* 2017;67(3):535–42.
7. Fung EB, Fischer R, Pakbaz Z, Fagaly RL, Vichinsky E, Starr TN, et al. The new SQUID biosusceptometer at Oakland: first year of experience. *Neurol Clin Neurophysiol.* 2004;2004:5.
8. Alústiza JM, Artetxe J, Castiella A, Agirre C, Emparanza JI, Otazua P, et al. MR quantification of hepatic iron concentration. *Radiology.* 2004;230(2):479–84.
9. Gandon Y, Olivie D, Guyader D, Aubé C, Oberti F, Seville V, et al. Non-invasive assessment of hepatic iron stores by MRI. *Lancet.* 2004;363(9406):357–62.
10. Castiella A, Alustiza JM, Artetxe J. Hereditary hemochromatosis. *N Engl J Med.* 2004;351(12):1263–4.
11. Wood MJ, Skoien R, Powell LW. The global burden of iron overload. *Hepatol Int.* 2009;3(3):434–44.
12. Froehlich F, Lamy O, Fried M, Gonvers JJ. Practice and complications of liver biopsy. *Dig Dis Sci.* 1993;38(8):1480–4.
13. Thampanitchawong P. Liver biopsy: complications and risk factors. *World J Gastroenterol.* 2000;5(4):301.
14. Bedossa P, Dargere D, Paradis V. Sampling variability of liver fibrosis in chronic hepatitis C. *Hepatology.* 2003;38(6):1449–57.
15. Millonig G, Muckenthaler MU, Mueller S. Hyperferritinaemia-cataract syndrome: worldwide mutations and phenotype of an increasingly diagnosed genetic disorder. *Hum Genomics.* 2010;4(4):250–62.
16. Mueller S, Seitz HK, Rausch V. Non-invasive diagnosis of alcoholic liver disease. *World J Gastroenterol.* 2014;20(40):14626–41.
17. Adhoute X, Foucher J, Laharie D, Terrebonne E, Vergniol J, Castéra L, et al. Diagnosis of liver fibrosis using FibroScan and other noninvasive methods in patients with hemochromatosis: a prospective study. *Gastroenterol Clin Biol.* 2008;32(2):180–7.
18. Legros L, Bardou-Jacquet E, Latournerie M, Guillygomarc’h A, Turlin B, Le Lan C, et al. Non-invasive assessment of liver fibrosis in C282Y homozygous HFE hemochromatosis. *Liver Int.* 2015;35(6):1731–8.
19. Paparo F, Cevasco L, Zefiro D, Biscaldi E, Bacigalupo L, Balocco M, et al. Diagnostic value of real-time elastography in the assessment of hepatic fibrosis in patients with liver iron overload. *Eur J Radiol.* 2013;82(12):e755–61.
20. Mirault T, Lucidarme D, Turlin B, Vandevenne P, Gosset P, Ernst O, et al. Non-invasive assessment of liver fibrosis by transient elastography in post transfusional iron overload. *Eur J Haematol.* 2008;80(4):337–40.
21. Fraquelli M, Cassinerio E, Roghi A, Rigamonti C, Casazza G, Colombo M, et al. Transient elastography in the assessment of liver fibrosis in adult thalassemia patients. *Am J Hematol.* 2010;85(8):564–8.

22. Muniz RLS, Esberard EBC, Guaraná T, Pollo P. Hepatic involvement by hemochromatosis. Ultrasound, doppler and ARFI elastography. *Ultrasound Med Biol.* 2013;39(5):S3.
23. Paparo F, Corradi F, Cevasco L, Revelli M, Marziano A, Molini L, et al. Real-time elastography in the assessment of liver fibrosis: a review of qualitative and semi-quantitative methods for elastogram analysis. *Ultrasound Med Biol.* 2014;40(9):1923–33.
24. Venkatesh SK, Yin M, Ehman RL. Magnetic resonance elastography of liver: technique, analysis, and clinical applications. *J Magn Reson Imaging.* 2013;37(3):544–55.
25. Mueller S, Rausch V. The role of iron in alcohol-mediated hepatocarcinogenesis. *Adv Exp Med Biol.* 2015;815:89–112.
26. Mariappan YK, Dzyubak B, Glaser KJ, Venkatesh SK, Sirlin CB, Hooker J, et al. Application of modified spin-echo-based sequences for hepatic MR elastography: evaluation, comparison with the conventional gradient-echo sequence, and preliminary clinical experience. *Radiology.* 2017;282(2):390–8.

# Chapter 20

## Liver Stiffness in Patients with Wilson's Disease



Thomas Karlas

### Introduction to Wilson's Disease

The homeostasis of copper, an essential micronutrient, is regulated by biliary excretion. Wilson's disease (WD) is a rare genetic disorder caused by mutations in the ATP7B gene, which plays a crucial role in copper-transporting in hepatocytes. The ATP7B defect results in copper accumulation in the brain and the liver [1]. The clinical presentation may vary, but neurological symptoms and/or hepatitis in younger patients in combination with eye involvement (Kayser–Fleischer ring) or hemolysis are typical for WD (Fig. 20.1). A minor proportion of patients presents with acute onset of liver failure, which may require emergent liver transplantation. The diagnosis is established by a scoring system (Leipzig score, see Appendix Table A.25) that combines presence of typical clinical symptoms, assessment of urinary copper excretion, serum ceruloplasmin levels, and tests of Coombs-negative hemolytic anemia. In doubtful cases, the measurement of liver copper content from a biopsy sample can confirm the diagnosis [1–4].

Improvement of copper excretion is the basis of therapy in WD. Chelating agents (D-penicillamine, triethylenetetramine) and inhibition of intestinal copper absorption by zinc formulations are recommended regimens for WD. A life-long adherence to medical therapy is essential to avoid complications of WD. Liver function regularly improves in treated patients and may completely normalize, whereas neurological symptoms frequently persist to some degree under treatment [3]. Therefore, early diagnosis is crucial to prevent chronic neurological impairment [1–4].

---

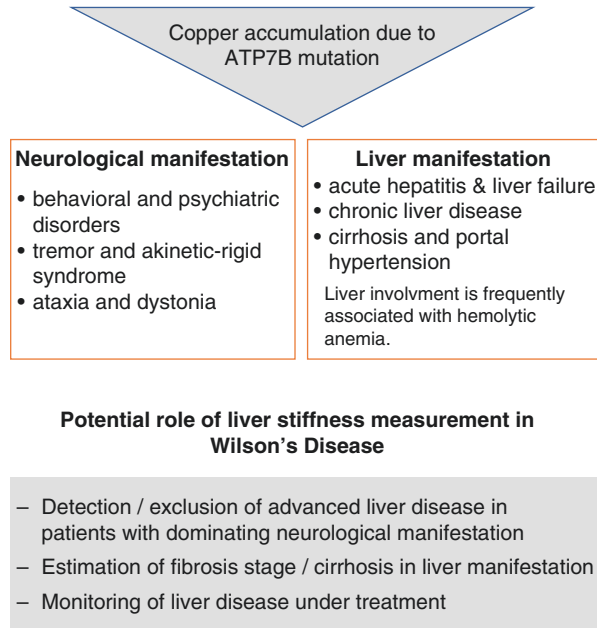
T. Karlas (✉)

Division of Gastroenterology, Medical Department II, University of Leipzig Medical Center, Leipzig, Germany

e-mail: [thomas.karlas@medizin.uni-leipzig.de](mailto:thomas.karlas@medizin.uni-leipzig.de)



**Fig. 20.1** Clinical features and potential applications of liver stiffness measurement in WD



## Considerations on the Use of Liver Stiffness Measurement in Wilson's Disease

Excess copper accumulates over a long period in the lysosomes of hepatocytes and is eventually released to the cytoplasm after disintegration of the lysosomal compartments [5]. This induces cell injury and death, probably due to the formation of free radicals. Depending on the rate of cell disintegration, this pathophysiological process may either result in life-threatening fulminant liver failure or present as chronic hepatitis. If untreated the latter usually progresses to fibrosis and ultimately cirrhosis with portal hypertension [1, 5].

Both acute liver failure, which histologically appears as necroinflammation, and fibrosis are major modulators of liver stiffness [2, 6–8]. There are three rationales for applying LSM in WD: (a) better discriminate between pure neurological manifestation and concomitant liver involvement; (b) detect advanced fibrosis and cirrhosis for assessing disease severity and prognosis, and (c) monitor the response to treatment in both acute and chronic liver diseases (Fig. 20.1).

Due to the low prevalence of symptomatic WD, which is estimated to be 1:~30.000, it is almost impossible to perform large biopsy-controlled studies [9, 10]. Within the last decade, only three pilot studies assessed the diagnostic properties of LSM in WD:

1. Sini et al. evaluated the transient elastography in 35 adult patients and compared the LSM results with liver histology [11]. This study proves the concept of a

positive correlation of LSM with the stage of fibrosis in WD, but the data are impaired by the small cohort size and technical limitations.

2. Karlas et al. evaluated both transient elastography and the ARFI-based point-shear wave elastography (pSWE) in a cohort of 50 adult patients with established diagnosis of WD [6]. The LSM results were compared with the clinical manifestation and correlated with the disease severity according to the Leipzig score. LSM values of both applied methods were lower in patients with dominant neurological involvement. Further, a correlation with disease severity was observed, although only advanced stages (i.e., cirrhosis) could be well discriminated with transient elastography. The main limitation of this study is the lack of a histological reference standard. In addition, the majority of patients had long-term therapy with chelating agents, which may explain the rather low cut-offs for cirrhosis [3].
3. Stefanescu et al. performed a long-term follow-up with transient elastography in nine pediatric patients with de novo diagnosis of WD [12]. They observed a continuous decline of LSM associated with improved urinary copper excretion in patients receiving either zinc or chelating agents.

These three reports prove the above-mentioned hypothesizes on the diagnostic use of LSM in WD (Fig. 20.1) but are insufficient to provide any standardized clinical recommendation. If available, LSM may compliment the diagnostic work-up of affected patients and may help to guide and monitor treatment decisions on an individual basis.

## Case Presentation

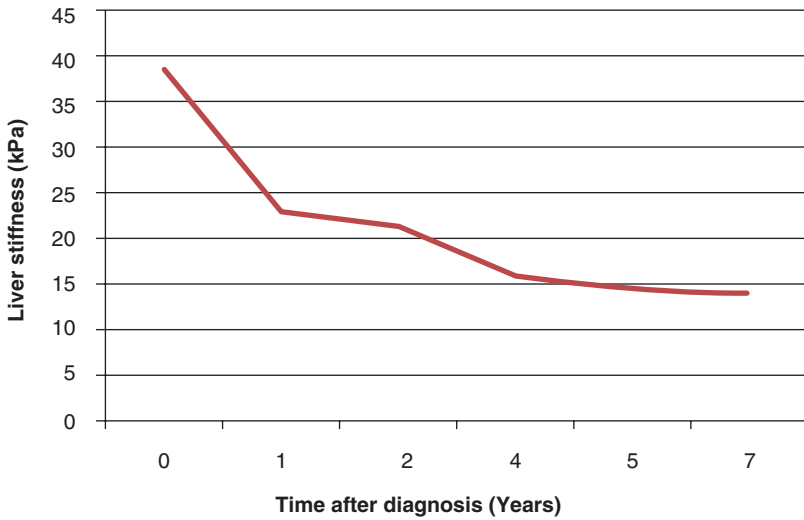
Considering the low prevalence of Wilson's disease, reports of individual cases are helpful to highlight the usefulness of LSM in this disorder. The following case gives an example of LSM as monitoring tool:

A 30-year-old man without any prior disease was diagnosed with liver cirrhosis and referred to a liver center for further diagnostics. Laboratory tests, imaging and further clinical evaluation revealed a compensated liver function (Child–Pugh A) with signs of portal hypertension (small esophageal varices). Further diagnostic work-up established the diagnosis of WD, and treatment with D-penicillamine was initiated.

The patient presented regularly for follow-up visits. Treatment was well tolerated, and no complications were observed within a period of 7 years. Liver function tests remained unchanged. Liver stiffness, which was highly elevated at the time of diagnosis (38.5 kPa), showed a continuous decline to a final value of 14.1 kPa. Notably, the sonographic appearance of the liver (irregular margins, coarse nodularity, rarefaction of peripheral portal, and liver veins) did not change over time (Fig. 20.2).

Increased LS values correlated with overall and liver-related mortality in patients with chronic liver disease [13]. In the present case, the decline of LS indicates a continuous reduction of mortality risk and, thus, proves the efficacy of treatment.

**Course of liver stiffness in a patient with Wilson's Disease**



**Ultrasound characteristics in the same patient**



**Fig. 20.2** Course of liver stiffness measurement (upper panel) and conventional ultrasound (lower panel) in a patient with Wilson's disease and compensated cirrhosis under treatment with D-penicillamine

Sonography and liver function tests were not capable to monitor this risk reduction. Hence, LSM is a promising technique for monitoring the treatment efficacy in patients with WD. For another interesting case of first-time diagnosis of WD in young male patients (case no. 19), see also book Part VII "How to Use LS in Clinical Practice" in the Chap. 53 "Clinical Cases" [14]. Here, an elevated LS was the first sign to insist on further diagnosis and LS normalized after 3 months of copper-chelation treatment.

## References

1. Ferenci P, Czlonkowska A, Stremmel W, Houwen R, Rosenberg W, Schilsky M, et al. EASL Clinical Practice Guidelines: Wilson's disease. *J Hepatol* 2012;56(3):671–85. <https://doi.org/10.1016/j.jhep.2011.11.007>.
2. Dietrich CF, Bamber J, Berzigotti A, Bota S, Cantisani V, Castera L, et al. EFSUMB guidelines and recommendations on the clinical use of liver ultrasound elastography, update 2017 (long version). *Ultraschall Med*. 2017;38(4):e16–47.
3. Bruha R, Marecek Z, Pospisilova L, Nevsimalova S, Vitek L, Martasek P, et al. Long-term follow-up of Wilson disease: natural history, treatment, mutations analysis and phenotypic correlation. *Liver Int*. 2010;31(1):83–91.
4. Huster D. Wilson disease. *Best Pract Res Clin Gastroenterol*. 2010;24(5):531–9.
5. Stremmel W, Merle U, Weiskirchen R. Clinical features of Wilson disease. *Ann Transl Med*. 2019;7(Suppl 2):S61.
6. Karlas T, Pfrepper C, Rosendahl J, Benckert C, Wittekind C, Jonas S, et al. Acoustic radiation force impulse (ARFI) elastography in acute liver failure: necrosis mimics cirrhosis. *Z Gastroenterol*. 2011;49(04):443–8.
7. Seo YS, Lee KG, Jung ES, An H, Park S, Keum B, et al. Dynamic changes in liver stiffness during the course of acute hepatitis A. *Scand J Gastroenterol*. 2010;45(4):449–56.
8. Mueller S, Sandrin L. Liver stiffness: a novel parameter for the diagnosis of liver disease. *Hepat Med*. 2010;2:49–67.
9. Isabelle Mohr KHW. Biochemical markers for the diagnosis and monitoring of Wilson disease. *Clin Biochem Rev*. 2019;40(2):59–77.
10. Karlas T, Hempel M, Tröltzsch M, Huster D, Günther P, Tenckhoff H, et al. Non-invasive evaluation of hepatic manifestation in Wilson disease with transient elastography, ARFI, and different fibrosis scores. *Scand J Gastroenterol*. 2012;47(11):1353–61.
11. Sini M, Sorbello O, Civolani A, Liggi M, Demelia L. Non-invasive assessment of hepatic fibrosis in a series of patients with Wilson's disease. *Dig Liver Dis*. 2012;44(6):487–91.
12. Stefanescu AC, Pop TL, Stefanescu H, Miu N. Transient elastography of the liver in children with Wilson's disease: preliminary results. *J Clin Ultrasound*. 2015;44(2):65–71.
13. Singh S, Fujii LL, Murad MH, Wang Z, Asrani SK, Ehman RL, et al. Liver stiffness is associated with risk of decompensation, liver cancer, and death in patients with chronic liver diseases: a systematic review and meta-analysis. *Clin Gastroenterol Hepatol*. 2013;11(12):1573–84.e2.
14. Mueller S. Personal observation. 2019.

**Part IV**  
**Important (Patho)physiological**  
**Confounders of Liver Stiffness**

# Chapter 21

## Introduction to Confounders of Elevated Liver Stiffness



Sebastian Mueller

### Introduction to Confounders of Elevated LS Irrespective of Cirrhosis

Since the introduction of TE, it has been rapidly learned that LS can be strongly affected by many (patho)physiological conditions irrespective of fibrosis stage (see Fig. 21.1) [1]. Some of the important confounders are separately discussed in detail in this book section (book Part IV). Initially, this has caused quite some confusion since many clinicians associate LS solely with fibrosis. However, common sense observation quickly reminds us that tissue stiffness such as skin stiffness is not only caused by induration due to deposited matrix proteins but also in response to inflammation (e.g., a bee sting). Major confounders of LS elevation encompass hepatic necroinflammation as found in acute hepatitis [2, 3], congestion [4], and mechanic cholestasis [5]. Namely the response of LS to liver congestion as seen in patients with right heart failure is quite impressive. Figure 21.2 demonstrates in an isolated pig liver that a 36 cm water pressure in the hepatic veins suffices to increase LS to 75 kPa, the detection limit of the FibroScan device [4]. Meanwhile, many other confounders have been identified (see a list in Table 21.1). Both Table 21.1 and Fig. 21.3 show the extent to which these confounders can increase LS in a non-cirrhotic liver. Of course, the awareness of these confounders is highly important for the interpretation of LS in daily clinical practice.

---

S. Mueller (✉)

Department of Medicine and Center for Alcohol Research and Liver Diseases, Salem Medical Center, University of Heidelberg, Heidelberg, Germany  
e-mail: [sebastian.mueller@urz.uni-heidelberg.de](mailto:sebastian.mueller@urz.uni-heidelberg.de)

**Fig. 21.1** Major clinical confounders of elevated liver stiffness

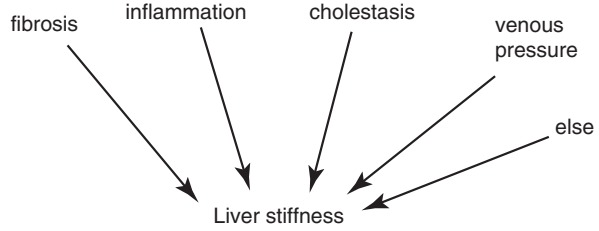


**Fig. 21.2** Dependence of liver stiffness on venous pressure. Note that 36 cm water pressure suffice to reach the detection limit of the Fibroscan device of 75 kPa

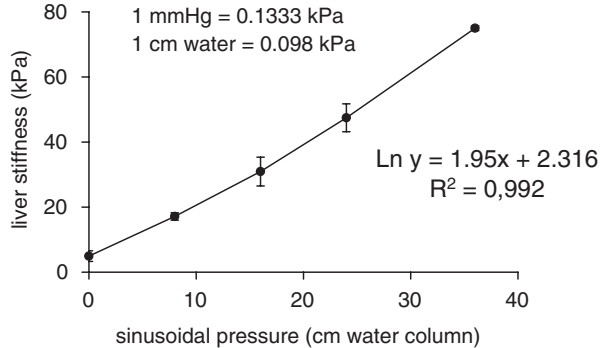


**Table 21.1** Maximum levels of liver stiffness reached by confounders irrespective of fibrosis

Confounder	LS elevation irrespective of fibrosis stage	References
Inflammation	30 kPa in acute hepatitis A	[6–8]
Mechanic cholestasis	25 kPa	[5]
Central venous pressure, congestion	75 kPa	[4]
Arterial pressure	8 kPa	[9]
Portal pressure	8 kPa	[10]
Mast cell infiltration	75 kPa	[11]
Alcohol consumption	25 kPa	[1]
Food intake	75 kPa	[12]
Water retention	75 kPa	[4]
Ballooning	30 kPa	[13]
Hepatic mast cell infiltration	75 kPa	[11]
Valsalva and orthostatic maneuvers	75 kPa	[14]
Amyloidosis	75 kPa	[15]

### Confounders of Elevated LS by Categories

Table 21.2 provides an overview of the various confounder categories ranging from pressure-related to histological and even intracellular factors. Pressure, namely the pressure within the hepatic sinus (sinusoidal pressure) has been a key feature in better understanding the molecular basis of LS. For more details see also book Part

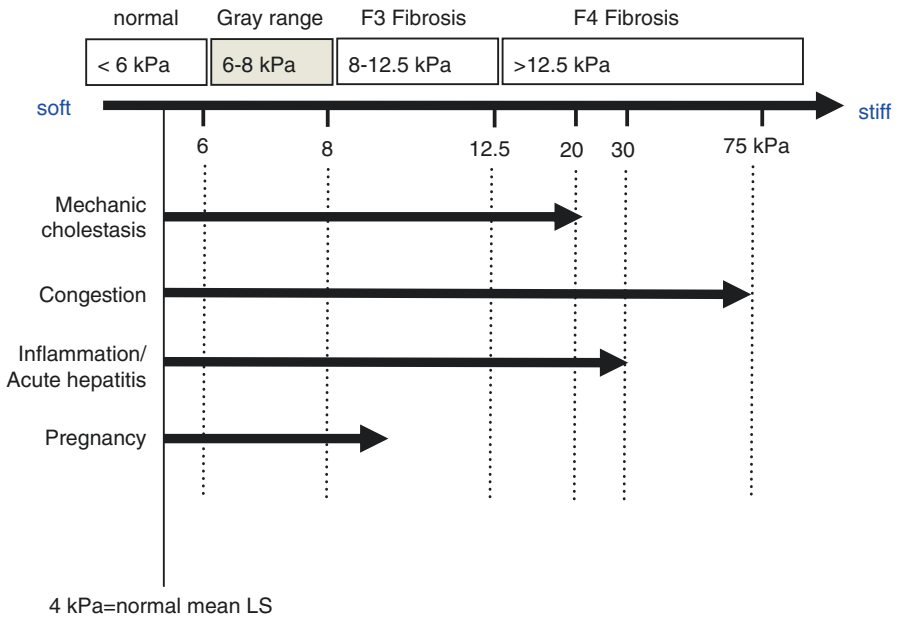


**Fig. 21.3** Extent of liver stiffness elevation to be reached by various confounding factors

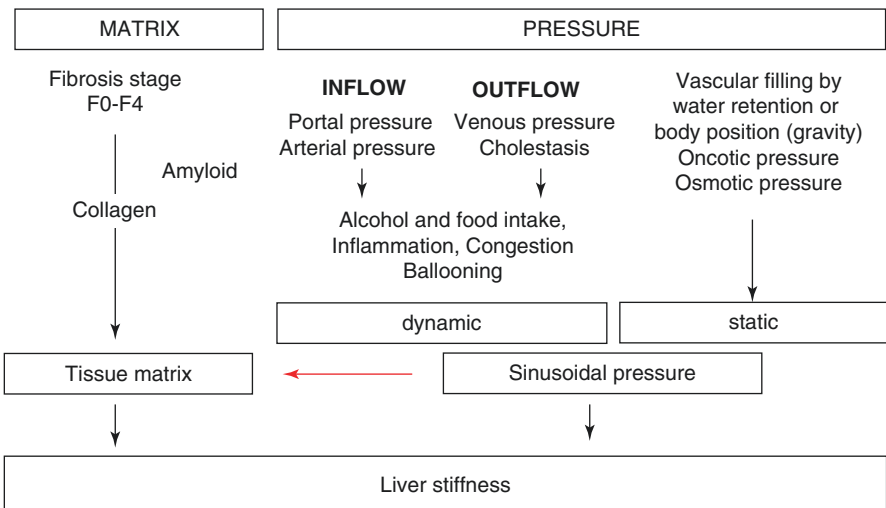
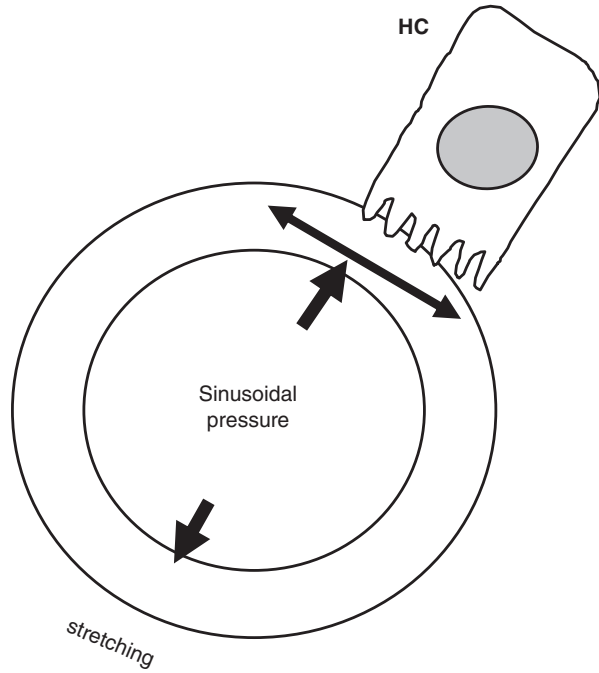
**Table 21.2** Confounders of elevated liver stiffness

Confounders	Examples
Matrix-associated	<ul style="list-style-type: none"> <li>• Collagen</li> <li>• Amyloid</li> </ul>
Hemodynamic	<ul style="list-style-type: none"> <li>• Arterial pressure</li> <li>• Portal pressure</li> <li>• Central venous pressure</li> </ul>
Histological	<ul style="list-style-type: none"> <li>• Ballooning</li> <li>• Inflammation</li> <li>• Intracellular inclusions</li> </ul>

VIII “Molecular Basis of Liver Stiffness and Cell Biology.” Figure 21.4 provides a simplified sketch how sinusoidal pressure stretches the perisinusoidal or perivascular wall structure, exposing aligning cells to stretch forces. Figure 21.5 provides a more complete scheme of the various matrix- and pressure-related confounders. Note that conditions such as alcohol [1] or food intake [16] but also inflammation are rather complex and relate to more than one molecular pathway (e.g., perfusion change, osmotic change, and infiltration of inflammatory cells in the case of hepatitis). The red arrow in Fig. 21.5 indicates that all these LS-elevating confounders are potentially unfavorable for the liver and can ultimately cause fibrosis. This has led to the introduction of pressure as important key component for fibrosis progression.



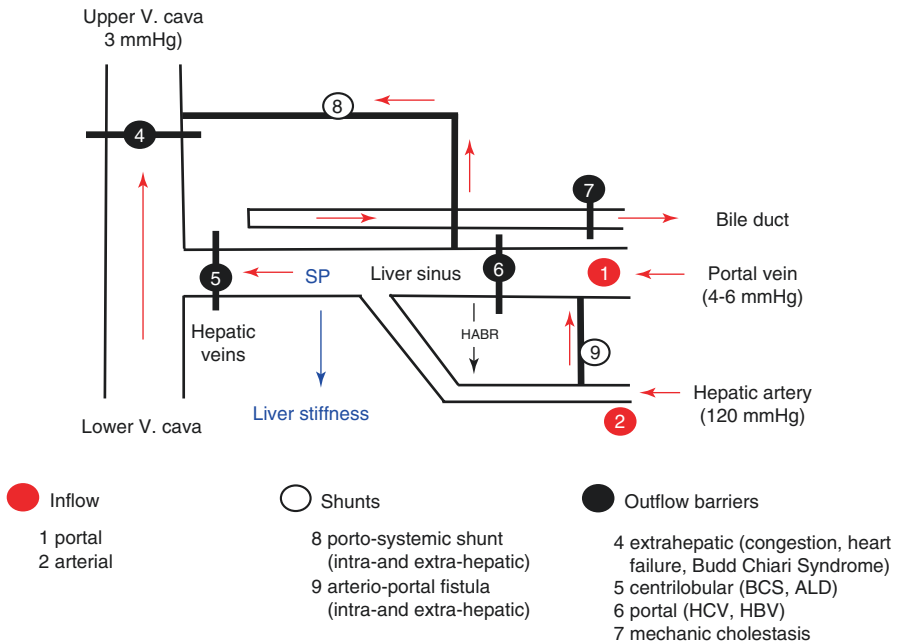
**Fig. 21.4** Schematic illustration of sinusoidal pressure and its role for LS elevation. Intrasinusoidal/intravascular pressure causes stretching of the perisinusoidal wall, increased wall stiffness, and eventually elevated liver stiffness. Many histological and molecular structures can contribute to the LS elevation and are still a matter of debate. *HC* hepatocyte



**Fig. 21.5** Overview of various confounders of liver stiffness elevation. The red arrow indicates that all these conditions eventually negatively impact on fibrosis. The resulting so called sinusoidal pressure hypothesis is discussed in more detail in Part IX

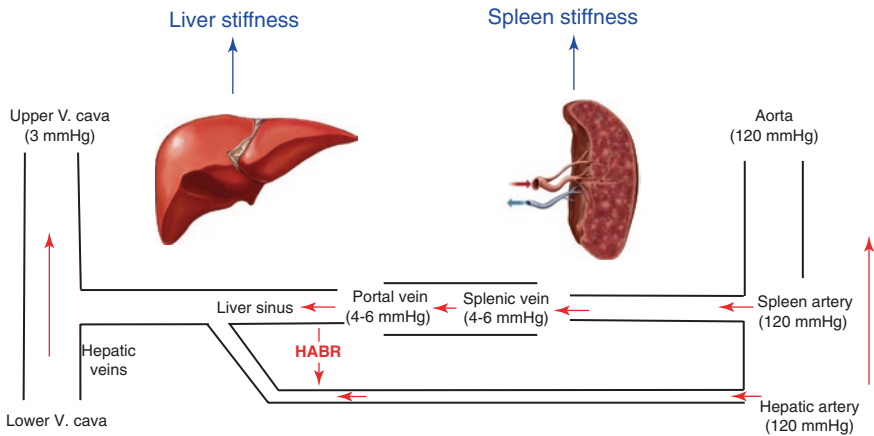
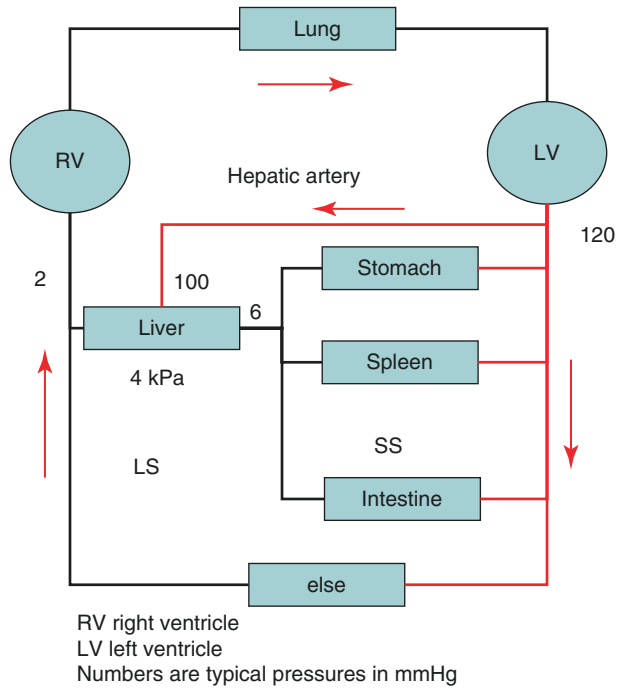
## The Inflow/Outflow Model to Explain Pressure-Related Confounders

Figure 21.6 eventually shows a simplified hemodynamic model of the liver to explain the role of various pressures on LS (inflow/outflow model) [17]. Accordingly, the hepatic outflow (bile flow, hepatic veins) and inflow (hepatic artery and portal vein) are important determinants of the sinusoidal pressure ultimately underlying LS. Pharmacological modulation with vasoactive substances in rodent models of cirrhosis has provided detailed insights into the complex interplay of inflow/outflow components depending not only on central venous, arterial, and portal pressure but also the heart rate [18]. Figure 21.7 schematically illustrates the integration of the liver in the systemic circulation which is often overlooked. It highlights the special vascular situation of the liver which is mainly (80%) supplied via low pressure (<6 mmHg) through the portal vein. This blood supply reverses in patients with liver cirrhosis where the hepatic artery will supply the liver with 80% of the blood at high pressure (120 mmHg). It also shows the specific position of the liver between right and left ventricle.



**Fig. 21.6** Hemodynamic scheme of liver vascularization to explain the inflow/outflow components that affect liver stiffness. Namely the role of shunts is still insufficiently understood. *HABR* hepatic arterial buffer response

**Fig. 21.7** Liver perfusion within the systemic circulation. The liver which is mainly supplied via low pressure (<6 mmHg) through the portal vein while the hepatic artery will take over in the diseased, stiff organ (see also Part VIII) . Liver hemodynamics are best understood when looking at it within one systemic circulation of two sequentially adjusted pumps (right and left ventricle)



**Fig. 21.8** Liver and spleen stiffness and its dependence on various hemodynamic conditions. Spleen stiffness is better reflecting portal hypertension but also the relation of LS and SS to each other provides useful information e.g., on the side of inflammation (portal versus lobular). *HABR* hepatic arterial buffer response

Taken together, liver hemodynamics is best understood when looking at it within one systemic circulation of two sequentially adjusted pumps (right and left ventricle). Figure 21.8 focuses both on liver and spleen stiffness and its dependence on various hemodynamic conditions. More details will be discussed in this book section. It will also explain why spleen stiffness is better reflecting portal hypertension as compared to liver stiffness.

While cardiac circulation is tightly connected to these components via the dynamic pressure, a static pressure component is also strongly affecting LS through water retention via hormonal, osmotic, or albumin-related conditions [17]. Finally, although not all subcellular factors (mitochondria, peroxisomes, etc.) associated with LS have been clarified yet, it is well established that histological features such as fibrosis, ballooning, and inflammation are associated with LS elevation [13, 19]. Controversies still continue about the role of fat that has been shown to lower LS in the absence of inflammation [19]. Why the molecular basis of LS-elevating confounders is still far from being understood, the consideration of these factors is highly important for the interpretation of LS in the clinical context.

## References

1. Mueller S, Millonig G, Sarovska L, Friedrich S, Reimann FM, Pritsch M, et al. Increased liver stiffness in alcoholic liver disease: differentiating fibrosis from steatohepatitis. *World J Gastroenterol.* 2010;16(8):966–72.
2. Sagir A, Erhardt A, Schmitt M, Haussinger D. Transient elastography is unreliable for detection of cirrhosis in patients with acute liver damage. *Hepatology.* 2008;47(2):592–5.
3. Dechêne A, Sowa J-P, Gieseler RK, Jochum C, Bechmann LP, El Fouly A, et al. Acute liver failure is associated with elevated liver stiffness and hepatic stellate cell activation. *Hepatology.* 2010;52(3):1008–16.
4. Millonig G, Friedrich S, Adolf S, Fonouni H, Golriz M, Mehrabi A, et al. Liver stiffness is directly influenced by central venous pressure. *J Hepatol.* 2010;52(2):206–10.
5. Millonig G, Reimann FM, Friedrich S, Fonouni H, Mehrabi A, Büchler MW, et al. Extrahepatic cholestasis increases liver stiffness (FibroScan) irrespective of fibrosis. *Hepatology.* 2008;48(5):1718–23.
6. Arena U, Vizzutti F, Corti G, Ambu S, Stasi C, Bresci S, et al. Acute viral hepatitis increases liver stiffness values measured by transient elastography. *Hepatology.* 2007;47(2):380–4.
7. Mueller S, Sandrin L. Liver stiffness: a novel parameter for the diagnosis of liver disease. *Hepat Med.* 2010;2:49–67.
8. Mueller S, Englert S, Seitz HK, Badea RI, Erhardt A, Bozaari B, et al. Inflammation-adapted liver stiffness values for improved fibrosis staging in patients with hepatitis C virus and alcoholic liver disease. *Liver Int.* 2015;35(12):2514–21.
9. Piecha F, Peccerella T, Bruckner T, Seitz HK, Rausch V, Mueller S. Arterial pressure suffices to increase liver stiffness. *Am J Physiol Gastrointest Liver Physiol.* 2016;311(5):G945–53.
10. Piecha F, Paech D, Sollors J, Seitz HK, Rossle M, Rausch V, et al. Rapid change of liver stiffness after variceal ligation and TIPS implantation. *Am J Physiol Gastrointest Liver Physiol.* 2018;314(2):G179–G87.
11. Adolf S, Millonig G, Seitz HK, Reiter A, Schirmacher P, Longerich T, et al. Systemic mastocytosis: a rare case of increased liver stiffness. *Case Reports Hepatol.* 2012;2012:1–6.
12. Mederacke I, Bahr MJ. Liver stiffness after meal intake at different stages of fibrotic evolution. *Hepatology.* 2014;59(2):734–5.
13. Mueller S, Nahon P, Rausch V, Peccerella T, Silva I, Yagmur E, et al. Caspase-cleaved keratin-18 fragments increase during alcohol withdrawal and predict liver-related death in patients with alcoholic liver disease. *Hepatology.* 2017;66(1):96–107.
14. Adolf S, Millonig G, Friedrich S, Seitz HK, Mueller S. Valsalva and orthostatic maneuvers increase liver stiffness in healthy volunteers. *Z Gastroenterol.* 2010;48:1.

15. Bastard C, Bosisio MR, Chabert M, Kalopissis AD, Mahrouf-Yorgov M, Gilgenkrantz H, et al. Transient micro-elastography: a novel non-invasive approach to measure liver stiffness in mice. *World J Gastroenterol.* 2011;17(8):968–75.
16. Mederacke I, Wurstthorn K, Kirschner J, Rifai K, Manns MP, Wedemeyer H, et al. Food intake increases liver stiffness in patients with chronic or resolved hepatitis C virus infection. *Liver Int.* 2009;29(10):1500–6.
17. Mueller S. Does pressure cause liver cirrhosis? The sinusoidal pressure hypothesis. *World J Gastroenterol.* 2016;22(48):10482.
18. Piecha F, Mandorfer M, Peccerella T, Ozga AK, Poth T, Vonbank A, et al. Pharmacological decrease of liver stiffness is pressure-related and predicts long term clinical outcome. *Am J Physiol Gastrointest Liver Physiol.* 2018;315(4):G484–94.
19. Rausch V, Peccerella T, Lackner C, Yagmur E, Seitz HK, Longerich T, et al. Primary liver injury and delayed resolution of liver stiffness after alcohol detoxification in heavy drinkers with the PNPLA3 variant I148M. *World J Hepatol.* 2016;8(35):1547–56.

# Chapter 22

## Histological Confounders of Liver Stiffness



Sebastian Mueller and Carolin Lackner

### Introduction to Histological Confounders of Liver Stiffness

Liver histology still provides an important diagnostic information that cannot be fully replaced by noninvasive means [1, 2]. In the daily clinical routine, however, liver biopsy is often limited due to technical requirements (cylinder size smaller than 15 mm), interobserver variability and sampling errors with regard to fibrosis staging which can reach 30% [3–7] or mild (pain and small bleedings in 6%) or severe complications (fatal perforations and bleedings in 0.1% [8, 9]).

Because of newly introduced elastographic techniques such as transient elastography (TE), liver biopsy should no longer be regularly performed to quantitate fibrosis stage or steatosis except in complex cases or cases with more than a single etiology of liver disease.

One striking advantage of TE in comparison to biopsy cohorts is the fact that more if not all patients can be classified for fibrosis stage. Thus, an almost complete distribution of fibrosis stages for the whole population can be obtained as shown in Fig. 22.1 (ALD cohort from Heidelberg) [11]. In the biopsy-proven group ( $n = 102$ ), ca. 54% were F3–4 while almost no one was F0 (5.2%). In patients staged by transient elastography ( $n = 675$ ) 42% were classified as F0 and 30% were F3–4. These data indicate that biopsy-proven studies are naturally biased missing especially many patients with normal livers.

In this chapter, we will briefly summarize the rather limited and complex data on LS and histology. To facilitate the understanding, we start with original data taken

---

S. Mueller (✉)

Department of Medicine and Center for Alcohol Research and Liver Diseases, Salem Medical Center, University of Heidelberg, Heidelberg, Germany  
e-mail: [sebastian.mueller@urz.uni-heidelberg.de](mailto:sebastian.mueller@urz.uni-heidelberg.de)

C. Lackner

Diagnostik & Forschungsinstitut für Pathologie, Medizinische Universität Graz, Graz, Austria  
e-mail: [karoline.lackner@medunigraz.at](mailto:karoline.lackner@medunigraz.at)

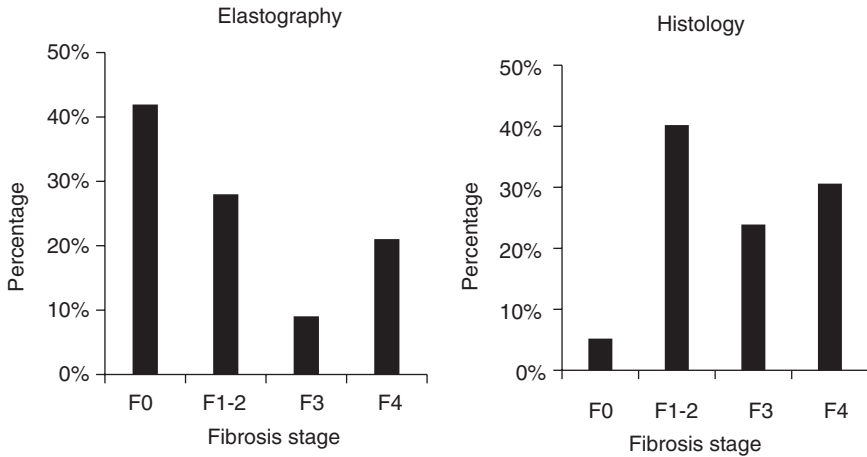


**Fig. 22.1** Histologically characterized patient cohorts have significantly more diseased patients and almost no patients without fibrosis. Left panel shows the elastographically characterized cohort with  $n = 675$  using TE with GOT-adapted cutoff values [10]. The right panel shows the  $n = 102$  (15.1%) patients that have been scored by liver biopsy

from the over 10 year ongoing Heidelberg cohort of heavy drinkers [10–15] since alcoholic liver disease (ALD) shows a diverse range of histologic features. These elementary histological features in ALD include steatosis, with macro- and micro-vesicles, hepatocellular ballooning, inflammatory infiltrates (neutrophils) that predominate in the lobules and variable degrees of fibrosis including pericellular fibrosis and lobular distortion perhaps progressing to cirrhosis [16]. We will finally discuss still inconclusive data on LS and histology.

## Correlation of Histological Parameters with Liver Stiffness: Correlation Data from Heavy Drinkers

To date, there are not many data available that study in detail histological features and liver stiffness. Therefore, we first present raw original data from patients with ALD of the above mentioned ongoing ALD cohort from Heidelberg (see also Fig. 22.1). As mentioned above, ALD is especially suited for understanding the association of LS with histology, since it shows all features ranging from steatosis, steatohepatitis, and fibrosis (see Fig. 22.2). In addition, important intracellular features can be demonstrated such as Mallory–Denk bodies, megamitochondria or deposits such as glycogen or iron. Despite heavy drinking (ca. 200 g alcohol per day over 15 years), more than 40% did not develop even early signs of fibrosis (see Fig. 22.1). The prevalence of the histological features is given in Table 22.1. Almost 70% showed steatosis, 75.3% steatohepatitis, 39% lobular inflammation, and ca.

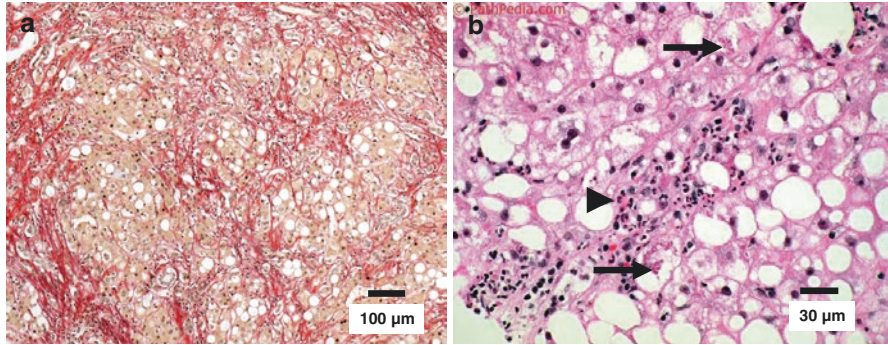


**Fig. 22.2** Histological confounders of elevated liver stiffness. **(a)** Sirius red to stain collagen fibers. A micronodular cirrhosis is shown with small modules that are surrounded by connective tissue. Additional pericellular fibrosis is also visible. Fibrosis is the histological marker that correlates best with LS ( $r$  typically  $>0.8$ ). **(b)** Hematoxyline Eosine stain. Liver section of a patient with alcoholic steatohepatitis is shown with all three key histologic findings: steatosis ( $>5\%$ ), Inflammation, and hepatocyte injury. Macro-steatosis is obvious and two ballooned hepatocytes are shown containing Mallory–Denk bodies (top and bottom arrows). The arrowhead shows hepatocellular inflammation. Correlation of these features with LS is more complex. While steatohepatitis and ballooning are positively correlated with stiffness, steatosis does not show any or sometimes even negative correlation

**Table 22.1** Relative distribution of histological features in ALD patients

Kleiner score (range)	considered elevated	Percentage
Kleiner steatosis 0–3	$>1$	69.4
Lobular inflammation 0–3	$>1$	38.8
Portal inflammation 0–1	$>0$	15.3
Ballooning 0–2	$>1$	15.3
Megamitochondria 0–1	$>0$	1.6
Mallory hyaline 0–1	$>0$	25.9
Classification steatohepatitis 0–2	$>0$	75.3

Preliminary data from Salem Medical Center ( $n = 102$ )

15% portal inflammation and ballooning. Steatosis is also an early sign in ALD and is most frequently seen in injured livers [17]. Nevertheless, it is still not clear whether simple steatosis is a benign condition, a prerequisite for further progression toward steatohepatitis or even a compensatory protective reaction. Alcoholic steatohepatitis (ASH) is characterized by steatosis in combination with hepatocyte ballooning, hepatocellular damage, and tissue inflammation represented by infiltrates of polymorphonuclear cells [18]. Among ASH, steatosis, and the extent of fibrosis, ASH demonstrated the highest risk for cirrhosis development in at least 40% of cases [19–23].

Table 22.2 shows the Spearman correlation of these histological features with LS. Clearly, features of *fibrosis* show the closest association with LS ranging from



**Table 22.2** Correlation of LS with various histological parameters from the Kleiner score [24] and Chevallier score [25] from a large biopsy group ( $n = 242$ )

Histological parameter (scores)	Spearman rho with liver stiffness ( $n = 242$ )	
	$r$	$p$
Chevallier score	0.785	1.1E-40
Septa number	0.777	1.6E-39
Width of septa	0.727	2.4E-32
Kleiner fibrosis score 0–4	0.727	5.3E-41
Mallory–Denk body 0–1	0.392	3.5E-10
Ballooning 0–2	0.371	3.6E-09
Lobular inflammation 0–3	0.345	5.2E-08
Classification steatohepatitis 0–2	0.303	4.0E-06
NAFLD activity Score (NAS)	0.279	1.3E-05
Portal inflammation 0–1	0.252	8.6E-05
Microgranulomas 0–1	0.198	2.1E-03
Acidophil bodies 0–1	0.183	4.6E-03
Megamitochondria 0–1	0.182	4.9E-03
CLV	0.151	3.8E-02
Glycogenated nuclei 0–1	0.131	4.3E-02
Large lipogranulomas 0–1	0.127	5.0E-02
Microvesicular steatosis 0–1	0.054	4.1E-01
Kleiner steatosis score 0–3	0.020	7.5E-01
Pigmented macrophages 0–1	–0.011	8.6E-01

About 70% represent patients with ALD, the rest has other etiologies

0.7 to 0.8. These fibrosis features include width and number of septa or the known Kleiner fibrosis and Chevalier scores [24, 25]. Fibrosis features are followed by signs of *ballooning* which, among other features, is characterized by accumulation of undergraded material such as Mallory’s hyaline in the now called Mallory–Denk bodies that are largely stuffed with CK18 cytokeratin filaments. Since ballooned hepatocytes represent apoptotic, damaged but still living enlarged cells, it is conceivable that the cellular volume increase contributes to elevated LS. Features of ballooning are followed by *signs of inflammation* such as infiltrates of neutrophils or other inflammatory cells. In the context of inflammation, it is highly plausible that both recruitment of more cells and more perfusion (pressure) will cause a LS elevation. Inflammation is followed by other histological features that are still positively and significantly associated with LS: microgranulomas, acidophil bodies, megamitochondria, glycogenated nuclei, and large lipogranulomas. These mostly intracellular histological parameters are all features of apoptotic cell damage or death. Notably, *steatosis* itself such as lipid droplets are not significantly correlated with LS, in some cohorts even *slightly negatively*. These findings are better visualized in Fig. 22.2a, b and schematically shown in Fig. 22.3a, b. For more details see also book Part VI “Assessment of Hepatic Steatosis Using CAP.”

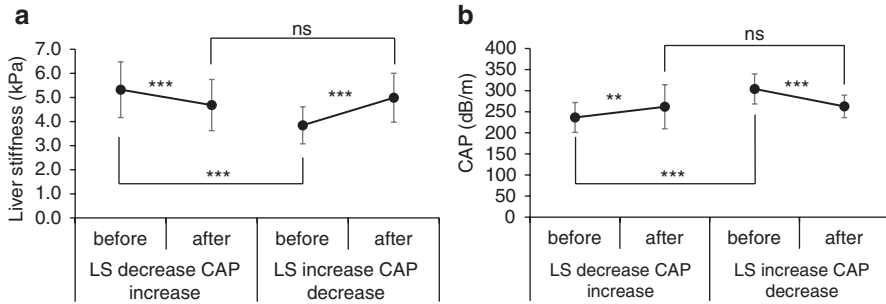


**Fig. 22.3** Change of LS and CAP in patients with simple steatosis (without inflammation) after alcohol withdrawal. First group ( $N = 13$ ) showed significant decrease of LS and increase of CAP after alcohol withdrawal. However, the opposite happened in the second group ( $N = 18$ ) where LS increased and CAP decreased after alcohol withdrawal. (a) shows the change in LS (kPa) in both groups while (b) shows the change in CAP (dB/m)

## Liver Stiffness and Steatosis

The presence of *macro vesicular fat* in hepatocytes is a very frequent finding in liver biopsy. Therefore, the question to what extent—if at all—liver stiffness may be modulated by *steatosis* besides fibrosis stage is clinically very relevant for noninvasive staging of any liver disease. As briefly discussed above, a negative association between LS and steatosis is seen in heavy drinkers. However, a search of the literature shows a more complex and partially controversial picture. Recently, it has been suggested that higher steatosis values assessed by CAP leads to overestimation of fibrosis staging by LS [26]. Boursier et al. used digital image analysis (morphometry) to assess steatosis, inflammation, and fibrosis in histological sections and investigated their impact on LS in 650 HCV patients also showing an overestimation of fibrosis stage due to steatosis [27]. However, another prospective study by Eddowes et al. with 450 NAFLD patients found no effect of steatosis on the fibrosis stage assessed by TE in multivariate analysis and after adjustment for histological stage [28]. The conflicting data may be partly explained by other coexisting confounders such as ballooning or inflammation [28–30]. For more details see also book Part VI “Assessment of Hepatic Steatosis Using CAP.”

An explanation for the controversy could be the fact that association studies are never causal but show a mere association not being able to clearly dissect which confounder is responsible for elevated LS. As mentioned above, steatosis is so common that a positive association could be simply due to coexisting inflammation. There are observations in individual patients with follow-up and treatment interventions that clearly suggest a negative impact of steatosis on LS.

For instance, in patients without inflammation but increased steatosis on follow-up, a decrease of LS has been observed (see Fig. 22.3). Moreover, small unpublished case observations suggest that a decrease of steatosis can lead to LS elevation.

To better understand the role of steatosis, prospective follow-up studies are needed with a careful characterization of steatosis, fibrosis, ballooning, and inflammation. Even better, the mere role of steatosis in noninflammatory liver should be studied.

## **Liver Stiffness and Inflammation**

As already mentioned in the introduction to book Part IV, “Important (Patho) Physiological Confounders of LS,” inflammation either by infiltration with inflammatory cells or increased blood flow as well as edematous tissue reactions are associated with increased LS. Moreover, therapeutic interventions to cure inflammation such as antiviral treatment, alcohol detoxification etc. cause a rapid decrease of LS which is related to viral load, transaminase levels, and LS at baseline before treatment [31, 32].

Among fatty liver diseases, liver stiffness in NAFLD seems to be influenced by inflammation to a lesser degree [29, 30] as compared to ALD [12]. As in viral hepatitis, the use of adapted LS cutoff has also been proposed for noninvasive staging of patients with ALD and elevated transaminases [33]. The utility of adapted cutoffs for noninvasive staging in settings of inflammation should be evaluated in further studies.

## **Role of Fibrosis Type on Liver Stiffness**

In contrast to most other chronic liver diseases which are associated by dense septa extending from the on histology (portal-based dense fibrous septa), the fibrosis type in ALD as well as NAFLD is characterized by a predominantly centrilobular and pericellular distribution. In early stages of fatty liver disease (FLD) so-called pericellular fibrosis (PCF) develops around the central veins involving single or small groups of hepatocytes presumably as a consequence of steatohepatitis-associated hepatocellular injury (i.e., ballooning) and inflammation [34, 35]. Therefore, PCF is a parenchymal feature and in progressive disease septal structures consisting of areas with PCF (“septal pericellular fibrosis”) may form and link central and/or portal vascular structures. Septal pericellular fibrosis is different from the dense fibrous septa which extend from portal areas in viral, autoimmune, and toxic hepatitis as well as biliary liver diseases [35, 36]. Particularly in ALD, PCF can be a very prominent feature and may contribute to LS to a greater degree than portal-based septal fibrosis [10, 37, 38]. The implications of PCF on the clinical course of FLD are not known. However, the impact of PCF and septal fibrosis types on survival of patients with ALD may differ. Recently published data indicate that patients with alcohol related steatohepatitis or decompensated ALD and severe PCF may enjoy

better outcome than patients with bridging fibrosis or cirrhosis [39, 40]. The cause for these observations is unknown but extensive PCF may represent an earlier stage in the progression to a more advanced fibrosis stage characterized by abundant dense fibrous septa. The relative contribution of PCF and septal fibrosis types to LS and their prognostic potential remains to be studied.

## Other Morphological Factors

Other morphological factors associated with an increased tension within the Glisson capsule are cholestasis and congestion. Extrahepatic cholestasis may contribute to liver stiffness via increased hydrostatic and intracellular pressure, inflammation, and edema [41]. Elevated bilirubin levels are highly correlated to total serum bilirubin and decrease as an effect of biliary drainage [41, 42]. Congestion due to left- or right-sided heart failure and acute decompensated heart failure have been shown to contribute to elevated LS obscuring and overestimating the histological fibrosis stage due to increased intrahepatic pressure [43–45]. In diseases associated with hepatic congestion, LS values decrease with successful treatment [43]. Studies in patients with acute liver failure (ALF) suggest that hepatic stellate cell activation is correlated with LS [46] and that LS is increased as a combination of hepatocyte edema, bilirubin elevation, and intrahepatic collagen deposition. In these ALF patients, LS was significantly increased compared to healthy controls. A significant correlation was found after 7 days in patients with TIMP-1, MMP-2, hyaluronic acid, and M65. Interestingly the MMP-1 expression on admission was negatively correlated with LS. This could indicate an early influence of MMP-1 expression on recovery from fibrosis.

## Conclusions

Taken together, a mechanic explanation seems to be justified when trying to understand our present knowledge of LS and histology (see Fig. 22.4a, b). Volume expansion by inflammation and ballooning but also deposition of collagen or amyloid [47, 48] will all stiffen the organ. It remains unclear, however, why fat is not more positively associated since oil is incompressible like water. The findings on fat may point to a special interaction of its hydrophobic parts with water that may allow special viscoelastic properties and fluidity. As discussed in book Part II on physical aspects of stiffness, the viscoelastic properties and their effect of stiffness is still largely unexplored and should be targeted in future studies. It is also highly attractive to envision novel targeted therapies to lower stiffness in tissues.

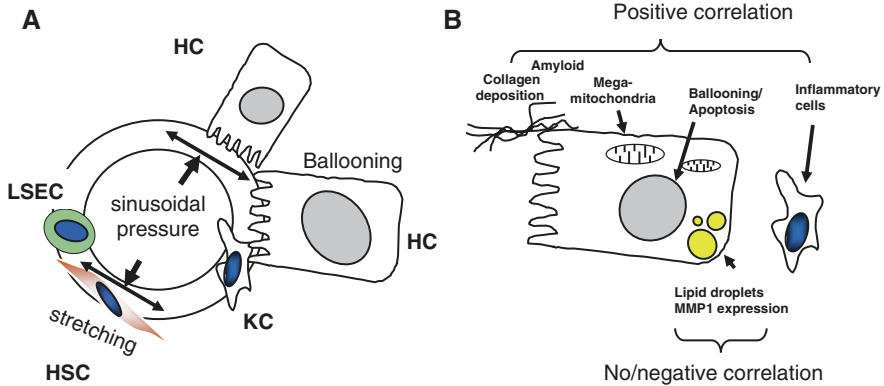


**Fig. 22.4** Liver histology and stiffness. **(A)** Both cell properties (number, size) and sinusoidal perfusion (pressure) affect LS. Thus, infiltration with inflammatory cells or enlargement of cells (Ballooning) cause LS elevation. **(B)** Typical histological features are shown that either increase or decrease LS. *HC* hepatocytes, *KC* Kupffer cells, *LSEC* liver sinus endothelial cells, *HSC* hepatic stellate cells

## References

1. Lefkowitz JH. Morphology of alcoholic liver disease. *Clin Liver Dis.* 2005;9(1):37–53.
2. Hall PD. Pathological spectrum of alcoholic liver disease. *Alcohol Alcohol Suppl.* 1994;2:303–13.
3. Abdi W, Millan JC, Mezey E. Sampling variability on percutaneous liver biopsy. *Arch Intern Med.* 1979;139(6):667–9.
4. Bedossa P, Dargere D, Paradis V. Sampling variability of liver fibrosis in chronic hepatitis C. *Hepatology.* 2003;38(6):1449–57.
5. Cadranet JF, Rufat P, Degos F. Practices of liver biopsy in France: results of a prospective nationwide survey. For the Group of Epidemiology of the French Association for the Study of the Liver (AFEF). *Hepatology.* 2000;32(3):477–81.
6. Maharaj B, Maharaj RJ, Leary WP, Cooppan RM, Naran AD, Pirie D, et al. Sampling variability and its influence on the diagnostic yield of percutaneous needle biopsy of the liver. *Lancet.* 1986;1(8480):523–5.
7. Regev A, Berho M, Jeffers LJ, Milikowski C, Molina EG, Pylsopoulos NT, et al. Sampling error and intraobserver variation in liver biopsy in patients with chronic HCV infection. *Am J Gastroenterol.* 2002;97(10):2614–8.
8. Gilmore IT, Burroughs A, Murray-Lyon IM, Williams R, Jenkins D, Hopkins A. Indications, methods, and outcomes of percutaneous liver biopsy in England and Wales: an audit by the British Society of Gastroenterology and the Royal College of Physicians of London. *Gut.* 1995;36(3):437–41.
9. McGill DB, Rakela J, Zinsmeister AR, Ott BJ. A 21-year experience with major hemorrhage after percutaneous liver biopsy. *Gastroenterology.* 1990;99(5):1396–400.
10. Mueller S, Englert S, Seitz HK, Badea RI, Erhardt A, Bozaari B, et al. Inflammation-adapted liver stiffness values for improved fibrosis staging in patients with hepatitis C virus and alcoholic liver disease. *Liver Int.* 2015;35(12):2514–21.
11. Rausch V, Peccerella T, Lackner C, Yagmur E, Seitz HK, Longerich T, et al. Primary liver injury and delayed resolution of liver stiffness after alcohol detoxification in heavy drinkers with the PNPLA3 variant I148M. *World J Hepatol.* 2016;8(35):1547–56.

12. Mueller S, Millonig G, Sarovska L, Friedrich S, Reimann FM, Pritsch M, et al. Increased liver stiffness in alcoholic liver disease: differentiating fibrosis from steatohepatitis. *World J Gastroenterol.* 2010;16(8):966–72.
13. Mueller S, Nahon P, Rausch V, Peccerella T, Silva I, Yagmur E, et al. Caspase-cleaved keratin-18 fragments increase during alcohol withdrawal and predict liver-related death in patients with alcoholic liver disease. *Hepatology.* 2017;66(1):96–107.
14. Mueller S. Non-invasive assessment of patients with alcoholic liver disease. *Clin Liver Dis.* 2013;2:68–71.
15. Mueller J, Rausch V, Silva I, Peccerella T, Piecha F, Dietrich C, et al. PS-171-Survival in a 10 year prospective cohort of heavy drinkers: liver stiffness is the best long-term prognostic parameter. *J Hepatol.* 2019;70(1):E107-E.
16. MacSween RNB. Histologic spectrum of alcoholic liver disease. *Semin Liver Dis.* 1986;6(3):221–32.
17. Edmondson HAPR, Frankel HH, Borowsky S. The early stage of liver injury in the alcoholic. *Medicine (Baltimore).* 1967;46(2):119–29.
18. EASL clinical practical guidelines: management of alcoholic liver disease. *J Hepatol.* 2012;57(2):399–420.
19. Galambos JTSR. Natural history of alcoholic hepatitis. *J Clin Invest.* 1973;52:2952–62.
20. Marbet UABL, Meury U, Stalder GA. Long-term histological evaluation of the natural history and prognostic factors of alcoholic liver disease. *J Hepatol.* 1987;4:364–72.
21. Pares ACJ, Bruguera M, Torres M, Rodes J. Histological course of alcoholic hepatitis. Influence of abstinence, sex and extent of hepatic damage. *J Hepatol.* 1986;2:33–42.
22. Sorensen TIOM, Bentsen KD, Hoybye G, Eghoje K, Christoffersen P. Prospective evaluation of alcohol abuse and alcoholic liver injury in men as predictors of development of cirrhosis. *Lancet.* 1984;2:241–4.
23. Mathurin PBF, Louvet A, Carrie-Ganne N, Balian A, Trinchet JC, Dalsoglio D, Prevot S, Naveau S. Fibrosis progression occurs in a subgroup of heavy drinkers with typical histological features. *Aliment Pharmacol Ther.* 2007;25(9):1047–54.
24. Kleiner DE, Brunt EM, Van Natta M, Behling C, Contos MJ, Cummings OW, et al. Design and validation of a histological scoring system for nonalcoholic fatty liver disease. *Hepatology.* 2005;41(6):1313–21.
25. Chevallier M, Guerret S, Chossegros P, Gerard F, Grimaud J-A. A histological semiquantitative scoring system for evaluation of hepatic fibrosis in needle liver biopsy specimens: comparison with morphometric studies. *Hepatology.* 1994;20(2):349–55.
26. Petta S, Wong VW, Camma C, Hiriart JB, Wong GL, Marra F, et al. Improved noninvasive prediction of liver fibrosis by liver stiffness measurement in patients with nonalcoholic fatty liver disease accounting for controlled attenuation parameter values. *Hepatology.* 2017;65(4):1145–55.
27. Boursier J, de Ledinghen V, Sturm N, Amrani L, Bacq Y, Sandrini J, et al. Precise evaluation of liver histology by computerized morphometry shows that steatosis influences liver stiffness measured by transient elastography in chronic hepatitis C. *J Gastroenterol.* 2014;49(3):527–37.
28. Eddowes PJ, Sasso M, Allison M, Tsochatzis E, Anstee QM, Sheridan D, et al. Accuracy of FibroScan controlled attenuation parameter and liver stiffness measurement in assessing steatosis and fibrosis in patients with nonalcoholic fatty liver disease. *Gastroenterology.* 2019;156(6):1717–30.
29. Wong VW, Vergniol J, Wong GL, Foucher J, Chan HL, Le Bail B, et al. Diagnosis of fibrosis and cirrhosis using liver stiffness measurement in nonalcoholic fatty liver disease. *Hepatology.* 2010;51(2):454–62.
30. Cassinotto C, Boursier J, de Ledinghen V, Lebigot J, Lapuyade B, Cales P, et al. Liver stiffness in nonalcoholic fatty liver disease: a comparison of supersonic shear imaging, FibroScan, and ARFI with liver biopsy. *Hepatology.* 2016;63(6):1817–27.

31. Facciorusso A, Garcia Perdomo HA, Muscatiello N, Buccino RV, Wong VW, Singh S. Systematic review with meta-analysis: change in liver stiffness during anti-viral therapy in patients with hepatitis B. *Dig Liver Dis.* 2018;50(8):787–94.
32. Singh S, Facciorusso A, Loomba R, Falck-Ytter YT. Magnitude and kinetics of decrease in liver stiffness after antiviral therapy in patients with chronic hepatitis C: a systematic review and meta-analysis. *Clin Gastroenterol Hepatol.* 2018;16(1):27–38. e4
33. Seitz HK, Bataller R, Cortez-Pinto H, Gao B, Gual A, Lackner C, et al. Alcoholic liver disease. *Nat Rev Dis Primers.* 2018;4(1):16.
34. Rangwala F, Guy CD, Lu J, Suzuki A, Burchette JL, Abdelmalek MF, et al. Increased production of sonic hedgehog by ballooned hepatocytes. *J Pathol.* 2011;224(3):401–10.
35. Lackner C, Tiniakos D. Fibrosis and alcohol-related liver disease. *J Hepatol.* 2019;70(2):294–304.
36. Lackner C, Bataller R, Burt A, Miquel R, Schuppan D, Tiniakos D, et al. Fibrosis evaluation by transient elastography in alcoholic liver disease: is the histological scoring system impacting cutoff values? *Hepatology.* 2017;65(5):1758–61.
37. Wong GL, Wong VW, Choi PC, Chan AW, Chum RH, Chan HK, et al. Assessment of fibrosis by transient elastography compared with liver biopsy and morphometry in chronic liver diseases. *Clin Gastroenterol Hepatol.* 2008;6(9):1027–35.
38. Elshaarawy O, Mueller J, Guha IN, Chalmers J, Harris R, Krag A, et al. Spleen stiffness to liver stiffness ratio significantly differs between ALD and HCV and predicts disease-specific complications. *JHEP Rep.* 2019;1(2):99–106.
39. Lackner C, Spindelboeck W, Haybaeck J, Douschan P, Rainer F, Terracciano L, et al. Histological parameters and alcohol abstinence determine long-term prognosis in patients with alcoholic liver disease. *J Hepatol.* 2017;66(3):610–8.
40. Altamirano J, Miquel R, Katoonizadeh A, Abraldes JG, Duarte-Rojo A, Louvet A, et al. A histologic scoring system for prognosis of patients with alcoholic hepatitis. *Gastroenterology.* 2014;146(5):1231–9.e1-6.
41. Millonig G, Reimann FM, Friedrich S, Fonouni H, Mehrabi A, Büchler MW, et al. Extrahepatic cholestasis increases liver stiffness (FibroScan) irrespective of fibrosis. *Hepatology.* 2008;48(5):1718–23.
42. Trifan A, Sfarti C, Cojocariu C, Dimache M, Cretu M, Hutanasu C, et al. Increased liver stiffness in extrahepatic cholestasis caused by choledocholithiasis. *Hepat Mon.* 2011;11(5):372–5.
43. Millonig G, Friedrich S, Adolf S, Fonouni H, Golriz M, Mehrabi A, et al. Liver stiffness is directly influenced by central venous pressure. *J Hepatol.* 2010;52(2):206–10.
44. Colli A, Pozzoni P, Berzuini A, Gerosa A, Canovi C, Molteni EE, et al. Decompensated chronic heart failure: increased liver stiffness measured by means of transient elastography. *Radiology.* 2010;257(3):872–8.
45. Hopper I, Kemp W, Porapakham P, Sata Y, Condon E, Skiba M, et al. Impact of heart failure and changes to volume status on liver stiffness: non-invasive assessment using transient elastography. *Eur J Heart Fail.* 2012;14(6):621–7.
46. Dechêne A, Sowa J-P, Gieseler RK, Jochum C, Bechmann LP, El Fouly A, et al. Acute liver failure is associated with elevated liver stiffness and hepatic stellate cell activation. *Hepatology.* 2010;52(3):1008–16.
47. Bastard C, Bosisio MR, Chabert M, Kalopissis AD, Mahrouf-Yorgov M, Gilgenkrantz H, et al. Transient micro-elastography: a novel non-invasive approach to measure liver stiffness in mice. *World J Gastroenterol.* 2011;17(8):968–75.
48. Lanzi A, Gianstefani A, Mirarchi MG, Pini P, Conti F, Bolondi L. Liver AL amyloidosis as a possible cause of high liver stiffness values. *Eur J Gastroenterol Hepatol.* 2010;22(7):895–7.

# Chapter 23

## Liver Stiffness Elevation in Patients with Heart Failure and Liver Congestion



Gunda Millonig

### Introduction

Heart failure (HF) manifests in many forms, ranging from overt left ventricular (LV) systolic dysfunction (low output failure) to isolated right ventricular (RV) diastolic dysfunction. Clinical correlation comprises a wide range of symptoms from edema of the lower extremities due to chronic fluid retention to acute multiorgan failure and death. The RV functions as low-pressure, high-volume pump compared to the LV which may be defined as a high-pressure, high-volume pump [1]. Its importance on circulation has long been overlooked because most research as well as clinical studies focused on LV failure. The RV was considered a dispensable chamber, rather a “passive partner” to the actively pumping LV, and with no relevance to the patient’s prognosis.

As diagnostic technologies advanced, an improved understanding developed regarding RV function in heart diseases. Determining RV systolic and diastolic function is important in the management of many cardiac conditions, including acute decompensated heart failure, chronic heart failure especially in the setting of ventricular dys-synchrony, pulmonary hypertension, heart transplantation, and congenital heart disease [2].

### Function of the RV and Ventricular Interdependence

While the anatomy of the RV is different from that of the LV, they act as mechanically interdependent units [1]. The shape of the RV is of a more complex geometry being best described as crescent-shaped while the LV may be described concentric.

---

G. Millonig (✉)

Ordination für Gastroenterologie und Innere Medizin, Innsbruck, Austria



During intrauterine development, the RV acts as the systemic ventricle. At birth with the transition from fetal to postnatal circulation, the RV adapts to a low resistance circulation becoming a thin-walled ventricle that is able to perform the same cardiac output as the LV at 20% of energy expenditure [3]. The entire heart is wrapped into the pericardium, a capsule of little elasticity, increasing the inextricably intertwined action of the two ventricles to a closed functional unit. Therefore, in this relatively “closed” system, acute cardiac alterations in volume or pressure in either ventricle can affect the other ventricle. It was proven in animal experiments early on that hypertrophy or dilatation of the LV leads to compression of the RV and thus to a secondary RV dysfunction [4, 5]. The most striking examples of acute ventricular interaction occur in the setting of acute pulmonary embolus, implantation of an LVAD (left ventricular assist device), acute RV failure after cardiac transplantation, or RV myocardial infarction. In each case, the cause of low cardiac output is RV distension in the stiff pericardium, resulting in decreased LV preload [1].

## RV Function and Prognosis

Numerous studies have underlined the importance of RV function. It has been shown that RV dysfunction is an important predictor of overall survival and morbidity in various clinical settings [2, 6, 7]. Despite low clinical consideration, the incidence of RV failure is similar to LV failure [8–10]. A reduced RV ejection fraction can predict prognosis: In patients with advanced systolic heart failure, a right ventricular ejection fraction (RVEF) less than 20% independently of LVEF predicts an increased risk of hospitalization and death [11]. Perioperative mortality is higher in RV failure than in left ventricular failure [8–10]. RV failure is an underdiagnosed entity in the noncardiac surgery perioperative setting [8–10] due to the lack of awareness and the difficulties in diagnosis.

## Diagnostic Approaches to RV Function

Echocardiography is the diagnostic approach of choice in patients with suspected HF since it is readily available, relatively cheap, noninvasive, and works with no radiation. The recognition of the importance of the RV on prognosis of patients with HF has increased the need of specialized RV evaluation regarding size and function. Two-dimensional echocardiography was the first step toward improved RV imaging and allowed standardized follow-up of RV size and function over time [12].

Standardized RV parameters in routine echocardiography focus on RV size and wall thickness as static parameters. RV function is represented by the TAPSE, measuring the distance of tricuspid annular movement between end-diastole to end-systole. In addition, the velocity of this movement can be measured with tissue

**Table 23.1** Echocardiography parameters in RV evaluation (adapted from Rudski [13] and Pleister [14])

Method of RV function	Abnormal	Limitations
RVEF on 2D	<44%	Unreliable
Fractional area change (FAC)	<35%	Endocardial border needs to be accurately traced
TAPSE	<1.6 cm	Load and angle dependent
RIMP	Pulsed >0.40 Tissue >0.55	Not reliable in elevated right atrium pressures of irregular heart rates (atrial fibrillation)
Isovolumetric Acceleration (IVA)	Not defined	Load and angle dependent, varies with age and heart rate
$S'$ (pulsed)	<10 cm/s	Angle dependent, limited data in elderly
RVEF on 3D	<44%	Not readily available

*RFEF* RV ejection fraction, *TAPSE* tricuspid annular plane systolic excursion, *RIMP* right ventricular index of myocardial performance,  $S'$  myocardial systolic velocity

Doppler imaging resulting in the  $S'$ -value. While RVEF in 2D-echocardiography is unreliable, measurements in 3D-echocardiography are more reliable but not readily available in routine echocardiography. Detailed RV measurements and its pros and cons are given in Table 23.1. Echocardiographic evaluation of the RV has several impediments: the retrosternal position of the RV preventing good accessibility in some patients, the complex shape of the RV that cannot be fitted into a mathematical model to calculate RV volume and function and the strong trabecularization that makes it difficult to trace the endocardial border [15].

Other imaging approaches comprise the radionuclide ventriculography using  $^{99m}\text{Tc}$  with calculation of the RVEF. While CT scans play an important role in diagnostic of pulmonary embolism, evaluation of the RV function is limited because of the high amount of radiocontrast agent and radiation dose. Cardiac magnetic imaging (MRI) is an important tool in RV evaluation and currently considered the gold standard in RV assessment since it can assess RV function as well as changes in the wall e.g., fatty deposits, myocarditis, or fibrosis [16]. Its drawbacks are the relatively high costs, reduced availability, and the fact that patients with medical devices (e.g., cardiac pacemaker) are unable to undergo MRI.

Cardiac catheterization is the invasive test of choice. Besides evaluation of RV function, it also allows to determine hemodynamic parameters or to perform pulmonary angiography at the same time and, thus, is considered the gold standard. Given the availability of other imaging techniques and the risk of an invasive procedure with significant iodinated contrast load, RV angiography is rarely used in routine evaluation of the RV size and function.

Early diagnosis of RV failure is paramount in improving patient outcomes. However, most imaging findings of RV failure, particularly those associated with poor outcomes, identify only end-stage disease. For example, in patients with pulmonary hypertension, the echocardiographic finding of TAPSE of <1.8 cm predicts

a 1-year survival of just 60% [17]. Similarly, RV end-diastolic volume index  $\geq 84$  mL/m<sup>2</sup> on MRI predicts a 3-year survival of approximately 60% in patients with pulmonary arterial hypertension [18].

## Pathophysiology of the Liver Lobule During Congestion and Liver Enzyme Patterns

The liver lobule is the physiological liver unit. It consists of a central vein and the portal tracts containing the liver triad (portal vein, bile canaliculus, and hepatic artery) (Fig. 23.1a). The functional unit of the liver is the liver acinus which is subdivided into three zones depending on their distance from the portal triad and thus differing in oxygen supply. Zone 3 is the furthest zone located around the central vein with the lowest oxygen supply and thus the most sensitive to hypoxia [19]. Increased pressure in the RV translates to increased pressure in the hepatic veins and the central veins leading to dilatation of the sinusoids in zone 3 and compression of the hepatocytes in combination with hypoxia. This mechanism is responsible for liver swelling followed by atrophy, centrilobular necrosis in case of acute HF and fibrotic changes in case of chronic HF [20].

Functional changes in the local circulation are present in acute decompensated or advanced HF. Hepatic microvasculature contains adrenergic receptors: Sympathetic activation causes portal vasoconstriction, splanchnic congestion, and

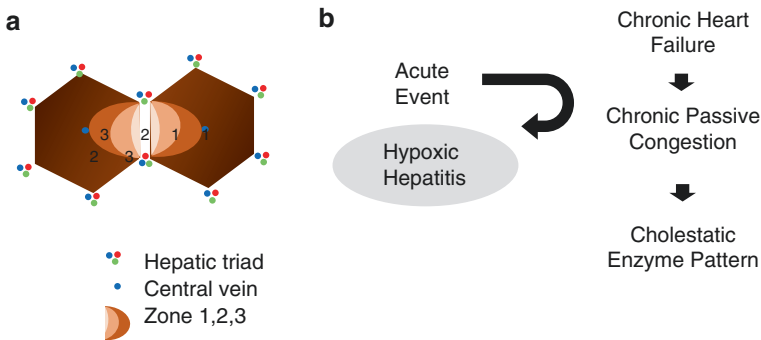


**Fig. 23.1** (a) Schematic representation of the liver lobule with the central vein surrounded by the portal triads. Functionally, the lobule can be divided into three zones, based upon oxygen supply. Zone 1 encircles the portal tracts where the oxygenated blood from hepatic arteries enters. Zone 3 is located around central veins, where oxygenation is poor. Zone 2 is located in between. Zone 3 is the zone at risk for damage in congestive heart disease. (b) Chronic passive congestions leads to elevation of the cholestatic liver enzymes (GGT, AP, and bilirubin). Hypoxic hepatitis is precipitated by acute forward failure with low cardiac output and hypoperfusion

further deteriorating liver ischemia leading finally to centrilobular necrosis, the pathological correlate of liver disease in acute HF. If HF worsens, the necrosis spreads further into zone 2.

Chronic severe hepatic congestion leads to bridging fibrosis called cardiac cirrhosis. The gross pathological appearance of a chronically congested liver reminds of a grated nutmeg thus called “nutmeg liver.” The elevated systemic pressures are transmitted directly to the hepatic veins and venules and proportionally backward to the portal vein, resulting in normal hepatic venous pressure gradient (HVPG) [21]. This implies that in contrast to primary liver diseases (e.g., chronic hepatitis or alcoholic liver damage), there is no portal hypertension (splenomegaly, oesophageal varices) until the very final stage of congestive liver disease with irreversible cardiac cirrhosis [22].

Interestingly enough, chronic congestion with a change in microcirculation of the liver sinusoids has also been suggested in several patho-mechanisms characteristic for advanced HF e.g., a decreased clearance of endotoxin thus tipping the balance to a more proinflammatory change but also a change in e.g., in iron metabolism leading to HF-associated anemia and cardiac cachexia [23].

Liver damage in HF has been described in the 1930s for the first time. Jolliffe reported that 80% of patients with congestive HF had elevated levels of bilirubin, and more than 90% had an impaired hepatic function [20]. Recent publications with a modern diagnostic approach to HF show that among patients with chronic HF, bilirubin was increased in 13% and transaminases were increased in 3.1% of the patients. Hypoalbuminemia was detected in 18.3% of the patients [24]. Other authors published similar results showing that a cholestatic profile (i.e., at least two cholestatic enzymes elevated) was found in 19.2% of patients whereas transaminases were elevated in 8.3%. A mixed profile of elevated liver enzyme counts was observed in 3.5% of patients [25]. In contrast to the typical mild cholestatic pattern in congestive liver disease, additional acute forward failure with low cardiac output leading to hypoperfusion leads to hypoxic hepatitis with a predominant transaminase elevation in the magnitude of 1000–5000 IU/mL (Fig. 23.1b, Table 23.2).

**Table 23.2** Changes in blood tests depending on type of heart failure

Laboratory parameter	Congestion (increased CVP)	Hypoperfusion (low cardiac output)
AST	0/↑	↑↑↑
ALT	0/↑	↑↑
Total bilirubin	↑	↑/↑↑
Direct bilirubin	↑/↑↑	↑
GGT	↑↑	0/↑
AP	↑/↑↑	0/↑
LDH	↑	↑↑

## Liver Stiffness in Patients with Liver Congestion and Cardiac Recompensation

When transient elastography (TE) was introduced in hepatological diagnostics it was first noted by Lebray and colleagues that LS was not a reliable parameter for fibrosis quantification in patients with congestive heart disease [26]. Since then, LS developed from being a confounder in fibrosis assessment to being used as additional parameter in patients with congestive HF.

The first study to systematically address interaction of LS and HF was our own where we showed in animal data that there is an almost linear correlation between central venous pressure (CVP) in the inferior caval vein and LS (Fig. 23.2a) [27]. LS elevation was drastic reaching the detection limit of the Fibroscan device of 75 kPa at a central venous pressure of 36 cm water column. In addition, LS elevation was reversible and rapidly normalized within 30 min (Fig. 23.2b).

The study by Deorsola et al. in patients undergoing Fontan surgery is a recapitulation of the animal data. Fontan surgery is performed in children with univentricular hearts. Surgical palliation comprises a diversion of arriving blood from the inferior caval vein directly to the pulmonary arteries without passing through a right atrium and ventricle. The single ventricle is saved for systemic circulation doing the pumping work for both ventricles. It is known that after live saving surgery these children develop liver congestion and finally cardiac cirrhosis at an early age. Before Fontan procedure mean LS was 6.2 kPa in these patients. Already at 4 month post-surgery, LS was increased to a mean value of 11.2 kPa [28]. The authors attributed that increase to a change in pressure only since a slow process such as

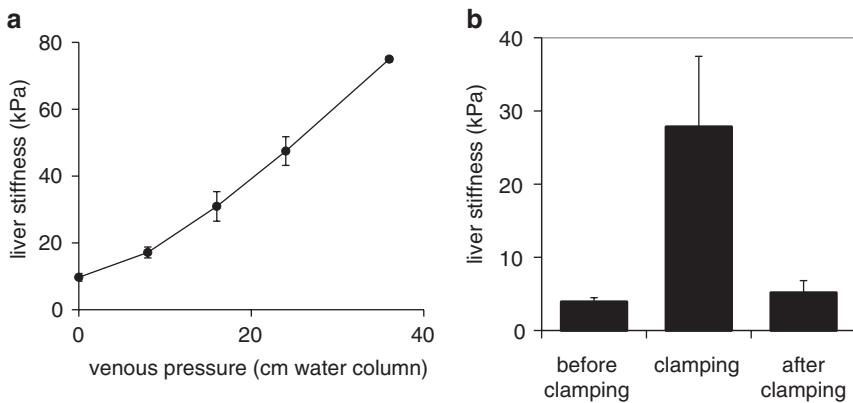


**Fig. 23.2** (a) Liver stiffness almost linearly increases with increased central venous pressure in pig liver. The liver was isolated *in situ* by clamping inferior caval vein, portal vein, and hepatic artery and the pressure increased stepwise by infusing isotonic saline. (b) Acute liver congestion leads to a significant increase in liver stiffness that is reversible. Hepatic congestion was mimicked in narcotized pigs by clamping the inferior caval vein and reopening the drainage to the right atrium after 5 min

noninflammation-driven fibrogenesis is unlikely to take place within 4 months (especially since transaminase were slightly but not dramatically altered after the procedure).

Patients with acute HF have significantly elevated LS values at the time of decompensation [27]. Following up these patients when recompensated with weight loss and disappearance of edema showed a decreased LS in all patients. This showed the effect of cardiac recompensation on liver congestion. However, in our study all patients but one still had significantly elevated LS values at the time of recompensation, leaving the question unanswered whether this was due to persisting elevated RV filling pressure or already established cardiac cirrhosis [27]. These data were independently reproduced by other groups and independent elastography techniques (vibration controlled elastography, shear wave elastography) [29, 30].

## Correlation of LS with Parameters of RV Function

A thorough cardiological approach to LS measurements and its correlation to echocardiographic parameters was presented by Saito and colleagues [31]. They showed in their study with 105 patients that as expected high LS values correlated significantly with several RV function parameters, among them low level of TAPSE, increased caval vein diameter, larger RV diastolic diameter, and higher estimated right atrial pressure as well as higher prevalence of tricuspid regurgitation [31, 32]. The same results were shown by Hopper et al. who showed that stable LV failure has a much lower impact on LS compared to stable RV failure [32].

Taniguchi et al. have been able to correlate LS with estimated RV filling pressure and showed that a LS of 5.6 kPa was equivalent to an estimated RV filling pressure of 5.7 mmHg [33]. These numbers fit nicely to the previously published numbers of change in LS depending on central venous pressure in porcine livers [27]. These data were corroborated by simultaneous determination of invasive CVP-measurements by right heart catheterization and shear wave elastography in children with congenital heart diseases [34, 35]. In one of the two studies, pre- and post-volume-loading during catheterization was additionally performed. The results showed identical slopes to studies with animal data and those with echocardiographically estimated pressures stating that the optimal cutoff to detect CVP > 10 mmHg was an LS of 10.8 kPa [34]. Inferior vena cava diameter, pulsed-Doppler profile of hepatic veins, and N-terminal pro-B-type natriuretic peptide were less robust than LS to estimate CVP [34]. Taniguchi et al. found to the identical cutoff value for RAP (right atrial pressure) (10.6 kPa for CVP > 10mmHg) [36], emphasizing the reproducibility of these results. They showed in addition that LS correlates even stronger with RAP than echocardiography [36], pointing out the fact that although echocardiography is the technique of choice to assess RV due to availability, it is not the gold standard for the determination of RV function and is associated with inaccuracies is to be kept in mind (Table 23.3).

**Table 23.3** Overview of cardiac parameters correlating with LS

Parameters correlated with LS	Parameters didn't correlate with LS
Central venous pressure (CVP)	LVEF
Caval vein diameter	NT-proBNP
RV diastolic diameter	
Right atrial pressure	
RV filling pressure (estimated)	
Tricuspid regurgitation	
TAPSE (negative correlation)	
Mortality (cardiac events, all-cause mortality)	
Readmission for HF-worsening	

## Liver Stiffness and Outcome

Since it has been recognized that RV failure has a relevant impact on clinical outcome, the question was if LS could predict prognosis in RV failure. Saito showed that in two cohorts of HF patients LS values at the time of admission had a prognostic relevance in regard to cardiac death (24% in the high LS-group versus 11% in the low LS-group) as well as in regard to readmission rates for HF (37% in the high LS-group versus 21% in the low LS-group). The significant association of high  $LS \geq 8.8$  kPa with the incidence of death from cardiovascular disease and readmission for HF persisted in models adjusted for age, sex, and indices related to organ congestion (NT-proBNP, urea, glomerular filtration rate, total bilirubin, GGT, and estimated right atrial pressure) [31].

Another publication by Omote and colleagues showed the same results: During a median follow-up period of 272 days, adverse events (death or worsening of HF) occurred in 37% of patients. Based on ROC analysis, the optimal cutoff value of LS for the development of adverse events was 1.50 m/s (equivalent to 7.1 kPa). At this cutoff value, the sensitivity and specificity for predicting cardiac events were 81% and 70%, respectively. Kaplan–Meier analysis revealed that composite adverse occurred events more frequently in patients with high LS ( $\geq 1.50$  m/s, i.e., 7.1 kPa) compared to those with low LS ( $< 1.50$  m/s i.e., 7.1 kPa). Multivariable Cox regression analyses showed that higher LS was associated independently of all other parameters with increased subsequent risk of adverse events [37].

A significant correlation between LS and overall mortality has not only been described in critically ill patients with HF but also in unselected patients in the ICU (intensive care unit) with various conditions [38]. In their study, Koch and colleagues showed that LS at the time of admission predicted mortality. In contrast to the selected HF patient cohorts, the cutoff value to discriminate survivors from non-survivors in the ICU study was much higher (18 kPa compared to around 7 kPa in the studies with only HF patients). This remained valid even after exclusion of cirrhotic patients. Neither subsequent LS measurements at days 3 and 7 during ICU

treatment nor individual changes of LS within the first week of ICU treatment were indicative of prognosis. The reason for the discrepancy of the cutoff values in this study remains unanswered, but most likely attributable to a mix of volume overload and positive-pressure ventilation leading to an increased CVP [38].

A Danish study performed in the emergency room also showed a prognostic value of LS. Among 212 patients admitted to the hospital the authors found an increased LS value ( $>8$  kPa) in 22.6%. The 30-day mortality among patients with LS values  $>8$  kPa was 20.8% compared to patients with LS values  $<8$  kPa 3.7%, and LS values  $>8$  kPa were an independent predictor of death [39].

## Liver Stiffness and Cardiac Surgery

An interesting study of Chon and colleagues demonstrated that patients undergoing successful valvular repair surgery had a decrease in LS in the long-term follow-up examination postoperatively (8.4 kPa shortly after surgery to 6.0 kPa 3 month later) while two patients that died despite heart transplantation remained at elevated levels [40].

Another cardiosurgical pilot study explored the usefulness of LS in the perioperative assessment during VAD implantation (ventricular assist device). Nishi et al. have studied LS in HF patients and concluded that no patient with LS  $<7$  kPa needed a RVAD, thus demonstrating that a LS  $<7$  kPa precludes RV failure. In contrast, those patients with high LS (around 35 kPa) required a biventricular VAD due to concurrent RV failure. Perioperative morbidity and mortality was also closely related to an increased LS  $> 12.5$  kPa [41].

Kashiyama and colleagues have also studied LS after implantation of LVAD. In this procedure one of the dreaded complications is secondary RV failure which occurs in 5–44% of patients [42]. Predicting RV failure is difficult before and after LVAD implantation, but right-sided filling pressure measurements such as the CVP/pulmonary capillary wedge pressure ratio are important predictive factors of RVF after LVAD implantation [43]. In their pilot study the authors showed that LS was significantly elevated in patients with RV failure after LVAD compared to those without RV failure [44]. In this cohort, patients who had RV failure or needed RVAD support following LVAD implantation were characterized by significantly higher LS. Because LS is immediately influenced by changes in CVP, serial assessments of LS would contribute to perioperative optimization of right-sided filling pressure without a pulmonary catheter study. Interestingly, the cases with higher LS than expected from preoperative CVP tended to undergo RVF or RVAD implantation after LVAD implantation, which implies that LS may indicate not only CVP but also other factors such as chronicity of RV failure or RV compliance. In patients with greater LS, there may be a more negative effect by an increase in preload rather than a positive effect by a decrease in afterload on the RV by LVAD support, suggesting that RV with impaired compliance may increase RV filling pressure easily by elevating preload by LVAD flow [44].



## Conclusion

Liver stiffness has made an evolution from being identified as an annoying interference in liver fibrosis assessment to a recognized parameter in evaluating RV function. LS elevation is of course nonspecific and other confounders such as primary liver diseases [45], cholestasis [46], and acute hepatitis [47]) have to be excluded before attributing LS to liver congestion. Once this is done, however, LS assessment opens a new window to functional assessment of the RV function without the need for invasive hemodynamic monitoring. This in turn might allow a close follow-up in RV hemodynamics during pharmacological intervention as well as surgical interventions but also a risk assessment in patients prior to cardio-surgery. It is interesting to note that the cutoff values in HF resemble very much those in liver fibrosis assessment:

- LS < 7 kPa: normal RV filling pressure and exclusion of RV failure
- LS 7–8 kPa: “grey zone”
- LS 8–12.5 kPa: increased risk for morbidity and mortality due to HF or cardiac death; in case of LVAD-implantation increased risk for RV failure
- LS > 35 kPa: BiVAD needed due to RV failure

So far, all published studies were pilot studies with only a small number of patients included. Close collaboration between hepatologists, cardiologists, and cardio-surgeons as well as larger numbers of patients and prospective study designs are needed to proceed from appreciating LS as a relevant parameter in RV investigation in a close circle of elastography adepts to LS as an integral part of RV evaluation.

## References

1. Dell'Italia LJ. Anatomy and physiology of the right ventricle. *Cardiol Clin.* 2012;30(2):167–87.
2. Haddad F, Doyle R, Murphy DJ, Hunt SA. Right ventricular function in cardiovascular disease, part II: pathophysiology, clinical importance, and management of right ventricular failure. *Circulation.* 2008;117(13):1717–31.
3. Mertens LL, Friedberg MK. Imaging the right ventricle--current state of the art. *Nat Rev Cardiol.* 2010;7(10):551–63.
4. Henderson YPA. The relative systolic discharges of the right and left ventricles and their bearing on pulmonary congestion and depletion. *Heart.* 1914;5:217–26.
5. Maruyama Y, Ashikawa K, Isoyama S, Kanatsuka H, Ino-Oka E, Takishima T. Mechanical interactions between four heart chambers with and without the pericardium in canine hearts. *Circ Res.* 1982;50(1):86–100.
6. Gavazzi A, Berzuini C, Campana C, Inserra C, Ponzetta M, Sebastiani R, et al. Value of right ventricular ejection fraction in predicting short-term prognosis of patients with severe chronic heart failure. *J Heart Lung Transplant.* 1997;16(7):774–85.
7. Monchi M, Bellenfant F, Cariou A, Joly LM, Thebert D, Laurent I, et al. Early predictive factors of survival in the acute respiratory distress syndrome. A multivariate analysis. *Am J Respir Crit Care Med.* 1998;158(4):1076–81.

8. Reichert CL, Visser CA, van den Brink RB, Koolen JJ, van Wezel HB, Moulijn AC, et al. Prognostic value of biventricular function in hypotensive patients after cardiac surgery as assessed by transesophageal echocardiography. *J Cardiothorac Vasc Anesth*. 1992;6(4):429–32.
9. Maslow AD, Regan MM, Panzica P, Heindel S, Mashikian J, Comunale ME. Precardiopulmonary bypass right ventricular function is associated with poor outcome after coronary artery bypass grafting in patients with severe left ventricular systolic dysfunction. *Anesth Analg*. 2002;95(6):1507–18, table of contents.
10. Szabo G, Soos P, Bahrle S, Radovits T, Weigang E, Kekesi V, et al. Adaptation of the right ventricle to an increased afterload in the chronically volume overloaded heart. *Ann Thorac Surg*. 2006;82(3):989–95.
11. Meyer P, Filippatos GS, Ahmed MI, Iskandrian AE, Bittner V, Perry GJ, et al. Effects of right ventricular ejection fraction on outcomes in chronic systolic heart failure. *Circulation*. 2010;121(2):252–8.
12. Ling LF, Marwick TH. Echocardiographic assessment of right ventricular function: how to account for tricuspid regurgitation and pulmonary hypertension. *JACC Cardiovasc Imaging*. 2012;5(7):747–53.
13. Rudski LG, Lai WW, Afilalo J, Hua L, Handschumacher MD, Chandrasekaran K, et al. Guidelines for the echocardiographic assessment of the right heart in adults: a report from the American Society of Echocardiography endorsed by the European Association of Echocardiography, a registered branch of the European Society of Cardiology, and the Canadian Society of Echocardiography. *J Am Soc Echocardiogr*. 2010;23(7):685–713; quiz 786–8.
14. Pleister A, Kahwash R, Haas G, Ghio S, Cittadini A, Baliga RR. Echocardiography and heart failure: a glimpse of the right heart. *Echocardiography*. 2015;32(Suppl 1):S95–107.
15. Sanz J, Conroy J, Narula J. Imaging of the right ventricle. *Cardiol Clin*. 2012;30(2):189–203.
16. Champion HC, Michelakis ED, Hassoun PM. Comprehensive invasive and noninvasive approach to the right ventricle-pulmonary circulation unit: state of the art and clinical and research implications. *Circulation*. 2009;120(11):992–1007.
17. Eidem BW, O’Leary PW, Tei C, Seward JB. Usefulness of the myocardial performance index for assessing right ventricular function in congenital heart disease. *Am J Cardiol*. 2000;86(6):654–8.
18. Damy T, Kallvikbacka-Bennett A, Goode K, Khaleva O, Lewinter C, Hobkirk J, et al. Prevalence of, associations with, and prognostic value of tricuspid annular plane systolic excursion (TAPSE) among out-patients referred for the evaluation of heart failure. *J Card Fail*. 2012;18(3):216–25.
19. Kietzmann T. Liver zonation in health and disease: hypoxia and hypoxia-inducible transcription factors as concert masters. *Int J Mol Sci*. 2019;20(9):2347.
20. Jolliffe N. Liver function in congestive heart failure. *J Clin Invest*. 1930;8(3):419–33.
21. Sherlock S. The liver in heart failure; relation of anatomical, functional, and circulatory changes. *Br Heart J*. 1951;13(3):273–93.
22. Moller S, Bernardi M. Interactions of the heart and the liver. *Eur Heart J*. 2013;34(36):2804–11.
23. Valentova M, von Haehling S, Doehner W, Murin J, Anker SD, Sandek A. Liver dysfunction and its nutritional implications in heart failure. *Nutrition*. 2013;29(2):370–8.
24. Allen LA, Felker GM, Pocock S, McMurray JJ, Pfeffer MA, Swedberg K, et al. Liver function abnormalities and outcome in patients with chronic heart failure: data from the Candesartan in Heart Failure: Assessment of Reduction in Mortality and Morbidity (CHARM) program. *Eur J Heart Fail*. 2009;11(2):170–7.
25. Poelzl G, Ess M, Mussner-Seeber C, Pachinger O, Frick M, Ulmer H. Liver dysfunction in chronic heart failure: prevalence, characteristics and prognostic significance. *Eur J Clin Invest*. 2012;42(2):153–63.
26. Lebray P, Varnous S, Charlotte F, Varaut A, Poynard T, Ratziu V. Liver stiffness is an unreliable marker of liver fibrosis in patients with cardiac insufficiency. *Hepatology*. 2008;48(6):2089.

27. Millonig G, Friedrich S, Adolf S, Fonouni H, Golriz M, Mehrabi A, et al. Liver stiffness is directly influenced by central venous pressure. *J Hepatol.* 2010;52(2):206–10.
28. Deorsola L, Aidala E, Cascarano MT, Valori A, Agnoletti G, Pace Napoleone C. Liver stiffness modifications shortly after total cavopulmonary connection. *Interact Cardiovasc Thorac Surg.* 2016;23(4):513–8.
29. Yoshitani T, Asakawa N, Sakakibara M, Noguchi K, Tokuda Y, Kamiya K, et al. Value of virtual touch quantification elastography for assessing liver congestion in patients with heart failure. *Circ J.* 2016;80(5):1187–95.
30. Soloveva A, Kobalava Z, Fudim M, Ambrosy AP, Villevalde S, Bayarsaikhan M, et al. Relationship of liver stiffness with congestion in patients presenting with acute decompensated heart failure. *J Card Fail.* 2019;25(3):176–87.
31. Saito Y, Kato M, Nagashima K, Monno K, Aizawa Y, Okumura Y, et al. Prognostic relevance of liver stiffness assessed by transient elastography in patients with acute decompensated heart failure. *Circ J.* 2018;82(7):1822–9.
32. Hopper I, Kemp W, Porapakkham P, Sata Y, Condon E, Skiba M, et al. Impact of heart failure and changes to volume status on liver stiffness: non-invasive assessment using transient elastography. *Eur J Heart Fail.* 2012;14(6):621–7.
33. Taniguchi T, Ohtani T, Kioka H, Tsukamoto Y, Onishi T, Nakamoto K, et al. Liver stiffness reflecting right-sided filling pressure can predict adverse outcomes in patients with heart failure. *JACC Cardiovasc Imaging.* 2019;12(6):955–64.
34. Villemain O, Sitefane F, Pernot M, Malekzadeh-Milani S, Tanter M, Bonnet D, et al. Toward noninvasive assessment of CVP variations using real-time and quantitative liver stiffness estimation. *JACC Cardiovasc Imaging.* 2017;10(10 Pt B):1285–6.
35. Terashi E, Kodama Y, Kuraoka A, Ishikawa Y, Nakamura M, Sagawa K, et al. Usefulness of liver stiffness on ultrasound shear-wave elastography for the evaluation of central venous pressure in children with heart diseases. *Circ J.* 2019;83(6):1338–41.
36. Taniguchi T, Sakata Y, Ohtani T, Mizote I, Takeda Y, Asano Y, et al. Usefulness of transient elastography for noninvasive and reliable estimation of right-sided filling pressure in heart failure. *Am J Cardiol.* 2014;113(3):552–8.
37. Omote K, Nagai T, Asakawa N, Kamiya K, Tokuda Y, Aikawa T, et al. Impact of admission liver stiffness on long-term clinical outcomes in patients with acute decompensated heart failure. *Heart Vessels.* 2019;34(6):984–91.
38. Koch A, Horn A, Dückers H, Yagmur E, Sanson E, Bruensing J, et al. Increased liver stiffness denotes hepatic dysfunction and mortality risk in critically ill non-cirrhotic patients at a medical ICU. *Crit Care.* 2011;15(6):R266.
39. Lindvig K, Mossner BK, Pedersen C, Lillevang ST, Christensen PB. Liver stiffness and 30-day mortality in a cohort of patients admitted to hospital. *Eur J Clin Invest.* 2012;42(2):146–52.
40. Chon YE, Kim SU, Park JY, Kim DY, Ahn SH, Han KH, et al. Dynamics of the liver stiffness value using transient elastography during the perioperative period in patients with valvular heart disease. *PLoS One.* 2014;9(3):e92795.
41. Nishi H, Toda K, Miyagawa S, Yoshikawa Y, Fukushima S, Kawamura M, et al. Novel method of evaluating liver stiffness using transient elastography to evaluate perioperative status in severe heart failure. *Circ J.* 2015;79(2):391–7.
42. Lampert BC, Teuteberg JJ. Right ventricular failure after left ventricular assist devices. *J Heart Lung Transplant.* 2015;34(9):1123–30.
43. Kormos RL, Teuteberg JJ, Pagani FD, Russell SD, John R, Miller LW, et al. Right ventricular failure in patients with the HeartMate II continuous-flow left ventricular assist device: incidence, risk factors, and effect on outcomes. *J Thorac Cardiovasc Surg.* 2010;139(5):1316–24.
44. Kashiwama N, Toda K, Nakamura T, Miyagawa S, Nishi H, Yoshikawa Y, et al. Evaluation of right ventricular function using liver stiffness in patients with left ventricular assist device. *Eur J Cardiothorac Surg.* 2017;51(4):715–21.

45. Sandrin L, Fourquet B, Hasquenoph J-M, Yon S, Fournier C, Mal F, et al. Transient elastography: a new non-invasive method for assessment of hepatic fibrosis. *Ultrasound Med Biol.* 2003;29(12):1705–13.
46. Millonig G, Reimann FM, Friedrich S, Fonouni H, Mehrabi A, Büchler MW, et al. Extrahepatic cholestasis increases liver stiffness (FibroScan) irrespective of fibrosis. *Hepatology.* 2008;48(5):1718–23.
47. Arena U, Vizzutti F, Abraldes JG, Corti G, Stasi C, Moscarella S, et al. Reliability of transient elastography for the diagnosis of advanced fibrosis in chronic hepatitis C. *Gut.* 2008;57(9):1288–93.

# Chapter 24

## Modulation of Liver Stiffness by Arterial and Portal Pressure



Felix Piecha and Sebastian Mueller

### Introduction

The liver is—apart from the hypophysis—the only organ with both an arterial and a venous blood supply. Under physiological conditions, about 80% of the hepatic blood flow is transported to the liver via the portal vein, whereas the arterial perfusion contributes about 20% [1]. Both perfusion systems merge within the hepatic sinusoids and the blood then flows toward the central vein and further on to the heart. Additionally, the dual hepatic perfusion is physiologically maintained at a constant level by an autoregulatory mechanism called the hepatic arterial buffer response (HABR) [2]. This means that changes in the portal venous perfusion are buffered by counterwise changes of the hepatic arterial perfusion [3, 4]. However, HABR functions in a unidirectional way so that changes in the arterial perfusion do not provoke changes in the portal venous blood flow [5].

Liver cirrhosis is characterized by structural changes of the liver architecture. During fibrosis progression, extracellular matrix is deposited by predominantly hepatic stellate cells (HSCs), and liver sinus endothelial cells (LSECs) lose their fenestration, thus undergoing a process called capillarization [6, 7]. As a consequence, the liver becomes stiffer which in turn affects the hepatic and ultimately the systemic blood circulation [8, 9]. At this stage, complications of portal hypertension may become apparent such as ascites and formation of collaterals like esophageal varices [10]. During fibrosis progression, due to stiffening and elevated vascular

---

F. Piecha (✉)

I. Department of Medicine, University Medical Center Hamburg-Eppendorf,  
Hamburg, Germany  
e-mail: [f.piecha@uke.de](mailto:f.piecha@uke.de)

S. Mueller

Department of Medicine and Center for Alcohol Research and Liver Diseases, Salem Medical  
Center, University of Heidelberg, Heidelberg, Germany  
e-mail: [sebastian.mueller@urz.uni-heidelberg.de](mailto:sebastian.mueller@urz.uni-heidelberg.de)

resistance, hepatic blood supply is increasingly taken over by the hepatic artery, a process called arterialization [1] leading ultimately to a predominant arterially perfused liver. In some cases, a so-called hepatofugal portal blood flow may even be observed where the hepatic artery accounts for the total hepatic blood supply while blood leaves the liver through both hepatic veins and the portal vein [11]. However, even in patients with end-stage liver disease, the autoregulatory mechanisms of hepatic perfusion remain intact [12]. Arterialization eventually exposes the liver to high pressure values, which seems to be a key factor for the self-perpetuation of cirrhosis. For more details see also book Part VIII “Molecular Basis of Liver Stiffness and Cell Biology.”

Due to the tight pathophysiological relationship between fibrosis development and hepatic perfusion, liver stiffness (LS) has early been evaluated as a non-invasive screening tool for the presence of esophageal varices [13] and portal hypertension [14]. These studies found a positive correlation between LS values and portal hypertension as measured by the hepatic venous pressure gradient (HVPG), but the impact of changes in the arterial and portal perfusion pressures on LS remained uncertain. In addition, several studies reporting an LS elevation after a meal intake hypothesized an influence of changes in the hepatic arterial blood flow [15]. Table 24.1 provides an overview of the present data on portal and arterial pressure modulation and the response to LS.

**Table 24.1** LS changes in response to pressure modulation

Intervention	LS change	Species	Explanations	References
Epinephrine	↑	Rat	Elevated arterial pressure	[16]
Variceal ligation	↑	Human	Increased portal pressure	[17]
TIPS insertion	↓	Human	Decreased portal pressure, which is not completely compensated by HABR	[17, 18]
Norepinephrine	↑	Rat	Elevated arterial pressure	[16]
Losartan	↓/↓↓	Rat	Decrease in both arterial and portal pressure	[16]
Glyceroltrinitrate (NO)	↓	Rat		
Propranolol	→	Rat	Decrease in heart rate, whereas arterial and portal pressure as well as LS remain stable	[16]
Propranolol	↓	Human	Decrease in arterial pressure and heart rate, followed by a decrease in portal pressure	[19, 20]
Carvedilol	↓↓	Rat		[21]
Metoprolol	↓	Rat		[21]
Enalapril	↓↓	Rat		[21]
Udenafil	↓	Rat	Decrease in both arterial and portal pressure	[21]
Terlipressin	→	Rat	Decrease in portal pressure, but most likely compensated by the HABR	[21]

## Arterial Pressure and LS

As perfusion changes and invasive pressure measurements in the liver-relevant compartments cannot be monitored in humans, we recently performed a set of experiments in rats to further clarify the role of arterial and portal pressure on LS [16, 17, 19]. First, we administered the adrenergic agents epinephrine, norepinephrine, and dobutamine as well as 1 mL saline solution as a control in healthy Wistar rats under continuous monitoring of the central venous, portal, and systemic arterial pressure as well as LS [16]. Figure 24.1 shows a representative real-time experiment of LS and other parameters in response to administration of epinephrine. While volume did not change the assessed parameters to a statistically significant extent, epinephrine injection immediately and drastically increased arterial pressure and LS. Importantly, both central venous and portal pressure remained unchanged, pointing to solely arterial pressure as the reason for the LS increase. This finding was further confirmed by the administration of norepinephrine, as LS and arterial pressure concomitantly increased, while portal pressure increased with a relevant delay of several seconds. Dobutamine, on the other hand, had the strongest effect on heart rate, but neither the arterial pressure nor LS changed to a statistically significant extent. This important finding showed that, first, an increase in heart rate alone does not seem to suffice to increase LS and that, second, direct hepatocellular mechanisms of the administered adrenergic agents [22] are unlikely to explain the observed changes in LS.

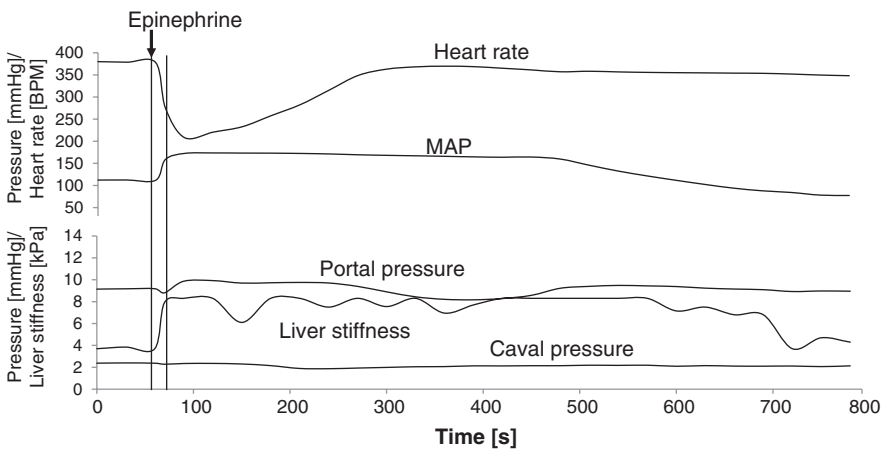
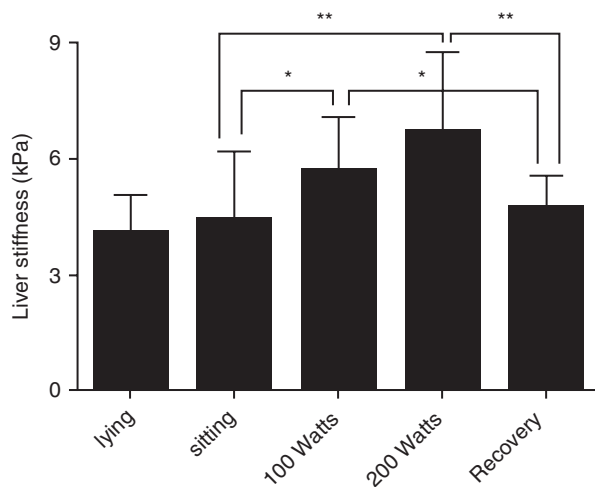


**Fig. 24.1** Real-time measurements of LS and pressures for epinephrine (modified from [16]). Representative measurements are shown from 4 to 6 independent measurements. Arrows indicate the time point of drug injection. Notably, LS increases synchronically with arterial pressure while portal pressure follows with a delay of several seconds. Vertical lines assist to better see the delay and only slight elevation of portal pressure. *MAP* mean arterial pressure, *BPM* beats per minute

In a second step, epinephrine was also administered in rats that had previously undergone fibrosis induction via thioacetamide (TAA). Under these circumstances, epinephrine evoked a comparable increase in systemic arterial pressure while portal pressure again remained stable. However, the increase in LS observed in the diseased organ was more prominent as compared to healthy livers (169% vs. 100%). This more pronounced increase in LS can be explained by the overall higher grade of arterIALIZATION in the diseased liver and is in line with reports on a stronger response of LS to food intake [23] or inflammation [24] in patients with advanced liver disease.

Importantly, these results of an LS increase due to an increase in arterial pressure were confirmed in a translational way [16]. In healthy male volunteers with normal baseline LS values, LS increased in a stepwise fashion while undergoing continuous exercise at 100 and 200 W on an ergometer, also returning to baseline values after a recovery phase of 10 min (see Fig. 24.2). Under these circumstances, LS correlated best with the systolic blood pressure ( $r = 0.527$ ,  $p$ -value  $< 0.01$ ), and 4/11 (36%) of the volunteers even surpassed 7.5 kPa and therefore the cut-off value for F2 fibrosis. Importantly, these results have been reproduced by a second work group using a different elastography technique [25]. Additionally, the systolic blood pressure at examination time was confirmed as an important confounder of LS values in apparently healthy individuals in a recent large meta-analysis comprising over 16,000 individuals [26]. Therefore, the systolic blood pressure should be taken into consideration when interpreting LS results and patients should undergo LS measurement after an adequate resting phase. Notably, this association of LS with arterial pressure cannot be observed in patients with arterial hypertension {Mueller, 2019 #26852, unpublished observation}.

**Fig. 24.2** Response of LS to physical exercise (modified from [16]). Healthy volunteers ( $n = 11$ ) underwent spinning for 10 min at 100 and 200 W, respectively. Bar diagrams show means and means of the interquartile range. Levels of significance are  $p$ -value  $< 0.05$  (\*) and  $p$ -value  $< 0.01$  (\*\*)





### Portal Pressure and LS

Due to the dual perfusion system of the liver, it is difficult to assess the sole impact of changes in portal pressure on LS. However, a multimodal approach both in humans and in animals helped to clarify the role of portal pressure changes on LS [17]. A transjugular intrahepatic portosystemic shunt (TIPS) is an elegant treatment option in patients with end-stage liver disease suffering from complications of portal hypertension and it is used to treat patients with bleeding from esophageal varices, refractory ascites or hepato-renal syndrome. By creating a shunt between the portal and the hepatic vein, a TIPS diverts blood flow to bypass the liver, resulting in an immediate and sustained decrease of portal pressure. Endoscopic band ligation of esophageal varices, on the other hand, diverts collateral blood flow back to the portal venous system with a consecutive increase in portal pressure [27]. Therefore, these interventions seemed feasible options for the assessment of the impact of portal pressure changes on LS.

Consequently, as shown in Fig. 24.3, LS was measured in patients undergoing variceal endoscopic band ligation (Fig. 24.3a) or TIPS implantation (Fig. 24.3b) directly before and 5 min after the procedure under otherwise stable hemodynamic conditions [17]. In this set-up, most patients (12/14, 85%) receiving a TIPS showed

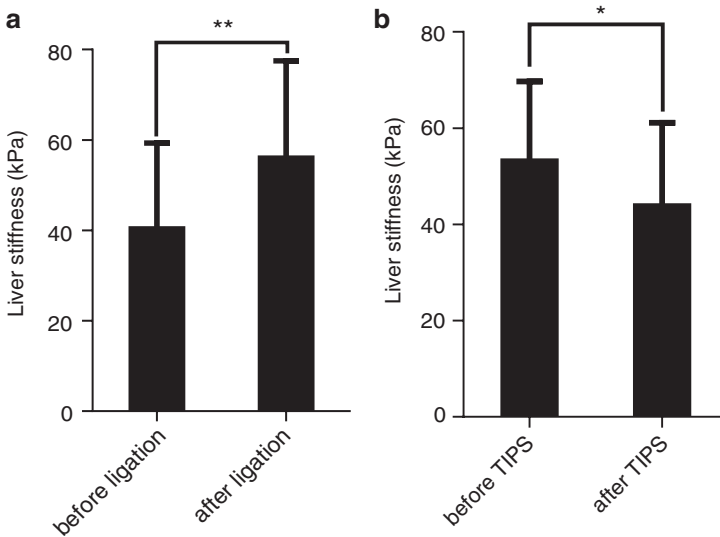


**Fig. 24.3** Change of LS in response to portal pressure modulation. (a) Immediate increase of LS after variceal ligation. Mean values of all patients receiving variceal ligation with the corresponding standard deviation.  $**p$ -value  $< 0.01$  (Student's *T*-Test). (b) LS significantly and immediately decreases after TIPS placement. Mean values with the corresponding standard deviation.  $*p$ -value  $< 0.05$  (Student's *T*-Test). Modified from [17]. *TIPS* transjugular intrahepatic portosystemic shunt

an immediate LS decrease, whereas all 11 patients undergoing variceal band ligation showed an increase in LS values. Importantly, LS and portal pressure were positively correlated ( $r = 0.558$ ) in patients receiving a TIPS, thus underlining the association between both parameters. The reason why LS increased in 2/14 (15%) of patients after TIPS-placement remains unclear, but both a higher grade of hepatic congestion [28] due to an increase in right atrial pressure as well as an increase in the hepatic arterial perfusion due to the HABR [12] are possible explanations.

The effect of portal pressure changes on LS was further confirmed in a set of experiments in non-cirrhotic rats undergoing single liver lobe ligation. This experimental procedure provokes similar hemodynamic changes as a variceal band ligation, as portal venous blood flow is diverted to the remaining perfused liver lobes. Under these conditions, both portal pressure as well as LS significantly increased in the remaining perfused lobes [17], and these data also parallel a recent report of an LS increase after a partial hepatectomy in humans [29]. Importantly, the direct impact of portal pressure changes on LS in patients receiving a TIPS have been reproduced by other authors [18, 30] and also in a different animal model [31].

### *LS Changes in Response to Portal-Pressure Lowering Drugs*

Both changes in solely arterial and portal pressure have a direct impact on LS. Consequently, conditions provoking a change both in arterial and portal pressure also directly influence LS, as demonstrated in TAA treated rats with advanced liver fibrosis undergoing a pharmacological pressure modulation [19]: In a set of experiments of acute injection of the vasodilating drugs glyceroltrinitrate (NO) or losartan, both arterial and portal pressure decreased with a concomitant decrease in LS. Controversially, an acute administration of propranolol only decreased heart rate, whereas arterial and portal pressure as well as LS remained stable. However, this observation is analogous to the above-mentioned dobutamine experiments, in which an increase in heart rate alone was not able to increase LS. Lately, these data have been confirmed in humans undergoing serial LS measurements after the initiation on a non-selective betablocker (NSBB) treatment [19, 20], and a decrease in LS upon pressure-lowering interventions may even be prognostically relevant for patients [18, 19].

## **Conclusion**

LS is strongly modulated by both arterial and portal pressure. Therefore, the systemic arterial pressure at the time of LS assessment as well as interventions like variceal ligation, TIPS-placement, or the beginning of an NSBB treatment need to be considered for the correct interpretation of LS values.

## References

1. Lautt WW. Hepatic circulation: physiology and pathophysiology. In: Colloquium Series on integrated systems physiology: from molecule to function to disease. San Rafael: Morgan & Claypool Life Sciences; 2009.
2. El-Shabrawi MH, Mohsen NA, Sherif MM, El-Karakasy HM, Abou-Yosef H, El-Sayed HM, et al. Noninvasive assessment of hepatic fibrosis and necroinflammatory activity in Egyptian children with chronic hepatitis C virus infection using FibroTest and ActiTest. *Eur J Gastroenterol Hepatol.* 2010;22:946–51.
3. Lautt WW. Mechanism and role of intrinsic regulation of hepatic arterial blood flow: hepatic arterial buffer response. *Am J Physiol.* 1985;249(5 Pt 1):G549–56.
4. Lautt WW. Relationship between hepatic blood-flow and overall metabolism - the hepatic arterial buffer response. *Fed Proc.* 1983;42(6):1662–6.
5. Jakab F, Rath S, Schmal F, Nagy P, Faller J. The interaction between hepatic arterial and portal venous-blood flows - simultaneous measurement by transit-time ultrasonic volume flowmetry. *Hepatogastroenterology.* 1995;42(1):18–21.
6. Olaso E, Friedman SL. Molecular regulation of hepatic fibrogenesis. *J Hepatol.* 1998;29(5):836–47.
7. Iwakiri Y, Groszmann RJ. Vascular endothelial dysfunction in cirrhosis. *J Hepatol.* 2007;46(5):927–34.
8. Garcia-Pagan JC, Gracia-Sancho J, Bosch J. Functional aspects on the pathophysiology of portal hypertension in cirrhosis. *J Hepatol.* 2012;57(2):458–61.
9. Iwakiri Y, Groszmann RJ. The hyperdynamic circulation of chronic liver diseases: from the patient to the molecule. *Hepatology.* 2006;43(2 Suppl 1):S121–31.
10. D'Amico G, Morabito A, D'Amico M, Pasta L, Malizia G, Rebora P, et al. Clinical states of cirrhosis and competing risks. *J Hepatol.* 2018;68(3):563–76.
11. Rector WG Jr, Hoefs JC, Hossack KF, Everson GT. Hepatofugal portal flow in cirrhosis: observations on hepatic hemodynamics and the nature of the arterioportal communications. *Hepatology.* 1988;8(1):16–20.
12. Gülberg V. Hepatic arterial buffer response in patients with advanced cirrhosis. *Hepatology.* 2002;35(3):630–4.
13. Kazemi F, Kettaneh A, N'Kontchou G, Pinto E, Ganne-Carrie N, Trinchet JC, et al. Liver stiffness measurement selects patients with cirrhosis at risk of bearing large oesophageal varices. *J Hepatol.* 2006;45(2):230–5.
14. Vizzutti F, Arena U, Romanelli RG, Rega L, Foschi M, Colagrande S, et al. Liver stiffness measurement predicts severe portal hypertension in patients with HCV-related cirrhosis. *Hepatology.* 2007;45(5):1290–7.
15. Berzigotti A, De Gottardi A, Vukotic R, Siramolpiwat S, Abraldes JG, Garcia-Pagan JC, et al. Effect of meal ingestion on liver stiffness in patients with cirrhosis and portal hypertension. *PLoS One.* 2013;8(3):e58742.
16. Piecha F, Peccerella T, Bruckner T, Seitz HK, Rausch V, Mueller S. Arterial pressure suffices to increase liver stiffness. *Am J Physiol Gastrointest Liver Physiol.* 2016;311(5):G945–G953.
17. Piecha F, Paech D, Sollors J, Seitz HK, Rossle M, Rausch V, et al. Rapid change of liver stiffness after variceal ligation and TIPS implantation. *Am J Physiol Gastrointest Liver Physiol.* 2018;314(2):G179–G87.
18. Jansen C, Moller P, Meyer C, Kolbe CC, Bogs C, Pohlmann A, et al. Increase in liver stiffness after transjugular intrahepatic portosystemic shunt is associated with inflammation and predicts mortality. *Hepatology.* 2018;67(4):1472–84.
19. Piecha F, Mandorfer M, Peccerella T, Ozga AK, Poth T, Vonbank A, et al. Pharmacological decrease of liver stiffness is pressure-related and predicts long-term clinical outcome. *Am J Physiol Gastrointest Liver Physiol.* 2018;315(4):G484–G94.
20. Choi SY, Jeong WK, Kim Y, Kim J, Kim TY, Sohn JH. Shear-wave elastography: a noninvasive tool for monitoring changing hepatic venous pressure gradients in patients with cirrhosis. *Radiology.* 2014;273(3):917–26.

21. Elshaarawy O, Alquzi S, Mueller J, Rausch V, Silva I, Peccerella T, et al. Response of liver and spleen stiffness to portal pressure lowering drugs in a rat model of cirrhosis. *J Hepatol.* 2019;70:E14–E5.
22. Ballet F, Chretien Y, Rey C, Poupon R. Differential response of normal and cirrhotic liver to vasoactive agents. A study in the isolated perfused rat liver. *J Pharmacol Exp Ther.* 1988;244(1):283–9.
23. Arena U, Lupsor Platon M, Stasi C, Moscarella S, Assarat A, Bedogni G, et al. Liver stiffness is influenced by a standardized meal in patients with chronic hepatitis C virus at different stages of fibrotic evolution. *Hepatology.* 2013;58(1):65–72.
24. Mueller S, Englert S, Seitz HK, Badea RI, Erhardt A, Bozaari B, et al. Inflammation-adapted liver stiffness values for improved fibrosis staging in patients with hepatitis C virus and alcoholic liver disease. *Liver Int.* 2015;35(12):2514–21.
25. Gersak MM, Sorantin E, Windhaber J, Dudea SM, Riccabona M. The influence of acute physical effort on liver stiffness estimation using Virtual Touch Quantification (VTQ). Preliminary results. *Med Ultrason.* 2016;18(2):151–6.
26. Bazerbachi F, Haffar S, Wang Z, Cabezas J, Arias-Loste MT, Crespo J, et al. Range of normal liver stiffness and factors associated with increased stiffness measurements in apparently healthy individuals. *Clin Gastroenterol Hepatol.* 2019;17(1):54–64.e1.
27. Lo GH, Liang HL, Lai KH, Chang CF, Hwu JH, Chen SM, et al. The impact of endoscopic variceal ligation on the pressure of the portal venous system. *J Hepatol.* 1996;24(1):74–80.
28. Millonig G, Friedrich S, Adolf S, Fonouni H, Golriz M, Mehrabi A, et al. Liver stiffness is directly influenced by central venous pressure. *J Hepatol.* 2010;52(2):206–10.
29. Ninomiya M, Shirabe K, Ijichi H, Toshima T, Harada N, Uchiyama H, et al. Temporal changes in the stiffness of the remnant liver and spleen after donor hepatectomy as assessed by acoustic radiation force impulse: a preliminary study. *Hepatol Res.* 2011;41(6):579–86.
30. Buechter M, Manka P, Theysohn JM, Reinboldt M, Canbay A, Kahraman A. Spleen stiffness is positively correlated with HVPg and decreases significantly after TIPS implantation. *Dig Liver Dis.* 2018;50(1):54–60.
31. Tang WB, Xu QH, Jiao ZY, Wu R, Song Q, Luo YK. Effect of pressure on liver stiffness during the development of liver fibrosis in rabbits. *Ultrasound Med Biol.* 2016;42(1):282–9.

# Chapter 25

## Liver Stiffness and Cholestasis



Sebastian Mueller

### Influence of Cholestasis on Liver Stiffness

Cholestasis is defined as a defect in bile secretion. First, it can result from various mechanisms that include the mechanic obstruction of the common bile duct by gallstones, tumors, or strictures (extrahepatic or mechanic cholestasis). Second, hepatocellular and/or small bile duct injuries within the liver can result in cholestasis (intrahepatic cholestasis). Both mechanisms cause accumulation of toxic bile acids and other compounds in the liver eventually leading to cell apoptosis, necro-inflammatory reactions, and ductular proliferation. These events will ultimately promote fibrosis development or cancer if cholestasis is not cured. PBC is typically associated with intrahepatic cholestasis while PSC can be associated with intra- or extrahepatic cholestasis. For more details on PBC/PSC see also the respective Chap. 18 in book Part III “Liver Stiffness and Various Etiologies of Liver Diseases.”

It was first noted in 2008 that cholestasis could elevate liver stiffness independent of fibrosis [1]. In this study, 15 patients with extrahepatic cholestasis mostly due to neoplastic invasion of the biliary tree (pancreas carcinoma, Klatskin tumor, liver metastases, and GIST) were analyzed. All patients underwent LSM by TE prior to and after successful biliary drainage by ERCP. Initial LS values above 12.5 kPa, which are otherwise suggestive of liver cirrhosis, were measured in four patients (26.6%) although none of these patients showed any signs of liver cirrhosis (clinical setting, liver imaging). With two exceptions, LS decreased in all patients after successful biliary drainage or stone extraction. As shown in Table 25.1, LS correlated significantly with a decrease in bilirubin but not with GGT, AP, AST, or ALT. The two patients in whom liver stiffness did not fall despite successful biliary drainage had both other causes that explained the persistently increased LS. One patient had

---

S. Mueller (✉)

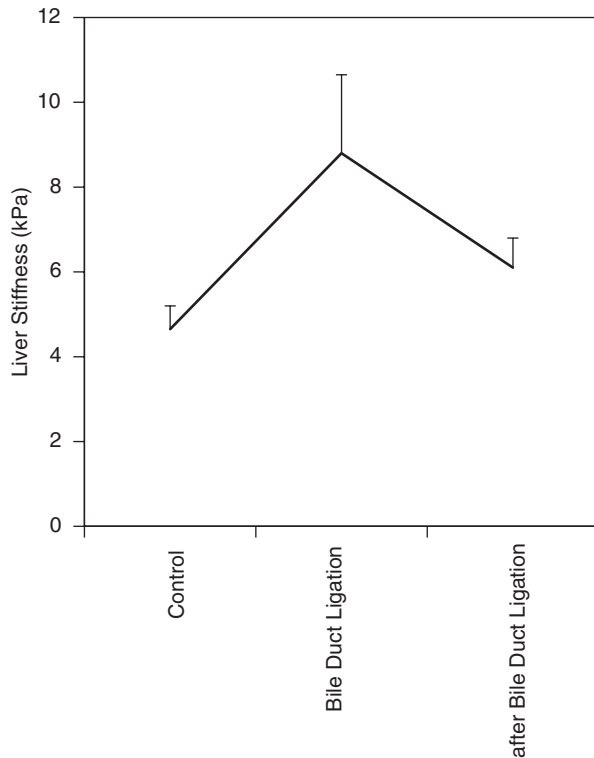
Department of Medicine and Center for Alcohol Research and Liver Diseases, Salem Medical Center, University of Heidelberg, Heidelberg, Germany  
e-mail: [sebastian.mueller@urz.uni-heidelberg.de](mailto:sebastian.mueller@urz.uni-heidelberg.de)

**Table 25.1** Spearman rho correlation of liver stiffness and routine laboratory parameters in patients with mechanic, extrahepatic choletasis

Spearman's rho						
	Fibroscan	Bilirubin	GOT	GPT	GGT	AP
Fibroscan	1.00	<b>0.67</b>	-0.02	-0.13	0.57	0.35
bilirubin	<b>0.67</b>	1.00	0.07	0.13	0.22	-0.03
GOT	-0.02	0.07	1.00	0.38	0.23	0.40
GPT	-0.13	0.13	0.38	1.00	-0.08	0.22
GGT	0.57	0.22	0.23	-0.08	1.00	0.30
AP	0.35	-0.03	0.40	0.22	0.30	1.00

LS only and highly correlates with direct bilirubin  
 bold = correlation is significant at the 0.05 level (2-tailed)  
 n = 10

**Fig. 25.1** Liver stiffness in response to bile duct ligation in German landrace pigs. (Modified from [1])



progressed alcoholic liver cirrhosis and the other had multiple liver metastasis due to colon carcinoma.

The effect of extrahepatic cholestasis on LS was proven by clamping experiments of the common bile duct in animal studies [1]. Bile duct ligation for 120 min was performed on pigs and compared the change in LS with sham operated animals. The ligation period of 120 min led to a significant swelling of the liver and a tightly

palpable gall bladder as compared to humans. LS values doubled during bile duct ligation and reached values suggesting F3 fibrosis (see Fig. 25.1). After removal of the bile duct ligation and a recovery period of 30 min, LS returned to almost normal values around 6.1 kPa.

This study confirmed that bile duct obstruction interferes with the determination of liver fibrosis by LSM in patients with extrahepatic cholestasis and may erroneously suggest the presence of liver cirrhosis. Meanwhile, it has been confirmed by other studies regardless of the assessment method used [2–5]. This effect, which is strongly correlated with serum levels of total bilirubin, likely results from the increased hydrostatic pressure into the liver since the increase in LS is quickly and fully reversible after biliary drainage.

## **Cholestasis-Mediated Elevation of Liver Stiffness in Other Liver Diseases**

There are also strong indications that cholestasis contributes at least in part to LS elevation in other liver diseases. Particularly in patients with PSC and elevated total bilirubin level, liver imaging must absolutely be performed prior to assessing LS to exclude a dominant stricture of the common bile duct [6]. Interestingly, liver stiffness has recently been shown to be increased in pregnant women with intrahepatic cholestasis of pregnancy, a transient condition characterized by pure, estrogen-induced, and reversible hepatocellular cholestasis, as compared to healthy pregnancies with similar gestation time [7]. This observation strongly supports that bile acid overload in hepatocytes and related hepatocellular changes (cell ballooning and clarification, Mallory bodies, etc.) may be sufficient to increase liver stiffness without requiring other superimposed factors.

In addition, intrahepatic cholestasis has been shown to correlate strongly with liver stiffness in patients with acute hepatitis [8]. Moreover, although AST levels are most important modulating parameter in patients with alcoholic liver disease (ALD), bilirubin elevation has been demonstrated as additional confounder of elevated LS [9]. Since ALD patients typically have elevated direct (conjugated) bilirubin this could provide a first hint toward more a mechanic cholestasis in these patients most likely associated with the obstructed bile canaliculi due to hepatocyte ballooning.

## **Conclusions and Clinical Implications**

Mechanic cholestasis is an established important clinical and independent confounder of LS elevation. As rule of thumb, during mechanic cholestasis, an elevation of bilirubin by 1 mg/dL corresponds to an increase of LS by 1 kPa. This information can be very helpful when looking at patients with a combination of established liver cirrhosis and additional bile stone.

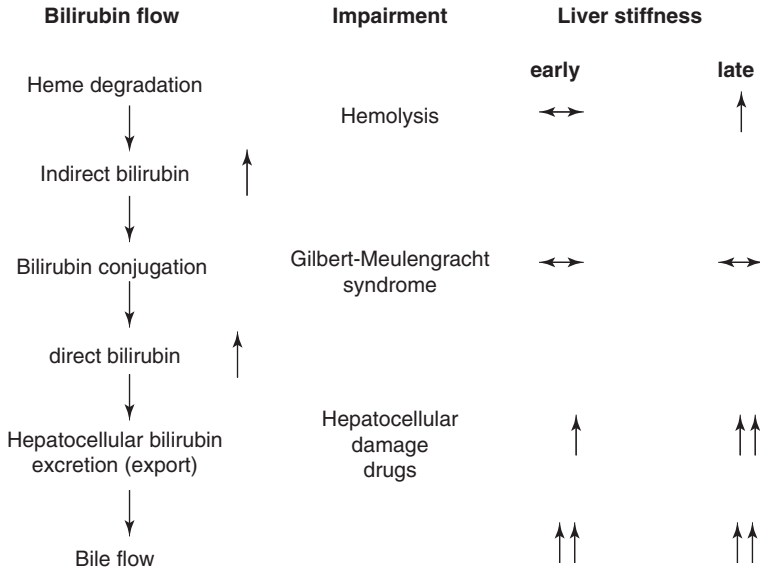


**Fig. 25.2** Simplified scheme of bile/bilirubin flow and corresponding diseases/pathologies and liver stiffness. Notably, severe hemolysis does not increase LS initially but only later due to hepatocellular damage

Due to the elevated LS, imaging studies will not show dilatation of the bile ducts in patients with fibrosis/cirrhosis. Here, comparison of bilirubin with LS can help to dissect cirrhosis from mechanic cholestasis.

Figure 25.2 shows a simplified scheme of bile/bilirubin flow and corresponding diseases/pathologies and liver stiffness. Notably, severe hemolysis should not increase LS in the acute setting. However, since hemolysis will later cause hepatocellular damage, it will ultimately lead to LS elevation. Although data of rare genetic cholestatic diseases are scarce (e.g., Alagille syndrome) all disease with impaired bile and bilirubin excretion are expected to show elevated LS including DILI (drug induced liver injury) of the cholestatic type. In contrast, conjugation problems such as the rather common Gilbert–Meulengracht syndrome are not causing LS elevation. Mechanic cholestasis even of the small canaliculi also contributes to LS elevation in more common etiologies such as PSC/PBC but also alcoholic liver disease.

## References

1. Millonig G, Reimann FM, Friedrich S, Fonouni H, Mehrabi A, Büchler MW, et al. Extrahepatic cholestasis increases liver stiffness (FibroScan) irrespective of fibrosis. *Hepatology*. 2008;48(5):1718–23.
2. Harata M, Hashimoto S, Kawabe N, Nitta Y, Murao M, Nakano T, et al. Liver stiffness in extrahepatic cholestasis correlates positively with bilirubin and negatively with alanine aminotransferase. *Hepatol Res*. 2011;41(5):423–9.



3. Trifan A, Sfarti C, Cojocariu C, Dimache M, Cretu M, Hutanasu C, et al. Increased liver stiffness in extrahepatic cholestasis caused by choledocholithiasis. *Hepat Mon.* 2011;11(5):372–5.
4. Attia D, Pischke S, Negm AA, Rifai K, Manns MP, Gebel MJ, et al. Changes in liver stiffness using acoustic radiation force impulse imaging in patients with obstructive cholestasis and cholangitis. *Dig Liver Dis.* 2014;46(7):625–31.
5. Pfeifer L, Strobel D, Neurath MF, Wildner D. Liver stiffness assessed by acoustic radiation force impulse (ARFI) technology is considerably increased in patients with cholestasis. *Ultraschall Med.* 2014;35(4):364–7.
6. Ehlken H, Lohse AW, Schramm C. Transient elastography in primary sclerosing cholangitis—the value as a prognostic factor and limitations. *Gastroenterology.* 2014;147(2):542–3.
7. Cetin O, Karaman E, Arslan H, Akbudak I, Yildizhan R, Kolusari A. Maternal liver elasticity determined by acoustic radiation force impulse elastosonography in intrahepatic cholestasis of pregnancy. *J Med Ultrason (2001).* 2017;44(3):255–61.
8. Sagir A, Erhardt A, Schmitt M, Haussinger D. Transient elastography is unreliable for detection of cirrhosis in patients with acute liver damage. *Hepatology.* 2008;47(2):592–5.
9. Nguyen-Khac E, Thiele M, Voican C, Nahon P, Moreno C, Boursier J, et al. Non-invasive diagnosis of liver fibrosis in patients with alcohol-related liver disease by transient elastography: an individual patient data meta-analysis. *Lancet Gastroenterol Hepatol.* 2018;3(9):614–25.

# Chapter 26

## Liver Stiffness and Nutrition



Sebastian Mueller, Felix Piecha, and Omar Elshaarawy

### Nutritional Intake, LS Elevation, and Potential Mechanisms

Several studies have evaluated the effect of meal intake on elastography results. Most of these studies are based on transient elastography and show an LS increase after meal intake in approximately half of the patients [1]. Generally, an increase of 2–3 kPa was observed with a peak increase time of 30 min [1–6]. LS required 2–3 h to normalize after. More details about other elastographic techniques are provided in Table 41.1 in the Chap. 41 “Quality criteria for LS measurements,” book Part VII. Generally, LS increases 17–40% of the baseline value after meal intake [2, 3, 5, 7].

The portal blood flow increases after eating [3–5, 7, 8]; however, conflicting data have been obtained between both portal blood flow and liver stiffness variations [3–5, 7, 8]. However, according to the hepatic arterial buffer response (HABR) [9], arterial hepatic blood flow is physiologically decreased in response to increased portal blood flow after a meal (adenosine wash out hypothesis). In a study conducted in 19 cirrhotic patients, the increase in liver stiffness was more pronounced in patients lacking this post-prandial buffer response, suggesting it is an important factor modulating post-prandial changes in liver stiffness [3]. Increased LS values

---

S. Mueller (✉) · O. Elshaarawy  
Department of Medicine and Center for Alcohol Research and Liver Diseases, Salem Medical Center, University of Heidelberg, Heidelberg, Germany  
e-mail: [sebastian.mueller@urz.uni-heidelberg.de](mailto:sebastian.mueller@urz.uni-heidelberg.de); [oelshaarawy@liver.menofia.edu.eg](mailto:oelshaarawy@liver.menofia.edu.eg)

F. Piecha  
I. Department of Medicine, University Medical Center Hamburg-Eppendorf,  
Hamburg, Germany  
e-mail: [f.piecha@uke.de](mailto:f.piecha@uke.de)

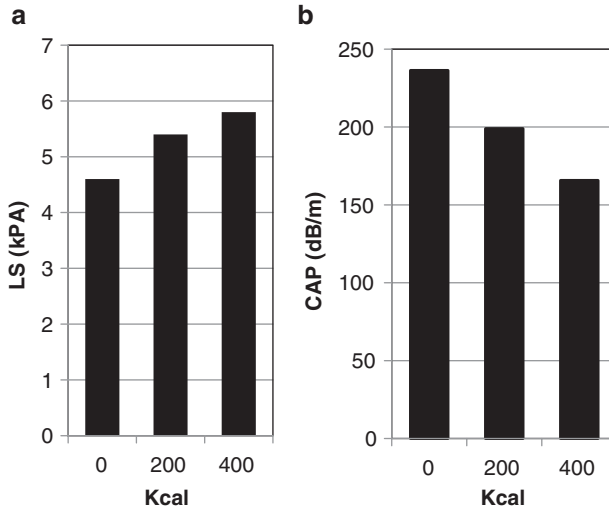


**Fig. 26.1** Short-term response of LS and CAP to intake of 200 and 400 kcal cream cake after 15 and 30 min. Healthy volunteers ( $n = 5$ ). Standard deviations was  $<20\%$  for all LS and CAP data and are not depicted. Note the seemingly paradox decrease of CAP (steatosis) in response to this short-term metabolic load. Whether CAP really mirrors hepatic steatosis under such conditions or is affected, e.g., by perfusion effects remains questionable

after meal intake can lead to fibrosis stage overestimation and 11% of healthy volunteers with normal liver stiffness shift to  $>6.0$  kPa [1, 10] after food intake. In addition, fibrosis stage is also overestimated in patients with chronic liver disease in  $\sim 30\%$  after meal intake [1, 7]. Guidelines therefore recommend fasting for at least 2 h prior to LSM [11, 12]. Figure 26.1 shows the short-term response of LS after intake of 200–400 kcal cream cake over 15 and 30 min in five healthy volunteers [13]. LS increased by 1.5 kPa within 30 min. As demonstrated in Fig. 26.2a, LS did not change significantly after a short-term intake of high percentage alcohol for 30 min.

## CAP and Nutritional Intake

The controlled attenuation parameter (CAP) included in the FibroScan device evaluates liver steatosis through quantification of the ultrasound attenuation during transient elastography examination [14, 15]. The data available about CAP evolution after meal intake remain conflicting with some works having shown a significant decrease [6], while others demonstrated a significant increase [7] or no modification [16, 17]. Interestingly and as shown in Fig. 26.1b, CAP significantly decreased in all five volunteers in response to short-term high caloric intake. Thus, CAP measurement could be affected by other physiological changes of the ingesting liver requiring some time to balance out. Interestingly and in line with high-caloric

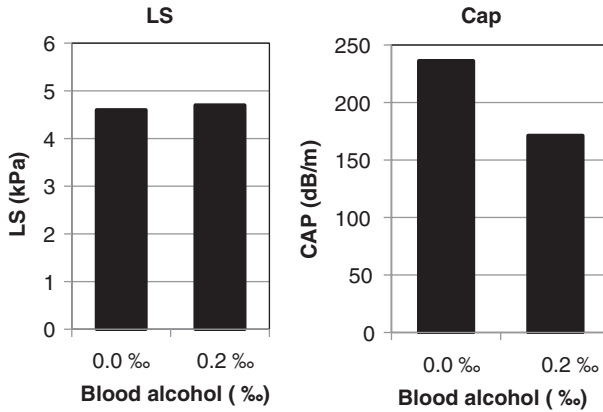


**Fig. 26.2** Short-term response of LS and CAP to intake of 200 mL 40% alcohol after 30 min. Blood alcohol concentration in ‰. Healthy volunteers ( $n = 5$ ). Standard deviations were <20% for all LS and CAP data and are not depicted

response in Fig. 26.1b, CAP decreased in response to alcohol within 30 min (Fig. 26.2b). In contrast, alcohol withdrawal in heavy drinkers causes not only a robust and consistent decrease of LS [18–21] but CAP also significantly decreases in 78% of the patients by ~30 dB/m within 1 week [22]. Taken together, CAP better reflects hepatic steatosis as compared to bright echo pattern in conventional ultrasound. However, the underlying molecular mechanisms of short-term responses of CAP are poorly understood, and fasting state for 2 h is recommended for reliable measurement.

## LS and SS in Response to Various Nutrients in Preliminary Animal Models

Using the  $\mu$ FibroScan device (see also book Part II) [23–26], we have been able to collect first preliminary data on invasive pressure changes, LS and SS in response to direct injection of nutrients into the portal vein including glucose and alcohol. Male Wistar rats were narcotized, and pressure sensors were placed as described recently [24–26]. LS and SS were recorded using the  $\mu$ FibroScan (Echosens, Paris, France) according to recently established conditions [24–27]. After injection of 1 mL 40% glucose, LS and portal pressure values increased (see Fig. 26.3). Correlation confirmed a significant association between LS and portal pressure. However, whether this short-term effect of glucose is due to osmolarity changes, transient hepatocyte swelling, or metabolic consequences remains to be studied. In another set of experiments, the direct effect on LS, SS, portal vein pressure (PVP), and mean arterial pressure (MAP) was studied following injection of 1 mL of 20% ethanol into the portal vein. As shown in Fig. 26.4, all parameters increased although this elevation was not significant for MAP. No change was observed for the heart rate (not shown).

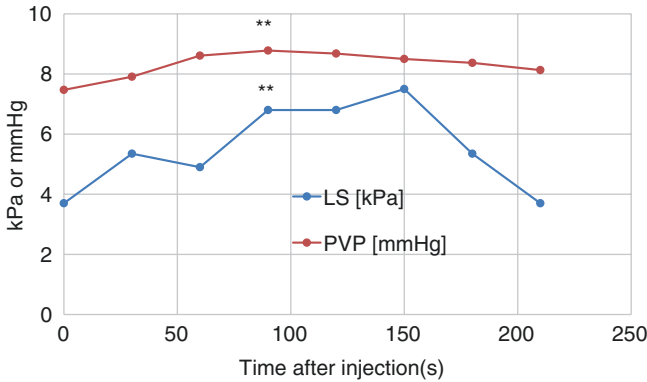


**Fig. 26.3** Effect of 1 mL 40% glucose into the portal veins of Wistar rats on LS and portal vein pressure (PVP). PVP and LS increased immediately after glucose injection. No LS elevation was observed with an identical volume of physiological sodium chloride (control). Note: \*\*significance levels were calculated with a Student's *t*-test with  $P < 0.001$

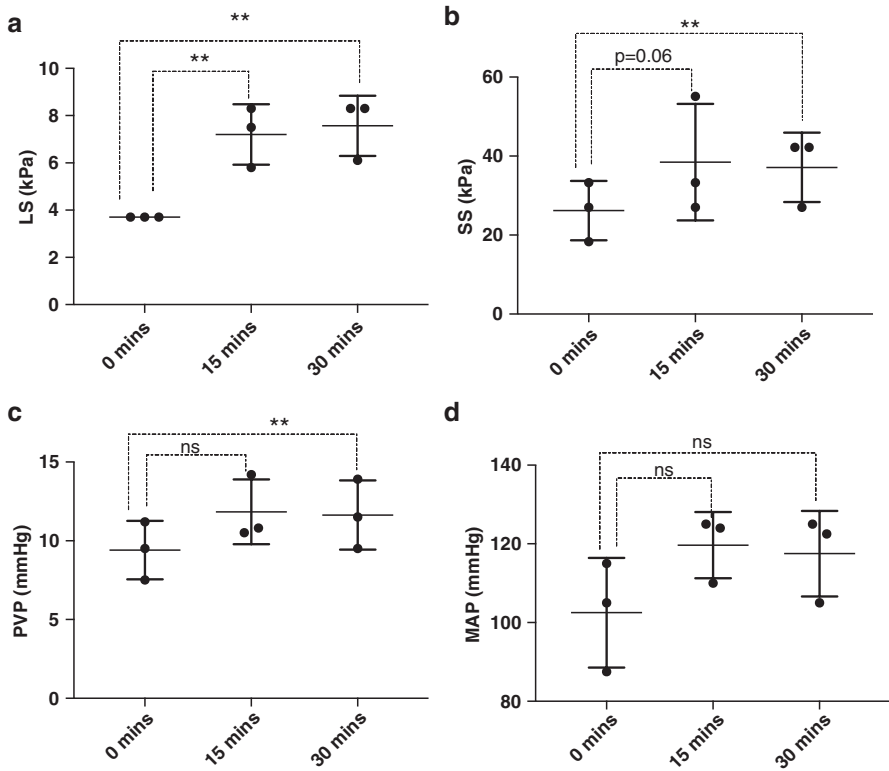


**Fig. 26.4** Effect of alcohol injection (1 mL of 20% alcohol) in control rats on (a) LS, (b) SS, (c) PVP, and (d) MAP. No change was observed with control injections of 1 mL 0.9 NaCl. PVP portal vein pressure, MAP mean arterial pressure. Mean and standard deviation are shown for  $n = 5$

Taken together, isolated portal injection of glucose and ethanol causes rapid elevation of LS within minutes. These rapid responses rather suggest that metabolic or osmotic effects are most likely increasing hepatic vascular resistance, eventually leading to LS and SS elevation. Therefore, these preliminary animal studies provide a first metabolic rationale for the commonly observed LS elevation after intake of meal or alcohol.

## References

1. Mederacke I, Wurstthorn K, Kirschner J, Rifai K, Manns MP, Wedemeyer H, et al. Food intake increases liver stiffness in patients with chronic or resolved hepatitis C virus infection. *Liver Int.* 2009;29(10):1500–6.
2. Arena U, Lupson Platon M, Stasi C, Moscarella S, Assarat A, Bedogni G, et al. Liver stiffness is influenced by a standardized meal in patients with chronic hepatitis C virus at different stages of fibrotic evolution. *Hepatology.* 2013;58(1):65–72.
3. Berzigotti A, De Gottardi A, Vukotic R, Siramolpiwat S, Abraldes JG, Garcia-Pagan JC, et al. Effect of meal ingestion on liver stiffness in patients with cirrhosis and portal hypertension. *PLoS One.* 2013;8(3):e58742.
4. Alvarez D, Orozco F, Mella JM, Anders M, Antinucci F, Mastai R. Meal ingestion markedly increases liver stiffness suggesting the need for liver stiffness determination in fasting conditions. *Gastroenterol Hepatol.* 2015;38(7):431–5.
5. Barone M, Iannone A, Brunetti ND, Sebastiani F, Cecere O, Berardi E, et al. Liver stiffness and portal blood flow modifications induced by a liquid meal consumption: pathogenetic mechanisms and clinical relevance. *Scand J Gastroenterol.* 2015;50(5):560–6.
6. Ratchatassetakul K, Rattanasiri S, Promson K, Sringam P, Sobhonslidsuk A. The inverse effect of meal intake on controlled attenuation parameter and liver stiffness as assessed by transient elastography. *BMC Gastroenterol.* 2017;17(1):50.
7. Kjaergaard M, Thiele M, Jansen C, Staehr Madsen B, Gortzen J, Strassburg C, et al. High risk of misinterpreting liver and spleen stiffness using 2D shear-wave and transient elastography after a moderate or high calorie meal. *PLoS One.* 2017;12(4):e0173992.
8. Jajamovich GH, Dyvorne H, Donnerhack C, Taouli B. Quantitative liver MRI combining phase contrast imaging, elastography, and DWI: assessment of reproducibility and postprandial effect at 3.0 T. *PLoS One.* 2014;9(5):e97355.
9. Lauth WW. Hepatic circulation: physiology and pathophysiology. Colloquium series on integrated systems physiology: from molecule to function to disease. San Rafael: Morgan & Claypool Life Sciences; 2009.
10. Petzold G, Porsche M, Ellenrieder V, Kunsch S, Neeße A. Impact of food intake on liver stiffness determined by 2-D shear wave elastography: prospective interventional study in 100 healthy patients. *Ultrasound Med Biol.* 2019;45(2):402–10.
11. EASL-ALEH Clinical Practice Guidelines: non-invasive tests for evaluation of liver disease severity and prognosis. *J Hepatol.* 2015;63(1):237–64.
12. Dietrich CF, Bamber J, Berzigotti A, Bota S, Cantisani V, Castera L, et al. EFSUMB Guidelines and recommendations on the clinical use of liver ultrasound elastography, update 2017 (long version). *Ultraschall Med.* 2017;38(4):e16–47.
13. Mueller S. Personal observation. 2019.
14. Sasso M, Beaugrand M, de Ledinghen V, Douvin C, Marcellin P, Poupon R, et al. Controlled attenuation parameter (CAP): a novel VCTE™ guided ultrasonic attenuation measurement for the evaluation of hepatic steatosis: preliminary study and validation in a cohort of patients with chronic liver disease from various causes. *Ultrasound Med Biol.* 2010;36(11):1825–35.

15. Karlas T, Petroff D, Sasso M, Fan JG, Mi YQ, de Ledinghen V, et al. Individual patient data meta-analysis of controlled attenuation parameter (CAP) technology for assessing steatosis. *J Hepatol.* 2017;66(5):1022–30.
16. Silva M, Costa Moreira P, Peixoto A, Santos AL, Lopes S, Goncalves R, et al. Effect of meal ingestion on liver stiffness and controlled attenuation parameter. *GE Port J Gastroenterol.* 2019;26(2):99–104.
17. Vuppalanchi R, Weber R, Russell S, Gawrieh S, Samala N, Slaven JE, et al. Is fasting necessary for individuals with nonalcoholic fatty liver disease to undergo vibration-controlled transient elastography? *Am J Gastroenterol.* 2019;114(6):995–7.
18. Mueller S, Millonig G, Sarovska L, Friedrich S, Reimann FM, Pritsch M, et al. Increased liver stiffness in alcoholic liver disease: differentiating fibrosis from steatohepatitis. *World J Gastroenterol.* 2010;16(8):966–72.
19. Trabut JB, Thepot V, Nalpas B, Lavielle B, Cosconea S, Corouge M, et al. Rapid decline of liver stiffness following alcohol withdrawal in heavy drinkers. *Alcohol Clin Exp Res.* 2012;36(8):1407–11.
20. Gelsi E, Dainese R, Truchi R, Marine-Barjoan E, Anty R, Autuori M, et al. Effect of detoxification on liver stiffness assessed by fibroscan(R) in alcoholic patients. *Alcohol Clin Exp Res.* 2011;35(3):566–70.
21. Gianni E, Forte P, Galli V, Razzolini G, Bardazzi G, Annese V. Prospective evaluation of liver stiffness using transient elastography in alcoholic patients following abstinence. *Alcohol Alcohol.* 2017;52(1):42–7.
22. Thiele M, Rausch V, Fluhr G, Kjærgaard M, Piecha F, Mueller J, et al. Controlled attenuation parameter and alcoholic hepatic steatosis: diagnostic accuracy and role of alcohol detoxification. *J Hepatol.* 2018;68(5):1025–32.
23. Bastard C, Bosisio MR, Chabert M, Kalopissis AD, Mahrouf-Yorgov M, Gilgenkrantz H, et al. Transient micro-elastography: a novel non-invasive approach to measure liver stiffness in mice. *World J Gastroenterol.* 2011;17(8):968–75.
24. Piecha F, Peccerella T, Bruckner T, Seitz HK, Rausch V, Mueller S. Arterial pressure suffices to increase liver stiffness. *Am J Physiol Gastrointest Liver Physiol.* 2016;311(5):G945–G53.
25. Piecha F, Mandorfer M, Peccerella T, Ozga AK, Poth T, Vonbank A, et al. Pharmacological decrease of liver stiffness is pressure-related and predicts long-term clinical outcome. *Am J Physiol Gastrointest Liver Physiol.* 2018;315(4):G484–G94.
26. Piecha F, Paech D, Sollors J, Seitz HK, Rossle M, Rausch V, et al. Rapid change of liver stiffness after variceal ligation and TIPS implantation. *Am J Physiol Gastrointest Liver Physiol.* 2018;314(2):G179–G87.
27. Elshaarawy O, Alquzi S, Mueller J, Rausch V, Silva I, Peccerella T, et al. Response of liver and spleen stiffness to portal pressure lowering drugs in a rat model of cirrhosis. *J Hepatol.* 2019;70:E14–E5.

# Chapter 27

## Genetic Confounders of Liver Stiffness and Controlled Attenuation Parameter



Vanessa Rausch, Johannes Mueller, and Sebastian Mueller

### Genetic Determinants of Liver Stiffness

Hepatic fibrosis, a hallmark of all chronic liver disease including non-alcoholic fatty liver disease (NAFLD), alcoholic fatty liver disease (ALD), as well as viral hepatitis, is characterized by excessive collagen deposition in the liver [1, 2]. Irrespective of the etiology, only ~15% develop end-stage cirrhosis underlining the importance of genetic determinants for disease progression [3, 4]. Genome-wide association studies (GWAS) allow to analyze the relationship between a given phenotype/disease and millions of small nucleotide polymorphisms (SNPs) in thousands of different individuals [5]. Using this hypothesis-free approach, an association between patatin-like phospholipase domain containing 3 (PNPLA3/adiponutrin) and steatosis, enhanced transaminase levels, fibrosis as well as HCC development has been recently identified in patients with NAFLD and ALD [6]. Other polymorphisms associated with alcoholic cirrhosis and alcoholic hepatitis are membrane-bound O-acyltransferase domain-containing protein 7 (MBOAT7) and transmembrane 6 superfamily 2 (TM6SF2) [7]. More recently, hydroxysteroid 17-beta dehydrogenase 13 (HSD17B13) was found to be associated with cirrhosis and hepatocellular cancer [8, 9]. The majority of these studies aiming to define the genetic background of fibrosis were based on biopsies and thus hampered by a small study size [10, 11]. Although liver biopsy represents the “gold standard” for staging liver fibrosis, it has limitations such as procedure-related complications, e.g., bleeding, sampling error,

---

V. Rausch · J. Mueller · S. Mueller (✉)  
Department of Medicine and Center for Alcohol Research and Liver Diseases, Salem Medical Center, University of Heidelberg, Heidelberg, Germany  
e-mail: [sebastian.mueller@urz.uni-heidelberg.de](mailto:sebastian.mueller@urz.uni-heidelberg.de)



observer variability, and costs [12, 13], which renders recruiting large cohorts for well-powered genetic analyses troublesome. With the development of non-invasive methods to measure liver stiffness (LS) such as transient elastography (TE, FibroScan), larger patient cohorts can be analyzed in genetic studies. However, important confounders need to be considered when interpreting an elevated LS such as inflammation, ballooning, or congestion [14]. For more details, see also book Part IV “Important (Patho)Physiological Confounders of LS.” In addition, appropriate algorithms should be applied to optimally translate LS values in histological fibrosis stages. In the following, we summarize and discuss genetic determinants of elevated LS.

## Function and Regulation of Adiponutrin/PNPLA3

So far, the physiological function of PNPLA3 and the effect of the I148M amino acid substitution are controversially discussed [15], and the molecular mechanisms leading to steatosis and inflammation remain largely unexplained. All studies mentioned above establish the PNPLA3 p.I148M variant as a common determinant of chronic liver injury leading to steatosis and progressive fibrosis [16]. Furthermore, recent *in vitro* studies point towards an important role for PNPLA3 in regulating lipolysis by repressing the lipolytic activity of PNPLA2 (ATGL) in a lipid droplet (perilipin-5) associated manner. This is most likely mediated by a disruption of active PNPLA2 complexes, thereby increasing the accumulation of toxic lipids [17]. Inactivation or overexpression of the wild-type protein in mice does not lead to steatosis [18]. In contrast, overexpression of a catalytically inactive form of PNPLA3 (I148M) induces the accumulation of both PNPLA3 and TGs on hepatic lipid droplets in sucrose-fed mice leading to steatosis [19, 20]. This is contrary to earlier findings by Kumari et al. who suggested that PNPLA3 p.I148M is a “gain-of-function” variant, resulting in higher lysophosphatidic acid acyltransferase activity and increased hepatic diacylglycerol synthesis [21]. Moreover, further genetic studies as well as our own work associated the p.I148M variant with some metabolic traits, in particular related to lipid metabolism [22–26]. A very basic scheme of the functions of some of the most important genes is shown in Fig. 27.1.

Of note and as mentioned above, PNPLA3 expression is changed in altered metabolic status, such as obesity, and its expression is regulated by nutritional intake, in both hepatocytes and adipocytes [15]. For example, in hepatocytes, PNPLA3 expression is highly induced by carbohydrate feeding and insulin treatment. Detailed mouse PNPLA3 promoter studies revealed two specific consensus sites for the carbohydrate responsive-element binding protein (ChREBP) and the sterol regulatory element-binding protein 1c (SREBP-1c). SREBP-1c is a member of a transcription factor family regulating lipid and cholesterol metabolism and the major isoform expressed in the liver [27]. It is likewise highly regulated by fasting and re-feeding regimen [28]. SREBP-1c is involved in fatty acid synthesis by activating several genes in the biosynthetic pathway. Insulin enhances SREBP-1c gene expression and its protein cleavage, therefore favoring its binding to sterol-response element in

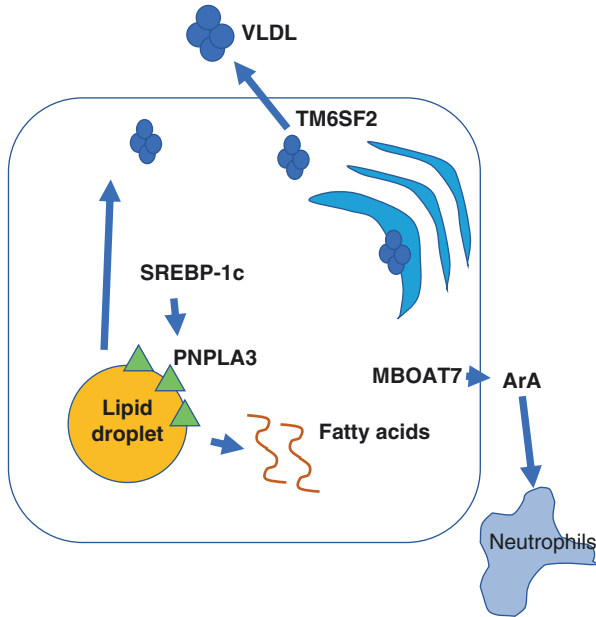


**Fig. 27.1** Simplified scheme of known and potential functions of PNPLA3, MBOAT7, and TM6SF2. PNPLA3 is regulated by SREBP-1c, located at the surface of lipid droplets and contributes to the hydrolysis of triglycerides. MBOAT7 regulates the transfer of polyunsaturated fatty acids such as arachidonic acid (ArA), while TM6SF2 is involved in the secretion of very low density lipoproteins (VLDL)

the promoter of target genes [15]. PNPLA3 mRNA levels were increased in SREBP-1c transgenic mice with an expression pattern resembling that of fatty acid synthase (FAS) [29]. The induction of SREBP-1c by carbohydrate feeding is mediated by liver X receptor (LXR), and it was discovered that LXR agonist treatment (T0901317) increased PNPLA3 mRNA expression. Furthermore, experiments indicated that SREBP-1c interacts directly with a response element in the PNPLA3 gene and that overexpression of SREBP-1c in mouse hepatocytes led to an increase in PNPLA3 gene expression [30]. All this data suggests a close interaction of SREBP-1c with PNPLA3 for its regulation.

## Impact of Adiponutrin/PNPLA3 on Liver Stiffness in Patients with ALD/NAFLD

The PNPLA3 rs738409 polymorphism was identified in a GWAS with 2111 multi-ethnic participants (Dallas Heart study), showing that carriers of the risk allele are prone to steatosis development (triglyceride levels,  $P = 5.9 \times 10^{-10}$ ) and hepatic inflammation ( $P = 3.7 \times 10^{-4}$ ). The risk allele was most common in Hispanics, the ethnic group with highest susceptibility to NAFLD [31]. The association was

replicated and confirmed in additional population-based studies around the world in different ethnicities [32] and also extended to ALD [33–35]. In addition, Sookoian et al. showed that carrying the risk allele predisposes towards all stages of liver damage starting from simple steatosis to steatohepatitis resulting in progressive fibrosis in patients with NAFLD [36]. Finally, patients with advanced fibrosis/cirrhosis with different underlying liver disease carrying the PNPLA3 risk allele are at increased risk of hepatocellular carcinoma (HCC) [37–41]. In patients suffering from HCC, this variant is also associated with poor prognosis [42].

Krawczyk et al. first studied in nearly 900 patients with different chronic liver diseases the impact of PNPLA3 p.I148M variant on the development of severe forms of NAFLD and ALD based on non-invasive liver stiffness measurements (LS) by TE (Fibroscan). This study demonstrated that distinct p.I148M PNPLA3 genotypes show significantly different LS values ( $P = 0.017$ , ANOVA) and that carriers of the G allele are at higher risk to develop liver cirrhosis defined by LS values  $>13.0$  kPa (OR = 1.56;  $P = 0.005$ ) [16].

## Impact of SREBP1c on Liver Stiffness

Dubuquoy et al. showed that SREBP-1c is also the master regulator of hepatic PNPLA3 expression in humans [30]. In addition, previous studies suggested a contribution of two SREBP-1c variants, namely rs2297508 and rs11868035, on alterations in glucose and lipid metabolism in humans [43]. By using a candidate-gene approach, Krawczyk et al. showed that the SREBP-1c rs11868035 variant is associated with LS in 899 patients with chronic liver disease especially in patients with low TE levels (5.0–8.0 kPa) [43]. Moreover, carriers of both SREBP1c and PNPLA3 polymorphisms displayed significantly ( $P = 0.005$ ) higher median LS, as compared to patients carrying none of these variants. The authors suggested that the SREBP-1c variant may affect early stages of liver fibrosis (LS  $< 8$  kPa) and a combined effect of SREBP-1c-PNPLA3-specific pathway on liver stiffness and hepatic fibrogenesis. Additional studies are needed to assess the association between SREBP-1c variant and liver disease progression in a prospective manner and to confirm its proposed role in hepatic steatosis development.

## Impact of MBOAT7 on Liver Stiffness

Membrane-bound O-acyltransferase domain containing 7 (MBOAT7, also known as LPIAT1) is a protein involved in the acyl chain remodeling of phospholipids via the Lands' cycle. It has been shown that MBOAT7 is associated with membranes. A recent study by Caddeo et al. revealed that MBOAT7 is a six-transmembrane protein and remodels the acyl chain composition of endo-membranes [44]. In addition, MBOAT7 was identified as a susceptibility risk gene for the development and progression of NAFLD and ALD as well as HCV. Mancina et al. found that the genotype rs641738 at

the MBOAT7-TMC4 locus was associated with increased hepatic fat content, with more severe liver damage and increased histological fibrosis in European NAFLD patients [45]. Furthermore, the MBOAT7 rs641738 T allele was associated with lower hepatic protein expression and changes in phosphatidylinositol species detected in the plasma consistent with decreased MBOAT7 enzyme function [45]. This may favor hepatic steatosis and the production of inflammatory mediators [45]. These findings were expanded towards an approximately 80% increased risk of MBOAT7 rs641738 T allele carriers to develop HCC, especially in non-cirrhotic NAFLD patients (histological fibrosis stage  $\leq$ F2 or in  $n = 3$  cases LS measurements  $\leq$ 8.4 kPa) (OR = 1.65; 95% CI = 1.08–2.55;  $P < 0.001$ ) [46]. Krawczyk et al. analyzed in a multicenter biopsy-based study cohort of  $n = 515$  patients the impact of MBOAT7 rs641738 variant on NAFLD severity and found that MBOAT7 variant was solely associated with increased fibrosis ( $P = 0.046$ ) [47]. Buch et al. was the first who identified in a two-stage GWAS that MBOAT7 is also a significant risk locus for alcohol-related cirrhosis ( $P = 1.03 \times 10^{-9}$ ) as defined by histological fibrosis score (Ishak fibrosis stage 5 or 6) and clinical or laboratory evidence for the presence of cirrhosis. A meta-analysis identified a cluster of variants in high linkage disequilibrium covering the 5'-regions of the neighboring TMC4 and MBOAT7 loci. Here, the top MBOAT7 variant identified through fine mapping, rs641738, is in high linkage disequilibrium with rs626283 ( $r^2 = 0.98$ ).

Finally, Donati and colleagues also showed in a combined cohort of non-cirrhotic patients with ALD or HCV ( $n = 1121$ ) that the MBOAT7 T allele was independently associated with HCC risk (OR = 1.93; 95% CI = 1.07–3.58;  $P < 0.028$ ) [46].

## Impact of TM6SF2 on Liver Stiffness

Like MBOAT7, the transmembrane 6 superfamily 2 gene (TM6SF2) is located on chromosome 19. The exact function of TM6SF2 is still not completely known. In an exome-wide association study, TM6SF2 rs58542926 C/T was identified together with PNPLA3 to be associated with NAFLD, especially with increased hepatic fat content, elevated transaminase levels, and lower serum lipoprotein levels [48]. It is suggested that the E167K amino acid substitution encodes a loss-of-function protein and predisposes to progressive NAFLD (steatohepatitis and fibrogenesis) by impairing the secretion of low-density lipoproteins (VLDLs) such as apolipoprotein B by hepatocytes [49, 50]. Indeed, the mutation is associated with a reduced fasting circulating lipoprotein concentration [48]. In a multicenter biopsy proofed study on NAFLD severity [47], TM6SF2 was associated with steatosis and elevated transaminase levels but not fibrosis as detected by histological analysis. In 2018, Petta et al. was the first who studied the effect of TM6SF2 on TE in 890 NAFLD patients. They found that the TM6SF2 T variant was independently associated with advanced fibrosis as determined by LS  $> 9.6$  kPa with an odds ratio of 3.06 (95% CI = 1.08–8.65;  $P < 0.05$ ) [51].

Table 27.1 summarizes all studies on non-invasive fibrosis determination based on liver stiffness measurements and the association with the most relevant genetic variants. The genetic variants identified as risk factors for NAFLD overlap with

**Table 27.1** Literature overview of most important genetic determinants of LS

Reference	Etiology	Median LS (kPa)	Gene	Freq.	OR type	LS cut-off (kPa)	Univariate		Multivariate		Adjustment
							P	OR	P	OR	
Krawzik et al. 2011 [16]	CLD	6.8	<i>PNPLA3</i> rs738409	CC 485 CG 351 GG 63	C->GG	13	0.005 (1.14–2.15)	1.57 (1.14–2.15)	0.001 (1.30–2.67)	1.86 (1.30–2.67)	Age, alcohol
Krawzik et al. 2013 [43]	CLD	6.8	<i>SREBP1c</i> rs11868035	CC 87 CT 384 TT 421	CC->T	7	0.035	1.66 (1.04–2.66)	0.036 (1.03–2.70)	1.67 (1.03–2.70)	Age
			<i>SREBP1c</i> rs2297508	GG 140 GC 436 CC 315	CC->T	7	>0.05	–	>0.05	–	
			<i>PNPLA3</i> rs738409	CC 481 CG 348 GG 63	CC->G	7	>0.05	1.18 (0.96–1.46)	>0.05	–	
Lundbo et al. 2014 [54]	HCV	7.4	<i>IL28B</i>	CC 129 CT 183 TT 38	T->CC	17.1	>0.05	–	>0.05	–	
Petta et al. 2018 [51]	NAFLD	–	<i>TM6SF2</i> rs58542926	890	CC->CT/TT	9.3	0.03	1.34 (1.02–1.76)	0.04	1.33 (1.01–1.81)	Age, gender, obesity, ALT, diabetes, HDL cholesterol, triglycerides
			<i>PNPLA3</i> rs738409	890	CC->CG->GG	9.3	–	–	0.62	0.81 (0.35–1.84)	

2019, own data (unpublished)	ALD	6.2	PNPLA3 rs738409	CC 188 CG 235 GG 43	CC->CG->GG	12.5	0.019	1.39 (1.06-1.82)	0.193	1.21 (0.91-1.61)	Age, BMI, gender, alcohol consumption
			MBOAT7 rs626283	GG 152 GC 271 CC 96	GG->GC->CC	12.5	0.002	1.51 (1.17-1.95)	0.001	1.61 (1.22-2.13)	
			TM6SF2 rs58542926	CC 427 CT 71 TT 3	CC->CT/TT	12.5	0.968	1.01 (0.63-1.61)	0.469	1.21 (0.72-2.03)	

*CLD* chronic liver disease, *ALD* alcoholic liver disease, *NAFLD* non-alcoholic fatty liver disease, *HCV* hepatitis C, *LS* liver stiffness, *OR* odds ratio

ALD indicating similar or shared pathological mechanisms. They may serve as therapeutic targets in the future in both liver diseases.

## Genetic Determinants of Liver Stiffness in the Context of Chronic Hepatitis C

In addition, recent studies also analyzed the association of different SNPs and the progression of liver fibrosis by non-invasive techniques in patients infected with hepatitis C virus (HCV). Recently, GWAS studies have revealed that SNPs in proximity of the interleukin (IL)28-B gene might predict spontaneous clearance of the HCV infection as well as outcome following interferon and ribavirin therapy among genotype 1-infected patients [52, 53]. In addition, the rs12979860 C/T polymorphism in the IL28-B gene has been linked to progression towards cirrhosis in mono-infected HCV patients. Lundbo et al. investigated in detail the relation between HCV genotypes and IL28-B and the development of liver fibrosis assessed by TE [54]. They found that infection with HCV genotype 3 was associated with cirrhosis (simplified cut-off value for cirrhosis was 17.1 kPa). Interestingly, the IL28-B genotype was not an independent predictor of fibrosis development in their study. Next, Lutz et al. investigated in a cross-sectional study the impact of rs12979860 T allele in the IL28-B gene on fibrosis progression in HIV/HCV co-infected patients measured by TE, since co-infection is characterized by accelerated progression of liver disease. The authors found that although the progression of liver fibrosis was low under highly active antiretroviral therapy (HAART) in the patient cohort, the progression was more pronounced in HIV/HCV genotype 1 co-infected patients with the T allele ( $P = 0.047$ ) [55]. Another study evaluated in over 770 HCV-infected patients in a real-life trial the impact of rs12979860 variability in the IL28-B gene on LS measurements and HCV genotype [56]. The authors found that the CC variant of rs12979860 was more common among HCV genotype 2- and 3-infected patients and is associated with higher LS values among HCV genotype 3-infected patients. In summary, rs12979860 CC seems to be associated with more pronounced liver pathology in patients with HCV genotype 3 as compared to genotype 1, suggesting that the IL28-B variant differently regulates HCV infection across HCV genotypes.

IL-7 and its receptor play an important role in the homeostasis and development of T cells, and this interaction is critical for T-cell mediated antiviral responses. HCV clearance is related to the early expression of IL-7RA on T cells during acute phase of infection. IL-7RA polymorphisms have been related to homeostasis and development of T cells, thereby eventually having an impact on the immune system. Therefore, Jimenez-Sousa et al. analyzed the relationship between **IL-7RA polymorphisms** rs6897932, rs987106, and rs3194051 and the progression of liver fibrosis in 187 patients infected with HCV with repeated LS measurements [57]. They found that baseline LS values did not show significant statistical differences for IL-7RA genotypes ( $P > 0.05$ ). In univariate analysis, the rs6897932 T allele was associated with increased LS ( $P = 0.001$ ), progression to advanced fibrosis ( $F \geq 3$ , 9.5–12.4 kPa) (OR = 2.51; 95% CI = 1.29–4.88;  $P = 0.006$ ) and progression to cir-

rhosis ( $F4 \geq 12.5$  kPa) (OR = 2.71; 95% CI = 0.94–5.03;  $P = 0.069$ ). In multivariate analysis, the rs6897932 T allele was also related to a higher increase of LS values during follow-up and higher odds of progression to advanced fibrosis (adjusted OR = 4.46; 95% CI = 1.87–10.62;  $P = 0.001$ ), and progression to cirrhosis (adjusted OR = 3.92; 95% CI = 1.30–11.77;  $P = 0.015$ ). Regarding IL-7RA rs987106 and rs3194051 polymorphisms, the authors did not find significant results except for the relationship between IL-7RA rs987106 and the increase in LS (adjusted OR = 1.12; 95% CI = 1.02–1.23;  $P = 0.015$ ). To conclude, the IL-7RA rs6897932 polymorphism seems to be associated with increased risk of liver fibrosis progression in HCV-infected patients detected by LS.

Since contradictory data about the impact of PNPLA3 rs738409 polymorphism on liver fibrosis progression in HIV/HCV co-infected patients have been reported, a recent study was undertaken to test whether PNPLA3 rs738409 and other polymorphisms previously related to fatty liver disease in HIV-infected patients linked to SAMM50 or LPPR4 genes influence liver fibrosis progression in HIV/HCV co-infected individuals [58]. The study included 323 patients from four Spanish study sites and was conducted between 2011 and 2013. The authors also analyzed the progression of LS in 171 individuals with two available LS determinations without anti-HCV treatment between the measurements. The study revealed that rs738409 was associated with cirrhosis in 29.6% of G allele carriers, whereas 20.0% of CC carriers showed cirrhosis (adjusted OR = 1.98; 95% CI = 1.12–3.50;  $P = 0.018$ ). Also, 30.4% of G carriers versus only 15.7% of CC carriers showed significant liver stiffness progression (adjusted OR = 2.89; 95% CI = 1.23–6.83;  $P = 0.015$ ). These results suggest that the rs738409 polymorphism in PNPLA3 is also associated with liver fibrosis progression in HIV/HCV co-infected patients.

## Genetic Determinants of Steatosis Determined by CAP

Early steatosis screening can be carried out by various methods including ultrasonography (US), computed tomography (CT), and magnetic resonance imaging (MRI) [59]. Among those, hepatic steatosis assessment via US is well-established and a lower-cost imaging technique for the diagnosis of hepatic steatosis. However, in patients with mild steatosis, it has limited analytical sensitivity and specificity and is highly operator dependent. CT has also poor sensitivity to detect mild steatosis as well as small changes in fat content and presents a potential radiation hazard. Nowadays, MRI and MR spectroscopy are the imaging tools of choice allowing the most accurate quantitative methods for measuring hepatic steatosis in clinical practice, especially for follow-up studies, but limited by the lack of established standardization of sequence characteristics and their high cost [60, 61]. Recently, controlled attenuation parameter (CAP) has been introduced to measure steatosis. For more details, see also book Part VI “Assessment of Hepatic Steatosis Using CAP.”

CAP is obtained on the FibroScan platform, highly reproducible and quantitative with an AUROC up to 90% for fatty liver [62].



## Genetic Determinants of Steatosis Determined by CAP in Patients with ALD/NAFLD: Impact of PNPLA3, MBOAT7, and TM6SF2

As mentioned before, the PNPLA3 p.I148M variant has been identified as common genetic modifier of hepatic steatosis and consecutive inflammation in humans consuming western diets. Therefore, researcher started to evaluate the impact of PNPLA3 p.I148M on non-invasively quantified hepatic fat content assessed by CAP. Arslanow and colleagues showed in an observational study including 174 patients with chronic liver disease 70.7% diagnosed with NAFLD, 21.8% presented with cryptogenic chronic liver disease (CLD), and 7.5% with ALD that PNPLA3 genotype is associated with increased hepatic CAP measurements using thresholds between 190 and 340 dB/m ( $P < 0.05$ ) [63]. Furthermore, the p.148 M risk allele increased the odds of developing liver steatosis (OR = 2.39,  $P = 0.023$ ). In multivariate models, BMI and PNPLA3 mutations were both independently associated with CAP values ( $P < 0.001$  and  $P = 0.007$ , respectively). In addition, the authors analyzed the newly detected genetic risk factor TM6SF2 for NAFLD but clearly showed that carriage of the TM6SF2-risk allele did not affect CAP values.

## Impact of Variants in Genes Controlling Vitamin D Metabolism and APOC3 on CAP

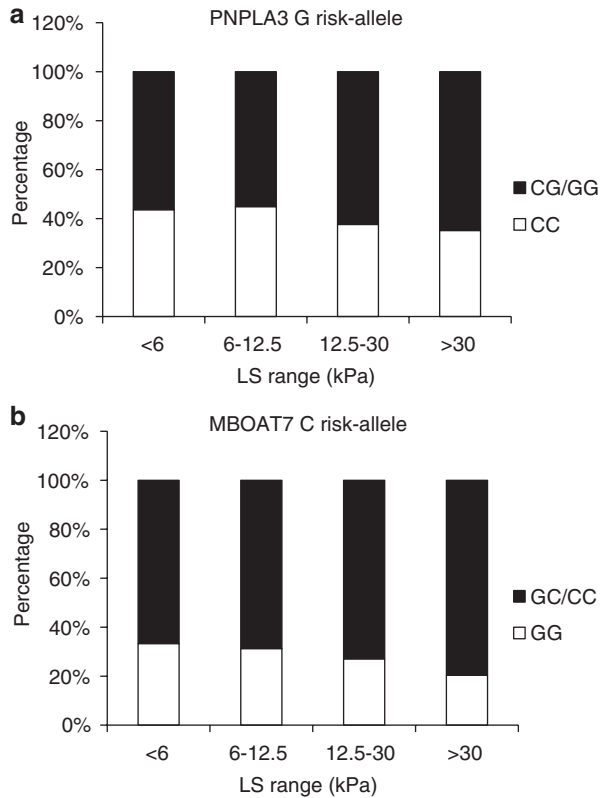
Vitamin D and its active form 1 $\alpha$ -25-dihydroxyvitamin D [1,25(OH) $_2$ D] is a steroid hormone and has been suggested to play an important role in the pathogenesis of fatty liver disease especially in immune modulation and inflammatory responses [64]. Serum 1,25(OH) $_2$ D concentrations have been shown to be negatively correlated with hepatic steatosis. Therefore, Jamka and colleagues analyzed in 241 patients (median BMI 29.4 kg/m $^2$ ) with CLD the impact of three SNPs in the vitamin D-binding group-specific component (GC rs7041), 7-dehydrocholesterol reductase (DHCR7 rs12785878), and cytochrome P450 family 2 subfamily R member 1 genes (CYP2R1 rs10741657) on CAP and 1,25(OH) $_2$ D concentrations [65]. The researcher claimed that patients with advanced steatosis (CAP $\geq$ 280 dB/m) had significantly lower 1,25(OH) $_2$ D levels as compared to patients with CAP<280 dB/m ( $P = 0.033$ ). Moreover, the T allele in GC rs7041 was significantly associated with higher 1,25(OH) $_2$ D levels in patients with CAP<280 dB/m ( $P = 0.018$ ). The authors suggest that higher CAP values are associated with low serum 1,25(OH) $_2$ D concentrations but not with common vitamin D gene variants. Another study analyzed the controversial discussed association between apolipoprotein C3 SNPs and NAFLD [66]. Here, the authors studied in 59 patients and 72 healthy controls the impact of the rs2070666 variant and found that after adjusting for sex, age, serum triglycerides, total cholesterol, BMI, and the PNPLA3 rs738409 polymorphism, the APOC3 rs2070666 A allele was an independent risk factor for NAFLD (OR = 3.683; 95%

CI = 1.037–13.084). Furthermore, the APOC3 rs2070666 A allele was linked to the fourth quartile of CAP values (OR = 2.769; 95% CI = 1.002–7.651) in 131 individuals, but not to hepatic fibrosis as detected by LS measurements and histology. They conclude that APOC3 rs2070666 variant might contribute to increased liver fat content in Chinese Han population. These results should be confirmed in larger studies and evaluated in various populations in future.

## **Preliminary Data on PNPLA3, MBOAT7, and TM6SF2 in Heavy Alcohol Drinkers from the Heidelberg Cohort**

Here, we show some preliminary data of the effect of genes and alcohol withdrawal on LS and CAP in 516 Caucasian heavy alcohol drinkers who were hospitalized for alcohol withdrawal at Salem Medical Center in Heidelberg. Parts of the data on PNPLA3 were already published in 2016 [6]. The patients were genotyped for PNPLA3 rs738409, TM6SF2 rs58542926, and MBOAT7 rs626283. All patients had LS, CAP, and routine laboratory before and after alcohol withdrawal. The minor allele frequencies were 0.31, 0.45, and 0.08 for PNPLA3, MBOAT7, and TM6SF2, respectively. Median age of the total cohort was 52 years, median alcohol intake was 163 g per day, and mean duration of alcohol withdrawal was 6.3 days. For parameters at the day of admission, no difference was observed for age, BMI, alcohol intake, and transaminase levels between the genotypes of the three genes. LS differed significantly between PNPLA3 genotypes ( $P = 0.019$ , ANOVA) and MBOAT7 genotypes ( $P = 0.004$ , ANOVA) while CAP values were only significantly different in PNPLA3 ( $P = 0.039$ , ANOVA). The percentage of risk-allele carriers for PNPLA3 and MBOAT7 (G for PNPLA3 and C for MBOAT7) with respect to LS value ranges can be seen in Fig. 27.2. This figure shows that the prevalence of the risk alleles increases with increasing LS for both PNPLA3 and MBOAT7. No differences between TM6SF2 genotypes regarding LS and CAP could be observed. Alcohol withdrawal revealed interesting differences between PNPLA3 and MBOAT7. In PNPLA3, after alcohol withdrawal, LS was significantly decreased in the CC and CG genotype while LS did not significantly decrease in the GG genotype (see Fig. 27.3a). This could be an effect of the low number of patients with this genotype; however, AST levels were significantly elevated after alcohol withdrawal in the GG genotype with respect to the CC type ( $P < 0.001$ ) (see Fig. 27.3b). M30 levels were also increased after withdrawal (not shown). This is an indication of prolonged inflammation and inflammation-associated LS increase in the GG type [67] instead of a direct influence on fibrosis development. For MBOAT7 on the other hand, LS decreased in all genotypes significantly after withdrawal but in the CC type LS stayed significantly elevated ( $P < 0.001$ ) (see Fig. 27.4a). AST levels also decreased in all MBOAT7 genotypes, and no difference could be observed before or after withdrawal (see Fig. 27.4b). Since here no differences in inflammation associated parameters could be observed, the difference in LS values before and after withdrawal indicates a direct effect of MBOAT7 on fibrosis devel-

**Fig. 27.2** Proportional distribution of (a) PNPLA3 G risk-allele vs. non-risk-allele carriers and (b) MBOAT7 C risk-allele vs. non-risk-allele carriers in four groups stratified by non-invasive LS measurements



opment but not on inflammation and liver injury. Steatosis as measured by CAP decreased significantly after withdrawal in all PNPLA3, MBOAT7, and TM6SF2 genotypes, and for MBOAT7 and TM6SF2, no differences between the genotypes could be observed. In PNPLA3 however, an increased CAP in GG with respect to CC could also be seen after alcohol withdrawal. Furthermore, the decrease in CAP was stronger in the GG type with 37 dB/m vs. 32 dB/m in the CC type. Since steatosis seems to have a decreasing effect on LS (see also book Part VI “Assessment of Hepatic Steatosis Using CAP”), this could also have an effect on LS and partially explain the smaller decrease in LS after withdrawal in the PNPLA3 GG genotype. In a multivariate logistic regression model including PNPLA3, MBOAT7, age, gender, BMI, and alcohol consumption, it was found that PNPLA3 is an independent risk factor for elevated AST >50 IU/L after withdrawal (OR = 1.32; 95% CI = 1.00–1.74;  $P = 0.048$ ) and steatosis as measured by CAP >250 dB/m after withdrawal (OR = 1.54; 95% CI = 1.08–2.17;  $P = 0.019$ ). The association with elevated LS > 17 kPa disappeared after also correcting for AST values. MBOAT7 on the other hand was only an independent risk factor for fibrosis/cirrhosis as expressed by LS > 17 kPa. This association stayed significant even after correcting for AST levels (OR = 1.70; 95% CI = 1.11–2.60;  $P = 0.014$ ). This is another proof of the

**Fig. 27.3** Comparison of (a) liver stiffness, (b) AST, and (c) CAP levels prior and after 7 days of alcohol detoxification according to PNPLA3 rs738409 variants. \* $P < 0.05$ ; \*\* $P < 0.01$ ; \*\*\* $P < 0.001$

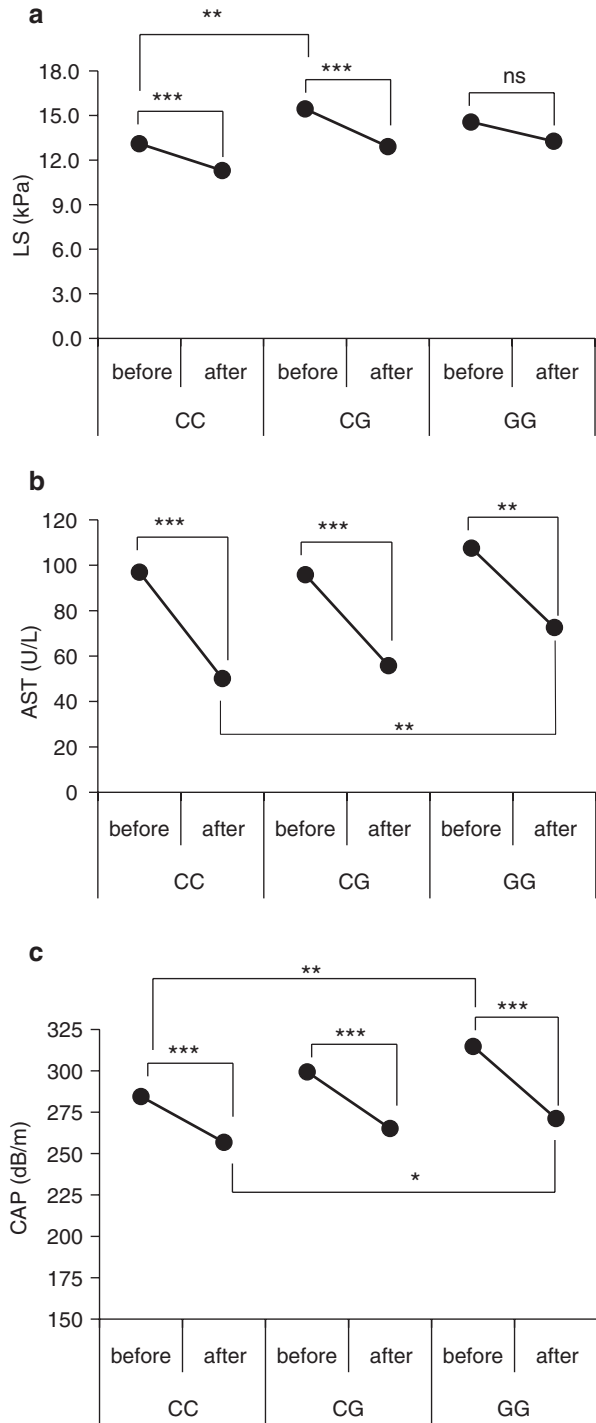
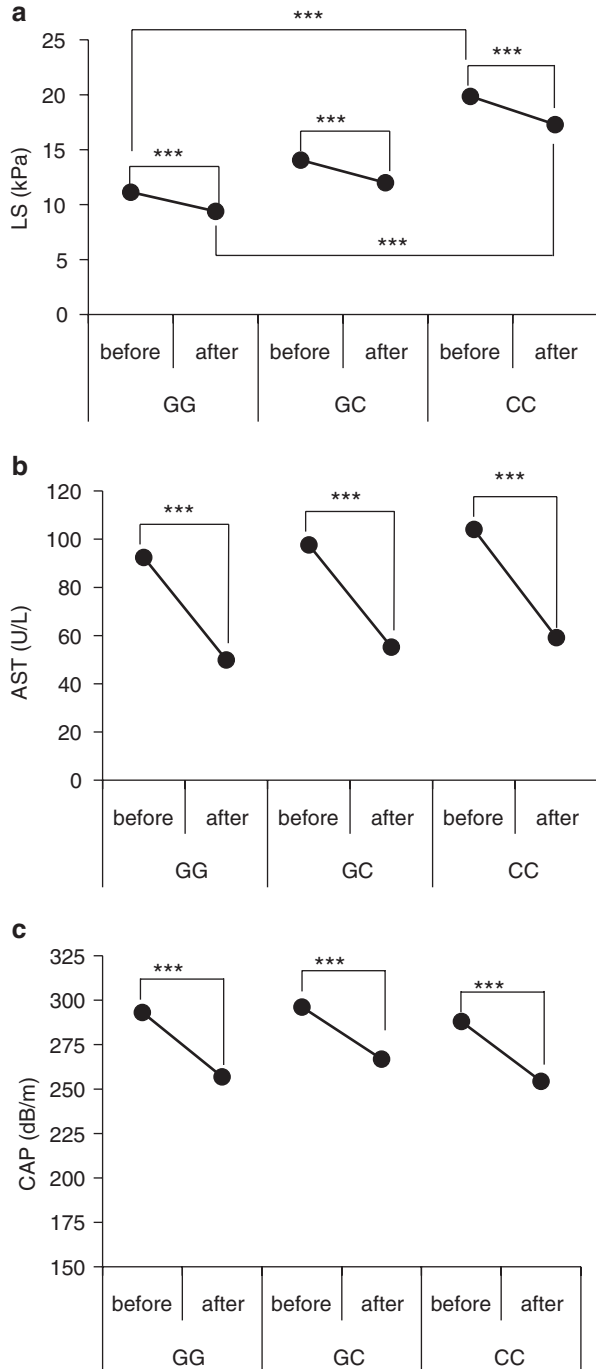


**Fig. 27.4** Comparison of (a) liver stiffness, (b) AST, and (c) CAP levels prior and after 7 days of alcohol detoxification according to MBOAT7 rs626283 variants. \* $P < 0.05$ ; \*\* $P < 0.01$ ; \*\*\* $P < 0.001$



findings above that PNPLA3 is more associated with steatosis development, inflammation and liver injury, which leads to fibrosis later on while MBOAT7 seems to be directly associated with fibrosis development without significant effects on liver injury, inflammation, or steatosis. This finding is new, and the molecular mechanism should be investigated further in the future.

## Conclusion

Different gene variants have been identified as underlying risk factors for the development of various liver diseases. The PNPLA3 p.I148M variant represents the most important pro-steatotic genetic risk factor. PNPLA3 seems to be mainly involved in liver inflammation but shows only a moderate effect on fibrosis development. In contrast, MBOAT7 seems to solely effect fibrosis (see Fig. 27.5). The results for TM6SF2 are controversially discussed, but mainly suggest an effect on steatosis.

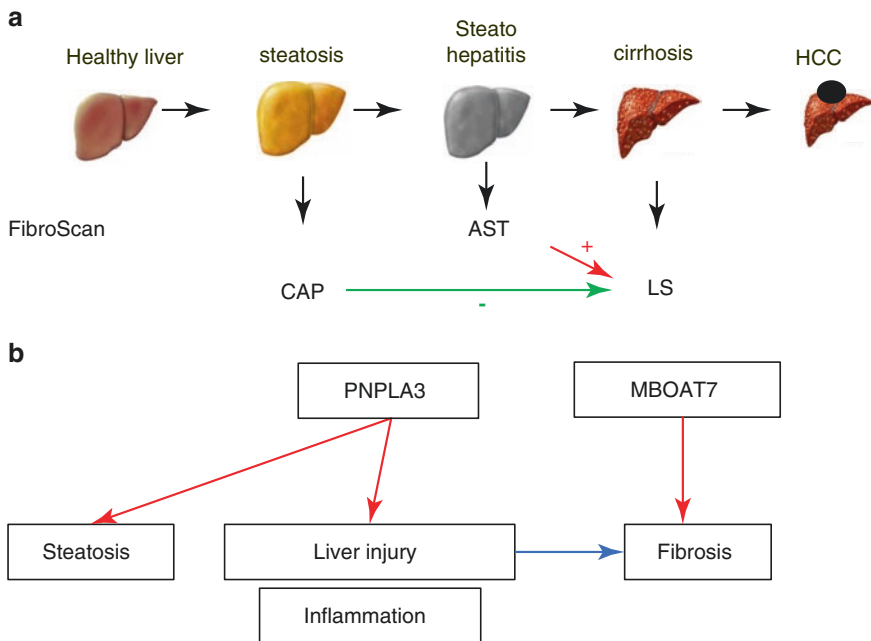


**Fig. 27.5** Conclusions from the Heidelberg genotype alcohol withdrawal study using non-invasive fibrosis assessment based on LS measurements. Inflammation, steatosis, and fibrosis were studied by transaminase levels (AST), CAP, and LS measurements. **(a)** Note that there are interactions between AST, CAP, and LS. While inflammation as measured by AST levels cause LS elevation, steatosis (CAP) has a negative impact on LS. This needs to be considered when interpreting LS-based studies. **(b)** Major lessons learnt from the Heidelberg alcohol withdrawal study (preliminary data 2020, unpublished): PNPLA3 mainly causes fibrosis by inflammation/apoptosis. MBOAT7 seems to have a direct effect on pro-fibrogenic signaling pathways irrespective of inflammation

Since most risk variants involved in lipid metabolism and are clinically relevant for both NAFLD and ALD, common pathological pathways can be assumed. However, the exact underlying molecular mechanisms as well as the effects of the amino acid substitutions are not completely understood and require further investigations. To conclude, the recent established non-invasive techniques such as liver stiffness and CAP measurements are ideal to diagnose and follow up liver disease patients carrying a risk allele.

## References

1. Bataller R, Brenner DA. Liver fibrosis. *J Clin Invest*. 2005;115(2):209–18.
2. Friedman SL. Mechanisms of hepatic fibrogenesis. *Gastroenterology*. 2008;134(6):1655–69.
3. Krawczyk M, Mullenbach R, Weber SN, Zimmer V, Lammert F. Genome-wide association studies and genetic risk assessment of liver diseases. *Nat Rev Gastroenterol Hepatol*. 2010;7(12):669–81.
4. Mueller S, Rausch V. The role of iron in alcohol-mediated hepatocarcinogenesis. *Adv Exp Med Biol*. 2015;815:89–112.
5. Manolio TA. Genomewide association studies and assessment of the risk of disease. *N Engl J Med*. 2010;363(2):166–76.
6. Rausch V, Peccerella T, Lackner C, Yagmur E, Seitz HK, Longerich T, et al. Primary liver injury and delayed resolution of liver stiffness after alcohol detoxification in heavy drinkers with the PNPLA3 variant I148M. *World J Hepatol*. 2016;8(35):1547–56.
7. Buch S, Stickel F, Trepo E, Way M, Herrmann A, Nischalke HD, et al. A genome-wide association study confirms PNPLA3 and identifies TM6SF2 and MBOAT7 as risk loci for alcohol-related cirrhosis. *Nat Genet*. 2015;47(12):1443–8.
8. Yang J, Trepo E, Nahon P, Cao Q, Moreno C, Letouze E, et al. A 17-Beta-hydroxysteroid dehydrogenase 13 variant protects from hepatocellular carcinoma development in alcoholic liver disease. *Hepatology*. 2019;70(1):231–40.
9. Stickel F, Lutz P, Buch S, Nischalke HD, Silva I, Rausch V, et al. Genetic variation in HSD17B13 reduces the risk of developing cirrhosis and hepatocellular carcinoma in alcohol misusers. *Hepatology*. 2019. <https://doi.org/10.1002/hep.30996>.
10. Weber S, Grunhage F, Hall R, Lammert F. Genome-wide association studies in hepatology. *Z Gastroenterol*. 2010;48(1):56–64.
11. Bataller R, North KE, Brenner DA. Genetic polymorphisms and the progression of liver fibrosis: a critical appraisal. *Hepatology*. 2003;37(3):493–503.
12. Castera L, Pinzani M. Biopsy and non-invasive methods for the diagnosis of liver fibrosis: does it take two to tango? *Gut*. 2010;59(7):861–6.
13. Mueller S, Seitz HK, Rausch V. Non-invasive diagnosis of alcoholic liver disease. *World J Gastroenterol*. 2014;20(40):14626–41.
14. Mueller S, Sandrin L. Liver stiffness: a novel parameter for the diagnosis of liver disease. *Hepat Med*. 2010;2:49–67.
15. Bruschi FV, Tardelli M, Claudel T, Trauner M. PNPLA3 expression and its impact on the liver: current perspectives. *Hepat Med*. 2017;9:55–66.
16. Krawczyk M, Grunhage F, Zimmer V, Lammert F. Variant adiponutrin (PNPLA3) represents a common fibrosis risk gene: non-invasive elastography-based study in chronic liver disease. *J Hepatol*. 2011;55(2):299–306.
17. Witzel H, Schwittai I, Pawella L, Rausch V, Mueller S, Schattenberg J, et al. Lipid droplet-associated proteins in alcoholic and non-alcoholic steatohepatitis in patients with polymorphisms in PNPLA3. *Z Gastroenterol*. 2019;57(01):e55.

18. Li JZ, Huang Y, Karaman R, Ivanova PT, Brown HA, Roddy T, et al. Chronic over-expression of PNPLA3I148M in mouse liver causes hepatic steatosis. *J Clin Invest.* 2012;122(11):4130–44.
19. BasuRay S, Wang Y, Smagris E, Cohen JC, Hobbs HH. Accumulation of PNPLA3 on lipid droplets is the basis of associated hepatic steatosis. *Proc Natl Acad Sci.* 2019;116(19):9521–6.
20. Smagris E, BasuRay S, Li J, Huang Y, Lai KM, Gromada J, et al. Pnpla3I148M knockin mice accumulate PNPLA3 on lipid droplets and develop hepatic steatosis. *Hepatology.* 2015;61(1):108–18.
21. Kumari M, Schoiswohl G, Chitraju C, Paar M, Cornaciu I, Rangrez AY, et al. Adiponutrin functions as a nutritionally regulated lysophosphatidic acid acyltransferase. *Cell Metab.* 2012;15(5):691–702.
22. Kollerits B, Coassin S, Beckmann ND, Teumer A, Kiechl S, Doring A, et al. Genetic evidence for a role of adiponutrin in the metabolism of apolipoprotein B-containing lipoproteins. *Hum Mol Genet.* 2009;18(23):4669–76.
23. Krawczyk M, Gruenhage F, Mahler M, Tirziu S, Acalovschi M, Lammert F. The common adiponutrin variant p.I148M does not confer gallstone risk but affects fasting glucose and triglyceride levels. *J Physiol Pharmacol.* 2011;62(3):369–75.
24. Palmer CN, Maglio C, Pirazzi C, Burza MA, Adiels M, Burch L, et al. Paradoxical lower serum triglyceride levels and higher type 2 diabetes mellitus susceptibility in obese individuals with the PNPLA3 148M variant. *PLoS One.* 2012;7(6):e39362.
25. Pirazzi C, Adiels M, Burza MA, Mancina RM, Levin M, Stahlman M, et al. Patatin-like phospholipase domain-containing 3 (PNPLA3) I148M (rs738409) affects hepatic VLDL secretion in humans and in vitro. *J Hepatol.* 2012;57(6):1276–82.
26. Rausch V, Mueller S. Suppressed fat mobilization due to PNPLA3 rs738409-associated liver damage in heavy drinkers: the liver damage feedback hypothesis. *Adv Exp Med Biol.* 2018;1032:153–72.
27. Hua X, Wu J, Goldstein JL, Brown MS, Hobbs HH. Structure of the human gene encoding sterol regulatory element binding protein-1 (SREBF1) and localization of SREBF1 and SREBF2 to chromosomes 17p11.2 and 22q13. *Genomics.* 1995;25(3):667–73.
28. Horton JD, Bashmakov Y, Shimomura I, Shimano H. Regulation of sterol regulatory element binding proteins in livers of fasted and refed mice. *Proc Natl Acad Sci U S A.* 1998;95(11):5987–92.
29. Huang Y, He S, Li JZ, Seo YK, Osborne TF, Cohen JC, et al. A feed-forward loop amplifies nutritional regulation of PNPLA3. *Proc Natl Acad Sci U S A.* 2010;107(17):7892–7.
30. Dubuquoy C, Robichon C, Lasnier F, Langlois C, Dugail I, Foufelle F, et al. Distinct regulation of adiponutrin/PNPLA3 gene expression by the transcription factors ChREBP and SREBP1c in mouse and human hepatocytes. *J Hepatol.* 2011;55(1):145–53.
31. Romeo S, Kozlitina J, Xing C, Pertsemlidis A, Cox D, Pennacchio LA, et al. Genetic variation in PNPLA3 confers susceptibility to nonalcoholic fatty liver disease. *Nat Genet.* 2008;40(12):1461–5.
32. Anstee QM, Day CP. The genetics of NAFLD. *Nat Rev Gastroenterol Hepatol.* 2013;10(11):645–55.
33. Tian C, Stokowski RP, Kershenobich D, Ballinger DG, Hinds DA. Variant in PNPLA3 is associated with alcoholic liver disease. *Nat Genet.* 2010;42(1):21–3.
34. Stickel F, Buch S, Lau K, Meyer zu Schwabedissen H, Berg T, Ridinger M, et al. Genetic variation in the PNPLA3 gene is associated with alcoholic liver injury in caucasians. *Hepatology.* 2011;53(1):86–95.
35. Trepo E, Gustot T, Degre D, Lemmers A, Verset L, Demetter P, et al. Common polymorphism in the PNPLA3/adiponutrin gene confers higher risk of cirrhosis and liver damage in alcoholic liver disease. *J Hepatol.* 2011;55(4):906–12.
36. Sookoian S, Castano GO, Burgueno AL, Gianotti TF, Rosselli MS, Pirola CJ. A nonsynonymous gene variant in the adiponutrin gene is associated with nonalcoholic fatty liver disease severity. *J Lipid Res.* 2009;50(10):2111–6.



37. Singal AG, Manjunath H, Yopp AC, Beg MS, Marrero JA, Gopal P, et al. The effect of PNPLA3 on fibrosis progression and development of hepatocellular carcinoma: a meta-analysis. *Am J Gastroenterol.* 2014;109(3):325–34.
38. Nischalke HD, Berger C, Luda C, Berg T, Muller T, Grunhage F, et al. The PNPLA3 rs738409 148M/M genotype is a risk factor for liver cancer in alcoholic cirrhosis but shows no or weak association in hepatitis C cirrhosis. *PLoS One.* 2011;6(11):e27087.
39. Valenti L, Rumi M, Galmozzi E, Aghemo A, Del Menico B, De Nicola S, et al. Patatin-like phospholipase domain-containing 3 I148M polymorphism, steatosis, and liver damage in chronic hepatitis C. *Hepatology.* 2011;53(3):791–9.
40. Falletti E, Fabris C, Cmet S, Cussigh A, Bitetto D, Fontanini E, et al. PNPLA3 rs738409C/G polymorphism in cirrhosis: relationship with the aetiology of liver disease and hepatocellular carcinoma occurrence. *Liver Int.* 2011;31(8):1137–43.
41. Burza MA, Pirazzi C, Maglio C, Sjöholm K, Mancina RM, Svensson PA, et al. PNPLA3 I148M (rs738409) genetic variant is associated with hepatocellular carcinoma in obese individuals. *Dig Liver Dis.* 2012;44(12):1037–41.
42. Hassan MM, Kaseb A, Etzel CJ, El-Serag H, Spitz MR, Chang P, et al. Genetic variation in the PNPLA3 gene and hepatocellular carcinoma in USA: risk and prognosis prediction. *Mol Carcinog.* 2013;52(Suppl 1):E139–47.
43. Krawczyk M, Grunhage F, Lammert F. Identification of combined genetic determinants of liver stiffness within the SREBP1c-PNPLA3 pathway. *Int J Mol Sci.* 2013;14(10):21153–66.
44. Caddeo A, Jamialahmadi O, Solinas G, Pujia A, Mancina RM, Pingitore P, et al. MBOAT7 is anchored to endomembranes by six transmembrane domains. *J Struct Biol.* 2019;206(3):349–60.
45. Mancina RM, Dongiovanni P, Petta S, Pingitore P, Meroni M, Rametta R, et al. The MBOAT7-TMC4 variant rs641738 increases risk of nonalcoholic fatty liver disease in individuals of European descent. *Gastroenterology.* 2016;150(5):1219–30 e6.
46. Donati B, Dongiovanni P, Romeo S, Meroni M, McCain M, Miele L, et al. MBOAT7 rs641738 variant and hepatocellular carcinoma in non-cirrhotic individuals. *Sci Rep.* 2017;7(1):4492.
47. Krawczyk M, Rau M, Schattenberg JM, Bantel H, Pathil A, Demir M, et al. Combined effects of the PNPLA3 rs738409, TM6SF2 rs58542926, and MBOAT7 rs641738 variants on NAFLD severity: a multicenter biopsy-based study. *J Lipid Res.* 2017;58(1):247–55.
48. Kozlitina J, Smagris E, Stender S, Nordestgaard BG, Zhou HH, Tybjaerg-Hansen A, et al. Exome-wide association study identifies a TM6SF2 variant that confers susceptibility to non-alcoholic fatty liver disease. *Nat Genet.* 2014;46(4):352–6.
49. Liu YL, Reeves HL, Burt AD, Tiniakos D, McPherson S, Leathart JB, et al. TM6SF2 rs58542926 influences hepatic fibrosis progression in patients with non-alcoholic fatty liver disease. *Nat Commun.* 2014;5:4309.
50. Dongiovanni P, Petta S, Maglio C, Fracanzani AL, Pipitone R, Mozzi E, et al. Transmembrane 6 superfamily member 2 gene variant disentangles nonalcoholic steatohepatitis from cardiovascular disease. *Hepatology.* 2015;61(2):506–14.
51. Petta S, Di Marco V, Pipitone RM, Grimaudo S, Buscemi C, Craxi A, et al. Prevalence and severity of nonalcoholic fatty liver disease by transient elastography: genetic and metabolic risk factors in a general population. *Liver Int.* 2018;38(11):2060–8.
52. Rauch A, Kutalik Z, Descombes P, Cai T, Di Iulio J, Mueller T, et al. Genetic variation in IL28B is associated with chronic hepatitis C and treatment failure: a genome-wide association study. *Gastroenterology.* 2010;138(4):1338–45, 45 e1–7.
53. Thomas DL, Thio CL, Martin MP, Qi Y, Ge D, O’Huigin C, et al. Genetic variation in IL28B and spontaneous clearance of hepatitis C virus. *Nature.* 2009;461(7265):798–801.
54. Lundbo LF, Clausen LN, Weis N, Schonning K, Rosenorn L, Benfield T, et al. Influence of hepatitis C virus and IL28B genotypes on liver stiffness. *PLoS One.* 2014;9(12):e115882.
55. Lutz P, Wasmuth JC, Nischalke HD, Vidovic N, Grunhage F, Lammert F, et al. Progression of liver fibrosis in HIV/HCV genotype 1 co-infected patients is related to the T allele of the rs12979860 polymorphism of the IL28B gene. *Eur J Med Res.* 2011;16(8):335–41.

56. Ydreborg M, Westin J, Rembeck K, Lindh M, Norrgren H, Holmberg A, et al. Impact of I128b-related single nucleotide polymorphisms on liver transient elastography in chronic hepatitis C infection. *PLoS One*. 2013;8(11):e80172.
57. Jimenez-Sousa MA, Gomez-Moreno AZ, Pineda-Tenor D, Medrano LM, Sanchez-Ruano JJ, Fernandez-Rodriguez A, et al. The IL7RA rs6897932 polymorphism is associated with progression of liver fibrosis in patients with chronic hepatitis C: repeated measurements design. *PLoS One*. 2018;13(5):e0197115.
58. Nunez-Torres R, Macias J, Mancebo M, Frias M, Dolci G, Tellez F, et al. The PNPLA3 genetic variant rs738409 influences the progression to cirrhosis in HIV/hepatitis C virus coinfecting patients. *PLoS One*. 2016;11(12):e0168265.
59. Schwenzer NF, Springer F, Schraml C, Stefan N, Machann J, Schick F. Non-invasive assessment and quantification of liver steatosis by ultrasound, computed tomography and magnetic resonance. *J Hepatol*. 2009;51(3):433–45.
60. d'Assignies GRM, Khiat A, Lepanto L, Chagnon M, Kauffmann C, et al. Noninvasive quantification of human liver steatosis using magnetic resonance and bioassay methods. *Eur Radiol*. 2009;19:2033–40.
61. Mancini M, Prinster A, Annuzzi G, Liuzzi R, Giacco R, Medagli C, Cremonese M, Clemente G, Maurea S, Riccardi G, Rivellesse AA, Salvatore M. Sonographic hepatic-renal ratio as indicator of hepatic steatosis: comparison with (1)H magnetic resonance spectroscopy. *Metabolism*. 2009;58(12):1724–30.
62. Sasso M, Beaugrand M, de Ledinghen V, Douvin C, Marcellin P, Poupon R, et al. Controlled attenuation parameter (CAP): a novel VCTE™ guided ultrasonic attenuation measurement for the evaluation of hepatic steatosis: preliminary study and validation in a cohort of patients with chronic liver disease from various causes. *Ultrasound Med Biol*. 2010;36(11):1825–35.
63. Arslanow A, Stokes CS, Weber SN, Grunhage F, Lammert F, Krawczyk M. The common PNPLA3 variant p.I148M is associated with liver fat contents as quantified by controlled attenuation parameter (CAP). *Liver Int*. 2016;36(3):418–26.
64. Eliades M, Spyrou E. Vitamin D: a new player in non-alcoholic fatty liver disease? *World J Gastroenterol*. 2015;21(6):1718–27.
65. Jamka M, Arslanow A, Bohner A, Krawczyk M, Weber SN, Grunhage F, et al. Effects of gene variants controlling vitamin D metabolism and serum levels on hepatic steatosis. *Digestion*. 2018;97(4):298–308.
66. Zhang RN, Zheng RD, Mi YQ, Zhou D, Shen F, Chen GY, et al. APOC3 rs2070666 is associated with the hepatic steatosis independently of PNPLA3 rs738409 in Chinese han patients with nonalcoholic fatty liver diseases. *Dig Dis Sci*. 2016;61(8):2284–93.
67. Mueller S, Englert S, Seitz HK, Badea RI, Erhardt A, Bozaari B, et al. Inflammation-adapted liver stiffness values for improved fibrosis staging in patients with hepatitis C virus and alcoholic liver disease. *Liver Int*. 2015;35(12):2514–21.

# Chapter 28

## Liver Stiffness and Acute Liver Failure



Aline Gottlieb and Ali Canbay

### Liver Stiffness During Liver Failure

Liver stiffness (LS) has been measured in a few studies during ALF with differing results and conclusions. ALF should be clearly separated from entities such as acute-on-chronic-liver failure which encompasses acute liver injury in a patient with pre-existing liver disease which will be covered at the end of this chapter. Other entities such as acute-on-cirrhotic-liver failure, however, will not be covered here. It is important to understand the difference between all three entities to take appropriate diagnostic/therapeutic actions [1]. The following main questions will be addressed:

- Why should LS be measured in patients with ALF?
- What is the underlying cause for elevated LS in ALF?
- What techniques can be used to measure LS in ALF?
- Is there an increase in LS in acute-on-chronic liver failure?
- Future directions?

### Why Should LS Be Measured in Patients with ALF?

ALF is a rare, but severe clinical syndrome associated with high mortality if no immediate state-of-the-art intensive care or liver transplantation is performed. The etiologies for ALF are very diverse encompassing viral hepatitis, drug toxicity, autoimmune, mycotoxicosis, Wilsons disease, Budd–Chiari syndrome and several

---

A. Gottlieb · A. Canbay (✉)

Department of Gastroenterology, Hepatology and Infectious Diseases, University Magdeburg, Magdeburg, Germany

e-mail: [aline.gottlieb@med.ovgu.de](mailto:aline.gottlieb@med.ovgu.de); [ali.canbay@med.ovgu.de](mailto:ali.canbay@med.ovgu.de)

**Table 28.1** Acute liver failure etiologies

Etiology	
Virus hepatitis (Southern Europe, Africa, Asia ~50%; USA, England, Scandinavia ~10%; Germany ~20%)	Frequency: <ul style="list-style-type: none"> <li>– HAV: 0.2%</li> <li>– HBV: 1%</li> <li>– HDV: ~5% (more with co-infection)</li> <li>– HEV: up to 3%, in pregnant women up to 20%</li> <li>– Rarely double infections with two different virus strains</li> <li>– Rarely herpesviruses (CMV, EBV, HSV)</li> </ul>
Pharmacological-toxic (depending on region between 20 and 40%)	<ul style="list-style-type: none"> <li>– <i>Medication</i>: acetaminophen-intoxication, halothane, phenprocoumon</li> <li>– <i>Drugs</i>: ecstasy for example</li> <li>– <i>Deadly amanita</i> (<i>Amanita phalloides</i>)</li> <li>– <i>Phytotherapeutics</i> (amber, kava kava, ...)</li> <li>– <i>Chemicals</i> (e.g., carbon tetrachloride)</li> </ul>
Other causes (5%)	<ul style="list-style-type: none"> <li>– HELLP syndrome</li> <li>– Autoimmune hepatitis</li> <li>– Shock liver</li> <li>– Wilsons disease</li> <li>– Budd–Chiari syndrome</li> <li>– Acute fatty liver in pregnancy</li> </ul>
Cryptogenic (up to 20% of cases)	

**Table 28.2** Typical lab result changes in patients with ALF

Increased	Decreased
ASAT, ALAT	pH (metabolic alkalosis)
Bilirubin	Glucose levels
INR	Platelets
Ammonium – Causing hepatic encephalopathy (HE) ranging from minimal change in HE to HE IV	
PTT	

others (see Table 28.1). ALF can also occur as a side effect of acute heart failure where the heart usually determines the prognosis. ALF in its “pure” state is characterized by an acute to sub-acute onset of liver failure, without a pre-existing liver disease with the following symptoms: jaundice, hepatic encephalopathy, and hemorrhagic diathesis. Typical laboratory and histological characteristics of ALF are shown in Tables 28.2 and 28.3. In non-fatal cases of ALF, the liver is able to recover completely. Nevertheless, ALF is associated with massive cell death and impaired liver function [2, 3]. At the onset of ALF, predicting mortality remains difficult.

Clichy criteria, King’s college criteria (KCC), and MELD are widely recognized scoring systems to predict death in ALF patients. Nevertheless, further improvements are urgently needed since the prognosis is highly dependent on quick and appropriate treatment initiation. Moreover, identification of patients in need of liver transplantation is required, especially in light of organ shortage. First promising

**Table 28.3** Histological features of ALF

<b>Histological features of ALF</b>
• Confluent hepatocyte loss
• Terminology: coagulative, eosinophilic, zonal, panlobular, multiacinar, massive
• Centro-midlobular with periportal sparing
• Periportal necrosis
• Apoptosis in portal areas
• (Necroptosis, pyroptosis might also play a role)
• Activation of HSCs
• No residual hepatocytes
• Venous outflow block
• Map-like
• Microvesicular steatosis
• “Giant cell” hepatitis and neonatal haemochromatosis
• Geographic/random with viral inclusions
• Malignant infiltration

data have been obtained with novel markers such as levels of M30 and M65 which represent either caspase 3-cleaved or non-cleaved cytokeratine 18 filaments which are highly abundant in the liver [4]. M30 seems to predict which patients will not undergo spontaneous remission. A higher proliferation rate (measured by ki-67 expression for example) identifies patients who will have a spontaneous remission [5]. Even though mini-laparoscopy is a safe procedure for ALF patients and used in some centers to discriminate ALF from AOCLF [6], it is invasive and not all patients are eligible for it. Figure 28.1 shows several examples of macroscopic alterations of the liver surface as seen by mini-laparoscopy [5]. Liver biopsy should always be a consideration in patients with ALF to rapidly confirm the diagnosis or to measure levels of iron or copper (see also Table 28.3). However, rapid decline of coagulation parameters due to liver failure can be a limiting factor for biopsy despite trans-jugular options. Hence, it is necessary to establish other methods that are able to predict outcome/likelihood of a spontaneous remission or the need for a liver transplantation, such as measuring LS.

## What Is the Underlying Cause for Elevated LS in ALF?

LS measurement has been explored in a few studies in patients with ALF starting in 2008 [7, 8], and a summary of the findings is provided in Table 28.4. In chronic liver disease, progressive hepatocyte apoptosis will eventually lead to liver fibrosis over longer time periods. Hepatic stellate cells (HSC) differentiate into contractile myofibroblasts, which lead to tissue repair alongside regions of cellular collapse [7, 8]. Already in these first publications, it was suspected that LS elevation in this setting in ALF is rather due to liver edema, inflammatory infiltration, and tissue necrosis than fibrosis itself (see Fig. 28.2) [9].

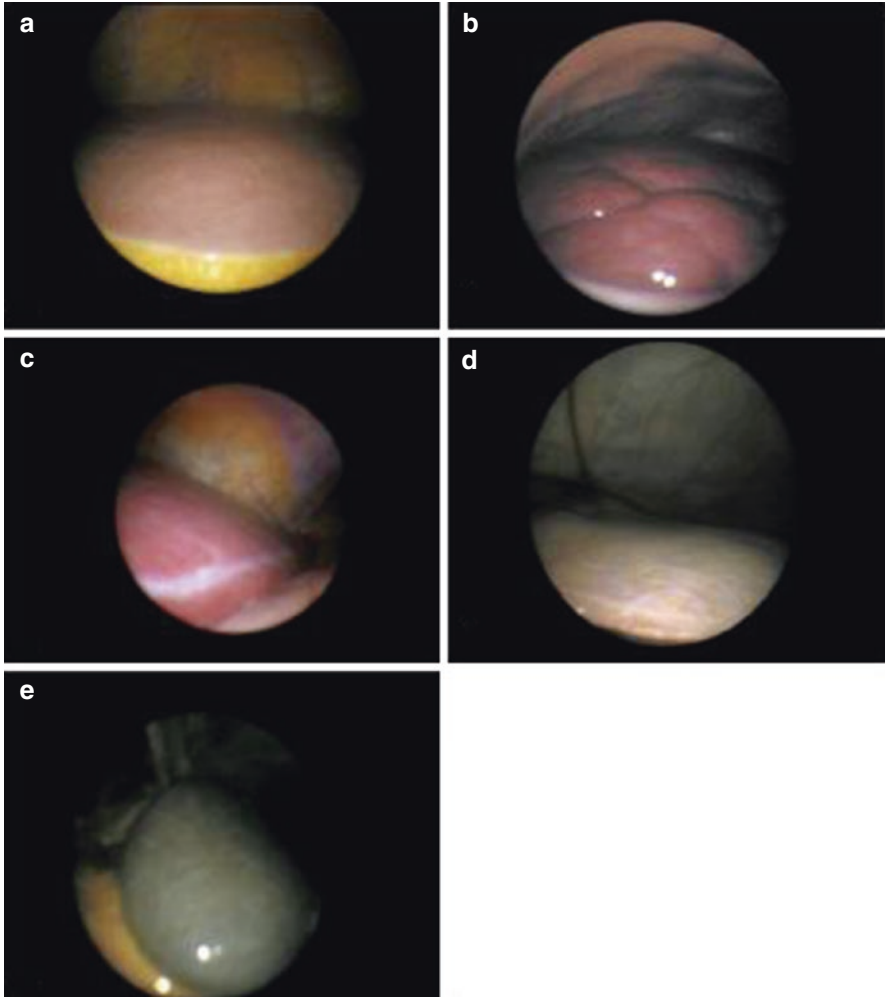


**Fig. 28.1** Typical macroscopic alterations of the liver surface. Depicted are (a) a healthy liver, (b) regenerative nodules, mild (c) and severe (d) capsular fibrosis, and (e) cholestasis [5]

In a study [6] conducted at the University Hospital Essen, it was tested if hepatocellular death activates HSCs and fibrogenesis, if an ongoing fibrogenesis is associated with increased LS, and if the remodeling of the extracellular matrix is indicative of a positive outcome in ALF. Twenty-nine (29) ALF patients were examined on their day of admission and after 1 week of hospitalization. The tests included standard laboratory parameters, fibrogenesis and cell death markers, LS measurements using FibroScan<sup>®</sup>, and liver biopsy in 13 out of 29 patients. The study cohort could then be split according to LS development during the first week: either decreased or increased LS. Compared to healthy controls, the cytokeratin-18 (M65) and caspase-cleaved cytokeratin-18 neo-epitope (M30) were significantly increased in both groups, indicating massive cell death due to necrosis and apoptosis.

**Table 28.4** LS and lab parameters

	Reference for healthy individuals	Total	Group 1: increase in FibroScan (n = 11)	Group 2: decrease in FibroScan (n = 16)
LS at ALF diagnosis (kPa)	Up to 6 (*Foucher et al., Gut, 2006;55:403–408)	25.6 ± 3.0	22.2 ± 4.8	32.4 ± 5.9
LS 7 days after diagnosis (kPa)		20.9 ± 3.2	26.3 ± 4.3	12.9 ± 2.1
Bilirubin (mg/dL)	0.3–1.2	14.8 ± 8.7	20 ± 7.7	10 ± 6.8
INR	1.0	2.7 ± 2.4	3 ± 3.4	2 ± 0.6
AST (IU/L)	0–34	4169 ± 5083	4043 ± 3637	4273 ± 6065
ALT (IU/L)	0–34	3372 ± 3201	3589 ± 2383	3196 ± 1679
γGT (IU/L)	0–34	264 ± 258	312 ± 250	225 ± 267
AP (IU/L)	25–100	224 ± 202	348 ± 271	223 ± 252
Creatinine (mg/dL)	0.6–1.1	1.8 ± 1.9	2.0 ± 2.7	1.0 ± 0.7
MELD	–	25 ± 9	25 ± 11	24 ± 5
HSC activation score	–	–	6.4 (3.94–8.93) <sup>a</sup>	2.1 (0.96–8.9) <sup>a</sup>

Data are presented as means of peak values and standard deviations, Dechene et al. [6]

<sup>a</sup>P = 0.04 (independent t-test)

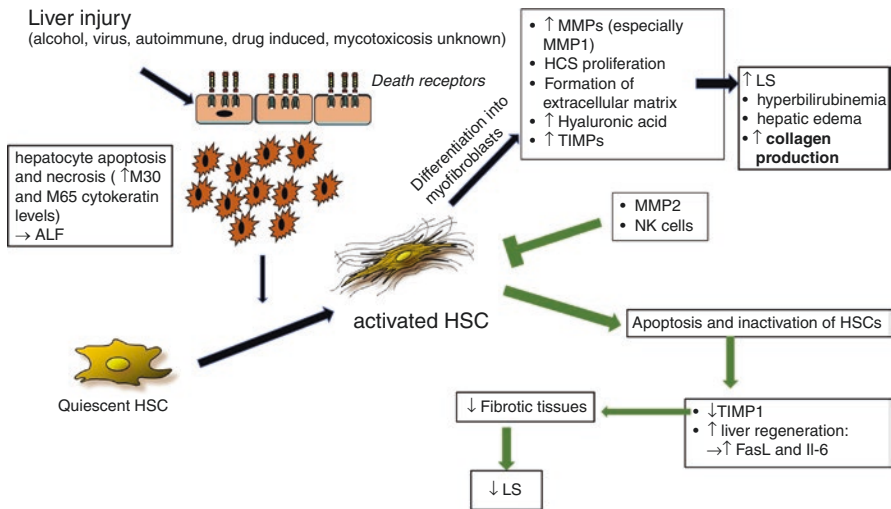


**Fig. 28.2** Pathomechanism in acute liver failure. Shown are fibrotic mechanisms/serum marker changes during ALF (black arrows) and restoration after ALF (green arrow)

After a week, these markers were not elevated significantly anymore in both groups. Signs of liver regeneration were evident by testing for interleukin-6 (IL-6) and Fas (CD95) and Fas ligand (FasL) being known as well-established parameters of liver regeneration [10, 11]. A significant increase of fibrogenic markers such as TIMP-1 and TIMP-2, MMP-1 and MMP-2 as well as hyaluronic acid was observed.

Histological analysis showed collagen fibers around apoptotic/necrotic regions as well as an abundant HSC activation in areas of liver tissues with widespread cell death. Notably, HSC activation was correlated with LS. A schematic overview of serum marker changes in ALF is shown in Fig. 28.2.

LS seems to be increased as a combination of hepatocyte edema, bilirubin elevation, and intrahepatic collagen deposition. In both groups, the LS was significantly increased compared to healthy controls. Interestingly, the increased LS was measured in those patients who also showed higher cell death levels and TIMP-1 values.

A significant correlation was found after 7 days in patients with TIMP-1, MMP-2, hyaluronic acid, and M65. Additionally, the MMP-1 expression on admission was negatively correlated with LS. This could indicate an early influence of MMP-1 expression on recovery from fibrosis.

This study shows at several levels that fibrogenesis is a part of ALF and can contribute to increased LS. The fibrosis might serve as a wound-healing process by transiently conserving the organ's structure until the defective tissue areas are replaced by functional hepatocytes and accessory cells. The resolution of fibrosis is linked to apoptosis of activated HSCs [12]. This in return seems possible because of natural killer cells, which eliminate TIMP-1 [13]. Another finding of this study is that LS was decreasing in patients being compromised through a short-term liver damage such as toxicity or mycotoxicosis. The LS increased in patients with a continuous liver injury through viral hepatitis or heart failure. Meanwhile, these results could be confirmed by others [14].

## **What Techniques Can Be Used to Measure Liver Stiffness in ALF?**

So far, transient elastography (FibroScan<sup>®</sup>) and acoustic radiation force impulse elastography (ARFI elastography, pSWE) have been explored in the setting of ALF. A challenge with LS measurement is the fact that it is affected by other confounders that may be relevant in patients with ALF. For example, cardiac failure [15], portal hypertension [16], and acute inflammatory infiltrates can also increase the LS [17, 18]. For more details see also book Part IV "Important (Patho) Physiological Confounders of LS." Nevertheless, caution should be taken to judge a patient's liver function solely based on LS.

## **Is There an Increase in Liver Stiffness in Acute-on-Chronic Liver Failure?**

Several studies have shown [19, 20] that LS increases in patients with AOCLF. However, since LS will decrease again to their basal LS after the acute injury has stopped or has been treated, its prognostic power remains unclear. AOCLF can occur due to an infection, relapse of alcohol consumption, or non-compliance



regarding medication (for instance stopping HBV/HCV medication). Pathophysiologically, an increased LS in these cases could be due to an acute (aminotransferase) flare or due to necro-inflammatory activity [21]. For more details, see also book Part IV “Important (Patho)Physiological Confounders of LS.”

## Future Directions

Measuring LS in patients with ALF can be used as a precise and an early biomarker of fulminant hepatitis in combination with total bilirubin, hepatocyte growth factor, and platelet count [22, 23]. It correlates with ALT [24] and an increase in total bilirubin in acute hepatitis is also associated with LS elevation [25]. By measuring LS at two time points (for example, day 0 and 7 of hospital admission), a better prognosis estimation can be achieved. Interestingly, different etiologies of ALF can be grouped into different behaviors of LS development. This could also be a potential tool to estimate prognosis. LS can also be used as a discriminatory tool to decide which patients need to undergo liver biopsy. However, further studies are necessary to decide on a stiffness threshold [26]. Quite established, LS can be used as a measurement of treatment success in patients with ALF. One challenge especially of transient elastography is the poor performance in severely obese individuals. The incidence of obese patients with ALF will most likely be an increasing problem in the future.

## Conclusion

1. ALF is associated with fibrogenesis, which is probably necessary for liver regeneration.
2. LS correlates with the severity of ALF cases.
3. LS development over the course of a week allows to estimate the prognostic outcome.
4. It is important to differ between ALF and AOCLF patients.
5. Prognosis in ALF should be made through a multi-methodological approach: serum markers, LS measurement.
6. LS measurement is not feasible in AOCLF cases.

## References

1. Gottlieb A, Kottmann M, Manka P, Bedreli S, Hadem J, Bechmann L, et al. How to define acute liver failure patients with pre-existing liver disease without signs of cirrhosis. *Dig Dis*. 2018;37(2):147–54.
2. Stephen M, Riordan RW. Mechanisms of hepatocyte injury, multiorgan failure, and prognostic criteria in acute liver failure. *Semin Liver Dis*. 2003;23(3):203–16.

3. Rutherford A, Chung R. Acute liver failure: mechanisms of hepatocyte injury and regeneration. *Semin Liver Dis.* 2008;28(2):167–74.
4. Bechmann LP, Jochum C, Kocabayoglu P, Sowa JP, Kassalik M, Gieseler RK, et al. Cytokeratin 18-based modification of the MELD score improves prediction of spontaneous survival after acute liver injury. *J Hepatol.* 2010;53(4):639–47.
5. Dechene A, Sowa JP, Schlattjan M, Wree A, Blomeyer S, Best J, et al. Mini-laparoscopy guided liver biopsy increases diagnostic accuracy in acute liver failure. *Digestion.* 2014;90(4):240–7.
6. Dechêne A, Sowa J-P, Gieseler RK, Jochum C, Bechmann LP, El Fouly A, et al. Acute liver failure is associated with elevated liver stiffness and hepatic stellate cell activation. *Hepatology.* 2010;52(3):1008–16.
7. Parola M, Marra F, Pinzani M. Myofibroblast—like cells and liver fibrogenesis: emerging concepts in a rapidly moving scenario. *Mol Asp Med.* 2008;29(1–2):58–66.
8. Wirz W, Antoine M, Tag CG, Gressner AM, Korff T, Hellerbrand C, et al. Hepatic stellate cells display a functional vascular smooth muscle cell phenotype in a three-dimensional co-culture model with endothelial cells. *Differentiation.* 2008;76(7):784–94.
9. Arena U, Vizzutti F, Corti G, Ambu S, Stasi C, Bresci S, et al. Acute viral hepatitis increases liver stiffness values measured by transient elastography. *Hepatology.* 2007;47(2):380–4.
10. Desbarats J, Newell MK. Fas engagement accelerates liver regeneration after partial hepatectomy. *Nat Med.* 2000;6(8):920–3.
11. Volkman X, Anstaett M, Hadem J, Stiefel P, Bahr MJ, Lehner F, et al. Caspase activation is associated with spontaneous recovery from acute liver failure. *Hepatology.* 2008;47(5):1624–33.
12. Jeong W-I, Park O, Radaeva S, Gao B. STAT1 inhibits liver fibrosis in mice by inhibiting stellate cell proliferation and stimulating NK cell cytotoxicity. *Hepatology.* 2006;44(6):1441–51.
13. Gao B, Radaeva S. Natural killer and natural killer T cells in liver fibrosis. *Biochim Biophys Acta.* 2013;1832(7):1061–9.
14. He Y, Jin L, Wang J, Yan Z, Chen T, Zhao Y. Mechanisms of fibrosis in acute liver failure. *Liver Int.* 2015;35(7):1877–85.
15. Millonig G, Friedrich S, Adolf S, Fonouni H, Golriz M, Mehrabi A, et al. Liver stiffness is directly influenced by central venous pressure. *J Hepatol.* 2010;52(2):206–10.
16. Piecha F, Paech D, Sollors J, Seitz HK, Rossle M, Rausch V, et al. Rapid change of liver stiffness after variceal ligation and TIPS implantation. *Am J Physiol Gastrointest Liver Physiol.* 2018;314(2):G179–G87.
17. Pinzani M, Vizzutti F, Arena U, Marra F. Technology insight: noninvasive assessment of liver fibrosis by biochemical scores and elastography. *Nat Clin Pract Gastroenterol Hepatol.* 2008;5(2):95–106.
18. Mueller S, Sandrin L. Liver stiffness: a novel parameter for the diagnosis of liver disease. *Hepat Med.* 2010;2:49–67.
19. Sagir A, Glaubach B, Sahin K, Graf D, Erhardt A, Oette M, et al. Transient elastography for the detection of liver damage in patients with HIV. *Infect Dis Ther.* 2015;4(3):355–64.
20. Sagir A, Ney D, Oh J, Pandey S, Kircheis G, Mayatepek E, et al. Evaluation of acoustic radiation force impulse imaging (ARFI) for the determination of liver stiffness using transient elastography as a reference in children. *Ultrasound Int Open.* 2015;01(01):E2–7.
21. Cobbold JFL, Taylor-Robinson SD. Transient elastography in acute hepatitis: all that's stiff is not fibrosis. *Hepatology.* 2008;47(2):370–2.
22. Friedrich-Rust M, Lupsor M, de Knegt R, Dries V, Buggisch P, Gebel M, et al. Point shear wave elastography by acoustic radiation force impulse quantification in comparison to transient elastography for the noninvasive assessment of liver fibrosis in chronic hepatitis C: a prospective international multicenter study. *Ultraschall Med.* 2015;36(03):239–47.
23. Kuroda H, Kakisaka K, Oikawa T, Onodera M, Miyamoto Y, Sawara K, et al. Liver stiffness measured by acoustic radiation force impulse elastography reflects the severity of liver damage and prognosis in patients with acute liver failure. *Hepatol Res.* 2014;45(5):571–7.

24. Coco B, Oliveri F, Maina AM, Ciccorossi P, Sacco R, Colombatto P, et al. Transient elastography: a new surrogate marker of liver fibrosis influenced by major changes of transaminases. *J Viral Hepat.* 2007;14(5):360–9.
25. Sagir A, Heintges T, Akyazi Z, Oette M, Erhardt A, Haussinger D. Therapy outcome in patients with chronic hepatitis C: role of therapy supervision by expert hepatologists. *J Viral Hepat.* 2007;14(9):633–8.
26. Taylor-Robinson SD, Cobbold JFL, Thomas HC. Liver stiffness measurements in acute hepatitis B: implications for clinical practice. *Eur J Gastroenterol Hepatol.* 2010;22(2):133–4.

# Chapter 29

## Liver Stiffness and Pregnancy



Omar Elshaarawy, Johannes Mueller, and Sebastian Mueller

### Introduction

Although complications during pregnancy have been significantly decreased over the decades, problematic pregnancies still occur and lead to death in 1 per 4000 pregnancies in developed countries [1]. Besides postpartum bleeding and embolic complications, liver-related complications are observed in ~3% of all pregnancies and can lead to high maternal and perinatal mortality [2–4]. Most pregnancy complications, besides hyperemesis gravidarum, occur usually in the last 3 months of pregnancy, for example, intrahepatic cholestasis (ICP) and HELLP syndrome. These complications can be accompanied by increased portal pressure. Management of these complications can be challenging since treatment decisions need to consider both the health of the mother and the fetus, and it becomes even more complicated if the pregnant woman has an already existing liver disease.

Screening for these liver-related complications involves normally lab testing of liver transaminases and gGT, only if abnormalities are found and liver sonography is performed. However, the usefulness of these parameters for the prediction of severe complications during pregnancy is limited [5]. So far, no screening test is established for the early prediction of these pregnancy complications since liver tests can be elevated during normal pregnancy [6, 7].

---

O. Elshaarawy · J. Mueller · S. Mueller (✉)

Department of Medicine and Center for Alcohol Research and Liver Diseases, Salem Medical Center, University of Heidelberg, Heidelberg, Germany

e-mail: [oelshaarawy@liver.menofia.edu.eg](mailto:oelshaarawy@liver.menofia.edu.eg); [Sebastian.Mueller@urz.uni-heidelberg.de](mailto:Sebastian.Mueller@urz.uni-heidelberg.de)

In chronic liver disease, apart from pregnancy, measurement of liver stiffness (LS) has become the parameter of choice to assess liver fibrosis in a non-invasive manner [8–10]. The advantages are that it is easy to learn and does not require a dedicated ultrasound device [11]. Furthermore, it is non-invasive, has a lower sampling error and better interobserver reliability as compared to liver biopsy, which ideally render it for follow-up measurements [8, 12].

## Spectrum of Liver Diseases During Pregnancy

Liver disease during pregnancy is a challenging clinical issue that includes pregnancy-specific liver diseases in addition to any liver disease that could affect a pregnant woman. Pregnancy-specific liver diseases are listed in Table 29.1 and include:

1. Hyperemesis gravidarum which is defined as nausea and intractable vomiting resulting in dehydration, ketosis, and weight loss of more than 5% [13];
2. Intrahepatic cholestasis of pregnancy (ICP) which typically presents in the last two trimesters and is characterized by persistent pruritus, typically in the palms and soles, and more severe overnight [14];
3. Acute fatty liver of pregnancy which is rare but highly threatening hepatic disease occurring during the last trimester of pregnancy [15]. This pathology is characterized by micro-vesicular steatosis in the hepatocytes of zone 3 (centri-lobular), rapid loss of liver function, jaundice, and coagulopathy requiring maternal supportive care;
4. Preeclampsia that is a pregnancy-specific systemic disorder characterized by new onset hypertension (systolic blood pressure 140 mmHg or diastolic blood pressure 90 mmHg) and proteinuria (300 mg/d) after 20 weeks of gestation [16];
5. The HELLP syndrome which is considered to be a complication of preeclampsia and occurs in approximately 10% of women with severe preeclampsia. This syndrome is characterized by hemolytic anemia, increased liver enzyme levels, and low platelet count [17].

## LS in Uncomplicated Pregnancy

So far, two studies exist which investigated the development of LS during normal pregnancy and the feasibility for the prediction of liver-related complications [18, 19]. These studies did not observe any complications due to elastography-related energy transfer. Thus, pregnancy should not be considered a contraindication for transient elastography. Whether ARFI or SSI is applicable in pregnant women needs to be clarified since higher ultrasound energy can be applied locally. In a large study from our center, 537 pregnant women were investigated with TE. About 91% of the women could be measured with the M probe and in 9% the XL probe had to be used. Using both probes, LSM could be obtained in all women. This study showed that LS

**Table 29.1** Liver stiffness and characteristic findings of liver-associated complications during pregnancy [14–18]

Disease	HG	ICP	AFLP	Pre-eclampsia	HELLP syndrome
Trimester	First	Second–third	Third–postpartum	>20 weeks	Third–postpartum
Frequency	0.3–2%	0.1–5%	0.01%	5–10%	0.2–0.6%
Clinical features	Vomiting, dehydration, weight loss, ketosis	Pruritus, jaundice (25%)	Abdominal pain, vomiting, polydipsia/polyuria, encephalopathy	Abdominal pain, hypertension, proteinuria, headache, blurred vision, peripheral edema	Abdominal pain, vomiting, proteinuria, headache, peripheral edema
Liver stiffness	–	↑	no data available	↑	↑↑ (case observations [24])
Ascites	–	–	+/-	–	–
Platelets	–	–	↓	↓	↓
Hemolysis	–	–	–	↑	+/- ↑
Bilirubin	<4 mg/dL	<5 mg/dL	<10 mg/dL	<5 mg/dL	<5 mg/dL
Bile acids	–	30–100×	–	–	–
AST levels	1–2× (50%)	1–5×	5–10×	1–100× (20–30%)	1–100×
LDH	–	–	↑	↑	≥600 IU/L
ALP	–	↑	↑	↑ mild	↑
Hypoglycemia	–	–	+/-	–	–
Uric acid	–	–	↑ (80%)	↑	↑
Creatinine	–	–	↑	↑	–
Proteinuria	–	–	+/- ↑	↑	+/- ↑
Liver imaging (US, CT)	Normal parenchyma without biliary obstruction	Should excluded cholelithiasis	Fatty infiltration, bright liver	Hepatic infarcts, hematomas, rupture	Hepatic infarcts, hematomas, rupture

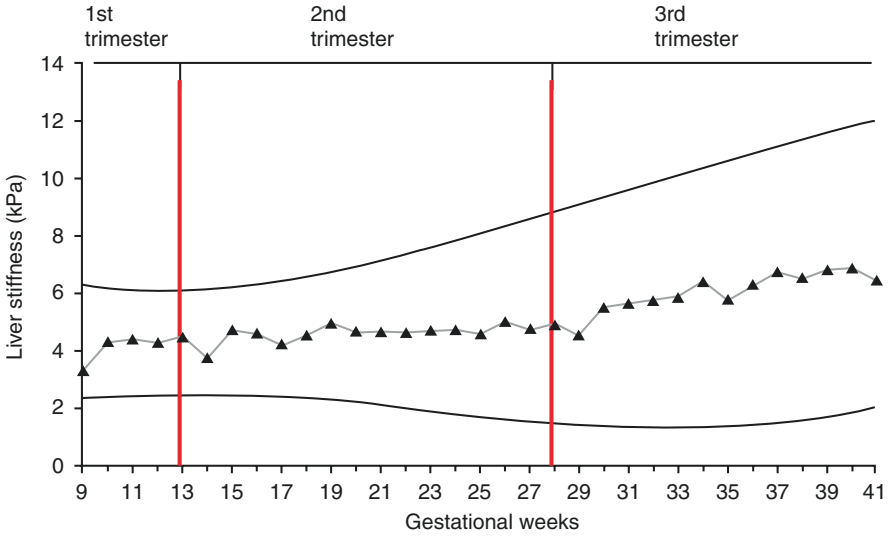
(continued)

Table 29.1 (continued)

Disease	HG	ICP	AFLP	Pre-eclampsia	HELLP syndrome
Liver histopathology	–	Hepatocellular bile and canalicular bile plugs, cholestasis without parenchymal inflammation	Micro vesicular steatosis, foamy hepatocytes, hepatic necrosis	Fibrin deposition, hemorrhage, hepatocellular necrosis	Fibrin deposition, hemorrhage, hepatocellular necrosis
Complications	Usually resolves by 18 weeks without complications	Late intrauterine death	Maternal and fetal/perinatal mortality. 50% will have evidence of PE	Liver rupture and necrosis. Maternal and fetal/perinatal mortality	Maternal and fetal/perinatal mortality
Treatment	Supportive, rehydration, antiemetics, vitamins supplementation: B1, B6, B12, C	Ursodesoxycholic acid and delivery at 37 weeks	Delivery at 34 weeks	Control of hypertension and urgent delivery to avoid eclampsia	Delivery at 34 weeks or even before 24–34 weeks given corticosteroids for fetal lung maturation
Recurrence	+++	+++	Rarely 25% risk in defects of fatty acids oxidation	++	++ (4–19%)

Abbreviations: *AFLP* acute fatty liver of pregnancy, *HELLP syndrome* hemolysis, elevated liver enzymes and low platelets, *HG* hyperemesis gravidarum, *ICP* intrahepatic cholestasis of pregnancy

increases with gestational age in normal uncomplicated pregnancies and can be elevated above the 6 kPa limit, which is usually considered as normal LS cut-off value (see Fig. 29.1). 25% of all women and ~40% of women in the final trimester showed an LS higher than 6 kPa. In detail, median LS in the first trimester was 4.3 kPa, in the second trimester 4.5 kPa, and in the third trimester, it raised to 5.4 kPa. The highest value observed was 20.7 kPa. Notably, LS rapidly normalized in all women within 24 h after delivery (Fig. 29.2). Thus, LS can be elevated during



**Fig. 29.1** Liver stiffness during uncomplicated pregnancy. In the third trimester, liver stiffness exceeds 6 kPa in 41% of pregnancies. Mean LS is given per gestational week. (Modified from [1])

**Fig. 29.2** LS in normal pregnancies in the third trimester and 24 h after delivery (n=26). Shown are mean and standard deviation. (Modified from [1])

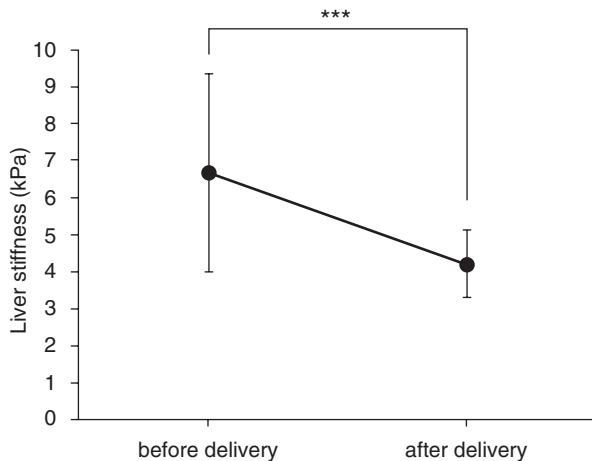
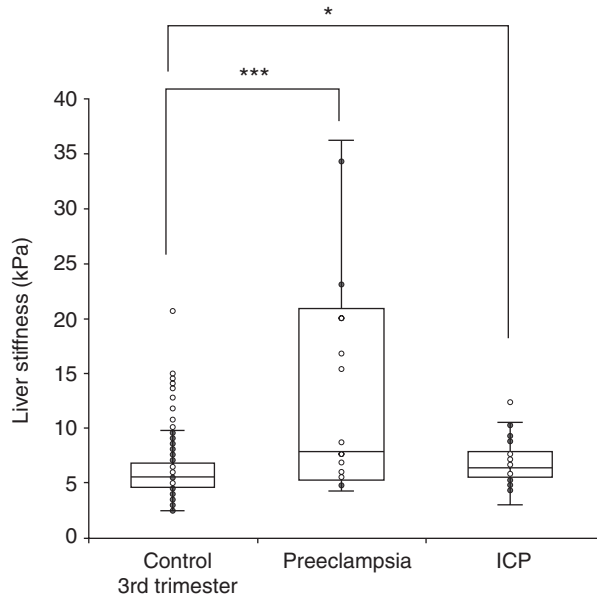




**Fig. 29.3** Comparison of LS between normal pregnancies, women with preeclampsia and intrahepatic cholestasis of pregnancy (ICP). Data are from the third trimester only. (Modified from [1])



normal pregnancy which should not be mistaken for a manifest liver disorder (Fig. 29.3).

The cause for the LS elevation, however, could not be identified in the study. Correlations were seen with increased body weight and BMI, weak correlations with spleen size, and nulliparous state. In multivariate analysis, gestational age and fetus weight were independent predictors for a LS increase beyond 6 kPa. One can only speculate about the reason for the increase in LS. Earlier studies showed that a mere increase in intraabdominal pressure per se does not lead to increased LS [20]. This rapid decrease of LS after delivery points towards a mechanical cause such as hemodynamic changes since liver inflammation or apoptosis usually do not resolve within 1 day. The weak correlation of LS with spleen size is highly suggestive of increased portal pressure [21, 22]. LS association of nulliparous state, typically a condition that favors pregnancy complications, further points towards potential mechanic issues encountered during the pregnancy. It is well known that uncomplicated pregnancies lower the risk for complications in following pregnancies, and it could point towards a “training” effect. Although not confirmed in this study, an impaired hepatic venous outflow could be another explanation causing liver congestion and LS elevation [23]. Finally, no elevation of controlled attenuation parameter (CAP) as surrogate marker for hepatic steatosis was observed in this large study.

In a recent study, Stinberg Riobero et al. could confirm the above findings in a much smaller cohort [19]. In this study from Denmark, 24 healthy women with normal pregnancies were prospectively followed up. All women underwent transient elastography at gestational week 18–20, week 26–28, and week 36–38, as well as after a minimum of 8 weeks postpartum. Mean age at baseline was 30.6 years, mean BMI was 22.3 kg/m<sup>2</sup>, and 14 women (58%) were nulliparous.

Pregnancy outcome was normal, and no cases of preeclampsia or gestational diabetes were observed. Mean LS increased from 3.8 kPa during the second trimester to 5.9 kPa during the third trimester. In the third trimester, LS increased in two women to more than 7.9 kPa. In confirmation of the earlier report, LS had normalized in 8 weeks after delivery. In contrast to the German study, CAP increased from 186 dB/m in the second trimester to 215 dB/m in the third trimester.

## LS as a Predictor for Pregnancy Complications

In the German study, two subgroups with complications were analyzed encompassing preeclampsia ( $n = 22$ ) and ICP ( $n = 40$ ). Both groups had an increased LS as compared to normal pregnancies in the third trimester with a mean LS of 17.9 kPa for preeclampsia and 6.9 kPa for ICP (AUROC 0.82). In the multivariate model, LS together with leucocytes were independent predictors of preeclampsia. Women with LS greater than 8 kPa had a twice higher risk to develop preeclampsia. In contrast, pruritus and ALT levels were significant predictors for ICP but not LS. Although LS also decreased in women with preeclampsia, it did not resolve to normal levels below 6 kPa.

## Conclusion

LS increases during pregnancy in 25% of all women, almost exclusively in the third trimester and rapidly normalizes within 24 h after delivery. Therefore, an elevated LS during pregnancy should not be mistaken as liver fibrosis or disease. On the other side, LS is significantly associated with complications of pregnancy such as preeclampsia or ICP.

## References

1. Hill K, AbouZhar C, Wardlaw T. Estimates of maternal mortality for 1995. *Bull World Health Organ.* 2001;79(3):182–93.
2. Clark SL, Belfort MA, Dildy GA, Herbst MA, Meyers JA, Hankins GD. Maternal death in the 21st century: causes, prevention, and relationship to cesarean delivery. *Am J Obstet Gynecol.* 2008;199(1):36 e1–5. discussion 91–2 e7–11.
3. Steegers EA, von Dadelszen P, Duvekot JJ, Pijnenborg R. Pre-eclampsia. *Lancet.* 2010;376(9741):631–44.
4. Westbrook RH, Dusheiko G, Williamson C. Pregnancy and liver disease. *J Hepatol.* 2016;64(4):933–45.
5. Suresh I, Tr V, Hp N. Predictors of fetal and maternal outcome in the crucible of hepatic dysfunction during pregnancy. *Gastroenterology Res.* 2017;10(1):21–7.

6. Poon LC, Kametas NA, Chelemen T, Leal A, Nicolaides KH. Maternal risk factors for hypertensive disorders in pregnancy: a multivariate approach. *J Hum Hypertens*. 2010;24(2):104–10.
7. Tran TT, Ahn J, Reau NS. ACG clinical guideline: liver disease and pregnancy. *Am J Gastroenterol*. 2016;111(2):176–94. quiz 96.
8. Mueller S, Sandrin L. Liver stiffness: a novel parameter for the diagnosis of liver disease. *Hepat Med*. 2010;2:49–67.
9. Sandrin L, Fourquet B, Hasquenoph J-M, Yon S, Fournier C, Mal F, et al. Transient elastography: a new non-invasive method for assessment of hepatic fibrosis. *Ultrasound Med Biol*. 2003;29(12):1705–13.
10. Foucher J, Chanteloup E, Vergniol J, Castera L, Le Bail B, Adhoute X, et al. Diagnosis of cirrhosis by transient elastography (FibroScan): a prospective study. *Gut*. 2006;55(3):403–8.
11. Nahon P, Thabut G, Ziol M, Htar MT, Cesaro F, Barget N, et al. Liver stiffness measurement versus clinicians' prediction or both for the assessment of liver fibrosis in patients with chronic hepatitis C. *Am J Gastroenterol*. 2006;101(12):2744–51.
12. Colletta C, Smirne C, Fabris C, Toniutto P, Rapetti R, Minisini R, et al. Value of two noninvasive methods to detect progression of fibrosis among HCV carriers with normal aminotransferases. *Hepatology*. 2005;42(4):838–45.
13. Kamimura K, Abe H, Kawai H, Kamimura H, Kobayashi Y, Nomoto M, et al. Advances in understanding and treating liver diseases during pregnancy: a review. *World J Gastroenterol*. 2015;21(17):5183–90.
14. Shekhar S, Diddi G. Liver disease in pregnancy. *Taiwan J Obstet Gynecol*. 2015;54(5):475–82.
15. Liu J, Ghaziani TT, Wolf JL. Acute fatty liver disease of pregnancy: updates in pathogenesis, diagnosis, and management. *Am J Gastroenterol*. 2017;112(6):838–46.
16. Gomes CF, Sousa M, Lourenço I, Martins D, Torres J. Gastrointestinal diseases during pregnancy: what does the gastroenterologist need to know? *Ann Gastroenterol*. 2018;31(4):385–94.
17. Kelly C, Pericleous M. Pregnancy-associated liver disease: a curriculum-based review. *Frontline Gastroenterol*. 2018;9(3):170–4.
18. Ammon FJ, Kohlhaas A, Elshaarawy O, Mueller J, Bruckner T, Sohn C, et al. Liver stiffness reversibly increases during pregnancy and independently predicts preeclampsia. *World J Gastroenterol*. 2018;24(38):4393–402.
19. Stenberg Ribeiro M, Hagström H, Stål P, Ajne G. Transient liver elastography in normal pregnancy—a longitudinal cohort study. *Scand J Gastroenterol*. 2019;54(6):761–5.
20. Kohlhaas A, Durango E, Millonig G, Bastard C, Sandrin L, Golriz M, et al. Transient elastography with the XL probe rapidly identifies patients with non-hepatic ascites. *Hepat Med*. 2012;4:11–8.
21. Augustin S, Millan L, Gonzalez A, Martell M, Gelabert A, Segarra A, et al. Detection of early portal hypertension with routine data and liver stiffness in patients with asymptomatic liver disease: a prospective study. *J Hepatol*. 2014;60(3):561–9.
22. Elshaarawy O, Mueller J, Guha IN, Chalmers J, Harris R, Krag A, et al. Spleen stiffness to liver stiffness ratio significantly differs between ALD and HCV and predicts disease-specific complications. *JHEP Rep*. 2019;1(2):99–106.
23. Millonig G, Friedrich S, Adolf S, Fonouni H, Golriz M, Mehrabi A, et al. Liver stiffness is directly influenced by central venous pressure. *J Hepatol*. 2010;52(2):206–10.
24. Mueller S. Personal observation. 2019.

**Part V**  
**Liver Stiffness and Important Clinical**  
**Endpoints**

# Chapter 30

## Liver Stiffness and Important Clinical Endpoints



Sebastian Mueller

### Introduction

Liver cirrhosis is among the top leading causes of death worldwide. As shown in Fig. 30.1, it has two clinically-defined conditions consisting of *compensated* and *decompensated* cirrhosis [1]. Decompensation is defined as the onset of severe clinical symptoms including ascites, bleeding, hepatic encephalopathy, hepatorenal syndrome, or jaundice that are all associated with unfavorable prognosis [2–4]. The management of cirrhotic patients depends on the liver function reservoir and the presence of these liver cirrhosis-related events. The progression toward decompensation is the leading cause of morbidity and mortality among those cirrhotic patients [5]. Hepatic decompensation is considered to be an impairment of blood flow through the portal vein and increased portal pressure [6]. In this book section, various chapters will cover these major endpoints including decompensation (bleeding, encephalopathy, ascites, liver failure), HCC, liver-related death, or all-cause related death.

### LS Cutoff Values and Clinical Endpoints

Although several studies have explored these endpoints, still more studies are required for definite answers. A summary of important cutoff values taken from various studies of the following chapters are depicted in Fig. 30.2. While a LS of 6–8 kPa almost excludes hepatic complications (exception e.g., HBV-related

---

S. Mueller (✉)

Department of Medicine and Center for Alcohol Research and Liver Diseases,  
Salem Medical Center, University of Heidelberg, Heidelberg, Germany  
e-mail: [sebastian.mueller@urz.uni-heidelberg.de](mailto:sebastian.mueller@urz.uni-heidelberg.de)

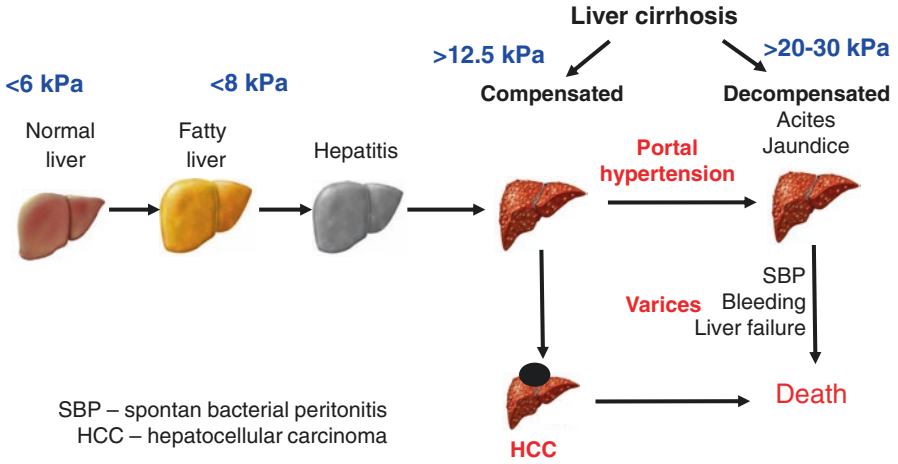


**Fig. 30.1** Progression of liver fibrosis and important clinical endpoints such as decompensation, HCC and liver-related, and all-cause death

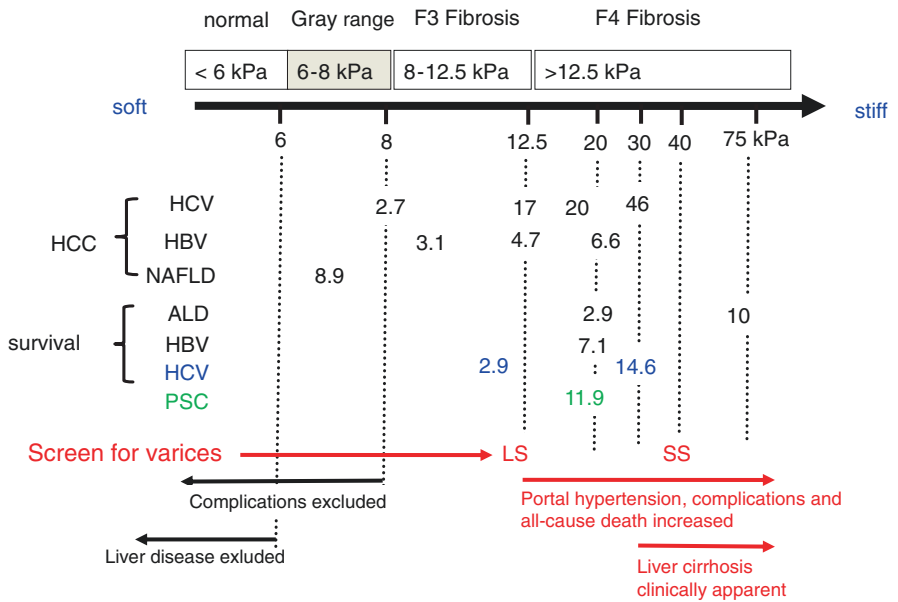


**Fig. 30.2** Liver stiffness cutoff values and reported hazard ratios for various clinical endpoints

liver cancer), it becomes increasingly clear that a LS > 12.5 kPa not only defines the onset of clinically significant portal hypertension but also above-mentioned complications and all-cause mortality. At LS values >30 kPa, liver cirrhosis becomes usually clinically apparent, ascites will be omnipresent and serum markers are better predictors of death within the 12 months range. Therefore, these LS values represent important screening cutoff values. The additional assessment of spleen stiffness (SS) further increases the prediction of portal hypertension while further studies on survival and outcome are required. It should be also noted that LS is good predictor of HCC and could be helpful to optimize patient selection in the liver transplant setting. Here, novel data are of high interest that show HCC incidence already at lower LS values (12 kPa range). Whether this is related to portal versus lobular inflammation and can be elucidated e.g., by the SS/LS ratio, remains to be studied [7, 8].

### **Pathology of Liver Diseases and Relation to LS, SS, and the LS/SS Ratio**

Liver cirrhosis encompasses a huge variety of different dysfunctions and better standardized classifications are required to categorize the various subtypes of cirrhosis [9]. For instance, cirrhosis can present clinically either as liver failure (synthesis impairment) or with complications of portal hypertension (see Fig. 30.3). Both conditions can occur independently and determine individual prognosis. These chains of thoughts suggest that **novel subgroups** of liver cirrhosis should be defined in order to better predict distinct complications in individual patients. For instance, the degree of synthesis impairment and portal hypertension should be evaluated separately to better determine the natural course, prognosis, potential complications, and therapeutic interventions. In practice, patients can be seen with normal synthesis parameters but pronounced portal hypertension. Despite normal INR and albumin levels, they can develop massive ascites and may later die from spontaneous bacterial peritonitis or variceal bleeding. Such patients have a stiff liver and show vast matrix deposition in the biopsy. In contrast, other patients show rather early signs of jaundice and impaired coagulation tests, but portal hypertension is less pronounced.

More research needs to be done to better understand genetic determinants of these individual natural courses. As shown in Fig. 30.3, this may explain why conventional laboratory-based scores rather detect cirrhotic patients with impaired synthetic functions but overlook patients with portal hypertension. By contrast, elastographic techniques are highly sensitive to identify patients with portal hypertension as also suggested in a recent Korean study by Hong et al. [10]. The combination of LS [1, 11, 12] and SS [13–18] is an excellent predictor of portal hypertension,

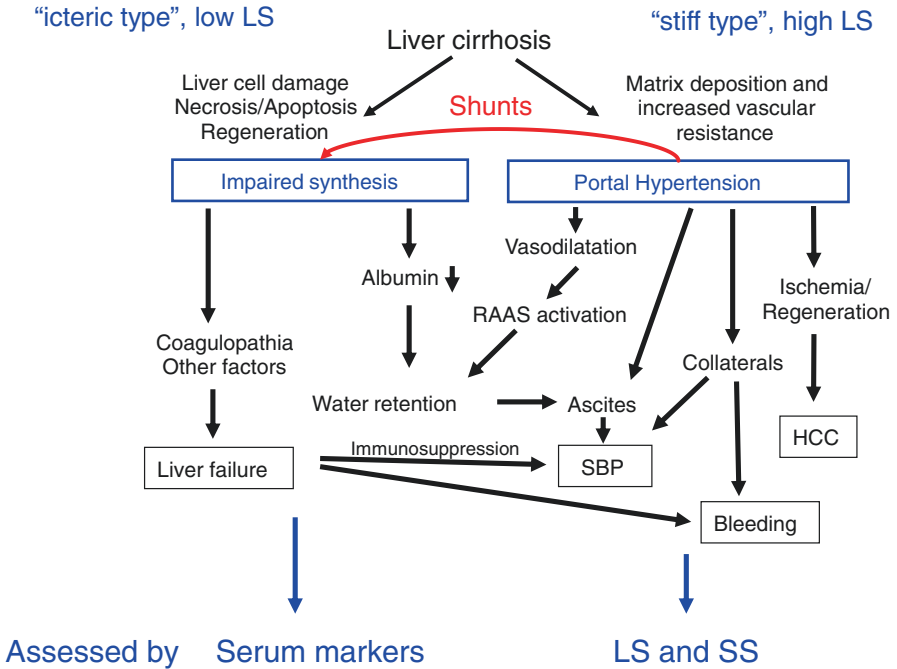


**Fig. 30.3** Liver cirrhosis encompasses a huge variety of different dysfunctions and better standardized classifications are required to categorize the various subtypes of cirrhosis. For instance, cirrhosis can present clinically either as liver failure (synthesis impairment) or complications of portal hypertension. Both conditions can occur independently in cirrhotic patients and determine individual prognosis. While synthesis is easily assessed by lab tests, elastographic techniques are the future method of choice to identify patients with portal hypertension. Both extra- and intrahepatic shunts (red arrow) not only lower portal hypertension but also the functional hepatic capacity. Ultimately, shunts lower SS and LS while serum markers of liver function will worsen. Abbreviations: *HCC* hepatocellular cancer, *LS* liver stiffness, *RAAS* renin-angiotensin converting enzyme system, *SBP* spontaneous bacterial peritonitis, *SS* spleen stiffness

esophageal varices, and even variceal bleeding. For more details see also the chapter entitled “Liver and spleen stiffness to predict portal hypertension and its complications.” While the additional assessment of spleen stiffness (SS) further increases the prediction of portal hypertension, the ratio of SS/LS seems also to provide information about disease etiology and likeliness of disease-specific complications [8].

A simplified perfusion scheme of the liver is shown in Fig. 30.4. It shows the different effects of posthepatic versus prehepatic (e.g., heart failure versus portal vein thrombosis) and lobular versus portal diseases (e.g., ALD versus HCV) on LS, SS and the SS/LS ratio. For more details see also Appendix Figs. A.8 and A.9. More work is necessary to better understand the role and pharmacological management of the so-called hepatic arterial buffer response (HABR) that steers hepatic arterial flow though portal flow in an autonomous manner [19].



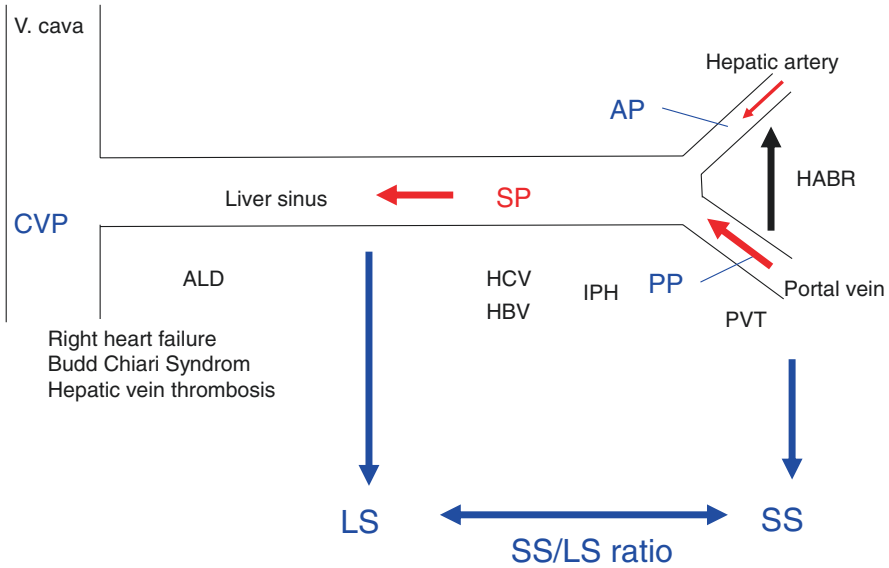


**Fig. 30.4** Simplified hemodynamic scheme of liver vascularization to explain post- versus prehepatic lesions and portal versus lobular lesions and their relation to LS, SS, and SS/LS ratio. Abbreviations: *ALD* alcoholic liver disease, *CVP* central venous pressure, *HBV* hepatitis B virus infection, *HCV* hepatitis C virus infection, *HABR* hepatic arterial buffer response, *IPH* idiopathic portal hypertension, *LS* liver stiffness, *PP* portal pressure, *PVT* portal vein thrombosis, *SS* spleen stiffness

## Role of Hepatic Shunts and Its Relation to Liver Stiffness and Fibrosis Progression

Recently, as shown in Fig. 30.5, the development of porto-systemic shunts whether of intra- or extrahepatic nature, has been proposed as underlying mechanism to explain the two major subtypes of cirrhosis (stiff versus icteric) [9]. For more details, see also the chapter on “Sinusoidal pressure hypothesis” in book section VIII “Molecular basis of liver stiffness and cell biology.” Although still in a premature stage, a first relation between formation of intra- and extrahepatic shunts becomes evident: while shunts lower portal pressure (and both LS and SS), they will decrease the exposure of blood to hepatocytes and, thus, the functional liver reserve (see also Fig. 30.3). In contrast, patients with minimal shunt volume will show soon all complications of portal pressure elevation and pressure-driven fibrosis progression but maintain good liver synthesis for a rather long time. Consequently, liver cirrhosis could be described as a body’s continued and desperate decision-making between pressure-mediated fibrogenesis and shunt-related liver failure, a jump out of the frying pan into the fire. It seems appropriate to discriminate a so-called “stiff” from an “icteric” phenotype of liver cirrhosis. It remains to be studied how an individual

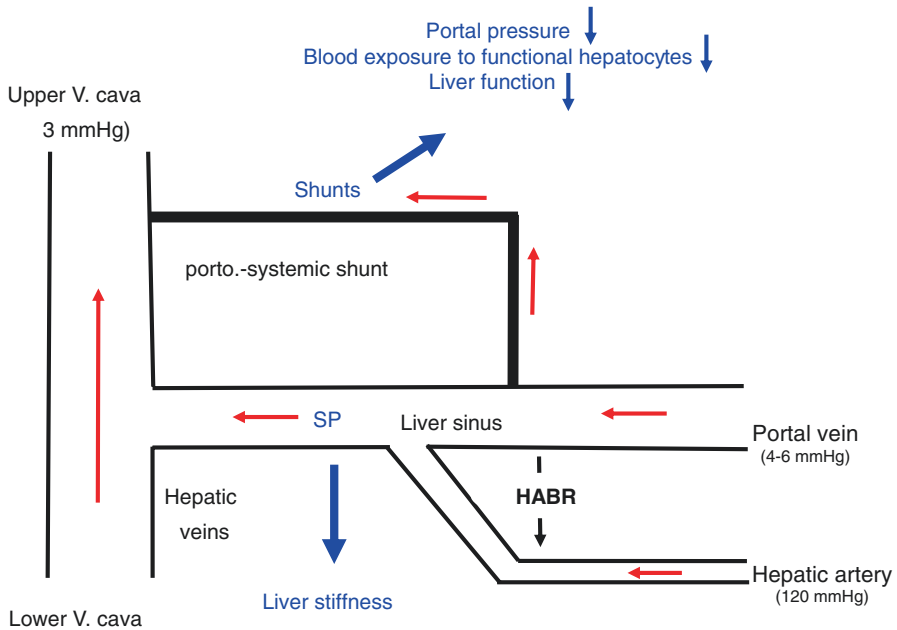


**Fig. 30.5** Simplified scheme of hepatic perfusion and role of porto-systemic shunts versus arterIALIZATION in defining the two major subtypes of liver cirrhosis (stiff type versus icteric type). Shunt formation, although ameliorating portal hypertension, will eventually bypass blood from hepatocytes and consequently decrease liver function. Decreased shunt formation will increase hepatic perfusion but expose the liver to detrimentally elevated pressure (for details see also [9])

profiling of cirrhotic patients by LSM and SSM will help to optimize the therapeutic management (e.g., by TIPS or portal pressure lowering drugs) in the future. Finally, the underlying molecular mechanisms need to be elucidated further.

## References

1. Foucher J, Chanteloup E, Vergniol J, Castera L, Le Bail B, Adhoute X, et al. Diagnosis of cirrhosis by transient elastography (FibroScan): a prospective study. *Gut*. 2006;55(3):403–8.
2. Hernandez-Gea V, Berzigotti A. Clinical evaluation and prognosis. *Dig Dis*. 2015;33(4): 515–23.
3. Ge PS, Runyon BA. Treatment of patients with cirrhosis. *N Engl J Med*. 2016;375(8):767–77.
4. Angeli P, Bernardi M, Villanueva C, Francoz C, Mookerjee RP, Trebicka J, et al. EASL Clinical Practice Guidelines for the management of patients with decompensated cirrhosis. *J Hepatol*. 2018;69(2):406–60.
5. Tsochatzis EA, Bosch J, Burroughs AK. New therapeutic paradigm for patients with cirrhosis. *Hepatology*. 2012;56(5):1983–92.
6. Sanyal AJ, Bosch J, Blei A, Arroyo V. Portal hypertension and its complications. *Gastroenterology*. 2008;134(6):1715–28.

7. Mueller S, Englert S, Seitz HK, Badea RI, Erhardt A, Bozaari B, et al. Inflammation-adapted liver stiffness values for improved fibrosis staging in patients with hepatitis C virus and alcoholic liver disease. *Liver Int.* 2015;35(12):2514–21.
8. Elshaarawy O, Mueller J, Guha IN, Chalmers J, Harris R, Krag A, et al. Spleen stiffness to liver stiffness ratio significantly differs between ALD and HCV and predicts disease-specific complications. *JHEP Rep.* 2019;1(2):99–106.
9. Mueller S. Does pressure cause liver cirrhosis? The sinusoidal pressure hypothesis. *World J Gastroenterol.* 2016;22(48):10482.
10. Hong WK, Kim MY, Baik SK, Shin SY, Kim JM, Kang YS, et al. The usefulness of non-invasive liver stiffness measurements in predicting clinically significant portal hypertension in cirrhotic patients: Korean data. *Clin Mol Hepatol.* 2013;19(4):370–5.
11. Llop E, Berzigotti A, Reig M, Erice E, Reverter E, Seijo S, et al. Assessment of portal hypertension by transient elastography in patients with compensated cirrhosis and potentially resectable liver tumors. *J Hepatol.* 2012;56(1):103–8.
12. Frulio N, Balabaud C, Bioulac-Sage P. Can elastometry be used for a better identification of cirrhosis? *Clin Res Hepatol Gastroenterol.* 2011;35(3):166–8.
13. Takuma Y, Nouse K, Morimoto Y, Tomokuni J, Sahara A, Takabatake H, et al. Prediction of oesophageal variceal bleeding by measuring spleen stiffness in patients with liver cirrhosis. *Gut.* 2016;65(2):354.
14. Sharma P, Kirnake V, Tyagi P, Bansal N, Singla V, Kumar A, et al. Spleen stiffness in patients with cirrhosis in predicting esophageal varices. *Am J Gastroenterol.* 2013;108(7):1101–7.
15. Colecchia A, Colli A, Casazza G, Mandolesi D, Schiumerini R, Reggiani LB, et al. Spleen stiffness measurement can predict clinical complications in compensated HCV-related cirrhosis: a prospective study. *J Hepatol.* 2014;60(6):1158–64.
16. Stefanescu H, Grigorescu M, Lupsor M, Maniu A, Crisan D, Procopet B, et al. A new and simple algorithm for the noninvasive assessment of esophageal varices in cirrhotic patients using serum fibrosis markers and transient elastography. *J Gastrointestin Liver Dis.* 2011;20(1):57–64.
17. Stefanescu H, Grigorescu M, Lupsor M, Procopet B, Maniu A, Badea R. Spleen stiffness measurement using Fibroscan for the noninvasive assessment of esophageal varices in liver cirrhosis patients. *J Gastroenterol Hepatol.* 2011;26(1):164–70.
18. Wang X-K, Wang P, Zhang Y, Qi S-L, Chi K, Wang G-C. A study on spleen transient elastography in predicting the degree of esophageal varices and bleeding. *Medicine.* 2019;98(9):e14615.
19. Lauth WW. Hepatic circulation: physiology and pathophysiology. Colloquium series on integrated systems physiology: from molecule to function to disease. San Rafael: Morgan and Claypool; 2009.

## Chapter 31

# Liver and Spleen Stiffness to Predict Portal Hypertension and Its Complications



Yuly P. Mendoza, Giuseppe Murgia, Susana G. Rodrigues, Maria G. Delgado, and Annalisa Berzigotti

### Introduction to Portal Hypertension: Definition and Terminology

Portal hypertension (PH) is a frequent clinical syndrome characterized by an increase in portal pressure and in the pressure gradient through the liver (i.e., between the portal venous system and the inferior vena cava or portal pressure gradient, PPG). From a hemodynamic point of view, pressure in a hydraulic system is the result of the interaction of resistance and flow ( $P = \text{resistance} \times \text{flow}$ ; Ohm's law). PH can occur due to obstacles to portal venous flow occurring at the pre-hepatic, intrahepatic, or post-hepatic sites.

From an epidemiological point of view, advanced chronic liver disease constitutes the most prevalent cause of PH in the Western World. Irrespective of its cause, PH can cause severe clinical manifestations, such as development and bleeding of esophagogastric varices, ascites, hepatorenal syndrome (HRS), and hepatic encephalopathy, which are associated with high morbidity and mortality [1, 2]. The complications of PH are the most common clinical manifestation in patients with advanced chronic liver disease (cirrhosis), and define the “decompensated” stage [3].

In the early, compensated phases of cirrhosis, portal hypertension is mostly a consequence of an increased intrahepatic resistance to portal blood flow due to the architectural distortion and intrahepatic vasoconstriction [4]. Later on, as the disease advances, portal pressure further increases due to an increase in portal inflow,

---

Y. P. Mendoza · G. Murgia · S. G. Rodrigues · M. G. Delgado · A. Berzigotti (✉)  
Swiss Liver Center, Hepatology, University Clinic for Visceral Surgery and Medicine  
(UVC/M), Inselspital, University of Bern, Bern, Switzerland

Department of Biomedical Research (DBMR), University of Bern, Bern, Switzerland  
e-mail: [yuly.mendoza@extern.insel.ch](mailto:yuly.mendoza@extern.insel.ch); [giuseppe.murgia@insel.ch](mailto:giuseppe.murgia@insel.ch); [Susana.GomesRodrigues@insel.ch](mailto:Susana.GomesRodrigues@insel.ch); [mariagabriela.delgado@insel.ch](mailto:mariagabriela.delgado@insel.ch); [Annalisa.Berzigotti@insel.ch](mailto:Annalisa.Berzigotti@insel.ch)

mediated by a progressive splanchnic vasodilation and by the development of porto-systemic collateral circulation.

In cirrhosis, the **hepatic venous pressure gradient (HVPG)**, measured as the difference between the “wedged” (or “occluded”) and the “free” hepatic vein pressure [3], is equivalent to PPG, and it is considered the best available method to assess the presence and severity of portal hypertension in this scenario [5]. Only under specific conditions such as heart failure, HVPG and PH may differ from each other. The method is described in detail in the following paragraph.

HVPG is considered normal up to 5 mmHg; subclinical PH is defined by an increase in HVPG from 6 to 9 mmHg [6]; and once the HVPG exceeds a critical threshold value of 10 mmHg, the patient becomes susceptible to develop esophageal varices (EV) [7], clinical decompensation [8, 9], postsurgical decompensation [10], and hepatocellular carcinoma (HCC) [11]. Therefore, this HVPG threshold is defined “clinically significant portal hypertension (CSPH).” Other HVPG thresholds are relevant from a clinical point of view; an HVPG  $\geq 12$  mmHg identifies risk of variceal hemorrhage (VH). An HVPG  $\geq 16$  mmHg denotes a higher risk of mortality and an HVPG  $\geq 20$  mmHg predicts treatment failure in acute VH, early rebleeding, and mortality during acute VH [3, 12].

In **compensated advanced chronic liver disease (cACLD)**, which comprises early compensated cirrhosis and severe fibrosis [13], the presence of CSPH has a major prognostic significance and should be identified early. Among patients with CSPH, two further substages with different prognosis can be distinguished according to the absence or presence of gastroesophageal varices (GEV) [2, 14, 15]. The presence of ascites, and/or the first episode of portal hypertensive bleeding, and/or hepatic encephalopathy, marks the transition from the **compensated to the decompensated stage**, which carries a much higher risk of further progression and mortality [16]. Obviously, all patients with decompensated disease have CSPH, which does not need to be hemodynamically diagnosed in these cases (present in 100% of cases). Finally, a stage of late or further decompensation is defined by refractory ascites, hepato-renal syndrome (HRS), recurrent/persistent encephalopathy, jaundice, or recurrent variceal bleeding [2].

According to different international clinical practice guidelines, this staging system not only is important for prognosis but points out the main pathophysiological mechanisms driving progression and complications. Consequently, it is important to guide clinical management [2, 17]. Stages of PH in cirrhosis and goals of therapy at each stage are shown in Fig. 31.1.

## Reference Standard Method to Assess Portal Hypertension in Cirrhosis

As mentioned above, the measurement of HVPG is the reference standard for the assessment of portal pressure in chronic liver disease [13]. As stated previously, HVPG is the difference between the “wedged” and the “free” hepatic vein pressure

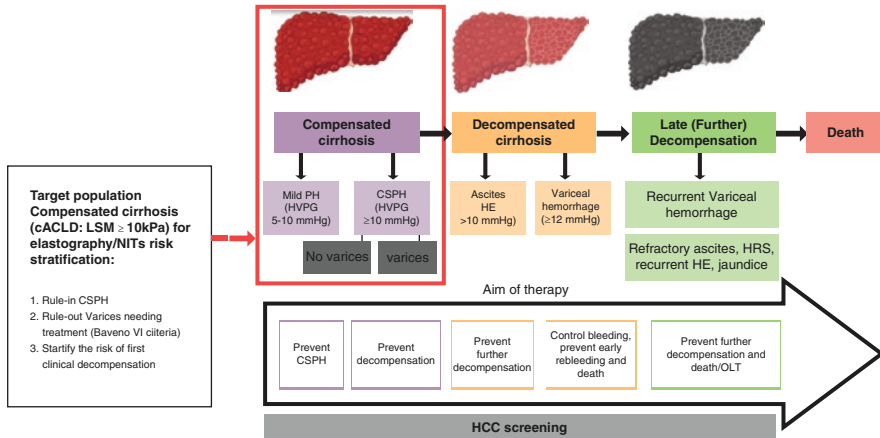


**Fig. 31.1** Natural history of chronic liver disease and aim of therapy of portal hypertension. As shown, patients with compensated advanced chronic liver disease are the target population for the use of elastography aiming at detecting clinically significant portal hypertension (CSPH) and identifying patients most likely not at risk for varices needing treatment. cACLD: compensated advanced chronic liver disease

(WHVP and FHVP respectively) at hepatic vein catheterization. The venous system is accessed most often through the right jugular vein or right femoral vein or right antecubital vein under local anesthesia, using the Seldinger technique and a hydrophilic guidewire. Then, a balloon-tipped catheter is introduced under fluoroscopic control into the inferior vena cava and a large hepatic vein [3, 18]. Once the catheter is inside the hepatic vein, the balloon at the tip of the catheter is inflated, and a small amount of iodine contrast is injected to confirm an appropriate block of the hepatic venous flow. Once confirmed that no veno-venous communicant vessels exist, the catheter is connected to the pressure measurement system (polygraph similar to that used for any other invasive pressure measurement). After reaching the pressure plateau (usually after 1–2 min), the occlusion pressure at the tip of the catheter equals that of the hepatic sinusoidal pressure; hence, in the presence of a sinusoidal cause of portal hypertension, this pressure equals portal pressure. The FHVP is measured by deflating the balloon and measuring the pressure at 2–3 cm from the hepatic vein ostium. Its value is generally very close to that of the inferior vena cava pressure [19], and this pressure should be used to measure the HVPG [20, 21].

## Need for Non-invasive Tests in the Field of Portal Hypertension

Although HVPG is the best method to identify CSPH and to further stratify the risk of complications in cACLD, this method is relatively expensive, not available at the bedside or non-specialized centers, requires personnel with adequate training, and may be

associated with procedural complications [3]. Therefore, reliable, reproducible, and easy to perform non-invasive tests [22] are needed to assess PH. Ideally, a quantification of HVPG should be provided by the non-invasive diagnostic method. If not feasible, non-invasive tests should at least discriminate between patients having or not CSPH, and those with or without varices needing treatment, since these are major prognostic determinants, which trigger-specific management actions.

## **Pathophysiological Rationale for the Measurement of Liver Stiffness as a Surrogate of Portal Pressure in cACLD**

Liver fibrosis is the major source of increased intrahepatic vascular resistance in cACLD, and portal pressure is mostly due to this increase in the early phases of PH development [3]. Liver stiffness (LS) is a physical property of the tissue, mostly reflecting liver fibrosis content. In the absence of confounding factors in cACLD, liver stiffness measurement (LSM) initially using transient elastography (TE) (and more recently using other ultrasound elastography techniques) has been evaluated as a possible non-invasive surrogate for portal hypertension. The initial data showed an excellent correlation between the HVPG and LS below the threshold of 10 mmHg, while for higher values the relationship between the reference standard and LSM diverges. This has been attributed to a component of portal pressure depending on increased porto-collateral flow, which cannot be properly mirrored by LSM [23]. On the other hand, Mueller et al. studied LS in detail in relation to several complex non-static components, which include hepatic congestion, necroinflammation, arterial pressure, cholestasis, and food intake, as well as portal pressure pharmacological (or mechanical) modulation [24]. Thus, in addition to the structure-dependent component of LS due to liver fibrosis, the pressure balance between inflow and outflow from the hepatic sinusoidal system influences LSM, creating a dynamic component [12, 25, 26]. Importantly, this implies that changes in portal pressure can be reflected by changes in LSM. For more details, see also book Part IV “Important (patho) physiological confounders of LS.”

## **Liver Stiffness Measurement and Clinically Significant Portal Hypertension**

### ***Transient Elastography***

The reliability of LSM by TE to identify the presence of CSPH has been assessed in patients with cACLD due to different etiologies; the vast majority of data relates to cACLD due to chronic hepatitis B and C. Table 31.1 provides an overview on LS and CSPH as measured by TE. LSM obtained by TE correlates significantly with HVPG in patients with cACLD, showing a correlation coefficient ranging between

**Table 31.1** Accuracy of liver stiffness measurement using transient elastography for the diagnosis of clinically significant portal hypertension

Study	Year	Study design	Population	Correlation coefficient between LSM and HVPG	AUROC for CSPH	Cut-off for CSPH	Sensitivity	Specificity
Vizzutti et al. [23]	2007	Retrospective	61 patients with HCV ACLD	0.781	0.99	13.6 kPa	97%	92%
Bureau et al. [28]	2008	Prospective	144 patients with HCV or alcoholic cirrhosis	0.858	0.945	21 kPa	89.9%	93.2%
Lemoine et al. [137]	2008	Retrospective	92 patients with compensated HCV or alcoholic cirrhosis	0.728	0.84 (all) 0.94 [138]	NA (all) 34.9 kPa [138]	NA	NA 88%
Sanchez-Conde et al. [139]	2011	Prospective	38 patients with HCV cirrhosis and HIV co-infection	0.678	0.80	14 kPa	92.8%	52%
Colecchia et al. [77]	2012	Prospective	100 patients with HCV cirrhosis	0.836	0.836	24.2 kPa	52.3%	97.1%
Llop et al. [18]	2012	Prospective	79 Child A patients (mostly viral) with resectable HCC	0.552	0.84	Rule out: 13.6 kPa Rule in: 21 kPa	91% 58%	57% 91%
Reiberger et al. [140]	2012	Retrospective	502 patients with/without cirrhosis, some decompensated (mixed etiologies)	0.794	0.871	18 kPa	82.2%	83.4%
Hong et al. [141]	2013	Retrospective	59 patients with cirrhosis	0.704	0.851	21.9 kPa	82.5%	73.7%
Augustin et al. [142]	2014	Prospective	40 patients with ACLD	NA	NA	25 kPa	65%	93%
Schwabl et al. [143]	2015	Retrospective	188 patients with chronic liver disease	0.846	0.957	16.1 kPa	94.8%	86.9%

(continued)



**Table 31.1** (continued)

Study	Year	Study design	Population	Correlation coefficient between LSM and HVPG	AUROC for CSPH	Cut-off for CSPH	Sensitivity	Specificity
Kitson et al. [90]	2015	Prospective	95 patients with cirrhosis	NA	0.90	29 kPa	71.9%	100%
Cho et al. [144]	2015	Retrospective	219 patients with alcoholic cirrhosis (some decompensated)	NA	0.85	NA	NA	NA
Zyklus et al. [145]	2015	Prospective	107 patients with cirrhosis (mixed etiologies)	0.750	0.949	17.4 kPa	88%	87.5%
Hametner et al. [146]	2015	Retrospective	236 cirrhotic patients (mixed etiologies)	NA	0.92	24.8 kPa	81%	93%
Kumar et al. [147]	2017	Retrospective	326 cirrhotic patients (mixed etiologies)	NA	0.74	21.46 kPa	79%	67%
Salavrakos et al. [35]	2018	Retrospective	118 patients with alcoholic liver disease	0.753	0.925	30.6 kPa	81%	94%

LSM liver stiffness measurement, HVPG hepatic venous pressure gradient, AUROC area under receiver operator curve, CSPH clinically significant portal hypertension, HCV hepatitis C virus, ACLD advanced chronic liver disease, HCC hepatocellular carcinoma

0.55 and 0.82 in the studies published so far [27]. As previously mentioned, the correlation between the HVPG and LS is excellent below the threshold of 10 mmHg, while it decreases in patients with HVPG above the threshold for CSPH, likely due to a flow-dependent increase in portal pressure, not mirrored by LSM [23]. Given this limitation, LSM does not allow a sufficiently accurate estimation of the exact value of HVPG [12, 26]. However, LS is a reliable non-invasive parameter to accurately identify patients with CSPH, showing an area under the receiver operating curve (AUROC) ranging between 0.74 and 0.94 for this aim [27]. The most recent meta-analysis confirmed the diagnostic capability of this method, reporting a summary AUROC of 0.93 with a sensitivity of 87.5% (CI 75.8–93.9%) and a specificity of 85.3% (95% CI 76.9–90.9%). The summary correlation coefficient was 0.783 (95% CI 0.737–0.823) [27].

Several LS cut-off values have been proposed to identify the presence of CSPH. The cut-off of 21 kPa demonstrated a high specificity (over 90%) for HVPG >10 mmHg [18, 23, 28]. According to this data, in 2015 the Baveno VI consensus stated that LS >20–25 kPa can be used to identify the presence of CSPH in patients with untreated HCV or HBV cACLD [13]. The specificity of this cut-off has been shown to be over 90% in the meta-analysis by You et al. [27]. In another recent meta-analysis [29] performed exclusively in patients with chronic viral hepatitis, it was suggested that two cut-offs can be used, namely <13.6 kPa to rule out CSPH (pooled sensitivity 96%; CI 95% 93–97%) and >22 kPa to rule in CSPH (pooled specificity 94% (95% CI 86–97%); this data confirms the recommendations provided by the Baveno VI consensus [29].

As for patients who underwent antiviral treatment for HCV, it has been shown that portal pressure usually decreases after obtaining sustained virological response (SVR) and LS quickly and sometimes dramatically decreases as well [30–34]. Despite being statistically significant, the correlation between the decrease of LS and HVPG was weak in the largest study published on this topic so far [33]. Consequently, the previously identified 13.6 kPa cut-off to rule out CSPH performed poorly after SVR, since almost half of patients with LS <13.6 kPa still showed HVPG  $\geq$ 10 mmHg. On the other hand, LSM >21 kPa accurately rule in CSPH even after SVR [33].

According to all these reported findings, for the aim of confirming the presence of CSPH, the invasive assessment of HVPG would be avoidable in a fair proportion of patients with ACLD due to viral hepatitis, before and after antiviral treatment. However, the current data do not clarify which value of LS could be used to safely rule out persistence of CSPH, in patients with SVR after HCV therapy.

An additional limitation regards the rather limited proportion of non-viral hepatitis etiology included in the studies focusing on portal hypertension and LS. Since the etiology of the underlying liver disease influences LS, it has been postulated that LSM accuracy may be limited in patients with non-viral ACLD [24]. LS demonstrated a good correlation to HVPG in patients with alcoholic liver disease (ALD) in a recent retrospective study (correlation coefficient 0.753; AUROC 0.925) [35]. The cut-off of 30.6 kPa showed the best capacity to rule in CSPH

(sensitivity 81%, specificity 94%) [35]. In a recent meta-analysis focused on ALD including nine studies, the authors identified a cut-off value of 21.8 kPa for CSPH [36]. Despite a good pooled sensitivity (0.89, 95% CI 0.83–0.93), both specificity (0.71, 95% CI 0.64–0.78) and positive likelihood ratio (3.1, 95% CI 2.4–4) were modest [36]. Therefore, the cut-off value of 21.8 kPa has a good performance in ruling out CSPH, but it is not satisfactory in ruling in CSPH (similarly to what has been described for the 13.6 kPa cut-off in viral ACLD) [29, 36]. According to these data, the cut-off value to be used to rule in CSPH in ALD seems to be higher than that for viral ACLD. Data on the accuracy of LSM for CSPH in cholestatic liver disease (in which a pre-sinusoidal component of PH is invariably present) are currently lacking and require specific studies. Recent data suggest that the location of the liver inflammation (portal versus lobular) seems to affect the ratio between liver and spleen stiffness [37]. In this paper, patients with portal HCV showed not only higher spleen stiffness as compared to ALD but suffered also more from PH-related complications [37].

### ***Point Shear Wave Elastography (pSWE)***

Three studies investigated the use of pSWE (acoustic radiation force impulse imaging, Acuson Siemens 2000, Germany) for diagnosing CSPH. Similarly to TE, pSWE showed a significant correlation with HVPG ( $r$  0.609–0.650) and demonstrated a good diagnostic accuracy for CSPH (AUROC 0.83–0.93) [38–40]. However, the data is currently insufficient to identify an accurate cut-off value to rule in and rule out CSPH. The current cut-offs are highly variable (ranging 2.17–2.58 m/s), likely due to the heterogeneity of included population. Due to these limitations, pSWE cannot yet be recommended for the diagnosis of CSPH [26] (Table 31.2).

### ***Two-Dimensional Shear Wave Elastography (2D-SWE)***

2D-SWE has been tested for CSPH in eight studies so far and showed a good discriminative capacity (AUROC 0.80–0.87), with sensitivity and specificity ranging between 80 and 90% in most of the studies. In a meta-analysis including published studies up to February 2017 on point-SWE and 2D-SWE, Suh et al. [41] confirmed the good diagnostic performance of this elastographic method for CSPH (AUROC 0.88, 95% CI 0.85–0.91). The summary sensitivity and summary specificity were 85% (95% CI 75–91%) and 85% (95% CI 77–90%), respectively. The correlation between LS by 2D-SWE and HVPG was high (summary correlation coefficient 0.741; 95% CI 0.658–0.825) [41].

In the specific context of HBV-related cACLD, the discriminative ability of this method seems to be slightly lower (AUROC 0.72, 95% CI 0.49–0.95), but a cut-off

**Table 31.2** Accuracy of liver stiffness measurement using point shear wave elastography for the diagnosis of clinically significant portal hypertension

Study	Year	Study design	Population	Correlation coefficient between LSM and HVPG	AUROC for CSPH	Cut-off for CSPH	Sensitivity	Specificity
Salzi et al. [38]	2014	Prospective	88 patients with liver cirrhosis	0.646	0.855	2.58 m/s	71.4%	87.5%
Attia et al. [39]	2015	Prospective	78 patients with chronic liver disease	0.650	0.93	2.17 m/s	97%	89%
Takuma et al. [40]	2016	Prospective	60 patients with liver cirrhosis	0.609	0.83	NA	NA	NA

LSM liver stiffness measurement, HVPG hepatic venous pressure gradient, AUROC area under receiver operator curve, CSPH clinically significant portal hypertension, HCV hepatitis C virus, ACLD advanced chronic liver disease

of <13.2 kPa ruled out CSPH with a sensitivity >90% and a cut-off >24.9 kPa ruled in CSPH with a specificity >90% [42].

Jansen et al. developed two algorithms to non-invasively rule in and rule out CSPH using 2D-SWE using LSM followed by spleen stiffness measurement (SSM) [43, 44]. LS <16 kPa and SS <26.6 were able to rule out CSPH with a sensitivity of 98.6% [43]. LS >38 kPa correctly ruled in CSPH in all patients. In patients with LS <38 kPa, SS >27.9 kPa was able to rule in CSPH with a specificity of 91.4%. Combining both algorithms, patients were correctly classified as having or not having CSPH in 91.6% of cases with a sensitivity of 98.3% and a specificity of 96.3% [44].

Unfortunately, the performance of both algorithms was not confirmed by Elkrief et al. [45] in a large independent cohort of 191 cirrhotic patients, showing that their accuracy was insufficient for the application in clinical practice. Importantly, since the study included both compensated and decompensated patients, the performance of the algorithms was tested in patients without previous history of decompensation, without improvement [45]. Overall, LSM performance using 2D-SWE for CSPH is likely consistent with that of TE [27]. However, there is marked heterogeneity of cut-offs (2D-SWE 16–38 kPa), possibly underlining a lack of standardization. While LSM by 2D-SWE for CSPH is currently unaccepted in clinical practice, the method seems promising, and further data is awaited [26] (Table 31.3).

## **Liver Stiffness Measurement Alone or Combined with Other Noninvasive Methods to Diagnose Gastroesophageal Varices**

The risk of esophageal varices (EV) rupture in cirrhosis is closely linked to the size of varices [46]. Given this observation, screening endoscopy for EV in patients with a diagnosis of ACLD is a crucial part of the management, since it can precisely identify varices need treatment (VNT) aimed at reducing the risk of bleeding [47]. VNT is defined as (1) small varices with red wale marks or occurring in patients in Child–Pugh C class (decompensated patients) or (2) medium or large varices [13]. LSM has been amply proven to accurately predict the presence and size of EV. On its own, it is the single most valid non-invasive tool to predict the presence of EV and VNT in patients with compensated advanced chronic liver disease (cACLD), although it is not as accurate as for defining the presence of clinically significant portal hypertension (CSPH) [48]. In a recent meta-analysis spanning 18 studies with a total of 3644 patients, it was concluded that for EV or VNT, the probability of a correct diagnosis following a positive measurement of LS (with variable cut-offs) did not exceed 70% [48].

Due to the lack of precision, it is not recommended to rely on LSM as a single tool for the prediction of EV/VNT. This left room for improvement, where the combination of other non-invasive markers of portal hypertension such as spleen size and platelet count could be used to increase the diagnostic accuracy of LSM. In fact,

**Table 31.3** Accuracy of liver stiffness measurement using 2D-SWE for the diagnosis of clinically significant portal hypertension

Study	Year	Study design	Population	Correlation coefficient between LSM and HVPG	AUROC for CSPH	Cut-off for CSPH	Sensitivity	Specificity
Choi et al. [148]	2014	Retrospective	95 cirrhotic patients (mixed etiologies)	0.593	NA	NA	NA	NA
Elkrief et al. [68]	2015	Prospective	79 cirrhotic patients (mixed etiologies)	0.578	24.6 kPa	0.87	81%	88%
Kim et al. [149]	2015	Prospective	92 cirrhotic patients (mixed etiologies)	0.646	15.2 kPa	0.819	85.7%	80%
Procopet et al. [85]	2015	Prospective	88 cirrhotic patients	0.611	17 kPa	0.858	80.8%	82.1%
Jansen et al. [44]	2017	Prospective	158 cirrhotic patients (mixed etiologies)	0.626	24.6 kPa <16 kPa rule out >29.5 kPa rule in	0.86	68.3%	80.4%
Maruyama et al. [150]	2016	Prospective	22 patients with chronic hepatitis or cirrhosis (mixed etiologies)	0.435	15.4 kPa	0.844	87.5%	83.3%
Elkrief et al. [45]	2017	Prospective	191 patients with liver cirrhosis (mixed etiologies) 77 included in a previous study [68]	NA	NA	0.80	NA	NA
Zhu et al. [42]	2019	Retrospective	104 hepatitis B-related cirrhotic patients	0.607	16.1 kPa <13.2 kPa rule out >24.9 kPa rule in	0.72	81%	83%

LSM liver stiffness measurement, HVPG hepatic venous pressure gradient, AUROC area under receiver operator curve, CSPH clinically significant portal hypertension, HCV hepatitis C virus, ACLD advanced chronic liver disease

a previous study using LSM-spleen diameter to platelet ratio score (LSPS) showed an increment in diagnostic accuracy to 90% for VNT, clearly outperforming LSM alone (AUROC: 0.95 vs. 0.88,  $P < 0.001$ ) [49]. A recent meta-analysis assessed and compared the performance of LSM, SSM, and LSPS for the detection of EV and VNT. The authors conclude that for EV detection, LSPS and SSM were superior to LSM [50].

Furthermore, in a prospective cohort of patients with cACLD, LSPS correctly classified the presence of EV in around 80% of patients [5]. Subsequently, the Baveno VI Consensus conference on portal hypertension suggested that a simple combination of non-invasive tests, i.e., platelet count  $>150$  g/L and LSM  $<20$  kPa, could be applied to identify patients with cACLD but with a very low risk ( $<5\%$ ) of VNT, as such, suitable to skip endoscopic screening (unnecessary) [13].

This section will highlight the most recent evidence of use of LSM using TE, pSWE, and 2D SWE  $\pm$  other unrelated parameters in predicting varices and VNT, primarily following the publication of the Baveno VI consensus report (Fig. 31.2).

## Transient Elastography $\pm$ Other Unrelated Noninvasive Tests

Following the publications of the Baveno VI Consensus report, there was a plethora of studies validating the findings in various etiologies. The results of the most relevant studies are summarized in Table 31.4. The “Anticipate” study showed that none of the tests identified those with very low risk of *all-size* varices, but both LSPS and a model combining TE and platelet count detect patients with very low risk ( $<5\%$ ) of VNT [51]. Another group showed that LS alone at a cut-off of 20 kPa had an AUC of 0.686 for EV and LSM (20 kPa) and platelet count (150 G/L) combined increased the AUC to 0.746 [52]. A meta-analysis of 15 studies, all except 5 using the Baveno VI criteria, concluded that VNT is found in no more than 4% of patients when LS  $<20$  kPa and platelet count is normal [53]. Another meta-analysis stated LSM could not provide high accuracy for the size of EV due to the various cut-offs and different etiologies and that widespread use in clinical practice at the time should be limited [54]. Moreover, another study tested earlier non-invasive test-based algorithms and Baveno VI and found that EV is misdiagnosed when using platelets in 3.1%, TE in 3.7%, LSPS in 10%, Variceal risk index (VRI) in 11.3%, Baveno VI in 1.8%, and Augustin algorithm in 3.7% of patients. The rate of unnecessary gastroscopies was 46% for platelet count, 25% for TE, 13% for LSPS, 6% for VRI, 53% for Baveno VI 53%, and 39.1% for Augustin algorithm [55].

This data prompted researchers to refine the Baveno VI criteria particularly to reduce the number of unnecessary endoscopies. Jangouk et al. reported a 12% increase in spared endoscopies (with no additional VNT missed) by expanding the Baveno VI criteria to patients with MELD = 6. Additionally, a stepwise strategy using platelet count  $>150$  G/L and MELD = 6 without LSM substantially increased the number of endoscopies avoided to 54%, with a very low rate of missing VNT [56]. Other authors could not validate these findings without LSM, because it led to

Strategies of screening for varices needing treatment	
Based on Liver Stiffness Measurement	Based on Liver and spleen Stiffness Measurement
<p><b>STANDARD BAVENO VI CRITERIA</b> (de Francis R et al. J Hepatol 2015)</p> <p><b>cACLD (LSM <math>\geq 10</math>kPa)</b></p> <p><b>Yes</b> → safely avoid endoscopic screening of varices</p> <p><b>No</b> → Perform endoscopy</p> <p>LSM <math>\geq 20</math>kPa and PLT <math>&gt; 150</math></p>	<p><b>LSSM-GUIDED STRATEGY</b> (Wong GLH et al. Liver int 2018)</p> <p><b>cACLD (LSM <math>\geq 10</math>kPa)</b></p> <p><b>Yes</b> → safely avoid endoscopic screening of varices</p> <p><b>No</b> → Perform endoscopy</p> <p>LSM <math>\geq 12.5</math> kPa and SSM <math>\leq 41.3</math> kPa</p>
<p><b>EXPANDED BAVENO VI CRITERIA</b> (Augustin S et al. J Hepatol 2017)</p> <p><b>cACLD (LSM <math>\geq 10</math>kPa)</b></p> <p><b>Yes</b> → safely avoid endoscopic screening of varices</p> <p><b>No</b> → Perform endoscopy</p> <p>LSM <math>\geq 25</math>kPa and PLT <math>&gt; 110</math></p>	<p><b>SPLEEN STIFFNESS AND BAVENO VI</b> (Colecchia A et al. J Hepatol 2018)</p> <p><b>cACLD (LSM <math>\geq 10</math>kPa)</b></p> <p><b>Yes</b> → safely avoid endoscopic screening of varices</p> <p><b>No</b> → Perform endoscopy</p> <p>LSM <math>\geq 20</math>kPa and PLT <math>&gt; 150</math> and SSM <math>\leq 46</math>kPa</p>
<p>~20-25% of endoscopies are spared</p> <p>Limited proportion of endoscopies spared with this strategy</p>	<p>40% of endoscopies are spared</p> <p>In some studies &gt; 5% varices needing treatment are missed</p>
<p><b>Advantages</b></p>	<p>50% of endoscopies are spared</p>
<p><b>Drawbacks</b></p>	<p>Lacks validation in non-viral etiology of cACLD</p>

**Fig. 31.2** Liver and spleen stiffness-based strategies to spare endoscopic screening in patients with compensated advanced chronic liver disease (cACLD)



**Table 31.4** Accuracy of liver stiffness measurement using ultrasound elastography techniques (TE, pSWE, and 2D SWE) for the diagnosis of gastroesophageal varices in the post-Baveno VI era

Study	Year	Design	Type of ultrasound elastography method ± other combined	Patient population: Number of EV, Number VNT	TE cut-offs and AUC EV/VNT	Conclusions
Maurice et al. [52]	2016	Retrospective	TE + platelet count	310 mixed	LSM: 20 kPa, AUC 0.686 LSM (20 kPa) and PLT (150 G/L): AUC 0.746	SENS 67%, SPEC 55%, PPV 7%, NPV 97% SENS 87%, SPEC 34%, PPV 6%, NPV 98%
Abraldes et al. [51]	2016	Retrospective	TE + platelet count ± spleen size; liver stiffness to spleen/platelet score (LSPS) score and platelet-spleen ratio (PSR)	518 mixed	LSM: 14.0 kPa (AUC 0.67) LSM (20 kPa) and PLT (150 G/L): AUC 0.76	LSM and a model with TE and platelet count identified patients with very low risk (<5%) risk of VNT
Marot et al. [53]	2017	Meta-analysis	TE ± platelet count or TE alone	3364 mixed	<20 kPa; PLT >150 G/L	LSM + PLT (150 G/L): SENS 89%, SPEC 38%, PPV 43%, NPV 86%, SENS 93%, SPEC 30%, PPV 14%, NPV 97%
Pu et al. [54]	2017	Meta-analysis	TE alone	2697 mixed	LSM (pooled): 20 kPa, AUC 0.83; 30 kPa, AUC: 0.83	LSM: Pooled: SENS 84%, SPEC 62% Cut-off 20 kPa: SENS 83%, SPEC 68% Pooled: SENS 78%, SPEC 76% Cut-off 30 kPa: SENS 73%, SPEC 74%
Llop et al. [55]	2017	Retrospective analysis of prospective data	TE alone and Baveno VI (LSM 20 kPa, PLT >150 G/L)	161 mixed	LSM: 20.0 kPa, LSM (20 kPa) and PLT >150 G/L	LSM alone: SENS 76%, SPEC 71%, PPV 32%, NPV 94% LSM + PLT: SENS 88%, SPEC 38%, PPV 21%, NPV 94%

Jangouk et al. [56]	2017	Retrospective	Baveno VI (LSM 20 kPa, PLT >150 G/L), MELD = 6	262 mixed	LSM (20 kPa) and PLT >150 G/L; MELD = 6 (150 G/L)	Baveno criteria 26% (US) and 16% (Italy) spared. SENS and NPV were 100%. PLT >150 G/L and MELD = 6, increased the number of endoscopies avoided to 54% (US) while maintaining a SENS. and NPV of 100%
Agustin et al. [57]	2017	Retrospective	TE ± PLT, expanded Baveno	925 mixed	LSM (25 kPa) and PLT >110 G/L	Expanded Baveno VI: spare 40%; missing VNT of 1.6%
Petta et al. [58]	2018	Retrospective analysis of prospective data	Baveno VI and expanded Baveno VI (TE ± PLT)	790 NAFLD/ NASH	LSM: 20 kPa + PLT 150 G/L LSM 25 kPa + PLT 110 G/L LSM 30 kPa + PLT 110 G/L	Best cut-offs to rule out VNT: PLT >110 G/L + LSM <30 kPa (M probe), PLT >110 G/L + LSM <2.5 kPa (XL probe)
Manatsathit et al. [50]	2018	Meta-analysis 45 studies	LSM alone vs. SSM alone vs. LSPS	4337 mixed	AUC SSM and LSPS vs. LSM: 0.899 and 0.851 vs. 0.817	For EV detection: SSM and LSPS vs. LSM (0.90 and 0.91 vs. 0.85), specificity (0.73 and 0.76 vs. 0.64) For VNT: SSM (0.87) > LSM (0.85) > LSPS (0.82); LSM, SSM, and LSPS cannot be recommended for detection of VNT
Bae et al. [61]	2018	Cross-sectional	TE	282 mixed (60% HBV)	LSM (20 kPa) and PLT >150 G/L; LSM (25 kPa) and PLT >110 G/L	Expanded Baveno VI criteria spare more (51.7%) than (27.6%), expanded missed VNT (6.8%) than the original criteria (3.8%), Baveno VI: NPV HBV 0.92, HCV 1.00, ARLD 1.00, NAFLD 1.00

(continued)

Table 31.4 (continued)

Study	Year	Design	Type of ultrasound elastography method $\pm$ other combined	Patient population; Number of EV, Number VNT	TE cut-offs and AUC EV/VNT	Conclusions
Lee et al. [60]	2018	Retrospective	Baveno VI and expanded Baveno VI (TE $\pm$ PLT)	1218 (40% HBV)	LSM (20 kPa) and PLT >150 G/L; LSM (25 kPa) and PLT >110 G/L AUC LSPS: 0.780 (95% CI: 0.774–0.820)	Baveno VI: 25.7% saved endoscopy; VNT miss rate: 1.9%. Expanded Baveno VI: saved endoscopy: 39.1%; VNT miss rate <5%
Moctezuma-Velazquez et al. [59]	2018	Cross-sectional	TE $\pm$ PLT Baveno VI and expanded Baveno VI	227 cholestatic PBC ( $n = 147$ ) PSC ( $n = 80$ )		Baveno-VI criteria 0% false-negative rate in PBC and PSC, saving 39 and 30% of endoscopies. In PBC the other LSM-TE: FNRS >5%. In PSC the expanded Baveno: adequate performance. In both conditions
Thabut et al. [62]	2019	Prospective ancillary study ANRS CO12 CirVir cohort	TE $\pm$ PLT (Baveno VI)	200 HBV ( $n = 98$ ) or HCV ( $n = 94$ ) or both ( $n = 8$ ) with SVR to antivirals		Baveno VI valid patients with compensated viral cirrhosis, even SVR. Endoscopy is no longer necessary in the subgroup of low-risk patients
Salzi et al. [38]	2014	Cross-sectional	pSWE; Acuson S2000	88 mixed	L-SWE: 2.74 m/s (0.743)	For EV: 62.5%/89.5%/PPV: 91.5%/NPV: 56.9%
Takuma et al. [40]	2016	Cross-sectional	pSWE; Acuson S2000	340 mixed	For EV: AUC: 0.789; VNT: AUC 0.788	
Attia et al. [39]	2015	Cross-sectional	pSWE; Acuson S2000	78 mixed		LSM in both groups of patients (SSM: 0.90 and 0.93 vs. LSM: 0.84 and 0.88, respectively)
Lucchina et al. [63]	2018	Cross-sectional	pSWE; iU22	42 mixed	L-SWE: 12.27 kPa AUC: 0.913	SENS 100%/SPEC 66.67%

Grgurević et al. [65]	2015	Retrospective	2D-SWE, Aixplorer	44 mixed	Cut-off 19.7 for EV (AUC 0.796)	Any EV: 19.7 for L-SWE
Cassinotto et al. [64]	2015	Prospective	2D-SWE, Aixplorer	401 mixed	L-SWE: AUC 0.80 LSM: AUC 0.73	L-SWE: SENS 92%/SPEC 36%
Kasai et al. [66]	2015	Retrospective	2D-SWE, Aixplorer	273 mixed	0.807	
Kim et al. [67]	2016	Retrospective	2D-SWE, Aixplorer	103 mixed	For EV: L-SWE: 13.9 kPa AUC 0.887; VNT cut-off 16.1 kPa; AUC 0.887 for any EV and 0.880 VNT; L-SWE: All patients: 26.3 kPa; AUC:0.683 cACL: 14.2 kPa (0.925)	EV: SENS 75%/SPEC 88.9%/ VNT: 84.6%/85.6%
Elkrief et al. [68]	2015	Prospective	2D-SWE; Aixplorer	79 mixed	For VNT: LS (TE):0.60 (cut-off 32.4 kPa) L-SWE: 0.63 (cut-off 24.7 kPa)	LS (TE) VNT SENS 0.85, SPEC 0.50, PPV 0.71, NPV 0.70, Diagnostic accuracy 0.77; LS (SWE) VNT SENS 0.82, SPEC 0.44, PPV 0.74, NPV 0.55; Diagnostic accuracy: 0.69
Stefanescu et al. [69]	2017	Prospective	2D-SWE; Aixplorer SSI	73 mixed	L-SWE: AUC 0.753	L-2D SWE (SSI) <19 kPa; PLT >100 G/L Refined algorithm for EV, were ruled-out with 83% accuracy (77.8% PPV; 85% SPEC; 87% NPV; 81% SENS) and 74% endoscopies spared

(continued)

**Table 31.4** (continued)

Study	Year	Design	Type of ultrasound elastography method ± other combined	Patient population; Number of EV, Number VNT	TE cut-offs and AUC EV/VNT	Conclusions
Jansen et al. [44]	2017	Prospective	2D-SWE; Aixplorer SSI	158 mixed		Rule-out for EV SENS 0.98, SPEC 0.50, PPV 0.80, NPV 0.93, diagnostic accuracy: 0.83 Rule-in for EV SENS 0.90, SPEC 0.60, PPV 0.83, NPV 0.73, diagnostic accuracy: 0.81
Petzold et al. [70]	2019	Prospective	2D-SWE; GE Logiq E9	100 mixed	L-SWE: AUC: 0.781	L-SWE combined with gallbladder wall thickness (GBWT) for EV: SENS 86.3% SPEC 71.4%; at L-SWE >9 kPa or GBWT >4 mm: SENS 100% (NPV 1.0)

TE transient elastography, pSWE point shear wave elastography, 2D-SWE two-dimensional shear wave elastography, EV esophageal varices, VNT varices needing treatment, AUC area under the curve, SENS sensibility, SPEC specificity, kPa kilopascal, L-SWE liver stiffness by shear wave elastography

an unacceptable high rate of missed VNT [57]. The “Expanded Baveno VI criteria” used a platelet count  $>110$  G/L and LSM  $<25$  kPa to rule out the need for endoscopy. It would potentially spare 40% of endoscopies (21% with Baveno VI criteria) with a risk of missing VNT of 1.6% in patients within the criteria and 0.6 in the overall 925 patients evaluated [57].

The Baveno VI and expanded criteria were primarily validated in patients with viral, namely hepatitis C and/or ALD. NAFLD-related cirrhosis was explored [58] and found that expanded criteria worked better than the Baveno VI criteria for ruling out VNT, sparing unnecessary procedures. Cholestatic liver diseases (PBC and PSC) have a known pre-sinusoidal component of portal hypertension that could affect the applicability of Baveno VI criteria. The authors concluded that Baveno VI criteria can be applied in these patients, resulting in 30–40% of saved endoscopies. Baveno VI criteria had a 0% false-negative rate in PBC and PSC, saving 39% and 30% of EGDs, respectively. In PSC, the expanded Baveno VI criteria had an adequate performance. Additionally, expanded criteria in PBC would lead to false-negative rate  $>5\%$  [59]. Two Asian studies explored cohorts with hepatitis B as the major etiology. Lee et al. found a VNT missed rate of 1.9% with a 25.7% saved endoscopy rate with Baveno VI criteria and saved endoscopy rate of 39.1% with a VNT missed rate  $<5\%$  for the expanded criteria [60]. Bae et al. demonstrated that expanded criteria could spare more endoscopies (51.7%) than the original criteria (27.6%) in predominantly HBV-associated cACLD. Nevertheless, the expanded criteria missed more frequently VNT (6.8%) than the original criteria (3.8%) [61]. These last studies suggest that the expanded Baveno VI criteria, in some settings, can lead to a missed rate of VNT  $>5\%$ . A French multicenter cohort study indicated that the Baveno VI criteria were valid in patients with HBV- or HCV-associated cACLD even after sustained virological response (SVR) to antiviral therapy [62].

## *pSWE*

pSWE has been widely evaluated for the prediction of EV. Overall, in the last 5 years, studies have shown mixed results. A 2014 cohort study reported an AUROC of 0.743 for the prediction of EV using pSWE (vs. TE with an AUROC of 0.802) [38]. Later, a Japanese study showed an AUROC of 0.789 for any varices and an AUROC of 0.788 for VNT, respectively [40]. A recent, small study detected an AUROC of 0.913 using pSWE-LSM for EV detection versus pSWE-based SSM with an AUROC of 0.675, with the drawback that none of the varices were VNT [63]. Currently, evidence is not strong enough to recommend pSWE to rule in or rule out VNT.

## **2D-SWE**

Over the last 5 years, there has been data supporting the use of 2D-SWE for EV/VNT screening. Three studies showed an AUROC around 0.80 for LSM in patients with cACLD [64–66]. LSM yielded an AUROC of 0.887 for any EV and 0.880 (cut-off 16.1 kPa) for VNT [67], which was not confirmed in another study including 79 patients revealing no difference between LSM and SSM values (L-2D-SWE and by TE) between patients for VNT [68]. Stefanescu et al. demonstrated that with a stepwise approach combining LSM at a cut-off <19 kPa with a cut-off of PLT >100 G/L, EV were ruled out with 83% accuracy [69]. Another cohort study of cACLD patients supported this data [44]. A single-center study reported that LSM  $\geq 10$  kPa or gallbladder wall thickness measured >4 mm measured at the same time had a 100% sensitivity for the presence of EV [70].

To conclude, most of the extensive published data on the diagnostic performance of elastography-based methods for EV/VNTs are based on TE. In particular after the publication of the Baveno VI report, these studies validated the criteria. Overall, TE and platelet combined approaches are highly applicable in all major liver disease etiologies, and most studies report a fair to good diagnostic capacity for EV/VNT. Some studies have eliminated LSM in the screening algorithm, relying solely upon simple blood-based tests (platelets and MELD score), but further validation is warranted. Both pSWE- and 2D-SWE-based LSM have shown encouraging results for variceal screening, but large-scale studies are needed to overcome significant discrepancies between among reported cut-offs. Currently, there is solid evidence to support the use of LSM and platelet count, but future studies aim to implement SSM and other non-invasive tests to further enhance EV screening strategies in cACLD.

## **Measurement of Spleen Stiffness by Ultrasound Elastography**

The spleen has an anatomical connection to the portal system (venous drainage through the splenic vein, which is one of the tributary veins of the portal system), and diseases leading to an increase in portal pressure influence the spleen structure. Splenomegaly is the most common finding in patients with portal hypertension, and it is due not only to venous congestion but also to the activation of lymphoid tissue and angiogenic and fibrogenic factors [71]. These changes can lead to an increase in the stiffness of the organ, providing a rationale for the use of elastography in this field.

Using TE, the normal SS ranges from  $13.8 \pm 2.9$  to  $17.3 \pm 2.6$  kPa [72, 73]. SS is not influenced by gender, age, or spleen size [73]. The reproducibility of this method is excellent, with an intra-class correlation coefficient of 0.94 for intra-observer concordance and 0.87 for inter-observer concordance [64]. SSM by TE using the conventional probe has a high measurement failure rate, which has been estimated around 20–29% [73]. Recently, a dedicated exam type was developed to perform SSM on the Fibroscan platform with improved performance [74]. SSM can be also

measured using pSWE with higher success (~95% of cases) [40]. 2D-SWE seems to have technical limitations in measuring SS [75].

SSM by TE has been shown to accurately reflect the presence of CSPH [76] and to be accurate for EV detection [77, 78]. A cut-off value of SSM <40 kPa ruled out CSPH with 98% sensitivity and SSM >52.8 kPa ruled it in with 97% specificity in patients with HCV-related cirrhosis [76]. In addition, SS <41.3 kPa is highly sensitive to rule out EV, and SS >55 kPa is highly specific to rule in EV [79]. The combination of SSM (41.3 kPa cut-off) and LSM (27.3 kPa cut-off) increases the diagnostic accuracy [80]. A recent meta-analysis showed that the combination of LSM and SSM is highly sensitive and specific for the prediction of EV [50]. In the only randomized controlled trial (RCT) published to date in this field, Wong and colleagues compared a strategy based on LSM and SSM to guide endoscopic screening of EV (patients with LS  $\geq$ 12.5 kPa or SS  $\geq$ 41.3 kPa were taken to endoscopy) vs. universal endoscopic screening, reporting no inferiority in the detection of high-risk varices [79]. According to this recent clinical trial, LSM-guided strategy spared more endoscopies than the Baveno VI criteria, reducing up to 50% of examinations, compared with 33% according to the Baveno VI criteria. Another multicentric, European study using a strategy based on both LS and SS ( $\geq$ 46 kPa) revealed again a higher proportion of spared endoscopies compared to the Baveno VI strategy [81]. Interestingly, in a study performed in children, SS was the best non-invasive marker to predict high-risk varices; a cut-off of 38 kPa was clinically meaningful to identify this important endpoint [82]. Taken together, all these results suggest that SSM by TE could be implemented in clinical practice to refine the selection of patients requiring endoscopy for screening of varices. A dedicated probe has entered the market in 2019, and studies validating the use of this device for SSM are expected soon [74]. For more details, see also book Part II “Techniques to Measure Liver Stiffness.”

As for SSM by pSWE, its accuracy for CSPH and varices prediction has been assessed in a limited number of studies, apparently with results similar to those reported for TE [83]. Different studies have shown that SSM measured by pSWE is a good predictor of clinically significant portal hypertension (CSPH), with AUROC between 0.80 and 0.90 [39, 40, 84]. Takuma et al. demonstrated that SSM by pSWE has a better correlation with HVPG than LSM [40]. A cut-off value of 3.51 cm/s has a sensitivity of 94% to exclude esophageal varices with risk of rupture [40].

As for 2D-SWE, few studies focused on SS [43, 68, 85]. Recently, a multicenter study showed that a cut-off value  $\leq$ 21.7 kPa or  $\geq$ 35.6 kPa of SS-SWE had a sensitivity of 90% and specificity of 91% to exclude or diagnose CSPH [44].

In conclusion, SSM by TE, pSWE and 2D-SWE is a promising and increasingly used method to assess the presence of CSPH, EV and VNT in patients with compensated ACLD, and, in the view of the authors of this chapter, it is sufficiently established to be included among the standard non-invasive tests to be used in this population.



## Prediction of Clinical Decompensation by Liver and Spleen Stiffness Measurement

The prognosis of compensated and decompensated liver cirrhosis is significantly different, and the aim of therapy is to prevent clinical decompensation in patients with cACLD. To do so, it is essential to recognize those compensated patients at higher risk of developing decompensation [16]. As previously discussed, CSPH is a key predictor of progressive liver disease and of risk of clinical decompensation [8]. Robic et al. [86] measured LS by TE and HVPG in 100 patients with cACLD, and followed them up for 2 years. They demonstrated that LS and HVPG were similarly accurate in predicting the first episode of decompensation. All of the clinical events occurred in patients with  $LS \geq 21.1$  kPa, which is currently considered the best cut-off value to identify CSPH.

Different studies [86–91] have shown that in patients with cACLD, LS holds prognostic value for liver-related events, including not only clinical decompensation but also onset of HCC, and death. Despite the limitations of these studies such as a limited sample size, short follow-up, and heterogeneous rate of events, all coincide in identifying LSM as an independent predictor of prognosis. Recently, this was confirmed in a systematic review and meta-analysis [92] of 17 prospective cohort studies, including 7058 patients with chronic liver disease. The baseline LSM was associated significantly with the risk of hepatic decompensation (relative risk, 1.07; 95% confidence interval [CI], 1.03–1.11) and death (relative risk, 1.22; 95% CI, 1.05–1.43). In another large meta-analysis (35,249 participants), LS displayed a nonlinear relationship with the risk of liver-related events [93]. Despite the possibility of calibrating LS vs. risk of clinical events factoring other variables (e.g., albumin, bilirubin, INR), models for this personalized risk-stratification are still lacking and should be object of future research.

LS increase of  $>1.5$  kPa per year seems to add prognostic value to baseline LS in patients with PBC [94] and in HCV [95].

As for the combination of LSM with other NITs, LSPS predicted first decompensation in patients with HBV-related cACLD better than LSM alone [96]. Recently, our group has shown that in patients with overweight/obesity and NASH as the main etiology of liver disease, LSM-spleen diameter to platelet ratio score was superior to LSM (using XL probe) and PH risk score to predict the first clinical decompensation [97].

SS also predicts clinical decompensation in cACLD due to chronic hepatitis C and B. Colecchia et al. [98] showed that SS, alone or combined with MELD, predicted decompensation in a 2-year follow-up similarly to HVPG and better than LS. The best SS cut-off to predict decompensation was  $>54$  kPa. Subsequently, other studies validated the predictive value of SS (either by TE or by pSWE or 2D-SWE) for liver-related events [65, 99–103].

For the specific aim of predicting the first episode of variceal hemorrhage, SS in combination with LS seems to provide the best results [104, 105]. Wong et al. [105] showed in 548 patients with cACLD followed-up for 3 years that an LSM/SSM

(LSSM) guided screening strategy for varices had a similar low risk of incident variceal hemorrhage as compared to universal screening. These findings support that the use of the LSSM-guide screening might serve at the same time to predict the risk of varices requiring treatment and the occurrence of variceal hemorrhage. For instance, a cACLD patient with a low risk of clinically significant EV by LSSM would have minimal risk (<1% in 3 year) of incident variceal hemorrhage [105].

As far as HCC prediction is concerned, PH is one of the factors involved in HCC development and recurrence [11]. A number of prospective studies have identified that LSM in patients with viral cirrhosis is associated with the risk of incidence of HCC [106–110]. Jung et al. [110] validated a previously described cut-off of LS (>8 kPa) in 1130 patients with chronic hepatitis B. Additional larger longitudinal prospective studies including diverse etiologies of chronic liver disease are needed to assess whether LSM can be used in combination with other variables to better stratify the risk of HCC in cACLD.

Finally, LSM [111] and SSM [112] have been investigated in the setting of HCC recurrence after effective therapy. Marzano et al. [112] identified SSM (hazard ratio 1.046, 95% CI 1.020–1.073) as the only independent predictor of late HCC recurrence (>24 months) after liver resection.

## Liver and Spleen Stiffness Measurement to Follow-Up Patients Treated for PH

While the strength of correlation between LSM and HVPG is improved under non-selective beta-blockers (NSBB) [113], likely to a reduced impact of flow-dependent factors on LSM [114], LSM changes in patients with PH undergoing therapy with NSBB do not correlate with changes in HVPG [113]. Since LS cannot be used to monitor PH under NSBB, Kim et al. [115] studied SS for this purpose. They measured SS by pSWE (Virtual Touch, Siemens, Germany) in 106 patients with cirrhosis and high-risk esophageal varices, both before and after titration of NSBB. They also assessed the hemodynamic response to NSBB by measuring the HVPG at the same time points.  $\Delta$ SSM ( $\Delta$ SSM [=SSM2 – SSM1]) significantly predicted the HVPG response (OR 0.039; 95% CI 0.008–0.135;  $P < 0.0001$ ) to carvedilol. Based on the calculated prediction model (Model =  $0.0490 - 2.8345 * \Delta$ SSM) and using 0.530 as the cut-off value, the hemodynamic response could be predicted with a good performance (AUROC 0.803). In the validation cohort, the model maintained a high discriminative ability (AUROC 0.848). If externally validated, SS changes by pSWE would be the first non-invasive test able to predict the hemodynamic response to NSBB.

In addition, changes in LS and SS after placement of a transjugular intrahepatic portosystemic shunt (TIPS) may be used in the follow-up. As for SS, in a preliminary work, Novelli et al. [116] found that the SS significantly decreases after TIPS; however, SS decreased in only 58% of cases, and SS showed no correlation with

portal pressure. In contrast, several more recent studies [117–122] have indicated a positive correlation between changes in SS and changes in portal venous pressure ( $\Delta$ PVP) after TIPS placement (e.g., in the largest:  $\Delta$ SSM and  $\Delta$ PVP  $r = 0.871$ ,  $p \leq 0.001$ ) [122]. Using pSWE, Ran et al. suggested that the cut-off value  $\Delta$ SSM  $>0.36$  m/s could predict a good TIPS performance (AUC 0.869; sensitivity: 77%; specificity: 100%).

As for LSM after TIPS placement, studies showed overall a decrease after TIPS [123], but no significant correlation between the decrease in LS and that in portal pressure was detected [120, 122, 124, 125]. More recently, it has been postulated that LS would decrease after TIPS in only a part of patients; patients with early decrease in LS would show a good outcome after TIPS, while patients showing increase in LS early after TIPS would have a poor prognosis [125]. LS increase after TIPS could be due to inflammatory response, triggering acute on chronic liver failure and death in this population. Further data is awaited to confirm this preliminary report.

## **LS and SS in Patients with Portal Hypertension of Unknown Cause or No Cirrhosis**







In patients presenting with clear signs of portal hypertension, the first step is to diagnose the primary cause. In Western countries, over 90% of cases of PH are due to cACLD/cirrhosis, but nonetheless, other types of PH exist and need to be identified correctly.

Pre-hepatic PH is frequent in children and in the Asian countries, and it is mostly due to thrombosis of the portal vein (extrahepatic portal vein obstruction—EHPVO) which can evolve into cavernous transformation. Thrombosis of the hepatic veins/vena cava inferior (Budd–Chiari syndrome, BCS) is the most common cause of post-hepatic PH. These diseases are usually diagnosed by imaging (ultrasound, CT scan, and MRI).

Intrahepatic, non-cirrhotic portal hypertension is a heterogeneous group of diseases characterized by the elevation of portal pressure without liver cirrhosis. Among the causes of non-cirrhotic portal hypertension, porto-sinusoidal vascular disease (PSVD) [126] a new term that encompasses from a clinical perspective: idiopathic portal hypertension and non-cirrhotic portal hypertension, and from a histological standpoint: idiopathic portal fibrosis, obliterative venopathy, nodular regenerative hyperplasia-NRH, non-cirrhotic portal fibrosis, hepatoportal sclerosis, and incomplete septal cirrhosis. It is frequent in the Western world; in other geographical areas, schistosomiasis is a frequent cause of intrahepatic, non-cirrhotic PH. The clinical manifestations are similar to those observed in cirrhotic PH and include thrombocytopenia due to splenomegaly, onset of varices, and variceal bleeding, which is usually better tolerated than in cirrhosis, due to a preserved liver function [127]. The diagnosis of intrahepatic non-cirrhotic portal hypertension, and

in particular that of PSVD, requires liver biopsy and HVPG measurement, since non-cirrhotic portal hypertension can be indistinguishable from cirrhosis on imaging. For more details, see also book Part III “Liver Stiffness and Various Etiologies of Liver Diseases.”

Several observations suggest that combined elastography of the liver and of the spleen can play a role in improving the differential diagnosis of cirrhosis and intrahepatic non-cirrhotic portal hypertension. Many patients with non-cirrhotic portal hypertension have LS values above the threshold usually taken as that for the diagnosis of cACLD (10 kPa). In a study comprising pre-hepatic PH, PSVD, and post-hepatic-PH, 31% of patients with EHPVO, 50% of patients with NRH, and 75% of patients with other causes (Budd–Chiari syndrome, sarcoidosis, etc.) showed LS >10 kPa. Importantly, 95% of them did not present significant fibrosis on liver biopsy, suggesting that LS is increased due to other factors [128]. Another prospective study that included 30 patients with NRH found LS ≥7.1 kPa (compatible with significant fibrosis) in 47% of cases, but no fibrosis on liver biopsy. As expected, LS and HVPG show no correlation in these patients [129]. Seijo et al. demonstrated that in comparison to patients with cACLD and with similar manifestations of PH (similar size of varices, etc.), LS values in patients with idiopathic PH are much lower; however, LS values are significantly higher in patients with idiopathic PH than in patients with EHPVO [130], who more often have completely normal livers. On the other hand, SS is increased similarly in all categories of PH, irrespective of the cause. Hence, the finding of a disproportionate increase in SS vs. LS in a patient with signs of PH and the finding of LS <20 kPa in a patient suspected of cirrhosis due to PH should prompt further investigations to rule out PSVD and other causes of non-cirrhotic intrahepatic PH. Figure 31.3 summarizes these concepts.

Type of PH	Pre-hepatic PH		Hepatic (sinusoidal) PH (cACLD)		Post-hepatic PH	
Stiffness measurement patterns						
	Normal LSM	High SSM	High LSM	High SSM	High LSM	High SSM
Examples	Extrahepatic portal vein obstruction		Liver cirrhosis		Budd-Chiari syndrome Congestive liver (heart)	

PH, portal hypertension; LSM, liver stiffness measurement; SSM, spleen stiffness measurement; cACLD, compensated advanced chronic liver disease

**Fig. 31.3** Liver and spleen stiffness patterns in pre-hepatic, intrahepatic and post-hepatic portal hypertension (PH). Please note that contrarily to sinusoidal forms of PH (cirrhosis) pre-sinusoidal forms of intrahepatic portal hypertension, such as porto-sinusoidal vascular disease, usually show a mild–moderate increase in liver stiffness despite a marked increase in spleen stiffness (similar to that observed in cirrhosis)

In the specific context of patients at risk of developing sinusoidal obstruction syndrome (SOS), Colecchia et al. demonstrated that LS by TE increases significantly days before the development of symptoms or signs. In the authors' view, this could be explained by pre-clinical liver congestion due to initial sinusoidal obstruction, which later on progresses and leads to the classical syndrome. The increase in LS was observed between days 2 and 12, and LS had a 75% sensitivity and 98% specificity for the diagnosis of SOS [131].

As for pre-hepatic causes of PH, LS is usually normal or minimally increased, while SS is very much elevated in patients with EHPVO (who often have normal or slightly elevated LSM), and SS by TE was higher in patients who had a previous history of variceal bleeding [132]. This data suggests that SS might be a prognostic tool in EHPVO. However, a study using 2D-SWE to measure SS did not observe differences between patients experiencing or not experiencing variceal bleeding [133].

As for post-hepatic causes of PH, in patients with BCS, a study on seven cases showed that, on presentation, LS and SS were close to the maximum measurable values [134]. In a recent case series [134], LS and SS values could stratify the severity of BCS and in particular SS was more accurate predicting patients who required TIPS intervention. Interestingly, two studies (in 7 and in 25 patients, respectively) reported a significant decrease in LS after endovascular treatment [134, 135]. These differences in LS were not related to changes in the stage of fibrosis measured by METAVIR score and suggest that high LS in BCS is primarily due to liver congestion. In a recent study, Wang found similar results using 2D-SWE-based LS, which correlated with the decrease in HVPG after endovascular treatment [136].

In conclusion, LS and SS used in combination seem to provide diagnostic and prognostic data in patients with non-cirrhotic forms of PH. However, the exact use of ultrasound elastography in this context remains to be defined.

**Acknowledgment** Yuly P. Mendoza is supported by the Swiss Government Excellence Scholarship ESKAS-Nr: 2018.0666; Susana G. Rodrigues receives financial support from the Stiftung für Leberkrankheiten Bern.

## References

1. Bosch J, Garcia-Pagán JC, Berzigotti A, Abraldes JG. Measurement of portal pressure and its role in the management of chronic liver disease. *Semin Liver Dis.* 2006;26(4):348–62.
2. Garcia-Tsao G, Abraldes JG, Berzigotti A, Bosch J. Portal hypertensive bleeding in cirrhosis: risk stratification, diagnosis, and management: 2016 practice guidance by the American Association for the study of liver diseases. *Hepatology.* 2017;65(1):310–35.
3. Bosch J, Abraldes JG, Berzigotti A, García-Pagan JC. The clinical use of HVPG measurements in chronic liver disease. *Nat Rev Gastroenterol Hepatol.* 2009;6(10):573–82.
4. Bosch J, Groszmann RJ, Shah VH. Evolution in the understanding of the pathophysiological basis of portal hypertension: How changes in paradigm are leading to successful new treatments. *J Hepatol.* 2015;62(1 Suppl):S121–30.
5. Berzigotti A, Seijo S, Reverter E, Bosch J. Assessing portal hypertension in liver diseases. *Expert Rev Gastroenterol Hepatol.* 2013;7(2):141–55.

6. Berzigotti A, Ashkenazi E, Reverter E, Abraldes JG, Bosch J. Non-invasive diagnostic and prognostic evaluation of liver cirrhosis and portal hypertension. *Dis Markers*. 2011;31(3):129–38.
7. Groszmann RJ, Garcia-Tsao G, Bosch J, Grace ND, Burroughs AK, Planas R, et al. Beta-blockers to prevent gastroesophageal varices in patients with cirrhosis. *N Engl J Med*. 2005;353(21):2254–61.
8. Ripoll C, Groszmann R, Garcia-Tsao G, Grace N, Burroughs A, Planas R, et al. Hepatic venous pressure gradient predicts clinical decompensation in patients with compensated cirrhosis. *Gastroenterology*. 2007;133(2):481–8.
9. Hernandez-Gea V, Berzigotti A. Clinical evaluation and prognosis. *Dig Dis*. 2015;33(4):515–23.
10. Berzigotti A, Reig M, Abraldes JG, Bosch J, Bruix J. Portal hypertension and the outcome of surgery for hepatocellular carcinoma in compensated cirrhosis: a systematic review and meta-analysis. *Hepatology*. 2015;61(2):526–36.
11. Ripoll C, Groszmann RJ, Garcia-Tsao G, Bosch J, Grace N, Burroughs A, et al. Hepatic venous pressure gradient predicts development of hepatocellular carcinoma independently of severity of cirrhosis. *J Hepatol*. 2009;50(5):923–8.
12. Berzigotti A. Non-invasive evaluation of portal hypertension using ultrasound elastography. *J Hepatol*. 2017;67(2):399–411.
13. de Franchis R. Expanding Consensus in Portal Hypertension—Report of the Baveno VI Consensus Workshop: Stratifying risk and individualizing care for portal hypertension. *J Hepatol*. 2015;63(3):743–52.
14. Bruno S, Zuin M, Crosignani A, Rossi S, Zadra F, Roffi L, et al. Predicting mortality risk in patients with compensated HCV-induced cirrhosis: a long-term prospective study. *Am J Gastroenterol*. 2009;104(5):1147–58.
15. Zipprich A, Garcia-Tsao G, Rogowski S, Fleig WE, Seufferlein T, Dollinger MM. Prognostic indicators of survival in patients with compensated and decompensated cirrhosis. *Liver Int*. 2012;32(9):1407–14.
16. D’Amico G, Garcia-Tsao G, Pagliaro L. Natural history and prognostic indicators of survival in cirrhosis: a systematic review of 118 studies. *J Hepatol*. 2006;44(1):217–31.
17. Qi X, Berzigotti A, Cardenas A, Sarin SK. Emerging non-invasive approaches for diagnosis and monitoring of portal hypertension. *Lancet Gastroenterol Hepatol*. 2018;3(10):708–19.
18. Llop E, Berzigotti A, Reig M, Erice E, Reverter E, Seijo S, et al. Assessment of portal hypertension by transient elastography in patients with compensated cirrhosis and potentially resectable liver tumors. *J Hepatol*. 2012;56(1):103–8.
19. Procopet B, Berzigotti A. Diagnosis of cirrhosis and portal hypertension: imaging, non-invasive markers of fibrosis and liver biopsy. *Gastroenterol Rep*. 2017;5(2):79–89.
20. Silva-Junior G, Baiges A, Turon F, Torres F, Hernández-Gea V, Bosch J, et al. The prognostic value of hepatic venous pressure gradient in patients with cirrhosis is highly dependent on the accuracy of the technique. *Hepatology*. 2015;62(5):1584–92.
21. La Mura V, Abraldes JG, Berzigotti A, Erice E, Flores-Arroyo A, García-Pagán JC, et al. Right atrial pressure is not adequate to calculate portal pressure gradient in cirrhosis: a clinical-hemodynamic correlation study. *Hepatology*. 2010;51(6):2108–16.
22. Lossnitzer D, Steen H, Zahn A, Lehrke S, Weiss C, Weiss KH, et al. Myocardial late gadolinium enhancement cardiovascular magnetic resonance in patients with cirrhosis. *J Cardiovasc Magn Reson*. 2010;12:47.
23. Vizzutti F, Arena U, Romanelli RG, Rega L, Foschi M, Colagrande S, et al. Liver stiffness measurement predicts severe portal hypertension in patients with HCV-related cirrhosis. *Hepatology*. 2007;45(5):1290–7.
24. Dietrich CF, Bamber JF, Berzigotti A, Bota S, Cantisani V, Castera L, et al. EFSUMB guidelines and recommendations on the clinical use of liver ultrasound elastography, update 2017 (Long Version). *Ultraschall Med*. 2017;38(4):e16–47.
25. Mueller S. Does pressure cause liver cirrhosis? The sinusoidal pressure hypothesis. *World J Gastroenterol*. 2016;22(48):10482.



26. Ferraioli G, Wong VW, Castera L, Berzigotti A, Sporea I, Dietrich CF, et al. Liver ultrasound elastography: an update to the World Federation for Ultrasound in Medicine and Biology guidelines and recommendations. *Ultrasound Med Biol.* 2018;44(12):2419–40.
27. You MW, Kim KW, Pyo J, Huh J, Kim HJ, Lee SJ, et al. A meta-analysis for the diagnostic performance of transient elastography for clinically significant portal hypertension. *Ultrasound Med Biol.* 2017;43(1):59–68.
28. Bureau C, Metivier S, Peron JM, Selves J, Robic MA, Gourraud PA, et al. Transient elastography accurately predicts presence of significant portal hypertension in patients with chronic liver disease. *Aliment Pharmacol Ther.* 2008;27(12):1261–8.
29. Song J, Ma Z, Huang J, Liu S, Luo Y, Lu Q, et al. Comparison of three cut-offs to diagnose clinically significant portal hypertension by liver stiffness in chronic viral liver diseases: a meta-analysis. *Eur Radiol.* 2018;28(12):5221–30.
30. Pons M, Santos B, Simon-Talero M, Ventura-Cots M, Riveiro-Barciela M, Esteban R, et al. Rapid liver and spleen stiffness improvement in compensated advanced chronic liver disease patients treated with oral antivirals. *Therap Adv Gastroenterol.* 2017;10(8):619–29.
31. Mandorfer M, Kozbial K, Schwabl P, Freissmuth C, Schwarzer R, Stern R, et al. Sustained virologic response to interferon-free therapies ameliorates HCV-induced portal hypertension. *J Hepatol.* 2016;65(4):692–9.
32. Rincon D, Ripoll C, Lo Iacono O, Salcedo M, Catalina MV, Alvarez E, et al. Antiviral therapy decreases hepatic venous pressure gradient in patients with chronic hepatitis C and advanced fibrosis. *Am J Gastroenterol.* 2006;101(10):2269–74.
33. Lens S, Alvarado-Tapias E, Marino Z, Londono MC, Llop E, Martinez J, et al. Effects of All-Oral Anti-Viral Therapy on HVPg and systemic hemodynamics in patients with hepatitis C Virus-associated cirrhosis. *Gastroenterology.* 2017;153(5):1273–83 e1.
34. Radu C, Stancu O, Sav R, Bugariu A, Suci A, Grigoras C, et al. Liver stiffness better predicts portal hypertension after HCV eradication. *J Gastrointest Liver Dis.* 2018;27(2):204.
35. Salavrakos M, Piessevaux H, Komuta M, Lanthier N, Starkel P. Fibroscan reliably rules out advanced liver fibrosis and significant portal hypertension in alcoholic patients. *J Clin Gastroenterol.* 2019;53(10):772–8.
36. Song J, Ma Z, Huang J, Luo Y, Zyklus R, Kumar A, et al. Reliability of transient elastography-based liver stiffness for diagnosing portal hypertension in patients with alcoholic liver disease: a diagnostic meta-analysis with specific cut-off values. *Ultraschall Med.* 2019.
37. Elshaarawy O, Mueller J, Guha IN, Chalmers J, Harris R, Krag A, et al. Spleen stiffness to liver stiffness ratio significantly differs between ALD and HCV and predicts disease-specific complications. *JHEP Rep.* 2019;1(2):99–106.
38. Salzl P, Reiberger T, Ferlitsch M, Payer BA, Schwengerer B, Trauner M, et al. Evaluation of portal hypertension and varices by acoustic radiation force impulse imaging of the liver compared to transient elastography and AST to platelet ratio index. *Ultraschall Med.* 2014;35(6):528–33.
39. Attia D, Schoenemeier B, Rodt T, Negm AA, Lenzen H, Lankisch TO, et al. Evaluation of liver and spleen stiffness with acoustic radiation force impulse quantification elastography for diagnosing clinically significant portal hypertension. *Ultraschall Med.* 2015;36(6):603–10.
40. Takuma Y, Nouse K, Morimoto Y, Tomokuni J, Sahara A, Takabatake H, et al. Portal hypertension in patients with liver cirrhosis: diagnostic accuracy of spleen stiffness. *Radiology.* 2016;279(2):609–19.
41. Suh CH, Kim KW, Park SH, Lee SS, Kim HS, Tirumani SH, et al. Shear wave elastography as a quantitative biomarker of clinically significant portal hypertension: a systematic review and meta-analysis. *Am J Roentgenol.* 2018;210(5):W185–W95.
42. Zhu YL, Ding H, Fu TT, Peng SY, Chen SY, Luo JJ, et al. Portal hypertension in hepatitis B-related cirrhosis: diagnostic accuracy of liver and spleen stiffness by 2-D shear-wave elastography. *Hepatol Res.* 2019;49(5):540–9.
43. Jansen C, Bogs C, Verlinden W, Thiele M, Moller P, Gortzen J, et al. Algorithm to rule out clinically significant portal hypertension combining Shear-wave elastography of liver and spleen: a prospective multicentre study. *Gut.* 2016;65(6):1057–8.

44. Jansen C, Bogs C, Verlinden W, Thiele M, Moller P, Gortzen J, et al. Shear-wave elastography of the liver and spleen identifies clinically significant portal hypertension: a prospective multicentre study. *Liver Int.* 2017;37(3):396–405.
45. Elkrief L, Ronot M, Andrade F, Dioguardi Burgio M, Issoufaly T, Zappa M, et al. Non-invasive evaluation of portal hypertension using shear-wave elastography: analysis of two algorithms combining liver and spleen stiffness in 191 patients with cirrhosis. *Aliment Pharmacol Ther.* 2018;47(5):621–30.
46. Dell'era A, Bosch J. Review article: the relevance of portal pressure and other risk factors in acute gastro-oesophageal variceal bleeding. *Aliment Pharmacol Ther.* 2004;20(Suppl 3):8–15; discussion 6-7.
47. Angeli P, Bernardi M, Villanueva C, Francoz C, Mookerjee RP, Trebicka J, et al. EASL Clinical Practice Guidelines for the management of patients with decompensated cirrhosis. *J Hepatol.* 2018;69(2):406–60.
48. Shi KQ, Fan YC, Pan ZZ, Lin XF, Liu WY, Chen YP, et al. Transient elastography: a meta-analysis of diagnostic accuracy in evaluation of portal hypertension in chronic liver disease. *Liver Int.* 2013;33(1):62–71.
49. Kim BK, Han KH, Park JY, Ahn SH, Kim JK, Paik YH, et al. A liver stiffness measurement-based, noninvasive prediction model for high-risk esophageal varices in B-viral liver cirrhosis. *Am J Gastroenterol.* 2010;105(6):1382–90.
50. Manatsathit W, Samant H, Kapur S, Ingviya T, Esmadi M, Wijarnprecha K, et al. Accuracy of liver stiffness, spleen stiffness, and LS-spleen diameter to platelet ratio score in detection of esophageal varices: Systemic review and meta-analysis. *J Gastroenterol Hepatol.* 2018;33(10):1696–706.
51. Abraldes JG, Bureau C, Stefanescu H, Augustin S, Ney M, Blasco H, et al. Noninvasive tools and risk of clinically significant portal hypertension and varices in compensated cirrhosis: the “Anticipate” study. *Hepatology.* 2016;64(6):2173–84.
52. Maurice JB, Brodtkin E, Arnold F, Navaratnam A, Paine H, Khawar S, et al. Validation of the Baveno VI criteria to identify low risk cirrhotic patients not requiring endoscopic surveillance for varices. *J Hepatol.* 2016;65(5):899–905.
53. Marot A, Trepo E, Doerig C, Schoepfer A, Moreno C, Deltenre P. Liver stiffness and platelet count for identifying patients with compensated liver disease at low risk of variceal bleeding. *Liver Int.* 2017;37(5):707–16.
54. Pu K, Shi JH, Wang X, Tang Q, Wang XJ, Tang KL, et al. Diagnostic accuracy of transient elastography (FibroScan) in detection of esophageal varices in patients with cirrhosis: a meta-analysis. *World J Gastroenterol.* 2017;23(2):345–56.
55. Llop E, Lopez M, de la Revilla J, Fernandez N, Trapero M, Hernandez M, et al. Validation of noninvasive methods to predict the presence of gastroesophageal varices in a cohort of patients with compensated advanced chronic liver disease. *J Gastroenterol Hepatol.* 2017;32(11):1867–72.
56. Jangouk P, Turco L, De Oliveira A, Schepis F, Villa E, Garcia-Tsao G. Validating, deconstructing and refining Baveno criteria for ruling out high-risk varices in patients with compensated cirrhosis. *Liver Int.* 2017;37(8):1177–83.
57. Augustin S, Pons M, Maurice JB, Bureau C, Stefanescu H, Ney M, et al. Expanding the Baveno VI criteria for the screening of varices in patients with compensated advanced chronic liver disease. *Hepatology.* 2017;66(6):1980–8.
58. Petta S, Sebastiani G, Bugianesi E, Viganò M, Wong VW, Berzigotti A, et al. Non-invasive prediction of esophageal varices by stiffness and platelet in non-alcoholic fatty liver disease cirrhosis. *J Hepatol.* 2018;69(4):878–85.
59. Moctezuma-Velazquez C, Saffiotti F, Tasayco-Huaman S, Casu S, Mason A, Roccarina D, et al. Non-invasive prediction of high-risk varices in patients with primary biliary cholangitis and primary sclerosing cholangitis. *Am J Gastroenterol.* 2019;114(3):446–52.
60. Lee HA, Kim SU, Seo YS, Lee YS, Kang SH, Jung YK, et al. Prediction of the varices needing treatment with non-invasive tests in patients with compensated advanced chronic liver disease. *Liver Int.* 2018;39(6):1071–9.



61. Bae J, Sinn DH, Kang W, Gwak GY, Choi MS, Paik YH, et al. Validation of the Baveno VI and the expanded Baveno VI criteria to identify patients who could avoid screening endoscopy. *Liver Int.* 2018;38(8):1442–8.
62. Thabut D, Bureau C, Layese R, Bourcier V, Hammouche M, Cagnot C, et al. Validation of Baveno VI criteria for screening and surveillance of esophageal varices in patients with compensated cirrhosis and a sustained response to antiviral therapy. *Gastroenterology.* 2019;156(4):997–1009 e5.
63. Lucchina N, Recaldini C, Macchi M, Molinelli V, Montanari M, Segato S, et al. Point shear wave elastography of the spleen: its role in patients with portal hypertension. *Ultrasound Med Biol.* 2018;44(4):771–8.
64. Cassinotto C, Charrie A, Mouries A, Lapuyade B, Hiriart J-B, Vergniol J, et al. Liver and spleen elastography using supersonic shear imaging for the non-invasive diagnosis of cirrhosis severity and oesophageal varices. *Dig Liver Dis.* 2015;47(8):695–701.
65. Grgurevic I, Bokun T, Mustapic S, Trkulja V, Heinzl R, Banic M, et al. Real-time two-dimensional shear wave ultrasound elastography of the liver is a reliable predictor of clinical outcomes and the presence of esophageal varices in patients with compensated liver cirrhosis. *Croat Med J.* 2015;56(5):470–81.
66. Kasai Y, Moriyasu F, Saito K, Hara T, Kobayashi Y, Nakamura I, et al. Value of shear wave elastography for predicting hepatocellular carcinoma and esophagogastric varices in patients with chronic liver disease. *J Med Ultrason (2001).* 2015;42(3):349–55.
67. Kim TY, Kim TY, Kim Y, Lim S, Jeong WK, Sohn JH. Diagnostic performance of shear wave elastography for predicting esophageal varices in patients with compensated liver cirrhosis. *J Ultrasound Med.* 2016;35(7):1373–81.
68. Elkrief L, Rautou PE, Ronot M, Lambert S, Dioguardi Burgio M, Francoz C, et al. Prospective comparison of spleen and liver stiffness by using shear-wave and transient elastography for detection of portal hypertension in cirrhosis. *Radiology.* 2015;275(2):589–98.
69. Stefanescu H, Allegretti G, Salvatore V, Piscaglia F. Bidimensional shear wave ultrasound elastography with supersonic imaging to predict presence of oesophageal varices in cirrhosis. *Liver Int.* 2017;37(9):1405.
70. Petzold G, Tsaknakis B, Bremer SCB, Knoop RF, Goetze R, Amanzada A, et al. Evaluation of liver stiffness by 2D-SWE in combination with non-invasive parameters as predictors for esophageal varices in patients with advanced chronic liver disease. *Scand J Gastroenterol.* 2019;54(3):342–9.
71. Mejias M, Garcia-Pras E, Gallego J, Mendez R, Bosch J, Fernandez M. Relevance of the mTOR signaling pathway in the pathophysiology of splenomegaly in rats with chronic portal hypertension. *J Hepatol.* 2010;52(4):529–39.
72. Pawlus A, Ingot M, Chabowski M, Szymanska K, Ingot M, Patyk M, et al. Shear wave elastography (SWE) of the spleen in patients with hepatitis B and C but without significant liver fibrosis. *Br J Radiol.* 2016;89(1066):20160423.
73. Albayrak E, Server S. The relationship of spleen stiffness value measured by shear wave elastography with age, gender, and spleen size in healthy volunteers. *J Med Ultrason (2001).* 2019;46(2):195–9.
74. Bastard C, Miette V, Cales P, Stefanescu H, Festi D, Sandrin L. A novel fibroscan examination dedicated to spleen stiffness measurement. *Ultrasound Med Biol.* 2018;44(8):1616–26.
75. Berzigotti A, Ferraioli G, Bota S, Gilja OH, Dietrich CF. Novel ultrasound-based methods to assess liver disease: the game has just begun. *Dig Liver Dis.* 2018;50(2):107–12.
76. Cescon M, Colecchia A, Cucchetti A, Peri E, Montrone L, Ercolani G, et al. Value of transient elastography measured with FibroScan in predicting the outcome of hepatic resection for hepatocellular carcinoma. *Ann Surg.* 2012;256(5):706–12; discussion 12–3.
77. Colecchia A, Montrone L, Scaiola E, Bacchi-Reggiani ML, Colli A, Casazza G, et al. Measurement of spleen stiffness to evaluate portal hypertension and the presence of esophageal varices in patients with HCV-related cirrhosis. *Gastroenterology.* 2012;143(3):646–54.

78. Mazur R, Celmer M, Silicki J, Holownia D, Pozowski P, Miedzybrodzki K. Clinical applications of spleen ultrasound elastography—a review. *J Ultrasonogr.* 2018;18(72):37–41.
79. Wong GLH, Kwok R, Hui AJ, Tse YK, Ho KT, Lo AOS, et al. A new screening strategy for varices by liver and spleen stiffness measurement (LSSM) in cirrhotic patients: a randomized trial. *Liver Int.* 2018;38(4):636–44.
80. Sharma P, Kimake V, Tyagi P, Bansal N, Singla V, Kumar A, et al. Spleen stiffness in patients with cirrhosis in predicting esophageal varices. *Am J Gastroenterol.* 2013;108(7):1101–7.
81. Colecchia A, Ravaioli F, Marasco G, Colli A, Dajti E, Di Biase AR, et al. A combined model based on spleen stiffness measurement and Baveno VI criteria to rule out high-risk varices in advanced chronic liver disease. *J Hepatol.* 2018;69(2):308–17.
82. Sutton H, Fitzpatrick E, Davenport M, Burford C, Alexander E, Dhawan A, et al. Transient elastography measurements of spleen stiffness as a predictor of clinically significant varices in children. *J Pediatr Gastroenterol Nutr.* 2018;67(4):446–51.
83. Leung VY, Shen J, Wong VW, Abrigo J, Wong GL, Chim AM, et al. Quantitative elastography of liver fibrosis and spleen stiffness in chronic hepatitis B carriers: comparison of shear-wave elastography and transient elastography with liver biopsy correlation. *Radiology.* 2013;269(3):910–8.
84. Rifai K, Cornberg J, Bahr M, Mederacke I, Potthoff A, Wedemeyer H, et al. ARFI elastography of the spleen is inferior to liver elastography for the detection of portal hypertension. *Ultraschall Med.* 2011;32(Suppl 2):E24–30.
85. Procopet B, Berzigotti A, Abralde JG, Turon F, Hernandez-Gea V, Garcia-Pagan JC, et al. Real-time shear-wave elastography: applicability, reliability and accuracy for clinically significant portal hypertension. *J Hepatol.* 2015;62(5):1068–75.
86. Robic MA, Procopet B, Metivier S, Peron JM, Selves J, Vinel JP, et al. Liver stiffness accurately predicts portal hypertension related complications in patients with chronic liver disease: a prospective study. *J Hepatol.* 2011;55(5):1017–24.
87. Merchante N, Rivero-Juarez A, Tellez F, Merino D, Jose Rios-Villegas M, Marquez-Solero M, et al. Liver stiffness predicts clinical outcome in human immunodeficiency virus/hepatitis C virus-coinfected patients with compensated liver cirrhosis. *Hepatology.* 2012;56(1):228–38.
88. Macías J, Camacho A, Von Wichmann MA, López-Cortés LF, Ortega E, Tural C, et al. Liver stiffness measurement versus liver biopsy to predict survival and decompensations of cirrhosis among HIV/hepatitis C virus-coinfected patients. *AIDS.* 2013;27(16):2541–9.
89. Wang JH, Chuah SK, Lu SN, Hung CH, Kuo CM, Tai WC, et al. Baseline and serial liver stiffness measurement in prediction of portal hypertension progression for patients with compensated cirrhosis. *Liver Int.* 2014;34(9):1340–8.
90. Kitson MT, Roberts SK, Colman JC, Paul E, Button P, Kemp W. Liver stiffness and the prediction of clinically significant portal hypertension and portal hypertensive complications. *Scand J Gastroenterol.* 2015;50(4):462–9.
91. Merchante N, Rivero-Juárez A, Téllez F, Merino D, Ríos-Villegas MJ, Ojeda-Burgos G, et al. Liver stiffness predicts variceal bleeding in HIV/HCV-coinfected patients with compensated cirrhosis. *AIDS.* 2017;31(4):493–500.
92. Singh S, Fujii LL, Murad MH, Wang Z, Asrani SK, Ehman RL, et al. Liver stiffness is associated with risk of decompensation, liver cancer, and death in patients with chronic liver diseases: a systematic review and meta-analysis. *Clin Gastroenterol Hepatol.* 2013;11(12):1573–84.e2.
93. Wang J, Li J, Zhou Q, Zhang D, Bi Q, Wu Y, et al. Liver stiffness measurement predicted liver-related events and all-cause mortality: a systematic review and nonlinear dose-response meta-analysis. *Hepatol Commun.* 2018;2(4):467–76.
94. Corpechot C, Gaouar F, El Nagggar A, Kemgang A, Wendum D, Poupon R, et al. Baseline values and changes in liver stiffness measured by transient elastography are associated

- with severity of fibrosis and outcomes of patients with primary sclerosing cholangitis. *Gastroenterology*. 2014;146(4):970–9; quiz e15–6.
95. Vergniol J, Boursier J, Coutzac C, Bertrais S, Foucher J, Angel C, et al. Evolution of non-invasive tests of liver fibrosis is associated with prognosis in patients with chronic hepatitis C. *Hepatology*. 2014;60(1):65–76.
  96. Kim BK, Park YN, Kim DY, Park JY, Chon CY, Han KH, et al. Risk assessment of development of hepatic decompensation in histologically proven hepatitis B viral cirrhosis using liver stiffness measurement. *Digestion*. 2012;85(3):219–27.
  97. Mendoza YCS, Murgia G, Chen T, Margini C, Sebastiani G, Berzigotti A. Simple non-invasive surrogates of portal hypertension predict clinical decompensation in overweight/obese patients with cACLD. *EASL*. 2019;70:e664.
  98. Colecchia A, Colli A, Casazza G, Mandolesi D, Schiumerini R, Reggiani LB, et al. Spleen stiffness measurement can predict clinical complications in compensated HCV-related cirrhosis: a prospective study. *J Hepatol*. 2014;60(6):1158–64.
  99. Grgurevic I, Puljiz Z, Brnic D, Bokun T, Heinzl R, Lukic A, et al. Liver and spleen stiffness and their ratio assessed by real-time two dimensional-shear wave elastography in patients with liver fibrosis and cirrhosis due to chronic viral hepatitis. *Eur Radiol*. 2015;25(11):3214–21.
  100. Takuma Y, Morimoto Y, Takabatake H, Toshikuni N, Tomokuni J, Sahara A, et al. Measurement of spleen stiffness with acoustic radiation force impulse imaging predicts mortality and hepatic decompensation in patients with liver cirrhosis. *Clin Gastroenterol Hepatol*. 2017;15(11):1782–90.e4.
  101. Radu C, Stefanescu H, Procopet B, Lupsor Platon M, Tantau M, Grigorescu M. Is spleen stiffness a predictor of clinical decompensation in cirrhotic patients? *J Gastrointest Liver Dis*. 2014;23(2):223–4.
  102. Mori K, Arai H, Abe T, Takayama H, Toyoda M, Ueno T, et al. Spleen stiffness correlates with the presence of ascites but not esophageal varices in chronic hepatitis C patients. *Biomed Res Int*. 2013;2013:857862.
  103. Meister P, Dechene A, Buchter M, Kalsch J, Gerken G, Canbay A, et al. Spleen stiffness differentiates between acute and chronic liver damage and predicts hepatic decompensation. *J Clin Gastroenterol*. 2019;53(6):457–63.
  104. Buechter M, Kahraman A, Manka P, Gerken G, Jochum C, Canbay A, et al. Spleen and liver stiffness is positively correlated with the risk of esophageal variceal bleeding. *Digestion*. 2016;94(3):138–44.
  105. Wong GL, Liang LY, Kwok R, Hui AJ, Tse YK, Chan HL, et al. Low risk of variceal bleeding in patients with cirrhosis after variceal screening stratified by liver/spleen stiffness. *Hepatology*. 2019;70(3):971–81.
  106. Masuzaki R, Tateishi R, Yoshida H, Goto E, Sato T, Ohki T, et al. Prospective risk assessment for hepatocellular carcinoma development in patients with chronic hepatitis C by transient elastography. *Hepatology*. 2009;49(6):1954–61.
  107. Narita Y, Genda T, Tsuzura H, Sato S, Kanemitsu Y, Ishikawa S, et al. Prediction of liver stiffness hepatocellular carcinoma in chronic hepatitis C patients on interferon-based anti-viral therapy. *J Gastroenterol Hepatol*. 2014;29(1):137–43.
  108. Wang HM, Hung CH, Lu SN, Chen CH, Lee CM, Hu TH, et al. Liver stiffness measurement as an alternative to fibrotic stage in risk assessment of hepatocellular carcinoma incidence for chronic hepatitis C patients. *Liver Int*. 2013;33(5):756–61.
  109. Kim DY, Song KJ, Kim SU, Yoo EJ, Park JY, Ahn SH, et al. Transient elastography-based risk estimation of hepatitis B virus-related occurrence of hepatocellular carcinoma: development and validation of a predictive model. *Onco Targets Ther*. 2013;6:1463–9.
  110. Jung KS, Kim SU, Ahn SH, Park YN, Kim DY, Park JY, et al. Risk assessment of hepatitis B virus-related hepatocellular carcinoma development using liver stiffness measurement (FibroScan). *Hepatology*. 2011;53(3):885–94.

111. Jung KS, Kim SU, Choi GH, Park JY, Park YN, Kim DY, et al. Prediction of recurrence after curative resection of hepatocellular carcinoma using liver stiffness measurement (FibroScan(R)). *Ann Surg Oncol*. 2012;19(13):4278–86.
112. Marzano A, Tucci A, Chiala C, Saracco GM, Fadda M, Debernardi VW. Liver stiffness-based model for portal hypertension and hepatocellular cancer risk in HBV responsive to antivirals. *Minerva Gastroenterol Dietol*. 2019;65(1):11–9.
113. Reiberger T, Ferlitsch A, Payer BA, Pinter M, Homoncik M, Peck-Radosavljevic M, et al. Non-selective beta-blockers improve the correlation of liver stiffness and portal pressure in advanced cirrhosis. *J Gastroenterol*. 2012;47(5):561–8.
114. Piecha F, Mandorfer M, Peccerella T, Ozga AK, Poth T, Vonbank A, et al. Pharmacological decrease of liver stiffness is pressure-related and predicts long-term clinical outcome. *Am J Physiol Gastrointest Liver Physiol*. 2018;315(4):G484–G94.
115. Kim HY, So YH, Kim W, Ahn DW, Jung YJ, Woo H, et al. Non-invasive response prediction in prophylactic carvedilol therapy for cirrhotic patients with esophageal varices. *J Hepatol*. 2019;70(3):412–22.
116. Novelli PM, Cho K, Rubin JM. Sonographic assessment of spleen stiffness before and after transjugular intrahepatic portosystemic shunt placement with or without concurrent embolization of portal systemic collateral veins in patients with cirrhosis and portal hypertension: a feasibility study. *J Ultrasound Med*. 2015;34(3):443–9.
117. Gao J, Ran HT, Ye XP, Zheng YY, Zhang DZ, Wang ZG. The stiffness of the liver and spleen on ARFI Imaging pre and post TIPS placement: a preliminary observation. *Clin Imaging*. 2012;36(2):135–41.
118. Ran HT, Ye XP, Zheng YY, Zhang DZ, Wang ZG, Chen J, et al. Spleen stiffness and spleno-portal venous flow: assessment before and after transjugular intrahepatic portosystemic shunt placement. *J Ultrasound Med*. 2013;32(2):221–8.
119. Gao J, Zheng X, Zheng YY, Zuo GQ, Ran HT, Auh YH, et al. Shear wave elastography of the spleen for monitoring transjugular intrahepatic portosystemic shunt function: a pilot study. *J Ultrasound Med*. 2016;35(5):951–8.
120. De Santis A, Nardelli S, Bassanelli C, Lupo M, Iegri C, Di Ciesco CA, et al. Modification of splenic stiffness on acoustic radiation force impulse parallels the variation of portal pressure induced by transjugular intrahepatic portosystemic shunt. *J Gastroenterol Hepatol*. 2018;33(3):704–9.
121. Buechter M, Manka P, Theysohn JM, Reinboldt M, Canbay A, Kahraman A. Spleen stiffness is positively correlated with HVPG and decreases significantly after TIPS implantation. *Dig Liver Dis*. 2018;50(1):54–60.
122. Han H, Yang J, Zhuge YZ, Zhang M, Wu M. Point shear wave elastography to evaluate and monitor changing portal venous pressure in patients with decompensated cirrhosis. *Ultrasound Med Biol*. 2017;43(6):1134–40.
123. Tzschätzsch H, Sack I, Marticorena Garcia SR, Ipek-Ugay S, Braun J, Hamm B, et al. Time-harmonic elastography of the liver is sensitive to intrahepatic pressure gradient and liver decompression after transjugular intrahepatic portosystemic shunt (TIPS) implantation. *Ultrasound Med Biol*. 2017;43(3):595–600.
124. Attia D, Rodt T, Marquardt S, Hinrichs J, Meyer BC, Gebel M, et al. Shear wave elastography prior to transjugular intrahepatic portosystemic shunt may predict the decrease in hepatic vein pressure gradient. *Abdom Radiol (NY)*. 2019;44(3):1127–34.
125. Jansen C, Moller P, Meyer C, Kolbe CC, Bogs C, Pohlmann A, et al. Increase in liver stiffness after transjugular intrahepatic portosystemic shunt is associated with inflammation and predicts mortality. *Hepatology*. 2018;67(4):1472–84.
126. De Gottardi A, Rautou PE, Schouten J, Rubbia-Brandt L, Leebeek F, Trebicka J, et al. Portosinusoidal vascular disease: proposal and description of a novel entity. *Lancet Gastroenterol Hepatol*. 2019;4(5):399–411.

127. Khanna R, Sarin SK. Idiopathic portal hypertension and extrahepatic portal venous obstruction. *Hepatology*. 2018;12(S1):148–67.
128. Vuppalanchi R, Mathur K, Pyko M, Samala N, Chalasani N. Liver stiffness measurements in patients with noncirrhotic portal hypertension—the devil is in the details. *Hepatology*. 2018;68(6):2438–40.
129. Laharie D, Vergniol J, Bioulac-Sage P, Diris B, Poli J, Foucher J, et al. Usefulness of non-invasive tests in nodular regenerative hyperplasia of the liver. *Eur J Gastroenterol Hepatol*. 2010;22(4):487–93.
130. Seijo S, Reverter E, Miquel R, Berzigotti A, Abraldes JG, Bosch J, et al. Role of hepatic vein catheterisation and transient elastography in the diagnosis of idiopathic portal hypertension. *Dig Liver Dis*. 2012;44(10):855–60.
131. Colecchia A, Ravaioli F, Sessa M, Alemanni VL, Dajti E, Marasco G, et al. Liver stiffness measurement allows early diagnosis of veno-occlusive disease/sinusoidal obstruction syndrome in adult patients who undergo hematopoietic stem cell transplantation: results from a monocentric prospective study. *Biol Blood Marrow Transplant*. 2019;25(5):995–1003.
132. Sharma P, Mishra SR, Kumar M, Sharma BC, Sarin SK. Liver and spleen stiffness in patients with extrahepatic portal vein obstruction. *Radiology*. 2012;263(3):893–9.
133. Madhusudhan KS, Kilambi R, Shalimar SP, Sharma R, Srivastava DN, et al. Measurement of splenic stiffness by 2D-shear wave elastography in patients with extrahepatic portal vein obstruction. *Br J Radiol*. 2018;91(1092):20180401.
134. Dajti E, Ravaioli F, Colecchia A, Marasco G, Vestito A, Festi D. Liver and spleen stiffness measurements for assessment of portal hypertension severity in patients with Budd Chiari syndrome. *Can J Gastroenterol Hepatol*. 2019;2019:1673197.
135. Mukund A, Pargewar SS, Desai SN, Rajesh S, Sarin SK. Changes in liver congestion in patients with Budd–Chiari syndrome following endovascular interventions: assessment with transient elastography. *J Vasc Interv Radiol*. 2017;28(5):683–7.
136. Wang HW, Shi HN, Cheng J, Xie F, Luo YK, Tang J. Real-time shear wave elastography (SWE) assessment of short- and long-term treatment outcome in Budd-Chiari syndrome: a pilot study. *PLoS One*. 2018;13(5):e0197550.
137. Lemoine M, Katsahian S, Ziolo M, Nahon P, Ganne-Carrie N, Kazemi F, et al. Liver stiffness measurement as a predictive tool of clinically significant portal hypertension in patients with compensated hepatitis C virus or alcohol-related cirrhosis. *Aliment Pharmacol Ther*. 2008;28(9):1102–10.
138. Kawaguchi T, Sumida Y, Umemura A, Matsuo K, Takahashi M, Takamura T, et al. Genetic polymorphisms of the human PNPLA3 gene are strongly associated with severity of non-alcoholic fatty liver disease in Japanese. *PLoS One*. 2012;7(6):e38322.
139. Sanchez-Conde M, Miralles P, Bellon JM, Rincon D, Ramirez M, Gutierrez I, et al. Use of transient elastography (FibroScan(R)) for the noninvasive assessment of portal hypertension in HIV/HCV-coinfected patients. *J Viral Hepat*. 2011;18(10):685–91.
140. Reiberger T, Ferlitsch A, Payer BA, Pinter M, Schwabl P, Stift J, et al. Noninvasive screening for liver fibrosis and portal hypertension by transient elastography—a large single center experience. *Wien Klin Wochenschr*. 2012;124(11-12):395–402.
141. Hong WK, Kim MY, Baik SK, Shin SY, Kim JM, Kang YS, et al. The usefulness of non-invasive liver stiffness measurements in predicting clinically significant portal hypertension in cirrhotic patients: Korean data. *Clin Mol Hepatol*. 2013;19(4):370–5.
142. Augustin S, Millan L, Gonzalez A, Martell M, Gelabert A, Segarra A, et al. Detection of early portal hypertension with routine data and liver stiffness in patients with asymptomatic liver disease: a prospective study. *J Hepatol*. 2014;60(3):561–9.
143. Schwabl P, Bota S, Salzl P, Mandorfer M, Payer BA, Ferlitsch A, et al. New reliability criteria for transient elastography increase the number of accurate measurements for screening of cirrhosis and portal hypertension. *Liver Int*. 2015;35(2):381–90.

144. Cho EJ, Kim MY, Lee JH, Lee IY, Lim YL, Choi DH, et al. Diagnostic and prognostic values of noninvasive predictors of portal hypertension in patients with alcoholic cirrhosis. *PLoS One*. 2015;10(7):e0133935.
145. Zykus R, Jonaitis L, Petrenkiene V, Pranculis A, Kupcinskas L. Liver and spleen transient elastography predicts portal hypertension in patients with chronic liver disease: a prospective cohort study. *BMC Gastroenterol*. 2015;15:183.
146. Hametner S, Ferlitsch A, Ferlitsch M, Etschmaier A, Schofl R, Ziachehabi A, et al. The VITRO Score (Von Willebrand Factor Antigen/Thrombocyte Ratio) as a new marker for clinically significant portal hypertension in comparison to other non-invasive parameters of fibrosis including ELF test. *PLoS One*. 2016;11(2):e0149230.
147. Kumar A, Khan NM, Anikhindi SA, Sharma P, Bansal N, Singla V, et al. Correlation of transient elastography with hepatic venous pressure gradient in patients with cirrhotic portal hypertension: a study of 326 patients from India. *World J Gastroenterol*. 2017;23(4):687–96.
148. Choi SY, Jeong WK, Kim Y, Kim J, Kim TY, Sohn JH. Shear-wave elastography: a noninvasive tool for monitoring changing hepatic venous pressure gradients in patients with cirrhosis. *Radiology*. 2014;273(3):917–26.
149. Kim TY, Jeong WK, Sohn JH, Kim J, Kim MY, Kim Y. Evaluation of portal hypertension by real-time shear wave elastography in cirrhotic patients. *Liver Int*. 2015;35(11):2416–24.
150. Maruyama H, Kobayashi K, Kiyono S, Sekimoto T, Kanda T, Yokosuka O. Two-dimensional shear wave elastography with propagation-based reliability assessment for grading hepatic fibrosis and portal hypertension. *J Hepatobiliary Pancreat Sci*. 2016;23(9):595–602.

# Chapter 32

## Liver Stiffness and Hepatic Decompensation



Omar Elshaarawy and Sebastian Mueller

### Liver Stiffness and Hepatic Decompensation

Several studies have assessed the relation of LS and hepatic decompensation (see Table 32.1), and LS was found to be highly predictive for hepatic decompensation. In a cohort study by Gomez-Moreno et al. on 343 patients with chronic liver disease, 60 patients had liver cirrhosis, for all patients, each incremental unit in the natural logarithm (Ln) of LS was associated with 14.7 times higher risk of developing liver-related events ( $P < 0.001$ ) [1]. Patients with LS  $>25$  kPa had a greater risk to develop decompensation than those with a LS  $<25$  kPa and the hazard ratio was 30.9 ( $P < 0.001$ ). Of note, LS performed well in predicting decompensation events with an AUROC of 0.876 in all patients while the predictive power of LS decreased when only considering patients with cirrhosis (AUROC 0.729). In a similar study by Kim et al., LS was found to be an independent predictor of decompensation in a cohort of 26 cirrhotic patients [2]. They stratified the patients according to LS into three stages:  $<13$  kPa, 13–18 kPa, and  $>18$  kPa. This study concluded that patients with LS 13–18 kPa have a hazard ratio (HR) of 4.5 to develop decompensation ( $P = 0.044$ ) while patients with LS  $>18$  kPa have a higher HR of 12.4 in order to progress to liver decompensation ( $P < 0.001$ ). In a systematic review and meta-analysis, Singh et al. in 2013 included 17 studies on 7508 patients with chronic liver disease. They concluded that LS was significantly associated with the risk of hepatic decompensation

---

O. Elshaarawy · S. Mueller (✉)

Department of Medicine and Center for Alcohol Research and Liver Diseases,

Salem Medical Center, University of Heidelberg, Heidelberg, Germany

e-mail: [oelshaarawy@liver.menofia.edu.eg](mailto:oelshaarawy@liver.menofia.edu.eg); [sebastian.mueller@urz.uni-heidelberg.de](mailto:sebastian.mueller@urz.uni-heidelberg.de)



**Table 32.1** Liver stiffness cut-off values for various decompensation states

Study	Etiology	Stage of CLD	Decompensation endpoints	Liver stiffness (kPa)	Cases	N	HR/RR (95% CI)	Adjustments
Park et al. (2011) [16]	HBV	NP	HD (variceal bleeding, ascites, HE, SBP, or HRS)	Per unit kPa	47	1126	1.03 (1.01–1.06)	NP
				≤8	8	595	1	Age, male sex, alcohol consumption, serum albumin level, and HBeAg positivity
				8.1–13	13	285	3.07 (1.01–9.31)	
Jung et al. (2011) [17]	HBV	Cirrhosis 197 (17.4)	HCC	13.1–18	10	130	4.68 (1.40–15.64)	
				18.1–23	10	53	5.55 (1.53–20.04)	
				>23	16	67	6.60 (1.83–23.84)	
Kim et al. (2012) [18]	HBV	F4 217 (100)	HD (ascites, HE, variceal hemorrhage, and deterioration of liver function to Child–Pugh class B or C)	<13	NP	110	1	Age, albumin, bilirubin, PLT, spleen size, MELD score
				13–18		52	4.55 (1.14–19.81)	
				≥18		55	12.45 (3.06–50.65)	
Merchante et al. (2012) [19]	HIV-HCV	Cirrhosis 239 (100)	HD and/or HCC	Per unit kPa	31	239	1.03 (1.01–1.05)	Hepatitis B virus surface antigen, HCV RNA load, CDC stage C, CD4 cell count, PLT, Child–Turcotte–Pugh class, MELD score, age, sex, and the achievement of SVR
Chon et al. (2012) [20]	HBV	Cirrhosis 197 (17.5)	HD (variceal bleeding, ascites, HE, SBP, or HRS)	Per unit kPa	68	1126	1.03 (1.01–1.06)	Age, male, liver cirrhosis, Child–Pugh score, PT, PLT
Calvaruso et al. (2012) [21]	HCV	Cirrhosis 239 (100)	HD (ascites, variceal bleeding, or HE)	Per unit kPa	20	239	1.06 (1.03–1.09)	NP



Kim et al. (2013) [22]	HBV	F3 15 (14.5); F4A 12 (11.7); F4B 60 (58.3); F4C 16 (15.5)	HD (ascites, variceal bleeding, HE, SBP, and HRS)	<11.6	2	51	1	Unadjusted
				11.6–18.2	2	31	1.65 (0.24–11.09)	
				≥18.2	5	21	6.07 (1.28–28.87)	
Calvaruso et al. (2013) [23]	HCV	Cirrhosis 155 (100)	HD (ascites, variceal bleeding, HE)	Per unit kPa	16	155	1.06 (1.01–1.10)	NP
Macias et al. (2013) [24]	HIV-HCV	NP	HD	Per 5 kPa	NP	NP	1.37 (1.21–1.54)	NP
Poynard et al. (2014) [25]	HCV	F0 1127 (29); F1 733 (19); F2 377 (10); F3 644 (16); F4 1046 [27]	HD	≤5	7	790	1	Unadjusted
				5–7.1	25	1049	2.69 (1.17–6.19)	
				7.1–9.5	14	505	3.13 (1.27–7.70)	
				9.5–12.5	8	276	3.27 (1.20–8.94)	
				12.5–20	27	210	14.51 (6.41–32.86)	
Colecchia et al. (2014) [12]	HCV	Cirrhosis 92 (100)	HD	20–50	42	184	25.76 (11.80–56.42)	Unadjusted
				>50	5	17	33.19 (11.71–94.12)	
				Per unit kPa	30	92	1.10 (1.04–1.16)	
Merchante et al. (2015) [26]	HIV-HCV	Cirrhosis 275 (100)	HD (PHGB, ascites, HRS, SBP, and HE) and/or HCC	<21	7	145	1	Age, sex, SVR during follow-up, PLT, Child–Turcotte–Pugh class A
				≥21	12	130	1.9 (0.59–6.07)	

(continued)

Table 32.1 (continued)

Study	Etiology	Stage of CLD	Decompensation endpoints	Liver stiffness (kPa)	Cases	N	HR/RR (95% CI)	Adjustments
Bihari et al. (2016) [27]	HBV	F0 250 (26); F1 328 (34); F2 135 (14); F3 138 (14.3); F4 113 (11.7)	HD (ascites, HE, HRS, variceal bleeding, SBP, a Child-Turcotte-Pugh score value of >7)	Per unit kPa	57	964	1.11 (1.08–1.14)	
Macías et al. (2013) [24]	HIV-HCV	F3 149 (47); F4 168 (53)	HD (SBP, PHGB, ascites, HRS, HE, nonobstructive jaundice, and HCC)	9.5–14.5 ≥14.6	NP	NP	1 5.67 (2.27–14.1)	Age, gender, CDC stage C, CD4 cell count, serum ALT, PLT
Macías et al. (2013) [24]	HIV-HCV	F0 42 (14); F1 97 (33); F2 79 (27); F3 39 (13); F4 40 (14)	HD (SBP, PHGB, ascites, HRS, HE, nonobstructive jaundice, and HCC)	≤6 6.1–8.9 9–14.5 14.6–21 >21	2 0 1 4 14	86 99 49 26 37	1 0.43 (0.04–4.71) 0.88 (0.08–9.43) 6.62 (1.28–34.09) 16.27 (3.89–68.03)	Unadjusted
Pérez-Latorre et al. (2014) [28]	HCV (24), HIV-HCV (36)	Cirrhosis 60 (100)	HD (ascites, HE, variceal bleeding, and jaundice), HCC, and death HD (ascites, HE, variceal bleeding, and jaundice) or HCC HD (ascites, HE, variceal bleeding, and jaundice)	<25 ≥25 Per unit kPa	1 11 12	32 28 60	1 12.57 (1.73–91.35) 1.07 (1.01–1.13)	Unadjusted HIV status, albumin concentration
				Per unit kPa	8	60	1.06 (0.99–1.13)	

PHGB portal hypertensive gastrointestinal bleeding, HE hepatic encephalopathy, CLD chronic liver disease, HD hepatic decompensation, NP not provided, SBP spontaneous bacterial peritonitis, SVR sustained viral response, HRS hepatorenal syndrome

(RR, 1.07; 95% CI, 1.03–1.11) and the development of HCC (9 studies; RR, 1.11; 95% CI, 1.05–1.18) [3]. Recently, Lee et al. assessed LS by magnetic resonance elastography in 217 patients with compensated chronic liver disease. Accordingly, each incremental unit in LS is associated with a 1.59 hazard ratio to develop HCC and a 2.02 hazard ratio to develop hepatic decompensation [4].

## Spleen Stiffness Can Predict Hepatic Decompensation as Well as Variceal Bleeding

Several studies investigated the utility of spleen stiffness (SS) to predict esophageal varices or even the incidence of variceal bleeding [5–13]. Accordingly, SS was able to predict hepatic decompensation with almost 70% accuracy and AUROCs up to 0.843 have been reported by e.g. Takuma et al. [9]. A SS cut-off of 3.25 m/s (~31.6 kPa) identified patients with decompensation with a negative predictive value of 98.8% and 68.9% accuracy. Moreover, a SS cut-off value of 3.64 m/s (~39.7 kPa) is an accurate predictor of esophageal variceal bleeding (EVB) in compensated cirrhotic patients while a cut-off value of 3.75 m/s (~42.2 kPa) in decompensated patients. Noteworthy, SS had better AUROC values in predicting EVB in comparison to spleen diameter, platelet count, and LS (0.857, 0.746, 0.720, and 0.688, respectively) [9]. In a recent study by Wang et al., similar SS cut-off values for EVB (SS = 45.5 kPa and AUROC = 0.923 vs. LS = 29.6 kPa and AUROC = 0.860) were identified with SS being superior to LS in predicting EVB [13]. In a cohort of 210 patients, Meister et al. reported an SS cut-off value of 39 kPa for hepatic decompensation. They also reported the utility of SS to differentiate between acute and chronic liver damage as SS was significantly higher in patients with chronic liver damage than acute ones with the same LS values [14].

Recently, SS/LS ratio has been proposed to determine the histological side of inflammation and predict disease-specific complications [15]. It was reported that HCV patients have a higher SS/LS ratio than the ALD patients. Of note, 73% of the HCV patients had more variceal bleeding as the mode of first decompensation while, in contrast, 65% of the ALD patients had hepatocellular jaundice as the mode of first decompensation. Taken together, LS and SS both add valuable information in predicting disease-specific complications of liver diseased patients, namely various forms of hepatic decompensation. Prospective long-term studies are encouraged to further validate the utility of these elastographic parameters and their its performance.

## References

1. Gomez-Moreno AZ, Pineda-Tenor D, Jimenez-Sousa MA, Sánchez-Ruano JJ, Artaza-Varasa T, Saura-Montalban J, et al. Liver stiffness measurement predicts liver-related events in patients with chronic hepatitis C: a retrospective study. *PLoS One*. 2017;12(9):e0184404.

2. Kim BK, Kim do Y, Han KH, Park JY, Kim JK, Paik YH, et al. Risk assessment of esophageal variceal bleeding in B-viral liver cirrhosis by a liver stiffness measurement-based model. *Am J Gastroenterol.* 2011;106(9):1654–62, 730.
3. Singh S, Fujii LL, Murad MH, Wang Z, Asrani SK, Ehman RL, et al. Liver stiffness is associated with risk of decompensation, liver cancer, and death in patients with chronic liver diseases: a systematic review and meta-analysis. *Clin Gastroenterol Hepatol.* 2013;11(12):1573–84.e2.
4. Lee DH, Lee JM, Chang W, Yoon J-H, Kim YJ, Lee J-H, et al. Prognostic role of liver stiffness measurements using magnetic resonance elastography in patients with compensated chronic liver disease. *Eur Radiol.* 2018;28(8):3513–21.
5. Singh S, Eaton JE, Murad MH, Tanaka H, Iijima H, Talwalkar JA. Accuracy of spleen stiffness measurement in detection of esophageal varices in patients with chronic liver disease: systematic review and meta-analysis. *Clin Gastroenterol Hepatol.* 2014;12(6):935–45.e4.
6. Paternostro R, Reiberger T, Bucsics T. Elastography-based screening for esophageal varices in patients with advanced chronic liver disease. *World J Gastroenterol.* 2019;25(3):308–29.
7. Colecchia A, Montrone L, Scaiola E, Bacchi-Reggiani ML, Colli A, Casazza G, et al. Measurement of spleen stiffness to evaluate portal hypertension and the presence of esophageal varices in patients with HCV-related cirrhosis. *Gastroenterology.* 2012;143(3):646–54.
8. Colecchia A, Di Biase AR, Scaiola E, Predieri B, Iughetti L, Reggiani ML, et al. Non-invasive methods can predict oesophageal varices in patients with biliary atresia after a Kasai procedure. *Dig Liver Dis.* 2011;43(8):659–63.
9. Takuma Y, Nouse K, Morimoto Y, Tomokuni J, Sahara A, Takabatake H, et al. Prediction of esophageal variceal bleeding by measuring spleen stiffness in patients with liver cirrhosis. *Gut.* 2016;65(2):354.
10. Elkrief L, Rautou PE, Ronot M, Lambert S, Dioguardi Burgio M, Francoz C, et al. Prospective comparison of spleen and liver stiffness by using shear-wave and transient elastography for detection of portal hypertension in cirrhosis. *Radiology.* 2015;275(2):589–98.
11. Sharma P, Kirnake V, Tyagi P, Bansal N, Singla V, Kumar A, et al. Spleen stiffness in patients with cirrhosis in predicting esophageal varices. *Am J Gastroenterol.* 2013;108(7):1101–7.
12. Colecchia A, Colli A, Casazza G, Mandolesi D, Schiumerini R, Reggiani LB, et al. Spleen stiffness measurement can predict clinical complications in compensated HCV-related cirrhosis: a prospective study. *J Hepatol.* 2014;60(6):1158–64.
13. Wang X-K, Wang P, Zhang Y, Qi S-L, Chi K, Wang G-C. A study on spleen transient elastography in predicting the degree of esophageal varices and bleeding. *Medicine.* 2019;98(9):e14615.
14. Meister P, Dechene A, Buchter M, Kalsch J, Gerken G, Canbay A, et al. Spleen stiffness differentiates between acute and chronic liver damage and predicts hepatic decompensation. *J Clin Gastroenterol.* 2019;53(6):457–63.
15. Elshaarawy O, Mueller J, Guha IN, Chalmers J, Harris R, Krag A, et al. Spleen stiffness to liver stiffness ratio significantly differs between ALD and HCV and predicts disease-specific complications. *JHEP Rep.* 2019;1(2):99–106.
16. Park JJ, Park JY, Kim do Y, Park YN, Ahn SH, Chon CY, et al. Prediction of significant fibrosis in chronic hepatitis C patients with normal ALT. *Hepatogastroenterology.* 2011;58(109):1321–7.
17. Jung KS, Kim SU, Ahn SH, Park YN, Kim DY, Park JY, et al. Risk assessment of hepatitis B virus-related hepatocellular carcinoma development using liver stiffness measurement (FibroScan). *Hepatology.* 2011;53(3):885–94.
18. Kim BK, Park YN, Kim DY, Park JY, Chon CY, Han KH, et al. Risk assessment of development of hepatic decompensation in histologically proven hepatitis B viral cirrhosis using liver stiffness measurement. *Digestion.* 2012;85(3):219–27.
19. Merchante N, Rivero-Juarez A, Tellez F, Merino D, Jose Rios-Villegas M, Marquez-Solero M, et al. Liver stiffness predicts clinical outcome in human immunodeficiency virus/hepatitis C virus-coinfected patients with compensated liver cirrhosis. *Hepatology.* 2012;56(1):228–38.
20. Chon YE, Jung ES, Park JY, Kim DY, Ahn SH, Han KH, et al. The accuracy of noninvasive methods in predicting the development of hepatocellular carcinoma and hepatic decompensation in patients with chronic hepatitis B. *J Clin Gastroenterol.* 2012;46(6):518–25.

21. Calvaruso V, Dhillon AP, Tsochatzis E, Manousou P, Grillo F, Germani G, et al. Liver collagen proportionate area predicts decompensation in patients with recurrent hepatitis C virus cirrhosis after liver transplantation. *J Gastroenterol Hepatol.* 2012;27(7):1227–32.
22. Kim DY, Song KJ, Kim SU, Yoo EJ, Park JY, Ahn SH, et al. Transient elastography-based risk estimation of hepatitis B virus-related occurrence of hepatocellular carcinoma: development and validation of a predictive model. *Onco Targets Ther.* 2013;6:1463–9.
23. Calvaruso V, Bronte F, Conte E, Simone F, Craxi A, Di Marco V. Modified spleen stiffness measurement by transient elastography is associated with presence of large oesophageal varices in patients with compensated hepatitis C virus cirrhosis. *J Viral Hepat.* 2013;20(12):867–74.
24. Macías J, Camacho A, Von Wichmann MA, López-Cortés LF, Ortega E, Tural C, et al. Liver stiffness measurement versus liver biopsy to predict survival and decompensations of cirrhosis among HIV/hepatitis C virus-coinfected patients. *AIDS.* 2013;27(16):2541–9.
25. Poynard T, Vergniol J, Ngo Y, Foucher J, Munteanu M, Merrouche W, et al. Staging chronic hepatitis C in seven categories using fibrosis biomarker (FibroTest) and transient elastography (FibroScan(R)). *J Hepatol.* 2014;60(4):706–14.
26. Merchante N, Tellez F, Rivero-Juarez A, Rios-Villegas MJ, Merino D, Marquez-Solero M, et al. Progression of liver stiffness predicts clinical events in HIV/HCV-coinfected patients with compensated cirrhosis. *BMC Infect Dis.* 2015;15:557.
27. Bihari C, Rastogi A, Sen B, Bhadoria AS, Maiwall R, Sarin SK. Quantitative fibrosis estimation by image analysis predicts development of decompensation, composite events and defines event-free survival in chronic hepatitis B patients. *Hum Pathol.* 2016;55:63–71.
28. Perez-Latorre L, Sanchez-Conde M, Rincon D, Miralles P, Aldamiz-Echevarria T, Carrero A, et al. Prediction of liver complications in patients with hepatitis C virus-related cirrhosis with and without HIV coinfection: comparison of hepatic venous pressure gradient and transient elastography. *Clin Infect Dis.* 2014;58(5):713–8.

# Chapter 33

## Spleen Stiffness to Liver Stiffness Ratio and Disease Etiology



Omar Elshaarawy, Johannes Mueller, and Sebastian Mueller

### Introduction

Spleen stiffness (SS) is now widely used as novel noninvasive parameter to screen for portal hypertension [1, 2]. Moreover, SS has been demonstrated to outscore liver stiffness or platelet count in predicting complications of portal hypertension such as the presence of esophageal varices and the risk of variceal bleeding [3–9]. A combination of LS and SS is currently considered the best predictor of portal hypertension [1, 10]. Although transient elastography has been originally designed to measure LS, it can well be explored to assess SS [1, 11]. Limitations are small normal sized spleens and obesity. In addition, since SS is typically higher as LS, the upper detection limit of the Fibroscan device at 75 kPa is more rapidly reached which has presently resulted in commercially available technically modified dedicated spleen examinations [12]. The presence of clinically significant portal hypertension (CSPH) is correlated with worse outcome, liver decompensation, and the presence of hepatocellular carcinoma (HCC) [13, 14].

However, less attention has been paid to the relation of SS and disease etiology. With regard to LS, it has been rapidly learnt that it clearly depends on disease etiology resulting in different cutoff values, e.g., for F4 cirrhosis [15, 16]. While the exact identification of LS cutoff values is still an ongoing debate, it has been well settled that inflammation is a key modifier of LS for common liver diseases such as viral hepatitis or ALD. Moreover, resolution of inflammation has been demonstrated

---

O. Elshaarawy · J. Mueller

Center for Alcohol Research and Liver Diseases, Salem Medical Center,  
University of Heidelberg, Heidelberg, Germany  
e-mail: [oelshaarawy@liver.menofia.edu.eg](mailto:oelshaarawy@liver.menofia.edu.eg)

S. Mueller (✉)

Department of Medicine and Center for Alcohol Research and Liver Diseases,  
Salem Medical Center, University of Heidelberg, Heidelberg, Germany  
e-mail: [sebastian.mueller@urz.uni-heidelberg.de](mailto:sebastian.mueller@urz.uni-heidelberg.de)

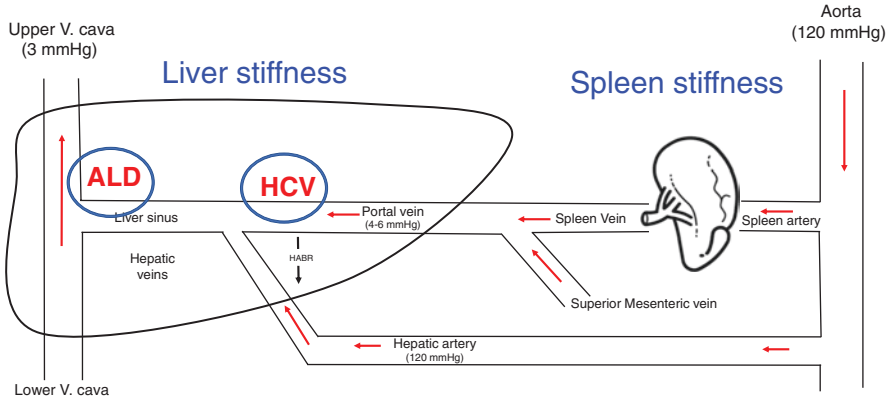


**Fig. 33.1** Effect of disease etiology and localization of inflammation (lobular versus portal disease) on liver and spleen stiffness. (Modified from [15])

to result in lowered LS both upon viral clearance in HCV patients [17] and alcohol detoxification in patients with ALD treatment [18, 19]. In a recent large multicenter trial of more than 1500 biopsy proven patients with HCV and ALD, it was shown that inflammation had a different impact on LS strongly depending on disease etiology. Thus, HCV patients with identical high transaminases and fibrosis stage had clearly lower LS values compared to patients with lobular ALD [15]. It has been therefore suggested that the localization of inflammation (portal versus lobular) could be an additional critical factor that determines LS (see Fig. 33.1). These observations have been also taken up and integrated in the recently introduced sinusoidal pressure hypothesis that identifies the sinusoidal pressure as a key factor for liver stiffness and fibrosis progression [20].

### SS/LS Ratio Significantly Differs in ALD and HCV

Recently, we conducted a study that analyzed and compared SS and LS in patients with portal (HCV) and lobular (ALD) chronic liver disease [21]. Our findings clearly show that patients with portal HCV have a significantly higher SS and SS/LS ratio. Figure 33.2 shows LS, SS, and spleen size both for HCV and ALD in cohorts matched for LS to rule out cohort-specific differences. Cohorts were also matched for age and gender. Although no significant differences were observed with regard to LS (19.0 vs. 19.8 kPa,  $P = 0.63$ ), Fig. 33.2 demonstrates that spleens were significantly larger and SS was higher in HCV. Of note, these patients are also significantly more likely to develop and to die from complications of portal hypertension. In contrast, patients with lobular ALD showed more elevated LS and are more prone to develop signs of synthetic liver failure such as jaundice. In addition, our

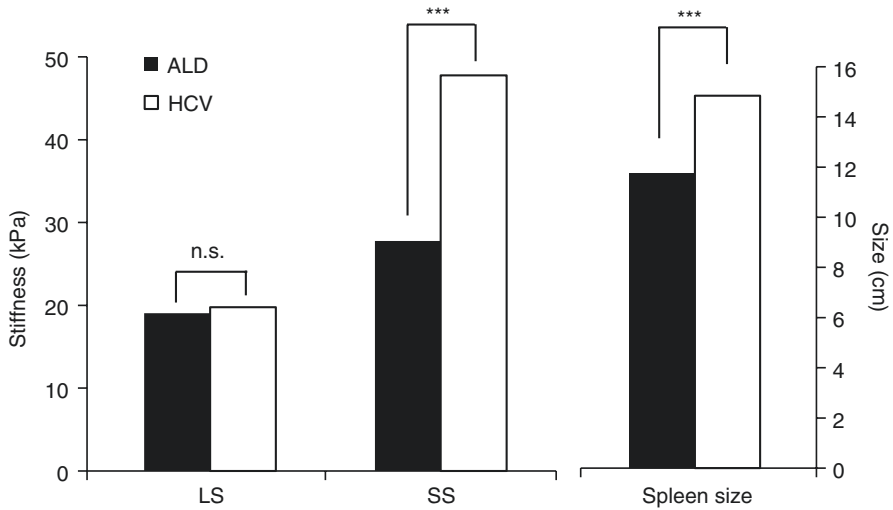


**Fig. 33.2** Spleen stiffness and spleen size are significantly higher in patients with portal hepatitis C infection (HCV) as compared to lobular alcoholic liver disease (ALD). Both ALD (n = 191) and HCV (n = 220) were matched for liver stiffness, age, gender and BMI. Modified from [21]

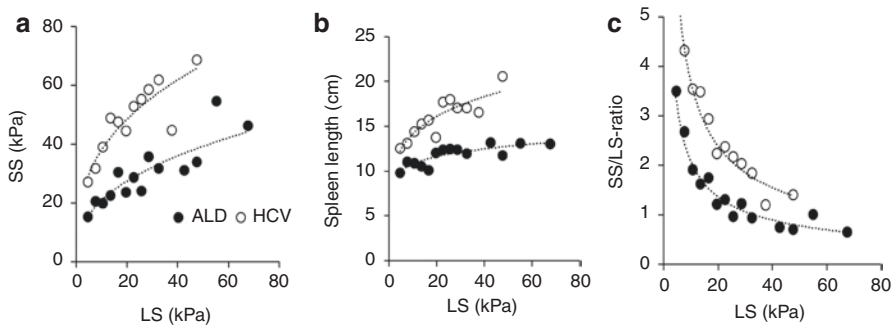


**Fig. 33.3** Development of SS (a), spleen length (b), and SS/LS (c) along increasing LS

data indicated that combined use of LS and SS is not only associated with the degree of fibrosis or portal hypertension but may also provide useful information about the intrahepatic localization of inflammation and, consequently, the likeliness of potential future complications.

Surprisingly, the SS/LS ratio showed a significant difference in both cohorts (ALD and HCV) with 1.7 in ALD versus 3.8 in the HCV cohort ( $P < 0.001$ ). Also, the spleen length to LS ratio reflected the same relation (0.95 vs. 1.46,  $P < 0.0001$ ). These findings suggest that the portal localization of inflammation in HCV could explain the higher SS as compared to higher LS in patients with ALD and pronounced lobular disease. Since the side of inflammation is strongly dependent on fibrosis stage and will eventually encompass the whole liver in both diseases, it



**Table 33.1** Differences in the SS/LS ratio in groups stratified according to SS cutoff values for clinically significant portal hypertension (Colecchia et al. [1])

Cohorts/SS	SS <40 kPa	SS ≥40 kPa	P value
ALD	1.8	1.34	<0.001
HCV	4.19	3.32	<0.001
P value	<0.001	<0.001	

was important to study the effect of fibrosis stages on SS/LS ratio. In both cohorts, the ratios declined with the progression of fibrosis being significantly different in all stages. Interestingly, all spleen-related parameters were higher for the total LS range in HCV patients. Figure 33.3b underlines that even the simple spleen length performs well. Taken together, SS/LS ratio is higher in HCV over all fibrosis stages. Also, SS/LS ratio was also significantly higher in HCV than ALD patients on stratifying patients according to the SS cutoff values for clinically significant portal hypertension (see Table 33.1) and significant decrease in both etiologies with the progression of portal hypertension [1]. Consequently, the SS/LS ratio provides additional information about the localization of inflammation/fibrosis (see also Appendix Figs. A.8 and A.9).

## SS and Spleen Length

Data in humans indicate that SS and spleen length are linearly related to each other independent of the underlying liver disease [21]. In particular, no differences were observed between ALD and HCV regarding SS and spleen length. Similar data have been demonstrated in animal models with TAA-induced liver fibrosis. This indicates that SS and spleen length seem to be the sole result of portal hypertension while additional, e.g., extrahepatic, disease-specific confounders are neglectable. In confirmation, spleen length correlated highly with SS following a linear function with a coefficient of determination of 0.91 and no significant differences between both diseases [21]. Of note, spleen length and stiffness, the actual portal pressure (invasively assessed), and portal hypertension-related complications were always higher or more frequent in HCV patients. Also, liver size to LS ratio clearly differs between HCV and ALD. While, during fibrosis progression, liver size continuously decreased in patients with HCV, it rather increased in patients with ALD up to a LS of 30 kPa and only thereafter started to decrease. These findings also emphasize that the liver is the primary side to show the differences of SS/LS ratio between HCV and ALD. Notably, these observations are also in line with an earlier study that demonstrated significantly higher LS values for ALD as compared to NAFLD patients (40.4 vs. 25.7 kPa) for the detection of large esophageal varices [22].

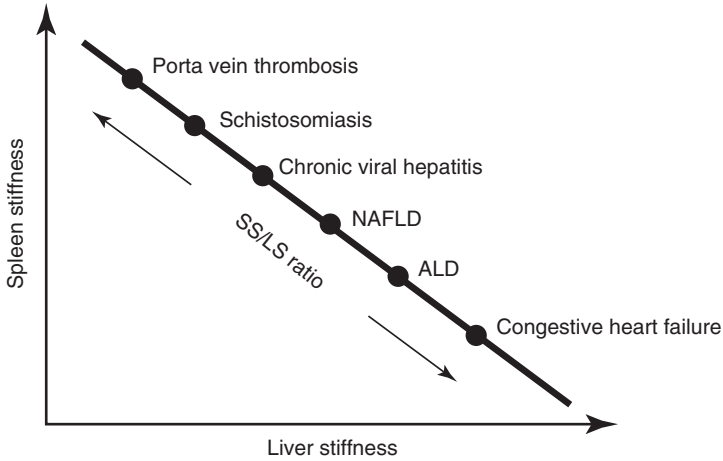


**Fig. 33.4** SS/LS ratio according to the underlying liver disease, histological localization of inflammation or side of pressure elevation

## Future Applications of SS/LS Ratio

Since mean SS/LS ratio did not overlap between ALD and HCV, the SS/LS ratio may be also a useful tool to better emphasize the role of alcohol consumption in HCV patients. No prospective data are yet available on portal vein thrombosis and other forms of viral hepatitis including HBV or even diseases such as schistosomiasis and congestive heart failure. However, it is expected that distinct liver diseases will show specific SS/LS ratios as shown in Fig. 33.4 but also Appendix Figs. A.8 and A.9. Thus, pre-hepatic pathologies such as portal vein thrombosis yield very high SS/LS ratios (17 in individual cases) while a post-hepatic pathology such as liver congestion in heart failure will lead to SS/LS ratio as low as 0.3. Taken together, SS/LS ratios seem to provide additional valuable and noninvasive information for the differential diagnosis of liver disease.

## References

1. Colecchia A, Montrone L, Scaioli E, Bacchi-Reggiani ML, Colli A, Casazza G, et al. Measurement of spleen stiffness to evaluate portal hypertension and the presence of esophageal varices in patients with HCV-related cirrhosis. *Gastroenterology*. 2012;143(3):646–54.
2. Abraldes JG, Reverter E, Berzigotti A. Spleen stiffness: toward a noninvasive portal sphygmomanometer? *Hepatology*. 2013;57(3):1278–80.
3. Abraldes JG, Villanueva C, Aracil C, Turnes J, Hernandez-Guerra M, Genesca J, et al. Addition of simvastatin to standard therapy for the prevention of variceal rebleeding does not reduce rebleeding but increases survival in patients with cirrhosis. *Gastroenterology*. 2016;150(5):1160–70.e3.

4. Kim HY, Jin EH, Kim W, Lee JY, Woo H, Oh S, et al. The role of spleen stiffness in determining the severity and bleeding risk of esophageal varices in cirrhotic patients. *Medicine (Baltimore)*. 2015;94(24):e1031.
5. Takuma Y, Nouse K, Morimoto Y, Tomokuni J, Sahara A, Takabatake H, et al. Prediction of oesophageal variceal bleeding by measuring spleen stiffness in patients with liver cirrhosis. *Gut*. 2016;65(2):354.
6. Takuma Y, Nouse K, Morimoto Y, Tomokuni J, Sahara A, Takabatake H, et al. Portal hypertension in patients with liver cirrhosis: diagnostic accuracy of spleen stiffness. *Radiology*. 2016;279(2):609–19.
7. Sharma P, Kirnake V, Tyagi P, Bansal N, Singla V, Kumar A, et al. Spleen stiffness in patients with cirrhosis in predicting esophageal varices. *Am J Gastroenterol*. 2013;108(7):1101–7.
8. Stefanescu H, Grigorescu M, Lupsor M, Procopet B, Maniu A, Badea R. Spleen stiffness measurement using Fibrosan for the noninvasive assessment of esophageal varices in liver cirrhosis patients. *J Gastroenterol Hepatol*. 2011;26(1):164–70.
9. Abraldes JG, Bureau C, Stefanescu H, Augustin S, Ney M, Blasco H, et al. Noninvasive tools and risk of clinically significant portal hypertension and varices in compensated cirrhosis: the “Anticipate” study. *Hepatology*. 2016;64(6):2173–84.
10. Colecchia A, Colli A, Casazza G, Mandolesi D, Schiumerini R, Reggiani LB, et al. Spleen stiffness measurement can predict clinical complications in compensated HCV-related cirrhosis: a prospective study. *J Hepatol*. 2014;60(6):1158–64.
11. Stefanescu H, Grigorescu M, Lupsor M, Maniu A, Crisan D, Procopet B, et al. A new and simple algorithm for the noninvasive assessment of esophageal varices in cirrhotic patients using serum fibrosis markers and transient elastography. *J Gastrointest Liver Dis*. 2011;20(1):57–64.
12. Bastard C, Miette V, Cales P, Stefanescu H, Festi D, Sandrin L. A novel FibroScan examination dedicated to spleen stiffness measurement. *Ultrasound Med Biol*. 2018;44(8):1616–26.
13. D’Amico G, Garcia-Pagan JC, Luca A, Bosch J. Hepatic vein pressure gradient reduction and prevention of variceal bleeding in cirrhosis: a systematic review. *Gastroenterology*. 2006;131(5):1611–24.
14. Abraldes JG, Araujo IK, Turón F, Berzigotti A. Diagnosing and monitoring cirrhosis: liver biopsy, hepatic venous pressure gradient and elastography. *Gastroenterol Hepatol*. 2012;35(7):488–95.
15. Mueller S, Englert S, Seitz HK, Badea RI, Erhardt A, Bozaari B, et al. Inflammation-adapted liver stiffness values for improved fibrosis staging in patients with hepatitis C virus and alcoholic liver disease. *Liver Int*. 2015;35(12):2514–21.
16. Castera L, Forns X, Alberti A. Non-invasive evaluation of liver fibrosis using transient elastography. *J Hepatol*. 2008;48(5):835–47.
17. Pons M, Santos B, Simon-Talero M, Ventura-Cots M, Riveiro-Barciela M, Esteban R, et al. Rapid liver and spleen stiffness improvement in compensated advanced chronic liver disease patients treated with oral antivirals. *Therap Adv Gastroenterol*. 2017;10(8):619–29.
18. Gelsi E, Dainese R, Truchi R, Marine-Barjoan E, Anty R, Autuori M, et al. Effect of detoxification on liver stiffness assessed by fibrosan((R)) in alcoholic patients. *Alcohol Clin Exp Res*. 2011;35(3):566–70.
19. Mueller S, Millonig G, Sarovska L, Friedrich S, Reimann FM, Pritsch M, et al. Increased liver stiffness in alcoholic liver disease: differentiating fibrosis from steatohepatitis. *World J Gastroenterol*. 2010;16(8):966–72.
20. Mueller S. Does pressure cause liver cirrhosis? The sinusoidal pressure hypothesis. *World J Gastroenterol*. 2016;22(48):10482.
21. Elshaarawy O, Mueller J, Guha IN, Chalmers J, Harris R, Krag A, et al. Spleen stiffness to liver stiffness ratio significantly differs between ALD and HCV and predicts disease-specific complications. *JHEP Rep*. 2019;1(2):99–106.
22. Nguyen-Khac E, Saint-Leger P, Tramier B, Coevoet H, Capron D, Dupas JL. Noninvasive diagnosis of large esophageal varices by Fibrosan: strong influence of the cirrhosis etiology. *Alcohol Clin Exp Res*. 2010;34(7):1146–53.

# Chapter 34

## Prediction of HCC Using Liver Stiffness Measurements



Grace Lai-Hung Wong

### Introduction

Liver fibrosis is a pivotal component of all chronic liver diseases. It is the formation of scar tissue in response to parenchymal injury secondary to chronic liver disease, e.g., chronic hepatitis B and C, non-alcoholic fatty liver disease (NAFLD), or alcoholism [1]. The continuous and progressive replacement of hepatocytes by extracellular matrix and fibrous tissue leads to liver cirrhosis, which is a key risk factor for hepatocellular carcinoma (HCC) [2]. Liver stiffness measurement (LSM) with transient elastography has been proven to predict various liver-related complications, in particular hepatocellular carcinoma (HCC). The LS data on HCC prediction will be discussed in detail in this chapter.

### LSM Predicts HCC Occurrence

The dose–response relationship between LSM and incident HCC was first described in the end of last decade. In a Japanese cohort of 866 patients with chronic hepatitis C (CHC), the hazard ratios (HRs) of incident HCC were 17, 21, 26, and 46 in patients with LS at 10.1–15.0 kPa, 15.1–20.0 kPa, 20.1–25.0 kPa, and >25.0 kPa, respectively (LS  $\leq$  10.0 kPa as reference) [3]. Subsequently, with slightly lower cutoffs for patients with chronic hepatitis B (CHB), the HRs of developing HCC were 3.1, 4.7,

---

G. L.-H. Wong (✉)

Institute of Digestive Disease, The Chinese University of Hong Kong, Shatin, Hong Kong

Department of Medicine and Therapeutics, Prince of Wales Hospital, Shatin, Hong Kong

State Key Laboratory of Digestive Disease, The Chinese University of Hong Kong, Shatin, Hong Kong

e-mail: [wonglaihung@cuhk.edu.hk](mailto:wonglaihung@cuhk.edu.hk)

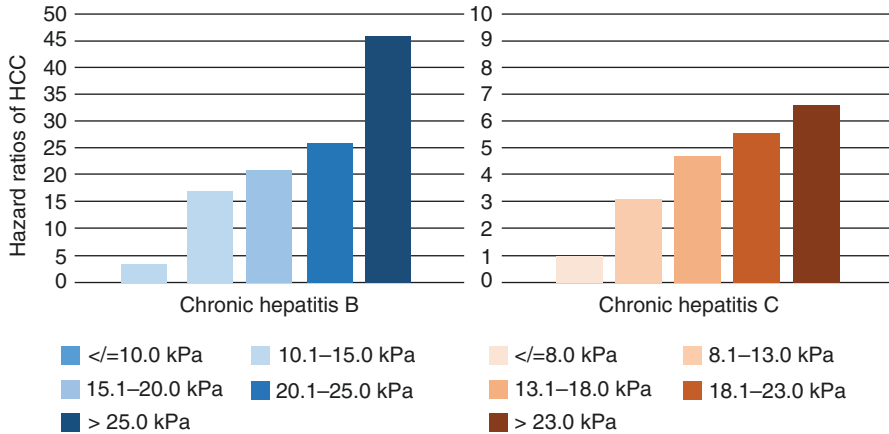


**Fig. 34.1** The dose–response relationship between LS and incident hepatocellular carcinoma (HCC) in patients with chronic hepatitis B or C. Note that the risk of HCC is ca. 6x higher in CHB at LS values higher than 25 kPa as compared to CHC

5.6, and 6.6 in patients with LSM at 8.1–13.0 kPa, 13.1–18.0 kPa, 18.1–23.0 kPa, and >23.0 kPa, respectively (LSM  $\leq$  8.0 kPa as reference), in a Korean cohort of 1130 CHB patients (Fig. 34.1) [4]. In patients with CHB-related cirrhosis, patients of sub-cirrhotic range of LS (defined as <13.0 kPa) would have more than 50% lower risk of HCC development compared to those with cirrhotic range of LS [5].

Apart from patients with chronic viral hepatitis, this relationship was also confirmed in the cirrhotic patients of mixed etiologies in a European multicenter study. In this retrospective cohort of 432 cirrhosis patients with baseline LSM  $\geq$  20 kPa, there was again a dose–response relationship between LSM and HCC risk: the 30–40 kPa group had a HR of 3.0; and the >40 kPa group had a HR of 4.8 (LSM 20–25 kPa as reference) [6].

There is also a diagnostic role of elastography for HCC. Point shear wave elastography (ARFI-pSWE) is used for differentiating benign and malignant liver tumors by the assessment of virtual touch tissue imaging (VTI) and virtual touch tissue quantification (VTQ), as VTI appears to be stiffer and VTQ is higher in malignant lesion than its benign counterpart [7]. For magnetic resonance elastography (MRE), a higher loss modulus has been described for malignant tumors as compared to benign lesions [8].

### *Prediction After Antiviral Therapy*

LSM is not just useful to predict HCC at a single time point; it may also facilitate the dynamic prediction of HCC at different time points, in particular before and after antiviral therapy.

## Interferon-Based Treatment

In general, a significant LSM reduction was observed in CHC patients who had received antiviral therapy [9].  $LS \geq 14.0$  kPa, on top of platelet count and lack of sustained virologic response (SVR), is an independent risk factor of HCC in CHC patients receiving interferon-based treatment [10]. After achieving SVR, a risk-score system (from 0 to 4) combining advanced fibrosis/cirrhosis, presence of diabetes mellitus, and a  $LS > 12$  kPa predicted HCC [11].

## DAA Treatment

In recent years, direct-acting antivirals (DAA) have improved treatment effectiveness in CHC patients with cirrhosis, because of the much higher SVR rates and optimal drug safety profile, allowing treatment scaling up in patients suffering from advanced cirrhosis [12, 13]. However, early reports concerning de novo or recurrent HCC risk in patients with cirrhosis treated with DAAs have shown conflicting results; a few studies showed a protective SVR effect on incident HCC [14–16]. Hence, this calls for a need to predict de novo or recurrent HCC after DAA treatment. In a retrospective cohort study of 565 CHC patients with cirrhosis, LS together with male gender, diabetes mellitus, and FIB-4 score were independent risk factors for de novo HCC [17]. Patients with baseline  $LS > 30$  kPa had an estimated incidence rate of 20% de novo HCC at 3 years (compared to 5% in  $LSM < 30$  kPa) [17]. Interestingly, CHC patients with cirrhosis and HCC showed a larger decrease of LS after DAA treatments as compared to those that did not develop HCC (−18.0% vs. −28.9%). A decrease of LS more than 30% was an independent risk factor for HCC development [18].

## *LSM-Based HCC Risk Prediction Models*

Based on the robust relationship between LS and HCC risk, various prediction models have been developed based on LS and other clinical parameters. Hence, LS has become an important part of some HCC risk score.

## LSM-HCC Score

LSM-HCC score [19] is optimized from the CU-HCC score [20] by replacing clinical cirrhosis with LS; this optimization further increases the negative predictive value close to 100% for the 3–5-year HCC prediction in CHB patients. The LSM-HCC score ranges from 0 to 30. Using  $LS < 11$  kPa as the cutoff value, 706 (68.2%) and 329 (31.8%) patients were in the low- and high-risk categories; 4 (0.6%) and 29 (8.8%) patients developed HCC over 5 years. The areas under the receiver operating characteristic curve (AUROCs) of the LSM-HCC score were higher than those of

the CU-HCC score (0.83–0.89 vs 0.75–0.81). The sensitivity for identifying HCC was 87.9% and the NPV was 99.4% at 5 years [19].

### **Korean Model**

A Korean study developed a sophisticated prediction model with four parameters, namely LS, age, male gender, and baseline serum HBV DNA >20,000 IU/L [21]. The formula for a 3-year probability of HCC occurrence is as follows: Probability =  $1 - PA$  [ $A = \exp(0.05306 \times \text{age} + 1.106 \times \text{male gender} + 0.04858 \times \text{liver stiffness values} + 0.50969 \times \text{HBV DNA} \geq 20,000 \text{ IU/L})$ ]. In bootstrap analyses, the AUROC remained largely unchanged between iterations, with an average value of 0.802 [21].

### **Modified REACH-B (mREACH-B) Score**

The REACH-B scoring system, which was developed and validated as a simple HCC prediction model prior to the era of antiviral therapy, showed suboptimal predictive performance [22]. Therefore, an alternative predictor of long-term prognosis is required particularly in CHB patients who had achieved CVR from antiviral treatment, because levels of HBV DNA are no longer useful at the time of complete viral suppression. In the modified REACH-B model (**mREACH-B model**), the serum levels of HBV DNA were substituted by LS, and had better predictive performance among patients who achieved complete viral suppression with entecavir [23]. The authors reassessed the scores at complete viral suppression, replacing suppressed HBV DNA with LS. The AUROC value for risk at the 3-year follow-up was 0.805, compared to 0.629 using the original REACH-B scoring system, when 0, 1, and 2 points were assigned to LS values of <8.0, 8.0–13.0, and >13.0 kPa, respectively, and 0.814 (95%CI: 0.709–0.912) when 0, 2, and 4 points were assigned to LS values of <8.0, 8.0–13.0, and >13.0 kPa, respectively [23]. The mREACH-B score had better performance for prediction of HCC development at 3 and 5 years, compared to the LSM-HCC, as well as other conventional, non-LSM-based prediction models (e.g., GAG-HCC, REACH-B, and CU-HCC) [24, 25]. The mREACH-B score has better predictive value for HCC compared to LSM-HCC score, irrespective of follow-up period and baseline ALT levels [26].

### ***LS Predicts HCC Outcome***

#### ***HCC Recurrence***

LS is also an important prognostic parameter in patients with confirmed HCC. In 150 CHC patients who had HCC and underwent different HCC treatments, LS increased significantly after transarterial chemoembolization (TACE) but not after microwave ablation (MWA); a lower pre-ablation LS predicted complete ablation of

tumor [27]. In HCC patients receiving partial hepatectomy or TACE, LS and AST to Platelet Ratio Index (APRI) are two independent prognostic factors of survival [28–30]. LS is also found useful to predict de novo recurrence after curative treatment, e.g., resection [31] or radiofrequency ablation [32, 33] for HCC. Another study of 133 HCC patients revealed that patients of  $LS \geq 13.4$  kPa had a nearly twofold increase in the risk of HCC late recurrence compared to those with  $LS < 13.4$  kPa [34].

In contrast, a recent Italian study found that spleen stiffness measurement (SSM) was found to be the only predictor of late HCC recurrence [35]. In this study, a positive correlation between LS and late HCC recurrence was identified only at univariate analysis, while at multivariate analysis only SSM remained significantly correlated which was not measured in the previous Korean study [34]. A possible explanation for these different results is the known better accuracy of SSM to predict portal hypertension, which plays an important role in HCC development and recurrence [36]. More information on spleen stiffness and portal hypertension is provided in book section V.

### *Postoperative Complications in HCC Patients*

A prospective study of 105 HCC patients demonstrated that a LS cutoff of 12.0 kPa had the sensitivity of 86% and specificity of 72% in predicting major postoperative complications [37]. This cutoff may also identify patients with more severe operative blood loss and higher transfusion rate [37]. In a cohort of 51 patients with early HCC undergoing liver resection, LSM had an equally good performance compared to hepatic venous pressure gradient (HVPG) in predicting decompensation within the next 3 months [38].

### *Postoperative Survival*

In a study of 263 Chinese patients who underwent curative resection for HBV-positive HCC, preoperative  $LS \geq 13.2$  kPa predicted poorer overall survival (median, 61.3 vs. 48.2 months) and recurrence-free survival (median, 60.4 vs. 47.0 months) when compared to those with a preoperative  $LS < 13.2$  kPa [39]. In the same study, LS was correlated with Barcelona Clinic Liver Cancer (BCLC) stage and TNM stage, which suggests that patients with higher LS tend to have a more advanced tumor [39]. A meta-analysis of 13 (12 prospective and one retrospective) cohort studies with a total of 1942 subjects demonstrated that preoperative LS is significantly associated with the occurrence of overall postoperative complications (OR 1.76, 95% CI 1.46 ± 2.11) [40]. The authors further analyzed the LS cutoffs based on ethnicities; a weighted mean LS value of 14.2 kPa and 11.3 kPa were suggested as the optimal LS cutoffs for predicting overall postoperative complications in Asian and European countries, respectively [40].



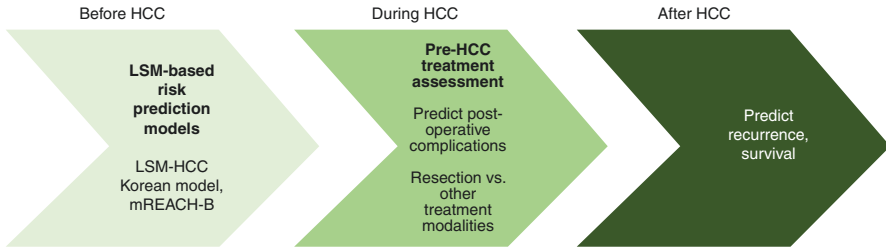


**Fig. 34.2** Role of LSM to predict HCC risk, HCC survival and to guide HCC management

## Conclusions

In conclusion, LSM plays an important role before, during, and after HCC treatment (Fig. 34.2). LSM-based risk prediction models provide an accurate risk-stratification before and after antiviral treatment. LSM also helps in predicting HCC treatment outcomes, including HCC recurrence, postoperative complications and survival. Hence patients either at risk of HCC or already developed HCC should receive LSM on a regular basis.

**Authorship Statement** Grace Wong had full access to all of the data and take responsibility for the integrity of the data and the accuracy of the data analysis. She was also responsible for the interpretation of data, the drafting, and critical revision of the manuscript for important intellectual content.

**Financial Support** None.

**Statement of Interests** Grace Wong has served as an advisory committee member for Gilead Sciences, and as a speaker for Abbott, Abbvie, Bristol-Myers Squibb, Echosens, Furui, Gilead Sciences, Janssen, and Roche.

## References

1. Cheng JY, Wong GL. Advances in the diagnosis and treatment of liver fibrosis. *Hepatoma Res.* 2017;3:156–69.
2. Pinter M, Trauner M, Peck-Radosavljevic M, Sieghart W. Cancer and liver cirrhosis: implications on prognosis and management. *ESMO Open.* 2016;1(2):e000042.
3. Masuzaki R, Tateishi R, Yoshida H, Goto E, Sato T, Ohki T, et al. Prospective risk assessment for hepatocellular carcinoma development in patients with chronic hepatitis C by transient elastography. *Hepatology.* 2009;49(6):1954–61.
4. Jung KS, Kim SU, Ahn SH, Park YN, Kim DY, Park JY, et al. Risk assessment of hepatitis B virus-related hepatocellular carcinoma development using liver stiffness measurement (FibroScan). *Hepatology.* 2011;53(3):885–94.
5. Jeon MY, Lee HW, Kim SU, Heo JY, Han S, Kim BK, et al. Subcirrhotic liver stiffness by FibroScan correlates with lower risk of hepatocellular carcinoma in patients with HBV-related cirrhosis. *Hepatol Int.* 2017;11(3):268–76.

6. Adler M, Larocca L, Trovato FM, Marcinkowski H, Pasha Y, Taylor-Robinson SD. Evaluating the risk of hepatocellular carcinoma in patients with prominently elevated liver stiffness measurements by FibroScan: a multicentre study. *HPB (Oxford)*. 2016;18(8):678–83.
7. Shuang-Ming T, Ping Z, Ying Q, Li-Rong C, Ping Z, Rui-Zhen L. Usefulness of acoustic radiation force impulse imaging in the differential diagnosis of benign and malignant liver lesions. *Acad Radiol*. 2011;18(7):810–5.
8. Garteiser P, Doblas S, Daire JL, Wagner M, Leitao H, Vilgrain V, et al. MR elastography of liver tumours: value of viscoelastic properties for tumour characterisation. *Eur Radiol*. 2012;22(10):2169–77.
9. Subramaniam S, Wong VW, Tse YK, Yip TC, Chan HL, Wong GL. Impact of diabetes mellitus and hepatitis B virus coinfection on patients with chronic hepatitis C: A territory-wide cohort study. *J Gastroenterol Hepatol*. 2018;33(4):934–41.
10. Narita Y, Genda T, Tsuzura H, Sato S, Kanemitsu Y, Ishikawa S, et al. Prediction of liver stiffness hepatocellular carcinoma in chronic hepatitis C patients on interferon-based anti-viral therapy. *J Gastroenterol Hepatol*. 2014;29(1):137–43.
11. Wang JH, Yen YH, Yao CC, Hung CH, Chen CH, Hu TH, et al. Liver stiffness-based score in hepatoma risk assessment for chronic hepatitis C patients after successful antiviral therapy. *Liver Int*. 2016;36(12):1793–9.
12. He T, Lopez-Olivo MA, Hur C, Chhatwal J. Systematic review: cost-effectiveness of direct-acting antivirals for treatment of hepatitis C genotypes 2-6. *Aliment Pharmacol Ther*. 2017;46(8):711–21.
13. Ji F, Wei B, Yeo YH, Ogawa E, Zou B, Stave CD, et al. Systematic review with meta-analysis: effectiveness and tolerability of interferon-free direct-acting antiviral regimens for chronic hepatitis C genotype 1 in routine clinical practice in Asia. *Aliment Pharmacol Ther*. 2018;47(5):550–62.
14. Cheung MCM, Walker AJ, Hudson BE, Verma S, McLauchlan J, Mutimer DJ, et al. Outcomes after successful direct-acting antiviral therapy for patients with chronic hepatitis C and decompensated cirrhosis. *J Hepatol*. 2016;65(4):741–7.
15. Romano A, Angeli P, Piovesan S, Noventa F, Anastassopoulos G, Chemello L, et al. Newly diagnosed hepatocellular carcinoma in patients with advanced hepatitis C treated with DAAs: a prospective population study. *J Hepatol*. 2018;69(2):345–52.
16. Anrs Collaborative Study Group on Hepatocellular Carcinoma. Lack of evidence of an effect of direct-acting antivirals on the recurrence of hepatocellular carcinoma: data from three ANRS cohorts. *J Hepatol*. 2016;65(4):734–40.
17. Degasperis E, D'Ambrosio R, Iavarone M, Sangiovanni A, Aghemo A, Soffredini R, et al. Factors associated with increased risk of de novo or recurrent hepatocellular carcinoma in patients with cirrhosis treated with direct-acting antivirals for hev infection. *Clin Gastroenterol Hepatol*. 2019;17(6):1183–91.e7.
18. Ravaioli F, Conti F, Brillanti S, Andreone P, Mazzella G, Buonfiglioli F, et al. Hepatocellular carcinoma risk assessment by the measurement of liver stiffness variations in HCV cirrhotics treated with direct acting antivirals. *Dig Liver Dis*. 2018;50(6):573–9.
19. Wong GL, Chan HL, Wong CK, Leung C, Chan CY, Ho PP, et al. Liver stiffness-based optimization of hepatocellular carcinoma risk score in patients with chronic hepatitis B. *J Hepatol*. 2014;60(2):339–45.
20. Wong VW, Chan SL, Mo F, Chan TC, Loong HH, Wong GL, et al. Clinical scoring system to predict hepatocellular carcinoma in chronic hepatitis B carriers. *J Clin Oncol*. 2010;28(10):1660–5.
21. Kim DY, Song KJ, Kim SU, Yoo EJ, Park JY, Ahn SH, et al. Transient elastography-based risk estimation of hepatitis B virus-related occurrence of hepatocellular carcinoma: development and validation of a predictive model. *Onco Targets Ther*. 2013;6:1463–9.
22. Yang H-I, Yuen M-F, Chan HL-Y, Han K-H, Chen P-J, Kim D-Y, et al. Risk estimation for hepatocellular carcinoma in chronic hepatitis B (REACH-B): development and validation of a predictive score. *Lancet Oncol*. 2011;12(6):568–74.
23. Lee HW, Ahn SH. Prediction models of hepatocellular carcinoma development in chronic hepatitis B patients. *World J Gastroenterol*. 2016;22(37):8314–21.

24. Jung KS, Kim SU, Song K, Park JY, Kim DY, Ahn SH, et al. Validation of hepatitis B virus-related hepatocellular carcinoma prediction models in the era of antiviral therapy. *Hepatology*. 2015;62(6):1757–66.
25. Seo YS, Jang BK, Um SH, Hwang JS, Han KH, Kim SG, et al. Validation of risk prediction models for the development of HBV-related HCC: a retrospective multi-center 10-year follow-up cohort study. *Oncotarget*. 2017;8(68):113213–24.
26. Jeon MY, Lee HW, Kim SU, Kim BK, Park JY, Kim DY, et al. Feasibility of dynamic risk prediction for hepatocellular carcinoma development in patients with chronic hepatitis B. *Liver Int*. 2018;38(4):676–86.
27. Abdelaziz AO, Abdelhalim H, Elsharkawy A, Shousha HI, Abdelmaksoud AH, Soliman ZA, et al. Liver stiffness measurement changes following hepatocellular carcinoma treatment with percutaneous microwave ablation or transarterial chemoembolization: a cohort study. *Eur J Gastroenterol Hepatol*. 2019;31(6):685–91.
28. Chong CC-N, Wong GL-H, Chan AW-H, Wong VW-S, Fong AK-W, Cheung Y-S, et al. Liver stiffness measurement predicts high-grade post-hepatectomy liver failure: a prospective cohort study. *J Gastroenterol Hepatol*. 2017;32(2):506–14.
29. Pang Q, Zhang JY, Xu XS, Song SD, Chen W, Zhou YY, et al. The prognostic values of 12 cirrhosis-related noninvasive models in patients with hepatocellular carcinoma. *Scand J Clin Lab Invest*. 2015;75(1):73–84.
30. Wong JS, Wong GL, Tsoi KK, Wong VW, Cheung SY, Chong CN, et al. Meta-analysis: the efficacy of anti-viral therapy in prevention of recurrence after curative treatment of chronic hepatitis B-related hepatocellular carcinoma. *Aliment Pharmacol Ther*. 2011;33(10):1104–12.
31. Kim BK, Kim HS, Yoo EJ, Oh EJ, Park JY, Kim DY, et al. Risk assessment of clinical outcomes in Asian patients with chronic hepatitis B using enhanced liver fibrosis test. *Hepatology*. 2014;60(6):1911–9.
32. Lee SH, Kim SU, Jang JW, Bae SH, Lee S, Kim BK, et al. Use of transient elastography to predict de novo recurrence after radiofrequency ablation for hepatocellular carcinoma. *Oncol Targets Ther*. 2015;8:347–56.
33. Lee YR, Park SY, Kim SU, Jang SY, Tak WY, Kweon YO, et al. Using transient elastography to predict hepatocellular carcinoma recurrence after radiofrequency ablation. *J Gastroenterol Hepatol*. 2017;32(5):1079–86.
34. Jung KS, Kim SU, Choi GH, Park JY, Park YN, Kim DY, et al. Prediction of recurrence after curative resection of hepatocellular carcinoma using liver stiffness measurement (FibroScan(R)). *Ann Surg Oncol*. 2012;19(13):4278–86.
35. Marasco G, Colecchia A, Colli A, Ravaioli F, Casazza G, Bacchi Reggiani ML, et al. Role of liver and spleen stiffness in predicting the recurrence of hepatocellular carcinoma after resection. *J Hepatol*. 2019;70(3):440–8.
36. Ripoll C, Groszmann RJ, Garcia-Tsao G, Bosch J, Grace N, Burroughs A, et al. Hepatic venous pressure gradient predicts development of hepatocellular carcinoma independently of severity of cirrhosis. *J Hepatol*. 2009;50(5):923–8.
37. Wong JS-W, Wong GL-H, Chan AW-H, Wong VW-S, Cheung Y-S, Chong C-N, et al. Liver stiffness measurement by transient elastography as a predictor on posthepatectomy outcomes. *Ann Surg*. 2013;257(5):922–8.
38. Procopet B, Fischer P, Horhat A, Mois E, Stefanescu H, Comsa M, et al. Good performance of liver stiffness measurement in the prediction of postoperative hepatic decompensation in patients with cirrhosis complicated with hepatocellular carcinoma. *Med Ultrason*. 2018;20(3):272.
39. Qi M, Chen Y, Zhang GQ, Meng YJ, Zhao FL, Wang J, et al. Clinical significance of preoperative liver stiffness measurements in primary HBV-positive hepatocellular carcinoma. *Future Oncol*. 2017;13(30):2799–810.
40. Huang Z, Huang J, Zhou T, Cao H, Tan B. Prognostic value of liver stiffness measurement for the liver-related surgical outcomes of patients under hepatic resection: a meta-analysis. *PLoS One*. 2018;13(1):e0190512.

# Chapter 35

## Liver Stiffness as a Predictor for Survival



Sebastian Mueller

### Introduction

Overall survival is the most important clinical endpoint. Other important endpoints in clinical hepatology include liver-related death and death due to specific complications such as HCC, liver failure, or decompensation. Most initial studies focused on the performance of LSM to assess fibrosis in comparison to other methods. Nevertheless, it is surprising that the number of prospective studies to assess LS and overall survival is still limited. The available data on LS and all-cause and liver-related mortality are shown Tables 35.1 and 35.2. In a recent meta-analysis that included studies published up to July 1, 2017, and that assessed the LS in predicting liver-related events and all-cause mortality among subjects with chronic liver disease, 54 observational cohort studies were identified [1]. Here, for each unit increment of liver stiffness, the summary relative ratio (RR) was 1.06 for all-cause mortality [1]. However, when having a closer look at the included 54 studies it rapidly becomes apparent that most studies have been performed in patients with viral hepatitis (see Table 35.1), mainly HCV/HBV and partly HIV and only a few addressed all-cause and liver-related mortality. Surprisingly and despite a major worldwide interest, no long-term follow-up data on NAFLD and ALD have been published yet. In a recent abstract [2] on 2251 prospectively recruited NAFLD patients, the median follow-up time was 27 months [IQR: 25–38]. The study reported that 55 patients died and 3 patients had liver transplantation. Only 0.9% of patients (21 patients) had liver-related event (either decompensation or HCC) while 142 (6.3%) developed can-

---

S. Mueller (✉)

Department of Medicine and Center for Alcohol Research and Liver Diseases, Salem Medical Center, University of Heidelberg, Heidelberg, Germany  
e-mail: [sebastian.mueller@urz.uni-heidelberg.de](mailto:sebastian.mueller@urz.uni-heidelberg.de)

**Table 35.1** Prediction of all-cause mortality by LS

Study	Etiologies	Fibrosis stages	N	Liver stiffness (kPa)	HR/RR (95% CI)	Adjustments
Vergniol et al. 2011 [13]	HCV	F0-2: 67.1%, F3-4: 32.9%	789	<9.5	1	FibroTest, ActiTest, treatment, age
				≥9.5	2.9 (2.0-4.3)	
				5-7.1	1.43 (0.67-3.06)	
				7.1-9.5	1.56 (0.66-3.73)	
				9.5-12.5	4.01 (1.80-8.92)	
				12.5-20	5.64 (2.57-12.38)	
				20-50	14.60 (7.35-29.00)	
>50	9.29 (2.20-39.23)					
Vergniol et al. 2014 [11]	HCV	NP	975	Per baseline LS (ln kPa)	5.76 (3.74-8.87)	Age, male gender, alcohol abuse, SVR, follow-up LSM, delta LSM
Hansen et al. 2019 [12]	HCV	<10 kPa (68.4%) 10-16.9 kPa (16.9%) 17-75 kPa (14.7%)	591	<10 kPa	1	Age, sex, alcohol and drug use
				10-16.9 kPa	1.33 (0.63-2.76)	
				17-75 kPa	6 (3.55-10)	
Cepeda et al. 2017 [14]	HCV/HIV-HCV	F0-F2 86%, F3-F4 14%	964	<8.0	1	Sociodemographics, behavioral, HIV infection, and comorbidities
				8.0-12.3	1.39 (0.92-2.09)	
				>12.3	2.19 (1.44-3.33)	
Mueller et al. (abstract) [3]	ALD	71% F0-2, 28% F3-F4	675	Per unit kPa	1.013 (1.003-1.023)	Age, AP, Hb
				<12.5	1	
				≥12.5 kPa	2.049 (1.367-3.072)	

Abbreviations: *CLD* chronic liver disease, *HR* hazard ratio, *NP* not provided, *RR* relative risk, *LRE* liver-related event, *HCV* hepatitis C, *HBV* hepatitis B, *HIV* human immune deficiency virus

**Table 35.2** Prediction of liver-related mortality by LS

Study	Etiologies	Stage of CLD	N	Liver stiffness (kPa)	HR/RR (95% CI)	Adjustments
Hansen et al. 2019 [12]	HCV	<10 kPa (68.4%)	560	<10 kPa	1	Age, sex, alcohol and drug use
		10–16.9 kPa (16.9%)		10–16.9 kPa	9.5 (0.98–91.3)	
		17–75 kPa (14.7%)		17–75 kPa	97 (13.2–713)	
Tuma et al. 2009 [15]	HIV	Cirrhosis	194	≤28.8	1	NP
				>28.8	3.5 (1.24–9.70)	
Cheng et al. 2016 [16]	HBV	NP		≤8.0	1	NP
				>8.0	1.9 (1.1–3.2)	
Mueller et al. (abstract) [3]	ALD	71% F0-2, 28% F3-F4	623	Per unit kPa	1.034 (1.017–1.054)	Total bilirubin
				<12.5	1	
				≥12.5 kPa	8.436 (2.697–26.395)	

Abbreviations: CLD chronic liver disease, HR hazard ratio, NP not provided, RR relative risk, LRE liver-related event, HCV hepatitis C, HBV hepatitis B, HIV human immune deficiency virus

cer (excluding HCC) and 151 (6.7%) had a cardiovascular event during follow-up. They also reported that the overall survival significantly declined with increasing baseline LS. Overall, 21 patients (0.9%) had a liver-related event, 142 (6.3%) developed cancer (excluding HCC) and 151 (6.7%) had a cardiovascular event during follow-up. On multivariate analysis, independent predictors of overall survival were: baseline LS (adjusted HR (aHR) = 2.85 [1.65–4.92],  $P = 0.0002$ ), age (aHR = 1.11[1.08–1.13],  $P < 0.0001$ ), and male sex (aHR = 2.05 [1.17–3.57],  $P = 0.012$ ). Patients with elevated LS showed more significant cardiovascular and liver events but no other cancers. The incidence of HCC increased with baseline LS (<12 kPa: 0.32%; 12–18 kPa: 0.58%; 18–38 kPa 9.26%, and >38 kPa: 13.3%). The authors concluded that prediction of survival, cardiovascular and liver complications should be based on initial evaluation of LSM [2].

Only some publications contain a few cases of non-viral diseases so that no etiology-specific statements can be derived. An exception has been our prospective 10-year follow-up study in heavy drinkers which has been published recently in abstract form [3]. Another challenge is the lack of characterization, standardization, information, and many studies use different criteria, cut-offs and look for different endpoints.

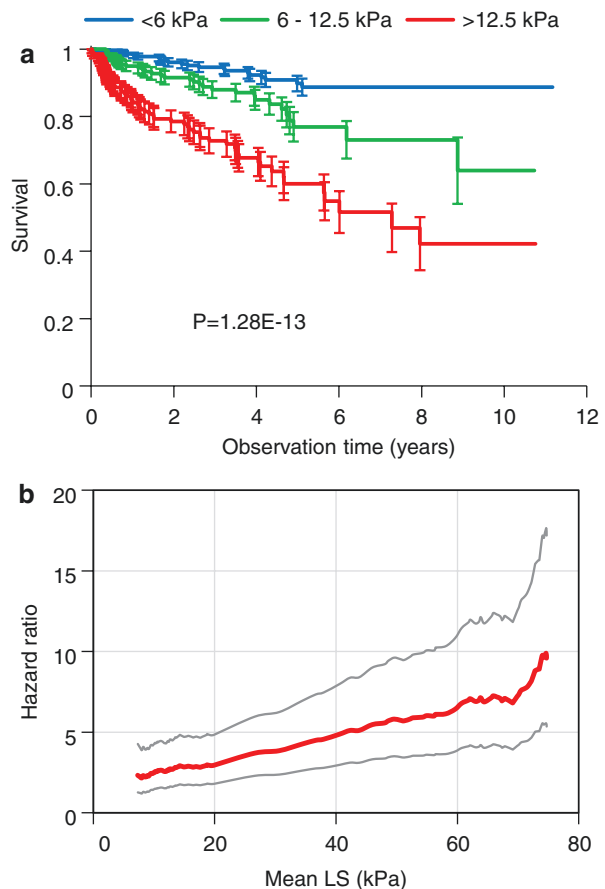
On the other side, there are interesting first data that suggest LS to be highly prognostic in very specific but highly relevant settings, e.g., predicting the 30-day overall mortality of patients admitted to the emergency room [4]. These first data underscore the many confounders of LS elevation. According to a Danish study, major causes of 30-day overall mortality were either related to heart failure or liver cirrhosis, mainly alcoholic liver cirrhosis. It should be also mentioned that there are first data on LS and heart failure [5] and in the setting of the intensive care unit [6]. Very few data have evaluated data on LS dynamics. Accordingly, a decreasing LS either after TIPS intervention [7] or treatment with non-selective  $\beta$ -blockers [8] predict a better outcome. Finally, almost no data are available on spleen stiffness (SS) that is considered to be a better predictor of portal hypertension. First data suggest that SS may provide additional information on hepatic decompensation and outcome [9, 10].

Taken together, data on overall survival and LS are still very limited and more prospective, disease-specific and multicenter studies are required to get a clear picture. The first available data indicate that LS will be clearly an important predictor of short- and long-term survival. There will be differences with regard to disease etiology and it will be also necessary to define the role of spleen stiffness and its relation to LS for the long-term outcome. In addition, first data suggest that LS kinetics may differ between different etiologies and that the response of LS to treatment interventions holds a prognostic value on its own. Finally, important but different clinical settings increasingly emerge where LS and SS assessment will play a major role in assessing not only liver-related but also all-cause mortality such as the emergency room and intensive care units. In the following, the available data on these specific topics will be discussed in more detail.

## LS and All-Cause Mortality

As mentioned above, 54 observational cohort studies with 35,249 participants were included in a recent first meta-analysis on all-cause mortality [1]. Summary relative risks (RRs) were calculated using a random-effects model, and a restricted cubic spline function was used to model the dose-response association. All-cause mortality was increased in subjects with a high LS (RR, 4.15) and for each unit increment of LS, the summary RR was 1.06 for all-cause mortality. A positive relationship with a nonlinear trend for LS with liver-related events and all-cause mortality was examined by a dose-response meta-analysis ( $P < 0.001$ ). When stratified by etiology, a nonlinear association was also found in patients infected with hepatitis C virus and those coinfecting with hepatitis C virus and human immunodeficiency virus. In contrast, there was no evidence of departure from linearity among patients with hepatitis B virus infection ( $P$ -Nonlinearity = 0.072). However, when having a closer look at the studies, only three remain that explicitly and prospectively assess all-cause mortality. They are shown in Table 35.1 together with our still unpublished survival study in heavy drinkers. It is

**Fig. 35.1** (a) Kaplan-Meier curves for different LS values and (b) Hazard ratios as a function of increasing LS from the prospective Heidelberg cohort ( $N = 675$ ) of heavy drinkers followed up for over 10 years





interesting to note that LS seems to predict all-cause mortality quite independent of the etiology. For both HCV and ALD, a cut-off from 9 to 12.5 kPa has a hazard ratio for all-cause mortality of ca. 2 [3, 11]. In heavy drinkers, LS was the best univariate predictor of death and remained an independent variable in multivariate analysis [3]. We analyzed LS in terms of predicting mortality in a large prospective cohort ( $N = 675$ ) of heavy alcohol drinkers recruited over an 11-year period. Figure 35.1a shows survival curves for patients with LS <6 kPa, between 6 and 12.5 kPa, and equal or greater than 12.5 kPa. Patients with LS greater than 12.5 kPa had a ca. 5.4 times higher risk for death than patients with LS less than 6 kPa. These results are unadjusted. In multivariate analysis, LS was also an independent predictor of all-cause and liver-related mortality. The risk increase per kPa in the multivariate model was 1.1% for all-cause mortality and 2.8% for liver-related mortality. Figure 35.1b shows the relative risk versus the average LS in comparison to patients with LS <6 kPa (unadjusted). It can be seen that patients with LS >70 kPa have an eight times higher risk for death from any cause. LS was also the best predictor of 5-year survival.

As shown in Fig. 35.1a, ca. half of heavy drinkers (ca. 180 g alcohol per day) will have passed away after 5 years, if baseline LS was >12.5 kPa [3]. Although the hazard ratio for death continuously increases with LS, there seems to be a nonlinear relation and at LS >50 kPa, other factors are more likely to predict death [11].

In a recent study [12] on 591 chronic hepatitis C patients, patients were grouped by baseline LS: <10, 10–16.9, and 17–75 kPa. Primary outcomes were all-cause mortality and liver-related mortality using cox regression and competing risk regression models, respectively. Median follow-up was 46.1 months. Median LS was 6.8 kPa (IQR 5.3–11.6) with 68.4% having a LS <10 kPa, 16.9% with a LS between 10 and 16.9 kPa, and 14.7% with a LS between 17 and 75 kPa. There were 69 deaths, 27 from liver-related disease. The mortality rate in the 17–75 kPa group was 9.7/100 person-years, compared to 2.2/100 person-years and 1.1/100 person-years in the 10–16.9 kPa and <10 kPa groups ( $P < 0.005$ ). Liver-related mortality increased tenfold for each group ( $P < 0.005$ ). Patients with a LS 17–75 kPa had significantly higher risks of death, liver-related death, and complications to cirrhosis if their hyaluronic acid measurement was more than or equal to 200 ng/mL at baseline, with hazard ratios of 3.2 (95% CI 1.48–7.25), 7.7 (95% CI 2.32–28), and 3.2 (95% CI 1.35–7.4), respectively. These data suggest that combination of LS and circulating levels of hyaluronic acid significantly improve the prognostic power, relative to LS alone. Thus, combined LS and serum markers of liver fibrosis could provide superior risk prediction.

## LS and Mortality in Emergency Room and Intensive Care Unit

One study addressed the question whether an initial LSM by TE in the **emergency room** setting was associated with increased 30-day mortality [4]. Patients  $\geq 18$  years of age were consecutively examined by TE at admission and outcome measure was 30-day mortality.

Among 568 patients admitted during 24 days, 289 (50.8%) were included in the study, 212 (73.4%) with valid TE measurement. Increased LS defined as >8 kPa was

found in 22.6% (48/212). This was independently associated with liver cirrhosis ( $P < 0.001$ ) and congestive heart failure (CHF) ( $P < 0.001$ ). The estimated prevalence of cirrhosis was 7%. The 30-day mortality among patients with TE value  $>8$  kPa was 20.8% compared to 3.7% in patients with a LS  $\leq 8$  kPa, and LS  $>8$  kPa was an independent predictor of death.

Another promising study comes from the **intensive care unit (ICU)** [6]. Hepatic dysfunction is a common finding in critically ill patients on the ICU and directly influences survival. Here, LS was prospectively evaluated in 108 consecutive critically ill patients at the ICU. LS was measured at admission, Day 3, Day 7, and weekly thereafter during the course of ICU treatment. Outcome was followed after discharge with a median observation time of 237 days. LS could be reliably measured in 71% of ICU patients at admission (65% at Day 3, 63% at Day 7). Critically ill patients had significantly increased LS compared to sex- and age-matched standard care patients ( $n = 25$ ). ICU patients with decompensated cirrhosis showed highest LS, whereas other critical diseases (for example, sepsis) and comorbidities (for example, diabetes, obesity) did not impact LS values. At admission to the ICU, LS was closely related to hepatic damage (liver synthesis, cholestasis, fibrosis markers). During the course of ICU treatment, fluid overload (renal failure, volume therapy) and increased central venous pressure (mechanical ventilation, heart failure) were major factors determining LS. LS values  $>18$  kPa at ICU admission were associated with increased ICU and long-term mortality, even in non-cirrhotic patients. In conclusion, both studies from the emergency room and the ICU suggest that LSM may be useful to identify liver dysfunction and predict mortality. Among the many confounders of elevated LS, heart failure and liver disease seem to be the major reasons. One important limitation in these clinical settings is still the rather high percentage (ca. 20–30%) of patients with invalid measurements.

## Prognostic Impact of LS Changes After Therapeutic Interventions

Interestingly, there are first indications that early response of LS to treat portal hypertension such as trans-jugular intrahepatic portosystemic shunt (TIPS) or portal-pressure lowering drugs hold prognostic value.

A recent prospective study investigated LS in patients receiving TIPS regardless of indication [7]. Of 83 included patients, 16 underwent TE immediately before and 30 min after TIPS (acute group), while 67 received shear wave elastography of liver and spleen 1 day before and 7 days after TIPS (chronic group) and were followed further. In 56 patients, LS decreased or remained unchanged ( $<10\%$ ). Importantly, spleen stiffness measured by shear wave elastography decreased in all patients (chronic group). None of the clinical or laboratory parameters differed between patients with increase in LS and those without. Of note, patients with increased LS showed higher overall and/or hepatic venous levels of proinflammatory cytokines at TIPS and higher incidence of organ failure and worse survival after TIPS. C-reactive

protein values and increase of >10% in liver stiffness after TIPS were the only independent predictors of mortality in these patients.

In another study, changes of LS and the hepatic venous pressure gradient (HVPG) under propranolol therapy were assessed with regard to clinical outcomes in a human cohort of  $n = 38$  cirrhotic patients [8]. Most patients ( $n = 25$ , 66%) showed a LS decrease after propranolol treatment initiation which significantly correlated to HVPG ( $r = 0.518$ ,  $P < 0.01$ ) but was not accompanied by statistically significant changes in transaminases or model of end-stage liver disease (MELD). On multivariate analysis, patients with decreasing LS on propranolol had a decreased risk for experiencing a transplantation or death than patients with increasing LS irrespective of HVPG.

Taken together, a LS decrease in response to interventions such as portal pressure-lowering drugs or TIPS may be predictive of improved outcome irrespective of MELD scores and may serve as an additional follow-up tool in the future.

## Mortality and Spleen Stiffness

In a recent study from Japan, spleen stiffness as measured by ARFI imaging was associated with mortality and decompensation in patients with cirrhosis and compared with liver stiffness and other markers [9]. Spleen stiffness (SS) was measured in 393 patients diagnosed with cirrhosis. Patients underwent biochemical, ARFI, ultrasonography, and endoscopy evaluations every 3 or 6 months to screen for liver-related complications until their death, liver transplantation, or the end of the study period. The primary outcome was the accuracy of spleen stiffness in predicting mortality and decompensation, measured by Cox proportional hazards model analysis. During a median follow-up period of 44.6 months, 67 patients died and 35 patients developed hepatic decompensation. In the multivariate analysis, spleen stiffness was an independent parameter associated with mortality, after adjustment for levels of alanine aminotransferase and serum sodium, and the MELD score ( $P < 0.001$ ). SS was associated independently with decompensation after adjustment for Child-Pugh and MELD score. Notably, SS predicted mortality and decompensation with greater accuracy than LS. A SS cut-off value of 3.43 m/s identified the death of patients with a 95.3% negative predictive value and 75.8% accuracy. A SS cut-off value of 3.25 m/s identified patients with decompensation with a 98.8% negative predictive value and 68.9% accuracy.

In addition to these emerging data, it could be recently shown that the SS to LS ratio depends on disease etiology and is able to predict disease-specific complications [10].

## Conclusion

Both LS and SS are independent predictors of all-cause and liver-related mortality in the first few prospective studies.

## References

1. Wang J, Li J, Zhou Q, Zhang D, Bi Q, Wu Y, et al. Liver stiffness measurement predicted liver-related events and all-cause mortality: a systematic review and nonlinear dose-response meta-analysis. *Hepatology*. 2018;2(4):467–76.
2. Shili S, Wong GL-H, Jean-Baptiste H, Liu K, Chermak F, Shu S, et al. SAT-288-liver stiffness measurement predicts long-term survival and complications in non-alcoholic fatty liver disease. *J Hepatol*. 2019;70(1):e763–e4.
3. Mueller J, Rausch V, Silva I, Peccerella T, Piecha F, Dietrich C, et al. PS-171-survival in a 10 year prospective cohort of heavy drinkers: Liver stiffness is the best long-term prognostic parameter. *J Hepatol*. 2019;70(1):E107.
4. Lindvig K, Mossner BK, Pedersen C, Lillevang ST, Christensen PB. Liver stiffness and 30-day mortality in a cohort of patients admitted to hospital. *Eur J Clin Invest*. 2012;42(2):146–52.
5. Sato Y, Yoshihisa A, Kanno Y, Watanabe S, Yokokawa T, Abe S, et al. Liver stiffness assessed by Fibrosis-4 index predicts mortality in patients with heart failure. *Open Heart*. 2017;4(1):e000598.
6. Koch A, Horn A, Duckers H, Yagmur E, Sanson E, Bruensing J, et al. Increased liver stiffness denotes hepatic dysfunction and mortality risk in critically ill non-cirrhotic patients at a medical ICU. *Crit Care*. 2011;15(6):R266.
7. Jansen C, Moller P, Meyer C, Kolbe CC, Bogs C, Pohlmann A, et al. Increase in liver stiffness after transjugular intrahepatic portosystemic shunt is associated with inflammation and predicts mortality. *Hepatology*. 2018;67(4):1472–84.
8. Piecha F, Mandorfer M, Peccerella T, Ozga AK, Poth T, Vonbank A, et al. Pharmacological decrease of liver stiffness is pressure-related and predicts long-term clinical outcome. *Am J Physiol Gastrointest Liver Physiol*. 2018;315(4):G484–G94.
9. Takuma Y, Morimoto Y, Takabatake H, Toshikuni N, Tomokuni J, Sahara A, et al. Measurement of spleen stiffness with acoustic radiation force impulse imaging predicts mortality and hepatic decompensation in patients with liver cirrhosis. *Clin Gastroenterol Hepatol*. 2017;15(11):1782–90 e4.
10. Elshaarawy O, Mueller J, Guha IN, Chalmers J, Harris R, Krag A, et al. Spleen stiffness to liver stiffness ratio significantly differs between ALD and HCV and predicts disease-specific complications. *JHEP Reports*. 2019;1(2):99–106.
11. Vergniol J, Boursier J, Coutzac C, Bertrais S, Foucher J, Angel C, et al. Evolution of non-invasive tests of liver fibrosis is associated with prognosis in patients with chronic hepatitis C. *Hepatology*. 2014;60(1):65–76.
12. Hansen JF, Christiansen KM, Staugaard B, Moessner BK, Lillevang S, Krag A, et al. Combining liver stiffness with hyaluronic acid provides superior prognostic performance in chronic hepatitis C. *PloS one*. 2019;14(2):e0212036.
13. Vergniol J, Foucher J, Terrebbonne E, Bernard PH, le Bail B, Merrouche W, et al. Noninvasive tests for fibrosis and liver stiffness predict 5-year outcomes of patients with chronic hepatitis C. *Gastroenterology*. 2011;140(7):1970–9, 9 e1-3.
14. Cepeda JA, Thomas DL, Astemborski J, Sulkowski MS, Kirk GD, Mehta SH. Increased mortality among persons with chronic hepatitis C with moderate or severe liver disease: a cohort study. *Clin Infect Dis*. 2017;65(2):235–43.

15. Tuma P, Jarrin I, Del Amo J, Vispo E, Medrano J, Martin-Carbonero L, et al. Survival of HIV-infected patients with compensated liver cirrhosis. *AIDS*. 2010;24(5):745–53.
16. Cheng JY, Wong VW, Tse YK, Chim AM, Chan HL, Wong GL. Metabolic syndrome increases cardiovascular events but not hepatic events and death in patients with chronic hepatitis B. *Hepatology*. 2016;64(5):1507–17.

# Chapter 36

## Role of Liver Stiffness in the Management of Liver Transplantation: First Experience and Clinical Practice



Guido Piai, Giovanna Valente, and Luca Rinaldi

### Abbreviations

AIH	Autoimmune hepatitis
ALD	Alcoholic liver disease
ALP	Alkaline phosphatase
ALT	Alanine aminotransferase
APRI	AST to platelet ratio index
ARFI	Acoustic radiation force impulse
AST	Aspartate aminotransferase
AUROC	Area under receiver operating characteristic
BMI	Body mass index
CAP	Controlled attenuation parameter
CI	Confidence interval
HCC	Hepatocellular carcinoma
HE	Hepatic steatosis
INR	International normalized ratio
LB	Liver biopsy
LDLT	Living donor liver transplantation
LS	Liver stiffness
LSM	Liver stiffness measurement
MELD	Model for end-stage liver disease
MRE	Magnetic resonance elastography

---

G. Piai (✉) · G. Valente

Department of Medical Sciences, Liver Unit for Transplant Management—SATTE, AORN Sant'Anna e San Sebastiano, Caserta, Italy

L. Rinaldi

Department of Advanced Medical and Surgical Sciences, University of Campania "Luigi Vanvitelli", Naples, Italy

NAFLD	Non-alcoholic fatty liver disease
PBC	Primary biliary cirrhosis
PSC	Primary sclerosing cholangitis
p-SWE	Point shear wave elastography
SWE	Shear wave elastography
TE	Transient elastography
ULN	Upper limit of normal

## Introduction to Liver Transplantation

In this review, we will briefly summarize liver transplantation (LTX) studies in which liver stiffness (LS) has been studied. Liver stiffness measurement (LSM) could virtually play a role in any context of the transplanted liver graft. This organ is subject both to diseases specific to the condition of the transplant and to those of the general population. Liver transplantation is the standard of care in patients with end-stage liver disease and in those with liver tumors that cannot be treated otherwise [1]. The number of liver transplants performed worldwide, according to the World Transplant Registry [2], has exceeded 30,000/year, and specialists, sonographers, and even radiologists who are not directly involved in the transplantation activity, are increasingly seeing patients with LTX. We have divided the process of liver transplantation into phases in which the liver has different functional aspects: liver stiffness (LS) has been studied before transplantation, from the first days after transplantation until stabilization, during long follow-up, and in the particular context of transplantation in pediatric age. The definition of LS and the numerous methods to detect it are described in other chapters of this book and in the guidelines of the major scientific societies [3]. For more details, see also book Part II “Techniques to Measure Liver Stiffness”.

The significance of LS evaluation in transplantation has been defined mostly by studies conducted with transient elastography (TE), the first and oldest available ultrasound-based method. In the real world, LS can now be measured during a liver transplant follow-up that last for years and by different methods in different places and also with different devices in the same single patient. Therefore, it is always better to maintain a certain degree of caution regarding the interchangeability of the various systems [4].

## Liver Stiffness in the Pre-transplant Management

### *Prognosis of the Patient in the Waiting List*

The value of MELD score is well established as prognostic predictor in patients with cirrhosis waiting for LTX. Nacif et al. compared [5] the mortality risk of end-stage cirrhotic patients with and without HCC on the LTX waiting list with transient

elastography. The study highlighted how increased LS is associated with higher mortality, just like the well-known MELD score. One hundred and three patients were included (without HCC  $n = 58$  (66%); HCC  $n = 45$  (44%)). The mean MELD score was  $14.7 \pm 6.4$ , the portal hypertension present in 83.9%, and the mean LS was  $32.7 \pm 22.5$  kPa. The survival group had a mean LS of  $31.6 \pm 22.2$  kPa vs.  $50.8 \pm 20.9$  kPa ( $P = 0.098$ ) and higher MELD scores ( $P = 0.035$ ). They concluded that elastography is an important noninvasive tool for cirrhosis and HCC and for predicting mortality although more prospective data are required.

### *Evaluation of the Living Donor Liver*

Cultural, religious, and social beliefs largely preclude deceased donor transplantation in Asia where living donor liver transplantation (LDLT) has become the predominant way of transplantation. In North American and European countries, however, due to the critical shortage of organs, LDLT is also becoming increasingly widespread. The selection of a healthy liver grafts is crucial for the success of transplantation. An elevated LS always seems to indicate an ongoing liver pathology. For more details see also book Part IV “Important (Patho)physiological Confounders of LS”. Thus, elastography may be ideal to screen the general population and to identify those who require further evaluation and subsequently to select potential candidates for LDLT.

The process of evaluation and selection of living liver donors, who are strictly volunteers, is very complex. After the initial full screening on donor’s motivation for donation and on social and psychiatric problems, all donors are completely examined with biochemical and imaging techniques. An abdominal Doppler ultrasonography is the first examination to check liver quality, including evaluation for hepatic fibrosis and steatosis. One of the main selection criteria of the quality of a liver graft is the degree of steatosis, which will determine the success of the transplantation, because fatty livers are vulnerable to preservation injury that results in a higher rate of primary nonfunction, of early allograft dysfunction, and of post-transplant vascular and biliary complications [6]. Donors are excluded based on ultrasound if there is an indication for severe steatosis or other unfavorable hepatic parenchymal, vascular, or biliary morphology prior to the surgery. Nowadays, liver donation is permitted if the donor livers have no more than 30% steatosis [6, 7], even in light of protective strategies, such as machine-based perfusion used to minimize preservation related injury. Preoperative liver biopsy becomes generally mandatory in cases of severe fatty liver.

A few small studies have been performed LSM in the preLTX selection of liver grafts. A study conducted in an Egyptian population [8] involved 50 individuals between 19 and 42 years of age who were candidate donors for LDLT. They passed all stages of evaluation for liver donation for their relatives and reached a strict definition of healthy condition based on clinical, chemical, radiological, and histological assessment without evidence of fatty liver or fibrosis. LS by TE ranged between 2.6 and 6.8 kPa, with a median stiffness of 4 kPa. Therefore, these LS values can be considered as normal reference values of an Arab population for further clinical applications.



The degree of fibrosis of a living donor may have clinical consequences after the transplant. In a retrospective study in LDLT, Lee et al. [9] have examined the correlation of LS by TE before transplant with perioperative clinical and laboratory parameters. They reviewed 48 subjects who underwent LDLT. All donors and recipients underwent TE, abdominal computed tomography (CT), and biochemical tests within 1 month before and at 1 week after transplantation. Using a cut-off LSM of 7.5 kPa, which they arbitrarily assigned to be indicative of significant fibrosis, they divided the study population into  $\leq 7.5$  kPa (group L;  $n = 15$ , 31.3%) vs.  $>7.5$  kPa (group H;  $n = 33$ , 68.8%). Pre-transplantation serum total bilirubin, international normalized ratio, and MELD scores of recipients were significantly higher in group H than group L. Regarding the pre-transplantation donor characteristics, the graft-recipient weight ratio was significantly smaller among those in group H ( $P = 0.039$ ). In addition, the post-transplantation 1-week serum total bilirubin level was significantly higher in group H (2.3 mg/dL vs. 1.2 mg/dL,  $P = 0.015$ ), although neither biliary complications nor hepatic congestion was identified by abdominal CT. They concluded that a high LS after LDLT suggests intrahepatic cholestasis and portal hyper-circulation in the graft, irrespective of liver fibrosis, outflow obstruction, or biliary obstruction. In addition, the 1-week post-transplantation serum total bilirubin level was significantly higher in group H, although abdominal CT identified neither biliary complications nor hepatic congestion. Only total bilirubin positively correlated with LSM. The authors suggested that a high LSM in the first period after LDLT might advise regeneration, intrahepatic cholestasis, and persistent portal hyper-circulation in the graft.

Hong et al. [10] evaluated the accuracy of controlled attenuation parameter (CAP) for detecting hepatic steatosis in potential living donor, who underwent a CAP assessment and ultrasonography-guided liver biopsy. For more details, see also book Part VI "Assessment of Hepatic Steatosis Using CAP". According to the liver biopsies, 19 patients (34.5%) had steatosis less than 5%, 30 patients (54.5%) had steatosis 5–33%, and 6 patients (11.0%) had steatosis 34–66%. The CAP value correlated positively with BMI, waist circumference, hip circumference, magnetic resonance fat signal fraction, and histologic steatosis grade. The AUROC was good with 0.88 for the diagnosis of significant steatosis ( $\geq S2$ ) by CAP. The authors concluded that CAP may be sufficient for identifying, and thus excluding significant hepatic steatosis ( $>33\%$ ) in potential liver donors.

### *Evaluation of the Deceased Donor Liver*

In the case of evaluation of a brain-dead donor, the time available to the expert team to assess the quality of liver grafts is limited and one of the difficulties is to be able to quickly determine objectively the degree of steatosis. Ideally, procurement teams should have access to a reliable, reproducible, noninvasive, simple, and rapid tool to objectively identify and quantify liver steatosis and finally to increase the number and the quality of liver grafts.

Mancia et al. [11] evaluated LS and CAP by TE for the assessment of steatosis and fibrosis in livers from brain-dead donors to be considered for LTX. Over a period of 10 months, 23 consecutive brain-dead donors screened for liver procurement underwent TE and a liver biopsy. The different predictive models of liver retrievability with liver biopsy as gold standard led to the following AUROCs: 76.6% (95% CI: 48.2–100%) when based solely on CAP, 75.0% (95% CI: 34.3–100%) when based solely on LS, and 96.7% (95% CI: 88.7–100%) when based on both CAP and LS. Consequently, these data suggest a good preoperative prediction of the donor quality of a potential liver graft by TE. Another small study with  $n = 16$  liver donors [12] was aimed to evaluate the feasibility of TE during the liver retrieval procedure. LS values were considered elevated in three donors (19%). The correlation with histology was excellent. The remaining 13 liver grafts with normal LS showed normal histology.

The accuracy of CAP for the quantitation of steatosis during LDLT was studied by Yen et al. [13] in another study on 54 liver donors. This study confirmed a good performance of CAP also in this East Asian living liver donors. No steatosis was found in 47 donors, while the remaining 7 donors showed steatosis ranging from 10 to 30%. The AUROC to predict steatosis was 0.96 (95% CI: 0.91–1;  $P < 0.001$ ) for CAP. The optimal cut-off value for steatosis was 257 dB/m, positive predictive value: 58.3%, and negative predictive value: 100%. Among the 42 candidates with CAP  $< 257$  dB/m, none had steatosis. By contrast, 7 of the 12 candidates with CAP  $\geq 257$  dB/m had confirmed steatosis. In a multivariate linear regression analyses, body mass index was found to be independently associated with CAP in those without steatosis.

Taken together, larger multicenter studies are required to consider TE as an objective instrument for the preoperative selection of liver graft. At present, LS alone should not be used to describe the suitability for donation of an apparently healthy liver.

## **Liver Stiffness in the Management of the Early Post-liver Transplant Period**

The newly transplanted liver is by definition a sufficiently healthy organ in terms of its structure and functions, but it is also an inflamed organ mainly due to ischemia/reperfusion injury, and inflammation is one of the classic states that affect liver stiffness preventing reliable conclusions from being drawn on fibrosis.

### ***Ischemia/Reperfusion Injury***

Ischemia/reperfusion injury (IRI) results from the damage of the liver during procurement, preservation, surgery, and reperfusion. IRI directly depends on the time of ischemia during prolonged surgical resection of the liver that uses perfusion

clamping and from the metabolic/immunological changes following reperfusion after revascularization. Clinically, IRI manifests with elevated liver enzymes and bilirubin just after transplantation. Usually, the liver enzyme levels normalize very quickly, typically within a week of LTX. Bilirubin levels follow a similar pattern but with some delay. However, if the graft has suffered severe preservation injury, return to normality may lag and the overall viability function of the liver requires to be carefully monitored because IRI is the pre-requisite for different degrees of functional graft impairment, i.e., poor early graft function up to primary nonfunction. TE has been shown to detect dynamic changes of LS in the general population associated with acute liver damage regardless of chronic structural changes [14, 15]. Thus, TE is hypothesized to be a noninvasive monitoring tool to trace dynamic LS changes in post-transplant liver for monitoring of graft function and complications in the peri-transplantation period.

Feasibility and usefulness of TE in the perioperative period of LDLT has been studied by Inoue et al. [16] in 24 living donors and corresponding recipients after LTX. LS values were the highest in the first postoperative week and slowly declined thereafter, remaining high compared with the preoperative values even 1 month after the transplantation. Recipients with complications had significantly higher LS values than those without complications in the fourth, fifth, or later postoperative week. All cases of acute cellular rejection had a concomitant sharp rise in LS and, in their experience, a rapidly depleted portal flow at Doppler ultrasound.

### ***Acute Cellular Rejection***

Acute cellular rejection (ACR) is an inflammatory process directed at endothelial and biliary epithelial cells, and ACR is typically diagnosed through liver biopsy. It occurs in approximately 30% of liver transplant recipients and requires prompt treatment. It takes place most often within the first week of transplantation and its incidence decreases as a function of time within the first year of liver transplantation. Late episodes, i.e., those occurring after the first year, are suspicious of insufficient immunosuppressive therapy. Some reports [17] showed elevated LS by TE in ACR patients, and cut-off values of >7.9 kPa have been proposed to define graft damage while LS <5.3 kPa excluded graft damage (AUROC 0.93;  $P < 0.001$ ). In a prospective study [18] on 27 patients with ACR, LS cut-off values >8.5 kPa predicted moderate to severe ACR (specificity 100%, AUROC 0.924), while LS <4.2 kPa excluded any ACR. LS improved in 7%, 21%, and 64% of patients with moderate/severe rejection at day 7, 30, and 90.

In another small study [19], attenuation measuring ultrasound shear wave elastography (AMUSE) was used to measure shear wave velocity and attenuation in 15 transplanted livers in patients with potential ACR, and the results were compared with the biopsy findings. The study showed excellent agreement and

suggests that AMUSE can be used to separate transplanted livers with acute rejection from livers with no rejection. According to these results, LSM should be used to monitor ACR.

## **Liver Stiffness in the Management of Liver Transplant Follow-Up**

LTX has become an established treatment option for end-stage liver diseases and survival outcomes have dramatically improved over the years. The challenge of managing thousands of liver transplant survivors, an ever-increasing number, is common in all developed countries.

Management of liver transplant patients aims to prevent and treat any graft disease as well as to improve the quality of patient's life. During post-transplant follow-up, transplant hepatologists routinely carry out a large variety of laboratory and instrumental controls to identify graft damage. Morbidity and mortality are closely related to liver fibrosis development, the common element of progression for all chronic liver diseases from any cause during the process that finally leads to cirrhosis and end-stage liver disease. Liver biopsy still plays a central role in the context of liver transplantation, mainly because, in addition to assessing fibrosis, it allows to exclude a phase of rejection and identify different etiologies of liver damage [1, 20]. However, liver biopsy has substantial limitations, including sampling error, intra- and inter-observer variability, infrequent but potentially severe complications, significant costs, and is hardly repeatable [3]. Thus, alternative noninvasive tools are necessary for the detection of graft fibrosis also in the liver transplant setting.

After LSM by TE has been shown to accurately predict liver fibrosis in patients with a variety of clinical conditions, LSM is now part of official guidelines with an explicit role in the evaluation of transplanted livers [1, 20].

TE introduction has partly coincided the specific challenge of patients suffering from chronic HCV infection. HCV was the first cause of diseases leading to transplantation. Unfortunately, these patients had the worst survival rate due to universal recurrence of HCV after liver transplant [21]. In fact, fibrosis progression of recurrent hepatitis C is accelerated in liver transplant recipients, as shown by studies with per protocol or on-demand liver biopsy [22]. Thus, 20%–54% of liver transplant recipients developed bridging fibrosis-cirrhosis within the first 5 years after LTX [23]. Consequently, early recognition and treatment of recipients with rapidly evolving recurrent hepatitis C following liver transplant is the only strategy to improve outcome of these patients.

Thanks to the availability of direct acting antivirals (DAAs) in the field of liver transplantation, the problem of recurrence of the C virus after liver transplant has been virtually solved [24]. Today, liver transplant recipients with HCV recurrence are no longer considered a difficult-to-treat population, and discussions are restricted to whether to eradicate the virus before transplantation or immediately after transplantation [25]. The survival after LTX in patients with HCV has become the same as for other causes of LTX [26].

## ***Comparison of Liver Stiffness Measurement and Liver Histology***

Several studies showed that TE is accurate in identifying patients with significant [27–29] and advanced fibrosis [27, 30, 31], in predicting the fibrosis progression both in HCV and non-HCV transplanted liver diseases [32–35] and in formulating prognosis of graft survival [36]. In these reports with TE, the optimal LS cut-off value varied between 7.0 and 12.3 for defining Metavir scores  $\geq$ F2 (significant fibrosis) and 12.6–17.6 for Metavir score F4 (cirrhosis).

LS was able to identify best candidates for antiviral therapy [37] and to predict long-term outcomes of mild hepatitis C [38]. Now, DAAs have become standard for the treatment of HCV recurrent hepatitis after liver transplant starting around 2014. To prevent overuse of initially expensive sofosbuvir for the treatment of recurrent hepatitis C [39] significant fibrosis (Metavir  $>$ F2) was defined as an indispensable inclusion criterion even in those liver transplant patients without liver biopsy. Italian guidelines at that time [40] suggested minimum LS cut-off values at 10 and 12 kPa to identify patients with significant (F3) fibrosis and cirrhosis, respectively.

## ***Role of Serial Liver Stiffness Measurements***

One of the advantages of TE compared to liver biopsy is that it can easily be repeated over time, as a routine or an on-demand procedure, offering repeated “dynamic” LS values. The procedure resulted of paramount importance in the management of hepatitis C recurrent after liver transplant.

Repeated LSM allowed to discriminate at 1-year after liver transplant between low and rapid “fibrosers” [35, 37]. The discrimination between patients with slow and rapid fibrosis progression avoided unnecessary antiviral therapy in patients with an expected good long-term survival, while urging early treatment in those at high risk of disease progression. After therapy, LS decreased over time in those with a sustained virologic response [33, 41] and increased in patients without a response [41, 42]. In a study on 162 transplanted patients, 80 with recurrent hepatitis C, Rinaldi et al. [43] were able to define a so-called trend over time parameter based on serial LSM in one patient (increase, stability, or decrease). Significant changes in serial LSM were related to the development of clinically relevant outcomes of the transplanted liver: all cases with a 20% increase in kPa values in at least three controls 3-months apart resulted in the detection of hepatic damage in the liver biopsy or in a clear clinical expression of cirrhosis development. The same has been described in the general population [44, 45]. LS decrease was observed in cases with fibrosis and necroinflammation regression after successful HCV therapy [46] and in the general population [47].

It is well known that LSM, however, is influenced by several frequent conditions in addition to fibrosis, including hepatitis-associated necro-inflammatory activity, cholestasis and vascular congestion [40], steatosis [48], measurements in post-prandial status [49], and extrahepatic obstructive cholestasis [50, 51].

All these factors can lead to overestimation of fibrosis stage. In our experience and with regard to LTX management, however, the noninvasiveness and high sensitivity of TE certainly outweigh a decreased specificity as an elevated LS is always suggestive for a liver pathology and should prompt follow-up measurements. For more details, see also book Part IV “Important (Patho)physiological Confounders of LS”.

A continuous increase of LS over time should prompt other diagnostic procedures such as liver biopsy. Biopsy can identify the cause of graft liver damage [43], e.g., re-infection by HCV, overlapping diseases such as unexpected cirrhosis, cholangitis, acute and chronic rejection, NASH, and alcohol abuse. In two cases, increased over time LSM suggested a liver injury despite normal or trivial results of biochemical tests, and a liver biopsy showed severe fibrosis. In one case with a baseline LSM suggestive of F4 fibrosis and an increasing over time LSM, the liver biopsy showed a F2 fibrosis. This patient, however, developed ascites during the follow-up, confirming the LSM result and underlining the quite high sampling error of liver biopsy up to 30%. One patient, with recurrent cholangitis episodes that were sometimes clinically severe, showed a gradual significant increase of baseline LS (6 kPa vs. 8.7 kPa); imaging did not diagnose a definite pathology of extra-hepatic ducts, and a liver biopsy showed severe chronic rejection. Thus, the information from serial LSM is quite different and cannot be substituted by a liver biopsy; the two methods are not competing with each other but should be considered complementary.

The potential limitation of TE to be influenced by factors other than fibrosis appears to be its strength in the context of surveillance, where it is necessary to easily detect early alarm signs. In conclusion, serial LSM is common in use to efficiently support clinical decisions, being an appropriate noninvasive procedure to sequentially assess the progression of liver fibrosis in patients after liver transplant [41] and to avoid protocol liver biopsy in patients with improved or stable LSM values during follow-up [35].

### ***Liver Steatosis After Transplantation***

Liver steatosis is becoming more and more important because cirrhosis due to NASH is currently the second indication for liver transplantation in the United States. On the other hand, the high mortality on the liver transplant waitlist and the organ shortage has forced transplant centers to consider suboptimal grafts, such as steatotic livers for transplantation. Liver transplanted patients frequently present NAFLD, recurrent after pre-transplant NASH-cirrhosis or de novo after liver transplantation. NAFLD is due to metabolic imbalance for weight gain and immunosuppressant drugs, favoring hyperglycemia, arterial hypertension, and hyperlipidemia. The largest part of patients who have undergone transplantation fulfill the criteria of metabolic syndrome [52]. Great attention is currently paid to know its clinical course after liver transplant [53] providing an important role for elastography.

Bhati et al. [54] retrospectively described disease recurrence and clinical course after liver transplant for NASH-cirrhosis, evaluating fibrosis by TE and steatosis by liver biopsy. Steatosis was detected in 49 (87.5%) patients who had a TE and were defined to have recurrent NAFLD. Most patients had LS values consistent with no fibrosis (42.9%) or F1-F2 fibrosis (30.4%). Advanced fibrosis was noted in 26.8%, whereas 5.4% had cirrhosis but were clinically compensated. In patients with liver biopsy, 88.2% had recurrent NAFLD, whereas 41.2% had recurrent NASH. Bridging fibrosis was noted in 20.6% of patients, but no patients had cirrhosis. Within the cohort, 32 patients died with cancer as leading cause of mortality (25%), infectious complications (25%), and cardiovascular disease (21.9%). Only 9% of deaths were attributable to graft cirrhosis. They concluded that recurrent NAFLD is common in the post-liver transplant setting, occurring in nearly 88% of all patients and nearly a quarter of patients have advanced fibrosis.

LS and controlled attenuation parameter (CAP) are nowadays recognized to be accurate in assessing fibrosis and steatosis in general patients with suspected NAFLD [55]. Karlas et al. [56] evaluated 204 liver transplant recipients (pre-transplant disease:  $n = 102$  nonalcoholic liver cirrhosis;  $n = 102$  alcoholic liver disease) by TE for liver graft fibrosis and CAP for steatosis. Results were correlated with clinical, ultrasound, and genetic risk factors (PNPLA3). Increased hepatic echogenicity at ultrasound was observed in 36% of patients, CAP values  $>252$  and  $>300$  dB/m indicated steatosis, and advanced steatosis in 44% and 24% of individuals. Advanced fibrosis (TE  $>7.9$  kPa) was associated with increased CAP results (266 vs. 229 dB/m,  $P = 0.012$ ). PNPLA3 G allele carriers had increased CAP values (257 vs. 222 dB/m,  $P = 0.032$ ), higher liver stiffness (TE 6.4 vs. 5.5 kPa,  $P = 0.005$ ), and prevalence of diabetes mellitus (40% vs. 22%,  $P = 0.016$ ). In conclusion, non-invasive liver graft assessment methods frequently detect hepatic steatosis, both alcoholic and non-alcoholic, which is associated with graft fibrosis, components of the metabolic syndrome, and recipient PNPLA3 rs738409 genotype, especially in alcoholic liver disease patients. Finally, LSM by TE showed a higher accuracy in identifying patients with post-transplant HCV significant ( $\geq F2$ ) fibrosis or cirrhosis than noninvasive clinical and serological indices in several studies [28, 30, 57].

### ***pSWE (ARFI) in LTX Setting***

TE has become the gold standard for novel elastographic techniques such as alternative SWE techniques [58]. Indeed, the concordance between most elastography machines and TE has been defined moderate in a study [59] or even good to excellent in another study [60]. Thus, TE cut-off values should not be automatically transferred to other techniques. For more details, see also book Part III “Liver Stiffness and Various Etiologies of Liver Diseases”. With this limitation in mind, several reports have been published on the role of pSWE (ARFI) after liver transplant that, globally, reproduce the results obtained with TE. First, in a study by Crespo et al. [61], pSWE was shown to provide higher technical success rate than TE. Significant



fibrosis ( $F \geq 2$ ) was diagnosed as accurate as TE both in transplanted patients (AUROCs 0.867 and 0.902, respectively) and non-transplanted patients (AUROCs 0.897 and 0.890, respectively). According to Hong et al. [10], 2D-SWE technique has the potential to reliably detect rejection or recurrent hepatitis early after LTX (4 week), in both HCV and non-HCV patients. Haberal et al. [62] evaluated the diagnostic efficiency of pSWE in assessing of fibrosis in 28 liver transplant patients. Fibrosis scores of 4 biopsies were evaluated as F0 (14.3%), 16 as F1 (57.1%), 4 as F2 (14.3%), and 4 as F3 (14.3%). Mean results of pSWE LSM  $1.4 \pm 0.07$  m/s in F0,  $1.74 \pm 0.57$  in F1,  $2.19 \pm 0.7$  in F2, and  $2.18 \pm 0.35$  in F3. There was no significant correlations of mean LS values between the F0 vs. F1 and F0 vs. F2 stages. A statistically significant correlation of mean LS values was found between the F0 and F3 fibrosis stages. They concluded that pSWE is a promising screening test for detecting significant liver fibrosis in liver transplant recipients. Other studies indicated that pSWE is reliable in significant fibrosis [62, 63] and is able to identify patients with a benign course of HCV recurrence [64].

Perry et al. [65] prospectively evaluated pSWE for the assessment of liver fibrosis and to determine the usefulness and optimal location for obtaining LSMs in native and transplanted livers from 100 consecutive patients presenting for percutaneous liver biopsy. Measurements were acquired within both the superior right hepatic lobe (segments VII/VIII) via an intercostal approach and the inferior right hepatic lobe (segments V/VI) via a subcostal approach: LSMs can be combined or taken separately from either the superior or inferior right hepatic lobe. The presence of hepatic steatosis did not affect the accuracy of pSWE, while it accurately differentiated between patients with no-to-mild hepatic fibrosis (F0–F1) and moderate-to-severe hepatic fibrosis ( $\geq F2$ ) with sensitivity of 72% and specificity of 69%. However, pSWE values in patients with body mass index higher than 40 kg/m<sup>2</sup> should be interpreted with caution.

A recent study [66] showed the utility of real-time 2D-SWE to differentiate low from advanced liver fibrosis in patients with recurrent hepatitis C virus infection after liver transplant. Valente et al. [67] compared pSWE to TE for liver fibrosis staging and evaluation in a cohort of 196 patients with liver transplant. Both methods showed 100% feasibility and reliability and concordance in 93% of cases to categorize a patient in the same fibrosis stage. The correlation between the LSM obtained with pSWE and TE was so strong that the minimal detected percentage of difference does not seem to have any practical clinical significance. To have an idea of the interchangeability of results between two techniques seems important because in the real-world situation it can happen that, during a follow-up which last for years, the controls are practiced with different devices and in different places. Nonetheless, the authors advise that it is better to maintain a certain degree of caution on the interchangeability of the systems, because, how large the overlapping of results of the two different techniques may be, it is never full [68]. In conclusion, all studies indicate that pSWE and 2D-SWE techniques can be used as a noninvasive method to assess liver stiffness in the practical clinical context of follow-up of liver transplant recipients. For more details, see also book Part II “Techniques to Measure Liver Stiffness”. See also Table A.4 for different LS cut-off values using different elastography techniques.



## ***Magnetic Resonance Elastography and Liver Transplant***

The utility of magnetic resonance elastography (MRE) to detect significant fibrosis after liver transplant was first shown by Lee [69] and the examination performed better than FIBROSpect II (an algorithm of serum  $\alpha$ 2M, PIIINP, and TIMP-1), APRI, and AST:ALT ratio. Singh et al. [70] studied the diagnostic accuracy of MRE to detect fibrosis stage in liver transplant recipients using liver biopsy as gold standard. The study reported data on 141 liver transplant recipients (mean age, 57 years; 75.2% male; mean BMI, 27.1 kg/m<sup>2</sup>). Fibrosis distribution in stages 0, 1, 2, 3, or 4 was 37.6%, 23.4%, 24.8%, 12%, and 2.2%, respectively. Mean AUROC values for diagnosis of any ( $\geq$ stage 1) significant advanced fibrosis and cirrhosis were 0.73 (0.66–0.81), 0.69 (0.62–0.74), 0.83 (0.61–0.88), and 0.96 (0.93–0.98), respectively. Similar diagnostic performance was observed in stratified analysis based on sex, obesity, and inflammation grade. They concluded that MRE has high diagnostic accuracy for the detection of advanced fibrosis in liver transplant recipients, independent of BMI, and degree of inflammation.

## **Liver Stiffness in Pediatric Liver Transplantation**

Outcome of liver disease in children is mainly determined by severity and progression of liver fibrosis. Graft fibrosis is present in two thirds of children 5–10 years after transplantation [71, 72] and usually develops silently in the presence of normal liver function tests and may lead to eventual graft loss. Protocol liver biopsy is the accepted standard for evaluating fibrosis, but biopsy should be repeated as time from transplant increases, and it is problematic because of the need for sedation in children, sampling error, and risks including bleeding. In 2013 Fitzpatrick et al. [73] compared TE with biopsy score for noninvasive assessment of liver fibrosis in a pediatric cohort including a subgroup of 16 post-transplant children with complex graft pathology (cases of acute cellular rejection, nonspecific hepatitis, de novo autoimmune hepatitis, post-transplant lymphoproliferative disease, late hepatic artery thrombosis, biliary stricture, hepatic arterial-portal vein fistula, and off immunosuppression at the time of biopsy). The median interval from transplant to biopsy/TE was 10.2 years (IQR 5.1–11.4 years). TE failed in 3 (19%), mainly because of the position of the graft (left lateral segment). TE was a good discriminator of significant fibrosis ( $\geq$ F2) ( $P < 0.001$ ), severe fibrosis ( $\geq$ F3) ( $P < 0.001$ ), and cirrhosis (F4) ( $P = 0.003$ ). TE showed good performance for the prediction of  $\geq$ F2,  $\geq$ F3, and F4 fibrosis stages (AUROC curves 0.78, 0.79, and 0.96, respectively).

In one study [74], TE was compared to serum noninvasive markers (FT, fibrotest; ELF, enhanced liver fibrosis) to diagnose liver allograft fibrosis in children. TE correlated best with histological degree of fibrosis. Liver stiffness values for transplanted children without fibrosis were significantly higher than those of healthy controls. Presence of rejection was a potent confounder for the performance of

TE. Both TE and FT reflected clinical changes (acute rejection, cholestasis, increasing fibrosis) in a total of 16 patients who underwent serial measurements. TE correlated better with histological degree of fibrosis in liver-transplanted children than FT or ELF, but an individual baseline value needed to be determined for each patient. In their experience, normal or cut-off values for pathological degrees of fibrosis cannot be transferred from non-transplanted children.

Vinciguerra et al. [75] evaluated the reliability of TE in children after liver transplant and compared both the TE and the APRI index results with the histological scores of fibrosis on liver biopsies. A total of 36 pediatric transplant recipients were studied. There was a statistically significant correlation between LS values by TE and Metavir scores ( $P = 0.005$ ). The diagnostic accuracy of TE for the diagnosis of significant fibrosis ( $F \geq 2$ ) demonstrated a good diagnostic performance, while APRI was not so accurate in assessing graft fibrosis when compared to Metavir. A LS cut-off value of 5.6 kPa was identified as the best predictor for a significant graft fibrosis on liver biopsy, with 75% sensitivity, 95.8% specificity, 90% positive predictive value, and 88.5% negative predictive value.

Taken together, these data suggest that TE represents a noninvasive, reliable tool for the assessment of graft fibrosis also in the setting of pediatric liver transplant, in the follow-up of transplanted children, alerting the clinicians to the indication for a liver biopsy, with the aim of reducing the number of protocol liver biopsies.

## Conclusions

To date, there is enough evidence to support that LSM by elastography is a useful way to monitor the transplanted liver, especially during the life-long follow-up. Moreover, the method has already become part of the usual clinical practice as an easy and easily repeatable monitoring tool. Serial LSM have been proven useful in identifying liver pathologies early on.

## References

1. EASL. EASL Clinical Practice Guidelines: liver transplantation. *J Hepatol.* 2016;64(2):433–85.
2. World Transplant Registry reports. La Moncloa. 2018. <https://www.lamoncloa.gob.es/lang/en/gobierno/news/Paginas/2018/20180829transplants.aspx>.
3. European Association for Study of Liver, Asociacion Latinoamericana para el Estudio del Hígado. EASL-ALEH Clinical Practice Guidelines: non-invasive tests for evaluation of liver disease severity and prognosis. *J Hepatol.* 2015;63(1):237–64.
4. Dietrich CF, Bamber J, Berzigotti A, Bota S, Cantisani V, Castera L, et al. EFSUMB Guidelines and Recommendations on the Clinical Use of Liver Ultrasound Elastography, Update 2017 (Long Version). *Ultraschall Med.* 2017;38(4):e16–47.
5. Nacif LS, Paranagua-Vezozzo DC, Matsuda A, Alves VAF, Carrilho FJ, Farias AQ, et al. Higher values in liver elastography and MELD score are mortality predictors on liver transplant waiting list. *Arquivos brasileiros de cirurgia digestiva.* 2018;31(1):e1360.

6. Chu MJ, Dare AJ, Phillips AR, Bartlett AS. Donor hepatic steatosis and outcome after liver transplantation: a systematic review. *J Gastrointest Surg.* 2015;19(9):1713–24.
7. Song ZZ. Acute viral hepatitis increases liver stiffness values measured by transient elastography. *Hepatology.* 2008;48(1):349–50; author reply 50.
8. Alsebaey A, Allam N, Alswat K, Waked I. Normal liver stiffness: a study in living donors with normal liver histology. *World J Hepatol.* 2015;7(8):1149–53.
9. Lee SH, Joo DJ, Kim SU, Kim MS, Lee AL, Choi GH, et al. Graft function measured by transient elastography in living donor liver transplantation: preliminary. *Transplant Proc.* 2013;45(8):3028–31.
10. Hong YM, Yoon KT, Cho M, Chu CW, Rhu JH, Yang KH, et al. Clinical usefulness of controlled attenuation parameter to screen hepatic steatosis for potential donor of living donor liver transplant. *Eur J Gastroenterol Hepatol.* 2017;29(7):805–10.
11. Mancina C, Loustaud-Ratti V, Carrier P, Naudet F, Bellissant E, Labrousse F, et al. Controlled attenuation parameter and liver stiffness measurements for steatosis assessment in the liver transplant of brain dead donors. *Transplantation.* 2015;99(8):1619–24.
12. Pichon N, Loustaud-Ratti V, Clavel M, Carrier P, Amiel JB, Labrousse F. Value of liver stiffness measured by transient elastography in the liver transplant pre-operative evaluation of the potential deceased liver donors: preliminary study. *Clin Transplant.* 2011;25(2):E205–10.
13. Yen YH, Kuo FY, Lin CC, Chen CL, Chang KC, Tsai MC, et al. Predicting hepatic steatosis in living liver donors via controlled attenuation parameter. *Transplant Proc.* 2018;50(10):3533–8.
14. Arena U, Vizzutti F, Corti G, Ambu S, Stasi C, Bresci S, et al. Acute viral hepatitis increases liver stiffness values measured by transient elastography. *Hepatology.* 2007;47(2):380–4.
15. Sagir A, Erhardt A, Schmitt M, Haussinger D. Transient elastography is unreliable for detection of cirrhosis in patients with acute liver damage. *Hepatology.* 2008;47(2):592–5.
16. Inoue Y, Sugawara Y, Tamura S, Ohtsu H, Taguri M, Makuuchi M, et al. Validity and feasibility of transient elastography for the transplanted liver in the peritransplantation period. *Transplantation.* 2009;88(1):103–9.
17. Nacif LS, Gomes CDC, Mischiatti MN, Kim V, Paranagua-Vezozzo D, Reinoso GL, et al. Transient elastography in acute cellular rejection following liver transplantation: systematic review. *Transplant Proc.* 2018;50(3):772–5.
18. Crespo G, Castro-Narro G, Garcia-Juarez I, Benitez C, Ruiz P, Sastre L, et al. Usefulness of liver stiffness measurement during acute cellular rejection in liver transplantation. *Liver Transpl.* 2016;22(3):298–304.
19. Nenadic IZ, Qiang B, Urban MW, Zhao H, Sanchez W, Greenleaf JF, et al. Attenuation measuring ultrasound shearwave elastography and in vivo application in post-transplant liver patients. *Phys Med Biol.* 2017;62(2):484–500.
20. Lucey MR, Terrault N, Ojo L, Hay JE, Neuberger J, Blumberg E, et al. Long-term management of the successful adult liver transplant: 2012 practice guideline by the American Association for the Study of Liver Diseases and the American Society of Transplantation. *Liver Transpl.* 2013;19(1):3–26.
21. Cotter TG, Paul S, Sandikci B, Couri T, Bodzin AS, Little EC, et al. Improved graft survival after liver transplantation for recipients with hepatitis C virus in the direct-acting antiviral era. *Liver Transpl.* 2019;25(4):598–609.
22. Gane EJ. The natural history of recurrent hepatitis C and what influences this. *Liver Transpl.* 2008;14(Suppl 2):S36–44.
23. Berenguer M, Schuppan D. Progression of liver fibrosis in post-transplant hepatitis C: mechanisms, assessment and treatment. *J Hepatol.* 2013;58(5):1028–41.
24. Terrault NA, Pageaux GP. A changing landscape of liver transplantation: king HCV is dethroned, ALD and NAFLD take over! *J Hepatol.* 2018;69(4):767–8.
25. Pawlotsky J-M, Negro F, Aghemo A, Berenguer M, Dalgard O, Dusheiko G, et al. EASL recommendations on treatment of hepatitis C 2018. *J Hepatol.* 2018;69(2):461–511.
26. Belli LS, Perricone G, Adam R, Cortesi PA, Strazzabosco M, Facchetti R, et al. Impact of DAAs on liver transplantation: major effects on the evolution of indications and results. An ELITA study based on the ELTR registry. *J Hepatol.* 2018;69(4):810–7.

27. Adebajo CO, Talwalkar JA, Poterucha JJ, Kim WR, Charlton MR. Ultrasound-based transient elastography for the detection of hepatic fibrosis in patients with recurrent hepatitis C virus after liver transplantation: a systematic review and meta-analysis. *Liver Transpl.* 2012;18(3):323–31.
28. Corradi F, Piscaglia F, Flori S, D'Errico-Grigioni A, Vasuri F, Tame MR, et al. Assessment of liver fibrosis in transplant recipients with recurrent HCV infection: usefulness of transient elastography. *Dig Liver Dis.* 2009;41(3):217–25.
29. Harada N, Soejima Y, Taketomi A, Yoshizumi T, Ikegami T, Yamashita Y, et al. Assessment of graft fibrosis by transient elastography in patients with recurrent hepatitis C after living donor liver transplantation. *Transplantation.* 2008;85(1):69–74.
30. Beckebaum S, Iacob S, Klein CG, Dechene A, Varghese J, Baba HA, et al. Assessment of allograft fibrosis by transient elastography and noninvasive biomarker scoring systems in liver transplant patients. *Transplantation.* 2010;89(8):983–93.
31. Kamphues C, Lotz K, Rocken C, Berg T, Eurich D, Pratschke J, et al. Chances and limitations of non-invasive tests in the assessment of liver fibrosis in liver transplant patients. *Clin Transplant.* 2010;24(5):652–9.
32. Barrault C, Roudot-Thoraval F, Tran Van Nhieu J, Atanasiu C, Kluger MD, Medkour F, et al. Non-invasive assessment of liver graft fibrosis by transient elastography after liver transplantation. *Clin Res Hepatol Gastroenterol.* 2013;37(4):347–52.
33. Bellido-Munoz F, Giraldez-Gallego A, Roca-Oporto C, Garcia-Cayuela T, Pascasio-Acevedo JM, Sousa-Martin JM. Monitoring the natural evolution and response to treatment of post liver transplant recurrent hepatitis C using transient elastography: preliminary results. *Transplant Proc.* 2012;44(7):2082–6.
34. Della-Guardia B, Evangelista AS, Felga GE, Marins LV, Salvalaggio PR, Almeida MD. Diagnostic accuracy of transient elastography for detecting liver fibrosis after liver transplantation: a specific cut-off value is really needed? *Dig Dis Sci.* 2017;62(1):264–72.
35. Rigamonti C, Fraquelli M, Bastiampillai AJ, Caccamo L, Reggiani P, Rossi G, et al. Transient elastography identifies liver recipients with nonviral graft disease after transplantation: a guide for liver biopsy. *Liver Transpl.* 2012;18(5):566–76.
36. Crespo G, Lens S, Gambato M, Carrion JA, Marino Z, Londono MC, et al. Liver stiffness 1 year after transplantation predicts clinical outcomes in patients with recurrent hepatitis C. *Am J Transplant.* 2014;14(2):375–83.
37. Carrion JA, Torres F, Crespo G, Miquel R, Garcia-Valdecasas JC, Navasa M, et al. Liver stiffness identifies two different patterns of fibrosis progression in patients with hepatitis C virus recurrence after liver transplantation. *Hepatology.* 2010;51(1):23–34.
38. Gambato M, Crespo G, Torres F, LL L, Carrion J, Londono M, et al. Simple prediction of long-term clinical outcomes in patients with mild hepatitis C recurrence after liver transplantation. *Transpl Int.* 2016;29(6):698–706.
39. Carrai P, Morelli C, Cordone G, Romano A, Tame M, Lionetti R, et al. The Italian compassionate use of sofosbuvir observational cohort study for the treatment of recurrent hepatitis C: clinical and virological outcomes. *Transpl Int.* 2017;30(12):1253–65.
40. Bonino F, Arena U, Brunetto MR, Coco B, Fraquelli M, Oliveri F, et al. Liver stiffness, a non-invasive marker of liver disease: a core study group report. *Antivir Ther.* 2010;15(Suppl 3):69–78.
41. Masuzaki R, Yamashiki N, Sugawara Y, Yoshida H, Tateishi R, Tamura S, et al. Assessment of liver stiffness in patients after living donor liver transplantation by transient elastography. *Scand J Gastroenterol.* 2009;44(9):1115–20.
42. Crespo G, Gambato M, Millan O, Casals G, Ruiz P, Londono MC, et al. Early non-invasive selection of patients at high risk of severe hepatitis C recurrence after liver transplantation. *Transpl Infect Dis.* 2016;18(3):471–9.
43. Rinaldi L, Valente G, Piai G. Serial liver stiffness measurements and monitoring of liver-transplanted patients in a real-life clinical practice. *Hepat Mon.* 2016;16(12):e41162.
44. Vergniol J, Boursier J, Coutzac C, Bertrais S, Foucher J, Angel C, et al. Evolution of non-invasive tests of liver fibrosis is associated with prognosis in patients with chronic hepatitis C. *Hepatology.* 2014;60(1):65–76.

45. Kim BK, Fung J, Yuen MF, Kim SU. Clinical application of liver stiffness measurement using transient elastography in chronic liver disease from longitudinal perspectives. *World J Gastroenterol.* 2013;19(12):1890–900.
46. Omar H, Said M, Eletreby R, Mehrez M, Bassam M, Abdellatif Z, et al. Longitudinal assessment of hepatic fibrosis in responders to direct-acting antivirals for recurrent hepatitis C after liver transplantation using noninvasive methods. *Clin Transplant.* 2018;32(8):e13334.
47. Stasi C, Arena U, Zignego AL, Corti G, Monti M, Triboli E, et al. Longitudinal assessment of liver stiffness in patients undergoing antiviral treatment for hepatitis C. *Dig Liver Dis.* 2013;45(10):840–3.
48. Petta S, Maida M, Macaluso FS, Di Marco V, Camma C, Cabibi D, et al. The severity of steatosis influences liver stiffness measurement in patients with nonalcoholic fatty liver disease. *Hepatology.* 2015;62(4):1101–10.
49. Berzigotti A, Abraldes JG, Bosch J. Regarding “Liver stiffness is influenced by a standardized meal in patients with chronic hepatitis C virus at different stages of fibrotic evolution”. *Hepatology.* 2014;59(1):350–1.
50. Millonig G, Reimann FM, Friedrich S, Fonouni H, Mehrabi A, Büchler MW, et al. Extrahepatic cholestasis increases liver stiffness (FibroScan) irrespective of fibrosis. *Hepatology.* 2008;48(5):1718–23.
51. Yashima Y, Tsujino T, Masuzaki R, Nakai Y, Hirano K, Tateishi R, et al. Increased liver elasticity in patients with biliary obstruction. *J Gastroenterol.* 2011;46(1):86–91.
52. Watt KD, Charlton MR. Metabolic syndrome and liver transplantation: a review and guide to management. *J Hepatol.* 2010;53(1):199–206.
53. Gitto S, de Maria N, di Benedetto F, Tarantino G, Serra V, Maroni L, et al. De-novo nonalcoholic steatohepatitis is associated with long-term increased mortality in liver transplant recipients. *Eur J Gastroenterol Hepatol.* 2018;30(7):766–73.
54. Bhati C, Idowu MO, Sanyal AJ, Rivera M, Driscoll C, Stravitz RT, et al. Long-term outcomes in patients undergoing liver transplantation for nonalcoholic steatohepatitis-related cirrhosis. *Transplantation.* 2017;101(8):1867–74.
55. Eddowes PJ, Sasso M, Allison M, Tsochatzis E, Anstee QM, Sheridan D, et al. Accuracy of FibroScan controlled attenuation parameter and liver stiffness measurement in assessing steatosis and fibrosis in patients with nonalcoholic fatty liver disease. *Gastroenterology.* 2019;156(6):1717–30.
56. Karlas T, Kollmeier J, Böhm S, Müller J, Kovacs P, Tröltzsch M, et al. Noninvasive characterization of graft steatosis after liver transplantation. *Scand J Gastroenterol.* 2015;50(2):224–32.
57. Piscaglia F, Cucchetti A, Terzi E, Gianstefani A. Validation of noninvasive methods for the assessment of liver fibrosis in patients with recurrent hepatitis C after transplantation. *Liver Transpl.* 2010;16(8):1006–7.
58. Parfieniuk-Kowerda A, Lapinski TW, Rogalska-Plonska M, Swiderska M, Panasiuk A, Jaroszewicz J, et al. Serum cytochrome c and m30-neoepitope of cytokeratin-18 in chronic hepatitis C. *Liver Int.* 2014;34(4):544–50.
59. Piscaglia F, Salvatore V, Mulazzani L, Cantisani V, Colecchia A, Di Donato R, et al. Differences in liver stiffness values obtained with new ultrasound elastography machines and Fibroscan: a comparative study. *Dig Liver Dis.* 2017;49(7):802–8.
60. Ferraioli G, De Silvestri A, Lissandrini R, Maiocchi L, Tinelli C, Filice C, et al. Evaluation of inter-system variability in liver stiffness measurements. *Ultraschall Med.* 2019;40(1):64–75.
61. Crespo G, Fernández-Varo G, Mariño Z, Casals G, Miquel R, Martínez SM, et al. ARFI, FibroScan, ELF, and their combinations in the assessment of liver fibrosis: a prospective study. *J Hepatol.* 2012;57(2):281–7.
62. Haberal KM, Turnaoglu H, Ozdemir A, Uslu N, Haberal Reyhan AN, Moray G, et al. Liver stiffness measurements using acoustic radiation force impulse in recipients of living-donor and deceased-donor orthotopic liver transplant. *Exp Clin Transplant.* 2017.
63. Abdelhaleem H, Gamal Eldeen H, Nabeel MM, Abdelmoniem R, Elakel W, Zayed N, et al. Evaluation of acoustic radiation force impulse (ARFI) elastography as non-invasive diagnostic tool in living donor liver transplantation. *Abdom Radiol (NY).* 2019;44(2):464–72.

64. Bignulin S, Falletti E, Cmet S, Cappello D, Cussigh A, Lenisa I, et al. Usefulness of acoustic radiation force impulse and fibrotest in liver fibrosis assessment after liver transplant. *Ann Hepatol.* 2016;15(2):200–6.
65. Perry MT, Savjani N, Bluth EI, Dornelles A, Therapondos G. Point shear wave elastography in assessment of hepatic fibrosis: diagnostic accuracy in subjects with native and transplanted livers referred for percutaneous biopsy. *Ultrasound Q.* 2016;32(3):201–7.
66. Rattansingh A, Amooshahi H, Menezes RJ, Wong F, Fischer S, Kirsch R, et al. Utility of shear-wave elastography to differentiate low from advanced degrees of liver fibrosis in patients with hepatitis C virus infection of native and transplant livers. *J Clin Ultrasound.* 2018;46(5):311–8.
67. Valente G, Rinaldi L, Moggio G, Piai G. Point Shear Wave Elastography and Vibration Controlled Transient Elastography for Estimating Liver Fibrosis in a Cohort of Liver Transplant Patients. Accepted for publication on *European Review for Medical and Pharmacological Sciences*, 2020.
68. Zeng J, Zheng J, Huang Z, Chen S, Liu J, Wu T, et al. Comparison of 2-D shear wave elastography and transient elastography for assessing liver fibrosis in chronic hepatitis B. *Ultrasound Med Biol.* 2017;43(8):1563–70.
69. Lee VS, Miller FH, Omary RA, Wang Y, Ganger DR, Wang E, et al. Magnetic resonance elastography and biomarkers to assess fibrosis from recurrent hepatitis C in liver transplant recipients. *Transplantation.* 2011;92(5):581–6.
70. Singh S, Venkatesh SK, Keaveny A, Adam S, Miller FH, Asbach P, et al. Diagnostic accuracy of magnetic resonance elastography in liver transplant recipients: a pooled analysis. *Ann Hepatol.* 2016;15(3):363–76.
71. Kelly D, Verkade HJ, Rajanayagam J, McKiernan P, Mazariegos G, Hubscher S. Late graft hepatitis and fibrosis in pediatric liver allograft recipients: current concepts and future developments. *Liver Transpl.* 2016;22(11):1593–602.
72. Varma SD, Devamanoharan PS. Hydrogen peroxide in human blood. *Free Radic Res Commun.* 1991;14(2):125–31.
73. Fitzpatrick E, Quaglia A, Vimalasvaran S, Basso MS, Dhawan A. Transient elastography is a useful noninvasive tool for the evaluation of fibrosis in paediatric chronic liver disease. *J Pediatr Gastroenterol Nutr.* 2013;56(1):72–6.
74. Goldschmidt I, Stieghorst H, Munteanu M, Poynard T, Schlue J, Streckenbach C, et al. The use of transient elastography and non-invasive serum markers of fibrosis in pediatric liver transplant recipients. *Pediatr Transplant.* 2013;17(6):525–34.
75. Vinciguerra T, Brunati A, David E, Longo F, Pinon M, Ricceri F, et al. Transient elastography for non-invasive evaluation of post-transplant liver graft fibrosis in children. *Pediatr Transplant.* 2018;22(2).

**Part VI**  
**Assessment of Hepatic Steatosis Using**  
**Controlled Attenuation Parameter (CAP)**

# Chapter 37

## Steatosis Assessment by Controlled Attenuation Parameter (CAP™)



Magali Sasso and Laurent Sandrin

### Introduction

Hepatic steatosis is a common histological feature, characterized by an accumulation of lipids—mainly triglycerides—in the hepatocytes. Steatosis is considered pathological when the hepatic fat content exceeds 5% of the liver weight and more practically when more than 5% of hepatocytes contain fatty droplets. Steatosis can be induced by several causes such as alcohol abuse, viral infection, or metabolic factors (obesity, type 2 diabetes, hyperglycemia, hypertriglyceridemia) [1]. Its prevalence is increasing with the worldwide epidemic of non-alcoholic fatty liver disease (NAFLD) [2]. The prevalence of NAFLD in the general population is estimated to be around 25% with worldwide heterogeneities, from a lower prevalence of 13% in Africa up to a prevalence of 32% in Middle East [2, 3]. In at risk population, the prevalence of steatosis can reach 46% in heavy drinkers [4], 50% in patients with chronic hepatitis C (CHC) [5, 6], 50–80% in obese population [7], and 86–96% in severely obese patients [8, 9].

Isolated steatosis is considered as a benign and reversible condition. However, recent studies have shown that the presence of steatosis is independently associated with fibrosis progression [10–12], a lower response rate to antiviral treatment [13, 14], or even the occurrence of hepatocellular carcinoma [15, 16]. For all these reasons, the identification and quantification of steatosis have an increasing clinical relevance for routine patient care but also in clinical studies [17].

Liver biopsy (LB) is considered the gold standard for steatosis assessment but it suffers from many drawbacks [18]. LB has potential sampling error [19], is an invasive and often painful procedure and can result in severe complications [20]. Furthermore, it can only be applied in selected subjects and not readily repeated to assess the follow-up of patients.

---

M. Sasso (✉) · L. Sandrin  
R&D Department, Echosens, Paris, France  
e-mail: [laurent.sandrin@echosens.com](mailto:laurent.sandrin@echosens.com)



Alternative non-invasive methods, mainly conventional imaging, have been proposed to detect steatosis, since fat accumulation alters the physical properties of the liver. B-mode ultrasound (US) is the most common liver-imaging technique because of its safety, accessibility, and low cost and is often used as first-line assessment for screening of fatty liver [21, 22]. However, US has limited sensitivity, does not reliably detect mild steatosis [21, 22] and is highly operator and machine dependent [21], and it has a limited applicability in case of morbid obesity. Conventional unenhanced computed tomography (CT) can be used to detect moderate to severe steatosis but is inaccurate at diagnosing mild steatosis and involves the use of radiation [23]. Magnetic resonance (MR) based techniques assess triglyceride specific signal intensity and is considered the most sensitive and specific technique for assessing steatosis [23–25]. Magnetic resonance spectroscopy (MRS) has been widely accepted as the non-invasive reference standard for steatosis evaluation [23] but requires complex post-processing by radiologists with specific expertise. MR imaging (MRI)-proton density fat fraction (PDFF) offers the possibility to cover the entire liver volume since the images needed for PDFF measurements can be acquired very quickly (in a single or two breath-holds) [23]. In addition, key confounders such as iron overload can be corrected using advanced sequences [23]. Despite the superior diagnostic performance of MRI-based techniques, they are not suitable as point-of-care methods due to high cost and lack of standardization among the different MR techniques [17, 21]. The software packages needed to process PDFF may not be available in all centers due to cost or hardware constraints [23]. Eventually, patient's factors such as claustrophobia, discomfort, implanted devices, or high body mass index (BMI) may limit its applicability [23].

More recently, a non-invasive parameter named CAP<sup>TM</sup> for controlled attenuation parameter, based on Vibration-Controlled Transient Elastography (VCTE<sup>TM</sup>), has been developed to assess liver steatosis using the FibroScan<sup>®</sup> device [26]. CAP is a promising technique that may overcome most of the limitations of the liver steatosis imaging techniques [17, 27]. In particular, CAP may be suitable for point-of-care diagnostic assessment [17]. CAP is recommended by the Asia-Pacific 2017 NAFLD guidelines as accurate alternative to abdominal ultrasonography for the detection of steatosis [28]. The American Association for the Study of Liver Diseases (AASLD) 2018 guidelines on the diagnosis and management of NAFLD mention CAP as a promising tool for quantifying hepatic fat in an ambulatory setting [29]. In its latest guidelines on liver ultrasound elastography, the World Federation for Ultrasound in Medicine and Biology (WFUMB) has recommended CAP as a point-of-care, standardized and reproducible technique, promising for the detection of liver steatosis [30].

This chapter is organized as follows. First, the CAP measurement principle and rationale will be explained. CAP performance will be given in detail for various chronic liver disease (CLD). Its performance comparison with non-invasive markers of steatosis will be summarized together with CAP results in monitoring or follow-up. Eventually, CAP reproducibility and factors influencing CAP will be discussed.

## CAP Principle

### *Ultrasound Attenuation for the Evaluation of Liver Steatosis*

CAP is a measure of ultrasound attenuation which has been developed to assess liver steatosis using FibroScan®. Measuring the ultrasound attenuation in biological tissues is of great interest because it may be related to the composition of tissues, reflecting a pathological state [31]. Ultrasound attenuation is a physical property of the medium of propagation which corresponds to the loss of energy as ultrasound propagates through this medium. Due to attenuation, the intensity of emitted ultrasound  $I_0$  decreases exponentially with depth  $z$ :

$$I_z = I_0 \exp^{-\alpha(f)z} \quad (37.1)$$

where  $I_z$  is the ultrasound intensity at depth  $z$  and  $\alpha$  is the frequency ( $f$ ) dependent attenuation coefficient. Ultrasound attenuation depends principally on the ultrasound frequency and the properties of the medium of propagation. At a given frequency, the ultrasound attenuation coefficient  $\alpha$  can be expressed in dB/m. Typical values of ultrasound attenuation at 3.5 MHz in a few human tissue are [32]: fat ~175–630 dB/m, liver ~140–245 dB/m, tendon ~315–385 dB/m, soft tissue ~105–280 dB/m.

Fat is known to be an attenuating medium and therefore many researchers have tried to implement quantitative attenuation parameters to characterize fatty liver in vivo, from the beginning of the 1980s [33, 34]. In particular, many studies have shown that ultrasound attenuation could be used to diagnose steatosis on human liver in vivo [35–40]. In most of the studies, the investigators have calibrated their measurement from reference material to consider effects such as beam diffraction, transducer focusing, and effect of gain.

### *CAP Measurement Principle*

The Controlled Attenuation Parameter (CAP) is a measure of ultrasound attenuation coefficient which is based on VCTE and implemented on the FibroScan device [26]. For more details on VCTE, see also book part II “Techniques to Measure Liver Stiffness.” This ultrasonic attenuation coefficient is an estimate of the total ultrasonic attenuation (go-and-return path) at 3.5 MHz—the center frequency of the M probe—and is expressed in dB/m. CAP is evaluated using the same radio-frequency data and in the same region of interest than the ones used for Liver Stiffness Measurement (LSM) and is only appraised if the acquisition is “valid.” CAP is therefore guided by VCTE, ensuring the operator to obtain an ultrasonic attenuation value of the liver automatically.

CAP has been first developed on the M probe of the FibroScan [26]. More recently, CAP has been developed on the XL probe of the FibroScan [41]. Since the center frequency of the XL probe is 2.5 MHz, CAP had to be adapted to be able to measure ultrasound attenuation at 3.5 MHz as it is done with the M probe and therefore have comparable values whatever the probe used is. Details of this adaptation are provided in Section “[Development and Validation of CAP on the XL Probe](#)”.

## **Validation of CAP as an Estimate of Ultrasound Attenuation**

### ***Results on Simulations***

The validity of CAP to estimate the attenuation coefficient at 3.5 MHz was initially appraised using ultrasonic Field II simulations [42] in homogeneous medium with attenuation varying from 100 dB/m to 350 dB/m [43]. CAP values were very close to the reference values set in the simulations. The root mean square error was very low (<2 dB/m which is lesser than 2% of the reference attenuation).

### ***Results on Tissue-Mimicking Phantoms***

The validity of CAP to estimate the attenuation coefficient at 3.5 MHz was further assessed on tissue-mimicking phantoms manufactured by CIRS (CIRS Inc., Norfolk, VA) [26]. Two types of phantoms were used. The first one is a custom-made elasticity phantom whose ultrasonic attenuation is equal to 0.48 dB/cm/MHz according to CIRS. The second one is the multi-purpose multi-tissue ultrasound phantom (model 040) with two different attenuation layers ( $0.50 \pm 0.05$  dB/cm/MHz and  $0.70 \pm 0.07$  dB/cm/MHz). In this phantom, the homogeneous zone of each layer was used. Acquisitions were performed using the FibroScan probe held fixed by a grip. To be able to compare CAP values with the attenuation values provided by the manufacturer, CAP was converted into dB/cm/MHz by dividing the CAP values by 3.5 MHz, using the hypothesis of an ultrasonic attenuation varying linearly with frequency and a null intercept. CAP measured in tissue-mimicking phantoms was 0.56 dB/cm/MHz for the custom-made phantom with reference attenuation of 0.48 dB/cm/MHz. CAP was 0.60 and 0.79 dB/cm/MHz in the bi-layer attenuation phantom with reference attenuation of 0.50 and 0.70 dB/cm/MHz, respectively. CAP values were slightly higher but in the same order of magnitude than the reference values given by the manufacturer. The slight difference can be explained by different experimental conditions which might influence the measured attenuation, e.g., the temperature, the transducer used (5 MHz center frequency transducer used by CIRS to characterize their phantoms), or even the approximation of an ultrasonic attenuation varying linearly with frequency with null intercept.

## ***Development and Validation of CAP on the XL Probe***

Initially, CAP had been developed on the M probe of the FibroScan only [26]. However, in some studies dealing with overweight and obese patients measured with the M probe only, it has been shown that CAP performance was impaired by an increased body mass index (BMI) [44, 45]. This phenomenon is attributed to the fact that overweight or obese patients have an increased skin-to-capsule distance (SCD) resulting from a high subcutaneous fat thickness. In these cases, the region of interest for CAP on the M probe will contain not only liver parenchyma but also a portion of the subcutaneous fat layer, which causes an overestimation of CAP, as it was illustrated on tissue-mimicking phantoms [41].

Since a dedicated probe for overweight and obese patients was developed and commercialized by Echosens [46], CAP was then adapted to be measured on XL probe [41]. For more details, see also book part II “Techniques to Measure Liver Stiffness.” Since the center frequency of the XL probe is 2.5 MHz, the tricky part of the development was to get CAP values around 3.5 MHz using the XL probe. This was necessary to obtain comparable CAP values between the M and XL probes and, thus, to enable physicians to have the same range of CAP values for interpretation and diagnostic purposes. This is particularly important from a clinical point of view to prevent any misdiagnosis. Indeed, attenuation values measured on the same medium using a 2.5 or 3.5 MHz center frequency do not differ greatly; therefore, if the physicians had to read off CAP values from different scales using the M and the XL probes, they might easily confuse the CAP values. The new development of CAP on signals acquired with the XL probe requires three steps [41]:

1. Evaluation of the raw attenuation around 2.5 MHz, the center frequency of the XL probe, using the same proprietary algorithm used on signals acquired on the M probe.
2. Evaluation of the frequency dependence of attenuation using a method similar to that described in Wear (2003) [47].
3. Estimation of CAP around 3.5 MHz using frequency dependent attenuation as a correction factor. In this step, attenuation was assumed to be linearly dependent with frequency.

As for the M probe, CAP on the XL probe was validated as an estimate of ultrasound attenuation on both simulated data and tissue-mimicking phantoms [41]. On Field II simulation, several simulations were performed on homogeneous attenuating media with attenuation values at 3.5 MHz set from 100 to 400 dB/m in 20 dB/m steps. The root mean square error for attenuation estimation at 3.5 MHz, using the M and XL probes, was 2.1 and 5.6 dB/m, respectively. On tissue-mimicking phantoms, the intra-class correlation coefficient (ICC) of variation was equal to 1 for both M and XL probes, showing perfect agreement [41].

## Steatosis Assessment Using CAP

### *Princeps Study*

Performance of CAP was first assessed in a precept study performed retrospectively on 115 patients with chronic liver disease from various causes [26]. In this study, steatosis was graded as follows: S0  $\leq 10\%$ , S1: 11–33%, S2: 34–66%, S3  $\geq 67\%$  of hepatocytes with fatty accumulation. CAP was shown to be significantly correlated to steatosis grade (Spearman  $\rho = 0.81$ ;  $P < 10^{-16}$ ). In addition, CAP was shown to be independent of fibrosis stage. Satisfactory performance was obtained to detect steatosis using CAP with area under the receiver operating curve (AUROC) of: 0.91 (95% CI 0.86–0.97), 0.95 (95% CI 0.91–1), and 0.89 (95% CI 0.75–1) for the diagnostic of steatosis ( $S \geq S1$ ,  $S \geq S2$ , and  $S = S3$ , respectively).

### *CAP Diagnostic Accuracy Taking Liver Biopsy as Reference*

Many studies using LB as reference have confirmed the results from princeps study. A summary of the study that has assessed the diagnostic performance using AUROC is provided in Table 37.1. In CLD, good to excellent performance was found for the diagnostic of steatosis. In viral hepatitis, mixed results were found with some studies confirming the good performance of the princeps study [43, 48–50] and others showing more moderate results [51–53]. In NAFLD, except for Runge et al. [54] and Siddiqui et al. [55], good to excellent performance was also found for the diagnostic of steatosis. In particular, Eddowes et al. [56] have reported, according to the standard for reporting of diagnostic accuracy (STARD) guidelines, good performance of CAP for the detection of steatosis in NAFLD. Only one study in ALD [57] has assessed the performance of CAP showing moderate results for the detection of steatosis ( $S \geq S1$  and  $S \geq S2$ ) but satisfactory results for the detection of massive steatosis. It can generally be observed from Table 37.1 that even if results were good for the detection of steatosis, they were generally lower for the detection of massive steatosis ( $S = S3$ ) showing a poor to moderate accuracy for the differentiation between moderate and massive steatosis.

Results could however be impaired by a large SCD (or BMI) in patient measured with the M probe as shown in Shen et al. [58]. Other factors may also impact the results such as a small cohort size [54], a large time interval between the FibroScan and the LB [59], the LB reading, or operator experience. Naveau et al. [60] have also shown in a study on morbidly obese patients that the quality of the FibroScan examination could have a significant impact on CAP performance. Indeed, a set of patients had been measured retrospectively (CAP was reprocessing on raw examination files when CAP on the XL probe was not yet commercially available of the device) showing moderate results for the diagnostic of steatosis and higher steatosis grades. When the patients with similar characteristics were measured prospectively

**Table 37.1** Summary of published study with diagnostic performance in terms of area under the receiver operation curve (AUROC) of controlled attenuation parameter (CAP) using liver histology as reference

Etiology	Reference	N	Probe used	BMI (kg/m <sup>2</sup> )	AUROC (95% CI) for S ≥ S1	AUROC (95% CI) for S ≥ S2	AUROC (95% CI) for S = S3
CLD	[26]	115	M	—	<b>0.91</b> (0.86–0.97)* Prevalence = 58%	<b>0.95</b> (0.91–1) Prevalence = 39%	<b>0.89</b> (0.75–1) Prevalence = 8%
	[67]	112	M	Mean: 25.8 ± 4.2	<b>0.84</b> (0.76–0.92)* Prevalence = 51%	<b>0.86</b> (0.78–0.95) Prevalence = 31%	<b>0.93</b> (0.84–1) Prevalence = 15%
	[45]	153	M	Median: 32 (IQR: 30–34)	<b>0.81</b> (0.74–0.88)* Prevalence = 75%	<b>0.76</b> (0.69–0.84) Prevalence = 35%	<b>0.70</b> (0.60–0.81) Prevalence = 10%
	[116]	155	M	Median: 24.4 (range: 15.4–39.2)	<b>0.88</b> (0.82–0.94) Prevalence = 35%	—	—
	[99]	423	M	Mean: 26.6 ± 5.9	<b>0.79</b> (0.75–0.84)* Prevalence = 52%	<b>0.84</b> (0.80–0.88) Prevalence = 32%	<b>0.84</b> (0.80–0.88) Prevalence = 15%
	[100]	135	M	Median: 24.4 (range: 14.3–33.5)	<b>0.89</b> (0.82–0.93) Prevalence = 69%	<b>0.89</b> (0.83–0.94) Prevalence = 25%	<b>0.80</b> (0.72–0.86) Prevalence = 7%
	[102]	161	M	Median: 24.4 (range: 14.3–34.3)	<b>0.86</b> (0.81–0.92) Prevalence = 74%	<b>0.90</b> (0.84–0.95) Prevalence = 24%	<b>0.74</b> (0.56–0.91) Prevalence = 4%
	[101]	151	M	Median: 26.0 (IQR: 24.4–29.3)	<b>0.92</b> (0.88–0.97) Prevalence = 59%	<b>0.92</b> (0.87–0.97) Prevalence = 30%	<b>0.88</b> (0.82–0.94) Prevalence = 9%
	[117]	201	M	Mean: 26.4 ± 4.6	<b>0.81</b> (0.75–0.86) Prevalence = 45%	<b>0.82</b> (0.76–0.87) Prevalence = 16%	<b>0.84</b> (0.78–0.88) Prevalence = 6%
	[58]	SCD <25 mm: 332 SCD ≥25 mm: 49	M	SCD <25 mm: median 24.3 (IQR: 21.9–26.5) SCD ≥25 mm: median: 27.7 (IQR: 25.1–29.6)	SCD <25 mm: <b>0.88</b> (0.84–0.92) Prevalence = 43% SCD ≥25 mm: <b>0.81</b> (0.66–0.96) Prevalence=90%	SCD <25 mm: <b>0.90</b> (0.86–0.95) Prevalence = 19% SCD ≥25 mm: <b>0.85</b> (0.74–0.96) Prevalence = 57%	SCD <25 mm: <b>0.84</b> (0.74–0.94) Prevalence = 5% SCD ≥25 mm: <b>0.72</b> (0.52–0.92) Prevalence = 20%
	[109]	754	M	Mean: 27.2 ± 5.3	<b>0.85</b> (0.82–0.88) Prevalence = 71%	—	—

(continued)

Table 37.1 (continued)

Etiology	Reference	N	Probe used	BMI (kg/m <sup>2</sup> )	AUROC (95% CI) for S ≥ S1	AUROC (95% CI) for S ≥ S2	AUROC (95% CI) for S = S3
	[64]	236	M and XL	Median: 24.4 (IQR: 6.3)	M: <b>0.82</b> (0.77–0.88) XL: <b>0.83</b> (0.77–0.88) Prevalence = 48%	M: <b>0.89</b> (0.84–0.93) XL: <b>0.88</b> (0.82–0.93) Prevalence = 26%	M: <b>0.92</b> (0.89–0.96) XL: <b>0.93</b> (0.89–0.97) Prevalence = 16%
	[69]	79	M	Mean: 26.0 ± 5.1	<b>0.90</b> (0.83–0.97) Prevalence = 48%	—	—
	[118]	159	M	17% with BMI >30 kg/m <sup>2</sup>	<b>0.82</b> (0.73–0.91) Prevalence = 81%	<b>0.96</b> (0.93–0.99) Prevalence = 48%	<b>0.98</b> (0.96–1.00) Prevalence = 26%
	[66]	180	M and XL	Mean: 29.5 ± 4.8	M: <b>0.84</b> (0.78–0.89) XL: <b>0.91</b> (0.85–0.94) Prevalence = 91%	M: <b>0.76</b> (0.69–0.82) XL: <b>0.78</b> (0.71–0.84) Prevalence = 62%	M: <b>0.61</b> (0.54–0.69) XL: <b>0.65</b> (0.58–0.72) Prevalence = 18%
	[72]	182	M	Median: 25.9 (IQR: 22.4–28.4)	<b>0.83</b> (0.74–0.91) Prevalence = 63%	<b>0.84</b> (0.73–0.95) Prevalence = 24%	<b>0.82</b> (0.70–0.93) Prevalence = 9%
	[119]	462	M or XL	Median: 23.4 (IQR: 20.8–26.4)	<b>0.88</b> (0.84–0.92) Prevalence = 28%	<b>0.89</b> (0.86–0.93) Prevalence = 12%	<b>0.88</b> (0.82–0.94) Prevalence = 4%
CHC	[43]	615	M	Mean: 24.1 ± 3.7	<b>0.80</b> (0.75–0.84)* Prevalence = 31%	<b>0.86</b> (0.81–0.92) Prevalence = 13%	<b>0.88</b> (0.73–1) Prevalence = 1%
	[51]	108	M	Mean: 24.7 ± 3.3	<b>0.66</b> (0.56–0.75) Prevalence = 52%	<b>0.67</b> (0.57–0.75) Prevalence = 22%	<b>0.92</b> (0.85–0.96) Prevalence = 7%
	[48]	312	M	Median: 27.2 (IQR: 24.0–28.6)	<b>0.94</b> Prevalence = 81%	—	—
CHB	[51]	146	M	Mean: 24.3 ± 3.6	<b>0.68</b> (0.60–0.76) Prevalence = 52%	<b>0.79</b> (0.72–0.86) Prevalence = 19%	<b>0.84</b> (0.77–0.90) Prevalence = 6%
	[52]	88	M	Mean: 24.2 ± 5.0	<b>0.71</b> (0.59–0.87) Prevalence = 54%	<b>0.87</b> (0.75–0.99) Prevalence = 28%	<b>0.97</b> (0.92–1) Prevalence = 9%
	[49]	136	M	Mean: 25 ± 4	<b>0.82</b> (0.73–0.92)* Prevalence = 22%	<b>0.82</b> (0.69–0.95) Prevalence = 12%	<b>0.97</b> (0.84–1) Prevalence = 3%
	[50]	189	M	Median: 22.5 (range: 16.9–30.1)	<b>0.88</b> (0.82–0.95) Prevalence = 52%	<b>0.92</b> (0.87–0.97) Prevalence = 20%	<b>0.94</b> (0.90–0.99) Prevalence = 7%

	[68]	366	M	Median: 23.4 (range: 17.2–30)	<b>0.78</b> (0.74–0.82) Prevalence = 38%	<b>0.93</b> (0.90–0.96) Prevalence = 4%	<b>0.99</b> (0.97–1) Prevalence = 1%
CHB and CHC	[53]	115	M	Mean: 24.8 ± 4.2	<b>0.76</b> (0.67–0.84) Prevalence = 53%	<b>0.82</b> (0.74–0.89) Prevalence = 14%	—
NAFLD	[59]	46	M	Mean: 28.0 ± 5.5	—	<b>0.78</b> (0.58–0.99) Prevalence = 74%	<b>0.72</b> (0.57–0.86) Prevalence = 46%
	[51]	63	M	Mean: 25.1 ± 2.0	—	<b>0.79</b> Prevalence = 59%	<b>0.76</b> Prevalence = 11%
	[44]	101 + 60 control	M	Mean: 29.4 ± 3.9 (20.8 ± 3.4 in control)	<b>0.97</b> Prevalence = 61%	<b>0.86</b> Prevalence = 40%	<b>0.75</b> Prevalence = 9%
	[120]	261	M	Mean: 30.2 ± 5.1	—	<b>0.80</b> (0.73–0.86) Prevalence = 70%	<b>0.66</b> (0.59–0.72) Prevalence = 32%
	[73]	127	M	Mean: 28.1 ± 4.6	<b>0.88</b> (0.80–0.95) Prevalence = 93%	<b>0.73</b> (0.64–0.81) Prevalence = 55%	<b>0.70</b> (0.58–0.83) Prevalence = 16%
	[92]	183	M	Mean: 27.9 ± 4.3	<b>0.95</b> (0.93–0.98) Prevalence = 95%	<b>0.86</b> (0.80–0.91) Prevalence = 54%	<b>0.73</b> (0.65–0.81) Prevalence = 18%
	[74]	104	M or XL	Mean: 30.4 ± 5.2	<b>0.85</b> (0.75–0.96) Prevalence = 91%	<b>0.70</b> (0.58–0.82) Prevalence = 38%	<b>0.73</b> (0.58–0.89) Prevalence = 14%
	[65]	57 +22 control	M and XL	Mean: 30.2 ± 5.0	M: <b>0.94</b> (0.86–0.98) XL: <b>0.97</b> (0.90–0.99) Prevalence = 99%	M: <b>0.80</b> (0.69–0.88) XL: <b>0.81</b> (0.71–0.89) Prevalence = 76%	M: <b>0.69</b> (0.57–0.79) XL: <b>0.67</b> (0.56–0.77) Prevalence = 26%
	[54]	55	M	Median: 27.8 (IQR: 26.0–33.1)	<b>0.77</b> (0.64–0.87) Prevalence = 91%	<b>0.78</b> (0.65–0.88) Prevalence = 47%	<b>0.79</b> (0.65–0.88) Prevalence = 16%
	[55]	393	M or XL	Mean: 34.4 ± 6.4	<b>0.76</b> (0.64–0.89) Prevalence = 95%	<b>0.70</b> (0.64–0.75) Prevalence = 58%	<b>0.58</b> (0.51–0.64) Prevalence = 27%
	[56]	380	M or XL	Median: 33.8 (IQR: 9.2)	<b>0.87</b> (0.82–0.92) Prevalence = 88%	<b>0.77</b> (0.71–0.82) Prevalence = 64%	<b>0.70</b> (0.64–0.75) Prevalence = 36%

(continued)



**Table 37.1** (continued)

Etiology	Reference	N	Probe used	BMI (kg/m <sup>2</sup> )	AUROC (95% CI) for S ≥ S1	AUROC (95% CI) for S ≥ S2	AUROC (95% CI) for S = S3
ALD	[57]	269	—	Mean: 26 ± 5	<b>0.77</b> (0.71–0.83) Prevalence = 72%	<b>0.78</b> (0.72–0.83) Prevalence = 37%	<b>0.82</b> (0.75–0.88) Prevalence = 13%
Bariatric surgery patients	[60] <sup>a</sup>	Retro: 194 Prosp: 123	M or XL	Retro Mean: 44 ± 0.4 Prosp Mean: 44 ± 0.6	Retrospective <b>0.73</b> (0.61–0.71) Prevalence = 82% Prospective <b>0.84</b> (0.71–0.91) <sup>b</sup> Prevalence = 81%	Retrospective <b>0.77</b> (0.69–0.83) Prevalence = 56% Prospective <b>0.83</b> (0.74–0.90) <sup>b</sup> Prevalence = 58%	Retrospective <b>0.79</b> (0.71–0.74) Prevalence = 36% Prospective <b>0.84</b> (0.75–0.90) <sup>a</sup> Prevalence = 37%
	[80]	76	XL	Mean: 45.2 ± 7.1	<b>0.75</b> (0.61–0.89) Prevalence = 92%	<b>0.74</b> (0.62–0.86) Prevalence = 30%	<b>0.82</b> (0.73–0.91) Prevalence = 5%
	[76]	182	XL	Mean: 45.1 ± 8.3	<b>0.75</b> (0.56–0.94) Prevalence = 83%	<b>0.69</b> (0.56–0.81) Prevalence = 46%	<b>0.54</b> (0.38–0.70) Prevalence = 14%
HIV	[121]	140		Median: 26 (IQR: 24–30)	<b>0.88</b> (0.76–0.99) Prevalence = 76%	—	—
Living liver donors	[122]	54	M	Mean: 24.0 ± 4.2	0.96 (0.91–1) Prevalence = 13%	—	—

ALD alcoholic liver disease, AUROC area under the receiver operating curve, BMI body mass index, CAP controlled attenuation parameter, CHB chronic hepatitis B, CHC chronic hepatitis C, CI confidence interval, CLD chronic liver disease, HIV human immunodeficiency virus, NAFLD non-alcoholic fatty liver disease, S steatosis, SCD skin capsular distance

<sup>a</sup>Patients were assessed for CAP either retrospectively by reprocessing the examination raw data (on patients measured when CAP on the XL probe and liver-targeting tool was not available on the machine), or prospectively when CAP on the XL and liver-targeting tool was available on the machine

<sup>b</sup>S1 corresponding to 5–33% steatosis

on a FibroScan device with the liver-targeting tool that allows the operator to perform CAP examination in a homogenous zone of the liver, performance was higher for the detection of each steatosis grade. Those results show the importance of performing the FibroScan examination properly in a liver parenchyma zone free of blood vessels or liver heterogeneities. Eventually, global performance of CAP was assessed in a few meta-analyses, robust cutoffs for the diagnostic of steatosis, and higher steatosis grades.

### ***CAP Accuracy and Cutoffs from Meta-Analyses***

Four meta-analyses have been published on the diagnostic accuracy of CAP for evaluating liver steatosis. Three were aggregated data meta-analyses [61–63] and one was an individual patient data meta-analysis [27]. Table 37.2 summarizes the diagnostic accuracy from the meta-analyses. While the first three meta-analyses were performed on patients with various CLD, the recent meta-analysis by Pu et al. [63] was focused only on NAFLD. The three meta-analyses in various CLD gave consistent results with good to excellent AUROC ranging from 0.82 to 0.85 for the diagnostic of  $S \geq S1$ , 0.87–0.88 for  $S \geq S2$ , and 0.87–0.94 for  $S = S3$ . Cutoffs were not exactly the same in the three studies but rather consistent. The individual patient's data meta-analysis provided the following cutoffs: 248 dB/m for the diagnostic of  $S \geq S1$ , 268 dB/m for  $S \geq S2$ , and 280 dB/m for  $S = S3$ . Unfortunately, the meta-analysis on NAFLD patients did not provide any cutoffs. In NAFLD, diagnostic accuracy was excellent for  $S \geq S1$ , good for  $S \geq S2$ , and moderate for  $S = S3$  (AUROCs equal to 0.96, 0.82, and 0.70, respectively).

## **Comparison Study with CAP**

### ***Comparison of CAP on M and XL Probes***

Three studies have compared CAP on M and CAP on XL probe. In the first validation study of CAP on the XL probe, 59 patients with CLD were assessed with both probes and their diagnostic performance was compared using MRI-PDFF as a reference (41). Diagnostic performance was similar with both probes ( $P > 0.50$ ) with good to excellent AUROCs (ranging between 0.84 (95% CI 0.73–0.94) and 0.92 (95% CI 0.84–0.99)) for the diagnostic of 1%, 5%, 10%, or 30% of fat fraction [41]. In addition, cutoffs were similar on both probes in this study.

Three other studies, using LB as reference, have compared CAP on the M and on the XL probes. The first one has been performed on 237 patients with CLD and a mean BMI of  $24 \pm 6 \text{ kg.m}^{-2}$  [64]. The second one was performed on 57 NAFLD patients + 22 controls with a higher mean BMI of  $30 \pm 5 \text{ kg.m}^{-2}$  [65]. CAP

**Table 37.2** Diagnostic accuracy of CAP for the evaluation of hepatic steatosis and CAP cutoffs, results from meta-analyses

Reference	Type of meta-analysis	Number of studies included	Total number of patients	Main liver diseases	Steatosis grade <sup>a</sup>	Diagnostic accuracy			
						AUROC (95% CI)	CAP cutoff (dB/m)	Summary sensitivity	Summary specificity
[61]	Aggregate data meta-analysis	9	1771	CHB, CHC, ALD, NAFLD	S ≥ S1	0.85 (0.81–0.88)	232.5	0.78 (0.69–0.84)	0.79 (0.68–0.86)
					S ≥ S2	0.88 (0.85–0.91)	255	0.85 (0.74–0.92)	0.79 (0.71–0.85)
					S = S3	0.87 (0.84–0.90)	290	0.83 (0.76–0.89)	0.79 (0.68–0.87)
[62]	Aggregate data meta-analysis	11	2076	CHB, CHC, ALD, NAFLD	S ≥ S1	0.86 (0.82–0.88)	244	0.78 (0.71–0.84)	0.79 (0.70–0.86)
					S ≥ S2	0.88 (0.85–0.90)	261	0.82 (0.74–0.88)	0.79 (0.73–0.85)
					S = S3	0.94 (0.91–0.96)	287	0.86 (0.82–0.89)	0.89 (0.86–0.92)
[27]	Individual patients data meta-analysis	19	2735	CHB, CHC, NAFLD	S ≥ S1	0.82 (0.81–0.84)	248	0.69 (0.60–0.75)	0.82 (0.76–0.90)
					S ≥ S2	0.87 (0.85–0.88)	268	0.77 (0.69–0.84)	0.81 (0.75–0.88)
					S = S3	0.88 (0.86–0.91)	280	0.88 (0.77–0.96)	0.78 (0.72–0.82)
[63]	Aggregate data meta-analysis	9	1297	NAFLD	S ≥ S1	0.96 (0.93–0.99)	–	0.87 (0.84–0.90)	0.91 (0.85–0.96)
					S ≥ S2	0.82 (0.76–0.88)		0.85 (0.82–0.88)	0.74 (0.69–0.78)
					S = S3	0.70 (0.65–0.75)		0.76 (0.71–0.80)	0.58 (0.55–0.61)

ALD alcoholic liver disease, AUROC area under the receiver operating curve, CAP controlled attenuation parameter, CHB chronic hepatitis B, CHC chronic hepatitis C, CI confidence interval, CLD chronic liver disease, NAFLD non-alcoholic fatty liver disease, S steatosis

<sup>a</sup>Steatosis grades correspond to: S1: 11–33%, S2: 34–66%, S3 ≥67% of hepatocytes with fatty infiltration

diagnostic accuracy was similar with both probes for the diagnostic of  $S \geq S1$ ,  $S \geq S2$ , and  $S = S3$ . de Ledinghen et al. have found similar cutoff values on both probe [64]. Chan et al. found marginally higher cutoffs for each of the steatosis grades when using the XL probe [65]. However, this cohort is quite small and determination of cutoffs in such a small cohort is not optimal. In addition, patients measured in this cohort had a higher BMI than in de Ledinghen et al. [64]. In most of those patients, the M probe may not be adapted to an increased skin capsular distance and in that case CAP with the M probe would have been overestimated as it is shown in [41].

Eventually, one study aimed to determine if the same cutoffs could be used on the M and the XL probes for diagnosis of steatosis using CAP [66]. In this study, 180 patients with a mean BMI of  $30 \pm 5 \text{ kg m}^{-2}$  were measured using both M and XL probes. Cutoffs determined for the M probe in the Karlas et al. meta-analysis [27] were applied on all patients measured with each probe. For each cutoff and the diagnostic of  $S \geq S1$ ,  $S \geq S2$ ,  $S = S3$ , the sensibility, specificity, positive and negative predictive values were either identical or similar, showing that the same cutoff values for CAP may be used for either the M or the XL probe for the diagnosis of hepatic steatosis grades.

### *Comparison with Steatosis Evaluation on US*

A few studies have performed a head-to-head comparison of CAP with the evaluation of steatosis using B-mode ultrasound using liver biopsy as a reference. de Ledinghen et al. [67] compared the accuracy of CAP and steatosis evaluation by ultrasound in 71 patients with CLD. Xu et al. [68] compared CAP and US on 137 chronic hepatitis B (CHB) patients. Both studies found that CAP was significantly better than US for the evaluation and grading of liver steatosis. Jun et al. [69] have compared CAP and US for diagnostic of steatosis in 79 patients with CLD, showing higher AUROC for CAP (0.90 (95% CI 0.83–0.97) vs 0.86 (95% CI 0.78–0.94), respectively). Thiele et al. [57] have compared CAP with US in a large cohort of 269 patients with alcoholic liver disease (ALD). CAP diagnosed steatosis with significantly higher diagnostic accuracies than US for higher stages of steatosis and at the limit of statistical significance for any steatosis ( $P = 0.051$ ).

Eventually, Ferraioli et al. have performed two studies using the imperfect gold standard methodology as reference (Bayesian latent class models). The first one was 726 subjects, 589 with chronic viral hepatitis, and 137 with no hepatitis [70]. In patients with chronic viral hepatitis, CAP performed better than US, whereas in patients with no hepatitis, US showed the best performance. In the second study on 305 overweight or obese children, CAP showed superior performance to US [71].

More recently, Fujiwara et al. [72] have compared CAP with the ultrasound-guided attenuation parameter (UGAP) which is a measure of an ultrasound coefficient which requires a calibration on an ultrasound tissue-mimicking phantom. AUROCs of UGAP were significantly higher than those of CAP for the identification of  $S \geq S2$  and  $S = S3$  only.

### ***Comparison with Steatosis Evaluation on MRI-Based Techniques***

CAP was shown to be outperformed by MRI-PDFF in studies using liver biopsy as reference, although it provides a rapid and inexpensive bedside assessment of liver steatosis. Imajo et al. [73] compared CAP to MRI-PDFF in a cohort of 127 NAFLD and 10 control. They showed that MRI-PDFF outperformed CAP for the diagnostic of steatosis (AUROC = 0.96 (95% CI 0.92–1.00) vs 0.88 (95% CI 0.80–0.95);  $P = 0.048$ ) and for moderate and severe steatosis as well ( $P < 0.001$  and  $P = 0.01$ , respectively). Park et al. [74] have shown similar results on 104 NAFLD patients with an AUROC for the detection of any steatosis of 0.99 (95% CI 0.98–1.00), which was significantly higher than that of CAP (0.85 (95% CI, 0.75–0.96)). Runge et al. [54] found consistent results on 55 NAFLD for the detection of steatosis where MRI-PDFF outperformed CAP (AUROC = 0.99 vs 0.77, respectively;  $P = 0.03$ ). Recently, CAP has also been compared with MRI-PDFF in a cohort of HIV-mono-infected patient at risk of NAFLD. In this cohort, patients with suspected significant fibrosis (LSM by VCTE  $\geq 7.1$  kPa and/or FibroTest  $\geq 0.49$ ) were sent to LB ( $N = 140$ ). MRI-PDFF had excellent and CAP good performances with AUROCs at 0.98 (95% CI 0.96–1.00) and 0.88 (95% CI 0.76–0.99), respectively.

Eventually one study compared CAP to  $^1\text{H}$ -magnetic resonance spectroscopy magnetic resonance spectroscopy ( $^1\text{H}$ -MRS) on 50 NAFLD patients and 15 controls, suggesting comparable diagnostic value for both method for hepatic steatosis quantification [75]. Another study compared CAP and  $^1\text{H}$ -MRS in morbidly obese patients [76]. In patients with successful MRI examination,  $^1\text{H}$ -MRS was excellent for the evaluation of steatosis. However, due to a very low applicability of MRI examination (65%), its performance was outperformed by CAP in intention-to-diagnose analysis.

### ***Comparison with Other Non-invasive Tests of Steatosis***

de Ledinghen et al. [67] have compared in a cohort of 112 patients with CLD CAP with SteatoTest, and fatty liver index (FLI) using liver biopsy as reference. CAP outperformed both SteatoTest and FLI for the diagnostic of  $S \geq S1$  ( $P = 0.04$  and  $P = 0.02$ , respectively), of  $S \geq S2$  ( $P = 0.02$  and  $P < 0.001$ , respectively), and of  $S = S3$  ( $P < 0.001$ ). The same group have compared performance of CAP vs SteatoTest and FLI in a larger cohort of 423 patients with CLD; AUROC for CAP was 0.79 (95% CI 0.75–0.84), 0.84 (95% CI 0.80–0.88), 0.84 (95% CI 0.80–0.88) for  $S \geq S1$ ,  $S \geq S2$ , and  $S = S3$ , respectively. AUROCs of FLI score were 0.74 (95% CI 0.69–0.79), 0.79 (95% CI 0.75–0.84), and 0.76 (95% CI 0.70–0.82),  $S \geq S1$ ,  $S \geq S2$ , and  $S = S3$ , respectively. Myer et al. [45] have compared the CAP performance to FLI and HSI for the diagnostic of steatosis. The AUROC of the CAP was 0.81 (95%

CI 0.74–0.88) compared with 0.65 (95% CI 0.57–0.74;  $P = 0.02$ ) for the HSI and 0.72 (95% CI 0.63–0.82;  $P = 0.12$ ) for the FLI. Xu et al. [68] compared CAP and hepatic steatosis index (HSI) on 366 CHB patients. CAP outperformed HSI for the diagnostic of each steatosis grade ( $P < 0.002$ ). Jun et al. [69] have compared CAP and HSI for the diagnostic of steatosis on 79 patients with CLD. CAP had a significantly higher AUROC (0.90 (95% CI 0.83–0.97) vs 0.77 (95% CI 0.66–0.88), respectively;  $P = 0.039$ ). Eddowes et al. [56] compared CAP to HSI in their cohort of 380 NAFLD patients showing significantly higher performance for CAP for all steatosis grades ( $P < 0.01$ ). In the study on HIV-mono-infected patients at risk of NAFLD sent to LB for suspicion of significant fibrosis, CAP had better diagnostic performance for the detection of steatosis than SteatoTest (0.88 (95% CI 0.76–0.99) vs 0.68 (95% CI 0.51–0.85), respectively).

## CAP for Monitoring

### *Non-pharmacological Interventions*

A study have assessed the influence of hypocaloric diet on 60 NAFLD patients after a 14 days follow-up [77]. At the end of the study, CAP had significantly decreased ( $P < 0.001$ ) together with weight, LSM, GGT, and lipids. Similarly, Rezende et al. [78] evaluated the effects of aerobic physical activity on reducing hepatic steatosis in 40 sedentary post-menopausal women with NAFLD. In this study, the patients were randomly divided into two groups: an exercise group and a control group, and the exercise group underwent a supervised aerobic physical activity program for 24 weeks. However, the CAP analysis did not reveal a significant decrease in hepatic steatosis in this group. Another study had been performed in 20 obese patients who had EndoBarrier® gastrointestinal liner as an experimental treatment for type 2 diabetes [79]. After explantation at  $11.6 \pm 0.5$  months, CAP had significantly decreased ( $P < 0.05$ ), together with LSM, weight, and HbA1c. Garg et al. [80] assessed the effect of bariatric surgery on liver steatosis and CAP on 32 patients using paired liver biopsy. At 1-year follow-up, CAP was significantly reduced ( $P < 0.001$ ) together with liver steatosis ( $P = 0.001$ ).

Eventually, a study on lifestyle intervention was performed on 37 participants with NAFLD who were advised to perform exercise of moderate intensity at least 3 days per week, for 45 min each time for 6 months [81]. In addition, their caloric intake was restricted to 25–30 kcal/kg/day of ideal body weight. After 6 months, the mean CAP value was significantly improved ( $P = 0.03$ ), demonstrating that lifestyle modifications, improved hepatic steatosis.

Thiele et al. [57] have shown in a cohort of 293 ALD patients admitted for detoxification that CAP significantly decreased by  $32 \pm 47$  dB/m ( $P < 0.001$ ) after a detoxification of 6.3 (IQR 4–6) days. However, they observed that CAP in obese patients did not decrease significantly during detoxification ( $P = 0.30$ ).

## ***Pharmacological Treatment***

A few studies had been performed, mainly on small sample size, on the influence of pharmacological treatment on CAP. In [82], 40 NAFLD patients with NAFLD deficiency are supplemented for steatosis for 6 months. At 6 months, restoration of serum vitamin D levels was observed, and CAP had decreased significantly from baseline ( $P = 0.007$ ). In [83], the hepatic effect of Lobeglitazone, a new thiazolidinedione, was investigated in 42 patients with type 2 diabetes and NAFLD. After 24 weeks of treatment, CAP had significantly decreased ( $P = 0.02$ ) together with HbA1c, lipid, and hepatic profiles. Another single arm pilot study was performed to assess the effect of glutathione for the treatment of NAFLD in 29 patients [84]. At the end of the study, patients were dichotomized in ALT responders (patients with significant disease in ALT) and the ALT non-responder with no significant modification from baseline. CAP had significantly decreased from baseline in the ALT responders ( $P < 0.05$ ) and was not significantly different from baseline in the non-responders ( $P = 0.31$ ). Ogasawara et al. [85] investigated the impact of direct-acting antiviral (DAA) therapy (24-week dual oral therapy of daclatasvir and asunaprevir) on changes in liver fibrosis and steatosis using LSM by VCTE and CAP in 214 elderly patients with HCV genotype 1b. While LSM by VCTE was significantly lower at the end of treatment compared with baseline, CAP significantly increased from baseline at 48 weeks post end of treatment ( $P = 0.02$ ). Together with CAP, total cholesterol was also significantly increased post-treatment. Kobayashi et al. [86] investigated sequential changes in LSM by VCTE and CAP in 57 HCV patients who received DAA therapy and achieved sustained virologic response. CAP at 48 weeks after the end of treatment was significantly different from baseline ( $P = 0.02$ ).

Shizumu et al. [87] performed a randomized, open-label trial on 57 patients with type 2 diabetes and NAFLD on a sodium-glucose co-transporter-2 (SGLT2) inhibitor. After 24 weeks of treatment, CAP showed a significant decrease in the treatment group as compared with the control group ( $P = 0.04$ ). Same significant decrease was observed in the treatment group for ALT, GGT, and visceral fat mass.

Leite et al. [88] recently investigated the effect of diacerein, an anti-inflammatory drug, on 84 patients with type 2 diabetes and NAFLD in a 24 months randomized double-blind, placebo-controlled trial. No difference in CAP from baseline was observed in the placebo group and treatment group ( $P = 0.32$ ).

## **Prognostic Value of CAP**

Studies on prognostic values of CAP are scarce with conflicting results. Liu et al. [89] aimed to determine the prognostic value of CAP for liver-related events, non-hepatocellular carcinoma (HCC) cancers, and cardiovascular events in a study on 4282 patients with a median follow-up of 26 months. They reported that neither the presence nor the severity of hepatic steatosis predicted liver-related



events, cancer, or cardiovascular events, while LSM by VCTE and etiology independently predicted liver-related events. Sub-group analysis of viral hepatitis and NAFLD patients revealed similar results. Margini et al. [90] evaluated the prognostic significance of CAP in patients with compensated advanced chronic liver disease in a retrospective study on 193 patients. At the end of a median follow-up of 18 months, 18 patients had developed clinically relevant events (decompensation or severe bacterial infection). All events were present in patients with CAP > 220 dB/m. Multivariable analysis revealed that CAP > 220 dB/m was significantly associated with clinically relevant events independently of LSM by VCTE. Scheiner et al. [91] performed a similar retrospective study on 430 patients with advanced chronic liver disease and decompensated cirrhosis. In this study, the CAP cutoff of 248 dB/m for Karlas et al. meta-analysis was used [27] and CAP was not associated with the development of first or further decompensation.

### ***CAP in Combination with LSM by VCTE for the Diagnostic of Non-alcoholic Steato-hepatitis***

Imajo et al. [73] have combined LSM by VCTE and CAP for the diagnostic of non-alcoholic steato-hepatitis (NASH) in their cohort of 127 NAFLD patients. They reported an AUROC of 0.80 (95% CI 0.73–0.88) for the diagnostic of NASH and 0.65 (95% CI 0.73–0.88) for the diagnostic of NAS  $\geq$  5. When combined with CK-18 or ALT AUROCs were not significantly different: 0.82 (95% CI 0.75–0.89) and 0.80 (95% CI 0.72–0.88), respectively, for the diagnostic of NASH and 0.66 (95% CI 0.54–0.78) and 0.67 (95% CI 0.56–0.78), respectively, for the diagnostic of NAS  $\geq$  5. Lee et al. [92] have developed a score combining LSM by VCTE, CAP, and ALT for the diagnostic of NASH showing good performance in the derivation cohort (AUROC = 0.81 (95% CI 0.72–0.88)) and good bootstrap interval validation (AUROC = 0.83 (95% CI 0.74–0.89)). Eventually, Echosens has recently developed a novel score combining LSM by VCTE, CAP, and AST to identify at risk fibrotic NASH showing good diagnostic performance in the derivation cohort and good to excellent performance in external validation cohorts from different clinical setting and geographical origins [93, 94].

### **CAP Reproducibility**

Intra-operator reproducibility has been assessed using intra-class correlation coefficient (ICC) for the M probe of the FibroScan in 22 NAFLD patients with ICC of 0.92 (95% CI 0.83–0.97) within session and 0.65 (95% CI 0.33–0.84) within weeks [54]. ICC has been assessed and compared using both the M and XL probe on 59



patients with CLD [41]. ICCs were excellent and comparable for both probes (ICC = 0.83 (95% CI 0.76–0.89) and 0.84 (95% CI 0.77–0.90) for the M and XL probes, respectively. Eventually, a recent study was performed from the NASH-CRN group on 838 patients in whom both the M and XL probes were used, according to the automatic probe selection [95]. Intra-observer correlation was high overall  $r = 0.82$  but significantly different when compared between probes ( $r = 0.85$  for the M probe vs 0.75 for the XL probe;  $P = 0.003$ ).

Inter-operator reproducibility has been assessed on the M probe in three independent studies, both showing excellent results. In Ferraioli et al. [96], the concordance correlation coefficient was 0.82 (95% CI 0.78–0.85) on 335 healthy patients or with CLD. In Recio et al. [97], ICC was 0.84 (95% CI 0.77–0.88) in 118 patients with CHC or HIV. In Runge et al. [54], similar results were found on 16 NAFLD patients with an ICC of 0.83 (95% CI 0.57–0.93). In Vuppalachchi et al. [95], the inter-observer correlation was 0.64 for the M probe and 0.68 for the XL probe ( $P = 0.71$ ).

## Factors Influencing CAP

### *Fibrosis, Inflammation, and Other Covariates*

Several studies have performed multivariable analyses to appraise factors influencing CAP. Steatosis and BMI have been shown to influence CAP [26, 44, 45, 51, 53, 98–104]. CAP has been consistently shown to be independent of fibrosis [26, 44, 45, 51, 100, 102], inflammation [26, 44, 45, 51, 100, 102, 104], liver function tests [44, 51, 98, 100–104], lipidic profile [44, 51, 53, 98, 100, 101, 103, 104], glycemic blood parameters [44, 98–100, 103], hypertension [98, 99, 103], age [26, 44, 51, 53, 98, 103, 104], gender [26, 44, 51, 98, 103], and waist circumference [26, 98, 99] when adjusted on steatosis. In the Karlas et al. meta-analysis, the relevant covariates influencing CAP were the etiology, diabetes, and BMI [27].

### *Influence of Meal Intake on CAP*

Four studies assessed the influence of meal intake on CAP values with conflicting results. In Ratchasettakul et al. [105], 40 patients with CLD who have had a liver biopsy in the previous month had a FibroScan after an overnight fast which was repeated a few times after a standard commercial meal. Significant decrease in CAP values was observed in all patients 15–120 min after meals, with the CAP peak value at 60 min and the mean post-meal delta reduction of 18.1 dB/m. Post-meal CAP values returned to baseline within 150 min following meals. In Kjargaard et al. [106], 60 patients with CLD ingested a 625 kcal and a 1250 kcal liquid meal on two consecutive days. CAP increased slightly after both meals (overall increase: +22 dB/m with both meals). Mean proportional increase was 7% after the 625-kcal

meal and 10% after the 1250 kcal with highest CAP observed at 60 min and 120 min, respectively. Eventually, a study was performed on 85 patients with CLD and healthy volunteer who had CAP measured before an overnight fasting and 30 min after intake of a standardized breakfast. In this study, CAP values did not increase significantly after food intake but no follow-up was performed after 30 min. In Vuppalanchi et al. [107], 24 patients were measured at baseline and serially for 6 h after meal intake. CAP changed minimally with a maximal change of 3% ( $P > 0.1$ ). Thus, further studies are necessary to properly understand the influence of meal intake on CAP values and draw any conclusions.

## CAP Quality Criteria

No quality criteria are recommended for CAP by the manufacturer. A study has indicated that a steatosis grade of S and high CAP values independently affect CAP performance [102]. Similarly, Galaski et al. [108] have shown that high CAP value ( $>300$  dB/m) has high specificity for steatosis but failed to stratify between steatosis grade S1 and S3, concluding that high CAP measurements need to be interpreted with care and with regard to clinical parameters, in particular when high IQR values are registered.

Two studies tried to assess the quality criteria for CAP. Wong et al. [109] have performed a large retrospective study on 754 consecutive patients with CLD from four centers. CAP was measured in all patients by the M probe. They reported that the accuracy of CAP was lower for an IQR  $>40$  dB/m (AUROC = 0.77 for  $S \geq S1$  for IQR  $>40$  dB/m vs 0.90 in patients with IQR  $<40$  dB/m,  $P = 0.004$ ). The authors therefore suggested that an IQR  $<40$  dB/m could be used as a quality criterion. Another study from Caussy et al. [110] found similar results but with an IQR of 30 dB/m. Recently, Eddowes et al. [56] tried to validate both those criteria in their large cohort of NAFLD patients. They could not confirm the results from both Wong et al. [109] and Caussy et al. [110] studies since they found lower performance in patients with an IQR  $<30$  or 40 dB/m. Same observation was found by Thiele et al. [57] in ALD patients. Further studies are needed to really appraise the CAP quality criteria or validate the ones that have been proposed.

## Liver Steatosis as a Modifier of LSM by VCTE

A few studies had suggested that the presence of massive steatosis [111] was associated with higher LSM by VCTE in patients with low fibrosis stage, leading to an overestimation of liver fibrosis. However, those studies were performed using the M probe only in overweight or obese patients. Some of those patients are very likely to have a skin-to-capsule distance higher than 25 mm, which may induce an overestimation of LSM. The same patients being overweight or obese have also a higher likelihood of having steatosis. Therefore, important confounding factors were not

taken into account, together with other methodological issues [112, 113]. The impact of steatosis on LSM was still uncertain [114]. Eddowes et al. [56] have however very recently shown that when the proper probe is used for each patient, according to the automatic probe recommendation tool embedded in the FibroScan device, the only histological factor influencing LSM by VCTE is the liver fibrosis. Karlas et al. [115] tried to appraise if CAP could be used to enhance LSM by VCTE interpretation, finding negligible to slight impact of using CAP values for fibrosis evaluation.

## Conclusion

CAP provides a rapid and inexpensive bedside assessment of liver steatosis. Its performance for the diagnostic of steatosis was shown to be satisfactory in various etiologies especially in cohorts of patients with various CLD, in viral hepatitis and in NAFLD exceeding conventional ultrasound. CAP has however a moderate accuracy for the differentiation between higher grades of steatosis. CAP being embedded on the FibroScan device, it has the advantage to provide an assessment of steatosis together with LSM by VCTE. Both steatosis and fibrosis can therefore be assessed simultaneously, in the same zone of the liver and the physician has access to both parameters which is especially relevant in the context of NAFLD. Studies have shown that the same cutoffs could be applied for both M and XL probes. More recent studies have shown that CAP is sensitive to both lifestyle intervention and pharmacological treatment. Recent data suggest that CAP, in combination with LSM by VCTE and possibly other bio-clinical parameters such as transaminase levels, might be very useful for the evaluation of NASH or NASH-related histological lesions.

## References

1. Farrell GC. Fatty liver disease: NASH and related disorders. Malden: Blackwell Publishing; 2004.
2. Chalasani N, Younossi Z, Lavine JE, Diehl AM, Brunt EM, Cusi K, et al. The diagnosis and management of non-alcoholic fatty liver disease: practice Guideline by the American Association for the Study of Liver Diseases, American College of Gastroenterology, and the American Gastroenterological Association. *Hepatology*. 2012;55(6):2005–23.
3. Younossi ZM, Koenig AB, Abdelatif D, Fazel Y, Henry L, Wymer M. Global epidemiology of nonalcoholic fatty liver disease-meta-analytic assessment of prevalence, incidence, and outcomes. *Hepatology*. 2016;64(1):73–84.
4. Bellentani S, Saccoccio G, Masutti F, Croce LS, Brandi G, Sasso F, et al. Prevalence of and risk factors for hepatic steatosis in Northern Italy. *Ann Intern Med*. 2000;132(2):112–7.
5. Leandro G, Mangia A, Hui J, Fabris P, Rubbia-Brandt L, Collorero G, et al. Relationship between steatosis, inflammation, and fibrosis in chronic hepatitis C: a meta-analysis of individual patient data. *Gastroenterology*. 2006;130(6):1636–42.

6. Asselah T, Rubbia-Brandt L, Marcellin P, Negro F. Steatosis in chronic hepatitis C: why does it really matter? *Gut*. 2006;55(1):123–30.
7. Farrell GC, Larter CZ. Nonalcoholic fatty liver disease: from steatosis to cirrhosis. *Hepatology*. 2006;43(2 Suppl 1):S99–S112.
8. Dixon JB, Bhathal PS, O'Brien PE. Nonalcoholic fatty liver disease: predictors of non-alcoholic steatohepatitis and liver fibrosis in the severely obese. *Gastroenterology*. 2001;121(1):91–100.
9. Gholam PM, Flancbaum L, Machan JT, Charney DA, Kotler DP. Nonalcoholic fatty liver disease in severely obese subjects. *Am J Gastroenterol*. 2007;102(2):399–408.
10. Singh S, Allen AM, Wang Z, Prokop LJ, Murad MH, Loomba R. Fibrosis progression in non-alcoholic fatty liver vs nonalcoholic steatohepatitis: a systematic review and meta-analysis of paired-biopsy studies. *Clin Gastroenterol Hepatol*. 2015;13(4):643–54; quiz e39–40.
11. Castera L, Hezode C, Roudot-Thoraval F, Bastie A, Zafarani ES, Pawlotsky JM, et al. Worsening of steatosis is an independent factor of fibrosis progression in untreated patients with chronic hepatitis C and paired liver biopsies. *Gut*. 2003;52(2):288–92.
12. Fartoux L, Chazouilleres O, Wendum D, Poupon R, Serfaty L. Impact of steatosis on progression of fibrosis in patients with mild hepatitis C. *Hepatology*. 2005;41(1):82–7.
13. Poynard T, Ratziu V, McHutchison J, Manns M, Goodman Z, Zeuzem S, et al. Effect of treatment with peginterferon or interferon alfa-2b and ribavirin on steatosis in patients infected with hepatitis C. *Hepatology*. 2003;38(1):75–85.
14. Harrison SA, Brunt EM, Qazi RA, Oliver DA, Neuschwander-Tetri BA, Di Bisceglie AM, et al. Effect of significant histologic steatosis or steatohepatitis on response to antiviral therapy in patients with chronic hepatitis C. *Clin Gastroenterol Hepatol*. 2005;3(6):604–9.
15. Ohata K, Hamasaki K, Toriyama K, Matsumoto K, Saeki A, Yanagi K, et al. Hepatic steatosis is a risk factor for hepatocellular carcinoma in patients with chronic hepatitis C virus infection. *Cancer*. 2003;97(12):3036–43.
16. Kurosaki M, Hosokawa T, Matsunaga K, Hirayama I, Tanaka T, Sato M, et al. Hepatic steatosis in chronic hepatitis C is a significant risk factor for developing hepatocellular carcinoma independent of age, sex, obesity, fibrosis stage and response to interferon therapy. *Hepatol Res*. 2010;40(9):870–7.
17. Berzigotti A. Getting closer to a point-of-care diagnostic assessment in patients with chronic liver disease: controlled attenuation parameter for steatosis. *J Hepatol*. 2014;60(5):910–2.
18. Bravo AA, Sheth SG, Chopra S. Liver biopsy. *N Engl J Med*. 2001;344(7):495–500.
19. Ratziu V, Charlotte F, Heurtier A, Gombert S, Giral P, Bruckert E, et al. Sampling variability of liver biopsy in nonalcoholic fatty liver disease. *Gastroenterology*. 2005;128(7):1898–906.
20. Grant A, Neuberger J. Guidelines on the use of liver biopsy in clinical practice. *British Society of Gastroenterology*. *Gut*. 1999;45(Suppl 4):1–11.
21. Schwenzler NF, Springer F, Schraml C, Stefan N, Machann J, Schick F. Non-invasive assessment and quantification of liver steatosis by ultrasound, computed tomography and magnetic resonance. *J Hepatol*. 2009;51(3):433–45.
22. EASL. EASL-EASD-EASO clinical practice guidelines for the management of non-alcoholic fatty liver disease. *J Hepatol*. 2016;64(6):1388–402.
23. Zhang YN, Fowler KJ, Hamilton G, Cui JY, Sy EZ, Balanay M, et al. Liver fat imaging—clinical overview of ultrasound, CT, and MR imaging. *Br J Radiol*. 2018;91(1089):20170959.
24. Bohte AE, van Werven JR, Bipat S, Stoker J. The diagnostic accuracy of US, CT, MRI and 1H-MRS for the evaluation of hepatic steatosis compared with liver biopsy: a meta-analysis. *Eur Radiol*. 2011;21(1):87–97.
25. Uhrig M, Mueller J, Longeric T, Straub BK, Buschle LR, Schlemmer HP, et al. Susceptibility based multiparametric quantification of liver disease: non-invasive evaluation of steatosis and iron overload. *Magn Reson Imaging*. 2019;63:114–22.
26. Sasso M, Beaugrand M, de Ledinghen V, Douvin C, Marcellin P, Poupon R, et al. Controlled attenuation parameter (CAP): a novel VCTE™ guided ultrasonic attenuation measurement for the evaluation of hepatic steatosis: preliminary study and validation in

- a cohort of patients with chronic liver disease from various causes. *Ultrasound Med Biol.* 2010;36(11):1825–35.
27. Karlas T, Petroff D, Sasso M, Fan JG, Mi YQ, de Ledinghen V, et al. Individual patient data meta-analysis of controlled attenuation parameter (CAP) technology for assessing steatosis. *J Hepatol.* 2017;66(5):1022–30.
  28. Wong VW, Chan WK, Chitturi S, Chawla Y, Dan YY, Duseja A, et al. Asia-Pacific working party on non-alcoholic fatty liver disease guidelines 2017-part 1: definition, risk factors and assessment. *J Gastroenterol Hepatol.* 2018;33(1):70–85.
  29. Chalasani N, Younossi Z, Lavine JE, Charlton M, Cusi K, Rinella M, et al. The diagnosis and management of nonalcoholic fatty liver disease: practice guidance from the American Association for the study of liver diseases. *Hepatology.* 2018;67(1):328–57.
  30. Ferraioli G, Wong VW, Castera L, Berzigotti A, Sporea I, Dietrich CF, et al. Liver ultrasound elastography: an update to the World Federation for ultrasound in medicine and biology guidelines and recommendations. *Ultrasound Med Biol.* 2018;44(12):2419–40.
  31. Szabo TL. *Diagnostic ultrasound imaging : inside out.* Boston: Elsevier Academic Press; 2004.
  32. Bushberg JT. *The essential physics of medical imaging.* 2nd ed. Philadelphia: Lippincott Williams & Wilkins; 2001. p. 848.
  33. Kuc R. Clinical application of an ultrasound attenuation coefficient estimation technique for liver pathology characterization. *IEEE Trans Biomed Eng.* 1980;27(6):312–9.
  34. Fink M, Hottier F, Cardoso JF. Ultrasonic signal processing for in vivo attenuation measurement: short time Fourier analysis. *Ultrasound Imaging.* 1983;5(2):117–35.
  35. Maklad NF, Ophir J, Balsara V. Attenuation of ultrasound in normal liver and diffuse liver disease in vivo. *Ultrasound Imaging.* 1984;6(2):117–25.
  36. Taylor KJ, Riely CA, Hammers L, Flax S, Weltin G, Garcia-Tsao G, et al. Quantitative US attenuation in normal liver and in patients with diffuse liver disease: importance of fat. *Radiology.* 1986;160(1):65–71.
  37. Garra BS, Insana MF, Shawker TH, Russell MA. Quantitative estimation of liver attenuation and echogenicity: normal state versus diffuse liver disease. *Radiology.* 1987;162(1 Pt 1):61–7.
  38. Wilson LS, Robinson DE, Griffiths KA, Manoharan A, Doust BD. Evaluation of ultrasonic attenuation in diffuse diseases of spleen and liver. *Ultrasound Imaging.* 1987;9(4):236–47.
  39. Lu ZF, Zagzebski JA, Lee FT. Ultrasound backscatter and attenuation in human liver with diffuse disease. *Ultrasound Med Biol.* 1999;25(7):1047–54.
  40. Fujii Y, Taniguchi N, Itoh K, Shigeta K, Wang Y, Tsao JW, et al. A new method for attenuation coefficient measurement in the liver: comparison with the spectral shift central frequency method. *J Ultrasound Med.* 2002;21(7):783–8.
  41. Sasso M, Audiere S, Kemgang A, Gaouar F, Corpechot C, Chazouilleres O, et al. Liver steatosis assessed by controlled attenuation parameter (CAP) measured with the XL probe of the fibroscan: a pilot study assessing diagnostic accuracy. *Ultrasound Med Biol.* 2016;42(1):92–103.
  42. Jensen JA. Field: a program for simulating ultrasound systems. In: 10th Nordicbaltic conference on biomedical Imaging, vol. 4. 1996. pp. 351–3.
  43. Sasso M, Tengher-Barna I, Ziol M, Miette V, Fournier C, Sandrin L, et al. Novel controlled attenuation parameter for noninvasive assessment of steatosis using Fibroscan®: validation in chronic hepatitis C. *J Viral Hepat.* 2012;19(4):244–53.
  44. Chan WK, Nik Mustapha NR, Mahadeva S. Controlled attenuation parameter for the detection and quantification of hepatic steatosis in nonalcoholic fatty liver disease. *J Gastroenterol Hepatol.* 2014;29(7):1470–6.
  45. Myers RP, Pollett A, Kirsch R, Pomier-Layrargues G, Beaton M, Levstik M, et al. Controlled attenuation parameter (CAP): a noninvasive method for the detection of hepatic steatosis based on transient elastography. *Liver Int.* 2012;32(6):902–10.

46. Myers RP, Pomier-Layrargues G, Kirsch R, Pollett A, Duarte-Rojo A, Wong D, et al. Feasibility and diagnostic performance of the FibroScan XL probe for liver stiffness measurement in overweight and obese patients. *Hepatology*. 2012;55(1):199–208.
47. Wear KA. The effect of trabecular material properties on the frequency dependence of backscatter from cancellous bone. *J Acoust Soc Am*. 2003;114(1):62–5.
48. Mendes LC, Ferreira PA, Miotto N, Zanaga L, Goncales ESL, Pedro MN, et al. Elastogram quality assessment score in vibration-controlled transient elastography: diagnostic performance compared to digital morphometric analysis of liver biopsy in chronic hepatitis C. *J Viral Hepat*. 2018;25(4):335–43.
49. Cardoso AC, Beaugrand M, de Ledinghen V, Douvin C, Poupon R, Trinchet JC, et al. Diagnostic performance of controlled attenuation parameter for predicting steatosis grade in chronic hepatitis B. *Ann Hepatol*. 2015;14(6):826–36.
50. Chen J, Wu D, Wang M, Chen E, Bai L, Liu C, et al. Controlled attenuation parameter for the detection of hepatic steatosis in patients with chronic hepatitis B. *Infect Dis*. 2016;48(9):670–5.
51. Kumar M, Rastogi A, Singh T, Behari C, Gupta E, Garg H, et al. Controlled attenuation parameter for non-invasive assessment of hepatic steatosis: does etiology affect performance? *J Gastroenterol Hepatol*. 2013;28(7):1194–201.
52. Wang CY, Lu W, Hu DS, Wang GD, Cheng XJ. Diagnostic value of controlled attenuation parameter for liver steatosis in patients with chronic hepatitis B. *World J Gastroenterol*. 2014;20(30):10585–90.
53. Ferraioli G, Tinelli C, Lissandrini R, Zicchetti M, Dal Bello B, Filice G, et al. Controlled attenuation parameter for evaluating liver steatosis in chronic viral hepatitis. *World J Gastroenterol*. 2014;20(21):6626–31.
54. Runge JH, Smits LP, Verheij J, Depla A, Kuiken SD, Baak BC, et al. MR spectroscopy-derived proton density fat fraction is superior to controlled attenuation parameter for detecting and grading hepatic steatosis. *Radiology*. 2018;286(2):547–56.
55. Siddiqui MS, Vuppalanchi R, Van Natta ML, Hallinan E, Kowdley KV, Abdelmalek M, et al. Vibration-controlled transient elastography to assess fibrosis and steatosis in patients with nonalcoholic fatty liver disease. *Clin Gastroenterol Hepatol*. 2018;17(1):156–63.
56. Eddowes PJ, Sasso M, Allison M, Tsochatzis E, Anstee QM, Sheridan D, et al. Accuracy of FibroScan controlled attenuation parameter and liver stiffness measurement in assessing steatosis and fibrosis in patients with nonalcoholic fatty liver disease. *Gastroenterology*. 2019;156(6):1717–30.
57. Thiele M, Rausch V, Fluhr G, Kjærgaard M, Piecha F, Mueller J, et al. Controlled attenuation parameter and alcoholic hepatic steatosis: diagnostic accuracy and role of alcohol detoxification. *J Hepatol*. 2018;68(5):1025–32.
58. Shen F, Zheng RD, Shi JP, Mi YQ, Chen GF, Hu X, et al. Impact of skin capsular distance on the performance of controlled attenuation parameter in patients with chronic liver disease. *Liver Int*. 2015;35(11):2392–400.
59. Friedrich-Rust M, Romen D, Vermehren J, Kriener S, Sadet D, Herrmann E, et al. Acoustic radiation force impulse-imaging and transient elastography for non-invasive assessment of liver fibrosis and steatosis in NAFLD. *Eur J Radiol*. 2012;81(3):e325–31.
60. Naveau S, Voican CS, Lebrun A, Gaillard M, Lamouri K, Njike-Nakseu M, et al. Controlled attenuation parameter for diagnosing steatosis in bariatric surgery candidates with suspected nonalcoholic fatty liver disease. *Eur J Gastroenterol Hepatol*. 2017;29(9):1022–30.
61. Shi KQ, Tang JZ, Zhu XL, Ying L, Li DW, Gao J, et al. Controlled attenuation parameter for the detection of steatosis severity in chronic liver disease: a meta-analysis of diagnostic accuracy. *J Gastroenterol Hepatol*. 2014;29(6):1149–58.
62. Wang Y, Fan Q, Wang T, Wen J, Wang H, Zhang T. Controlled attenuation parameter for assessment of hepatic steatosis grades: a diagnostic meta-analysis. *Int J Clin Exp Med*. 2015;8(10):17654–63.



63. Pu K, Wang Y, Bai S, Wei H, Zhou Y, Fan J, et al. Diagnostic accuracy of controlled attenuation parameter (CAP) as a non-invasive test for steatosis in suspected non-alcoholic fatty liver disease: a systematic review and meta-analysis. *BMC Gastroenterol.* 2019;19(1):51.
64. de Ledinghen V, Hiriart JB, Vergniol J, Merrouche W, Bedossa P, Paradis V. Controlled attenuation parameter (CAP) with the XL probe of the Fibroscan®: a comparative study with the M probe and liver biopsy. *Dig Dis Sci.* 2017;62(9):2569–77.
65. Chan WK, Nik Mustapha NR, Wong GL, Wong VW, Mahadeva S. Controlled attenuation parameter using the FibroScan® XL probe for quantification of hepatic steatosis for non-alcoholic fatty liver disease in an Asian population. *United European Gastroenterol J.* 2017;5(1):76–85.
66. Chan WK, Nik Mustapha NR, Mahadeva S, Wong VW, Cheng JY, Wong GL. Can the same controlled attenuation parameter cut-offs be used for M and XL probes for diagnosing hepatic steatosis? *J Gastroenterol Hepatol.* 2018;33(10):1787–94.
67. de Ledinghen V, Vergniol J, Foucher J, Merrouche W, le Bail B. Non-invasive diagnosis of liver steatosis using controlled attenuation parameter (CAP) and transient elastography. *Liver Int.* 2012;32(6):911–8.
68. Xu L, Lu W, Li P, Shen F, Mi YQ, Fan JG. A comparison of hepatic steatosis index, controlled attenuation parameter and ultrasound as noninvasive diagnostic tools for steatosis in chronic hepatitis B. *Dig Liver Dis.* 2017;49(8):910–7.
69. Jun BG, Park WY, Park EJ, Jang JY, Jeong SW, Lee SH, et al. A prospective comparative assessment of the accuracy of the FibroScan in evaluating liver steatosis. *PLoS One.* 2017;12(8):e0182784.
70. Ferraioli G, Tinelli C, De Silvestri A, Lissandrin R, Above E, Dellafiore C, et al. The clinical value of controlled attenuation parameter for the noninvasive assessment of liver steatosis. *Liver Int.* 2016;36(12):1860–6.
71. Ferraioli G, Calcaterra V, Lissandrin R, Guazzotti M, Maiocchi L, Tinelli C, et al. Noninvasive assessment of liver steatosis in children: the clinical value of controlled attenuation parameter. *BMC Gastroenterol.* 2017;17(1):61.
72. Fujiwara Y, Kuroda H, Abe T, Ishida K, Oguri T, Noguchi S, et al. The B-mode image-guided ultrasound attenuation parameter accurately detects hepatic steatosis in chronic liver disease. *Ultrasound Med Biol.* 2018;44(11):2223–32.
73. Imajo K, Kessoku T, Honda Y, Tomeno W, Ogawa Y, Mawatari H, et al. Magnetic resonance imaging more accurately classifies steatosis and fibrosis in patients with nonalcoholic fatty liver disease than transient elastography. *Gastroenterology.* 2016;150(3):626–37.
74. Park CC, Nguyen P, Hernandez C, Bettencourt R, Ramirez K, Fortney L, et al. Magnetic resonance elastography vs transient elastography in detection of fibrosis and noninvasive measurement of steatosis in patients with biopsy-proven nonalcoholic fatty liver disease. *Gastroenterology.* 2017;152(3):598–607.
75. Karlas T, Petroff D, Garnov N, Bohm S, Tenckhoff H, Wittekind C, et al. Non-invasive assessment of hepatic steatosis in patients with NAFLD using controlled attenuation parameter and 1H-MR spectroscopy. *PLoS One.* 2014;9(3):e91987.
76. Ooi GJ, Earnest A, Kemp WW, Burton PR, Laurie C, Majeed A, et al. Evaluating feasibility and accuracy of non-invasive tests for nonalcoholic fatty liver disease in severe and morbid obesity. *Int J Obes.* 2018;42(11):1900–11.
77. Arslanow A, Teutsch M, Walle H, Grunhage F, Lammert F, Stokes CS. Short-term hypocaloric high-fiber and high-protein diet improves hepatic steatosis assessed by controlled attenuation parameter. *Clin Transl Gastroenterol.* 2016;7(6):e176.
78. Rezende RE, Duarte SM, Stefano JT, Roschel H, Gualano B, de Sa Pinto AL, et al. Randomized clinical trial: benefits of aerobic physical activity for 24 weeks in postmenopausal women with nonalcoholic fatty liver disease. *Menopause.* 2016;23(8):876–83.
79. Gollisch KS, Lindhorst A, Raddatz D. EndoBarrier gastrointestinal liner in type 2 diabetic patients improves liver fibrosis as assessed by liver elastography. *Exp Clin Endocrinol Diabetes.* 2017;125(2):116–21.

80. Garg H, Aggarwal S, Shalimar YR, Datta Gupta S, Agarwal L, et al. Utility of transient elastography (fibroscan) and impact of bariatric surgery on nonalcoholic fatty liver disease (NAFLD) in morbidly obese patients. *Surg Obes Relat Dis.* 2018;14(1):81–91.
81. Paul J, Venugopal RV, Peter L, Shetty KNK, Shetti MP. Measurement of controlled attenuation parameter: a surrogate marker of hepatic steatosis in patients of nonalcoholic fatty liver disease on lifestyle modification - a prospective follow-up study. *Arq Gastroenterol.* 2018;55(1):7–13.
82. Papapostoli I, Lammert F, Stokes CS. Effect of short-term vitamin D correction on hepatic steatosis as quantified by controlled attenuation parameter (CAP). *J Gastrointestin Liver Dis.* 2016;25(2):175–81.
83. Lee YH, Kim JH, Kim SR, Jin HY, Rhee EJ, Cho YM, et al. Lobeglitazone, a novel thiazolidinedione, improves non-alcoholic fatty liver disease in type 2 diabetes: its efficacy and predictive factors related to responsiveness. *J Korean Med Sci.* 2017;32(1):60–9.
84. Honda Y, Kessoku T, Sumida Y, Kobayashi T, Kato T, Ogawa Y, et al. Efficacy of glutathione for the treatment of nonalcoholic fatty liver disease: an open-label, single-arm, multicenter, pilot study. *BMC Gastroenterol.* 2017;17(1):96.
85. Ogasawara N, Kobayashi M, Akuta N, Kominami Y, Fujiyama S, Kawamura Y, et al. Serial changes in liver stiffness and controlled attenuation parameter following direct-acting antiviral therapy against hepatitis C virus genotype 1b. *J Med Virol.* 2018;90(2):313–9.
86. Kobayashi N, Iijima H, Tada T, Kumada T, Yoshida M, Aoki T, et al. Changes in liver stiffness and steatosis among patients with hepatitis C virus infection who received direct-acting antiviral therapy and achieved sustained virological response. *Eur J Gastroenterol Hepatol.* 2018;30(5):546–51.
87. Shimizu M, Suzuki K, Kato K, Jojima T, Iijima T, Murohisa T, et al. Evaluation of the effects of dapagliflozin, a sodium-glucose co-transporter-2 inhibitor, on hepatic steatosis and fibrosis using transient elastography in patients with type 2 diabetes and non-alcoholic fatty liver disease. *Diabetes Obes Metab.* 2019;21(2):285–92.
88. Leite NC, Viegas BB, Villela-Nogueira CA, Carlos FO, Cardoso CRL, Salles GF. Efficacy of diacerein in reducing liver steatosis and fibrosis in patients with type 2 diabetes and non-alcoholic fatty liver disease: a randomized, placebo-controlled trial. *Diabetes Obes Metab.* 2019;21(5):1266–70.
89. Liu K, Wong VW, Lau K, Liu SD, Tse YK, Yip TC, et al. Prognostic value of controlled attenuation parameter by transient elastography. *Am J Gastroenterol.* 2017;112(12):1812–23.
90. Margini C, Murgia G, Stirnimann G, De Gottardi A, Semmo N, Casu S, et al. Prognostic significance of controlled attenuation parameter in patients with compensated advanced chronic liver disease. *Hepatol Commun.* 2018;2(8):929–40.
91. Scheiner B, Steininger L, Semmler G, Unger LW, Schwabl P, Bucsics T, et al. Controlled attenuation parameter does not predict hepatic decompensation in patients with advanced chronic liver disease. *Liver Int.* 2019;39(1):127–35.
92. Lee HW, Park SY, Kim SU, Jang JY, Park H, Kim JK, et al. Discrimination of nonalcoholic steatohepatitis using transient elastography in patients with nonalcoholic fatty liver disease. *PLoS One.* 2016;11(6):e0157358.
93. Sasso M, Chan WK, Harrison SA, Czernichow S, Allison M, Tsochatzis E, et al. FS3 FibroScan-based score to identify NASH patients with NAS $\geq$ 4 AND F $\geq$ 2 Development in a NAFLD UK cohort - external validation in a Malaysian NAFLD cohort, a US screening cohort and a French bariatric surgery cohort. Liver meeting of the American Association for the Study of Liver Disease (AASLD); San Francisco, CA, USA; 2018.
94. Boursier J, Zheng M-H, Wong VW, Michalak S, Li Y, Chan AW, et al. External validation in NAFLD cohorts of a FibroScan-based score combining liver stiffness, controlled attenuation parameter and AST to identify patients with active NASH (NAS $\geq$ 4) and significant fibrosis (F $\geq$ 2). International Liver Congress (ILC), European Association for the Study of the Liver (EASL); Vienna, Austria; 2019.



95. Vuppalanchi R, Siddiqui MS, Van Natta ML, Hallinan E, Brandman D, Kowdley K, et al. Performance characteristics of vibration-controlled transient elastography for evaluation of nonalcoholic fatty liver disease. *Hepatology*. 2018;67(1):134–44.
96. Ferraioli G, Tinelli C, Lissandrin R, Zicchetti M, Rondanelli M, Perani G, et al. Interobserver reproducibility of the controlled attenuation parameter (CAP) for quantifying liver steatosis. *Hepatol Int*. 2014;8(4):576–81.
97. Recio E, Cifuentes C, Macias J, Mira JA, Parra-Sanchez M, Rivero-Juarez A, et al. Interobserver concordance in controlled attenuation parameter measurement, a novel tool for the assessment of hepatic steatosis on the basis of transient elastography. *Eur J Gastroenterol Hepatol*. 2013;25(8):905–11.
98. Yilmaz Y, Ergelen R, Akin H, Imeryuz N. Noninvasive detection of hepatic steatosis in patients without ultrasonographic evidence of fatty liver using the controlled attenuation parameter evaluated with transient elastography. *Eur J Gastroenterol Hepatol*. 2013;25(11):1330–4.
99. de Ledinghen V, Vergniol J, Capdepon M, Chermak F, Hiriart JB, Cassinotto C, et al. Controlled attenuation parameter (CAP) for the diagnosis of steatosis: a prospective study of 5323 examinations. *J Hepatol*. 2014;60(5):1026–31.
100. Chon YE, Jung KS, Kim SU, Park JY, Park YN, Kim DY, et al. Controlled attenuation parameter (CAP) for detection of hepatic steatosis in patients with chronic liver diseases: a prospective study of a native Korean population. *Liver Int*. 2014;34(1):102–9.
101. Shen F, Zheng RD, Mi YQ, Wang XY, Pan Q, Chen GY, et al. Controlled attenuation parameter for non-invasive assessment of hepatic steatosis in Chinese patients. *World J Gastroenterol*. 2014;20(16):4702–11.
102. Jung KS, Kim BK, Kim SU, Chon YE, Chun KH, Kim SB, et al. Factors affecting the accuracy of controlled attenuation parameter (CAP) in assessing hepatic steatosis in patients with chronic liver disease. *PLoS One*. 2014;9(6):e98689.
103. Chon YE, Jung KS, Kim KJ, Joo DJ, Kim BK, Park JY, et al. Normal controlled attenuation parameter values: a prospective study of healthy subjects undergoing health checkups and liver donors in Korea. *Dig Dis Sci*. 2015;60(1):234–42.
104. Mi YQ, Shi QY, Xu L, Shi RF, Liu YG, Li P, et al. Controlled attenuation parameter for non-invasive assessment of hepatic steatosis using Fibroscan(R): validation in chronic hepatitis B. *Dig Dis Sci*. 2015;60(1):243–51.
105. Ratchasettakul K, Rattanasiri S, Promson K, Sringam P, Sobhonslidsuk A. The inverse effect of meal intake on controlled attenuation parameter and liver stiffness as assessed by transient elastography. *BMC Gastroenterol*. 2017;17(1):50.
106. Kjaergaard M, Thiele M, Jansen C, Staehr Madsen B, Gortzen J, Strassburg C, et al. High risk of misinterpreting liver and spleen stiffness using 2D shear-wave and transient elastography after a moderate or high calorie meal. *PLoS One*. 2017;12(4):e0173992.
107. Vuppalanchi R, Weber R, Russell S, Gawrieh S, Samala N, Slaven JE, et al. Is fasting necessary for individuals with nonalcoholic fatty liver disease to undergo vibration-controlled transient elastography? *Am J Gastroenterol*. 2019;114(6):995–7.
108. Galaski J, Schulz L, Krause J, Lohse AW. Discordance in steatosis classification between liver biopsy and transient elastography for high controlled attenuation parameter (CAP) values. *Z Gastroenterol*. 2018;56(1):36–42.
109. Wong VW, Petta S, Hiriart JB, Camma C, Wong GL, Marra F, et al. Validity criteria for the diagnosis of fatty liver by M probe-based controlled attenuation parameter. *J Hepatol*. 2017;67(3):577–84.
110. Caussy C, Alquraish MH, Nguyen P, Hernandez C, Cepin S, Fortney LE, et al. Optimal threshold of controlled attenuation parameter with MRI-PDFF as the gold standard for the detection of hepatic steatosis. *Hepatology*. 2018;67(4):1348–59.
111. Petta S, Maida M, Macaluso FS, Di Marco V, Camma C, Cabibi D, et al. The severity of steatosis influences liver stiffness measurement in patients with nonalcoholic fatty liver disease. *Hepatology*. 2015;62(4):1101–10.

112. Eddowes P, Sasso M, Fournier C, Vuppalanchi R, Newsome P. Steatosis and liver stiffness measurements using transient elastography. *Hepatology*. 2016;64(2):700.
113. Karlas T, Beer S, Babel J, Busse H, Schaudinn A, Linder N, et al. Do we need controlled attenuation parameter adjustment for fibrosis estimation in nonalcoholic fatty liver disease patients? *Hepatology*. 2017;65(6):2126–8.
114. Ferraioli G, Filice C, Castera L, Choi BI, Sporea I, Wilson SR, et al. WFUMB guidelines and recommendations for clinical use of ultrasound elastography: part 3: liver. *Ultrasound Med Biol*. 2015;41(5):1161–79.
115. Karlas T, Petroff D, Sasso M, Fan JG, Mi YQ, de Ledinghen V, et al. Impact of controlled attenuation parameter on detecting fibrosis using liver stiffness measurement. *Aliment Pharmacol Ther*. 2018;47(7):989–1000.
116. Masaki K, Takaki S, Hyogo H, Kobayashi T, Fukuhara T, Naeshiro N, et al. Utility of controlled attenuation parameter measurement for assessing liver steatosis in Japanese patients with chronic liver diseases. *Hepatol Res*. 2013;43(11):1182–9.
117. Lupsor-Platon M, Feier D, Stefanescu H, Tamas A, Botan E, Sparchez Z, et al. Diagnostic accuracy of controlled attenuation parameter measured by transient elastography for the non-invasive assessment of liver steatosis: a prospective study. *J Gastrointest Liver Dis*. 2015;24(1):35–42.
118. Andrade P, Rodrigues S, Rodrigues-Pinto E, Gaspar R, Lopes J, Lopes S, et al. Diagnostic accuracy of controlled attenuation parameter for detecting hepatic steatosis in patients with chronic liver disease. *GE Port J Gastroenterol*. 2017;24(4):161–8.
119. Rout G, Kedia S, Nayak B, Yadav R, Das P, Acharya SK, et al. Controlled attenuation parameter for assessment of hepatic steatosis in Indian patients. *J Clin Exp Hepatol*. 2019;9(1):13–21.
120. de Ledinghen V, Wong GL, Vergniol J, Chan HL, Hiriart JB, Chan AW, et al. Controlled attenuation parameter for the diagnosis of steatosis in non-alcoholic fatty liver disease. *J Gastroenterol Hepatol*. 2016;31(4):848–55.
121. Lemoine M, Assoumou L, De Wit S, Girard PM, Valantin MA, Katlama C, et al. Diagnostic accuracy of noninvasive markers of steatosis, NASH, and liver fibrosis in HIV-monoinfected individuals at risk of nonalcoholic fatty liver disease (NAFLD): results from the ECHAM study. *J Acquir Immune Defic Syndr*. 2019;80(4):e86–94.
122. Yen YH, Kuo FY, Lin CC, Chen CL, Chang KC, Tsai MC, et al. Predicting hepatic steatosis in living liver donors via controlled attenuation parameter. *Transplant Proc*. 2018;50(10):3533–8.

# Chapter 38

## Steatosis Assessment with Controlled Attenuation Parameter (CAP) in Various Diseases



Charlotte Wernberg, Mie Balle Hugger, and Maja Thiele

### The Role of Steatosis in Liver Disease

Liver steatosis is the accumulation of lipid droplets, mainly triglycerides, in the hepatocytes. It can be defined histologically, which necessitates a liver biopsy, by the presence of fat droplets in  $\geq 5\%$  of hepatocytes; or radiologically/chemically by the wet mass of the liver parenchyma consisting of  $\geq 5\%$  lipid mass [1]. Steatosis represents imbalanced hepatic lipid metabolism due to liver injury in a variety of chronic and acute liver diseases, including drug-induced liver injury, alcoholic liver disease (ALD), and chronic viral hepatitis B and C (HBV, HCV). In particular, liver steatosis is the hallmark of non-alcoholic fatty liver disease (NAFLD) which is, by definition, lipid accumulation in the liver, in the absence of excess alcoholic consumption and other known causes of chronic liver disease [2]. Being able to easily assess steatosis is therefore crucial for diagnosing NAFLD. The high prevalence of NAFLD in the western world and the fact that NAFLD is the fastest growing chronic liver disease is one reason for the focus on finding noninvasive methods for diagnosing and grading steatosis in patients at risk of NAFLD. Beyond NAFLD, noninvasive modalities that can diagnose and quantify steatosis may be used for screening, follow-up, and assessment of efficacy of intervention in other chronic liver diseases where liver fat accumulation is an indicator of hepatocyte dysfunction [3].

---

C. Wernberg · M. B. Hugger · M. Thiele (✉)

Department of Gastroenterology and Hepatology, Odense University Hospital, Odense, Denmark

Institute for Clinical Research, University of Southern Denmark, Odense, Denmark

e-mail: [Charlotte.Wilhelmina.Wernberg@rsyd.dk](mailto:Charlotte.Wilhelmina.Wernberg@rsyd.dk); [mie.balle.hugger@rsyd.dk](mailto:mie.balle.hugger@rsyd.dk); [majath@dadlnet.dk](mailto:majath@dadlnet.dk)

## Ultrasonography, Serum Markers, Computed Tomography, and Magnetic Resonance Imaging as Noninvasive Markers of Steatosis

The gold standard for evaluation of fatty liver is still liver biopsy despite the method's imperfections [2, 4]. Liver biopsy is subject to sampling error, and to intra- and inter-observer variation [5]. A biopsy is further an invasive procedure, time consuming, and only available in specialist centers. Ultrasound (US) has been, and is still, the most common tool to diagnose liver steatosis, due to its wide availability and low cost. However, US has low sensitivity for mild steatosis, since bright liver echo pattern (BLEP) with or without attenuation of the US beam can only adequately detect a hepatic lipid content above 20% [6, 7]. Bright liver echo pattern is a diffuse increase in liver echogenicity, when compared to the right renal cortex, while US beam attenuation is blurring of the deep liver vein margins and loss of definition of the diaphragm. A meta-analysis on 49 studies showed an AUROC of 0.93 of BLEP with or without attenuation for the diagnosis of moderate-severe steatosis [8]. In addition to the low sensitivity, BLEP's main limitations are observer variability and false positives due to a hyperechoic liver parenchyma in liver disease patients with fibrosis or inflammation [9]. Additionally, US quality is vastly impaired by large skin-capsule distance in obese patients. Novel post-processing computerized analyses of US images such as the hepatorenal sonographic index [10] have shown excellent accuracy for diagnosing  $\geq S1$  steatosis with an AUROC of 0.99, 100% sensitivity, and 91% specificity. Other studies have verified these results [11, 12].

Several serum-based biomarkers for steatosis have been developed and validated against ultrasound, MRS, or liver biopsy (Table 38.1) [13, 14]. However, the serum markers for steatosis are not routinely used, probably because of wide access to ultrasound imaging that have similar or better accuracy which work as point-of-care and therefore outplay the serum markers.

Computed tomography (CT) has the advantage that the whole liver is evaluated but it uses ionizing radiation and its sensitivity is low when steatosis is  $<30\%$  [15]. Therefore, CT is not routinely used for steatosis assessment, but steatosis may be described as an incidental finding after CT for other indications.

In contrast, magnetic resonance imaging (MRI) based techniques quantify liver fat with excellent sensitivity, especially MR spectroscopy (MRS) and MRI with proton-density-fat-fraction (PDFF) [16–18]. MRI-PDFF and MRS accurately differentiate moderate/severe steatosis ( $\geq S2$ ) from mild/no hepatic steatosis with similar accuracy between techniques, and closely correlated to histological steatosis score [17]. Despite the superior diagnostic accuracy, the MRI modalities are currently restricted to tertiary clinics and research due to cost and demands for specialist equipment and trained personnel.

**Table 38.1** Algorithms combining clinical information with serum blood tests for diagnosing liver steatosis

Scores	Score components							
	Sex	BMI	DM	ALT	AST/ ALT ratio	GGT	TG	Other
Fatty liver index (FLI)		x				x	x	Waist circumference
Hepatic steatosis index (HSI)		x	x		x			
Index of NASH (ION)	x			x			x	Waist-to-hip ratio, HOMA
Lipid accumulation product (LAP)	x						x	Waist circumference
NAFLD-liver fat score (NAFLD-LFS)			x		x			MetS and insulin
SteatoTest™	x	x		x		x	x	Age, A2M, ApoA1, haptoglobin, bilirubin, cholesterol, glucose

™=patented, all other scores are non-patented

A2M a2-macroglobulin, ALT alanine transaminase, AST aspartate transaminase, ApoA1 apolipoprotein A-1, BMI body mass index, DM diabetes mellitus, GGT gamma-glutamyl transferase, MetS metabolic syndrome, TG triglycerides

## Controlled Attenuation Parameter Is a Novel Ultrasound Technique for Diagnosing Steatosis in Liver Disease Patients

Transient elastography with the FibroScan device has revolutionized our ability to diagnose liver fibrosis in patients with chronic liver disease of various etiologies [19]. Controlled attenuation parameter was added to the FibroScan software in 2010 [20]. With CAP, it is possible to obtain a measure of liver parenchyma attenuation (in dB/m) in parallel with the liver stiffness measurement. An additional advantage is CAP’s continuous nature, which increases resolution more than the ultrasound steatosis staging from 0 to 3.

Initially, CAP measurements relied on the FibroScan M-probe, which was a disadvantage due to the high failure rate in patients with central obesity or BMI >30 kg/m<sup>2</sup>. In a prospective study with 5323 CAP examinations using the M-probe, 7.7% of measurements failed [21]. Fortunately, CAP for the XL-probe was made available from 2015, which substantially reduced the failure rate [22]. In a 2018 study utilizing both the M- and XL-probes, failure rate was down to 3.2% in 992 NAFLD patients [23]. Whether probe type should be considered, when interpreting CAP values, is however still debated: In a study with 992 NAFLD patients, Vuppalanchi

et al. [23] found that CAP values obtained in the same patient with the XL-probe were on average 16 dB/m higher compared with the M-probe, adjusted for BMI and histological steatosis severity [23]. However, in a recent study by Eddowes and colleagues of similar size, probe type was not a predictor of either false positives or false negatives [24].

Eight studies from 2010 to 2016 investigated the overall performance of CAP to diagnose liver steatosis, using liver biopsy as gold standard [20, 25–31]. In these studies, CAP had sensitivities ranging from 64 to 91% for detecting any steatosis ( $\geq S1$ ) and specificities ranging from 64 to 94%. Similarly, studies reported a broad range of optimal cutoff values for any steatosis, from 214 to 289 dB/m. Cutoffs for  $\geq S2$  and  $\geq S3$  also varied. The between-study heterogeneity indicates substantial spectrum bias, probably due to patient selection. Consequently, an individual-patient data meta-analysis including data from 2735 patients from 19 studies with different etiologies tried to establish common CAP cutoff values for the M-probe (they excluded studies where subjects had BMI above 30 kg/m<sup>2</sup> or a skin to liver capsule distance above 2.5 cm) [32]. The steatosis distribution was 51%/27%/16%/6% for S0/S1/S2/S3. Optimal cutoff for diagnosing any steatosis ( $\geq S1$ ) was 248 dB/m (AUROC 0.82, sensitivity 69%), moderate steatosis ( $\geq S2$ ) was 268 dB/m (AUROC 0.87, sensitivity 77%) and severe steatosis ( $=S3$ ) was 280 dB/m (AUROC 0.88, sensitivity 88%).

## CAP in Non-alcoholic Fatty Liver Disease

Controlled attenuation parameter in patients suspected of NAFLD is of particular interest, as a noninvasive tool which affordably can identify and monitor people at risk for NAFLD.

Fifteen studies to date have examined the performance of CAP for diagnosing steatosis (Table 38.2).

From the evidence so far, CAP does not seem to reliably diagnose severe steatosis ( $\geq S3$ ), as AUROCs are consistently below 0.80. However, on average CAP has good accuracy for diagnosing any steatosis ( $\geq S1$ ), with AUROCs in the large studies above 0.85, except in the American multicenter study by Siddiqui and colleagues [33]. However, cutoffs vary highly, which limits generalizability of results. Additionally, sensitivities and specificities for the optimal cutoffs are well below 90% for  $\geq S1$  across studies. This means that from the existing evidence, it is not possible to derive universal cutoffs that can reliably rule-out any steatosis (cutoff with sensitivity above 90% would result in 10% false positive classifications) or rule-in any steatosis (specificity above 90% would result in 10% false negatives).

The vast majority of existing studies on NAFLD have analyzed CAP in secondary and tertiary settings with a high prevalence of steatosis. It is therefore not yet clear how CAP performs in primary care settings where the prevalence of steatosis is much lower.

**Table 38.2** Studies evaluating CAP performance with liver biopsy as reference in people with NAFLD

Authors	Year	NAFLD patients	Distribution of steatosis (%)	Probe	Mean ± SD or median (IQR) CAP (dB/m)	Optimal cutoff value (dB/m)	AUROC (95% CI)	Se (%)	Sp (%)
Friedrich-Rust [51]	2012	46	S0 = 1 (2)	M	S1 = 241 ± 71	≥S2 = 245	0.78 (0.58–0.99)	97	67
			S1 = 11 (24)						
			S2 = 13 (28)						
Kumar [52]	2013	63	S3 = 21 (46)	-	S3 = 314 ± 39	≥S3 = 301	0.72 (0.57–0.86)	76	68
			S0 = 0 (0)						
			S1 = 26 (41)						
Chan [53]	2014	101	S2 = 30 (48)	M	S1 = 213 (100–324)	≥S2 = 258	0.79	78	73
			S3 = 7 (11)						
			S0 = 3 (3)						
Karlus [54]	2014	46	S1 = 33 (33)	M	S2 = 248 (117–359)	≥S1 = 263	0.97	92	94
			S2 = 51 (51)						
			S3 = 14 (14)						
Karlus [54]	2014	46	S0 = 0 (0)	M	S3 = 291 (266–373)	≥S2 = 263	0.86	97	68
			S1 = 18 (36)						
			S2 = 20 (40)						
Karlus [54]	2014	46	S3 = 12 (24)	M	S1 = 253 ± 43	≥S3 = 281	0.75	100	53
			S0 = 0 (0)						
			S2 = 20 (40)						
Karlus [54]	2014	46	S1 = 18 (36)	M	S2 = 321 ± 42	≥S1 = 233	0.93 (0.86–1.00)	93	87
			S2 = 20 (40)						
			S3 = 12 (24)						
Karlus [54]	2014	46	S0 = 0 (0)	M	S3 = 335 ± 43	≥S2 = 268	0.94 (0.88–0.99)	97	81
			S1 = 18 (36)						
			S2 = 20 (40)						
Karlus [54]	2014	46	S2 = 20 (40)	M	S3 = 335 ± 43	≥S3 = 301	0.82 (0.70–0.93)	82	76
			S3 = 12 (24)						
			S0 = 0 (0)						

(continued)

Table 38.2 (continued)

Authors	Year	NAFLD patients	Distribution of steatosis (%)	Probe	Mean $\pm$ SD or median (IQR) CAP (dB/m)	Optimal cutoff value (dB/m)	AUROC (95% CI)	Se (%)	Sp (%)
Imajo [30]	2016	127	S0 = 0 (0)	M					
		+10C	S1 = 59 (42)		S1 = 263	$\geq$ S1 = 236	0.88 (0.80–0.95)	82	91
			S2 = 59 (42)		S2 = 290	$\geq$ S2 = 270	0.73 (0.64–0.81)	78	80
			S3 = 24 (17)		S3 = 305	$\geq$ S3 = 302	0.70 (0.58–0.83)	64	74
de Ledinghen [55]	2016	261	S0 = 0 (0)	M					
			S1 = 78 (30)		S1 = 264 $\pm$ 45				
			S2 = 100 (38)		S2 = 298 $\pm$ 48	$\geq$ S2 = 310	0.80 (0.73–0.86)	79	71
			S3 = 83 (32)		S3 = 331 $\pm$ 37	$\geq$ S3 = 311	0.66 (0.59–0.72)	87	47
Lee [56]	2016	183	S0 = 9 (5)	–					
			S1 = 76 (42)		S1 = 265 (173–377)	$\geq$ S1 = 247	0.95 (0.93–0.98)	88	100
			S2 = 65 (36)		S2 = 313 (192–350)	$\geq$ S2 = 280	0.85 (0.80–0.91)	85	80
			S3 = 33 (18)		S3 = 322 (230–400)	$\geq$ S3 = 300	0.73 (0.65–0.81)	73	61



Chan [57]

2017	57		S0 = 1 (2)	M	S1 = 324 (268–350)	≥S1 = 266	0.94 (0.86–0.98)	91	87
		+22C	S1 = 13 (23)		S2 = 321 (299–341)	≥S2 = 266	0.80 (0.69–0.88)	91	87
			S2 = 28 (49)		S3 = 330 (299–344)	≥S3 = 267	0.69 (0.57–0.79)	100	41
			S3 = 15 (26)	XL	S1 = 339 (302–368)	≥S1 = 271	0.97 (0.90–0.99)	95	91
					S2 = 345 (298–389)	≥S2 = 271	0.81 (0.71–0.89)	95	61
					S3 = 345 (305–368)	≥S3 = 304	0.67 (0.56–0.77)	80	55
2017	78		S0 = 9 (9)	M, XL					
			S1 = 49 (48)			≥S1 = 261	0.85 (0.75–0.96)	72	86
			S2 = 29 (28)			≥S2 = 305	0.70 (0.58–0.82)	63	69
			S3 = 16 (16)			≥S3 = 312	0.73 (0.58–0.89)	64	70

(continued)

Park [35]

Table 38.2 (continued)

Authors	Year	NAFLD patients	Distribution of steatosis (%)	Probe	Mean $\pm$ SD or median (IQR) CAP (dB/m)	Optimal cutoff value (dB/m)	AUROC (95% CI)	Se (%)	Sp (%)
Naveau [58]	2017	123	S0 = 23 (19)	XL					
			S1 = 29 (24)		S1 = 323 $\pm$ 10	$\geq$ S1 = 298	0.84 (0.71–0.91)	78	83
			S2 = 25 (20)		S2 = 358 $\pm$ 8	$\geq$ S2 = 303	0.83 (0.74–0.90)	90	69
			S3 = 46 (37)		S3 = 358 $\pm$ 8	$\geq$ S3 = 326	0.84 (0.75–0.90)	83	71
Siddiqui [33]	2018	358	S0 = 19 (5)	M, XL					
			S1 = 150 (38)		S1 = 306 (270–338)	$\geq$ S1 = 285	0.76 (0.64–0.89)	80	77
			S2 = 119 (30)		S2 = 340 (312–369)	$\geq$ S2 = 311	0.70 (0.64–0.75)	77	57
			S3 = 105 (27)		S3 = 340 (311–360)	$\geq$ S3 = 306	0.58 (0.51–0.64)	80	40
Garg [59]	2018	76	S0 = 6 (8)	XL					
			S1 = 47 (62)		S1 = 320 (296–345)	$\geq$ S1 = 323	0.75 (0.61–0.89)	59	83
			S2 = 19 (25)		S2 = 354 (328–366)	$\geq$ S2 = 336	0.74 (0.62–0.86)	74	76
			S3 = 4 (5)		S3 = 362 (361–369)	$\geq$ S3 = 357	0.82 (0.73–0.91)	100	78

Runge [36]	2018	55	S0 = 5 (9) S1 = 24 (44)	M		≥S1 = 260	0.77 (0.64–0.88)	90	60
			S2 = 17 (31)			≥S2 = 296	0.78 (0.65–0.88)	92	55
			S3 = 9 (16)			≥S3 = 334	0.79 (0.65–0.88)	79	76
Darweesh [60]	2019	60	S0 = 0 (0) S1 = 22 (37) S2 = 25 (42) S3 = 13 (22)	–	S1 = 262 (245–299) S2 = 323 (278–345) S3 = 378 (366–400)	≥S2 = 297 ≥S3 = 366	0.77 (1.01–1.03) 0.92 (1.01–1.08)	81 73	85 96
	2019	380	S0 = 47 (12) S1 = 89 (23) S2 = 107 (28) S3 = 137 (36)	M, XL		≥S1 = 302 ≥S2 = 331 ≥S3 = 337	0.87 (0.82–0.92) 0.77 (0.71–0.82) 0.70 (0.64–0.75)	80 70 72	83 76 63

AUROC area under the receiver operating curve, C controls without NAFLD without liver biopsy, CAP controlled attenuation parameter, NAFLD non-alcoholic fatty liver disease, Se sensitivity, Sp specificity, 95% CI 95% confidence interval, IQR interquartile range, S1, S2, S3 fat accumulation in 5%–33%, >33%–66%, >66% of hepatocytes

Two studies have suggested quality criteria for the measurement of CAP [18, 34]. A study from Wong and colleagues recommended using an IQR of CAP below 40 dB/m together with 10 valid measurements [34]. Another study from Caussy et al. with 119 MRI-PDFF-proven NAFLD patients recommended using IQR below 30 dB/m and 10 valid measurements [18]. However, both these studies do not take into account an increase in IQR when median CAP increases. Consequently, the quality criteria that use low IQR will be biased towards patients with lower CAP values. Therefore, common quality criteria that can be applied to the full range of CAP measurement from 100 to 400 dB/m are still needed. Three studies have directly compared CAP with MRI-PDFF (Table 38.3). They all show that CAP is significantly inferior to MRI-PDFF in differentiating all steatosis grades [30, 35, 36].

**Table 38.3** Studies comparing diagnostic accuracy of CAP versus MRI-PDFF in NAFLD, with liver biopsy as reference

Author	Year	Steatosis level	CAP				MRI-PDFF			
			Cutoff (dB/m)	AUROC (95% CI)	Se (%)	Sp (%)	Cutoff (%)	AUROC (95% CI)	Se (%)	Sp (%)
Imajo [30]	2016	≥S1	236	0.88 (0.80–0.95)	82	91	5.2	0.98 (0.96–1.00)	90	93
		≥S2	270	0.73 (0.64–0.81)	78	80	11.3	0.90 (0.81–0.98)	79	84
		≥S3	302	0.70 (0.58–0.83)	64	74	17.1	0.79 (0.64–0.95)	74	81
Park [35]	2017	≥S1	261	0.85 (0.75–0.96)	72	86	3.7	0.99 (0.98–1.00)	96	100
		≥S2	305	0.70 (0.58–0.82)	63	69	13.1	0.90 (0.82–0.97)	80	83
		≥S3	312	0.73 (0.58–0.89)	64	70	16.4	0.92 (0.84–0.99)	82	84
Runge [36]	2018	≥S1	260	0.77 (0.64–0.88)	90	60	4.1	0.99 (0.91–1.00)	94	100
		≥S2	296	0.78 (0.65–0.88)	92	55	15.7	0.98 (0.89–0.99)	92	97
		≥S3	334	0.79 (0.65–0.88)	79	76	20.9	0.96 (0.86–0.99)	100	83

AUROC area under the receiver operating curve, CAP controlled attenuation parameter, MRI-PDFF magnetic resonance imaging proton-density-fat-fraction, NAFLD non-alcoholic fatty liver disease, Se sensitivity, Sp specificity, 95% CI 95% confidence interval, S1, S2, S3 fat accumulation in 5%–33%, >33%–66%, >66% of hepatocytes

## CAP in Chronic Viral Hepatitis

Steatosis is a common histological finding in patients with chronic HCV infection. To some extent also in HBV, but liver fat accumulation linked to metabolic comorbidity, alcohol overuse or the viral infection itself seems to play a role in HCV in particular [37]. The prevalence of steatosis is 1.5–3 times higher in HCV patients than in the general population, at 40–86% vs. 25–30% [38, 39]. The presence of steatosis is not only associated with a lower response rate to anti-viral treatment [40], but may also increase fibrosis progression [41, 42] and risk of HCC development [43].

In contrast to HCV, liver steatosis in HBV seems to be comparable to the general population, at approximately 30% [44]. The same meta-analysis found an association between hepatic steatosis in HBV and metabolic comorbidity (obesity, BMI, diabetes), but not viral load.

Seven studies have investigated the use of CAP in chronic viral hepatitis using liver biopsy as diagnostic gold standard (Table 38.4).

**Table 38.4** Studies evaluating CAP performance with liver biopsy as reference in people with either HBV or HCV

Authors	Year	Patients	Etiology	Probe	Steatosis prevalence (%)	Optimal cutoff value (dB/m)	AUROC	Se (%)	Sp (%)	
Sasso [61]	2012	615	HCV	M	S0 = 55					
					S1 = 31	≥S1 = 222	0.80	76	71	
					S2 = 13	≥S2 = 233	0.86	87	74	
					S3 = 1	≥S3 = 290	0.88	78	93	
Wang [62]	2014	88	HBV	M	S0 = 9					
					S1 = 54	≥S1 = 219	0.71	70	72	
					S2 = 28	≥S2 = 230	0.87	83	78	
					S3 = 9	≥S3 = 283	0.97	100	97	
Ferraioli [63]	2014	115	HBV/ HCV	M	S0 = 29					
					4	S1 = 53	≥S1 = 219	0.76	91	52
						S2 = 14	≥S2 = 296	0.82	60	91
						S3 = 4				
Cardoso [64]	2015	136	HBV	M	S0 = 63					
						S1 = 22		0.82		
						S2 = 12		0.82		
						S3 = 3		0.97		
Mi [65]	2015	340	HBV	M	S0 = 58					
						S1 = 34	≥S1 = 224	0.81	73	76
						S2 = 5	≥S2 = 236	0.90	92	70
						S3 = 2.6	≥S3 = 285	0.97	100	93

(continued)

**Table 38.4** (continued)

Authors	Year	Patients	Etiology	Probe	Steatosis prevalence (%)	Optimal cutoff value (dB/m)	AUROC	Se (%)	Sp (%)
Chen [66]	2016	189	HBV	M	S = 49				
					S1 = 32	≥S1 = 222	0.90	89	85
					S2 = 12	≥S2 = 247	0.92	91	93
					S3 = 7	≥S3 = 274	0.94	100	86
Xu [67]	2016	366	HBV	M	S0 = 56				
					S1 = 40	≥S1 = 224	0.78	69	76
					S2 = 2.2	≥S2 = 246	0.93	100	78
					S3 = 1.4	≥S3 = 284	0.99	100	96

Overall, the prevalence of severe steatosis is much lower in HCV and HBV patients compared to NAFLD patients; only in two studies does S3 prevalence exceed 5%. It may be due to these differences that the optimal cutoff values in general are lower than for NAFLD, while the AUROCs are generally higher, particularly moderate (≥S2) and severe (≥S3) steatosis. We speculate that other factors influencing CAP in fatty liver diseases may also diminish the diagnostic accuracy of CAP in NAFLD, compared to chronic viral hepatitis.

### CAP in Alcohol-Related Liver Disease

Simple steatosis is seen in almost all patients who drink excess amounts of alcohol for a sustained period. However, the role of hepatic fat accumulation in ALD is not clear. Many consider alcohol-related fatty liver as relatively benign. However, 7% of patients with biopsy-proven simple steatosis may progress to cirrhosis [45].

The role of CAP for diagnosing and monitoring liver fat in ALD has been scarcely investigated. Only one single-etiology study has assessed the diagnostic accuracy of CAP and CAP changes as an effect of abstinence [46]. In this study, 269 patients received a liver biopsy (steatosis scores S0, S1, S2, S3 = 28%, 35%, 24%, 13%) to address diagnostic accuracy, while 293 patients had dual CAP measurements at the beginning and end of hospital admission for alcohol use, to test the effect of detoxification. CAP diagnostic accuracies were comparable to NAFLD: AUROC ≥S1 = 0.77, ≥S2 = 0.78, and S3 = 0.82. CAP was superior to BLEP by ultrasound, while MRI was not performed. CAP above 290 dB/m ruled-in any steatosis with 88% specificity and 92% positive predictive value. In the 293 patients who were admitted 6 days (IQR 4–6) for detoxification, CAP decreased significantly, except in obese patients with a BMI above 30 kg/m<sup>2</sup>. Similarly, the study found that CAP was significantly lower in patients who had abstained from alcohol more than 4 weeks from inclusion, in comparison to ongoing drinkers (253 ± 56 dB/m vs. 284 ± 59 dB/m). The latter is in agreement with another study where low CAP correlated negatively with alcohol use [47].

## CAP as a Prognostic Marker

Patients with compensated advanced chronic liver disease and concomitant obesity and steatosis may be at higher risk for progressing to decompensation than normal-weight patients [48]. Therefore, CAP may be a predictive marker of the development of decompensation in patients with compensated advanced chronic liver disease. However, results of two retrospective studies are conflicting. One Swiss study investigated 193 patients for median 18 months (viral etiology = 58%; transient elastography = 15.1 kPa; CAP =  $255 \pm 62$  dB/m; CAP above 220 dB/m sensitivity). They showed a potentially harmful effect of higher CAP, independent of BMI. CAP was  $275 \pm 46$  dB/m in the 18 patients who experienced an event, versus  $252 \pm 63$  dB/m ( $P = 0.07$ ) in the 175 patients who did not progress. Body mass index was similar in the two groups. All events were more frequent in patients with CAP  $\geq 220$  dB/m (12.9% vs. 1.6%;  $P = 0.013$ ). However, these findings could not be validated in a later study, from Austria, involving 430 patients with compensated ( $n = 292$ ) or decompensated ( $n = 138$ ) advanced chronic liver disease [49]. CAP neither predicted of first decompensation (hazard ratio = 0.97; 95% CI 0.91–1.03), nor further hepatic decompensation (hazard ratio = 0.99; 0.94–1.03). Using a CAP cutoff of 248 dB/m for hepatic steatosis, the event rate was similar in patients with hepatic steatosis or without. Consequently, longitudinal data and prospective studies in patients with advanced liver disease are still highly needed to evaluate whether CAP can be used as prognostic marker for liver-related outcomes.

In pre-cirrhotic patients, one large Asian study suggests that CAP holds no prognostic value for predicting short-term liver-related events, hepatocellular carcinoma, non-HCC malignancy, or cardiovascular events. The study followed 4282 patients (median age 57 years; median liver stiffness 6.1 kPa; 41% NAFLD; CAP median 250 dB/m) [50]. During 8540 patient-years of follow-up, there were however few liver-related events: 34 patients developed HCC and 33 decompensations.

The foremost question for the coming years is whether CAP can be used as a surrogate marker for steatosis regression in phase II and III antifibrotic trials, and whether steatosis regression or progression represents any clinical value for patients.

## References

1. Vuppalanchi R, Chalasani N. Nonalcoholic fatty liver disease and nonalcoholic steatohepatitis: selected practical issues in their evaluation and management. *Hepatology*. 2009;49(1):306–17.
2. Chalasani N, Younossi Z, Lavine JE, Charlton M, Cusi K, Rinella M, et al. The diagnosis and management of nonalcoholic fatty liver disease: practice guidance from the American Association for the Study of Liver Diseases. *Hepatology*. 2018;67(1):328–57.
3. Gluchowski NL, Becuwe M, Walther TC, Farese RV Jr. Lipid droplets and liver disease: from basic biology to clinical implications. *Nat Rev Gastroenterol Hepatol*. 2017;14(6):343–55.
4. Bedossa P, Patel K. Biopsy and noninvasive methods to assess progression of nonalcoholic fatty liver disease. *Gastroenterology*. 2016;150(8):1811–22.e4.
5. Ratziu V, Charlotte F, Heurtier A, Gombert S, Giral P, Bruckert E, et al. Sampling variability of liver biopsy in nonalcoholic fatty liver disease. *Gastroenterology*. 2005;128(7):1898–906.

6. Dasarathy S, Dasarathy J, Khiyami A, Joseph R, Lopez R, McCullough AJ. Validity of real time ultrasound in the diagnosis of hepatic steatosis: a prospective study. *J Hepatol.* 2009;51(6):1061–7.
7. Taylor KJ, Riely CA, Hammers L, Flax S, Weltin G, Garcia-Tsao G, et al. Quantitative US attenuation in normal liver and in patients with diffuse liver disease: importance of fat. *Radiology.* 1986;160(1):65–71.
8. Hernaez R, Lazo M, Bonekamp S, Kamel I, Brancati FL, Guallar E, et al. Diagnostic accuracy and reliability of ultrasonography for the detection of fatty liver: a meta-analysis. *Hepatology.* 2011;54(3):1082–90.
9. Perez NE, Siddiqui FA, Mutchnick MG, Dhar R, Tobi M, Ullah N, et al. Ultrasound diagnosis of fatty liver in patients with chronic liver disease: a retrospective observational study. *J Clin Gastroenterol.* 2007;41(6):624–9.
10. Webb M, Yeshua H, Zelber-Sagi S, Santo E, Brazowski E, Halpern Z, et al. Diagnostic value of a computerized hepatorenal index for sonographic quantification of liver steatosis. *AJR Am J Roentgenol.* 2009;192(4):909–14.
11. Chauhan A, Sultan LR, Furth EE, Jones LP, Khungar V, Sehgal CM. Diagnostic accuracy of hepatorenal index in the detection and grading of hepatic steatosis. *J Clin Ultrasound.* 2016;44(9):580–6.
12. Marshall RH, Eissa M, Bluth EI, Gulotta PM, Davis NK. Hepatorenal index as an accurate, simple, and effective tool in screening for steatosis. *Am J Roentgenol.* 2012;199(5):997–1002.
13. Stern C, Castera L. Non-invasive diagnosis of hepatic steatosis. *Hepatol Int.* 2017;11(1):70–8.
14. Castera L, Friedrich-Rust M, Loomba R. Noninvasive assessment of liver disease in patients with nonalcoholic fatty liver disease. *Gastroenterology.* 2019;156(5):1264–81 e4.
15. Castera L, Vilgrain V, Angulo P. Noninvasive evaluation of NAFLD. *Nat Rev Gastroenterol Hepatol.* 2013;10(11):666–75.
16. Ozturk A, Grajo JR, Gee MS, Benjamin A, Zubajlo RE, Thomenius KE, et al. Quantitative hepatic fat quantification in non-alcoholic fatty liver disease using ultrasound-based techniques: a review of literature and their diagnostic performance. *Ultrasound Med Biol.* 2018;44(12):2461–75.
17. Idilman IS, Keskin O, Celik A, Savas B, Halil Elhan A, Idilman R, et al. A comparison of liver fat content as determined by magnetic resonance imaging-proton density fat fraction and MRS versus liver histology in non-alcoholic fatty liver disease. *Acta Radiol.* 2015;57(3):271–8.
18. Caussy C, Alquraish MH, Nguyen P, Hernandez C, Cepin S, Fortney LE, et al. Optimal threshold of controlled attenuation parameter with MRI-PDFF as the gold standard for the detection of hepatic steatosis. *Hepatology.* 2018;67(4):1348–59.
19. Dietrich CF, Bamber J, Berzigotti A, Bota S, Cantisani V, Castera L, et al. EFSUMB guidelines and recommendations on the clinical use of liver ultrasound elastography, update 2017 (Long Version). *Ultraschall Med.* 2017;38(4):e16–47.
20. Sasso M, Beaugrand M, de Ledingham V, Douvin C, Marcellin P, Poupon R, et al. Controlled attenuation parameter (CAP): a Novel VCTE™ guided ultrasonic attenuation measurement for the evaluation of hepatic steatosis: preliminary study and validation in a cohort of patients with chronic liver disease from various causes. *Ultrasound Med Biol.* 2010;36(11):1825–35.
21. de Ledingham V, Vergniol J, Capdepon M, Chermak F, Hiriart JB, Cassinotto C, et al. Controlled attenuation parameter (CAP) for the diagnosis of steatosis: a prospective study of 5323 examinations. *J Hepatol.* 2014;60(5):1026–31.
22. Sasso M, Audiere S, Kengang A, Gaouar F, Corpechot C, Chazouilleres O, et al. Liver steatosis assessed by controlled attenuation parameter (CAP) measured with the XL probe of the FibroScan: a pilot study assessing diagnostic accuracy. *Ultrasound Med Biol.* 2016;42(1):92–103.
23. Vuppalanchi R, Siddiqui MS, Van Natta ML, Hallinan E, Brandman D, Kowdley K, et al. Performance characteristics of vibration-controlled transient elastography for evaluation of nonalcoholic fatty liver disease. *Hepatology.* 2018;67(1):134–44.
24. Eddowes PJ, Sasso M, Allison M, Tsochatzis E, Anstee QM, Sheridan D, et al. Accuracy of FibroScan controlled attenuation parameter and liver stiffness measurement in assess-



- ing steatosis and fibrosis in patients with nonalcoholic fatty liver disease. *Gastroenterology*. 2019;156(6):1717–30.
25. de Ledinghen V, Vergniol J, Foucher J, Merrouche W, le Bail B. Non-invasive diagnosis of liver steatosis using controlled attenuation parameter (CAP) and transient elastography. *Liver Int*. 2012;32(6):911–8.
  26. Shen F, Zheng RD, Mi YQ, Wang XY, Pan Q, Chen GY, et al. Controlled attenuation parameter for non-invasive assessment of hepatic steatosis in Chinese patients. *World J Gastroenterol*. 2014;20(16):4702–11.
  27. Kumar M, Rastogi A, Singh T, Behari C, Gupta E, Garg H, et al. Controlled attenuation parameter for non-invasive assessment of hepatic steatosis: does etiology affect performance? *J Gastroenterol Hepatol*. 2013;28(7):1194–201.
  28. Myers RP, Pollett A, Kirsch R, Pomier-Layrargues G, Beaton M, Levstik M, et al. Controlled attenuation parameter (CAP): a noninvasive method for the detection of hepatic steatosis based on transient elastography. *Liver Int*. 2012;32(6):902–10.
  29. Chan WK, Nik Mustapha NR, Mahadeva S. Controlled attenuation parameter for the detection and quantification of hepatic steatosis in nonalcoholic fatty liver disease. *J Gastroenterol Hepatol*. 2014;29(7):1470–6.
  30. Imajo K, Kessoku T, Honda Y, Tomeno W, Ogawa Y, Mawatari H, et al. Magnetic resonance imaging more accurately classifies steatosis and fibrosis in patients with nonalcoholic fatty liver disease than transient elastography. *Gastroenterology*. 2016;150(3):626–37.e7.
  31. Lupsor-Platon M, Feier D, Stefanescu H, Tamas A, Botan E, Sparchez Z, et al. Diagnostic accuracy of controlled attenuation parameter measured by transient elastography for the non-invasive assessment of liver steatosis: a prospective study. *J Gastrointestin Liver Dis*. 2015;24(1):35–42.
  32. Karlas T, Petroff D, Sasso M, Fan JG, Mi YQ, de Ledinghen V, et al. Individual patient data meta-analysis of controlled attenuation parameter (CAP) technology for assessing steatosis. *J Hepatol*. 2017;66(5):1022–30.
  33. Siddiqui MS, Yamada G, Vuppalanchi R, Van Natta M, Loomba R, Guy C, et al. Diagnostic accuracy of noninvasive fibrosis models to detect change in fibrosis stage. *Clin Gastroenterol Hepatol*. 2019;17(9):1877–85.e5.
  34. Wong VW, Petta S, Hiriart JB, Camma C, Wong GL, Marra F, et al. Validity criteria for the diagnosis of fatty liver by M probe-based controlled attenuation parameter. *J Hepatol*. 2017;67(3):577–84.
  35. Park CC, Nguyen P, Hernandez C, Bettencourt R, Ramirez K, Fortney L, et al. Magnetic resonance elastography vs transient elastography in detection of fibrosis and noninvasive measurement of steatosis in patients with biopsy-proven nonalcoholic fatty liver disease. *Gastroenterology*. 2017;152(3):598–607.e2.
  36. Runge JH, Smits LP, Verheij J, Depla A, Kuiken SD, Baak BC, et al. MR spectroscopy-derived proton density fat fraction is superior to controlled attenuation parameter for detecting and grading hepatic steatosis. *Radiology*. 2018;286(2):547–56.
  37. Asselah T, Rubbia-Brandt L, Marcellin P, Negro F. Steatosis in chronic hepatitis C: why does it really matter? *Gut*. 2006;55(1):123–30.
  38. Leandro G, Mangia A, Hui J, Fabris P, Rubbia-Brandt L, Colloredo G, et al. Relationship between steatosis, inflammation, and fibrosis in chronic hepatitis C: a meta-analysis of individual patient data. *Gastroenterology*. 2006;130(6):1636–42.
  39. Younossi ZM, Koenig AB, Abdelatif D, Fazel Y, Henry L, Wymer M. Global epidemiology of nonalcoholic fatty liver disease-Meta-analytic assessment of prevalence, incidence, and outcomes. *Hepatology*. 2016;64(1):73–84.
  40. Harrison SA, Brunt EM, Qazi RA, Oliver DA, Neuschwander-Tetri BA, Di Bisceglie AM, et al. Effect of significant histologic steatosis or steatohepatitis on response to antiviral therapy in patients with chronic hepatitis C. *Clin Gastroenterol Hepatol*. 2005;3(6):604–9.
  41. Fartoux L, Chazouilleres O, Wendum D, Poupon R, Serfaty L. Impact of steatosis on progression of fibrosis in patients with mild hepatitis C. *Hepatology*. 2005;41(1):82–7.

42. Castera L, Hezode C, Roudot-Thoraval F, Bastie A, Zafrani ES, Pawlotsky JM, et al. Worsening of steatosis is an independent factor of fibrosis progression in untreated patients with chronic hepatitis C and paired liver biopsies. *Gut*. 2003;52(2):288–92.
43. Kurosaki M, Hosokawa T, Matsunaga K, Hirayama I, Tanaka T, Sato M, et al. Hepatic steatosis in chronic hepatitis C is a significant risk factor for developing hepatocellular carcinoma independent of age, sex, obesity, fibrosis stage and response to interferon therapy. *Hepatol Res*. 2010;40(9):870–7.
44. Machado MV, Oliveira AG, Cortez-Pinto H. Hepatic steatosis in hepatitis B virus infected patients: meta-analysis of risk factors and comparison with hepatitis C infected patients. *J Gastroenterol Hepatol*. 2011;26(9):1361–7.
45. Deleuran T, Grønbaek H, Vilstrup H, Jepsen P. Cirrhosis and mortality risks of biopsy-verified alcoholic pure steatosis and steatohepatitis: a nationwide registry-based study. *Aliment Pharmacol Ther*. 2012;35(11):1336–42.
46. Thiele M, Rausch V, Fluhr G, Kjærsgaard M, Piecha F, Mueller J, et al. Controlled attenuation parameter and alcoholic hepatic steatosis: diagnostic accuracy and role of alcohol detoxification. *J Hepatol*. 2018;68(5):1025–32.
47. de Ledinghen V, Hiriart JB, Vergniol J, Merrouche W, Bedossa P, Paradis V. Controlled attenuation parameter (CAP) with the XL probe of the Fibroscan (R): a comparative study with the M probe and liver biopsy. *Dig Dis Sci*. 2017;62(9):2569–77.
48. Berzigotti A, Garcia-Tsao G, Bosch J, Grace ND, Burroughs AK, Morillas R, et al. Obesity is an independent risk factor for clinical decompensation in patients with cirrhosis. *Hepatology*. 2011;54(2):555–61.
49. Scheiner B, Steininger L, Semmler G, Unger LW, Schwabl P, Bucsiacs T, et al. Controlled attenuation parameter does not predict hepatic decompensation in patients with advanced chronic liver disease. *Liver Int*. 2019;39(1):127–35.
50. Liu K, Wong VW, Lau K, Liu SD, Tse YK, Yip TC, et al. Prognostic value of controlled attenuation parameter by transient elastography. *Am J Gastroenterol*. 2017;112(12):1812–23.
51. Friedrich-Rust M, Romen D, Vermehren J, Kriener S, Sadet D, Herrmann E, et al. Acoustic radiation force impulse-imaging and transient elastography for non-invasive assessment of liver fibrosis and steatosis in NAFLD. *Eur J Radiol*. 2012;81(3):e325–31.
52. Kumar M, Rastogi A, Singh T, Behari C, Gupta E, Garg H, et al. Controlled attenuation parameter for non-invasive assessment of hepatic steatosis: does aetiology affect performance. *J Gastroenterol Hepatol*. 2013;28(7):1194–201.
53. Chan WK, Nik Mustapha NR, Mahadeva S. Controlled attenuation parameter for the detection and quantification of hepatic steatosis in non-alcoholic fatty liver disease. *J Gastroenterol Hepatol*. 2014;29(7):1470–6.
54. Karlas T, Petroff D, Garnov N, Bohm S, Tenckhoff H, Wittekind C, et al. Non-invasive assessment of hepatic steatosis in patients with NAFLD using controlled attenuation parameter and 1H-MR spectroscopy. *PLoS One*. 2014;9(3):e91987.
55. de Ledinghen V, Wong GL, Vergniol J, Chan HL, Hiriart JB, Chan AW, et al. Controlled attenuation parameter for the diagnosis of steatosis in non-alcoholic fatty liver disease. *J Gastroenterol Hepatol*. 2016;31(4):848–55.
56. Lee HW, Park SY, Kim SU, Jang JY, Park H, Kim JK, et al. Discrimination of nonalcoholic steatohepatitis using transient elastography in patients with nonalcoholic fatty liver disease. *PLoS One*. 2016;11(6):e0157358.
57. Chan WK, Nik Mustapha NR, Wong GL, Wong VW, Mahadeva S. Controlled attenuation parameter using the FibroScan(R) XL probe for quantification of hepatic steatosis for non-alcoholic fatty liver disease in an Asian population. *United Eur Gastroenterol J*. 2017;5(1):76–85.
58. Naveau S, Voican CS, Lebrun A, Gaillard M, Lamouri K, Njike-Nakseu M, et al. Controlled attenuation parameter for diagnosing steatosis in bariatric surgery candidates with suspected nonalcoholic fatty liver disease. *Eur J Gastroenterol Hepatol*. 2017;29(9):1022–30.

59. Garg H, Aggarwal S, Shalimar YR, Datta Gupta S, Agarwal L, et al. Utility of transient elastography (fibrosan) and impact of bariatric surgery on nonalcoholic fatty liver disease (NAFLD) in morbidly obese patients. *Surg Obes Relat Dis.* 2018;14(1):81–91.
60. Darweesh SK, Omar H, Medhat E, Abd-Al Aziz RA, Ayman H, Saad Y, et al. The clinical usefulness of elastography in the evaluation of nonalcoholic fatty liver disease patients: a biopsy-controlled study. *Eur J Gastroenterol Hepatol.* 2019;31(8):1010–6.
61. Sasso M, Tengher-Barna I, Ziol M, Miette V, Fournier C, Sandrin L, et al. Novel controlled attenuation parameter for noninvasive assessment of steatosis using Fibrosan((R)): validation in chronic hepatitis C. *J Viral Hepat.* 2012;19(4):244–53.
62. Wang CY, Lu W, Hu DS, Wang GD, Cheng XJ. Diagnostic value of controlled attenuation parameter for liver steatosis in patients with chronic hepatitis B. *World J Gastroenterol.* 2014;20(30):10585–90.
63. Ferraioli G, Tinelli C, Lissandrin R, Zicchetti M, Dal Bello B, Filice G, et al. Controlled attenuation parameter for evaluating liver steatosis in chronic viral hepatitis. *World J Gastroenterol.* 2014;20(21):6626–31.
64. Cardoso AC, Beaugrand M, de Ledinghen V, Douvin C, Poupon R, Trinchet JC, et al. Diagnostic performance of controlled attenuation parameter for predicting steatosis grade in chronic hepatitis B. *Ann Hepatol.* 2015;14(6):826–36.
65. Mi YQ, Shi QY, Xu L, Shi RF, Liu YG, Li P, et al. Controlled attenuation parameter for non-invasive assessment of hepatic steatosis using Fibrosan(R): validation in chronic hepatitis B. *Dig Dis Sci.* 2015;60(1):243–51.
66. Chen J, Wu D, Wang M, Chen E, Bai L, Liu C, et al. Controlled attenuation parameter for the detection of hepatic steatosis in patients with chronic hepatitis B. *Infect Dis (Lond).* 2016;48(9):670–5.
67. Xu L, Lu W, Li P, Shen F, Mi YQ, Fan JG. A comparison of hepatic steatosis index, controlled attenuation parameter and ultrasound as noninvasive diagnostic tools for steatosis in chronic hepatitis B. *Dig Liver Dis.* 2017;49(8):910–7.

# Chapter 39

## Liver Steatosis (CAP) as Modifier of Liver Stiffness



Thomas Karlas and Sebastian Mueller

### Modulation of Liver Stiffness by Hepatic Steatosis

Hepatic steatosis is defined by the accumulation of lipid droplets within the hepatocytes. This process is often driven by metabolic factors associated with diabetes mellitus and obesity but may also occur occasionally in lean subjects with unremarkable anthropometry. Steatosis is traditionally classified according to histology: the relative number of affected hepatocytes is used to determine the grade of steatosis, whereas neither absolute nor relative lipid content of the liver is currently considered for definition of disease severity [1, 2]. Lipid droplets modify the ultrasound signal propagation in the liver:

1. The more lipid droplets within the hepatocytes the more ultrasound signal reflection. In conventional ultrasound, this mechanism causes the typical bright echo pattern in superficial parts of the liver as well as attenuation of ultrasound signals from more profound parenchyma areas. For ultrasound-based elastography, the attenuation of tracking signals may impair the measurement quality and reliability [1, 3, 4].
2. Ultrasound-based elastography methods apply complex algorithms that include assumptions of physical tissue properties. For example, a density of  $1 \text{ g/cm}^3$  is assumed for conversion formulas for shearwave speed and the elasticity modulus [5]. Such assumptions become imprecise in advanced steatosis and may thus alter the results of liver stiffness measurement [LSM].

---

T. Karlas (✉)

Division of Gastroenterology, Medical Department II, University of Leipzig Medical Center, Leipzig, Germany  
e-mail: [thomas.karlas@medizin.uni-leipzig.de](mailto:thomas.karlas@medizin.uni-leipzig.de)

S. Mueller

Department of Medicine and Center for Alcohol Research and Liver Diseases, Salem Medical Center, University of Heidelberg, Heidelberg, Germany  
e-mail: [sebastian.mueller@urz.uni-heidelberg.de](mailto:sebastian.mueller@urz.uni-heidelberg.de)

Besides these direct effects of steatosis on LS, the associated metabolic conditions influence ultrasound signal quality and propagation of mechanical impulses to the liver. Most importantly, subcutaneous fat deposits increase the skin-to-liver capsule distance at the measuring site and impair any signal propagation to the liver tissue [6]. There are also indications that fat can decrease LS [7]. For more details, see also book section II “Techniques to measure liver stiffness.” The molecular basis of the interplay between LS and steatosis is not yet completely understood. For example, in cohorts of heavy drinkers, LS was not at all or even slightly negatively associated with steatosis [8, 9].

## Impact of Steatosis on Different Methods for Assessing Liver Stiffness

The putative impact of steatosis on LS has been analyzed in several studies that provide inconsistent results. This can be partly explained by further modulators of LS such as the etiology of liver disease, heterogeneous definitions of the reference standard, and application of different methods for LSM that cannot easily be compared with each other [10, 11]. In addition, some studies fail to differentiate clearly between true effects of steatosis and associated modulations of LS by anthropometry and/or metabolic conditions. Table 39.1 gives an overview on relevant publications in the field. In addition, inflammatory activity in steatotic hepatic tissue (i.e., steatohepatitis) represents an important confounding factor for liver stiffness assessment: inflammation is positively associated with liver stiffness and may mimic steatosis-induced effects unless it is properly considered in multivariate analysis [9]. For more details, see also book section IV “Important (patho)physiological confounders of LS.”

## Ultrasound-Based Steatosis Estimation: A Guide for Liver Stiffness Interpretation?

Encouraged by the data summarized in Table 39.1, several studies aimed to defining rules for LSM interpretation taking the severity of hepatic steatosis into account. As a logical consequence of the noninvasive nature of fibrosis assessment with ultrasound-based methods, histological analyses of steatosis seem unsuitable for such an approach. In the same line, magnetic resonance methods are not convenient for clinical practice. Ultrasound-based techniques, however, potentially enable simultaneous steatosis and LSM assessment for large cohorts [12, 13].

Two ultrasound-based approaches for steatosis estimation have been developed and evaluated in the last decade:

1. Analysis of the **ultrasound signal attenuation**. The intensity of the bright liver parenchyma echo pattern correlates with the grade of liver steatosis. Several tools

**Table 39.1** Studies assessing the impact of steatosis on liver stiffness

Author[s]/ year	Method[s]	Main finding	Commentary
Boursier et al. 2013 [22]	650 patients with chronic hepatitis C Fibrosis: transient elastography, histology Steatosis: METAVIR, computerized morphometric analysis	Liver stiffness measurement [LSM] with transient elastography is associated with fibrosis, inflammatory activity, and steatosis. High-grade steatosis is associated with poor diagnostic performance of LSM	This report proves the concept of steatosis as modifier of LSM. Impact if steatosis is limited to variation within few kPa units. Higher steatosis is associated with higher variation of measurements [=poor reliability]
Macaluso et al. 2014 [23]	618 patients with chronic hepatitis C Fibrosis: transient elastography, histology Steatosis: histology [Scheuer score] and conventional ultrasound	Patients with steatosis had higher mean LSM values. Steatosis was associated with higher risk of false positive measurements	Only the M probe of the transient elastography device was used, although more than half of the cohort was overweight or obese
Petta et al. 2015 [24]	253 patients with biopsy-proven NAFLD Fibrosis: transient elastography, histology Steatosis: histology [Kleiner score] and conventional ultrasound	Presence of steatosis was associated with higher liver stiffness, especially in patients without significant fibrosis. This observation was associated with higher risk of false positive LSM	All patients of this obese cohort [BMI >25 in 80%] were examined with the M probe of transient elastography. The observed effect is likely related to anthropometric measures
Karlas et al. 2015 [25]	41 patients with morbid obesity [40 without significant fibrosis] and biopsy-proven NAFLD Fibrosis: transient elastography, point-shearwave elastography [pSWE], ELF score, histology Steatosis: MR spectroscopy, histology	Both pSWE and transient elastography [M and XL probe] had a high rate of invalid and/or unreliable measurements. The remainder results were significantly higher than reported cutoffs for advanced fibrosis	Data are not stratified according to steatosis or anthropometric parameters. Elastography results from severely obese patients demand careful interpretation

(continued)

**Table 39.1** (continued)

Author[s]/ year	Method[s]	Main finding	Commentary
Harris et al. 2016 [26]	349 patients with liver steatosis [53 with biopsy] Fibrosis: biopsy, pSWE [published cutoffs] Steatosis: biopsy and conventional ultrasound	Low stages of fibrosis were frequently overestimated by pSWE. Higher failure rate of pSWE in patients with steatosis	No anthropometric data provided Conclusion: the study “does not show conclusively if the presence of steatosis or its severity independently alters” pSWE
Conti et al. 2016 [27]	211 patients with hepatitis C and liver biopsy Fibrosis: elastography point quantification, histology [METAVIR] Steatosis: histology, ultrasound	Liver stiffness was similar in patients with and without steatosis. Obesity was associated with higher risk of misclassification	Identifies obesity as relevant factor for incorrect liver elasticity evaluation

have been suggested for a standardized assessment, e.g., computer-aided comparison of liver and renal parenchyma. A software algorithm implemented in the transient elastography device calculates the controlled attenuation parameter (CAP) [14]. CAP has shown a good accuracy for noninvasive grading of liver steatosis [15]. Recently, Attenuation Imaging (ATI) has been proposed as a CAP alternative integrated in a conventional ultrasound device [16], which merits further evaluation.

2. Analysis of the **echo pattern distribution**. The speckle pattern of the liver parenchyma is modulated by steatosis. Acoustic structure quantification (ASQ) is a software tool that compares the parenchyma structure of a patient with an ideal parenchyma model. The deviation from the ideal curve correlates with the degree of steatosis [17, 18] but can also be modulated by the presence of fibrosis [19].

To date, only CAP has been intensively investigated as a modifier of LSM, whereas the role of ATI and ASQ needs to be defined in further biopsy-controlled studies. However, most data on CAP derives from cohorts assessed with the M probe which is dedicated to lean subjects. This impairs the transition of the results to obese NAFLD patients where steatosis adjusted LSM is of special interest. Table 39.2 summarizes the available data. These studies do not provide a definitive conclusion on the role of CAP for adjustment of LSM, but higher CAP values are associated with a higher risk of imprecise fibrosis assessment using established cutoffs for LSM. Such cases should be evaluated very carefully (Fig. 39.1). In addition, Fig. 39.2 shows two cases of patients with alcoholic fatty liver in the absence of inflammation (see normal transaminase levels). During detoxification, CAP values (steatosis) clearly decreased while LS increased [20]. Such cases have been observed by both of us and warrant further confirmation.

**Table 39.2** Studies assessing the role of controlled attenuation parameter (CAP) for interpretation of liver stiffness measurement (LSM)

Author[s]/year	Method[s]	Main finding	Commentary on Fibroscan probe type
Petta et al. 2016 [28]	324 biopsy-proven NAFLD patients LSM values for each fibrosis stage were stratified according to CAP tertiles	LSM increased in patients with low fibrosis [F0-F2, Kleiner score] according to steatosis severity. In consequence, the diagnostic accuracy for detection of advanced steatosis was reduced in patients with high CAP values A decisional flowchart for combining LSM and CAP values is provided	CAP and LSM were measured with the M probe although 40% patients were obese. Hence, the reduced diagnostic accuracy of LSM in severe steatosis may be related to a true modulation of LSM but can also represent a mere correlation of altered anthropometry [high skin-to-liver capsule distance at the measuring site] with steatosis
Karlas et al. 2018 [29]	Individual patient data from 19 studies The impact of steatosis [defined by histology and/or CAP] on LSM [M probe] was analyzed in 2058 patients	LSM had a low positive predictive value for the detection of cirrhosis or advanced fibrosis, especially in NAFLD Controlled attenuation parameter slightly improved LSM interpretation	Only M probe data were available. Therefore, patients with high BMI and/or high skin-to-liver capsule distance were not considered for the analysis
Eddowes et al. 2019 [30]	Prospective multicentric biopsy-controlled study assessing the value of CAP and LSM in patients at risk for NAFLD	450 patients with liver biopsy [assessed according to NASH CRN] were included. LSM had a good diagnostic accuracy but showed a limited positive predictive value for detection of higher fibrosis stages. Steatosis or probe type [M or XL] did not affect LSM	M and XL probe were used according to the manufacturer recommendation. The XL probe was used in 67% of cases
Shen et al. 2019 [31]	Consecutive patients [ $n = 593$ ] with chronic hepatitis B CAP and LSM were compared with histology [METAVIR]	LSM was higher in patients without significant fibrosis when steatosis [S2–3 according to histology or CAP class] was present Hence, CAP $\geq 268$ dB/m slightly affected LSM for ruling in significant fibrosis	Only M probe data. Patients with high body mass index $>30$ kg/m <sup>2</sup> or high skin-to-liver-capsule distance [ $>25$ mm] were excluded



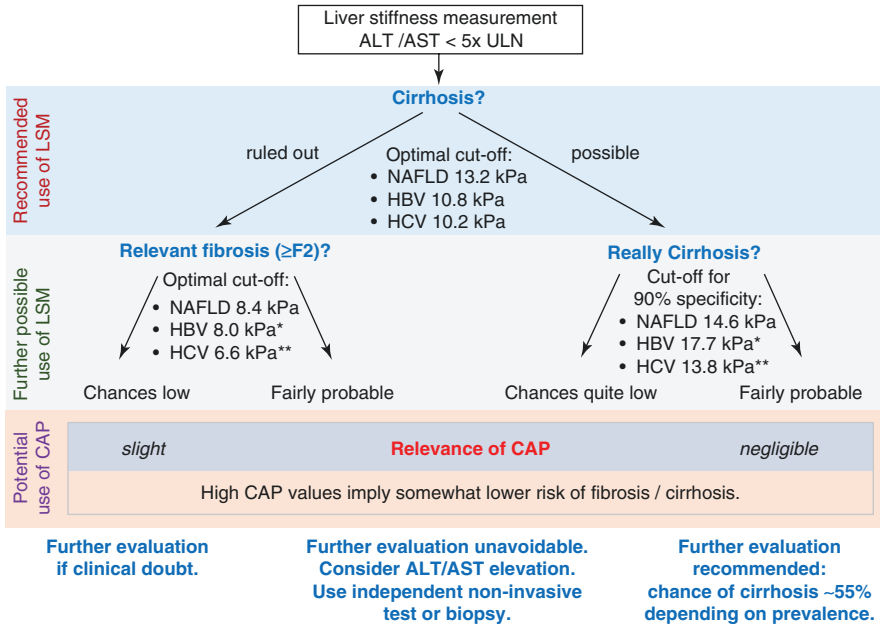


**Fig. 39.1** Example of controlled attenuation parameter (CAP) guided interpretation of liver stiffness measurement. (Figure has been adapted from [29] with permission of John Wiley & Sons Ltd. (© 2018))

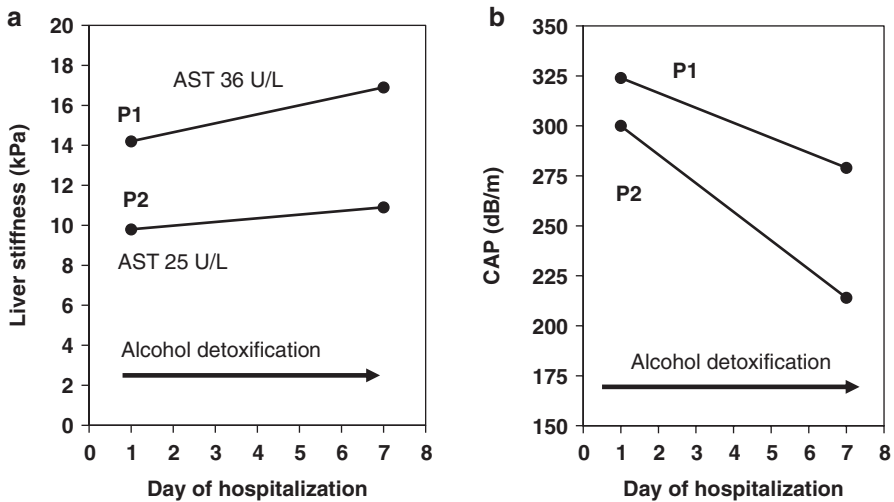


**Fig. 39.2** LS and CAP of two patients (P1 and P2) during alcohol detoxification. Here, in the absence of inflammation (see normal AST levels), LS increased while steatosis/CAP decreased. Such observations suggest that steatosis can lower stiffness which is in line with correlation data and the common observation that fat tissue is soft. More studies are required to better understand the complex interplay between fat and stiffness at the molecular level

## Conclusion

The relevance of steatosis-induced modulation of LS remains a topic of ongoing debate. Although no specific recommendation can be given, the majority of studies indicate a reduced diagnostic precision of LSM in patients with severe steatosis and obesity, which especially impairs the positive predictive value of LSM for ruling in advanced fibrosis. This effect seems to be more pronounced for the use of TE compared to 2D-SWE [21]. This should be considered when interpreting LSM results, especially in obese patients with NAFLD. High CAP values may help to identify cases at risk for impaired elastography precision. The application of proper ultrasound/elastography transducers remains crucial for optimal LSM in patients with obesity. At the molecular level, steatosis and fat tissue is soft and there are indications that elevated fat content lowers LS in the absence of confounders such as inflammation/ballooning. More prospective studies are required to better understand the complex interplay between fat content and stiffness.

## References

1. EASL-EASD-EASO Clinical EASL. Practice guidelines for the management of non-alcoholic fatty liver disease. *J Hepatol.* 2016;64(6):1388–402.
2. Bedossa P, Biopsy PK. Noninvasive methods to assess progression of nonalcoholic fatty liver disease. *Gastroenterology.* 2016;150(8):1811–22.e4.
3. Dyson JK, McPherson S, Anstee QM. Non-alcoholic fatty liver disease: non-invasive investigation and risk stratification. *J Clin Pathol.* 2013;66(12):1033–45.
4. Hirche TO, Ignee A, Hirche H, Schneider A, Dietrich CF. Evaluation of hepatic steatosis by ultrasound in patients with chronic hepatitis C virus infection. *Liver Int.* 2007;27(6):748–57.
5. Nightingale K, Rouze N, Rosenzweig S, Wang M, Abdelmalek M, Guy C, et al. Derivation and analysis of viscoelastic properties in human liver: impact of frequency on fibrosis and steatosis staging. *IEEE Trans Ultrason Ferroelectr Freq Control.* 2015;62(1):165–75.
6. Shen F, Zheng RD, Shi JP, Mi YQ, Chen GF, Hu X, et al. Impact of skin capsular distance on the performance of controlled attenuation parameter in patients with chronic liver disease. *Liver Int.* 2015;35(11):2392–400.
7. Mueller S. Does pressure cause liver cirrhosis? The sinusoidal pressure hypothesis. *World J Gastroenterol.* 2016;22(48):10482.
8. Mueller S, Nahon P, Rausch V, Peccerella T, Silva I, Yagmur E, et al. Caspase-cleaved keratin-18 fragments increase during alcohol withdrawal and predict liver-related death in patients with alcoholic liver disease. *Hepatology.* 2017;66(1):96–107.
9. Rausch V, Peccerella T, Lackner C, Yagmur E, Seitz HK, Longerich T, et al. Primary liver injury and delayed resolution of liver stiffness after alcohol detoxification in heavy drinkers with the PNPLA3 variant I148M. *World J Hepatol.* 2016;8(35):1547–56.
10. Ballestri S, Nascimbeni F, Lugari S, Lonardo A, Francica G. A critical appraisal of the use of ultrasound in hepatic steatosis. *Expert Rev Gastroenterol Hepatol.* 2019;13(7):667–81.
11. Piscaglia F, Salvatore V, Mulazzani L, Cantisani V, Schiavone C. Ultrasound shear wave elastography for liver disease. a critical appraisal of the many actors on the stage. *Eur J Ultrasound.* 2016;37(01):1–5.

12. Berzigotti A. Getting closer to a point-of-care diagnostic assessment in patients with chronic liver disease: controlled attenuation parameter for steatosis. *J Hepatol.* 2014;60(5):910–2.
13. Karlas T, Petroff D, Wiegand J. Collaboration, not competition: the role of magnetic resonance, transient elastography, and liver biopsy in the diagnosis of nonalcoholic fatty liver disease. *Gastroenterology.* 2017;152(3):479–81.
14. Sasso M, Beaugrand M, de Ledinghen V, Douvin C, Marcellin P, Poupon R, et al. Controlled attenuation parameter (CAP): a Novel VCTE™ guided ultrasonic attenuation measurement for the evaluation of hepatic steatosis: preliminary study and validation in a cohort of patients with chronic liver disease from various causes. *Ultrasound Med Biol.* 2010;36(11):1825–35.
15. Karlas T, Petroff D, Sasso M, Fan JG, Mi YQ, de Ledinghen V, et al. Individual patient data meta-analysis of controlled attenuation parameter (CAP) technology for assessing steatosis. *J Hepatol.* 2017;66(5):1022–30.
16. Tada T, Iijima H, Kobayashi N, Yoshida M, Nishimura T, Kumada T, et al. Usefulness of attenuation imaging with an ultrasound scanner for the evaluation of hepatic steatosis. *Ultrasound Med Biol.* 2019;45(10):2679–87.
17. Karlas T. Estimating steatosis and fibrosis: Comparison of acoustic structure quantification with established techniques. *World J Gastroenterol.* 2015;21(16):4894.
18. Keller J, Kaltenbach TEM, Haenle MM, Oeztuerk S, Graeter T, Mason RA, et al. Comparison of Acoustic Structure Quantification (ASQ), shearwave elastography and histology in patients with diffuse hepatopathies. *BMC Med Imaging.* 2015;15(1).
19. Liu J, Ren W, Ai H, Dun G, Ji Y, Zhang Y, et al. Acoustic structure quantification versus point shear wave speed measurement for the assessment of liver fibrosis in viral hepatitis B. *Ultrasound Med Biol.* 2018;44(6):1177–86.
20. Mueller S. Personal observation. 2019.
21. Poynard T, Pham T, Perazzo H, Munteanu M, Luckina E, Elaribi D, et al. Real-time shear wave versus transient elastography for predicting fibrosis: applicability, and impact of inflammation and steatosis. A non-invasive comparison. *PLoS One.* 2016;11(10):e0163276.
22. Boursier J, Zarski JP, de Ledinghen V, Rousselet MC, Sturm N, Lebaill B, et al. Determination of reliability criteria for liver stiffness evaluation by transient elastography. *Hepatology.* 2013;57(3):1182–91.
23. Macaluso FS, Maida M, Cammà C, Cabibbo G, Cabibi D, Alduino R, et al. Steatosis affects the performance of liver stiffness measurement for fibrosis assessment in patients with genotype 1 chronic hepatitis C. *J Hepatol.* 2014;61(3):523–9.
24. Petta S, Maida M, Macaluso FS, Di Marco V, Camma C, Cabibi D, et al. The severity of steatosis influences liver stiffness measurement in patients with nonalcoholic fatty liver disease. *Hepatology.* 2015;62(4):1101–10.
25. Karlas T, Dietrich A, Peter V, Wittekind C, Lichtiginghen R, Garnov N, et al. Evaluation of transient elastography, acoustic radiation force impulse imaging (ARFI), and enhanced liver function (ELF) score for detection of fibrosis in morbidly obese patients. *PLoS One.* 2015;10(11):e0141649.
26. Harris N, Nadebaum D, Christie M, Gorelik A, Nicoll A, Sood S, et al. Acoustic radiation force impulse accuracy and the impact of hepatic steatosis on liver fibrosis staging. *J Med Imaging Radiat Oncol.* 2016;60(5):587–92.
27. Conti F, Serra C, Vukotic R, Fiorini E, Felicani C, Mazzotta E, et al. Accuracy of elastography point quantification and steatosis influence on assessing liver fibrosis in patients with chronic hepatitis C. *Liver Int.* 2016;37(2):187–95.
28. Petta S, Wong VW, Camma C, Hiriart JB, Wong GL, Marra F, et al. Improved noninvasive prediction of liver fibrosis by liver stiffness measurement in patients with nonalcoholic fatty liver disease accounting for controlled attenuation parameter values. *Hepatology.* 2017;65(4):1145–55.
29. Karlas T, Petroff D, Sasso M, Fan JG, Mi YQ, de Ledinghen V, et al. Impact of controlled attenuation parameter on detecting fibrosis using liver stiffness measurement. *Aliment Pharmacol Ther.* 2018;47(7):989–1000.

30. Eddowes PJ, Sasso M, Allison M, Tsochatzis E, Anstee QM, Sheridan D, et al. Accuracy of FibroScan controlled attenuation parameter and liver stiffness measurement in assessing steatosis and fibrosis in patients with nonalcoholic fatty liver disease. *Gastroenterology*. 2019;156(6):1717–30.
31. Shen F, Mi YQ, Xu L, Liu YG, Wang XY, Pan Q, et al. Moderate to severe hepatic steatosis leads to overestimation of liver stiffness measurement in chronic hepatitis B patients without significant fibrosis. *Aliment Pharmacol Ther*. 2019;50(1):93–102.

**Part VII**  
**How to Use Liver Stiffness in**  
**Clinical Practice**

# Chapter 40

## Introducing to Liver Stiffness Measurement in Clinical Practice



Sebastian Mueller

### Introduction

In clinical practice, new applicants of elastographic devices are often confused since they are confronted with many questions at one time: Which device should I use? What does the LSM mean for my patient? How do LSM from different devices relate to each other? Can I really trust the LSM or is it due to a measuring artifact, a clinical confounder or indeed liver fibrosis?

In the following book section VII, various chapters address these practical questions including points to consider for high-quality LSM and patient preparation.

### Selection of Elastographic Techniques

The decision for one or the other technique depends on many aspects that include price, geographic particularities of the health care structure, reimbursement by health care providers and personal experience e.g. in ultrasound. For instance, in many countries such as France, the UK and the USA, abdominal ultrasound is performed by radiologists while in others (Germany, Austria), GI specialists or practitioners are able to do it onside and in time. The latter has the clear advantage that elastographic findings will be seen within the context of the ultrasound results. In addition, quality of LSM improves with dedicated ultrasound knowledge.

**1D-elastographic techniques** such as the FibroScan can be performed by everybody after a rather short learning time. Normally, first measurements can be performed after measuring a few patients. After ca. 1 week, routine measurements are

---

S. Mueller (✉)

Department of Medicine and Center for Alcohol Research and Liver Diseases,  
Salem Medical Center, University of Heidelberg, Heidelberg, Germany  
e-mail: [Sebastian.Mueller@urz.uni-heidelberg.de](mailto:Sebastian.Mueller@urz.uni-heidelberg.de)

possible and only occasionally, questions and problems arise that require further training or discussions. It is quite helpful that the FibroScan device has an internal quality algorithm to reject invalid LSM and it is certainly one of the reasons why elastography has had its breakthrough in the last 15 years worldwide. A **2D-SWE** platform requires basic or even advanced ultrasound knowledge. On the other side, the degree of freedom is high which also increases the risk of measurement artifacts. As a simple example, although 2D-SWE devices allow the definition of a so-called regions of interest (ROI), this ROI can be placed at tissues or organ borders and within liquids (gall bladder, vascular structures) which will lead to completely artificial stiffness numbers. In other words: These devices offer more opportunities, but the user should know more about pitfalls, limitations and standard procedures. Costs for elastographic devices are still changing in short time and even leasing models are increasingly discussed by some companies on a monthly basis.

The almost exponential increase of commercially available platforms on the market has not made selections easier for physicians. In my opinion, it clearly means that elastography will evolve as a subspeciality with its own dedicated knowledge and expertise. It will be also clearly different from imaging survey and require more “Clinical context knowledge”. In other words, in the long run, elastographic techniques will become an essential diagnostic methodology within many different clinical disciplines. On a final note, MRE is often propagated has the “all-in-one-solution” and MRE certainly holds great promises for the future, especially if one considers the future role of artificial intelligence and machine learning for medical image processing. However, so far, it has been the “simple” bedside TE that first unraveled the role of clinical confounders of elevated LS and paved the way for the worldwide success of LSM.

## **Standardization, Ascites, Obesity and Elastogram Evaluation**

One of the challenges of LSM is the lack of standardization, mainly due to the following reasons:

1. rapid evolution of elastographic techniques since 2003 with primarily commercial competition
2. the many commercially available devices without clear specifications/validations/comparisons with established techniques leaving its usage and interpretation “to the physicians”
3. The complexity of LS as physical parameter, still leaving many open questions to the experts.

Several standards for successful LSM are listed in Table 40.1. More details about the various elastographic techniques are given in Appendix Tables A.13 and A.14. These quality criteria will be extensively discussed in the next chapter by Jérôme Boursier, followed by a discussion of shear wave propagation maps that are briefly called “elastograms”. Next, limiting pathophysiological conditions such as obesity and ascites are covered in detail. Other chapters are aimed at shedding more light on

**Table 40.1** Optimal standardized conditions for liver stiffness measurements for all techniques

No.	Conditions
1	Standardized patient conditions and positioning. Horizontal positioning for at least 5 min. Normal breathing. Fasting status. Stabilized hemodynamics e.g. after physical exercise. Note that some SWE specifications require breath holding which may affect LSM itself.
2	Correct training of the examiner depending upon the elastographic technique used. Short learning curve for 1D-SWE such as TE, dedicated ultrasound knowledge for 2D-SWE. Specific radiology training for 3D-MRE
3	Correct physical LS measurement: basic anatomical and specific knowledge such as choice of probe, probe pressure, localization of liver region for LSM
4	Correct and standardized analysis of shear wave speed which may necessitate additional interpretation of e.g. elastograms. Additional factors in 2D-SWE such as viscosity and sound speed
5	Correct statistical interpretation e.g. median LS and IQR
6	Correct interpretation of LS within the clinical context including the influence of confounders such as inflammation, congestion, cholestasis or others. These confounders require additional information such as an on-time abdominal ultrasound or laboratory parameters. Critical discussion of potential measurement artefacts
7	Definition whether LSM is used in screening or expert mode. The screening mode is primarily designed to rule out any liver abnormalities. The expert mode is thought to confirm an elevated LS, to rule out potential confounders or artifacts and to ultimately link the elevated LS either to fibrosis stage, prognostic evaluation or to guide therapies

the consideration of clinical confounders of LS elevation, use of other noninvasive markers such as serum markers in combination with LS to screen large populations. At the end of the book section, a collection of clinical case examples will be presented to more practically demonstrate the usage of LSM in many clinical situations.

## Screening and Expert Mode

As shown in Fig. 40.1, a **screening mode** can be differentiated from an **expert mode**. The screening mode is primarily designed to rule out chronic liver diseases. It is mainly justified for the following reasons:

1. LSM has an excellent negative predictive value. In other words, a normal LS rules out any liver disease or potential confounders (see Fig. 40.1 or Appendix Fig. A.4).
2. All potential confounders cause LS elevation but not LS decrease. In addition, technical artefacts will only lead to higher LS. Taken together, this is an important, often underestimated cause for the worldwide and rapid success of LSM: Only LS elevation requires careful differential diagnosis of potential confounders or the consideration of potential artefacts while a normal LS can be taken as it is.
3. Especially, 1D-SWE such as TE does not require dedicated ultrasound knowledge. TE can be performed noninvasively in less than 5 min with a small sample error by untrained medical assistant personnel with a fast learning curve.



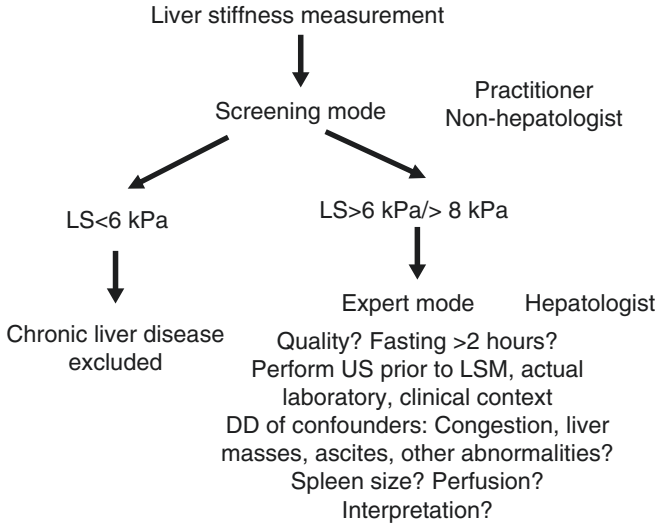


**Fig. 40.1** Introducing the concept of **Screening mode** and **Expert mode**. Accordingly, TE is ideally designed for screening large populations even by practitioners as no ultrasound knowledge is required, the learning curve for assistance personnel is short and a normal LS clearly rules out manifest liver disease and cannot be caused by technical artefacts. In contrast, the expert mode should be applied in cases of an elevated LS, optimally by a trained hepatologist with dedicated ultrasound knowledge. At this stage, all potential artefacts should be ruled out and all (patho)physiological confounders need to be discussed that may cause LS elevation

In contrast, the **expert mode** should be applied in case of an elevated LS, optimally by a trained hepatologist with dedicated ultrasound knowledge. At this stage, all potential artefacts should be ruled out and all (patho)physiological confounders need to be discussed. It is hoped that more affordable devices or new business models will drastically increase the accessibility of patients to LSM. These business models could include leasing or freemium models.

## Algorithms to Interpret LSM

Figure 40.2 shows a typical interpretation of LS if ultrasound and laboratory testing is available (expert mode). TE is performed directly after the abdominal ultrasound and routine blood tests. A minimum time of 5 min in horizontal position should be allowed for stable hemodynamics and LS stabilization. During the ultrasound, liver size, spleen size, morphology, abnormalities such as congestion, cholestasis, morphological signs of cirrhosis, the presence of ascites and the diameter of the inferior vena cava are assessed. In case of heart failure, interventions such as treatment with diuretics should be considered [1]. Biliary drainage is required in cases of mechanic cholestasis [2]. TE is then performed either with the M probe or in cases of M probe failure, obvious obesity (BMI>30) [3–5] or ascites [6] with the XL probe. If LS is

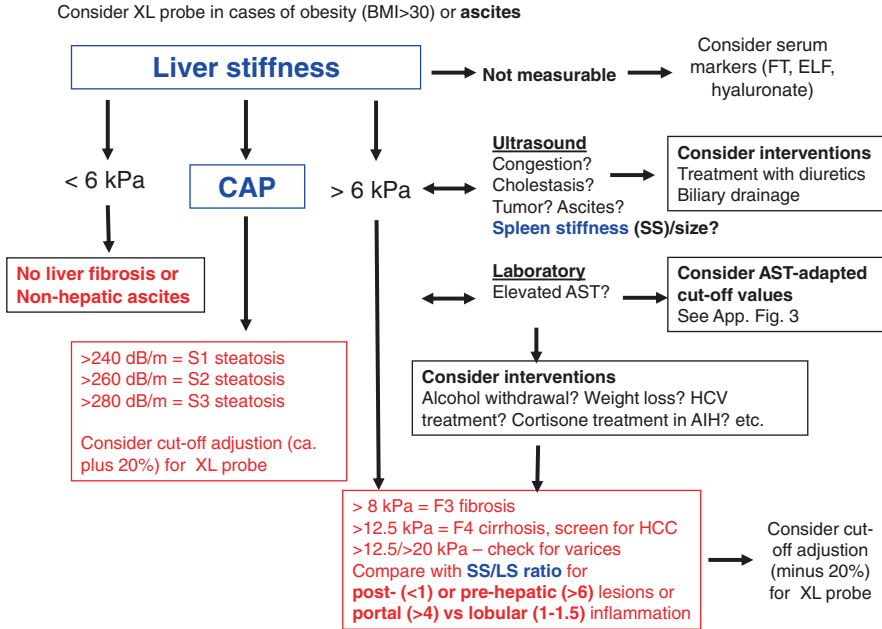


**Fig. 40.2** Practical algorithm for interpretation of liver stiffness and controlled attenuation parameter (CAP) within the clinical context. In cases of severe obesity (BMI >30) or ascites, the XL probe should be used. A normal LS <6 kPa excludes even early fibrosis stages or hepatic causes of ascites. An elevated LS requires an on-time abdominal ultrasound and an actual laboratory (AST levels, etc.). In cases of congestion or cholestasis, interventions such as biliary drainage or diuretics should be considered. Under conditions of hepatic inflammation (AST levels >50/100 U/L), AST-adapted cutoff values should be applied or the underlying cause should be treated and LS should be then remeasured. Note that for the XL probe, 20% smaller cutoff values for LSM and 20% higher cutoff values for CAP measurements apply. Spleen size or spleen stiffness (SS) further adds important information about portal hypertension and the SS/LS ratio allows further confirmation of pre- vs. posthepatic lesions or portal vs. lobular inflammation. Thus, LS, SS, SS/LS ratio and CAP should be always interpreted within the full clinical context

elevated and patients have AST>50 or even >100 U/mL, treatment interventions should be considered according to the underlying liver disease. This could be alcohol withdrawal for at least 2 weeks in drinkers, weight loss in patients with NAFLD, corticosteroid therapy in patients with AIH or antiviral therapy in patients with HCV or HBV. After normalization of transaminases, a delay period of 2–4 weeks should be kept before remeasuring LS. In patients with LS >30 kPa, the diagnosis of cirrhosis is settled despite steatohepatitis as measured by elevated transaminase levels. At these levels, the development of ascites is very likely.

This approach allows definitive noninvasive assessment of fibrosis stage in ca. 95%. Compared to conventional routine ultrasound, TE identifies twice as many patients with advanced fibrosis/cirrhosis (Mueller S, unpublished) and has a smaller sample error as compared to histology (3–5% vs. 20–50%). So-called AST-adapted cutoff values allow immediated decisions without the need of rescheduling

follow-up visits [7]. Additional measurement of spleen stiffness (SS) has further improved the assessment of portal hypertension and its complications [8–13]. Finally, the SS/LS ratio [14] will shed further light on disease etiologies. Taken together, this practical algorithm requires ultrasound and hepatology knowledge, but no simplified algorithms or formulas can be recommended at this stage.

## **Additional Assessment of Spleen Stiffness and LSM in Established Cirrhotics**

Additional measurement of spleen stiffness (SS) has further improved the assessment of portal hypertension and its complications [8–13]. It is quite exciting that more recent studies even demonstrated that the ratio of both SS and LS are providing further information on the disease etiology and even predict disease-specific complications [14]. Here, SS/LS ratio was shown to be significantly higher in patients with portal HCV as compared to lobular ALD. It was concluded that combined LS and SS/SL measurements provide additional information about disease etiology and disease-specific complications. The respective chapter entitled “Spleen to liver stiffness ratio and disease etiology” from book section V is recommended for further reading as well as Appendix Figs. A.8 and A.9.

The final two chapters will address novel findings on LSM in patients with established cirrhosis. For instance, a decreasing LS in cirrhotic patients may not always predict a good prognosis as it may be related to newly formed esophageal varices [15] as could be also demonstrated in patients undergoing TIPS implantation [15, 16]. Notably, therapeutic interventions targeting hepatic hemodynamics and therefore a decrease in portal hypertension also lead to decreasing LS values in most patients, and a decrease of LS is generally associated with an improved prognosis. Therefore, serial LS measurements are a valuable follow-up tool for patients with liver cirrhosis and may help in the decision-making of patient monitoring.

## **References**

1. Millonig G, Friedrich S, Adolf S, Fonouni H, Golriz M, Mehrabi A, et al. Liver stiffness is directly influenced by central venous pressure. *J Hepatol.* 2010;52(2):206–10.
2. Millonig G, Reimann FM, Friedrich S, Fonouni H, Mehrabi A, Büchler MW, et al. Extrahepatic cholestasis increases liver stiffness (FibroScan) irrespective of fibrosis. *Hepatology.* 2008;48(5):1718–23.
3. de Ledinghen V, Vergniol J, Foucher J, El-Hajji F, Merrouche W, Rigalleau V. Feasibility of liver transient elastography with FibroScan using a new probe for obese patients. *Liver Int.* 2010;30(7):1043–8.
4. Myers RP, Pomier-Layrargues G, Kirsch R, Pollett A, Duarte-Rojo A, Wong D, et al. Feasibility and diagnostic performance of the FibroScan XL probe for liver stiffness measurement in overweight and obese patients. *Hepatology.* 2012;55(1):199–208.

5. Durango E, Dietrich C, Seitz HK, Kunz CU, Pomier-Layrargues GT, Duarte-Rojo A, et al. Direct comparison of the FibroScan XL and M probes for assessment of liver fibrosis in obese and nonobese patients. *Hepat Med.* 2013;5:43–52.
6. Kohlhaas A, Durango E, Millonig G, Bastard C, Sandrin L, Golriz M, et al. Transient elastography with the XL probe rapidly identifies patients with non-hepatic ascites. *Hepat Med.* 2012;4:11–8.
7. Mueller S, Englert S, Seitz HK, Badea RI, Erhardt A, Bozaari B, et al. Inflammation-adapted liver stiffness values for improved fibrosis staging in patients with hepatitis C virus and alcoholic liver disease. *Liver Int.* 2015;35(12):2514–21.
8. Cescon M, Colecchia A, Cucchetti A, Peri E, Montrone L, Ercolani G, et al. Value of transient elastography measured with FibroScan in predicting the outcome of hepatic resection for hepatocellular carcinoma. *Ann Surg.* 2012;256(5):706–12; discussion 12–3.
9. Colecchia A, Montrone L, Scaiola E, Bacchi-Reggiani ML, Colli A, Casazza G, et al. Measurement of spleen stiffness to evaluate portal hypertension and the presence of esophageal varices in patients with HCV-related cirrhosis. *Gastroenterology.* 2012;143(3):646–54.
10. Mazur R, Celmer M, Silicki J, Holownia D, Pozowski P, Miedzybrodzki K. Clinical applications of spleen ultrasound elastography—a review. *J Ultrasonogr.* 2018;18(72):37–41.
11. Wong GLH, Kwok R, Hui AJ, Tse YK, Ho KT, Lo AOS, et al. A new screening strategy for varices by liver and spleen stiffness measurement (LSSM) in cirrhotic patients: a randomized trial. *Liver Int.* 2018;38(4):636–44.
12. Sharma P, Kirnake V, Tyagi P, Bansal N, Singla V, Kumar A, et al. Spleen stiffness in patients with cirrhosis in predicting esophageal varices. *Am J Gastroenterol.* 2013;108(7):1101–7.
13. Manatsathit W, Samant H, Kapur S, Ingviya T, Esmadi M, Wijarnpreecha K, et al. Accuracy of liver stiffness, spleen stiffness, and LS-spleen diameter to platelet ratio score in detection of esophageal varices: Systemic review and meta-analysis. *J Gastroenterol Hepatol.* 2018;33(10):1696–706.
14. Elshaarawy O, Mueller J, Guha IN, Chalmers J, Harris R, Krag A, et al. Spleen stiffness to liver stiffness ratio significantly differs between ALD and HCV and predicts disease-specific complications. *JHEP Rep.* 2019;1(2):99–106.
15. Piecha F, Paech D, Sollors J, Seitz HK, Rossle M, Rausch V, et al. Rapid change of liver stiffness after variceal ligation and TIPS implantation. *Am J Physiol Gastrointest Liver Physiol.* 2018;314(2):G179–G87.
16. Jansen C, Moller P, Meyer C, Kolbe CC, Bogs C, Pohlmann A, et al. Increase in liver stiffness after transjugular intrahepatic portosystemic shunt is associated with inflammation and predicts mortality. *Hepatology.* 2018;67(4):1472–84.

# Chapter 41

## Quality Criteria for Liver Stiffness Measurement by Transient Elastography



Jérôme Boursier

### Abbreviations

2D-SWE	Two-dimensional shear wave elastography
CAP	Controlled Attenuation Parameter
pSWE	Point shear wave elastography
IQR/M	Interquartile range/median ratio
SD/M	Standard deviation/mean ratio

### Introduction

The principle of hepatic elastography is to generate an elastic shear wave and to measure its speed through the liver, from which is calculated the liver stiffness (LS) itself correlated with the severity of chronic liver diseases. For more details, see also book section II “Techniques to measure liver stiffness.” As for all medical exams, some precautions must be taken before and during liver stiffness measurement (LSM) to ensure that the most relevant and clinically meaningful results are obtained. Therefore, conditions related to the patient (fasting, alcohol withdrawal status), to the operator (experience with the device), and to the procedure of examination (measurement site, choice of the FibroScan probe, intrinsic characteristic of the examination) must be carefully controlled to reach the highest quality of liver stiffness measurement.

---

J. Boursier (✉)

Service d’Hépatogastroentérologie, Centre Hospitalier Universitaire d’Angers, Angers, France

Laboratoire HIFIH, UPRES EA3859, SFR 4208, Université d’Angers, Angers, France

e-mail: [JeBoursier@chu-angers.fr](mailto:JeBoursier@chu-angers.fr)

## Fasting

Several studies have evaluated the effect of meal intake on elastography results (Table 41.1). Most of these works evaluated TE whose results significantly increase after eating in half of the patients [1]. The peak increase in LS occurs between 15 and 60 min after meal intake [2–5], and the increase rises up to 20–40% of the

**Table 41.1** Impact of meal intake on liver stiffness measurement

Study	Patients	Device	Type of meal	Time of evaluation after meal intake	Evolution of liver stiffness	Time to recovery
Mederacke 2009 [1]	56 CHC	TE	Standardized breakfast	15, 30, 60, 90, 120, and 180 min	+2 to +3 kPa in 22 of the 43 patients having baseline stiffness $\leq 10$ kPa	3 h
Yin 2011 [12]	25 CLD 20 HV	MRE	Liquid test meal	30 min	>10% increase in 22 of the 25 CLD patients (overall: $+21.1 \pm 14.5\%$ ) >10% increase in 7 of the 20 HV (overall: $+8.1 \pm 10.3\%$ )	–
Arena 2013 [2]	125 CHC	TE	Standardized liquid meal	15, 30, 45, 60, and 120 min	Peak increase in liver stiffness occurred at 15–45 min, with +17% (F4 patients) to +34% (F0-1 patients)	2 h
Berzigotti 2013 [7]	19 cirrhotics	TE	Standard mixed liquid meal	30 min	Mean increase in liver stiffness: +27%	–
Popescu 2013 [67]	57 HV	pSWE	Standard solid meal	1 and 3 h	>15% increase in 26 of the 57 patients	3 h
Jajamovich 2014 [11]	19 CHC 11 HV	MRE	Standardized liquid meal	20 min	Mean increase in liver stiffness: $+4.5\% \pm 10.1\%$ (CHC patients) and $+9.3\% \pm 12.6\%$ (HV)	–
Alvarez 2015 [8]	24 CLD	TE	Standard liquid meal	30 min	Significant increase from $7.8 \pm 3.3$ kPa (baseline) to $10.3 \pm 4.1$ kPa (time of evaluation)	2 h

**Table 41.1** (continued)

Study	Patients	Device	Type of meal	Time of evaluation after meal intake	Evolution of liver stiffness	Time to recovery
Barone 2015 [6]	54 CLD	TE	Standardized liquid meal	30 min	Mean increase in liver stiffness: $16 \pm 4\%$	–
Zhang 2016 [13]	20 HV	MRE	Standardized solid meal	30 and 60 min	$+13.4 \pm 18.0\%$ mean increase when measured in the foot-head direction; $+9.9 \pm 25.0\%$ in the right-left direction. No significant difference in the anterior-posterior direction	–
Gersak 2016 [9]	31 HV	2D-SWE	Standardized solid meal	20, 40, 60, 80, 100 and 120 min	Peak increase in liver stiffness occurred at 20 to 40 min, with $+7\%$ in female and $+12\%$ in males	2 h
Ratchasettakul 2017 [4]	40 CLD	TE CAP	Standardized liquid meal	15, 30, 45, 60, 90, and 120 min	TE: peak increase at 15 min, with $+2.4$ kPa CAP: peak decrease at 60 min, with $-18.1$ dB/m	2.5 h
Kjaergaard 2017 [3]	60 CLD	TE 2D-SWE CAP	Standardized liquid meal	20, 40, 60, 120, and 180 min	TE: peak increase at 60 min, with $+37\%$ 2D-SWE: peak increase at 60 min, with $+19\%$ ; CAP: peak increase at 60 min, with $+7.4\%$ to $+9.9\%$	–
Simkin 2018 [68]	20 HV	2D-SWE	Solid meal, no standardized	30–40 min	No significant contribution of the prandial state on liver stiffness measurement	–
Vuppalanchi 2019 [5]	16 NAFLD	TE CAP	Solid meal	30 min, 1, 2, 3, 4, 5, and 6 h	TE: peak increase at 2 h, with $+26 \pm 25\%$ increase CAP: no significant modification after the meal	3 h

(continued)

**Table 41.1** (continued)

Study	Patients	Device	Type of meal	Time of evaluation after meal intake	Evolution of liver stiffness	Time to recovery
Silva 2019 [18]	59 CLD 22 HV	TE CAP	Standardized breakfast	30 min	TE: Significant increase from 6.1 kPa (baseline) to 6.8 kPa (30 min) in CLD, no significant difference in HV CAP: no significant difference between baseline and 30 min	–
Petzold 2019 [10]	100 HV	2D-SWE	Standardized liquid meal	30–40 min	Mean increase in liver stiffness: +21.6%	–

*CHC* chronic hepatitis C, *TE* transient elastography, *min* minutes, *kPa* kiloPascal, *CLD* chronic liver disease, *HV* healthy volunteers, *MRE* magnetic resonance elastography, *pSWE* point shear wave elastography, *2D-SWE* two dimensional shear wave elastography, *CAP* controlled attenuation parameter, *NAFLD* nonalcoholic fatty liver disease

baseline value [2, 3, 6, 7]. LS recovers to initial level within 2–3 h [1, 2, 5, 8]. LS measured with two-dimensional shear wave elastography (2D-SWE) shows also a peak increase before the first hour after meal intake [3, 9], but at lesser extent with a mean 10–20% increase [3, 9, 10]. As for TE, LS recovers to the initial level within 2 h [9]. When measured with magnetic resonance elastography (MRE), LS increases by 5–20% after meal intake [11–13].

The portal blood flow increases after eating [3, 6–8, 11], and some studies have highlighted a significant correlation between both portal blood flow and LS variations [6, 11]. However, others failed to replicate these findings [3, 7, 8]. The decrease in arterial hepatic blood flow is a physiologic response to increased portal blood flow after a meal (hepatic arterial buffer response; HABR). In a study conducted in 19 cirrhotic patients, the increase in LS was more pronounced in patients lacking this postprandial HABR, suggesting it is an important factor modulating postprandial change in LS [7]. Increasing LS after a meal has a significant impact on the diagnosis of liver fibrosis at the individual level. 11% of healthy volunteers with normal LS shift to >6.0 kPa [1] or to >6.7 kPa [10] after meal intake. In patients with chronic liver disease, performing LSM with TE early after eating leads to overestimation of liver fibrosis in around one-third of the patients [1, 3]. As a consequence, international guidelines recommend to perform LSM after fasting for at least 2 h [14, 15].

The Controlled Attenuation Parameter (CAP) included in the FibroScan device evaluates liver steatosis through quantification of the ultrasound attenuation during TE examination on the FibroScan platform [16, 17]. For more details, see also book section VI “Assessment of hepatic steatosis using CAP.” The data available about



CAP evolution after meal intake remains conflicting (Table 41.1): some works have shown a significant decrease [4], whereas others demonstrated a significant increase [3] or no modification [5, 18].

## Alcohol Withdrawal

Liver stiffness has been shown to significantly and rapidly decrease after curing the cause of chronic liver diseases, especially in chronic viral hepatitis [19, 20]. In fact, this early decrease is mainly due to inflammation regression rather than immediate fibrosis improvement. This is also the case in alcoholic liver disease, with studies showing around 3 kPa decrease in LS within the month after alcohol withdrawal in half of the patients [21–24]. LS could continue to decrease 6 months after alcohol withdrawal, up to 6 kPa [24]. Therefore, LS results should be interpreted with caution in this situation to avoid underestimation of liver fibrosis [22, 24]. Inflammation-adapted cutoff values may be used for optimal LS interpretation [25]. A recent study has shown that CAP also significantly decreases in 78% of the patients who stop alcohol consumption [26]. For more details, see also book section IV “Important (patho)physiological confounders of LS.”

## Operator Experience

An important point for clinical practice is to assess when an operator is sufficiently trained to perform liver stiffness measurement (Table 41.2). In a large series of 13,369 liver stiffness examinations with FibroScan, operator experience fewer than 500 examinations was independently associated with a higher rate of measurement failure and a higher rate of unreliable examinations [27]. However, two other works performed in 2335 patients with chronic liver disease [28] and 992 NAFLD patients [29] found no independent association between the operator experience and the reliability of FibroScan examination.

**Table 41.2** Impact of operator experience on liver stiffness measurement

Reference	Device	Patients	Operators	Results
Boursier 2008 [31]	TE	250 CLD	5 novices with different medical status, comparison with experts	Progressive increase in the success rate of liver stiffness measurements performed by the novices, especially the two non-physicians. For liver stiffness results, excellent novice-expert agreement from the ten first examinations
Boursier 2010 [35]	pSWE	101 CLD	One novice compared to an expert	Very good agreement between the novice and the expert for liver stiffness results and success rate

(continued)

**Table 41.2** (continued)

Reference	Device	Patients	Operators	Results
Castera 2010 [27]	TE	13,369 exams in patients with CLD	Seven operators with various level of experience	Operator experience fewer than 500 examinations was independently associated with a higher rate of measurement failure (no value obtained after at least 10 shots) and a higher rate of unreliable examinations (<10 valid measurement or success rate <60% or IQR/M >30%)
Grădinaru-Tașcău 2013 [33]	2D-SWE	371 CLD and HV	One novice (<300 exams) compared to an expert (>500 exams)	Higher rate of unreliable examinations with the novice in obese patients, no significant difference between the novice and the expert in patients with normal weight and in overweight patients
Pang 2014 [28]	TE	2335 CLD	Two operators with different level of experience	Operator experience (<500 vs. ≥500 examinations) was not an independent predictor of poorly reliable examination (IQR/M >30% with LSM ≥7.1 kPa)
Carrion 2015 [32]	TE	334 CLD	Three operators with different level of experience	The accuracy (AUROC) to diagnose significant fibrosis slightly but significantly improved from 0.89 (moderate experience: 50–500 examinations) to 0.91 (experienced operator >500 examinations). No significant difference for the diagnosis of cirrhosis
Fraquelli 2016 [36]	pSWE	186 CLD	Two investigators expert in TE examinations (>3 years) and no previous experience in pSWE	The overall diagnostic accuracy (AUROC) values for the diagnosis of $F \geq 2$ , $F \geq 3$ , and F4 were, respectively, 0.77, 0.85, and 0.88. A 1-year learning curve was required to optimize pSWE diagnostic accuracy, the AUROC for the diagnosis of $F \geq 2$ , $F \geq 3$ , and F4 being 0.86, 0.94, and 0.91, respectively, during the second year of the investigation
Perazzo 2016 [30]	TE	276 CHC and/or HIV	One novice compared to an expert (>500 exams)	No increase in interobserver agreement between the novice and the trained operator with increasing examinations (ICC = 0.95 for the 100 first examinations, ICC = 0.96 for the 200 next examinations)
Lee 2017 [34]	2D-SWE	115 CLD	One novice compared to a 9-years experienced operator	Excellent interobserver agreement for SWE measurements between the novice and the expert with ICC = 0.88 (CI: 0.82–0.92)

**Table 41.2** (continued)

Reference	Device	Patients	Operators	Results
Vuppalanchi 2018 [29]	TE	992 NAFLD	Operators with various level of experience	Operator experience was not an independent predictor of unreliable examinations (IQR/M >30%) after adjustment on BMI, ethnicity, and age
Simkin 2018 [68]	2D-SWE	20 HV	One novice compared to an expert (>500 exams)	Individual differences between the subjects accounted for 86.3% of the variation in median stiffness values, with no statistical influence of the operator experience

TE transient elastography, CLD chronic liver disease, pSWE point shear wave elastography, IQR/M interquartile range/median, 2D-SWE two-dimensional shear wave elastography, HV healthy volunteers, kPa kiloPascal, CHC chronic hepatitis C, ICC intraclass correlation coefficient, NAFLD nonalcoholic fatty liver disease, BMI body mass index

Beyond reliability of the examination, training can also be evaluated through interobserver reproducibility between novice and experienced operators. A recent study showed an excellent novice-expert agreement for the FibroScan result as early as the first 100 examinations [30]. Due to its high ease of use, LSM with FibroScan could be delegated to nonmedical staff such as nurse or specialized technicians. To explore this possibility, the training with FibroScan has been evaluated in five novices having different medical status: a physician specializing in hepatology, a medical intern, a third-year medical student, a nurse, and a non-physician clinical research assistant [31]. The novices showed a progressive increase in the success rate of their LSM, especially the two non-physicians who finally required 50 examinations training. Interestingly, novice-expert agreement for LS results was excellent from the ten first patients with no learning curve for any of the five novices. Taken together, these results suggest that increasing experience allow to perform LSM more easily, but that results are relevant from the first examinations. In line with these findings, a study performed in patients with biopsy-proven chronic liver disease showed that operators with moderate experience (50–500 LSM) were as accurate as experienced operators for the diagnosis of cirrhosis using FibroScan (respective AUROC: 0.93 vs. 0.94), and only slightly less accurate for the diagnosis of significant fibrosis (AUROC: 0.89 vs. 0.91) [32].

There are few data available about the training with 2D-SWE or point shear wave elastography (pSWE). The rate of unreliable examinations with 2D-SWE in obese patients is higher for a novice compared to an experimented operator, but the difference is no longer significant in patients with normal weight and in overweight patients [33]. Interobserver agreement for liver stiffness results between novice and expert operators are very good for 2D-SWE [34] as for pSWE [35, 36]. However, one study that used liver biopsy as reference has suggested that around 130 examinations with pSWE are required to optimize diagnostic accuracy [36]. Since both technologies are run on conventional ultrasound machines, normally a dedicated ultrasound knowledge is required.

In summary, it can be considered that around 100 liver stiffness examinations are required before considering an operator as totally trained in the use of an elastography device.

## FibroScan Probe

The classic FibroScan M probe is impaired by measurement failure rates reaching 8% in overweight patients and 17% in obese patients [27]. To circumvent this limitation, the manufacturer has developed the XL probe specifically dedicated for obese patients with skin-liver capsule distance >25 mm. Compared with the classic M probe, the XL probe uses a lower central frequency (2.5 vs. 3.5 MHz for the M probe), has a larger tip diameter (12 vs. 9 mm), and measures more deeply below the skin surface (3.5–7.5 cm vs. 2.5–6.5 cm with the M probe). The XL probe provides a lower rate of measurement failure and a similar diagnostic accuracy than the M probe [37–40]. However, the XL probe result is lower than that of the M probe with consequently a potential risk of underestimation of liver fibrosis. In contrast with the phantoms, the XL probe consistently produced approximately 20% lower liver stiffness values in humans compared with the M probe [40]. In addition to a long skin-liver capsule distance, a high degree of steatosis was also responsible for this discordance. Adjustment of cutoff values for the XL probe (<5.5, 5.5–7, 7–10, and <10 kPa for F0, F1–2, F3, and F4 fibrosis, respectively) significantly improved agreement between the two probes from  $r = 0.655$  to  $0.679$  [40]. However, a recent work has shown that liver stiffness results obtained with the M probe in patients with BMI <30 kg/m<sup>2</sup> are not significantly different from those obtained with the XL probe in obese patients (BMI ≥30 kg/m<sup>2</sup>) [41]. Therefore, by following the EASL-ALEH Clinical Practice Guidelines (M probe in patients with BMI <30 kg/m<sup>2</sup> and XL probe in obese patients) [14], the same diagnostic cutoffs for both probes displayed similar diagnostic accuracy [41]. These results have been confirmed by another study which also evaluated the Automatic Probe Selection tool included in the recent versions of the FibroScan software [42]. The Automatic Probe Selection tool automatically measures the skin-liver capsule distance and indicates the probe to be used as a function of the patient's morphology. According to their study results, the authors proposed to use the M probe first in patients with BMI <32 kg/m<sup>2</sup> and eventually switch to the XL probe according to the recommendation made by the Automatic Probe Selection tool, and to use the XL probe in all patients with BMI ≥32 kg/m<sup>2</sup>.

## Measurement Site

Liver stiffness measurement is performed in patients lying in dorsal decubitus with the right arm behind the head in maximal abduction. The operator has first to choose the correct measurement site, between two ribs at the level of the right lobe of the liver. By evaluating four different measurement sites, it has been suggested that the interobserver reproducibility for FibroScan results is the highest when the measurement is performed at the crossing of the median axillary line and the first intercostal space under the upper limit of the liver dullness [43] (Table 41.3). Another work showed no significant difference in liver stiffness result, AUROC for significant

**Table 41.3** Impact of the measurement site on liver stiffness measurement

Reference	Device	Patients	Measurement site tested	Results
Boursier 2008 [43]	TE	46 CLD	Median axillary line/1st ICS under the ULLD; Median axillary line/2nd ICS under the ULLD; Anterior axillary line/1st ICS under the ULLD	Interobserver agreement for liver stiffness result was excellent when the measurement was performed at the crossing between the median axillary line and the first intercostal space under the upper limit of the liver dullness
Kim 2010 [44]	TE	91 CHB	Between median and anterior axillary line: fifth ICS, sixth ICS, seventh ICS, same site as liver biopsy	No significant difference in liver stiffness results, AUROC for significant fibrosis and AUROC for cirrhosis between the measurement sites evaluated
Kaminuma 2011 [45]	pSWE	20 HV	Lateral segment (3.5 cm from the probe) vs. superficial portion of the right hepatic lobe (3.5 cm) vs. deep portion of the right hepatic lobe (5.5 cm). Intercostal vs. subcostal approach	Liver stiffness results significantly lower when measured in the deep portion of the right lobe compared to the superficial portion. Liver stiffness results obtained on the intercostal exams tended to be lower than those obtained on the subcostal exams
Koizumi 2011 [69]	Real-time tissue elastography	70 CHC	Median axillary line/1st ICS under the ULLD; Median axillary line/2nd ICS under the ULLD; Anterior axillary line/1st ICS under the ULLD	Excellent interobserver agreement whatever the measurement site (ICC between 0.91 and 0.95)
Beland 2014 [46]	2D-SWE	50 CLD	One in the left lobe using a subxyphoid approach; Two in the right lobe at two different craniocaudal locations with the patient in a supine or slight right anterior oblique position; One in the area planned for liver biopsy	Nonsignificant decrease in diagnostic accuracy for significant fibrosis when the measure was performed in the left lobe, especially in the subgroup of CHC patients
Samir 2015 [47]	2D-SWE	136 CLD	Left lobe; Upper right lobe; Lower right lobe; Liver biopsy site	Mean results at all sites showed a significant correlation with fibrosis stage, except those from the left lobe

TE transient elastography, CLD chronic liver disease, ICS intercostal space, ULLD upper limit of liver dullness, CHB chronic hepatitis B, pSWE point shear wave elastography, HV healthy volunteer, CHC chronic hepatitis C, ICC intraclass correlation coefficient, 2D-SWE two dimensional shear wave elastography

fibrosis or AUROC for cirrhosis among the different measurement sites evaluated [44]. In fact, it is important to correctly place the probe in front of the liver and to ensure a measurement in a liver portion at least 6 cm thick free of large vascular structures. To do this with FibroScan, the operator should control the real-time ultrasound signal on the screen of the device to obtain a typical acoustic signature of the liver characterized by a layered TM mode without heterogeneity and a linear decrease of the A mode. After the shot, the operator must also control that the elastogram displayed on the FibroScan screen is visible throughout the entire window with parallel margins.

Imaging devices including elastography modulus have the advantage to allow the visual selection of the best region of interest within the liver parenchyma. However, liver stiffness results obtained with pSWE are significantly lower when the measurement is performed in the deep portion compared to the superficial portion of the right lobe of the liver, and by intercostal compared to subcostal approach [45]. 2D-SWE seems to perform less for the diagnosis of significant fibrosis when the measurement is performed in the left lobe of the liver [46, 47].

## Reliability Criteria

The correct interpretation of elastography results is crucial to ensure appropriate patient management but remains a challenge for physicians because several conditions other than liver fibrosis can increase liver stiffness: liver inflammation [48, 49], cholestasis [50], and central venous pressure [51]. Conflicting data have been observed on steatosis [52–55] and they are discussed in more detail in chapter “Histological confounders of liver stiffness” in book section IV and in chapter “Liver steatosis (CAP) as modifier of liver stiffness” in book section VI. In addition, intrinsic characteristics of elastography examination should also be carefully considered for the best interpretation of elastography result.

## *FibroScan*

A reliable FibroScan examination has initially been defined as an exam with  $\geq 10$  valid shots and  $\geq 60\%$  success rate and an interquartile range/median ratio (IQR/M)  $\leq 30\%$ . However, some works have found that this “classical” definition does not lead to a significant improvement of the noninvasive diagnosis of liver fibrosis [56, 57]. The first study which specifically evaluated the intrinsic characteristics of FibroScan examination demonstrated that IQR/M is a key parameter to consider [58]. Liver stiffness was converted into fibrosis stage according to published cutoffs, discordance was defined as  $\geq 2$  stages difference with liver biopsy result, and the multivariate analysis identified IQR/M as independently associated with discordances. There was a 15% discordance rate in FibroScan examinations with IQR/M  $\geq 0.21$  vs. 7% in those with IQR/M  $< 0.21$ . These results were confirmed by another

**Table 41.4** New reliability criteria for liver stiffness measurement with FibroScan

Liver stiffness result (kPa)	Interquartile range/median ratio		
	≤0.10	0.11–0.30	0.30<
<7.1	Very reliable	Reliable	Reliable
≥7.1			Poorly reliable

Poorly reliable examinations are associated with decreased diagnostic accuracy and should not be used to decide the patient management in clinical practice

work in which the discordance rate was 22% for FibroScan examinations with IQR/M  $\geq 0.17$  vs. 7% for those with IQR/M  $< 0.17$  [57]. In this last work, neither the criteria  $< 10$  valid shots nor the success rate was associated with discordance between FibroScan and liver biopsy.

The effect of IQR/M on the discordance rate observed in the Lucidarme and Myers studies did not translate in a significant effect on diagnostic accuracy as evaluated with the AUROC [57, 58]. Therefore, another work has used diagnostic accuracy as endpoint rather than discordance between FibroScan and liver biopsy [56]. Multivariate analysis demonstrated that IQR/M independently interacted with the level of liver stiffness to predict liver fibrosis, leading the authors to define three new categories of reliability (Table 41.4): “very reliable” (IQR/M  $\leq 0.10$ ), “reliable” ( $0.10 < \text{IQR/M} \leq 0.30$ , or IQR/M  $> 0.30$  with liver stiffness  $< 7.1$  kPa), and “poorly reliable” (IQR/M  $> 0.30$  with liver stiffness  $\geq 7.1$  kPa). AUROCs and rate of well classified patients were significantly lower in poorly reliable examinations compared to the two other very reliable and reliable categories. 9.1% of FibroScan examinations were poorly reliable versus 24.3% unreliable examination with the classical definition ( $\geq 10$  valid shots,  $\geq 60\%$  success rate, and IQR/M  $\leq 30\%$ ). The IQR/M ratio reflects the dispersion of the valid acquisitions obtained during the examination and, when increased, it indicates a limitation in correctly assessing the true level of liver stiffness. However, by definition, a high IQR/M implies a smaller interval in low liver stiffness levels. For example, an IQR/M at 0.30 represents a 1.5 kPa interval when liver stiffness is 5.0 kPa, but a 4.5 kPa interval when liver stiffness is 15.0 kPa. Consequently, IQR/M has little impact in low liver stiffness levels, thus explaining why FibroScan examination with IQR/M  $> 0.30$  can be considered “reliable” when liver stiffness is  $< 7.1$  kPa. Therefore, reliability criteria based only on IQR/M without consideration for the level of LS erroneously exclude reliable examinations and artificially increase the rate of unreliable examinations. An independent validation study has confirmed that the new reliability criteria increase the number of patients with valid FibroScan examinations without compromising the diagnostic accuracy [59]. In this work including 55% cirrhotic patients, the rate of reliable examinations according to the classical definition was 71.6% versus 83.2% of very reliable/reliable examinations according to the new criteria. Compared to classically defined reliable examinations, reliable/very reliable examinations according to the new criteria yielded a similar correlation with fibrosis stages and hepatic venous pressure gradient and showed the same diagnostic accuracy for significant fibrosis or cirrhosis. The new reliability criteria for FibroScan have recently been validated in a cohort of 938 NAFLD patients [60].



### ***Point Shear Wave Elastography (pSWE)***

pSWE examinations with  $\text{IQR/M} \geq 0.30$  have a higher rate of discordance with liver biopsy and a lower diagnostic accuracy for significant fibrosis and for severe fibrosis/cirrhosis [61]. The same methodology used for FibroScan has been applied in 1094 patients with biopsy-proven chronic liver disease to define three categories of reliability for pSWE: “very reliable” ( $\text{IQR/M} < 0.15$ ), “reliable” ( $0.15 \leq \text{IQR/M} < 0.35$ , or  $\text{IQR/M} \geq 0.35$  with pSWE result  $< 1.37$  m/s), and “poorly reliable” ( $\text{IQR/M} \geq 0.35$  with pSWE result  $\geq 1.37$  m/s) [60]. Unreliable examinations produced a very low diagnostic accuracy for advanced fibrosis (AUROC: 0.657, rate of well classified patients: 57.8%) as well as for cirrhosis (AUROC: 0.659, rate of well classified patients: 50.0%), which made these exams as not suitable for the evaluation of liver fibrosis in clinical practice. Unreliable examinations accounted for 21.4% of all exams and, interestingly, the rate of unreliable examinations significantly increased with the skin-liver capsule distance to reach 52.7% in patients with a distance higher than 30 mm. These reliability criteria for pSWE examination need now to be independently validated.

### ***2D Shear Wave Elastography (2D-SWE)***

A recent work performed in a small series of 88 patients with chronic liver disease took clinically significant portal hypertension defined by hepatic venous pressure gradient  $\geq 10$  mmHg as endpoint and proposed three categories of reliability for 2D-SWE examination using the standard deviation/mean ratio (SD) and the depth of measurement: “highly reliable” ( $\text{SD} \leq 0.10$  and depth  $< 5.6$  cm), “reliable” ( $\text{SD} > 0.10$  or depth  $\geq 5.6$  cm), “unreliable” ( $\text{SD} > 0.10$  and depth  $\geq 5.6$  cm) [62]. Accuracy of 2D-SWE for the noninvasive diagnosis of clinically significant portal hypertension was significantly different between highly reliable, reliable, and unreliable examinations, with respectively 96%, 76%, and 44% correctly classified patients. Another study performed in 142 patients with alcoholic liver disease or chronic viral hepatitis C did not find any association between reliability and SD below 10% [63]. In this work, 2D-SWE measurements with both  $\text{SD} \leq 1.75$  kPa and a ROI diameter  $\geq 18$  mm had excellent accuracy for the diagnosis of cirrhosis (AUROC = 0.99) whereas AUROC was only 0.75 for the exams with  $\text{SD} > 1.75$  kPa and diameter  $< 18$  mm. Finally, it seems that the SD is an important factor to consider for the interpretation of 2D-SWE results, but further studies performed in large cohorts are required to clearly define and validate the reliability criteria of 2D-SWE.

### ***Controlled Attenuation Parameter (CAP)***

It has been recently suggested that CAP examinations with an  $\text{IQR/M} > 30$  dB/m [64] or  $> 40$  dB/m [65] are less accurate for the diagnosis of fatty liver. The interest of using  $\text{IQR/M} > 40$  dB/m as criteria to identify unreliable CAP examinations has



been replicated in a study including patients with alcoholic liver disease [26], but not in another work performed in NAFLD [66]. Further studies are required to determine and validate the reliability criteria for CAP examination.

## References

1. Mederacke I, Wursthorn K, Kirschner J, Rifai K, Manns MP, Wedemeyer H, et al. Food intake increases liver stiffness in patients with chronic or resolved hepatitis C virus infection. *Liver Int.* 2009;29(10):1500–6.
2. Arena U, Lupsor Platon M, Stasi C, Moscarella S, Assarat A, Bedogni G, et al. Liver stiffness is influenced by a standardized meal in patients with chronic hepatitis C virus at different stages of fibrotic evolution. *Hepatology.* 2013;58(1):65–72.
3. Kjaergaard M, Thiele M, Jansen C, Staehr Madsen B, Gortzen J, Strassburg C, et al. High risk of misinterpreting liver and spleen stiffness using 2D shear-wave and transient elastography after a moderate or high calorie meal. *PLoS One.* 2017;12(4):e0173992.
4. Ratchatasettakul K, Rattanasiri S, Promson K, Sringam P, Sobhonslidsuk A. The inverse effect of meal intake on controlled attenuation parameter and liver stiffness as assessed by transient elastography. *BMC Gastroenterol.* 2017;17(1):50.
5. Vuppalanchi R, Weber R, Russell S, Gawrieh S, Samala N, Slaven JE, et al. Is fasting necessary for individuals with nonalcoholic fatty liver disease to undergo vibration-controlled transient elastography? *Am J Gastroenterol.* 2019;114(6):995–7.
6. Barone M, Iannone A, Brunetti ND, Sebastiani F, Cecere O, Berardi E, et al. Liver stiffness and portal blood flow modifications induced by a liquid meal consumption: pathogenetic mechanisms and clinical relevance. *Scand J Gastroenterol.* 2015;50(5):560–6.
7. Berzigotti A, De Gottardi A, Vukotic R, Siramolpiwat S, Abraldes JG, Garcia-Pagan JC, et al. Effect of meal ingestion on liver stiffness in patients with cirrhosis and portal hypertension. *PLoS One.* 2013;8(3):e58742.
8. Alvarez D, Orozco F, Mella JM, Anders M, Antinucci F, Mastai R. Meal ingestion markedly increases liver stiffness suggesting the need for liver stiffness determination in fasting conditions. *Gastroenterol Hepatol.* 2015;38(7):431–5.
9. Gersak MM, Badea R, Lenghel LM, Vasilescu D, Botar-Jid C, Dudea SM. Influence of food intake on 2-D shear wave elastography assessment of liver stiffness in healthy subjects. *Ultrasound Med Biol.* 2016;42(6):1295–302.
10. Petzold G, Porsche M, Ellenrieder V, Kunsch S, Neesse A. Impact of food intake on liver stiffness determined by 2-D shear wave elastography: prospective interventional study in 100 healthy patients. *Ultrasound Med Biol.* 2019;45(2):402–10.
11. Jajamovich GH, Dyvorne H, Donnerhack C, Taouli B. Quantitative liver MRI combining phase contrast imaging, elastography, and DWI: assessment of reproducibility and postprandial effect at 3.0 T. *PLoS One.* 2014;9(5):e97355.
12. Yin M, Talwalkar JA, Glaser KJ, Venkatesh SK, Chen J, Manduca A, et al. Dynamic postprandial hepatic stiffness augmentation assessed with MR elastography in patients with chronic liver disease. *Am J Roentgenol.* 2011;197(1):64–70.
13. Zhang J, Arena C, Pednekar A, Lambert B, Dees D, Lee VV, et al. Short-term repeatability of magnetic resonance elastography at 3.0T: effects of motion-encoding gradient direction, slice position, and meal ingestion. *J Magn Reson Imaging.* 2016;43(3):704–12.
14. EASL-ALEH Clinical Practice Guidelines. Non-invasive tests for evaluation of liver disease severity and prognosis. *J Hepatol.* 2015;63(1):237–64.
15. Dietrich CF, Bamber J, Berzigotti A, Bota S, Cantisani V, Castera L, et al. EFSUMB guidelines and recommendations on the clinical use of liver ultrasound elastography, update 2017 (Long Version). *Ultraschall Med.* 2017;38(4):e16–47.

16. Sasso M, Beaugrand M, de Ledinghen V, Douvin C, Marcellin P, Poupon R, et al. Controlled attenuation parameter (CAP): A novel VCTE™ guided ultrasonic attenuation measurement for the evaluation of hepatic steatosis: preliminary study and validation in a cohort of patients with chronic liver disease from various causes. *Ultrasound Med Biol*. 2010;36(11):1825–35.
17. Karlas T, Petroff D, Sasso M, Fan JG, Mi YQ, de Ledinghen V, et al. Individual patient data meta-analysis of controlled attenuation parameter (CAP) technology for assessing steatosis. *J Hepatol*. 2017;66(5):1022–30.
18. Silva M, Costa Moreira P, Peixoto A, Santos AL, Lopes S, Goncalves R, et al. Effect of meal ingestion on liver stiffness and controlled attenuation parameter. *GE Port J Gastroenterol*. 2019;26(2):99–104.
19. Singh S, Facciorusso A, Loomba R, Falck-Ytter YT. Magnitude and kinetics of decrease in liver stiffness after antiviral therapy in patients with chronic hepatitis C: a systematic review and meta-analysis. *Clin Gastroenterol Hepatol*. 2018;16(1):27–38. e4
20. Facciorusso A, Garcia Perdomo HA, Muscatiello N, Buccino RV, Wong VW, Singh S. Systematic review with meta-analysis: change in liver stiffness during anti-viral therapy in patients with hepatitis B. *Dig Liver Dis*. 2018;50(8):787–94.
21. Mueller S, Millonig G, Sarovska L, Friedrich S, Reimann FM, Pritsch M, et al. Increased liver stiffness in alcoholic liver disease: differentiating fibrosis from steatohepatitis. *World J Gastroenterol*. 2010;16(8):966–72.
22. Trabut JB, Thepot V, Nalpas B, Lavielle B, Coscone S, Corouge M, et al. Rapid decline of liver stiffness following alcohol withdrawal in heavy drinkers. *Alcohol Clin Exp Res*. 2012;36(8):1407–11.
23. Gelsi E, Dainese R, Truchi R, Marine-Barjoan E, Anty R, Autuori M, et al. Effect of detoxification on liver stiffness assessed by fibroscan(R) in alcoholic patients. *Alcohol Clin Exp Res*. 2011;35(3):566–70.
24. Gianni E, Forte P, Galli V, Razzolini G, Bardazzi G, Annese V. Prospective evaluation of liver stiffness using transient elastography in alcoholic patients following abstinence. *Alcohol*. 2017;52(1):42–7.
25. Mueller S, Englert S, Seitz HK, Badea RI, Erhardt A, Bozaari B, et al. Inflammation-adapted liver stiffness values for improved fibrosis staging in patients with hepatitis C virus and alcoholic liver disease. *Liver Int*. 2015;35(12):2514–21.
26. Thiele M, Rausch V, Fluhr G, Kjærsgaard M, Piecha F, Mueller J, et al. Controlled attenuation parameter and alcoholic hepatic steatosis: diagnostic accuracy and role of alcohol detoxification. *J Hepatol*. 2018;68(5):1025–32.
27. Castéra L, Foucher J, Bernard P-H, Carvalho F, Allaix D, Merrouche W, et al. Pitfalls of liver stiffness measurement: a 5-year prospective study of 13,369 examinations. *Hepatology*. 2010;51(3):828–35.
28. Pang JX, Pradhan F, Zimmer S, Niu S, Crotty P, Tracey J, et al. The feasibility and reliability of transient elastography using Fibroscan(R): a practice audit of 2335 examinations. *Can J Gastroenterol Hepatol*. 2014;28(3):143–9.
29. Vuppalanchi R, Siddiqui MS, Van Natta ML, Hallinan E, Brandman D, Kowdley K, et al. Performance characteristics of vibration-controlled transient elastography for evaluation of nonalcoholic fatty liver disease. *Hepatology*. 2018;67(1):134–44.
30. Perazzo H, Fernandes FF, Soares JC, Fittipaldi J, Cardoso SW, Grinsztejn B, et al. Learning curve and intra/interobserver agreement of transient elastography in chronic hepatitis C patients with or without HIV co-infection. *Clin Res Hepatol Gastroenterol*. 2016;40(1):73–82.
31. Boursier J, Konate A, Guilly M, Gorea G, Sawadogo A, Quemener E, et al. Learning curve and interobserver reproducibility evaluation of liver stiffness measurement by transient elastography. *Eur J Gastroenterol Hepatol*. 2008;20(7):693–701.
32. Carrion JA, Puigvehi M, Coll S, Garcia-Retortillo M, Canete N, Fernandez R, et al. Applicability and accuracy improvement of transient elastography using the M and XL probes by experienced operators. *J Viral Hepat*. 2015;22(3):297–306.
33. Gradinaru-Tascau O, Sporea I, Bota S, Jurchis A, Popescu A, Popescu M, et al. Does experience play a role in the ability to perform liver stiffness measurements by means of supersonic shear imaging (SSI)? *Med Ultrason*. 2013;15(3):180–3.

34. Lee ES, Lee JB, Park HR, Yoo J, Choi JI, Lee HW, et al. shear wave liver elastography with a propagation map: diagnostic performance and inter-observer correlation for hepatic fibrosis in chronic hepatitis. *Ultrasound Med Biol.* 2017;43(7):1355–63.
35. Boursier J, Isselin G, Fouchard-Hubert I, Oberti F, Dib N, Lebigot J, et al. Acoustic radiation force impulse: a new ultrasonographic technology for the widespread noninvasive diagnosis of liver fibrosis. *Eur J Gastroenterol Hepatol.* 2009;22(9):1074–84.
36. Fraquelli M, Baccarin A, Casazza G, Conti CB, Giunta M, Massironi S, et al. Liver stiffness measurement reliability and main determinants of point shear-wave elastography in patients with chronic liver disease. *Aliment Pharmacol Ther.* 2016;44(4):356–65.
37. Wong VW, Vergniol J, Wong GL, Foucher J, Chan AW, Chermak F, et al. Liver stiffness measurement using XL probe in patients with nonalcoholic fatty liver disease. *Am J Gastroenterol.* 2012;107(12):1862–71.
38. de Ledinghen V, Wong VW, Vergniol J, Wong GL, Foucher J, Chu SH, et al. Diagnosis of liver fibrosis and cirrhosis using liver stiffness measurement: comparison between M and XL probe of FibroScan(R). *J Hepatol.* 2012;56(4):833–9.
39. Myers RP, Pomier-Layrargues G, Kirsch R, Pollett A, Duarte-Rojo A, Wong D, et al. Feasibility and diagnostic performance of the FibroScan XL probe for liver stiffness measurement in overweight and obese patients. *Hepatology.* 2012;55(1):199–208.
40. Durango E, Dietrich C, Seitz HK, Kunz CU, Pomier-Layrargues GT, Duarte-Rojo A, et al. Direct comparison of the FibroScan XL and M probes for assessment of liver fibrosis in obese and nonobese patients. *Hepat Med.* 2013;5:43–52.
41. Wong VW, Irlles M, Wong GL, Shili S, Chan AW, Merrouche W, et al. Unified interpretation of liver stiffness measurement by M and XL probes in non-alcoholic fatty liver disease. *Gut.* 2019;68(11):2057–64.
42. Berger A, Shili S, Zuberbuhler F, Hiriart JB, Lannes A, Chermak F, et al. Liver stiffness measurement with fibroscan: use the right probe in the right conditions! *Clin Transl Gastroenterol.* 2019;10(4):e00023.
43. Boursier J, Konate A, Gorea G, Reaud S, Quemener E, Oberti F, et al. Reproducibility of liver stiffness measurement by ultrasonographic elastometry. *Clin Gastroenterol Hepatol.* 2008;6(11):1263–9.
44. Kim SU, Kim JK, Park JY, Ahn SH, Lee JM, Baatarkhuu O, et al. Variability in liver stiffness values from different intercostal spaces. *Liver Int.* 2009;29(5):760–6.
45. Kaminuma K, Tsushima Y, Matsumoto N, Kurabayashi T, Taketomi-Takahashi A, Endo K. Reliable measurement procedure of virtual touch tissue quantification with acoustic radiation force impulse imaging. *J Ultrasound Med.* 2011;30(6):745–51.
46. Beland MD, Brown SF, Machan JT, Taliano RJ, Promrat K, Cronan JJ. A pilot study estimating liver fibrosis with ultrasound shear-wave elastography: does the cause of liver disease or location of measurement affect performance? *AJR Am J Roentgenol.* 2014;203(3):W267–73.
47. Samir AE, Dhyani M, Vij A, Bhan AK, Halpern EF, Mendez-Navarro J, et al. Shear-wave elastography for the estimation of liver fibrosis in chronic liver disease: determining accuracy and ideal site for measurement. *Radiology.* 2015;274(3):888–96.
48. Coco B, Oliveri F, Maina AM, Ciccorossi P, Sacco R, Colombatto P, et al. Transient elastography: a new surrogate marker of liver fibrosis influenced by major changes of transaminases. *J Viral Hepat.* 2007;14(5):360–9.
49. Arena U, Vizzutti F, Abralde JG, Corti G, Stasi C, Moscarella S, et al. Reliability of transient elastography for the diagnosis of advanced fibrosis in chronic hepatitis C. *Gut.* 2008;57(9):1288–93.
50. Millonig G, Reimann FM, Friedrich S, Fonouni H, Mehrabi A, Büchler MW, et al. Extrahepatic cholestasis increases liver stiffness (FibroScan) irrespective of fibrosis. *Hepatology.* 2008;48(5):1718–23.
51. Millonig G, Friedrich S, Adolf S, Fonouni H, Golriz M, Mehrabi A, et al. Liver stiffness is directly influenced by central venous pressure. *J Hepatol.* 2010;52(2):206–10.
52. Petta S, Maida M, Macaluso FS, Di Marco V, Camma C, Cabibi D, et al. The severity of steatosis influences liver stiffness measurement in patients with nonalcoholic fatty liver disease. *Hepatology.* 2015;62(4):1101–10.

53. Boursier J, de Ledinghen V, Sturm N, Amrani L, Bacq Y, Sandrini J, et al. Precise evaluation of liver histology by computerized morphometry shows that steatosis influences liver stiffness measured by transient elastography in chronic hepatitis C. *J Gastroenterol.* 2014;49(3):527–37.
54. Rausch V, Peccerella T, Lackner C, Yagmur E, Seitz HK, Longrich T, et al. Primary liver injury and delayed resolution of liver stiffness after alcohol detoxification in heavy drinkers with the PNPLA3 variant I148M. *World J Hepatol.* 2016;8(35):1547–56.
55. Mueller S, Nahon P, Rausch V, Peccerella T, Silva I, Yagmur E, et al. Caspase-cleaved keratin-18 fragments increase during alcohol withdrawal and predict liver-related death in patients with alcoholic liver disease. *Hepatology.* 2017;66(1):96–107.
56. Boursier J, Zarski JP, de Ledinghen V, Rousselet MC, Sturm N, Lebaill B, et al. Determination of reliability criteria for liver stiffness evaluation by transient elastography. *Hepatology.* 2013;57(3):1182–91.
57. Myers RP, Crotty P, Pomier-Layrargues G, Ma M, Urbanski SJ, Elkashab M. Prevalence, risk factors and causes of discordance in fibrosis staging by transient elastography and liver biopsy. *Liver Int.* 2010;30(10):1471–80.
58. Lucidarme D, Foucher J, Le Bail B, Vergniol J, Castera L, Duburque C, et al. Factors of accuracy of transient elastography (fibroscan) for the diagnosis of liver fibrosis in chronic hepatitis C. *Hepatology.* 2009;49(4):1083–9.
59. Schwabl P, Bota S, Salzl P, Mandorfer M, Payer BA, Ferlitsch A, et al. New reliability criteria for transient elastography increase the number of accurate measurements for screening of cirrhosis and portal hypertension. *Liver Int.* 2015;35(2):381–90.
60. Boursier J, Cassinotto C, Hunault G, Shili S, Lebigot J, Lapuyade B, et al. Criteria to determine reliability of noninvasive assessment of liver fibrosis with virtual touch quantification. *Clin Gastroenterol Hepatol.* 2019;17(1):164–71. e5
61. Fang C, Jaffer OS, Yusuf GT, Konstantatou E, Quinlan DJ, Agarwal K, et al. Reducing the number of measurements in liver point shear-wave elastography: factors that influence the number and reliability of measurements in assessment of liver fibrosis in clinical practice. *Radiology.* 2018;287(3):844–52.
62. Procopet B, Berzigotti A, Abraldes JG, Turon F, Hernandez-Gea V, Garcia-Pagan JC, et al. Real-time shear-wave elastography: applicability, reliability and accuracy for clinically significant portal hypertension. *J Hepatol.* 2015;62(5):1068–75.
63. Thiele M, Madsen BS, Procopet B, Hansen JF, Moller LMS, Detlefsen S, et al. Reliability criteria for liver stiffness measurements with real-time 2D shear wave elastography in different clinical scenarios of chronic liver disease. *Ultraschall Med.* 2017;38(6):648–54.
64. Caussy C, Alquraish MH, Nguyen P, Hernandez C, Cepin S, Fortney LE, et al. Optimal threshold of controlled attenuation parameter with MRI-PDFF as the gold standard for the detection of hepatic steatosis. *Hepatology.* 2018;67(4):1348–59.
65. Wong VW, Petta S, Hiriart JB, Camma C, Wong GL, Marra F, et al. Validity criteria for the diagnosis of fatty liver by M probe-based controlled attenuation parameter. *J Hepatol.* 2017;67(3):577–84.
66. Eddowes PJ, Sasso M, Allison M, Tsochatzis E, Anstee QM, Sheridan D, et al. Accuracy of FibroScan controlled attenuation parameter and liver stiffness measurement in assessing steatosis and fibrosis in patients with nonalcoholic fatty liver disease. *Gastroenterology.* 2019;156(6):1717–30.
67. Popescu A, Bota S, Sporea I, Sirli R, Danila M, Racean S, et al. The influence of food intake on liver stiffness values assessed by acoustic radiation force impulse elastography—preliminary results. *Ultrasound Med Biol.* 2013;39(4):579–84.
68. Simkin P, Rattansingh A, Liu K, Hudson JM, Atri M, Jang HJ, et al. Reproducibility of 2 liver 2-dimensional shear wave elastographic techniques in the fasting and postprandial states. *J Ultrasound Med.* 2019;38(7):1739–45.
69. Koizumi Y, Hirooka M, Kisaka Y, Konishi I, Abe M, Murakami H, et al. Liver fibrosis in patients with chronic hepatitis C: noninvasive diagnosis by means of real-time tissue elastography—establishment of the method for measurement. *Radiology.* 2011;258(2):610–7.

# Chapter 42

## Interpretation of Shear Wave Propagation Maps (Elastogram) Using Transient Elastography



Sebastian Mueller, Johannes Mueller, and Omar Elshaarawy

### Introduction

Transient elastography relies on a transient mechanical vibration which is used to induce a shear wave into the tissue [1, 2]. For more details, see also book section II “Techniques to measure liver stiffness.” The propagation of the shear wave is tracked using ultrasound in order to assess the shear wave speed from which the Young’s modulus is deduced under the assumption of homogeneity, isotropy, and pure elasticity. Transient elastography gives a quantitative one-dimensional (i.e. a line) image of tissue stiffness. The progression of the shear wave is imaged as it passes deeper into the body using a 1D ultrasound beam. The ultrasound images per time are then displayed in a two-dimensional diagram which is called shear wave propagation map or **elastogram**. From the elastogram, the shear wave speed is automatically derived with software-based algorithms and converted into the Young’s modulus or liver stiffness.

In ca. 80%, valid and automated measurements are obtained using TE. There have been several reasons for the great success of TE worldwide. First, the learning curve for the operator is fast, second, no dedicated ultrasound knowledge is required, and third, the device uses an automatic algorithm to decide whether the shear wave speed and hence the LS is calculated or not. With a few exceptions, this allows for reliable and reproducible measurements and to compare the results within a patient in follow-up studies and between different institutions. It is also a reason why TE is preferred for multicenter or pharmacological studies.

---

S. Mueller (✉) · J. Mueller · O. Elshaarawy  
Department of Medicine and Center for Alcohol Research and Liver Diseases,  
Salem Medical Center, University of Heidelberg, Heidelberg, Germany  
e-mail: [sebastian.mueller@urz.uni-heidelberg.de](mailto:sebastian.mueller@urz.uni-heidelberg.de); [oelshaarawy@liver.menofia.edu.eg](mailto:oelshaarawy@liver.menofia.edu.eg)

## Normal Elastogram

Unfortunately, the elastogram (see Fig. 42.1) is rarely studied in detail although it provides important information about the shear wave propagation within the liver tissues. Once a measurement has been done and a LS value is provided by the device there are still opportunities of completely false or not accurate measurements that could be validated by inspection of the elastogram. It is understandable that the manufacturer resists to allow manual corrections since the objective, automated LS calculation is one of the success stories of the FibroScan device. Nevertheless, some experienced hepatologists would find it very helpful to manually adjust e.g., the aligning of the slope of the regression analysis in cases of dispersions. There are sometimes clinical cases of heavily sick patients where only a few (3 to 4 valid measurements) are obtained while other diagnostic alternatives such as biopsy or CT are restricted for reasons such as ethics, time restrictions, anatomy, or renal failure. In such desperate moments, a few (less < 10) measurements with accurate elastograms would be a tremendous help. Of course, the responsibility in such cases should not be with the manufacturer but the performing clinician and this should also be saved to the measurement protocol.

In Fig. 42.1a, a normal elastogram is shown. The M-mode ultrasound image demonstrates a typical liver texture resolved over time and the A-mode shows the real-time ultrasound signal which is a linear ultrasound attenuation (decay) without disturbances in this example. Although the initial compression wave is not well seen and slightly dispersed, a beautiful shear wave is generated, actually followed by other late shear waves. Figure 42.1b demonstrates a simplified elastogram scheme (compression wave in gray and shear wave in red) that is used within this chapter to visualize potential shear and compression wave perturbances. Although the elastogram seems to be straight forward it is actually a rather complex recording of wave patterns over time that can be prone to wave diffractions, reflections, superpositions, and dispersion not always easy to interpret even for experts in acoustic imaging. The ultrasound radio frequency (RF) signal should actually be not able to detect compression waves, as they travel at the same speed of 1450 m/s in water/liver. It should be noted that there are still discussions, to what extent the first wave is indeed a compression wave. Since compression waves are as fast as the ultrasound imaging signal, there are also good arguments that the first wave is more an image artifact of the compression shear wave. It has been also shown that in the near field of a point source vibrator, longitudinal compression waves can be observed propagating at the same speed as the shear wave [3]. In contrast, normal speed of shear waves in the liver range between 1 and 1.1 m/s. Figure 42.1c shows another perfect elastogram with normal compression and shear waves in a patient with liver cirrhosis. The resulting liver stiffness of  $73.9 \pm 2.8$  kPa is shown in orange while the CAP is  $217 \pm 30$  dB/m is given in light blue. The regression



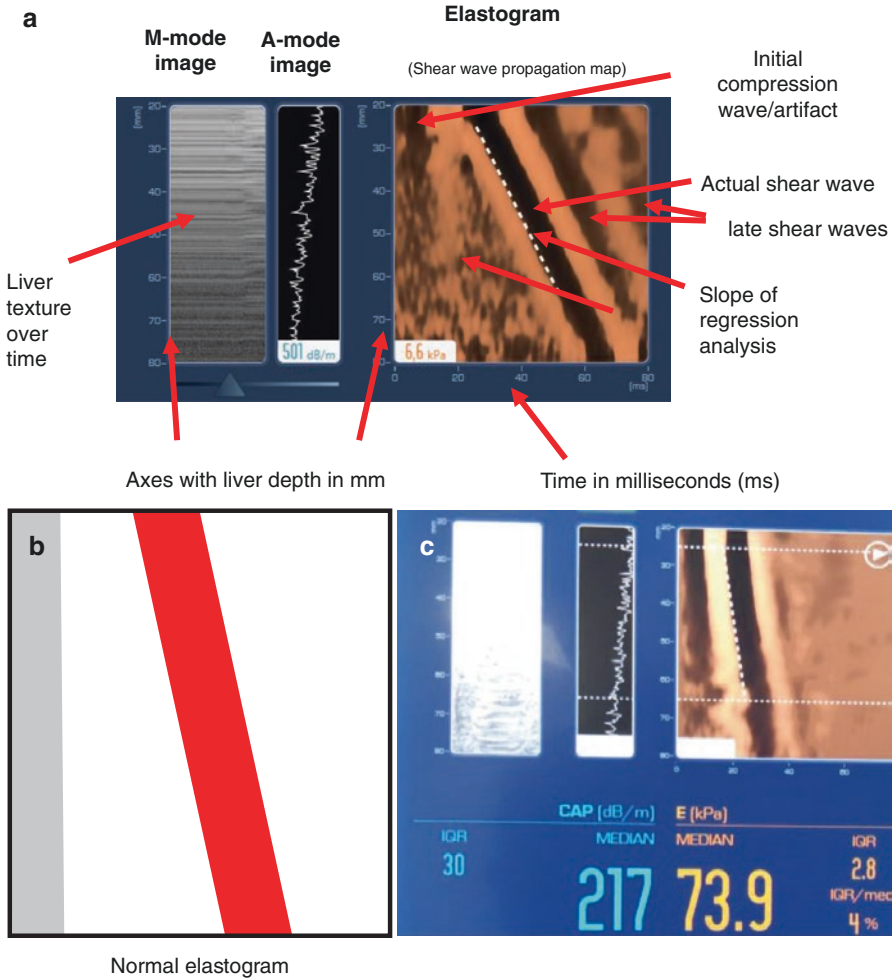


**Fig. 42.1** Normal elastogram. (a) Elastogram (or shear wave propagation map) with details, (b) scheme of normal elastogram, (c) normal elastogram in patient with manifest cirrhosis in the absence of fat (low CAP). While the initial compression travels at 1450 m/s in liver/water, shear wave speed in normal liver is more than 1000 times slower ranging between 1 and 1.1 m/s. Therefore, radio frequency ultrasound signals are able to measure the speed of shear wave propagation. Duplicated shear waves are displaced by 20 ms and due to late shear waves induced by the 50 Hz TE-probe vibration

algorithms also show a perfectly aligned regression line (dashed white line). The high shear wave propagation speed indicates a high liver stiffness in the cirrhotic range. The absence of any steatosis (low CAP value) is also in line with the presence of cirrhosis.

## Interpretation of A and M-Mode Images for Quality Control

First, A and M-mode images should be inspected to assure a high-quality LS measurement (Fig. 42.2). In Fig. 42.2a, an optimal M-mode with typical liver texture and a good A-mode image with linear decay is depicted. In contrast, in Fig. 42.2b, the decay of the A-mode is not linear which will increase the risk of nonvalid measurements or lower quality. Figure 42.2c demonstrates an example of M and A-mode at an improper measuring side due to interfering vascular structures and corresponding perturbations. Likewise, a disruption is caused as shown in Fig. 42.2d, most likely caused by a smaller vessel. Figure 42.2e, f show nonlinear A-mode images in two cases of non-perpendicular probe positioning (see also Fig. 42.3). Here, A-mode inspection is especially important as wrong probe positioning can often not be seen in the final elastogram. Taken together, an optimal A and M-mode image should be obtained prior to initiate LS measurements.

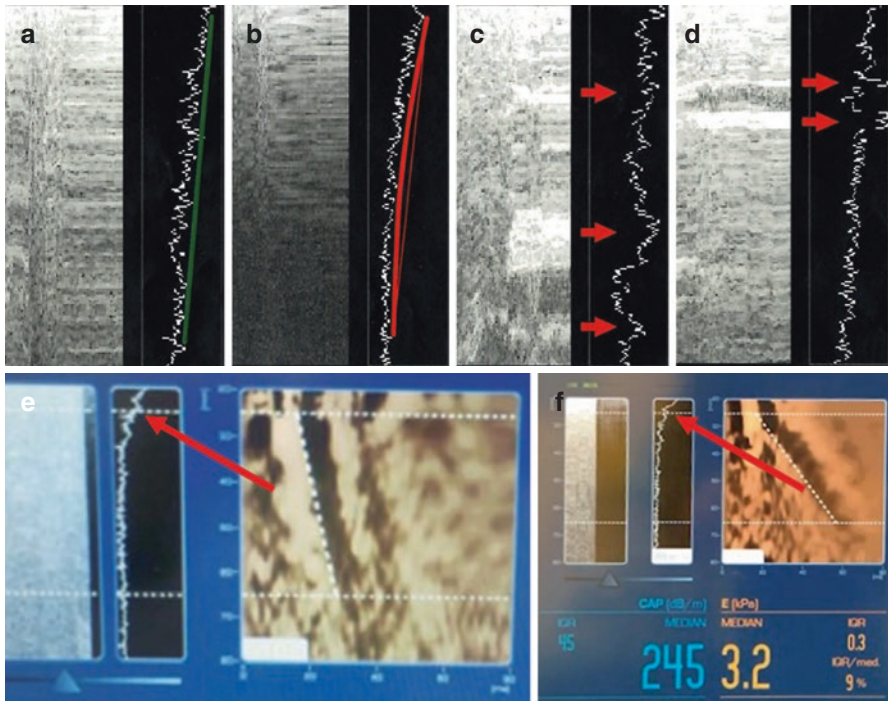


**Fig. 42.2** A-mode and M-mode images are critical for quality confirmation of LSM. **(a)** Optimum A-mode image with linear decay. **(b)** Decay of the A-mode image is not linear which will increase the risk of invalid LSM. **(c)** and **(d)** Perturbation due to vascular or nodular obstacles (red arrows). **(e)** and **(f)** Nonlinear decay of A-mode due to wrong probe positioning



## Probe Positioning

Incorrect LS values can be obtained due to wrong probe positioning. It is important to mention that these inaccuracies are not always visible in the elastograms but can severely impact them. Figure 42.3a represents an optimum measurement where the probe was positioned perpendicularly to the skin surface. The A-mode is homogenous and shows a linear decay. In contrast, Fig. 42.3b shows an incorrect measurement in the same patient due to non-perpendicular placement of the probe which results in nonlinear decay of the A-mode. LS is overestimated by more than 50% although the elastogram looks fine. Figure 42.3c explains the impact of wrong probe positioning on LS measurement. As a matter of fact, the shear wave tends to propagate perpendicularly to the surface of the rib cage. It is important that the probe be perpendicular too so that the two axes are parallel. If not, the measured shear wave speed is overestimated. A simple geometrical model shows that the measured speed is the real shear wave speed divided by the cosines of the angle in between the two axes.

Ribs can also cause perturbations with the LS assessment that are not easily visible in the elastogram. In such cases, the superimposition of two shear waves may be observed. Figure 42.4a shows a normal measurement whereas Fig. 42.4b shows the measurement of the same patient with probe positioning too close to the rib. LS is doubled and only slight compression and shear wave perturbations are visible. Therefore, ribs should be avoided from the very beginning by manual palpation. LS measurement errors due to wrong probe positioning are also listed in Table 42.1 together with potential explanations and typical examples. A new FibroScan software has been developed which includes improved algorithms that can distinguish the primary shear wave from rib echoes.

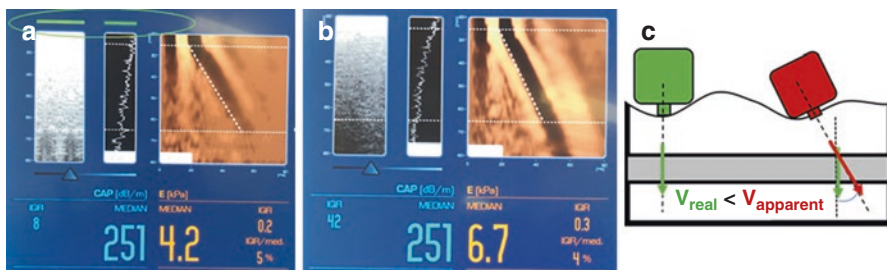


**Fig. 42.3** Effect of non-perpendicular probe positioning on LSM by TE. (a) Correct LSM. The probe was positioned perpendicularly to the skin surface. The A-mode image is homogenous and shows a linear decay. (b) This figure is showing an incorrect measurement of the same patient using a non-perpendicular placement of the probe. (c) Scheme to explain overestimation of shear wave propagation speed due to non-perpendicular probe positioning

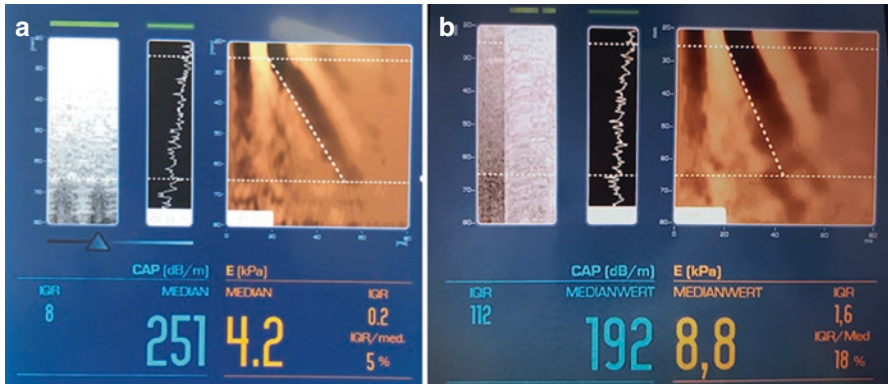


**Fig. 42.4** (a) Normal versus (b) rib effect on elastogram. A too close positioning of the TE probe to the rib can cause a superimposed shear wave by the rib and eventually lead to LS overestimation

**Table 42.1** List of various elastograms, affected compression or shear waves and explanations

Elastogram feature	Compression wave	Shear wave	Explanation	Figures	LS overestimation
<i>Normal</i>	Normal	Normal		Fig. 42.1	
Duplication	Normal	Duplicated	Late shear wave	Figs. 42.1 and 42.7	
<i>Probe positioning</i>					
Not perpendicular	Normal or disturbed	Normal or disturbed	Wrong calculation of shear wave speed (see Fig. 42.3c)	Figs. 42.2 and 42.3	Yes
Rib contact	Normal	Normal	shear wave super positioning	Fig. 42.4	Yes
XL vs. M probe	Normal or disturbed	Normal or disturbed	1. Regression algorithm of M probe starts in the extrahepatic, compressed part of shear wave 2. M probe too weak, leading to dispersion and conical shape with too steep alignment of regression algorithm	Fig. 42.5	Yes (by M probe)

**Table 42.1** (continued)

Elastogram feature	Compression wave	Shear wave	Explanation	Figures	LS overestimation
<i>Disturbances of shear or compression waves or both</i>					
Compression-shear wave conversion	Normal	Normal	Liquid phases (ascites) do not transmit shear waves. After passing to normal tissue, the compression wave is converted back to shear waves. Both ascites and intraabdominal pressure do not affect shear wave speed in the liver [4]	Fig. 42.8	Yes
Interruptions of shear and compression waves	Normal or interrupted	Normal or interrupted	A target (vessel, calcification) can interrupt the wave propagation	Fig. 42.9	
Reflections of shear waves	Normal	Reflected	Shear wave hits a target (e.g. bone) that causes reflection	Fig. 42.10	
Bifurcation of shear waves	Normal	Bifurcated	Offspringing compression wave or superimposed shear wave which can cause wrong alignment by the regression algorithm	Fig. 42.11	Yes
Dispersion of shear and compression waves	Normal or dispersed	Normal or dispersed	Heterogenous tissue structures or fat can cause dispersion. Dispersion of compression waves is most likely imaging artifacts	Fig. 42.12	Yes
Displacement or reflection of compression waves	Displaced/ reflected	Always disturbed	A displaced compression wave (most likely through back reflection) causes severe disturbances of the shear wave	Fig. 42.13	Yes

## Probe Selection

Another important issue is the probe selection. Since this is discussed in more detail in the chap. 44 entitled “Use of XL probe in obese and non-obese patients” in this book section, it is only briefly mentioned here for completeness. Figure 42.5 shows a representative elastogram obtained by either by the M probe (Fig. 42.5a) or XL

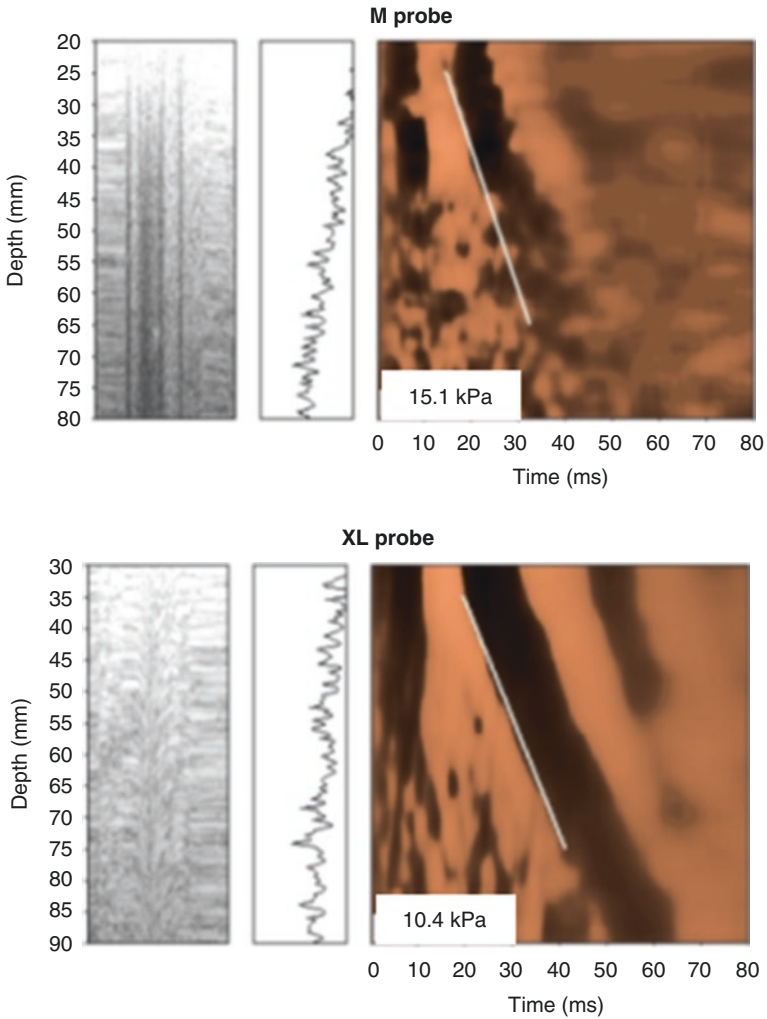


**Fig. 42.5** Representative elastogram obtained by (a) the M probe and (b) XL probe. The less energetic M probe causes shear wave dispersion and overestimation of LS. In addition, the M probe algorithm does not penetrate deeply enough into liver tissue in obese patients causing a premature alignment of the regression algorithm still in the compression section

probe (Fig. 42.5b). It can be seen that the M probe initiated the shear wave in the extrahepatic region of this obese patient causing overestimation of LS. Moreover, the shear wave of the less energetic M probe is rapidly attenuated and dispersed which further contributes to LS overestimation. In addition, the depth of the M probe is smaller. In contrast, in all of these patients the XL probe yielded a well-defined shear wave and correctly calculates the LS.

## Elastogram Disturbances: Overview

There are common disturbances to be seen in elastograms that can involve either compression and shear waves or just shear waves alone. Figure 42.6 provides an overview of these typical disturbances. Figure 42.6a shows a normal elastogram for comparison. Figure 42.6b can be called a **duplication**. It actually represents a normal elastogram but shows on the right of the primary shear wave another later shear wave typically 20 ms displaced (due to the 50 Hz vibration of the TE probe). It most likely is caused by a longer excitation due to poor damping. Other examples of a duplication are shown in Figs. 42.1 and 42.7. Figure 42.6c–e demonstrates three forms of **shear wave interruptions** that are all involving both compression and shear waves. Main reasons are inhomogeneities in the liver due to vessels, calcifications, or nodules. Figure 42.6c is typical for the presence of a vessel. Figure 42.6f shows a reflected shear wave without obvious perturbations of the compression wave. The shear wave is likely to have rebounded at the lower surface of the liver. These **reflections** can be due to compartment borders e.g., bone which cannot be passed by shear waves. Another important feature is the **bifurcation** of a shear wave that usually only involves the shear wave. It seems to be due to transformation of a shear wave into a compression wave caused by liver tissue inhomogeneities for still poorly understood reasons. Figure 42.6h, i represent dispersions of shear waves

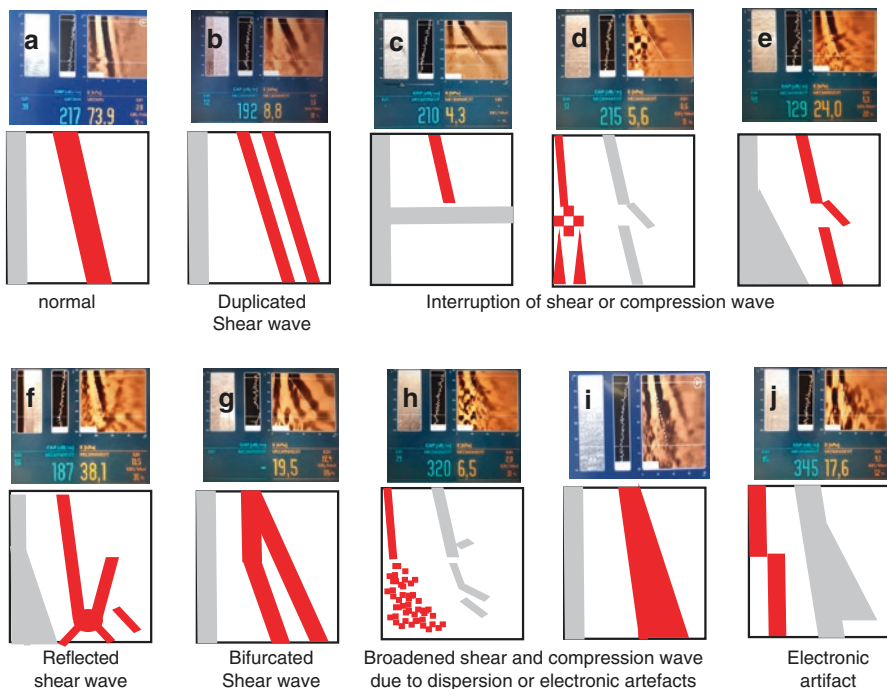
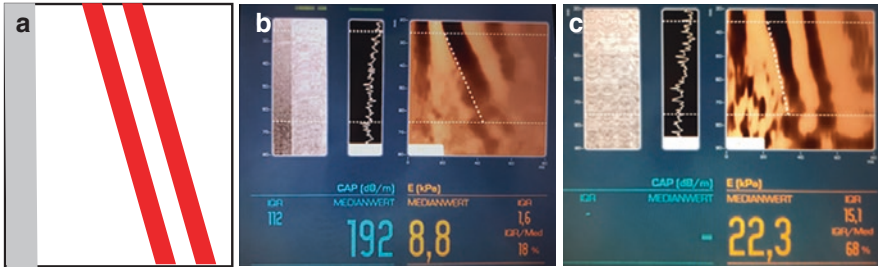


Fig. 42.6 Overview of various elastograms with normal variants and disturbances



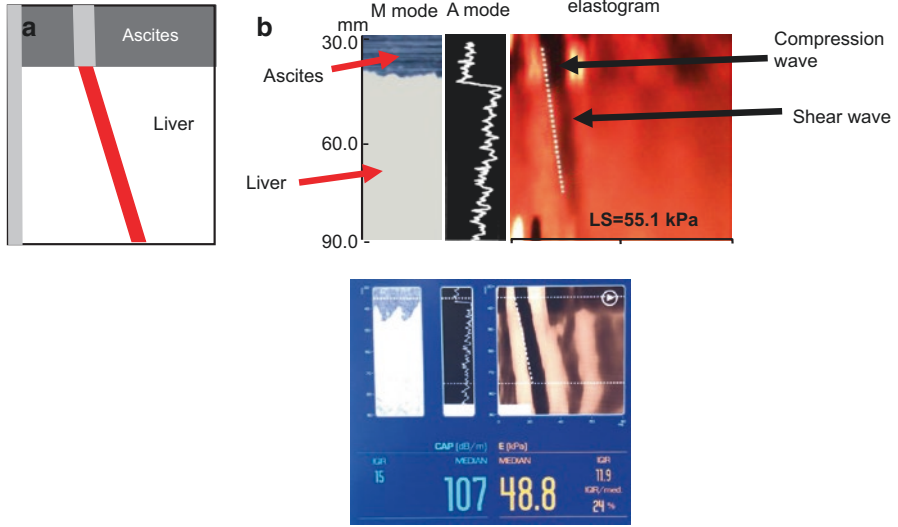
**Fig. 42.7** Duplication of shear waves

most likely due to evenly distributed perturbations within the liver tissue. As already mentioned above, it is questionable whether the here called compression is indeed reflecting the real compression wave and broadening of these elastogram structures could also be due to electronic artifacts. Finally, Fig. 42.6j shows a sharp compression wave displacement most likely caused by a compression wave reflection. This will always cause shear wave perturbations and, consequently, affect the LS measurement.

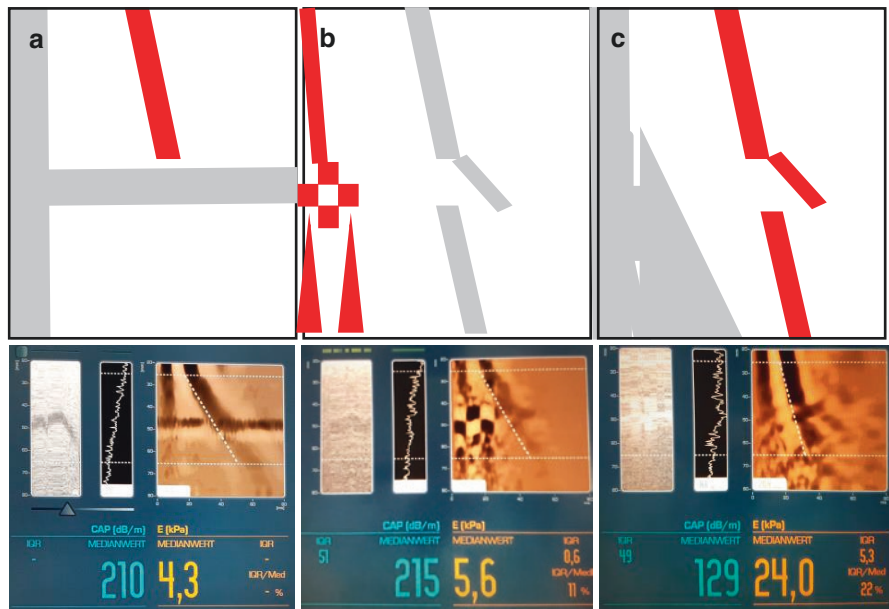
## Detailed Discussions of Shear Wave Disturbances

Table 42.1 lists all disturbances, references example figures, and provides explanations. An important feature is the **conversion of compression and shear waves** when passing liquid and tissue phases as already discussed in chap. 43 entitled “LS measurement in patients with hepatic vs non-hepatic ascites” in this book section. As shown in Fig. 42.8 and in the chapter on ascites, initial compression waves pass through or vibration passes around liquid phases and are then converted to shear waves which further propagate through liver tissue. Liquids do not have any shear strength and so a shear wave cannot propagate through a liquid. When they reach the surface they cause horizontal shaking. As already discussed in the ascites chap. 43 and based on phantom measurements [4], the liquid phase and the intraabdominal pressure do not alter the LS. Moreover, hepatic shear wave propagation speed is identical in the presence or absence of surrounding ascites and elevated intraabdominal pressure [4]. Although this has not been studied in more detail, this observation could have important implications for shear wave propagation in tissues such as liver since many vascular structures of different size can be hit. It is assumed that an enrichment of vascular structures such as the congested liver could cause an elevation of shear wave speed by multiple conversions between compression and shear waves. Moreover, such conversions could be responsible for the wave dispersions seen in Fig. 42.6h, i.

Figure 42.9 demonstrates various examples of shear **wave interruptions** by propagation obstacles in the liver tissue. They can easily be identified and cause incorrect LSM. Notably, interruptions can be already detected in the M-mode



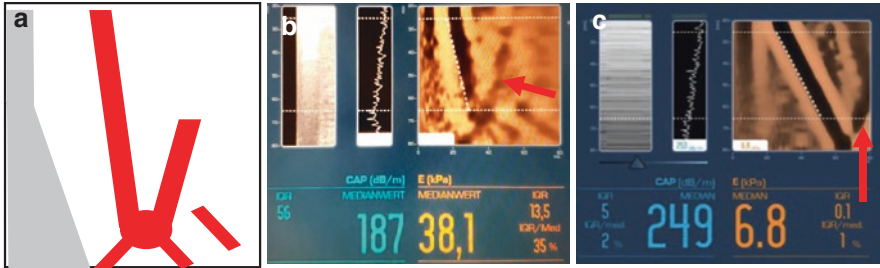
**Fig. 42.8** Conversion between compression and shear waves at a liquid-to-solid interface. A compression waves travels through the ascites layer and is converted into a shear wave when entering solid liver tissue. In contrast, shear waves cannot pass through liquids



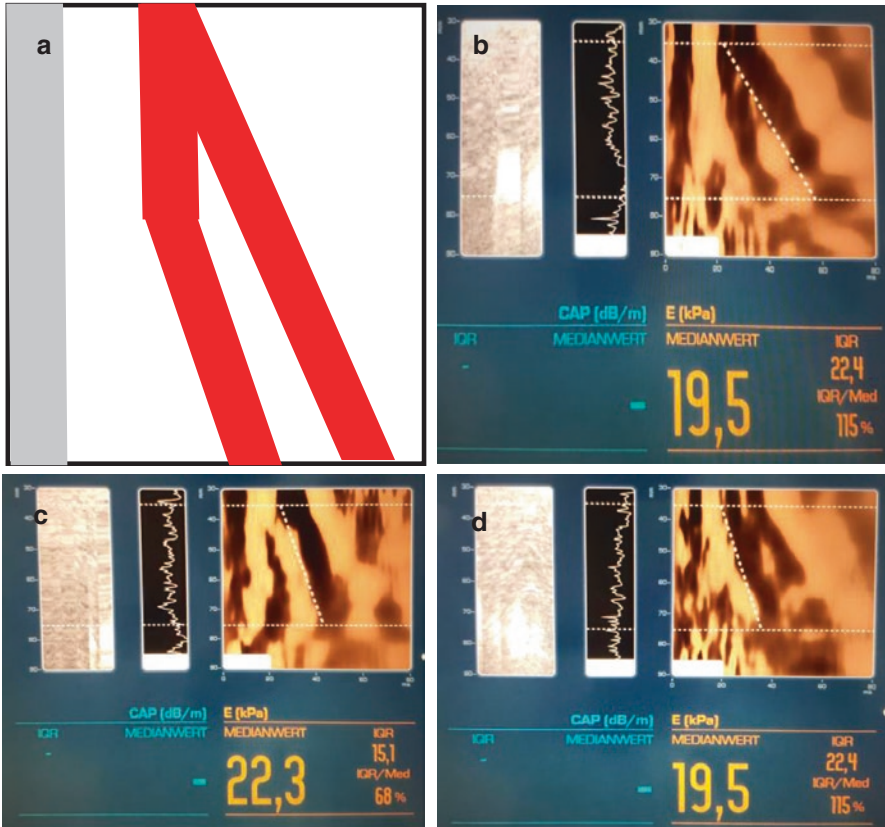
**Fig. 42.9** Various examples (a–c) of shear wave interruptions both of compression and *shear* waves. Note that the term compression wave may not be completely correct since only an image artifact of the compression wave is recorded. Imaging of compression waves may be impossible by ultrasound since they travel at the same speed as the ultrasound RF signal used for imaging



image and seem to be always involved in compression wave perturbations. In contrast, only shear waves seem to be affected by **reflections** (Fig. 42.10) following typical physical laws of wave propagation e.g., at rapid density changes. Reflections can but not necessarily cause wrong calculations of LS. **Bifurcations**



**Fig. 42.10** Reflections of shear waves. Typically, no disturbances of compression waves are observed



**Fig. 42.11** Bifurcation of shear waves. These disturbances are caused due to offspringing compression waves and are commonly leading to LS overestimation. Correct shear wave alignment is done in (b) and (c), while the slope is calculated wrongly in (d) from an interfering compression wave artifact



(Fig. 42.11) seem to be caused by rib echoes. Bifurcations are a severe and common reason for LS overestimation and can be falsely taken for a shear wave by the device-internal regression algorithm. Here, the above-mentioned expert mode with manual adaptation of the shear wave slope would improve LSM performance in some patients. Figure 42.11a, b shows the correct slope alignment to the shear wave. In Fig. 42.11c, however, the slope has been aligned to an offspringing compression wave and severely overestimates LS. **Broadening of waves** can occur both for compression (Fig. 42.12a–c) or predominantly shear waves (Fig. 42.12d, e). They continuously lead to overestimation of LSM since the regression algorithm will be aligned to the steeper left rim of the broadened shear wave. Again, manual adaptation could improve LSM in such rather common cases. Figure 42.13 seems to be a mere electronic artifact shown as an abrupt **displacement** of the compression wave. Such disturbances should be either taken off the LSM or allow for manual adaptation.

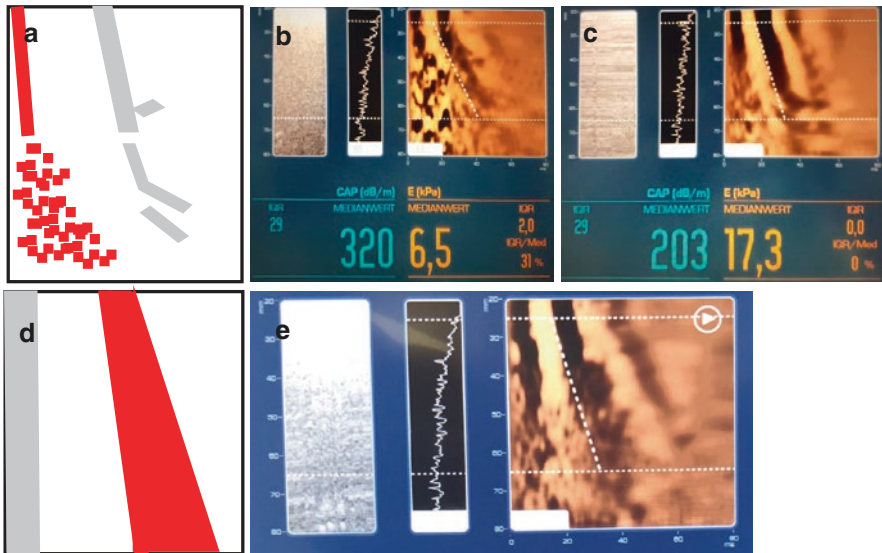


**Fig. 42.12** Broadening of (a–c) compression waves and (d–e) shear waves. Broadening of shear waves is mostly due to dispersions that can easily lead to LS overestimation. Broadening of compression waves may be due to image artifacts

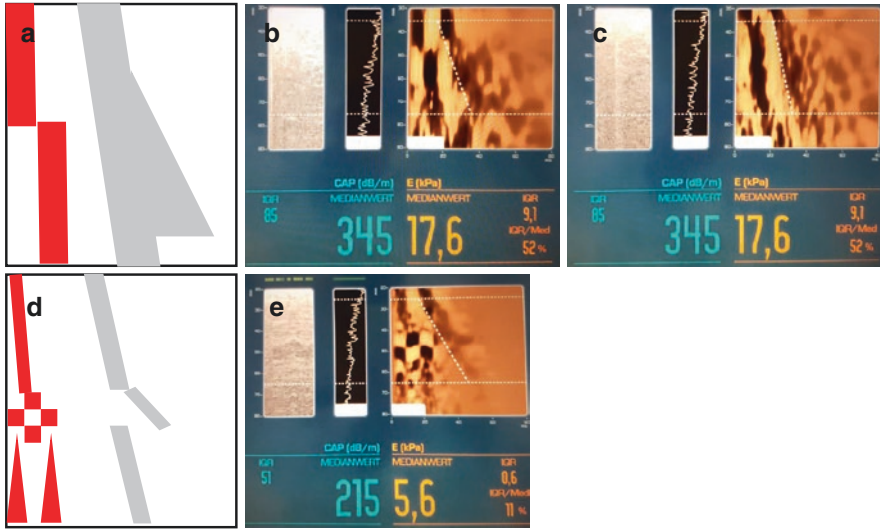


**Fig. 42.13** Various examples of compression wave displacements causing shear wave dispersion and LS overestimation. Compression wave displacements are most likely caused by electronic imaging artifacts

## Conclusions

Taken together, this chapter lists and classifies for the first time typical perturbations of compression and shear waves as regularly seen in elastograms of a FibroScan device. While incorrect probe positioning is usually not visible in elastograms (but only in M and A-mode images), interruptions, reflections, broadenings, displacements, and bifurcations are easily detectable. Namely dispersions and bifurcations are common disturbances of the shear wave leading to LS overestimation. Here, a manual adaptation in a so-called expert mode should further help to improve LSM by TE.

## References

1. Sandrin L, Cassereau D, Fink M. The role of the coupling term in transient elastography. *J Acoust Soc Am.* 2004;115(1):73–83.
2. Sandrin L, Fourquet B, Hasquenoph J-M, Yon S, Fournier C, Mal F, et al. Transient elastography: a new non-invasive method for assessment of hepatic fibrosis. *Ultrasound Med Biol.* 2003;29(12):1705–13.
3. Sandrin L, Cassereau D, Fink M. The role of the coupling term in transient elastography. *J Acoust Soc Am.* 2003;115(1):73–83.
4. Kohlhaas A, Durango E, Millonig G, Bastard C, Sandrin L, Golriz M, et al. Transient elastography with the XL probe rapidly identifies patients with non-hepatic ascites. *Hepat Med.* 2012;4:11–8.

# Chapter 43

## Liver Stiffness Measurement in Patients with Hepatic Versus Non-hepatic Ascites



Sebastian Mueller

### Introduction

The diagnosis of the underlying cause of ascites is still a difficult challenge. The disease spectrum potentially leading to ascites is broad and ranges from various liver diseases such as cirrhosis, liver cancer, hepatic venous occlusion to non-hepatic entities like pancreatitis, tuberculosis, serositis, portal vein thrombosis, and peritoneal carcinomatosis. Although decompensated liver cirrhosis has been established as the major cause of ascites in ca. 80% [1], there remains a significant number of patients that often undergo long and intensive clinical examinations before the non-hepatic cause can be established.

At present, unfortunately, clinical tools to rule out liver cirrhosis are not specific and sensitive enough to make a precise diagnosis. About 40% of patients with cirrhosis are asymptomatic and routine laboratory tests are normal [2, 3]. Likewise, modern ultrasound devices and other imaging techniques allow to establish the diagnosis of cirrhosis only in the presence of so-called definite or sure signs of cirrhosis. These signs include a nodular aspect of the liver surface or a recanalized umbilical vein but not e.g. an enlarged spleen [4]. The diagnostic procedure is further complicated in some patients since ascites can cause sparseness of hepatic veins in imaging studies that may be suggestive of cirrhosis. Although the serum-ascites albumin gradient has been an improvement compared to the old exudate-transudate concept in discriminating ascites due to portal hypertension from other causes, this parameter can be modulated by superinfections [5].

---

S. Mueller (✉)

Department of Medicine and Center for Alcohol Research and Liver Diseases, Salem Medical Center, University of Heidelberg, Heidelberg, Germany  
e-mail: [sebastian.mueller@urz.uni-heidelberg.de](mailto:sebastian.mueller@urz.uni-heidelberg.de)

## Validation of LSM in Liver-Mimicking Phantoms Surrounded by Water

It has been demonstrated in liver-ascites mimicking copolymer-in-oil phantom surrounded by water that this artificial ascites lamella does not disturb the physical measurement of LS by TE [6]. All phantoms had three different degrees of stiffness (4.8, 11 and 40 kPa) representing various stages of fibrosis (F0, F3 and F4) [7]. Figure 43.1a, b shows the elastographs and M mode results of two representative measurements using the 4.8 and 40 kPa phantoms and a ca. 20 mm water lamella between XL probe and phantom. First, clear shear wave formation can be seen despite the presence of water which, secondly, corresponds well to the phantom stiffness obtained without ascites. These studies also showed that probe positioning namely angulation towards the phantom is very critical as has been shown for TE in general [8]. A strict perpendicular position of the probe is required to prevent an overestimation of stiffness. Sometimes diffractions and reflections were observed arising from the novel borders generated by water (water-phantom, water-wall of plastic bag) that could alter the shear wave through superposition. Taken together, these phantom studies indicate that a shear wave can be generated in a solid liver-mimicking phantom through a liquid phase that corresponds well with the stiffness obtained under conditions without surrounding water.

## Liver Stiffness Measurement in Patients with Ascites

Using the XL probe, it was recently demonstrated that LS can be determined by TE and remains unaffected by the ascites lamella and increased intra-abdominal pressure, thus allowing to identify patients with non-hepatic ascites. Figure 43.2a demonstrates a successful measurement of LS using the FibroScan device (left panels: M and A mode ultrasound, right panel: elastogram) in a patient with established alcoholic liver cirrhosis and ascites. Despite the massive ascites lamella of 39 mm which is visible in the M mode graph (arrow), a strong shear wave was observed without diffraction artifacts. The rather high LS of 55.1 kPa clearly confirmed liver cirrhosis. Figure 43.2b shows normal LS measurement of 6.4 kPa in a patient with mild ascites due to portal vein thrombosis.

## Ascites and Concomitant Elevated Intra-abdominal Pressure Do Not Increase Liver Stiffness

It has been also ruled out that an increased intra-abdominal pressure affects LS [6]. To study the influence of ascites and intra-abdominal pressure (IAP) of LS, a large animal model of ascites was used [9, 10]. Using a laparoscopic trocar, isotonic saline solution was installed to generate artificial ascites and to modulate the

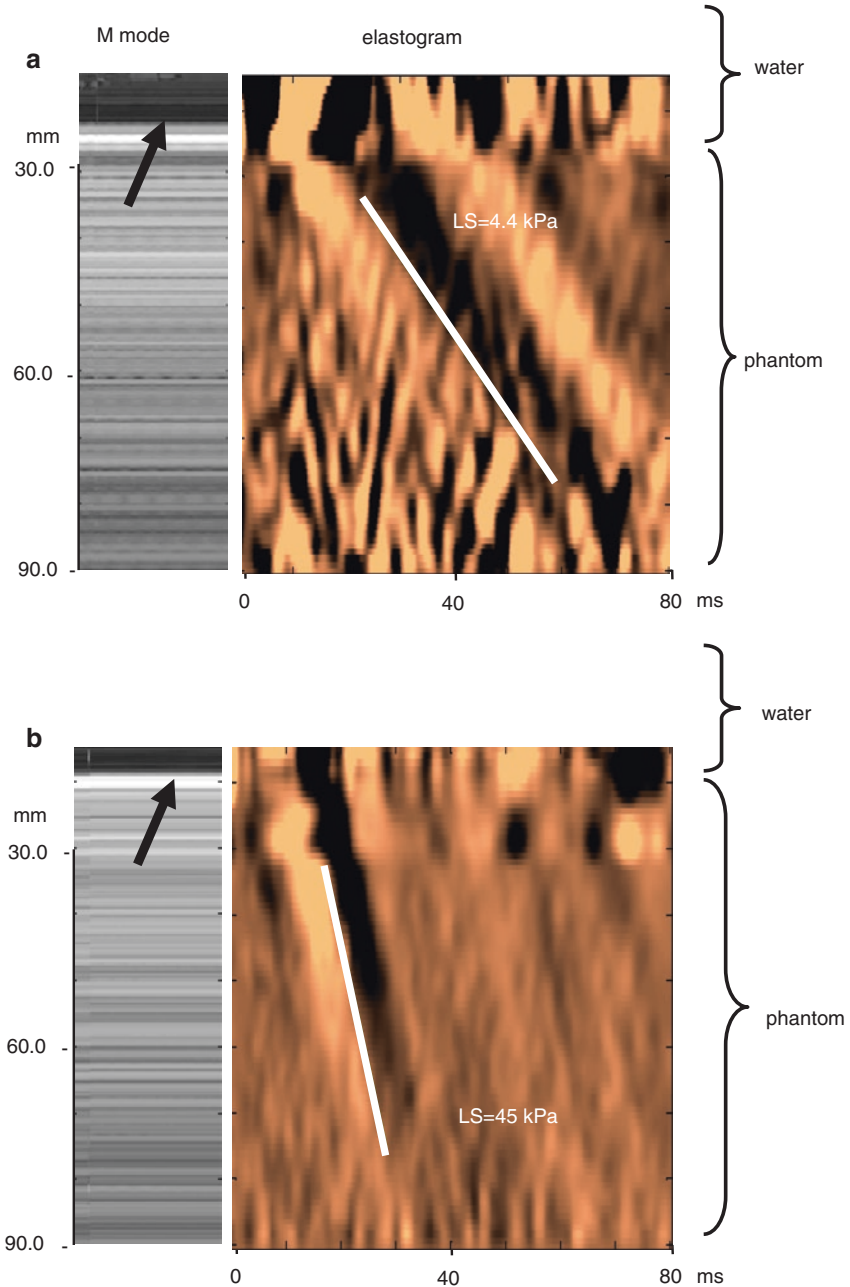


**Fig. 43.1** Shear wave propagation map (elastogram) and stiffness measurements in liver-mimicking copolymer phantoms surrounded by water (modified from [6]). A representative M mode image and elastogram with shear wave propagation is shown in liver-ascites mimicking copolymer-in-oil phantoms surrounded by 20 mm water (arrow) using stiffness of (a) 4.8 kPa and (b) 40 kPa. The shear wave propagation can be clearly seen despite the presence of water. Notably, stiffness corresponds well to the phantom stiffness obtained without ascites. Some wave reflections can be seen in the water phase in the upper panel

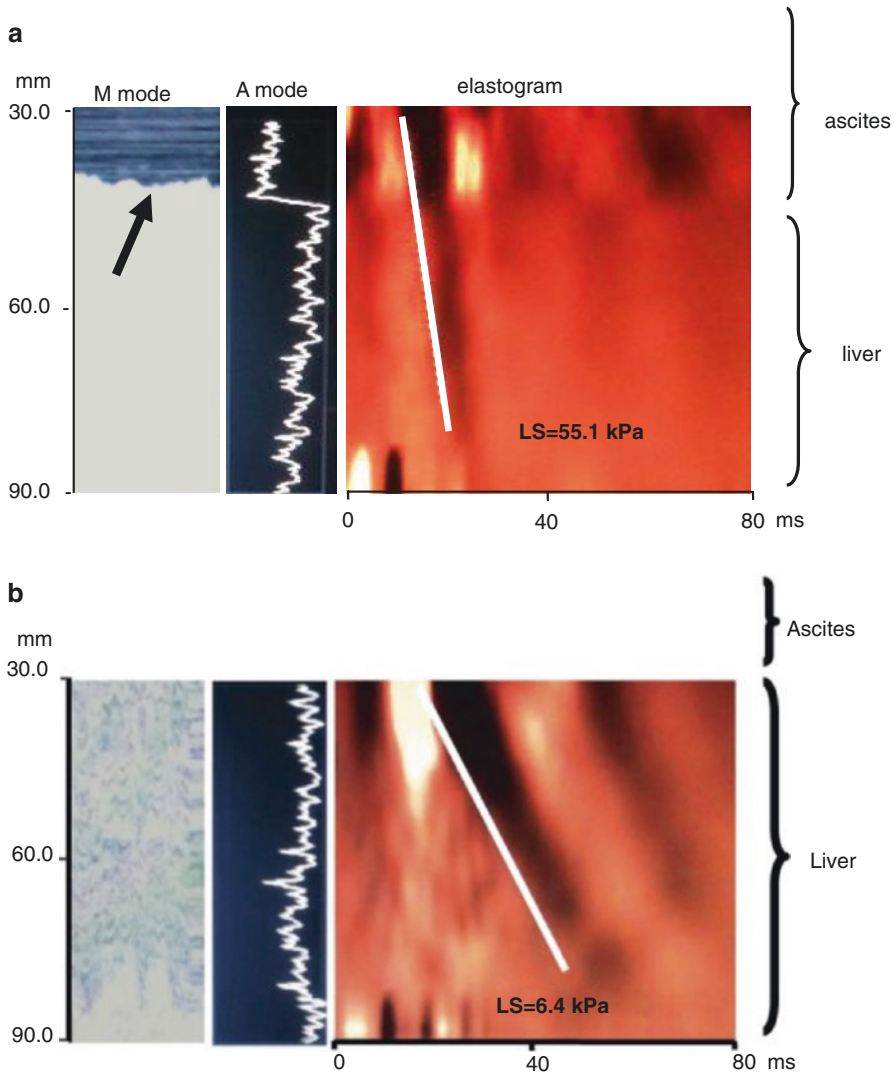


**Fig. 43.2** Example elastograms in patients with (a) hepatic or (b) non-hepatic ascites. (a) Patient with alcoholic liver cirrhosis with a massive ascites lamella of 39 mm using XL probe. Despite ascites which can be seen in the M mode graph (arrow), a strong shear wave is seen corresponding to cirrhotic stiffness values of 55.1 kPa. (b) Example elastogram of a patient with portal vein thrombosis and a smaller ascites lamella of 11 mm shows an almost normal LS measurement of 6.4 kPa

IAP. IAP and central venous pressure (CVP) were continuously monitored. One representative example is shown in Fig. 43.2. IAP continuously increased over 140 min up to 18 mmHg. Importantly, LS did not increase despite a drastically increased IAP. CVP also increased over the time probably to prevent collapse of central veins and to maintain circulation [11, 12]. Similar to the phantom experiments described above, these studies underline that surrounding ascites or increased IAP do not affect LS in the absence of liver congestion (Fig. 43.3).

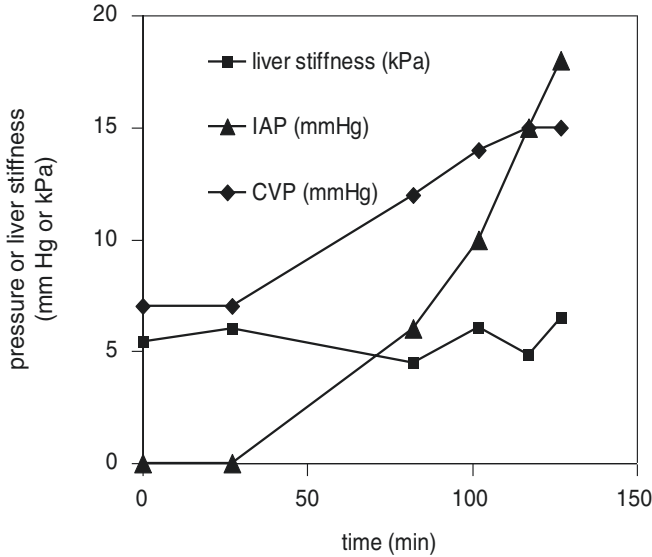


**Fig. 43.3** Elevation of intra-abdominal pressure does not increase liver stiffness in an animal model of ascites (modified from [6]). Using a laparoscopic trocar in narcotized German landrace pigs, isotonic saline solution was installed to generate artificial ascites and to modulate the intra-abdominal pressure (IAP) up to 18 mmHg. LS remained normal despite increased IAP. Note that central venous pressure (CVP) also increased over time to prevent compression of central veins and to maintain blood circulation. LS of each time point is the result of ten measurements. IQR was less than 30% in all measurements. Figure is a representative of three independent experiments

## LSM Identify Patients with Non-hepatic Causes of Ascites

So far and as shown in Table 43.1, three studies have been performed to explore the diagnostic value of LSM for patients with ascites [6, 13, 14]. In the first study, Bota et al. [13] assessed the feasibility of performing acoustic radiation force impulse (ARFI) elastography in patients with ascites and its predictive value for the cirrhotic or non-cirrhotic etiology of ascites. The study included 153 patients with ascites with a mean age of 58.8 years. 75.2% had hepatic ascites, mostly in the context of cirrhosis, while 18.9% had non-cirrhotic ascites. Cirrhosis was ruled out by clinical, ultrasound, endoscopic and/or laparoscopic criteria but could not be clarified in 5.9%. Invalid LSM of 3.2% were seen. Mean LSM were significantly higher in patients with hepatic ascites (3.04 vs 1.45 m/s;  $P < 0.001$ ). Using a cutoff value of 1.8 m/s for predicting ascites in the context of cirrhosis, ARFI had 98.1% sensitivity and 86.2% specificity. The study by Kohlhaas et al. [6] was the first to prove that LS can be measured by TE in patients with ascites by using the XL probe. In fact, LS could be measured in 95.8% with the XL probe and in 45.8% with the conventional M probe. All 24% with non-cirrhotic ascites had an almost normal LS of less than 8 kPa. Patients with hepatic ascites had a LS  $> 30$  kPa.

Another study by Lindner evaluated the predictive value of LSM and SSM in patients with refractory ascites treated with TIPS insertion or receiving

**Table 43.1** Liver stiffness measurements allow discrimination between hepatic and non-hepatic ascites both by TE and pSWE

Study	LS method	Patient number	LS non-hepatic ascites		LS hepatic ascites		LSM failure Ascites lamella (mm)	Valid LSM (%)
			Mean	Cutoff	Mean	Cutoff		
Bota et al., 2011 [13]	ARFI/pSWE	n = 153	n = 29		n = 115			97
Kohlhaas et al., 2012 [6]	TE XL probe	n = 23	1.45 ± 0.59 m/s		3.04 ± 0.70	1.8 m/s		
Lindner et al., 2018 [14]	TE XL probe	n = 20/TIPS	5.4 ± 1.3 kPa	<8 kPa	66.2 ± 13.2 kPa	>30 kPa	>37	>90
					46.8 kPa		>27	>90
		n = 23/paraceteses			55.2 kPa			
	pSWE	n = 20/TIPS			3.21 m/s		>27	>90
		n = 23/paraceteses			3.48 m/s			

LS values and patient characteristics of three studies are shown



conservative therapy [14]. Although the authors concluded that LS and SS cannot be recommended for risk stratification in cirrhotic patients with refractory ascites, it confirmed the valid LSM both using pSWE and TE.

## Conclusion

Ascites should no longer be regarded as exclusion criterion for TE. Liver stiffness can be accurately assessed by pSWE and TE despite the presence of ascites. For TE, the XL probe should be used. It is important to know that surrounding ascites and elevated intra-abdominal pressure is not increasing LS per se. Using TE, a LS < 8 kPa suggests the presence of non-hepatic ascites while a LS > 30 kPa is highly suggestive for hepatic ascites. Using pSWE, a cutoff value of 1.8 m/s predicts ascites in the context of cirrhosis. Taken together, LSM is an early diagnostic tool to rapidly identify non-hepatic causes of ascites. It requires further careful clinical, laboratory, endoscopic, or imaging examinations since, in addition to cirrhosis, other rare causes such as liver metastasis or extramedullary hematopoiesis may be present.

## References

1. Runyon BA. Care of patients with ascites. *N Engl J Med.* 1994;330(5):337–42.
2. Naveau S, Perlemuter G, Balian A. Epidemiology and natural history of cirrhosis. *Rev Prat.* 2005;55(14):1527–32.
3. Mueller S, Sandrin L. Liver stiffness: a novel parameter for the diagnosis of liver disease. *Hepat Med.* 2010;2:49–67.
4. Di Lelio A, Cestari C, Lomazzi A, Beretta L. Cirrhosis: diagnosis with sonographic study of the liver surface. *Radiology.* 1989;172(2):389–92.
5. Runyon BA, Montano AA, Akriviadis EA, Antillon MR, Irving MA, McHutchison JG. The serum-ascites albumin gradient is superior to the exudate-transudate concept in the differential diagnosis of ascites. *Ann Intern Med.* 1992;117(3):215–20.
6. Kohlhaas A, Durango E, Millonig G, Bastard C, Sandrin L, Golriz M, et al. Transient elastography with the XL probe rapidly identifies patients with non-hepatic ascites. *Hepat Med.* 2012;4:11–8.
7. Oudry J, Vappou J, Choquet P, Willinger R, Sandrin L, Constantinesco A. Ultrasound-based transient elastography compared to magnetic resonance elastography in soft tissue-mimicking gels. *Phys Med Biol.* 2009;54(22):6979–90.
8. Sandrin L, Fourquet B, Hasquenoph J-M, Yon S, Fournier C, Mal F, et al. Transient elastography: a new non-invasive method for assessment of hepatic fibrosis. *Ultrasound Med Biol.* 2003;29(12):1705–13.
9. Millonig G, Friedrich S, Adolf S, Fonouni H, Golriz M, Mehrabi A, et al. Liver stiffness is directly influenced by central venous pressure. *J Hepatol.* 2010;52(2):206–10.
10. Millonig G, Reimann FM, Friedrich S, Fonouni H, Mehrabi A, Büchler MW, et al. Extrahepatic cholestasis increases liver stiffness (FibroScan) irrespective of fibrosis. *Hepatology.* 2008;48(5):1718–23.

11. Zink J, Greenway CV. Control of ascites absorption in anesthetized cats: effects of intraperitoneal pressure, protein, and furosemide diuresis. *Gastroenterology*. 1977;73(5):1119–24.
12. Zink J, Greenway CV. Intraperitoneal pressure in formation and reabsorption of ascites in cats. *Am J Phys*. 1977;233(2):H185–90.
13. Bota S, Sporea I, Sirli R, Popescu A, Danila M, Sendroiu M. Value of acoustic radiation force impulse elastography for the assessment of ascites syndrome. *World J Radiol*. 2011;3(8):205–9.
14. Lindner F, Muhlberg R, Wiegand J, Troltsch M, Hoffmeister A, Keim V, et al. Predictive value of liver and spleen stiffness in advanced alcoholic cirrhosis with refractory ascites. *Z Gastroenterol*. 2018;56(6):561–8.

# Chapter 44

## Use of XL Probe in Obese and Non-obese Patients



Omar Elshaarawy and Sebastian Mueller

### Introduction

Transient elastography (TE) is the most popular and rapid tool to measure liver stiffness. It reliably allows to diagnose cirrhosis or exclude significant fibrosis when performed in an appropriate clinical setting and optimum conditions [1, 2]. However, type and position of the probe and operator experience can have an impact TE [3–6]. Currently, Echosens has a spectrum of three probes (S, M, and XL) for liver stiffness measurements and one dedicated spleen stiffness probe. An enlarged skin-capsular distance and thoracic fold measurements are important determinants of LSM failure. The classic FibroScan M probe is impaired by measurement failure rates reaching 8% in overweight patients and 17% in obese patients [7]. Figure 44.1 shows measurement failure rates in a previous study that compared XL and M probe directly [8]. To circumvent this limitation, the manufacturer has developed the XL probe specifically dedicated for obese patients with a skin-liver capsule distance >25 mm. Compared with the classic M probe, the XL probe uses a lower central frequency (2.5 vs 3.5 MHz for the M probe), has a larger tip diameter (12 vs 9 mm), and measures more deeply below the skin surface (3.5–7.5 cm vs 2.5–6.5 cm with the M probe). The XL probe provides a lower rate of measurement failure and a similar diagnostic accuracy than the M probe [8–11]. However, as shown in Fig. 44.2 and as is discussed below, the XL probe results in lower LS values as compared to the conventional M probe. The S probe has a shallower range of measurement

---

O. Elshaarawy · S. Mueller (✉)

Department of Medicine and Center for Alcohol Research and Liver Diseases, Salem Medical Center, University of Heidelberg, Heidelberg, Germany

e-mail: [oelshaarawy@liver.menofia.edu.eg](mailto:oelshaarawy@liver.menofia.edu.eg); [sebastian.mueller@urz.uni-heidelberg.de](mailto:sebastian.mueller@urz.uni-heidelberg.de)

XL probe	M probe			M and XL probes
	Failure	Unreliable	Reliable	
	14.8%	28.0%	57.1%	
Failure 1.6%	1.6%	0%	0%	1.6%
Unreliable 25.3%	6.7%	7.5%	11%	14.3%
Reliable 73.0%	6.4%	20.5%	46.1%	84.1%

**Fig. 44.1** Comparison between M and XL probe. (Modified from Durango E et al., 2013 [8])

acquisition that ranges from 15 to 40 mm and a higher transducer frequency to suit pediatric patients [12]. A Chinese study conducted a comparison between S and M probe in 100 pediatric patients with biliary atresia and recommended the S probe only in pediatric patients with thorax perimeter of <45 cm [13].

## XL Probe

Several studies reported that LSM acquired with XL probe are 1–2 kPa lower than those for M probe. In 2014, a study conducted by Şirli et al. [14] with 216 patients with chronic liver disease, paired measurements were performed using the M (3.5 MHz) and XL (2.5 MHz) probes in the same session for all patients. They were not able to obtain reliable LSM in 127 patients by standard M probe, 10 of them had normal weight, 25 of them were overweight, and 92 were obese. Using the XL probe, reliable measurements could be obtained in 80/127(63%) of these patients: 8/10 (80%) of the normal weights, 17/25 (68%) of the overweight, and 55/92 (59.8%) of the obese patients. In 98 patients, reliable measurements were obtained by both M probe and XL probe. The LSM obtained by the XL probe were significantly correlated with those obtained by the M probe (Spearman  $r = 0.789$ ,  $P < 0.00001$ ), but were significantly lower [median 6.4 kPa (range 3.1–53.8) vs 7.7 kPa (range 3.7–69.1), Wilcoxon paired  $t$  test  $P < 0.001$ ]. Şirli and her colleagues concluded that the XL probe underestimated the LSM in comparison to the standard M probe [14].

In another study by Myers et al. [11], XL and M probe were compared in overweight/obese patients with chronic liver disease (either viral hepatitis related or non-viral related as NASH). Measurement failure occurred only in 1% of patients

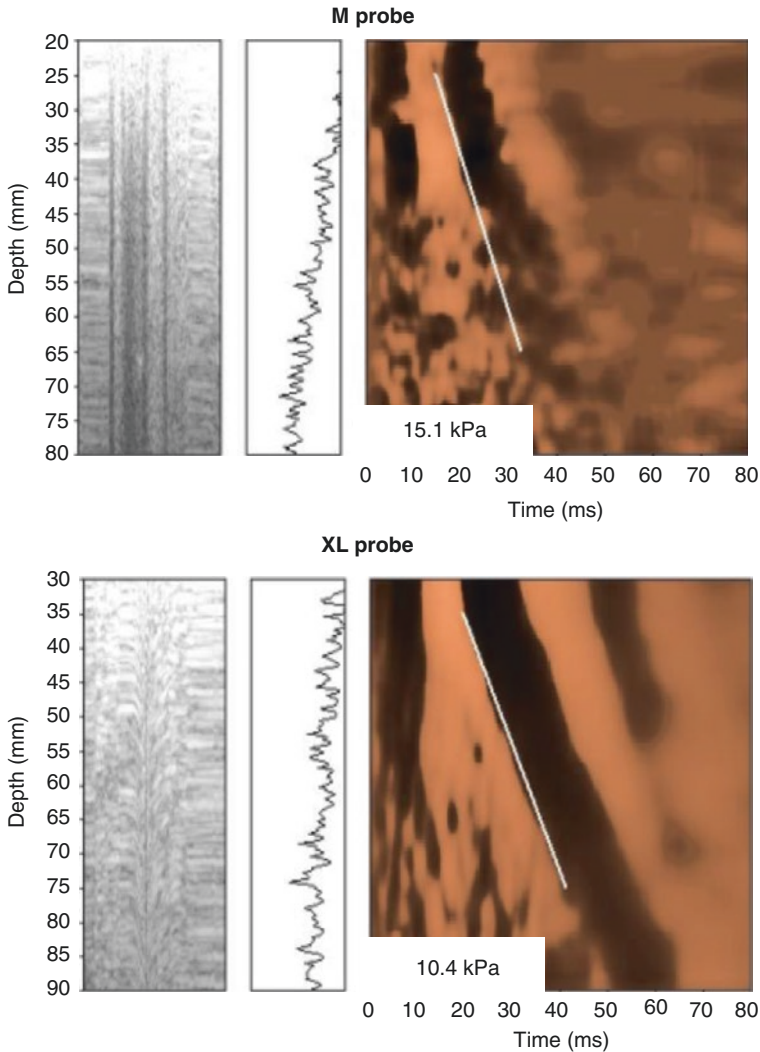


**Fig. 44.2** Representative elastogram obtained by (a) the M probe and (b) XL probe of a patient whose LS markedly differed between the two probes. (a) M probe yields a scattered broad shear wave probably due to diffraction effects. The regression algorithm of the FibroScan device clearly preferred the left rim of the shear wave with the higher velocity eventually leading to an overestimation of LS. (b) In contrast, in all of these patients the XL probe yielded a well-defined shear wave and correctly calculates the LS

with the XL probe as compared with 16% using the M probe. These findings were confirmed in a large cohort-based study from the UK by Harris et al. on 477 patients [15]. Here, 21% had no valid measurements with the M probe. There was a significant difference between the probes in the proportion achieving  $\geq 10$  valid

readings (M versus XL probe: 66.2% versus 90.2%;  $p \leq 0.001$ ) and in their reliability (M versus XL probe: 77.4% versus 98.5%;  $P = 0.028$ ). Unreliable results with the M probe were associated with an elevated BMI [15].

Durango et al. compared XL to M probe to assess liver fibrosis in obese but also non-obese patients [8]. Both probes were also directly compared first in copolymer phantoms of varying stiffness (4.8, 11, and 40 kPa) and then in 371 obese and non-obese patients (body mass index, range 17.2–72.4) from German ( $n = 129$ ) and Canadian ( $n = 242$ ) centers. Liver stiffness values for both probes correlated better in phantoms than in patients ( $r = 0.98$  versus  $0.82$ ,  $P < 0.001$ ). Significantly more patients could be measured successfully using the XL probe than the M probe (98.4% versus 85.2%, respectively,  $P < 0.001$ ) while the M probe produced a smaller interquartile range (21% versus 32%). Failure of the M probe to measure liver stiffness was not only observed in patients with a high body mass index and long skin-liver capsule distance but also in some non-obese patients ( $n = 10$ ) due to attenuating the signal from subcutaneous fat tissue. In contrast with the phantoms, the XL probe consistently produced approximately 20% lower liver stiffness values in humans compared with the M probe. A long skin-liver capsule distance and a high degree of steatosis were responsible for this discordance. Adjustment of cutoff values for the XL probe (<5.5 kPa, 5.5–7 kPa, 7–10 kPa, and >10 kPa for F0, F1–2, F3, and F4 fibrosis, respectively) significantly improved agreement between the two probes from  $r = 0.655$  to  $0.679$ . They concluded that liver stiffness can be measured in significantly more obese and non-obese patients using the XL probe than the M probe. However, the XL probe is less accurate and adjusted cutoff values are required [8]. Detailed data are provided in Tables 44.1 and 44.2.

However, a recent work has shown that liver stiffness results obtained with the M probe in patients with BMI <30 kg/m<sup>2</sup> are not significantly different from those obtained with the XL probe in obese patients (BMI  $\geq 30$  kg/m<sup>2</sup>) [16]. Therefore, by following the EASL-ALEH Clinical Practice Guidelines (M probe in patients with BMI <30 kg/m<sup>2</sup> and XL probe in obese patients) [17], the same diagnostic cutoffs for both probes displayed similar diagnostic accuracy [16]. These results have been confirmed by another

**Table 44.1** Classification of fibrosis stages by LS values using optimized cutoff values (XL probe) (modified from [8])

M probe		XL probe			
LS (kPa)		<5.5	5.5–7	>7–10	>10
<6	61	51	9	1	
6–8	40	18	15	7	
>8–12.5	30		6	16	8
>12.5	34			4	30
	<b>165</b>	69	30	28	38

Cutoff values used for classification of F0, F1–2, F3, and F4 fibrosis stage are <5.5, 5.5–7, 7–10, and >10 kPa. No further cutoff value was introduced for F1 and F2 fibrosis stage, since resolution in this low LS range is very low due to other confounders

**Table 44.2** Agreement between both probes for different cutoff values (modified from [8])

Cutoff values for XL probe (kPa)				Agreement				Discrepancy (> two fibrosis stages)	
F0	F1–F2	F3	F4	Overall	No fibrosis	No advanced fibrosis	Advanced fibrosis	F0–4	F4
<6	6–8	8–12.5	>12.5	0.65	0.62	0.87	0.77	1	0
<6	6–8	8–10	>10	0.60	0.62	0.87	0.77	1	0
<6	6–7	7–10	>10	0.66	0.62	0.87	0.81	2	0
<b>&lt;5.5</b>	<b>5.5–7</b>	<b>7–10</b>	<b>&gt;10</b>	<b>0.68</b>	<b>0.65</b>	<b>0.87</b>	<b>0.81</b>	<b>1</b>	<b>0</b>

Agreement was calculated as ratio of agreeing LS values divided by the sum of all LS values. The left columns describe the chosen cutoff values for fibrosis stages F0–F4. The new optimized cutoff values (lane 5) significantly improve agreement for both low and advanced fibrosis stage. Data were calculated from all 165 patients with reliable LS measurements by both probes [8]

study which also evaluated the automatic probe selection tool included in the recent versions of the FibroScan software [18]. The automatic probe selection tool automatically measures the skin-liver capsule distance and indicates the probe to be used as a function of the patient’s morphology. According to their study results, the authors proposed to use the M probe first in patients with BMI <32 kg/m<sup>2</sup> and eventually switch to the XL probe according to the recommendation made by the automatic probe selection tool, and to use the XL probe in all patients with BMI ≥32 kg/m<sup>2</sup>.

## Conclusion

The XL probe (FibroScan) has been introduced and validated for obese patients with comparable diagnostic accuracy to the standard M probe. The XL probe allows to measure almost 15% more patients than the M probe which shows a 10% smaller interquartile range. LS measurement failure of the M probe is not only observed in patients with high BMI and long skin-liver capsule distance (SCD) but also in some non-obese patients. Since ca. 20% lower LS values are measured in humans compared to the M probe, a correction of cutoff values is advisable, namely in cases of doubt.

## References

1. Sandrin L, Fournier C, Miette V, Millonig G, Mueller S, editors. Fibroscan in hepatology: a clinically-validated tool using vibration-controlled transient elastography. Ultrasonics symposium (IUS), 2009 IEEE international, 20–23 Sept. 2009; 2009.
2. Mueller S, Sandrin L. Liver stiffness: a novel parameter for the diagnosis of liver disease. *Hepat Med.* 2010;2:49–67.

3. Berrutti M, Ciancio A, Smedile A, Brunello F, Bonardi R, Pellicano R, et al. Assessment of liver fibrosis in the clinical setting: something is changing? *Minerva Gastroenterol Dietol.* 2007;53(1):111–4.
4. Lamproye A, Belaiche J, Delwaide J. The FibroScan: a new non invasive method of liver fibrosis evaluation. *Rev Med Liege.* 2007;62 Spec No:68–72.
5. Horvath G. New non-invasive tool for assessment of liver fibrosis: transient elastography. *Orv Hetil.* 2011;152(22):860–5.
6. Murtagh J, Foerster V. Transient elastography (FibroScan) for non-invasive assessment of liver fibrosis. *Issues Emerg Health Technol.* 2006;90:1–4.
7. Castéra L, Foucher J, Bernard P-H, Carvalho F, Allaix D, Merrouche W, et al. Pitfalls of liver stiffness measurement: a 5-year prospective study of 13,369 examinations. *Hepatology.* 2010;51:828–35.
8. Durango E, Dietrich C, Seitz HK, Kunz CU, Pomier-Layrargues GT, Duarte-Rojo A, et al. Direct comparison of the FibroScan XL and M probes for assessment of liver fibrosis in obese and nonobese patients. *Hepat Med.* 2013;5:43–52.
9. Wong VW, Vergniol J, Wong GL, Foucher J, Chan AW, Chermak F, et al. Liver stiffness measurement using XL probe in patients with nonalcoholic fatty liver disease. *Am J Gastroenterol.* 2012;107(12):1862–71.
10. de Ledinghen V, Wong VW, Vergniol J, Wong GL, Foucher J, Chu SH, et al. Diagnosis of liver fibrosis and cirrhosis using liver stiffness measurement: comparison between M and XL probe of FibroScan(R). *J Hepatol.* 2012;56(4):833–9.
11. Myers RP, Pomier-Layrargues G, Kirsch R, Pollett A, Duarte-Rojo A, Wong D, et al. Feasibility and diagnostic performance of the FibroScan XL probe for liver stiffness measurement in overweight and obese patients. *Hepatology.* 2012;55(1):199–208.
12. Lai-Hung Wong G. Transient elastography (Fibroscan®): a new look of liver fibrosis and beyond. *Eur J Hepato Gastroenterol.* 2013;3:70–7.
13. Kim S, Kang Y, Lee MJ, Kim MJ, Han SJ, Koh H. Points to be considered when applying FibroScan S probe in children with biliary atresia. *J Pediatr Gastroenterol Nutr.* 2014;59(5):624–8.
14. Şirli R, Sporea I, Deleanu A, Culcea L, Szilaski M, Popescu A, et al. Comparison between the M and XL probes for liver fibrosis assessment by transient elastography. *Med Ultrason.* 2014;16(2):119–22.
15. Harris R, Card TR, Delahooke T, Aithal GP, Guha IN. The XL probe: a luxury or a necessity? Risk stratification in an obese community cohort using transient elastography. *United European Gastroenterol J.* 2018;6(9):1372–9.
16. Wong VW, Irls M, Wong GL, Shili S, Chan AW, Merrouche W, et al. Unified interpretation of liver stiffness measurement by M and XL probes in non-alcoholic fatty liver disease. *GUT.* 2019;68(11):2057–64.
17. EASL-ALEH Clinical Practice Guidelines: Non-invasive tests for evaluation of liver disease severity and prognosis. *J Hepatol.* 2015;63(1):237–64.
18. Berger A, Shili S, Zuberbuhler F, Hiriart JB, Lannes A, Chermak F, et al. Liver stiffness measurement with FibroScan: use the right probe in the right conditions! *Clin Transl Gastroenterol.* 2019;10(4):e00023.



# Chapter 45

## Comparison of Various Elastographic Techniques for Liver Fibrosis Assessment



Ioan Sporea

### Introduction

Following the development of so many elastographic methods, it is a legitimate question to compare their value for the use in clinical practice. Liver elastography can be performed by measuring shear wave speed either by ultrasound (ultrasound-based elastography) or magnetic resonance imaging (magnetic resonance elastography, MRE). In addition, recently published guidelines, by EFSUMB [1] and WFUMB [2], respectively, classified liver elastography into shear wave elastography (SWE) and strain elastography (SE). Both guidelines underline that only SWE is ready for clinical use for liver fibrosis (LF) assessment, despite the fact that some Japanese studies revealed good results for strain elastography for LF evaluation [3].

In this chapter, we will focus on comparing SWE methods. In all SWE methods, the US probe generates shear waves into the liver that will be used for elastographic measurements. The results are expressed in meters/seconds or in kPa. SWE can be subclassified into transient elastography (TE) and ARFI techniques (using acoustic radiation force impulse): point SWE (pSWE) and 2D-SWE (Real-time SWE) (see Fig. 45.1 and Appendix Tables A.2, A.3 and A.4). For more details, see also book Part II “Techniques to Measure Liver Stiffness.”

---

I. Sporea (✉)

Department of Gastroenterology and Hepatology, “Victor Babeş” University of Medicine and Pharmacy, Timișoara, Romania  
e-mail: [isporea@umft.ro](mailto:isporea@umft.ro)

**Fig. 45.1** Classification of ultrasound-based elastographic techniques

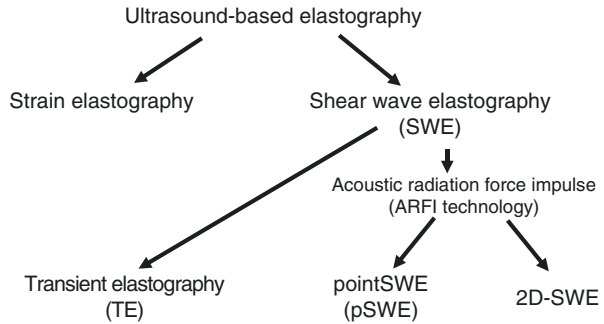


**Table 45.1** Feasibility of different elastography techniques

Study	Elastography method	No. of subjects	Feasibility (%)
Castera. L 2015 [4]	TE	12949	TE: 10903(86.4%)
Sirli. R 2013 [5]	TE	8218	TE: 5827 (71.9%)
Sporea. I 2016 [6]	TE	3235	TE: 3024 (93.5%)
Grădinaru-Tascău. O [33]	SSI	371	SSI: 324 (87.1%)
Bota. S 2013 [12]	TE, ARFI	1163	TE: 1087 (93.4%) pSWE: 1138 (97.9%)
Cassinotto. C 2016 [14]	TE, SSI, ARFI	291	TE: 223 (76.6%) 2D-SWE: 232 (79.7%) pSWE: 236 (81%)
Lee. MS 2018 [34]	TE, SSI, ARFI	94	TE: 74 (78.7%) 2D-SWE: 69 (73.4%) pSWE: 82 (88.3%)

### Feasibility of Different Elastographic Techniques

For ultrasound-based elastographic methods, a very important parameter is the feasibility which is influenced by factors such as obesity, abdominal circumference, or gender. The feasibility of TE using only the M probe (in normal weight subjects) is only 70–85% [4, 5]. Using both M and XL probes, it can reach 93.5% [6]. For pSWE where the measuring box is small, the feasibility is usually higher than 95%. For 2D-SWE where the box is larger, the feasibility is lower. This is especially the case in patients with advanced fibrosis with a rather heterogenous liver. In addition, experienced knowledge in abdominal ultrasound is needed for good acquisitions [5] (see also Table 45.1). As is discussed in Chap. 42, a specific analysis of shear wave propagation maps (elastograms) may further increase feasibility.

### Comparison Between the Techniques

Several studies have been published regarding the comparison between elastographic techniques. Some of these studies were performed considering liver biopsy as the gold standard. In later studies, this was no longer possible due to the sharp

decrease of the number of liver biopsies performed after noninvasive methods appeared on the market [7]. On the other hand, considering that TE was validated and part of many guidelines, including EASL (European Association for the Study of the Liver) guidelines [8], TE was considered as the novel reference method.

EFSUMB and WFUMB guidelines [1, 2] underline that the cutoff values of liver elastography for different stages of fibrosis are system-dependent, and that they must be known for every system used in practice. The cutoff values for the newly developed elastographic techniques (and in this moment all the important ultrasound companies implemented elastographic modules on their systems) have been calculated considering either liver biopsy or TE as the reference method. For more details, see also book Part II “Techniques to Measure Liver Stiffness.”

From a temporal point of view, TE was the first liver elastographic method on the market. More than 1500 published papers proved this method’s value for liver fibrosis evaluation in HCV and HBV chronic hepatitis, in NAFLD, in ALD, in cholestatic diseases, in post-transplant patients, mainly considering liver biopsy as the gold standard. The second-generation elastographic methods that appeared on the market was point SWE (pSWE). The first system with this technology (ARFI technique) was Virtual Touch Quantification (VTQ) from Siemens. Many comparative studies between different ultrasound-based elastographic methods have been published during the time.

### ***Point SWE (Table 45.2)***

A comparison between TE and VTQ (ARFI) was performed by Lupşor M et al. [9] in chronic hepatitis C using liver biopsy as the gold standard. In the cohort of 112 consecutive patients, the diagnostic accuracy of these two elastographic methods was comparable only for prediction of severe fibrosis and cirrhosis, but for earlier stages of fibrosis, TE performed better.

In a multicenter study in 400 chronic HCV patients, with liver biopsy as gold standard, VTQ was compared to TE [10]. In this study, the correlation with histological fibrosis was similar between VTQ and TE (0.689 vs 0.728, with a  $P = 0.28$ ).

In a prospective European multicenter study, VTQ was compared with TE, also with liver biopsy as gold standard [11]. A total of 241 HCV patients from seven European centers were evaluated. Comparison between the accuracy of pSWE and TE revealed no significant difference between the methods for all stages of fibrosis (0.81 vs 0.85 for  $F \geq 2$ ;  $P = 0.15$ ; 0.88 vs 0.92 for  $F \geq 3$ ;  $P = 0.11$ ; and 0.89 vs 0.94 for cirrhosis;  $P = 0.19$ ). The conclusion of the study was that the diagnostic accuracy of TE and pSWE (VTQ) was comparable in HCV patients.

Later, a meta-analysis was performed to compare TE with pSWE (VTQ) [12]. In this meta-analysis, 1163 patients with chronic hepatopathies were analyzed. The feasibility of VTQ was 97.9%, and for TE it was 93.4% ( $P < 0.001$ ). For predicting significant fibrosis ( $F \geq 2$ ), TE had 0.78 (95% CI: 0.72–0.83) sensitivity and a specificity of 0.84 (95% CI: 0.75–0.90), while for VTQ the sensitivity was 0.74 (95% CI: 0.66–0.80) and the specificity was 0.83 (95% CI: 0.75–0.90). For the diagnosis of

**Table 45.2** Performance of pSWE

Study	Elastography techniques	No. of subjects etiology	Performance of methods	
			TE(AUROC)	VTQ (AUROC)
Lupşor. M 2009; JGLD [9]	VTQ vs TE	112 HCV	TE(AUROC)	VTQ (AUROC)
			≥F1:0.918 ≥F2:0.961 ≥F3:0.957 F4:0.970	≥F1:0.725 ≥F2:0.869 ≥F3:0.900 F4:0.936
Sporea. I 2012; EJR [10]	VTQ vs TE	400 HCV		VTQ (AUROC)
				≥F1: 0.779 ≥F2:0.792 ≥F3:0.829 F4:0.842
Friedrich-Rust. M 2015; Ultraschall Med [11]	VTQ vs TE	241 HCV	TE(Spearman's r)	VTQ (Spearman's r)
			≥F2:0.85 ≥F3:0.92 F4:0.94	≥F2:0.81 ≥F3:0.88 F4:0.89
Bota. S 2013; Liver Int [12]	VTQ vs TE	1163 CLD	TE(sROC)	VTQ (sROC)
			≥F2:0.87 F4:0.93	≥F2:0.85 F4:0.93
Conti. F 2019; Clin Gastroenterol Hepatol [13]		406 CLD	TE(AUROC)	ELASTPQ (AUROC)
			SUPERIMPOSABLE	≥F2:0.856 ≥F3:0.951 F4:0.965

liver cirrhosis, the sensitivity was 0.89 (95% CI: 0.80–0.94) for TE and the specificity 0.87 (95% CI: 0.81–0.91), while for VTQ the sensitivity was 0.87 (95% CI: 0.79–0.92) and the specificity 0.87 (95% CI:0.75–0.90). There were no significant differences between the diagnostic odds ratio of these two methods regarding the detection of significant fibrosis [mean difference in rDOR = 0.27 (95% CI:0.69–0.14)] or cirrhosis [mean difference in rDOR = 0.12n (0.95 CI: 0.29–0.52)]. The results of this meta-analysis in a quite large cohort underline its utility for clinical use.

In a recently published paper, an Italian group compared TE with ElastPQ (a pSWE method) [13]. In a cohort of 406 patients with chronic liver diseases of diverse etiology who underwent liver biopsy, liver stiffness measurements with ElastPQ and TE have been obtained in 361 patients. In this comparative study, ElastPQ values correlated well with the histologic fibrosis score ( $r = 0.718$ ;  $P < 0.001$ ). For ElastPQ, the AUROC values were 0.856 for significant fibrosis ( $F \geq 2$ ), 0.951 for advanced fibrosis ( $F \geq 3$ ), and 0.965 for cirrhosis. There was a superimposable diagnostic accuracy of ElastPQ and TE for each stage of liver fibrosis. The conclusion of this comparative study was that ElastPQ and TE identified patients with fibrosis and liver cirrhosis with a similar level of accuracy.

**2D-SWE** (Table 45.3)

In 2D-SWE, a color-coded image and numeric value are displayed as the result of elastographic assessment. The advantages of 2D-SWE are the following: its multi-point evaluation, real-time evaluation, large area of interrogation, and high rate frame acquisition (in SuperSonic Image from Aixplorer). For more details, see also book Part II “Techniques to Measure Liver Stiffness.” Several comparative studies have been performed, two of them by a French group (Cassinotto et al.) in chronic viral hepatitis [14] and NAFLD patients [15], respectively. In the first one, including

**Table 45.3** Performance of 2D-SWE

Reference	Elastography techniques	No. of subjects etiology	Performance of methods		
			TE(AUROC)	VTQ(ARFI) (AUROC)	SSI(AUROC)
Cassinotto. C 2014 [14]	VTQ(ARFI) vs TE vs SSI	349 CLD	TE(AUROC)	VTQ(ARFI) (AUROC)	SSI(AUROC)
			≥F1:0.86 ≥F2:0.84 ≥F3:0.87 F4:0.90	≥F1:0.84 ≥F2:0.81 ≥F3:0.89 F4:0.90	≥F1:0.89 ≥F2:0.88 ≥F3:0.93 F4:0.93
Cassinotto. C 2016 [15]	VTQ(ARFI) vs TE vs SSI	291 NAFLD	TE(AUROC)	VTQ(ARFI)	SSI(AUROC)
			≥F2:0.82 ≥F3:0.86 F4:0.87	≥F2:0.77 ≥F3:0.84 F4:0.84	≥F2:0.86 ≥F3:0.89 F4:0.88
Lee. MS 2017 [16]	VTQ(ARFI) vs TE vs SSI	94 NAFLD	TE(AUROC)	VTQ(ARFI)	SSI(AUROC)
			≥F2:0.757 ≥F3:0.870	≥F2:0.657 ≥F3:0.873	≥F2:0.759 ≥F3:0.809
Hermann. E 2018 [17]	TE vs SSI	665 CLD	TE(differences in AUROC)	SSI(AUROC)	
			≥F2: -5.3% ≥F3: -3.4% F4:-1.8%	≥F2:0.864 ≥F3:0.908 F4:0.931	
Sporea. I 2013 [18]	VTQ(ARFI) vs SSI	334 CLD	VTQ(ARFI) (accuracy%)	SSI(accuracy%)	
			≥F2:72.2 F4:78.2	≥F2:74.4 F4:85.8	
Mulazzani. L 2017 [19]	pSWE.Esaote vs SSI	108 CLD	2D.SWE.SSI vs pSWE.ESA (Lin’s analysis)		
			<15.2 kPa Precision: 0.737 Accuracy: 0.861	>15.2 kPa Precision: 0.559 Accuracy: 0.998	
Yongyan. G 2018 [20]	TE vs SSI	402 VHB	TE(AUROC)	SSI(AUROC)	
			F4:0.80	F4:0.87	
Sporea. I 2018 [21]	VTQ vs SSI vs ElastPQ	127 CLD	VTQ (accuracy%)	ElastPQ (accuracy%)	SSI (accuracy%)
			F < 2:82 F2/F3:84.1 F4:93.9	F < 2:86 F2/F3:84 F4:94	F < 2:80 F2/F3:85.3 F4:94

a cohort of 349 patients with chronic hepatopathies in whom liver biopsy was performed to assess liver fibrosis, three ultrasound-based elastography methods were compared: TE with M and XL probe, 2D-SWE, and pSWE (VTQ with ARFI technology). All three elastographic techniques significantly correlated with histological fibrosis:  $r = 0.79$ ,  $P < 0.00001$  for SSI,  $r = 0.70$ ,  $P < 0.00001$  for TE, and  $r = 0.64$ ,  $P < 0.00001$  for VTQ. The AUROCs for different methods and stages of fibrosis were: 0.88 for SSI, 0.84 for TE, and 0.81 for VTQ for significant fibrosis, while for cirrhosis they were 0.93 for SSI, 0.90 for TE, and 0.90 for VTQ. The conclusion of this study was that there were no significant differences between the systems for significant fibrosis and cirrhosis.

In the second paper of the same group, in which the performance of elastographic systems were compared in NAFLD patients, 291 patients have been included [15]. All have been evaluated by means of liver biopsy in two French university hospitals, by 2D-SWE (SSI), TE, and pSWE (VTQ). For significant fibrosis ( $F \geq 2$ ), the AUROCs were 0.86, 0.82, and 0.77 and for cirrhosis 0.88, 0.87, and 0.84, respectively. Regarding feasibility, VTQ (ARFI) had the highest one—99.3%, vs. SSI—87% and TE—85.6%. The factors associated with failed measurements were waist circumference, BMI, and intercostal wall thickness. Cutoff values for 2D-SWE and TE were quite similar to predict the same stages of fibrosis. A similar study was performed by Lee et al. [16], comparing TE, SSI, and VTQ with liver biopsy in 94 patients with NAFLD. The rate of unreliable and failed results was 21.3% for TE, 26.6% for SSI, and for VTQ only 11.7%. In this study, the AUROCs for significant fibrosis ( $F \geq 2$ ) were 0.757, 0.759, and 0.657, and for advanced fibrosis ( $F \geq 3$ ) they were 0.870, 0.809, and 0.873, respectively. This study also concluded that all three elastographic methods had similar diagnostic performance in NAFLD patients.

In a multicenter study (13 centers from 9 countries) published by Hermann et al. [17], the accuracy of SSI for staging liver fibrosis (liver biopsy as reference) was evaluated in 1134 patients with viral and non-viral chronic liver diseases. In 665 subjects, SSI was also compared to TE. In the comparative study group, 2D-SWE (SSI) performed better than TE for all stages of fibrosis, and significantly better for  $F \geq 2$  and liver cirrhosis ( $P < 0.001$  and  $P = 0.007$ ). In a comparative study between VTQ (ARFI) and 2D-SWE (SSI), considering TE as reference (18), 332 consecutive patients have been evaluated in the same day by the three methods, but reliable liver stiffness measurements were obtained only in 184 cases (55.4%) by all three. Higher body mass index and older age were associated with unreliable measurements. Reliable measurements have been obtained in a significantly higher percentage of cases by VTQ than by TE (M probe), or by SSI: 92.1% vs 72.2% ( $P < 0.0001$ ) and vs. 71.3%; ( $P < 0.0001$ ). This study also demonstrated that VTQ and SSI have similar accuracy in diagnosing significant fibrosis and liver cirrhosis.

A comparison between pSWE from Esaote (pSWE.ESA) and SSI, considering TE as reference, was performed in a cohort of 81 patients with chronic liver diseases [19]. Spearman's correlation coefficients between TE and pSWE.EAS and SSI were 0.849 and 0.878, respectively. According to this study, the correlation was less strict in higher liver stiffness values ( $>15.2$  kPa), but this does not influence the staging of

fibrosis, since all are in the cirrhotic range. In another study, a comparison between 2D-SWE (SSI) and TE was performed in HBV patients, considering liver biopsy as the gold standard [20]. The study included a cohort of 402 subjects with chronic hepatitis B (154 with chronic infection and 248 with chronic hepatitis). The AUROC of 2D-SWE to predict cirrhosis was 0.87 (95% confidence interval [CI]: 0.83–0.90) higher than that of TE—0.80 (95% CI: 0.68–0.88).

Another comparative paper between elastographic methods was published by a Romanian group [21]. It was a prospective study on 127 consecutive patients with chronic liver diseases of mixed etiologies. In the same day, these patients were evaluated by four elastographic methods: TE, VTQ (pSWE), ElastPQ (pSWE), and SSI (2D-SWE), TE being the reference method. Regarding feasibility, valid measurements were obtained in 116/127 cases with VTQ, in 108/127 with SSI, in 111/127 with TE, and in 109/127 with ElastPQ, so that the final analysis was performed in 82 subjects who had reliable measurements by all four methods. This study showed that the accuracies of VTQ, SSI, and ElastPQ for diagnosing significant/severe fibrosis and liver cirrhosis were quite similar: 84.1%, 85.3%, 84% ( $P > 0.05$ ) and 93.9%, 94% and 94% ( $P > 0.05$ ), respectively.

Considering the results of all the published studies that showed similar performance of various ultrasound-based liver elastography methods, it is safe to consider that any of them can be used for liver fibrosis assessment [22], keeping in mind that specific cutoff values should be used for each system.

### **MRE (Table 45.4)**

Comparative studies have also been performed between ultrasound-based elastographic methods and magnetic resonance elastography (MRE). The first one was published in 2008 by Huwart L et al. [23] in a prospective cohort of 141 patients with chronic liver diseases, all evaluated by liver biopsy, MRE, and TE. Reliable values were obtained in 133/141 patients (94%) by MRE and in 118/141 subjects (84%) with the M probe by TE, so that the comparison was performed in 96 cases. The AUROCs for MRE were larger as compared to TE (0.994 for  $F \geq 2$ ; 0.985 for  $F \geq 3$ ; and 0.998 for  $F = 4$  for MRE and 0.837, 0.709, and 0.849 for TE). The conclusion of this study was that the feasibility and the accuracy of MRE are superior to TE.

A comparative study regarding the performance of MRE and TE in chronic hepatitis B and C was performed in 103 patients with liver biopsy [24]. The comparison was possible in 85 subjects (65 HBV, 19 HCV, and 1 co-infected). In this study, TE and MRE had comparable accuracies (AUROC for  $F \geq 2$ : 0.914 TE vs. 0.909 MRE,  $P = 0.89$ ; for  $F \geq 3$ : 0.895 TE vs. 0.928 MRE,  $P = 0.42$ ).

In a retrospective study on 113 patients with chronic liver diseases, all with liver biopsy or liver resection [25], the AUROCs of MRE for all the stages of fibrosis were higher than for TE (0.98 vs 0.87 for  $F \geq 2$ :  $P = 0.0003$ ; 0.97 vs 0.93 for cirrhosis:  $P < 0.0308$ ).

**Table 45.4** Performance of MRE

Study	Elastography techniques	No. of subjects etiology	Performance of methods		
			TE(AUROC)	MRE(AUROC)	
Huwart. L 2008 [23]	MRE vs TE	96 CLD	TE(AUROC)	MRE(AUROC)	
			≥F2:0.837 ≥F3:0.709 F4:0.849	≥F2:0.994 ≥F3:0.985 F4:0.998	
Bohte. AE 2014 [24]	MRE vs TE	85 HBV, HCV	TE(AUROC)	MRE(AUROC)	
			≥F2:0.914 ≥F3:0.895	≥F2:0.909 ≥F3:0.928	
Ichikawa. S 2015 [25]	MRE vs TE	113 CLD	TE(AUROC)	MRE(AUROC)	
			≥F1:0.87 ≥F2:0.87 F4:0.93	≥F1:0.97 ≥F2:0.98 F4:0.97	
Xiao. H 2017 [26]	MRE vs TE	3641 CLD	TE(AUROC)	MRE(AUROC)	
			≥F2:0.796 ≥F3:0.893 F4:0.905	≥F2:0.981 ≥F3:0.972 F4:0.972	
Xiao. G 2017 [27]	MRE vs TE vs SSI	13046 NAFLD	TE(AUROC)	SSI(AUROC)	MRE(AUROC)
			≥F2:0.83(M) ≥F3:0.87(M) F4:0.92(M)	≥F2:0.89 ≥F3:0.91 F4:0.97	≥F2:0.88 ≥F3:0.93 F4:0.92
			≥F2:0.82(XL) ≥F3:0.86(XL) F4:0.94(XL)		
Imajo. K 2016 [28]	MRE vs TE	142 NAFLD	TE(AUROC)	MRE(AUROC)	
			≥F2:0.82	≥F2:0.91	
Park. CC 2017 [29]	MRE vs TE	104 NAFLD	TE(AUROC)	MRE(AUROC)	
			≥F1:0.67 ≥F2:0.86 ≥F3:0.80 F4:0.69	≥F1:0.82 ≥F2:0.89 ≥F3:0.87 F4:0.87	
Cui. J 2016 [30]	MRE vs VTQ(ARFI)	125 NAFLD	VTQ(ARFI) (AUROC)	MRE(AUROC)	
			≥F1:0.664 ≥F2:0.848 ≥F3:0.896 F4:0.862	≥F1:0.799 ≥F2:0.885 ≥F3:0.934 F4:0.882	

In a systematic meta-analysis in patients with chronic HBV [26], the performance of MRE was evaluated in 1470 patients and of TE in 3641 patients. AUROC values for MRE and TE for detecting significant fibrosis, advanced fibrosis, and cirrhosis were 0.981 vs. 0.796 ( $P < 0.001$ ), 0.972 vs. 0.893 ( $P < 0.001$ ), and 0.972 vs. 0.905 ( $P < 0.001$ ). The conclusion of this meta-analysis was that MRE is more accurate than TE for the assessment of liver fibrosis in HBV patients.



Another meta-analysis that compared TE and 2D-SWE (SSI) with MRE was performed in patients with NAFLD [27]. A total of 13,046 NAFLD subjects were included, the prevalence of significant fibrosis, advanced fibrosis, and cirrhosis being 45.0%, 24.0%, and 9.4%, respectively. The sensitivities and specificities of TE, 2D-SWE, and MRE for detecting advanced fibrosis were 0.87 and 0.79, 0.90 and 0.93, and 0.84 and 0.90, respectively. In this meta-analysis, the AUROC values for TE with M probe, XL probe, 2D-SWE, and MRE for diagnosing  $F \geq 3$  were 0.88, 0.85, 0.95, and 0.96, respectively. The conclusion of this study was that MRE and 2D-SWE have the highest accuracy for correct staging of fibrosis in NAFLD patients.

Another study compared MRE with TE in NAFLD patients [28]. This study included 142 patients with NAFLD and a mean body mass index of 28.1 kg/m<sup>2</sup>, all with liver biopsy. The AUROC of TE to predict  $F \geq 2$  was 0.82 (95% CI: 0.74–0.89), whereas MRE had an AUROC value of 0.91 (95% CI: 0.86–0.96),  $P = 0.001$ . In the same study, the authors compared CAP (controlled attenuation parameter) from FibroScan, with PDFF (proton density fat fraction) from MRI. CAP measurements identified patients with hepatic steatosis grade  $\geq 2$  with an AUROC value of 0.73 (95% CI: 0.64–0.81) and PDFF identified them with an AUROC value of 0.90 (95% CI: 0.82–0.97),  $P < 0.001$ .

In a study performed by Park CC et al. [29], a cohort of 104 patients with NAFLD was included. All patients were evaluated by liver biopsy, TE and MRE. MRE detected any fibrosis (stage 1 or more) with an AUROC of 0.82 (95% CI, 0.74–0.91), which was significantly higher than that of TE (AUROC, 0.67; 95% CI, 0.56–0.78). Regarding different stages of fibrosis, MRE detected fibrosis stage 2, 3, or 4 with AUROC values of 0.89 (95% CI, 0.83–0.96), 0.87 (95% CI, 0.78–0.96), and 0.87 (95% CI, 0.71–1.00), respectively; TE detected fibrosis stage 2, 3, or 4 with AUROC values of 0.86 (95% CI, 0.77–0.95), 0.80 (95% CI, 0.67–0.93), and 0.69 (95% CI, 0.45–0.94). Regarding steatosis assessment, MRI-PDFF detected any steatosis with an AUROC of 0.99 (95% CI, 0.98–1.00), significantly higher than that of CAP (AUROC, 0.85; 95% CI, 0.75–0.96). In the same time, MRI-PDFF identified steatosis grade 2 or 3 with AUROC values of 0.90 (95% CI, 0.82–0.97) and 0.92 (95% CI, 0.84–0.99) and CAP identified steatosis grade 2 or 3 with AUROC values of 0.70 (95% CI, 0.58–0.82) and 0.73 (95% CI, 0.58–0.89). The conclusion of this study was that MRE with PDFF is more accurate than TE with CAP for the evaluation of fibrosis and steatosis in NAFLD patients.

Another comparison was performed between MRE and a pSWE technique—VTQ(ARFI) [30] in a cohort of 125 patients with NAFLD, with a mean BMI of 31.8 ( $\pm 7.0$ ) kg/m<sup>2</sup>. MRE AUROCs for diagnosing  $F \geq 2$ ,  $F \geq 3$ , and  $F = 4$  were 0.885 (95% CI 0.816–0.953), 0.934 (95% CI 0.863–1.000), and 0.882 (95% CI 0.729–1.000), while for VTQ (ARFI) the AUROCs were 0.848 (95% CI 0.776–0.921), 0.896 (95% CI 0.824–0.968), and 0.862 (95% CI 0.721–1.000). Considering the influence of obesity, MRE was superior to TE in obese subjects, but not in non-obese ( $P = 0.722$ ). The conclusion of this study was that MRE is more accurate than pSWE for liver fibrosis assessment in NAFLD patients, especially in obese subjects.

## Advantages and Limitations

1. TE—is easy to perform, does not require dedicated US knowledge (in some countries it is performed by technicians), only provides LS values under controlled conditions in a highly controlled manner.
2. pSWE—is quite easy to perform, it uses ultrasound image for measurement, the region of interest can be chosen by the operator (avoiding the capsule of the liver and the big vessels), but the measuring box is quite small (around 10/5 mm). There are still open questions with regard to measuring depth and LS (standardization).
3. For 2D-SWE, more experience in ultrasound is necessary [4]. The investigational area is larger and can be selected with B-mode ultrasound image. The elastographic assessment is displayed in a color-coded system and with numeric values.

In 2015, EASL issued guidelines regarding the noninvasive methods for liver diseases severity assessment [8] in which the advantages and disadvantages of all these methods are presented (Table 45.5). In contrast to earlier reports, TE is able to be used in patients with ascites by applying the XL probe [31].

**Table 45.5** Advantages and disadvantages of noninvasive tools for fibrosis assessment in chronic hepatitis (modified from EASL-ALEH Clinical Practice Guidelines [8])

Serum biomarkers	Measurement of liver stiffness			
	Transient elastography	ARFI (pSWE)	2D-SWE	MR elastography
<i>Advantages</i>				
<ul style="list-style-type: none"> <li>• Good reproducibility</li> <li>• High applicability (95%)</li> <li>• No cost and wide availability (non-patented)</li> <li>• Well validated</li> <li>• Can be performed in the outpatient clinic</li> </ul>	<ul style="list-style-type: none"> <li>• Most widely used and validated technique: standard to be beaten</li> <li>• User-friendly (performed at bedside; rapid, easy to learn)</li> <li>• High range of values (2–75 kPa)</li> <li>• Quality criteria well defined</li> <li>• Good reproducibility</li> <li>• High performance for cirrhosis (AUROC &gt;0.9)</li> <li>• Prognostic value in cirrhosis</li> </ul>	<ul style="list-style-type: none"> <li>• Can be implemented on a regular US machine</li> <li>• ROI smaller than TE but location chosen by the operator</li> <li>• Higher applicability than TE (ascites and obesity)</li> <li>• Performance equivalent to that of TE for significant fibrosis and cirrhosis</li> </ul>	<ul style="list-style-type: none"> <li>• Can be implemented on a regular US machine</li> <li>• ROI can be adjusted in size and location and chosen by the operator</li> <li>• Measures liver stiffness in real time</li> <li>• High range of values (2–150 kPa)</li> <li>• Good applicability</li> <li>• High performance for cirrhosis</li> </ul>	<ul style="list-style-type: none"> <li>• Can be implemented on a regular MRI machine</li> <li>• Examination of the whole liver</li> <li>• Higher applicability than TE (ascites and obesity)</li> <li>• High performance for cirrhosis</li> </ul>

**Table 45.5** (continued)

Serum biomarkers	Measurement of liver stiffness			
	Transient elastography	ARFI (pSWE)	2D-SWE	MR elastography
<i>Disadvantages</i>				
<ul style="list-style-type: none"> <li>• Non-specific of the liver</li> <li>• Unable to discriminate between intermediate stages of fibrosis</li> <li>• Performance not as good as TE for cirrhosis</li> <li>• Cost and limited availability (proprietary)</li> <li>• Limitations (hemolysis, Gilbert syndrome, inflammation...)</li> </ul>	<ul style="list-style-type: none"> <li>• Requires a dedicated device</li> <li>• ROI cannot be chosen</li> <li>• Applicability (80%) lower than serum biomarker: (obesity, operator experience)</li> <li>• Confounders of elevated LS to be considered for all elastographic techniques</li> </ul>	<ul style="list-style-type: none"> <li>• Unable to discriminate between intermediate stages of fibrosis</li> <li>• Units (m/sec) different from that of TE (kPa)</li> <li>• Narrow range of values (0.5–4.4 m/sec)</li> <li>• Quality criteria not well defined</li> <li>• Prognostic value in cirrhosis?</li> </ul>	<ul style="list-style-type: none"> <li>• Further validation warranted</li> <li>• Quality criteria not well defined</li> <li>• Learning curve?</li> </ul>	<ul style="list-style-type: none"> <li>• Further validation warranted especially in comparison with TE</li> <li>• Not applicable in case of iron overload</li> <li>• Requires a MRI facility</li> <li>• Time-consuming</li> <li>• Costly</li> </ul>

## Conclusions

Feasibility and performance seem to be similar for the different ultrasound-based elastographic methods. Consequently, all ultrasound-based elastographic methods (TE, pSWE, and 2D-SWE) can be used in clinical practice [1, 2]; however, different cutoff values should be used for each system. In addition, some techniques require a deeper ultrasound knowledge (pSWE and 2D-SWE) in comparison to TE. The reports of LS change at varying liver depths on pSWE have not seen so far with 2D-SWE or TE and require further studies [32]. MRE seems to be superior to ultrasound-based elastographic systems but has limited availability, is cost-intensive and can only be performed by radiologists. In contrast, US-based elastography can be performed by clinicians and radiologists, in a point of care setting. Nowadays, quite all the high end and even some of the medium class ultrasound systems (Philips, GE, Siemens, and others) include ultrasound-based elastographic modules (pSWE or 2D-SWE). This enables the practitioner to perform elastography at the end of an ultrasound examination, when he or she already has all the clinical information, avoiding confounding factors (such as non-fasting patient, obstructive jaundice, increased aminotransferases, right hearth failure) [2].

## References

1. Dietrich CF, Bamber J, Berzigotti A, Bota S, Cantisani V, Castera L, et al. EFSUMB Guidelines and recommendations on the clinical use of liver ultrasound elastography, update 2017 (long version). *Ultraschall Med.* 2017;38(4):e16–47.
2. Ferraioli G, Wong VW, Castera L, Berzigotti A, Sporea I, Dietrich CF, et al. Liver ultrasound elastography: an update to the world federation for ultrasound in medicine and biology guidelines and recommendations. *Ultrasound Med Biol.* 2018;44(12):2419–40.
3. Fujimoto K, Kato M, Kudo M, Yada N, Shiina T, Ueshima K, et al. Novel image analysis method using ultrasound elastography for noninvasive evaluation of hepatic fibrosis in patients with chronic hepatitis C. *Oncology.* 2013;84(Suppl 1):3–12.
4. Castéra L, Foucher J, Bernard P-H, Carvalho F, Allaix D, Merrouche W, et al. Pitfalls of liver stiffness measurement: A 5-year prospective study of 13,369 examinations. *Hepatology.* 2010;54:828–35.
5. Sirli R, Sporea I, Bota S, Jurchis A. Factors influencing reliability of liver stiffness measurements using transient elastography (M-probe)-monocentric experience. *Eur J Radiol.* 2013;82(8):e313–6.
6. Sporea I, Sirli R, Mare R, Popescu A, Ivascu SC. Feasibility of transient elastography with M and XL probes in real life. *Med Ultrason.* 2016;18(1):7–10.
7. Sporea I, Popescu A, Gheorghe L, Cijevschi Prelipcean C, Sparchez Z, Voiosu R. “Quo vadis” liver biopsy? A multi-centre Romanian study regarding the number of liver biopsies performed for chronic viral hepatitis. *J Gastrointestin Liver Dis.* 2012;21(3):326.
8. European Association for Study of Liver; Asociacion Latinoamericana para el Estudio del Hígado. EASL-ALEH Clinical Practice Guidelines: Non-invasive tests for evaluation of liver disease severity and prognosis. *J Hepatol.* 2015;63(1):237–64. <https://doi.org/10.1016/j.jhep.2015.04.006>.
9. Lupsor M, Badea R, Stefanescu H, Sparchez Z, Branda H, Serban A, et al. Performance of a new elastographic method (ARFI technology) compared to unidimensional transient elastography in the noninvasive assessment of chronic hepatitis C. Preliminary results. *J Gastrointestin Liver Dis.* 2009;18(3):303–10.
10. Sporea I, Bota S, Peck-Radosavljevic M, Sirli R, Tanaka H, Iijima H, et al. Acoustic radiation force impulse elastography for fibrosis evaluation in patients with chronic hepatitis C: an international multicenter study. *Eur J Radiol.* 2012;81(12):4112–8.
11. Friedrich-Rust M, Lupsor M, de Knegt R, Dries V, Buggisch P, Gebel M, et al. Point shear wave elastography by acoustic radiation force impulse quantification in comparison to transient elastography for the noninvasive assessment of liver fibrosis in chronic hepatitis C: a prospective international multicenter study. *Ultraschall Med.* 2015;36(03):239–47.
12. Bota S, Herkner H, Sporea I, Salzl P, Sirli R, Neghina AM, et al. Meta-analysis: ARFI elastography versus transient elastography for the evaluation of liver fibrosis. *Liver Int.* 2013;33(8):1138–47.
13. Conti F, Serra C, Vukotic R, Felicani C, Mazzotta E, Gitto S, et al. Assessment of liver fibrosis with elastography point quantification vs other noninvasive methods. *Clin Gastroenterol Hepatol.* 2019;17(3):510–7 e3.
14. Cassinotto C, Lapuyade B, Mouries A, Hiriart JB, Vergniol J, Gaye D, et al. Non-invasive assessment of liver fibrosis with impulse elastography: comparison of supersonic shear imaging with ARFI and FibroScan(R). *J Hepatol.* 2014;61(3):550–7.
15. Cassinotto C, Boursier J, de Ledinghen V, Lebigot J, Lapuyade B, Cales P, et al. Liver stiffness in nonalcoholic fatty liver disease: a comparison of supersonic shear imaging, FibroScan, and ARFI with liver biopsy. *Hepatology.* 2016;63(6):1817–27.
16. Lee MS, Bae JM, Joo SK, Woo H, Lee DH, Jung YJ, et al. Prospective comparison among transient elastography, supersonic shear imaging, and ARFI imaging for predicting fibrosis in nonalcoholic fatty liver disease. *PLoS One.* 2017;12(11):e0188321.
17. Herrmann E, de Ledinghen V, Cassinotto C, Chu WC, Leung VY, Ferraioli G, et al. Assessment of biopsy-proven liver fibrosis by two-dimensional shear wave elastography: an individual patient data-based meta-analysis. *Hepatology.* 2018;67(1):260–72.

18. Sporea I, Bota S, Jurchis A, Sirli R, Gradinaru-Tascau O, Popescu A, et al. Acoustic radiation force impulse and supersonic shear imaging versus transient elastography for liver fibrosis assessment. *Ultrasound Med Biol*. 2013;39(11):1933–41.
19. Mulazzani L, Salvatore V, Ravaoli F, Allegretti G, Matassoni F, Granata R, et al. Point shear wave ultrasound elastography with Esaote compared to real-time 2D shear wave elastography with supersonic imagine for the quantification of liver stiffness. *J Ultrasound*. 2017;20(3):213–25.
20. Gao Y, Zheng J, Liang P, Tong M, Wang J, Wu C, et al. Liver fibrosis with two-dimensional US shear-wave elastography in participants with chronic hepatitis B: a prospective multicenter study. *Radiology*. 2018;289(2):407–15.
21. Sporea I, Mare R, Lupusoru R, Popescu A, Danila M, Bende F, et al. Comparative study between four ultrasound shear waves elastographic methods for liver fibrosis assessment. *Med Ultrason*. 2018;20(3):265–71.
22. Sporea I. One or more elastographic methods for liver fibrosis assessment? *Med Ultrason*. 2015;17(2):137–8.
23. Huwart L, Sempoux C, Vicaut E, Salameh N, Annet L, Danse E, et al. Magnetic resonance elastography for the noninvasive staging of liver fibrosis. *Gastroenterology*. 2008;135(1):32–40.
24. Bohte AE, de Niet A, Jansen L, Bipat S, Nederveen AJ, Verheij J, et al. Non-invasive evaluation of liver fibrosis: a comparison of ultrasound-based transient elastography and MR elastography in patients with viral hepatitis B and C. *Eur Radiol*. 2014;24(3):638–48.
25. Ichikawa S, Motosugi U, Morisaka H, Sano K, Ichikawa T, Tatsumi A, et al. Comparison of the diagnostic accuracies of magnetic resonance elastography and transient elastography for hepatic fibrosis. *Magn Reson Imaging*. 2015;33(1):26–30.
26. Xiao H, Shi M, Xie Y, Chi X. Comparison of diagnostic accuracy of magnetic resonance elastography and Fibroscan for detecting liver fibrosis in chronic hepatitis B patients: a systematic review and meta-analysis. *PLoS One*. 2017;12(11):e0186660.
27. Xiao G, Zhu S, Xiao X, Yan L, Yang J, Wu G. Comparison of laboratory tests, ultrasound, or magnetic resonance elastography to detect fibrosis in patients with nonalcoholic fatty liver disease: a meta-analysis. *Hepatology*. 2017;66(5):1486–501.
28. Imajo K, Kessoku T, Honda Y, Tomeno W, Ogawa Y, Mawatari H, et al. Magnetic resonance imaging more accurately classifies steatosis and fibrosis in patients with nonalcoholic fatty liver disease than transient elastography. *Gastroenterology*. 2016;150(3):626–37.e7.
29. Park CC, Nguyen P, Hernandez C, Bettencourt R, Ramirez K, Fortney L, et al. Magnetic resonance elastography vs transient elastography in detection of fibrosis and noninvasive measurement of steatosis in patients with biopsy-proven nonalcoholic fatty liver disease. *Gastroenterology*. 2017;152(3):598–607 e2.
30. Cui J, Heba E, Hernandez C, Haufe W, Hooker J, Andre MP, et al. Magnetic resonance elastography is superior to acoustic radiation force impulse for the diagnosis of fibrosis in patients with biopsy-proven nonalcoholic fatty liver disease: a prospective study. *Hepatology*. 2016;63(2):453–61.
31. Kohlhaas A, Durango E, Millonig G, Bastard C, Sandrin L, Golriz M, et al. Transient elastography with the XL probe rapidly identifies patients with non-hepatic ascites. *Hepat Med*. 2012;4:11–8.
32. Sporea I, Sirli RL, Deleanu A, Popescu A, Focsa M, Danila M, et al. Acoustic radiation force impulse elastography as compared to transient elastography and liver biopsy in patients with chronic hepatopathies. *Ultraschall Med*. 2011;32(Suppl 1):S46–52.
33. Gradinaru-Tascau O, Sporea I, Bota S, Jurchis A, Popescu A, Popescu M, et al. Does experience play a role in the ability to perform liver stiffness measurements by means of supersonic shear imaging (SSI)? *Med Ultrason*. 2013;15(3):180–3.
34. Jun BG, Park WY, Park EJ, Jang JY, Jeong SW, Lee SH, et al. A prospective comparative assessment of the accuracy of the FibroScan in evaluating liver steatosis. *PLoS One*. 2017;12(8):e0182784.

# Chapter 46

## Adaptation of Liver Stiffness Cutoff Values to Inflammation, Cholestasis, and Congestion



Sebastian Mueller

### Introduction

Various confounders can increase LS independent of fibrosis stage (see also book Part III and IV). This typically leads to an overestimation of fibrosis stages and, hence, a decreased diagnostic accuracy. Important confounders (see book Part III) include inflammation, congestion, or cholestasis. While these confounders may have their own therapeutic implications, it is often desirable to know whether a liver cirrhosis is present or not. In some situations, the patient may have two liver problems, for instance a gallstone in the common bile duct and a manifest liver cirrhosis. In such cases, it is difficult to dissect elevation of bilirubin and liver stiffness. It should be mentioned that these algorithms are still under discussion and some alternatives are covered in this book section by other authors. In contrast to, e.g., algorithms, this chapter is aimed at discussing how to deal with confounders in an individual patient by obtaining the maximum of information. As shown in Fig. 46.1, a valid LS of <6 kPa rules out a manifest liver disease. In case of elevated LS, an ultrasound should be performed first. An on-time ultrasound is normally very helpful since it can be quickly done and provides useful information such as signs of congestion, cholestasis, or tumor masses. In case of ascites, TE can be performed but the XL probe should be used (see the respective chapter in the same book section). In addition, an actual laboratory test should be available for correct LS interpretation. AST has been shown the most simple and best estimate to predict potential overestimation of fibrosis stage due to inflammation/hepatitis. In this case, either an intervention should be considered to efficiently treat the underlying cause of the hepatitis or so-called AST-adapted cutoff values can be applied for rapid decision-making. Both strategies will be discussed below. Moreover, several cases

---

S. Mueller (✉)

Department of Medicine and Center for Alcohol Research and Liver Diseases, Salem Medical Center, University of Heidelberg, Heidelberg, Germany  
e-mail: [sebastian.mueller@urz.uni-heidelberg.de](mailto:sebastian.mueller@urz.uni-heidelberg.de)

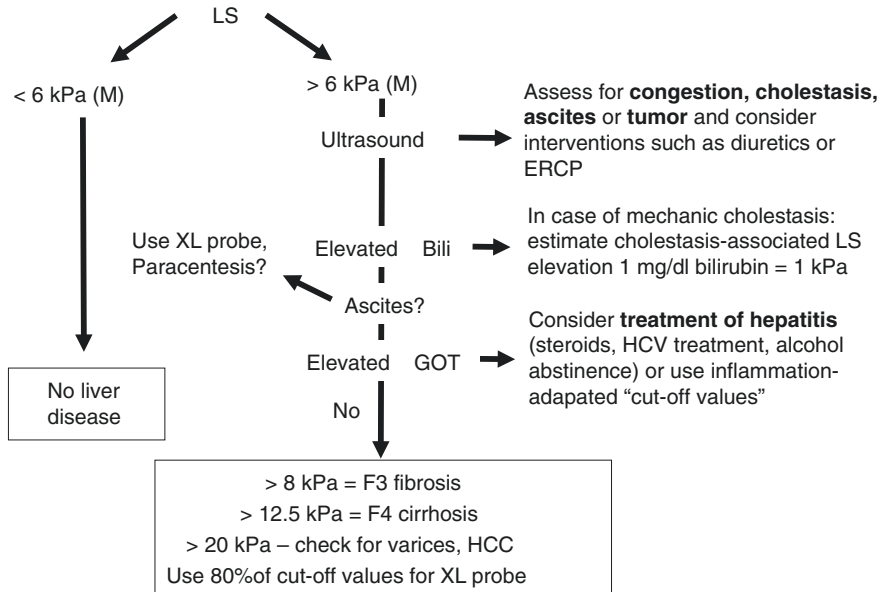


**Fig. 46.1** General workflow to interpret LS. A normal LS <6 kPa rules out any chronic liver disease, since all potential confounders and technical artifacts lead to LS elevation but never decrease LS. An on-time abdominal ultrasound and actual laboratory parameters (GOT/AST levels) are most helpful to rule out confounders such as congestion, cholestasis, nodular masses, or inflammation

are described in the clinical case chapter which can be studied for further illustration. Of course, patients can present with a combination of LS-modulating diseases which is especially the case in the elderly who can show a combination of e.g. heart failure, bile stones, and alcohol consumption. Here, combinatorial strategies as shown in Fig. 46.3 can be applied.

## Mechanic Cholestasis

Mechanic cholestasis can significantly increase LS up to 30 kPa whether it is due to an obstructing gall stone or a tumor obstruction of the common bile duct [1]. Depending on the degree of cholestasis and accompanying hepatitis, removal of the bile stone or implantation of a biliary stent can rapidly cause normalization of LS within days. Figure 46.2 shows both bilirubin and LS levels in a patient with a common bile duct obstructing GIST tumor. An ERCP with stent implantation normalized LS within 2 days till day 10. On day 15, a stent obstruction and cholangitis was diagnosed, causing LS to increase again to ca. 10 kPa. Bilirubin reached levels of 8.1 mg/dL. It could be also shown earlier [1] that in cases of mechanic cholestasis within an otherwise healthy liver, an increase of bilirubin by 1 mg/dL corresponds to ca. 1 kPa



**Fig. 46.2** Effect of mechanic cholestasis on LS in a patient with a bile duct obstructing GIST tumor. ERCP with stent implantation led to successful biliary drainage and decrease of LS within 2 days. After 10 days, re-obstruction of the bile duct/stent again caused rapid onset of jaundice and LS elevation

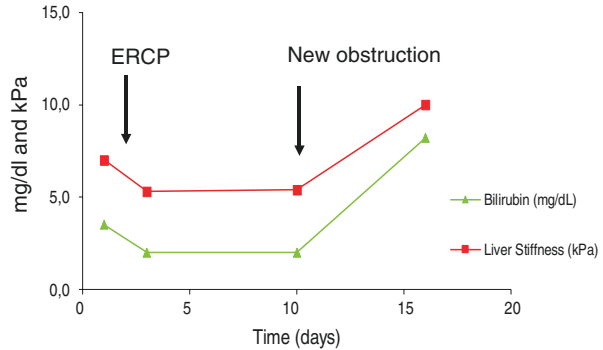
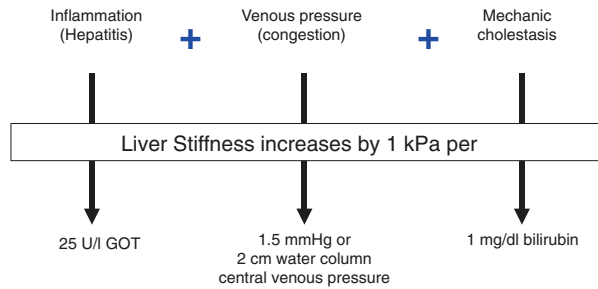


**Fig. 46.3** Rule of thumb for clinical practice to estimate the impact of inflammation (GOT/AST), congestion, and cholestasis to elevate LS by 1 kPa



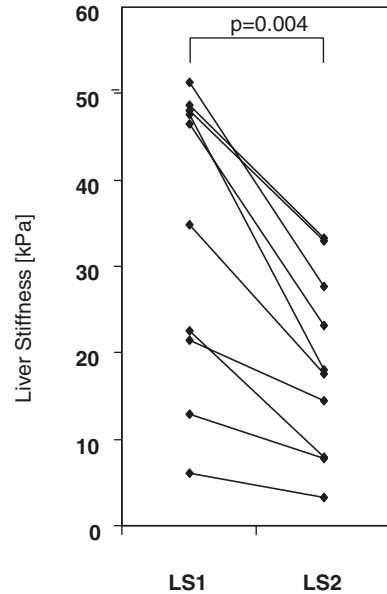
(see Fig. 46.3). This rule of thumb can be applied if one is not sure whether an icteric patient has liver cirrhosis and/or a bile stone. It is often overlooked in clinical practice that patients with manifest cirrhosis and a bile duct obstruction due to a gall stone will not show typical ultrasound signs of mechanic cholestasis since the stiff cirrhotic liver will not allow dilation of the common bile duct. In addition, both pathological conditions cause primarily an elevation of conjugated bilirubin. In the clinical case in Fig. 46.2, 8.1 mg/dL would correspond with an increase of LS by 8 kPa which is 4 kPa (normal LS) + 8 kPa = 12 kPa. Thus, a LS of 12 kPa could be simply explained by the mechanic cholestasis. In other words, the measured LS of 10 kPa completely rules out any fibrosis in this patient despite LS elevation.

### Liver Congestion

Liver congestion or an elevated central venous pressure is an important modulator of LS elevation [2]. Consequently, congestion should be especially suspected in the elder population aged >70 years since heart failure is the most common diagnosis in these patients. Heart failure, next to liver cirrhosis, has also been identified as important cause for LS elevation in the emergency room predicting 30 day mortality [3]. An often overlooked discrete sign of manifest cardiac cirrhosis is the presence of slightly elevated GGT in the 100–150 U/L range in older patients. Animal



**Fig. 46.4** Decrease of LS in ten patients with heart failure after successful therapy with diuretics. Heart failure in elder patients >70 years old is one of the main confounders of LS elevation. It is still difficult to clearly discriminate manifest cardiac cirrhosis from mere congestion in these patients since a combination is often present. Modified from [2]



experiments in pigs have demonstrated that 36 cm water column/26 mmHg of central venous pressure suffice to increase LS up to 75 kPa, the detection limit of the FibroScan device. Figure 46.4 shows sequential LS data in ten patients with right heart failure following treatment with diuretics for 7 days. Weight loss was 3 kg during this time. Median LS of 40.7 kPa decreased in all of them down to 17.8 kPa. As a rough rule of thumb, 2 cm water column (1.5 mmHg) of central venous pressure increase corresponds to 1 kPa LS elevation (see Fig. 46.3). These values can be used to estimate roughly whether a LS elevation in a heart failure patient is due to congestion. Unfortunately, LS does not seem to allow to differentiate between LS elevation due to cardiac cirrhosis or congestion. In an unpublished study of  $n = 23$  patients with heart failure, LS correlated both with ultrasound signs of cirrhosis and caval vein dilation before and after treatment with diuretics [4]. Cardiac cirrhosis can only be ruled out if LS completely normalizes after removal of water retention.

## LS Elevation by Inflammation

Inflammation is the most important clinical confounder of elevated LS which can cause significant overestimation of fibrosis stage by LSM [5–7]. Treatment of the underlying cause of various liver diseases can lead to significant LS decrease of up to 80% due to resolution of inflammation [2, 4, 6, 8–18]. Elevated LS has been in most detail analyzed in patients with alcoholic liver disease (ALD) where it correlates best with histological inflammation and ballooning next to fibrosis stage [19].

For clinical practice, there has been a long search for activity markers that can be used to estimate the LS elevation due to inflammation. Transaminases,

**Table 46.1** Liver disease, therapeutic measures, resolution of inflammation and time interval for efficient liver stiffness decrease

Liver disease	Treatment option	LS decrease (normal/extended)
ALD	Alcohol detoxification	7 days/4 weeks
NAFLD	Weight loss/bariatric surgery	3 months
Autoimmune hepatitis	Steroid therapy	7 days/4 weeks
Acute viral infection (hepatitis A, Epstein–Barr Virus)	Spontaneous remission	7 days/4 weeks
HCV	Antiviral treatment	4 weeks/3 months
Hemochromatosis	Phlebotomy	3 months/12 months
Wilson's disease	Copper chelation	3 months/12 months
PBC	Ursodeoxycholic acid	1 week/3 months

namely, AST levels, are the best serum marker to predict LS elevation due to inflammation [7, 20, 21]. Notably and as shown in Appendix Table A.8, AST levels are also better correlated with LS elevation by inflammation than any other laboratory marker [7]. Appendix Table A.9 is recommended for more details. Briefly, these tables show in a large cohort of ALD patients that the decrease of LS after alcohol detoxification is best correlated by AST. For further reading, Appendix Table A.8 is recommended that provides association of LS in both HCV and ALD for different fibrosis stages. Consideration of AST levels has significantly improved fibrosis assessment in patients with ALD [20] with an increase of AUROC from 0.91 to 0.94.

It still remains unclear why AST is so tightly associated with the LS decrease. Further studies are needed whether other serum markers, e.g., of ballooning or apoptosis such as levels of M65 or M30 (see also Appendix Table A.9) are better to predict LS decrease and are more accurately assessing fibrosis stage. Table 46.1 provides treatment periods of time for first efficient and sustained LS decrease for various liver diseases. For instance, to ultimately settle the remaining fibrosis stage, patients with elevated LS and chronic HCV infection should have a final LS measurement 3 months after successful antiviral treatment and complete HCV elimination to ultimately.

Long-term abstinence has been shown to further decrease LS by 50% in patients who consequently abstained from alcohol for 5 years [4]. Even a 2 months reduction of alcohol consumption by 40% significantly reduced LS by 17% as shown recently using the opioid antagonist nalmefene for better controlled drinking [22].

AST-adapted cutoff values allow an immediate assessment of fibrosis stage even in patients with pronounced steatohepatitis and avoid overestimation of fibrosis stages [7]. Appendix Fig. A.3 shows LS as a function of AST levels for both ALD and HCV for direct readout and it provides the formulas to calculate fibrosis stages, e.g., for clinical multicenter studies.

It should be taken into account that not all patients with an elevated AST have an increased LS. In patients with an initial AST >100 U/L, 30.1% show a decrease in LS, while the remaining ~70% did not show any change in LS [7].

## Conclusion

Most important confounders for elevated LS are inflammation, congestion, and cholestasis that are best considered/excluded by an on-time abdominal ultrasound and actual laboratory parameters.

## References

1. Millonig G, Reimann FM, Friedrich S, Fonouni H, Mehrabi A, Büchler MW, et al. Extrahepatic cholestasis increases liver stiffness (FibroScan) irrespective of fibrosis. *Hepatology*. 2008;48(5):1718–23.
2. Millonig G, Friedrich S, Adolf S, Fonouni H, Golriz M, Mehrabi A, et al. Liver stiffness is directly influenced by central venous pressure. *J Hepatol*. 2010;52(2):206–10.
3. Lindvig K, Mossner BK, Pedersen C, Lillevang ST, Christensen PB. Liver stiffness and 30-day mortality in a cohort of patients admitted to hospital. *Eur J Clin Investig*. 2012;42(2):146–52.
4. Mueller S. Personal observation. 2019.
5. Arena U, Vizzutti F, Corti G, Ambu S, Stasi C, Bresci S, et al. Acute viral hepatitis increases liver stiffness values measured by transient elastography. *Hepatology*. 2007;47(2):380–4.
6. Mueller S, Sandrin L. Liver stiffness: a novel parameter for the diagnosis of liver disease. *Hepat Med*. 2010;2:49–67.
7. Mueller S, Englert S, Seitz HK, Badea RI, Erhardt A, Bozaari B, et al. Inflammation-adapted liver stiffness values for improved fibrosis staging in patients with hepatitis C virus and alcoholic liver disease. *Liver Int*. 2015;35(12):2514–21.
8. Arima Y, Kawabe N, Hashimoto S, Harata M, Nitta Y, Murao M, et al. Reduction of liver stiffness by interferon treatment in the patients with chronic hepatitis C. *Hepatol Res*. 2010;40(4):383–92.
9. Macias J, del Valle J, Rivero A, Mira JA, Camacho A, Merchante N, et al. Changes in liver stiffness in patients with chronic hepatitis C with and without HIV co-infection treated with pegylated interferon plus ribavirin. *J Antimicrob Chemother*. 2010;65(10):2204–11.
10. Wang J-H, Changchien C-S, Hung C-H, Tung W-C, Kee K-M, Chen C-H, et al. Liver stiffness decrease after effective antiviral therapy in patients with chronic hepatitis C: longitudinal study using FibroScan. *J Gastroenterol Hepatol*. 2010;25(5):964–9.
11. Martinez SM, Foucher J, Combis J-M, Métivier S, Brunetto M, Capron D, et al. Longitudinal liver stiffness assessment in patients with chronic hepatitis C undergoing antiviral therapy. *PLoS One*. 2012;7(10):e47715.
12. Stasi C, Arena U, Zignego AL, Corti G, Monti M, Triboli E, et al. Longitudinal assessment of liver stiffness in patients undergoing antiviral treatment for hepatitis C. *Dig Liver Dis*. 2013;45(10):840–3.
13. Elshaarawy O, Mueller J, Guha IN, Chalmers J, Harris R, Krag A, et al. Spleen stiffness to liver stiffness ratio significantly differs between ALD and HCV and predicts disease-specific complications. *JHEP Rep*. 2019;1(2):99–106.
14. Ogawa E, Furusyo N, Murata M, Ohnishi H, Toyoda K, Taniai H, et al. Longitudinal assessment of liver stiffness by transient elastography for chronic hepatitis B patients treated with nucleoside analog. *Hepatol Res*. 2011;41(12):1178–88.
15. Stasi C, Salomoni E, Arena U, Corti G, Montalto P, Bartalesi F, et al. Non-invasive assessment of liver fibrosis in patients with HBV-related chronic liver disease undergoing antiviral treatment: a preliminary study. *Eur J Pharmacol*. 2017;806:105–9.

16. Hartl J, Ehlken H, Sebode M, Peiseler M, Krech T, Zenouzi R, et al. Usefulness of biochemical remission and transient elastography in monitoring disease course in autoimmune hepatitis. *J Hepatol.* 2018;68(4):754–63.
17. Nickel F, Tapking C, Benner L, Sollors J, Billeter AT, Kenngott HG, et al. Bariatric surgery as an efficient treatment for non-alcoholic fatty liver disease in a prospective study with 1-year follow-up: BariScan study. *Obes Surg.* 2018;28(5):1342–50.
18. Patel NS, Hooker J, Gonzalez M, Bhatt A, Nguyen P, Ramirez K, et al. Weight loss decreases magnetic resonance elastography estimated liver stiffness in nonalcoholic fatty liver disease. *Clin Gastroenterol Hepatol.* 2017;15(3):463–4.
19. Rausch V, Peccerella T, Lackner C, Yagmur E, Seitz HK, Longerich T, et al. Primary liver injury and delayed resolution of liver stiffness after alcohol detoxification in heavy drinkers with the PNPLA3 variant I148M. *World J Hepatol.* 2016;8(35):1547–56.
20. Mueller S, Millonig G, Sarovska L, Friedrich S, Reimann FM, Pritsch M, et al. Increased liver stiffness in alcoholic liver disease: differentiating fibrosis from steatohepatitis. *World J Gastroenterol.* 2010;16(8):966–72.
21. Trabut JB, Thepot V, Nalpas B, Lavielle B, Cosconea S, Corouge M, et al. Rapid decline of liver stiffness following alcohol withdrawal in heavy drinkers. *Alcohol Clin Exp Res.* 2012;36(8):1407–11.
22. Mueller S, Luderer M, Zhang D, Meulien D, Steiniger Brach B, Brix Schou M. Open-Label Study with Nalmefene as Needed Use in Alcohol-Dependent Patients with Evidence of Elevated Liver Stiffness and/or Hepatic Steatosis'. *Alcohol Alcohol.* 2019; 55(2020):63–70.

# Chapter 47

## Screening for Liver Fibrosis in General or At-Risk Populations Using Transient Elastography



Dominique Roulot

### Introduction

Cirrhosis, the final stage of chronic liver disease, is a major cause of death worldwide and accounts for a large number of hospitalizations. Deaths due to cirrhosis increased by 46% between 1990 and 2013, and it has become the fifth leading cause of death worldwide. The principal causes of liver cirrhosis are infection by hepatitis B and C viruses, alcoholic liver disease (ALD), and non-alcoholic fatty liver disease (NAFLD). Whereas the availability of highly effective antiviral drugs will rapidly reduce HCV infection and its consequences, the incidence of NAFLD is increasing dramatically in many areas of the world, associated with the epidemic of obesity and type-2 diabetes.

In general, cirrhosis progresses very slowly over a period of 2–3 decades and remains undiagnosed during this period because the disease is asymptomatic, and patients do not seek medical attention. Diagnosis most commonly occurs once the disease has reached the latest stages when complications appear, related to portal hypertension, liver failure, or development of hepatocellular carcinoma. Standard liver tests used to evaluate liver conditions such as serum aminotransferases levels or liver ultrasound examination are not sensitive methods to detect fibrosis. The diagnosis of patients at early stages of chronic liver diseases would allow identification of causal factors and subsequent application of specific targeted interventions. Given the high prevalence of chronic liver diseases, screening the general population for liver fibrosis would make sense in terms of public health. So far, however,

---

D. Roulot (✉)

Unité d'Hépatologie, Hôpital Avicenne, Assistance Publique-Hôpitaux de Paris, Université Paris 13, Bobigny, France

Inserm U955, équipe 18, Université Paris-Est, Créteil, France

e-mail: [dominique.roulot@aphp.fr](mailto:dominique.roulot@aphp.fr)

this objective has remained a very difficult challenge, because of the lack of appropriate tools [1].

Until recently, the only available method to detect liver fibrosis was liver biopsy. However, over the past decade, this procedure has been challenged by the development of alternative noninvasive methods. These new approaches rely either on blood tests or on liver stiffness measurement (LSM) by transient elastography (TE, Fibroscan<sup>®</sup>), which is currently the most commonly used and validated tool for staging of chronic liver disease. TE is a widely available technique which can be performed by doctors or nurses after a short training. This technique seems particularly suitable for the early detection of chronic liver diseases in the general population, particularly in high-risk populations, such as patients with obesity and/or diabetes. In this context, the recent introduction of new probes (XL-probes) specifically designed for obese patients has significantly improved measurability of liver stiffness.

## Screening for Liver Fibrosis in General Populations by Elastography

So far, a limited number of studies have reported results (summarized in Table 47.1) on systematic liver fibrosis screening in the general population using noninvasive methods [2]. The first study was conducted in France [3] on 1190 apparently healthy subjects older than 45 years attending a medical check-up in a primary care center. Among them, 7.5% showed LS values >8 kPa consistent with significant liver fibrosis and for 0.7% of the investigated persons LS values were above a threshold of 13 kPa considered to be indicative of liver cirrhosis. Subsequent evaluation showed that NAFLD was the most common cause of liver fibrosis, followed by ALD. A liver biopsy was obtained in almost one-third of the individuals with increased LS, and moderate-to-severe fibrosis was confirmed in 66% of the cases. Cirrhosis was confirmed histologically in the nine patients who displayed LS values above 13 kPa (100% positive predictive value).

Similar findings were reported in a subsequent general population-based study from the Netherlands conducted on 3041 people older than 45 years: 5.6% of them showed LS values >8 kPa. In 0.6% of the cases, LS was higher than 13 kPa [4]. Interestingly, in most cases, the increased LS was associated with components of the metabolic syndrome, suggesting that NAFLD was the principal cause of liver disease.

In a population-based study by Wong et al. from Hong Kong, 922 individuals, recruited by random selection from the government census database, were investigated for liver fat and fibrosis using an approach combining proton-magnetic resonance spectroscopy and TE [5]. NAFLD prevalence (defined by an intrahepatic triglyceride content greater than 5%) was 27.3%, and advanced fibrosis (defined by LS greater than 9.6 kPa) prevalence among patients with NAFLD was 3.7%.

**Table 47.1** Summary of studies screening for liver fibrosis in general or at-risk populations using TE

Reference	Population	Age (years)	Sample size	Prevalence of F $\geq$ 2	Prevalence of F $\geq$ 3	Prevalence of cirrhosis	Principal etiology
Roulot et al. 2011 [3]	Walk-in primary care	>45	1190	7.5% (>8 kPa)	NA	0.7% (>13 kPa)	NAFLD
Wong et al. 2012 [5]	Population-based	>18	922	NA	3.7% (>9.6 kPa)	NA	NAFLD
Koehler et al. 2016 [4]	Population-based	>45	3041	5.6% (>8 kPa)	NA	0.6% (>13 kPa)	NAFLD
Caballeria et al. 2018 [6]	Population-based	>18	3079	5.8% (>8 kPa)	3.6% (>9 kPa)	NA	NAFLD
Harman et al. 2015 [11]	Risk-related lifestyle factors	>18	378	27% (>8 kPa)	NA	NA	NAFLD. ALD
Kwok et al. 2016 [10]	Type 2 diabetics	>18	1918	NA	18% (>9.6 kPa)	11% (>11.5 kPa)	NAFLD
Rausch et al. 2016 [7]	20 year heavy drinkers 200 g alcohol per day	>18	512	NA	6.3% (AST-adapted cutoff values [8])	18.1% (AST-adapted cutoff values [8])	ALD

Recently, Caballeria et al. have investigated the prevalence of liver fibrosis in 3076 subjects older than 18 years in the Barcelona area [6]. LS values above 8 kPa were found in 5.8% of the subjects and values higher than 9 kPa were observed in 3.6% of the cases. Liver histology could be obtained from 92 subjects with increased LS; among them 81 had NAFLD and 7 alcoholic liver disease.

In a study on 521 heavy drinkers (ca. 200 g alcohol per day) presenting primarily for alcohol detoxification [7], ca. 25% showed advanced fibrosis or cirrhosis (F3-F4) based on AST-adapted LS cutoff values [8] after ca. 20 years of heavy drinking. This study underlines that only a minority of about one quarter will develop advanced liver disease despite two decades of heavy drinking. Notably, fibrosis distribution differed markedly in the noninvasively versus histologically assessed cohorts. Thus, histologically characterized patients showed only a small fraction of F0 stages as compared to the TE-assessed group (6% vs 47%). These data suggest that invasive screening procedure may be biased by recruiting more diseased patients.

## Screening for Liver Fibrosis in General Populations by Serum Markers

In comparison and by using serum biomarkers (FibroTest®), a study performed on 7463 apparently healthy individuals older than 40 years followed in two French social security centers, reported a presumed (not confirmed by liver biopsy) prevalence of 2.8% and 0.3% for advanced fibrosis and cirrhosis, respectively [9].

## Elastography Screening Studies in Selected Cohorts

Other studies screened for liver fibrosis in selected populations presenting risk factors for chronic liver diseases, specifically NAFLD and ALD. In a study conducted in Hong Kong [10] on 1918 patients with type 2 diabetes, the prevalence of LS values above 9.6 kPa, suggestive of a fibrosis stage  $\geq$ F3, was 18%. Approximately one-third of these patients had a liver biopsy: among them, 56% showed histological steatohepatitis, 21% advanced fibrosis, and 29% cirrhosis. Another study was conducted in the UK [11] on 378 patients attending primary care practices with either type 2 diabetes or excessive alcohol consumption associated with an abnormal blood biomarker (AST/ALT ratio for alcoholic liver disease and/or BARD score for NAFLD). Increased LS  $>$ 8 kPa was found in 27% of the cases and almost half of the patients who had liver biopsy showed liver cirrhosis. Notably, most of them had normal liver enzymes, indicating that the diagnosis of chronic liver disease would have been missed if patients had exclusively been assessed with the standard diagnostic algorithms used in primary care.

## Cost-Effectiveness

Whether a global screening strategy with noninvasive methods such as TE is cost-effective in terms of health outcomes and treatment costs is still a matter of debate.

Serra-Burriel et al. [12] analyzed individual data from 6 independent prospective cohorts including 6295 patients from 6 countries (five in Europe and one in Asia) with different healthcare systems with most of these studies mentioned above. This study suggests that a noninvasive screening strategy is cost-effective for identifying patients with liver fibrosis in primary care. The economic analyses showed that healthcare systems would need to invest between 2000€ (if targeting at-risk populations) and 7000€ (if targeting the general population) to gain an extra year of life, adjusted per quality of life. This meta-analysis concludes that large screening programs for liver fibrosis in the general population based on TE should be evaluated further.



The aim of the “Liverscreen project” is to assess the prevalence of liver fibrosis using Fibroscan in the general population above 40 years in several European countries. The study duration will be 24 months from the inclusion of the first patient and the number of included subjects will be 20,000. Patients with known chronic liver disease including cholestasis will be excluded, whereas patients with known liver steatosis but no diagnosis of fibrosis or cirrhosis will be included. Currently participating countries are Spain, France, Denmark, Italy, Germany, and United Kingdom.

Taken together, screening programs for liver fibrosis with TE in both the general population and in patients at risk for fibrosis development seems to be cost-effective and could be implemented across countries and different healthcare systems in Europe.

## Conclusion

Taken together, population-wide screening studies show a prevalence of elevated LS between 5.6 and 7.5% in the general adult population. Elevated LS was found between 18 and 27% among individuals with risk factors. These findings indicate an alarmingly high prevalence of chronic liver diseases in the general population, mainly related to NAFLD and ALD. However, whether a global screening strategy with noninvasive methods such as TE is cost-effective in terms of health outcomes and treatment costs is still a matter of debate. In conclusion, screening programs for liver fibrosis with TE in both the general population and in patients with risk factors for chronic liver diseases such as diabetes may be cost-effective and could be implemented across countries and different healthcare systems in Europe.

## References

1. Castera L. Screening the general population for cirrhosis using transient elastography: finding a needle in a haystack? *Gut*. 2011;60(7):883–4.
2. Gines P, Graupera I, Lammert F, Angeli P, Caballeria L, Krag A, et al. Screening for liver fibrosis in the general population: a call for action. *Lancet Gastroenterol Hepatol*. 2016;1(3):256–60.
3. Roulot D, Costes JL, Buyck JF, Warzocha U, Gambier N, Czernichow S, et al. Transient elastography as a screening tool for liver fibrosis and cirrhosis in a community-based population aged over 45 years. *Gut*. 2011;60(7):977–84.
4. Koehler EM, Plompen EP, Schouten JN, Hansen BE, Darwish Murad S, Taimr P, et al. Presence of diabetes mellitus and steatosis is associated with liver stiffness in a general population: the Rotterdam study. *Hepatology*. 2016;63(1):138–47.
5. Wong VW, Chu WC, Wong GL, Chan RS, Chim AM, Ong A, et al. Prevalence of non-alcoholic fatty liver disease and advanced fibrosis in Hong Kong Chinese: a population study using proton-magnetic resonance spectroscopy and transient elastography. *Gut*. 2012;61(3):409–15.
6. Caballeria L, Pera G, Arteaga I, Rodriguez L, Aluma A, Morillas RM, et al. High prevalence of liver fibrosis among European adults with unknown liver disease: a population-based study. *Clin Gastroenterol Hepatol*. 2018;16(7):1138–45.e5.

7. Rausch V, Peccerella T, Lackner C, Yagmur E, Seitz HK, Longerich T, et al. Primary liver injury and delayed resolution of liver stiffness after alcohol detoxification in heavy drinkers with the PNPLA3 variant I148M. *World J Hepatol.* 2016;8(35):1547–56.
8. Mueller S, Englert S, Seitz HK, Badea RI, Erhardt A, Bozaari B, et al. Inflammation-adapted liver stiffness values for improved fibrosis staging in patients with hepatitis C virus and alcoholic liver disease. *Liver Int.* 2015;35(12):2514–21.
9. Poynard T, Lebray P, Ingiliz P, Varaut A, Varsat B, Ngo Y, et al. Prevalence of liver fibrosis and risk factors in a general population using non-invasive biomarkers (FibroTest). *BMC Gastroenterol.* 2010;10:40.
10. Kwok R, Choi KC, Wong GL, Zhang Y, Chan HL, Luk AO, et al. Screening diabetic patients for non-alcoholic fatty liver disease with controlled attenuation parameter and liver stiffness measurements: a prospective cohort study. *Gut.* 2016;65(8):1359–68.
11. Harman DJ, Ryder SD, James MW, Jelpke M, Ottey DS, Wilkes EA, et al. Direct targeting of risk factors significantly increases the detection of liver cirrhosis in primary care: a cross-sectional diagnostic study utilising transient elastography. *BMJ Open.* 2015;5(4):e007516.
12. Serra-Burriel M, Graupera I, Torán P, Thiele M, Roulot D, Wai-Sun Wong V, et al. Transient elastography for screening of liver fibrosis: cost-effectiveness analysis from six prospective cohorts in Europe and Asia. *J Hepatol.* 2019;71(6):1141–51.

# Chapter 48

## Elastography in Combination with Other Biomarkers: Role of Algorithms



Maja Thiele and Katrine Prier Lindvig

### Algorithms Are Ideal to Combine Different Kinds of Information

An algorithm can be defined as a process, or set of rules, to be followed in problem-solving operations, especially by a computer. Any algorithm will follow a set of unambiguous instructions, typically to perform a calculation. In medicine, predictive algorithms are often derived from multivariable modelling and operate as diagnostic tests to stratify patients by risk and inform discrete decision-making [1]. Multivariable models are typical examples of parallel testing—two or more tests combined to provide one output result. An example of this is the liver stiffness, platelet count, spleen length test (LSPS; liver stiffness  $\times$  spleen diameter/platelet ratio) to diagnose portal hypertension [2]. Another option is sequential testing, where the result of an index test is used to guide what other test should follow, if any. The latter is often used in referral pathways from primary to secondary care, for example when the general physician orders a Fibrosis-4 test (FIB-4) and refers the NAFLD patient to elastography if FIB-4 exceeds a threshold of 1.3 (Fig. 48.1) [3].

Elastography of the liver provides data on liver stiffness (LS), the viscoelastic properties of the hepatic parenchyma. For more details, see also book Part II “Techniques to Measure Liver Stiffness.” Since liver fibrosis increases LS, elastography correlates highly with liver fibrosis. However, elastography is hampered by other factors that also increase liver stiffness, such as hepatic congestion, bile duct occlusion, and inflammation [4]. For more details, see also book Part IV “Important (Patho)physiological Confounders of LS.” In contrast, serum markers and imaging

---

M. Thiele (✉) · K. P. Lindvig

Fibrosis, Fatty Liver and Steatohepatitis Research Centre Odense (FLASH), Department of Gastroenterology and Hepatology, Odense University Hospital, Odense, Denmark

Department of Clinical Research, University of Southern Denmark, Odense, Denmark  
e-mail: [Maja.Thiele@rsyd.dk](mailto:Maja.Thiele@rsyd.dk); [Katrine.Prier.Lindvig@rsyd.dk](mailto:Katrine.Prier.Lindvig@rsyd.dk)

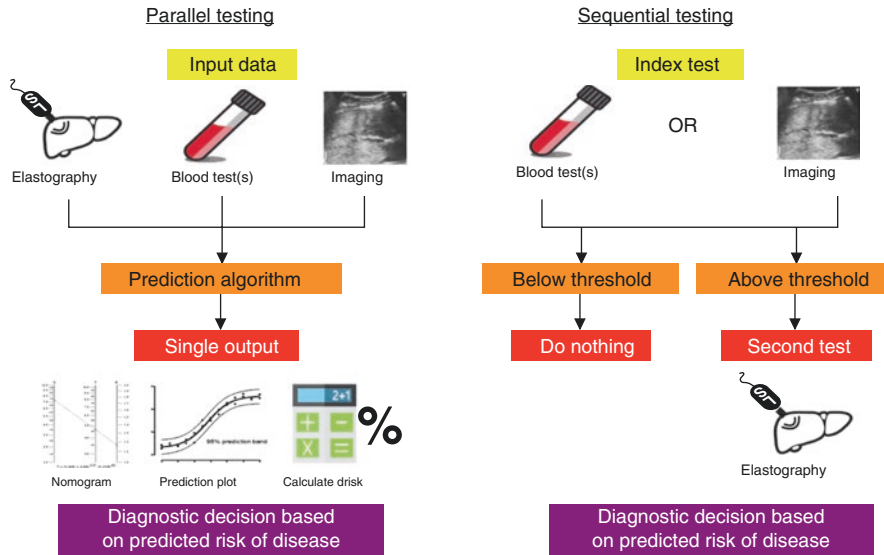


**Fig. 48.1** Two types of diagnostic algorithms, combining several diagnostic tests, either in parallel (left) or sequential (right). Both types of algorithms follow a set of rules to compute the predicted risk of a patient having the disease

techniques give other kinds of information, information that may also be of importance—either to correctly interpret the LS (for example to avoid false-negatives), to further increase the diagnostic accuracy of elastography, or to provide other types of information that is also of importance to the diagnosis and prognostication of liver disease. Information held by circulating biomarkers relate to hepatocellular or biliary damage (transaminases, gamma-glutamyl transferase), inflammation (ferritin, gamma-globulin), extracellular matrix remodelling (the ELF test, ProC3), liver function (INR, bilirubin, albumin, haptoglobin, cholesterol), or portal hypertension (platelet count, sodium), whereas imaging methods provide information on structural changes and hepatic hemodynamics. The combination of these three very different types of input data—from elastography, blood tests, and imaging—may provide knowledge and decision-making power that the individual test cannot provide alone. While the human brain exceeds even the most powerful supercomputers in processing speed and complex, cognitive work, humans are far behind even a simple smartphone when it comes to combining data into simple, calculated algorithms. When humans make a diagnostic prediction, we go through a process of reasoning. This diagnostic reasoning will be based on a number of data sources. We are somewhat limited in the number of data sources that can be taken into account, but we are particularly limited in the weight each data source is given to the final decision. In that sense, digital algorithms are more suited to capture complex, nonlinear patterns in all the available data. It is therefore very likely that computer-based algorithms to interpret LS will be decision tools for future hepatologists (Fig. 48.2).

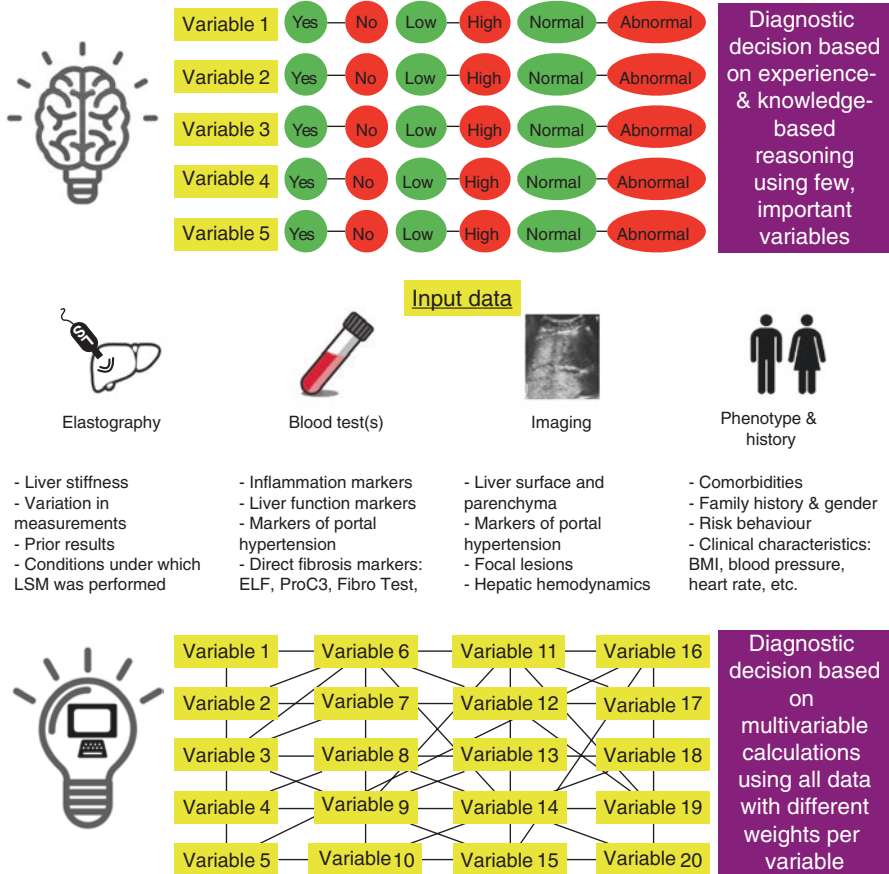


**Fig. 48.2** Rough depiction of human decision-making versus digital calculations. Humans tend to rely on few variables whose importance is based on prior knowledge and experience and appraise data dichotomously—above or below a threshold. Machine learning and other forms of computerized algorithms will seek patterns in the full dataset, considering the continuous nature of most variables and giving different weight to each variable. Unless supervised, the digital algorithm will however lack any mechanistic insight or understanding of the data, and digital algorithms should therefore be considered decision tools, up for interpretation, rather than automated truths

## Elastography Algorithms to Diagnose Fibrosis

Efforts have already been made towards improved diagnostics of elastography through the combination with other non-invasive tools (Table 48.1). However, due to the high accuracy of elastography for diagnosing liver fibrosis and cirrhosis, the addition of other non-invasive markers to elastography in multivariable models has been largely unsuccessful in improving the overall diagnostic accuracy, compared to elastography alone. In line with this, the EASL-ALEH clinical practice guideline on non-invasive tests supports the use of algorithms combining transient elastography

**Table 48.1** Examples of published elastography algorithms to risk stratify patients for liver fibrosis

Author, year	Algorithm	Patient population
Castera 2005 [13]	Multivariable model combining FibroTest with LSM; or parallel testing with FibroTest and LSM, concordance between tests confirms the diagnosis	HCV
Boursier 2009 [6]	Multivariable model (FibroMeter VCTE) including platelet count, prothrombin ratio, AST, Alpha-2-macroglobulin, GGT, and LSM	Mixed etiology
Wong 2014 [16]	Parallel testing with ELF and LSM. Either low ELF or low LSM excludes advanced fibrosis, agreement between high ELF and high LSM confirms the diagnosis	HBV
Chan 2015 [12]	Sequential testing with NAFLD fibrosis score (NFS) → LSM	NAFLD
Mueller 2015 [37]	Parallel testing with LSM cut-offs adapted according to AST above or below 40 U/L	Alcohol and HCV
Harman 2015 [18]	Sequential testing with AST:ALT ratio in excess drinkers or BARD score in patients with diabetes or elevated ALT → LSM	Primary care patients with risk factors
Boursier 2017 [38]	Sequential testing with eLIFT → FibroMeter VCTE	Mixed etiology
Calés 2017 [39]	Parallel testing with FibroMeter <sup>V2G</sup> and LSM. Concordance between tests confirms the diagnosis	HCV
Thiele 2018 [19]	Sequential testing with Forns index → ELF test → LSM	Alcohol-related liver disease

**Scores:** **BARD score** = BMI >28 = 1 point, AST:ALT ratio of >0.8 = 2 points, DM = 1 point. **eLIFT** = easy liver fibrosis test, which assigns points for age, male sex, AST, GGT, platelet count, and prothrombin time. **ELF test** = Commercial, multivariable model containing hyaluronic acid, N-terminal propeptide of collagen type 3 (PIIINP), and tissue inhibitor of metalloproteinase-1 (TIMP-1), calculated differently whether measured on an ADVIA Centaur XP/XPT or CP (Siemens healthcare). **FibroMeter<sup>V2G</sup>** = commercial, multivariable model, which combines age, gender, AST, urea, prothrombin ratio, platelet count, alpha-2-macroglobulin, and hyaluronic acid. The algorithms **FibroMeter VCTE** and **FibroMeter<sup>V2G</sup>** are owned and protected by Echosens. **FibroTest** = commercial, multivariable model combining **Forns index** =  $7.811 - 3.131 \cdot \ln(\text{platelets}) + 0.781 \cdot \ln(\text{GGT}) + 3.467 \cdot \ln(\text{age}) - 0.541 \cdot (\text{chol})$ , with cholesterol in mmol/L. **NFS** =  $-1.675 + 0.037 \cdot \text{age} + 0.094 \cdot \text{BMI} + 1.13 \cdot \text{IFG/diabetes}(\text{yes} = 1, \text{no} = 0) + 0.99 \cdot \text{AST/ALT ratio} - 0.013 \cdot \text{platelet count} - 0.66 \cdot \text{albumin}(\text{g/dL})$

**Abbreviations:** *ALT* alanine transaminase, *AST* aspartate transaminase, *GGT* gamma-glutamyltransferase, *HBV* chronic viral hepatitis B, *HCV* chronic viral hepatitis C, *LSM* liver stiffness measurement by transient elastography (FibroScan), *NAFLD* non-alcoholic fatty liver disease, *VCTE* vibration controlled transient elastography

(TE) and serum biomarkers, but does not recommend them over TE alone [5]. However, the guideline does recommend a strategy of parallel testing with TE and serum biomarkers, assessing whether results of the two are concordant or discordant. In case of unexplained discordance, a liver biopsy should be performed. This strategy is for now however only recommended for chronic viral hepatitis C (HCV), for lack of supporting evidence in other etiologies.

The multivariable model FibroMeter (Echosens, France) is an example of a commercial algorithm of circulating markers that can be combined with TE. FibroMeter contains platelet count, prothrombin ratio, alpha-2-macroglobulin, GGT, and AST and had an area under the receiver operating characteristics curve (AUROC) of 0.83 for the diagnosis of significant fibrosis ( $\geq F2$ ) in a cohort of liver disease patients of mixed etiology [6]. Transient elastography had a superior accuracy, with an AUROC of 0.87. When combined, the model containing FibroMeter and TE, FibroMeter VCTE, increased AUROC to 0.89. This was statistically significant, but whether it is clinically relevant remains to be debated.

In cohorts of alcohol-related liver disease (ALD), Voican and colleagues found that the combined use of TE with Fibrotest<sup>®</sup> or PGAA did not improve the performance of TE alone for the diagnosis of advanced fibrosis [7]. TE had an AUROC of 0.90, comparable to AUC = 0.91 and AUC = 0.90 for TE-FibroTest<sup>®</sup> and TE-PGAA, respectively. Similarly, in an earlier study of ALD by Mueller and colleagues, the accuracy of TE for diagnosing advanced fibrosis was AUC = 0.91 [8]. By excluding patients with AST >100 U/L, as a marker of steatohepatitis, the diagnostic accuracy of TE remained almost similar, at AUC = 0.92. The diagnostic accuracy of TE could be improved to AUC = 0.95 by restricting the analysis to patients without steatohepatitis, evidenced by AST <50 U/L. The gain in overall diagnostic accuracy as measured by the AUROC was of minimal clinical relevance, while statistically significant. However, the main advantage of adding a serum marker of hepatic inflammation to the algorithm is the possibility of increasing specificity of elastography, by decreasing the number of false positives. In the aforementioned study, exclusion of patients with AST >100 U/L increased specificity from 75 to 87%. Consequently, the 2018 EASL clinical practice guideline on alcohol-related liver disease does not recommend any diagnostic algorithms of elastography and other markers for evaluating fibrosis, but do recommend to interpret liver stiffness values in patients with AST >100 U/L with caution, due to the risk of falsely elevated liver stiffness caused by liver inflammation [9].

In the context of non-alcoholic fatty liver disease (NAFLD), elastography also correlates well with hepatic fibrosis and therefore little evidence favors algorithms combining elastography with circulating markers of fibrosis, over elastography alone. Boursier and colleagues compared eight blood fibrosis tests with TE [10]. They found that TE and FibroMeter<sup>V2G</sup> had similar, good diagnostic accuracies for advanced fibrosis (AUCs of 0.83 and 0.82, respectively). However, the use of TE resulted in fewer patients in the “grey zone” of fibrosis classification, where neither negative nor positive predictive value is above 90%. TE classified 44% in the grey zone, compared to 53% for FibroMeter<sup>V2G</sup>, overall favoring the use of TE alone. A similar study compared seven fibrosis blood tests with TE and found that the overall performance of FibroMeter VCTE was comparable to TE alone (AUROCs of 0.86 and 0.85) [11]. One study combined the non-commercial NAFLD-fibrosis-score (NFS) with LS measurement. The NFS score had poor sensitivity (40%), but high specificity (97%). Therefore, NFS combined with TE had no advantage over using TE alone, whereas a strategy of sequential testing with NFS to rule out advanced fibrosis, followed by TE in patients with indeterminate or high NFS scores, reduced

the number of patients requiring a liver biopsy while maintaining the accuracy to predict advanced fibrosis [12].

Chronic viral hepatitis, particularly HCV, is the etiology where most evidence supports the use of TE combination algorithms. For the first time in 2005, Castèra and colleagues showed that TE in combination with FibroTest was superior to stand-alone tests, with AUROCs for advanced fibrosis of 0.90 for TE and FibroTest alone, compared to 0.95 for a multivariable regression model combining the two [13]. Additionally, when the two tests were in accordance, 95% of patients were correctly classified.

While TE and other elastography methods have excellent diagnostic accuracy for advanced fibrosis and cirrhosis, the method is weaker for diagnosing significant fibrosis ( $\geq F2$ ). Therefore, combination algorithms or stepwise approaches have been tested, to increase the number of correct classifications for significant fibrosis. For example, Zarski and colleagues tested seven blood tests and TE in combination, for the diagnosis of significant fibrosis in HCV [14]. They found that the original ELF test (containing age in addition to three serum fibrosis markers) in parallel with TE had both the highest negative predictive value (90%) for excluding F0-1 fibrosis, and the highest positive predictive value for ruling in significant fibrosis (92%). Altogether the combination algorithm avoided 55% of liver biopsies. In contrast, a study in Asian HBV patients found TE to be superior to the ELF test to predict liver fibrosis without any more correctly classified patients, when combining ELF and TE. Yet when testing sequentially, the number of avoided liver biopsies increased slightly, from 64% with TE alone, to 69% using the two tests in sequence [15]. Another study have tested TE and ELF, but aimed at avoiding TE false positives by excluding [16]. Wong and colleagues used ALT-adapted TE cut-offs, and they found that an enhanced liver fibrosis-liver stiffness measurement algorithm could improve the accuracy of prediction of either ELF or LSM alone in patients with chronic hepatitis B.

A single study has combined elastography with serum markers and imaging: Two algorithms were proposed for cirrhosis diagnostics in chronic hepatitis B patients: CIR-4 consisting of TE, INR, platelet count and ultrasonic hepatic vessel appearance, and CIR-6 consisting of TE, INR, platelet count, albumin, ultrasonic hepatic vessel and liver parenchyma appearance. Both algorithms outperformed TE alone to detect cirrhosis (AUROC = 0.95 for both CIR-4 and CIR-6, versus AUC = 0.91 for TE) [17].

The primary care health sector needs cheaper options than elastography for detecting liver fibrosis in many patients with obesity, type 2 diabetes, elevated liver function tests, or harmful use of alcohol as risk factors for liver fibrosis. Therefore, the biggest opportunity for combination algorithms lies in sequential testing as referral pathways from primary to secondary care [3]. The feasibility of such a referral pathway has already been tested in the UK, where patients with excess alcohol consumption, type 2 diabetes, or persistently elevated liver enzymes were subjected first to the AST:ALT ratio (in case of excess drinking) or the BARD score (in case of risk of NAFLD), and subsequently subjected to TE in case of elevated serum scores [18]. An extended, three-step strategy was suggested in Danish primary care



patients with alcohol-related liver disease, whereby the cheap Forns index was used as first threshold, then the—somewhat more expensive—ELF test in those with elevated Forns index; and finally TE, in those with both elevated ELF test and Forns index [19]. While the sequential algorithm of serum test first followed by elastography in test positives may not have a higher diagnostic accuracy than elastography-for-all, it is a straightforward, cost-conscious way of saving expensive secondary care referrals. Indeed, preliminary evidence suggests that such a referral pathway may be cost-efficient [20].

In summary, combining elastography with other biomarkers in multivariable models has only discrete impact on the overall diagnostic accuracy for detecting liver fibrosis and cirrhosis across etiologies. A better approach is to address whether elastography and a serum test are in concordance or discordance. However, while this approach may decrease false positives, there is a risk of placing more patients in a “grey zone” of discordant results, than if using elastography alone. The most promising approach is in primary care, where we may greatly improve case finding while keeping screening costs down, by the systematic use of sequential algorithms with an initial, inexpensive serum test, followed by elastography only in case of a positive screening result.

## Elastography Algorithms to Diagnose Portal Hypertension

The development and progression of portal hypertension is not purely caused by accumulation of liver fibrosis, but by changes in the hepatic hemodynamics and systemic circulation. Therefore, elastography alone is unreliable for the diagnosis of portal hypertension above 10 mmHg and complications to portal hypertension [21]. Multivariable algorithms combining liver elastography with non-invasive markers, that reflect hemodynamic changes, have therefore been more successful than similar combinations for diagnosing fibrosis [22]. Best known is the Baveno VI algorithm for ruling out large varices in patients with compensated advanced chronic liver disease [22]. The strategy optimizes the number of spared endoscopies, while keeping the risk of missing varices needing treatment below 5%. Many groups have independently validated the first set of Baveno VI criteria—TE below 20 kPa and a platelet count above  $150 \times 10^9/L$  [23–26]. Recently, a set of extended criteria were suggested, using a 25 kPa TE cut-off and platelet count of  $110 \times 10^9/L$  [24, 26]. The Baveno VI original and extended criteria have been further validated in NAFLD specifically, accounting for use of the FibroScan XL probe in obese patients [27].

Algorithms developed to rule out or diagnose clinically significant portal hypertension (CSPH,  $\geq 10$  mmHg), severe portal hypertension ( $\geq 12$  mmHg), and esophageal varices use liver stiffness as a fibrosis measure, combined with markers that reflect hemodynamic-induced changes to the spleen. These changes are: (a) increased spleen diameter and (b) increased spleen stiffness, both caused by elevated splenic venous pressure that lead to spleen congestion, fibrosis, and hyperplasia; and (c) thrombocytopenia due to trapping and destruction of platelets in the

**Table 48.2** Common elastography algorithms to rule out varices needing treatment

Algorithm name	Algorithm components				Outcome
	Liver stiffness (kPa)	Spleen stiffness (kPa)	Spleen length (cm)	Platelet count 10 <sup>9</sup> /L	
Baveno VI [22]	TE < 20	–	–	>150	26% saved endoscopies while missing <1% of VNT [26]
Extended Baveno VI [24]	TE < 25	–	–	>110	43% saved endoscopies while missing 2% of VNT [26]
Baveno VI for NAFLD cirrhosis [27]	TE < 30 with M-probe TE < 25 with XL probe	–	–	>110	58% saved endoscopies while missing 4% of VNT
Anticipate [25]	+	–	+	+	LSPS* ≤ 1.33 saved 26% of endoscopies
Baveno VI/SSM [40]	TE < 20	TE ≤ 46	–	>150	37–44% saved endoscopies while missing 2% of VNT

**Abbreviations:** NAFLD non-alcoholic fatty liver disease, VNT varices needing treatment

\*LSPS: liver stiffness × spleen diameter/platelet ratio [41]

spleen, aggravated by a decrease in thrombopoietin. Table 48.2 provides an oversight of the best validated elastography algorithms to rule out varices needing treatment. For more details, see also book Part V “LS and Important Clinical Endpoints.”

Few studies have proposed algorithms to rule out CSPH using other elastography methods than TE. In patients with cirrhosis, point shear wave elastography (pSWE) and 2-dimensional shear wave elastography (2D-SWE) may have a particular advantage, since they provide additional morphological information such as spleen lengths, collateral development, or sure sign of cirrhosis. 2D-SWE and pSWE should not be considered anymore superior in patients with ascites, since TE also allows to measure LS in ascitic patients using the XL probe [28]. A European multicenter study proposed that a combination of liver 2D-SWE and spleen 2D-SWE could rule out CSPH [29]. However, this finding was refuted by an independent, single-center study from France that could not validate the multicenter results [30].

## Future Directions: Machine Learning and Artificial Intelligence

The combination of computer technology, artificial intelligence, and the concept of big data may provide solutions to complex problems in fields such as video surveillance, fraud detection, social media, and retail industry [31]. But especially in

healthcare, it is believed that machine-learning algorithms can improve the accuracy of diagnostic and prognostic predictions compared with conventional algorithms. The advantage of machine learning is its ability to capture complex, nonlinear relationships in the data and identify strong, hypothesis-free associations. Machine-learning approaches for detection of NAFLD have already been published [32]. Radiomics is a deep learning technique, whereby each pixel is treated as a data point and processed. Recently, Wang and colleagues developed a radiomics model that substantially improved diagnostic accuracy of 2D-SWE for detecting HBV fibrosis. The AUROC for advanced fibrosis increased from 0.81 with traditional 2D-SWE, to 0.99 with the radiomics model [33]. However, three or more image acquisitions were still needed from each subject, and for each acquisition, investigators needed to extract the 2D-SWE images, manually select the input layer, and run the radiomics software. Consequently, radiomics are still a long way from implementation. Radiomics efforts do continue, and the technique is particularly suited for 2D-SWE, which acquire a detailed elastogram [34]. Other studies have yielded less convincing results: One study added an artificial neural network to liver stiffness for diagnosing cirrhosis, portal hypertension and esophageal varices and found a high diagnostic performance; nonetheless the network was inferior to liver stiffness measurement alone [35]. Another study used a random forest machine-learning technique to develop an algorithm that combines INR, AST, platelet count, urea nitrogen, hemoglobin, and presence of ascites to spare 31% of patients from variceal screening endoscopy, while missing 3% of varices needing treatment [36]. These data are however fully comparable with the simpler Baveno VI criteria.

Machine learning attracts huge attention in healthcare research, largely driven by increases in computational power and the availability of massive new datasets. However, in hepatology we have yet to see artificial intelligence and deep neural networks provide real breakthroughs of true clinical importance and implementation to practice. Some elastography studies have been published with promising results; surely more will be seen in the future.

## References

1. Collins GS, Reitsma JB, Altman DG, Moons KGM. Transparent reporting of a multivariable prediction model for individual prognosis or diagnosis (TRIPOD): the TRIPOD statement. *The TRIPOD Statement. Ann Intern Med.* 2015;162(1):55–63.
2. Berzigotti A, Seijo S, Arena U, Abralles JG, Vizzutti F, García-Pagán JC, et al. Elastography, spleen size, and platelet count identify portal hypertension in patients with compensated cirrhosis. *Gastroenterology.* 2013;144(1):102–11.e1.
3. Castera L, Friedrich-Rust M, Loomba R. Noninvasive assessment of liver disease in patients with nonalcoholic fatty liver disease. *Gastroenterology.* 2019;156(5):1264–81.e4.
4. Mueller S, Sandrin L. Liver stiffness: a novel parameter for the diagnosis of liver disease. *Hepat Med.* 2010;2:49–67.
5. European Association for Study of Liver; Asociacion Latinoamericana para el Estudio del Hígado. EASL-ALEH Clinical Practice Guidelines: non-invasive tests for evaluation of liver disease severity and prognosis. *J Hepatol.* 2015;63(1):237–64.

6. Boursier J, Vergniol J, Sawadogo A, Dakka T, Michalak S, Gallois Y, et al. The combination of a blood test and Fibroscan improves the non-invasive diagnosis of liver fibrosis. *Liver Int.* 2009;29(10):1507–15.
7. Voican CS, Louvet A, Trabut JB, Njike-Nakseu M, Dharancy S, Sanchez A, et al. Transient elastography alone and in combination with FibroTest(R) for the diagnosis of hepatic fibrosis in alcoholic liver disease. *Liver Int.* 2017;37(11):1697–705.
8. Mueller S, Millonig G, Sarovska L, Friedrich S, Reimann FM, Pritsch M, et al. Increased liver stiffness in alcoholic liver disease: differentiating fibrosis from steatohepatitis. *World J Gastroenterol.* 2010;16(8):966–72.
9. EASL. EASL Clinical Practice Guidelines: management of alcohol-related liver disease. *J Hepatol.* 2018;69(1):154–81.
10. Boursier J, Vergniol J, Guillet A, Hiriart JB, Lannes A, Le Bail B, et al. Diagnostic accuracy and prognostic significance of blood fibrosis tests and liver stiffness measurement by FibroScan in non-alcoholic fatty liver disease. *J Hepatol.* 2016;65(3):570–8.
11. Loong TC, Wei JL, Leung JC, Wong GL, Shu SS, Chim AM, et al. Application of the combined FibroMeter vibration-controlled transient elastography algorithm in Chinese patients with non-alcoholic fatty liver disease. *J Gastroenterol Hepatol.* 2017;32(7):1363–9.
12. Chan WK, Nik Mustapha NR, Mahadeva S. A novel 2-step approach combining the NAFLD fibrosis score and liver stiffness measurement for predicting advanced fibrosis. *Hepatol Int.* 2015;9(4):594–602.
13. Castera L, Vergniol J, Foucher J, Le Bail B, Chanteloup E, Haaser M, et al. Prospective comparison of transient elastography, Fibrotest, APRI, and liver biopsy for the assessment of fibrosis in chronic hepatitis C. *Gastroenterology.* 2005;128(2):343–50.
14. Zarski JP, Sturm N, Guechot J, Zafrani ES, Vaubourdolle M, Thoret S, et al. Contribution of the ELFG test in algorithms of non-invasive markers towards the diagnosis of significant fibrosis in chronic hepatitis C. *PLoS One.* 2013;8(3):e59088.
15. Heo JY, Kim BK, Park JY, Kim DY, Ahn SH, Kim HS, et al. Combination of transient elastography and an enhanced liver fibrosis test to assess the degree of liver fibrosis in patients with chronic hepatitis B. *Gut Liver.* 2018;12(2):190–200.
16. Wong GL, Chan HL, Choi PC, Chan AW, Yu Z, Lai JW, et al. Non-invasive algorithm of enhanced liver fibrosis and liver stiffness measurement with transient elastography for advanced liver fibrosis in chronic hepatitis B. *Aliment Pharmacol Ther.* 2014;39(2):197–208.
17. Liang XE, Dai L, Yang SL, Zhong CX, Peng J, Zhu YF, et al. Combining routine markers improves the accuracy of transient elastography for hepatitis B cirrhosis detection. *Dig Liver Dis.* 2016;48(5):512–8.
18. Harman DJ, Ryder SD, James MW, Jelpke M, Ottey DS, Wilkes EA, et al. Direct targeting of risk factors significantly increases the detection of liver cirrhosis in primary care: a cross-sectional diagnostic study utilising transient elastography. *BMJ Open.* 2015;5(4):e007516.
19. Thiele M, Madsen BS, Hansen JF, Detlefsen S, Antonsen S, Krag A. Accuracy of the enhanced liver fibrosis test vs FibroTest, elastography, and indirect markers in detection of advanced fibrosis in patients with alcoholic liver disease. *Gastroenterology.* 2018;154(5):1369–79.
20. Tapper EB, Hunink MGM, Afdhal NH, Lai M, Sengupta N. Cost-effectiveness analysis: risk stratification of nonalcoholic fatty liver disease (NAFLD) by the primary care physician using the NAFLD fibrosis score. *PLoS One.* 2016;11(2):e0147237.
21. Colecchia A, Montrone L, Scaiola E, Bacchi-Reggiani ML, Colli A, Casazza G, et al. Measurement of spleen stiffness to evaluate portal hypertension and the presence of esophageal varices in patients with HCV-related cirrhosis. *Gastroenterology.* 2012;143(3):646–54.
22. de Franchis R. Expanding consensus in portal hypertension: report of the Baveno VI Consensus Workshop: stratifying risk and individualizing care for portal hypertension. *J Hepatol.* 2015;63(3):743–52.
23. Maurice JB, Brodtkin E, Arnold F, Navaratnam A, Paine H, Khawar S, et al. Validation of the Baveno VI criteria to identify low risk cirrhotic patients not requiring endoscopic surveillance for varices. *J Hepatol.* 2016;65(5):899–905.

24. Augustin S, Pons M, Maurice JB, Bureau C, Stefanescu H, Ney M, et al. Expanding the Baveno VI criteria for the screening of varices in patients with compensated advanced chronic liver disease. *Hepatology*. 2017;66(6):1980–8.
25. Abraldes JG, Bureau C, Stefanescu H, Augustin S, Ney M, Blasco H, et al. Noninvasive tools and risk of clinically significant portal hypertension and varices in compensated cirrhosis: the “Anticipate” study. *Hepatology*. 2016;64(6):2173–84.
26. Siddiqui MS, Yamada G, Vuppalanchi R, Van Natta M, Loomba R, Guy C, et al. Diagnostic accuracy of noninvasive fibrosis models to detect change in fibrosis stage. *Clin Gastroenterol Hepatol*. 2019;17(9):1877–85.e5.
27. Petta S, Sebastiani G, Bugianesi E, Viganò M, Wong VW, Berzigotti A, et al. Non-invasive prediction of esophageal varices by stiffness and platelet in non-alcoholic fatty liver disease cirrhosis. *J Hepatol*. 2018;69(4):878–85.
28. Kohlhaas A, Durango E, Millonig G, Bastard C, Sandrin L, Golriz M, et al. Transient elastography with the XL probe rapidly identifies patients with non-hepatic ascites. *Hepat Med*. 2012;4:11–8.
29. Jansen C, Bogs C, Verlinden W, Thiele M, Moller P, Gortzen J, et al. Shear-wave elastography of the liver and spleen identifies clinically significant portal hypertension: a prospective multicentre study. *Liver Int*. 2017;37(3):396–405.
30. Elkrief L, Ronot M, Andrade F, Burgio MD, Zappa M, Roux O, et al. Non-invasive evaluation of portal hypertension using shear-wave elastography: analysis of two algorithms combining liver and spleen stiffness in 191 patients with cirrhosis. *Aliment Pharmacol Ther*. 2018;47(5):621–30.
31. Chen JH, Asch SM. Machine learning and prediction in medicine—beyond the peak of inflated expectations. *N Engl J Med*. 2017;376(26):2507–9.
32. Yip TC, Ma AJ, Wong VW, Tse YK, Chan HL, Yuen PC, et al. Laboratory parameter-based machine learning model for excluding non-alcoholic fatty liver disease (NAFLD) in the general population. *Aliment Pharmacol Ther*. 2017;46(4):447–56.
33. Wang K, Lu X, Zhou H, Gao Y, Zheng J, Tong M, et al. Deep learning Radiomics of shear wave elastography significantly improved diagnostic performance for assessing liver fibrosis in chronic hepatitis B: a prospective multicentre study. *Gut*. 2019;68(4):729–41.
34. Gatos I, Tsantis S, Spiliopoulos S, Karnabatidis D, Theotokas I, Zoumpoulis P, et al. A machine-learning algorithm toward color analysis for chronic liver disease classification, employing ultrasound shear wave elastography. *Ultrasound Med Biol*. 2017;43(9):1797–810.
35. Procopet B, Cristea VM, Robic MA, Grigorescu M, Agachi PS, Metivier S, et al. Serum tests, liver stiffness and artificial neural networks for diagnosing cirrhosis and portal hypertension. *Dig Liver Dis*. 2015;47(5):411–6.
36. Dong TS, Kalani A, Aby ES, Le L, Luu K, Hauer M, et al. Machine learning-based development and validation of a scoring system for screening high-risk esophageal varices. *Clin Gastroenterol Hepatol*. 2019;17(9):1894–901.e1.
37. Mueller S, Englert S, Seitz HK, Badea RI, Erhardt A, Bozaari B, et al. Inflammation-adapted liver stiffness values for improved fibrosis staging in patients with hepatitis C virus and alcoholic liver disease. *Liver Int*. 2015;35(12):2514–21.
38. Boursier J, de Ledinghen V, Leroy V, Anty R, Francque S, Salmon D, et al. A stepwise algorithm using an at-a-glance first-line test for the non-invasive diagnosis of advanced liver fibrosis and cirrhosis. *J Hepatol*. 2017;66(6):1158–65.
39. Calés P, Boursier J, Lebigot J, de Ledinghen V, Aube C, Hubert I, et al. Liver fibrosis diagnosis by blood test and elastography in chronic hepatitis C: agreement or combination? *Aliment Pharmacol Ther*. 2017;45(7):991–1003.
40. Colecchia A, Ravaioli F, Marasco G, Colli A, Dajti E, Di Biase AR, et al. A combined model based on spleen stiffness measurement and Baveno VI criteria to rule out high-risk varices in advanced chronic liver disease. *J Hepatol*. 2018;69(2):308–17.
41. Kim BK, Han KH, Park JY, Ahn SH, Kim JK, Paik YH, et al. A liver stiffness measurement-based, noninvasive prediction model for high-risk esophageal varices in B-viral liver cirrhosis. *Am J Gastroenterol*. 2010;105(6):1382–90.

# Chapter 49

## Fibrosis Assessment via Liver Stiffness Measurements: How Many Patients Are Spared from a Liver Biopsy?



Amine Benmassaoud and Giada Sebastiani

### Introduction

The evaluation of patients with chronic liver disease is based on a global approach which includes a clinical exam, laboratory investigations, and radiological assessment. In some patients, a liver biopsy is required to identify the cause of liver disease, to grade the degree of inflammatory activity, and to stage fibrosis [1]. Information obtained from the liver biopsy allows to differentiate patients with an expected benign course from those at risk of progressive liver disease or pre-clinical cirrhosis [2]. For this reason, a lot of work has gone into developing and standardizing various histological classification systems [3]. From the original and complex Knodell histology activity index published in 1981 or the simplified Batts and Ludwig classification, to more disease-specific scoring systems such as the METAVIR and Ishak classification in patients with Hepatitis C Virus (HCV) infection, and the more recent Brunt and Kleiner classification for those with non-alcoholic steatohepatitis (NASH), the histological assessment of hepatic fibrosis is considered the gold standard to stage liver fibrosis [4–7]. For more details on histological fibrosis scores, see also Appendix Tables A.19, A.20, A.21, A.22, A.23 and A.24. Using a 5-level liver fibrosis staging system, such as in the METAVIR or the Batts and Ludwig classification, from F0 to F4, those with F2 are considered to have significant liver fibrosis which is likely to be progressive, whereas patients with F3 fibrosis have advanced or severe fibrosis, and F4 denotes the presence of cirrhosis.

From an epidemiology perspective, chronic liver diseases are the 11th cause of mortality worldwide, with nearly two million deaths annually [8]. Although

---

A. Benmassaoud · G. Sebastiani (✉)  
Division of Gastroenterology and Hepatology, Royal Victoria Hospital, McGill University  
Health Centre, Montreal, QC, Canada  
e-mail: [giada.sebastiani@mcgill.ca](mailto:giada.sebastiani@mcgill.ca)

geographic prevalence can be difficult to ascertain, the European HEPAAHEALTH project estimates that the median age-adjusted prevalence of cirrhosis and chronic liver disease in Europe is 833 cases per 100,000 individuals [9]. These estimates were derived from the Global Burden of Disease study from 2016 which unfortunately did not directly assess non-alcoholic fatty liver disease (NAFLD), but rather divided causes into alcohol-related liver disease (ALD), infection with Hepatitis B Virus (HBV) and HCV, and other causes. On the other hand, the National Health and Nutrition Examination Survey estimated that the prevalence rate of chronic liver diseases was 15% over a 4-year period, with NAFLD being the most common cause of liver disease in nearly 50% of cases [10]. In another prospective population-based cohort study from the USA, newly diagnosed chronic liver disease was estimated at 64 cases per 100,000, with nearly 20% of them having cirrhosis at presentation [11]. Once cirrhosis is present, the median survival of patients with compensated and decompensated cirrhosis is 10 and 2 years, respectively [12]. Considering these numbers, it is imperative to screen and identify patients with chronic liver disease early on, before cirrhosis is established, in order to treat the underlying cause of liver disease, prevent progression, and initiate appropriate surveillance programs when necessary.

These prevalence rates demonstrate that liver biopsy cannot be used for screening purposes, nor was it ever intended to be. In addition, there are multiple inherent limitations to the liver biopsy. Firstly, liver biopsy is estimated to reflect only 1:50,000 of the entire liver parenchyma [13]. This can therefore lead to sampling error leading to under-staging the degree of fibrosis especially in smaller biopsies with length and width under 15 mm and under 1.4 mm, respectively [14]. In fact, in some studies the misdiagnosis of cirrhosis occurred in 33% of cases [15]. In addition, the procedure itself is not without risk, with rates of complications in the order of 1%, and mortality between 0.1% and 0.01% [16].

In this context, noninvasive tests were developed to stage liver fibrosis and to potentially screen patients with chronic liver diseases. Noninvasive tests encompass non-patented simple serum markers, including the Aspartate aminotransferase to Platelet Ratio Index (APRI), FIB-4, or NAFLD Fibrosis Score (NFS), and patented serum markers, such as Fibrotest, Fibrometer, and Enhanced Liver Fibrosis (ELF) score. Moreover, several noninvasive physical methods have been developed for assessing liver stiffness (LS), such as transient elastography (TE) with Fibroscan, shear-wave elastography, and magnetic resonance elastography. The purpose of all the noninvasive tests is to maximize diagnostic accuracy to stage liver hepatic fibrosis while minimizing the number of liver biopsies necessary [17–22]. Serum fibrosis biomarkers have been progressively incorporated into clinical guidelines and are becoming first-line diagnostic tests for liver fibrosis staging, with significant reduction in the need for liver biopsy. We here provide an update on the diagnostic and screening algorithms based on noninvasive fibrosis tests and on their accuracy in clinical scenarios related to etiologies of chronic liver diseases.



## Optimizing a First Line of Screening

With increased awareness on the rising prevalence of NAFLD, affecting nearly 20–30% of individuals in Europe and the USA, a significant burden is placed on community general practitioners, which are the front line in this epidemic. As opposed to other etiologies of chronic liver disease, an important part of the management of patients with early NAFLD and ALD is rooted in primary practice through lifestyle modification and social support. In addition, it would not be possible for specialized clinics to assess all patients with NAFLD or ALD. Therefore, the prioritization of patients with at least significant fibrosis is necessary. General practitioners should identify and refer to specialized care patients with at least significant liver fibrosis [23, 24]. In cases with abnormal liver enzymes, a positive liver etiology screen or abnormal ultrasound, except for hepatic steatosis, a referral to specialist evaluation is recommended [25]. In the following section, we will describe NAFLD and ALD algorithms developed for first-line practitioners as this will lead to the largest number of spared liver biopsies in the real world.

### *Non-alcoholic Fatty Liver Disease (NAFLD)*

Both the British Society of Gastroenterology and the American College of Gastroenterology released recent guidelines addressing the evaluation of patients with abnormal liver enzymes [25, 26]. More specifically, the British Society of Gastroenterology has provided a two-step sequential algorithm for patients with suspected NAFLD incorporating simple biomarkers, such as FIB-4 and NFS (Fig. 49.1) [25]. If FIB-4 or NFS suggests a low risk of advanced fibrosis (F3), the patient should remain and be managed in primary care with periodical re-assessment every 2–5 years. Due to a lower specificity in patients above the age of 65, an adjusted FIB-4 and NFS cutoff were suggested to exclude advanced fibrosis at  $<2.0$  and  $<0.12$ , respectively [27]. Patients identified to be at high risk of F3 disease (FIB-4  $>3.25$  or NFS  $>0.675$ ), should be referred to a hepatology clinic where patients with an indeterminate result should have a second noninvasive test, either with ELF or LS measurement by TE. The result of this second test will determine if advanced fibrosis could be present and guide subsequent management. In cases of technical failure or unreliable measurement of TE, which occur in 5–25% of cases, the patient should still be referred to a specialist [28]. The chosen cutoffs for ELF and TE to trigger hepatology referral were  $>9.5$  and  $>7.8$  kPa, respectively [29]. The latter TE cutoff was actually validated for significant fibrosis and not advanced fibrosis [29]. This approach is likely to increase sensitivity and the negative predictive value of this test, making it safer to use by first-line physicians.

In a large UK primary care setting, this two-step sequential algorithm for patients with NAFLD, incorporating FIB-4 followed by ELF when necessary, was compared to standard care [30]. The application of this NAFLD pathway resulted in a fivefold



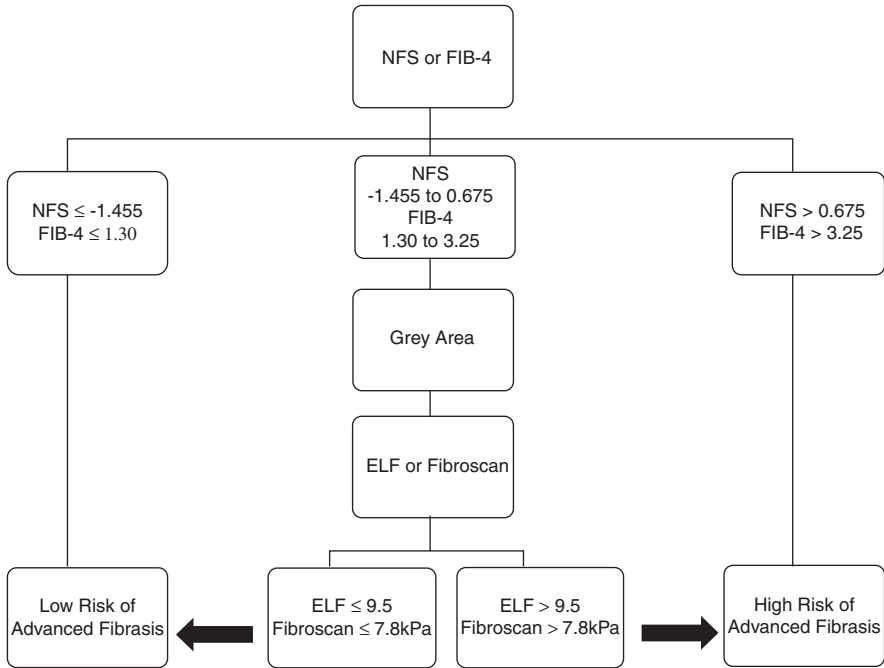


**Fig. 49.1** Two-step sequential algorithm assessing the degree of hepatic fibrosis in patients with suspected NAFLD evaluated in primary care. *ELF score* Enhanced Liver Fibrosis score, *NFS* NAFLD Fibrosis Score

improved detection of advanced fibrosis (Kleiner F3) or cirrhosis (F4) with an 81% reduction in unnecessary referral from primary care. For example, hepatologists detected cirrhosis in 14.5% of patients referred using the NAFLD pathway compared to 5.6% from standard care. This equated to a lower number of referrals required to detect one case of advanced fibrosis (3.4 vs. 12.6). Because this pathway was established before the impact of age was acknowledged as a confounder on FIB-4 cutoffs, a post-hoc analysis was performed for assessing its impact. A change in FIB-4 from  $<1.3$  to  $<2.0$  to exclude advanced fibrosis would have resulted in lower referrals, but also cases with advanced fibrosis and cirrhosis would have been missed. Similarly, a higher ELF cutoff, as advocated by the National Institute for Health and Care Excellence (NICE) guidelines ( $ELF > 10.5$ ) or the manufacturer ( $ELF > 9.8$ ), would have resulted in missed cases of advanced fibrosis and even cirrhosis [30, 31]. In this study, confirmation of advanced fibrosis was achieved through a global approach incorporating hepatologist review, radiological assessment, LS measurement and liver biopsy.

Another primary care-based referral pathway was developed in Canada, comparing a FIB-4 first strategy or TE in all patients to detect significant fibrosis [32]. Consistent with guidelines, patients with a non-NAFLD diagnosis were directly referred to hepatology care. Patients suspected to have NAFLD and advanced fibrosis with a TE  $\geq 8$  kPa were referred to a hepatologist. The other patients were provided lifestyle advice and repeat assessment was performed 1 or 2 years later. A

FIB-4 first strategy would have avoided 85% of referrals for TE, while a disagreement occurred in 10% of patients. In the 45 patients with FIB-4 and TE disagreement, including TE failure, 6 underwent a liver biopsy, and 2 were found to have advanced fibrosis. This approach is particularly interesting when physical noninvasive methods of fibrosis assessment are not available due to wide geographic population distribution like in Canada. Although the above pathways are promising, the repeat assessment interval of first-line testing is variable, between 1 and 5 years, and still needs to be validated, keeping in mind the impacts of delayed referral. Furthermore, for it to be used by primary practitioners, either ELF or TE should be more easily accessible to favor pathway application. For further reading on LS and NAFLD, Chap. 10 is also recommended.

### ***Alcoholic Liver Disease (ALD)***

ALD represents an important spectrum of patients that highly benefit from primary care management and timely specialist referral. More details on LS are provided in Chap. 11. In a detailed French study, all patients above the age of 45 who presented for regular medical check-up at their community practice received screening for liver disease with Fibroscan [33]. Using a cutoff of  $>8$  kPa to trigger a hepatology referral, 7.5% of patients were incidentally identified to have suspected liver disease with significant fibrosis, of which 42% were related to NAFLD and 30% to ALD [33]. For screening purposes, NICE guidance suggests that patients with harmful drinking or a full AUDIT score  $>19$  are at high risk of ALD and should be screened either with ELF or TE [34]. Referral to a specialized liver clinic was recommended if TE  $>8$  kPa as it is suggestive of advanced fibrosis, whereas a score above 16 kPa is suggestive of cirrhosis (Fig. 49.2) [25]. In patients with TE  $<8$  kPa, this pathway should be repeated in 3 to 5 years. This threshold was also endorsed in a recent review on the noninvasive diagnosis of fibrosis in ALD [35]. When compared to easy to calculate serum markers, TE by Fibroscan outperformed APRI, FIB-4, and Forns' index for the diagnosis of significant fibrosis, advanced fibrosis, and cirrhosis [36, 37]. Furthermore, the combination of LS measurement by TE and other noninvasive markers, such as ELF, Fibrotest, or Fibrometer, did not increase the diagnostic performance of TE alone [36–38]. Interestingly, in these studies, the established cutoffs for advanced fibrosis were 12.7 and 15 kPa, while it was 8.2 kPa for significant fibrosis [36, 37]. Unfortunately, the two studies staged fibrosis differently, with METAVIR in one and Kleiner in the other. In any case, with a TE  $\geq 15$  kPa, by intention-to-diagnose analysis, the sensitivity, specificity, positive (PPV) and negative predictive value (NPV) were 86%, 94%, 80% and 96%, respectively, meaning that below that threshold, a fibrosis stage  $F \geq 3$  by Kleiner could be excluded by TE alone [37]. In the other study, a fibrosis stage  $F \geq 2$  by METAVIR could be diagnosed with TE  $\geq 7.8$  kPa (sensitivity 80%, specificity 91%, PPV 93%, NPV 70%) [36]. For  $F \geq 3$  disease, the TE cutoff was 11 kPa (sensitivity 87%, specificity 81%, PPV 82%, NPV 84%) [39]. As discussed above for the NAFLD pathway, using a lower cutoff of 8 kPa in the guidelines to identify potential patients with advanced

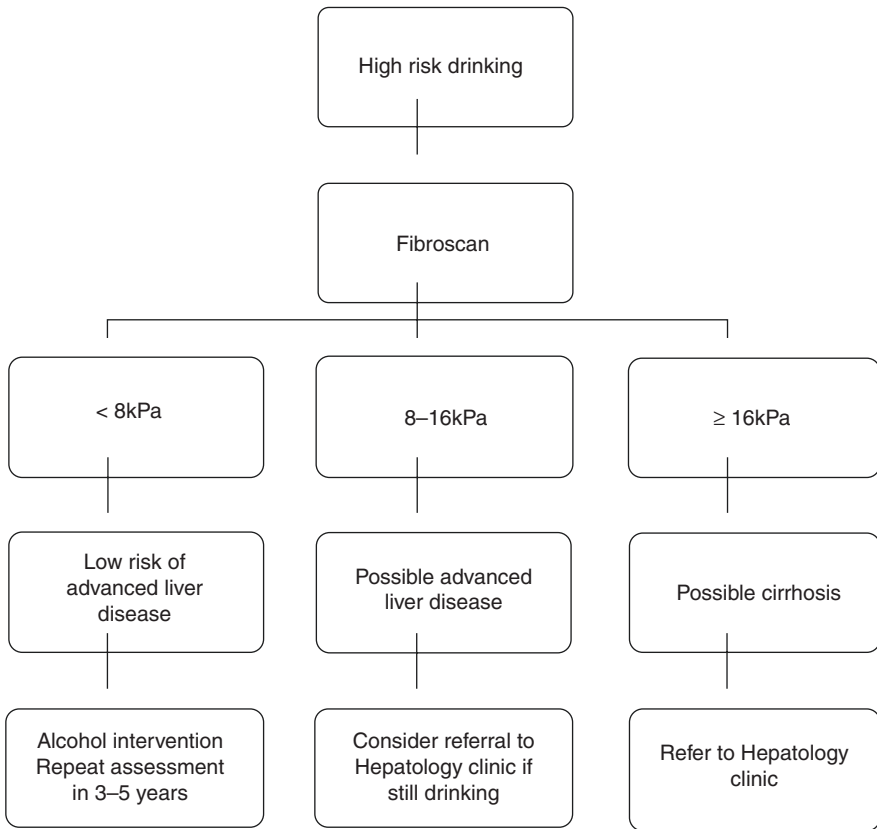


**Fig. 49.2** Noninvasive assessment of hepatic fibrosis in patients with suspected alcohol-related liver disease

fibrosis will increase the test's sensitivity and NPV for the diagnosis of advanced fibrosis. In this population, TE alone can be used to guide referral to specialized care. If unreliable, or not possible, patented serum markers such as ELF or Fibrotest should be considered given the poor diagnostic accuracy of non-patented serum markers in ALD. Considering these data, this pathway relies on a quick referral to TE capable centers. If LS measurement is below the critical threshold, the patient can be safely discharged back to primary care with a focus on alcohol abstinence. Standardized assessment sheets could help select appropriate patients for referral.

## Second Expertise Diagnosis by the Hepatologist

Patients with chronic liver disease under the care of a hepatologist are those at higher risk of progressive liver disease and cirrhosis where, in the latter case, hepatocellular carcinoma and variceal surveillance need to be initiated. These patients

will also be considered for disease-specific therapies, such as antivirals for HBV or HCV, corticosteroids for autoimmune hepatitis, vitamin E for non-diabetic patients with NASH, ursodeoxycholic acid for primary biliary cholangitis, while monitoring for response to therapy is performed during follow-up. To be able to perform their duty of care, hepatologists were often guided by the result of liver biopsies [1].

With the advent of noninvasive markers of fibrosis, physician behavior started to change as shown in our 2012 web-based survey investigating the practice of physicians treating patients with chronic liver disease in Canada [40]. Of the 104 physicians who responded, 81% were gastroenterologists or hepatologists. The primary method used for assessing liver fibrosis was liver biopsy in 46% of physicians, followed by TE in 39%. When stratified by etiology of chronic liver disease, there was a tendency toward increased use of noninvasive tests in viral hepatitis as compared to liver biopsy, while the opposite was true for cholestatic or autoimmune diseases (liver biopsy: 69% vs. noninvasive tests: 31%,  $P < 0.0001$ ). Overall, noninvasive tests led to an important reduction in liver biopsies as nearly 40% of physicians reduced by more than 50% the number of biopsies they ordered, but not in the cholestatic or autoimmune diseases. The main concern that physicians expressed about the use of noninvasive tests was related to the access/availability of the Fibroscan, as 60% did not have access to it in their clinics. Given that physicians systematically obtain liver fibrosis assessment in patients with chronic liver disease and that they think TE provides an accurate assessment of fibrosis, improving access to the device will have a major role in further sparing patients from liver biopsies. In addition, a clear disease-specific guidance on how to approach the noninvasive assessment of patients with chronic liver disease is needed as there has been a flourishing of serum-based and physical tools, with varying cutoffs, which can be confusing for everyday practice. Since our survey, EASL has published guidelines on the use of noninvasive tests in an attempt at trying to bridge this gap [41]. The following section will describe potential algorithms sparing liver biopsies for the different causes of chronic liver disease. These algorithms are also summarized in Table 49.1.

## *Hepatitis C Virus*

Historically, HCV represented an ideal etiology to develop noninvasive methods for fibrosis staging. With a standardized histological classification system and a large population requiring staging for treatment prioritization, the Sequential Algorithm for Fibrosis Evaluation (SAFE) biopsy was developed using a two-step algorithm combining APRI and Fibrotest [5, 39]. It was noted that the combination of APRI and Fibrotest was better than either tests alone. Three versions of the algorithm were developed to guide the diagnosis of fibrosis stages METAVIR  $F \geq 2$ ,  $F = 4$ , or both simultaneously [39] (Fig. 49.3). The number of biopsies spared was 36% for the simultaneous identification of patients with F2 and F4 disease, 46% for the detection of  $F \geq 2$ , and 81.5% for the detection of cirrhosis. Using the SAFE biopsy, the diagnostic accuracies were 90.1% for significant fibrosis, 92.5% for cirrhosis, and 97.4% for the simultaneous detection of significant fibrosis and cirrhosis.

**Table 49.1** Summary of available noninvasive algorithms to stage hepatic fibrosis separated by disease etiology

Disease (references)	Type of algorithm	Significant fibrosis ( $F \geq 2$ )			Advanced fibrosis ( $F \geq 3$ )			Cirrhosis (F4)			
		Noninvasive methods	AUC	Liver biopsies avoided	Accuracy	AUC	Liver biopsies avoided	Accuracy	AUC	Liver biopsies avoided	Accuracy
<b>HCV</b>											
SAFE [39, 42]	Sequential	APRI and Fibrotest	0.89-0.94	46-48%	90-97%	-	-	0.87-0.92	75-81%	89-92%	
Bordeaux [43, 42]	Synchronous	Fibrotest and Fibroscan	0.88-0.91	72-77%	84-88%	-	-	0.93-0.95	78-79%	94-96%	
Angers [45]	Synchronous	Fibrometer and Fibroscan	-	-	-	0.88	73%	-	-	-	
<b>HBV</b>											
SAFE [51]	Sequential	APRI and Fibrotest	0.96 (0.92-1.0)	48%	97%	-	-	0.95 (0.90-1.0)	81%	96%	
Chan [52]	Sequential	ALT and Fibroscan	-	-	-	0.87 (0.82-0.93)	62%	0.93 (0.89-0.97)	58%	63-91%	
Vigano [55]	Simple	Fibroscan	0.85 (0.77-0.91)	72%	92%	-	-	0.94 (0.90-0.98)	79%	96%	
<b>HIV/HCV</b>											
SAFE [63]	Sequential	APRI and Fibrotest	-	49.1%	65%	-	-	-	90%	85%	
Bordeaux [63]	Synchronous	Fibrotest and Fibroscan	-	69.0%	89%	-	-	-	78.4%	87%	

HIV									
Morse [66]	Simple	Fibroscan	0.93 (0.86–0.99)	48%	–	–	–	–	–
HIV/HBV									
Mitailhes [68]	Synchronous	Fibrotect and Fibroscan	–	67%	97%	–	71%	97%	–
NAFLD									
Petta [58]	Synchronous	NFS and Fibroscan	–	–	–	0.84–0.88	52–59%	93–99%	–
Petta [58]	Synchronous	Fib-4 and Fibroscan	–	–	–	0.85–0.89	54–62%	90–98%	–
Chan [59]	Sequential	NFS and Fibroscan	–	–	–	–	80–81%	91–96%	–
ALD									
Voican [69]	Simple	Fibroscan	–	–	–	–	–	0.93 (0.88–0.97)	86%
HFE-HC									
Legros [75]	Sequential	Ferritin and Fibroscan	–	–	–	0.97	61%	100%	–

95% confidence interval is provided between brackets when available for the AUC. *ALD* alcohol-related liver disease, *ALT* alanine aminotransferase, *APRI* AST to platelet ratio, *AUC* area under the curve, *HBV* hepatitis B virus, *HCV* hepatitis C virus, *HIV* human immunodeficiency virus, *NAFLD* non-alcoholic fatty liver disease, *HFE-HC* hereditary hemochromatosis

Castera et al. proposed two different algorithms using the concept of test concordance, where the diagnosis was established if both tests agreed (Fig. 49.4) [42]. To do so, they compared APRI combined with TE, Fibrotest combined with TE, or all three. The best area under the curve (AUC) was achieved when TE was combined

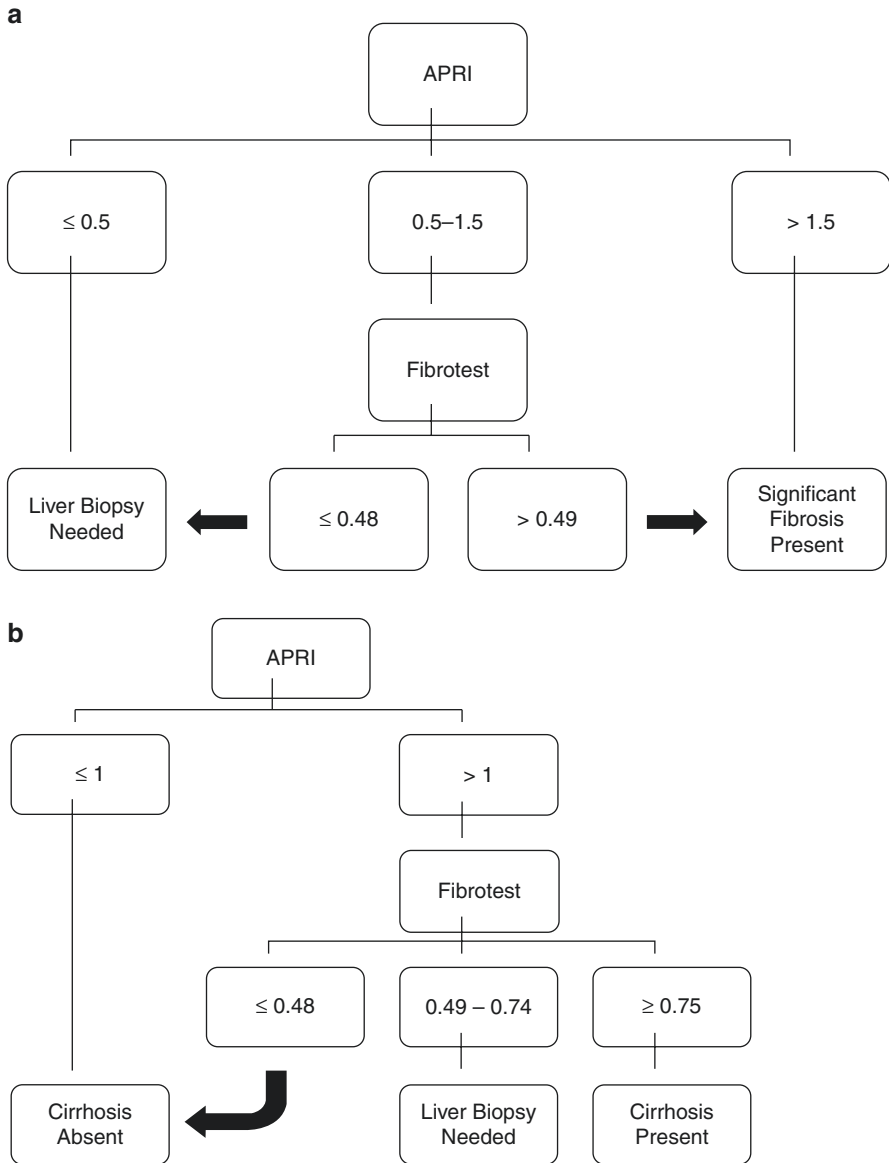


**Fig. 49.3** SAFE algorithm for the noninvasive assessment of (a) significant fibrosis, (b) cirrhosis, (c) significant fibrosis and in patients with Hepatitis C Virus. APRI AST to Platelet Ratio Index

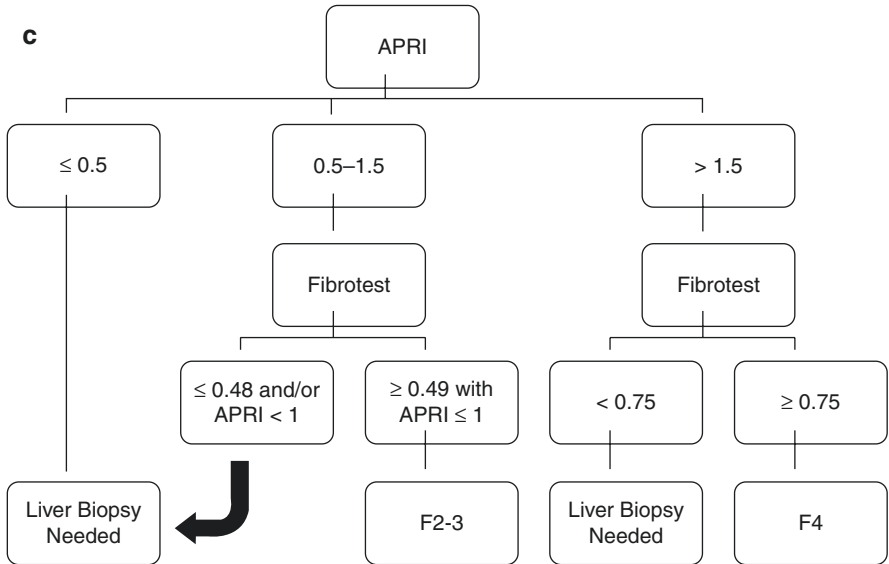


**Fig. 49.3** (continued)

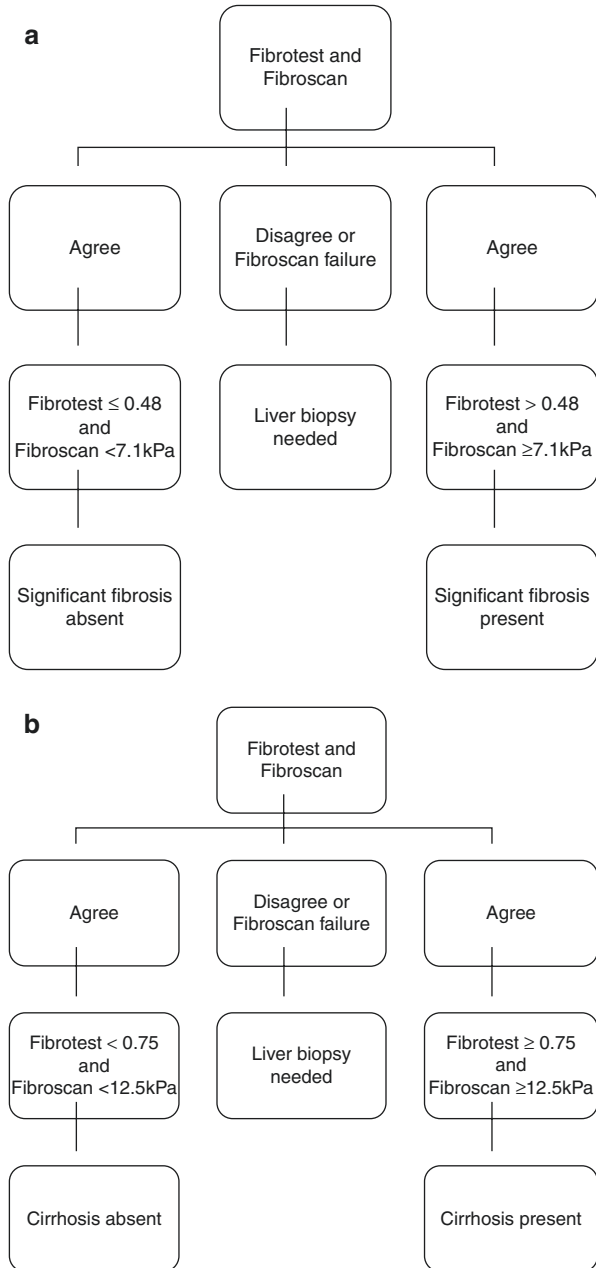
with Fibrotest for F2 (0.88; 95% CI 0.82–0.92); F3 (0.95; 95% CI 0.91–0.97); and F4 (0.95; 95% CI 0.91–0.97). The diagnostic accuracies were 84% for  $F \geq 2$ , 95% for  $F \geq 3$ , and 94% for  $F = 4$ . In addition, the rate of concordance was 77% for  $F \geq 2$ , 70% for  $F \geq 3$  disease, and 79% for  $F = 4$ . Therefore, the rate of biopsy spared would have been between 70 and 79%. The optimal cutoffs of LS measurement determined in this study were 7.1 kPa for F2, 9.5 kPa for F3, and 12.5 kPa for F4. They then proposed an algorithm for patients with HCV where patients with discordant TE and Fibrotest would be offered a liver biopsy. Patients with concordant results were provided either follow-up if F0–1, treatment if  $F \geq 2$ , or treatment with cirrhosis surveillance if  $F \geq 3$ .

In a later publication by one of us, the SAFE biopsy was compared to the Castera algorithm described above [43]. In this study, the rate of TE failure was 2.6%. Therefore, when compared head-to-head in an intention-to-diagnose analysis, the SAFE biopsy could have avoided 48% of liver biopsies compared to 72% with the Castera algorithm ( $P < 0.0001$ ) for the detection of significant fibrosis ( $F \geq 2$ ). Despite that, the SAFE algorithm was more accurate, 97% vs. 88% ( $P < 0.0001$ ). For the identification of patients with cirrhosis, both algorithms did not differ leading to 79% and 75% of spared biopsies, for the Castera algorithm and the SAFE biopsy, respectively. It remained that in this subgroup, the diagnostic accuracy of the Castera algorithm was superior in 96% vs. 89% ( $P < 0.0001$ ).

Another study assessed the performance of nine noninvasive blood tests and Fibroscan when applied in concordance [44]. In an intention-to-diagnose analysis for presence of cirrhosis, the percentage of well-classified patients was around 90%, and the number of biopsies spared around 85%. The best combination was achieved



**Fig. 49.4** Proposed concordance algorithms of both TE and a serum test for the noninvasive assessment of (a) significant fibrosis and (b) cirrhosis in patients with Hepatitis C Virus



with TE and any blood test, including APRI, Fibrometer, or Fibrotect. The best identified cutoff was 12.9 kPa for the detection of cirrhosis by LS measurement, 2.0 for APRI, 0.74 for Fibrotect, and 0.88 for Fibrometer. For significant fibrosis, the number of well-classified patients hovered between 76 and 82% when using

combined testing. The number of biopsies spared was between 54 and 66%. The cutoff for LS measurement was 5.2 kPa, APRI 0.5, Fibrotest 0.48, and Fibrometer 0.41. The percentage of well-classified patients for significant fibrosis was 78% with the combination of APRI and TE. This study shows that APRI has a role when combined with TE, if patented markers are unavailable.

The concept of score concordance was also evaluated by Cales et al. who looked at the performance of Fibrometer and TE [45]. In their study, the researchers looked at the ability of each test to predict severe fibrosis (METAVIR  $F \geq 3$ ) with cutoffs of 0.695 for Fibrometer and 9.15 kPa for LS measurement. They also combined the two tests in one formula called the Fibrometer<sup>VCTE2G</sup>. As in previous publications, concordance for severe fibrosis was noted in 73% of cases, and thereby avoiding liver biopsy, with an AUROC of 0.88 and accuracy of 79%. When Fibrometer<sup>V2G</sup> and TE were concordant, 88% of patients were correctly classified, with corresponding AUC above 0.90. When the two tests were discordant, about 50% of patients were correctly classified under each test, with AUCs between 0.53 and 0.60. For discordant cases, the authors assessed the benefit of calculating the Fibrometer<sup>VCTE2G</sup> score. When compared to the histologic scoring system using METAVIR classification, they found that the combined test only had a diagnostic accuracy of 62%. They then compared the combined test accuracy in a novel fibrosis classification they had previously developed [46, 47]. In this instance, when there is partial discordance between the two constitutive tests, the Fibrometer<sup>VCTE2G</sup> provided accurate classification in 93% of cases. In the rare instance of strict discordance between the two tests, which only happened in 3.2% of cases, they showed that the Fibrometer<sup>VCTE2G</sup> was unreliable if it predicted severe fibrosis, which only occurred in 1.4% of patients. In that instance, a liver biopsy should be performed. Therefore, based on their algorithm, patients would be spared a liver biopsy in 98.6% of cases for the identification of severe fibrosis. The significant drawback of this method is that it relies on a patented method, and therefore it is not easily done in most places.

Both the American Association for the Study of Liver Diseases (AASLD) and the European Association for the Study of the Liver (EASL) published guidelines in 2018 recommending treatment of all patients regardless of fibrosis stage, unless if there is non-liver related limited life expectancy [48, 49]. This approach was previously shown to be cost-effective [50]. Treatment should be initiated without delay in those with at least significant fibrosis [49]. Guidelines still recommend fibrosis staging when there is no evidence of cirrhosis as identification of patients with pre-clinical cirrhosis will lead to the initiation of HCC surveillance and screening for esophageal varices. It is recognized that if treatment is performed outside of specialty clinics or in low- or middle-income countries, APRI and FIB-4 can be used for identification of patients with cirrhosis as an APRI  $\geq 2$  and FIB-4  $\geq 3.25$  have a specificity of more than 92–94% [49]. Otherwise, as stated above, combination of a blood biomarkers and LS measurement in concordance improves diagnostic accuracy [41, 49]. Liver biopsy should still be performed in discordant cases or if there is suspected mixed etiologies, especially if it will lead to a change in management. Finally, an improved fibrosis assessment by TE has been also shown using so-called

inflammation-adapted cutoff values [51]. For more details, see also Appendix Fig. A.3 and book Part III “Liver stiffness and various etiologies of liver diseases.”

## Hepatitis B Virus

Algorithms staging hepatic fibrosis and linking it with treatment initiation have also been developed for patients with HBV [41]. Before the development of LS, the use of the SAFE algorithm in chronic HBV was able to decrease the need for liver biopsy by 48% for the detection of significant fibrosis (METAVIR  $F \geq 2$ ) (AUC 0.96, sensitivity 100%, specificity 91%, PPV 96%, NPV 100%, accuracy 97%) or 81% for cirrhosis (AUC 0.95, sensitivity 93%, specificity 96%, PPV 97%, NPV 98%, accuracy 96%) [52]. TE has also been validated in this setting with cutoffs taking into account the degree of alanine aminotransferase (ALT) elevation, as this is associated with a falsely increased LS measurement [53]. Chan et al. developed algorithms with high sensitivity to exclude bridging fibrosis, and high specificity to diagnose at least bridging fibrosis for patients with normal or elevated ALT (Fig. 49.5) [53]. Liver biopsy was recommended only in patients failing in the grey zone. This led to a rate of spared liver biopsy between 58% and 62%. In patients with normal ALT, the cutoff to exclude  $F \geq 3$  was 6 kPa (sensitivity 93%, NPV 88%, accuracy 69%), compared to 7.5 kPa (sensitivity 96%, NPV 94%, accuracy 77%) for those with an elevated ALT. For the diagnosis of bridging fibrosis, the cutoffs were 9 kPa (specificity 100%, PPV 100%, accuracy 86%) and 12 kPa (specificity

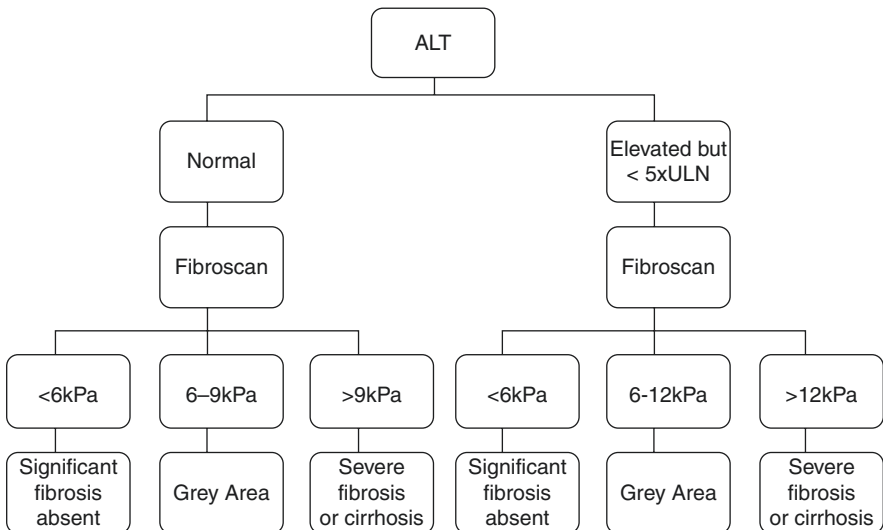


**Fig. 49.5** Algorithm for the noninvasive assessment of hepatic fibrosis in patients with Hepatitis B virus depending on the degree of ALT elevation

98%, PPV 96%, accuracy 76%) for those with a normal or elevated ALT, respectively. Subsequently, they attempted to confirm their findings in a validation cohort [54]. Unfortunately, although LS measurement by TE had sensitivity above 90% to rule out and specificity above 90% to rule in bridging fibrosis, this fell below that threshold in the validation cohort. From a serum biomarker point of view, Forns' index showed the best test characteristics, with sensitivity of 100% to rule out and specificity of 93% to rule in. When TE and Forns' index provided concordant results, high sensitivity and specificity were once again achieved in the validation cohort. For the exclusion of advanced fibrosis, the use of this algorithm increased the number of spared biopsies from 61% to 66%, while the number of incorrect diagnoses remained the same at 7%. In the confirmatory strategy, the number of spared biopsies decreased from 43% to 29%, with an even more impressive decrease in incorrect diagnosis from 38% to 0%. A sequential algorithm combining TE and ELF could avoid a significant number of biopsies. However, there was a large number of incorrect diagnoses, and biopsies wrongly avoided [55].

Vigano et al. also evaluated the performance of TE in a training and validation cohort of treatment naïve patients with HBV—unfortunately, not in an intention-to-diagnose fashion [56]. In their validation cohort, the use of a cutoff of  $\leq 9.4$  kPa correctly classified 98% of patients as not having cirrhosis, with 96% sensitivity. With a cutoff of  $>13.1$  kPa, TE correctly classified 89% of patients as having cirrhosis with a specificity of 97%. Based on their cutoffs to include and exclude cirrhosis, a diagnosis could be reached in 79% of patients, with consideration for biopsy in 21% to establish the diagnosis of cirrhosis. The use of TE  $\leq 6.2$  kPa excluded significant fibrosis with a diagnostic accuracy of 86%, while TE  $>9.4$  kPa confirmed the diagnosis with 97% accuracy. With this algorithm, about 28% of patients would have needed a liver biopsy and the overall diagnostic accuracy was 92%. The researchers also found that an elevated ALT was associated with a worse diagnostic accuracy in the evaluation of significant fibrosis, but not cirrhosis.

In conclusion, for HBV-infected treatment naïve patients, algorithms should take into consideration the degree of ALT elevation. The number of liver biopsies spared depends on whether the aim is to identify significant liver fibrosis or cirrhosis, as the algorithms are not as accurate for significant fibrosis. Regardless, rates of spared liver biopsy ranged between 60 and 80%. Again, liver biopsy should only be considered if it will change management. EASL has incorporated these findings in its noninvasive testing guidelines, whereas AASLD has not [41, 57].

## **NAFLD**

The development of algorithms capable of sparing patients from liver biopsies to stage hepatic fibrosis is crucial for those with NAFLD, as this is a highly prevalent condition. In order to develop hepatic fibrosis, patients with NAFLD need to progress from simple steatosis to steatohepatitis with histological evidence of lobular inflammation, ballooning hepatocytes, and of course hepatic steatosis. Unfortunately,

NASH is still diagnosed with a liver biopsy as serum biomarkers, or elastography techniques, cannot reliably distinguish it from simple steatosis [58]. For this reason, most pathways will focus on the assessment of fibrosis in patients with evidence of hepatic steatosis, without knowledge of the degree of steatohepatitis. As previously discussed, general practitioners can perform an initial screen of patients using some of the proposed pathways and only refer those with significant fibrosis [25, 30].

Petta et al. assessed retrospectively a cohort of patients with NAFLD in Northern (training set) and Southern Italy (validation set) [59]. The analysis was performed against adequate liver biopsies staged using the Kleiner histologic classification. TE was used and noninvasive biomarkers such as APRI, FIB-4, and NFS were also calculated. Following the separate analysis of each noninvasive test, the combination of TE and NFS provided the best overall accuracy. Using the concept of concordance, with TE <7.9 kPa and NFS <-1.455 to rule out  $F \geq 3$ , and with TE  $\geq 9.6$  kPa and NFS >0.676 to rule in  $F \geq 3$ , discordance occurred in 48% of cases, which would prompt a liver biopsy. In those classified, the rates of false positive and false negative were excellent at 0% and 1%, respectively. The combination of TE and FIB-4 could also be considered as it performed equally well in the validation cohort. In this study, authors used previously published cutoffs for TE and did not derive it from their population. Although TE alone performed better than when combined with FIB-4 or NFS, with lower uncertainty area, and higher diagnostic accuracy, it was not able to reliably confirm the diagnosis with a PPV below 60%.

Another algorithm was prospectively validated incorporating NFS and TE (Fig. 49.6) [60]. In patients with NFS <-1.455, advanced fibrosis was excluded with enough confidence and TE was unnecessary. This is consistent with the

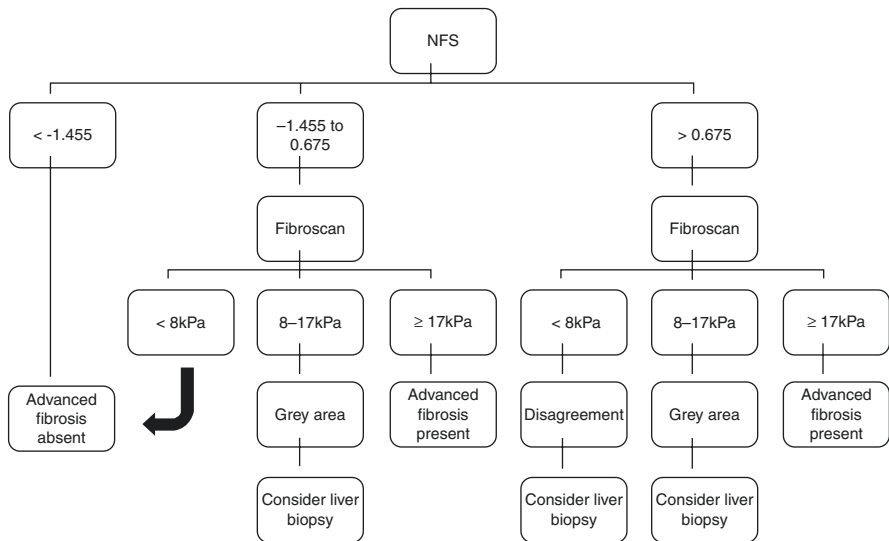


**Fig. 49.6** Noninvasive algorithm for the assessment of hepatic fibrosis in patients with suspected NAFLD. NFS NAFLD Fibrosis Score

recommendation to have patients with NFS  $< -1.455$  remain in primary care. Although they showed a discordance rate of 33% between NFS  $< -1.455$  and TE  $\geq 8$  kPa for the exclusion of advanced fibrosis, only 4.5% of patients were truly misclassified. In patients with NFS  $> -1.455$ , the researchers suggested to use TE. Patients remaining in the grey zone or with discordance between TE and NFS would have to undergo liver biopsy. Using this approach, only 19% of patients would need a liver biopsy and 9% were misclassified. The suggested cutoffs by TE were 8 kPa and 17 kPa to rule out or rule in advanced fibrosis, respectively. Using their algorithm, the overall sensitivity, specificity, PPV, and NPV were 66.7%, 100%, 100%, and 94.6%, respectively. Although this study is highly relevant, they did not perform an intention-to-diagnose analysis. False positives were also noted to increase with the severity of hepatic steatosis, as highlighted by higher Controlled Attenuation Parameter (CAP) values [61]. An adjustment to the algorithm was proposed taking into consideration CAP values when TE was performed with the M probe, as was the case in this study [61]. Furthermore, since the development of the XL probe to decrease technical failures and unreliable measurements in patients with high BMI, the median LS measurement per fibrosis stage was similar between patients with BMI under 30 kg/m<sup>2</sup> assessed by M probe, and those with BMI above 30 kg/m<sup>2</sup> assessed by XL probe [62]. Importantly, when performed on the same patient, values with the XL probe tended to be about 2 kPa lower than with the M probe. It remains to be seen if the cutoffs developed using the M probe can also be applied with the XL probe [62].

## **HIV**

Patients with HIV constitute a heterogeneous group at risk of chronic liver disease from multiple different causes. Beyond HBV and HCV, these patients can develop liver disease due to exposure to hepatotoxic medications, NAFLD, and HIV itself [63]. It is therefore important to consider potential confounders when assessing these patients. Moreover, the number of studies comparing noninvasive tests to liver biopsy in HIV-infected patients is limited. *Ad hoc* validation of noninvasive fibrosis tests is relevant in the setting of HIV infection as thrombocytopenia, encompassed in several fibrosis biomarkers, may be more frequently unrelated to hepatopathy in this population. Similar to patients with HCV mono-infection, the SAFE algorithm was compared to the Castera algorithm in HIV/HCV co-infected patients for the detection of significant fibrosis (METAVIR  $F \geq 2$ ) or cirrhosis (METAVIR  $F = 4$ ) (Figs. 49.3 and 49.4) [64]. For the detection of significant fibrosis, the SAFE algorithm was unreliable, correctly classifying only 32% of patients. The Castera algorithm fared much better by correctly classifying 61% of patients ( $P < 0.0001$ ), and 69% with saved biopsies. Nonetheless, TE  $\geq 7.1$  kPa had a higher rate of correctly classified patients at 80% ( $P < 0.0001$ ). The NPV of the Castera algorithm was better at excluding significant fibrosis at 94% compared to 88% for TE, 89% for Fibrotest, and 75% for APRI. All noninvasive methods assessed had poor PPV for

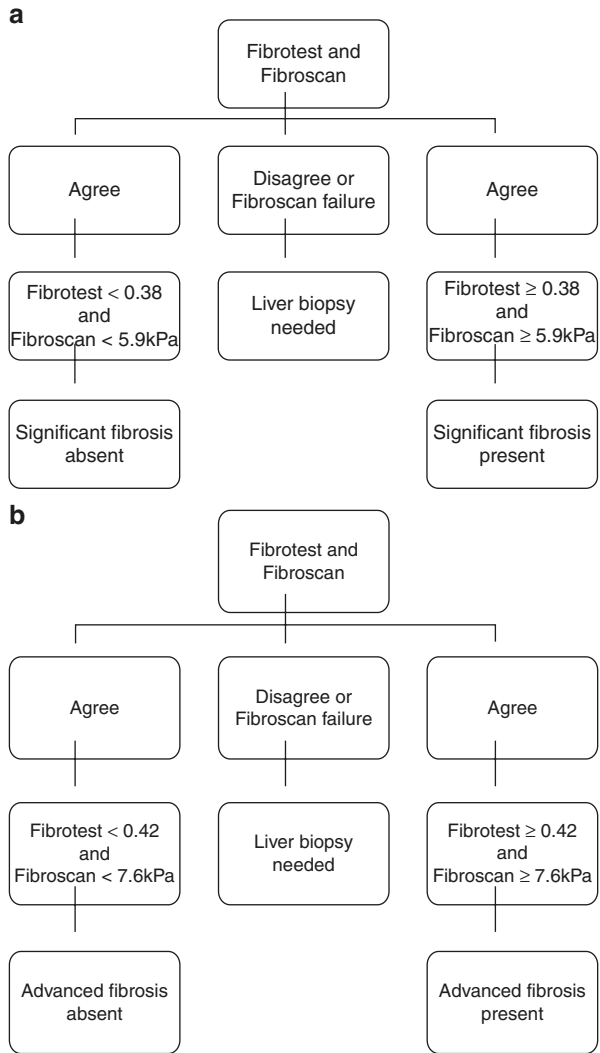
significant fibrosis. For the detection of cirrhosis, the conclusions were much different. The Castera algorithm performed poorly compared to the SAFE algorithm, the latter being able to save 91% of biopsies and correctly classified 77% of patients as compared to 78% and 68% for the former. A cutoff of 12.5 kPa of TE alone had the highest rate of correctly classified patients with cirrhosis at 85%, and worked best to rule out cirrhosis with 97% NPV. Therefore, significant fibrosis can be more safely excluded using the Castera algorithm as opposed to the SAFE algorithm. For the diagnosis of cirrhosis, TE alone had the best NPV.

In another HIV/HCV co-infected cohort, the combination of serum biomarkers and TE was not better than TE alone for the diagnosis of cirrhosis at a cutoff of 10.4 kPa, with correctly classified rate at 91% (sensitivity 100%, specificity 89%, PPV 61%, NPV 100%) [65]. A similar result was obtained using this time a cutoff of 11.8 kPa by TE which excluded cirrhosis in all cases (sensitivity 100%, specificity 93%, PPV 81%, NPV 100%) [66]. This approach would have avoided biopsies in 76% of patients. The performance of serum biomarkers and TE for the diagnosis of significant fibrosis was unfortunately not as good, with AUC 0.72 vs. 0.97 for cirrhosis.

In HIV mono-infected individuals, the current state of knowledge does not allow us to draw clear conclusions. In a prospective biopsy cohort of 66 patients with HIV mono-infection and abnormal liver enzymes on antiretroviral therapy, a TE cutoff of 7.1 kPa reliably excluded significant fibrosis (Ishak  $F \geq 2$ ) in an intention-to-diagnose analysis (AUC 0.93, sensitivity 93%, specificity 73%, PPV 52%, NPV 97%) [67]. Using this cutoff, 48% of biopsies could have been avoided. In this population, FIB-4 ( $>2.67$ ), APRI ( $>1.5$ ), and NFS ( $>0.676$ ) were not as reliable, with respective AUCs of 0.64, 0.61, and 0.70 [67]. Of note, these cutoffs have previously been used to confirm as opposed to exclude significant fibrosis, which might explain their lower performance. We also assessed the diagnostic accuracy of TE in the identification of significant fibrosis in patients with suspected NASH and HIV mono-infection based on a diagnostic algorithm combining cytokeratin-18 and TE [63]. Once again, in 17 patients with available liver biopsy, TE  $>7.1$  kPa had an AUROC of 0.91, confirming the presence of significant fibrosis (NASH CRN  $F \geq 2$ ) in all patients [63]. Unfortunately, since we did not perform a liver biopsy in patients with TE  $<7.1$  kPa, we could not assess the test's NPV. In another study, TE was not a reliable predictor of significant fibrosis (METAVIR  $F \geq 2$ ) with AUC 0.61 [68]. Although of interest, the results of this study cannot be generalized as only pre-selected patients with a Fibroscan above 7.1 kPa and/or Fibrotest  $>0.48$  were eligible. Furthermore, of the 35% of patients eligible for a liver biopsy, only 36% underwent the procedure. Interestingly, APRI performed better than Fibroscan to exclude significant fibrosis using a cutoff of 0.5 with AUC 0.86 ( $P < 0.02$ ) [68].

In HIV/HBV co-infected individuals, the combination of TE  $\geq 5.9$  kPa, and Fibrotest  $\geq 0.38$  resulted in all patients being adequately categorized as having at least significant fibrosis (METAVIR  $F \geq 2$ ) (Fig. 49.7) [69]. When both tests were

**Fig. 49.7** Noninvasive algorithm for the assessment of hepatic fibrosis in patients co-infected with HIV and HBV for the detection of (a) significant fibrosis and (b) advanced fibrosis



below the cutoffs, the NPV was 93% for significant fibrosis. In their cohort, 67% of biopsies could have been avoided for the detection of significant fibrosis. For advanced fibrosis, METAVIR  $F \geq 3$ , the same algorithm, combining TE, this with a cutoff of 7.6 kPa, and Fibrotest, at a cutoff of 0.42, had a PPV of 100% and NPV of 96%. This algorithm could also spare 71% of liver biopsies. Unfortunately, this study did not use accepted TE reliability criteria allowing eight successful measurements instead of 10 and a success rate >30% instead of >60%, which limits its applicability.



## **Alcoholic Liver Disease (ALD)**

As described above, patients at risk of ALD benefit from TE alone to stage the degree of hepatic fibrosis [25, 35]. The diagnostic accuracy of TE did not seem to improve with the addition of noninvasive biomarkers such as Fibrotest, or Fibrometer [36, 70, 71]. One study seemed to suggest that the combination of FIB-4 with Fibroscan improved the detection of patients with advanced fibrosis, but that the effect was marginal when excluding patients with obvious signs of cirrhosis, making this not clinically useful [71]. In addition, combining TE and ELF score did not lead to a higher diagnostic accuracy, nor did it increase classification of patients [37]. When TE and ELF tests were discordant, TE alone would have more appropriately classified patients.

For the diagnosis of cirrhosis, a TE cutoff of 15 kPa was considered optimal with a diagnostic accuracy of 86% (sensitivity 93%, specificity 85%, PPV 53%, NPV 99%) [70]. To obtain a NPV of 100%, the authors proposed a cutoff of 7 kPa. Considering this, similar to the British Society of Gastroenterology recommendations, if TE is below 7 kPa, cirrhosis is excluded and patients do not need a liver biopsy, which would decrease the need for a liver biopsy by nearly 50%. If the TE is between 7 and 15 kPa, with signs of cirrhosis, the authors suggest a liver biopsy while it can be postponed in the absence of cirrhosis signs. Finally, a LS above 15 kPa in patients that are actively drinking should be repeated after 1 month of abstinence [72, 73]. If the value remains elevated, cirrhosis should be confirmed with a liver biopsy, due to the low PPV [70]. It is important to note that some patients might have asymptomatic alcoholic hepatitis, often associated with a raised aspartate aminotransferase, or bilirubin, and decreased prothrombin activity. In these patients, TE might not be as useful, and cutoffs should be adjusted as shown in a meta-analysis of individual patient data [74]. Improved fibrosis assessment by TE has been also shown by so-called inflammation-adapted cutoff values [51]. For more details, see also Appendix Fig. A.3 and book Part III “Liver stiffness and various etiologies of liver diseases.”

## ***Autoimmune and Cholestatic Liver Diseases***

Although the diagnosis of autoimmune hepatitis (AIH) can be achieved using predictive scores, a histological assessment is still recommended by both AASLD and EASL to confirm the diagnosis [75, 76]. The initial liver biopsy will therefore also provide the stage of fibrosis and the degree of histological activity, both used to decide if treatment is necessary [76]. Because of these considerations and the paucity of data, recommendations on the use of noninvasive assessment to spare liver biopsies have not been made to date [41]. Promising data on liver fibrosis assessment using elastography techniques for AIH are being published and covered in another chapter. Conversely, in primary biliary cholangitis [77] and primary sclerosing cholangitis [78], the diagnosis can be made in the majority of patients without a

liver biopsy and the stage of fibrosis is often not required to guide initial medical therapy. Therefore, the noninvasive assessment of fibrosis in PBC and PSC should focus on identifying patients with worsening disease or cirrhosis in order to initiate appropriate surveillance. In a prospective cohort study including 95 patients diagnosed with either PBC or PSC and available liver biopsy, TE alone was highly predictive of advanced fibrosis (METAVIR  $F \geq 3$ ) and cirrhosis (METAVIR  $F = 4$ ), using cutoffs of 9.8 kPa (AUC 0.95, sensitivity 91%, specificity 90%, PPV 84%, NPV 95%) and 17.3 kPa (AUC 0.96, sensitivity 93%, specificity 95%, PPV 78%, NPV 99%), respectively, potentially avoiding liver biopsies [79]. This was consistent in PBC and PSC patients when analyzed separately. In a follow-up study from the same researchers, TE was confirmed as the best noninvasive tool in PBC with cutoffs of 10.7 kPa and 16.9 kPa for advanced fibrosis and cirrhosis, respectively, when compared to other serum markers, including APRI, FIB-4, and the Mayo Score [80]. For more details, see also book Part III “Liver stiffness and various etiologies of liver diseases.”

### *Genetic Liver Diseases*

Limited by overall low prevalence compared to other causes of chronic liver disease, data is scarce on the use of noninvasive tools to predict hepatic fibrosis in patients with HFE-hemochromatosis, Wilson’s disease, or alpha-1 Antitrypsin deficiency. Current AASLD and EASL guidelines advocate a liver biopsy in patients with HFE-hemochromatosis and a serum ferritin above 1000  $\mu\text{g/L}$  to assess for the presence of cirrhosis [81, 82]. In a prospective observational cohort study of C282Y homozygous HFE-hemochromatosis, TE was able to reliably exclude and diagnose severe liver fibrosis using cutoffs of 6.4 kPa (sensitivity 100%, specificity 81%, PPV 61%, NPV 100%) and 13.9 kPa (sensitivity 64%, specificity 100%, PPV 100%, NPV 90%), respectively [83]. When applying these TE cutoffs to patients with a serum ferritin  $>1000 \mu\text{g/L}$ , 61% of liver biopsies could have been avoided [83]. At this stage, these results need to be replicated before they can be recommended. For patients with Wilson’s disease, a single study showed that transient elastography was better than APRI or FIB-4 for the identification of advanced fibrosis (METAVIR  $F \geq 3$ ) [84], which could pave the way for further research in the field. Lastly, one study compared elastography to liver biopsy, utilizing magnetic resonance in this case, showing a good correlation [85]. Further studies are awaited.

### **Conclusions**

Serum biomarkers and LS measurement have dramatically changed the way we evaluate hepatic fibrosis in chronic liver diseases. For this reason and to provide advice to physicians, EASL has published a complete set of guidelines on the use of

these noninvasive tools that are still under debate and development [41]. From a clinical point of view, it is important to choose the right algorithm for the right cause of chronic liver disease, as patients with NAFLD or HCV are not assessed the same way. In HCV, the diagnostic accuracy of the algorithm tends to increase when two noninvasive tests, combining serum-based and physical methods, are applied in concordance. However, in other conditions like NAFLD or hemochromatosis, an algorithm using two tests in sequential manner seems to have the best result. In HBV and ALD, TE alone suffices to make decisions. With these algorithms, liver biopsies can be decreased in more than half of patients. Future research is still needed to identify better strategies to avoid further liver biopsies with tests that can be used in point-of-care settings. Improving access to TE will not only allow more individuals to be screened early, preventing late presentations, but by rapidly identifying patients with more advanced disease, they will be linked with appropriate care resources.

## References

1. Brunt EM. Grading and staging the histopathological lesions of chronic hepatitis: the Knodell histology activity index and beyond. *Hepatology*. 2000;31(1):241–6.
2. Poynard T, Bedossa P, Opolon P. Natural history of liver fibrosis progression in patients with chronic hepatitis C. The OBSVIRC, METAVIR, CLINIVIR, and DOSVIRC groups. *Lancet*. 1997;349(9055):825–32.
3. Desmet VJ, Knodell RG, Ishak KG, Black WC, Chen TS, Craig R, Kaplowitz N, Kiernan TW, Wollman J. Formulation and application of a numerical scoring system for assessing histological activity in asymptomatic chronic active hepatitis [Hepatology 1981;1:431-435]. *J Hepatol*. 2003;38(4):382–6.
4. Brunt EM, Janney CG, Di Bisceglie AM, Neuschwander-Tetri BA, Bacon BR. Nonalcoholic steatohepatitis: a proposal for grading and staging the histological lesions. *Am J Gastroenterol*. 1999;94(9):2467–74.
5. The French METAVIR Cooperative Study Group. Intraobserver and interobserver variations in liver biopsy interpretation in patients with chronic hepatitis C. *Hepatology*. 1994;20(1 Pt 1):15–20.
6. Knodell RG, Ishak KG, Black WC, Chen TS, Craig R, Kaplowitz N, et al. Formulation and application of a numerical scoring system for assessing histological activity in asymptomatic chronic active hepatitis. *Hepatology*. 1981;1(5):431–5.
7. Batts KP, Ludwig J, Chronic h. An update on terminology and reporting. *Am J Surg Pathol*. 1995;19(12):1409–17.
8. Asrani SK, Devarbhavi H, Eaton J, Kamath PS. Burden of liver diseases in the world. *J Hepatol*. 2019;70(1):151–71.
9. Pimpin L, Cortez-Pinto H, Negro F, Corbould E, Lazarus JV, Webber L, et al. Burden of liver disease in Europe: Epidemiology and analysis of risk factors to identify prevention policies. *J Hepatol*. 2018;69(3):718–35.
10. Younossi ZM, Stepanova M, Afendy M, Fang Y, Younossi Y, Mir H, et al. Changes in the prevalence of the most common causes of chronic liver diseases in the United States from 1988 to 2008. *Clin Gastroenterol Hepatol*. 2011;9(6):524–30 e1; quiz e60.
11. Bell BP, Manos MM, Zaman A, Terrault N, Thomas A, Navarro VJ, et al. The epidemiology of newly diagnosed chronic liver disease in gastroenterology practices in the United States:

- results from population-based surveillance. *Am J Gastroenterol.* 2008;103(11):2727–36; quiz 37.
12. D'Amico G, Garcia-Tsao G, Pagliaro L. Natural history and prognostic indicators of survival in cirrhosis: a systematic review of 118 studies. *J Hepatol.* 2006;44(1):217–31.
  13. Germani G, Hytioglou P, Fotiadu A, Burroughs AK, Dhillon AP. Assessment of fibrosis and cirrhosis in liver biopsies: an update. *Semin Liver Dis.* 2011;31(1):82–90.
  14. Colloredo G, Guido M, Sonzogni A, Leandro G. Impact of liver biopsy size on histological evaluation of chronic viral hepatitis: the smaller the sample, the milder the disease. *J Hepatol.* 2003;39(2):239–44.
  15. Afdhal NH, Nunes D. Evaluation of liver fibrosis: a concise review. *Am J Gastroenterol.* 2004;99(6):1160–74.
  16. Standish RA, Cholongitas E, Dhillon A, Burroughs AK, Dhillon AP. An appraisal of the histopathological assessment of liver fibrosis. *Gut.* 2006;55(4):569–78.
  17. Vallet-Pichard A, Mallet V, Nalpas B, Verkarre V, Nalpas A, Dhalluin-Venier V, et al. FIB-4: an inexpensive and accurate marker of fibrosis in HCV infection. Comparison with liver biopsy and fibrotest. *Hepatology.* 2007;46(1):32–6.
  18. Angulo P, Hui JM, Marchesini G, Bugianesi E, George J, Farrell GC, et al. The NAFLD fibrosis score: a noninvasive system that identifies liver fibrosis in patients with NAFLD. *Hepatology.* 2007;45(4):846–54.
  19. Wai CT, Greenon JK, Fontana RJ, Kalbfleisch JD, Marrero JA, Conjeevaram HS, et al. A simple noninvasive index can predict both significant fibrosis and cirrhosis in patients with chronic hepatitis C. *Hepatology.* 2003;38(2):518–26.
  20. Imbert-Bismut F, Ratziu V, Pieron L, Charlotte F, Benhamou Y, Poinard T, et al. Biochemical markers of liver fibrosis in patients with hepatitis C virus infection: a prospective study. *Lancet.* 2001;357(9262):1069–75.
  21. Rosenberg WM, Voelker M, Thiel R, Becka M, Burt A, Schuppan D, et al. Serum markers detect the presence of liver fibrosis: a cohort study. *Gastroenterology.* 2004;127(6):1704–13.
  22. Cales P, Oberti F, Michalak S, Hubert-Fouchard I, Rousset MC, Konate A, et al. A novel panel of blood markers to assess the degree of liver fibrosis. *Hepatology.* 2005;42(6):1373–81.
  23. Lazo M, Hernaez R, Eberhardt MS, Bonekamp S, Kamel I, Guallar E, et al. Prevalence of nonalcoholic fatty liver disease in the United States: the Third National Health and Nutrition Examination Survey, 1988-1994. *Am J Epidemiol.* 2013;178(1):38–45.
  24. Younossi ZM, Koenig AB, Abdelatif D, Fazel Y, Henry L, Wymer M. Global epidemiology of nonalcoholic fatty liver disease-Meta-analytic assessment of prevalence, incidence, and outcomes. *Hepatology.* 2016;64(1):73–84.
  25. Newsome PN, Cramb R, Davison SM, Dillon JF, Foulerton M, Godfrey EM, et al. Guidelines on the management of abnormal liver blood tests. *Gut.* 2018;67(1):6–19.
  26. Kwo PY, Cohen SM, Lim JK. ACG clinical guideline: evaluation of abnormal liver chemistries. *Am J Gastroenterol.* 2017;112(1):18–35.
  27. McPherson S, Hardy T, Dufour JF, Petta S, Romero-Gomez M, Allison M, et al. Age as a confounding factor for the accurate non-invasive diagnosis of advanced NAFLD fibrosis. *Am J Gastroenterol.* 2017;112(5):740–51.
  28. Chen T, Wong R, Wong P, Rollet-Kurhajec KC, Alshaalán R, Deschenes M, et al. Occult cirrhosis diagnosed by transient elastography is a frequent and under-monitored clinical entity. *Liver Int.* 2015;35(10):2285–93.
  29. Myers RP, Pomier-Layrargues G, Kirsch R, Pollett A, Duarte-Rojo A, Wong D, et al. Feasibility and diagnostic performance of the FibroScan XL probe for liver stiffness measurement in overweight and obese patients. *Hepatology.* 2012;55(1):199–208.
  30. Srivastava A, Gailer R, Tanwar S, Trembling P, Parkes J, Rodger A, et al. Prospective evaluation of a primary care referral pathway for patients with non-alcoholic fatty liver disease. *J Hepatol.* 2019;71(2):371–8.
  31. Glen J, Floros L, Day C, Pryke R, Guideline DG. Non-alcoholic fatty liver disease (NAFLD): summary of NICE guidance. *BMJ.* 2016;354:i4428.

32. Davyduke T, Abruñades JG, Tandon P, Ma MM. Impact of pre-screening with Fibrosis-4 index on a referral pathway for patients with suspected NAFLD. *Hepatology*. 2018;68(S1):44A.
33. Roulot D, Costes JL, Buyck JF, Warzocha U, Gambier N, Czernichow S, et al. Transient elastography as a screening tool for liver fibrosis and cirrhosis in a community-based population aged over 45 years. *Gut*. 2011;60(7):977–84.
34. Reinert DF, Allen JP. The alcohol use disorders identification test (AUDIT): a review of recent research. *Alcohol Clin Exp Res*. 2002;26(2):272–9.
35. Moreno C, Mueller S, Szabo G. Non-invasive diagnosis and biomarkers in alcohol-related liver disease. *J Hepatol*. 2019;70(2):273–83.
36. Nguyen-Khac E, Chatelain D, Tramier B, Decrombecque C, Robert B, Joly JP, et al. Assessment of asymptomatic liver fibrosis in alcoholic patients using fibroscan: prospective comparison with seven non-invasive laboratory tests. *Aliment Pharmacol Ther*. 2008;28(10):1188–98.
37. Thiele M, Madsen BS, Hansen JF, Detlefsen S, Antonsen S, Krag A. Accuracy of the enhanced liver fibrosis test vs fibrotest, elastography, and indirect markers in detection of advanced fibrosis in patients with alcoholic liver disease. *Gastroenterology*. 2018;154(5):1369–79.
38. Ducancelle A, Leroy V, Vergniol J, Sturm N, Le Bail B, Zarski JP, et al. A single test combining blood markers and elastography is more accurate than other fibrosis tests in the main causes of chronic liver diseases. *J Clin Gastroenterol*. 2017;51(7):639–49.
39. Sebastiani G, Halfon P, Castera L, Pol S, Thomas DL, Mangia A, et al. SAFE biopsy: a validated method for large-scale staging of liver fibrosis in chronic hepatitis C. *Hepatology*. 2009;49(6):1821–7.
40. Sebastiani G, Ghali P, Wong P, Klein MB, Deschenes M, Myers RP. Physicians' practices for diagnosing liver fibrosis in chronic liver diseases: a nationwide, Canadian survey. *Can J Gastroenterol Hepatol*. 2014;28(1):23–30.
41. EASL-ALEH Clinical Practice Guidelines. Non-invasive tests for evaluation of liver disease severity and prognosis. *J Hepatol*. 2015;63(1):237–64.
42. Castera L, Vergniol J, Foucher J, Le Bail B, Chanteloup E, Haaser M, et al. Prospective comparison of transient elastography, Fibrotest, APRI, and liver biopsy for the assessment of fibrosis in chronic hepatitis C. *Gastroenterology*. 2005;128(2):343–50.
43. Castera L, Sebastiani G, Le Bail B, de Ledinghen V, Couzigou P, Alberti A. Prospective comparison of two algorithms combining non-invasive methods for staging liver fibrosis in chronic hepatitis C. *J Hepatol*. 2010;52(2):191–8.
44. Zarski JP, Sturm N, Guechot J, Paris A, Zafrani ES, Asselah T, et al. Comparison of nine blood tests and transient elastography for liver fibrosis in chronic hepatitis C: the ANRS HCEP-23 study. *J Hepatol*. 2012;56(1):55–62.
45. Cales P, Boursier J, Lebigot J, de Ledinghen V, Aube C, Hubert I, et al. Liver fibrosis diagnosis by blood test and elastography in chronic hepatitis C: agreement or combination? *Aliment Pharmacol Ther*. 2017;45(7):991–1003.
46. Cales P, Boursier J, Ducancelle A, Oberti F, Hubert I, Hunault G, et al. Improved fibrosis staging by elastometry and blood test in chronic hepatitis C. *Liver Int*. 2014;34(6):907–17.
47. Boursier J, de Ledinghen V, Zarski JP, Rousselet MC, Sturm N, Foucher J, et al. A new combination of blood test and fibroscan for accurate non-invasive diagnosis of liver fibrosis stages in chronic hepatitis C. *Am J Gastroenterol*. 2011;106(7):1255–63.
48. A-IHG P. Hepatitis C. Guidance 2018 update: AASLD-IDS recommendations for testing, managing, and treating hepatitis C virus infection. *Clin Infect Dis*. 2018;67(10):1477–92.
49. Pawlotsky J-M, Negro F, Aghemo A, Berenguer M, Dalgard O, Dusheiko G, et al. EASL recommendations on treatment of hepatitis C 2018. *J Hepatol*. 2018;69(2):461–511.
50. Crossan C, Tsochatzis EA, Longworth L, Gurusamy K, Davidson B, Rodriguez-Peralvarez M, et al. Cost-effectiveness of non-invasive methods for assessment and monitoring of liver fibrosis and cirrhosis in patients with chronic liver disease: systematic review and economic evaluation. *Health Technol Assess*. 2015;19(9):1–409, v-vi.

51. Mueller S, Englert S, Seitz HK, Badea RI, Erhardt A, Bozaari B, et al. Inflammation-adapted liver stiffness values for improved fibrosis staging in patients with hepatitis C virus and alcoholic liver disease. *Liver Int.* 2015;35(12):2514–21.
52. Sebastiani G, Vario A, Guido M, Alberti A. Sequential algorithms combining non-invasive markers and biopsy for the assessment of liver fibrosis in chronic hepatitis B. *World J Gastroenterol.* 2007;13(4):525–31.
53. Chan HL, Wong GL, Choi PC, Chan AW, Chim AM, Yiu KK, et al. Alanine aminotransferase-based algorithms of liver stiffness measurement by transient elastography (Fibroscan) for liver fibrosis in chronic hepatitis B. *J Viral Hepat.* 2009;16(1):36–44.
54. Wong GL, Wong VW, Choi PC, Chan AW, Chan HL. Development of a non-invasive algorithm with transient elastography (Fibroscan) and serum test formula for advanced liver fibrosis in chronic hepatitis B. *Aliment Pharmacol Ther.* 2010;31(10):1095–103.
55. Wong GL, Chan HL, Choi PC, Chan AW, Yu Z, Lai JW, et al. Non-invasive algorithm of enhanced liver fibrosis and liver stiffness measurement with transient elastography for advanced liver fibrosis in chronic hepatitis B. *Aliment Pharmacol Ther.* 2014;39(2):197–208.
56. Vigano M, Paggi S, Lampertico P, Fraquelli M, Massironi S, Ronchi G, et al. Dual cut-off transient elastography to assess liver fibrosis in chronic hepatitis B: a cohort study with internal validation. *Aliment Pharmacol Ther.* 2011;34(3):353–62.
57. Terrault NA, Bzowej NH, Chang KM, Hwang JP, Jonas MM, Murad MH, et al. AASLD guidelines for treatment of chronic hepatitis B. *Hepatology.* 2016;63(1):261–83.
58. Castera L, Friedrich-Rust M, Loomba R. Noninvasive assessment of liver disease in patients with nonalcoholic fatty liver disease. *Gastroenterology.* 2019;156(5):1264–81 e4.
59. Petta S, Vanni E, Bugianesi E, Di Marco V, Camma C, Cabibi D, et al. The combination of liver stiffness measurement and NAFLD fibrosis score improves the noninvasive diagnostic accuracy for severe liver fibrosis in patients with nonalcoholic fatty liver disease. *Liver Int.* 2015;35(5):1566–73.
60. Chan WK, Nik Mustapha NR, Mahadeva S. A novel 2-step approach combining the NAFLD fibrosis score and liver stiffness measurement for predicting advanced fibrosis. *Hepatol Int.* 2015;9(4):594–602.
61. Petta S, Wong VW, Camma C, Hiriart JB, Wong GL, Marra F, et al. Improved noninvasive prediction of liver fibrosis by liver stiffness measurement in patients with nonalcoholic fatty liver disease accounting for controlled attenuation parameter values. *Hepatology.* 2017;65(4):1145–55.
62. Wong VW, Irls M, Wong GL, Shili S, Chan AW, Merrouche W, et al. Unified interpretation of liver stiffness measurement by M and XL probes in non-alcoholic fatty liver disease. *Gut.* 2019;68(11):2057–64.
63. Benmassaoud A, Ghali P, Cox J, Wong P, Szabo J, Deschenes M, et al. Screening for non-alcoholic steatohepatitis by using cytokeratin 18 and transient elastography in HIV mono-infection. *PLoS One.* 2018;13(1):e0191985.
64. Castera L, Winnock M, Pambrun E, Paradis V, Perez P, Loko MA, et al. Comparison of transient elastography (FibroScan), FibroTest, APRI and two algorithms combining these non-invasive tests for liver fibrosis staging in HIV/HCV coinfected patients: ANRS CO13 HEPAVIH and FIBROSTIC collaboration. *HIV Med.* 2014;15(1):30–9.
65. Schmid P, Bregenzer A, Huber M, Rauch A, Jochum W, Mullahtaupt B, et al. Progression of liver fibrosis in HIV/HCV Co-infection: a comparison between non-invasive assessment methods and liver biopsy. *PLoS One.* 2015;10(9):e0138838.
66. de Ledingham V, Douvin C, Kettaneh A, Zioli M, Roulot D, Marcellin P, et al. Diagnosis of hepatic fibrosis and cirrhosis by transient elastography in HIV/hepatitis C virus-coinfected patients. *J Acquir Immune Defic Syndr.* 2006;41(2):175–9.
67. Morse CG, McLaughlin M, Proschan M, Koh C, Kleiner DE, Heller T, et al. Transient elastography for the detection of hepatic fibrosis in HIV-monoinfected adults with elevated aminotransferases on antiretroviral therapy. *AIDS.* 2015;29(17):2297–302.



68. Lemoine M, Assoumou L, De Wit S, Girard PM, Valantin MA, Katlama C, et al. Diagnostic accuracy of noninvasive markers of steatosis, NASH, and liver fibrosis in HIV-monoinfected individuals at risk of nonalcoholic fatty liver disease (NAFLD): results from the ECHAM study. *J Acquir Immune Defic Syndr*. 2019;80(4):e86–94.
69. Miallhes P, Pradat P, Chevallier M, Lacombe K, Bailly F, Cotte L, et al. Proficiency of transient elastography compared to liver biopsy for the assessment of fibrosis in HIV/HBV-coinfected patients. *J Viral Hepat*. 2011;18(1):61–9.
70. Voican CS, Louvet A, Trabut JB, Njike-Nakseu M, Dharancy S, Sanchez A, et al. Transient elastography alone and in combination with FibroTest((R)) for the diagnosis of hepatic fibrosis in alcoholic liver disease. *Liver Int*. 2017;37(11):1697–705.
71. Lannerstedt H, Konopski Z, Sandvik L, Haaland T, Loberg EM, Haukeland JW. Combining transient elastography with FIB4 enhances sensitivity in detecting advanced fibrosis of the liver. *Scand J Gastroenterol*. 2013;48(1):93–100.
72. Mueller S, Millonig G, Sarovska L, Friedrich S, Reimann FM, Pritsch M, et al. Increased liver stiffness in alcoholic liver disease: differentiating fibrosis from steatohepatitis. *World J Gastroenterol*. 2010;16(8):966–72.
73. Trabut JB, Thepot V, Nalpas B, Lavielle B, Coscone S, Corouge M, et al. Rapid decline of liver stiffness following alcohol withdrawal in heavy drinkers. *Alcohol Clin Exp Res*. 2012;36(8):1407–11.
74. Nguyen-Khac E, Thiele M, Voican C, Nahon P, Moreno C, Boursier J, et al. Non-invasive diagnosis of liver fibrosis in patients with alcohol-related liver disease by transient elastography: an individual patient data meta-analysis. *Lancet Gastroenterol Hepatol*. 2018;3(9):614–25.
75. Manns MP, Czaja AJ, Gorham JD, Krawitt EL, Mieli-Vergani G, Vergani D, et al. Diagnosis and management of autoimmune hepatitis. *Hepatology*. 2010;51(6):2193–213.
76. European Association for the Study of the L. EASL clinical practice guidelines: autoimmune hepatitis. *J Hepatol*. 2015;63(4):971–1004.
77. Mells GF, Floyd JA, Morley KI, Cordell HJ, Franklin CS, Shin SY, et al. Genome-wide association study identifies 12 new susceptibility loci for primary biliary cirrhosis. *Nat Genet*. 2011;43(4):329–32.
78. Ehnert S, Lukoschek T, Bachmann A, Martinez Sanchez JJ, Damm G, Nussler NC, et al. The right choice of antihypertensives protects primary human hepatocytes from ethanol- and recombinant human TGF-beta1-induced cellular damage. *Hepat Med*. 2013;5:31–41.
79. Corpechot C, El Naggar A, Poujol-Robert A, Ziol M, Wendum D, Chazouilleres O, et al. Assessment of biliary fibrosis by transient elastography in patients with PBC and PSC. *Hepatology*. 2006;43(5):1118–24.
80. Corpechot C, Carrat F, Poujol-Robert A, Gaouar F, Wendum D, Chazouilleres O, et al. Noninvasive elastography-based assessment of liver fibrosis progression and prognosis in primary biliary cirrhosis. *Hepatology*. 2012;56(1):198–208.
81. Bacon BR, Adams PC, Kowdley KV, Powell LW, Tavill AS, American Association for the Study of Liver Diseases. Diagnosis and management of hemochromatosis: 2011 practice guideline by the American Association for the Study of Liver Diseases. *Hepatology*. 2011;54(1):328–43.
82. European Association for the Study of the L. EASL clinical practice guidelines for HFE hemochromatosis. *J Hepatol*. 2010;53(1):3–22.
83. Legros L, Bardou-Jacquet E, Latournerie M, Guillygomarch A, Turlin B, Le Lan C, et al. Non-invasive assessment of liver fibrosis in C282Y homozygous HFE hemochromatosis. *Liver Int*. 2015;35(6):1731–8.
84. Sini M, Sorbello O, Civolani A, Liggi M, Demelia L. Non-invasive assessment of hepatic fibrosis in a series of patients with Wilson’s disease. *Dig Liver Dis*. 2012;44(6):487–91.
85. Kim RG, Nguyen P, Bettencourt R, Dulai PS, Haufe W, Hooker J, et al. Magnetic resonance elastography identifies fibrosis in adults with alpha-1 antitrypsin deficiency liver disease: a prospective study. *Aliment Pharmacol Ther*. 2016;44(3):287–99.

# Chapter 50

## Performance of Liver and Spleen Stiffness Measurements in Predicting Postoperative Hepatic Decompensation After HCC Resection



Horia Stefanescu, Oana Nicoara-Farcau, Andreea Ardelean,  
and Bogdan Procopet

### Background

The management of hepatocellular carcinoma (HCC) evolved in the last years since better therapies are available. Barcelona Clinic Liver Cancer (BCLC) staging system and treatment strategy recommends surgical resection for HCC stage 0 and 1, if the patient is an optimal candidate [1]. The matter of “optimal candidate,” however, lays very much on the judgment of the physician/surgeon. A multiparametric assessment involving liver function (Child Pugh class A and MELD score <10), degree of portal hypertension (PH), and the estimation of liver remnant on imaging together with the possibility to adopt a minimally invasive (laparoscopic) strategy is needed [1].

Clinically significant PH (CSPH: hepatic venous pressure gradient—HVPG >10 mmHg) was shown to be associated with postoperative decompensation [2] and with decreased survival after resection in patients with HCC, especially if liver

---

H. Stefanescu (✉)

Liver Unit, Regional Institute of Gastroenterology and Hepatology, Cluj-Napoca, Romania

Liver Research Club, Cluj-Napoca, Romania

e-mail: [horia.stefanescu@irgh.ro](mailto:horia.stefanescu@irgh.ro)

O. Nicoara-Farcau · A. Ardelean

Liver Research Club, Cluj-Napoca, Romania

3rd Medical Clinic, Department of Internal Medicine, Cluj-Napoca University of Medicine and Pharmacy, Cluj-Napoca, Romania

B. Procopet

Liver Unit, Regional Institute of Gastroenterology and Hepatology, Cluj-Napoca, Romania

Liver Research Club, Cluj-Napoca, Romania

3rd Medical Clinic, Department of Internal Medicine, Cluj-Napoca University of Medicine and Pharmacy, Cluj-Napoca, Romania



function is also impaired (bilirubin >1 mg/dL) [3]. Despite this strong correlation (OR = 4.4;  $P = 0.00006$ ), the wide use of HVPG is limited. This is not mainly due to the invasiveness of the HVPG procedure [4], but mainly because the need for appropriate equipment, sufficient and reliable operators, and increased costs [5]. Therefore, it is rarely used outside Liver Units specifically devoted to the clinical management of portal hypertension.

Liver stiffness (LS) is highly correlated with HVPG, regardless the technique used for its measurement [6–9] and is a good predictor of CSPH [10–12], ruling out cirrhosis with high accuracy [11, 13–15]. For more details, see also book Part V “LS and Important Clinical Endpoints.” Therefore, LS measurement (LSM) is currently recommended by multiple societies guidelines as an accurate noninvasive method for the management of patients with advanced liver diseases [16, 17].

In this context, the use of LSM for the management of patients with HCC appears extremely attractive, fulfilling an important clinical need by combining noninvasiveness and good diagnostic performance in a category of patients in whom the edge between oncological safety and liver failure can be very thin.

## Portal Hypertension: A Major Player in HCC

Starting from the pivotal finding [3], the relationship between CSPH and the outcome of patients with HCC who underwent surgical resection was further analyzed. A meta-analysis that included 11 prospective studies and more than 1700 patients showed that CSPH increases two times the risk of death at 3 and 5 years after SR, while the risk of postoperative decompensation is increased three times [10]. Interestingly, only 5/11 studies used HVPG as standard method to assess CSPH, while the other studies used standard surrogate criteria: presence of esophageal varices or splenomegaly (>12 cm) and low platelets count (<100,000). Besides the heterogeneity included in the analysis, this fact demonstrates the predictive role of surrogates of CSPH in the setting of HCC resection.

A large prospective study that included more than 800 patients followed up for 5 years demonstrates that a patient resected for HCC has a higher risk of dying from tumor recurrence, rather than from hepatic decompensation [18]. The extent of hepatectomy was associated with worse survival in both situations, while the risk of death from hepatic decompensation was also associated with liver function (MELD score) and portal hypertension (presence of varices and low platelets). This competing risk analysis nicely demonstrates that the strict use of CSPH as exclusion criteria from resection has no significant impact on 3 years survival, occurrence of postoperative complications or decompensation, while denying a potential cure for almost 25% of the patients with compensated disease (MELD score <9).

## Liver Stiffness in the Settings of Liver Cancer

Although HCC is softer compared with other liver tumors [19], patients with HCC have an increased LS [20, 21]. This is expected, since HCC develops in patients with advanced liver diseases regardless of etiology with an incidence up to 8%/year [22] and is the most frequent event that occurs in the natural history [23]. Moreover, increased LS can predict the further development of HCC [20, 24].

LSM is the most validated method to estimate CSPH in compensated patients with advanced liver disease, and its use is endorsed by current guidelines which recommend the 21 kPa threshold to rule-in severe PH, and the another one at 13 kPa to rule it out [25]. LSM was also validated as a good surrogate marker for CSPH in the presence of resectable HCC. A slightly better negative predicting value (93%) was observed for the rule-out threshold, while for the rule-in limit, the positive predictive value was lower (76%) [23]. It is worth mentioning that in this study, which excluded from resection patients with HVPG >10 mmHg, neither LSM nor HVPG could predict the occurrence of postoperative complications. The most relevant endpoints to be assessed after SR in patients with HCC are post-hepatectomy liver failure (PHLF), HCC recurrence and survival. LSM was evaluated against all of them, and good correlation appears to exist in each scenario.

### *LSM and Post-hepatectomy Liver Failure (PHLF)*

The ability of LSM to predict PHLF was investigated in several studies [18, 26–36] and the detected AUROC varies from 0.60 [33] to 0.86 [27]. The latter found that none of the patients who experienced PHLF had a baseline LSM lower than 15.6 kPa, thus suggesting that it could be an optimal cutoff value [27]. However, only few of these studies performed a head-to-head comparison with preoperative HVPG measurement. One showed a significantly lower predictive power of LSM compared with HVPG (0.60 vs. 0.85 AUROCs) for PHLF, but similar performance for predicting 3-month decompensation (0.81 vs. 0.88 AUROCs;  $P = 0.21$ ) [33]. The other study, however, detected similar AUROC values for LS (0.81) and HVPG (0.79) for the prediction of PHLF [18]. Another study that compared LSM with intraoperative direct measurement of portal pressure found that the former is better in predicting 3-month decompensation (0.81 vs. 0.71 AUROCs), but in this study, only half of the patients were cirrhotics [34]. Interestingly, a French study did not find any association between preoperative LSM and neither PHLF nor 3-month mortality [26]. However, pooled data derived from a meta-analysis of studies that used surrogate markers to predict outcome after SR for HCC show odds ratios for the occurrence of PHLF not different from the overall assessment: 2.56 (95%CI: 1.73–3.80) vs. 3.02 (95%CI: 2.02–4.59), respectively [10].

LSM can be used as a continuous variable to predict the individual risk of PHLF. Considering 10% as an acceptable postoperative risk of decompensation, only patients with LSM <10 kPa should undergo resection. However, in everyday clinical practice decision-making is based on more than just one argument. Therefore, adding LSM to preoperative MELD score and clinical signs of PH (low platelets and presence or varices or splenomegaly) demonstrate net benefit, resulting in a reduction of PHLF of up to 39% by selecting and excluding patients at risk, without ruling out those who duly have an uncomplicated hepatic surgery outcome [29].

### ***LSM and Post-hepatectomy HCC Recurrence***

From the oncological perspective, overall and disease-free survival are the most important endpoints of any cancer treatment. In HCC, resection is considered a curative therapy with survival rates exceeding 5 years [1]. However, reported recurrence rates are as high as 70% at 5 years [1] and the 2 years limit separates early from late recurrence [36].

LSM was the sole preoperative independent predictor of late recurrence (apart from tumor factors) in a predominantly HBV cirrhosis cohort, with a HR of 1.065 [37]. The same study demonstrates a much higher cumulative rate of recurrence at 3 years (68% vs 43%, log-rank  $P = 0.009$ ) if baseline LSM was >13.4 kPa. This cutoff was also associated with higher rates of PHLF and major complications, as well as with 9 months less disease-free survival [37]. These findings were reproduced in another study, in which HBV etiology was predominant [38], making difficult to extrapolate the findings for all patients, regardless the cause of cirrhosis. Indeed, in a large multi-etiological European cohort, although LSM is associated with late recurrence after resection (HR = 1.036; 95%CI 1.005–1.067), it cannot independently predict its occurrence [39]. Increased baseline LSM (>13 kPa) appears to be the sole independent non-cancer-related predictor of late recurrence after radiofrequency ablation therapy [6] with a hazard ratio of 3.11 (95%CI: 1.23–7.84), and can also predict mortality in this settings (HR = 9.83; 95%CI: 1.14–84.21) [40].

In the last years, in the settings of direct acting antiviral therapy for HCV eradication, the issue of increased HCC occurrence and recurrence also emerged [41, 42]. LSM appears to be one of the independent predictors of de novo HCC occurrence (although the HR is only 1.03; 95%CI: 1.01–1.06), but is not associated with recurrence during the median follow-up of 25 months (of note, curative HCC treatment was performed at least 12 months prior the initiation of antiviral therapy, resulting a 3 years disease-free survival period) [43].

Lower baseline LSM as well as lower 6 month increase in LSM appears to be associated with increased rates of complete response after microwave ablation and TACE. The logistic regression analysis performed in this cohort of patients with HCC and HCV cirrhosis suggests that each unit increase in baseline stiffness is associated with 3% reduction in the odds of complete ablation [44].

## *LSM and Survival*

When assessing survival after SR in patients with HCC, we must acknowledge that there are two distinct events that are competing for the same endpoint: death from PHLF and death from HCC recurrence. In the first 16 months after resection, the risk of death from PHLF exceeds the one from recurrence, but in the long time, death from recurrence is more likely to occur [29]. In the absence of preoperative LSM, tumor and intraoperative variables are associated with the likelihood of dying from recurrence, while PH and liver function are associated with the risk of death from liver failure. Combination of these factors may result in a diagram for clinical judgment of surgical and oncological benefit and individual decision-making [29]. The previously demonstrated association between LSM and PH warrants its use to predict survival in patients with HCC proposed for resection.

Indeed, baseline LSM < 16.2 kPa was associated with increased overall survival (34 vs 29 months,  $P = 0.028$ ) in a cohort of Asian patients with predominantly HBV cirrhosis [45]. Absence of CSPH increases the odds ratio of 3 and 5 years survival by 2.09 (95%CI: 1.52–2.88) and 2.07 (95%CI: 1.51–2.84), respectively. The use of noninvasive methods (mainly LSM and clinical surrogates) to estimate PH show similar performance (1.76 (95%CI: 1.38–2.25) and 1.75 (95%CI: 1.36–2.26) odds ratios), as meta-analysis shows [10].

LS estimation by bi-dimensional shear wave elastography prior to RFA showed that LSM <13.3 kPa is associated with higher 3-year survival (96.3 vs. 76.8%, HR = 4.3 (95%CI: 1.26–14.7),  $P = 0.02$ ) [46]. Another study using MR elastography showed that baseline LSM is the only factor associated with overall survival and a value >4.02 kPa predicts poor outcome (65.4 vs. 95.6% 5-year survival,  $P = 0.015$ , with 5.56 (95%CI: 1.40–22.1) hazard ratio) [40].

## **Spleen Stiffness**

Spleen stiffness measurement (SSM) was demonstrated to be better correlated with HVPG [47] and therefore was investigated as a predictor of the outcome of patients with HCC undergoing curative therapies. The same group was able to demonstrate the good correlation between baseline SSM and post-hepatectomy outcomes: PHLF (OR = 1.057(95%CI: 1.016–1.099);  $P = 0.005$ ) [48] and late recurrence (OR = 1.046(95%CI: 1.02–1.07);  $P = 0.0005$ ) [39]. These findings were confirmed also in Asian population, in which preoperative SSM value (assessed by point shear-wave elastography) together with spleen volume to future liver remnant volume ratio were found to be independent predictors of PHLF (HR for SSM = 1.077 (95%CI: 1.01–1.14);  $P = 0.009$ ) [49]. Interestingly, another Chinese study that included a small number of patients—all with HBV etiology—did not replicate the findings; SSM was not found to be associated with neither PHLF (AUROC = 0.61;  $P = 0.3$ ), nor with overall survival (log-rank  $P = 0.37$ ) [45].

## Tumor Stiffness as Predictor of Response to Non-surgical Therapies

Early changes in tumor stiffness (i.e., tumor becoming softer) were found to be associated with treatment response in a murine model of HCC treated with sorafenib [50]. In humans, tumor elastography was only recently applied, demonstrating that various focal liver lesions have different stiffness [51, 52]. Only one study so far reported a significant 3 days increase in tumor stiffness after ablative therapy (either RFA, TACE, or both) in non-responders, while in responders it remained unchanged (as was the non-tumoral liver parenchyma) [53].

## Conclusions

In conclusion, LSM is validated as a valuable clinical tool in decision-making in patients with cirrhosis and resectable HCC. It can predict the occurrence of post-hepatectomy liver failure as well as late (>2 years) recurrence and overall survival. If used together with the MELD score—as an accurate estimation of liver function, it can help to navigate between oncological benefit and risk of decompensation and death. SSM appears to be a valuable additional noninvasive predictor of PHLF and late recurrence, with doubtful benefit in predicting overall survival. In patients who undergo local therapies, early changes in tumor stiffness may predict response. However, prospective randomized controlled trials are still needed to elucidate controversial findings.

## References

1. Galle PR, Forner A, Llovet JM, Mazzaferro V, Piscaglia F, Raoul J-L, et al. EASL Clinical Practice Guidelines: management of hepatocellular carcinoma. *J Hepatol*. 2018;69(1):182–236.
2. Bruix J, Castells A, Bosch J, Feu F, Fuster J, Garcia-Pagan JC, et al. Surgical resection of hepatocellular carcinoma in cirrhotic patients: prognostic value of preoperative portal pressure. *Gastroenterology*. 1996;111(4):1018–22.
3. Llovet JM, Fuster J, Bruix J. Intention-to-treat analysis of surgical treatment for early hepatocellular carcinoma: resection versus transplantation. *Hepatology*. 1999;30(6):1434–40.
4. Procopet B, Bureau C, Métivier S, Selves J, Robic MA, Christol C, et al. Tolerance of liver biopsy in a tertiary care center. *Eur J Gastroenterol Hepatol*. 2012;24(10):1209–13.
5. Thalheimer U, Bellis L, Puoti C, Burroughs AK. Should we routinely measure portal pressure in patients with cirrhosis, using hepatic venous pressure gradient (HVPG) as a guide for prophylaxis and therapy of bleeding and rebleeding? No. *Eur J Intern Med*. 2011;22(1):5–7.
6. Jung KS, Kim JH, Kim SU, Song K, Kim BK, Park JY, et al. Liver stiffness value-based risk estimation of late recurrence after curative resection of hepatocellular carcinoma: development and validation of a predictive model. *PLoS One*. 2014;9(6):e99167.
7. Bureau C, Metivier S, Peron JM, Selves J, Robic MA, Gourraud PA, et al. Transient elastography accurately predicts presence of significant portal hypertension in patients with chronic liver disease. *Aliment Pharmacol Ther*. 2008;27(12):1261–8.

8. Salzl P, Reiberger T, Ferlitsch M, Payer BA, Schwengerer B, Trauner M, et al. Evaluation of portal hypertension and varices by acoustic radiation force impulse imaging of the liver compared to transient elastography and AST to platelet ratio index. *Ultraschall Med.* 2014;35(6):528–33.
9. Vizzutti F, Arena U, Romanelli RG, Rega L, Foschi M, Colagrande S, et al. Liver stiffness measurement predicts severe portal hypertension in patients with HCV-related cirrhosis. *Hepatology.* 2007;45(5):1290–7.
10. Berzigotti A, Reig M, Abraldes JG, Bosch J, Bruix J. Portal hypertension and the outcome of surgery for hepatocellular carcinoma in compensated cirrhosis: a systematic review and meta-analysis. *Hepatology.* 2015;61(2):526–36.
11. Castera L. Liver stiffness by ultrasound elastography. Diagnostic methods for cirrhosis and portal hypertension. Springer International Publishing; 2018. p. 95–111.
12. You MW, Kim KW, Pyo J, Huh J, Kim HJ, Lee SJ, et al. A meta-analysis for the diagnostic performance of transient elastography for clinically significant portal hypertension. *Ultrasound Med Biol.* 2017;43(1):59–68.
13. Friedrich-Rust M, Ong MF, Martens S, Sarrazin C, Bojunga J, Zeuzem S, et al. Performance of transient elastography for the staging of liver fibrosis: a meta-analysis. *Gastroenterology.* 2008;134(4):960–74.e8.
14. Singh S, Fujii LL, Murad MH, Wang Z, Asrani SK, Ehman RL, et al. Liver stiffness is associated with risk of decompensation, liver cancer, and death in patients with chronic liver diseases: a systematic review and meta-analysis. *Clin Gastroenterol Hepatol.* 2013;11(12):1573–84.e2.
15. Tsochatzis EA, Gurusamy KS, Ntaoula S, Cholongitas E, Davidson BR, Burroughs AK. Elastography for the diagnosis of severity of fibrosis in chronic liver disease: a meta-analysis of diagnostic accuracy. *J Hepatol.* 2011;54(4):650–9.
16. Dietrich CF, Bamber J, Berzigotti A, Bota S, Cantisani V, Castera L, et al. EFSUMB guidelines and recommendations on the clinical use of liver ultrasound elastography, update 2017 (long version). *Ultraschall Med.* 2017;38(4):e16–47.
17. European Association for Study of Liver; Asociacion Latinoamericana para el Estudio del Hígado. EASL-ALEH Clinical Practice Guidelines: non-invasive tests for evaluation of liver disease severity and prognosis. *J Hepatol.* 2015;63(1):237–64.
18. Cucchetti A, Cescon M, Colecchia A, Neri F, Cappelli A, Ravaioli M, et al. Adding liver stiffness measurement to the routine evaluation of hepatocellular carcinoma resectability can optimize clinical outcome. *Ultraschall Med.* 2016;38(05):515–22.
19. Masuzaki R, Tateishi R, Yoshida H, Sato T, Ohki T, Goto T, et al. Assessing liver tumor stiffness by transient elastography. *Hepato Int.* 2007;1(3):394–7.
20. Akima T, Tamano M, Hiraishi H. Liver stiffness measured by transient elastography is a predictor of hepatocellular carcinoma development in viral hepatitis. *Hepato Res.* 2011;41(10):965–70.
21. Kusaka K, Harihara Y, Torzilli G, Kubota K, Takayama T, Makuuchi M, et al. Objective evaluation of liver consistency to estimate hepatic fibrosis and functional reserve for hepatectomy. *J Am Coll Surg.* 2000;191(1):47–53.
22. Ioannou GN, Splan MF, Weiss NS, McDonald GB, Beretta L, Lee SP. Incidence and predictors of hepatocellular carcinoma in patients with cirrhosis. *Clin Gastroenterol Hepatol.* 2007;5(8):938–45.e4.
23. Llop E, Berzigotti A, Reig M, Erice E, Reverter E, Seijo S, et al. Assessment of portal hypertension by transient elastography in patients with compensated cirrhosis and potentially resectable liver tumors. *J Hepatol.* 2012;56(1):103–8.
24. Masuzaki R, Tateishi R, Yoshida H, Goto E, Sato T, Ohki T, et al. Prospective risk assessment for hepatocellular carcinoma development in patients with chronic hepatitis C by transient elastography. *Hepatology.* 2009;49(6):1954–61.
25. de Franchis R. Expanding consensus in portal hypertension: report of the Baveno VI Consensus Workshop: stratifying risk and individualizing care for portal hypertension. *J Hepatol.* 2015;63(3):743–52.

26. Boleslawski E, Petrovai G, Truant S, Dharancy S, Duhamel A, Salleron J, et al. Hepatic venous pressure gradient in the assessment of portal hypertension before liver resection in patients with cirrhosis. *Br J Surg*. 2012;99(6):855–63.
27. Cescon M, Colecchia A, Cucchetti A, Peri E, Montrone L, Ercolani G, et al. Value of transient elastography measured with FibroScan in predicting the outcome of hepatic resection for hepatocellular carcinoma. *Ann Surg*. 2012;256(5):706–12; discussion 12–3.
28. Chong CC-N, Wong GL-H, Chan AW-H, Wong VW-S, Fong AK-W, Cheung Y-S, et al. Liver stiffness measurement predicts high-grade post-hepatectomy liver failure: a prospective cohort study. *J Gastroenterol Hepatol*. 2017;32(2):506–14.
29. Cucchetti A, Sposito C, Pinna AD, Citterio D, Cescon M, Bongini M, et al. Competing risk analysis on outcome after hepatic resection of hepatocellular carcinoma in cirrhotic patients. *World J Gastroenterol*. 2017;23(8):1469.
30. Fung J, Poon RTP, Yu W-C, Chan S-C, Chan ACY, Chok KSH, et al. Use of liver stiffness measurement for liver resection surgery: correlation with indocyanine green clearance testing and post-operative outcome. *PLoS One*. 2013;8(8):e72306.
31. Kim SU, Ahn SH, Park JY, Kim DY, Chon CY, Choi JS, et al. Prediction of postoperative hepatic insufficiency by liver stiffness measurement (FibroScan®) before curative resection of hepatocellular carcinoma: a pilot study. *Hepatol Int*. 2008;2(4):471–7.
32. Li C, Zhang J-Y, Zhang X-Y, Wen T-F, Yan L-N. FibroScan predicts ascites after liver resection for hepatitis B virus-related hepatocellular carcinoma: a prospective cohort study. *Int J Surg*. 2015;20:21–5.
33. Procopet B, Fischer P, Horhat A, Mois E, Stefanescu H, Comsa M, et al. Good performance of liver stiffness measurement in the prediction of postoperative hepatic decompensation in patients with cirrhosis complicated with hepatocellular carcinoma. *Med Ultrason*. 2018;20(3):272.
34. Rajakannu M, Cherqui D, Ciaccio O, Golse N, Pittau G, Allard MA, et al. Liver stiffness measurement by transient elastography predicts late posthepatectomy outcomes in patients undergoing resection for hepatocellular carcinoma. *Surgery*. 2017;162(4):766–74.
35. Wong JS-W, Wong GL-H, Chan AW-H, Wong VW-S, Cheung Y-S, Chong C-N, et al. Liver stiffness measurement by transient elastography as a predictor on posthepatectomy outcomes. *Ann Surg*. 2013;257(5):922–8.
36. Llovet JM, Di Bisceglie AM, Bruix J, Kramer BS, Lencioni R, Zhu AX, et al. Design and end-points of clinical trials in hepatocellular carcinoma. *J Natl Cancer Inst*. 2008;100(10):698–711.
37. Jung KS, Kim SU, Choi GH, Park JY, Park YN, Kim DY, et al. Prediction of recurrence after curative resection of hepatocellular carcinoma using liver stiffness measurement (FibroScan(R)). *Ann Surg Oncol*. 2012;19(13):4278–86.
38. Qi M, Chen Y, Zhang GQ, Meng YJ, Zhao FL, Wang J, et al. Clinical significance of preoperative liver stiffness measurements in primary HBV-positive hepatocellular carcinoma. *Future Oncol*. 2017;13(30):2799–810.
39. Marasco G, Colecchia A, Colli A, Ravaioli F, Casazza G, Bacchi Reggiani ML, et al. Role of liver and spleen stiffness in predicting the recurrence of hepatocellular carcinoma after resection. *J Hepatol*. 2019;70(3):440–8.
40. Lee YR, Park SY, Kim SU, Jang SY, Tak WY, Kweon YO, et al. Using transient elastography to predict hepatocellular carcinoma recurrence after radiofrequency ablation. *J Gastroenterol Hepatol*. 2017;32(5):1079–86.
41. Conti F, Buonfiglioli F, Scuteri A, Crespi C, Bolondi L, Caraceni P, et al. Early occurrence and recurrence of hepatocellular carcinoma in HCV-related cirrhosis treated with direct-acting antivirals. *J Hepatol*. 2016;65(4):727–33.
42. Reig M, Mariño Z, Perelló C, Iñáñirraegui M, Ribeiro A, Lens S, et al. Unexpected high rate of early tumor recurrence in patients with HCV-related HCC undergoing interferon-free therapy. *J Hepatol*. 2016;65(4):719–26.
43. Degasperis E, D'Ambrosio R, Iavarone M, Sangiovanni A, Aghemo A, Soffredini R, et al. Factors associated with increased risk of de novo or recurrent hepatocellular carcinoma in patients with



- cirrhosis treated with direct-acting antivirals for HCV infection. *Clin Gastroenterol Hepatol*. 2019;17(6):1183–91.e7.
44. Abdelaziz AO, Abdelhalim H, Elsharkawy A, Shousha HI, Abdelmaksoud AH, Soliman ZA, et al. Liver stiffness measurement changes following hepatocellular carcinoma treatment with percutaneous microwave ablation or transarterial chemoembolization: a cohort study. *Eur J Gastroenterol Hepatol*. 2019;31(6):685–91.
  45. Wu D, Chen E, Liang T, Wang M, Chen B, Lang B, et al. Predicting the risk of postoperative liver failure and overall survival using liver and spleen stiffness measurements in patients with hepatocellular carcinoma. *Medicine*. 2017;96(34):e7864.
  46. Lee DH, Lee JM, Yoon J-H, Kim YJ, Lee J-H, Yu SJ, et al. Liver stiffness measured by two-dimensional shear-wave elastography: prognostic value after radiofrequency ablation for hepatocellular carcinoma. *Liver Cancer*. 2018;7(1):65–75.
  47. Colecchia A, Montrone L, Scaiola E, Bacchi-Reggiani ML, Colli A, Casazza G, et al. Measurement of spleen stiffness to evaluate portal hypertension and the presence of esophageal varices in patients with HCV-related cirrhosis. *Gastroenterology*. 2012;143(3):646–54.
  48. Marasco G, Colecchia A, Dajti E, Ravaioli F, Cucchetti A, Cescon M, et al. Prediction of posthepatectomy liver failure: role of SSM and LSPS. *J Surg Oncol*. 2018;119(3):400–1.
  49. Peng W, Zhang XY, Li C, Wen TF, Yan LN, Yang JY. Spleen stiffness and volume help to predict posthepatectomy liver failure in patients with hepatocellular carcinoma. *Medicine (Baltimore)*. 2019;98(18):e15458.
  50. Salvatore V, Baron Toaldo M, Marinelli S, Milazzo M, Palamà C, Venerandi L, et al. Early prediction of treatment response to sorafenib with elastosonography in a mice xenograft model of hepatocellular carcinoma: a proof-of-concept study. *Ultraschall Med*. 2013;34(06):541–9.
  51. Zhang P, Zhou P, Tian S-M, Qian Y, Deng J, Zhang L. Application of acoustic radiation force impulse imaging for the evaluation of focal liver lesion elasticity. *Hepatobiliary Pancreat Dis Int*. 2013;12(2):165–70.
  52. Grgurevic I, Bokun T, Salkic NN, Brkljacic B, Vukelić-Markovic M, Stoos-Veic T, et al. Liver elastography malignancy prediction score for noninvasive characterization of focal liver lesions. *Liver Int*. 2017;38(6):1055–63.
  53. Praktijnjo M, Krabbe V, Pohlmann A, Sampels M, Jansen C, Meyer C, et al. Evolution of nodule stiffness might predict response to local ablative therapy: a series of patients with hepatocellular carcinoma. *PLoS One*. 2018;13(2):e0192897.



# Chapter 51

## Liver Stiffness Changes in Patients with Established Liver Cirrhosis



Felix Piecha and Sebastian Mueller

### Introduction

Liver stiffness (LS) measurement by transient elastography (TE) has evolved as the most commonly applied instrument for the non-invasive diagnosis of liver fibrosis. Even though cut-off values may vary according to the underlying disease etiology, values  $>12.5$  kPa are generally accepted for the diagnosis of liver cirrhosis [1, 2]. For more details, see also book Part III “Liver Stiffness and Various Etiologies of Liver Diseases.” However, the Fibroscan® device (Echosens, Paris, France) is able to continuously measure LS up to 75 kPa, thus allowing for a further discrimination of patients within the cirrhotic range. Large studies have shown that baseline LS is an independent predictor of complications of liver cirrhosis and patient outcome in various disease etiologies [3–8]. Due to its non-invasive nature, however, LS can be measured repeatedly and therefore be used as a follow-up tool. Especially in light of the dynamic component of LS, values may change over time and need to be carefully interpreted for the correct risk stratification of patients.

---

F. Piecha (✉)

I. Department of Medicine, University Medical Center Hamburg-Eppendorf,  
Hamburg, Germany  
e-mail: [f.piecha@uke.de](mailto:f.piecha@uke.de)

S. Mueller

Department of Medicine and Center for Alcohol Research and Liver Diseases, Salem Medical  
Center, University of Heidelberg, Heidelberg, Germany  
e-mail: [sebastian.mueller@urz.uni-heidelberg.de](mailto:sebastian.mueller@urz.uni-heidelberg.de)

## LS Changes in Patients with Established Liver Cirrhosis

### *Treatment of the Underlying Disease*

The most common reason for changes in LS in patients with liver cirrhosis is the treatment of the underlying liver disease. This has been shown for various disease etiologies, including alcohol detoxification in patients with an alcoholic liver disease (ALD) [9, 10], eradication of viral hepatitis [11, 12], immunosuppressive treatment of an autoimmune hepatitis (AIH) [13], or weight loss in patients with a non-alcoholic fatty liver disease (NAFLD) [14, 15]. More examples are given in Table 8.2 in Chap. 8. In general, this improvement of LS can be attributed to a decrease in the inflammatory component of LS and is usually correlated to an improvement in transaminase levels [16, 17]. However, recent studies suggest that this rapid first phase of LS improvement is followed by a sustained second phase of improvement attributed to a true regression in liver fibrosis [16, 18].

On the other hand, increases in LS have also been observed. In general, this should trigger further diagnostic measures and a closer clinical monitoring. Analogous to an LS decrease, changes in the behavioral patterns of patients may serve as an explanation of increased LS values, like ongoing alcohol consumption or weight gain, especially if the underlying liver disease is otherwise well controlled—e.g., in patients with a chronic hepatitis B virus (HBV) infection with an insignificant viral load. However, an increase in LS can also be a first hint of an acute deterioration of hepatic function [19] or an increase in the inflammatory activity of the underlying liver disease [16] and needs to be interpreted in the context of further clinical and laboratory parameters.

### *Changes of Hepatic Hemodynamics*

In patients with liver cirrhosis, the clinical presentation is dominated by complications of portal hypertension [20, 21]. At this stage, therapeutic interventions targeting hepatic hemodynamics and collateral blood flow are common, and all affect LS via its dynamic component [22]. Therefore, as also described in chapter “Modulation of LS by Arterial and Portal Pressure,” all measures with an impact on portal pressure like the insertion of a transjugular intrahepatic portosystemic shunt (TIPS), endoscopic band ligation [23, 24], or the beginning of a treatment with non-selective betablockers (NSBB) directly affect LS [25]. For more details, see also book Part IV “Important (Patho)physiological Confounders of LS.” However, under these circumstances, LS changes are not uniform, as a minority of patients shows a counterintuitive increase in LS after TIPS-placement or the beginning of a NSBB treatment [23–25]. The reason for this increase remains unclear, but both an increase in atrial pressure and therefore hepatic congestion [23] as well as a chronic inflammatory activity [24] have been discussed as possible explanations. Nevertheless, patients with an LS increase after a pressure-lowering intervention seem to have an inferior prognosis and should therefore undergo closer clinical monitoring [24, 25].

While an increase in LS is generally associated with a deterioration of liver function and prognosis, a decrease in LS seems to be related to improved outcomes. However, a short-term decrease in LS under otherwise stable conditions (meaning without the beginning of a therapeutic intervention, stable transaminases, and liver function scores) should also be interpreted with caution, as preliminary data suggest that this decrease could be associated with spontaneous shunt formation like esophageal varices [23]. The decrease in LS in this clinical scenario could be explained by the increasing amount of blood bypassing the liver during shunt development. Given the importance of spontaneous porto-systemic shunts (SPSS) on the prognosis of patients with liver cirrhosis [26] and their currently unclear impact on therapeutic interventions like TIPS-placement [27], the interdependency of LS, SPSS formation, and hepatic hemodynamics need to be addressed in future studies.

On a final note, disease etiology and localization of inflammation (portal versus lobular) also strongly affect the ratio of spleen stiffness to liver stiffness (SS/LS), the degree of portal hypertension, and its complications [28]. This study showed that lobular ALD had less portal hypertension and smaller SS and spleen size as compared to portal HCV-related liver disease at matched LS values [28]. In line with this, an earlier study demonstrated significantly higher LS values for ALD as compared to NAFLD patients (40.4 vs. 25.7 kPa) for the detection of large esophageal varices [29]. Thus, LS responses to portal flow changes will not only depend on the flow itself but also the underlying liver disease.

## Conclusion

In patients with liver cirrhosis, changes in LS need to be interpreted in the clinical context of therapeutic interventions and further laboratory and clinical data. In general, a decrease in LS after an intervention seems to be associated with an improved prognosis, but special attention needs to be paid to an LS decrease under otherwise stable conditions. Due to its non-invasive nature, serial LS measurements are a valuable follow-up tool for patients with liver cirrhosis and may help in the decision-making of patient monitoring.

## References

1. Mueller S, Sandrin L. Liver stiffness: a novel parameter for the diagnosis of liver disease. *Hepat Med.* 2010;2:49–67.
2. Friedrich-Rust M, Koch C, Rentzsch A, Sarrazin C, Schwarz P, Herrmann E, et al. Noninvasive assessment of liver fibrosis in patients with Fontan circulation using transient elastography and biochemical fibrosis markers. *J Thorac Cardiovasc Surg.* 2008;135(3):560–7.
3. Vergniol J, Foucher J, Terrebonne E, Bernard PH, le Bail B, Merrouche W, et al. Noninvasive tests for fibrosis and liver stiffness predict 5-year outcomes of patients with chronic hepatitis C. *Gastroenterology.* 2011;140(7):1970–9, 9.e1–3.
4. Dillon A, Galvin Z, Sultan AA, Harman D, Guha IN, Stewart S. Transient elastography can stratify patients with Child-Pugh A cirrhosis according to risk of early decompensation. *Eur J Gastroenterol Hepatol.* 2018;30(12):1434–40.

5. Omote K, Nagai T, Asakawa N, Kamiya K, Tokuda Y, Aikawa T, et al. Impact of admission liver stiffness on long-term clinical outcomes in patients with acute decompensated heart failure. *Heart Vessels*. 2019;34(6):984–91.
6. Chalouni M, Sogni P, Miallhes P, Lacombe K, Poizot-Martin I, Chas J, et al. Liver stiffness and fibrosis-4 alone better predict liver events compared with aspartate aminotransferase to platelet ratio index in a cohort of human immunodeficiency virus and hepatitis C virus co-infected patients from ANRS CO13 HEPAVIH cohort. *Eur J Gastroenterol Hepatol*. 2019;31(11):1387–96.
7. Karlas T, Weisse T, Petroff D, Beer S, Dohring C, Gnatzy F, et al. Predicting hepatic complications of allogeneic hematopoietic stem cell transplantation using liver stiffness measurement. *Bone Marrow Transplant*. 2019;54(11):1738–46.
8. Jung KS, Kim SU, Ahn SH, Park YN, Kim DY, Park JY, et al. Risk assessment of hepatitis B virus-related hepatocellular carcinoma development using liver stiffness measurement (FibroScan). *Hepatology*. 2011;53(3):885–94.
9. Gelsi E, Dainese R, Truchi R, Marine-Barjoan E, Anty R, Autuori M, et al. Effect of detoxification on liver stiffness assessed by Fibroscan((R)) in alcoholic patients. *Alcohol Clin Exp Res*. 2011;35(3):566–70.
10. Mueller S, Millonig G, Sarovska L, Friedrich S, Reimann FM, Pritsch M, et al. Increased liver stiffness in alcoholic liver disease: differentiating fibrosis from steatohepatitis. *World J Gastroenterol*. 2010;16(8):966–72.
11. Facciorusso A, Del Prete V, Turco A, Buccino RV, Nacchiero MC, Muscatello N. Long-term liver stiffness assessment in hepatitis C virus patients undergoing antiviral therapy: results from a 5-year cohort study. *J Gastroenterol Hepatol*. 2018;33(4):942–9.
12. Kim BK, Oh HJ, Park JY, Kim DY, Ahn SH, Han KH, et al. Early on-treatment change in liver stiffness predicts development of liver-related events in chronic hepatitis B patients receiving antiviral therapy. *Liver Int*. 2013;33(2):180–9.
13. Hartl J, Denzer U, Ehlken H, Zenouzi R, Peiseler M, Sebode M, et al. Transient elastography in autoimmune hepatitis: timing determines the impact of inflammation and fibrosis. *J Hepatol*. 2016;65(4):769–75.
14. Nickel F, Tapking C, Benner L, Sollors J, Billeter AT, Kenngott HG, et al. Bariatric surgery as an efficient treatment for non-alcoholic fatty liver disease in a prospective study with 1-year follow-up: BariScan study. *Obes Surg*. 2018;28(5):1342–50.
15. Nogami A, Yoneda M, Kobayashi T, Kessoku T, Honda Y, Ogawa Y, et al. Assessment of 10-year changes in liver stiffness using vibration-controlled transient elastography in non-alcoholic fatty liver disease. *Hepatol Res*. 2019;49(8):872–80.
16. Hartl J, Ehlken H, Sebode M, Peiseler M, Krech T, Zenouzi R, et al. Usefulness of biochemical remission and transient elastography in monitoring disease course in autoimmune hepatitis. *J Hepatol*. 2018;68(4):754–63.
17. Mueller S, Englert S, Seitz HK, Badea RI, Erhardt A, Bozaari B, et al. Inflammation-adapted liver stiffness values for improved fibrosis staging in patients with hepatitis C virus and alcoholic liver disease. *Liver Int*. 2015;35(12):2514–21.
18. Pan JJ, Bao F, Du E, Skillin C, Frenette CT, Waalen J, et al. Morphometry confirms fibrosis regression from sustained virologic response to direct-acting antivirals for hepatitis C. *Hepatol Commun*. 2018;2(11):1320–30.
19. Sharma P, Bansal R, Matin A, Tyagi P, Bansal N, Singla V, et al. Role of transient elastography (Fibroscan) in differentiating severe acute hepatitis and acute on chronic liver failure. *J Clin Exp Hepatol*. 2015;5(4):303–9.
20. Karkmann K, Piecha F, Runzi AC, Schulz L, von Wulffen M, Benten D, et al. [Management of compensated liver cirrhosis 2018—evidence based prophylactic measures]. *Z Gastroenterol*. 2018;56(1):55–69.
21. Arvaniti V, D'Amico G, Fede G, Manousou P, Tsochatzis E, Pleguezuelo M, et al. Infections in patients with cirrhosis increase mortality four-fold and should be used in determining prognosis. *Gastroenterology*. 2010;139(4):1246–56, 56.e1–5.

22. Moreno C, Mueller S, Szabo G. Non-invasive diagnosis and biomarkers in alcohol-related liver disease. *J Hepatol.* 2019;70(2):273–83.
23. Piecha F, Paech D, Sollors J, Seitz HK, Rossle M, Rausch V, et al. Rapid change of liver stiffness after variceal ligation and TIPS implantation. *Am J Physiol Gastrointest Liver Physiol.* 2018;314(2):G179–G87.
24. Jansen C, Moller P, Meyer C, Kolbe CC, Bogs C, Pohlmann A, et al. Increase in liver stiffness after transjugular intrahepatic portosystemic shunt is associated with inflammation and predicts mortality. *Hepatology.* 2018;67(4):1472–84.
25. Piecha F, Mandorfer M, Peccerella T, Ozga AK, Poth T, Vonbank A, et al. Pharmacological decrease of liver stiffness is pressure-related and predicts long-term clinical outcome. *Am J Physiol Gastrointest Liver Physiol.* 2018;315(4):G484–G94.
26. Simon-Talero M, Roccarina D, Martinez J, Lampichler K, Baiges A, Low G, et al. Association between portosystemic shunts and increased complications and mortality in patients with cirrhosis. *Gastroenterology.* 2018;154(6):1694–705.e4.
27. Piecha F, Radunski UK, Ozga A-K, Steins D, Drolz A, Horvatits T, et al. Ascites control by TIPS is more successful in patients with a lower paracentesis frequency and is associated with improved survival. *JHEP Rep.* 2019;1(2):90–8.
28. Elshaarawy O, Mueller J, Guha IN, Chalmers J, Harris R, Krag A, et al. Spleen stiffness to liver stiffness ratio significantly differs between ALD and HCV and predicts disease-specific complications. *JHEP Rep.* 2019;1(2):99–106.
29. Nguyen-Khac E, Saint-Leger P, Tramier B, Coevoet H, Capron D, Dupas JL. Noninvasive diagnosis of large esophageal varices by Fibroscan: strong influence of the cirrhosis etiology. *Alcohol Clin Exp Res.* 2010;34(7):1146–53.

# Chapter 52

## Therapeutic Monitoring of Portal Pressure Lowering Drugs Using Liver Stiffness



Omar Elshaarawy, Felix Piecha, and Sebastian Mueller

### Introduction

Monitoring of portal hypertension (PH) and its response to therapeutic interventions at different stages has a significant prognostic value. A “clinically significant portal hypertension” is defined at HVPg >10 mmHg which is associated with PH-related complications [1, 2]. However, the measurement of HVPg is an invasive and expensive procedure and not available in many centers. In 2010, the Baveno V Consensus conference included noninvasive methods to assess PH in order to monitor the response and compliance to treatment [3]. Many tools have been investigated for the noninvasive monitoring of PH comprising routine laboratory tests (e.g., platelets to spleen ratio) and ultrasound techniques especially transient elastography (TE) which included liver and spleen stiffness. Of note, the Baveno VI Consensus conference in 2015 concluded that patients with LS <20 kPa and platelet count more than  $150 \times 10^9$  cells/L can avoid screening endoscopy [4]. In 2017, expanded Baveno VI criteria reported that more endoscopies would be spared if patients with LS <25 kPa and platelet count  $>110 \times 10^9$  cells/L avoided screening without sacrificing the accuracy to detect varices needing treatment [5]. For more details see also the chapter on “Portal Hypertension” in book Part V “LS and Important Clinical Endpoints.”

TE to assess **liver stiffness** has been used to predict PH and esophageal varices, and the AUROC estimated for LS to predict manifested PH ( $\geq 12$  mmHg) was

---

O. Elshaarawy · S. Mueller (✉)

Department of Medicine and Center for Alcohol Research and Liver Diseases,  
Salem Medical Center, University of Heidelberg, Heidelberg, Germany  
e-mail: [oelshaarawy@liver.menofia.edu.eg](mailto:oelshaarawy@liver.menofia.edu.eg); [Sebastian.Mueller@urz.uni-heidelberg.de](mailto:Sebastian.Mueller@urz.uni-heidelberg.de)

F. Piecha

Department of Medicine, University Medical Center Hamburg-Eppendorf, Hamburg,  
Germany  
e-mail: [f.piecha@uke.de](mailto:f.piecha@uke.de)

0.94–0.99 corresponding to cut off values from 13.6 to 21 kPa. The LS cut-off value to predict esophageal varices grade 2 or 3 was 19.8–47.5 kPa with AUROC of 0.72–0.78 [6, 7]. Sporea et al. concluded in their study on 1000 patients that at least 8 from 10 patients with LS more than 40 kPa will have clinically significant portal hypertension. Consequently, half of the patients with LS less than 40 kPa have esophageal varices and thus require screening for esophageal varices (NPV 54.9%) while patients with LS less than 17 kPa do not require endoscopic evaluation (NPV 89.3%) [8].

**Spleen stiffness (SS)** has been frequently addressed as a non-invasive tool to assess PH [9, 10]. Many studies validated that SS can predict the presence of varices and the risk of variceal bleeding, and it can identify patients who require screening endoscopy [11–15]. Assessing spleen stiffness by TE emerged from the rationale that PH leads to spleen congestion. Colecchia et al. assessed 113 compensated cirrhotic patients for LS and SS using TE followed by HVPG measurement and upper endoscopy within 1 week. They reported higher correlation of SS ( $r = 0.89$ ) with HVPG than LS, and SS showed an AUROC of 0.966 to predict the presence of esophageal varices. They concluded that SS <41.3 kPa and LS <16.4 kPa would exclude the presence of esophageal varices (any varices) [9].

Based on the endoscopic classification of varices, esophageal varices were classified into grades from I to IV, or more intuitively, as small, medium, or large [16–18]. Recently, the Austrian Billroth III consensus conference simplified the grading of EV size just into small (<5 mm) and large ( $\geq 5$  mm) in diameter [19].

Several studies reported the superiority of SS over LS regarding the correlation with HVPG, and others recommended combining it with LS for better prediction of PH and esophageal varices (Table 52.1). However, the transducer used in most published SS studies was the regular liver probe which shows a high failure rate in small spleen length and obese patients [14, 20, 21]. The following table shows the cut-off values from several studies comparing LS versus SS with sensitivity, specificity, negative, and positive predictive values. It shows the superiority of SS in predicting the presence of esophageal varices specially the large ones (that needs treatment) over LS. Noteworthy, many studies reported that the prognostic performance of SS is significantly higher than LS [22, 23]. So far, however, SS has not replaced LS in guidelines such as the Baveno consensus criteria. Finally, there are first indications that a simple measurement of spleen length in the abdominal ultrasound performs almost as well as SS assessment [24].

## Portal-Lowering Drugs and Stiffness

It is a fundamental knowledge that portal pressure is a product of both the portal blood flow and the vascular resistance. This vascular resistance can be modulated by drugs in a range between 20 to 30% [25–28]. Several studies have shown that decreasing PH by 20% reduces the risk of decompensation [29, 30]. Pharmacological treatment of PH has been explored for decades. The list of drugs includes non-

**Table 52.1** LS and SS cut-off values to predict the presence of esophageal varices. TE was used except \* marked references that used MRE

Study ID	No. EV/ LEV	LS cutoff kPa	Sens.	Spec.	PPV	NPV	SS cutoff kPa	Sens.	Spec.	+ve PV	-ve PV
Stefanescu et al., 2011 [15]	EV: 116	28	0.74	0.62	0.91	0.30	46.4	0.84	0.71	0.94	0.44
	LEV: 47	38	0.89	0.56	0.70	0.62	53	0.89	0.51	0.67	0.81
Colecchia et al., 2012 [9]	EV: 53	21.4	0.83	0.81	0.83	0.81	46	0.94	0.77	0.82	0.92
Fraquelli et al., 2012 [43]	EV: 11	19	0.73	0.47	0.13	0.94	65	0.91	0.80	0.33	0.99
Sharma et al., 2013 [14]	EV: 124	27.3	0.86	0.70	0.89	0.77	40.8	0.85	0.79	0.91	0.84
Calvaruso et al., 2013 [44]	EV: 54	17.0	0.70	0.57	0.68	0.6	50.0	0.65	0.60	0.67	0.57
	LEV: 26	19.0	0.73	0.54	0.37	0.84	54.0	0.81	0.70	0.5	0.91
Shin et al., 2014 [45]*	EV: 78	4.58*	0.91	0.72	0.79	0.80	7.23*	0.94	0.76	0.84	0.8
	LEV: 45	4.81*	0.60	0.72	0.49	0.91	7.60*	0.76	0.66	0.52	0.85
Elkrief et al., 2015 [46]	LEV: 45	24.7	0.82	0.45	0.70	0.62	32.3	0.48	0.71	0.73	0.45
	EV: 54	19.7	0.83	0.67	0.80	0.71	30.3	0.80	0.76	0.84	0.69

EV esophageal varices, LEV large esophageal varices, Sens. sensitivity, Spec. specificity, PPV positive predictive value, NPV negative predictive value  
\* MRE

selective beta-blockers, vasopressin and somatostatin analogues. They act on the systemic circulation namely to attenuate consequences of the hyperdynamic circulation, to decrease the splanchnic hyper-perfusion but also to improve the effective blood volume [26, 28]. For instance, the use of beta-blockers has been shown to ameliorate the association between liver stiffness and portal pressure [31]. Table 52.2 shows a summary of the current and novel drugs in the treatment of portal hypertension. Other alternatives to decrease the portal pressure include decreasing the intra-hepatic resistance by nitric oxide donors, angiotensin-converting enzyme (ACE) inhibitors, or endothelin receptor antagonists. Some of these drugs, e.g., ACE inhibitors failed to improve PH in patients although good animal data were available. Recently, phosphodiesterase type 5 (PDE-5) inhibitors have been suggested to treat PH. Noteworthy, they improve erectile dysfunction which is a frequent problem in patients with cirrhosis [32, 33]. It has been noted that PDE-5 is upregulated in liver cirrhosis decreasing the vascular tone. In addition, PDE-5 inhibitors increase the



**Table 52.2** Summary of current and novel drugs for portal hypertension (PH)

Drug	References	Mode of action	Status
Metoprolol	[47–49]	Cardio-selective beta-blocker	Not recommended in guidelines
Propranolol	[29, 50–52]	Non-selective beta-blocker	Currently used to prevent complications of portal hypertension such as bleeding
Carvedilol	[26, 27, 53–57]	Non-selective beta-blocker with alpha 1 blocking action	Complications of portal hypertension such as bleeding
Nadolol	[58, 59]	Non-selective beta-blocker	Complications of portal hypertension such as bleeding
Nitrates	[60–62]	Vasodilatation through nitric oxide induction	Not recommended in guidelines
Terlipressin	[63–65]	Splanchnic arterial vasoconstriction through vasopressin-like action and reduction of portal flow	Complications of portal hypertension such as bleeding in acute settings
Octreotide	[66–69]	Reduces splanchnic blood flow through a somatostatin-like effect by blocking glucagon	Complications of portal hypertension such as bleeding in acute settings
Losartan	[70, 71]	Angiotensin receptor blockers	Not recommended in guidelines
Enalapril	[48, 72]	Angiotensin-converting enzyme inhibitors	Not recommended in guidelines
Udenafil	[32, 33]	PDE5 inhibition decreased intrahepatic resistance and increased hepatic parenchymal and hepatic arterial flow	Not approved to treat portal hypertension except in limited number of Asian countries
Obeticholic acid	[73, 74]	Farnesoid X receptor agonist leading to increased eNOS, thus NO	Novel therapy; no data available

portal flow, further leading to improved liver function and decreased sinusoidal resistance. Several studies have shown the long-term effect of nonselective beta-blockers on survival but not LS. Recently, Piecha et al. presented first animal data in a rat model of cirrhosis on LS [34], and first data were published in abstract form recently on SS in similar models [35].

## Monitoring of Portal Pressure-Lowering Drugs Using LS and SS

In 2018, Piecha et al. studied the effect of acute hemodynamic changes on LS (measured by  $\mu$ Fibroscan) in a rodent model of cirrhosis in response to pharmacological modulation of portal pressure (PP) by losartan, nitric oxide donors, and propranolol

[34]. After losartan or NO injection, the LS decreased by 25% which was strongly correlated with a concomitant decrease of the mean arterial pressure and portal pressure (PP). In contrary, acute injection of propranolol decreased heart rate but not MAP leading to no significant change in LS. In addition, they investigated the changes of LS and the hepatic venous pressure gradient (HVPG) in patients under propranolol therapy in terms of clinical outcome. The study included 38 cirrhotic patients. Of note, LS decreased in 66% of patients after propranolol initiation which was significantly correlated to HVPG ( $r = 0.518$ ,  $P < 0.01$ ). However, this decrease was not associated with statistically significant changes in transaminases or model of end-stage liver disease (MELD). Also, the multivariate analysis showed that patients with decreasing LS on propranolol showed a decreased risk for liver transplantation or death than those with increasing LS irrespective of the degree of HVPG. Finally, Piecha et al. concluded that LS is influenced by the hemodynamic effects on arterial and portal pressure after pharmacological intervention with propranolol. In addition, the decrease in LS after propranolol therapy may predict better outcome irrespective of MELD score and may serve as a tool to noninvasively monitor the response to portal pressure lowering drugs.

Recently, Elshaarawy et al. investigated five different PH-lowering drugs (metoprolol, udenafil, enalapril, carvedilol, and terlipressin) in TAA-induced cirrhosis rats [35]. The response to these drugs was monitored non-invasively by LS and SS using  $\mu$ Fibroscan and correlated to the portal and arterial pressures which were measured invasively using the PowerLab device [35]. LS and SS were significantly higher in TAA-treated rats than in the control group (23.8 vs. 3.8 kPa and 47.8 vs. 19.6 kPa,  $P < 0.0001$ ). In addition, they had significantly bigger and heavier spleens (6 vs. 4 cm and 2.7 vs. 1 g,  $P < 0.0001$ , respectively). Overall, LS and SS followed tightly the change of the portal vein pressure ( $r = 0.681$  and  $0.622$ ,  $P < 0.01$ , respectively). Also, SS was significantly correlated with spleen size and weight ( $r = 0.723$  and  $0.663$ , respectively,  $< 0.01$ ). Noteworthy, a significant decrease of portal vein pressure (PVP) ranging from 22 to 34% ( $P < 0.05$ ) was seen after 15–30 min with metoprolol, udenafil, enalapril, and carvedilol which was accompanied with a significant decrease in LS and SS ranging from 18.2 to 44% ( $P < 0.05$ ).

Overall, carvedilol showed the best response regarding the decrease of PVP, LS, and SS. Of note, the heart rate increased after metoprolol and udenafil injection ( $\sim 10\%$ ,  $P < 0.05$ ), while it decreased in response to terlipressin and carvedilol by  $\sim 30\%$  ( $P < 0.01$ ). In conclusion, all drugs showed significant decrease of portal pressure. Surprisingly, LS and SS significantly decreased in all drug groups except terlipressin. This could be explained in light of the hepatic arterial buffer response (HABR) [36]. Physiologically, the healthy liver is supplied with blood by about 80% via the portal vein [37]. The physiological basis for the HABR is the so-called adenosine washout hypothesis [38]. Adenosine has a direct vasodilator effect on the hepatic artery but not on the portal vein. It is secreted constantly into the space of Mall (periportal space) as a product of continuous metabolic processes and “washed out” into the portal vein. A decrease in portal flow causes adenosine accumulation which opens the hepatic artery for increased arterial blood supply [37]. HABR is thought to compensate the decrease in the portal blood flow [38, 39] and only func-

tions unidirectionally [40]. Consequently, HABR could be responsible for the observations of LS and SS response to terlipressin.

In 2017, McDonald et al. conducted a randomized parallel study to monitor the hemodynamic response to NSBB (propranolol or carvedilol) in 22 patients using phase-contrast MR angiography (PC-MRA) in selected intra-abdominal vessels data at baseline and after 4 weeks of treatment [41]. They reported a substantial reduction in mean average flow in the superior abdominal aorta after 4 weeks of NSBB therapy (versus L/min). However, they reported non-statistically significant differences in flow in any other vessels, even in patients with >25% decrease in heart rate which accounted 47% of patients. Of note, the mean percentage change in liver and spleen T1 following NSBB was minimal and highly variable. Finally, they concluded that PC-MRA was able to detect reduction in cardiac output by NSBB but did not detect significant changes in visceral blood flow or T1.

Recently, Kim et al. proposed a statistical model based only on the change in SS as a predictive model for the response carvedilol [42]. They measured SS by point shear wave elastography (pSWE, Virtual Touch, Siemens, Germany) in 106 patients with cirrhosis and high-risk esophageal varices, both before and after administration of NSBB. They also assessed the hemodynamic response to carvedilol by measuring the HVPG at the same time-points.  $\Delta SSM$  ( $\Delta SSM = SSM2 - SSM1$ ) significantly predicted the HVPG response (OR 0.039;  $P < 0.0001$ ) to carvedilol. The response to treatment could be predicted with an AUROC of 0.803. Noteworthy, internal validation showed good and reliable discriminative performance (AUROC 0.848).

## Conclusion

In conclusion, LS and SS show great promise for the non-invasive diagnosis, management, and prognostic evaluation of portal hypertension, namely the response to treatment.

## References

1. Groszmann RJ, Garcia-Tsao G, Bosch J, Grace ND, Burroughs AK, Planas R, et al. Beta-blockers to prevent gastroesophageal varices in patients with cirrhosis. *N Engl J Med.* 2005;353(21):2254–61.
2. Ripoll C, Groszmann R, Garcia-Tsao G, Grace N, Burroughs A, Planas R, et al. Hepatic venous pressure gradient predicts clinical decompensation in patients with compensated cirrhosis. *Gastroenterology.* 2007;133(2):481–8.
3. de Franchis R. Revising consensus in portal hypertension: report of the Baveno V consensus workshop on methodology of diagnosis and therapy in portal hypertension. *J Hepatol.* 2010;53(4):762–8.

4. de Franchis R. Expanding consensus in portal hypertension: report of the Baveno VI Consensus Workshop: stratifying risk and individualizing care for portal hypertension. *J Hepatol.* 2015;63(3):743–52.
5. Augustin S, Pons M, Maurice JB, Bureau C, Stefanescu H, Ney M, et al. Expanding the Baveno VI criteria for the screening of varices in patients with compensated advanced chronic liver disease. *Hepatology.* 2017;66(6):1980–8.
6. Pritchett S, Cardenas A, Manning D, Curry M, Afdhal NH. The optimal cut-off for predicting large oesophageal varices using transient elastography is disease specific. *J Viral Hepat.* 2011;18(4):e75–80.
7. Bureau C, Metivier S, Peron JM, Selves J, Robic MA, Gourraud PA, et al. Transient elastography accurately predicts presence of significant portal hypertension in patients with chronic liver disease. *Aliment Pharmacol Ther.* 2008;27(12):1261–8.
8. Sporea I, Ratiu I, Sirlu R, Popescu A, Bota S. Value of transient elastography for the prediction of variceal bleeding. *World J Gastroenterol.* 2011;17(17):2206–10.
9. Colecchia A, Montrone L, Scaioli E, Bacchi-Reggiani ML, Colli A, Casazza G, et al. Measurement of spleen stiffness to evaluate portal hypertension and the presence of esophageal varices in patients with HCV-related cirrhosis. *Gastroenterology.* 2012;143(3):646–54.
10. Abralde JG, Reverter E, Berzigotti A. Spleen stiffness: toward a noninvasive portal sphygmomanometer? *Hepatology.* 2013;57(3):1278–80.
11. Abralde JG, Bureau C, Stefanescu H, Augustin S, Ney M, Blasco H, et al. Noninvasive tools and risk of clinically significant portal hypertension and varices in compensated cirrhosis: the “Anticipate” study. *Hepatology.* 2016;64(6):2173–84.
12. Kim HY, Jin EH, Kim W, Lee JY, Woo H, Oh S, et al. The role of spleen stiffness in determining the severity and bleeding risk of esophageal varices in cirrhotic patients. *Medicine (Baltimore).* 2015;94(24):e1031.
13. Takuma Y, Nouse K, Morimoto Y, Tomokuni J, Sahara A, Takabatake H, et al. Prediction of oesophageal variceal bleeding by measuring spleen stiffness in patients with liver cirrhosis. *Gut.* 2016;65(2):354.
14. Sharma P, Kirmake V, Tyagi P, Bansal N, Singla V, Kumar A, et al. Spleen stiffness in patients with cirrhosis in predicting esophageal varices. *Am J Gastroenterol.* 2013;108(7):1101–7.
15. Stefanescu H, Grigorescu M, Lupșor M, Procopet B, Maniu A, Badea R. Spleen stiffness measurement using Fibroscan for the noninvasive assessment of esophageal varices in liver cirrhosis patients. *J Gastroenterol Hepatol.* 2011;26(1):164–70.
16. Dagradi AE, Stempien SJ, Owens LK. Bleeding esophagogastric varices. An endoscopic study of 50 cases. *Arch Surg.* 1966;92(6):944–7.
17. Paquet KJ. Prophylactic endoscopic sclerosing treatment of the esophageal wall in varices—a prospective controlled randomized trial. *Endoscopy.* 1982;14(1):4–5.
18. Brick IB, Palmer ED. One thousand cases of portal cirrhosis of the liver. Implications of esophageal varices and their management. *Arch Intern Med.* 1964;113:501–11.
19. Reiberger T, Puspok A, Schoder M, Baumann-Durchschein F, Bucsecs T, Datz C, et al. Austrian consensus guidelines on the management and treatment of portal hypertension (Billroth III). *Wien Klin Wochenschr.* 2017;129(Suppl 3):135–58.
20. Fraquelli M, Giunta M, Pozzi R, Rigamonti C, Della Valle S, Massironi S, et al. Feasibility and reproducibility of spleen transient elastography and its role in combination with liver transient elastography for predicting the severity of chronic viral hepatitis. *J Viral Hepat.* 2013;21(2):90–8.
21. Stefanescu H, Procopet B. Noninvasive assessment of portal hypertension in cirrhosis: liver stiffness and beyond. *World J Gastroenterol.* 2014;20(45):16811–9.
22. Bolondi L, Zironi G, Gaiani S, Bassi SL, Benzi G, Barbara L. Caliber of splenic and hepatic arteries and spleen size in cirrhosis of different etiology. *Liver.* 1991;11(4):198–205.
23. Takuma Y, Nouse K, Morimoto Y, Tomokuni J, Sahara A, Takabatake H, et al. Portal hypertension in patients with liver cirrhosis: diagnostic accuracy of spleen stiffness. *Radiology.* 2016;279(2):609–19.

24. Elshaarawy O, Mueller J, Guha IN, Chalmers J, Harris R, Krag A, et al. Spleen stiffness to liver stiffness ratio significantly differs between ALD and HCV and predicts disease-specific complications. *JHEP Rep.* 2019;1(2):99–106.
25. Ge PS, Runyon BA. The changing role of beta-blocker therapy in patients with cirrhosis. *J Hepatol.* 2014;60(3):643–53.
26. Li T, Ke W, Sun P, Chen X, Belgaumkar A, Huang Y, et al. Carvedilol for portal hypertension in cirrhosis: systematic review with meta-analysis. *BMJ Open.* 2016;6(5):e010902.
27. Mandorfer M, Reiberger T. Beta blockers and cirrhosis, 2016. *Dig Liver Dis.* 2017;49(1):3–10.
28. Schwabl P, Laleman W. Novel treatment options for portal hypertension. *Gastroenterol Rep (Oxf).* 2017;5(2):90–103.
29. Abraldes JG, Tarantino I, Turnes J, Garcia-Pagan JC, Rodes J, Bosch J. Hemodynamic response to pharmacological treatment of portal hypertension and long-term prognosis of cirrhosis. *Hepatology.* 2003;37(4):902–8.
30. D'Amico G, Garcia-Pagan JC, Luca A, Bosch J. Hepatic vein pressure gradient reduction and prevention of variceal bleeding in cirrhosis: a systematic review. *Gastroenterology.* 2006;131(5):1611–24.
31. Reiberger T, Ferlitsch A, Payer BA, Pinter M, Homoncik M, Peck-Radosavljevic M, et al. Non-selective beta-blockers improve the correlation of liver stiffness and portal pressure in advanced cirrhosis. *J Gastroenterol.* 2012;47(5):561–8.
32. Choi SM, Shin JH, Kim JM, Lee CH, Kang KK, Ahn BO, et al. Effect of udenafil on portal venous pressure and hepatic fibrosis in rats. A novel therapeutic option for portal hypertension. *Arzneimittelforschung.* 2009;59(12):641–6.
33. Kreisel W, Deibert P, Kupcinskas L, Sumskiene J, Appenrodt B, Roth S, et al. The phosphodiesterase-5-inhibitor udenafil lowers portal pressure in compensated preascitic liver cirrhosis. A dose-finding phase-II-study. *Dig Liver Dis.* 2015;47(2):144–50.
34. Piecha F, Mandorfer M, Peccerella T, Ozga AK, Poth T, Vonbank A, et al. Pharmacological decrease of liver stiffness is pressure-related and predicts long-term clinical outcome. *Am J Physiol Gastrointest Liver Physiol.* 2018;315(4):G484–G94.
35. Elshaarawy O, Alquzi S, Mueller J, Rausch V, Silva I, Peccerella T, et al. Response of liver and spleen stiffness to portal pressure lowering drugs in a rat model of cirrhosis. *J Hepatol.* 2019;70:E14–E5.
36. El-Shabrawi MH, Mohsen NA, Sherif MM, El-Karaksy HM, Abou-Yosef H, El-Sayed HM, et al. Noninvasive assessment of hepatic fibrosis and necroinflammatory activity in Egyptian children with chronic hepatitis C virus infection using FibroTest and ActiTest. *Eur J Gastroenterol Hepatol.* 2010;22:946.
37. Lauth WW. Hepatic circulation: physiology and pathophysiology. *Colloquium series on integrated systems physiology: from molecule to function to disease.* San Rafael; 2009.
38. Lauth WW. Mechanism and role of intrinsic regulation of hepatic arterial blood flow: hepatic arterial buffer response. *Am J Physiol.* 1985;249(5 Pt 1):G549–56.
39. Eipel C, Abshagen K, Vollmar B. Regulation of hepatic blood flow: the hepatic arterial buffer response revisited. *World J Gastroenterol.* 2010;16(48):6046–57.
40. Jakab F, Rath S, Schmal F, Nagy P, Faller J. The interaction between hepatic arterial and portal venous-blood flows—simultaneous measurement by transit-time ultrasonic volume flowmetry. *Hepatogastroenterology.* 1995;42(1):18–21.
41. McDonald N, Lilburn DML, Lachlan NJ, Macnaught G, Patel D, Jayaswal ANA, et al. Assessment of haemodynamic response to nonselective beta-blockers in portal hypertension by phase-contrast magnetic resonance angiography. *J BioMed Res Int.* 2017;2017:8.
42. Kim HY, So YH, Kim W, Ahn DW, Jung YJ, Woo H, et al. Non-invasive response prediction in prophylactic carvedilol therapy for cirrhotic patients with esophageal varices. *J Hepatol.* 2019;70(3):412–22.
43. Fraquelli M, Rigamonti C, Colombo M. Spleen stiffness measured by transient elastography accurately predicts esophageal varices in liver cirrhosis. *Gastroenterology.* 2012;143(4):e23; author reply e23–4.

44. Calvaruso V, Bronte F, Conte E, Simone F, Craxi A, Di Marco V. Modified spleen stiffness measurement by transient elastography is associated with presence of large oesophageal varices in patients with compensated hepatitis C virus cirrhosis. *J Viral Hepat.* 2013;20(12):867–74.
45. Shin SU, Lee J-M, Yu MH, Yoon JH, Han JK, Choi B-I, et al. Prediction of esophageal varices in patients with cirrhosis: usefulness of three-dimensional MR elastography with echo-planar imaging technique. *Radiology.* 2014;272(1):143–53.
46. Elkrif L, Rautou PE, Ronot M, Lambert S, Dioguardi Burgio M, Francoz C, et al. Prospective comparison of spleen and liver stiffness by using shear-wave and transient elastography for detection of portal hypertension in cirrhosis. *Radiology.* 2015;275(2):589–98.
47. Butzow GH, Remmecke J, Brauer A. Metoprolol in portal hypertension. A controlled study. *Klin Wochenschr.* 1982;60(20):1311–4.
48. Lazebnik LB, Mikheeva OM, Toporkov AS, Komissarenko IA, Vasnev OS, Fedulenkova LV. [Correction of portal hypertension by beta-adrenoblockers (atenolol and metoprolol) and inhibitors of ACE (lisinopril and enalapril) in liver cirrhosis]. *Eksp Klin Gastroenterol.* 2007;(5):57–66.
49. Uribe M, Orozco H, Moran S, Guevara L, Poo JL, Vargas-Vorackova F. Portal-systemic encephalopathy and gastrointestinal bleeding after cardioselective beta-blocker (metoprolol) administration to patients with portal hypertension. *Arch Med Res.* 1995;26(3):221–6.
50. Brito-Azevedo A, Perez Rde M, Coelho HS, Fernandes Ede S, Castiglione RC, Villela-Nogueira CA, et al. Propranolol improves endothelial dysfunction in advanced cirrhosis: the ‘endothelial exhaustion’ hypothesis. *Gut.* 2016;65(8):1391–2.
51. Lebrech D, Corbic M, Nouel O, Benhamou JP. Propranolol—a medical treatment for portal hypertension? *Lancet.* 1980;2(8187):180–2.
52. Perez-Paramo M, Munoz J, Albillos A, Freile I, Portero F, Santos M, et al. Effect of propranolol on the factors promoting bacterial translocation in cirrhotic rats with ascites. *Hepatology.* 2000;31(1):43–8.
53. Araujo Junior RF, Garcia VB, Leitao RF, Brito GA, Miguel Ede C, Guedes PM, et al. Carvedilol improves inflammatory response, oxidative stress and fibrosis in the alcohol-induced liver injury in rats by regulating Kupffer cells and hepatic stellate cells. *PLoS One.* 2016;11(2):e0148868.
54. Forrest EH, Bouchier IA, Hayes PC. Acute haemodynamic changes after oral carvedilol, a vasodilating beta-blocker, in patients with cirrhosis. *J Hepatol.* 1996;25(6):909–15.
55. Reiberger T, Ulbrich G, Ferlitsch A, Payer BA, Schwabl P, Pinter M, et al. Carvedilol for primary prophylaxis of variceal bleeding in cirrhotic patients with haemodynamic non-response to propranolol. *Gut.* 2013;62(11):1634–41.
56. Sinha R, Lockman KA, Mallawaarachchi N, Robertson M, Plevris JN, Hayes PC. Carvedilol use is associated with improved survival in patients with liver cirrhosis and ascites. *J Hepatol.* 2017;67(1):40–6.
57. Tripathi D, Therapondos G, Lui HF, Stanley AJ, Hayes PC. Haemodynamic effects of acute and chronic administration of low-dose carvedilol, a vasodilating beta-blocker, in patients with cirrhosis and portal hypertension. *Aliment Pharmacol Ther.* 2002;16(3):373–80.
58. Villanueva C, Aracil C, Colomo A, Hernandez-Gea V, Lopez-Balaguer JM, Alvarez-Urturi C, et al. Acute hemodynamic response to beta-blockers and prediction of long-term outcome in primary prophylaxis of variceal bleeding. *Gastroenterology.* 2009;137(1):119–28.
59. Gonzalez A, Augustin S, Perez M, Dot J, Saperas E, Tomasello A, et al. Hemodynamic response-guided therapy for prevention of variceal rebleeding: an uncontrolled pilot study. *Hepatology.* 2006;44(4):806–12.
60. Blei AT, Ganger D, Fung HL, Groszmann R. Organic nitrates in portal hypertension. *Eur Heart J.* 1988;9(Suppl A):205–11.
61. Merkel C. Nonselective beta-blockers plus nitrates in portal hypertension: an open question. *Hepatology.* 2003;37(6):1254–6.
62. Premaratna R, Sathishchandra H, Thilakarathna Y, Shantharaj W, de Silva H. Effects of propranolol and nitrates on exercise capacity, respiratory minute volume and capillary oxy-

- gen saturation during exercise in cirrhotic patients with portal hypertension. *Hepato Res.* 2002;24(2):152.
63. Escorsell A, Bandi JC, Moitinho E, Feu F, Garcia-Pagan JC, Bosch J, et al. Time profile of the haemodynamic effects of terlipressin in portal hypertension. *J Hepatol.* 1997;26(3):621–7.
  64. Ioannou GN, Doust J, Rockey DC. Terlipressin for acute esophageal variceal hemorrhage. *Cochrane Database Syst Rev.* 2003;(1):CD002147.
  65. Møller S, Hansen EF, Becker U, Brinch K, Henriksen JH, Bendtsen F. Central and systemic haemodynamic effects of terlipressin in portal hypertensive patients. *Liver.* 2001;20(1):51–9.
  66. Gao JH, Wen SL, Feng S, Yang WJ, Lu YY, Tong H, et al. Celecoxib and octreotide synergistically ameliorate portal hypertension via inhibition of angiogenesis in cirrhotic rats. *Angiogenesis.* 2016;19(4):501–11.
  67. Huang YT, Tsai JF, Liu TB, Hong CY, Yang MC, Lin HC. Chronic administration of octreotide increases vascular responsiveness in rats with portal hypertension. *Clin Sci (Lond).* 1996;91(5):601–6.
  68. Malesci A, Tacconi M, Valentini A, Basilico M, Lorenzano E, Salerno F. Octreotide long-term treatment in patients with portal hypertension: persistent inhibition of postprandial glucagon response without major changes in renal function. *J Hepatol.* 1997;26(4):816–25.
  69. Silvain C, Besson I, Beauchant M. [Somatostatin, octreotide and portal hypertension]. *Gastroenterol Clin Biol.* 1994;18(8–9):761–6.
  70. Croquet V, Moal F, Veal N, Oberti F, Chappard D, Cales P. Hemodynamic and antifibrotic effects of losartan in rats with liver fibrosis and/or portal hypertension. *J Hepatol.* 2002;37:773–80.
  71. Heller J, Shiozawa T, Trebicka J, Hennenberg M, Schepke M, Neef M, et al. Acute haemodynamic effects of losartan in anaesthetized cirrhotic rats. *Eur J Clin Invest.* 2003;33(11):1006–12.
  72. Svoboda P, Ochmann J, Kantorova I, Sefr R. [The ACE inhibitor, enalapril, in portal hypertension. A prospective placebo controlled study]. *Cas Lek Cesk.* 1992;131(6):170–3.
  73. Verbeke L, Farre R, Trebicka J, Komuta M, Roskams T, Klein S, et al. Obeticholic acid, a farnesoid X receptor agonist, improves portal hypertension by two distinct pathways in cirrhotic rats. *Hepatology.* 2014;59(6):2286–98.
  74. Xu W, Lu C, Zhang F, Shao J, Yao S, Zheng S. Dihydroartemisinin counteracts fibrotic portal hypertension via farnesoid X receptor-dependent inhibition of hepatic stellate cell contraction. *FEBS J.* 2017;284(1):114–33.



# Chapter 53

## Clinical Cases: Application and Interpretation of Liver Stiffness



Sebastian Mueller

### Introduction

In general, LSM has become essential for the screening and follow-up of patients with liver diseases. In addition, LS has proven quite useful in daily clinical decision making of patients suffering from internal medicine diseases. At the moment, prices are too high but LSM will certainly prove to be useful in the GP setting. This chapter presents a collection of clinical cases to visualize the application of LS, its interpretation and potentials. Below is a list of the cases for easier overview. Table 53.1 shows typical laboratory and ultrasound parameters used within this chapter as well as their normal range and abbreviations.

- Case 1: Exclusion of cirrhosis
- Case 2: Chronic HCV infection with successful treatment
- Case 3: ALD detox
- Case 4: Jaundice-patients with alcoholic acute-on-chronic liver disease
- Case 5: Jaundice due to autoimmune hemolytic anemia
- Case 6: Jaundice due to mechanic cholestasis
- Case 7: Jaundice due to Zieve syndrome
- Case 8: NAFLD with progression
- Case 9: NAFLD with no progression
- Case 10: NAFLD M versus XL probe
- Case 11: Acute hepatitis A infection
- Case 12: Acute EBV infection
- Case 13: Non-hepatic ascites with ovarian cancer
- Case 14: Liver congestion

---

S. Mueller (✉)

Department of Medicine and Center for Alcohol Research and Liver Diseases, Salem Medical Center, University of Heidelberg, Heidelberg, Germany  
e-mail: [sebastian.mueller@urz.uni-heidelberg.de](mailto:sebastian.mueller@urz.uni-heidelberg.de)



**Table 53.1** Laboratory and ultrasound parameters with normal range and abbreviations

Parameter/units	Normal value	Abbreviations
Erythrocytes (/pl) <sup>a</sup>	4.5–5.9/4.1–5.1	Ery
Hemoglobin (g/dL) <sup>a</sup>	13.5–17.5/12.0–16.0	Hb
MCV (fl)	80–96	MCV
Leucocytes (/nL)	3.7–10.0	Leuco
Platelets (10 <sup>9</sup> /L)	150–360	plt
AST (U/L)	<50	AST
ALT (U/L)	<50	ALT
GGT (U/L)	<60	GGT
AP (U/L)	40–130	AP
Bilirubin total (mg/dL)	<1.3	Bili
Bilirubin indirect (mg/dL)	<1.0	
Quick	70–120	Quick
INR	1	INR
Creatinine (mg/dL)	<1.3	Crea
Ferritin (ng/ml) <sup>a</sup>	30–400/13–150	Ferritin
LDH (U/L)	<250	LDH
CRP (mg/dL)	<5	CRP
Liver size (cm) <sup>b</sup>	<17	
Liver stiffness (kPa)	<6	LS
CAP (dB/m)	<250	CAP
Spleen size (cm)	<11.5	

<sup>a</sup>Only for some parameters male/gender normal values are given

<sup>b</sup>Measured from top to bottom at the mean axillar line and parallel to it

Case 15: Liver metastasis

Case 16: HCC

Case 17: Hepatic amyloidosis

Case 18: Patient with hereditary spherocytosis

Case 19: Initial diagnosis of Wilson's disease

Case 20: Budd–Chiari Syndrome

Case 21: Chronic HCV and response to DAAs

### Case 1: Exclusion of Cirrhosis

44-year-old male patient presents with pressure pain by palpation in the right upper quadrant and jaundice. He is known to have multiple sclerosis for 10 years. He is lean and has slightly reduced general condition, the pulse was 96 beats/min.

**Ultrasound:** Liver inhomogeneous, otherwise normal, spleen drastically enlarged 16.5 cm, US otherwise normal, LSM  $6.1 \pm 1.3$  kPa

**Laboratory:** Hb 7.7, MCV 89, Reticulocytes 96, AST 60, ALT 90, AP and GGT normal, **Bilirubin** 6.5 mg/dL, Direct bilirubin 0.8, Haptoglobin <0.08.

Viral serology was negative

**Results and lessons learnt:**

Autoimmune hemolytic anemia with warm autoantibodies was eventually diagnosed.

This is an example that an early LSM in an icteric patient can rule out a hepatic cause. In this case, severe hemolytic anemia occurred and LS was almost normal. According to book Part “IV Important (patho)physiological confounders of LS,” chapter “cholestasis,” a mechanic cholestasis increases LS about 1 kPa per 1 mg/dL elevated bilirubin. A bilirubin of 6.5 mg/dL would lead up to total stiffness = normal stiffness (4 kPa) + bilirubin\*1 kPa = 10 kPa. The measured 6.1 kPa is clearly below this estimate and suggests a non-hepatic cause. Diagnosis in hemolytic patients can be further complicated since it can also lead to liver damage.

**Case 2: Patient with Chronic HCV Infection and Successful Treatment**

54-year-old male from Afghanistan, perioperative HCV (Genotype IB infection) 17 years ago.

**Laboratory and liver stiffness:**

2015: good condition, ALT 55 IU/L, LS 32 kPa

2016: increase of LS to 35 kPa, no varices, spleen size normal

2017: HCV clearance due to oral DAA treatment, 3 months later LS 18.9 kPa

2019: LS 17.3 kPa

**Conclusions:** The case shows that HCV elimination can drastically improve LS despite histological cirrhosis stage has been reached. LS should be followed up every 12 months, ultrasound every 6 months for HCC screening.

**Case 3: ALD Detoxification**

45-year-old female patients and known established cirrhosis (Child A stage) presenting for alcohol detoxification and planned operation for abdominal hernia.

**Ultrasound:** spleen size was 12 cm, no ascites, enlarged liver with 18 cm size, echogenic inhomogeneous, no clear signs of cirrhosis. The patient had alcoholic polyneuropathy.

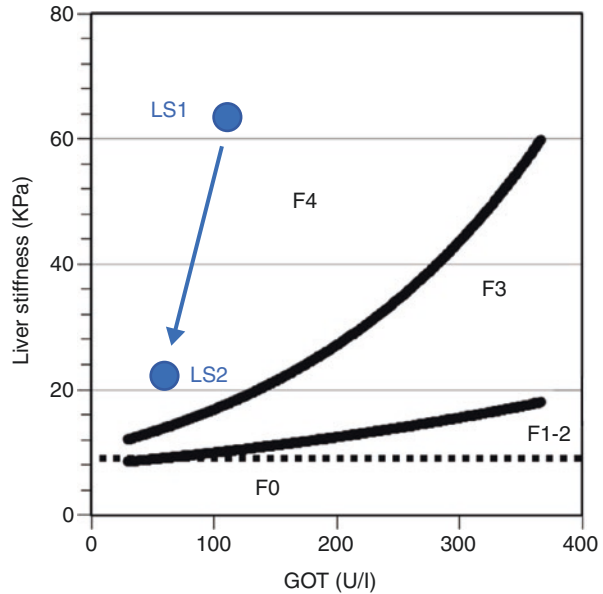
**Laboratory:** Bilirubin 1.8 mg/dL, AST 140 IU/L, ALT 36 IU/L, GGT 1107 IU/L, AP 135 IU/L, Alcohol 2.2 g/L, Quick 64%, Platelets 65 (109/L).

**Liver stiffness** was  $66.4 \pm 7.4$  kPa and AST was 98 IU/L at day of LSM, clearly indicating F4 cirrhosis as shown in Fig. 53.1 (see chapter “Fibrosis assessment in ALD” in book Part III “Liver stiffness and various etiologies of liver diseases”).

**Results and lessons:**

This patient was able to completely abstain from alcohol for 1 year. Ultrasound showed a much smaller liver (14 cm) without sure signs of cirrhosis. Now, LS had decreased to  $22 \pm 2.3$  kPa. Transaminases were normal except a GGT of 77 (see Fig. 53.1). This case underlines the drastic beneficial effect of abstinence in patients with manifest alcoholic cirrhosis. Since  $LS > 20$  kPa, this patient is at risk of developing HCC and variceal bleeding and should undergo diagnostic follow-up examinations. In some cases, continued abstinence can further decrease LS by 20–50%. Rare cases with complete LS normalization have been observed [1] (see also Fig. 52.2).

**Fig. 53.1** Change of LS/ fibrosis stage during alcohol detoxification. Although LS drastically improves, AST-adapted LS cutoff values still diagnose F4 cirrhosis. (GOT = AST)



#### Case 4: Patient with Jaundice and with Alcoholic Liver Cirrhosis and Acute-on-Chronic Liver Disease

51-year-old female patient presenting again for alcohol withdrawal after relapse

25 years of heavy drinking, obesity with a BMI of 34.6 kg/m<sup>2</sup> diabetes mellitus II for 10 years, otherwise, almost no symptoms at admission and no history of any chronic illness. Fully conscious and oriented with a tinge of jaundice

No detectable abnormalities in cardiac, respiratory, or nervous system examination

**Laboratory** Hb 11.8 g/L, MCV 110 fl, Erythrocytes 3.1/pL, Leucocytes/nL 6.1, Platelets 134, total bilirubin 5.9 mg/dL, AST 233 IU/L, ALT 91 IU/L, AP 410 IU/L, GGT 3359 IU/L, INR 0.84, Ferritin 2420 ng/mL.

All markers for HCV, HBV, and AIH were negative, B12 and folic acid were normal

**Ultrasound** Hepatomegaly 19 cm, Hepatic steatosis grade III, Splenomegaly 13.5 cm

No ascites

**Liver stiffness** 55.1 ± 21.6 kPa (XL), CAP 247 ± 37 dB/M

**Results and conclusions:** Liver biopsy showed severe steatohepatitis with concomitant hepatocellular siderosis. In addition to portal, peri-cellular, perisinusoidal, and septal fibrosis, findings are consistent with alcoholic hepatitis. Maddrey score was 16, and Glasgow AH score was 6. Taken together, the case was considered a beginning **acute-on-chronic liver disease**. Therapy consisted of thiamin substitution, alcohol detoxification with chlormethiazole using a tapering scheme. Serum bilirubin initially increased from 5.9 to 17.7 mg/dL in the first week while INR stayed within the normal range. LS increased to 75 kPa (see Fig. 53.2). Notably, this patient remained **abstinent** for almost 1 year. Figure 53.2 shows that LS further

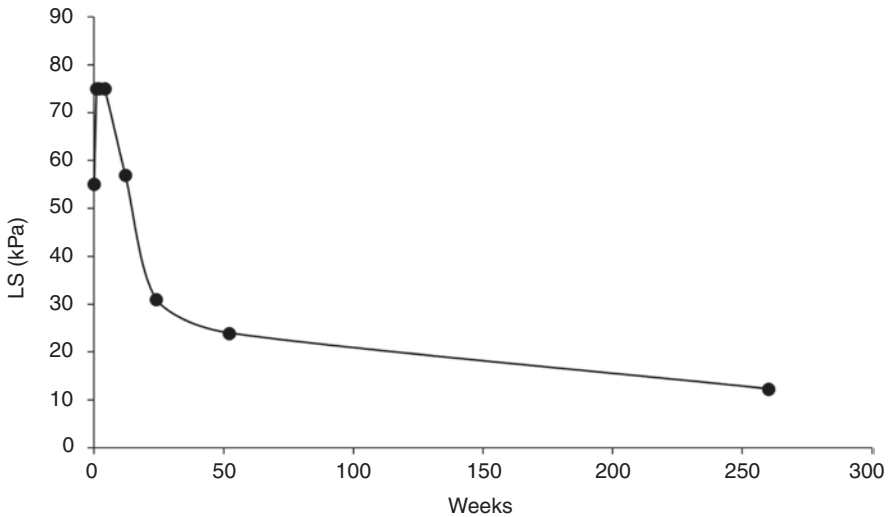


**Fig. 53.2** Development of LS of a patients with ALD and acute decompensation (jaundice) after 260 days of abstaining from alcohol. Note the continued improvement of LS

decreased during complete abstinence. Screening gastroscopy did not show any varices. This case underlines that LS can further resolve after elimination of the underlying cause of the liver disease. It remains to be determined whether this is partly due to fibrosis reversal or solely due to resolution of inflammation and ballooning since apoptotic markers further continued to fall.

#### **Case 5: Jaundice Caused by Autoimmune Hemolytic Anemia**

44-year-old male, asthenic, pulse 96/min, jaundice, abdominal pain in the right upper quadrant, multiple sclerosis since 1996

**Ultrasound:** Inhomogeneous ultrasound pattern in the liver, liver 16 cm in MAL, splenomegaly 16 cm, everything else was fine. Liver stiffness was  $6.1 \pm 0.5$  kPa

**Lab tests:** Hb 7.7 g/L, MCV normal, reticulocytes 96, AST 60, ALT 90 IU/L, AP and GGT normal, bilirubin 6.5 mg/dL, direct bilirubin 0.8 mg/dL, haptoglobin  $<0.08$ , viral serology were negative. Autoimmune hemolytic anemia (warm autoantibody type) was diagnosed.

**Conclusions:** Example of how a rapid LSM, done within 5 min and obtained before laboratory values, can support the suspicion of a pre-hepatic icterus. Although hemolysis itself can cause liver damage and elevated LS, in most cases LS is much lower as compared to comparable mechanic cholestasis.

#### **Case 6: Jaundice Due to Mechanic Cholestasis**

64-year-old male, referred from a psychiatrist with known schizophrenia and Parkinson's disease with increased transaminases and suspected acute hepatitis.

The patients had jaundice, poor nutritional state, otherwise good general condition. Abdominal examination revealed no tenderness, no pressure pain, normal bowel sounds, normal liver span, spleen was not palpable, and kidneys were not tender.

**Laboratory:** Bilirubin 6.7 mg/dL mostly direct bilirubin, AST 309 IU/L, ALT 432 IU/L, GGT 1006 IU/L, AP 677 IU/L, LDH 268 IU/L, erythrocytes 4.0/pL, Hb 12.3 g/L, leucocytes 10.5/nL, CRP 68 mg/dL, serum creatinine was normal

**Ultrasound:** pronounced meteorism, common bile duct not clearly visible

**Liver stiffness:** 11.8 kPa IQR 5.9 kPa success rate: 71%

**Results and conclusion:** Suspicion of choledocholithiasis with cholangitis and accompanying hepatitis. ERCP was done the next day with enlarged common bile duct 11 mm, sludge, multiple concretions. Papillotomy and removal of gallstones. This case underlines some general observations from the Chap. 25 “LS and Cholestasis” from book Part IV “Important (patho)physiological confounders of LS.” Accordingly, 1 mg/dL bilirubin elevation will cause an increase of LS by ca. 1 kPa leading to a cumulative LS = normal LS + bilirubin \* 1 kPa = 10 kPa.

### Case 7: Heavy Drinker with Zieve Syndrome

55-year-old patient with progressing jaundice, dizziness, vomiting, diarrhea, and fever till 39° for one day. Known heavy alcohol consumption.

**Laboratory:** Leucocytes 28/nL, Hb 7.9 g/L, MCV 102 fl, platelets  $78 \times 10^9/L$ , creatinine 4.1 mg/dL, Na 126 mEq/L, ALT 137 IU/L, **AST 872 IU/L**, GGT 185 IU/L, AP 138 IU/L, LDH 4850 IU/L, CK 221 U/L, **bilirubin 17.9 mg/dL**, TG 415 mg/dL

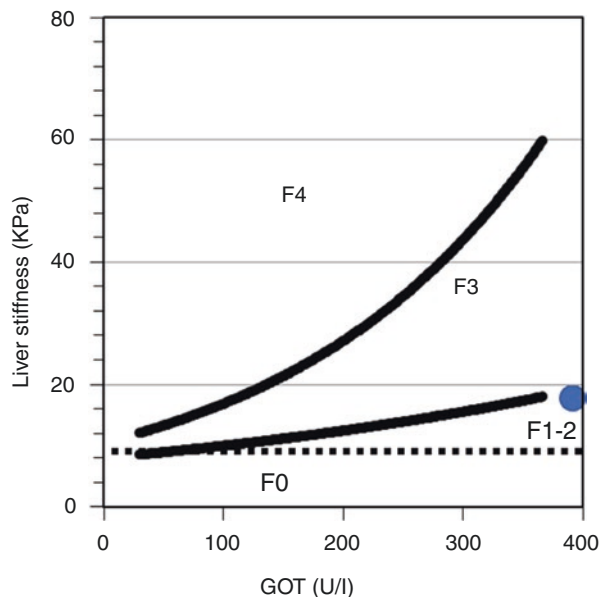
LS  $17.6 \pm 3.6$  kPa

**Ultrasound:** no ascites, spleen enlarged with 15 cm

Liver stiffness:  $17.6 \pm 3.4$  kPa

**Results and conclusions:** Patients rapidly improved after therapy with antibiotics, dialysis, i.v. supplementation with isotonic liquids. Diagnosis of Zieve syndrome was made (hemolysis, hypertriglyceridemia, icterus). A look at Fig. 53.3

**Fig. 53.3** Patients with LS of 17.6 kPa due to ALD and Zieve syndrome. Although LS was clearly higher as 12.5 kPa, it did not fulfill cirrhosis criteria according to the AST-adapted cutoff values. LS later normalized. (GOT = AST)



demonstrates that initial LSM did not fulfill criteria of cirrhosis although it was clearly higher as 12.5 kPa. After treatment, resolution of icterus, hemolysis, and transaminases, LS was in the normal range.

### Case 8: NAFLD

Two male patients (father and son) with 60 and 28 years presenting both with histologically confirmed NAFLD and NASH for the first time for liver stiffness measurements. Similar signs of liver inflammation with ALT 134 IU/L and AST 66 IU/L, no diabetes, no overweight, regular exercise.

**Ultrasound:** signs of fatty liver, no signs of cirrhosis in both patients

**Liver stiffness:** Father with  $22 \pm 3.4$  kPa and son with  $4.9 \pm 1$  kPa.

**Results and conclusions:** This is an example of non-insulin resistance-related NAFLD (<10% of NAFLD patients), perfect compliance with regard to nutrition, physical exercise and weight control but unfortunately an unfavorable genetic background. While LSM clearly establishes compensated liver cirrhosis in the father, any even early liver fibrosis could be ruled out in the 32 years younger son despite ongoing significant NASH. Both should undergo follow-up LSM every 12 months and laboratory testing once or twice a year and continue dietary and exercise measures. In addition, the father should undergo gastroscopy to rule out esophageal varices and HCC screening every 6 months. In this situation, LSM detects manifest cirrhosis and is crucial in controlling complications and progression of the disease.

### Case 9: NAFLD

61-year-old male patient with BMI 30, pronounced fatty liver in ultrasound, mother and grandmother also had fatty liver and obesity. External laboratory tests were OK except low platelets of 147 over 10 years. Occasional alcohol consumption.

**Ultrasound:** significantly increased echo density, local hypodensity around gall bladder, no ascites, no splenomegaly

**LS**  $6.7 \pm 0.8$  kPa

**Conclusion:** In this case, the patients suffered from an inherited thrombocytopenia and LSM helped to clearly rule out liver fibrosis which he was afraid of.

### Case 10: NAFLD

55-year-old female patient with known NAFLD for LS follow-up.

**Liver stiffness:** M probe revealed 10.4 kPa, XL probe 15.1 kPa (see elastograms in Fig. 53.4).

#### Conclusions:

The use of different probes with TE such as S for children and XL for obese patients has significantly improved measurability of these patient cohorts. However, care should be taken when applying different probes in a single patient. According to the Chap. 44 entitled “Use of XL probe in obese and non-obese patients” in book Part VII, XL probe can be directly applied to obese patients when BMI >30. If not sure, M probe should be first applied and XL only in case of measurement failure. In any case, patients should be followed up with the same probe. As can be nicely seen in Fig. 53.4, M probe shows higher LS values. This is due first to the shorter penetration depth in obese patients still measuring part of the compressed fat tissue/muscle tissue and calculation of LS from the lower conical rim of the shear wave.

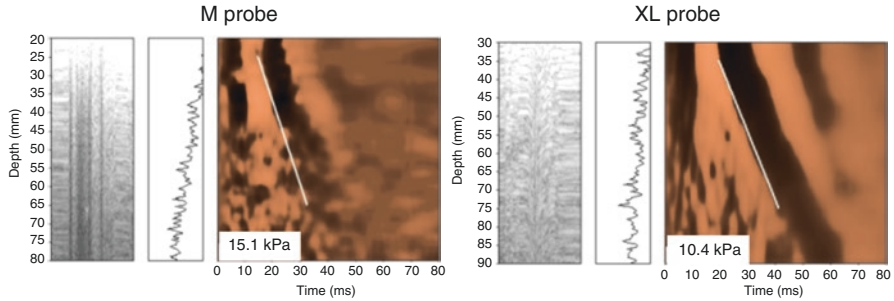


**Fig. 53.4** M and XL probe in same NAFLD patient. As shown in this representative example, XL probe typically yields 20% lower LS values

**Table 53.2** LS and transaminase levels in a patient with acute hepatitis A on days 1 and 5 of admission

Parameter/units	Day 1	Day 5
AST (U/L)	5577	1203
ALT (U/L)	2829	335
Liver stiffness (kPa)	26.3	13.9

As a rule of thumb, cutoff values for the XL probe are 20% lower as the M probe. As discussed in book Part VII, there are still ongoing controversies about whether this algorithm always applies.

**Case 11: Acute Hepatitis A Infection**

22-year-old male was transferred to the hospital with fatigue and suspicion of acute hepatitis A (see laboratory in Table 53.2). Enlarged spleen (13 cm) in the otherwise normal abdominal ultrasound. Acute hepatitis A was later established serologically. LSM was drastically elevated. Both transaminase levels and LS rapidly decreased within a few days (see Table 53.2).

**Results and conclusions:**

Acute hepatitis can cause LS elevation up to 30 kPa in the absence of fibrosis. Typical viral causes are HAV or EBV infection. If patients are at potential risk of spleen rupture, they can be followed up in the hospital till LS decreases and spleen size or SS does not increase further.

**Case 12: Acute EBV Infection**

25-year-old male with fever, left side pain, collapse, 64 kg, 177 cm, EBV quick test positive, later confirmed by serology

**Laboratory day 1:** AST 382 IU/L, ALT 299 IU/L, GGT 80 IU/L, AP 186 IU/L, LDH 1228 IU/L, CRP 8.2 mg/dL, Ferritin 2270 ng/mL

**Ultrasound day 1:** Liver size 17.5 cm, Spleen size 18 cm, LS 6.6 ± 1.1 kPa

**Laboratory day 5:** improvement with AST 96 IU/L, ALT 197 IU/L, LDH 778 IU/L

**Ultrasound day 5:** Liver size 17.5 cm, Spleen size 17 cm, LS 4.0 ± 0.5 kPa

**Conclusions:**

Hepatotropic viruses such as EBV can cause acute hepatitis, in some cases liver failure and spleen rupture. Since these are often young patients with discomfort,

noninvasive screening and follow-up is helpful. In this case, spleen size reduced on day 5 and LS had completely normalized. Patient was followed up by the GP.

### **Case 13 Non-hepatic Ascites with Ovarian Cancer**

70-year-old female presents with massive ascites, dyspnea, and edema of lower extremities.

Gastroscopy, colonoscopy, and gynecological exploration were normal. Echocardiography was normal.

**Laboratory:** Platelets  $381 \times 10^9/L$ , Hb 11.9 g/dL, serum protein 6.4 g/dL, CRP 54 mg/dL, Ferritin 180 ng/mL, all other liver values were normal

**Ultrasound:** Pronounced ascites, liver was 15 cm large, appeared normal, spleen was normal with 9.1 cm.

**Liver stiffness:** completely normal with  $4.9 \pm 0.5$  kPa

#### **Results and conclusions:**

This is an example of a patient with obviously non-hepatic ascites that is found in large cohorts in ca. 20% of all cases. As discussed in book Part VII How to use LS in clinical practice, Chap. 43 “LS and hepatic vs. non-hepatic ascites,” LS can be well determined using TE up to ascites lamella of 39 mm. A LS by 8 kPa clearly rules out hepatic causes of ascites. This is important to know since a rapid exclusion of a hepatic cause of ascites by LSM can avoid frustrated alternative diagnostic measures and loss of time. In this case, computer tomography was done and revealed peritoneal carcinomatosis and an ovarian cancer could be established. Both CA 125 and 19-9 were elevated. Cytology revealed adenocarcinoma.

### **Case 14: Liver Congestion**

79-year-old male patients with reduced general conditions and severe obesity. Known right heart failure with NYHA II-III and dyspnea on effort. Edema of lower extremities. Wet rattle noise in both lungs. Abdomen soft but examination limited.

**Echocardiography:** enlarged atria, left ventricular hypertrophy, contractility normal of left and right ventricle, systolic pulmonary arterial pressure with ca. 100 mmHg drastically increased, inferior vena cava was congested. Lung function with restrictions but no obstruction.

**Ultrasound:** Signs of liver congestion with enlarged inferior caval vein, nodular surface of the liver, inhomogeneous, gall bladder with multiple small gallstones.

**Laboratory:** normal except CRP 16 mg/dL and platelets  $136 \times 10^9/L$

**Liver stiffness:**  $22.1 \pm 5.6$  kPa

#### **Results and conclusions:**

Patients with right heart failure and decompensation. LS is increased due to liver congestion (see also Chap. 23 on “LS in patients with heart failure and liver congestions in Part “IV Important (patho)physiological confounders of LS”). The nodular aspects in US suggest cardiac cirrhosis and it is still difficult to discriminate elevated LS due to congestion or cirrhosis. Preliminary data indicate that GGT is a sign of manifest cardiac cirrhosis [1]. LS typically decreases rapidly after treatment with diuretics. Animal data have shown that a central venous pressure of 36 cm water column can cause LS elevation of 75 kPa, the detection limit of the Fibroscan device.



**Fig. 53.5** Multiple liver metastasis with high variability of LS between 26 kPa and 64 kPa



### Case 15: Liver Metastasis

60-year-old male patients after hernia operation, ascites, and suspicion of cirrhosis

**Ultrasound:** diffuse liver metastasis with some remaining areas of normal liver tissue (see Fig. 53.5). **Liver stiffness** varies drastically between 36 and 64 kPa with an IQR of 32 kPa.

**Conclusions:** Unusually high variation of LS (high IQR) are suspicious of nodular (malignant) liver masses. Such findings should trigger further imaging studies. See also the following case 16 with HCC.

### Case 16: Hepatocellular Carcinoma (HCC)

70-year-old male during routine check-up.

**Ultrasound:** Liver with normal size, no ascites, right liver lobe normal, left lobe from ventral with multiple nodule.

**Liver stiffness:** right liver lobe  $13.3 \pm 1$  kPa, left liver lobe  $75.0 \pm 5.2$  kPa

**Conclusions:** Later, CT confirms large 9 cm sized HCC in the left liver with liver cirrhosis. Sometimes, liver masses are not visible in ultrasound but may be first detected by an elevated LS with unusually high variability within different liver areas. There are some reports that have been tried to establish an increase of IQR as first sign of HCC or liver tumors which are typically very stiff [2, 3].

### Case 17: Hepatic Amyloidosis

72-year-old female patient with conditions after decompensated right heart failure, at time of admission no ascites and no liver congestion, known liver cysts. Gout, alcohol consumption, increase of serum creatine to 2.4 mg/dL.

**Liver stiffness:**  $32.2 \pm 6.3$  kPa

#### Conclusions:

Histology confirmed amyloidosis. Amyloidosis is a rare situation of LS elevation in the absence of cirrhosis or other confounders. This needs to be considered.

### Case 18: Patient with Hereditary Spherocytosis (Hereditary Hemolytic Anemia)

48-year-old female in good condition, autosomal recessive spherocytosis presenting with abdominal discomfort, upper endoscopy normal

**Laboratory:** Hb 12.1 g/dL, Ferritin 899 ng/mL, Monocytes 10.1%, MCV 89 fl. While serum AST, ALT, AP, and GGT were at normal levels, bilirubin was 1.3 mg/dL

**Liver iron measurement:** Liver iron 526  $\mu\text{g/g}$  liver wet weight (normal <300)

**Ultrasound:** Liver size was 22 cm while spleen was 18 cm

**Liver stiffness:**  $3.7 \pm 0.4$  kPa

**CAP:**  $276 \pm 39$  dB/m

**Spleen stiffness (SS):**  $48 \pm 12$  kPa

**Conclusion:** LS indicates no sustained liver affection by spherocytosis, phlebotomy recommended, elevated SS fits severe continued hemolysis, follow-up of LS in 12 months recommended.

### Case 19: Initial Diagnosis of Wilson's Disease

31-year-old male patients present with elevated transaminase levels, ALT > AST. Additionally, elevated ferritin, no improvement after 20 kg weight loss (now 1.95 m, 105 kg, BMI 27.6). Otherwise no symptoms.

**Laboratory:** AST 66 IU/L, ALT 158 IU/L, AP 77 IU/L, and GGT 106 IU/L while serum bilirubin level was 0.6 mg/dL. Also, Hb was 14.1 g/dL, ferritin was 660 ng/mL, and MCV was 78 fl

**Wilson's diagnosis:** Ceruloplasmin <0.01 (0.2–0.6), serum copper <100 (700–1400), urine copper **137** (10–80)

**Ultrasound:** Liver 19 cm, splenomegaly with spleen size 18 cm

**Liver stiffness:**  $39.0 \pm 1.1$  kPa

**CAP:**  $316 \pm 33$  dB/m

**Results and conclusions:** Liver biopsy was performed showing unspecific signs of NAFLD but elevated **liver copper levels with 416.9  $\mu\text{g/g}$  dry weight** (normal 0–50). Mutations c.2071G>A and c2720A>G in the ATP7B gene were detected. Brain MRI did not show any copper accumulation nor were other Wilson's disease related pathologies observed. Wilson's disease was diagnosed and treatment with Metalcaptase (Penicillamine) up to 1200 mg daily initiated. ALT decreased for the first time from 188 to 153, and after 6 months to 97. Ferritin fell to 278. Liver stiffness eventually decreased after 1 year down to 6.1 kPa. To date, the patient tolerates the therapy well and transaminase levels have become normal. This case illustrates that an elevated LS seems to be a quite early sign in patients with copper accumulation despite the otherwise inconclusive and unspecific tests. Thus, an elevated LS should trigger further diagnosis which should respond to treatment interventions accordingly. In this case, it almost took 1 year after weight loss and dietary measures that copper chelation treatment proved to be effective confirming the diagnosis. For more details, Chap. 20 on Wilson's disease is recommended.

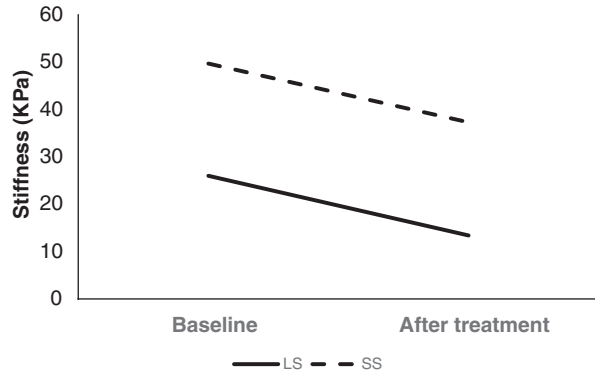
### Case 20: A Case of Budd–Chiari Syndrome (BCS)

A 34-year-old lady was diagnosed with Budd–Chiari syndrome with complete obstruction of the left hepatic vein as well as stenosis in the right hepatic vein. She had esophageal varices (grade II) and low platelet counts ( $98 \times 10^9/\text{L}$ ).

#### Results and conclusions:

She underwent percutaneous transluminal angioplasty (PTA) for the left hepatic vein. Liver stiffness decreased from 68.4 kPa before PTA to 14.8 kPa after 12 h and 9.4 kPa after 6 months with eradication of the esophageal varices and improvement of the platelet count ( $158 \times 10^9/\text{L}$ ) [4]. In addition, the serum level of hyaluronic acid decreased from 92 ng/mL before PTA to <8 ng/mL after 6 months. This is an example that rapid re-canalization of the obstructed vein in BCS is vital and LSM is an easy way to monitor immediate and sustained response. In this case, progression to cirrhosis could be prevented. See also Chap. 14 for more details on BCS.

**Fig. 53.6** Decline of LS and SS after treatment with DAAs for 3 months



### Case 21: A Case of Chronic HCV and DAAs

A 52-year-old man presented to us for assessment of hepatitis C. The physical examination revealed unremarkable findings for the presence of chronic liver disease, and virology investigations indicated hepatitis C infection. The laboratory investigations revealed the following: ALT = 79 IU/L, AST = 85 IU/L, albumin = 3.3 mg/dL, platelet count is  $139 \times 10^9/L$ , and an INR = 1.4. The abdominal ultrasound showed a diffusely fatty liver with normal size of 13 cm.

#### Results and conclusions

Liver stiffness was of 26 kPa with 100% success rate and CAP 335 db/m while spleen stiffness was 49.7 kPa. Screening upper endoscopy was ordered and revealed esophageal varices grade III where band ligation was done. Later, he was prescribed antiviral therapy for 3 months (sofosbuvir/ledipasvir combination) where LS and SS decreased (13.4 kPa and 37.3 kPa, respectively, Fig. 53.6) at the fourth week of therapy and viral clearance and HCV-PCR quantitation became negative. In addition, serum ALT and AST normalized after 4 weeks (ALT = 34 U/L and AST = 39 U/L). Surprisingly, the LS and SS continued to improve together with the liver functions after end of treatment to reach 8.8 kPa and 22.4 kPa, respectively, while CAP decreased 256 dB/m after end of treatment [5]. Of note, platelet count significantly improved after end of treatment to reach  $162 \times 10^9/L$ . Combined LS and SS measurements is mandatory to follow up the response to DAAs and the progression of portal hypertension especially in patients with advanced fibrosis. More details are provided in Chaps. 9 and 33 on LS and SS in patients with HCV.

## References

1. Mueller S. Personal observation; 2019.
2. Akima T, Tamano M, Hiraishi H. Liver stiffness measured by transient elastography is a predictor of hepatocellular carcinoma development in viral hepatitis. *Hepatol Res.* 2011;41(10):965–70.

3. Kusaka K, Harihara Y, Torzilli G, Kubota K, Takayama T, Makuuchi M, et al. Objective evaluation of liver consistency to estimate hepatic fibrosis and functional reserve for hepatectomy. *J Am Coll Surg*. 2000;191(1):47–53.
4. Millonig G, Reimann FM, Friedrich S, Fonouni H, Mehrabi A, Büchler MW, et al. Extrahepatic cholestasis increases liver stiffness (FibroScan) irrespective of fibrosis. *Hepatology*. 2008;48(5):1718–23.
5. Elshaarawy O, Mueller J, Guha IN, Chalmers J, Harris R, Krag A, et al. Spleen stiffness to liver stiffness ratio significantly differs between ALD and HCV and predicts disease-specific complications. *JHEP Rep*. 2019;1(2):99–106.

**Part VIII**  
**Molecular Basis of Liver Stiffness and**  
**Cell Biology**

# Chapter 54

## Introduction to the Molecular Basis of Liver Stiffness and Its Relation to Mechano-signaling



Sebastian Mueller

### Introduction

Liver stiffness (LS) appears to be a rather complex parameter that is modulated by many factors at the systemic, organ-, cellular, and intracellular level. This is primarily the matrix composition of the liver itself such as collagen deposition. Second, pressure-related factors contribute largely to LS and, third, liver perfusion. The dynamic component of pressure is associated with blood flow and eventually with an intact heart action. However, in combination with blood flow, the hepatic resistance and hemorheology also contribute to LS. Finally, there is also a static pressure component mainly derived from the vascular filling, e.g., through water retention but also characteristics of the vascular wall including muscle action and elastic properties. Figure 54.1 highlights all organ systems that are engaged in the control of LS. The following paragraphs are far from being complete but are thought to describe important aspects to be considered for a better understanding of LS in the future.

### Hepatic Blood Flow, Resistance, and Hemorheology

Many hemodynamic aspects of LS have been already discussed elsewhere in this book, e.g., in the chapter introducing the “Sinusoidal Pressure Hypothesis.” Some aspects listed in Fig. 54.2, however, are new and deserve some additional discussions. More details are also listed in Table 54.1. Thus, **capillary pressure** is expected

---

S. Mueller (✉)

Department of Medicine and Center for Alcohol Research and Liver Diseases,  
Salem Medical Center, University of Heidelberg, Heidelberg, Germany  
e-mail: [Sebastian.Mueller@urz.uni-heidelberg.de](mailto:Sebastian.Mueller@urz.uni-heidelberg.de)

**Fig. 54.1** Organ systems and liver stiffness

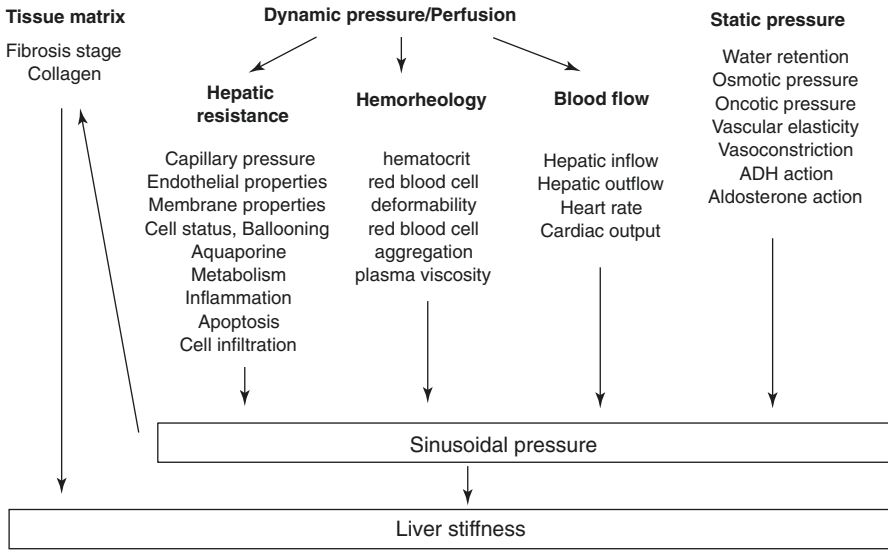
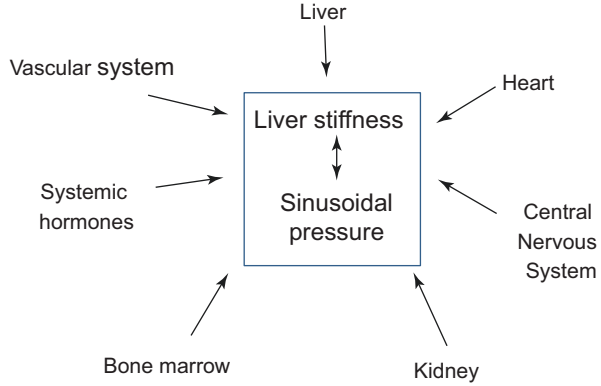


**Fig. 54.2** Liver stiffness at the systemic level. Liver stiffness is primarily modulated by matrix, blood flow, hepatic resistance, hemorheology, and static pressure

to contribute to LS, similar to its role in lungs. Capillary pressure is the pressure between two immiscible fluids in a thin tube, resulting from the interactions of forces between the fluids and solid walls of the tube. Capillary pressure can serve as both an opposing and driving force for fluid transport. The role of capillary pressure in liver sinusoids is still largely unexplored, so its role for LS and molecular factors. However, it can be assumed that both blood constituents and wall properties contribute to capillary pressure.

This links to **hemorheology** or blood rheology which is the study of flow properties of blood and its elements of plasma and cells. Proper tissue perfusion can occur only when blood's rheological properties are within certain levels and it has been

**Table 54.1** Major factors that affect liver stiffness and examples

LS factors		Examples	Example of LS elevation	Examples of LS decrease	
Tissue matrix		Collagen	Liver cirrhosis		
		Amyloid	Amyloidosis		
Pressure hemodynamics	Static	Elasticity of vascular bed	Vasoconstriction – Adrenaline – Noradrenaline	Vasodilatation – Nitrates – $\beta$ -blockers	
		Filling status	Water retention – RAAS – Aldosterone – Antidiuretic hormone	Treatment with diuretics – Furosemide – Spironolactone	
		Osmotic pressure	Hyponatremia		
		Oncotic pressure	Hypalbuminemia		
	Dynamic	<b>Hepatic inflow</b>			
		Hepatic artery	Elevated arterial pressure Increased cardiac output Increased heart rate Sympathetic action	Hypotonia Parasympathetic action	
		Portal vein	Elevated portal flow	Lowered portal pressure	
		<b>Hepatic outflow</b>			
		Hepatic veins	Congestion	Blood loss	
		Common bile duct	Cholestasis	Choleresis	
Hemorheology		Hematocrit Red blood cell deformability Red blood cell aggregation Plasma viscosity	Elevated blood viscosity – Dehydration	Lowered blood viscosity – Dilution, platelet inhibition, heparins	
Hepatic resistance	Capillary pressure	Endothelial properties			
		Membrane properties			
	Hepatocyte status	Ballooning	Ballooning		
		Aquaporin action			
		Metabolism			
		Steatosis		Steatosis?	
		Inflammation		Antiinflammatory treatment	
	Apoptosis	Apoptosis	Apoptosis inhibition		
	Cell infiltration	Macrophages	Inflammation		
		Neutrophils			



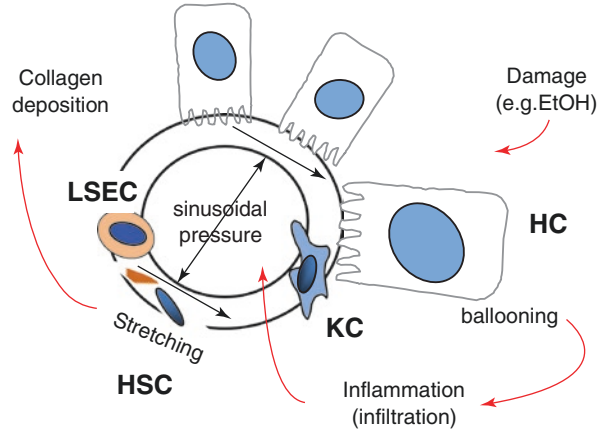
well conceived for a long time that alterations of these properties play a significant role in disease processes. **Blood viscosity** is determined by plasma protein concentration, hematocrit (volume fraction of red blood cells), temperature, and mechanical properties of red blood cells. These mechanical properties include erythrocyte deformability and erythrocyte aggregation. Blood can be considered as a non-Newtonian fluid as the viscosity of blood varies with shear rate. Blood becomes less viscous at high shear rates like those experienced with increased flow such as during exercise or in peak-systole. Contrarily, blood viscosity increases when shear rate goes down with increased vessel diameters or with low flow, such as downstream from an obstruction or in diastole. This decrease of blood viscosity in capillaries is called Fåhræus–Lindqvist effect [1].

Plasma viscosity is determined by water-content and macromolecular components. Nevertheless, hematocrit has the strongest impact on whole blood viscosity. One unit increase in hematocrit can cause up to a 4% increase in blood viscosity. This relationship becomes even stronger with increasing hematocrit. Thus, when the hematocrit rises from 40 to 60%, relative viscosity of the blood rises from 4 to 8, which is an increase by 100% [2]. In polycythemia, the blood viscosity can become as great as 10 times that of water, and its flow through blood vessels is greatly retarded because of increased resistance to flow.

## Stiffness at the Cellular Level

As already discussed in book Part IV in the chapter of “Histological Confounders,” several cellular conditions are known to be associated with LS. Fibrosis or collagen deposition shows the closest association with LS. Fibrosis is followed by features of hepatocyte injury including ballooning, lobular and portal inflammation, Mallory’s hyaline in the now called Mallory Denk bodies, and apoptosis. Inflammation is followed by other histological features that are positively and significantly associated with LS: microgranulomas, acidophil bodies, megamitochondria, glycogenated nuclei, and large lipo-granulomas. These mostly intracellular histological parameters are all features of apoptotic cell damage or death. Notably, steatosis itself such as lipid droplets are not significantly correlated with LS, in some cohorts even slightly negatively. The role of hemodynamic pressure is visualized in Fig. 54.3. It demonstrates how vascular pressure or sinusoidal pressure causes stretching of peri-vascular or perisinusoidal aligned structures or cells. These **stretch forces** will further elevate stiffness or LS but also engage in biomechanical signaling [3–6]. There will be also bidirectional interactions between pressure and peri-vascular structures. For instance, inflammation and ballooned hepatocytes will increase vascular resistance, increase pressure, and further stretch the surrounding.

**Fig. 54.3** Modulation of tissue stiffness by vascular or sinusoidal pressure. A liver sinus is shown schematically. Hepatocyte cell death, inflammation, or congestion all lead to increased sinusoidal pressure that causes stretching of, e.g., hepatic stellate cells (HSC), liver sinus endothelial cells (LSEC) or hepatocytes (HC)



## Intracellular Components and Stiffness

Figure 54.4 now briefly highlights cellular and intracellular structures that can affect cellular stiffness and organ stiffness such as LS. It should be noted, however, that our knowledge about these intracellular constituents are still largely unexplored and poorly validated. Apart from cellular “matrix constituents,” intracellular pressure will control wall tension and tension of intermediate filaments such as cytokeratin 18 (CK18). Many other cellular proteins are involved in anchoring cells to ECM or between cells. Thus, adherens junctions (AJ) are not only involved in anchoring the cell to the ECM but are also actively involved in transducing mechanical forces. AJ contain cadherins (such as E-Cadherin and N-Cadherin) that are linked to the cytoskeleton (F-actin) via linker proteins  $\beta$ -catenin and  $\alpha$ -catenin [7]. Cadherin-based cellular adhesions signal by a broad range of extra-, inter-, and intracellular mechanisms, which involve several kinases and phosphatases [8]. Tight junctions (TJ) are found at the apical membrane of all epithelia, thereby acting as barriers for lipids and proteins by preventing diffusion between apical and basolateral intramembrane domains (Fig. 54.5). TJ consist of transmembrane proteins including occludin, claudins, tricellulin, and junctional adhesion molecules (JAMs) as well as cytosolic proteins acting as scaffolding proteins that anchor membrane components to the actin cytoskeleton, e.g., ZO-1 to -3 or include signaling molecules and transcription factors (e.g., ZONAB) [9]. Their elevated expression, namely, occludin, claudin 1, 2, 4 and 7, has been observed in liver cirrhosis and HCC [10, 11]. Desmosomes are adhesive junctions consisting of transmembrane proteins (desmoglein and desmocollin) that interact with linker molecules of the armadillo family (plakoglobin, plakophilins, and desmoplakin) [12], thereby providing resistance to mechanical forces through direct interactions with cytokeratins, major proteins of the keratin-containing **intermediate filaments** (IF) [13, 14]. A recent study investigating mechanical

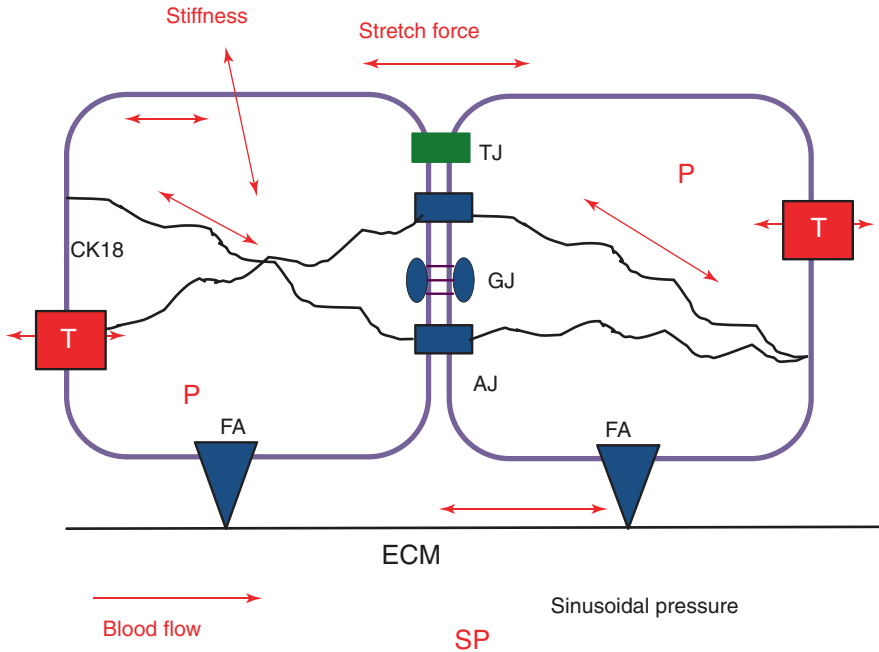


**Fig. 54.4** Stiffness and intracellular components. Stiffness is also affected by intracellular pressure (P) and stretch forces (red arrows) on the cellular membranes and intermediary filaments. Several intercellular junctions are schematically shown such as tight junctions (TJ), gap junctions (GJ), and adherence junctions (AJ). Intermediary filaments such as CK18 play an important role in liver disease. CK18 is interacting with intercellular junctions such as AJ. Finally, the intracellular pressure (P) is likewise controlled by many conditions including transport proteins (T) to control osmotic pressure, protein shuttles, or water influx, e.g., by aquaporins. Below, the blood flow direction and sinusoidal pressure are shown. We are only at the beginning to understand the role of all these cellular factors in defining stiffness and biomechanical signaling. Further abbreviations: *ECM* extracellular matrix, *SP* sinusoidal pressure

pressure (BDL rat model) and IF changes in liver demonstrated a disappearance of pericanalicular sheath and rearrangement of IF at the hepatocyte periphery [15]. IF in hepatocytes are mainly composed of CK18 and form a meshwork extending from desmosomes at the lateral cell membrane throughout the cytoplasm (Fig. 54.5). Desmosomal cadherins interact with each other and facilitate IF attachment. Furthermore, desmosomes are extremely stable and may play a role in reorganization of gap junctions (GJ) [16] that are important for intercellular communication. GJ are formed by hemichannels (connexons) of adjacent cells and are built up by six connexin proteins (Cx), which allow passive diffusion of small and hydrophilic molecules (<1 kDa) into neighboring cells. The most abundant connexins found in the liver are Cx 26, 32, 36, 40, and 43 [17]. GJ may contribute to modulation of portal pressure and intrahepatic vascular relaxation [17].

In summary, intracellular pressure in association with intercellular junctions, anchoring proteins, and intermediary filaments seem to play an important role in defining cellular stiffness and all these conditions are still largely unexplored.

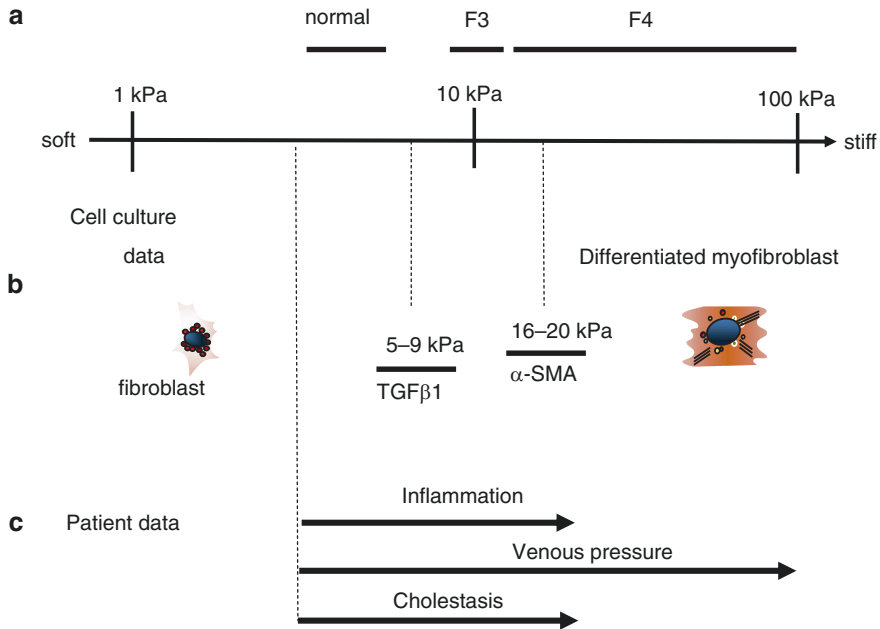


**Fig. 54.5** Similar stiffness values are found under pro-fibrogenic conditions in cellular and human studies. **(a)** Stiffness scale with cutoff values for normal, F3 and F4 fibrosis. **(b)** Known stiffness conditions to activate fibroblasts using atomic force microscopy (see [4]). **(c)** Known human LS values in various pathological conditions that ultimately cause liver fibrosis (see [45])

## How Do Cells Respond to Mechanical Stress?

Mechano-sensing has been studied for many decades and various underlying mechanisms seem to be involved. Cells must adhere to a solid. However, an understanding of how tissue cells—including fibroblasts, myocytes, neurons, and other cell types—sense matrix stiffness is just emerging with quantitative studies of cells adhering to gels (or to other cells) with which elasticity can be tuned to approximate that of tissues.

Key roles in molecular pathways are played by adhesion complexes and the actin-myosin cytoskeleton, whose contractile forces are transmitted through trans-cellular structures [18]. Potential sensing mechanisms include cation channels of the transient receptor potential (TRP) family, the actin-interacting protein zyxin and

G protein-coupled receptors that are activated in response to stretch [19, 20] while ion channel activation and alterations in cytoskeletal stability are part of the response to hydrostatic pressure [21]. Members of TRP family of cation channels are emerging as important players in mechanotransduction pathways. Localized within mechanosensory structures, they are activated by mechanical deformations/stretching and trigger fast as well as sustained cytoskeletal remodeling responses [20]. In HSCs, these channels have been shown to be upregulated during fibrosis development and if blocked, myofibroblast differentiation was attenuated, thus suggesting an important role in HSC activation [22]. Likewise, the stress fiber network within these cells structurally reinforces and provides tension to tissues such as those found in healing wounds. Stress fibers have been observed to polymerize in response to mechanical forces which involves calcium-signaling [23]. Furthermore, liver sinus endothelial cells (LSECs) are highly specialized endothelial cells, which line liver sinusoids and are likely to be the first to sense shear stress due to changes in sinusoidal pressure or elevated blood flow. Moreover, the cells contain fenestrae allowing passage of soluble factors smaller than 100–150 nm between the sinusoidal blood and parenchymal cells. A contractile cytoskeleton ring composed of actin and myosin supports the fenestrae. The size and density of fenestrae is affected by portal pressure and shear stress, as well as soluble factors [24–26]. A recent study suggests that the lack of fenestration plays an important role in fibrosis development and a restoration of LSEC differentiation was shown to promote HSC quiescence, enhances regression of fibrosis and prevents progression of cirrhosis in vivo [27]. Therefore, the role of LSECs in mechano-sensing and fibrosis development requires further investigation.

## **Role of Myofibroblasts and ECM in Mechano-signaling**

Myofibroblasts are regarded as major matrix generating cells in the liver but also in other tissues. In fact, besides HSCs, a large panel of cells can develop this phenotype upon activation including chondrocytes, osteoblasts, smooth muscle cells, pericytes, fibrocytes, or epithelial cells undergoing epithelial-to-mesenchymal transition. Neo-expression of the alpha isoform of smooth muscle actin ( $\alpha$ -SMA) is used as marker for activated myofibroblasts [28]. Fibroblasts without a contractile apparatus form only very small and immature adhesions with the ECM [29, 30]. During mechanic stress, these focal complexes mature into focal adhesions (FA) [4]. HSCs undergo myofibroblast transformation if coated on stiff matrices even in the absence of the pro-fibrogenic cytokine TGF- $\beta$  [31]. Most importantly, however, it was also shown that an increase in LS precedes histological matrix deposition in a rodent model [32]. In these concepts, the HSCs are described as sensing cells that respond to a stiff matrix by producing more matrix proteins. Indeed, HSCs have been known for a long time to be contractile and respond to changes in their environment [33]. In myofibroblasts, activated TGF- $\beta$  results in increased  $\alpha$ -SMA, which interacts with cellular myosin to contract and produce increased tension. TGF- $\beta$  is a common factor downstream of many mechanical forces; in addition to tension, other forces including shear forces mediated by interstitial fluid flow and stretch have been

implicated in TGF- $\beta$  activation and release [34, 35]. It is quite striking to see that comparable stiffness values have been observed in patients with various liver diseases and confounders (inflammation, cholestasis, congestion) obtained by transient elastography in humans and in cellular studies analyzing the pro-fibrogenic response of HSC and fibroblasts ( $\alpha$ -SMA activation and TGF- $\beta$  release) under culturing conditions with exactly defined stiffness as assessed by atomic force microscopy (for details, see Fig. 54.5a–c). The identical levels of stiffness and pro-fibrogenic conditions both in clinical and cellular studies are a strong argument for the role of sinusoidal pressure and pressure-mediated stiffness elevation in fibrosis progression [5]. Thus, pressure could be one of the long sought physiological correlates that modulate tissue stiffness (see Fig. 54.3 and Appendix Fig. A.14).

## Principles of Mechano-sensing: Lessons from Pressure-Sensing in Vessels and Cells

Physical forces of gravity, hemodynamic stresses, and movement play a critical role in tissue development and have been studied for a long time [36]. Yet, little is known about how cells convert these mechanical signals into a chemical response. In a model presented by Ingber in 1997, it was postulated that cells are hard-wired to respond immediately to mechanical stresses transmitted over cell surface receptors that physically couple the cytoskeleton to extracellular matrix (e.g., integrins) or to other cells (cadherins, selectins, CAMs). Many signal transducing molecules that are activated by cell binding to growth factors and extracellular matrix associate with cytoskeletal scaffolds within focal adhesion complexes. Mechanical signals, therefore, may be integrated with other environmental signals and transduced into a biochemical response through force-dependent changes in scaffold geometry or molecular mechanics. Myofibroblasts are regarded as major matrix generating cells in the liver but also in other tissues. In fact, besides HSCs, a large panel of cells can develop this phenotype upon activation including chondrocytes, osteoblasts, smooth muscle cells, pericytes, fibrocytes, or epithelial cells undergoing epithelial-to-mesenchymal transition. As already discussed above, neo-expression of the alpha isoform of smooth muscle actin ( $\alpha$ -SMA) is used as marker for activated myofibroblasts.

An important concept includes cell–matrix interactions such as **focal adhesions** (FAs). The cellular actin-myosin cytoskeleton exerts tension on ECM proteins via integrin attachments located within FAs that link the cell's actin cytoskeleton and plasma membrane to the underlying ECM (Fig. 54.6a). FAs change protein composition and dynamics and grow in size in response to tension [37, 38]. Mechano-sensing by focal adhesions during cell adhesion to the ECM can be, for instance, mediated by **talin** (Fig. 54.6a), a connecting protein between ECM-binding integrin receptors and the actin cytoskeleton. In response to this increased tension, vinculin can bind to talin resulting in a force- and direction-dependent focal adhesion reinforcement [39]. Another example is mechano-sensing through the **Latency Associated Peptide** (LAP) complex. Thus, TGF- $\beta$  that is stored in the LAP complex of the ECM can undergo activation as a direct result of mechanical tension. Through integrin

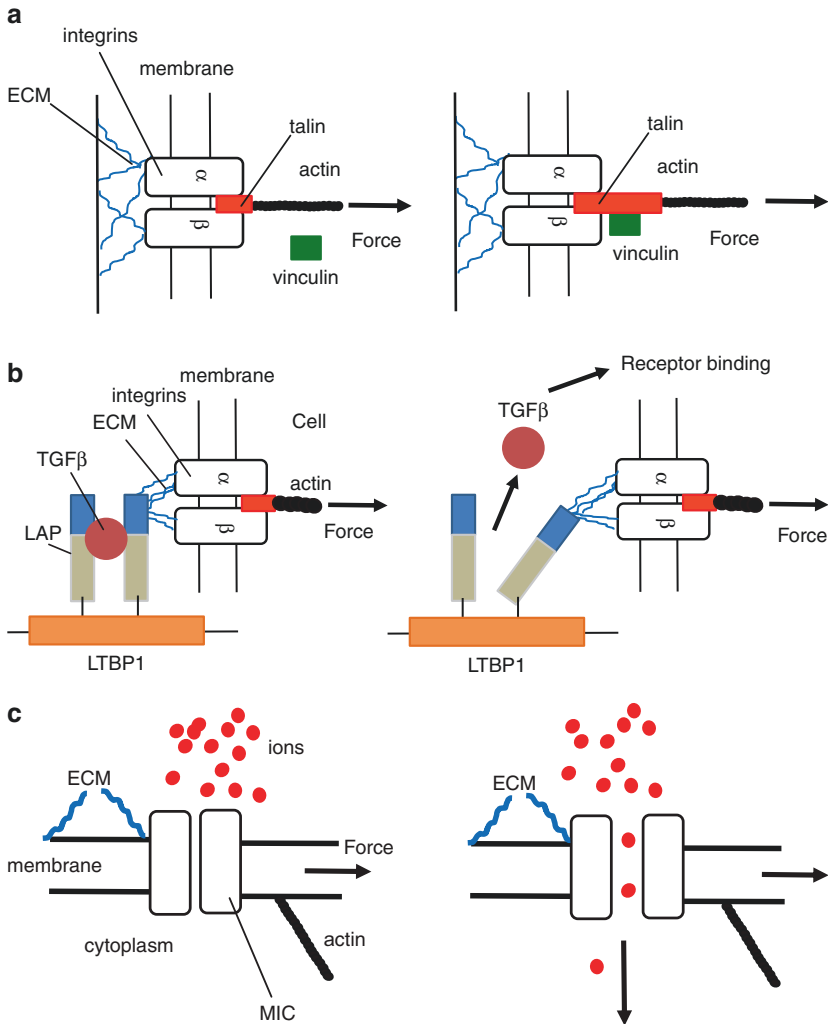


**Fig. 54.6** Molecular examples of mechano-sensing. These already established mechanisms could all contribute to sensing the sinusoidal pressure via intercellular or ECM-stretch forces ultimately causing matrix deposition to withstand the pressure. Many cells including HSC and fibroblasts have tactile properties and can sense the rigidity of the pressure-modulated tissues stiffness. **(a)** Mechano-sensing by focal adhesions during cell adhesion to the ECM. For instance, stretch forces free cryptic binding sides of talin, a connecting protein between ECM-binding integrin receptors and the actin cytoskeleton. In response this increased tension, vinculin can bind to talin resulting in a force- and direction-dependent focal adhesion reinforcement. **(b)** Stretch-sensing and pro-fibrogenic response by latent TGF- $\beta$  activation. Integrin binding to a specific RGD site in LAP transmits intracellular force to the latent TGF- $\beta$  complex consisting of LTBP1, TGF- $\beta$ , and LAP. In case of, e.g., pressure-induced stretch forces, RGD-linked ECM will pull LAP away and this conformation change will release TGF- $\beta$ . **(c)** Stretch-sensing by mechanosensitive ion channels (MIC). MIC perceive changes in plasma membrane tension, which can be modulated by the actin network. Mechanical forces are thought to gate ion channels by inducing a conformational switch resulting in pore opening and ion flux. Abbreviations: *ECM* extracellular matrix, *LAP* latency associated protein, *LTBP1* latent transforming growth factor  $\beta$  binding protein 1, *TGF- $\beta$*  transforming growth factor  $\beta$

attachments, cells are able to exert tension on the LAP. In a soft environment, it deforms in response to tension and the complex remains intact. If the matrix is stiff, however, resistance to cell-generated tension results in deformation of the LAP and the concomitant release of active TGF-β [40, 41]. A third example is **mechanosensitive ion channels** that perceive changes in plasma membrane tension, which can be modulated by the actin network [39]. Mechanical forces are thought to gate ion channels by inducing a conformational switch resulting in pore opening and ion flux.

Many lessons on mechano- and pressure-mediated signaling pathways and sensing have been learnt from vascular biology [3, 6, 42–44]. It is also interesting to note that mechano-induced gene expression profiles include hypoxia-regulated genes such as HIF1alpha [6]. This could be a further hint that **pressure changes are always associated with oxygen changes**. For example, elevation of vascular pressure in response to vascular resistance will be followed by a decrease in oxygen. Under extreme conditions of a complete blockage of blood flow, pressure will be maximized while oxygen rapidly decreases. Figure 54.7 schematically depicts potentially involved pathways in sinusoidal pressure and LS induced mechano-sensing in the liver. These should be addressed in future studies.

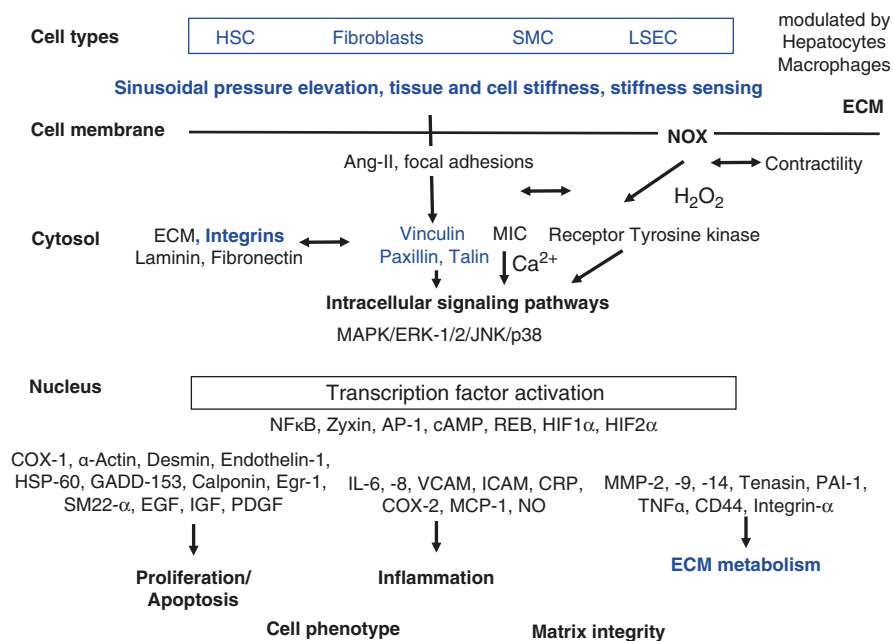


**Fig. 54.7** Potential sinusoidal pressure-induced pathways ultimately leading to liver fibrosis. Abbreviations: *AngII* Angiotensin II, *AP-1* Activator protein-1, *CAT* catalase, *Egr-1* early growth response gene-1, *ERK-1/2* extracellular signal regulated kinases 1 and 2, *FAK* focal adhesion kinase, *GADD-153* growth arrest and DNA damage-inducible gene 153, *JNK* c-Jun N-terminal kinase, *HSC* hepatic stellate cell, *HSP-60* heat shock protein-60, *LSEC* liver sinus endothelial cells, *MCA* monocyte chemotactic antigen, *MIC* Mechanosensitive ionic channels, *NO* nitric oxide, *NOX* NADPH-dependent oxidases, *PCNA* proliferating cell nuclear antigen, *REB* response element binding protein, *SGK* serum-glucocorticoid-induced protein kinase (a serine/threonine protein kinase), *SMC* smooth muscle cells, *SM22-α* smooth muscle cells specific protein, *TGF-β* transforming growth factor β, *THA-2* thromboxane synthase-A2, *TNF-α* tumor necrosis factor-α



## References

1. Fåhræus R. The suspension stability of the blood. *Physiol Rev.* 1929;9(2):241–74.
2. Wells RE Jr, Merrill EW. Influence of flow properties of blood upon viscosity-hematocrit relationships. *J Clin Invest.* 1962;41(8):1591–8.
3. Humphrey JD, Schwartz MA, Tellides G, Milewicz DM. Role of mechanotransduction in vascular biology: focus on thoracic aortic aneurysms and dissections. *Circ Res.* 2015;116(8):1448–61.
4. Hinz B. Tissue stiffness, latent TGF-beta1 activation, and mechanical signal transduction: implications for the pathogenesis and treatment of fibrosis. *Curr Rheumatol Rep.* 2009;11(2):120–6.
5. Mueller S. Does pressure cause liver cirrhosis? The sinusoidal pressure hypothesis. *World J Gastroenterol.* 2016;22(48):10482.
6. Anwar MA, Shalhoub J, Lim CS, Gohel MS, Davies AH. The effect of pressure-induced mechanical stretch on vascular wall differential gene expression. *J Vasc Res.* 2012;49(6):463–78.
7. Niessen CM, Leckband D, Yap AS. Tissue organization by cadherin adhesion molecules: dynamic molecular and cellular mechanisms of morphogenetic regulation. *Physiol Rev.* 2011;91(2):691–731.
8. Yap AS, Briehor WM, Gumbiner BM. Molecular and functional analysis of cadherin-based adherens junctions. *Annu Rev Cell Dev Biol.* 1997;13:119–46.
9. Balda MS, Matter K. Tight junctions and the regulation of gene expression. *Biochim Biophys Acta.* 2009;1788(4):761–7.
10. Holczbauer A, Gyongyosi B, Lotz G, Torzsok P, Kaposi-Novak P, Szijarto A, et al. Increased expression of claudin-1 and claudin-7 in liver cirrhosis and hepatocellular carcinoma. *Pathol Oncol Res.* 2014;20(3):493–502.
11. Yeh TH, Krauland L, Singh V, Zou B, Devaraj P, Stolz DB, et al. Liver-specific beta-catenin knockout mice have bile canalicular abnormalities, bile secretory defect, and intrahepatic cholestasis. *Hepatology.* 2010;52(4):1410–9.
12. Hatzfeld M. Plakophilins: multifunctional proteins or just regulators of desmosomal adhesion? *Biochim Biophys Acta.* 2007;1773(1):69–77.
13. Moll R, Franke WW. Intermediate filaments and their interaction with membranes. The desmosome-cytokeratin filament complex and epithelial differentiation. *Pathol Res Pract.* 1982;175(2–3):146–61.
14. Kroger C, Loschke F, Schwarz N, Windoffer R, Leube RE, Magin TM. Keratins control intercellular adhesion involving PKC-alpha-mediated desmoplakin phosphorylation. *J Cell Biol.* 2013;201(5):681–92.
15. Song JY, Van Noorden CJ, Frederiks WM. Alterations of hepatocellular intermediate filaments during extrahepatic cholestasis in rat liver. *Virchows Arch.* 1997;430(3):253–60.
16. Windoffer R, Beile B, Leibold A, Thomas S, Wilhelm U, Leube RE. Visualization of gap junction mobility in living cells. *Cell Tissue Res.* 2000;299(3):347–62.
17. Hernandez-Guerra M, Gonzalez-Mendez Y, de Ganzo ZA, Salido E, Garcia-Pagan JC, Abrante B, et al. Role of gap junctions modulating hepatic vascular tone in cirrhosis. *Liver Int.* 2014;34(6):859–68.
18. Discher DE. Tissue cells feel and respond to the stiffness of their substrate. *Science.* 2005;310(5751):1139–43.
19. Suresh Babu S, Wojtowicz A, Freichel M, Birnbaumer L, Hecker M, Cattaruzza M. Mechanism of stretch-induced activation of the mechanotransducer zyxin in vascular cells. *Sci Signal.* 2012;5(254):ra91.
20. Kuipers AJ, Middelbeek J, van Leeuwen FN. Mechanoregulation of cytoskeletal dynamics by TRP channels. *Eur J Cell Biol.* 2012;91(11–12):834–46.
21. Myers KA, Rattner JB, Shrive NG, Hart DA. Hydrostatic pressure sensation in cells: integration into the tensegrity model. *Biochem Cell Biol.* 2007;85(5):543–51.

22. Abhilash PA, Harikrishnan R, Indira M. Ascorbic acid suppresses endotoxemia and NF-kappaB signaling cascade in alcoholic liver fibrosis in guinea pigs: a mechanistic approach. *Toxicol Appl Pharmacol*. 2014;274(2):215–24.
23. Nekouzadeh A, Pryse KM, Elson EL, Genin GM. Stretch-activated force shedding, force recovery, and cytoskeletal remodeling in contractile fibroblasts. *J Biomech*. 2008;41(14):2964–71.
24. Morsiani E, Aleotti A, Ricci D. Haemodynamic and ultrastructural observations on the rat liver after two-thirds partial hepatectomy. *J Anat*. 1998;192(Pt 4):507–15.
25. Morsiani E, Mazzoni M, Aleotti A, Gorini P, Ricci D. Increased sinusoidal wall permeability and liver fatty change after two-thirds hepatectomy: an ultrastructural study in the rat. *Hepatology*. 1995;21(2):539–44.
26. Gatmaitan Z, Varticovski L, Ling L, Mikkelsen R, Steffan AM, Arias IM. Studies on fenestral contraction in rat liver endothelial cells in culture. *Am J Pathol*. 1996;148(6):2027–41.
27. DeLeve LD. Liver sinusoidal endothelial cells in hepatic fibrosis. *Hepatology*. 2015;61(5):1740–6.
28. Tomasek JJ, Gabbiani G, Hinz B, Chaponnier C, Brown RA. Myofibroblasts and mechano-regulation of connective tissue remodelling. *Nat Rev Mol Cell Biol*. 2002;3(5):349–63.
29. Tamariz E, Grinnell F. Modulation of fibroblast morphology and adhesion during collagen matrix remodeling. *Mol Biol Cell*. 2002;13(11):3915–29.
30. Yeung T, Georges PC, Flanagan LA, Marg B, Ortiz M, Funaki M, et al. Effects of substrate stiffness on cell morphology, cytoskeletal structure, and adhesion. *Cell Motil Cytoskeleton*. 2005;60(1):24–34.
31. Wells RG. The role of matrix stiffness in hepatic stellate cell activation and liver fibrosis. *J Clin Gastroenterol*. 2005;39(4 Suppl 2):S158–61.
32. Georges PC, Hui JJ, Gombos Z, McCormick ME, Wang AY, Uemura M, et al. Increased stiffness of the rat liver precedes matrix deposition: implications for fibrosis. *Am J Physiol Gastrointest Liver Physiol*. 2007;293(6):G1147–54.
33. Kawada N, Tran-Thi TA, Klein H, Decker K. The contraction of hepatic stellate (Ito) cells stimulated with vasoactive substances. Possible involvement of endothelin 1 and nitric oxide in the regulation of the sinusoidal tonus. *Eur J Biochem*. 1993;213(2):815–23.
34. Ng CP, Hinz B, Swartz MA. Interstitial fluid flow induces myofibroblast differentiation and collagen alignment in vitro. *J Cell Sci*. 2005;118(Pt 20):4731–9.
35. Sakata R, Ueno T, Nakamura T, Ueno H, Sata M. Mechanical stretch induces TGF-beta synthesis in hepatic stellate cells. *Eur J Clin Invest*. 2004;34(2):129–36.
36. Ingber DE. Tensegrity: the architectural basis of cellular mechanotransduction. *Annu Rev Physiol*. 1997;59:575–99.
37. Sagir A, Erhardt A, Schmitt M, Haussinger D. Transient elastography is unreliable for detection of cirrhosis in patients with acute liver damage. *Hepatology*. 2008;47(2):592–5.
38. Millonig G, Friedrich S, Adolf S, Fonouni H, Golriz M, Mehrabi A, et al. Liver stiffness is directly influenced by central venous pressure. *J Hepatol*. 2010;52(2):206–10.
39. Kanoldt V, Fischer L, Grashoff C. Unforgettable force—crosstalk and memory of mechano-sensitive structures. *Biol Chem*. 2019;400(6):687–98.
40. Buscemi L, Ramonet D, Klingberg F, Formey A, Smith-Clerc J, Meister JJ, et al. The single-molecule mechanics of the latent TGF-beta1 complex. *Curr Biol*. 2011;21(24):2046–54.
41. Wipff PJ, Rifkin DB, Meister JJ, Hinz B. Myofibroblast contraction activates latent TGF-beta1 from the extracellular matrix. *J Cell Biol*. 2007;179(6):1311–23.
42. Humphrey JD. Mechanisms of arterial remodeling in hypertension: coupled roles of wall shear and intramural stress. *Hypertension*. 2008;52(2):195–200.
43. Atta HM. Varicose veins: role of mechanotransduction of venous hypertension. *Int J Vasc Med*. 2012;2012:538627.
44. Pfisterer L, Konig G, Hecker M, Korff T. Pathogenesis of varicose veins—lessons from biomechanics. *Vasa*. 2014;43(2):88–99.
45. Mueller S, Sandrin L. Liver stiffness: a novel parameter for the diagnosis of liver disease. *Hepat Med*. 2010;2:49–67.

# Chapter 55

## Stiffness and Hepatocytes Function

### In Vitro



Srivatsan Kidambi

### Introduction

Liver damage as a consequence of liver injury or disease (e.g., chronic hepatitis C virus (HCV) infection, alcohol abuse, and nonalcoholic steatohepatitis (NASH)) is extremely prevalent worldwide and results in a huge economic burden on patients [1, 2]. Several liver diseases can lead to fibrosis, which results from an imbalance between production and resorption of extracellular matrix (ECM) and restructuring of the liver microenvironment (LME). The earliest changes in LME as a result of liver disease occur in response to ECM remodeling, resulting in accumulation of ECM proteins and an increase in liver stiffness. Furthermore, the balance of matrix production and degradation is compromised, leading to deleterious effects on the liver function. Clinically, stiffness measurement is considered as the best read-out to monitor, stage and diagnosis, clinical outcomes of new drugs, and survival correlation in liver diseases. Furthermore, clinical studies have shown that liver stiffening provides a permissive milieu for the development of cellular dysplasia and is a key

---

S. Kidambi (✉)

Department of Chemical and Biomolecular Engineering, University of Nebraska,  
Lincoln, NE, USA

Fred and Pamela Buffett Cancer Center, University of Nebraska Medical Center,  
Omaha, NE, USA

Nebraska Center for Integrated Biomolecular Communication, University of Nebraska,  
Lincoln, NE, USA

Nebraska Center for the Prevention of Obesity Diseases, University of Nebraska,  
Lincoln, NE, USA

Nebraska Center for Materials and Nanoscience, University of Nebraska, Lincoln, NE, USA

Mary and Dick Holland Regenerative Medicine Program, University of Nebraska Medical  
Center, Omaha, NE, USA

e-mail: [skidambi2@unl.edu](mailto:skidambi2@unl.edu)

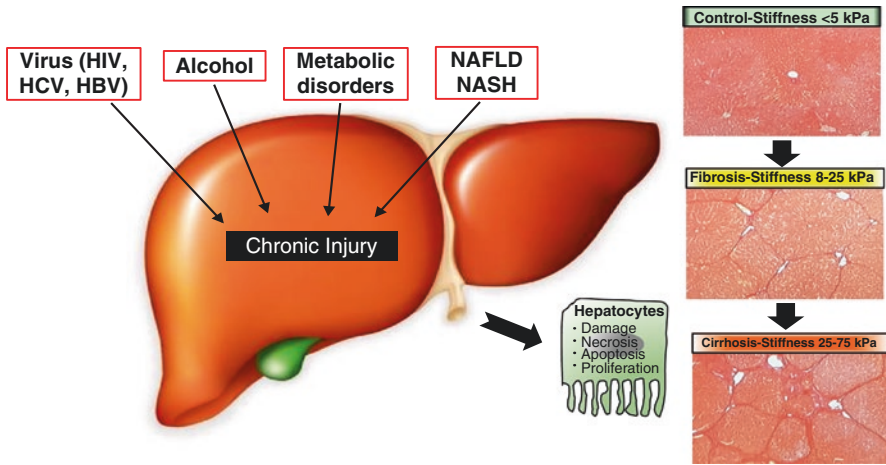


**Fig. 55.1** Etiologic factors and changes in liver stiffness in the pathogenic development of hepatic diseases. Increase in liver stiffness is the major pathogenic event occurring in several liver disorders. Chronic liver injury due to HBV and HCV infection, inadequate alcohol consumption, and metabolic disorders results in a gradual and dramatic increase in liver stiffness and corresponds to higher hepatocytes damage, necrosis, apoptosis, and proliferation. Instauration of hepatocyte oxidative stress condition results in liver fibrosis and cirrhosis, which may lead to hepatocellular carcinoma

feature of liver dysfunction that leads to cirrhosis and hepatocellular carcinoma (HCC) [3–5].

Noninvasive **elastography techniques** and **direct rheometry** measurements of the whole liver have established that the liver stiffness increases as fibrosis progresses [6–9]. Clinical research assessing liver stiffness by transient elastography has revealed that the stiffness of normal, early, and late stage liver fibrosis are <6 kPa, 6–12.5 kPa, and 12.5–75 kPa, respectively (Fig. 55.1) [10, 11]. For more details, see also other book parts, namely, book Part IV “Important (Patho)physiological Confounders of LS.” Studies of both humans and rats suggest that increased liver stiffness is associated with progression of fibrosis [12–14]. In patients with chronic hepatitis C infection, magnetic resonance elastography studies have shown that livers at stage F0 (with no detectable fibrosis) are stiffer than the livers of uninfected patients; similarly, in rats with carbon tetrachloride-mediated injury, increased liver stiffness preceded fibrosis [8]. Despite these data, there is lack in the complete understanding of the role of the mechanical cues elicited by the varying stiffness on the fate of liver cells, including hepatocytes.

## Hepatocytes as Key Players of Liver Parenchyma and Function

The liver is the largest solid organ in the body comprising about 3% of the adult body weight and can be considered the metabolic center that performs hundreds of vital functions necessary for maintaining homeostasis [15]. The different functional

roles of the liver can be grouped into categories of synthesis, storage, detoxification, and metabolism [16]. The highly metabolic nature of the organ demands approximately 30% of the total oxygen consumption. Some of the major functions carried out by the liver are bile synthesis, regulation of blood glucose, detoxification of xenobiotic substances, maintenance of serum oncotic pressure, nitrogen disposal, lipid synthesis and breakdown, and regulation of blood clotting [17]. The liver is a complex organ built by at least seven different resident cell types—hepatocytes, liver sinusoidal endothelial cells, dendritic cells, Kupffer cells, stellate cells, biliary epithelial cells, and lymphocytes of multiple types that are organized in a precise manner for maximal functional stability. Hepatocytes comprise the majority (~85%) of tissue mass in the liver as the liver parenchyma that performs several key liver functions. Hepatocytes perform the bulk of metabolic and synthetic functions of the organ. They synthesize the majority of circulating proteins in the plasma such as albumin, protease inhibitors, clotting factors, and inflammatory complexes [18]. They metabolize biomolecules such as cholesterol, heme, triglycerides, vitamins, glucose, and bilirubin for homeostasis [18]. Hepatocytes are large polygonal, multinucleated cells of about 20 microns in size and are connected to adjacent hepatocytes through adhesion complexes such as tight junctions, and desmosomes [15]. These cells have distinct polarity; along with a distinct signature of cell surface receptors, carrier proteins and pumps, the cell-layer surface that faces the space of Disse has microvilli extensions, allowing for maximum surface area for transport of molecules from the lumen. Due to their high metabolic nature, they contain a high density of intracellular machinery such as mitochondria, peroxisomes, lysosomes, and endoplasmic reticulum. In a healthy liver, hepatocytes possess a superior capacity for proliferation, thereby allowing for regeneration of the organ under manageable stress. Along with the complex functional profile, maintenance of the replicative capacity of hepatocytes is highly dependent upon the upkeep of the intricate elements of the liver microenvironment such as mechanical stresses, cell–cell interactions, and cell–ECM interactions. Consequently, primary hepatocytes isolated from the liver and disconnected from their natural environment experience a drastic loss in functions and a complete loss in proliferative capacity.

## Liver Microenvironment in Normal and Diseased Livers

The liver microenvironment (LME) is essential for the maintenance of tissue functionality. The various components that constitute the LME are the parenchymal cells, non-parenchymal cells, spatial organization of the heterogeneous cell population, liver-specific ECM, soluble factors, oxygen gradient, and several mechanical cues [19–22]. Numerous studies have investigated the various aspects of LME and incorporated the findings towards creating *in vitro* liver models. Uygun et al. employed derivative of decellularized liver matrix to demonstrate the importance of the chemical composition of the ECM in the maintenance of hepatocyte function for a prolonged duration [23]. Kidambi et al. established that high oxygen regulates the stability of hepatocyte function *in vitro*. Similarly, a study by Wong et al. showed

that the autocrine signaling between hepatocytes forming tight cell–cell junctions is essential towards maintaining their synthetic functions *in vitro* [24]. Paracrine signaling is equally important in prolonging the hepatocyte health, as shown through multiple co-culture studies of hepatocytes with the stellate cells, fibroblasts, and endothelial cells [21, 25–27]. Interestingly, the LME changes drastically in the event of liver pathological conditions such as fibrosis.

## Liver Fibrosis

Liver fibrosis is a sustained wound-healing response in the organ resultant of chronic stressors such as viral infections, autoimmune disorders, metabolic disorders, or alcohol abuse [28]. During liver fibrosis, stellate cells and other hepatic cell types acquire a pro-fibrogenic phenotype that primarily results in (1) excessive production of ECM molecules forming scar tissue (2) increased inflammatory response and (3) loss of parenchymal function [29]. The reversibility of liver fibrosis depends on the nature and severity of the stressor, and irreversible fibrosis can result in fatal conditions such as cirrhosis, kidney failure, and hepatocellular carcinoma [30]. The most critical challenges in liver fibrosis intervention are the following: (1) absence of noninvasive biomarkers, (2) lack of mechanistic studies on the reversibility of liver fibrosis, and (3) absence of effective anti-fibrosis therapies.

Functional maintenance of the liver in a healthy state and the rate of progression of liver fibrosis are both regulated by the complex factors of the LME. Researchers anticipate that restoration of the healthy liver milieu will determine the success of anti-fibrosis therapies. Establishing the role of these individual liver-specific cues such as mechanical stiffness on different hepatic cell types is crucial for a systematic bottom-up approach towards (1) functional tissue engineering and (2) creating physiologically relevant disease models. A gaping hole in the literature of LME is that a majority of these studies focused primarily on maintaining the hepatocyte functions but the correlation of stiffness on hepatocytes dysfunction is limited.

## Role of Mechanical Environment in Liver Function and Fibrosis

Tissue development and function are driven by several mechanical elements of the microenvironment such as shear stress, compression forces, surface tension, traction, and osmotic pressure [31]. In the context of the liver, matrix elasticity (stiffness) has been a particularly important aspect correlating to the healthy and the diseased state of the organ. Over the last decade, clinicians have routinely been using direct and noninvasive elastography techniques to determine the stiffness of the liver as a diagnostic measure for establishing the occurrence/severity of liver

fibrosis [9, 32–34]. The cells that build tissues are viscoelastic in nature, and their anchorage dependence with adjacent cells and matrix is essential for the regulation of events such as proliferation, apoptosis, differentiation, and stress response [35–37]. The short range forces that the cells experience as a result of this adhesion are sensed by the cells through focal adhesion and cytoskeleton-mediated pathways [38]. Studies demonstrate that **integrins**, the heterodimeric receptors on the cell surface that mediate anchorage with the ECM, are the principle **mechanosensors** of the cells. The bi-directional signaling between integrins and the cytoskeletal molecules regulates changes in the cellular phenotype [39, 40].

In the event of pathological conditions in the liver such as liver fibrosis, the stiffness of the organ can increase dramatically [28]. The occurrence of liver fibrosis is considered synonymous with a malfunctioning ECM production and maintenance. The increase in the stiffness of the organ can be attributed to the ECM changes, both through the sheer amount of ECM components such as collagen 1 and proteoglycans that are deposited and by the modification of the existing components through posttranslational modification and cross-linking [41, 42]. Research shows that adherent cells can sense mechanical changes, but the implications of mechanical changes that accompany liver fibrosis on hepatocytes are not well established.

## Significance of Mechanobiology for Hepatocyte Function

A majority of the mechanotransduction studies of the liver have focused on hepatic stellate cells due to their importance in liver fibrosis progression [43, 44]. Recent advancement in liver fibrosis research has established that the liver parenchyma and other non-parenchymal cells are also critical in the progression of liver disease. Zeisberg et al. demonstrated that epithelial to mesenchymal transition in hepatocytes results in an accumulation of activated fibroblasts in animal models with CCl<sub>4</sub>-induced liver fibrosis [45]. Similarly, a study shows that hepatocellular carcinoma cells have shown a difference in resistance towards chemotherapeutic drugs when subjected to varying mechanical stiffness [46]. These studies suggest that it is vital to establish the nature of **mechanosensitivity** in hepatocytes to provide a better understanding of the various mechanistic triggers that regulate liver fibrosis.

From a different perspective, consideration of the mechanical microenvironment is equally important for improving the functionality of **in vitro liver tissue model**. By mimicking the mechanical properties of the healthy liver, we could achieve **superior hepatotoxicity screening**, bio-artificial livers and potential to expand cellular population for cell-based therapies [47, 48]. The **conventional in vitro model** for these purposes is hepatocytes cultured on polystyrene dishes that are a few gigapascals in elastic modulus and cells exposed to such a physiologically irrelevant stiffness demonstrate a functional compromise. An in vitro model that recapitulates the mechanical stiffness of the liver as seen in physiological and pathological conditions will prove to be valuable towards (1) advancing the field of mechanobiology



of the liver, (2) modeling fibrotic phenotype in vitro, and (3) elucidating the role of stiffness on the phenotypic regulation of hepatocytes.

## Need for Bioengineered In Vitro Liver Models

Despite the accuracy of animal models in capturing several vital physiological parameters, it is challenging to capture the dynamic changes in physiological and pathological liver stiffness at various stages of disease progression. Functional in vitro liver models are alternative and simplistic research tools towards establishing a fundamental understanding of the microenvironmental regulation of the liver. Additionally, in vitro models provide the opportunity to utilize human-derived cells/tissues, which tremendously improves their physiological relevance. A vast section of novel drugs fail in the clinical trial phase due to rodent/human biological difference in the preclinical stage, and this could potentially be reduced by employing in vitro liver models as preclinical screening platforms [49]. Most popular in vitro model for the liver utilized in pharmaceutical industry and research setting is the **simple monoculture of primary hepatocytes or hepatic cell lines** (HepG2 or Huh7) [50, 51]. These models are typically used to study liver metabolism or drug screening, and they suffer from critical limitations in the form of altered **phenotypic drift** and loss in functions [52]. Advanced engineering techniques that can mimic the vital microenvironment elements of the liver will be required to create functional in vitro models of the liver.

## In Vitro Substrates for Recreating Liver Stiffness

In vitro tools have been instrumental in the advancement of mechanobiology research. A significant portion of these in vitro studies utilizes protein-based substrates for creating platforms of tunable stiffness [53, 54]. The impact of extracellular matrix on the differentiated functions of hepatocytes has been widely studied. In general, the efficiency of hepatocyte attachment is enhanced by **coating substrates with simple extracellular matrix proteins** (typically collagen); however, in most cases, a concomitant increase in hepatocyte spreading leads to a loss of liver-specific functions [55]. Presentation of extracellular matrices of different compositions and topologies can stabilize hepatocyte morphology and a limited set of phenotypic functions. For instance, hepatocyte culture on **biomatrix**, a complex mixture of extracellular matrix components extracted from liver, has been shown to improve hepatocyte function compared with monolayers on collagen [55, 56]. When **sandwiched** between two layers of gelled collagen whose stiffness parallels physiological liver stiffness, hepatocytes from a variety of species maintain a cuboidal shape, secrete albumin, and synthesize urea (marker of nitrogen metabolism) [57]. Rat hepatocytes, in particular, secrete albumin at a high rate for 40 days in



sandwich cultures, exhibit improved cytochrome P450 induction, and form a contiguous, anastomosing network of bile canaliculi indicative of polarity [52]. The disadvantages of using biological substrates to create tunable stiffness are their lack of reproducibility in the physical characteristics, cost-ineffectiveness and, most importantly, unwanted variability in chemical and topographic cues [27]. Recent study demonstrates that the liver during fibrosis experiences **shear strain softening** and **compression stiffening**, whereas collagen gels display the opposite phenomenon with respect to shear stress and compression [58].

Among the synthetic materials that are at our disposal for stiffness modeling, **polyacrylamide gels** have been a popular choice due to the tunability of stiffness in the physiologically relevant stiffness range [59–61]. The limitation of polyacrylamide gels lies in the possible toxicity of unpolymerized acrylamide and difficulty in uniform surface functionalization [62]. **Hyaluronic acid (HA)** gels were used for the stiffness study by altering the gel concentration through a cross-linking process. HA hydrogels contained liver extracellular matrix (ECM), which were used to study the cells morphology of human hepatocytes due to the tremendous medical applications of HA used [54, 63]. Just like HA hydrogels, **polyvinyl alcohol (PVA) hydrogels** were also developed to study the effect of stiffness on hepatocytes [64]. **Polydimethylsiloxane (PDMS)** has emerged as a novel alternative synthetic substrate to study mechanical properties of biological tissues. PDMS is a bio-inert, versatile inorganic silicone material widely used in micro/nano fabrication techniques [65, 66]. Conventionally, stiffness in PDMS substrates has been modified by varying the ratio of cross-linker to elastomer in Sylgard 184, but the drawback here is that the cellular toxicity due to non-crosslinked PDMS has not been established [67]. We have developed an attractive alternative to this stiffness tunability as well as developing a protein-free matrix for primary hepatocytes attachment to tease out the effect of stiffness as a sole parameter on hepatocytes function. Here we utilized **varying weight ratios of Sylgard 184 and Sylgard 527** to create resultant substrates of different stiffness and integrated a polymer-based interface on PDMS to overcome its hydrophobic and cell-resisting nature to facilitate cell-based studies (Fig. 55.2) [51, 68–70].

## Stiffness and Hepatocytes In Vitro

The in vitro culture of hepatocytes can exhibit many hepatic functions for a finite period. Studying the loss of hepatic functional markers such as urea and albumin, supplementing study of the non-specific end points, can be utilized as the tool to evaluate the effect of an external stimulus on the cellular behavior. Studies investigating the role of matrix stiffness on hepatocyte biology have observed that hepatocytes **remain differentiated (functional) on soft supports** and dedifferentiate (lose their functions) on stiff supports [71–73]. Studies have also demonstrated that when cultured on stiff, thin films of monomeric collagen, hepatocytes spread, proliferate, and otherwise adopt a dedifferentiated phenotype, whereas on soft gels of

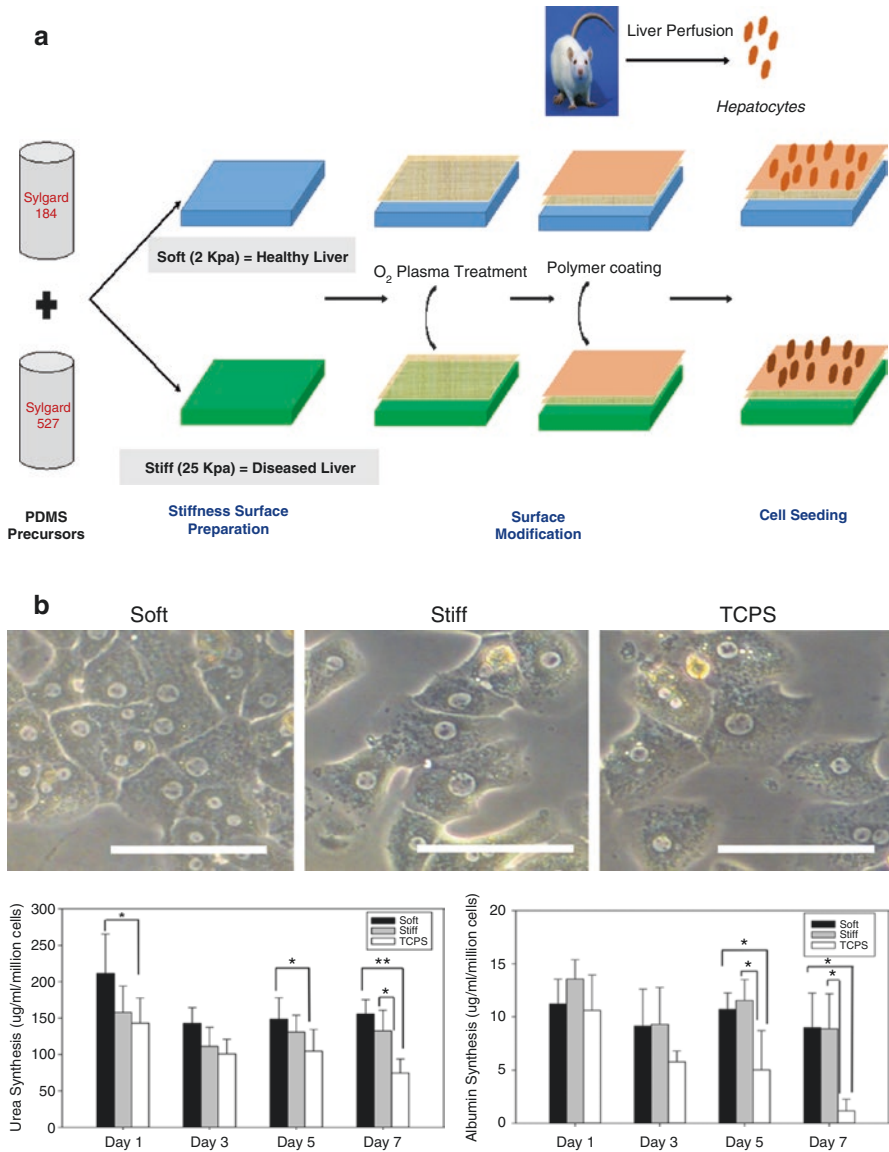


**Fig. 55.2** (a) Design of PDMS-based substrate coated with polymer films for tunable substrates for mechanical stimulation for primary hepatocytes. (b) Phase contrast images of primary hepatocytes on soft, stiff and TCPS substrates; Quantification of urea synthesis by primary hepatocytes on soft, stiff and TCPS substrates; Quantification of albumin synthesis by primary hepatocytes cultured on soft, stiff and TCPS substrates using ELISA

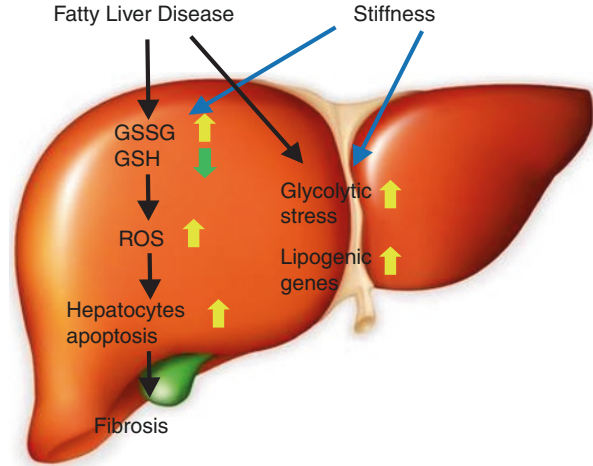
fibrillar collagen or **matrigel**, they remain differentiated and growth arrested [74, 75]. The primary goal of these studies was to extend the differentiated function of hepatocytes in order to use these as platforms for drug screening and toxicity studies and the effect of stiffness was not investigated in detail. Furthermore, it is inherently difficult to utilize bio-responsive materials to study the isolated effect of mechanical cues, independent of the ligand density. Accumulating evidence demonstrates the differential effect of matrix components on cultured hepatocytes. When isolated mature hepatocytes are cultured on type I collagen-coated dishes, the cells appear as a flattened monolayer and express low levels of liver function-specific mRNA and proteins. In dramatic contrast, when hepatocytes are cultured on a model basement membrane **Engelbreth–Holm–Swarm (EHS) gel**, hepatocytes retain their normal polarity and structure, and the products of liver-specific genes continue to be secreted for prolonged periods of culture [76, 77]. Cell–matrix interaction influences the determination of the differentiated phenotype of hepatocytes in cell culture, and maintains liver-specific functions for long-term culture, which effects have been associated with upregulation of liver-enriched transcription factors, including **hepatocyte nuclear factor (HNF)**. Upregulation of liver-specific genes induced by ECM is mediated via upregulation of HNF-4 $\alpha$  and HNF-1 induced by ECM. A collagen gel matrix increased the levels of HNF-3 $\alpha$  in the hepatocyte-derived cell line H2.35, but not those of HNF-3 $\beta$  and -3 $\gamma$ , responsible for the transcription of liver-specific genes. ECM regulates HNF-4 and tissue-specific gene expression in fetal hepatocytes as well as adult hepatocytes [78, 79].

Recently, there has been more study of the relationship between substrate stiffness and cellular functions, such as adhesion, migration, cell differentiation, and proliferation [13, 51, 61, 80–82]. Studies have explored the use of synthetic substrates of varying mechanical properties to examine hepatic phenotype expression. Chen and co-workers demonstrated that primary hepatocytes cultured on varying elastic modulus of polyelectrolyte multilayers had decreasing albumin production with increasing film stiffness [83]. Semler and co-workers investigated the effects of graded mechanical compliance on the function of primary hepatocytes using modified polyacrylamide gels with cell adhesive ligands and demonstrated that increasing hydrogel compliance resulted in increased albumin secretion [84]. You and co-workers utilized heparin-based hydrogels to investigate the effect of varying stiffness on primary hepatocytes function [54]. This study demonstrated that hepatocytes cultured on a softer heparin gel (10 kPa) were synthesizing five times higher levels of albumin compared to those on a stiffer heparin gel (110 kPa) after 5 days. Also, the study confirmed that softer gels promoted better maintenance of the hepatic phenotype as determined by hepatic markers (albumin and E-cadherin) demonstrating the importance of substrate mechanical properties on hepatocyte function. Xia and co-workers used RNA-Seq technology to study the transcriptome of hepatocytes cultured on soft, moderate, stiff, and plastic substrates [64]. Compared to soft substrate, their RNA-Seq results revealed 1131 genes that were

upregulated and 2534 that were downregulated on moderate substrate, 1370 genes that were upregulated and 2677 downregulated genes on stiff substrate. Further analysis indicated that differentially expressed genes were primarily associated with the regulation of actin cytoskeleton, focal adhesion, tight junction, adherens junction as well as antigen processing and presentation. In another study, three levels of stiffness were used that corresponded to the stiffness levels found in normal liver tissue (4.5 kPa), the early (19 kPa) and late stages (37 kPa) of fibrotic liver tissues [85]. This study showed that cytoskeleton of hepatocyte was influenced by substrate stiffness and soft substrates promoted the cellular migration and directionality. Integrin- $\beta$ 1 and  $\beta$ -catenin expression on cytomembrane were upregulated and downregulated with the increase of substrate stiffness, respectively. This study suggests that hepatocytes were sensitive to substrate stiffness and potential relationship among substrate stiffness, cellular Young's modulus and the dynamic balance of integrin- $\beta$ 1 and  $\beta$ -catenin pathways. Chang and co-workers demonstrated that fibrotic levels of matrix stiffness significantly inhibit hepatocyte-specific functions in part by inhibiting the HNF4 $\alpha$  transcriptional network mediated through the Rho/Rho-associated protein kinase pathway [80]. Fibrotic levels of matrix stiffness activated mechanotransduction in primary hepatocytes through focal adhesion kinase. In addition, blockade of the Rho/Rho-associated protein kinase pathway rescued HNF4 $\alpha$  expression from hepatocytes cultured on stiff matrix. However, these experiments were carried out using polyacrylamide gels which has few limitations: (1) covalently crosslink proteins using harsh chemicals is necessary for cell adhesion, (2) protein structure is regulated in varying stiffness [86–88], and (3) elastic creasing instability of the softer polyacrylamide gel that may lead to surface artifacts capable of contributing to non-specific cell behavior beyond stiffness [89].

Kidambi and co-workers demonstrated that stiffness impedes hepatic urea and albumin production, expression of drug transporter gene and epithelial cell phenotype marker, hepatocyte nuclear factor 4 alpha (HNF4 $\alpha$ ) (Fig. 55.2) [26, 51]. It was observed that hepatocytes cultured on soft substrates displayed a more differentiated and functional phenotype for a longer duration as compared to stiff substrates and TCPS. It was also demonstrated that hepatocytes on soft substrates exhibited higher urea and albumin synthesis. **Cytochrome P450 (CYP)** activity, another critical marker of hepatocytes, displayed a strong dependence on substrate stiffness, wherein hepatocytes on soft substrates retained 2.7-folds higher CYP activity on day 7 in culture, as compared to TCPS. Recently, Kidambi and co-workers further observed that increase in stiffness induces downregulation of key drug transporter genes (NTCP, UGT1A1, and GSTM-2). In addition, they observed that the epithelial cell phenotype was better maintained on soft substrates as indicated by higher expression of hepatocyte nuclear factor 4 $\alpha$ , **cytokeratin18**, and connexin 32. It was also demonstrated that hepatocytes cultured on NAFLD-like stiffness showed an induction of lipogenic genes, and lowered-oxidation genes expression, mitochondrial respiration, and glycolytic capacity, (2) increased ROS production, and (3) disruption of the mitochondrial fusion process and dynamics. Furthermore, significant increase in oxidized glutathione (GSSG) and reduced glutathione (GSH) in

**Fig. 55.3** Stiffness induces fatty liver-like metabolic dysfunction in primary hepatocytes



hepatocytes cultured on NAFLD-like stiffness compared to healthy liver stiffness was observed (Fig. 55.3) [90]. Similar effect was observed in hepatocytes isolated from fatty liver rat models indicating correlation to physiological conditions. Ganesan and co-workers demonstrated that levels of HIV and HCV mono- and co-infections were more prominent in primary hepatocytes cultured on substrates mimicking fibrotic stiffness (25 kPa-stiff) compared to substrates mimicking healthy liver (2.5 kPa-soft). Also the hepatocytes apoptosis due to viral infection was significantly higher in stiffer matrix compared to softer matrix. This study concluded that the increased matrix stiffness is not only a consequence of liver inflammation/fibrosis, but the condition that further accelerates liver fibrosis development. These studies suggest a plausible mechanism that increased stiffness modulates hepatocyte function causing liver functional failure. These results indicate that the substrate stiffness plays a significant role in modulating hepatocyte behavior. Understanding the impact of stiffness on hepatocytes biology will provide significantly more nuanced data to aid drug development for liver diseases.

## Conclusions and Future Directions

Although many challenges remain for the improvement of in vitro models to study the effect of stiffness on liver function, substantial progress has been made towards a thorough understanding of the necessary components. The parallel development of highly functional in vitro systems mimicking physiological and pathological liver stiffness is based on contributions from diverse disciplines, including regenerative medicine, developmental biology, transplant medicine, and bioengineering. In particular, novel technologies such as scaffold chemistries, high-throughput platforms, and micro/nano technologies represent enabling tools for investigating the

critical role of the liver microenvironment including stiffness in liver function and, subsequently, the development of structurally complex and clinically effective engineered liver systems. Despite these developments, the following things are still required to address this gap in knowledge; (1) the need to develop mechanically tunable technology capable of pressure-mimicking conditions with varying stiffness without any biochemical or protein intervention, (2) a better understanding of the effect of stiffness on hepatocyte metabolic changes during various stages of cirrhosis, (3) dissect the effect of stiffness in driving hepatocytes-mediated stellate cell activation, and (4) a high-throughput method to investigate the impact of stiffness on hepatocytes-non-parenchymal cell communication. Understanding the effect of increased matrix stiffness during the course of liver fibrosis on hepatocyte function will provide more insight in the role of matrix rigidity as a contributor to the disease progression and hepatic functional failure. Given that change in stiffness regulates cell function independent of the biochemical signals, *in vitro* study of stiffness and understanding its impact on hepatocytes function is critical for new therapeutic interventions for liver fibrosis and liver failure. Together, all these studies demonstrate the plausible role of stiffness in regulating hepatocytes function and contribute to metabolic dysregulation. Understanding the impact of stiffness on hepatocytes biology will provide significantly more nuanced data to aid drug development for liver diseases.

## References

1. Asrani SK, Larson JJ, Yawn B, Therneau TM, Kim WR. Underestimation of liver-related mortality in the United States. *Gastroenterology*. 2013;145(2):375–82.e1–2.
2. Liver disease in Europe. *Lancet*. 2013;381(9866):508.
3. Iredale JP, Thompson A, Henderson NC. Extracellular matrix degradation in liver fibrosis: biochemistry and regulation. *Biochim Biophys Acta*. 2013;1832(7):876–83.
4. Mederacke I. Liver fibrosis—mouse models and relevance in human liver diseases. *Z Gastroenterol*. 2013;51(1):55–62.
5. Ramachandran P, Iredale JP. Liver fibrosis: a bidirectional model of fibrogenesis and resolution. *QJM*. 2012;105(9):813–7.
6. Foucher J, Chanteloup E, Vergniol J, Castera L, Le Bail B, Adhoute X, et al. Diagnosis of cirrhosis by transient elastography (FibroScan): a prospective study. *Gut*. 2006;55(3):403–8.
7. Georges PC, Hui JJ, Gombos Z, McCormick ME, Wang AY, Uemura M, et al. Increased stiffness of the rat liver precedes matrix deposition: implications for fibrosis. *Am J Physiol Gastrointest Liver Physiol*. 2007;293(6):G1147–54.
8. Yin M, Kolipaka A, Woodrum DA, Glaser KJ, Romano AJ, Manduca A, et al. Hepatic and splenic stiffness augmentation assessed with MR elastography in an *in vivo* porcine portal hypertension model. *J Magn Reson Imaging*. 2013;38(4):809–15.
9. Yin M, Talwalkar JA, Glaser KJ, Manduca A, Grimm RC, Rossman PJ, et al. Assessment of hepatic fibrosis with magnetic resonance elastography. *Clin Gastroenterol Hepatol*. 2007;5(10):1207–13.e2.
10. Takeda T, Yasuda T, Nakayama Y, Nakaya M, Kimura M, Yamashita M, et al. Usefulness of noninvasive transient elastography for assessment of liver fibrosis stage in chronic hepatitis C. *World J Gastroenterol*. 2006;12(48):7768–73.



11. Mueller S, Sandrin L. Liver stiffness: a novel parameter for the diagnosis of liver disease. *Hepat Med.* 2010;2:49–67.
12. Henderson NC, Forbes SJ. Hepatic fibrogenesis: from within and outwith. *Toxicology.* 2008;254(3):130–5.
13. Lozoya OA, Wauthier E, Turner RA, Barbier C, Prestwich GD, Guilak F, et al. Regulation of hepatic stem/progenitor phenotype by microenvironment stiffness in hydrogel models of the human liver stem cell niche. *Biomaterials.* 2011;32(30):7389–402.
14. Wells RG. The role of matrix stiffness in regulating cell behavior. *Hepatology.* 2008;47(4):1394–400.
15. Arias I, Wolkoff A, Boyer J, Shafritz D, Fausto N, Alter H, et al. *The liver: biology and pathobiology.* Chichester: Wiley; 2011.
16. Arias IM, Boyer J, Shafritz D, Fausto N, Alter H, Cohen DE, Wolkoff A. *The liver: biology and pathology.* Hoboken: Wiley Blackwell; 2010. 1216 p.
17. Rouiller C. *The liver: morphology, biochemistry, physiology.* New York: Academic; 2013.
18. Zakim D, Boyer T, *Hepatology A. Textbook of liver disease.* Philadelphia: WB Saunders Company; 1996.
19. Pinzani M, Marra F, Carloni V. Signal transduction in hepatic stellate cells. *Liver.* 1998;18(1):2–13.
20. Van den Eynden GG, Majeed AW, Illemann M, Vermeulen PB, Bird NC, Høyer-Hansen G, et al. The multifaceted role of the microenvironment in liver metastasis: biology and clinical implications. *Cancer Res.* 2013;73(7):2031–43.
21. Kidambi S, Yarmush RS, Novik E, Chao P, Yarmush ML, Nahmias Y. Oxygen-mediated enhancement of primary hepatocyte metabolism, functional polarization, gene expression, and drug clearance. *Proc Natl Acad Sci.* 2009;106(37):15714–9.
22. Bhatia S, Balis U, Yarmush M, Toner M. Effect of cell–cell interactions in preservation of cellular phenotype: cocultivation of hepatocytes and nonparenchymal cells. *FASEB J.* 1999;13(14):1883–900.
23. Uygun BE, Soto-Gutierrez A, Yagi H, Izamis M-L, Guzzardi MA, Shulman C, et al. Organ reengineering through development of a transplantable recellularized liver graft using decellularized liver matrix. *Nat Med.* 2010;16(7):814–20.
24. Wong SF, Choi YY, Kim DS, Chung BG, Lee S-H. Concave microwell based size-controllable hepatosphere as a three-dimensional liver tissue model. *Biomaterials.* 2011;32(32):8087–96.
25. Bhandari RN, Riccalton LA, Lewis AL, Fry JR, Hammond AH, Tendler SJ, et al. Liver tissue engineering: a role for co-culture systems in modifying hepatocyte function and viability. *Tissue Eng.* 2001;7(3):345–57.
26. Kidambi S, Sheng LF, Yarmush ML, Toner M, Lee I, Chan C. Patterned co-culture of primary hepatocytes and fibroblasts using polyelectrolyte multilayer templates. *Macromol Biosci.* 2007;7(3):344–53.
27. Kidambi S, Lee I, Chan C. Controlling primary hepatocyte adhesion and spreading on protein-free polyelectrolyte multilayer films. *J Am Chem Soc.* 2004;126(50):16286–7.
28. Bataller R, Brenner DA. Liver fibrosis. *J Clin Invest.* 2005;115(2):209–18.
29. Friedman SL. Liver fibrosis—from bench to bedside. *J Hepatol.* 2003;38:38–53.
30. Hernandez-Gea V, Friedman SL. Pathogenesis of liver fibrosis. *Annu Rev Pathol.* 2011;6:425–56.
31. Mammoto T, Ingber DE. Mechanical control of tissue and organ development. *Development.* 2010;137(9):1407–20.
32. Ferraioli G, Tinelli C, Dal Bello B, Zicchetti M, Filice G, Filice C. Accuracy of real-time shear wave elastography for assessing liver fibrosis in chronic hepatitis C: a pilot study. *Hepatology.* 2012;56(6):2125–33.
33. Friedrich-Rust M, Ong MF, Martens S, Sarrazin C, Bojunga J, Zeuzem S, et al. Performance of transient elastography for the staging of liver fibrosis: a meta-analysis. *Gastroenterology.* 2008;134(4):960–74.e8.
34. Yin M, Woollard J, Wang X, Torres VE, Harris PC, Ward CJ, et al. Quantitative assessment of hepatic fibrosis in an animal model with magnetic resonance elastography. *Magn Reson Med.* 2007;58(2):346–53.

35. Wang H-B, Dembo M, Wang Y-L. Substrate flexibility regulates growth and apoptosis of normal but not transformed cells. *Am J Physiol Cell Physiol.* 2000;279(5):C1345–C50.
36. Hsiong SX, Carampin P, Kong HJ, Lee KY, Mooney DJ. Differentiation stage alters matrix control of stem cells. *J Biomed Mater Res A.* 2008;85(1):145–56.
37. Park JS, Chu JS, Tsou AD, Diop R, Tang Z, Wang A, et al. The effect of matrix stiffness on the differentiation of mesenchymal stem cells in response to TGF- $\beta$ . *Biomaterials.* 2011;32(16):3921–30.
38. Discher DE, Janney P, Wang YL. Tissue cells feel and respond to the stiffness of their substrate. *Science.* 2005;310(5751):1139–43.
39. Ingber DE. Cellular mechanotransduction: putting all the pieces together again. *FASEB J.* 2006;20(7):811–27.
40. McBeath R, Pirone DM, Nelson CM, Bhadriraju K, Chen CS. Cell shape, cytoskeletal tension, and RhoA regulate stem cell lineage commitment. *Dev Cell.* 2004;6(4):483–95.
41. Desmoulière A, Darby I, Costa A, Raccurt M, Tuchweber B, Sommer P, et al. Extracellular matrix deposition, lysyl oxidase expression, and myofibroblastic differentiation during the initial stages of cholestatic fibrosis in the rat. *Lab Invest.* 1997;76(6):765–78.
42. Brenner DA, Waterboer T, Choi SK, Lindquist JN, Stefanovic B, Burchardt E, et al. New aspects of hepatic fibrosis. *J Hepatol.* 2000;32:32–8.
43. Li Z, Dranoff JA, Chan EP, Uemura M, Sevigny J, Wells RG. Transforming growth factor-beta and substrate stiffness regulate portal fibroblast activation in culture. *Hepatology.* 2007;46(4):1246–56.
44. Sakata R, Ueno T, Nakamura T, Ueno H, Sata M. Mechanical stretch induces TGF- $\beta$  synthesis in hepatic stellate cells. *Eur J Clin Invest.* 2004;34(2):129–36.
45. Zeisberg M, Yang C, Martino M, Duncan MB, Rieder F, Tanjore H, et al. Fibroblasts derive from hepatocytes in liver fibrosis via epithelial to mesenchymal transition. *J Biol Chem.* 2007;282(32):23337–47.
46. Schrader J, Gordon-Walker TT, Aucott RL, van Deemter M, Quaas A, Walsh S, et al. Matrix stiffness modulates proliferation, chemotherapeutic response, and dormancy in hepatocellular carcinoma cells. *Hepatology.* 2011;53(4):1192–205.
47. Tateno C, Yoshizato K. Long-term cultivation of adult rat hepatocytes that undergo multiple cell divisions and express normal parenchymal phenotypes. *Am J Pathol.* 1996;148(2):383.
48. Clayton DF, Darnell J. Changes in liver-specific compared to common gene transcription during primary culture of mouse hepatocytes. *Mol Cell Biol.* 1983;3(9):1552–61.
49. Griffith LG, Swartz MA. Capturing complex 3D tissue physiology in vitro. *Nat Rev Mol Cell Biol.* 2006;7(3):211–24.
50. Sawada H, Takami K, Asahi S. A toxicogenomic approach to drug-induced phospholipidosis: analysis of its induction mechanism and establishment of a novel in vitro screening system. *Toxicol Sci.* 2005;83(2):282–92.
51. Natarajan V, Berglund EJ, Chen DX, Kidambi S. Substrate stiffness regulates primary hepatocyte functions. *RSC Adv.* 2015;5(99):80956–66.
52. Dunn JC, Yarmush ML, Koebe HG, Tompkins RG. Hepatocyte function and extracellular matrix geometry: long-term culture in a sandwich configuration. *FASEB J.* 1989;3(2):174–7.
53. Youssef J, Chen P, Shenoy VB, Morgan JR. Mechanotransduction is enhanced by the synergistic action of heterotypic cell interactions and TGF- $\beta$ 1. *FASEB J.* 2012;26(6):2522–30.
54. You J, Park SA, Shin DS, Patel D, Raghunathan VK, Kim M, et al. Characterizing the effects of heparin gel stiffness on function of primary hepatocytes. *Tissue Eng Part A.* 2013;19(23–24):2655–63.
55. LeCluyse E, Bullock P, Madan A, Carroll K, Parkinson A. Influence of extracellular matrix overlay and medium formulation on the induction of cytochrome P-450 2B enzymes in primary cultures of rat hepatocytes. *Drug Metab Dispos.* 1999;27(8):909–15.
56. Lin P, Chan WC, Badylak SF, Bhatia SN. Assessing porcine liver-derived biomatrix for hepatic tissue engineering. *Tissue Eng.* 2004;10(7–8):1046–53.



57. Guillouzo A. Liver cell models in in vitro toxicology. *Environ Health Perspect.* 1998;106(Suppl 2):511–32.
58. Peregelyuk M, Chin L, Cao X, van Oosten A, Shenoy VB, Janmey PA, et al. Normal and fibrotic rat livers demonstrate shear strain softening and compression stiffening: a model for soft tissue mechanics. *PLoS One.* 2016;11(1):e0146588.
59. Zustiak S, Nossal R, Sackett DL. Multiwell stiffness assay for the study of cell responsiveness to cytotoxic drugs. *Biotechnol Bioeng.* 2014;111(2):396–403.
60. Yeung T, Georges PC, Flanagan LA, Marg B, Ortiz M, Funaki M, et al. Effects of substrate stiffness on cell morphology, cytoskeletal structure, and adhesion. *Cell Motil Cytoskeleton.* 2005;60(1):24–34.
61. Engler AJ, Sen S, Sweeney HL, Discher DE. Matrix elasticity directs stem cell lineage specification. *Cell.* 2006;126(4):677–89.
62. Regehr KJ, Domenech M, Koepsel JT, Carver KC, Ellison-Zelski SJ, Murphy WL, et al. Biological implications of polydimethylsiloxane-based microfluidic cell culture. *Lab Chip.* 2009;9(15):2132–9.
63. Deegan DB, Zimmerman C, Skardal A, Atala A, Shupe TD. Stiffness of hyaluronic acid gels containing liver extracellular matrix supports human hepatocyte function and alters cell morphology. *J Mech Behav Biomed Mater.* 2015;55:87–103.
64. Xia T, Zhao R, Liu W, Huang Q, Chen P, Waju YN, et al. Effect of substrate stiffness on hepatocyte migration and cellular Young's modulus. *J Cell Physiol.* 2018;233(9):6996–7006.
65. Mata A, Fleischman AJ, Roy S. Characterization of polydimethylsiloxane (PDMS) properties for biomedical micro/nanosystems. *Biomed Microdevices.* 2005;7(4):281–93.
66. Dario P, Carrozza MC, Benvenuto A, Menciasci A. Micro-systems in biomedical applications. *J Micromech Microeng.* 2000;10(2):235.
67. Tzvetkova-Chevolleau T, Stéphanou A, Fuard D, Ohayon J, Schiavone P, Tracqui P. The motility of normal and cancer cells in response to the combined influence of the substrate rigidity and anisotropic microstructure. *Biomaterials.* 2008;29(10):1541–51.
68. Natarajan V, Moeller M, Casey CA, Harris EN, Kidambi S. Matrix Stiffness Regulates Liver Sinusoidal Endothelial Cell Function Mimicking Responses in Fatty Liver Disease. *bioRxiv*, 2020, <https://doi.org/10.1101/2020.01.27.921353>.
69. Daverey A, Mytty A, Kidambi S. Topography mediated regulation of HER-2 expression in breast cancer cells. *Nano LIFE.* 2012;2(3):1241009.
70. Kidambi S, Udpa N, Schroeder SA, Findlan R, Lee I, Chan C. Cell adhesion on polyelectrolyte multilayer coated polydimethylsiloxane surfaces with varying topographies. *Tissue Eng.* 2007;13(8):2105–17.
71. Huang X, Hang R, Wang X, Lin N, Zhang X, Tang B. Matrix stiffness in three-dimensional systems effects on the behavior of C3A cells. *Artif Organs.* 2013;37(2):166–74.
72. Ben-Ze'ev A, Robinson GS, Bucher N, Farmer SR. Cell-cell and cell-matrix interactions differentially regulate the expression of hepatic and cytoskeletal genes in primary cultures of rat hepatocytes. *Proc Natl Acad Sci.* 1988;85(7):2161–5.
73. Mooney D, Hansen L, Vacanti J, Langer R, Farmer S, Ingber D. Switching from differentiation to growth in hepatocytes: control by extracellular matrix. *J Cell Physiol.* 1992;151(3):497–505.
74. Hansen LK, Wilhelm J, Fassett JT. Regulation of hepatocyte cell cycle progression and differentiation by type I collagen structure. *Curr Top Dev Biol.* 2006;72:205–36, 1 plate.
75. Fassett J, Tobolt D, Hansen LK. Type I collagen structure regulates cell morphology and EGF signaling in primary rat hepatocytes through cAMP-dependent protein kinase A. *Mol Biol Cell.* 2005;17(1):345–56.
76. Nagaki M, Sugiyama A, Naiki T, Ohsawa Y, Moriwaki H. Control of cyclins, cyclin-dependent kinase inhibitors, p21 and p27, and cell cycle progression in rat hepatocytes by extracellular matrix. *J Hepatol.* 2000;32(3):488–96.
77. Nagaki M, Shidoji Y, Yamada Y, Sugiyama A, Tanaka M, Akaike T, et al. Regulation of hepatic genes and liver transcription factors in rat hepatocytes by extracellular matrix. *Biochem Biophys Res Commun.* 1995;210(1):38–43.

78. DiPersio CM, Jackson DA, Zaret KS. The extracellular matrix coordinately modulates liver transcription factors and hepatocyte morphology. *Mol Cell Biol.* 1991;11(9):4405–14.
79. Brill S, Zvibel I, Halpern Z, Oren R. The role of fetal and adult hepatocyte extracellular matrix in the regulation of tissue-specific gene expression in fetal and adult hepatocytes. *Eur J Cell Biol.* 2002;81(1):43–50.
80. Desai SS, Tung JC, Zhou VX, Grenert JP, Malato Y, Rezvani M, et al. Physiological ranges of matrix rigidity modulate primary mouse hepatocyte function in part through hepatocyte nuclear factor 4 alpha. *Hepatology.* 2016;64(1):261–75.
81. Wilson CL, Hayward SL, Kidambi S. Astrogliosis in a dish: substrate stiffness induces astrogliosis in primary rat astrocytes. *RSC Adv.* 2016;6(41):34447–57.
82. Cozzolino AM, Noce V, Battistelli C, Marchetti A, Grassi G, Cicchini C, et al. Modulating the substrate stiffness to manipulate differentiation of resident liver stem cells and to improve the differentiation state of hepatocytes. *Stem Cells Int.* 2016;2016:5481493.
83. Chen AA, Khetani SR, Lee S, Bhatia SN, Van Vliet KJ. Modulation of hepatocyte phenotype in vitro via chemomechanical tuning of polyelectrolyte multilayers. *Biomaterials.* 2009;30(6):1113–20.
84. Semler EJ, Lancin PA, Dasgupta A, Moghe PV. Engineering hepatocellular morphogenesis and function via ligand-presenting hydrogels with graded mechanical compliance. *Biotechnol Bioeng.* 2005;89(3):296–307.
85. Xia T, Zhao R, Feng F, Song Y, Zhang Y, Dong L, et al. Gene expression profiling of human hepatocytes grown on differing substrate stiffness. *Biotechnol Lett.* 2018;40(5):809–18.
86. Bowler BE. Thermodynamics of protein denatured states. *Mol BioSyst.* 2007;3(2):88–99.
87. Battle AR, Ridone P, Bavi N, Nakayama Y, Nikolaev YA, Martinac B. Lipid-protein interactions: lessons learned from stress. *Biochim Biophys Acta.* 2015;1848(9):1744–56.
88. Bordeleau F, Califano JP, Negron Abril YL, Mason BN, LaValley DJ, Shin SJ, et al. Tissue stiffness regulates serine/arginine-rich protein-mediated splicing of the extra domain B-fibronectin isoform in tumors. *Proc Natl Acad Sci U S A.* 2015;112(27):8314–9.
89. Saha K, Kim J, Irwin E, Yoon J, Momin F, Trujillo V, et al. Surface creasing instability of soft polyacrylamide cell culture substrates. *Biophys J.* 2010;99(12):L94–6.
90. Moeller M, Thulasingham S, Narasimhan M, Kidambi S. Stiffness Induces NAFLD-Like Metabolic Dysfunction in Primary Hepatocytes. *Hepatology.* 2019;70:119A.

# Chapter 56

## Liver Mechanics and the Profibrotic Response at the Cellular Level



Rebecca G. Wells

### Hepatic Stellate Cells and Other Cells of the Liver Are Mechanosensitive

The modern appreciation for the influence of mechanical factors on cell phenotype began 20 years ago with the publication of a seminal paper by Pelham and Wang showing that both epithelial cells and fibroblasts were more spread and less migratory, with increased dynamic focal adhesions, when cultured on soft rather than stiff polyacrylamide hydrogels [1]. Other groups went on to systematically validate the hydrogel method and demonstrate the critical importance of mechanics [2], often in combination with soluble factors, in determining the behavior of multiple cell types, including mesenchymal stem cells [2–4].

These concepts proved to be applicable to myofibroblasts in general and to hepatic stellate cell- and portal fibroblast-derived liver myofibroblasts in particular [5]. Both liver cell types underwent activation to fibrogenic myofibroblasts on stiff, but not soft hydrogels (Fig. 56.1); intermediate stiffnesses resulted in intermediate phenotypes, and all phenotypes were stable for weeks, suggesting that mechanosensing is an active and continuous process [6, 7]. Others have used a similar polyacrylamide hydrogel system to show that stiffness is inversely correlated with stellate cell production of MMP-9 and TIMP-1, which is postulated to contribute to the perpetuation of fibrosis [8]. While portal fibroblasts on polyacrylamide hydrogels had an additional requirement for transforming growth factor- $\beta$  (TGF- $\beta$ ), underscoring the cooperative role of soluble and mechanical factors in regulating cell phenotype, TGF- $\beta$  could not overcome the need for a stiff environment for activation for either kind of liver cell [6].

---

R. G. Wells (✉)  
University of Pennsylvania, Philadelphia, PA, USA  
e-mail: [rgwells@penncmedicine.upenn.edu](mailto:rgwells@penncmedicine.upenn.edu)

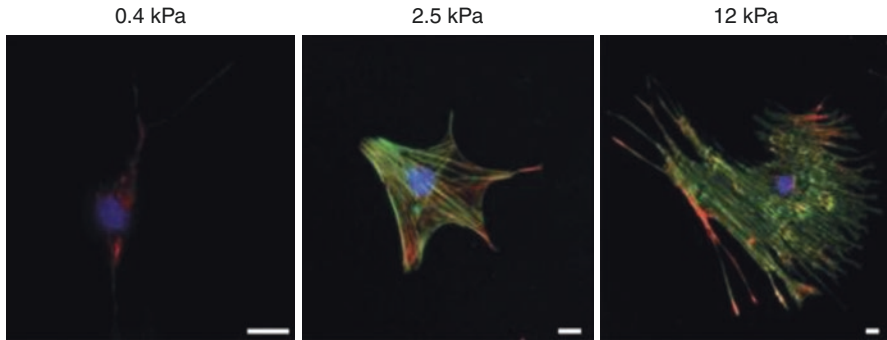


**Fig. 56.1** Hepatic stellate cells undergo myfibroblastic activation on stiff substrates. Primary rat hepatic stellate cells were isolated and cultured for 7 days on collagen-coated polyacrylamide hydrogels with shear elastic moduli ranging from 0.4 to 12 kPa, as shown. Cells were immunostained with antibodies against desmin (red) and  $\alpha$ -smooth muscle actin (green), and with the nuclear marker DAPI. Size bars, 10  $\mu$ m. (Reprinted from Olsen et al. [7])

The stiffness dependence of hepatic stellate cell activation has been validated using other mechanically tunable culture systems, including dynamically stiffening methacrylated hyaluronic acid-based gels. These demonstrate that freshly isolated stellate cells in culture require a period of recovery after isolation but then rapidly adapt their activation state to the stiffness of the gel—cells remain quiescent while the gels are soft but undergo myfibroblast activation within one day when the gels are stiffened [9, 10].

Stellate cells *in vivo* also require a stiff environment for myfibroblastic activation. In a rat carbon tetrachloride model of injury, livers became stiff early after injury, before significant matrix deposition. Notably, covalent cross-links mediated by members of the lysyl oxidase (LOX) family of enzymes began to increase soon after injury [11], and LOX inhibitors blunted the increase in stiffness as well as the initial wave of myfibroblast activation. This suggested that collagen cross-linking precedes fibrosis, causing the mechanical changes that drive myfibroblast activation [12]. Indeed, *in vitro*, increased covalent cross-linking enhanced collagen stiffness independent of concentration [13]. In lung fibrosis models, lung myfibroblasts were similarly dependent on collagen cross-link-mediated changes in stiffness, suggesting that mechanical changes in collagen precede fibrosis as a general phenomenon [14].

Hepatic stellate cells and portal fibroblasts are not the only mechanosensitive cells of the liver. Mechanics are particularly important to hepatocyte function and there are major functional ramifications when hepatocytes are exposed to the levels of stiffness seen in fibrosis (see Chap. 58). Hepatocytes exposed to stiff environments in 2D culture undergo rapid dedifferentiation, becoming highly proliferative [15, 16]. A recent detailed study using polyacrylamide hydrogels demonstrated that hepatocytes require very soft substrates (consistent with the stiffness of normal livers) to maintain a differentiated state as assessed by albumin production, glycogen storage, and HNF4 $\alpha$  expression [17]. Fibrotic levels of stiffness increased the activity of mechanotransduction pathways, which acted directly to decrease HNF4 $\alpha$  and led to dedifferentiation.

Sinusoidal endothelial cells, which are exposed to many of the same mechanical changes in fibrosis as hepatocytes, are also mechanosensitive, dedifferentiating at higher stiffnesses with a near-complete loss of fenestrae, increased surface expression of CD31 and podosome diameter, and marked actin cytoskeleton reorganization [18, 19]. The participation of sinusoidal endothelial cells in angiogenesis in fibrosis also appears to be stiffness sensitive [20]. For another cell type, bipotential liver progenitor cells, stiffness in combination with the chemical nature of the ECM regulates cell fate [21].

Almost all cells studied demonstrate phenotypic changes in response to stiffness; thus, while the mechano-responsiveness of some populations of cells of the liver has not necessarily been formally studied, the global mechanical changes in fibrosis are likely responsible for a similarly global cellular dysfunction throughout the fibrotic liver.

## Mechanotransduction Pathways in the Liver

Cells convert mechanical signals from the extracellular environment into biochemical intracellular signals via the process of mechanotransduction. While extracellular mechanical signals include fluid flow, stretch, and hydrostatic and osmotic pressure and are important in the regenerative as well as fibrotic responses to injury [22], we consider here mechanotransduction that results from cells exerting tension on substrates that, depending on how stiff they are, provide variable degrees of resistance.

There are significant differences between signaling by soluble (chemical) factors and by mechanical factors. Chief among these is that mechanical forces are directional, allowing for signals to be transmitted in three dimensions, while soluble forces diffuse radially, limiting the complexity of the signal. Mechanical signals are also more long-lived over distance, decaying as a function  $1/r$  (where  $r$  is the radius) through an elastic substrate (and over even longer distances in fibrous substrates), in comparison to soluble signals, which decay as  $1/r^2$  [2, 23, 24].

Mechanotransduction begins with the binding of cell surface receptors (primarily integrins) to the ECM, with subsequent integrin clustering [25]. ECM binding and clustering result in the recruitment of potentially hundreds of proteins, including vinculin and talin, to integrins at the cell membrane and the formation of large and dynamic force-sensitive macromolecular complexes termed focal adhesions. These complexes contain focal adhesion kinase as well as many src-family kinases that, through a series of tyrosine phosphorylations and docking events, transfer mechanical signals to the actin cytoskeleton, which is connected to integrins via their C-terminal tails. Cytoskeletal contractility, mediated by myosin and the activity of the Rho/Rho-associated protein kinase (ROCK) pathway, results in transmission of force to the nucleus [26, 27].

One of the most important transcriptional mediators is the HIPPO pathway effector Yes-associated protein (YAP) and the structurally similar protein transcriptional co-activator with PDZ-binding motif (TAZ), which demonstrate mechanosensitive movement into the nucleus [28, 29]. YAP nuclear localization reflects the degree of

hepatic stellate cell activation *in vitro* [9, 30] and it has also been shown to be a key driver of hepatic stellate cell activation [31]; its inhibition prevents fibrosis *in vivo* in a mouse carbon tetrachloride model [31]. Integrin  $\beta 1$ , likely with integrin  $\alpha 11$  as a binding partner, signals via p21-activated protein kinase (PAK) and YAP to mediate fibrosis; inhibition or inactivation of any of these pathway components abrogated fibrosis in a similar mouse model [32].

Another major mechanotransduction pathway is through myocardin-related transcription factor (MRTF)-A/MAL/MLK1, which undergoes mechanosensitive dissociation from G-actin in the cytoplasm, followed by movement into the nucleus and activation of serum response factor (SRF) [33, 34]. This pathway, like YAP pathways, may play a role in hepatic stellate cell activation, either directly or indirectly via hepatocytes [35, 36].

Although their intracellular signaling pathways differ, mechanical and soluble signals may potentiate or dampen each other [37]. As an example, the major pro-fibrotic soluble factor TGF- $\beta$ , which is secreted in latent form, undergoes activation in part through the application of mechanical force to its latent form when adherent to a stiff substrate [38, 39]. Another example is that of the G-protein-coupled estrogen receptor, which signals via RhoA and myosin to reduce stellate cell mechanosensing and YAP activation and induces regression to quiescence from the myofibroblastic state [40]. RhoA in some cases sends mechanical signals through the transcriptional co-activator p300 in hepatic stellate cells [41]. Future work on stellate cell mechanotransduction will need to determine whether the different reported pathways are linked and whether there is a universal pathway in fibrosis.

## **Mechanics of the ECM and Their Relevance to Liver Cells in Fibrosis**

Studies using variable-stiffness hydrogels like polyacrylamide have played an important role in broadening our understanding of the role of mechanics in cell behavior, but nonetheless fail to model many critical features of the mechanical environment *in vitro*. In particular, the ECM is not a homogenous, linearly elastic hydrogel (where the relationship between stress and strain, and therefore the elastic modulus, is constant), particularly in fibrosis [17], but rather a heterogeneous mixture of fibrous and gel-like components with significant nonlinearly elastic features (such that stiffness and therefore elastic modulus change nonlinearly in response to strain).

This heterogeneity has an important impact on cell phenotype. When hepatic stellate cells were plated on gels with patterns including both soft and stiff regions, cells on patterns large enough to permit spreading ( $>100 \mu\text{m}$ ) responded according to the local stiffness, even if close to a boundary [10]. However, engineered systems that mimic microscale mechanical heterogeneity (patches with diameters less than several  $\mu\text{m}^2$ ) suggest that the pattern of heterogeneity can influence phenotype, although these have not been tested with hepatic stellate cells [42, 43].

## Cross-Linking and Fibrous Networks

Cells in tissues reside in fibrous networks, defined as cross-linked webs of ECM proteins with large pore sizes relative to fiber diameter. Cells adhere to fibers and pull on them as they stiffness sense, causing—if the fibers permit mechanically—fiber rearrangements and enabling long-range transmission of force [24, 43, 44]; this is an important determinant of tissue mechanics [45]. Experimental work using synthetic fiber systems has added a nuance to the soft vs. stiff paradigm of cell phenotype identified using polyacrylamide and other hydrogels. A synthetic fiber system of methacrylated dextran in which cross-link density, fiber stiffness, fiber diameter, and functionalization could be varied showed that cells on soft fibers spread and proliferated more than cells on stiff [46], demonstrating that in fibrous systems there was a stiffness optimum. A hyaluronic acid-based fibrous gel system showed the same for hepatic stellate cells: soft substrates promoted spreading and activation, while cells on stiff fibers (with stronger and less breakable cross-links) were unable to reorganize the fibers and showed less activation (Fig. 56.2) [47]. Theoretical analyses suggest that fiber recruitment enables cells to increase ligand density (for adhesion), providing a way to reconcile different observations obtained using elastic substrates versus nonlinearly elastic fibrous substrates [48].

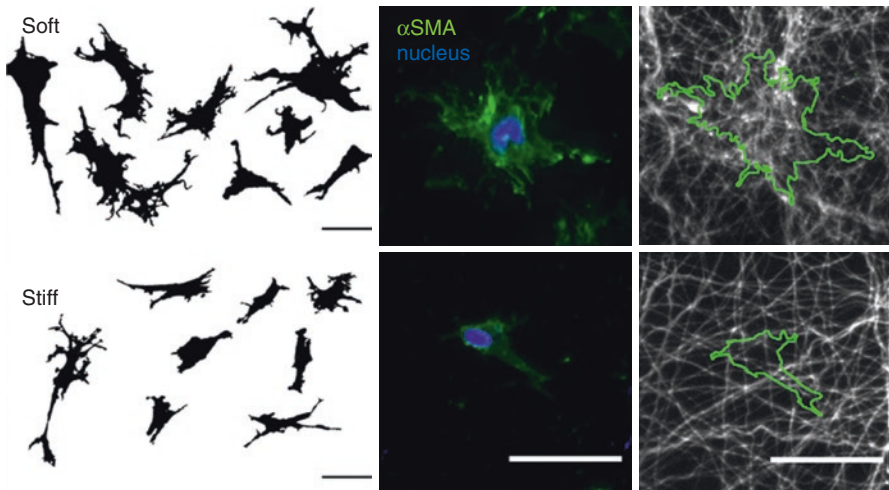


**Fig. 56.2** Hepatic stellate cells show more activated behavior on soft than on stiff fibers. Primary rat hepatic stellate cells were cultured on cross-linked hyaluronic acid-based fibers with varied mechanical properties. Cell masks (left) and  $\alpha$ -smooth muscle actin immunostains (green, with DAPI nuclear labeling in blue) show increased spreading on soft fibers (top) when compared to stiff fibers (bottom). Fluorescent images of the fiber system (right) with the cells from the middle panels outlined in green demonstrate increased recruitment of soft fibers. Size bars, 50  $\mu$ m. (Reprinted with permission from Davidson et al. [47])



Fibrous septa in liver fibrosis, as in bridging fibrosis or cirrhosis, are composed of aligned collagen fibrous networks. How heavily cross-linked these septa are and how local stellate cells and portal fibroblasts respond to and reorganize them is not known. In vitro studies show that cells cause plastic (permanent) rearrangements of collagen networks, with alignment and compaction of collagen fibers [49], but it has not yet been proven that stellate cells mediate these changes in vivo.

### *Proteoglycans and Glycosaminoglycans*

Glycosaminoglycans (GAGs), which are long linear carbohydrate chains, and proteoglycans (proteins with GAG modifications) are a major component of the ECM and make a significant contribution to the volume of ECM and tissues. With collagen, they increase markedly in liver fibrosis [50], with potentially significant mechanical implications that have not yet been fully explored. Hyaluronic acid, the major tissue GAG, and many proteoglycans bind to collagen and to each other to form large complexes, and experimental and theoretical work has shown that this increases collagen swelling and stiffness [51]. Liver fibrosis studies with mice lacking certain proteoglycans show variable but definite effects on fibrosis; although the mechanism of these effects is not known and may or may not be mechanical, this highlights the complexity of the matrix and its impact on cell phenotype in vivo [52, 53]. In vitro, the addition of lumican to collagen leads to increased hepatic stellate cell activation although, as in vivo, the role of mechanics was not studied [54].

### *Viscosity*

Although most mechanical studies in liver fibrosis have focused on the structural property of stiffness or the similar material property of elastic modulus, other mechanical properties of the ECM and tissues are of increasing interest, particularly viscosity. New polyacrylamide substrates that enable the separation of elastic and viscous properties have shown that hepatic stellate cells are highly responsive to viscosity. In one example, stellate cells demonstrate different degrees of myofibroblastic differentiation on substrates with the same elastic modulus, but different loss moduli (viscosities) [55]. Bulk liver viscosity is typically small (10–20%) in comparison to elasticity, although some reports have suggested that it changes in fibrosis and may be clinically relevant [11, 56]. Yet, both the details of viscosity sensing and the determinants of viscosity in tissues are unknown. In the future, it will be important to incorporate accurate and defined viscosities into in vitro culture systems in order to better understand the impact of this property on cell phenotype and signaling pathways.



## Conclusions

Stiffness of the liver is now—as this volume makes clear—firmly established as an important mechanistic, diagnostic, and prognostic factor in liver fibrosis. Similarly, a large number of studies have established that the stiffness of the organ translates to the cellular level and that mechanics are a key determinant not just of hepatic stellate cell fibrogenesis but of the phenotype of all other cells of the liver. Less clear are the specific mechanotransduction pathways that lead to phenotypic changes like fibrogenesis, the range of mechanical properties that cells respond to and, critically, the features and scale of the ECM that determine these properties. It will be important to understand these points in order to harness the potential for mechanical manipulation to treat disease.

## References

1. Pelham RJ, Wang Y. Cell locomotion and focal adhesions are regulated by substrate flexibility. *Proc Natl Acad Sci.* 1997;94(25):13661–5.
2. Wen JH, Vincent LG, Fuhrmann A, Choi YS, Hribar KC, Taylor-Weiner H, et al. Interplay of matrix stiffness and protein tethering in stem cell differentiation. *Nat Mater.* 2014;13(10):979–87.
3. Deroanne C. In vitro tubulogenesis of endothelial cells by relaxation of the coupling extracellular matrix-cytoskeleton. *Cardiovasc Res.* 2001;49(3):647–58.
4. Discher DE, Janmey P, Wang YL. Tissue cells feel and respond to the stiffness of their substrate. *Science.* 2005;310(5751):1139–43.
5. Wells RG. Tissue mechanics and fibrosis. *Biochim Biophys Acta.* 2013;1832(7):884–90.
6. Li Z, Dranoff JA, Chan EP, Uemura M, Sevigny J, Wells RG. Transforming growth factor-beta and substrate stiffness regulate portal fibroblast activation in culture. *Hepatology.* 2007;46(4):1246–56.
7. Olsen AL, Bloomer SA, Chan EP, Gaca MD, Georges PC, Sackey B, et al. Hepatic stellate cells require a stiff environment for myofibroblastic differentiation. *Am J Physiol Gastrointest Liver Physiol.* 2011;301(1):G110–8.
8. Lachowski D, Cortes E, Rice A, Pinato D, Rombouts K, del Rio Hernandez A. Matrix stiffness modulates the activity of MMP-9 and TIMP-1 in hepatic stellate cells to perpetuate fibrosis. *Sci Rep.* 2019;9(1):7299.
9. Caliani SR, Perepelyuk M, Soulas EM, Lee GY, Wells RG, Burdick JA. Gradually softening hydrogels for modeling hepatic stellate cell behavior during fibrosis regression. *Integr Biol.* 2016;8(6):720–8.
10. Guvendiren M, Perepelyuk M, Wells RG, Burdick JA. Hydrogels with differential and patterned mechanics to study stiffness-mediated myofibroblastic differentiation of hepatic stellate cells. *J Mech Behav Biomed Mater.* 2014;38:198–208.
11. Perepelyuk M, Terajima M, Wang AY, Georges PC, Janmey PA, Yamauchi M, et al. Hepatic stellate cells and portal fibroblasts are the major cellular sources of collagens and lysyl oxidases in normal liver and early after injury. *Am J Physiol Gastrointest Liver Physiol.* 2013;304(6):G605–G14.
12. Georges PC, Hui JJ, Gombos Z, McCormick ME, Wang AY, Uemura M, et al. Increased stiffness of the rat liver precedes matrix deposition: implications for fibrosis. *Am J Physiol Gastrointest Liver Physiol.* 2007;293(6):G1147–54.

13. Elbjeirami WM, Yonter EO, Starcher BC, West JL. Enhancing mechanical properties of tissue-engineered constructs via lysyl oxidase crosslinking activity. *J Biomed Mater Res.* 2003;66A(3):513–21.
14. Jones DP, Eklow L, Thor H, Orrenius S. Metabolism of hydrogen peroxide in isolated hepatocytes: relative contributions of catalase and glutathione peroxidase in decomposition of endogenously generated H<sub>2</sub>O<sub>2</sub>. *Arch Biochem Biophys.* 1981;210(2):505–16.
15. Semler EJ, Lancin PA, Dasgupta A, Moghe PV. Engineering hepatocellular morphogenesis and function via ligand-presenting hydrogels with graded mechanical compliance. *Biotechnol Bioeng.* 2005;89(3):296–307.
16. Sharp JA, Cane KN, Lefevre C, Arnould JPY, Nicholas KR. Fur seal adaptations to lactation: insights into mammary gland function. *Curr Top Dev Biol.* 2005;72:275–308.
17. Desai SS, Tung JC, Zhou VX, Grenert JP, Malato Y, Rezvani M, et al. Physiological ranges of matrix rigidity modulate primary mouse hepatocyte function in part through hepatocyte nuclear factor 4 alpha. *Hepatology.* 2016;64(1):261–75.
18. Juin A, Planus E, Guillemot F, Horakova P, Albiges-Rizo C, Génot E, et al. Extracellular matrix rigidity controls podosome induction in microvascular endothelial cells. *Biol Cell.* 2012;105(1):46–57.
19. Ford AJ, Jain G, Rajagopalan P. Designing a fibrotic microenvironment to investigate changes in human liver sinusoidal endothelial cell function. *Acta Biomater.* 2015;24:220–7.
20. Liu L, You Z, Yu H, Zhou L, Zhao H, Yan X, et al. Mechanotransduction-modulated fibrotic microniches reveal the contribution of angiogenesis in liver fibrosis. *Nat Mater.* 2017;16(12):1252–61.
21. Kourouklis AP, Kaylan KB, Underhill GH. Substrate stiffness and matrix composition coordinately control the differentiation of liver progenitor cells. *Biomaterials.* 2016;99:82–94.
22. Song Z, Gupta K, Ng IC, Xing J, Yang YA, Yu H. Mechanosensing in liver regeneration. *Semin Cell Dev Biol.* 2017;71:153–67.
23. Janmey PA, Miller RT. Mechanisms of mechanical signaling in development and disease. *J Cell Sci.* 2010;124(1):9–18.
24. Wang H, Abhilash AS, Chen Christopher S, Wells Rebecca G, Shenoy Vivek B. Long-range force transmission in fibrous matrices enabled by tension-driven alignment of fibers. *Biophys J.* 2014;107(11):2592–603.
25. Kechagia JZ, Ivaska J, Roca-Cusachs P. Integrins as biomechanical sensors of the microenvironment. *Nat Rev Mol Cell Biol.* 2019;20(8):457–73.
26. Wolfenson H, Yang B, Sheetz MP. Steps in mechanotransduction pathways that control cell morphology. *Annu Rev Physiol.* 2019;81(1):585–605.
27. Martino F, Perestrelo AR, Vinarský V, Pagliari S, Forte G. Cellular mechanotransduction: from tension to function. *Front Physiol.* 2018;9:824.
28. Dupont S, Morsut L, Aragona M, Enzo E, Giullitti S, Cordenonsi M, et al. Role of YAP/TAZ in mechanotransduction. *Nature.* 2011;474(7350):179–83.
29. Panciera T, Azzolin L, Cordenonsi M, Piccolo S. Mechanobiology of YAP and TAZ in physiology and disease. *Nat Rev Mol Cell Biol.* 2017;18(12):758–70.
30. Caliri SR, Perepelyuk M, Cosgrove BD, Tsai SJ, Lee GY, Mauck RL, et al. Stiffening hydrogels for investigating the dynamics of hepatic stellate cell mechanotransduction during myofibroblast activation. *Sci Rep.* 2016;6(1).
31. Mannaerts I, Leite SB, Verhulst S, Thoen LF, Claerhout S, Halder G, et al. P0444: the hippo pathway effector YAP controls mouse hepatic stellate cell activation. *J Hepatol.* 2015;62:S479.
32. Martin K, Pritchett J, Llewellyn J, Mullan AF, Athwal VS, Dobie R, et al. PAK proteins and YAP-1 signalling downstream of integrin beta-1 in myofibroblasts promote liver fibrosis. *Nat Commun.* 2016;7(1):12502.
33. Zhao XH, Laschinger C, Arora P, Szasz K, Kapus A, McCulloch CA. Force activates smooth muscle -actin promoter activity through the Rho signaling pathway. *J Cell Sci.* 2007;120(10):1801–9.

34. McGee KM, Vartiainen MK, Khaw PT, Treisman R, Bailly M. Nuclear transport of the serum response factor coactivator MRTF-A is downregulated at tensional homeostasis. *EMBO Rep.* 2011;12(9):963–70.
35. Tian W, Fan Z, Li J, Hao C, Li M, Xu H, et al. Myocardin-related transcription factor A (MRTF-A) plays an essential role in hepatic stellate cell activation by epigenetically modulating TGF- $\beta$  signaling. *Int J Biochem Cell Biol.* 2016;71:35–43.
36. Li Z, Li P, Lu Y, Sun D, Zhang X, Xu Y. A non-autonomous role of MKL1 in the activation of hepatic stellate cells. *Biochim Biophys Acta.* 2019;1862(6):609–18.
37. Totaro A, Panciera T, Piccolo S. YAP/TAZ upstream signals and downstream responses. *Nat Cell Biol.* 2018;20(8):888–99.
38. Buscemi L, Ramonet D, Klingberg F, Formey A, Smith-Clerc J, Meister J-J, et al. The single-molecule mechanics of the latent TGF- $\beta$ 1 complex. *Curr Biol.* 2011;21(24):2046–54.
39. Wipff P-J, Rifkin DB, Meister J-J, Hinz B. Myofibroblast contraction activates latent TGF- $\beta$ 1 from the extracellular matrix. *J Cell Biol.* 2007;179(6):1311–23.
40. Cortes E, Lachowski D, Rice A, Thorpe SD, Robinson B, Yeldag G, et al. Tamoxifen mechanically deactivates hepatic stellate cells via the G protein-coupled estrogen receptor. *Oncogene.* 2018;38(16):2910–22.
41. Dou C, Liu Z, Tu K, Zhang H, Chen C, Yaqoob U, et al. P300 acetyltransferase mediates stiffness-induced activation of hepatic stellate cells into tumor-promoting myofibroblasts. *Gastroenterology.* 2018;154(8):2209–21.e14.
42. Dingal PCDP, Bradshaw AM, Cho S, Raab M, Buxboim A, Swift J, et al. Fractal heterogeneity in minimal matrix models of scars modulates stiff-niche stem-cell responses via nuclear exit of a mechanorepressor. *Nat Mater.* 2015;14(9):951–60.
43. Ma H, Killaars AR, DelRio FW, Yang C, Anseth KS. Myofibroblastic activation of valvular interstitial cells is modulated by spatial variations in matrix elasticity and its organization. *Biomaterials.* 2017;131:131–44.
44. Abhilash AS, Baker Brendon M, Trappmann B, Chen Christopher S, Shenoy VB. Remodeling of fibrous extracellular matrices by contractile cells: predictions from discrete fiber network simulations. *Biophys J.* 2014;107(8):1829–40.
45. van Oosten ASG, Chen X, Chin L, Cruz K, Patteson AE, Pogoda K, et al. Emergence of tissue-like mechanics from fibrous networks confined by close-packed cells. *Nature.* 2019;573(7772):96–101.
46. Baker BM, Trappmann B, Wang WY, Sakar MS, Kim IL, Shenoy VB, et al. Cell-mediated fibre recruitment drives extracellular matrix mechanosensing in engineered fibrillar microenvironments. *Nat Mater.* 2015;14(12):1262–8.
47. Davidson MD, Song KH, Lee M-H, Llewellyn J, Du Y, Baker BM, et al. Engineered fibrous networks to investigate the influence of fiber mechanics on myofibroblast differentiation. *ACS Biomater Sci Eng.* 2019;5(8):3899–908.
48. Cao X, Ban E, Baker BM, Lin Y, Burdick JA, Chen CS, et al. Multiscale model predicts increasing focal adhesion size with decreasing stiffness in fibrous matrices. *Proc Natl Acad Sci.* 2017;114(23):E4549–E55.
49. Ban E, Franklin JM, Nam S, Smith LR, Wang H, Wells RG, et al. Mechanisms of plastic deformation in collagen networks induced by cellular forces. *Biophys J.* 2018;114(2):450–61.
50. Gressner AM, Krull N, Bachem MG. Regulation of proteoglycan expression in fibrotic liver and cultured fat-storing cells. *Pathol Res Pract.* 1994;190(9-10):864–82.
51. Lai VK, Nedrelov DS, Lake SP, Kim B, Weiss EM, Tranquillo RT, et al. Swelling of collagen-hyaluronic acid co-gels: an in vitro residual stress model. *Ann Biomed Eng.* 2016;44(10):2984–93.
52. Krishnan A, Li X, Kao W-Y, Viker K, Butters K, Masuoka H, et al. Lumican, an extracellular matrix proteoglycan, is a novel requisite for hepatic fibrosis. *Lab Invest.* 2012;92(12):1712–25.
53. Mormone E, Lu Y, Ge X, Fiel MI, Nieto N. Fibromodulin, an oxidative stress-sensitive proteoglycan, regulates the fibrogenic response to liver injury in mice. *Gastroenterology.* 2012;142(3):612–21.e5.

54. Saums MK, Wang W, Han B, Madhavan L, Han L, Lee D, et al. Mechanically and chemically tunable cell culture system for studying the myofibroblast phenotype. *Langmuir*. 2014;30(19):5481–7.
55. Charrier EE, Pogoda K, Wells RG, Janmey PA. Control of cell morphology and differentiation by substrates with independently tunable elasticity and viscous dissipation. *Nat Commun*. 2018;9(1):449.
56. Deffieux T, Gennisson J-L, Bousquet L, Corouge M, Coscinea S, Amroun D, et al. Investigating liver stiffness and viscosity for fibrosis, steatosis and activity staging using shear wave elastography. *J Hepatol*. 2015;62(2):317–24.

# Chapter 57

## Role of Sinusoidal Pressure and Arterialization in Driving Fibrosis Progression



Sebastian Mueller

### Introduction to Liver Cirrhosis

Chronic liver diseases ultimately lead to scarring (cirrhosis), a process in which the architectural organization of functional liver units becomes disrupted. Liver cirrhosis is the result of excessive accumulation of extracellular matrix (ECM) with increased liver stiffness (LS). This is often accompanied by a progressive loss of organ function despite the use of immunosuppressive, anti-viral, or anti-inflammatory agents [1, 2]. Excess ECM deposition also causes progressive elevation of the hepatic vascular resistance with important hemodynamic consequences including portal hypertension, the formation of vascular collaterals, and the so-called hyperdynamic circulation with elevated cardiac output and lowered arterial pressure [3]. Moreover, liver cirrhosis is an important pre-cancerogenic lesion finally resulting in hepatocellular cancer (HCC).

### Established Mechanisms of Liver Cirrhosis

The mechanisms of hepatic fibrosis are still poorly understood. Many different stimuli such as hepatotoxins, viruses, bile acids, and hypoxia can trigger fibrogenesis and so-called reactive oxygen species seem to play an important role in fibrosis progression [4]. The major proteins of the ECM are collagens forming important scaffolds and barriers. Collagens are the most abundant ECM components in the

---

S. Mueller (✉)

Department of Medicine and Center for Alcohol Research and Liver Diseases,  
Salem Medical Center, University of Heidelberg, Heidelberg, Germany  
e-mail: [Sebastian.Mueller@urz.uni-heidelberg.de](mailto:Sebastian.Mueller@urz.uni-heidelberg.de)

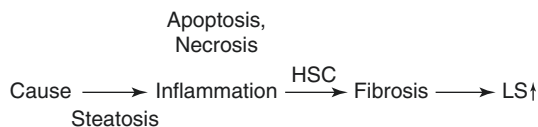
liver and their relative content increases up to tenfold in cirrhosis [5, 6]. Fibrogenesis is usually counterbalanced by fibrolysis, i.e., the removal of excess ECM by proteolytic enzymes, most importantly by matrix metalloproteinases (MMPs). With repeated injury or sufficient severity, fibrogenesis prevails over fibrolysis, resulting in excess ECM synthesis and deposition, a downregulation of MMP synthesis, secretion and activity along with an increase of the tissue inhibitors of MMPs (TIMPs, especially TIMP-1).

ECM components, MMPs and TIMPs are mainly produced by activated hepatic stellate cells (HSCs) and fibroblasts [7]. Activated macrophages (Kupffer cells) and also other cells are a major source for fibrogenic cytokines such as TGF- $\beta$ , also called the master cytokine of fibrosis development, that further stimulate HSCs and fibroblasts to transdifferentiate into activated myofibroblasts, the main cell type responsible for excess matrix deposition at sites of tissue repair.

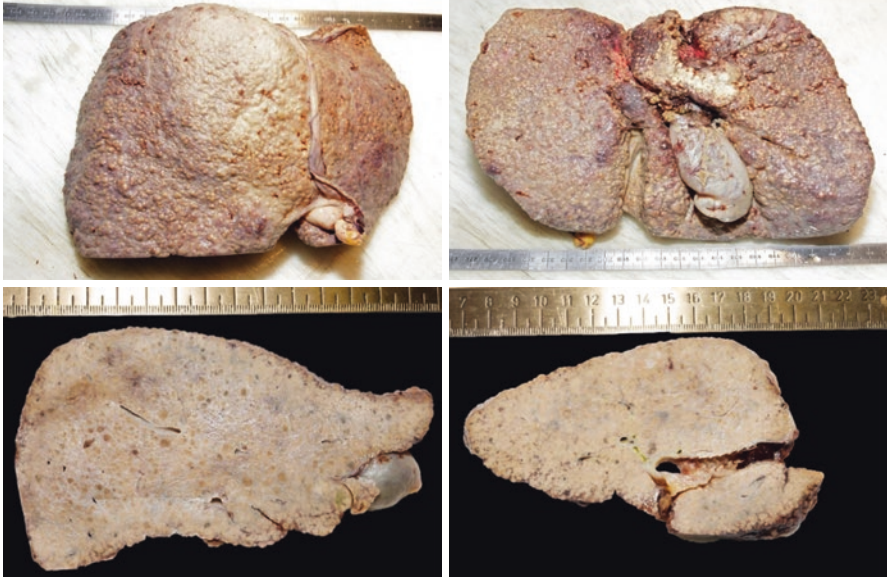
## Unresolved Key Observations in Patients with Liver Cirrhosis

Figure 57.1 depicts the conventional course of events ultimately leading to fibrosis where increased matrix deposition results in elevated liver stiffness that is the final consequence of liver fibrosis. Despite the enormous progress in understanding molecular mechanisms of fibrosis progression and its key players, we still lack a fundamental understanding of this disease. This becomes evident by established clinical key observations in patients with liver cirrhosis that cannot be explained by present concepts. These poorly understood characteristic features are the following three points:

- Highly uniform response of fibrosis progression despite very different stimuli such as inflammation, congestion, or cholestasis
- The macroscopic changes in cirrhotic livers with large fibrous septa spanning over several centimeters through the organ (see Fig. 57.2) not being plausibly explained by the action of local humoral factors
- The so-called “point of no return”: why is liver cirrhosis progressing further despite the elimination of the underlying cause (e.g., alcohol abstinence or HCV elimination)



**Fig. 57.1** Conventional sequence of fibrosis progression. Here, elevated liver stiffness (LS) is primarily regarded as correlate of matrix deposition (fibrosis stage). *HSC* hepatic stellate cells



**Fig. 57.2** Macroscopic aspect of a cirrhotic liver in a patient with alcoholic liver disease (courtesy of C. Lackner, University of Graz). Note the large fibrous septa spanning through the whole organ which are clearly visible at the macroscopic level. In the lower right panel, a TIPS channel can be seen

## Role of Pressure in Modulating Liver Stiffness: Introducing the Sinusoidal Pressure Hypothesis (SPH)

The potential role of sinusoidal pressure in mediating fibrosis progression has only recently been recognized mainly through novel *in vivo* data both from humans and animals on liver stiffness obtained by transient elastography (TE) [8]. During fibrosis progression, LS increases continuously from ca. 4 kPa up to 75 kPa. A threshold of 12.5 kPa is now widely considered as cut-off value of histological F4 cirrhosis stage [9]. However, as shown in Fig. 57.3, various other conditions are able to elevate LS irrespective of fibrosis, including liver inflammation (hepatitis) [10, 11], liver congestion [12], and mechanic obstruction of bile ducts (cholestasis) [13]. In addition to the findings mentioned above, well-established data from more than 500 clinical studies are most relevant for the concept of SPH that can be briefly summarized as follows [8]:

1. LS highly correlates with histological fibrosis stage independent of the underlying liver disease ( $r > 0.8$ ).
2. Elevated LS is also associated with other liver pathologies that ultimately lead to cirrhosis including inflammation, cholestasis, and congestion.

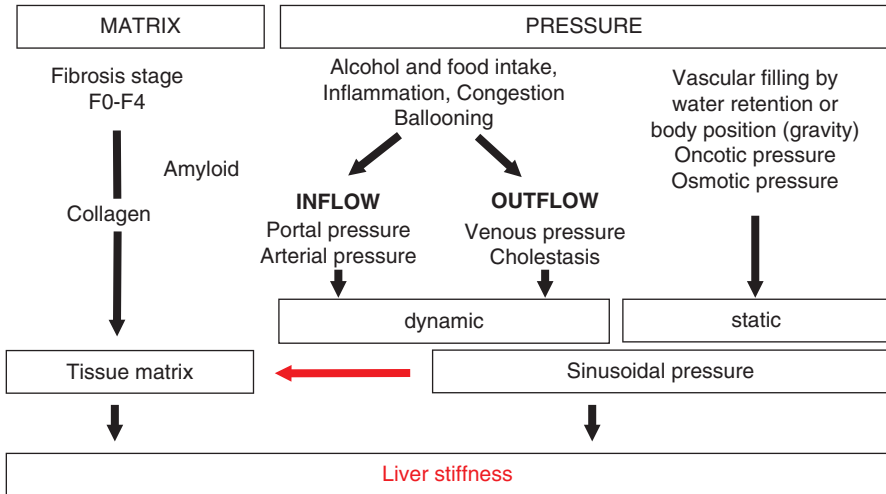


**Fig. 57.3** Established confounders of liver stiffness. Irrespective of fibrosis (left), many important and pressure-related confounders cause liver stiffness elevation through the sinusoidal pressure. Thus, in normal livers, liver stiffness reflects the sinusoidal pressure. According to the sinusoidal pressure hypothesis, this pressure drives fibrosis (red arrow)

3. LS is an independent predictor of liver-related mortality [14].
4. LS improves after elimination of liver pathology, e.g., after clearance of HCV, weight reduction, or alcohol withdrawal.
5. Genetic risk factors of liver disease increase LS.
6. A normal LS (<6 kPa) excludes liver pathology and liver fibrosis.

## Introducing the Role of Pressure in Driving Fibrosis Progression: The Sinusoidal Pressure Hypothesis

SPH provides an answer to all these open questions based on biomechanical considerations [15]. As shown in Table 57.1 and Fig. 57.4, they can be summarized in four key points. All potential causes of cirrhosis ultimately lead to an elevated sinusoidal pressure (SP). SP consists of dynamic and static components such as hepatic inflow and outflow balances or water retention. Even minimal increases of SP seem to be critical for the low-pressure organ liver which is typically exposed to ca. 5 mmHg via the portal vein. SP elevation may first develop in portal or central areas depending on the localization of the underlying disease (e.g., portal-tract disease such as HCV vs perivenular disease such as ALD). In contrast to conventional concepts (see Fig. 57.1), elevated LS is the consequence of both elevated SP and increased matrix deposition. This also means that LS almost exclusively mirrors SP in the absence of fibrosis. At the cellular level and as will be discussed below, SP is the actual driving force for the production of ECM by stretching of perisinusoidal cells, e.g., hepatic



**Table 57.1** Initiation and perpetuation of fibrosis driven by sinusoidal pressure*SPH Part I: Initiation of a pro-fibrogenic response by elevated sinusoidal pressure*

1. All liver diseases cause elevation of sinusoidal pressure (SP) which is the complex result of many factors (hemodynamics, intra- and extrahepatic shunts, inflammation, etc.)
2. LS represents the sum of matrix deposition (fibrosis) and SP. In non-cirrhotic livers, LS corresponds to SP
3. At the cellular level, SP elevation causes stretch forces on perisinusoidal cells that ultimately lead to collagen (matrix) deposition via inter- and intracellular biomechanical signaling. Dosage and time of elevated SP causes matrix generation (fibrosis) via biomechanical signaling. The matrix deposition ultimately matches SP (force = counter force)

*SPH Part II: Continued pressure elevation by arterialization of the fibrotic liver (Perpetuation)*

1. At a higher LS (ca. 12 kPa/12 mmHg), arterial blood supply becomes essential ultimately leading to arterialization of the liver via hypoxia signaling
2. Arterial supply is ultimately not reversible causing loss of endothelial fenestrae, capillarization, and sustained SP and LS elevation
3. Arterialization initiates a vicious cycle leading to further matrix deposition, eventual complete disconnection of hepatocytes from blood supply and ischemia with subsequent arterialization and nodular regeneration
4. Finally, the arterialized liver (high oxygen, high pressure) combined with cell death and enhanced regeneration will cause a pro-cancerogenic environment and HCC

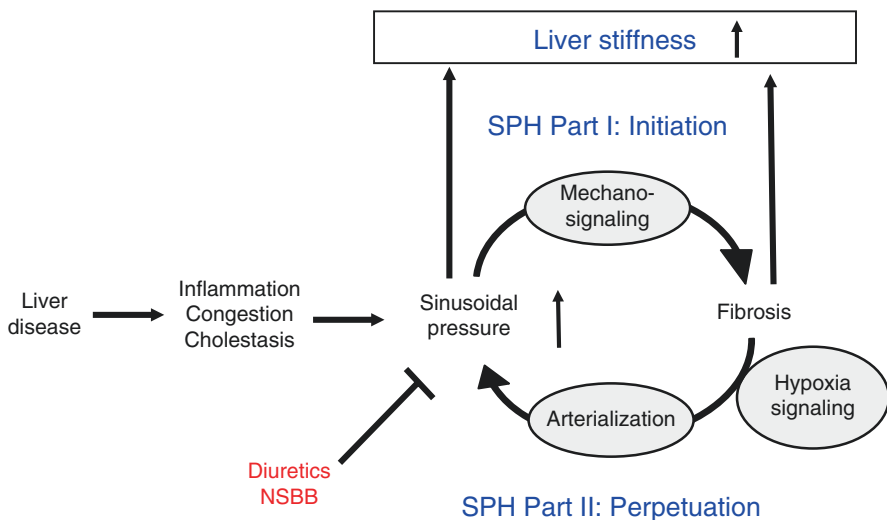


**Fig. 57.4** Sinusoidal pressure hypothesis (SPH) at the whole organ level and therapeutic target sides (red). SP is the driving force of matrix deposition. Irrespective of the etiology, all liver pathologies (shown in the left) increase the SP that initiates matrix deposition via specific inter- and intracellular biomechanical signaling pathways (SPH Part I, Initiation). LS should be regarded as the combined read-out of elevated pressure and fibrosis. Both SP elevation and matrix deposition increase vascular resistance that ultimately lead to elevated hepatic arterial flow and finally complete arterial blood supply. Depending on dosage (>12 mmHg) and time (>4 weeks), this vicious cycle will ultimately cause a complete arterialization leading to irreversible cirrhosis by exposing the low-pressure organ to permanent high pressure (SPH Part II, Perpetuation). According to SPH, non-selective beta blockers (NSBB) and diuretics are not only symptomatic therapies but interrupt the vicious cycle of pressure-driven fibrosis progression

stellate cells (HSCs), fibroblasts, and liver sinus endothelial cells (LSEC). It remains open whether these cells simply “feel” the surrounding pressure-mediated stiffness by dedicated sensing mechanisms [16] or whether they directly sense pressure-mediated stretch forces. So far, stiffness-mediated activation of HSC has not been linked to pressure or SP [6, 17]. According to the physics of mechanics, it is easily conceivable that pressure-induced stretch forces will overlay at the whole organ levels leading to regions with high trajectory forces and consequent large septa formation. SP-mediated stretch forces and matrix are in continuous equilibrium. Dosage and time of elevated SP/LS determine fibrosis progression (biomechanic signaling), eventually leading to a degree of matrix deposition that “matches” the pressure. Experimental and common clinical observations suggest that a SP >12 mmHg or a LS >12 kPa and a time period >4 weeks are critical thresholds.

## **Fibrosis Perpetuation by Arterialization of the Fibrotic Liver and Continuous Pressure Elevation**

The hepatic artery is directly connected to the sinusoidal bed via arteriole inlets and provides about 20% of blood in a normal healthy liver. The stiffer the liver becomes due to inflammation or fibrosis the more pressure is required to maintain sufficient blood flow. Although the elevation of portal pressure (portal hypertension >12 mmHg) can partly maintain some portal flow, it will hardly reach values higher than 30 mmHg. Under these conditions, the hepatic artery will be the only vessel with sufficiently high pressure to maintain hepatic blood supply. Elevation of hepatic arterial flow and subsequent arterialization is mainly driven by the hepatic arterial buffer response (HABR) [18] and hypoxia signaling [19]. SPH postulates that this arterialization defines the so-called “**point of no return.**” It provides a pressure-based rationale to explain the self-perpetuation of fibrosis progression and the uniform, etiology-independent progression of fibrosis. Arterialization of the fibrotic liver ultimately leads to a sustained exposure of the low-pressure organ liver (typically <6 mmHg) to higher pressures (see also Fig. 57.5). In ca. 7% of patients with cirrhosis, extreme flow changes can be observed such as complete reversal of the portal flow (so-called hepatofugal portal flow) [20]. Part II of SPH is summarized in Table 57.1 and depicted in Figs. 57.4 and 57.5. At the end, the arterialized liver (high oxygen, high pressure) together with massive matrix deposition will cause self-inflicted ischemia. The combination of these events stimulates the **formation of regenerative nodules**, finally causing the typical nodular aspect of cirrhotic livers. High pressure in combination with cell death and enhanced regeneration ultimately provides an ideal environment of genetic instability and formation of cancer (HCC). It is also postulated that the typical laboratory finding of cirrhotic livers, an increased AST/ALT ratio, and a slight GGT elevation [21] is indicative for the stage of arterialization [15].

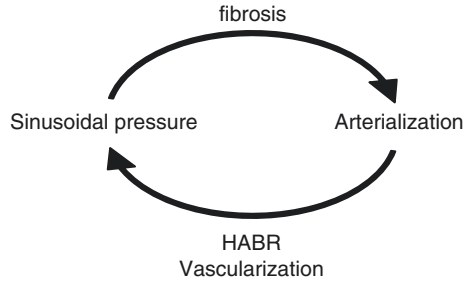
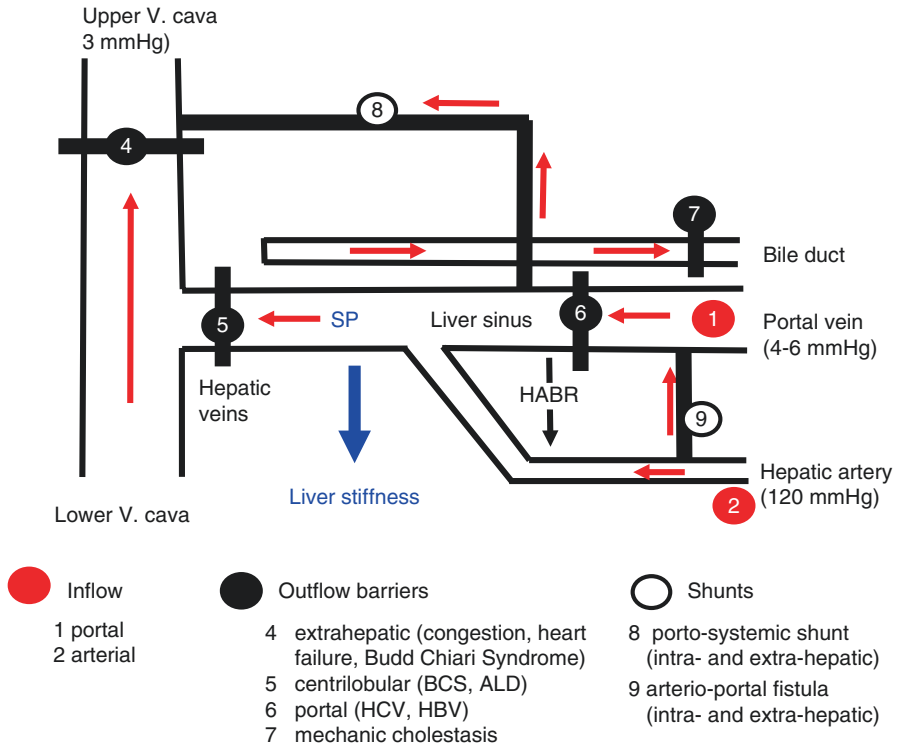


**Fig. 57.5** Vicious cycle of pressure elevation, matrix generation, and arterialization according to the sinusoidal pressure hypothesis. The arterial response is mainly driven by hypoxia signaling and metabolic demand. The hepatic arterial buffer response (HABR) is the first and most rapid step in increasing arterial blood flow in response to decrease portal flow according to the adenosine wash-out theory [18]. Later, other vascularization signals establish and secure arterial blood supply

## Sinusoidal Pressure as Consequence of the Hepatic Inflow/Outflow Balance

Figure 57.6 shows a simplified scheme of the vascular and biliary architecture of the liver to better illustrate the role of the various inflow, outflow, and shunt factors on SP. In general, the liver is a low-pressure organ. Pressure in the portal vein is ca. <math>6\text{ mmHg}</math>, while blood leaves the liver through the veins and is ca.  $2\text{ mmHg}$  in the caval vein (CVP) [22–24]. Close to the right atrium, this pressure can even reach negative values. Despite this low hepatic venous pressure gradient (HVP) of ca.  $3\text{--}6\text{ mmHg}$ , the liver is supplied with ca. 25% of the total cardiac output [24]. According to Ohm's law of streaming fluids, it also demonstrates the very low vascular resistance of the healthy liver that easily adapts to flow changes, e.g., from the splanchnic side [18]. The sinusoidal pressure is determined by static and dynamic components (see also Fig. 57.3). The **static part** of the SP is determined by the intravascular pressure and the elastic properties of the vessel walls and also exists in the absence of a functioning blood circulation. Osmotic, oncotic pressure as well as gravitational forces related to the body positioning further contribute to this component. In contrast, the **dynamic component** is represented by the kinetic energy of the blood flow and becomes only relevant under conditions of an operating blood circulation. The flow resistance of the liver, blood viscosity, and the blood flow rate all affect this dynamic component. The flow resistance, however, will be modulated by many conditions including cellular swelling or infiltration of inflammatory cells. Importantly, the localization of inflammation will increase the vascular resistance locally either in the portal or central areas. It explains why both a rapid increase of arterial [25] or portal [26] inflow or outflow barriers within the venous outflow tract (congestion) [12], bile ducts (mechanical cholestasis) [13], or the sinusoidal bed [27] are able to increase LS. Taken together, the introduction of pressure into the pathology of fibrosis allows various novel insights to understand fibrogenesis at the hemodynamic level.



Modified from Mueller S. *World J Gastroenterol.* 2016;22(48):10482-10501.

**Fig. 57.6** Simplified scheme of the hepatic vascular architecture and conditions that result in elevated sinusoidal pressure (SP) and liver stiffness (LS). A normal liver is supplied by blood from the hepatic artery (25%) with arterial pressure (AP) and the portal vein (75%) with the portal pressure (PP). Hepatic blood leads into the hepatic veins with a central venous pressure (CVP). The hepatic venous pressure gradient (HVPG) determines the flow through the sinusoidal bed. In contrast, the SP is determined by the outflow/inflow ratio and ultimately increases LS. According to the hepatic arterial buffer response (HABR), a reduced portal flow causes compensatory arterial blood supply in a liver-autonomous unidirectional fashion

## Sinusoidal Pressure Elevation at the Cellular Level

At the cellular level, sinusoidal pressure elevation induces stretch forces within the perisinusoidal cells that include hepatic stellate cells (HSC), endothelial cells, hepatocytes, and macrophages (Fig. 57.7a). Notably, fibroblasts and HSCs are known for a long time to contract and to respond to mechanic forces [16, 28, 29]. Taken together, the concept of SPH postulates that collagen deposition is a result of pressure elevation. The so-called pericellular fibrosis is not in contrast to SPH. **Pericellular fibrosis** describes collagen deposition around single ballooned hepatocytes and is commonly observed in heavy drinkers (see Fig. 57.7b). This pericellular fibrosis could be also explained by a pressure-stretch force concept. In contrast to perisinu-

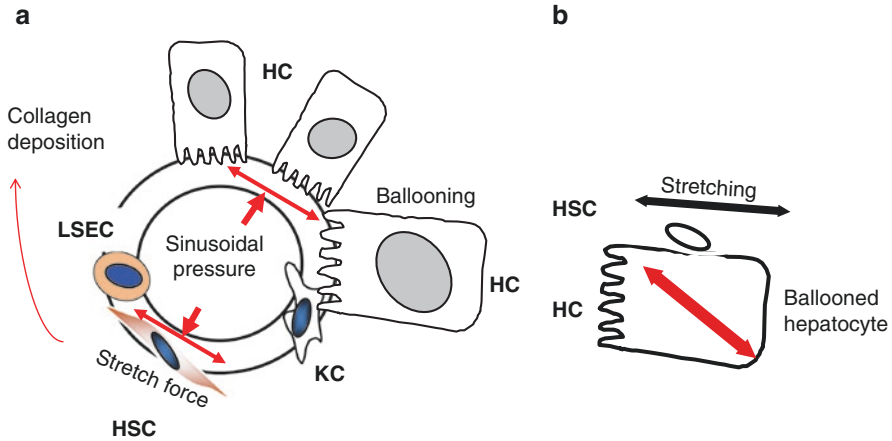


**Fig. 57.7** SPH at the cellular level. **(a)** According to SPH, SP predominantly translates into mechanic stretch forces within the perisinusoidal bed. Hepatocyte cell death, inflammation, or congestion all lead to increased SP that causes stretching of, for example, hepatic stellate cells (HSC), liver sinus endothelial cells (LSEC), Kupffer cells (KC) or hepatocytes (HC). **(b)** Moreover, intracellular pressure seen in ballooned hepatocytes can also cause stretch forces on the hepatocellular membrane and aligned HSC finally causing pericellular fibrosis

soidal fibrosis, pressure inside the ballooned hepatocyte causes stretch forces in pericellularly aligned HSC or fibroblasts and finally leads to mechanically induced collagen deposition. Thus, both intravascular and intracellular pressure can cause stretch forces at the hepatocyte membrane with consequent stretching of HSC and/or elevation of cellular stiffness.

## Future Clinical Impact of SPH

SPH could boost and stimulate basic and clinical research activities not only restricted to liver disease but also the bidirectional role of liver diseases within the whole organism and its relation to other organs such as the heart, kidney, or lung. Some important consequences of the SPH are listed in Table 57.2. It may further lead to a re-evaluation or optimization of established supportive standard therapies in cirrhotic patients. Thus, SPH could help to explain the widely discussed beneficial effects of pressure-lowering drugs such as NSBB and it could help to optimize treatment regimens, patient selection, and a better understanding of their mechanisms [30, 31]. Second, SPH sheds new light on the long-term therapy with diuretics in cirrhotic patients. Diuretics may not only remove excess water from the body but may also intercept with the viscous cycle of continued water retention, SP elevation (hydrostatic component, see Fig. 57.3), and fibrosis progression. It will also be quite exciting to learn whether the liver has a more immanent role in other diseases

**Table 57.2** Important consequences of SPH

1	<i>Awareness of mechanic forces and explanation of macroscopic organization of liver cirrhosis</i> Introducing pressure and stretch forces helps to explain why fibrous septa will span over several layers of liver tissue in the centimeter range. Many hemodynamics of the liver are poorly understood but should be relevant for biomechanic signaling. The liver is an organ exposed to a low-pressure environment (4–6 mmHg), which can be optionally put under high pressure by the hepatic artery. Capillary, adhesion, shear, and other forces are also insufficiently understood but could contribute to SP
2	<i>Uniform formation of end-stage liver cirrhosis by different etiologies</i> SPH could explain the uniform response of fibrosis formation to very different and heterogeneous liver pathologies and their combination
3	<i>Role of hepatic shunt formation and consequences for a novel typology of liver cirrhosis</i> Intra- and extrahepatic shunts will efficiently lower pressure gradients but also bypass liver cells. Shunts should efficiently lower SP and thus halt pressure-mediated fibrosis progression. It could also explain recently observed different types of patients with liver cirrhosis, those with high stiffness but excellent liver function (“stiff type”) and those with rather low LS but very limited liver function (“icteric type”) [32, 33] (see also Fig. 30.3). These considerations could eventually lead to a novel typology of liver cirrhosis if clinically meaningful
4	<i>Molecular and genetic basis of pressure-associated fibrogenesis</i> The concept of pressure-mediated fibrosis could help to better design, delineate, and interpret the so-far overwhelming and confusing data obtained by high throughput screening technologies. Pressure is a very complex, highly controlled and evolutionary conserved vital parameter in all mammals that is modulated by many genes engaging in expression of, for example, transporters that effect water and electrolyte metabolism, the vessel boundaries, pressure-controlling hormones but, of course, also the response of the biomechanical signal transduction cascade in response to elevated pressure
5	<i>Role of arterial pulse wave energy and energy absorption in the liver</i> Almost nothing is known about the consequences of pulse wave energy propagation in the liver. Stiffening of the liver could cause a much stronger, Tsunami-like release of mechanic energy in the liver and define a novel role of fat as “sound energy absorbing” factor
6	<i>Mechanic role of steatosis</i> SPH provides an alternative look at the role of fat on a mechanic basis. A mechanic approach towards hepatic steatosis provides a completely novel, partly unexpected but also fascinating and complex entrance to liver pathology
7	<i>Role of the intrahepatic localization of inflammation for fibrosis progression (portal versus lobular)</i> Zone III-localized hepatic diseases such as Budd–Chiari syndrome and schistosomiasis are known to rapidly produce cirrhosis and they are known to strongly increase LS [34–36]. It is also long known that, for example, ALD primarily starts in the region of the central vein causing so-called perivenular fibrosis [37]. Recent work shows that lobular inflammation translates to higher LS, while portal inflammation shows a more pronounced spleen stiffness elevation [38], elevated SS/LS ratio with pronounced complications of portal hypertension [38]. SPH provides a novel concept to better comprehend fibrosis progression based on the localization of the inflammatory disease

with water retention such as cardiac insufficiency. On the diagnostic level, noninvasive LS measurement may help to monitor and optimize the treatment of liver diseases especially with its direct link to SP. At the molecular level, the therapeutic desirable lowering of SP directly leads to a better understanding of hepatic mechanosignaling and the regulation of SP at the cellular level. Potential novel molecular

targets or strategies could be identified that may include mechanic conditioning or pharmacotherapy acting on mechanosignaling. The mechanic role of fat has been already discussed above and, based on preliminary observation, warrants further analysis. Further studies on SP will also require the implementation of liquid physics to better understand the dynamic component of SP and its role on fibrosis progression. Finally, the role of osmotic stress, the regulation of the hydration status of the cell, and the role of water channels such as aquaporins will be likewise highly interesting to study in the context of SP elevation and fibrosis progression.

## Conclusions

The Sinusoidal Pressure Hypothesis (SPH) identifies an elevation of sinusoidal pressure (SP) as cause of fibrosis and liver cirrhosis. It introduces pressure as driving force of fibrosis progression while pressure is typically associated with portal hypertension as a consequence of cirrhosis. SPH offers a plausible explanation for the uniform response of fibrosis progression to various stimuli, fibrosis reversal, and macroscopic changes. While fibrosis can still reverse if the underlying cause of SP elevation is eliminated, the increased matrix deposition requires increasing arterial blood supply. The final so-called arterialization of the liver permanently exposes the organ permanently to pathologically high pressures and initiates a vicious cycle of further matrix deposition and increased arterial pressure. Introducing biomechanics to the understanding of fibrosis progression offers novel treatment strategies that should help to better target this severe disease in the future.

## References

1. Bataller R, Brenner DA. Liver fibrosis. *J Clin Invest*. 2005;115(2):209–18.
2. Schuppan D, Afdhal NH. Liver cirrhosis. *Lancet*. 2008;371(9615):838–51.
3. Bosch J, Groszmann RJ, Shah VH. Evolution in the understanding of the pathophysiological basis of portal hypertension: how changes in paradigm are leading to successful new treatments. *J Hepatol*. 2015;62(1 Suppl):S121–30.
4. Benyon RC, Arthur MJ. Extracellular matrix degradation and the role of hepatic stellate cells. *Semin Liver Dis*. 2001;21(3):373–84.
5. Schuppan D, Gressner AM. Metabolism of collagen and other extracellular proteins. In: *Oxford textbook of clinical hepatology*; 1998. p. 381–408.
6. Wells RG. Tissue mechanics and fibrosis. *Biochim Biophys Acta*. 2013;1832(7):884–90.
7. Olaso E, Friedman SL. Molecular regulation of hepatic fibrogenesis. *J Hepatol*. 1998;29(5):836–47.
8. Mueller S, Sandrin L. Liver stiffness: a novel parameter for the diagnosis of liver disease. *Hepat Med*. 2010;2:49–67.
9. Friedrich-Rust M, Ong MF, Martens S, Sarrazin C, Bojunga J, Zeuzem S, et al. Performance of transient elastography for the staging of liver fibrosis: a meta-analysis. *Gastroenterology*. 2008;134(4):960–74.

10. Arena U, Vizzutti F, Abraldes JG, Corti G, Stasi C, Moscarella S, et al. Reliability of transient elastography for the diagnosis of advanced fibrosis in chronic hepatitis C. *Gut*. 2008;57(9):1288–93.
11. Sagir A, Erhardt A, Schmitt M, Haussinger D. Transient elastography is unreliable for detection of cirrhosis in patients with acute liver damage. *Hepatology*. 2008;47(2):592–5.
12. Millonig G, Friedrich S, Adolf S, Fonouni H, Golriz M, Mehrabi A, et al. Liver stiffness is directly influenced by central venous pressure. *J Hepatol*. 2010;52(2):206–10.
13. Millonig G, Reimann FM, Friedrich S, Fonouni H, Mehrabi A, Büchler MW, et al. Extrahepatic cholestasis increases liver stiffness (FibroScan) irrespective of fibrosis. *Hepatology*. 2008;48(5):1718–23.
14. Mueller J, Rausch V, Silva I, Peccerella T, Piecha F, Dietrich C, et al. PS-171-Survival in a 10 year prospective cohort of heavy drinkers: liver stiffness is the best long-term prognostic parameter. *J Hepatol*. 2019;70(1):e107.
15. Mueller S. Does pressure cause liver cirrhosis? The sinusoidal pressure hypothesis. *World J Gastroenterol*. 2016;22(48):10482.
16. Discher DE, Janmey P, Wang YL. Tissue cells feel and respond to the stiffness of their substrate. *Science*. 2005;310(5751):1139–43.
17. Hinz B. Tissue stiffness, latent TGF-beta1 activation, and mechanical signal transduction: implications for the pathogenesis and treatment of fibrosis. *Curr Rheumatol Rep*. 2009;11(2):120–6.
18. Lauth WW. Hepatic circulation: physiology and pathophysiology. Colloquium series on integrated systems physiology: from molecule to function to disease. San Rafael, CA; 2009.
19. Medina J, Arroyo AG, Sanchez-Madrid F, Moreno-Otero R. Angiogenesis in chronic inflammatory liver disease. *Hepatology*. 2004;39(5):1185–95.
20. Rector WG Jr, Hoefs JC, Hossack KF, Everson GT. Hepatofugal portal flow in cirrhosis: observations on hepatic hemodynamics and the nature of the arteriportal communications. *Hepatology*. 1988;8(1):16–20.
21. Mueller S, Englert S, Seitz HK, Badea RI, Erhardt A, Bozaari B, et al. Inflammation-adapted liver stiffness values for improved fibrosis staging in patients with hepatitis C virus and alcoholic liver disease. *Liver Int*. 2015;35(12):2514–21.
22. Balfour DC, Reynolds TB, Levinson DC, Mikkelsen WP, Pattison AC. Hepatic vein pressure studies for evaluation of intrahepatic portal hypertension. *AMA Arch Surg*. 1954;68(4):442–7.
23. Atkinson M, Sherlock S. Intrasplenic pressure as index of portal venous pressure. *Lancet*. 1954;266(6826):1325–7.
24. Schmidt RF, Thews G. *Physiologie des Menschen*. 23. Auflage ed. Heidelberg: Springer Verlag; 1987.
25. Piecha F, Peccerella T, Bruckner T, Seitz HK, Rausch V, Mueller S. Arterial pressure suffices to increase liver stiffness. *Am J Physiol Gastrointest Liver Physiol*. 2016;311(5):G945–G53.
26. Mueller S. Personal observation.
27. Arena U, Vizzutti F, Corti G, Ambu S, Stasi C, Bresci S, et al. Acute viral hepatitis increases liver stiffness values measured by transient elastography. *Hepatology*. 2008;47(2):380–4.
28. Anwar MA, Shalhoub J, Lim CS, Gohel MS, Davies AH. The effect of pressure-induced mechanical stretch on vascular wall differential gene expression. *J Vasc Res*. 2012;49(6):463–78.
29. Humphrey JD, Schwartz MA, Tellides G, Milewicz DM. Role of mechanotransduction in vascular biology: focus on thoracic aortic aneurysms and dissections. *Circ Res*. 2015;116(8):1448–61.
30. Garcia-Tsao G. Beta blockers in cirrhosis: the window re-opens. *J Hepatol*. 2016;64(3):532–4.
31. Mookerjee RP, Pavesi M, Thomsen KL, Mehta G, Macnaughtan J, Bendtsen F, et al. Treatment with non-selective beta blockers is associated with reduced severity of systemic inflammation and improved survival of patients with acute-on-chronic liver failure. *J Hepatol*. 2016;64(3):574–82.
32. Mueller S, Seitz HK, Schirmacher P, Straub BK. Nicht invasive versus invasive Beurteilung der Leberfibrose. *Gastroenterol Up2date*. 2014;3(10):51–67.



33. Mueller S, Seitz HK, Rausch V. Non-invasive diagnosis of alcoholic liver disease. *World J Gastroenterol.* 2014;20(40):14626–41.
34. de Carvalho BT, Coutinho Domingues AL, de Almeida Lopes EP, Brandao SC. Increased hepatic arterial blood flow measured by hepatic perfusion index in hepatosplenic schistosomiasis: new concepts for an old disease. *Dig Dis Sci.* 2016;61(7):2118–26.
35. Huang H, Deng M, Jin H, Liu A, Dirsch O, Dahmen U. Hepatic arterial perfusion is essential for the spontaneous recovery from focal hepatic venous outflow obstruction in rats. *Am J Transplant.* 2011;11(11):2342–52.
36. Shahin M, Schuppan D, Waldherr R, Risteli J, Risteli L, Savolainen ER, et al. Serum procollagen peptides and collagen type VI for the assessment of activity and degree of hepatic fibrosis in schistosomiasis and alcoholic liver disease. *Hepatology.* 1992;15(4):637–44.
37. Nakano M, Worner TM, Lieber CS. Perivenular fibrosis in alcoholic liver injury: ultrastructure and histologic progression. *Gastroenterology.* 1982;83(4):777–85.
38. Elshaarawy O, Mueller J, Guha IN, Chalmers J, Harris R, Krag A, et al. Spleen stiffness to liver stiffness ratio significantly differs between ALD and HCV and predicts disease-specific complications. *JHEP Rep.* 2019;1(2):99–106.

**Part IX**  
**Future Directions and Open Questions**

# Chapter 58

## Future Applications and Directions of Liver Stiffness Studies



Sebastian Mueller, Omar Elshaarawy, and Felix Piecha

### Future Applications of Tissues Stiffness in Medicine

Already the rather short history of liver stiffness measurements (LSM) has established the importance of tissue stiffness for medicine whether it is the earlier detection of tissue abnormalities, fibrosis, or complications including all-cause mortality. Moreover, due to the broad and complex interplay of liver stiffness with other organs, LSM will be used in many other medical areas and disciplines. Table 58.1 provides a list of either already established usages of LSM in other areas or very likely applications. Apart from liver diseases, specific and highly interesting areas for LSM will be intensive care unit, cardiology, hematology but also the monitoring and screening for potentially liver-harmful therapies by rheumatologists, neurologists, addiction specialists, psychiatrists, etc. Algorithms will further improve in line with novel technical opportunities and artificial intelligence/machine learning. Novel business models will also shape the landscape of elastographic applications to allow more and inexpensive access to many patients. Figures 58.1 and 58.2 demonstrate that more patients and individuals will have access to the so-called **low-cost screening mode** in order to rule out liver and other confounding pathologies while the **expert mode** will be restricted to specialists with profound ultrasound knowledge for the clarification of elevated LSM. Whether this will also lead to a continued modification of health care structures remains open but desirable since the on-time and onside noninvasive diagnosis with combined elastographic, ultrasound and laboratory testing appears to be an attractive vision for the near future.

---

S. Mueller (✉) · O. Elshaarawy  
Department of Medicine and Center for Alcohol Research and Liver Diseases,  
Salem Medical Center, University of Heidelberg, Heidelberg, Germany  
e-mail: [sebastian.mueller@urz.uni-heidelberg.de](mailto:sebastian.mueller@urz.uni-heidelberg.de); [oelshaarawy@liver.menofia.edu.eg](mailto:oelshaarawy@liver.menofia.edu.eg)

F. Piecha  
Department of Medicine, University Medical Center Hamburg-Eppendorf, Heidelberg,  
Germany  
e-mail: [f.piecha@uke.de](mailto:f.piecha@uke.de)

**Table 58.1** Future applications of LS and SS measurement in medicine

Discipline	Parameter	Questions to be answered by future studies
General care	LS	Exclude liver disease, combination with other markers, e.g., serum markers
General care	LS	Exclude right heart failure
General care	LS	Assess liver manifestation in the context of alcohol consumption
General care	LS	Assess liver manifestation in the context of obesity
General care	LS	Assess liver manifestation in the context of diabetes
Hepatology	LS	Monitoring liver transplant patients
Hepatology	LS	Assess liver fibrosis
Hepatology	LS and SS	Diagnosis and management of liver diseases
Hepatology	LS and SS	Predict all-cause mortality
Hepatology	LS and SS	Predict liver-related mortality
Hepatology	LS and SS	Portal hypertension
Hepatology	LS and SS	Predict esophageal varices
Hepatology	LS and SS	Monitor treatment interventions, e.g., to drugs or TIPS
Hepatology	SS LS and SS	Monitoring response to locoregional treatment for HCC
Gastroenterology	LS	Screen for drug-mediated liver damage, e.g., by methotrexate (MTX)
Gastroenterology	LS	Screen for hepatic manifestations of, e.g., chronic inflammatory bowel (CED) patients
Cardiology	LS	Assess right heart function
Cardiology	LS	Monitor response to treatment of liver diseases
Cardiology	LS	Assess chronic pulmonary disease
Cardiology	LS	Assess heart-related mortality
Intensive care unit	LS	Monitor right heart function and central venous pressure
Intensive care unit	LS	Study water retention and distribution
Intensive care unit	LS	Predict all-cause mortality
Intensive care unit	LS	Study hydration status during treatment with diuretics
Rheumatology, Oncology	LS	Screen for drug-mediated liver damage, e.g., by methotrexate (MTX) or anticancer drugs
Rheumatology	LS	Screen for hepatic manifestations of autoimmune diseases
Neurology	LS	Screen for drug-mediated liver damage, e.g., by carbamazepine
Neurology	LS	Screen for typical liver-related co-morbidities in the neurological setting
Hematology	LS	Assess graft versus host disease (GWHD)

(continued)

**Table 58.1** (continued)

Discipline	Parameter	Questions to be answered by future studies
Hematology	LS	Monitor patients after allogeneic stem cell transplantation
Nephrology	LS	Study hydration status, e.g., during dialysis
Pulmonology	LS	Study patients with pulmonary hypertension
Pulmonology	LS	Rule out right heart failure in patients with chronic obstructive pulmonary disease (COPD)

**Fig. 58.1** Future screening mode with low-cost business models (freemium, leasing) by general practitioners, nurses, or non-hepatologists

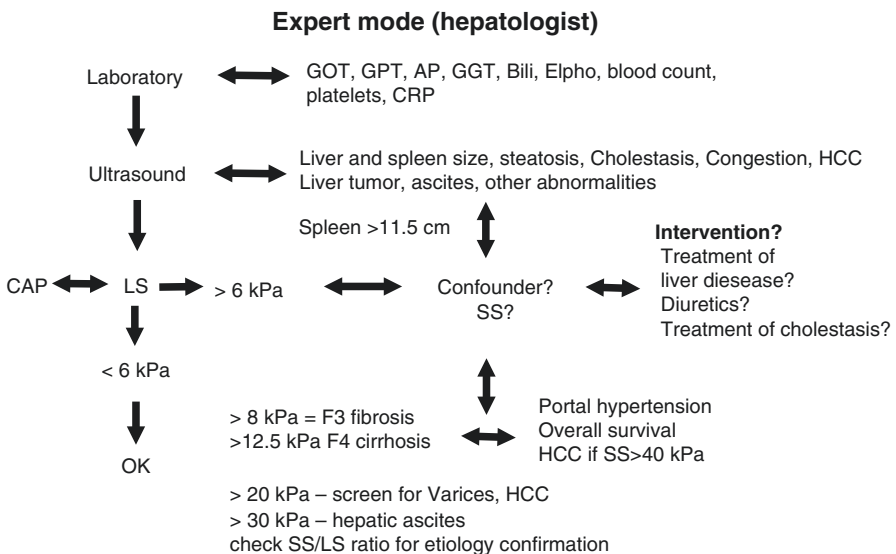
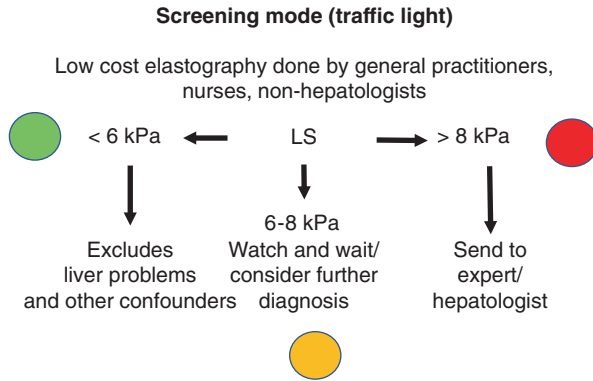


**Fig. 58.2** Future expert mode for hepatologists and experience in ultrasound with high end elastographic devices. The examination can be extended by information on hepatic steatosis (e.g., CAP), spleen stiffness, or other tissue stiffness values using 2D-SWE

## Directions of Future Technical, Clinical, and Experimental Studies

The noninvasive ability to measure liver stiffness has opened a new realm for both the diagnosis but also the molecular understanding of liver fibrosis. We will observe a rapid technical improvement of ultrasound and MRI based elastography techniques (Table 58.2). In addition, stiffness measurements of other organs such as spleen, heart, muscle, pancreas, or kidney and even brain will be possible. Hopefully, miniaturization will open stiffness measurements via endoscopic procedures. With regard to liver stiffness, upcoming studies have to clarify the open

**Table 58.2** Future technical studies and questions to be answered

Technical questions and studies
1. Standardization of techniques
2. Further standardization of elastographic examination and used “units”
3. Development of elastography phantoms for standardization
4. Better physical understanding of the different techniques, limitations, advantages
5. Comparison of different techniques
6. Establishment of other tissue stiffness measurements (kidney, brain, muscle, skin, fat, pancreas, brain, intestine, fat tissue)
7. Role and relation between stiffness, steatosis, and viscosity
8. Better discrimination between tissue stiffness and LS elevation due to confounders, e.g., pressure

**Table 58.3** Liver stiffness-specific and CAP-specific questions to be addressed by future studies

LS-specific questions to be answered by future clinical studies
1. Can we identify a direct quantitative relation between type and histological localization of hepatitis, serum transaminases, and liver stiffness?
2. What is the diagnostic value of LS in more complex clinical settings, e.g., a patient with combined alcoholic liver fibrosis and steatohepatitis and cardiomyopathy?
3. Could LS be part of prognostic scores for patients on the liver transplantation waiting list?
4. What other factors or rare diseases increase LS?
5. Could we use LS as a novel parameter to measure venous pressure in the context of intensive care setting or cardiology?
6. How valuable is LS in the neonatal screening for inborn liver diseases?
7. What are the gender- and age-specific normal stiffness values?
8. What are the population-wide prevalence rates of increased LS and fibrosis?
9. What are the genetic and molecular determinants of liver stiffness?
10. What is the kinetics of LS in various fibrosis models?
11. What is the kinetics of stiffness resolution in these models and is there a point of no return?

(continued)

**Table 58.3** (continued)

LS-specific questions to be answered by future clinical studies
12. Is there a critical cut-off value for stiffness that causes fibrosis?
13. What is the role of vasoactive hormones, mechanosensing channels, water channels such as aquaporins on liver stiffness and fibrosis?
14. Are there pharmacological or other therapeutic approaches to modulate liver stiffness and treat liver fibrosis?
15. SS/LS ratio and spleen size and their relation to disease etiology and stage?
16. LS control in patients with arterial hypertension?
17. Short seemingly paradox responses of CAP to food and alcohol intake?
18. Discrepancy between XL and M probe for CAP measurements?

questions listed in Table 58.3. On the other side, the area of liver stiffness will boost many basic research activities and novel miniaturized equipment is urgently required that will allow LS measurements on small animals such as mice.

### Potential Future Experimental Strategies to Validate the Role of Biomechanics in Liver Diseases/Stiffness

Much more needs to be learned about the complex interplay of liver stiffness and the various systemic, cellular, and intracellular confounders (Table 58.4). Pressure seems to be the physiological key process of mammals for LS which is controlled by many cellular, neural, and hormonal conditions [1–3]. The epithelial boundaries are critical for pressure maintenance and they put all aligning cells of the vascular system whether they are veins, arteries, capillaries, or specialized vascular entities such as the hepatic sinusoidal bed on stage. For instance, while focal adhesions (FA) and ECM-cell mechano-signaling have been intensively studied [4, 5], intercellular mechanotransduction (intercellular junctions of parenchymal cells and intermediate filaments) and its relation to pressure is largely unknown and would require adequate animal models for validation. Therefore, future studies should address these molecular mechanisms. A list of such potential studies is provided in Table 58.4. One potential strategy is well established in *in vitro* models under pressure-mimicking conditions with varying stiffness using viscoelastic gels (e.g., polyacrylamide) [6, 7]. The stiffness of these gels should be comparable to human fibrosis stages and validated using the  $\mu$ Fibroscan or atomic force microscopy [6]. The various liver-associated cells could be studied independently, individually, or in combination using co-culture approaches. Important cells should not be restricted to HSC and fibroblasts, but also endothelial cells, hepatocytes, and macrophages. The role of intercellular junctions and important molecules responsible for mechano-signaling could be examined in 2D versus 3D cell cultures.

**Table 58.4** Potential future experimental studies in order to better understand liver stiffness, biomechanic signaling, and liver diseases

Potential experimental studies to understand the LS
1. Matrix-modulating effects of pressure-lowering or modulating drugs
2. Physical aspects of pressure formation in biological tissues including the role of cardiac pulse wave energy and its mechanic absorption by fat
3. Effect of water metabolism, water channels (aquaporins), electrolyte transporters and other transporters, and osmotic pressure on matrix formation
4. Role of central nervous system and neuroendocrine hormones in controlling LS
5. Role of blood viscosity/hemorheology on LS
6. Role of anticoagulation and platelet inhibitors on LS
7. Role of pressure-mediated biomechanic signaling for matrix formation
8. Role of ECM, cellular and intercellular junctions on pressure-mediated matrix formation
9. Role of SP on gap junctions and matrix formation [8]
10. Role of vasoactive systems/substances, such as nitric oxide, cyclooxygenase-derivatives, carbon monoxide, and endogenous cannabinoids on SP and fibrosis [9]
11. Role of vasoconstrictor systems, such as the sympathetic nervous system, vasopressin, angiotensin, and endothelin-1 on SP and fibrosis [10, 11]
12. Optimization of pressure sensors, e.g., for the liver sinus including the development of molecular stretch force measuring sensors [12]
13. Association of pressure, tissue/cellular stiffness, and matrix formation at various organizational levels (cell, organ, and whole organism)
14. Interplay of organ systems involved in water and pressure regulation (e.g., heart, brain, kidney, and liver) for pressure regulation and matrix development
15. Role of liver size and lobulation of liver in various species in order to better sustain stretch forces of SP elevation
16. Mechanisms and modulation of vessel and shunt formation in the liver

For more details, see also [3]

## References

1. Anwar MA, Shalhoub J, Lim CS, Gohel MS, Davies AH. The effect of pressure-induced mechanical stretch on vascular wall differential gene expression. *J Vasc Res.* 2012;49(6):463–78.
2. Humphrey JD, Schwartz MA, Tellides G, Milewicz DM. Role of mechanotransduction in vascular biology: focus on thoracic aortic aneurysms and dissections. *Circ Res.* 2015;116(8):1448–61.
3. Mueller S. Does pressure cause liver cirrhosis? The sinusoidal pressure hypothesis. *World J Gastroenterol.* 2016;22(48):10482.
4. Hinz B. Tissue stiffness, latent TGF-beta1 activation, and mechanical signal transduction: implications for the pathogenesis and treatment of fibrosis. *Curr Rheumatol Rep.* 2009;11(2):120–6.
5. Wells RG. Tissue mechanics and fibrosis. *Biochim Biophys Acta.* 2013;1832(7):884–90.
6. Du Y, Han R, Wen F, Ng San San S, Xia L, Wohland T, et al. Synthetic sandwich culture of 3D hepatocyte monolayer. *Biomaterials.* 2008;29(3):290–301.
7. Chen S, Shi J, Xu X, Ding J, Zhong W, Zhang L, et al. Study of stiffness effects of poly(amidoamine)-poly(n-isopropyl acrylamide) hydrogel on wound healing. *Colloids Surf B Biointerfaces.* 2016;140:574–82.



8. Hernandez-Guerra M, Gonzalez-Mendez Y, de Ganzo ZA, Salido E, Garcia-Pagan JC, Abrante B, et al. Role of gap junctions modulating hepatic vascular tone in cirrhosis. *Liver Int.* 2014;34(6):859–68.
9. Bolognesi M, Di Pascoli M, Verardo A, Gatta A. Splanchnic vasodilation and hyperdynamic circulatory syndrome in cirrhosis. *World J Gastroenterol.* 2014;20(10):2555–63.
10. Bataller R, Schwabe RF, Choi YH, Yang L, Paik YH, Lindquist J, et al. NADPH oxidase signal transduces angiotensin II in hepatic stellate cells and is critical in hepatic fibrosis. *J Clin Invest.* 2003;112(9):1383–94.
11. Yokohama S, Yoneda M, Haneda M, Okamoto S, Okada M, Aso K, et al. Therapeutic efficacy of an angiotensin II receptor antagonist in patients with nonalcoholic steatohepatitis. *Hepatology.* 2004;40(5):1222–5.
12. Cost AL, Ringer P, Chrostek-Grashoff A, Grashoff C. How to measure molecular forces in cells: a guide to evaluating genetically-encoded FRET-based tension sensors. *Cell Mol Bioeng.* 2015;8(1):96–105.

# Appendix

## Figures

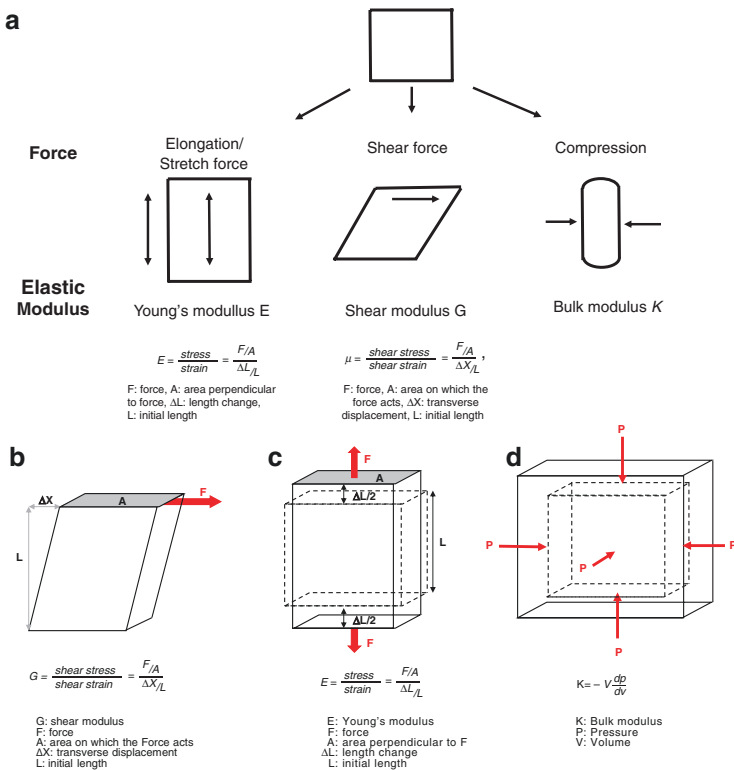
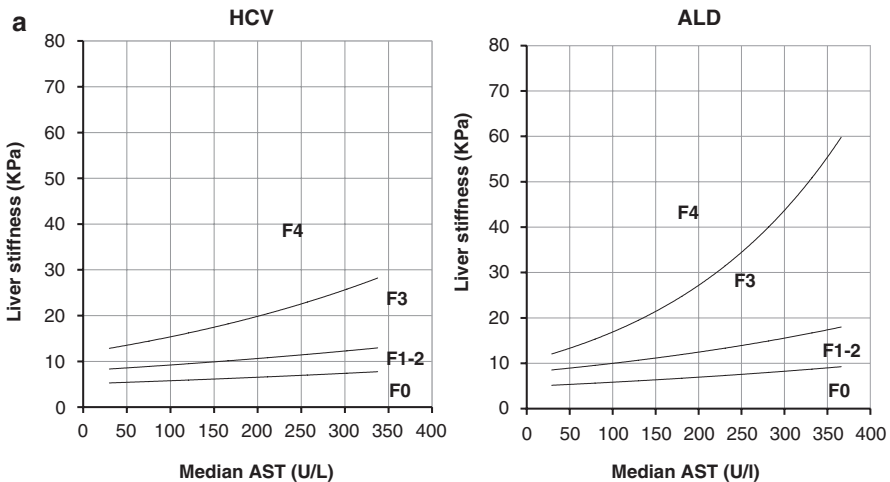


**Fig. A.1** (a) Overview of the various applied forces to liver tissue and resulting moduli. Typically, the Young's modulus E is considered the liver stiffness, e.g., by TE while some techniques such as MRE calculate the shear modulus G. (b) Visualization of the shear modulus. A force parallel to area A (shear stress) causes a shearing of the object and a transverse displacement (shear strain). (c) Visualization of the Young's modulus. A force perpendicular to the area A (stress) causes a length change (strain). (d) Visualization of the bulk modulus K. It is a measure of the resistance of a substance to compression

**Fig. A.2** Transient elastography outperforms serum fibrosis markers for all fibrosis stages. This pioneering study was performed on patients with alcoholic liver disease. No further algorithms were applied

Fibrosis stage	F ≥ 1	F ≥ 2	F ≥ 3	F = 4
<b>Fibroscan</b>	<b>0.84</b>	<b>0.91</b>	<b>0.90</b>	<b>0.94</b>
<b>Fibrometer</b>	0.72	0.82	0.88	0.85
<b>Fibrotest</b>	0.77	0.79	0.80	0.84
<b>Hepascore</b>	0.70	0.76	0.83	0.76
<b>Hyaluronic acid</b>	0.76	0.80	0.83	0.80
<b>PGA</b>	0.66	0.78	0.84	0.89
<b>PGAA</b>	0.74	0.81	0.86	0.83
<b>APRI</b>	0.76	0.54	0.43	0.56

Modified from Nguyen-Khac et al. *Alim Pharm Ther* 2008;28: 1188



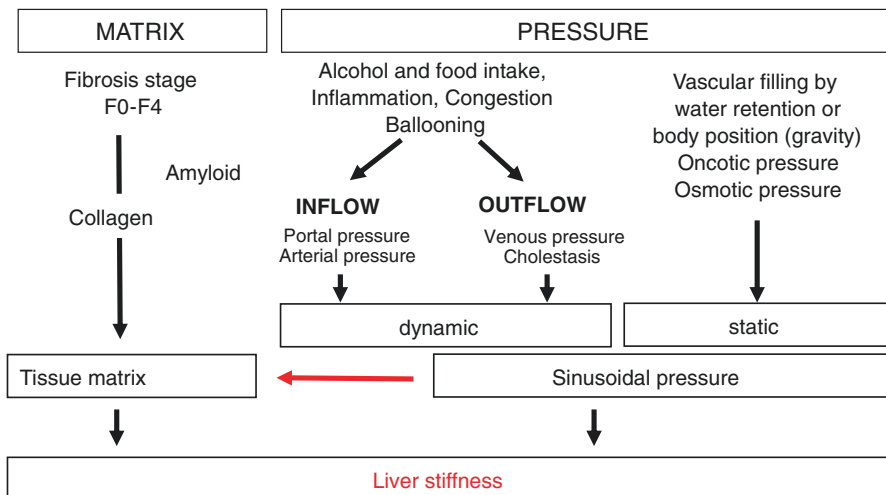
Modified from Mueller S et al *Liver Int.* 2015;35(12):2514-2521

**b**

Fibrosis stage	Cut-off for Liver Stiffness (kPa) in HCV	Cut-off for Liver Stiffness (kPa) in ALD
F0 vs F1-2	$\geq 5.1 \times \exp(0.0018 \times \text{AST})$	$\geq 4.9 \times \exp(0.0022 \times \text{AST})$
F1-2 vs F3	$\geq 9.0 \times \exp(0.0023 \times \text{AST})$	$\geq 8.1 \times \exp(0.0046 \times \text{AST})$
F3 vs F4	$\geq 11.9 \times \exp(0.0035 \times \text{AST})$	$\geq 10.5 \times \exp(0.0069 \times \text{AST})$

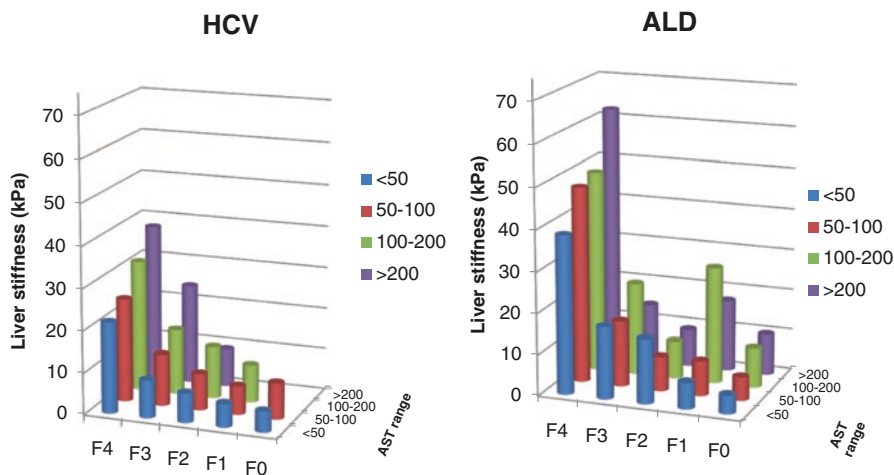
Modified from Mueller S et al *Liver Int.* 2015;35(12):2514-2521

**Fig. A.3** (a) AST-adapted cutoff values for alcoholic liver disease (ALD) and HCV. Note that identical AST levels cause higher LS elevation in ALD as compared to HCV. These graphs allow for instant fibrosis stage reading based on LSM and laboratory markers. A more precise assessment of fibrosis stage requires treatment interventions to remove the inflammation component such as alcohol detoxification or antiviral therapy. (b) Calculation of AST-adapted cutoff values for alcoholic liver disease (ALD) and HCV. These formulas are useful for multicenter studies to calculate fibrosis stages based on TE and AST levels



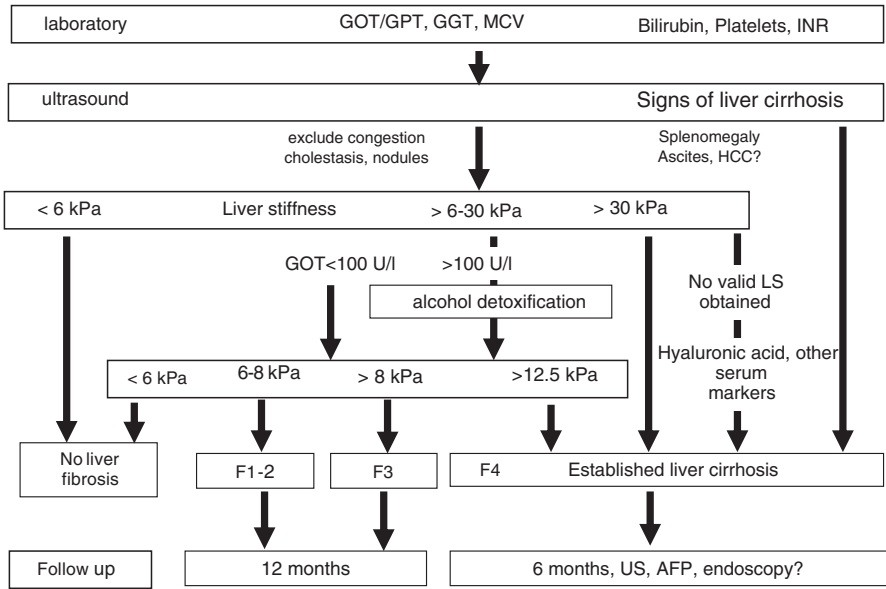
Modified from Mueller S. World J Gastroenterol. 2016;22(48):10482-10501.

**Fig. A.4** Established confounders of liver stiffness. Irrespective of fibrosis (left), many important and pressure-related confounders cause liver stiffness elevation through the sinusoidal pressure. Thus, in normal livers, liver stiffness reflects the sinusoidal pressure. According to the sinusoidal pressure hypothesis, this pressure drives fibrosis (red arrow)



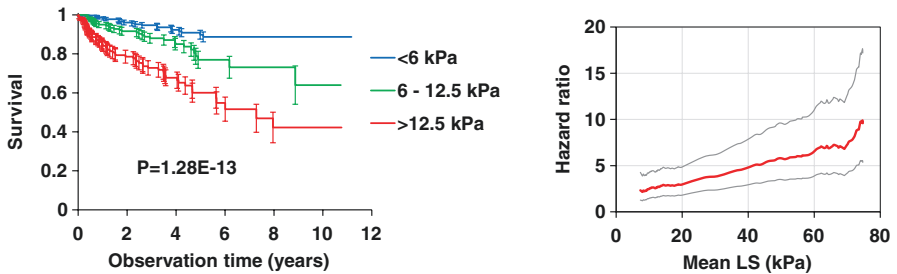
Modified from Mueller et al, 2015, Liver international; 35:2514–2521.

**Fig. A.5** Mean AST and LS levels according to histological fibrosis stage. While there is a clear relation between fibrosis stage and AST levels in HCV, this relation is more complex in ALD. Consequently, this needs to be considered when interpreting AST levels, e.g., within fibrosis scores



Modified from Mueller S et al *World J Gastroenterol.* 2014;20(40):14626-14641.

**Fig. A.6** Example of diagnostic flow chart for the diagnosis of alcoholic liver disease using liver stiffness (Heidelberg algorithm)



LS Cut-off (kPa)	3-year survival rate	5-year survival rate
<6	94%	90%
6-12.5	88%	78%
>12.5	74%	64%

**Fig. A.7** Liver stiffness (LS) is a novel independent long-term predictor of all-cause death. Data are from a prospective 10-year cohort of heavy drinkers. Kaplan-Meier curve and hazard ratio in comparison to patients with LS < 6 kPa (plotted vs the mean LS of the group with 95% C.I.) in a 10-year follow-up study (preliminary (n = 574) unpublished analysis)

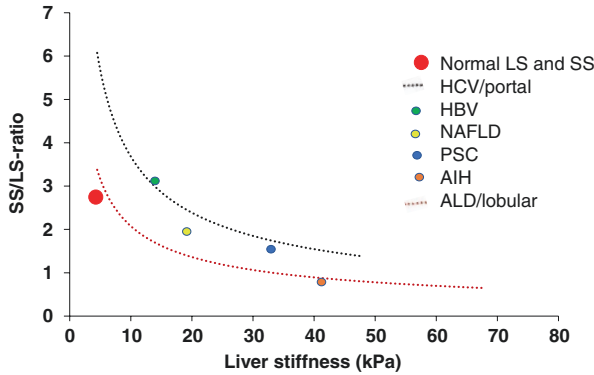
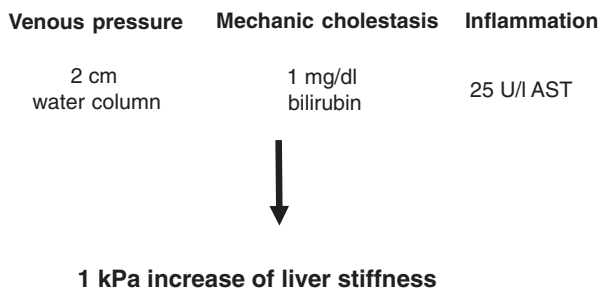


**Fig. A.8** Progression of the spleen stiffness to liver stiffness (SS/LS) ratio over increasing LS values in different etiologies. Portal diseases such as HCV show larger spleens and higher SS at comparable LS values. This can be used to confirm disease etiologies by noninvasive means. While SS/LS ratios are well settled for ALD and HCV, preliminary data are presented for NAFLD, PSC, HBV, and AIH

Parameter	Normal liver	Type of portal hypertension						
		post-hepatic		hepatic			pre-hepatic	
Example		heart failure	Budd-Chiari syndrome	manifest liver cirrhosis	non-cirrhotic lobular inflammation (e.g. F3 ALD)	non-cirrhotic portal inflammation (e.g. F3 HCV)	idiopathic portal hypertension	portal vein thrombosis
SS/LS ratio*	3	0.3	0.5-1	1-1.5	2.5	5	9	17
spleen length/LS ratio (cm/kPa)	2.3	0.13	0.15	0.3-0.5	1.3	1.8	2.7	3.7

**Fig. A.9** Spleen stiffness (SS) and liver stiffness (LS) in different liver pathologies. Note that SS/LS increases the more the pathology is localized at the portal or even prehepatic side. The simple parameter spleen length (SL) performs quite well. Thus, the SS/LS or SL/LS ratio can be used to provide further information about the disease etiology. Please also note that SS/LS decreases with progression of liver fibrosis. Therefore, SS/LS should be seen together with the absolute LS values. \* examples are given with typical values

**Fig. A.10** Estimated effect of important clinical confounders on LS



Modified from Mueller S, Sandrin L. *Hepatic Medicine: Evidence and Research* 2010;2:49-67.

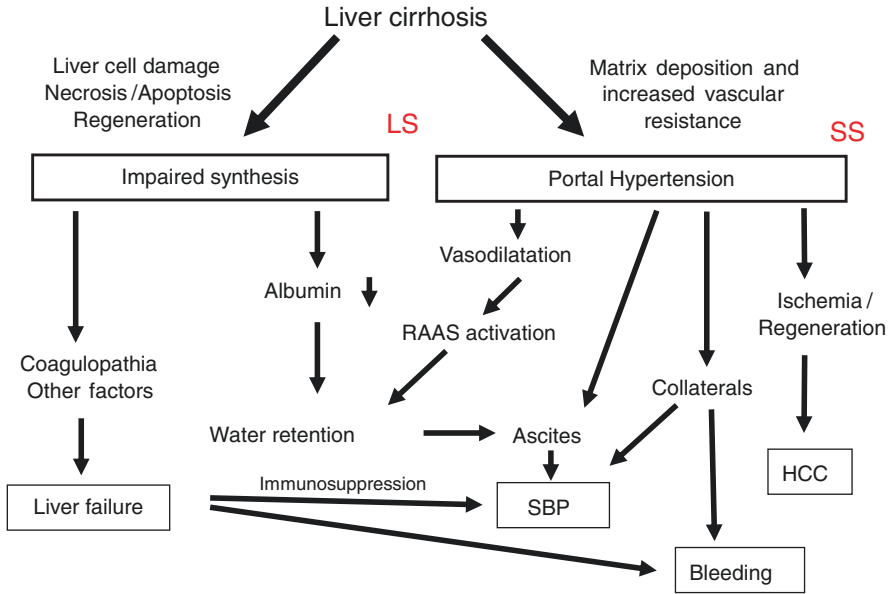
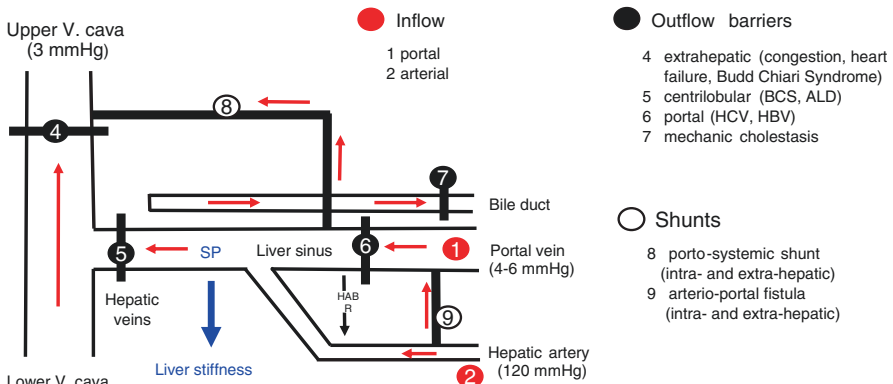


**Fig. A.11** Clinical significance of synthesis impairment and portal hypertension in cirrhotics. Both factors are independently and individually occurring in cirrhotic patients and determine the individual risk of severe complications (framed). While synthesis is easily assessed by lab tests, elastographic techniques are the future highly sensitive method of choice to identify patients with portal hypertension through measurement of liver stiffness (LS) and spleen stiffness (SS)



Modified from Mueller S. *World J Gastroenterol.* 2016;22(48):10482-10501.

**Fig. A.12** Hemodynamics of the low-pressure organ liver in the context of systemic circulation. Cirrhosis causes an increased vascular resistance, collateral formation, and increased hepatic arterial flow to maintain hepatic perfusion. Elevated hepatic arterial flow can be observed already before the onset of fibrosis. It eventually leads to a complete arterialization of the cirrhotic liver, sometimes even with hepatofugal flow through the portal vein

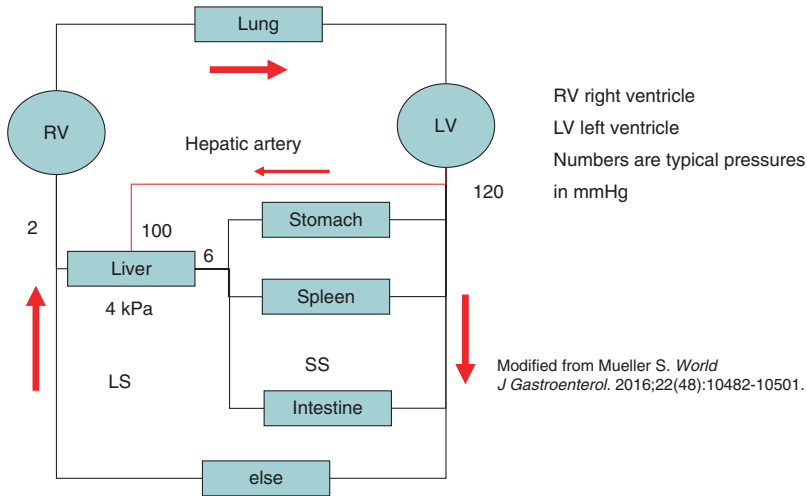


**Fig. A.13** Liver perfusion within the systemic circulation. The liver which is mainly supplied via low pressure (<6 mmHg) through the portal vein while the hepatic artery will take over in the diseased, stiff organ (see also Part VIII. Liver hemodynamics is best understood when looking at it within one systemic circulation of two sequentially adjusted pumps (right and left ventricle). Note that the blood circulation (red arrows) is maintained by two serial pumps (RV right ventricle, LV left ventricle). A dysbalance of these two pumps such as observed during right heart failure can also cause higher SP (congestion) and ultimately cardiac liver cirrhosis

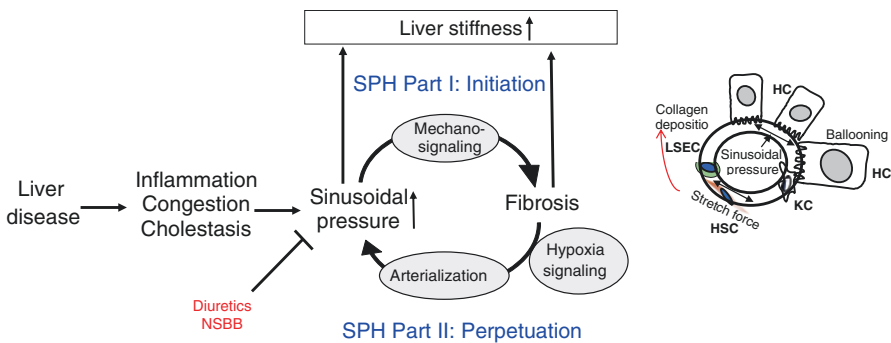


**Fig. A.14** Fig. A.4 Sinusoidal pressure hypothesis (SPH) at the whole organ level and therapeutic target sides (red). SP is the driving force of matrix deposition. Irrespective of the etiology, all liver pathologies (shown in the left) increase the SP that initiates matrix deposition via specific inter- and intracellular biomechanic signaling pathways (SPH Part I, Initiation). LS should be regarded as the combined readout of elevated pressure and fibrosis. Both SP elevation and matrix deposition increase vascular resistance that ultimately lead to elevated hepatic arterial flow and finally complete arterial blood supply. Depending on dosage (>12 mmHg) and time (>4 weeks), this vicious cycle will ultimately cause a complete arterialization leading to irreversible cirrhosis by exposing the low pressure organ to permanent high pressure (SPH Part II, Perpetuation). According to SPH, nonselective beta blockers (NSBB) and diuretics are not only symptomatic therapies but interrupt the vicious cycle of pressure-driven fibrosis progression. The right panel demonstrates how elevated sinusoidal pressure causes stretching of perisinusoidal aligned cells to induce mechano-signaling



## Tables

**Table A.1** Comparison of different methods to assess liver cirrhosis

Parameter	Biopsy	Ultrasound	Elastography	Serum markers
Invasive	Yes	No	No	No (blood sample)
Structures established	Decades	Decades	<10 years	Decades
Costs	High	Low	Low	Low
Immediacy	1–3 days	15 min	5 min	1–72 h
Patient at diagnostic side	No	Yes	Yes	No
Availability	Almost everywhere (mail)	Broadly available	Restricted to centers	Almost everywhere (mail)
Repeatable	After interval	Immediately	Immediately	Immediately
Sampling error	<30%	Subjective	<3%	<3%
Required expertise	High	High	Low	Low
Information	Multiple	Multiple	Few	Multiple
Limitations	Compliance, coagulation, ascites	Obesity, others	Obesity, others	Almost no
Direct liver read out	Yes	Yes	Yes	No
Future directions	Automated scanning and evaluation	Miniaturization, resolution, combination with elastography/Duplex	Miniaturization, part of whole body MRI analysis, co-integration in most US devices	High through put panels, novel marker profiles
Green points	4	7	7	8

The performance of various tests depends on many factors including whether to screen or provide a definite diagnosis. Various parameters are listed and highlighted in “green” if favorable. These “green points” are added in the final line. Elastography is noninvasive, the most immediate technology and able to rule out cirrhosis. On the other side, it is not available everywhere and has measurement failures. In contrast, blood samples can be obtained everywhere and shipped anywhere. For these reasons, serum markers are ideal for worldwide screening purposes








**Table A.2** Types of elastography: excitation mode, dimensions, and producers

Type of elastography	Excitation	Elastography type	Dimension	Company/brand
Strain imaging/ elastography	Manual compression	<i>Strain elastography</i>	2D	
		ElaXto	2D	Esaote
		Real-time elastography	2D	Hitachi Aloka
		Elastography	2D	GE, Philips, Mindray
		ElastoScan	2D	Samsung
		eSieTouch elasticity imaging	2D	Siemens
	Controlled compression	<i>Atomic force microscopy</i>	2D	Bruker, Hitachi, etc.
	Acoustic radiation force (single focus)	<i>Acoustic radiation force impulse (ARFI) strain imaging</i>	2D	
Virtual touch imaging (VTI/ARFI)		2D	Siemens	

**Table A.2** (continued)

Type of elastography	Excitation	Elastography type	Dimension	Company/brand
Shear wave imaging/ elastography	Acoustic radiation force (single focus)	<i>Point shear wave speed measurements (pSWE/ARFI quantification)</i>	2D	
		Virtual touch quantification (VTQ/ARFI)	2D	Siemens
		ElastPQ	2D	Philips
	Acoustic radiation force (single focus)	Virtual touch image quantification (VTIQ/ARFI)	2D	Siemens 2008, Philips, Toshiba 2013, GE
	Acoustic radiation force (multiple-zonated focus)	<i>2D-shear wave elastography (2D-SWE)</i>	2D	SuperSonic imagine
		<i>Or Supersonic shear imaging (SSI)</i>		
	Controlled external vibration	<i>Transient elastography (TE)</i>	1D	
Fibroscan		1D	Echosens 2003	
		<i>Magnetic resonance elastography</i>	3D	Hitachi, Siemens, etc.

Table A.3 Overview of elastographic methods and technical principles

Method	Ref	Abb	Measurement method		Displayed physical quantity	Excitation	Freq.	Units	Manufacturers
Transient elastography	[1]	TE	Shear wave speed, 1D		Young's modulus $E$ , stiffness	Controlled external vibration	50 Hz	kPa	Echosens (Fibroscan)
Magnetic resonance elastography	[2, 3]	MRE	Shear wave speed, 3D		Shear modulus $G$ , stiffness	Controlled external vibration (electromechanical, piezoelectrical, acoustic coupling)	60 Hz	kPa	Siemens, GE, Resoundant, Philips
Shear wave elasticity imaging	[4] <sup>a</sup>	SWEI SWE	Shear wave speed, 2D		Shear wave speed	Acoustic radiation force excitation	100–500 Hz	m/s	Siemens (VTQ), Philips (ElastPQ), GE (2D SWI GE)
Supersonic shear imaging	[5]	SSI 2D-SWE	Shear wave speed, 2D		Young's modulus $E$ , stiffness	Acoustic radiation force excitation	100–500 Hz	kPa	Supersonic imagine (Aixplorer)
Acoustic radiation force impulse strain imaging	[6]	ARFI	Displacement, 2D		Qualitative, contrast mapping	Acoustic radiation force excitation	–	Qualitative	Siemens, Phillips, Hitachi Aloka
Strain elastography and strain rate imaging			Palpation/ displacement, 2D		Qualitative, contrast mapping	Steady compression with transducer, heart beats, respiration	–	Qualitative	Hitachi, Toshiba, Siemens, GE, Samsung

$P$  density,  $V$  speed/velocity,  $E$  Young's modulus,  $\mu$  shear modulus ( $E = \mu(1 + \nu)$ ,  $\nu$  Poisson's ratio)

<sup>a</sup>Often also referred to as ARFI, especially VTQ

**Table A.4** Comparison of LS cutoff values between different elastography techniques

Technique	TE	pSWE/ARFI	2D-SWE/SSI	MRE	Reference
Estimated equation <sup>a</sup>	LS = $V * V * 3$ kPa	TE = ARFI*ARFI*3 + 2 m/s	LS = $V * V * 3$ m/s	TE = MRE*2.44 kPa	
Units	kPa	m/s	m/s	kPa	
Mean normal liver	4.5	1.14		4.4	[7-12]
Cutoff normal liver	<6	<1.16		<6.0	[7-11]
F3 fibrosis	8.0	1.6	1.9	11.0	[13-17]
F4 cirrhosis	12.5	1.9	2.1	15.0	[13-17]
Complications of cirrhosis	>20.0	>2.0		> 23.0	[18-20]
Detection limit FS	75.0			75	

This table has been prepared in order to allow comparison of the different LS cutoff values from different technologies. Estimated formulas are provided to convert LS values from one technique to the other

<sup>a</sup>Young's modulus  $E$  (as measured by Fibrosan/VCTE/FS) is three times higher than the MRE-measured shear stiffness  $\mu$  according to the following equation:  $\mu = E/3$

**Table A.5** Reliability criteria for liver stiffness measurement with FibroScan

Liver stiffness	Interquartile range/median ratio		
Result (kPa)	≤0.10	0.11 – 0.30	0.30<
<7.1	Very reliable	Reliable	Poorly reliable
≥7.1			

Poorly reliable examinations are associated with decreased diagnostic accuracy and should not be used to decide the patient management in clinical practice

**Table A.6** Definition and examples of waves

Wave/synonym	Definition	Example
Mechanical wave	Oscillation of matter. Mechanical waves transport energy. Can be produced only in media (in contrast to electromagnetic waves) which possess elasticity and inertia	Water waves, sound waves, and seismic waves
Elastic waves	An elastic disturbance that propagates in a solid, liquid, or gaseous medium. When elastic waves propagate, the energy of elastic deformation is transferred in the absence of a flow of matter. Every harmonic elastic wave is characterized by the amplitude and vibration frequency of the particles of the medium, a wavelength, phase and group velocities, and a law governing the distribution of displacements and stresses over the wave front. A special feature of elastic waves is that their phase and group velocities are independent of the wave amplitude and the wave geometry. An elastic wave may be a plane, spherical, or cylindrical wave	Sound waves
Acoustic waves	Mechanical waves. Type of energy propagation through a medium by means of adiabatic compression and decompression. Acoustic waves travel with a characteristic acoustic velocity that depends on the medium. Their speed is ca. 1450 m/s liver/water. Examples of acoustic waves are ultrasound used for medical imaging (waves traveling through the body)	Sound waves from loudspeakers Ultrasound imaging
Electromagnetic waves	Electromagnetic waves require no medium but can still travel through one	Radio waves, microwaves, infrared, (visible) light, ultraviolet, X-rays, and gamma rays
Body waves	These waves travel through the interior of a body along paths controlled by the material properties in terms of density and modulus (stiffness). The density and modulus according to temperature, composition, and material phase. Two types of particle motion result in two types of body waves: Primary and secondary waves	

**Table A.6** (continued)

Wave/synonym	Definition	Example
P-wave Primary waves Compressional waves Pressure waves	P-wave longitudinally ca. 1.7 times faster than other waves hence the name “primary.” In air, they travel at the speed of sound. Typical speeds are 330 m/s in air, 1450 m/s in water, and about 5000 m/s in granite	Sound waves
S-wave Secondary waves Transverse waves	S-waves are shear waves displace the ground perpendicular to the direction of propagation. S-waves can travel only through solids, as fluids (liquids and gases) do not support shear stresses. S-waves are typically around 60% of that of P-waves in any given material	
Surface waves	Surface waves, which are generally called Rayleigh waves, can propagate at the boundary between a solid half space and a vacuum, liquid, or gas; such waves are a combination of nonuniform longitudinal and shear waves whose amplitudes decrease exponentially with distance from the boundary. They travel more slowly than P and S waves	Water waves

**Table A.7** Normal stiffness values for various organs as measured by different elastography techniques

	Organ	TE	SWE	MRE	ARFI	Reference
Kidney			4.3 kPa			[21]
				6.4–7.3 kPa (90 Hz)		[22, 23]
	Transplant kidney	33.2–35 kPa			2.24 m/s	[24–27]
Uterus	Cervix		18.9 kPa			[29]
	Myometrium		40.2 kPa			[29]
	Endometrium		25.4 kPa			[29]
Pancreas				1.1–2.0 kPa (60 Hz)		[23, 30, 31]
					1.2–1.4 m/s	[24–27, 32]
Prostate	Whole gland		27.3 kPa			[33]
Spleen				3.5–3.6 kPa		[23, 34]
		22.0 kPa 13.8–17.3 kPa			2.4 m/s	[24–27, 35] [36–38]

**Table A.8** Association of serum markers with liver stiffness

Parameter	Spearman correlation coefficients with liver stiffness								
	F0-4			F=0-2		F3-4		all	
	HCV	ALD	Sum	HCV	ALD	HCV	ALD	Sum	
Fibrosis stage (histology)	0.69	0.78	1.46	0.33	0.38	0.61	0.59	1.91	
AST	0.54	0.35	0.89	0.36	0.43	0.45	0.13	1.38	
GGT	0.43	0.37	0.80	0.36	0.32	0.38	0.05	1.11	
ALT	0.35	0.13	0.48	0.33	0.31	0.14	-0.03	0.75	
Bilirubin	0.21	0.57	0.78	0.08	0.35	0.32	0.65	1.39	
APRI	0.50	0.49	0.99	0.41	0.39	0.62	0.40	1.83	
Platelets	-0.43	-0.45	-0.88	-0.20	-0.30	-0.61	-0.46	-1.57	
BMI	0.23	0.13	0.36	0.22	0.11	0.19	0.06	0.58	
Age	0.29	0.20	0.50	0.13	0.13	0.11	0.00	0.38	
AST/ALT ratio	0.17	0.31	0.47	-0.08	0.13	0.49	0.23	0.77	

■ Positive correlation (P<0.05)  
■ Negative correlation (P<0.05)  
 No significant correlation (P>0.05)

Correlation analysis with liver stiffness was performed for both HCV and ALD for (a) all fibrosis stages F0-4 (b) F0-2 and (c) F3-4. The sum of these correlation coefficients was determined to estimate which serum marker would best explain LS independent of fibrosis stage and etiology. Here, AST performs best. (From [39])

**Table A.9** Correlation of various serum markers with change of LS, LS and change of GOT in patients with ALD (n = 544). Note that changes of LS and GOT refer to changes prior and after alcohol detoxification. GOT correlates best with change of LS but not with absolute LS values. Here, GGT, M65, and AP are better associated. Also note: AST = GOT, ALT = GPT

Correlation with change of LS		
Parameter	Spearman Rho correlation with change of LS	
	r	p
Liver stiffness (kPa)	0.466	3.0E-31
CAP (dB/m)	0.235	2.8E-06
GOT (U/L)	0.182	1.6E-05
Delta GOT (U/L)	0.177	2.8E-05
GGT (U/L)	0.177	3.3E-05
IL-6 (ng/mL)	0.543	4.2E-04
GPT (U/L)	0.146	5.9E-04
Platelets (/nL)	-0.136	1.3E-03

Correlation with LS		
Parameter	Spearman Rho correlation with LS	
	r	p
GGT (U/L)	0.564	2.4E-47
M65 (U/L)	0.547	4.9E-38
AP (U/L)	0.504	4.6E-37
Quick (%)	-0.491	8.8E-35
INR	0.488	2.6E-34
GOT (U/L)	0.478	6.6E-33
Quick (%)	-0.491	8.8E-35
Platelets (/nL)	-0.427	7.2E-26

**Table A.9** (continued)

Correlation with change of AST/GOT		
Parameter	Spearman Rho correlation with change of GOT	
	<i>r</i>	<i>p</i>
GOT (U/L)	0.778	1.1E-113
GPT (U/L)	0.642	1.1E-65
GGT (U/L)	0.547	4.4E-44
M65 (U/L)	0.563	1.1E-40
M30 (U/L)	0.506	6.4E-32
Ferritin (ng/mL)	0.421	4.1E-25
AP (U/IL)	0.354	8.6E-18
Platelets (/nL)	-0.306	1.9E-13

**Table A.10** Estimated cutoff values for F3 fibrosis and F4 cirrhosis for different etiologies

Etiology	F3 LS cutoff value (kPa)	F4 LS cutoff value (kPa)	References
NASH	9.6 (8–11.4)	13.7 (10.2–14)	[40–43]
ALD	10.5 (8–12.9)	17.6 (11.5–22.6)	[44–47]
HCV	10.8	14.8	[48–50]
HBV	8.1	10.9	[51–54]
AIH	10.4	16	[55, 56]
PSC	9.6	14.4	[57]
PBC	10.7	16.3 (15.6–16.9)	[58, 59]
HFE	13.9	17.9	[60]
Wilson’s disease	8.25	13	[61]
Cardiac hepatopathy	7.6	13.0	[62]
AATD	7.8 (7.2–8.4)	14	[63, 64]
Cystic fibrosis		7.95	[65]
<b>ALL<sup>a</sup></b>	<b>9.6 kPa</b>	<b>14.0 kPa</b>	
<b>ALL<sup>b</sup></b>	<b>8 kPa</b>	<b>12.5 kPa</b>	

<sup>a</sup>Mean values of this table

<sup>b</sup>Mean values in the absence of inflammation

Note that mean values are shown from selected studies not being complete but representative. For some etiologies such as NAFLD or HCV, a range is provided. This range gives an impression of the variability between studies most likely due to confounders such as inflammation (e.g., ALD) and or cholestasis (e.g., PBC)



**Table A.11** Normal LS values according to different age groups

Age	TE (kPa)	LS			CAP (dB/m)
		2D-SWE GE Logiq (kPa)	2D-SWE kPa	p-SWE Samsung (m/s)	
1–5 <sup>a</sup>	3.4 [66]	2.9 [67]	4.63 ± 0.6 [68]	1.14 [67]	180
5–11 <sup>a</sup>	3.8 [66]	3.4 [67]	4.05 ± 0.57 [68]	1.17 [67]	181
12–18 <sup>a</sup>	4.1 [66]	3.8–3.9 [67]	4.39 ± 0.55 [68]	1.2 [67]	190
18 to >70	4.5 [7–12]				
Healthy pregnant women	4.5 [69]				226 [69]

<sup>a</sup>Since not all age ranges were identical in the studies some have been estimated. Note that it is still a challenge to consider a population as “liver normal” and, therefore, to define normal liver stiffness levels. However, taken together studies and daily clinical experience, normal values should be 3.4 kPa for children, 3.8 kPa for adolescents, and 4.2 kPa for adults. On the other side, soft livers at 3 kPa can be also observed sometimes in adults and this is then an excellent result. In contrast, 5.5 kPa can already be an indication of an elevated liver stiffness in a young adult. The generally accepted cutoff for normal LS (<6 kPa) takes heavily into account uncontrollable confounders in daily application such as food intake, positioning, breathing, etc. In some cases, optimal conditions should be applied (see book Part VII) and LS measurement should be repeated.

**Table A.12** Normal LS in different species

Species	Mean normal LS	Reference
Humans	4.5–4.7 kPa	[69, 70]
Pigs	3.1–4.1 kPa	[71, 72]
Rats	3.8–4.1 kPa	[73, 74]
Mice	4.4 kPa	[75]

**Table A.13** Characteristics of different Fibroscan probes (Adopted from EchoSens manufacturer's manual)

Parameter	S probe	M probe	XL probe	Spleen examination	TME
Size	158 × 52 mm	158 × 52 mm	158 × 52 mm		182 × 32 mm
Weight	0.5 kg	0.5 kg	0.5 kg		260 g
Transducer diameter	5 mm	7 mm	10 mm		2 mm
Vibration frequency	50 Hz	50 Hz	50 Hz	100 Hz	50 Hz
US frequency	5 MHz	3.5 MHz	2.5 MHz		Adjustable up from 1 to 60 MHz
Measurement depth	15–45/55 mm	25–65 mm	35–75 mm		Adjustable up from 1 to 200 mm
Static force range (N)	1–8	4–8	4–8		Adjustable from 1 to 12

*TME* transient micro elastography

**Table A.14** Clinical and technical considerations regarding L-S measurements using different techniques

TE [76]	ARFI [76]	SSI [76]	MRE [76]
<ol style="list-style-type: none"> <li>The investigation should be performed with the patient in the supine or slight left lateral position with the arm raised above the head to increase the intercostal space [77, 78]</li> <li>Measurements should be taken through an intercostal approach at the location of the best acoustical window [77, 78]</li> <li>Measurements should be taken 1.5–2.0 cm below the liver capsule to avoid reverberation artifact. The optimal location for maximum shear wave generation is 4.0–4.5 cm from the transducer [78, 79]</li> <li>The transducer should be perpendicular to the liver capsule [1, 80].</li> <li>Placement of the region of interests should avoid large blood vessels, bile ducts, and masses. The operator, assisted by ultrasound A-mode images provided by the system, locates a portion of the liver at least 6 cm thick and free of large vascular structures [81]</li> <li>For transient elastography, the appropriate transducer should be selected based on patient's body habitus</li> <li>Ten measurements should be obtained from 10 independent images, in the same location, with the median value used for transient elastography [78]</li> <li>The IQR/M (interquartile range/median) should be used as a measure of quality. For kPa measurements the IQR/M should be &lt;0.3 [78]</li> </ol>	<ol style="list-style-type: none"> <li>The right lobe should be scanned by an intercostal approach with normal breathing, which leads to a low measurement variability [82]</li> <li>The manufacturer recommendations to obtain the best results has to be considered as applying minimal scan pressure; excluding data that varies significantly; minimizing breathing and avoiding cardiac motion, and using the proper site (intercostal right lobe, segment 8 or 5) [83]</li> <li>According to the recent EFSUMB guidelines, measurement of liver stiffness by ARFI should be performed through a right intercostal space in supine position, with the right arm in extension, during breath hold, avoiding deep inspiration prior to the breath hold [84]</li> <li>According to the guidelines, the optimum depth could differ according to the used transducer and frequency. For convex transducers, depth is 4–5 cm and average frequency of 2.6 MHz are the optimum settings. However, the linear transducers require less depth range of 2–3 cm and higher frequency of 4 MHz [85]</li> </ol>	<ol style="list-style-type: none"> <li>The operator places the region of interest in an area without large vessels, at a depth more than 2 cm, but no deeper than 8 cm [86–88]</li> <li>The latest EFSUMB guidelines recommend that for 2D-SWE/SSI, a minimum of three measurements should be obtained; the result should be expressed as the median together with the interquartile range [76, 89]</li> <li>Initially no quality criteria were recommended by the manufacturer, but some authors use as quality control standard deviation/median liver stiffness <math>\leq 0.10</math> and measurement depth <math>&lt; 5.6</math> cm [90, 91]</li> <li>The measurement is performed with the patient in supine position, in intermediate breathing, through an intercostal space</li> <li>The right liver lobe is scanned and a region of interest (ROI) is placed at least, 10 mm below the liver capsule, in a region free of vessels [91, 92]</li> </ol>	<ol style="list-style-type: none"> <li>The mechanical waves are produced by a wave generator (also named as active driver), which is located outside the MRI examination room and shielded from the imaging magnet [93]</li> <li>The mechanical waves (vibrational energy, pressure waves) are sent to the passive driver through the flexible plastic connecting tube. The passive driver is placed on the external abdominal wall and is positioned across the lower chest or on the right lobe of the liver [22]</li> <li>This measurement shows both the properties of tissue elasticity and tissue viscosity (i.e., viscoelasticity) in units of kilopascals (kPa). Currently, all major brands offer commercially available elastograms using the same standard color scale of 0–8 kPa [94]</li> <li>Liver stiffness is assessed by drawing free-hand region of interest (ROI) in the elastograms</li> <li>The ROIs should be placed in areas with adequate wave amplitude. The edge of the liver should not be approached more than half a wavelength as it may cause edge effects. Hot spots (coded with red color), which are typically found under the passive driver, should be excluded [94]</li> <li>In addition, special care should be taken when placing an ROI to avoid regions of wave interference, large vessels (&gt;3 mm), severely dilated bile ducts, gallbladder fossa, widened liver fissures, and obvious image artifacts within the liver [95]</li> <li>Mean stiffness from each ROI is obtained. Mean value obtained from four different levels of the liver and range of measurements are reported [95]</li> </ol>

**Table A.15** Optimal standardized conditions for liver stiffness measurements for all techniques

No.	Conditions
1	Standardized patient conditions and positioning. Horizontal positioning for at least 5 min. Normal breathing. Fasting status. Stabilized hemodynamics e.g., after physical exercise
2	Correct training of the examiner depending upon the elastographic technique used. Small learning curve for 1D-SWE such as TE, dedicated ultrasound knowledge for 2D-SWE. Specific radiology training for 3D-MRE
3	Correct physical LS measurement: basic anatomical and specific knowledge such as choice of probe, probe pressure, localization of liver region for LSM
4	Correct and standardized analysis of shear wave speed which may necessitate additional interpretation of e.g., elastograms. Additional factors in 2D-SWE such as viscosity and sound speed
5	Correct statistical interpretation e.g., median LS and IQR
6	Correct interpretation of LS within the clinical context including the influence of confounders such as inflammation, congestion, cholestasis, or others. These confounders require additional information such as an on-time ultrasound or laboratory parameters. Critical discussion of potential measurement artifacts
7	Definition whether LSM is used in screening or expert mode. The screening mode is primarily designed to rule out any liver abnormalities. The expert mode is thought to confirm an elevated LS, to rule out potential confounders or artifacts and to ultimately link the elevated LS either to fibrosis stage or prognostic evaluation and guiding therapies

**Table A.16** General clinical and technical considerations regarding liver elastography

Recommendations	References
1. Experienced operators should perform measurement of liver stiffness	[76]
2. Measurement of liver stiffness (specially ultrasound-based techniques) should be performed through a right intercostal space in supine position, with the right arm in extension, during breath hold, avoiding deep inspiration prior to the breath hold	[78, 96]
3. Patients should fast for a minimum of 2 h and rest for a minimum of 5–10 min before undergoing liver stiffness measurement. Watch for stable LS	[97–103]
4. The major potential confounding factors (liver inflammation indicated by AST and/or ALT elevation >5 times the normal limits, arterial pressure, obstructive cholestasis, liver congestion, acute hepatitis and infiltrative liver diseases) should be excluded before performing LSM by ultrasound	[39, 71–73, 104, 105]

**Table A.17** Spearman rank correlation of important histological parameters (fibrosis, ballooning, steatosis, steatohepatitis) with physical, serum and clinical parameters

Parameter	Fibrosis (Chevallier)	Ballooning	Steatosis	Steatohepatitis
M30 (U/L)	0.291**	0.544**	0.467**	0.557**
M65 (U/L)	0.285**	0.540**	0.431**	0.554**
Liver stiffness (kPa)	0.828**	0.516**	0.096	0.391**
AST (U/L)	0.167	0.453**	0.415**	0.435**
GGT (U/L)	0.273**	0.429**	0.350**	0.474**
AP (U/L)	0.524**	0.425**	0.117	0.294**
Hyaluronic acid (ng/mL)	0.645**	0.365**	-0.044	0.236
Signs of cirrhosis (US)	0.573**	0.342**	0.008	0.227*
Hepatic steatosis (US)	0.040	0.327**	0.327**	0.452**
PNPLA3 GG	0.131	0.319**	0.264*	0.404**
CAP(dB/m)	-0.069	0.301	0.593**	0.432*
BMI (kg/m <sup>2</sup> )	0.182	0.220	0.076	0.089
PIIINP (ng/mL)	0.276*	0.214	0.014	0.147
ALT (U/L)	-0.232*	0.184	0.339**	0.256**
Alcohol consumption (g/day)	-0.074	-0.026	0.224*	0.123
Gender (male:1)	-0.106	-0.120	-0.094	-0.119

Parameters are sorted in descending order using the correlations coefficients for ballooning. \* $P < 0.05$ ; \*\* $P < 0.01$  [106] in a large cohort of heavy drinkers. Note that LS is the best noninvasive marker for fibrosis, M30/65 for steatohepatitis and ballooning, and CAP for steatosis (all highlighted in yellow). US: ultrasound. Data are from [106]

**Table A.18** Spleen stiffness (SS) cutoff values for the standard M probe vs the dedicated spleen probe to detect esophageal varices [107]

Esophageal varices grade	SS with standard M probe in kPa (IQR)	SS with dedicated spleen probe in kPa (IQR)
No varices	52.5 (32.5)	34.4 (15.4)
1	62.9 (28.7)	45.8 (19.1)
2	73.9 (19.6)	53.4 (13.7)
3	75.0 (2.5)	57.4 (11.5)

**Table A.19** Knodell histology activity index (HAI) [108]

Knodell histology activity index (HAI)			Points
<i>A. Periportal necrosis (PN) with or without bridging necrosis</i>			0
1. None			1
2. Mild piecemeal necrosis			2
3. Moderate PN (<1/2 circumference)			3
4. Marked PN (>1/2 circumference)			4
5. Moderate PN + bridging necrosis			5
6. Marked PNB + bridging necrosis			6
7. Multilobular necrosis			10
<i>B. Intralobular degeneration and focal necrosis</i>	<i>C. Portal inflammation</i>	<i>D. Fibrosis</i>	
1. None	1. None	1. None	0
2. Mild (1/3 of lobular)	2. Mild (1/3 of portal tract)	2. Fibrous portal expansion	1
3. Moderate (1/3–2/3)	3. Moderate (1/3–2/3)	3. Bridging fibrosis	3
4. Marked (>2/3)	4. Marked (>2/3)	4. Cirrhosis	4

**Table A.20** Scheuer histological activity index score [109]

Scheuer histological activity index		Points
<i>A. Portal/periportal activity</i>		
1. None/minimal		0
2. Portal inflammation		1
3. Mild portal necrosis (PN)		2
4. Moderate PN		3
5. Severe PN		4
<i>B. Lobular activity</i>	<i>C. Fibrosis</i>	
1. None	1. None	0
2. Inflammation no necrosis	2. Enlarged, fibrotic portal tracts	1
3. Focal necrosis/acidophil boding	3 Periportal or portal septa	2
4. Severe focal cell damage	4. Fibrosis, architectural distortion, no cirrhosis	3
5. Damage includes bridging necrosis	5. Probable/definite cirrhosis and necrosis	4

**Table A.21** Histopathological scores for assessment of liver fibrosis [110–112]

Ishak score	Batt and Ludwig	Metavir	Points
Inflammation and necrosis: Absent No fibrosis	Mild portal inflammation or no inflammation, either interface necrosis or lobular inflammation. <i>No fibrosis</i>	A0: no inflammation or necrosis F0: no fibrosis	0
Portal and periportal inflammation in some areas, with focal necrosis 1 focus/10×. Fibrous expansion of some portal areas with or without short septa	Minimum portal inflammation, patchy interface-necrosis, and occasionally apoptotic hepatocytes. <i>Portal fibrosis</i>	A1: mild necro-inflammatory activity F1: portal fibrosis	1
Mild swelling in portal areas with necrosis shown in zone 3 and some in zone 2. Focal necrosis 2–4 × 10×. Fibrous expansion of most portal areas, with or without short septa	Mild portal inflammation with interface hepatitis in some portal tracts and mild apoptosis. <i>Periportal fibrosis</i>	A2: moderate necro-inflammatory activity F2: portal fibrosis with few septa	2
50% or moderate inflammation with necrosis in most of zone 1, and focal necrosis 5–10 × 10×. Fibrous expansion of most portal areas with occasional P-P bridges.	Moderate portal inflammation, interface and lobular hepatitis, frequent necrotic hepatocytes. <i>Septal fibrosis</i>	A3: severe necro-inflammatory activity F3: portal fibrosis with numerous septa	3
Severe swelling in most portal tracts with necrosis in zone 1, occasional PC, bridges and focal necrosis 10 × 10×. Fibrous expansion of most portal areas with frequent PP and PC bridges	Severe portal inflammation, interface hepatitis with necrosis prominent on bridges and diffuse hepatocellular damage. <i>Cirrhosis</i>	F4: cirrhosis	4
Portal and lobular inflammation, necrosis in zone 1 with multiple PC areas numerous PP and PC bridges with incomplete cirrhosis or incomplete nodules.			5
Portal inflammation, lobular and pan-glandular necrosis. Cirrhosis			6

**Table A.22** Chevallier semiquantitative scoring system (SSS) [113]

Chevallier (SSS) score		Points
<i>A. Central lobular vein (CLV)</i>		
1. Normal vein or absence of vein		0
2. Moderately thickened (stellate aspect of vein wall)		1
3. Markedly thickened (annular aspect of vein wall with numerous fibrous intercellular extensions)		2
<i>B. Portal tract (PT)</i>	<i>C. Perisinusoidal space (PS)</i>	
1. Normal	1. Normal	0
2. Enlarged without septa	2. Localized fibrosis	1
3. Enlarged with septa	3. Diffuse fibrosis	2
4. Cirrhosis		3
<i>D. Number of septa (NS)</i>	<i>E. Width of septa (WS)</i>	
1. Absence	1. Thin and or incomplete	0
2. ≤6 septa/10 mm	2. Thick and loose connective matrix	1
3. >6 septa/10 mm	3. Very thick and dense connective matrix	2
4. Nodular organization	4. >2/3 of biopsy area	3
<i>Score expression: SSS = CLV + PS + PT + 2(WS × NS)</i>		

**Table A.23** NASH Clinical Research Network score (modified by Kleiner et al. 2005) [114]

NASH Clinical Research Network scoring system definitions			
<i>A. Steatosis grade</i>	<i>B. Location (predominant)</i>	<i>C. Lobular inflammation</i>	<i>Points</i>
1. <5%	1. Zone 3	1. No foci	0
2. 5–33%	2. Zone 1	2. <2 foci per 200 × field	1
3. >33–66%	3. Azonal	3. 2–4 foci per 200 × field	2
4. >66%	4. Panacinar	4. >4 foci per 200 × field	3
<i>D. Micro vesicular steatosis</i>	<i>E. Microgranulomas</i>	<i>F. Large lipogranuloma</i>	
1. Absent	1. Absent	1. Absent	0
2. Present	2. Present	2. Present	1
<i>G. Fibrosis stages</i>			
1. None			0
2. Perisinusoidal or periportal			1
3. Mild, zone 3, perisinusoidal			1A
4. Moderate, zone 3, perisinusoidal			1B
5. Portal/periportal			1C
6. Perisinusoidal and portal/periportal			2
7. Bridging fibrosis			3
8. Cirrhosis			4
<i>H. Portal inflammation</i>	<i>I. Pigmented macrophages</i>	<i>J. Mega mitochondria</i>	
1. None to minimal	1. None to rare	1. None to rare	0
2. More than minimal	2. Many	2. Many	1
<i>K. Ballooning</i>	<i>L. Glycogenated nuclei</i>	<i>M. Acidophil bodies</i>	
1. None	1. None to rare	1. None to rare	0
2. Few ballooned cells	2. Many	2. Many	1
3. Many cells/ prominent ballooning			2



**Table A.24** Desmet and Scheuer staging system for chronic hepatitis [115]

Score	Description	Histology
0	No fibrosis	No fiber multiplication
1	Mild/low fibrosis	Fiber propagation portal, no septa
2	Moderate fibrosis	Incomplete/complete portoportal septa, architecture preserved
3	High grade fibrosis	Connective tissue septa with architectural disorder (portocentral septa, shifting acinar structures), no complete cirrhosis
4	Cirrhosis	Probable or definitive cirrhotic remodeling

**Table A.25** Leipzig score for Wilson's disease [116]

Clinical symptoms and signs		Other investigations	
Kayser–Fleischer rings		Liver copper (in the absence of cholestasis)	
Present	2	>5× ULN (>4 μmol/g)	2
Absent	0	0.8–4 μmol/g	1
		Normal (<0.8 μmol/g)	–1
		Rhodamine-positive granules	1
Neurological symptoms		Urinary copper (in the absence of acute hepatitis)	
Severe	2	Normal	0
Mild	1	1–2× ULN	1
Absent	0	>2 ULN	2
		Normal, but >5× ULN after D-penicillamine	2
Serum ceruloplasmin		Mutation analysis	
Normal (>0.2 g/L)	0	Detected on both chromosomes	4
0.1–0.2 g/L	1	Detected on only one chromosome	1
<0.1 g/L	2	No mutations detected	0
Coombs-negative hemolytic anemia			
Present	1		
Absent	0		

## References of Appendix

1. Sandrin L, Fourquet B, Hasquenoph JM, Yon S, Fournier C, Mal F, et al. Transient elastography: a new noninvasive method for assessment of hepatic fibrosis. *Ultrasound Med Biol*. 2003;29(12):1705–13.
2. Muthupillai R, Lomas DJ, Rossman PJ, Greenleaf JF, Manduca A, Ehman RL. Magnetic resonance elastography by direct visualization of propagating acoustic strain waves. *Science*. 1995;269(5232):1854–7.
3. Venkatesh S, Yin M, Talwalkar J, Ehman R. Application of liver MR elastography in clinical practice. *Proceedings of the international society for magnetic resonance in medicine*, Toronto, Ontario, Canada; 2008. p. 2611.
4. Sarvazyan AP, Rudenko OV, Swanson SD, Fowlkes JB, Emelianov SY. Shear wave elasticity imaging: a new ultrasonic technology of medical diagnostics. *Ultrasound Med Biol*. 1998;24(9):1419–35.
5. Bercoff J, Tanter M, Fink M. Supersonic shear imaging: a new technique for soft tissue elasticity mapping. *IEEE Trans Ultrason Ferroelectr Freq Control*. 2004;51(4):396–409.
6. Nightingale KR, Palmeri ML, Nightingale RW, Trahey GE. On the feasibility of remote palpation using acoustic radiation force. *J Acoust Soc Am*. 2001;110(1):625–34.
7. Sirlin R, Sporea I, Bota S, Jurchis A. Factors influencing reliability of liver stiffness measurements using transient elastography (M-probe)-monocentric experience. *Eur J Radiol*. 2013;82(8):e313–6.
8. Rouviere O, Yin M, Dresner MA, Rossman PJ, Burgart LJ, Fidler JL, et al. MR elastography of the liver: preliminary results. *Radiology*. 2006;240(2):440–8.
9. Sporea I, Bota S, Peck-Radosavljevic M, Sirlin R, Tanaka H, Iijima H, et al. Acoustic Radiation Force Impulse elastography for fibrosis evaluation in patients with chronic hepatitis C: an international multicenter study. *Eur J Radiol*. 2012;81(12):4112–8.
10. Suh CH, Kim SY, Kim KW, Lim Y-S, Lee SJ, Lee M-G, et al. Determination of normal hepatic elasticity by using real-time shear-wave elastography. *Radiology*. 2014;271(3):895–900.
11. Barr RG, Ferraioli G, Palmeri ML, Goodman ZD, Garcia-Tsao G, Rubin J, et al. Elastography assessment of liver fibrosis: society of radiologists in ultrasound consensus conference statement. *Ultrasound Q*. 2016;32(2):94–107.
12. Sirlin R, Sporea I, Tudora A, Deleanu A, Popescu A. Transient elastographic evaluation of subjects without known hepatic pathology: does age change the liver stiffness? *J Gastrointest Liver Dis*. 2009;18(1):57–60.
13. Guibal A, Renosi G, Rode A, Scoazec JY, Guillaud O, Chardon L, et al. Shear wave elastography: an accurate technique to stage liver fibrosis in chronic liver diseases. *Diagn Interv Imaging*. 2016;97(1):91–9.
14. Sporea I, Bota S, Gradinaru-Tascau O, Sirlin R, Popescu A, Jurchis A. Which are the cut-off values of 2D-shear wave elastography (2D-SWE) liver stiffness measurements predicting different stages of liver fibrosis, considering transient elastography (TE) as the reference method? *Eur J Radiol*. 2014;83(3):e118–22.
15. Lee MS, Bae JM, Joo SK, Woo H, Lee DH, Jung YJ, et al. Prospective comparison among transient elastography, supersonic shear imaging, and ARFI imaging for predicting fibrosis in nonalcoholic fatty liver disease. *PLoS One*. 2017;12(11):e0188321.
16. Kim SU, Jang HW, Cheong JY, Kim JK, Lee MH, Kim DJ, et al. The usefulness of liver stiffness measurement using FibroScan in chronic hepatitis C in South Korea: a multicenter, prospective study. *J Gastroenterol Hepatol*. 2011;26(1):171–8.
17. Wu W-P, Chou C-T, Chen R-C, Lee C-W, Lee K-W, Wu H-K. Non-invasive evaluation of hepatic fibrosis: the diagnostic performance of magnetic resonance elastography in patients with viral hepatitis B or C. *PLoS One*. 2015;10(10):e0140068.

18. Jansen C, Bogs C, Verlinden W, Thiele M, Moller P, Gortzen J, et al. Shear-wave elastography of the liver and spleen identifies clinically significant portal hypertension: a prospective multicentre study. *Liver Int.* 2017;37(3):396–405.
19. Rizzo L, Pinzone MR, L'Abbate L, Attanasio M, Nunnari G, Cacopardo B. Quantitative ARFI elastography predicts short-term decompensation in HCV-related cirrhosis. *Infect Dis Tropical Med.* 2016;2(4):e345.
20. Grgurevic I, Bokun T, Salkic NN, Brkljacic B, Vukelić-Markovic M, Stoos-Veic T, et al. Liver elastography malignancy prediction score for noninvasive characterization of focal liver lesions. *Liver Int.* 2017;38(6):1055–63.
21. Leong SS, Wong JHD, Md Shah MN, Vijayanathan A, Jalalonmuhali M, Ng KH. Shear wave elastography in the evaluation of renal parenchymal stiffness in patients with chronic kidney disease. *Br J Radiol.* 2018;91(1089):20180235.
22. Venkatesh SK, Ehman RL. Magnetic resonance elastography of abdomen. *Abdom Imaging.* 2015;40(4):745–59.
23. Talwalkar JA, Yin M, Venkatesh S, Rossman PJ, Grimm RC, Manduca A, et al. Feasibility of in vivo MR elastographic splenic stiffness measurements in the assessment of portal hypertension. *AJR Am J Roentgenol.* 2009;193(1):122–7.
24. Gallotti A, D'Onofrio M, Mucelli RP. Acoustic radiation force impulse (ARFI) technique in ultrasound with virtual touch tissue quantification of the upper abdomen. *Radiol Med.* 2010;115(6):889–97.
25. Tomeno W, Yoneda M, Nozaki Y, Fujita K, Kirikoshi H, Saito S, et al. Novel ultrasound-based acoustic radiation force elastography in patients with non-alcoholic fatty liver disease (NAFLD). *Hepatology.* 2009;50(4):1035.
26. Hsu SJ, Liu CH, Kao JH, Chen DS. Acoustic radiation force impulse imaging predicts advanced fibrosis and cirrhosis in chronic hepatitis C patients. *Hepatology.* 2009;50(4):1623.
27. Piscaglia F, Salvatore V, Borghi A, Conti F, Peri E, Pietromartire F, et al. Virtual touch assessment of liver stiffness: virtual liver palpation. *Hepatology.* 2009;50(4):1088.
28. Sommerer C, Scharf M, Seitz C, Millonig G, Seitz HK, Zeier M, et al. Assessment of renal allograft fibrosis by transient elastography. *Transpl Int.* 2013;26(5):545–51.
29. Manchanda S, Vora Z, Sharma R, Hari S, Das CJ, Kumar S, et al. Quantitative sonoelastographic assessment of the normal uterus using shear wave elastography: an initial experience. *J Ultrasound Med.* 2019;38(12):3183–9.
30. Kolipaka A, Schroeder S, Mo X, Shah Z, Hart PA, Conwell DL. Magnetic resonance elastography of the pancreas: measurement reproducibility and relationship with age. *Magn Reson Imaging.* 2017;42:1–7.
31. Shi Y, Glaser KJ, Venkatesh SK, Ben-Abraham EI, Ehman RL. Feasibility of using 3D MR elastography to determine pancreatic stiffness in healthy volunteers. *J Magn Reson Imaging.* 2015;41(2):369–75.
32. Zaro R, Lupsor-Platon M, Cheviet A, Badea R. The pursuit of normal reference values of pancreas stiffness by using acoustic radiation force impulse (ARFI) elastography. *Med Ultrason.* 2016;18(4):425–30.
33. Harvey H, Morgan V, Fromageau J, O'Shea T, Bamber J, de Souza NM. Ultrasound shear wave elastography of the normal prostate: interobserver reproducibility and comparison with functional magnetic resonance tissue characteristics. *Ultrasound Imaging.* 2018;40(3):158–70.
34. Mannelli L, Godfrey E, Joubert I, Patterson AJ, Graves MJ, Gallagher FA, et al. MR elastography: spleen stiffness measurements in healthy volunteers—preliminary experience. *AJR Am J Roentgenol.* 2010;195(2):387–92.
35. Karlas T, Lindner F, Troltzsch M, Keim V. Assessment of spleen stiffness using acoustic radiation force impulse imaging (ARFI): definition of examination standards and impact of breathing maneuvers. *Ultraschall Med.* 2014;35(1):38–43.
36. Stefanescu H, Grigorescu M, Lupsor M, Procopet B, Maniu A, Badea R. Spleen stiffness measurement using Fibroscan for the noninvasive assessment of esophageal varices in liver cirrhosis patients. *J Gastroenterol Hepatol.* 2011;26(1):164–70.

37. Pawlus A, Inglot M, Chabowski M, Szymanska K, Inglot M, Patyk M, et al. Shear wave elastography (SWE) of the spleen in patients with hepatitis B and C but without significant liver fibrosis. *Br J Radiol.* 2016;89(1066):20160423.
38. Albayrak E, Server S. The relationship of spleen stiffness value measured by shear wave elastography with age, gender, and spleen size in healthy volunteers. *J Med Ultrason* (2001). 2019;46(2):195–9.
39. Mueller S, Englert S, Seitz HK, Badea RI, Erhardt A, Bozaari B, et al. Inflammation-adapted liver stiffness values for improved fibrosis staging in patients with hepatitis C virus and alcoholic liver disease. *Liver Int.* 2015;35(12):2514–21.
40. Eddowes PJ, Sasso M, Allison M, Tsochatzis E, Anstee QM, Sheridan D, et al. Accuracy of FibroScan controlled attenuation parameter and liver stiffness measurement in assessing steatosis and fibrosis in patients with nonalcoholic fatty liver disease. *Gastroenterology.* 2019;156(6):1717–30.
41. Yoneda M, Mawatari H, Fujita K, Endo H, Iida H, Nozaki Y, et al. Noninvasive assessment of liver fibrosis by measurement of stiffness in patients with nonalcoholic fatty liver disease (NAFLD). *Dig Liver Dis.* 2008;40(5):371–8.
42. Cassinotto C, Boursier J, de Ledinghen V, Lebigot J, Lapuyade B, Cales P, et al. Liver stiffness in nonalcoholic fatty liver disease: a comparison of supersonic shear imaging, FibroScan, and ARFI with liver biopsy. *Hepatology.* 2016;63(6):1817–27.
43. Imajo K, Kessoku T, Honda Y, Tomeno W, Ogawa Y, Mawatari H, et al. Magnetic resonance imaging more accurately classifies steatosis and fibrosis in patients with nonalcoholic fatty liver disease than transient elastography. *Gastroenterology.* 2016;150(3):626–37.e7.
44. Nahon P, Kettaneh A, Tengher-Barna I, Ziol M, de Ledinghen V, Douvin C, et al. Assessment of liver fibrosis using transient elastography in patients with alcoholic liver disease. *J Hepatol.* 2008;49(6):1062–8.
45. Nguyen-Khac E, Chatelain D, Tramier B, Decrombecque C, Robert B, Joly JP, et al. Assessment of asymptomatic liver fibrosis in alcoholic patients using fibroscan: prospective comparison with seven non-invasive laboratory tests. *Aliment Pharmacol Ther.* 2008;28(10):1188–98.
46. Thiele M, Detlefsen S, Sevelsted Møller L, Madsen BS, Fuglsang Hansen J, Fialla AD, et al. Transient and 2-dimensional shear-wave elastography provide comparable assessment of alcoholic liver fibrosis and cirrhosis. *Gastroenterology.* 2016;150(1):123–33.
47. Mueller S, Millonig G, Sarovska L, Friedrich S, Reimann FM, Pritsch M, et al. Increased liver stiffness in alcoholic liver disease: differentiating fibrosis from steatohepatitis. *World J Gastroenterol.* 2010;16(8):966–72.
48. Arena U, Vizzutti F, Abraldes JG, Corti G, Stasi C, Moscarella S, et al. Reliability of transient elastography for the diagnosis of advanced fibrosis in chronic hepatitis C. *Gut.* 2008;57(9):1288–93.
49. Castera L, Vergniol J, Foucher J, Le Bail B, Chanteloup E, Haaser M, et al. Prospective comparison of transient elastography, fibrotest, APRI, and liver biopsy for the assessment of fibrosis in chronic hepatitis C. *Gastroenterology.* 2005;128(2):343–50.
50. Ferraioli G, Tinelli C, Dal Bello B, Zicchetti M, Lissandrin R, Filice G, et al. Performance of liver stiffness measurements by transient elastography in chronic hepatitis. *World J Gastroenterol.* 2013;19(1):49–56.
51. Cai YJ, Dong JJ, Wang XD, Huang SS, Chen RC, Chen Y, et al. A diagnostic algorithm for assessment of liver fibrosis by liver stiffness measurement in patients with chronic hepatitis B. *J Viral Hepat.* 2017;24(11):1005–15.
52. Marcellin P, Ziol M, Bedossa P, Douvin C, Poupon R, de Ledinghen V, et al. Non-invasive assessment of liver fibrosis by stiffness measurement in patients with chronic hepatitis B. *Liver Int.* 2009;29(2):242–7.
53. Sporea I, Sirlu R, Deleanu A, Tudora A, Popescu A, Curescu M, et al. Liver stiffness measurements in patients with HBV vs HCV chronic hepatitis: a comparative study. *World J Gastroenterol.* 2010;16(38):4832–7.

54. Zhang D, Zhang S, Wan M, Wang S. A fast tissue stiffness-dependent elastography for HIFU-induced lesions inspection. *Ultrasonics*. 2011;51(8):857–69.
55. Sun LL, Dong G, Wang B, Zheng Q, Wang S, Zhang RF. Real-time shear wave elastography and APRI index for evaluating autoimmune hepatitis fibrosis. *J Biol Regul Homeost Agents*. 2016;30(4):1019–21.
56. Hartl J, Denzer U, Ehlken H, Zenouzi R, Peiseler M, Sebode M, et al. Transient elastography in autoimmune hepatitis: timing determines the impact of inflammation and fibrosis. *J Hepatol*. 2016;65(4):769–75.
57. Corpechot C, Gaouar F, El Naggar A, Kemgang A, Wendum D, Poupon R, et al. Baseline values and changes in liver stiffness measured by transient elastography are associated with severity of fibrosis and outcomes of patients with primary sclerosing cholangitis. *Gastroenterology*. 2014;146(4):970–9. quiz e15–6.
58. Corpechot C, Carrat F, Poujol-Robert A, Gaouar F, Wendum D, Chazouilleres O, et al. Noninvasive elastography-based assessment of liver fibrosis progression and prognosis in primary biliary cirrhosis. *Hepatology*. 2012;56(1):198–208.
59. Gomez-Dominguez E, Mendoza J, Garcia-Buey L, Trapero M, Gisbert JP, Jones EA, et al. Transient elastography to assess hepatic fibrosis in primary biliary cirrhosis. *Aliment Pharmacol Ther*. 2008;27(5):441–7.
60. Legros L, Bardou-Jacquet E, Latournerie M, Guillygomarc'h A, Turlin B, Le Lan C, et al. Non-invasive assessment of liver fibrosis in C282Y homozygous HFE hemochromatosis. *Liver Int*. 2015;35(6):1731–8.
61. Behairy BE-S, Sira MM, Zalata KR, Salama E-SE, Abd-Allah MA. Transient elastography compared to liver biopsy and morphometry for predicting fibrosis in pediatric chronic liver disease: does etiology matter? *World J Gastroenterol*. 2016;22(16):4238–49.
62. Colli A, Pozzoni P, Berzuini A, Gerosa A, Canovi C, Molteni EE, et al. Decompensated chronic heart failure: increased liver stiffness measured by means of transient elastography. *Radiology*. 2010;257(3):872–8.
63. Guillaud O, Dumortier J, Traclet J, Restier L, Joly P, Chapuis-Cellier C, et al. Assessment of liver fibrosis by transient elastography (Fibroscan((R))) in patients with A1AT deficiency. *Clin Res Hepatol Gastroenterol*. 2019;43(1):77–81.
64. Clark VC, Marek G, Liu C, Collinworth A, Shuster J, Kurtz T, et al. Clinical and histologic features of adults with alpha-1 antitrypsin deficiency in a non-cirrhotic cohort. *J Hepatol*. 2018;69(6):1357–64.
65. Karlas T, Neuschulz M, Oltmanns A, Guttler A, Petroff D, Wirtz H, et al. Non-invasive evaluation of cystic fibrosis related liver disease in adults with ARFI, transient elastography and different fibrosis scores. *PLoS One*. 2012;7(7):e42139.
66. Tokuhara D, Cho Y, Shintaku H. Transient elastography-based liver stiffness age-dependently increases in children. *PLoS One*. 2016;11(11):e0166683.
67. Mjelle AB, Mulabecirovic A, Havre RF, Rosendahl K, Juliusson PB, Olafsdottir E, et al. Normal liver stiffness values in children: a comparison of three different elastography methods. *J Pediatr Gastroenterol Nutr*. 2019;68(5):706–12.
68. Galina P, Alexopoulou E, Zellos A, Grigoraki V, Sihanidou T, Kelekis NL, et al. Performance of two-dimensional ultrasound shear wave elastography: reference values of normal liver stiffness in children. *Pediatr Radiol*. 2019;49(1):91–8.
69. Ammon FJ, Kohlhaas A, Elshaarawy O, Mueller J, Bruckner T, Sohn C, et al. Liver stiffness reversibly increases during pregnancy and independently predicts preeclampsia. *World J Gastroenterol*. 2018;24(38):4393–402.
70. Bazerbachi F, Haffar S, Wang Z, Cabezas J, Arias-Loste MT, Crespo J, et al. Range of normal liver stiffness and factors associated with increased stiffness measurements in apparently healthy individuals. *Clin Gastroenterol Hepatol*. 2019;17(1):54–64 e1.
71. Millionig G, Friedrich S, Adolf S, Fonouni H, Golriz M, Mehrabi A, et al. Liver stiffness is directly influenced by central venous pressure. *J Hepatol*. 2010;52(2):206–10.

72. Millonig G, Reimann FM, Friedrich S, Fonouni H, Mehrabi A, Büchler MW, et al. Extrahepatic cholestasis increases liver stiffness (FibroScan) irrespective of fibrosis. *Hepatology*. 2008;48(5):1718–23.
73. Piecha F, Peccerella T, Bruckner T, Seitz HK, Rausch V, Mueller S. Arterial pressure suffices to increase liver stiffness. *Am J Physiol Gastrointest Liver Physiol*. 2016;311(5):G945–G53.
74. Piecha F, Mandorfer M, Peccerella T, Ozga AK, Poth T, Vonbank A, et al. Pharmacological decrease of liver stiffness is pressure-related and predicts long-term clinical outcome. *Am J Physiol Gastrointest Liver Physiol*. 2018;315(4):G484–G94.
75. Bastard C, Bosisio MR, Chabert M, Kalopissis AD, Mahrouf-Yorgov M, Gilgenkrantz H, et al. Transient micro-elastography: a novel non-invasive approach to measure liver stiffness in mice. *World J Gastroenterol*. 2011;17(8):968–75.
76. Dietrich CF, Bamber J, Berzigotti A, Bota S, Cantisani V, Castera L, et al. EFSUMB guidelines and recommendations on the clinical use of liver ultrasound elastography, update 2017 (long version). *Ultraschall Med*. 2017;38(4):e16–47.
77. Boursier J, Konate A, Gorea G, Reaud S, Quemener E, Oberti F, et al. Reproducibility of liver stiffness measurement by ultrasonographic elastometry. *Clin Gastroenterol Hepatol*. 2008;6(11):1263–9.
78. Boursier J, Zarski JP, de Ledinghen V, Rousselet MC, Sturm N, Lebaill B, et al. Determination of reliability criteria for liver stiffness evaluation by transient elastography. *Hepatology*. 2013;57(3):1182–91.
79. Castéra L, Foucher J, Bernard P-H, Carvalho F, Allaix D, Merrouche W, et al. Pitfalls of liver stiffness measurement: A 5-year prospective study of 13,369 examinations. *Hepatology*. 2010;51(3):828–35.
80. Sandrin L, Fournier C, Miette V, Millonig G, Mueller S, editors. Fibroscan in hepatology: a clinically-validated tool using vibration-controlled transient elastography. *Ultrasonics symposium (IUS), 2009 IEEE international*, 20–23 Sept 2009; 2009.
81. Bamber J, Cosgrove D, Dietrich CF, Fromageau J, Bojunga J, Calliada F, et al. EFSUMB guidelines and recommendations on the clinical use of ultrasound elastography. Part 1: basic principles and technology. *Ultraschall Med*. 2013;34(2):169–84.
82. Bota S, Sporea I, Sirlu R, Popescu A, Danila M, Costachescu D. Intra- and interoperator reproducibility of acoustic radiation force impulse (ARFI) elastography—preliminary results. *Ultrasound Med Biol*. 2012;38(7):1103–8.
83. D’Onofrio M, Crosara S, De Robertis R, Canestrini S, Demozzi E, Gallotti A, et al. Acoustic radiation force impulse of the liver. *World J Gastroenterol*. 2013;19(30):4841–9.
84. Bota S, Sporea I, Sirlu R, Popescu A, Danila M, Sendroiu M. Factors that influence the correlation of acoustic radiation force impulse (ARFI), elastography with liver fibrosis. *Med Ultrason*. 2011;13(2):135–40.
85. Chang S, Kim MJ, Kim J, Lee MJ. Variability of shear wave velocity using different frequencies in acoustic radiation force impulse (ARFI) elastography: a phantom and normal liver study. *Ultraschall Med*. 2013;34(3):260–5.
86. Leung VY, Shen J, Wong VW, Abrigo J, Wong GL, Chim AM, et al. Quantitative elastography of liver fibrosis and spleen stiffness in chronic hepatitis B carriers: comparison of shear-wave elastography and transient elastography with liver biopsy correlation. *Radiology*. 2013;269(3):910–8.
87. Muller M, Gennisson JL, Deffieux T, Tanter M, Fink M. Quantitative viscoelasticity mapping of human liver using supersonic shear imaging: preliminary in vivo feasibility study. *Ultrasound Med Biol*. 2009;35(2):219–29.
88. Ferraioli G, Tinelli C, Dal Bello B, Zicchetti M, Filice G, Filice C. Accuracy of real-time shear wave elastography for assessing liver fibrosis in chronic hepatitis C: a pilot study. *Hepatology*. 2012;56(6):2125–33.
89. Sporea I, Gradinaru-Tascau O, Bota S, Popescu A, Sirlu R, Jurchis A, et al. How many measurements are needed for liver stiffness assessment by 2D-shear wave elastography (2D-SWE) and which value should be used: the mean or median? *Med Ultrason*. 2013;15(4):268–72.

90. Sporea I, Bota S, Jurchis A, Sirli R, Gradinaru-Tascau O, Popescu A, et al. Acoustic radiation force impulse and supersonic shear imaging versus transient elastography for liver fibrosis assessment. *Ultrasound Med Biol*. 2013;39(11):1933–41.
91. Procopet B, Berzigotti A, Abralde JG, Turon F, Hernandez-Gea V, Garcia-Pagan JC, et al. Real-time shear-wave elastography: applicability, reliability and accuracy for clinically significant portal hypertension. *J Hepatol*. 2015;62(5):1068–75.
92. Hudson JM, Milot L, Parry C, Williams R, Burns PN. Inter- and intra-operator reliability and repeatability of shear wave elastography in the liver: a study in healthy volunteers. *Ultrasound Med Biol*. 2013;39(6):950–5.
93. Srinivasa Babu A, Wells ML, Teytelboym OM, Mackey JE, Miller FH, Yeh BM, et al. Elastography in chronic liver disease: modalities, techniques, limitations, and future directions. *Radiographics*. 2016;36(7):1987–2006.
94. Silva AM, Grimm RC, Glaser KJ, Fu Y, Wu T, Ehman RL, et al. Magnetic resonance elastography: evaluation of new inversion algorithm and quantitative analysis method. *Abdom Imaging*. 2015;40(4):810–7.
95. Venkatesh SK, Yin M, Ehman RL. Magnetic resonance elastography of liver: technique, analysis, and clinical applications. *J Magn Reson Imaging*. 2013;37(3):544–55.
96. Ingiliz P, Chhay KP, Munteanu M, Lebray P, Ngo Y, Roulot D, et al. Applicability and variability of liver stiffness measurements according to probe position. *World J Gastroenterol*. 2009;15(27):3398–404.
97. Petzold G, Porsche M, Ellenrieder V, Kunsch S, Neesse A. Impact of food intake on liver stiffness determined by 2-D shear wave elastography: prospective interventional study in 100 healthy patients. *Ultrasound Med Biol*. 2019;45(2):402–10.
98. Mederacke I, Wursthorn K, Kirschner J, Rifai K, Manns MP, Wedemeyer H, et al. Food intake increases liver stiffness in patients with chronic or resolved hepatitis C virus infection. *Liver Int*. 2009;29(10):1500–6.
99. Popescu A, Bota S, Sporea I, Sirli R, Danila M, Racean S, et al. The influence of food intake on liver stiffness values assessed by acoustic radiation force impulse elastography—preliminary results. *Ultrasound Med Biol*. 2013;39(4):579–84.
100. Lemoine M, Shimakawa Y, Njie R, Njai HF, Nayagam S, Khalil M, et al. Food intake increases liver stiffness measurements and hampers reliable values in patients with chronic hepatitis B and healthy controls: the PROLIFICA experience in the Gambia. *Aliment Pharmacol Ther*. 2014;39(2):188–96.
101. Alvarez D, Orozco F, Mella JM, Anders M, Antinucci F, Mastai R. Meal ingestion markedly increases liver stiffness suggesting the need for liver stiffness determination in fasting conditions. *Gastroenterol Hepatol*. 2015;38(7):431–5.
102. Gersak MM, Badea R, Lenghel LM, Vasilescu D, Botar-Jid C, Ducea SM. Influence of food intake on 2-D shear wave elastography assessment of liver stiffness in healthy subjects. *Ultrasound Med Biol*. 2016;42(6):1295–302.
103. Berzigotti A, De Gottardi A, Vukotic R, Siramolpiwat S, Abralde JG, Garcia-Pagan JC, et al. Effect of meal ingestion on liver stiffness in patients with cirrhosis and portal hypertension. *PLoS One*. 2013;8(3):e58742.
104. Arena U, Vizzutti F, Corti G, Ambu S, Stasi C, Bresci S, et al. Acute viral hepatitis increases liver stiffness values measured by transient elastography. *Hepatology*. 2007;47(2):380–4.
105. Song ZZ. Acute viral hepatitis increases liver stiffness values measured by transient elastography. *Hepatology*. 2008;48(1):349–50. author reply 50.
106. Mueller S, Nahon P, Rausch V, Peccerella T, Silva I, Yagmur E, et al. Caspase-cleaved keratin-18 fragments increase during alcohol withdrawal and predict liver-related death in patients with alcoholic liver disease. *Hepatology*. 2017;66(1):96–107.
107. Bastard C, Miette V, Calès P, Stefanescu H, Festi D, Sandrin L. A novel FibroScan examination dedicated to spleen stiffness measurement. *Ultrasound Med Biol*. 2018;44(8):1616–26.



108. Knodell RG, Ishak KG, Black WC, Chen TS, Craig R, Kaplowitz N, et al. Formulation and application of a numerical scoring system for assessing histological activity in asymptomatic chronic active hepatitis. *Hepatology*. 1981;1(5):431–5.
109. Scheuer PJ. Classification of chronic viral hepatitis: a need for reassessment. *J Hepatol*. 1991;13(3):372–4.
110. Bedossa P, Poynard T. An algorithm for the grading of activity in chronic hepatitis C. The METAVIR Cooperative Study Group. *Hepatology*. 1996;24(2):289–93.
111. Ishak K, Baptista A, Bianchi L, Callea F, De Groote J, Gudat F, et al. Histological grading and staging of chronic hepatitis. *J Hepatol*. 1995;22(6):696–9.
112. Batts KP, Ludwig J. Chronic hepatitis. An update on terminology and reporting. *Am J Surg Pathol*. 1995;19(12):1409–17.
113. Chevallier M, Guerret S, Chossegros P, Gerard F, Grimaud J-A. A histological semiquantitative scoring system for evaluation of hepatic fibrosis in needle liver biopsy specimens: comparison with morphometric studies. *Hepatology*. 1994;20(2):349–55.
114. Kleiner DE, Brunt EM, Van Natta M, Behling C, Contos MJ, Cummings OW, et al. Design and validation of a histological scoring system for nonalcoholic fatty liver disease. *Hepatology*. 2005;41(6):1313–21.
115. Desmet VJ, Gerber M, Hoofnagle JH, Manns M, Scheuer PJ. Classification of chronic hepatitis: diagnosis, grading and staging. *Hepatology*. 1994;19(6):1513–20.
116. Ferenci P, Caca K, Loudianos G, Mieli-Vergani G, Tanner S, Sternlieb I, et al. Diagnosis and phenotypic classification of Wilson disease I. *Liver Int*. 2003;23(3):139–42.



# Index

## A

AATD, *see* Alpha1-antitrypsin deficiency

Acoustic radiation force

application, 42

ARFI imaging, 42–43

commercial implementations, 42

definition, 42

direction and magnitude, 42

shear wave elasticity imaging, 43–46

Acoustic radiation force impulse (ARFI) imaging, 42–43

in ascites patients, 513

shear wave elasticity imaging, 24

supersonic shear imaging, 24–25

*See also* Point shear wave elastography

Acute cellular rejection (ACR), 398–399

Acute liver failure (ALF)

acoustic radiation force impulse elastography, 302

etiology, 297–298

laboratory and histological characteristics, 298, 299

lab parameters, 299, 301

macroscopic alterations of liver surface, 299, 300

pathomechanism, 301–302

transient elastography, 302

Acute-on-chronic liver failure (AOCLF), 302–303, 616

AIH, *see* Autoimmune hepatitis

Alcohol detoxification, 598

Alcohol-related liver disease (ALD), 582–583

AST-adapted cutoff values, 105, 145, 541, 694

controlled attenuation parameter, 149–150  
detoxification, 615, 616

diagnosis, 141–142, 696

elastographic assessment

alcohol withdrawal/relapse, 144–145

asymptomatic and non-severe alcoholic hepatitis, 146

biopsy-proven studies, 143, 144

fibrosis stages, 144, 145

histological parameters, 146

lobular-pronounced ALD *v.s.* portal tract-localized HCV, 145, 146

fibrosis assessment

clinical practice with

ultrasound, 147–148

with transient elastography, 148–149

follow-up, 149

natural course, 143

steatosis, 149

“sure morphological signs of cirrhosis,” 143

ALD, *see* Alcohol-related liver disease

ALF, *see* Acute liver failure

Allogeneic stem cell transplantation (alloSCT), 171

Alpha1-antitrypsin deficiency (AATD)

gain-of-function toxicity, 188

genetic variants, 187, 188

liver disease, 188–189

noninvasive methods, 189–193

noninvasive screening, steatosis, 193

Anti-fibrosis therapies, 646

Arterial pressure

adrenergic agents epinephrine, 259

direct hepatocellular mechanisms, 259

dobutamine, 259

epinephrine, 260

heart rate, increase in, 259

- Arterial pressure (*cont.*)  
 modulation, 258  
 norepinephrine, 259  
 real-time experiment, 259  
 systolic blood pressure, 260
- Autoimmune hemolytic anemia, 614–615
- Autoimmune hepatitis (AIH), 582–583, 598  
 biochemical remission, 184, 185  
 disease progression, 183, 184  
 fibrosis staging, 181–182, 184, 185  
 follow-up liver stiffness measurement, 184  
 hepatic inflammation, 182–183  
 treatment monitoring, 184
- B**
- Barcelona Clinic Liver Cancer (BCLC)  
 staging system, 587
- Baveno VI Consensus conference, 603
- Bioengineered in vitro liver models, 648
- Biomatrix, 648
- B-mode ultrasound (US), 414
- Bright liver echo pattern (BLEP), 442
- Budd–Chiari syndrome (BCS), 170–171, 623
- C**
- CAP, *see* Controlled attenuation parameter
- Castera algorithm, 573
- CF, *see* Cystic fibrosis
- Chevalier semiquantitative scoring system  
 (SSS), 715
- Cholestasis, 198  
 bile/bilirubin flow, 268  
 bile duct ligation, 266, 267  
 cholestasis-mediated elevation, 267  
 clinical implications, 267–268  
 extrahepatic cholestasis, 266–267  
 Spearman rho correlation, 265, 266
- Cirrhosis, 72, 74, 76–77  
 compensated/decompensated cirrhosis, 317  
 ECM components, 670  
 fibrogenesis, 670  
 fibrosis progression, 670  
 macroscopic aspect, 670, 671  
 pathology, 319–321  
 pre-cancerogenic lesion, 669  
 screening tools, 7, 700  
 synthesis impairment and portal  
 hypertension, 698
- Clinically significant portal hypertension  
 (CSPH), 61, 334
- Compensated advanced chronic liver disease  
 (cACLD), 326
- Compression stiffening, 649
- Compression waves, 20
- Controlled attenuation parameter  
 (CAP™), 4, 23  
 AASLD 2018 guidelines, 414  
 in alcohol-related liver disease,  
 149–150, 452  
 AUROC, 418–422, 426  
 in chronic viral hepatitis, 451–452  
 cutoff values, 423, 444  
 cystic fibrosis, 166  
 development and validation, 417  
 diagnostic accuracy, 423, 424, 450  
 FibroScan device, 33, 34, 443  
 fibrosis, inflammation and  
 covariates, 430  
 final stiffness result, 37  
 genetic determinants, 286  
 intra-operator reproducibility, 429–430  
 liver localization and probe  
 selection, 34–36  
 on M and XL probes, 423, 425  
 meal intake, 430–431  
 measurement principle, 415–416  
 measurement sequence, 35–37  
 on NAFLD, 444–450  
 of NASH, 429  
 non-pharmacological interventions, 427  
 nutrition, 272–273  
 pharmacological treatment, 428  
 for point-of-care diagnostic  
 assessment, 414  
 Princeps study, 418  
 prognostic values, 428–429  
 quality criteria, 431  
 sensitivities, 444  
 STARD guidelines, 418  
 SteatoTest, 426  
 tissue-mimicking phantoms, 416  
 ultrasonic field II simulations, 416  
 ultrasound attenuation, 415  
 VCTE™, 414  
 vitamin D metabolism and  
 APOC3, 286–287  
 WFUMB, 414
- Cystic fibrosis (CF)  
 controlled attenuation parameter, 166  
 hepatic involvement, 161  
 transient elastography  
 diagnostic methods, 162–164  
 long-term follow-up, 164–165  
 in other organs, 166
- Cystic fibrosis associated liver disease  
 (CFLD), *see* Cystic fibrosis

**D**

- Desmet and Scheuer staging system, 716
- Direct-acting antivirals (DAA), 377, 399, 624
- Direct rheometry measurements, 644
- 2D-SWE, *see* Two-dimensional shear wave elastography
- Durotaxis, 15

**E**

- ECM mechanics, *see* Extracellular matrix mechanics
- EHPVO, *see* Extrahepatic portal vein obstruction
- Elastographic assessment, 702
  - advantages and limitations, 471, 532, 533
  - alcohol-related liver disease
    - alcohol withdrawal/relapse, 144–145
    - asymptomatic and non-severe alcoholic hepatitis, 146
    - biopsy-proven studies, 143, 144
    - fibrosis stages, 144, 145
    - histological parameters, 146
    - lobular-pronounced ALD *vs.* portal tract-localized HCV, 145, 146
  - big data, 558
  - clinical and technical considerations, 711
  - clinical context knowledge, 472
  - cutoff values, 525
  - diagnostic reasoning, 552
  - EASL-ALEH clinical practice guideline, 520
  - EFSUMB and WFUMB guidelines, 525
  - excitation mode, dimensions, and producers, 523, 700
  - feasibility, 524
  - FIB-4, 551
  - guidelines, 45–46
  - history of, 4
  - human decision-making *vs.* digital calculations, 552, 553
  - interpretation, 474–476
  - for liver fibrosis, 553–557
  - LS cutoff values, 25, 703
  - machine-learning algorithms, 559
  - by modes of excitation, 16, 17
  - by modes of reading/imaging, 17
  - multivariable models, 551, 555
  - normal stiffness values, 705
  - parallel testing, 551, 552
  - pathophysiological conditions, 472
  - portal hypertension diagnosis, 557–558
  - quality criteria, 472
  - screening and expert mode, 473–474

- sequential testing, 551, 552
- SS/LS ratio, 476
- standardization, 472, 473
- strain, 18–20
- types, 18, 19
- One-dimensional elastographic techniques, 471–472
- Elevated liver stiffness
  - clinical confounders, 225, 226
  - confounder categories, 226, 227
  - confounding factors, 225, 227
  - inflow/outflow model, 229–231
  - sinusoidal pressure hypothesis, 227, 228
  - venous pressure, 225, 226
- Engelbreth–Holm–Swarm (EHS) gel, 651
- Epstein–Barr virus (EBV) infection, 620–621
- European HEPAHEALTH project, 564
- Extracellular matrix (ECM) mechanics
  - cross-linking and fibrous networks, 663–664
  - glycosaminoglycans, 664
  - linearly elastic hydrogel, 662
  - proteoglycans, 664
  - viscosity, 664
- Extrahepatic cholestasis, 266–267
- Extrahepatic portal vein obstruction (EHPVO), 177, 178, 348

**F**

- Fåhræus–Lindqvist effect, 632
- F3 fibrosis and F4 cirrhosis, 707
- Fibrogenic myofibroblasts, 659, 660
- Fibrometer<sup>v2g</sup>, 555, 575
- Fibroscan-based scores, 37–38
- FibroScan device, 31, 33, 34, 415, 443
- FibroScan M probe, 517
- FibroScan platform, 482, 485, 488–489
- Fibroscan probes, 33, 709
- Fibrosis assessment
  - alcoholic liver disease, 147–149, 582–583
  - in chronic HBV infection
    - baseline assessment, 116–117
    - longitudinal evaluation, 117–118
  - in chronic HCV infection
    - baseline assessment, 114–115
    - longitudinal evaluation, 115–116
  - cutoff values *vs.* disease-specific cutoff values, 105–108
  - first line of screening, 565–568
  - NAFLD (*see* Non-alcoholic fatty liver disease (NAFLD))
  - noninvasive tests, 564, 569–571
  - primary biliary cholangitis

Fibrosis assessment (*cont.*)

- diagnostic VCTE thresholds, 199–200
  - elastography-based techniques, 198, 199
  - liver stiffness measurement, 199
  - prognosis, LSM, 200–201
  - primary sclerosing cholangitis
    - diagnostic VCTE thresholds, 203
    - elastography-based techniques, 201, 202
    - liver stiffness measurement, 201–204
    - prognosis, LSM, 203, 205–206
  - second expertise diagnosis
    - AASLD and EASL guidelines, 575
    - hepatitis B virus, 576–577
    - hepatitis C virus, 569, 572–576
    - HIV, 579–581
  - serum fibrosis biomarkers, 564
- Fibrosis progression, 321–322
- Fibrosis-4 test (FIB-4), 551
- FibroTest<sup>®</sup>, 548
- Forns index, 557

**G**

- Gastroesophageal varices (GEV), 326
- Genetic determinants
- adiponutrin/PNPLA3, 286
    - with ALD/NAFLD, 279–280, 286
    - function and regulation of, 278–279
  - chronic hepatitis C, 284–285
  - liver stiffness, 277–278
- MBOAT7
- impact, 280–281
  - preliminary data, 287–291
  - steatosis, 286
- PNPLA3
- preliminary data, 287–291
  - steatosis, 286
- preliminary data, 287–291
- SREBP-1c, impact, 280
- steatosis, 285
- TM6SF2
- impact, 281–283
  - preliminary data, 287–291
  - steatosis, 286
- Genetic liver diseases, 583
- Genome-wide association studies (GWAS), 277
- Glycosaminoglycans (GAGs), 664
- G-protein-coupled estrogen receptor, 662

**H**

- HABR, *see* Hepatic arterial buffer response
- HBV infection, *see* Hepatitis B virus infection
- HCC, *see* Hepatocellular carcinoma
- HCV infection, *see* Hepatitis C virus infection
- Hematological disorders
- allogeneic stem cell transplantation, 171
  - Budd–Chiari syndrome, 170–171
  - monitoring and guiding therapeutic decisions, 169, 170
  - predictive value, 173
  - sinusoidal obstruction syndrome, 171–173
- Hepatic amyloidosis, 622
- Hepatic arterial buffer response (HABR), 178, 257, 320, 674
- Hepatic decompensation
- cut-off values, 361–364
  - spleen stiffness, 365
- Hepatic hemodynamics, 598–599
- Hepatic shunts, 321–322
- Hepatic stellate cells (HSCs), 257, 659–661
- Hepatic venous pressure gradient (HVPG), 258, 326
- Hepatic vs. non-hepatic ascites
- ARFI elastography, 513
  - causes, 509
  - clinical tools, 509
  - diagnostic procedure, 509
  - elastograms, 510, 512
  - intra-abdominal pressure, 510, 512, 513
  - isotonic saline solution, 510
  - liver-mimicking phantoms, 510, 511
  - TE and pSWE, 513, 514
- Hepatitis A infection, 620
- Hepatitis B virus (HBV) infection
- baseline assessment, 116–117
  - longitudinal evaluation, 117–118
- Hepatitis C virus (HCV) infection, 615, 624
- AST-adapted cutoff values, 105, 145, 541, 694
  - baseline assessment, 114–115
  - longitudinal evaluation, 115–116
- Hepatocellular carcinoma (HCC), 622
- after antiviral therapy, 376–377
  - dose–response relationship, 375, 376
  - Korean model, 378
  - LSM-HCC score, 377–378
  - mREACH-B score, 378
  - postoperative complications, 379
  - postoperative survival, 379
  - recurrence, 378–379

- Hepatocyte nuclear factor (HNF), 651
- Hepatocytes
- adhesion complexes, 645
  - compression stiffening, 649
  - culture on biomatrix, 648
  - cytochrome P450 activity, 652
  - cytochrome P450 induction, 649
  - cytoskeleton of, 652
  - EHS gel, 651
  - extracellular matrices, 648
  - fatty liver-like metabolic dysfunction, 653
  - hepatocyte nuclear factor 4 alpha, 651, 652
  - hyaluronic acid gels, 649
  - in vitro culture, 649–653
  - intracellular machinery, 645
  - matrigel, 651
  - mechanosensitivity, 647–648
  - metabolic and synthetic functions, 645
  - PDMS, 649, 650
  - polyacrylamide gels, 649
  - PVA hydrogels, 649
  - Rho/Rho-associated protein kinase pathway, 652
  - RNA-Seq technology, 651
  - shear strain softening, 649
  - softer heparin gel, 651
- Hepatofugal portal blood flow, 258
- Hepatosplenic schistosomiasis (HES), 154–155
- Hereditary hemochromatosis (HH)
- ARFI elastography, 213
  - diagnostic algorithm, 214
  - hyperferritinaemia, 210
  - liver stiffness, 210, 211
  - MR elastography, 213
  - real-time elastography, 213
  - transient elastography, 211–212
- Hereditary spherocytosis, 622–623
- HH, *see* Hereditary hemochromatosis
- Histological confounders
- biopsy-proven studies, 233
  - fibrosis type, 238–239
  - inflammation, 238
  - liver stiffness, 233–234
  - morphological factors, 239
  - parameters, 234–237
  - prevalence, 234, 235
  - steatosis, 237–238
- <sup>1</sup>H-magnetic resonance spectroscopy magnetic resonance spectroscopy (<sup>1</sup>H-MRS), 426
- Hyaluronic acid-based fibrous gel system, 649, 663
- Hyperferritinaemia, 210
- I**
- Interferon-based treatment, 377
  - Inter-operator reproducibility, 59
  - Intra-operator reproducibility, 59
  - Ischemia/reperfusion injury (IRI), 397–398
- J**
- Jaundice, 616–617
    - caused by autoimmune hemolytic anemia, 617
    - due to mechanical cholestasis, 617–618
- K**
- Kaplan Meier curve, 149, 696
  - Knodell histology activity index (HAI), 563, 713
- L**
- Latency associated peptide (LAP) complex, 637
  - Leipzig score, 716
  - 5-level liver fibrosis staging system, 563
  - Liver cancer, 80–84
    - post-hepatectomy HCC recurrence, 590
    - post-hepatectomy liver failure, 589–590
    - survival, 591
  - Liver congestion, 539–540, 621
    - cardiac recompensation, 248–249
    - liver lobule, pathophysiology of, 246–247
  - Liver fibrosis
    - alpha1-antitrypsin deficiency
      - gain-of-function toxicity, 188
      - genetic variants, 187, 188
      - liver disease, 188–189
      - noninvasive methods, 189–193
    - histopathological scores, 714
  - Liver lobule, 246–247
  - Liver metastasis, 622
  - Liver microenvironment (LME), 645–646
  - Liver perfusion, 699
  - Liverscreen project, 549
  - Liver sinusoidal endothelial cells (LSECs), 257

- Liver stiffness (LS)
- all-cause mortality, 383–385, 387–388
  - blood viscosity, 632
  - capillary pressure, 629–630
  - at cellular level, 632, 633
  - clinical and technical considerations, 710
  - collagen deposition, 629
  - cutoff values and clinical endpoints, 317–318
  - of different age groups, 708
  - in different species, 97, 708
  - elevation, 540–541
  - in emergency room and intensive care unit, 388–389
  - fundamental dependence, 6
  - intracellular components, 633–635
  - liver-related mortality, 383–385
  - markers, 7
  - measurements
    - accuracy, 336, 338–342
    - biomechanical parameters, 13, 14
    - elasticity, 15
    - esophageal varices, 334
    - factors, 16
    - forces *vs.* elastic modulus, 14, 15
    - liver and spleen stiffness-based strategies, 337
    - metal spring, 13, 14
    - pliability/simplified softness, 15
    - point shear wave elastography, 332, 333, 343
    - shear waves, 20–23
    - in small animal models, 97
    - transient elastography, 328–330
    - two-dimensional shear wave elastography, 332, 334, 335, 343–344
    - unknown cause or no cirrhosis, 348–350
    - varices need treatment, 334
    - viscosity, 15–16
  - multivariate analysis, 386
  - organ systems and, 629, 630
  - plasma viscosity, 632
  - pressure-related factors, 629
  - relative ratio, 383
  - reliability criteria, 704
  - serum biomarkers, 706, 707
  - sinusoidal pressure hypothesis, 629
  - standardization of elastography, 27
  - standardized conditions, 711
  - technical, clinical, and experimental studies, 685–690
  - after therapeutic interventions, 389–390
  - values, 6
- Liver transplantation (LTX)
- direct acting antivirals, 399
  - early post-liver transplant period management
    - acute cellular rejection, 398–399
    - ischemia/reperfusion injury, 397–398
  - functional aspects, 394
  - liver biopsy, 399
  - and liver histology, 400
  - liver steatosis, 401–402
  - magnetic resonance elastography, 404
  - noninvasive tools, 399
  - in pediatric liver transplantation, 404–405
  - post-transplant follow-up, 399
  - in pre-transplant management
    - deceased donor liver evaluation, 396–397
    - LDLT, 395–396
    - patient in waiting list, 394–395
    - pSWE (ARFI), 402–403
    - trend over time parameter, 400
    - World Transplant Registry, 394
- Living donor liver transplantation (LDLT), 395–396
- Lobular *vs.* portal disease, 370
- Localization of inflammation, 370
- LS, *see* Liver stiffness
- LSM-spleen diameter to platelet ratio score (LSPS), 334
- LTX, *see* Liver transplantation
- M**
- Magnetic resonance elastography (MRE), 3, 5, 472
- description, 25
  - driver, sequences, and post-processing, 70–71
  - elasticity and viscosity, 71
  - for hemosiderosis-hemochromatosis, 213–214
  - liver fibrosis, 529–531
    - advanced imaging modalities, 72
    - compensated and decompensated cirrhosis, 72, 74, 76–77
    - detecting significant and advanced fibrosis, 74, 76–77
    - extracellular matrix elements, 72
    - histopathological analysis, 72

- quantitative, biophysical, and system-independent parameters, 72
  - staging, 72, 74, 75
  - T2w images and shear wave speed maps, 73
- liver transplantation, 404
- in liver tumors, 80–84
- in NAFLD/NASH, 77–80, 127–129
- in portal hypertension, 84–87
- vs. ultrasound-based elastography, 74
- in viral hepatitis, 80
- Magnetic resonance spectroscopy (MRS), 414, 442
- Matrigel, 651
- Mechanic cholestasis, 538–539
- Mechano-sensing
  - cell–matrix interactions, 637
  - LAP complex, 637
  - LSEC differentiation, 636
  - mechanical deformations/stretching, 636
  - mechano-induced gene expression profiles, 639
  - mechanosensitive ion channels, 639
  - molecular examples, 637, 638
  - myofibroblasts and ECM, 636–637
  - potential sensing mechanisms, 635
  - potential sinusoidal pressure-induced pathways, 639
  - stress fiber network, 636
- Modified REACH-B (mREACH-B) score, 378
- MR imaging (MRI)-proton density fat fraction (PDFF), 414
- Myocardin-related transcription factor (MRTF)-A/MAL/MLK1, 662
  
- N**
- NASH Clinical Research Network score, 715
- National Health and Nutrition Examination Survey, 564
- National Institute for Health and Care Excellence (NICE) guidelines, 566
- Non-alcoholic fatty liver disease (NAFLD), 413, 619–620
  - CAP™, 444–450
  - in children, 131–132
  - clinical practice, 133–134
  - diagnosis, 124
  - first line of screening, 565–567
  - follow-up with or without treatment, 134–135
  - liver stiffness measurement
    - acoustic radiation force impulse, 125–126
    - blood marker, 129–130
    - TE/FibroScan, 124–125
  - magnetic resonance elastography, 77–80, 127–129
  - multiparametric MRI, 128
  - prognosis, 130–131
  - risk of complications, 135
  - risk of fibrosis progression, 135
  - screening tool, 132–133
  - second expertise diagnosis, 577–579
  - steatosis assessment, 441
  - two-dimensional shear wave elastography, 126–127
- Nonalcoholic steatohepatitis (NASH), 77–80, 123, 124, 127–129, 133–135, 346, 401, 429, 563, 578, 643
- Non-hepatic ascites, 621
- Noninvasive elastography techniques, 644, 646
- Normal liver stiffness frequency dependence, 32
- Nutrition
  - alcohol injection, 273, 274
  - controlled attenuation parameter, 272–273
  - glucose, LS and portal pressure values, 273, 274
  - LS elevation, 271
  - potential mechanisms, 271
  - short-term response, 272, 273
  
- P**
- PBC, *see* Primary biliary cholangitis
- PH, *see* Portal hypertension
- Phosphodiesterase type 5 (PDE-5) inhibitors, 605
- Polyacrylamide hydrogel system, 659
- Point shear wave elastography (ARFI-pSWE), 376
- Point shear wave elastography (pSWE), 24, 44, 125
  - hepatic vs. non-hepatic ascites, 513, 514
  - liver fibrosis assessment, 525–526
  - liver transplantation, 402–403
  - portal hypertension, 332, 333, 343
  - reliability criteria, 490
  - schistosomiasis, 157
- Polyacrylamide gels, 649
- Polydimethylsiloxane (PDMS), 649
- Polyvinyl alcohol (PVA) hydrogels, 649

- Portal hypertension (PH), 84–87, 588  
 complications, 325  
 definition, 325  
 diagnosis, 603  
 epidemiology, 325  
 hepatic venous pressure gradient, 326  
 HVPG measurement, 603  
 liver stiffness, 603–605  
   accuracy, 336, 338–342  
   esophageal varices, 334  
   liver and spleen stiffness-based strategies, 337  
   point shear wave elastography, 332, 333, 343  
   transient elastography, 328–330  
   two-dimensional shear wave elastography, 332, 334, 335, 343–344  
   unknown cause or no cirrhosis, 348–350  
   varices need treatment, 334  
 non-invasive tests, 327–328  
 pathophysiological rationale, 328  
 portal pressure lowering drugs, 604–608  
 reference standard method, 326–327  
 routine laboratory tests, 603  
 schistosomiasis, 155  
 spleen stiffness, 604, 605  
   clinical decompensation, 345–347  
   follow-up, 347–348  
   by ultrasound elastography, 344–345  
   unknown cause or no cirrhosis, 348–350  
 stages, 326, 327
- Portal pressure  
 complications, 257  
 endoscopic band ligation, 261  
 lowering drugs, 262  
   list of, 604–606  
   monitoring, 606–608  
   PDE-5 inhibitors, 605  
 modulation, 261  
 transjugular intrahepatic portosystemic shunt, 261
- Portal vein thrombosis (PVT), 177–179
- Post-hepatectomy liver failure (PHLF), 589–590
- Pregnancy  
 complications, 313  
 normal vs. preeclampsia and intrahepatic cholestasis of pregnancy, 311–312  
 spectrum of liver diseases, 308–310  
 uncomplicated pregnancy, 311
- Primary biliary cholangitis (PBC)  
 diagnostic VCTE thresholds, 199–200  
 elastography-based techniques, 198, 199  
 liver stiffness measurement, 199  
 prognosis, LSM, 200–201
- Primary sclerosing cholangitis (PSC)  
 diagnostic VCTE thresholds, 203  
 elastography-based techniques, 201, 202  
 liver stiffness measurement, 201–204  
 prognosis, LSM, 203, 205–206
- Probe-to-capsula distance (PCD), 34
- Proteoglycans, 664
- PSC, *see* Primary sclerosing cholangitis
- pSWE, *see* Point shear wave elastography
- PUBMED, 4
- Q**
- Quantitative Imaging Biomarkers Alliance (QIBA), 25
- R**
- Radiomics, 559
- Real-time elastography (RTE), 213
- Right ventricular (RV)  
 cardiac surgery, 252  
 clinical outcomes, 250–251  
 diagnostic approaches, 244–246  
 function, 243–244  
 parameters, 249–250  
 ventricular interdependence, 243–244
- Rigidity, 13
- Room temperature susceptometry (RTS), 209
- S**
- Scheuer histological activity index score, 713
- Schistosomiasis  
 diagnosis, 154  
 hepatosplenic schistosomiasis, 154–155  
 liver elastography, 155–157  
 socioeconomic impact, 153  
 spleen elastography, 157–158
- Secondary hemochromatosis, 212–213
- Sequential algorithm for fibrosis evaluation (SAFE) biopsy, 569, 572, 573
- Serum response factor (SRF), 662
- Shear strain softening, 649
- Shear wave elasticity imaging (SWEI), 24, 43–46
- Two-dimensional shear wave elastography (2D-SWE), 3, 24–25, 44, 472, 490, 45  
 automatic and supersonic shear wave generation, 52–54  
 clinical impact



- diagnostic cut-off values, 60–62
  - diagnostic performance, 60–62
  - fast acquisition protocol, 59–60
  - liver fibrosis assessment, 60–61
  - reliable and reproducible measurements, 59
  - sensitivity and specificity, 60–62
- ease of use and reliability, 52
- for liver fibrosis, 527–529
- liver stiffness assessment, 56–58
- in NAFLD patients, 126–127
- portal hypertension, 332, 334, 335, 343–344
- reinventing ultrasound technology, 55–56
- ultrafast ultrasound imaging, 54–55
- ultrasound attenuation, 63
- ultrasound speed of sound, 63
- vascularization, 63
- viscosity, 62–63
- Shear wave propagation maps, 36
  - bifurcation, 503
  - definition, 495
  - A and M-mode images interpretation, 498
  - normal elastogram, 496–497
  - with normal variants and disturbances, 503
  - probe positioning, 499–501
  - probe selection, 501–502
  - reflections, 503
  - shear wave interruptions
    - bifurcation, 503, 506, 507
    - broadening of waves, 507
    - displacement, 507, 508
    - duplication of shear waves, 504
    - examples, 504, 505
    - horizontal shaking, 504
    - reflections, 503, 506
    - sharp compression wave displacement, 504
    - slope alignment, 507
- Shear waves
  - classification, 20, 21
  - vs. compression, 20, 22
  - vs. ultrasound techniques, 20, 22, 23
- Shear wave speed estimation methods, 44
- Sinusoidal obstruction syndrome (SOS), 171–173
- Sinusoidal pressure hypothesis (SPH), 699
  - at cellular level, 676–677
  - clinical impact, 677–679
  - clinical studies, 671
  - dynamic and static components, 672
  - formation of regenerative nodules, 674
  - HABR, 674
  - hepatic inflow/outflow balance, 675, 676
  - initiation and perpetuation of fibrosis, 373, 672
  - point of no return, 674
  - pressure elevation, matrix generation, and arterialization cycle, 674, 675
  - SP-mediated stretch forces and matrix, 674
  - stiffness-mediated activation, 674
- Small nucleotide polymorphisms (SNPs), 277
- Spearman rank correlation, 712
- SPH, *see* Sinusoidal pressure hypothesis
- Spleen elastography, 157–158
- Spleen stiffness (SS), 319, 390
  - cutoff values, 712
  - hepatic decompensation, 365
- Spleen stiffness measurements (SSM), 37, 379, 591
  - clinical decompensation, 345–347
  - follow-up, 347–348
  - in rats, 97–99
  - by ultrasound elastography, 344–345
  - unknown cause or no cirrhosis, 348–350
- Spleen stiffness to liver stiffness (SS/LS) ratio, 697
  - in animal models with TAA-induced liver fibrosis, 372
  - for clinically significant portal hypertension, 372
  - effect of fibrosis stages, 372
  - intrahepatic localization of inflammation, 371
  - in portal (HCV) and lobular (ALD) chronic liver disease, 370–372
- Spontaneous porto-systemic shunts (SPSS), 599
- Standard for reporting of diagnostic accuracy (STARD) guidelines, 418
- Steatosis assessment, 149
  - BLEP, 442
  - CAP<sup>TM</sup> (*see* Controlled attenuation parameter (CAP<sup>TM</sup>))
  - causes, 413
  - computed tomography, 442
  - imbalanced hepatic lipid metabolism, 441
  - inflammatory activity, 460
  - liver biopsy, 442
  - MRI, 442
  - NAFLD diagnosis, 441
  - non-invasive tests, 426–427
  - serum-based biomarkers, 442, 443
  - ultrasonography, 442
  - ultrasound-based elastography, 459
  - ultrasound-based steatosis estimation, 460–464
  - on US, 425
  - VCTE<sup>TM</sup>, 414, 431–432

SteatoTest, 426  
 Strain elastography, 18–20, 52  
 Superconducting quantum interference device (SQUID), 209  
 Supersonic shear imaging technique, *see*  
 Two-dimensional shear wave  
 elastography (2D-SWE)  
 SuperSonic Shear Wave™ Elastography, 44

## T

TE, *see* Transient elastography  
 Tissue stiffness  
 distortion/mechanic stress, 16, 17  
 elastographic techniques, 17  
 by modes of excitation, 16, 17  
 by modes of reading/imaging, 17  
 physical principles, 18  
 radiation force, 16  
 TME, *see* Transient micro-elastography  
 Transarterial chemoembolization (TACE), 378  
 Transient elastography (TE), 52, 369, 525  
 acute liver failure, 302  
 alcoholic liver disease, 483  
 automatic probe selection tool, 486  
 cost-effectiveness, 548–549  
 cystic fibrosis  
 diagnostic methods, 162–164  
 long-term follow-up, 164–165  
 in other organs, 166  
 description, 23  
 hereditary hemochromatosis, 211–212  
 history, 29–30  
 liver fibrosis screening  
 in general populations, 546–547  
 by serum markers, 548  
 meal intake, 480–482  
 measurement site, 486–488  
 operator experience, 483–485  
 portal hypertension, 328–330  
 principle of, 479  
 reliability  
 CAP, 490–491  
 FibroScan, 488–489  
 point shear wave elastography, 490  
 two-dimensional shear wave  
 elastography, 490  
 in secondary hemochromatosis, 212–213  
 serum biomarkers, 105, 694  
 shear wave propagation maps (*see* Shear  
 wave propagation maps)  
 XL and M probe, 517–521  
 XL-probes, 546

Transient micro-elastography (TME)  
 cirrhosis, 100  
 experimental applications, 101  
 measurements, in rats, 98  
 $\mu$ FibroScan lab processing unit, 95, 97  
 $\mu$ FibroScan probe, 95, 96  
 pharmacological modulation  
 experiments, 99–100  
 portal hypertension assessment, 100  
 Transjugular intrahepatic portosystemic shunt  
 (TIPS), 261, 598  
 Tumor stiffness, 592

## U

Ultrafast ultrasound imaging, 54–55  
 Ultrasound attenuation, 63  
 Ultrasound-based elastography (USE), 5, 74,  
 459, 524, 525, 528, 529  
 Ultrasound-based steatosis estimation  
 during alcohol detoxification, 462, 464  
 attenuation imaging, 462  
 cutoffs for LSM, 462, 463  
 echo pattern distribution, 462  
 ultrasound signal attenuation, 460, 462  
 Ultrasound-based transient elastography  
 (TE), 3, 5–7  
 Ultrasound speed of sound, 63  
 USE, *see* Ultrasound-based elastography

## V

Varices need treatment (VNT), 334  
 Vibration-controlled transient elastography  
 (VCTE™) technology  
 acoustic output power, 32  
 CAP™, 414  
 force applied by operator, 31–32  
 measurements validity, 33  
 steatosis assessment, 431–432  
 transient excitation, shape and  
 frequency of, 32  
 Viral hepatitis, 80  
 Virtual touch quantification (VTQ),  
 376, 525  
 Virtual touch tissue imaging (VTI), 376  
 Viscosity, 15–16, 45

## W

Wilson's disease (WD), 623  
 ATP7B gene, 217  
 clinical cases, 219–220

clinical features and applications,  
217, 218  
liver stiffness measurement, 218–219  
World Federation for Ultrasound in  
Medicine and Biology  
(WFUMB), 414  
World Transplant Registry, 394

**Y**

Yes-associated protein (YAP), 661–662

**Z**

Zero viscosity, 15–16

Zieve syndrome, 618–619